G R
HONI SOIT QUI MAL Y PENSE
DIEU ET MON DROIT

IMPERIAL INSTITUTE
OF
AGRICULTURAL RESEARCH, PUSA.

PROCEEDINGS

OF THE

ROYAL SOCIETY OF LONDON

SERIES A

CONTAINING PAPERS OF A MATHEMATICAL AND
PHYSICAL CHARACTER.

VOL. CXXV.

LONDON:
PRINTED FOR THE ROYAL SOCIETY AND SOLD BY
HARRISON AND SONS, LTD., ST. MARTIN'S LANE,
PRINTERS IN ORDINARY TO HIS MAJESTY.

NOVEMBER, 1929.

LONDON:
HARRISON AND SONS, LTD., PRINTERS IN ORDINARY TO HIS MAJESTY,
ST. MARTIN'S LANE.

CONTENTS.

SERIES A. VOL. CXXV.

No. 796.—August 1, 1929.

PAGE

Fluorescent and Phosphorescent Excitation of Mercury Vapour by the Resonance Frequency and by Lower Frequencies. By Lord Rayleigh, F.R.S. (Plates 1–3) 1

The Energy Functions of the H_2 Molecules. By O. W. Richardson, F.R.S., and P. M. Davidson 23

The Spark Spectrum of Thallium, Tl III. By J. C. McLennan, F.R.S., A. B. McLay and M. F. Crawford 50

Tests of Significance in Harmonic Analysis. By R. A. Fisher, F.R.S. 54

The Arc Spectrum of Chlorine. By K. Majumdar. Communicated by M. Saha, F.R.S. 60

On the Numerical Solution of Equations with Complex Roots. By R. A. Frazer and W. J. Duncan. Communicated by H. Lamb, F.R.S. 68

High Frequency Fatigue. By C. F. Jenkin and G. D. Lehmann. Communicated by Sir Richard Glazebrook, F.R.S. 83

Gaseous Combustion at High Pressures.—Part XIII. The Molecular Heats of Nitrogen, Steam and Carbon Dioxide at High Temperatures. By D. M. Newitt. Communicated by W. A. Bone, F.R.S. 119

The Absorption Coefficient for Slow Electrons in Mercury Vapour. By R. B. Brode. Communicated by F. A. Lindeman, F.R.S. 134

A Mechanism of Gelatinisation. By F. L. Usher. (Plates 4 and 5.) Communicated by R. Whytlaw-Gray, F.R.S. 143

The Second Order Wave Equations of the Spinning Electron. By G. Temple. Communicated by S. Chapman, F.R.S. 152

The Ultra-Violet Spectrum of Magnesium Hydride.—II. The Many-Lined γ-System. By R. W. B. Pearse. Communicated by A. Fowler, F.R.S. 157

On the Criterion for Stability of a Layer of Viscous Fluid Heated from Below. By A. R. Low. Communicated by L. N. G. Filon, F.R.S. 180

The Determination of Molecular Forces from the Viscosity of a Gas. By H. R. Hassé and W. R. Cook. Communicated by S. Chapman, F.R.S. 196

PAGE

The Exclusion Principle and Aperiodic Systems. By N. F. Mott. Communicated by R. H. Fowler, F.R.S. 222

The Compton Scattering and the New Statistics. By S. Chandrasekhar. Communicated by R. H. Fowler, F.R.S. 231

Regularities in the Arc Spectrum of Arsenic. By. K. R. Rao. Communicated by A. Fowler, F.R.S. 238

No. 797.—September 2, 1929.

The Action of High Speed Cathode Rays on Acetylene. By J. C. McLennan, F.R.S., M. W. Perrin and H. J. C. Ireton 246

Kronecker's Fundamental Limit Formula in the Theory of Numbers and Elliptic Functions and Similar Theorems. By L. J. Mordell, F.R.S. 262

The Kinetics of the Oxidation of Ethylene. By H. W. Thompson and C. N. Hinshelwood, F.R.S. 277

Observations of the Height of the Ozone in the Upper Atmosphere.—Part II. By F. W. P. Götz and G. M. B. Dobson, F.R.S. 292

The Oxidation of Phosphine at Low Pressures. By R. H. Dalton and C. N. Hinshelwood, F.R.S. 294

The Spectrum of H_2: The Bands Analogous to the Orthohelium Line Spectrum.—Part II. By O. W. Richardson, F.R.S., and K. Das 309

The Isotherms of Hydrogen, Carbon Monoxide and their Mixtures. By G. A. Scott. Communicated by W. A. Bone, F.R.S. 330

The Effect of a Transverse Magnetic Field on the Propagation of Light in vacuo. By W. H. Watson. (Plate 6A.) Communicated by Sir Ernest Rutherford, P.R.S. 345

Diffraction of Cathode Rays.—III. By G. P. Thomson. (Pate 6B.) Communicated by Sir Joseph Thomson, F.R.S. 352

The Growth of Silver Iodide Films. By U. R. Evans and L. C. Bannister. Communicated by Sir Harold Carpenter, F.R.S. 370

No. 798.—October 1, 1929.

The Electrical Conductivity Caused by Insoluble Monomolecular Films of Fatty Acid on Water. By J. W. McBain, F.R.S., and C. R. Peaker 394

A Quantitative Study of the Reflexion of X-Rays from Crystals of Aluminium. By R. W. James, G. W. Brindley and R. G. Wood. Communicated by Sir William Bragg, F.R.S. 401

The Straggling of β-Particles. By E. J. Williams. Communicated by Sir Ernest Rutherford, P.R.S. 420

PAGE

The Amount of Hydrogen and Oxygen present on the Surface of a Metallic Electrode. By F. P. Bowden. Communicated by T. M. Lowry, F.R.S. 446

Infra-Red Investigations of Molecular Structure. Part III.—The Molecule of Carbon Monoxide. By C. P. Snow and E. K. Rideal. Communicated by T. M. Lowry, F.R.S. 462

The Structure of the Band Spectrum of *Helium*.—VI. By W. E. Curtis and A. Harvey. Communicated by T. H. Havelock, F.R.S. 484

A "Spinning Target X-Ray Generator" and its Input Limit. By A. Müller. Communicated by Sir William Bragg, F.R.S. 507

The Melting Point of Palladium. By F. H. Schofield. Communicated by Sir Joseph Petavel, F.R.S. 517

Gaseous Combustion in Electric Discharges. Part IV.—The Effect of Moisture upon the Cathodic Combustion of Carbonic Oxide Detonating Gas. By G. I. Finch and D. L. Hodge. Communicated by W. A. Bone, F.R.S. 532

An X-Ray Investigation of the Structure of Naphthalene and Anthracene. By J. M. Robertson. (*Plates 7 and 8.*) *Communicated by Sir William Bragg, F.R.S.* 542

The Spark Spectrum of Thallium, Tl II—Term Analysis.—Fine Structure of Lines. By J. C. McLennan, F.R.S., A. B. McLay and M. F. Crawford 570

No. 799.—November 1, 1929.

A Robust Microbalance of High Sensitivity, Suitable for Weighing Sorbed Films. By Prof. James W. McBain, F.R.S., and Dr. H. G. Tanner 579

Further Studies on Intertraction. By Sir Almroth E. Wright, F.R.S. (Plates 9 and 10) 587

Notes on a Differential Equation which occurs in the Two-Dimensional Motion of a Compressible Fluid and the Associated Variational Problems. By H. Bateman, F.R.S. 598

A new form of Calorimeter suitable for Determining Heats of Solution, with an Application to Worked and Annealed Metals. By C. J. Smith. Communicated by Prof. C. H. Desch, F.R.S. 619

Sulphide Colours on Metallic Copper. By F. Hurn Constable. Communicated by T. M. Lowry, F.R.S. 630

The Decomposition of Potassium Hydrogen Oxalate Hemihydrate. By J. Hume and J. Colvin. Communicated by R. Whytlaw-Gray, F.R.S. 635

On the Turbulent Wake behind a Body of Revolution. By L. M. Swain. Communicated by L. Prandtl, For.Mem.R.S. 647

Electron Scattering in Mercury Vapour. By F. L. Arnot. Communicated by J. Chadwick, F.R.S. 660

PAGE

The Crystal Structure of Ice between 0° C. and − 183° C. By W. H. Barnes. (Plates 11 and 12.) Communicated by Sir William Bragg, F.R.S. 670

The Behaviour of Electrolytes in Mixed Solvents. Part I.—The Free Energies and Heat Contents of Hydrogen Chloride in Water-Ethyl Alcohol Solutions. By J. A. V. Butler and C. M. Robertson. Communicated by J. Kendall, F.R.S. ... 694

The Rate of Emission of Alpha Particles from Radium. By F. A. B. Ward, C. E. Wynn-Williams and H. M. Cave. Communicated by J. Chadwick, F.R.S. 713

Index 731

PROCEEDINGS OF
THE ROYAL SOCIETY.

Section A.—Mathematical and Physical Sciences.

Fluorescent and Phosphorescent Excitation of Mercury Vapour by the Resonance Frequency and by Lower Frequencies.

By Lord Rayleigh, F.R.S.

(Received June 17, 1929.)

(Plates 1–3.)

§ 1. *Introduction. Absorption by Wave-lengths longer than the Resonance Line.*

It is known that the fluorescence of mercury vapour can be excited by absorption in the region λ 1850, situated near the resonance line $1\,{}^1S_0 - 1\,{}^1P_1$, and in the region of band absorption λ 2345. It can also be excited by absorption in the region of the resonance line $1\,{}^1S_0 - 2\,{}^3P_1$ 2536·52. In this latter case it has, I believe, been generally supposed that fluorescence is not obtained unless excitation is fairly close to the resonance line. Thus Pringsheim and Terenin* found that a hot mercury lamp (punktlampe of Heraeus) or an overloaded ordinary 220-volt mercury lamp does not give band fluorescence of any kind. In the hot lamp the core of the resonance line is removed by self reversal.

It is, however, well known that unexcited mercury vapour has an absorption band beginning near the resonance line 2537, and extending, if the vapour is dense, to a distance of some hundreds of Ångströms towards longer waves. The question arises whether this absorption is accompanied by fluorescent emission or not.

The following experiment was made in January, 1927, much before the rest of the investigation, with a view to seeing how far from the resonance line the absorption could be pushed. A quartz tube about 10 cm. long and 1 cm. diameter contained a drop of mercury sealed up *in vacuo*. The ends were made as clear and transparent as practicable so that a beam of light could be sent axially along the length.

---

* 'Z. Physik,' vol. 47, p. 338 (1928).

The silica tube was placed in a simple form of electrically heated tube furnace. The source of illumination was burning sulphur (carbon disulphide in a spirit lamp) which gives a convenient approximately continuous spectrum over the range required (Plate 1, No. I*a*). The heating current was increased by steps until the tube exploded. At each step the absorption spectrum was photographed with a reference spectrum from a glass mercury lamp. The tube endured, for a few minutes at all events, a current of 2·5 amps. in the furnace, but on increasing the current to 2·75 it burst, about a minute after the increase. The exposure at 2·5 amps. heating current showed transmission beginning at λ 3650 (Plate 1, No. I*b*). The exposure in progress at the time of explosion showed transmission from λ 3750. The tube was then nearly white hot.

It appears that under these conditions absorption is complete for a range of 1200 Å. from the resonance line: with a tube of double the length the absorption range could doubtless be pushed still further.

It is of interest to notice that this absorption progresses continuously from the resonance line, until it covers the range of the continuous band 3130 to 3650 (maximum 3300) which is so well known in fluorescent emission.

At no stage is a maximum absorption at λ 3300 to be seen on the photographs.

§ 2. *Fluorescence under Long Wave-Excitation. "Antistokes" Effect.*

In the past experiments on the fluorescence of mercury vapour have been made for the most part with vapour of low density, into which the high frequencies from the aluminium spark, or the frequencies in the immediate neighbourhood of the resonance line 2537 could penetrate. To detect the fluorescence (if any) under much lower frequencies, it was evidently desirable to try vapour dense enough sensibly to absorb these frequencies.

Mercury was boiled at atmospheric pressure in a rectangular box built up from sheets of silica fused together at the edges. The spectrum from a suitable source was focussed on the side of the silica box, using a quartz train. The lines could be identified on a fluorescent screen, and when this was withdrawn, and the light traversed the mercury vapour, the tracks of lines lying within a certain spectral range could be traced through the vapour by the green visual fluorescence.

In this way a cadmium spark source showed a conspicuous track along the line λ 2573, and a less conspicuous one along λ 2748.

A mercury lamp of the type working at atmospheric pressure, in spite of the strong reversal of λ 2537, showed conspicuous fluorescence about this position, and also along the track of lines of shorter wave-length, including the blend 3125–3132. Fluorescence at λ 3341 or λ 3650 was not observed with this arrangement.

The line 3125 is within the range transmitted by Jena blue uviol glass, which cuts at about λ 2890. This offers great advantages over the monochromator for getting rid of green and yellow components from the source, which contribute false light without helping the excitation.

Mercury may be boiled in a silica flask at atmospheric pressure with reflux condensation. The beam from an "atmospheric" mercury lamp, or an iron arc, filtered through the blue uviol, and concentrated upon the vapour by a quartz condensing lens, is marked by a bluish green track bright enough to be shown to a fairly large audience.*

It was desired, if possible, to excite the vapour with still lower frequencies. To do this it is best to work at pressures above atmosphere so as to increase the absorption. A silica bulb was used of about 4 cm. diameter, containing a drop of mercury, exhausted and sealed. This was heated over a Bunsen burner, the lower part being nearly or quite red hot and the upper part bathed in hot air. To see the fluorescence to the best advantage, visual light should be excluded as far as possible. This was done by supplementing the blue uviol glass with a silica cell containing bromine vapour. The combination was opaque to the whole visual region, except the deep red.

Many experiments were made by stimulating the vapour with the light of isolated lines from various spectra. But the best success was gained by using a nickel arc as source, limiting it on the short wave side by filters giving a sharp cut. This arc shows a strong and well distributed group of lines from about λ 3360 to λ 3620. Thus the maximum frequency transmitted is practically determined by the properties of the filter.

The filters used were alcoholic solutions of organic substances in a silica cell. They were chosen from the data given by Hartley and Huntingdon on organic absorption spectra, but the absorption limits were determined from the actual filters used. A filter of natural (ortho) salicylic acid, 1 cm. thick, containing 1 gram in 280 c.c. of alcohol, was found to cut the spectrum at λ 3360. Using this filter the green fluorescence was easily seen along the track of the beam.

---

* A preliminary notice of these experiments was published in 'Nature,' August 18, 1923.

A solution of quinine hydrate cutting at λ 3450 was next tried. The silica bulb was smaller (2·5 cm. diameter) and was made very hot. The green fluorescence was again seen without difficulty.

I pass now to the spectrum of the fluorescence. This was examined with a small Hilger quartz spectrograph, using a rather wide slit.

In this work it is to be noticed that the exciting light is extremely powerful compared with the fluorescence, and that the spherical bulb used, though suited to resist internal pressure, was not of favourable shape for avoiding stray light. The fluorescence spectrum is therefore overlaid to a considerable extent by false light from the source, and is only examined to advantage in those regions where the light from the latter is cut off by the filters used, thus outside the region of excitation.

The primary beam viewed laterally was focussed on the slit of the spectrograph by a quartz-fluorite achromat, the image of the beam occupying only a strip of the vertical range of the spectrum. It is distinguished by this limited breadth of spectrum from the spectrum of the stray exciting light, and light from the burner used to heat the bulb.

Various spectra are reproduced with different limits of excitation. In Plate 1, No. II, the excitation is by the light of the iron arc filtered through blue-purple corex glass,[*] with a tube of chlorine 28 cm. long and a cell of bromine vapour 8 cm. long. These filters transmit the most effective part of the spectrum for excitation of fluorescence including the region of the resonance line, but cut off everything of longer wave-length than 2650, thus leaving the rest of the spectrum clear for observing the fluorescence.

This exhibits the broad structureless bands—

3130–3650—maximum 3300;
4300–green—maximum 4850;[†]

with the intervening minimum at 3800.

It will be shown presently that there are features in the neighbourhood of the resonance line. These cannot be made out on the present photograph owing to stray light, and to absorption by the large quantity of mercury vapour which has to be traversed by the emerging fluorescent beam. Only stray light from the source is seen in this region. Plate 1, No. III, represents the fluorescence excited by the iron arc filtered by Chance's vita glass and bromine (exciting wave-length 2850 upwards). The fluorescent spectrum is overlaid and somewhat obscured by the exciting light until we come to the region which is protected by the bromine filtration. The features are similar to those of the previous spectrum. It is clear from this photograph that both the broad bands 3300 and 4850 can be excited by wave-lengths hundreds of Ångströms greater than the resonance line.

---

[*] See *infra*.

[†] The position assumed for this maximum is very arbitrary, everything depends on whether photographic or visual intensities are taken. I follow previous writers, and refer to the bands as 3300 and 4850.

Plate 1, No. IV, is of special interest. Excitation in this case is by the nickel arc, filtered by salicylic acid, and an (inadequate) bromine cell. The same two broad bands are still present and discernible, though seriously overlaid by the stray light from the source. But the interesting point is that while excitation begins only at λ 3360, the narrow fluorescent spectrum stretches out into the region of shorter waves with marked violation of Stokes' law. The excitation is applied in the middle of the band 3300. It might be expected that this band would be as it were cut in half. But this does not occur. So far as the photographs allow of a judgment being formed it seems to be complete. The "antistokes" portion is seen to better advantage than the rest, owing to the absence of stray light. Whether any discontinuity of intensity sets in at the wave-length 3360 where the exciting spectrum begins, it is difficult to say, owing to the complication due to false light. On the negative the fluorescence is easily traceable as far as the wave-length 3130 which I have somewhat arbitrarily given as the limit of the band.* That is to say, it extends 230 A. on the short wave side of λ 3360, the shortest wave-length of the exciting light.†

It was attempted to photograph the fluorescence with yet lower excitation, using the quinine filter which cuts at λ 3450. Though, as already mentioned, this excitation gave an easily perceptible green fluroescence, I did not succeed in getting definite photographic results.

§ 3. *Fluorescence in the Neighbourhood of the Resonance Line. Iron Arc Excitation.*

The experiments so far described deal with the two broad maxima 3300 and 4850. We have now to consider the fluorescence in the neighbourhood of the resonance line λ 2537·52. It is to be remarked that in this neighbourhood the absorption of the vapour is strong, and therefore it is useless to attempt to observe through a thick stratum of dense vapour. On the other hand, the avoidance of false light is here all important, and for this the exciting beam must be kept away from the wall of the containing vessel, a condition which makes it difficult to avoid an intervening stratum of some thickness. The best compromise achieved so far is to keep the density of the vapour fairly low, and to work with a beam well defined by the use of lenses and diaphragms, and passing as close to the wall of the vessel as may be, without actually touching it. In the final experiments on this part of the work a tall rectangular blown silica vessel, measuring 7 × 7 × 18 cm. has been used almost exclusively.

---

* The limit is really quite indefinite, depending on the exposure. It extends much further in the photograph, Plate 1, No. II.

† A preliminary note of this result was published in 'Nature,' January 26, 1929.

Since the fluorescence in this region cannot be seen, it is much more difficult to arrive at the proper experimental conditions, and it is not claimed that anything like a complete survey has been made.

The iron arc was used as a source. It has the advantage of a small bright radiant, favourable to the formation of a concentrated and well defined beam in the vapour. Further, we have the very great advantage that the spectrum of the source is distinctive, and incapable of being confused with that of the fluorescence.

It is important in this and other parts of the present investigation to have an accurate knowledge of the spectrum of the iron arc in the neighbourhood of the mercury resonance line. Plate 1, No. V, shows these spectra photographed in comparison with a Hilger Littrow spectrograph. The mercury line is from a water cooled lamp of low voltage.

The wave-lengths are :—

		Interval from the mercury line.
Fe	2535·610	
		0·91
Hg	2536·52	
		0·30
Fe	2536·82	
		0·66
Fe	2537·180	
		2·30
Fe	2538·82	
		2·44
Fe	2538·96	

The comparison photograph V (Plate 1) confirms clearly enough that the mercury line *when narrow* does not overlap any one of the iron lines.

The fluorescence excited by the iron arc was photographed with a Hilger spectrograph of medium size, giving a dispersion of 0·12 mm. per Ångström at this part of the spectrum. The exposures were not more than 2 hours.

The spectra show the resonance line 2537 and the narrow band 2540·5, which extends from this position to the resonance line. As the pressure was diminished the line becomes more conspicuous relative to the band. This may be due in part to the lesser density of absorption vapour to be traversed. At pressures below 5 mm. the band is invisible.

Pressure, mm.	Line 2537.	Band 2540.
40	Absent	Present
20	Present	Strong
10	Strong	Strong
5	Strong	Suspected
2	Strong	Absent
1	Visible	Absent

These results are illustrated by Plate 1, Nos. IX and X.

No. IX shows the result at 10 mm. pressure, in comparison with the iron spectrum which forms the exciting light, and which is shown above. It will be observed that contamination with the exciting light has been successfully avoided. The total range of iron spectrum shown is about 55 Å.

Plate 1, No. X, shows the result at 2 mm. pressure.

At the higher pressures the *apparent* breadth of the line on the plate was 1 Å., while at the lower pressures it had an apparent breadth of less than half this amount. I suspect that these breadths are real, and not merely instrumental. But investigation of this point with higher resolving power is desirable, and should present no insuperable difficulty. However this may be, the centre of the resonance line is of higher frequency than the nearest iron line, and its excitation involves a violation of Stokes' law. The iron line on the side of higher frequency than the mercury line is not in question, as it is not absorbed except by dense vapour.

It is probable that the mercury vapour actually traversed in this vessel cuts out the iron line 2536·82 before the exciting light reaches the point where the lateral emission is examined. But to make sure, the exciting light was filtered by an independent absorption cell 3·2 cm. thick, containing mercury boiling at 1 cm. pressure. It was independently verified that this cut out the line in question. The mercury resonance line, and also the band 2540, were again obtained. In this case we have a clear interval of 0·66 Å. between the centre of the mercury resonance line, and the nearest exciting iron line.

The excitation could perhaps be observed with an interval considerably more than 0·66 Å., but I have not attempted anything further in this direction.

§ 4. *Core Effect and Wing Effect. Due probably to Atomic and Molecular Absorption.*

It is seen from the above experiments that both the visual fluorescence and the line 2537 can be obtained with exciting frequencies which are not coincident with that of the resonance line, but which are *less*, and in the case of the continuous spectrum of fluoresence, including the visual, *very much less*.

On the other hand, absorption is very strong at the actual position of the resonance line, and gives rise to the phenomenon called resonance radiation, as well as to visual fluorescence.

It is important to determine, if possible, whether sharp distinction exists between these two cases.

A priori we should certainly expect such a distinction, though Pienkowski has suggested* that at the resonance line, the secondary visual fluorescence is due to molecular absorption, the *atomic* absorption operating merely to use up the available energy and thus producing the illusion that the fluorescence-absorption is very energetic.

It seems clear that emission of the resonance line is not in itself a proof that the primary excitation or the chief absorption is atomic. This will, perhaps, be most readily admitted if we consider the case of sodium vapour, where molecular excitation in the blue-green region causes emission of the D lines.

It is instructive to excite mercury vapour by a source which extends continuously over the region of the resonance line and beyond it. Such a source is provided by the widened line of a mercury vapour lamp which is *not fully cooled*. This source is not indeed ideally continuous, since the resonance line is always seen reversed under a sufficiently great resolving power, but if this reversal is not so complete as to cut out altogether the core of the line, it will serve the purpose. I have used a water-cooled lamp of small diameter (7 mm.) and also an air-cooled lamp of larger diameter. The latter is convenient, in that the temperature and with it the terminal voltage can be regulated by moving the cooling fan closer or further off. A magnet is used as usual to press the discharge forward.

With 23 volts at the terminals the line is narrow and self-reversal cannot be detected, even with the Littrow spectrograph giving 0·36 mm. per Ångström. Allowing the voltage to increase to 50 or 60 volts, the breadth of the line increases sufficiently for the experiments about to be described.

---

* 'Z. Physik,' vol. 50, p. 791 (1928).

If we examine the visual fluorescence in mercury vapour saturated at, say, 10 cm. pressure, using the cold lamp we see nothing but a bright layer close to the wall of the vessel (Plate 1, No. XI). Allowing the lamp to warm up until it takes 50 or 60 volts, we find that this layer still subsists, but that beyond it the path of the incident beam is marked out by a fainter luminosity (Plate 1, No. XII). The point which I wish to emphasise is that as we go along the beam, the intensity does not fall off gradually but *suddenly*. There is a discontinuity of *intensity*, not perhaps in the full mathematical sense of the word, but in the same sense that we encounter a discontinuity of intensity in the spectrum of a salted spirit flame if we pass from the centre of one of the D lines to the continuous background of the spectrum.

The first emission, seen alone in Plate 1, No. XI, is due to the core of the resonance line, and I distinguish it as the *core effect*. The lateral emission along the further course of the beam, observed when the lamp is hot and the exciting line broadened, I call the *wing effect* (Plate 1, No. XII).

The discontinuity is very noticeable in visual observation ; the photographs show it less satisfactorily.*

We have seen that both line absorption and band absorption exist, and give rise to visual fluorescence. It is almost inevitable to attribute the core effect to line absorption and the wing effect to band absorption. The former must then result (indirectly no doubt) from atomic absorption. The latter from molecular absorption.

It is evidently important to determine what range of wave-lengths is active in producing the core effect. This was determined as follows. Two flat-sided silica cells were used in series, here called the absorption cell and the observation cell. The absorption cell was 5 mm. thick, the observation cell much more. Each contained mercury boiling under a reflux condenser, the lower part of the condenser containing mercury vapour in pressure equilibrium with the air filling the upper part. The latter was connected in each case to a separate low pressure reservoir. The pressure of mercury vapour in the observation cell was 1 cm., and in the absorption cell it was adjustable at pleasure. The beam from the mercury lamp at 55 volts, filtered by blue-purple corex glass, was passed through both cells, and when the absorption cell was cold it produced both wing and core effect in the observation cell. Thus more than the extreme range of wave-lengths which can contribute to the core effect was present.

---

* As is known, photography is at some disadvantage when extreme intensity contrasts are to be represented. It is difficult, *e.g.*, to deal with windows in photographing an architectural interior.

It was found by repeated experiments that if the vapour pressure in the absorption cell exceeded 3 mm., the core effect was not seen in the observation cell, all the radiation capable of producing it having been absorbed. With 2 mm. pressure in the absorption cell some core effect was seen in the observation cell. 2·5 mm. was adopted as the critical pressure.

The observation cell was then put aside, and the absorption cell alone at 2·5 mm. mercury vapour pressure was arranged between the source and the large Littrow spectrograph. The spectrum obtained is shown by Plate 1, No. VIII. The breadth of the reversal was measured as 0·1 Å., or, assuming symmetry, 0·05 Å., on either side of the centre of the resonance line. The photographs VI and VII, Plate 1, are generally confirmatory of this conclusion. VI is from a lamp hot enough to give both wing and core effect. The total width of the line, itself slightly reversed, exceeds the width of the artificially increased reversal in No. VIII. VI is from a fully cooled lamp which gives the core effect only, and shows a line which could go inside the reversal of No. VIII.*

The nearest iron line in No. V, Plate 1, is 0·30 Å. from the centre of the resonance line, and is therefore much beyond the limits within which the core effect is produced. In agreement with this, excitation by the iron arc is in fact found to give the wing effect alone without the core effect.

So far we have spoken of wing and core effect in the visual region alone. We shall see later that the same distinction is apparent in the region of the resonance line 2537.

The discontinuity distinguishing wing and core effect, which is so well seen in emission, must exist also in absorption, but is necessarily more difficult to detect. For lack of space this point is not discussed.

5. *Fluorescence carried along by a Moving Stream of Vapour. Different Behaviour of Visual and Ultra-violet Regions.*

One of the most interesting phenomena in connection with mercury fluorescence is the relatively long duration of the visual luminosity when the vapour is made to move away from the point of excitation. This was first described by F. S. Phillips.† Special attention has been paid to this effect, and some unexpected results have emerged.

---

* The photographs VI, VII, VIII, Plate 1, were taken independently, and are not in accurate relative position.

† Phillips, 'Roy. Soc. Proc.,' A, vol. 89, p. 39 (1913). See also Houtermans, 'Z. f. Phys.,' vol. 41, p. 140 (1927); Pienkowski, 'Zeit. f. Phys.,' vol. 50, p. 791 (1928). For analogous phenomena produced by electrical excitation see Rayleigh, 'Roy. Soc. Proc.,' A, vol. 108, p. 263 (1925), and A, vol. 114, p. 620 (1927).

In these experiments, everything depends on the avoidance of stray light from the source. A great step is made in this direction if we use a square silica tube instead of a round one. Such tubes have been drawn for me by the Thermal Syndicate, Wallsend. They can also be built up from silica sheet, which gives fairly satisfactory results even without being ground and polished. The advantages of a square tube are that a flat metal diaphragm can be applied to it to limit the entering beam; that the view is through a flat surface; that there is little tendency for the entering beam to be reflected internally round the tube in the thickness of the walls, with consequent scattering by striæ and bubbles, and above all, that no reflected image of the entrance or exit of the exciting beam is seen on the back surface of the tube, which would obscure the phenomenon of lateral emission. No one who tries square tubes in this class of work will willingly go back to round ones.

In observing the visual fluorescence, it is very desirable to avoid admitting the light of the visual mercury lines into the vessel at all. Until lately this could only be prevented by the use of a prismatic monochromator, but the "blue-purple corex" glass introduced by the Corning Company, which has already been mentioned, transmits a considerable fraction of the light of λ 2537, while cutting out altogether the green and yellow lines. For many purposes this is enough. If a bromine vapour cell be added we get rid of all the blue light from the mercury lamp as well, and the mercury vapour fluorescence can be observed in complete darkness, except for the inevitable fluorescence of the silica vessel where the exciting beam traverses it. This, however, is usually of little consequence. Two 3½-inch quartz condensing lenses of short focus were used between the lamp and the observing vessel.

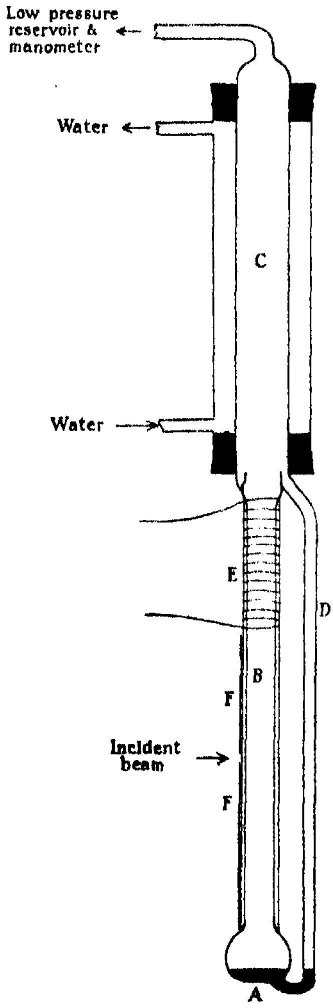

FIG. 1.—½ natural size.

The experimental vessel chiefly used is shown in fig. 1. The mercury is boiled by a source of heat placed at A. The vapour current rises into the square tube B and condenses in the water jacketted tube C. The condensed liquid runs back by the side tube D, which, though represented in the plane of the diagram, is in fact somewhat below, so that it should not scatter light from the emergent beam.

The square tube was made longer than experience afterwards showed to be desirable. This resulted in premature condensation of the vapour. The electrical heater indicated at E served to prevent this.

An iron plate F served as a screen to define the entering beam; it was somewhat broader than the square tube, so that the latter was in its shadow. The aperture was 2 × 4 mm., the longer dimension being vertical. A larger diaphragm placed 2 cm. away gave additional protection.

If this apparatus is exhausted the density and velocity of the vapour stream are obviously indeterminate, depending within wide limits on the rate at which heat is supplied. If we assume that the pressure of vapour in the condenser is effectively maintained at zero, the frictional resistance to the flow in the tube will absorb the driving difference of pressure between the boiler and the condenser; but the velocity and density at a given point cannot be determined without further data. The density cannot exceed the saturation density at the temperature of the mercury; and the velocity cannot exceed the molecular velocity. But either may be much less. In the future, it is hoped to elaborate the method of working to give precise information on these points. In the present work I have not been able to give particular attention to them.

If the condenser is connected above to a reservoir containing a few millimetres pressure of gas or vapour, then clearly before heat is applied the rarefied atmosphere will fill the entire apparatus. But as soon as the mercury boils vigorously, and the vapour issued from the long and comparatively narrow tube, and liquefies in the condenser, then the permanent gas is driven completely out. The conditions are apparently very similar to those in a mercury condensation pump. A surface of separation between the mercury vapour and the permanent gas must occur in the condenser. If, as in the present case, the condenser tube is of moderate diameter this surface may be somewhat indefinite. If the tube is narrow (say 4 mm.) as in some of my earlier experiments on absorption spectra of mercury boiling under various pressures, then the surface of separation is well defined, and in the case of an accessible air-cooled tube, can be readily located within a few millimetres by feeling the temperature with the hand.

Some experimenters who have not apparently themselves used the method suspect that under these conditions the mercury vapour is liable to be mixed with gas.* No doubt in theory there is some counter-diffusion of permanent gas against the mercury vapour current. I am convinced that under the conditions here used it is negligible. It is known that mercury fluorescence stimulated by the resonance line is very sensitive to the presence of air. The definite manner in which the fluorescence appears as the apparatus is heating up shows that the air is effectively removed as soon as condensation of mercury drops ceases to occur below the level of entrance of the exciting beam.†

By this device of allowing the mercury to boil under an external atmosphere the pressure of which can be varied, we can control the density of the mercury stream itself at the outflow end. If the pressure is diminished, the density of the mercury stream in the tube is diminished and the velocity increased. Although the control is not of that perfect kind which would allow us to assign predetermined values to the density and velocity, it is nevertheless enough to allow important conclusions to be drawn from experiments made under varied conditions.

As we have seen, the spectrum of the fluorescence may be divided into two portions. These are separated by a wide interval in which there is little or no emission, and this circumstance suggests, and at the same time makes easy, a separate investigation of them by using appropriate filters.

What I shall call, for brevity, the ultra-violet fluorescence, includes the resonance line 2537 and the band 2540 (Plate 1, No. IX), but not the band 3300, which of course is also in the ultra-violet. The filter used to isolate it consists of 28 cm. of chlorine, and 8 cm. of unsaturated bromine vapour. This compound filter cuts off all radiation of shorter wave-length than 2650, with the exception of red, to which the plates used are not sensitive. Photographs of the fluorescence taken through it with a quartz lens are due to the resonance line and the band 2540 near this line, since this part alone of the fluorescence spectrum is able appreciably to penetrate the filter.

---

* See for instance Walter and Barratt, 'Roy. Soc. Proc.,' A, vol. 122, p. 209 (1929).

† If, as in some experiments, not here described, the vessel consists of a wide flask or bottle with an internally cooled test tube projecting right into it, then the vapour current is less brisk, and air is more easily trapped. If the heat momentarily fails owing to draughts, etc., air may get in, and the fluorescence becomes unsteady. In vessels such as fig. 1 this *never* occurs in my experience, under a wide range of conditions. See further Pringsheim and Terenin, 'Zeit. f. Phys.,' vol. 47, p. 338 (1928); also Wood and Voss, 'Roy. Soc. Proc.,' A, vol. 119, p. 699 (1928).

On the other hand, photographs taken through a glass kinematograph lens (usually with an orthochromatic plate and yellow filter) represent the visual effects only. The effects of the broad maximum at 3300 (see Plate 1, No. II) are not represented in either. It is probable that they would show the same phenomena as the visual region.

The series of photographs on Plate 2 sums up this part of the work, and gives varied information. These photographs can be classified in several ways. The actual method of arrangement has been chosen so as to exhibit the progressive changes and contrasts of behaviour as clearly as may be. The core effects (top row) are distinguished from the wing effects (bottom row). The pressure of the atmosphere of permanent gas above—under which the various effects occur—diminishes from left to right, while the phenomena photographed in visual and in ultra-violet light under given conditions of pressure and excitation are placed side by side within a common margin.

These photographs have been trimmed so as to show the whole external breadth of the square tube B, fig. 1. The entrance and exit point of the beam are in most cases more or less conspicuously seen at the edges of the picture. They are made visible by the fluorescence of the silica tube. It is believed that no difficulty will be felt by the reader in distinguishing this effect from the fluorescence of the vapour. The latter is, of course, within the tube whereas the former is in the thickness of the tube wall. This is clearly apparent in No. XII in which, owing to an exceptionally long exposure, the tube walls have themselves been depicted, probably by light diffused in the course of repeated internal reflexions. In the photographs generally, when two or more or less separate luminous effects are observed at the left of the photograph where the beam enters; the first is due to stray light and fluorescence of the silica, the second to the vapour fluorescence.

Coming now to the fluorescent phenomena themselves, and beginning with the core effect, we notice in comparing Nos. I, II, IV and VI (Plate 2) that as the pressure is reduced the visual core effect begins to be perceptibly prolonged upwards (*i.e.*, out of the icident beam, and along the vapour stream) at 5 mm. pressure. For brevity this phenomenon will be referred to as "persistence."

Making a similar comparison for the ultra-violet core effect (Plate 2, Nos. III, V, VII, VIII) we observe that this, too, eventually shows persistence, though it only becomes apparent in VIII where the pressure above is reduced to a fraction of a millimetre.* There is, then, a range of conditions over which the visual fluorescence shows persistence and the ultra-violet shows none.

---

* Preliminary notes were published in 'Nature,' March 30, 1929, and April 13, 1929.

This is illustrated by comparing on Plate 2, No. IV, with Plate 3, No. V, and still more conspicuously by comparing VI with VII on this plate. As the superincumbent pressure in the condenser is reduced, the visual intensity becomes more and more diluted and difficult to see. At the stage of VIII (Plate 2) when the condenser is in communication with the air pump, there is no perceptible visual effect, even with well rested eyes, and all stray light from extraneous sources carefully excluded.

At one stage of the work I was tempted to doubt whether the ultra-violet fluorescence would show persistence under any circumstances, though in the light of earlier work by several investigators, including myself, it was difficult to suppose that it could not. Eventually it was found that if the external atmosphere was pumped down to a fraction of a millimetre or less, this did occur. (Plate 2, No. VIII.)

Coming next to the wing effect obtained with the hot lamp, we find substantially the same course of changes. Here again persistence sets in sooner for the visual than for the ultra-violet (compare on Plate 2, X with XI, and XII with XIII).

Under the experimental conditions used, the core effect occurs close to the wall of the experimental tube. Owing to viscosity the vapour current is more rapid in the middle of the tube than near the walls. We should expect therefore to find that persistence in the wing effect shows itself at higher pressures and therefore lower mean linear velocities than does persistence in the core effect.

This agrees with observation. At 9 mm. pressure persistence in the core effect is not apparent (Plate 2, No. II) but in the wing effect it is conspicuous (No. X). At low pressures the wing effect, like the core effect, shows persistence (No. XIV).

Another result of the greater velocity in the middle of the tube is the arching up of the visual wing effect seen in X and in XII.* This illustrates the delay in the appearance of the luminosity which has been investigated by Wood† in the case of aluminium spark excitation and by Pienkowski‡ for resonance line excitation. This is not equally conspicuous in the ultra-violet wing effect, but I am not prepared to say that it is absent altogether. Further investigation is needed on this point.

---

* The spotted appearance seen in No. XII, Plate 2, at the level of the incident beam is due to false light from optical imperfections in the tube. They are seen in this photograph because of the exceptionally long exposure which has also brought out the outline of the tube walls.

† 'Roy. Soc. Proc.,' A, vol. 99, p. 365 (1921).

‡ *Loc. cit.*

The above experiments on the *wing effect* show persistence when excitation definitely departs from the position of the atomic resonance line. We have seen, however, in the earlier part of this paper that visual fluorescence may be excited wave-lengths as much as 800 Ångströms greater than this, and the important question arises whether *persistence* is potentially observable over the whole of this range.

Much time was spent during the earlier part of the work in experimenting on this, and a note was published* in which it was stated that persistence could be observed for exciting wave-lengths up to, at any rate, wave-lengths 2650. These observations were made with a monochromator, the mercury vessel being traversed along the spectrum to the limit at which the effect could be observed. Further experimenting has led me to the conclusion that they cannot be relied on. The results were probably due to impurity of the spectrum due to scattered light, and to the aberration of the large aperture lens of the monochromator. On substituting for the monochromator a cell containing a dilute solution of benzene in alcohol, which cuts at λ 2650, no trace of fluorescence could be seen at pressures of 1 cm. or lower, such as are necessary for bringing persistence into evidence.

The difficulty is that denser vapour is needed for bringing into evidence the fluorescence at the longer wave-lengths, on account of the rapidly falling absorption coefficient for increasing wave-length; and in a tube of uniform bore dense vapour is unfavourable to higher linear speeds. It is planned to experiment further by allowing dense vapour from a nozzle to expand into an exhausted space, illuminating it at the mouth of the nozzle. Something has already been done on these lines, filtering the exciting light through mercury vapour so as to remove the wave-lengths near the resonance line. In this way persistence was shown for excitation 8 Å. away from the resonance line. But the arrangements were not well designed, and it should be possible to go much further.

§ 6. *Transition from Resonance Radiation at Room Temperature to the Persistent Ultra-Violet Core Effect.*

The photographs on Plate 2, classed as ultra-violet, are due to the aggregate effect of the resonance line λ 2537 and the neighbouring band 2540, if the latter contributes. We have seen, however, that even when the source (iron arc) contains no component in accurate coincidence with the line 2537, the line

---

* 'Nature,' November 10, 1928.

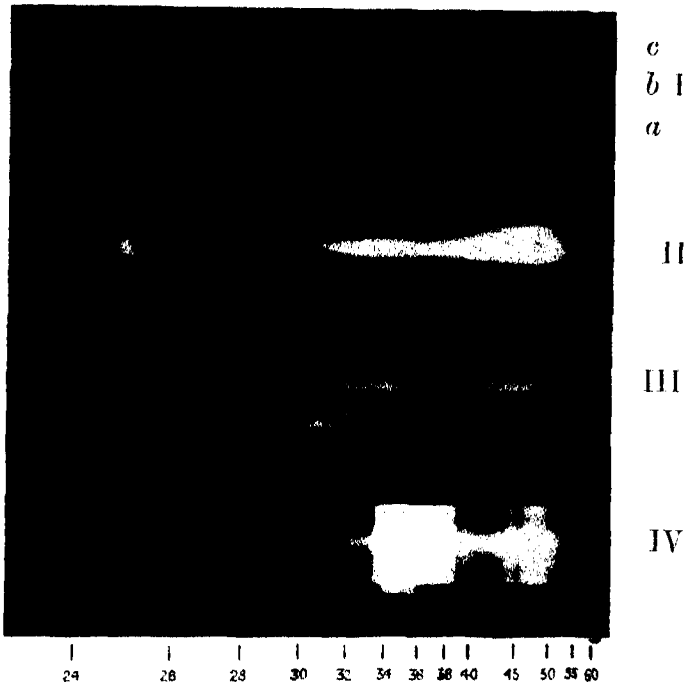
c
b I
a
II
III
IV
24
26
28
30
32
34
36
38
40
45
50
55
60

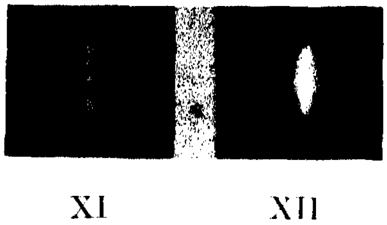
XI
XII

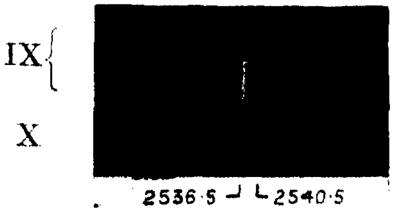
IX
X
2536·5
2540·5

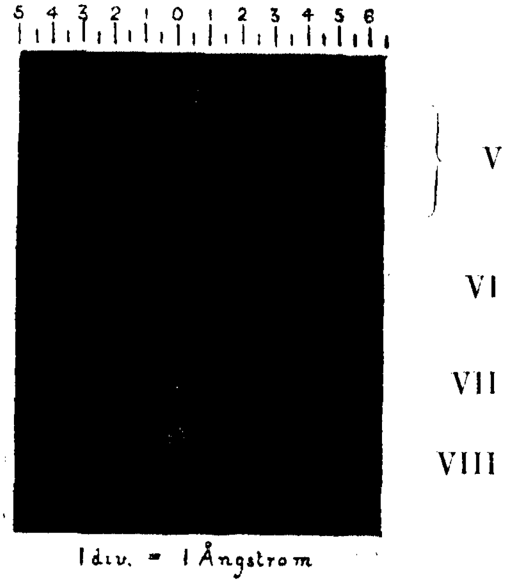
5 4 3 2 1 0 1 2 3 4 5 6
V
VI
VII
VIII
1 div. = 1 Ångstrom

(*Facing p.* 16.)

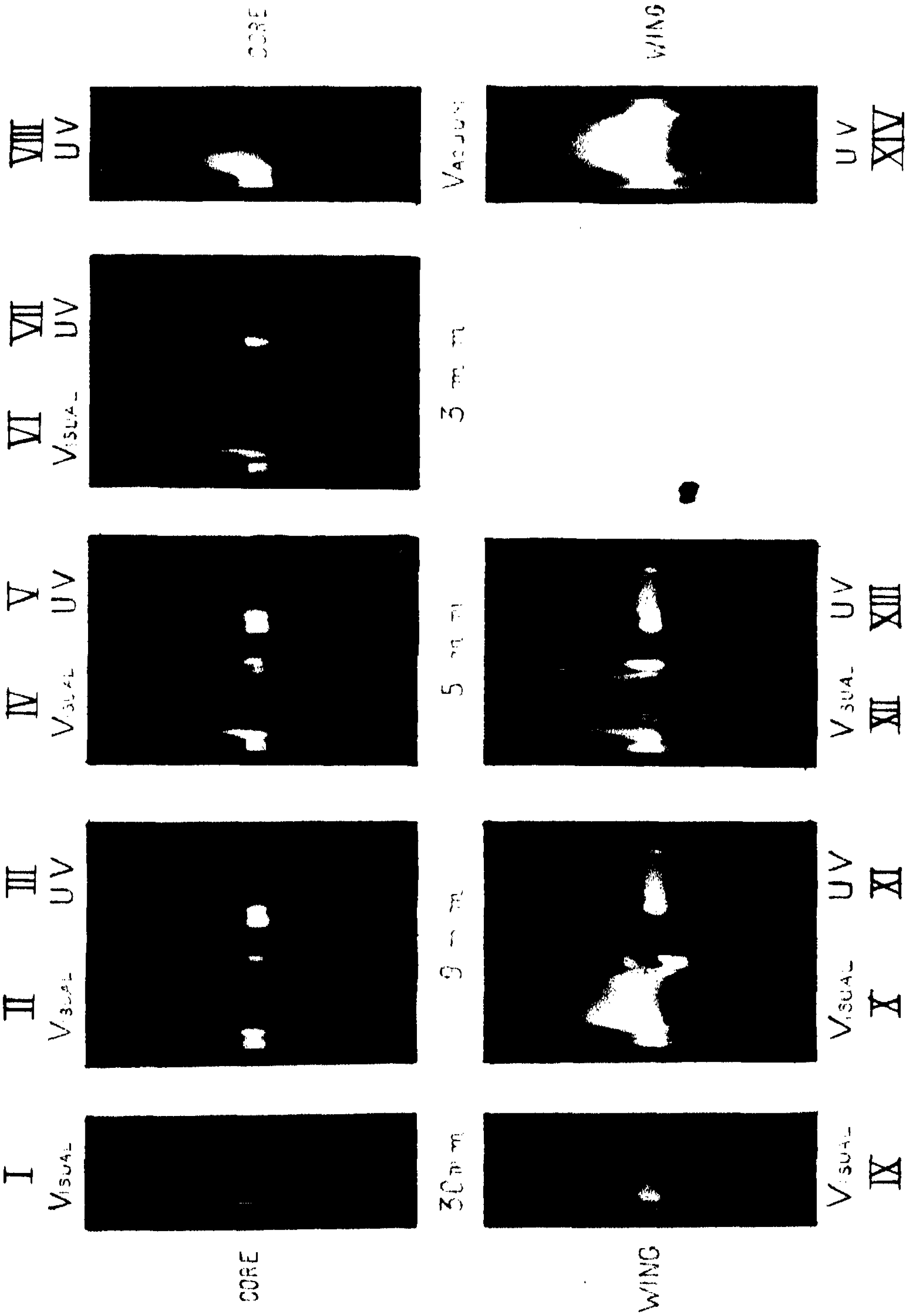
CORE
I
VISUAL
30 mm
II
VISUAL
III
UV
9 mm
IV
VISUAL
V
UV
5 mm
VI
VISUAL
VII
UV
3 mm
VIII
UV
CORE
WING
IX
VISUAL
X
VISUAL
XI
UV
XII
VISUAL
XIII
UV
XIV
UV
VACUUM
WING

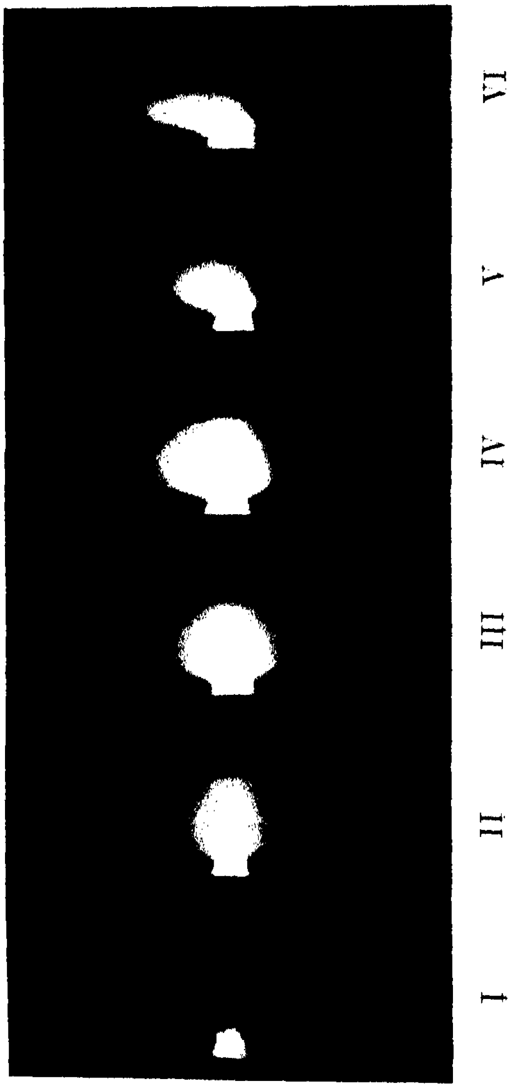
VI
V
IV
III
II
I

becomes predominant to the exclusion of the band, at pressures of 2 mm. or less. *A fortiori* it is concluded that the result of Plate 2, No. VIII, which is at a much lower pressure, and is excited by the core of the resonance line, is due to this line only to the exclusion of the band. This conclusion has been checked by photography through a mercury layer in another cell, which absorbed a breadth of about 1 A. at the resonance line. This cut out the whole phenomenon. Moreover, nothing is seen in the visual part of the spectrum under these conditions. There is apparently nothing but the line 2537, the same wave length as the exciting light. *Prima facie* therefore, we have the simple re-emission of the exciting radiation, though the possibility of complications not directly in evidence must be kept in view.

The re-emission of λ 2537 when this radiation falls on mercury vapour was observed by R. W. Wood in 1912, and called by him "resonance radiation." The question presents itself whether the effect here shown is of the same character as Wood's "resonance radiation" or not. This question may be investigated without reference to the theoretical views that may be taken of either phenomenon, by attempting to trace continuously the transition between the two.

Plate 3 shows the result and seems to afford satisfactory evidence that such continuous transition can be traced. Wood's resonance radiation is typically shown at atmospheric temperature, *in vacuo*. We may raise the temperature by successive steps and observe the sequence of phenomena, photographing always through the chlorine and bromine combined filter. Plate 3, No. I, is taken with the mercury cold and with air in the vessel (fig. 1, p. 11). No resonance radiation is obtained under these circumstances, and we have only the fluorescence of the silica wall where the radiation traverses it.

On exhausting the vessel, which, however, remains at room temperature, we get typical resonance radiation (Plate 3, No. II).

The temperature was then raised by enclosing the bottom part of the vessel in an electrically heated oven with a thermometer. It would have been preferable to take the temperature of the mercury directly, but it was unfortunately not practicable to put a thermometer inside the silica apparatus as actually constructed.

Plate 3, No. III, shows the effect when the oven was at 88° C.; the effects are not noticeably different from No. II, except that it is more difficult to see the distinction between primary and secondary resonance radiation.

Plate 3, No. IV, is obtained with the oven at 150° C. It begins to show a motion upwards and persistence.

Plate 3, No. V.—The oven is here at 177° C. Upward motion more conspicuous.

Plate 3, No. VI.—The oven was removed, and the full heat of a Bunsen burner substituted. This is the same photograph as Plate 2, No. VIII, reproduced here to complete the sequence on Plate 3.

As already emphasised, the temperatures in these experiments are merely arbitrary parameters, and can by no means be identified with the temperature of the mercury vapour; any more than we could identify the temperature of steam from a kettle with the temperature of a thermometer placed in the fire.

In another series of experiments carried out with a much larger boiling vessel, and also a larger tube, persistence was conspicuous with the external heating bath at 130° C. In this case also the actual temperature of the mercury was not determined.

It is intended to determine what is the lowest density of the mercury vapour stream at which persistence can be traced. This can probably be done by measuring independently the breadth of the absorption line in the emergent primary beam from a continuous source with the evaporation going on under working conditions.

§ 7. *Discussion.*

This work was undertaken from an observational standpoint, without many theoretical preconceptions; the results have been to me surprising, and difficult to reconcile with any of the more or less tentative theories which have been put forward by previous workers in the same field. I should prefer to let them speak for themselves as a contribution to the subject, because, though definite enough, they are of a qualitative nature, and at the best cannot afford a decisive check on any proposed theory. Some discussion will, however, be expected, and the following remarks are the best I can do at present to meet the demand.

As regards the long duration of the ultra-violet core effect, even under low densities, the issues are comparatively restricted. As so often happens in experimental work, the consideration of what has been done opens fresh questions for investigation, though under modern conditions publication cannot well be deferred. Thus the importance of determining the minimum vapour density at which persistence can be traced was not realised until the immediate opportunity for further experiment had passed. The pictures on Plate 3 decidedly indicate, I think, that we can pass continuously from a typical case of resonance radiation in stationary vapour to persistence in moving vapour.

Now resonance radiation as ordinarily interpreted means (in the relevant case) direct transition to the $^3P_1$ state by absorption, and direct return to the normal $^1S_0$ state. According to current views the return occurs in 10^{-7} seconds, and clearly does not allow enough time for visible persistence in the moving stream. If therefore we are to hold by the continuity shown in Plate 3, we must assume either that the elementary process described takes much longer than has been assumed, or, alternatively, that as we pass along the series of conditions, it is gradually replaced by a process which takes much longer before the ultimate emission occurs. The first alternative is difficult, and it is not expected that the evidence of these experiments at their present stage will be considered strong enough to shake the strong prepossession that exists on varied grounds in favour of the short duration. Nevertheless it would be the more direct interpretation, and I do not feel able at present to dismiss it as entirely out of court. It would seem that most of our information on the duration of excited states is derived by rather indirect methods, and that although it is difficult to avoid the view that the mean duration of an excited atom, isolated from other atoms and from radiation, is a definite constant independent of the circumstances of excitation, yet this has rather been assumed than proved.

The second alternative is that in Plate 3 :—simple resonance radiation passes over gradually to more complicated processes before persistence becomes apparent. That this is to a certain extent the case must, I think, be admitted. Two processes are to be considered. The "imprisonment" of radiation and the passage down to a metastable state and up again.

"Imprisonment" of radiation, *i.e.*, repeated handing on of radiation from an atom to its neighbours, is certainly operative to some extent even at room temperature. We can distinguish in Wood's early photographs, and also in the original of Plate 3, No. II (though not perhaps in the reproduction), the distinction between secondary radiation in the path of the primary beam, and tertiary radiation out of that path.

Zeemansky[*] who experimented on the duration of resonance radiation in static mercury vapour up to densities comparable to those here used, and found duration of the order of 10^{-4} seconds, interpreted them entirely on the basis of imprisonment of radiation.

If this interpretation is adopted for the more conspicuous cases of persistence, *e.g.*, Plate 3, No. VI, the failure of the radiation to be propagated downward, would be explained by assuming that the spreading of the imprisoned radiation is unable to make headway against the vapour stream, on account of the greater velocity of the latter, while in the upward direction the two velocities are added. In the lateral direction the stream of luminous vapour should tend to spread so as to fill the cross section of the tube. Nothing of this sort is apparent on photographs such as Plate 3, No. VI, which certainly suggest that the lateral spreading, if any, is very slow compared with the velocity of the stream.

---

[*] 'Physical Review,' vol. 29, p. 513 (1927).

There is another alternative to be considered. This is the passage of $^3P_1$ atoms to the metastable state $^3P_0$ by a collision of the second kind, a duration in the metastable state of the order of 10^{-4} seconds, and a return to $^3P_1$ by an exceptionally energetic collision of the first kind.

It has been shown by Asada* that a process of this kind does in fact occur in a mixture of mercury vapour at room temperature with 14 mm. of nitrogen, and accounts for an observed afterglow when this mixture (static) is illuminated by the resonance line.

It may be that in the present experiment the excess of mercury vapour itself takes the part of the added nitrogen, though it seems probable that in some of the experiments the density is too small to make this explanation satisfactory. In some forms experiments on the luminous vapour arising from a discharge in mercury alone† I found that the "forbidden" line $1\,^1S_0$—$2\,^3P_0$ 2656 was strongly developed. In that case we may assume that a considerable accumulation of $1\,^3P_0$ atoms is present, but that experiment, unlike the present ones, is not free from complication arising from the presence of higher excitation than the resonance line. A close search for this forbidden line with mercury vapour only, and excitation by the resonance line, is suggested by these considerations and is on my programme.

Although it does not seem possible to decide at present between the alternatives suggested, yet I must confess that it seems to me unattractive to adopt one kind of mechanism to explain persistence in the visual luminosity, and a quite different kind of mechanism to explain it for the 2537 radiation. It is only in the case of the latter that imprisonment of radiation could help us, and therefore I am not drawn to this explanation. For persistence of the visual luminosity it would seem that we must resort to some hypothesis of a long lived excited molecule because, as we have seen (*cf.* Plate 2, Nos. VI and VII *e.g.*), the visual emission can under suitable conditions be observed at a distance from the source, *after all phenomena which can be attributed to excited atoms have died away.*

---

* 'Phys. Zeit.,' vol. 29, p. 709 (1928). My attention was drawn to this work by Prof. R. Ladenburg, whom I wish to thank for valued suggestions, without, of course, making him responsible for any opinion here expressed.

† 'Roy. Soc. Proc.,' A, vol. 114, p. 620 (1927).

It has been suggested by Houtermans* that the $^3P_0$ metastable state of the mercury atom can be invoked in this case also to give persistence by an indirect process. If, however, this state of the atom is regarded as readily passing over to $^3P_1$, emission of λ 2537 would necessarily accompany the visual luminosity, which in fact it does not, as we see in comparing VI and VII, Plate 2.

Again, the fact that the green radiation can be excited by long waves up to at any rate λ 3450 seems to show that atomic excitation need not intervene in its production. It is true that persistence has not yet been demonstrated for these long wave excitations. I am inclined to think, however, that this has only been prevented by technical difficulties.

It seems difficult to carry the discussion much further until the true nature of the absorption band extending from about λ 2537 to long waves has been more definitely determined. For simplicity of discussion I have hitherto referred to this as molecular absorption, but Houtermans (*loc. cit.*), adopting views similar to those of Born and Franck,† considers that at a distance from the resonance line the absorption is not really molecular, but due to triple collisions between two atoms and a light quantum, with formation of an excited molecule at about the same energy level as a $^3P_1$ excited atom. In favour of this view is his observation that this absorption is not diminished by strong superheating, which should dissociate molecules, and thus reduce true molecular absorption.

Against it is the fluted structure in this band found about the same time by myself and by Mohler and Moore.‡

Walter and Barratt (*loc. cit.*) have attributed this structure to an oxide molecule; they found that it is only present in the presence of a trace of oxygen. My own experience would not lead me to think this probable, but similar questions have proved very difficult to settle experimentally in the past, and I should wish to re-examine the question in the light of their work.

Again, let us consider the experiments on p. 4 in which visual fluorescence is excited by wave-lengths as long as λ 3450 acting by absorption in this band. It is a somewhat violent assumption that the true mechanism involves ascent to a level 1·14 volts higher than the excitation, though it is true that in the dense mercury vapour atomic collisions able to supply the additional energy required do occur sometimes, if rarely.*

---

* *Loc. cit.*, p. 147.

† 'Z. Physik,' vol. 31, p. 411 (1925).

‡ Rayleigh, 'Nature,' vol. 119, p. 778 (1927); 'Roy. Soc. Proc,' A, vol. 116, p. 702 (1927); Mohler and Moore, 'J. Opt. Soc. Am.,' vol. 15, p. 74 (1927).

The strong "antistokes" fluorescence shown in Plate 1, No. IV, apparently proves however that there is an ascent of at least 0·27 volts above the optical excitation, whatever view may be taken of the mechanism. In this experiment the fluorescent intensity appears to depend on the first power of the exciting intensity. This was determined by Wood's test with a wire gauze, which produces the same effect whether used to reduce the former or the latter. It seems, therefore, that we cannot assume that two quanta are absorbed in succession by the same system.

§ 8. *Summary.*

This paper deals with fluorescence of mercury under frequencies equal to or less than that of the resonance line λ 2537.

Complete absorption can be traced in a column of dense vapour 10 cm. long from the resonance line as far as λ 3750

The green visual fluorescence has been traced in dense vapour with excitation beginning only at λ 3450.

The spectrum of the fluorescence, consisting of the broad bands λ 3300 and λ 4850, has been photographed with excitation beginning at λ 3360 upwards. In this case Stokes' law is strongly violated, the fluorescence spectrum beginning at wave-lengths 230 A. shorter than the excitation.

In the neighbourhood of the resonance line, the spectrum has only been photographed in less dense vapour. At 10 mm. pressure it shows the line λ 2537 and the band λ 2540. At 2 mm. pressure only the line. Excitation began 0·66 A. on the long wave side of the line.

When excitation extends over the resonance line, the fluorescence is sharply divided into core effect, excited by a range of 0·1 A. at the resonance line and wing effect excited by the region beyond the atomic line. The wing effect penetrates furthest into the vapour. This distinction is observed whether we examine visually (including photo-visually) or by photography, in the region of the resonance line (referred to as ultra-violet).

---

* Using Foote's method of calculation ('Phys. Review,' vol. 30, p. 293 (1927)) I find that in mercury vapour boiling at atmospheric pressure, 5×10^{-8} of the whole number of collisions have enough energy to pass from the exciting wave-length λ 3125 to λ 2537. Unfortunately the temperature of the denser vapour that was used in exciting with still longer waves was not determined at the time when the experiments were made.

These various effects are examined in a moving stream of vapour (Phillip's effect) with some control over the velocity of the stream. It is found that the visual core effect begins to pass along the stream at lower velocities than the ultra-violet core effect. The same applies to the wing effect. Thus the visual and ultra-violet effects can be *separated in space.*

With increased velocity of the stream the ultra-violet fluorescence moves also, in both cases.

Starting with Wood's "resonance radiation" at atmospheric temperatures *in vacuo*, and raising the temperature of the mercury, it is shown that we can pass continuously to the phenomenon of the moving ultra-violet core effect.

Photographs of the various phenomena are reproduced and the bearing of them discussed.

The Energy Functions of the H_2 *Molecules.*

By O. W. Richardson, F.R.S., Yarrow Research Professor of the Royal Society, and P. M. Davidson, B.A., King's College, London.

(Received April 26, 1929.)

§ 1. *Comparison of Vibrational and Rotational Determinations of the Terms in the Expansion of the Force Function near the Equilibrium Position.*

Owing to the progress which has recently been made in the analysis of the spectrum of H_2[*] we now have a good deal of information about the energy functions of some of the more stable H_2 molecules. In dealing with this material we shall first compare the results given by the formulæ of Kratzer,[†] Born and Hückel[‡] and Kemble,[§] which depend mainly on vibration data and only in a secondary degree on rotational data, with those given by the method of Birge[||] which involve only rotational data. It is satisfactory to find that the two methods do give a reasonably good agreement. This is important because without such agreement it is not possible to attack this problem by existing methods. In addition it shows that the analysis of the spectrum has proceeded along sound lines. A convenient account of these two methods will be found in the Report on Molecular Spectra in Gases.*

---

[*] Richardson, 'Roy. Soc. Proc.,' A, vol. 113, p. 368 (1926), and vol. 115, p. 528 (1927); Richardson and Das, *ibid.*, vol. 122, p. 688 (1929); Richardson and Davidson, *ibid.*, vol. 123, pp. 54, 466 (1929); vol. 124, pp. 50, 69 (1929).

[†] 'Z. Physik,' vol 3, p. 289 (1920).

[‡] 'Phys. Z. Jahrg.,' vol. 24, p. 1 (1923).

[§] 'J. Opt. Soc. America,' vol. 12, p. 1 (1926).

[||] 'Nature,' vol. 116, p. 783 (1925).

Assuming that in the neighbourhood of the equilibrium position the mutual force F between the nuclei can be expressed as a series of powers of the displacement, we can write

$$F = k_1(r - r_0) + k_2(r - r_0)^2 + k_3(r - r_0)^3 + \ldots \qquad (1)$$

where r is the instantaneous and r_0 the equilibrium separation and k_1, k_2, k_3, etc., are constants whose units are dynes per centimetre, square centimetre, cubic centimetre, etc. By the "vibration method"

$$k_1 = c^2\mu(2\pi\omega_0)^2. \qquad (2)$$

$$k_2 = -\frac{3k_1}{2r_0}\left(\frac{\alpha\omega_0}{6B_0^2} + 1\right), \qquad (3)$$

$$k_3 = \frac{1}{3k_1}\left(\frac{10k_2^2}{3} - \frac{8k_1^3x}{ch\omega_0}\right). \qquad (4)$$

Here $c = 2{\cdot}99796 \times 10^{10}$ cm. sec.$^{-1}$, $\mu = 1{\cdot}650 . 10^{-24} \times m_1m_2/(m_1 + m_2)$, where m_1 amd m_2 are the atomic weights of the atoms, ω_0 is the vibrational frequency at zero amplitude, in wave-numbers per centimetre, $2B_0 = h/4\pi^2I_0c$ where $I_0 = \mu r_0^2$ and $h = 6{\cdot}547 \times 10^{-27}$ erg sec., α is the constant in $B_n = B_0 - \alpha n +$, etc., and x is derived from the expression $n\omega_0(1 - xn + \ldots)$. B_0 and α are expressed in wave-numbers per centimetre. In the "rotation method" we set out from the following expression for the rotational energy $F_0(m)$ of the mth rotational vibrationless state

$$F_0(m) = B_0m^2 + D_0m^4 + F_0m^6 + H_0m^8, \qquad (5)$$

in which B_0, D_0, F_0 and H_0 are constants. In terms of these constants those in equation (1) are given by

$$k_1 = -2hcB_0^2/D_0r_0^2, \qquad (6)$$

$$k_2 = -\frac{3k_1}{2r_0}\left(3 - \frac{B_0F_0}{D_0^2}\right), \qquad (7)$$

$$k_3 = -\frac{k_1}{2r_0^2}\left(18\frac{F_0B_0}{D_0^2} - 25 - 9\frac{F_0^2B_0^2}{D_0^4} + 4\frac{H_0B_0^2}{D_0^3}\right). \qquad (8)$$

We shall now apply these formulæ to the data which have been obtained for the lower level $2\,^1S$ of the parhelium-like band systems and for the lower and upper levels $2\,^3S$ and $3\,^3P$ of the α system.

---

* 'Bull. Nat. Research Council,' vol. 11, p. 235 (1926).

The data for $2\,{}^1S$ are given in a previous paper* (§ 3). Taking the atomic weight of H to be 1·00777 we have $\mu = 8\cdot 314 \times 10^{-25}$. The value of ω_0 is 1337·726, so that the vibration method gives

$$k_1 = c^2\mu\,(2\pi\omega_0)^2 = 5\cdot 28\,.\,10^4 \text{ dyne cm.}^{-1}.$$

The rotational analysis gave $B_0 = 19\cdot 456$ and $D_0 = -0\cdot 0157$ so that the rotational method equation (6) gives

$$k_1 = 5\cdot 49\,.\,10^4 \text{ dyne cm.}^{-1}.$$

The vibrational analysis gave $\alpha = 0\cdot 96$, so that equation (3) gives

$$k_2 = -0\cdot 944\,.\,10^{13} \text{ dyne cm.}^{-2}.$$

The rotational analysis (*loc. cit.*, p. 71) gave $F_0 = 1\cdot 3\,.\,10^{-5}$, so that from equation (7) we have

$$k_2 = -1\cdot 2_{38}\,.\,10^{13}.$$

An alternative value found was $F_0 = 2\,.\,10^{-5}$ which would give a better agreement. The value of $x\omega_0$ was found to be 19·54, so that from equation (4)

$$k_3 = 1\cdot 464\,.\,10^{21} \text{ dyne cm.}^{-3}.$$

The value of k_3 on the rotation method depends on H_0 and there are not enough rotation data to determine this constant. Here in computing each k the k's previously got by the *same* method are used.

For the $2\,{}^3S$ state Richardson and Das (*loc. cit.*) give the following data

$$\omega_0 = 2594\cdot 06, \quad B_0 = 33\cdot 387, \quad D_0 = -0\cdot 0217, \quad \alpha = 1\cdot 6497$$

and

$$r_0 = 0\cdot 998\,.\,10^{-8}.$$

We must now attempt, however, to treat the data so as to obtain a value of F_0. The effect of the H_0 term is small, so we assume

$$F(m) = B_0 m^2 + D_0 m^4 + F_0 m^6.$$

The $(F_{m+2} - F_m)$'s have differences

$$\text{2nd diff.} = 48\,(m+2)\,D_0 + 120\,(2m^3 + 12m^2 + 27m + 22)\,F_0 = L, \text{ say}, \quad (9)$$

$$\text{3rd diff.} = 48D_0 + 120\,(6m^2 + 30m + 41)\,F_0 = M, \quad (10)$$

$$\text{4th diff.} = 1440\,(m+3)\,F_0 = N. \quad (11)$$

From Richardson and Das, p. 693, the values of these three quantities for $2\,{}^3S$ for $m = \frac{1}{2}$, are $-2\cdot 611$, $-0\cdot 842$, and $+0\cdot 044$. The equation $N = 0\cdot 044$

---

* 'Roy. Soc. Proc.,' A, vol. **123**, pp. **62** *et seq.* (1929).

gives $F_0 = 9 \,.\, 10^{-6}$. The effect of the m^8 term, which is here becoming appreciable, suggests the correction $F_0 \sim 10^{-5}$. The simultaneous equations $L = -2{\cdot}611$, $M = -0{\cdot}842$, give $F_0 = 4 \,.\, 10^{-5}$, $D_0 = -0{\cdot}0233$. The first method of finding F_0 involves using two $(F_{m+2} - F_m)$'s which are not mean values; the second method involves one. Gale, Monk and Lee's possible errors thus make the discrepancy not surprising, and we may as well take the average value $2{\cdot}5 \,.\, 10^{-5}$ for F_0. Actually the second method is likely to give the more accurate value, because, among other reasons, the contribution of F_0 to the quantities is larger.

The vibrational method gives for k_1, $1{\cdot}984_5 \,.\, 10^5$ dyne cm.$^{-1}$, for k_2 $-4{\cdot}86_7 \times 10^{13}$ dyne cm.$^{-2}$, and for k_3, $0{\cdot}769 \,.\, 10^{22}$ dyne cm.$^{-3}$. The rotational method gives for k_1, $1{\cdot}88 \,.\, 10^5$ dyne cm.$^{-1}$, and for k_2, $-4{\cdot}1 \,.\, 10^{13}$ dyne cm.$^{-2}$.

For $3\,^3P$ Richardson and Das (*loc. cit.*) find $\omega_0 = 2307{\cdot}63$, $x\omega_0 = 61{\cdot}68_5$, $B_0 = 29{\cdot}825$, $D_0 = -0{\cdot}02041$, $\alpha = 1{\cdot}3634$ and $r_0 = 1{\cdot}056 \,.\, 10^{-8}$. These data are for the levels from which the R′ P′ lines come. The values for the Q levels are so similar that it seems unnecessary to work out the data for both levels.

Using the previous notation, we have from page 692, Richardson and Das, $L = -3{\cdot}390$, $M = -0{\cdot}875$, m having its lowest value $1\frac{1}{2}$. This simultaneous equation gives $F_0 = 1{\cdot}1 \,.\, 10^{-5}$, $D_0 = -0{\cdot}0209_6$. These equations depend on two $(F_{m+2} - F_m)$'s which are not mean values.

With these data we find by the vibrational method

$$k_1 = 1{\cdot}570 \,.\, 10^5 \text{ dyne cm.}^{-1}, \quad k_2 = -3{\cdot}54_5 \,.\, 10^{13} \text{ dyne cm.}^{-2},$$
$$k_3 = 5{\cdot}01_7 \,.\, 10^{21} \text{ dyne cm.}^{-3}.$$

The rotational method gives

$$k_1 = 1{\cdot}494 \,.\, 10^5 \text{ dyne cm.}^{-1}, \quad k_2 = -4{\cdot}8 \,.\, 10^{13} \text{ dyne cm.}^{-2}.$$

Another way of expressing the agreement between the vibrational and rotational data is to calculate the values of D_0, F_0 and H_0 from B_0 and the vibrational constants by means of the equations

$$D_0 = -4B_0^3/\omega_0^2, \tag{12}$$

$$F_0 = \frac{D_0^2}{B_0}\left(2 - \frac{\alpha\omega_0}{6B_0^2}\right), \tag{13}$$

$$H_0 = \frac{1}{B_0^2 D_0}\left(3B_0F_0D_0^2 - 5D_0^4 + B_0^2F_0^2 - \frac{8D_0^3B_0^2x}{3\omega_0}\right). \tag{13A}$$

These values are compared with the observed values in Table IA.

Table IA.

		D_0.	F_0.	H_0.
$2\,^1S$	Measured	$-1\cdot5_7\,.\,10^{-2}$	Between $1\cdot3$ and $2\,.\,10^{-5}$	—
	Calculated	$-1\cdot646\,.\,10^{-2}$	$2\cdot0\,.\,10^{-5}$	$-2\cdot4\,.\,10^{-6}$
$2\,^3S$	Measured	$-2\cdot3\,.\,10^{-2}$	About $2\cdot5\,.\,10^{-5}$	—
	Calculated	$-2\cdot212\,.\,10^{-2}$	$2\cdot0\,.\,10^{-5}$	$-2\cdot27\,.\,10^{-6}$
$3\,^3P$	Measured	$-2\cdot1\,.\,10^{-2}$	About $1\cdot1\,.\,10^{-5}$	—
	Calculated	$-1\cdot99\,.\,10^{-2}$	$1\cdot8_8\,.\,10^{-5}$	$-2\cdot3\,.\,10^{-6}$

The measured values of F_0 are seen to be as close to their theoretical values as can be expected with the possible errors of measurement.

It is clear from these calculations that in this spectrum, as in others, the vibrational method permits far greater accuracy than the rotational, so we shall keep to it in the rest of the paper.

First, however, we should like to make a correction to one of the calculations on p. 71, Part I. The theoretical value of β in the formula $C_n = C_0 + \beta n$ (or in the present terminology $D_n = D_0 + \beta n$) is there computed as $-0\cdot39\,D_0$. The method is sensitive to the values of F_0 and H_0 employed, and if we give them their theoretical values from the above table, we find for β the value $-0\cdot13_7\,D_0$, which is in far better agreement with the observed value.

§ 2. *Comparison with* HCl *Data.*

These were originally worked out by Kratzer, but they have been carried further using more recent and improved observational material by Kemble (*loc. cit.*). He gives the following values $I_0 = \mu r_0^2 = 2\cdot65\,.\,10^{-40}$, $r_0 = 1\cdot28\,.\,10^{-8}$, $B_0 = 10\cdot447$, D_0 (observed) $= -0\cdot000514$, $\omega_0 = 2940\cdot77$, $x\omega_0 = 53\cdot58$ and $\alpha = +0\cdot30795$.* The data seem too inaccurate to deduce F_0 or H_0.

With these data the vibration method gives $k_1 = +4\cdot97\,.\,10^5$, $k_2 = -1\cdot39\,.\,10^{14}$ dyne cm.$^{-2}$ and $k_3 = +2\cdot23\,.\,10^{22}$. The rotational method gives $k_1 = 5\cdot10\,.\,10^5$. The value of F_0 given by equation (13) is $1\cdot64\,.\,10^{-8}$ and with this value equation (13A) gives $H_0 = -8\cdot7\,.\,10^{-13}$.

The values of the coefficients k_1, k_2, k_3 and of the ratios of successive pairs and similar data for the coefficients B_0, D_0, etc., for each of the three excited

---

* Kemble also gives a value $\alpha = 0\cdot3042$ which he seems to consider more accurate than this. This would alter our k_2 and k_3 but only by about 1 unit in the last place.

H_2 molecules $2\,{}^1S$, $2\,{}^3S$ and $3\,{}^3P$, as well as of the unexcited HCl molecule are collected in Table I.

Table I.

	k_1.	k_1/k_2.	k_2.	k_2/k_3.	k_3.	B_0.
$2\,{}^1S$	$5 \cdot 28 \,.\, 10^4$	$-5 \cdot 6 \,.\, 10^{-9}$	$-0 \cdot 944 \,.\, 10^{13}$	$-6 \cdot 5 \,.\, 10^{-9}$	$1 \cdot 464 \,.\, 10^{21}$	$1 \cdot 9456 \,.\, 10$
$2\,{}^3S$	$1 \cdot 98 \,.\, 10^5$	$-4 \cdot 0 \,.\, 10^{-9}$	$-4 \cdot 87 \,.\, 10^{13}$	$-6 \cdot 3 \,.\, 10^{-9}$	$0 \cdot 77 \,.\, 10^{22}$	$3 \cdot 3387 \,.\, 10$
$3\,{}^3P$	$1 \cdot 57 \,.\, 10^5$	$-4 \cdot 5 \,.\, 10^{-9}$	$-3 \cdot 54 \,.\, 10^{13}$	$-7 \cdot 1 \,.\, 10^{-9}$	$5 \cdot 02 \,.\, 10^{21}$	$2 \cdot 9825 \,.\, 10$
HCl	$4 \cdot 97 \,.\, 10^5$	$-3 \cdot 6 \,.\, 10^{-9}$	$-1 \cdot 39 \,.\, 10^{14}$	$-6 \cdot 4 \,.\, 10^{-9}$	$2 \cdot 23 \,.\, 10^{22}$	$1 \cdot 0447 \,.\, 10$

	B_0/D_0.	D_0.	D_0/F_0.	F_0.	F_0/H_0.	H_0.
$2\,{}^1S$	$-1 \cdot 22 \,.\, 10^3$	$-1 \cdot 6 \,.\, 10^{-2}$	$-0 \cdot 8 \,.\, 10^3$	$2 \cdot 0 \,.\, 10^{-5}$	$-0 \cdot 83 \,.\, 10^3$	$-2 \cdot 4 \,.\, 10^{-8}$
$2\,{}^3S$	$-1 \cdot 52 \,.\, 10^3$	$-2 \cdot 2 \,.\, 10^{-2}$	$-1 \cdot 1 \,.\, 10^3$	$2 \cdot 0 \,.\, 10^{-5}$	$-0 \cdot 87 \,.\, 10^3$	$-2 \cdot 3 \,.\, 10^{-8}$
$3\,{}^3P$	$-1 \cdot 49 \,.\, 10^3$	$-2 \cdot 0 \,.\, 10^{-2}$	$-1 \cdot 1 \,.\, 10^3$	$1 \cdot 88 \,.\, 10^{-5}$	$-0 \cdot 82 \,.\, 10^3$	$-2 \cdot 3 \,.\, 10^{-8}$
HCl	$-1 \cdot 98 \,.\, 10^4$	$-5 \cdot 27 \,.\, 10^{-4}$	$-3 \cdot 2 \,.\, 10^4$	$1 \cdot 64 \,.\, 10^{-8}$	$-1 \cdot 9 \,.\, 10^4$	$-8 \cdot 7 \,.\, 10^{-13}$

It will be seen from Table I that the successive coefficients in both sets always alternate in sign so that the ratios of successive coefficients are always negative. The ratio k_1/k_2 is nearly equal to k_2/k_3 in every case, and these ratios have very similar values for all four molecules. There is not a great difference in the absolute values either. This is another illustration of the close similarity between the structure of the H_2 and HCl molecules which was pointed out by one of us some time ago.* The ratios B_0/D_0, D_0/F_0 and F_0/H_0 are all nearly equal for each substance; they may in fact be equal, as the estimations of F_0 and H_0 are necessarily inaccurate. They also have very similar values for all the three H_2 molecules but the values for HCl are very much higher.

---

* O. W. Richardson, 'Roy. Soc. Proc.,' A, vol. 113, p. 416 (1926).

§ 3. *The Potential Energy Functions* U (ξ) *of* $2\,{}^1S$, $2\,{}^3S$, $3\,{}^3P$, $3\,{}^1B$ *and* H_2+.

We now proceed to a more complete determination of the expansion of the potential energy function of the molecules in the neighbourhood of the equilibrium value r_0 of the internuclear distance r. We adopt a notation slightly different from that in § 1 as it is more compact and convenient. The treatment, in fact, follows closely that of Kemble.* Let the potential energy U of the molecule be expressed as a power series in the form

$$U\,(\text{ergs}) = k\xi^2(1 + a\xi + b\xi^2 + c\xi^3 + d\xi^4 + \ldots) \tag{14}$$

where $\xi = r/r_0 - 1$. Then if $c\omega_0$ is the frequency for infinitesimal amplitude we have

$$\omega_0 = (2k/I_0)^{\frac{1}{2}}/2\pi c, \tag{15}$$

and we shall write $\omega_1 = h/4\pi^2 I_0 c = 2B_0$, $u = \omega_1/\omega_0$. Then the term values being expressed in wave-numbers in the form

$$F_n(j) = A_n + B_n m^2 + D_n m^4$$

where

$$\left.\begin{aligned} A_n &= \omega_0 n + \gamma n^2 + \delta n^3 + \ldots \\ B_n &= B_0 - \alpha' n + \gamma' n^2 + \ldots \\ D_n &= \alpha'' + \beta'' n + \gamma'' n^2 + \ldots \end{aligned}\right\} \tag{16}$$

formulæ are found for the constants in (16) in terms of k, a, b, c, etc. Of these there are four which include a and b but are free from c and d. The first two are

$$\gamma = \tfrac{3}{4}\omega_0 u\,(b - \tfrac{5}{4}a^2) \tag{17}$$

and

$$\alpha' = -\tfrac{3}{2}\omega_1 u\,(1 + a), \tag{18}$$

from which we can find a and b. The other two are the formulæ for β'' and for F_0, the coefficient of m^6 (see § 1), and the information which they provide is not accurate. The only formula involving a, b and c without d is

$$\gamma' = \tfrac{3}{4}\omega_1 u^2\left[5 + 10a - 3b + 5c - 13ab + \frac{15}{2}(a^2 + a^3)\right] \tag{19}$$

from which we determine c; and finally d is obtained from

$$\delta = \frac{\omega_0 u^2}{8}\left[10d - 35ac - \frac{17}{2}b^2 + \frac{225}{4}a^2 b - \frac{705}{32}a^4\right]. \tag{20}$$

We consider first the data for $2\,{}^1S$.

We have from (15) $k = 2\pi^2 c^2 I_0 \omega_0^2$ and putting $I_0 = 1{\cdot}42 \,.\, 10^{-40}$, $c = 3$.

---

* 'J. Opt. Soc. America,' vol. 12, p. 1 (1926).

10^{10} and $\omega_0 = 1337$, which are accurate enough for the present purpose, we find $k = 4\cdot515 \,.\, 10^{-12}$ ergs. It is more convenient to express U in "volts." To do this we have to multiply k by $0\cdot629 \,.\, 10^{12}$ and instead of the constant k outside the bracket in (14) we have $0\cdot629 \,.\, 10^{12} \times k = 2\cdot84$.

The bands are well represented by

$$A_n = 1338\cdot136n - 20\cdot26n^2 + 0\cdot7975n^3 - 0\cdot0946n^4 + 0\cdot005n^5$$

$$B_n = 19\cdot455 - 1\cdot067n + 0\cdot0875n^2 - 0\cdot007n^3 \ldots .$$

If the expression for A_n were replaced by the more approximate 4-terms series given in a previous paper (Part I), the terms of U would only be affected very slightly.

We shall not need the last term of either equation. Substitution of the others in equations (17) to (20) gives

$$\begin{aligned} U(2\,{}^1S) &= 2\cdot84\,(\xi^2 - 1\cdot63\xi^3 + 2\cdot63\xi^4 - 4\cdot1\xi^5 + 6\xi^6 \ldots) \\ &= 2\cdot84\xi^2 - 4\cdot63\xi^3 + 7\cdot46\xi^4 - 11\cdot6\xi^5 + 17\xi^6 \ldots \end{aligned} \qquad (21)$$

It is to be noted that here and in other cases such inaccuracies as are possible in the formulæ for A_n and B_n have little effect on the formulæ found for U; also that though the last two terms in the U formula appear to be computed from a small term in the A_n and B_n formulæ, the percentage error in the U term is in no way *proportional* to the percentage error in the small term: the magnitude of that term is rather to be regarded as determining the small *departure* of the U term from the value which it would have if the small term were neglected altogether. In the above case, for example, an error of 20 per cent. in the value 0·0875 for the coefficient of n^2 in B_n only causes an error of about 2 per cent. in the ξ^5 term in (21). This will lead, however, to an error of about 10 per cent. in the ξ^6 term, which is, unfortunately, rather sensitive to the value of the previous coefficient. It is, of course, the least accurate, and the least important term in the series.

For $2\,{}^3S$ we find

$$\left.\begin{aligned} A_n &= 2594\cdot30n - 70\cdot43n^2 + 0\cdot90n^3 + 0\cdot04n^4 \ldots \\ B_n &= 33\cdot386 \quad - 1\cdot6497n + 0\cdot0212n^2 \ldots \end{aligned}\right\} \qquad (22)$$

The coefficients in A differ very slightly from those given by Richardson and Das,* owing to a different method of extraction. We have worked out the formulæ for U using each of the alternative formulæ, and the difference proves very small. We find

---

* 'Roy. Soc. Proc.,' A, vol. 133, p. 716 (1929).

$$\begin{aligned} U(2\,{}^3S) &= 6\cdot24\xi^2(1 - 1\cdot637_5\xi + 1\cdot943\xi^2 - 2\cdot15\xi^3 + 2\cdot5\xi^4 \ldots) \\ &= 6\cdot24\xi^2 - 10\cdot21\xi^3 + 12\cdot12\xi^4 - 13\cdot4\xi^5 + 15\tfrac{1}{2}\xi^6 \ldots \end{aligned} \tag{23}$$

We now consider the $3\,{}^3P$ level.

The data are for the upper level of the α bands from which the P′ R′ lines (not the Q lines) come. We have $2B_0 = 59\cdot65$, $2B_2 = 54\cdot20$, $2B_3 = 51\cdot25$. Owing to a perturbation in the $n' = 1$ level we cannot measure $2B_1$ from the lines so we take it to be $57\cdot0$ which makes the second differences regular. To fit these data we require

$$B_n = 29\cdot825 - 1\cdot287n - 0\cdot038n^2,$$

and Richardson and Das (*loc. cit.*) give

$$A_n = 2307\cdot52n - 65\cdot013n^2 + 0\cdot845n^3 - 0\cdot029n^4.$$

$B_0 = 29\cdot825$ gives $I_0 = 9\cdot266\,.\,10^{-41}$ and $r_0 = 1\cdot056\,.\,10^{-8}$. The formulæ now give

$$\begin{aligned} U &= 5\cdot37\xi^2(1 - 1\cdot556\xi + 1\cdot575\xi^2 - 1\cdot56\xi^3) \\ &= 5\cdot37\xi^2 - 8\cdot361\xi^3 + 8\cdot461\xi^4 - 8\cdot38\xi^5 \text{ volts.} \end{aligned} \tag{24}$$

We now consider the $3\,{}^1B$ level.

The data for this are taken from Part I, Table III,* and Part II, Table XIII.† We have used

$$\left.\begin{aligned} B_n &= 28\cdot3 - 2\cdot225n + 0\cdot075n^2 \\ A_n &= 2175\cdot06n - 77\cdot83n^2 \end{aligned}\right\} \tag{25}$$

The exact value of the coefficient of n^2 in B_n is not important. This gives

$$\begin{aligned} U\,(\text{volts}) &= 5\cdot16\xi^2(1 - 2\cdot01\xi + 3\cdot19\xi^2 - 7\xi^3) \\ &= 5\cdot16\xi^2 - 10\cdot4\xi^3 + 16\cdot5\xi^4 - 36\xi^5 \end{aligned} \tag{26}$$

§ 4. *The Total Energy of the* H_2 *Molecules, the manner in which they Dissociate and some Related Matters.*

We consider first the case of $2\,{}^1S$. In Part I‡ we found, by extrapolation of the vibration levels, the energy necessary to dissociate this in the rotationless vibrationless state to be $3\cdot418$ volts, let us say $3\cdot42$ volts. We now have two atoms whose total energy Q must be the sum of two of the quantities R, $\frac{1}{4}$R, $\frac{1}{9}$R, etc., where R is Rydberg's constant, since each must have electronic $n = 1$ or 2 or 3, etc. Thus to break up the molecule completely from the $2\,^1S$ state requires energy $3\cdot42 + Q$ volts.

---

* 'Roy. Soc. Proc.,' A, vol. 123, p. 60 (1929).

† *Ibid.*, p. 473 (1929).

‡ 'Roy. Soc. Proc.,' A, vol. 123, p. 65 (1929).

The same breaking up can be done by first ionising the $2\,^1S$ state from its ground level to the $\bar{\nu}$ of the ion, the necessary energy being according to us, since for $2\,^1S$ $\bar{\nu}_e = 33876$ and the vibrational zero point energy is $s = 674$,* $33876 - 674 = 33202$ wave-numbers (on the *wave mechanics*) $= 4\cdot10$ volts, and then breaking up the ion; which requires the amount of energy necessary to destroy the ion from its $\bar{\nu}$ level. Assuming Burrau's† value $16\cdot30$ for this

$$3\cdot42 + Q = 4\cdot10 + 16\cdot30 = 20\cdot40 \quad \text{or} \quad Q = 16\cdot98 \text{ volts}.$$

As just stated, Q must be the sum of two of the quantities R, $\frac{1}{4}$R, $\frac{1}{9}$R, etc., that is $13\cdot542$, $3\cdot385$, $1\cdot505$, etc., volts. This shows unambiguously that one atom has $n = 1$ and one has $n = 2$ (as would be expected for the products of $2\,^1S$), giving

$$Q = 13\cdot542 + 3\cdot385 = \underline{16\cdot927}.$$

This differs from $16\cdot98$ by $0\cdot053$ volts which is within the accuracy of the extrapolation by which the energy of dissociation D ($2\,^1S$) of $2\,^1S$ was obtained. It is also almost within the probable error $\pm\,0\cdot03$ which Burrau assigns to his computation of $16\cdot30$; so that we can claim this as a further verification of the results of the wave-mechanics, in addition to the one given in Part II (*loc. cit.*).

We can check this by using the data from the interpretation of the spectrum by the formulæ of the old quantum mechanics. On that interpretation we found in Part II that ν_e ($2\,^1S$) = 34365 wave-numbers = $4\cdot24$ volts as the interval from the ground level of $2\,^1S$ to the ground level of the molecule ion, and $16\cdot16$ volts is required to ionise the ion from that state. Thus the total energy, say E ($2\,^1S$), needed to destroy a molecule at the $n = 0$ level of the $2\,^1S$ state is $16\cdot16 + 4\cdot24 = 20\cdot40$ volts. This is the same value of E ($2\,^1S$) as was got by the wave-mechanics formulæ above.

If we assume Burrau's value to be correct, we can reverse this process so as to redetermine the dissociation energy. In this way we find D ($2\,^1S$) = $3\cdot47$ volts.

Turning to $2\,^3S$ we have $\nu_0 = 29340$ wave-numbers = $3\cdot61$ volts and $Q = 3\cdot61 + 16\cdot16 - D\,(2\,^3S)$ where $16\cdot16$ is the value of I (H_2+) (see Part

---

* 'Roy. Soc. Proc.,' A, vol. 123, p. 485 (1929).

† 'K. Danske Vid. Selsk., math-fys.,' vol. 7, p. 14 (1927).

II*) on the old mechanics, to which system $\nu_0 = 29340$ refers. The value of D $(2\,{}^3S)$ as recomputed by Birge† is 3·02 volts from which

$$Q = 19\cdot77 - 3\cdot02 = 16\cdot75 \text{ volts.}$$

This result shows that this molecule also dissociates into one unexcited atom and one atom in the $n = 2$ state as we should expect. The total energy E $(2\,{}^3S)$ defined as for $2\,{}^1S$ is taken as 19·77 volts (assuming Burrau's value to be correct) and subtracting $\frac{5}{4}R = 16\cdot927$ we redetermine D $(2\,{}^3S)$ as 2·843 volts.

E $(3\,{}^3P)$ the work to destroy the $3\,{}^3P$ molecule, with no vibrational or rotational energy, can readily be found from the value 19·77 for E $(2\,{}^3S)$. The $3\,{}^3P$ level lies 16620 wave-numbers = 2·04 volts above $2\,{}^3S$, so that

$$E\,(3\,{}^3P) = 19\cdot77 - 2\cdot04 = 17\cdot73 \text{ volts.}$$

According to Birge's remeasurement (*loc. cit.*) of the dissociation energy of this level, it is 21,120 cm.$^{-1}$ = 2·607 volts. Thus for this molecule we have

$$Q = 17\cdot73 - 2\cdot61 = 15\cdot12 \text{ volts.}$$

Now

$$R + \tfrac{1}{9}R = 13\cdot542 + 1\cdot504 = 15\cdot046 \text{ volts.}$$

This shows unambiguously that this molecule dissociates into one unexcited atom and one atom excited to $n = 3$, as we should expect. Using the theoretical value of $R + \frac{1}{9}R$ to correct the value of D $(3\,{}^3P)$ we find

$$D\,(3\,{}^3P) = 17\cdot73 - 15\cdot046 = 2\cdot684 \text{ volts.}$$

Again $4\,{}^3P$ lies 22263 wave-numbers = 2·75 volts above $2\,{}^3S$, so that the work to destroy it is E $(4\,{}^3P) = 19\cdot77 - 2\cdot75 = 17\cdot02$ volts. According to Birge's remeasurement (*loc. cit.*) the dissociation energy of this level is 20,520 cm.$^{-1}$ = 2·535 volts. Thus for this molecule we have

$$Q = 17\cdot02 - 2\cdot535 = 14\cdot485 \text{ volts.}$$

Now

$$R + \tfrac{1}{16}R = 13\cdot542 + 0\cdot846 = 14\cdot388 \text{ volts.}$$

Here again we have a direct and unambiguous proof that the molecule in which the electron has total quantum number n breaks up into an unexcited atom and an atom in which the electron is excited to quantum number n. In the present case $n = 4$. Using the theoretical value of $\mathrm{R} + \frac{1}{16}\mathrm{R}$ to correct $\mathrm{D}\,(4\,{}^3\mathrm{P})$ we find

---

* 'Roy. Soc. Proc.,' A, vol. 123, p. 466 (1929).

† 'Proc. Nat. Acad. Sci.,' vol. 14, p. 12 (1928).

$$\mathrm{D}\,(4\,{}^3\mathrm{P}) = 17 \cdot 02 - 14 \cdot 388 = 2 \cdot 632 \text{ volts.}$$

$3\,{}^1\mathrm{B}$ lies 21850 wave-numbers $= 2 \cdot 70$ volts above $2\,{}^1\mathrm{S}$; so that the total energy $\mathrm{E}\,(3\,{}^1\mathrm{B})$ to destroy $3\,{}^1\mathrm{B}$ is given by

$$\mathrm{E}\,(3\,{}^1\mathrm{B}) = \mathrm{E}\,(2\,{}^1\mathrm{S}) - 2 \cdot 70 = 20 \cdot 40 - 2 \cdot 70 = 17 \cdot 70 \text{ volts.}$$

As we have found that all the other excited molecules dissociate into an unexcited atom and an atom with the same excitation as the electronic excitation of the original molecule, it seems safe to assume that this applies also to $3\,{}^1\mathrm{B}$. If so we have

$$\mathrm{E}\,(3\,{}^1\mathrm{B}) = 17 \cdot 70 = \mathrm{D}\,(3\,{}^1\mathrm{B}) + \mathrm{R} + \tfrac{1}{9}\mathrm{R} = \mathrm{D}\,(3\,{}^1\mathrm{B}) + 15 \cdot 046$$

giving for the dissociation energy of this molecule

$$\mathrm{D}\,(3\,{}^1\mathrm{B}) = 2 \cdot 654 \text{ volts.}$$

The vibrational properties of this level are not incompatible with such a value.

If we assume that this method is applicable generally we can use it to estimate the dissociation energy of all the known electronic levels of the H_2 molecule. These, together with the total negative energy values E, all in equivalent volts, are collected together in Table II. To make the table more complete various other important constants of the levels have been added.

In this table ν_e is the n, $m = 0$ electronic term in wave-numbers. All are measured from either $2\,{}^1\mathrm{S} = 34365$ (Part II) or $2\,{}^3\mathrm{S} = 29340$ (Richardson, *loc. cit.*). Dieke and Hopfield's A and C involve Hori's measures, the remainder rest on the measures of Gale, Monk and Lee. " den " is the value of z if $\nu_e =$ Rydberg constant $\div z^2$. ω_0 is the vibration frequency (wave-numbers) at infinitesimal amplitude. $\omega_0 x$ and $2\mathrm{B}_0$ are the usual band system constants. r_0 is the equilibrium nuclear separation. ε is the constant required to express the rotational terms as $\mathrm{B}\,(j - \varepsilon)^2$ with j half-integral. σ is the number of missing rotational levels. v means variable. Uncertain figures are depressed. Owing to peculiarities of the electronic levels many of the band constants, especially those of the upper levels of bands ending on $2\,{}^1\mathrm{S}_1$ are estimated subject to particular assumptions. For a complete interpretation of the table reference should be made to our previous papers (Parts I–IV), and to the papers by Richardson (*loc. cit.*) and Richardson and Das (*loc. cit.*).

Table II.

Level.	ν_e.	den.	E.	D.	ω_0.	$\omega_0 x$.	$2B_0$	$r_0 \times 10^8$.	ϵ.	σ.
$1\,^1S$ Dieke and Hopfield's A	124569	0·934	31·54	4·465	4262	113·5		0·76	0	0
$2\,^1S$,, B	34365	1·959	20·40	3·47	1337·726	19·54	38·91	1·313	0	0
,, C	25475	2·075	19·30	2·37	2380	66·5	59	1·06		
$2\,^3S$	29340	1·933	19·78	2·85	2594	70·5	66·773	0·998	0	0
3(?) ^3S (2^3S^1)¶	17733	$2{\cdot}48_5$	18·35	$1{\cdot}42_5$	2130	67	53·08	1·119	0	0
$3\,^3P$ (Q)	12719	2·937	17·73	$2{\cdot}68_5$	2307·5	65·01	59·09	1·061	0	1
$3\,^3P$ (R′)	12719	2·937	17·73	$2{\cdot}68_5$	2307·5		59·65	1·056	0	1
$3\,^1A$	12546	2·957	17·70	$2{\cdot}65_5$	2143·00	40·33	40 *		$-\frac{1}{2}$	0
$3\,^1B$	$12515{\cdot}_5$	2·960	17·70	$2{\cdot}65_5$	2175·06	77·84	56·6† 50 *		$+\frac{1}{2}$	1
$3\,^1C$	$12758{\cdot}_5$	2·932	17·73	2·68	2340·60	114·85	56·6† 40 *		$+1\frac{1}{2}$	0
$3\,^1K$	$12937{\cdot}_5$	2·913	17·755	2·71	2239	$6{\cdot}_4$	21·8*		0	0
$3\,^1L$	1130_5.	3·118	17·55	2·50	ca. 1830		19·4*		0	0
$3\,^1M$	1117_3.	3·138	17·53	2·48	219_3.	1_6.	26 *		0 ?	v
$3\,^1N$	9469	3·403	17·33	2·28‡	ca. 2000		36 *		0	0
$3\,^1O$	11614	3·07	17·59	2·54	2414	124	59 *		0	0
$3\,^1Q$	12525	2·958	17·70	2·65			75 *		0	?
λ 4142·801 (upper)	10000	3·31	17·39	2·34‡			75 * or 52 *		$+1\frac{1}{2}$?	>1
λ 4097·433 (upper)	9935	3·328	17·38	2·33‡					0 ?	>0
$4\,^3P$ (Q)	7067	3·942	17·03	2·64	2276·5	6_0.	58·80	1·064	0	1
$4\,^3P$ (R′)	7067	3·942	17·03	2·64			58·575	1·066	0	1
$4\,^1A$	7008	3·956	17·02	2·63			about 60	about 1·05	$-\frac{1}{2}$	0
$4\,^1B$	$6991{\cdot}_5$	3·961	17·02	2·63	ca. 2200		about 60	about 1·05	$+\frac{1}{2}$?	0
$4\,^1C$	$7152{\cdot}_5$	3·915	17·04	2·65			about 60	about 1·05	$+1\frac{1}{2}$	1
$4\,^1\chi$	$6761{\cdot}_5$	4·03	16·99	2·60			about 60	about 1·05	$+2\frac{1}{2}$?	2
$4\,^1E$	7187	3·91	17·05	2·66			about 60	about 1·05	2 ?	1
$5\,^3P$	4493	4·96	16·71	2·63	2251	5_8	5_7			
$6\,^3P$	3107	5·95	16·55	2·63	2236	5_7	5_7			
$7\,^3P$	2276	6·95	16·45	2·63						
Infra-red system (upper state)§	253_{00}.	$2{\cdot}08_4$	19·28	2·35	23_{50}.	1_{00}.	ca. 50	ca. 1·2	0	0
Infra-red system (upper state)‖	21009	2·286	18·75	$3{\cdot}70_5$	1900		4_0.	$1{\cdot}_2$	0	0
H_2+	0	∞	16·16	2·62	2280	60	59	1·06		

---

* Value for *m* small.

† Value for *m* large.

‡ These data assume that the relevant level ($3\,^1N$, upper of λ 4142·801 or upper of λ 4097·433) is a 3-electronic level.

§ These data assume the upper level to be a $n = 2$ electronic level and that 11310 is the $n' = 1$ band.

‖ These data assume the upper level to be a $n = 3$ electronic level and that 13402·1 is the $n' = 0$ band. It seems pretty certain from these figures that the assumption (electronic $n = 3$) is untenable.

¶ The data for this level are from an unpublished paper by Richardson and Das.

§ 5. *The Range of Validity of the Expansions.*

In fig. 1, curve A is the graph of

$$U = 6{\cdot}238\xi^2 - 10{\cdot}21\xi^3 + 12{\cdot}12\xi^4 - 13{\cdot}4_5\xi^5 + 15\tfrac{1}{2}\xi^6$$

and curve B that of

$$U = 6{\cdot}238\xi^2 - 10{\cdot}21\xi^3 + 12{\cdot}12\xi^4 - 13{\cdot}4_5\xi^5 + 15\tfrac{1}{2}\xi^6 - 15\tfrac{1}{2}\xi^7.$$

This is the expansion for 2 ^{3}S. The data give the coefficients as far as ξ^6 and the ξ^7 term is the extrapolation to give a second limit. In all cases it is seen that the signs of the terms are alternating and the absolute magnitudes either continue to increase or at least do not perceptibly diminish at the higher powers of ξ. These properties are also shown by the data for the HCl bands. These alternating signs are bound to arise and mean that the force between the nuclei increases rapidly as they approach each other. In the energy curves it will appear that the amplitude inwards is not nearly so large as the amplitude outwards, except when n is very small. If it were not so we could hardly get the eight or nine vibrational states which 2 ^{1}S, 2 ^{3}S and 3 ^{3}P each possess. When the first two vibrational energy levels ($1318\frac{1}{2}$ and 2600 wave-numbers) are drawn for 2 ^{1}S (see fig. 3) it is seen that at $n = 1$ each nucleus swings inwards through about 20 per cent. of its normal distance from the centre, and outwards through nearly 30 per cent. of the distance. At $n = 2$ these values become 26 per cent. and over 40 per cent. The outward amplitude at the $n = 8$ level is presumably very large.

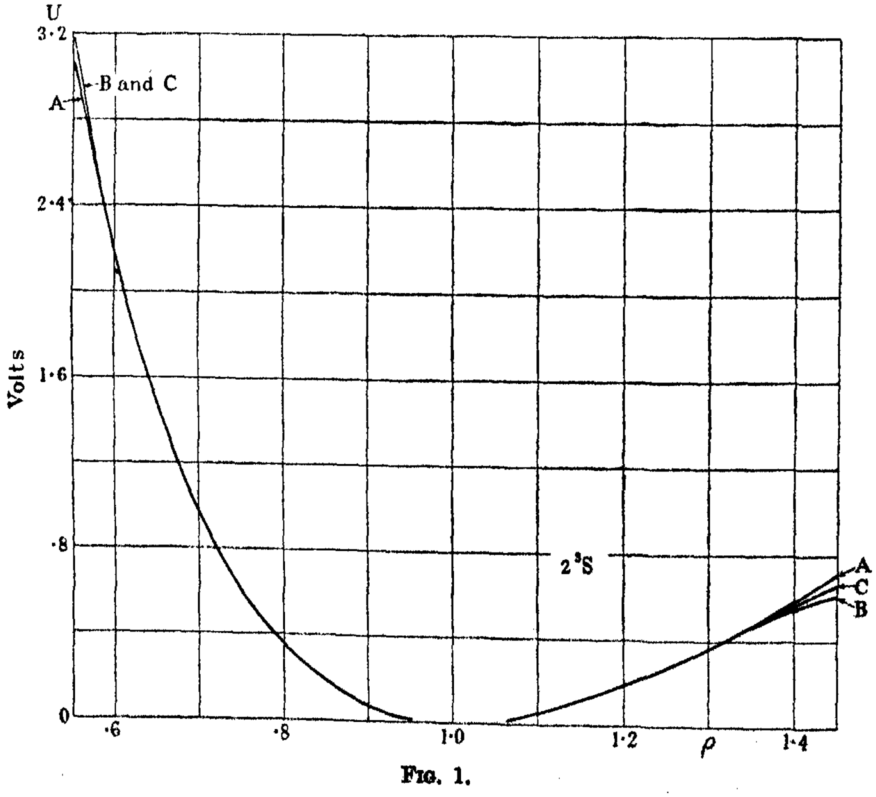

FIG. 1.

In fig. 1 in curve A we stop at a positive and in curve B at a negative term, so that the true curve is likely to lie between them for $\xi = 0$.

The possibility of drawing a single U curve for the various nuclear swings in the neighbourhood of $r = r_0$ involves the assumption that the force on the nuclei (and thus the configuration of the electronic orbits) at a given r is practically independent of the particular swing, and thus of the instantaneous nuclear velocity. This is to be expected, since the nuclear motion is slow compared to the electronic motion.

The forces exerted by the electrons on the nuclei are thus the same as if the nuclei were held at rest at the particular r, and U may be regarded as measuring (apart from a constant) the work done to bring the nuclei adiabatically to this particular separation, without giving them any velocity. The value of *this* quantity may be considered for quite small values of r, even though the nuclei, if released from such positions, would pass through the neighbourhood of r_0 with velocities by no means small. We shall refer to this quantity as U in the present paragraph, remembering that in the region of $r = r_0$ it is identical with our ξ series.

It is interesting to consider how it behaves as r tends to zero, *i.e.*, as the nuclei come very close together. The force on each of them must consist primarily of the repulsion of the other, so that the equal and opposite inward forces on them will be of the form

$$F(r) = -e^2/r^2 + ar + br^2 + \ldots \tag{27}$$

The series of positive powers are due to the electrons, which can give no constant term, since when the nuclei come together the electrons cannot exert equal and opposite forces on them. On the other hand the expression $-e^2/r^2$ is an artificial simplification for the internuclear force at small distances. With this proviso $U(r)$ for moderately small values of r may be represented by a power series

$$U(r) = \frac{e^2/r_0}{r/r_0} + B + D\frac{r^2}{r_0^2} + E\frac{r^3}{r_0^3} + \ldots = \frac{A}{\rho} + B + D\rho^2 + E\rho^3 + \ldots \text{ volts,} \tag{28}$$

where $\rho = r/r_0 = 1 + \xi$ and $A = e^2/r_0$. The values of A and B can be calculated for the states with which we are concerned. A, being equal to e^2/r_0 expressed in volts has the values $10 \cdot 9$ for $2\,^1S$, $14 \cdot 3$ for $2\,^3S$, $13 \cdot 5$ for $3\,^3P$, $13 \cdot 4$ for $4\,^3P$, $13 \cdot 1_5$ for $3\,^1B$ and $13 \cdot 5$ for H_2+. To calculate B we note that, when the nuclei are held very close together, we have, as far as the electrons are concerned, the 2S states of par- and orthohelium in the case of $2\,^1S$ and $2\,^3S$. The amount of work to remove the first electron in the case of parhelium is: for 2S, 3·95; for 3P, 1·496; for 4P, 0·842; and in the case of orthohelium: for 2S, 4·75; for 3S, 1·86; for 3P, 1·575; for 4P, 0·876; for 5P, 0·557; and for 6P, 0·386 volts. These data are got from the helium term values given in Fowler's Report on Series in Line Spectra. To remove the second electron from each of these and also from H_2+ when the nuclei are kept at a fixed sufficiently small distance requires an amount of work 4R. Taking $2\,^1S$ as a typical case the work to remove the two electrons with the nuclei fixed very close together is thus

$$4R + 3\cdot95 = 58\cdot12 \text{ volts.}$$

We may then separate the nuclei, requiring work $-e^2/r = -A/\rho$. Thus the total work done is $-A/\rho + 58\cdot12$. The negative of this would be the value of U if the latter were defined so as to be equal to the total energy; actually, however, the U's are defined so as to be zero in the equilibrium position, where for $2\,^1S$ the total energy is $-20\cdot40$ volts. Thus as $\rho \rightarrow 0$,

$$U(2\,^1S) \rightarrow A2\,^1S/\rho - 58\cdot12 + 20\cdot40 = 10\cdot9/\rho - 37\cdot72 \text{ volts.}$$

Similarly, $U(2\,^3S) \rightarrow A2\,^3S/\rho - 58\cdot92 + 19\cdot77 = 14\cdot27/\rho - 39\cdot15$ volts.

To each is to be added the series of positive powers of ρ due to the electrons.

Similarly for the molecule ion H_2 + Burrau's E which gives the actual total energy for various values of r (*i.e.*, is not defined so as to be zero in the equilibrium position), should tend to $e^2/r - 4R$ as $r \rightarrow 0$. It does so, as may be seen from his table.

If the ρ and ξ series were to hold from $\rho = 0$ to $\rho = 1$ it is easy to show by binomial expansion that the coefficients of the powers of ξ cannot tend to zero. They would eventually tend, with alternate signs, to the value of A, if to anything. Our formulæ in ξ show that this is not improbable.

If, without assuming the values of A and B we form a series of the type of equation (28) containing seven terms such that, when expressed in terms of ξ by the relation $\rho = 1 + \xi$, they agree with the ξ formulæ (21) and (23) for $2\,^1S$ and $2\,^3S$, as far as those formulæ go, *i.e.*, to ξ^6, we find for $2\,^1S$

$$U = 9\cdot9719/\rho - 26\cdot2733 + 83\cdot4735\rho^2 - 141\cdot4535\rho^3 + 111\cdot05\rho^4 - 43\cdot7967\rho^5 + 7\cdot0281\rho^6. \quad (29\text{A})$$

Similarly for $2\,^3S$

$$U = 12\cdot021/\rho - 26\cdot527 + 57\cdot363\rho^2 - 84\cdot465\rho^3 + 60\cdot934\rho^4 - 22\cdot905\rho^5 + 3\cdot579\rho^6 \quad (29\text{B})$$

This is the function (for $2\,{}^3S$) which is plotted in fig. 1 and gives the curve marked C. It will be recalled that curve A in fig. 1 is the graph of the right-hand side of (23) stopping at $+15\frac{1}{2}\xi^6$ and curve B is the same series with the extrapolated term$-15\frac{1}{2}\xi^7$. The abscissæ in fig. 1 are the values of $\rho = r/r_0$ where r_0 is the equilibrium nuclear distance for $2\,{}^3S$. The ordinates are the values of U in volts. The graph C coincides with A and B where they agree with each other and lies between them when they branch apart on the right-hand side of the diagram ; on the left-hand side B and C are too close together to be distinguishable but C is higher than B and, of course, than A. Moreover, this function (equation (29)) goes to ∞ as $r \rightarrow 0$ and for these reasons the graph C probably covers the actual U over a more extensive range than B or A. We have found this to hold also for the other states ; so that in the other diagrams in figs. 2 and 3 the function used is of the type given in equations (29), *i.e.*, an expansion in terms of $\rho = r/r_0$ made to agree with the ξ functions over the range over which these are reliable. In other words, we add to the ξ terms found theoretically, further terms with alternate sign and equal magnitude. As soon as ξ attains a value (positive or negative) for which the added terms contribute about 8 per cent. to the value U, we bring the curve to an end.

The curve for H_2+ is taken from Burrau's paper (*loc. cit.*).

Reverting to the discussion of equations (28) and (29) we see that the values of A are not very different from their theoretical values, but the discrepancies in the values of B show that the above procedure was not justified. This is not surprising when we remember that besides assuming that the formulæ in ρ hold from the region of $\rho = 0$ to the region of $\rho = 1$, we have, by curtailing the ρ formulæ after seven terms, imposed arbitrary values for all the later coefficients of ξ after those actually known. If, for example, we had taken ρ series having nine terms, we could have given to A and B their theoretical values as $r \rightarrow 0$, and could still have obtained (on converting to powers of ξ) agreement with the ξ formulæ as far as those formulæ go. This procedure would amount to imposing a different set of arbitrary values for the later coefficients in the ξ series.

No conclusions can thus be drawn from the individual coefficients in (29). Nevertheless we have used such formulæ as (29) for drawing the graphs of U since in the ranges considered they differ very slightly from the ξ curves called A and B, fig. 1, and satisfy the desirable conditions of lying between them for $\xi > 0$ and above them both for $\xi < 0$.

As we have seen the U curves go to ∞ as $r/r_H \rightarrow 0$. They should go to the heats of dissociation as $r/r_H \to \infty$. The magnitudes of these quantities for all the H_2 molecules are given in Table II *ante*. U (H_2+), being on the wave-mechanics, should, and does, go to (16·3 — R). This can be seen from fig. 2 on p. 15 of Burrau's paper, which is his E curve, and differs from that in our fig. 2 only in having the energy axis shifted by 16·3 volts, making the equilibrium position give a reading equal to the total energy — 16·3, instead of the arbitrary value zero to which all our curves are reduced.

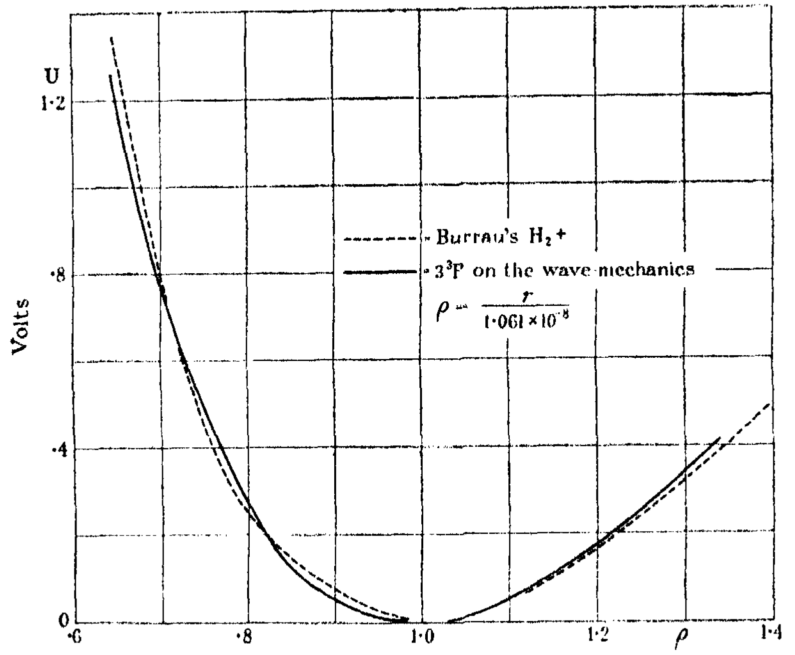

FIG. 2.

[*Note added in proof.*—The ideas of this paragraph may be illustrated by computing the U formula for the Bohr model, which, though yielding different dissociation products has a U formula not unlike those above. We find

$$U = e^2/r_0 (0{\cdot}5835\xi^2 - 0{\cdot}874\xi^3 + 1{\cdot}02\xi^4 - 1{\cdot}08\xi^5 + \ldots). \qquad (29c)$$

At the next term, not given, the coefficient is returning towards e^2/r_0, that is, towards unity inside the bracket. This may be compared with the formulæ above by writing them in the form

$$U(2^3S) = e^2/r_0 (0{\cdot}437\xi^2 - 0{\cdot}715\xi^3 + 0{\cdot}849\xi^4 - 0{\cdot}943\xi^5 + 1{\cdot}09\xi^6 - \ldots)$$

$$U(2^1S) = e^2/r_0 (0{\cdot}261\xi^2 - 0{\cdot}420\xi^3 + 0{\cdot}675\xi^4 - 1{\cdot}07\xi^5 + 1{\cdot}4\xi^6 - \ldots)$$

in each of which r_0 has the appropriate value for the particular state. Converting the ξ series for the Bohr model to a ρ series in the manner used for the others, which is equivalent to adding an infinite number of terms whose equal and opposite coefficients are nearly unity (inside the bracket), we obtain a series which represents the true U curve well throughout a considerably greater range than does the original series (29c).]

§ 6. *The Mean Kinetic Energy of the Electrons.*

The ordinary band formulæ are derived by assuming that the forces on the nuclei, and therefore also the potential of those forces, can be represented as a function of the nuclear separation r, independent of the vibration quantum number, and therefore of the velocity which the nuclei have for this value of r. This implies that the electronic motions depend only on r, independently of the velocity of the nuclei. We should expect this, as we have stated already, on account of the comparatively slow motion of the nuclei, and the assumption is justified by the success of the band formulæ.

We may thus speak of the mean kinetic energy $\overline{T}$ of the electrons (the time average over their motion) for a given value of r. It will be the same whether the nuclei are passing through this position in their swing, or whether they are brought to rest there (by applying external forces), and held stationary.

In the " Report on Molecular Spectra in Gases " (*loc. cit.*, p. 294) a formula is found for this mean kinetic energy, on an assumption (see footnote on that page), which is regarded as a special case of the general law that in a system of *unconstrained* particles in periodic motion, subject to the inverse square law, the mean kinetic energy is the negative of the total energy. It is stated that if some of the particles are held fixed the mean kinetic energy of the others is still equal to the negative of the total energy, provided that the mutual potential energy of the fixed particles is not counted in that total energy.

That this is not the case may be seen by considering a simple example such as the unvibrating Bohr model of H_2, or, indeed, any molecule in which the nuclei are in their equilibrium position. The nuclei being in equilibrium, it does not matter whether we imagine them held there or not. For the first case, the general theorem says that the kinetic energy of the electrons is equal to the negative of the total energy, whereas for the second case (*i.e.*, imagining the nuclei held), the statement in the report says that the kinetic energy is the negative of this total energy without the mutual potential energy e^2/r of the nuclei. The result from the general theorem is, of course, the correct one, and it remains to determine the correct law for a system of particles of which some are held fixed.

We have done this in an appendix to this paper. For the application to the case of two nuclei, with which alone we are concerned in this paper, the correct theorem is

$$-\overline{\mathrm{T}}(r) = \mathrm{W}(r) - r\mathrm{F} = \mathrm{W}(r) + r\,.\,d\mathrm{U}/dr = \mathrm{W}(\rho) + \rho\,.\,d\mathrm{U}/d\rho, \quad (30)$$

where W (r) is the total energy required to form the system with the nuclei at rest at separation r, and F is the mean outward force on each nucleus at separation r. These formulæ give the same answer to both forms of the question put to the Bohr model, since $\mathrm{F} = -d\mathrm{U}/dr = 0$, as the nuclei are in a position of equilibrium. Such formulæ do not use the idea of the spinning electron. The magnetic energy would introduce a correction term.

W (r) exceeds the energy needed to form a molecule with nuclei at rest at separation r_0 (*i.e.*, to form the state $n = 0$, $m = 0$) by the energy needed to change the separation from r_0 to r without giving the nuclei any velocity. This latter energy is U (as in the graphs), since we have chosen U as zero when $r = r_0$. If E is the work to *take to pieces* a molecule with $n = m = 0$, we have

$$\mathrm{W}(r) = -\mathrm{E} + \mathrm{U}(r) \quad (31)$$

and thus

$$\overline{\mathrm{T}}(r) = \mathrm{E} - \mathrm{U}(r) - r\,.\,d\mathrm{U}/dr = \mathrm{E} - d(\mathrm{U}\rho)/d\rho, \quad (32)$$

the differentials having their values at separation r.

The equations (32) have the following necessary properties :—

(1) For the equilibrium state ($n = m = 0$) we have $r = r_0$ and both U and $d\mathrm{U}/dr$ zero. Thus $\overline{\mathrm{T}}(r) = \mathrm{E}$, the negative total energy. This agrees with the general theorem since no constraint is required in the equilibrium position.

(2) When $\rho \rightarrow \infty$, and therefore U → the dissociation energy D, the force $\mathrm{F} = (-d\mathrm{U}/dr)$ on each nucleus is proportional to r^{-n} where n is certainly greater than 1. Therefore $r\,.\,d\mathrm{U}/dr \rightarrow 0$ and from (32), $\mathrm{T} \rightarrow \mathrm{E} - \mathrm{D}$. We have verified experimentally in § 4 that in a number of cases $\mathrm{E} - \mathrm{D}$ is equal to $\mathrm{R} + \mathrm{R}/n^2$ where R is Rydberg's constant and n is the electronic quantum number of the molecule. As this means dissociation into an unexcited + an n-excited atom at rest at infinity, the equation $\overline{\mathrm{T}}_\infty = (1 + 1/n^2)\mathrm{R}$ is correct.

When $\rho \rightarrow 0$, using (28) $\rho\mathrm{U} = \mathrm{A} + \mathrm{B}\rho + \mathrm{D}\rho^3 + \ldots$ and $d(\rho\mathrm{U})/d\rho = \mathrm{B} + 3\mathrm{D}\rho^2 + \text{etc.} \rightarrow \mathrm{B}$ at $\rho = 0$. Thus from (32) $\overline{\mathrm{T}} = \mathrm{E} - \mathrm{B}$ at $\rho = 0$. In

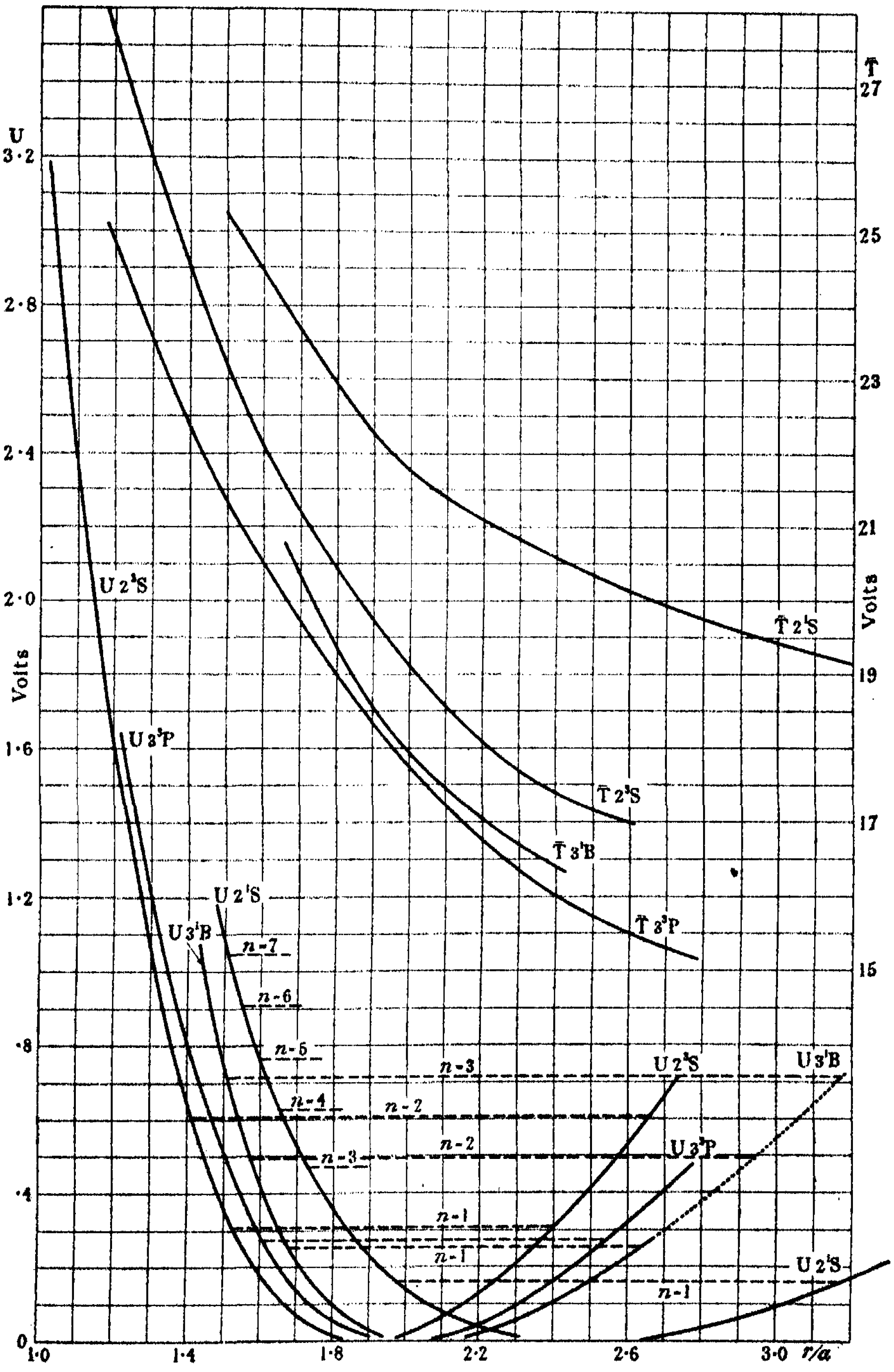
U
3·2
2·8
2·4
2·0
Volts
1·6
1·2
·8
·4
0
1·0
1·4
1·8
2·2
2·6
3·0
r/a
$\bar{T}$
27
25
23
21
Volts
19
17
15
$\bar{T}\ 2^1S$
$\bar{T}\ 2^3S$
$\bar{T}\ 3^1B$
$\bar{T}\ 3^3P$
$U\ 2^3S$
$U\ 3^3P$
$U\ 2^1S$
$U\ 3^1B$
n=7
n=6
n=5
n=4
n=3
n=2
n=3
n=2
n=1
n=1
n=1
$U\ 2^3S$
$U\ 3^1B$
$U\ 3^3P$
$U\ 2^1S$

Fig. 3.

§ 5 we found $B = -26 \cdot 27$ which would give $\bar{T} = 46 \cdot 67$ volts at $\rho = r = 0$. However, as we have pointed out, the series is very rough and B might be 100 per cent. wrong. We may instead use the theoretical formula $E - B = 4R + W(\mathrm{He})$ already mentioned where W (He) means the work to remove an electron from the corresponding helium atom. Thus $\bar{T}$ at $r = 0$ is equal to *the total work needed to disrupt the double atom leaving the nuclei joined.* The (joined) nucleus requires no external forces to hold it in position, so that the general theorem, $\bar{T} = -W$ gives the equation $\bar{T} = 4R + W(\mathrm{He})$ and thus confirms it.

In fig. 3 we have plotted the $\bar{T}$ curves in equivalent volts for $2\,{}^1S$, $3\,{}^1B$ (strong Q), and $2\,{}^3S$ and $3\,{}^3P$. These have been got by graphical methods from the corresponding U curves and are less accurate than the latter. The abscissæ in fig. 3 are the values of $\rho = r/r_H$ where r_H is the radius of the first Bohr circle for the hydrogen atom and is $= 0 \cdot 532 \, . \, 10^{-8}$ cm.

The values of E and D for about 30 states of H_2 are given in Table II.

§ 7. *General Comparison of the States of* H_2 *and of the* H_2 *Molecule Ion. The Intensity Distribution in the Band Systems.*

In fig. 3 we have plotted, in addition to the $\bar{T}$ functions, the U functions for $2\,{}^1S$, $3\,{}^1B$, $2\,{}^3S$ and $3\,{}^3P$ in equivalent volts against r/r_H, r_H being the radius of the first Bohr circle. For these graphs all the data were extracted by the formulæ of the old quantum mechanics, the actual expansions used being :—

For $2\,{}^1S$ $$U(\rho) = 9 \cdot 9719/\rho - 26 \cdot 2733 + 83 \cdot 4735\rho^2 - 141 \cdot 4535\rho^3 + 111 \cdot 05\rho^4 - 43 \cdot 7967\rho^5 + 7 \cdot 0281\rho^6.$$

For $2\,{}^3S$ $$U(\rho) = 12 \cdot 021/\rho - 26 \cdot 527 + 57 \cdot 363\rho^2 - 84 \cdot 465\rho^3 + 60 \cdot 934\rho^4 - 22 \cdot 905\rho^5 + 3 \cdot 579\rho^6.$$

For the others we used the exactly equivalent ξ functions, which are far more convenient for numerical calculation, viz. :—

For $3\,{}^3P$ $$U(\xi) = 5 \cdot 372\xi^2 - 8 \cdot 361\xi^3 + 8 \cdot 461\xi^4 - 8 \cdot 38\xi^5 + 8\xi^6 - 8\xi^7 \ldots$$

For $3\,{}^1B$ $$U(\xi) = 5 \cdot 16\xi^2 - 10 \cdot 4\xi^3 + 16 \cdot 5\xi^4 - 36\xi^5 + 19\xi^6 - 19\xi^7 \ldots$$

These series have, of course, to be adapted to the co-ordinates used in the graphs. The functions are a good deal alike and are very similar to Burrau's graph for the molecule ion. The one which deviates most from the rest is $2\,{}^1S$ which is broader and has a higher r_0 than the others. This is a reflection of the exceptionally low ω_0 and high moment of inertia of this molecule. The horizontal dotted lines indicate a number of the vibrational levels corresponding to the values of n which are given. It is obvious that the vibrations are very unsymmetrical even for the lowest values of n.

The U curve for 3 ^{3}P is very close indeed to that for the molecule ion. It was felt possible that some of this similarity might be unreal as Burrau's curve is calculated on the wave-mechanics and our data are got by the formulæ of the old quantum mechanics. Accordingly we re-calculated U for 3 ^{3}P in terms of the wave-mechanics using the transcription formulæ

$$\bar{\omega}_0 = \omega_0 - \gamma - \tfrac{1}{4}\alpha, \quad \bar{\alpha} = \alpha, \quad \bar{\gamma} = \gamma, \quad \bar{B}_0 = B_0 + \tfrac{1}{2}\alpha + \tfrac{1}{2}D, \quad \bar{D} = D, \tag{33}$$

where the quantities on the wave-mechanics are distinguished from the others by a bar. These make Fues's* formula for the molecular energy levels identical with the one we have used and his expressions for $\bar{\omega}_0$, $\bar{\alpha}$, $\bar{\gamma}$, ..., in terms of $\bar{k}$, $\bar{a}$, $\bar{b}$, $\bar{c}$, ..., are the same as ours for ω_0, α, γ ..., in terms of k, a, b, c, ... We therefore repeated the calculations using $\bar{\omega}_0$, $\bar{\alpha}$ ..., given by (33) instead of ω_0, α, ... This changed the expansion for 3 ^{3}P from

$$\begin{aligned} U &= 5 \cdot 50\xi^2 (1 - 1 \cdot 556\xi + 1 \cdot 58\xi^2 - 1 \cdot 56\xi^3) \\ &= 5 \cdot 50\xi^2 - 8 \cdot 56\xi^3 + 8 \cdot 69\xi^4 - 8 \cdot 58\xi^5 \end{aligned}$$

on the old quantum mechanics to

$$\begin{aligned} U &= 5 \cdot 71\xi^2 (1 - 1 \cdot 55\xi + 1 \cdot 58\xi^2 - 1 \cdot 59\xi^3) \\ &= 5 \cdot 71\xi^2 - 8 \cdot 85\xi^3 + 9 \cdot 02\xi^4 - 9 \cdot 08\xi^5 \end{aligned}$$

on the wave-mechanics.

In fig. 2 we have plotted U for 3 ^{3}P and also for the H_2 molecule ion, both calculated on the formulæ of the wave-mechanics. It is seen that *the curves are actually so close together that they cross each other three times.* The data for H_2+ are got from Burrau's paper (*loc. cit.*). In fig. 2 the ordinates are in equivalent volts and the abscissæ $\rho = r/1 \cdot 061 \,.\, 10^{-8}$. (For the purpose of the above comparison, it is evidently immaterial what constant we use for the denominator of ρ.)

From any pair of the U curves, such as those for 3 ^{1}B and 2 ^{1}S, we can determine the curve of intensity maxima in the vibration diagram for the corresponding band system, in this case 3 ^{1}B → 2 ^{1}S, by Condon's† method. The experimentally determined curve has been given in Part I of the spectrum of H_2‡ (the bands analogous to the parhelium line spectrum), fig. 1, for this system.

---

* 'Ann. Physik,' vol. 80, p. 367 (1926).

† 'Phys. Rev.,' vol. 28, p. 1182 (1926).

‡ 'Roy. Soc. Proc.,' A, vol. 123, p. 61 (1929).

The method involves the assumption that the electronic switch in a molecule occurs so rapidly, or in such a way, that there is no opportunity for the nuclear motions to accommodate themselves to the changed conditions. The effect is the same as if in fig. 3 the nuclei belonging to one of the curves, such as $3\,^1B$, suddenly found themselves in the field pertaining to the other, such as $2\,^1S$. They would thus acquire an additional vibrational energy given by moving from their separation in $3\,^1B$ to the same separation in $2\,^1S$, *i.e.*, along a vertical line until $2\,^1S$ was intersected. So far as is known there is nothing which tends to make such an electronic transition more likely at any one time interval in a vibrational swing than at any other; so that, as the molecule spends most time near the ends of its swings, the most probable jumps will be those from them. Thus to find the most probable jumps from, say, $n = 1$ of $3\,^1B$ we draw vertical lines from the ends of the dotted line for $n = 1$ for $3\,^1B$ in fig. 3 and find their intersections with $2\,^1S$. These points give the two final n's which are most probable when the initial $n' = 1$. We can then repeat this treatment for the other values of n'. The points so ascertained have been marked thus × on the diagram which we originally published* (fig. 1 of Part I), and which is reproduced here as fig. 4A of this paper. It will be seen that

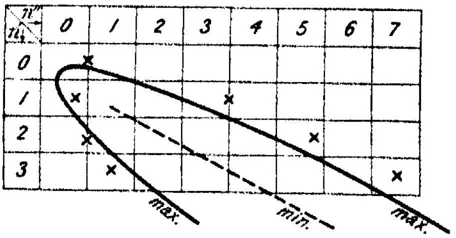

FIG. 4A.

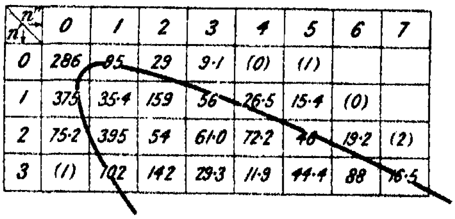

n' \ n''	0	1	2	3	4	5	6	7
0	286	85	29	9·1	(0)	(1)		
1	375	35·4	159	56	26·5	15·4	(0)	
2	75·2	395	54	61·0	72·2	46	19·2	(2)
3	(1)	102	142	29·3	11·9	44·4	88	16·5

FIG. 4B.†

the agreement is very good and, in fact, as nearly perfect as could be expected by such a method. Fig. 4B shows the calculated curve of intensity maxima with Kapuscinski and Eymers' measured intensities of the strong Q (3) lines of this system in the squares. A few intensities were given erroneously in Part I. The figures in brackets are Gale, Monk and Lee's eye estimates, actual measurements being lacking.

A similar computation has been made by Mr. Das for the α-bands ($3\,^3P \rightarrow 2\,^3S$). This covers fairly well the known line of intensity maxima in these bands, but suggests that there should be some strength further out in the infra-red than the present data cover. This may well be so.

---

* 'Roy. Soc. Proc.,' A, vol. 123, p. 61 (1929).

† The intensity for 2 → 2 *should read* 5·4 *not* 54.

Some of the $\bar{T}$ curves in fig. 3 have a trend, on the right-hand side of the diagram, towards values lower than $(1 + 1/n^2)R$ which we have seen is the limiting value as $r \rightarrow \infty$. For $2\,{}^1S$ and $2\,{}^3S$, for example, the value of this is $5R/4 = 16 \cdot 927$ volts. This may easily happen. U has to reach the constant limit D, the heat of dissociation, at r (or ρ) $= \infty$. Thus the U curve in passing from $\rho = 1$ to $\rho = \infty$ will have a slope which begins by being zero, increases, and falls to zero again. From the expression $\bar{T} = E - (U + \rho\, dU/d\rho)$ it is evident that if the slope $dU/d\rho$ attains a sufficient value, $\bar{T}$ may fall to quite low values in such parts of the range.

This does not prove that $dU/d\rho$ actually does attain such values in the present instances, and the effect may arise from the uncertainty of $dU/d\rho$ in the extreme region of the graphs. The values of $dU/d\rho$ for the curves A and B in fig. 1 are obviously considerably different here. The curve for H_2+ may be regarded as the U curve for ∞ P or ∞ S.

The values of the separations r_0 are: for H_2+, $1 \cdot 064 \,.\, 10^{-8}$; for $2\,{}^3S$, $0 \cdot 998 \,.\, 10^{-8}$; for $2\,{}^1S$, $1 \cdot 313 \,.\, 10^{-8}$; for $3\,{}^3P$, $1 \cdot 056 \,.\, 10^{-8}$; and for $3\,{}^1B$, $1 \cdot 088 \,.\, 10^{-8}$.

From the graphs, for both $2\,{}^1S$ and $2\,{}^3S$, at $n = 1$, each nucleus swings inwards from its equilibrium position by about $18\frac{1}{2}$ per cent. of its equilibrium distance from the centre, and outwards by 27 per cent. At $n = 2$ the values are 25 per cent. and 42 per cent. The corresponding figures for the other states are similar.

APPENDIX.

On the Mean Kinetic Energy of a System of Particles in Motion under their Mutual Forces, some of the Particles being held fixed and the others remaining in their neighbourhood.

Let there be n particles of which s are fixed. Let $\mathbf{F}_{pq}$ be the vectorial force on the pth particle due to the qth, vectors being indicated by heavy type, and time-averages by a bar above. Then the equation

$$m\ddot{\mathbf{r}}_p = \sum_{q=1}^{n} \mathbf{F}_{pq},$$

where $\mathbf{r}_p$ is the vectorial distance of the pth particle from the origin (see fig. 5), is true for all the moving particles, *i.e.*, for all values of p from $s + 1$ to n. It may be written

$$m\frac{d}{dt}(\mathbf{r}_p\dot{\mathbf{r}}_p) = m\dot{\mathbf{r}}_p\dot{\mathbf{r}}_p + \sum_{q=1}^{n} \mathbf{F}_{pq}\mathbf{r}_p = 2T_p + \sum_{q=1}^{n} \mathbf{F}_{pq}\mathbf{r}_p.$$

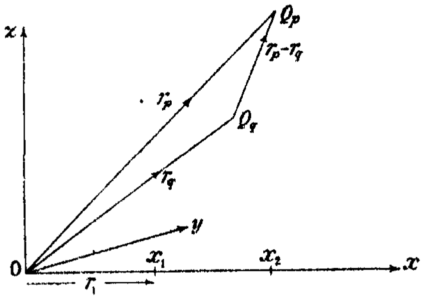

FIG. 5.

Hence, summing over the moving particles ($p = s + 1 \dots n$) and taking a time average of sufficient duration,

$$-2\overline{\mathrm{T}} = \sum_{p=s+1}^{n} \sum_{q=1}^{n} \overline{\mathbf{F}_{pq}\mathbf{r}_p} \tag{34}$$

where $\overline{\mathrm{T}}$ is the mean kinetic energy of all the moving particles, and therefore of the whole system. Equation (34) may be regarded as a special case of the virial theorem in the kinetic theory of gases. It may be written

$$-2\overline{\mathrm{T}} = \sum_{p=1}^{n} \sum_{q=1}^{n} \overline{\mathbf{F}_{pq}\mathbf{r}_p} - \sum_{p=1}^{s} \sum_{q=1}^{n} \overline{\mathbf{F}}_{pq}\mathbf{r}_p, \tag{35}$$

since $\mathbf{r}_p$ is constant for $p = 1 \dots s$.

$\mathbf{F}_{pq}$ may be written $\mathrm{Q}_p\mathrm{Q}_q f(r_{pq})(\mathbf{r}_p - \mathbf{r}_q)/r_{pq}$, where Q_p, Q_q are constants, and r_{pq}, the magnitude of $\mathbf{r}_p - \mathbf{r}_q$ is taken positive. In the first term of (35), $\mathbf{F}_{pq}$ the force on Q_p due to Q_q contributes a term

$$\mathrm{Q}_p\mathrm{Q}_q \overline{f(r_{pq})(\mathbf{r}_p - \mathbf{r}_q)\,\mathbf{r}_p/r_{pq}},$$

while $\mathbf{F}_{qp}$, the force on Q_q due to Q_p, contributes

$$\mathrm{Q}_p\mathrm{Q}_q \overline{f(r_{pq})(\mathbf{r}_q - \mathbf{r}_p)\,\mathbf{r}_q/r_{pq}}.$$

Thus their joint contribution to the first term of (35) is

$$\mathrm{Q}_p\mathrm{Q}_q \overline{f(r_{pq})(\mathbf{r}_p - \mathbf{r}_q)(\mathbf{r}_p - \mathbf{r}_q)/r_{pq}} = \mathrm{Q}_p\mathrm{Q}_q \overline{f(r_{pq})\,r_{pq}}.$$

Hence the term is

$$\sum_{p=1}^{n} \sum_{q=1}^{n} \mathrm{Q}_p\mathrm{Q}_q \overline{f(r_{pq})\,r_{pq}}, \tag{36}$$

in which each pair is counted once only.

The second term is

$$-\sum_{p=1}^{s} \overline{\mathbf{F}}_p\mathbf{r}_p, \tag{37}$$

where $\mathbf{F}_p$ is the total vectorial force on the *p*th particle, due to all the other particles, fixed or moving.

Thus we have altogether for (35)

$$-2\overline{T} = \sum_{p=1}^{n}\sum_{q=1}^{n} Q_pQ_q\overline{f(r_{pq})\,r_{pq}} - \sum_{p=1}^{s}\overline{\mathbf{F}}_p\mathbf{r}_p, \tag{38}$$

each pair in the first term being taken once only.

Since the magnitude of the repulsive force between Q_p and Q_q is $Q_pQ_q f(r_{pq})$ the mutual potential energy of the two particles is, if

$$f(r_{pq}) = r_{pq}{}^{-l},$$

given by $Q_pQ_qf(r_{pq})r_{pq}/(l-1)$. Thus the first term in (38) is $(l-1)\overline{V}$, where $\overline{V}$ is the mean total potential energy of the system, and the equation becomes

$$-2\overline{T} = (l-1)\,\overline{V} - \sum_{p=1}^{s}\overline{\mathbf{F}}_p\mathbf{r}_p. \tag{39}$$

We now apply this to the case of two nuclei fixed at points x_1 and x_2 on the x-axis. Since the inverse square law holds, $l = 2$; also Q_1 and Q_2 are the nuclear charges. Adding T to each side of (39) we have

$$-\overline{T} = W - F_1x_1 - F_2x_2 \tag{40}$$

where F_q is the mean component, along the positive x-axis of the total force on the *q*th nucleus, due to the other nucleus and the electrons. Hence F_1+F_2 is the total mean x-force on the nuclear system due to the electrons, and is therefore equal and opposite to the total mean x-force on the electronic system due to the nuclei. Accordingly, since the electrons remain in the vicinity of the nuclei, we must have $F_1 + F_2 = 0$. Hence equation (40) may be written

$$-\overline{T} = W - F_2(x_2 - x_1) = W - rF_2 = W - rF, \tag{41}$$

where r means the internuclear distance, and $F = F_2 = -F_1$ is the total mean x-force acting away from the origin on the second nucleus (or towards the origin on the first nucleus) due to all the particles of the system, including the other nucleus. In other words, it is the mean repulsive force between the nuclei, as modified by the presence of the electrons.

We will illustrate the final equation,

$$-\overline{T} = W - rF,$$

by two simple examples in which the motion may be solved completely.

(1) Bohr's model of the hydrogen molecule, the nuclei being held at arbitrary separation $2a$ and the electrons moving in circular orbits of radius b, not

necessarily quantised. Each side of the equation is easily shown to be equal to

$$e^2/4b - 2e^2b^2/(a^2+b^2)^{3/2}.$$

(2) Two nuclei, each with charge $+E$, held at separation $2c$, while a particle with charge $+e$ performs a linear oscillation (unstable laterally) along the internuclear axis, about a point midway between the nuclei, with amplitude k ($<c$). Writing the equation in the form

$$2\int \mathrm{T}\,dt = -\left[\int \mathrm{V}\,dt - r\int \mathrm{F}\,dt\right]$$

for a complete period, each side may be shown to be equal to

$$2\pi k^2\left[\frac{\mathrm{E}em}{c(c^2-k^2)}\right]^{\frac{1}{2}}\left[1+\tfrac{1}{2}\left(\tfrac{1}{2}\right)^2\frac{k^2}{c^2}\ldots+\frac{1}{n+1}\left(\frac{1\cdot3\ldots2n-1}{2^n\,.\,n\,!}\right)^2\frac{k^{2n}}{c^{2n}}+\ldots\right].$$

It is evident from the left-hand side of the equation that this is the action integral of the motion.

The Spark Spectrum of Thallium, Tl III.

By Prof. J. C. McLennan, F.R.S., A. B. McLay, Ph.D., and M. F. Crawford, M.A.*

(Received June 3, 1929.)

The term structure of the second spark spectrum of thallium, Tl III, was investigated by Carroll† in 1926. He found it to be a simple doublet spectrum by the identification of the first member of an S, a P and a D term sequence and of a tentative F and a G first member. Carroll also found analogous features in each of the iso-electronic spectra Hg II and Pb IV and showed that these and Tl III were similar in character to that of Au I that had been analysed by Thorsen.‡ The doublet structure of each of these spectra is now known to be built on the ^1S ($5d^{10}$) state of the next higher ion.

The authors examined the spark spectrum of thallium last spring and assigned a number of wave-lengths to the spectrum, Tl II, of the singly ionised atom. Two wave-lengths, namely, λ 2530·88 A. and λ 2452·00 A., that were shown to belong without doubt to Tl II, had previously been used by Carroll to establish the tentative ^{2}F term of Tl III mentioned above. The ^{2}F term therefore was invalidated and with it also the dependent ^{2}G. A subsequent investigation of Tl III was undertaken by us and has resulted in the identification of the real F and G first members and of members of each of the S, P and D series higher than those already located by Carroll. We also sought at the same time to extend the knowledge of the Hg II spectrum and made some progress in this direction. But the recent extensive analysis of Hg II by Paschen† has made it unnecessary for us to continue our examination. Our term scheme for Hg II in so far as it was worked out corresponded to Paschen's.

---

* Mr. Crawford was enabled to participate in this investigation through the award of a studentship to him by the National Research Council of Canada. I am also indebted to the Council for financial aid that enabled us to carry through this investigation and a number of others of the same character—J. C. McL.

† 'Phil. Trans.,' A. vol. 225, p. 357 (1926).

‡ 'Naturwiss.,' vol. 25, p. 500 (1923).

The results of the term analysis of Tl III are given in Table I. The term designations used are those suggested by Russell, Turner and Shenstone in a recent report on spectroscopic notation that should be adopted generally in a short time. Each term prefix 6*s*, etc., indicates the total quantum number "*n*" (numeral) and the azimuthal quantum number "*l*" (denoted by the usual letter *s*, *p*, etc.) of the orbit occupied by the single electron outside closed shells. The terms have been separated into two groups in the table, namely, even ones at left and odd ones at right (Σl even and odd respectively). The latter are distinguished from the former by the upper right superscript "*o*."

Table I.—Terms of Tl III.

Term.	Value $\Delta\nu$.		n^*.	Term.	Value $\Delta\nu$.		n^*.
$6s\ ^2S_{\frac{1}{2}}$	240600		2·026	$6p\ ^2P^o_{\frac{1}{2}}$	176443	14813	2·366
$7s\ ^2S_{\frac{1}{2}}$	101391		3·121	$6p\ ^2P^o_{1\frac{1}{2}}$	161300		2·472
$6d\ ^2D_{1\frac{1}{2}}$	95245	1314	3·220	$7p\ ^2P^o_{\frac{1}{2}}$	82748	5682	3·455
$6d\ ^2D_{2\frac{1}{2}}$	93931		3·243	$7p\ ^2P^o_{1\frac{1}{2}}$	77066		3·580
$8s\ ^2S_{\frac{1}{2}}$	57413		4·148	$5f\ ^2F^o_{3\frac{1}{2}}$	65007	1362	3·898
$7d\ ^2D_{1\frac{1}{2}}$	54244	592	4·267	$5f\ ^2F^o_{2\frac{1}{2}}$	63645		3·939
$7d\ ^2D_{2\frac{1}{2}}$	53652		4·290				
$5g\ ^2G$	39589	0	4·995				

---

† Paschen, 'Sitz. Preuss. Akad. Wiss.,' vol. 32, p. 536.

The term subscript is the value of the inner quantum number j of that component.

The term values are based on the value zero for the state ^1S ($5d^{10}$) reached at ionisation. This state is the limit common to all series given in Table I. The values were deduced as follows. A Hicks' series formula was applied to the known first three members of the sharp series and a value 240,300 was obtained for $6s\,^2S_{\frac{1}{2}}$. However this is probably a little too low since lower numbers than those fixed exactly from series with more than three members were arrived at when the same formula was applied to the corresponding members of Au I† and of Hg II. The value calculated above was therefore raised by 300 cm.$^{-1}$. Justification for a change of this amount is obtained from the fact that the resultant n^* (effective total quantum number) value of $5\,^2G$ is 4·995, *i.e.*, the level is nearly hydrogenic, in good agreement with a similar feature of the G term sequence of Hg II. It seems probable therefore that the values assigned by us to Tl III terms are not in error by more than 100 units. The n^* value for each term is noted in Table I. The progression of the values in each term sequence is qualitatively similar to that in the corresponding one of Au I and of Hg II. The ionisation potential of Tl III, computed from the value 240600 cm.$^{-1}$ for the $6s\,^2S_{\frac{1}{2}}$ term, is 29·7 volts.

The wave-lengths assigned to Tl III are recorded in Table II together with their wave-numbers, intensities and their series designations. The wave-lengths of many of the lines are from the published lists of Carroll (*loc. cit.*) and the rest were measured by the authors. The intensities of all lines recorded in Table II were estimated visually by us from plates of the thallium spark spectrum taken with various types of spectrographs.

We have sought also for the inverted ^2D ($5d^96s^2$) term of the doublet-quartet system of Tl III that is built on the $^{3,1}D$ ($5d^96s$) state of Tl^{+++}, but so far without success. Two of us established the corresponding term of Au I‡ and Paschen identified it in Hg II. We had also located the term in the latter spectrum before we noted Paschen's communication. The position of this term of Tl III has been found approximately by extrapolation of $\sqrt{\nu/R}$ values from Au I and Hg II. The deeper component $^2D_{2\frac{1}{2}}$ should lie between the components of the known $6p\,^2P^0$ term and the ^2D interval should be about 18000 cm.$^{-1}$. These predictions indicate that in all probability two of the

---

† Thorsen, 'Naturwiss.,' vol. 25, p. 500 (1923); McLennan, McLay, 'Roy. Soc. Proc.,' A, vol. 108, p. 571 (1925), vol. 112, p. 95 (1926).

‡ McLennan and McLay, 'Roy. Soc. Proc.,' A, vol. 108, p. 571 (1925), and vol. 112, p. 95 (1926); Paschen, 'Sitz. Preuss. Akad. Wiss.,' vol. 32, p. 536 (1928).

Table II.—Classified Lines of Tl III.

Int.	λ (I.A.).	ν.	Designation.	Auth.	Int.	λ (I.A.).	ν.	Designation.	Auth.
4	8001	12495	$7p\ ^2P^0_{\frac{1}{2}} - 6d\ ^2D_{1\frac{1}{2}}$	M.	9	3456·34	28924	$6d\ ^2D_{2\frac{1}{2}} - 5f\ ^2F^0_{3\frac{1}{2}}$	C.
5	5927·8	16865	$7p\ ^2P^0_{1\frac{1}{2}} - 6d\ ^2D_{2\frac{1}{2}}$	M.	3	3300·80	30287	$6d\ ^2D_{2\frac{1}{2}} - 5f\ ^2F^0_{2\frac{1}{2}}$	C.
2	5499·4	18179	$7p\ ^2P^0_{1\frac{1}{2}} - 6d\ ^2D_{1\frac{1}{2}}$	M.	6	3163·53	31600	$6d\ ^2D_{1\frac{1}{2}} - 5f\ ^2F^0_{2\frac{1}{2}}$	C.
4	5362·40	18643	$7s\ ^2S_{\frac{1}{2}} - 7p\ ^2P^0_{\frac{1}{2}}$	C.		λ (I vac)			
4	5086·99	19653	$7p\ ^2P^0_{1\frac{1}{2}} - 8s\ ^2S_{\frac{1}{2}}$	C.	8	1660·05	60239	$6p\ ^2P^0_{1\frac{1}{2}} - 7a\ ^2S_{\frac{1}{2}}$	M.
2	4380·57	22822	$7p\ ^2P^0_{1\frac{1}{2}} - 7d\ ^2D_{1\frac{1}{2}}$	C.	8	1558·67	64157	$6s\ ^2S_{\frac{1}{2}} - 6p\ ^2P^0_{\frac{1}{2}}$	M.
6	4269·81	23414	$7p\ ^2P^0_{1\frac{1}{2}} - 7d\ ^2D_{2\frac{1}{2}}$	C.	4	1506·37	66385	$6p\ ^2P^0_{1\frac{1}{2}} - 6d\ ^2D_{1\frac{1}{2}}$	M.
4	4155·75	24056	$5f\ ^2F^0_{2\frac{1}{2}} - 5g\ ^2G$	C.	10	1477·14	67699	$6p\ ^2P^0_{1\frac{1}{2}} - 6d\ ^2D_{2\frac{1}{2}}$	M
7	4109·85	24325	$7s\ ^2S_{\frac{1}{2}} - 7p\ ^2P^0_{1\frac{1}{2}}$	C.	4	1332·36	75055	$6p\ ^2P^0_{\frac{1}{2}} - 7s\ ^2S_{\frac{1}{2}}$	C.
2	3946·02	25335	$7p\ ^2P^0_{\frac{1}{2}} - 8s\ ^2S_{\frac{1}{2}}$	C.	10	1266·33	78968	$6s\ ^2S_{\frac{1}{2}} - 6p\ ^2P^0_{1\frac{1}{2}}$	C.
6	3933·05	25418	$5f\ ^2F^0_{3\frac{1}{2}} - 5g\ ^2G$	C.	7	1231·57	81197	$6p\ ^2P^0_{\frac{1}{2}} - 6d\ ^2D_{1\frac{1}{2}}$	C.
4	3507·41	28503	$7p\ ^2P^0_{\frac{1}{2}} - 7d\ ^2D_{1\frac{1}{2}}$	C.					

M. = McLennan, McLay and Crawford.
C. = Carroll.

three lines of the $6p\ ^2P^0 - 5d^96s^2\ ^2D$ multiplet are in the extreme infra-red region. At any rate, we have not been able to identify such a multiplet in Tl III. We hope, however, to establish the inverted ^2D term by its combinations with other terms of the spectrum. If we are successful in this undertaking the results will be published in a later report together with those on the corresponding inverted ^2D terms that we have located in the analogous Ga III and In III spectra.

Tests of Significance in Harmonic Analysis.

By R. A. FISHER, F.R.S.

(Received June 5, 1929.)

1. *Schuster's Test.*

If a series $u_1, u_2, \ldots, u_{2n+1}$ constitute a random sample from a normally distributed population, then any linear function

$$A = \overset{2n+1}{\underset{1}{S}} (a_r u_r)$$

will also be normally distributed; moreover its mean will be zero if $S(a_r) = 0$, and its variance will be equal to that of the original population if

$$S(a_r^2) = 1.$$

Any other linear function

$$B = \overset{2n+1}{\underset{1}{S}} (b_r u_r)$$

will be distributed independently of the first if

$$S(a_r b_r) = 0,$$

and in this case the sum of the squares,

$$x = A^2 + B^2,$$

will be distributed so that the chance of exceeding any particular value of x is

$$e^{-\frac{x}{c}},$$

where c is the mean value of x, equal to twice the variance of the population sampled.

This proposition, which gives the χ^2 distribution for the particular case $n = 2$, is the basis of Schuster's test of the significance of any particular term in the harmonic analysis of a series. For the coefficients

$$a_r = \sqrt{\frac{2}{2n+1}} \cos \frac{2\pi pr}{2n+1},$$

$$b_r = \sqrt{\frac{2}{2n+1}} \sin \frac{2\pi pr}{2n+1},$$

fulfil the necessary conditions for all integral values of p. Values of p from 1 to n give independently distributed values of x and, if the variance of the population were known *a priori*, the test would be rigorous for any one of these chosen in advance.

2. *Allowance for Selection of the Largest Term.*

The practice of picking out the larger values of x, not in advance, but by reason of their exceptional magnitude, requires, as Sir Gilbert Walker has shown, an important modification of the test of significance. For, if we wish to test the significance of the largest observed value of x, we must compare the value observed with the sampling distribution of the largest of n independent values, and not with that of any one value chosen in advance. If P stand for the probability which we adopt, as sufficiently small to be used as a criterion of significance, the corresponding value of x will be given by

$$e^{-\frac{x}{c}} = \mathrm{P},$$

for any particular term, but if x is chosen to be the largest of n independent values, it is necessary that the probability should be $1 - \mathrm{P}$ that all the n values shall be less than x, so that

$$\left(1 - e^{-\frac{x}{c}}\right)^n = 1 - \mathrm{P}$$

is the equation which determines the least value of x to be judged significant. This is the criterion derived by Walker.

3. *Allowance for the Sampling Error of the Estimated Variance.*

In the practical application of this criterion, when c is not known *a priori*, it is necessary to substitute for c an estimate of it derived from the data, and, for an exact test, to take into account the sampling error of this estimate. The estimate of c will necessarily be based on the variance observed in the original sample, or, what comes to the same thing, on the average value of x for the n possible periods; and, whether we take, as our actual estimate, the average of all the n values, or the average of the $(n - 1)$ values other than that to be tested, all that is required for an exact solution, in either case, is the frequency distribution of the largest of n values of x, expressed as a fraction of the total of the sample of n of which it is the largest member.

If $x_1, \ldots, x_n$ are the co-ordinates of a point in Euclidian space of n dimensions, the simultaneous distribution of the n values will be represented by a density function

$$e^{-\frac{1}{c}(x_1 + x_2 + \ldots + x_n)}$$

which is constant over plane finite regions of $n-1$ dimensions, bounded by the n-surfaces

$$x_r = 0$$

in the form of a generalised tetrahedron. In every such region, the distribution of the ratio of the largest co-ordinate to the sum of all co-ordinates will be the same, and, since the density is constant over each such region, the distribution is to be found merely from the elements of generalised volume, into which the region is divided for fixed values of the ratio. Any particular co-ordinate, *e.g.*, x_1, will be the greatest in one nth of the whole region, this fraction being bounded on the one hand by the loci, at which it ceases to be greatest,

$$x_1 = x_2, \quad x_1 = x_3, \quad \ldots, \quad x_1 = x_n,$$

and, on the other, by the boundaries,

$$x_2 = 0, \quad x_3 = 0, \quad \ldots, \quad x_n = 0\,;$$

within this region it is required to find the distribution of the ratio

$$g = \frac{x_1}{x_1 + x_2 + \ldots + x_n}.$$

4. *The Discontinuities of the Distribution.*

The distribution defined geometrically by the dissection of a generalised tetrahedron exhibits a number of discontinuities; the linear regions which constitute its boundary intersect $n-1$ at a time at the sets of points typified by

$$\begin{array}{l}
x_1 = x_2 = x_3 = \ldots\ldots\ldots = x_n \\
x_2 = 0, \quad x_1 = x_3 = \ldots\ldots = x_n \\
x_2 = x_3 = 0, \quad x_1 = x_4 = \ldots = x_n \\
\ldots\ldots\ldots\ldots\ldots\ldots\ldots\ldots \\
x_2 = x_3 = \ldots\ldots\ldots\ldots = x_n = 0,
\end{array}$$

at which it is evident that the values of g are

$$\frac{1}{n}, \quad \frac{1}{n-1}, \quad \ldots, \quad \tfrac{1}{2}, \quad 1,$$

representing in succession, the centre of the generalised tetrahedron, the centres of all its bounding faces, of successively lower dimensions, which meet in the point, $g = 1$, the middle points of the edges running from this point, and finally the limiting point, $g = 1$, itself. Hence g is distributed over the range from $1/n$ to 1; and for an exact test of significance we require to know the probability with which any particular value between these limits is exceeded.

5. *The Exact Distribution.*

A point about the distribution which greatly facilitates the solution, is that within the region between any two discontinuities the probability integral of the distribution is merely a polynomial in g of degree $n - 1$. For the boundaries of any region, $g = g_0$, change the magnitude of their elements continuously at rates determined by the magnitude of their boundaries, and so on down to the bounding edges, the lengths of which are linear functions of g; consequently the probability integral is in each region a polynomial of degree $n - 1$, but from region to region the $(n - 1)$th differential coefficient with respect to g changes discontinuously.

We may therefore represent the probability integral by the form

$$\mathrm{P} = \alpha_1 (1 - g)^{n-1} + \alpha_2 (1 - 2g)^{n-1} + \dots + \alpha_n (1 - ng)^{n-1},$$

in which as many terms are to be taken as have positive quantities within the brackets. The last term is therefore included for no possible value of g, but is written above in order to utilise the condition that when $g < 1/n$ the probability integral shall be unity. This condition is sufficient to determine the n coefficients by equation of the coefficients of $g^0, g^1, \dots, g^{n-1}$.

To determine their actual values let

$$f = -1 + \alpha_1 t + \alpha_2 t^2 + \dots + \alpha_n t^n,$$

then the equations of the successive coefficients give

$$f = 0, \quad \left(t \frac{d}{dt}\right) f = 0, \quad \dots, \quad \left(t \frac{d}{dt}\right)^{n-1} f = 0,$$

at the values $t = 1$. These are evidently equivalent to

$$f = 0, \quad \frac{d}{dt} f = 0, \quad \dots, \quad \frac{d^{n-1}}{dt^{n-1}} f = 0,$$

for the same value, so that f, being of degree n, must be a numerical multiple of $(t - 1)^n$, or, in view of its first term,

$$f = -(1 - t)^n.$$

We have therefore the probability integral in the form

$$P = n\,(1-g)^{n-1} - \frac{n\,(n-1)}{2}\,(1-2g)^{n-1} + \ldots + (-)^{k-1}\frac{n\,!}{k!\,(n-k)\,!}\,(1-kg)^{n-1},$$

where k is the greatest integer less than $1/g$.

6. *Summary and Table of 5 per cent. Values.*

A practical convenience of the form which has been obtained for the probability integral, is that for small values of P, such as are needed in tests of significance, the magnitude of the successive terms decreases very rapidly, so that even when, as at the 5 per cent. point for $n = 50$, as many as seven terms exist, very high precision is obtained from the first three terms only. Indeed the first term alone gives a very satisfactory approximate test of significance. The first term has, moreover, a simple meaning in relation to a related statistical problem. There are, in fact four related distributions each of which is the appropriate solution of one of four problems.

(I) The distribution of any one harmonic term obtained from a random sample of numbers drawn from a population of known variance. Schuster's solution of this is given by the distribution of the form

$$P = e^{-x}. \tag{1}$$

(II) The distribution of the largest of the n harmonic terms obtained from a similar sample; for this we have Walker's solution

$$P = 1 - (1 - e^{-x})^{n}. \tag{2}$$

(III) We may ask what is the distribution of any one harmonic term as a fraction of the total (or mean) of the terms obtained from the same sample; here there is no restriction that our term should be the largest, and all points within the generalised tetrahedron are available, so that

$$P = (1 - g)^{n-1} \tag{3}$$

where g is the chosen term expressed as a fraction of the whole.

(IV) Finally the probability that the largest of the n terms should exceed g is, so long as this probability is small, naturally not far from n times the value given by (3), and has been shown to be exactly

$$P = n\,(1 - g)^{n-1} - \ldots + (-)^{n-1}\frac{n\,!}{k\,!\,(n-k)\,!}\,(1 - kg)^{n-1}, \tag{4}$$

where k is the largest integer less than $1/g$.

How good an approximation is obtained by using the first term only, is shown by the following table giving the 5 per cent. values of g for values of n from 5 to 50 in a parallel column with those obtained by ignoring all terms after the first.

n.	g (by exact formula).	g (by first term only).
5	0·68377	0·68377
10	0·44495	0·44495
15	0·33462	0·33463
20	0·27040	0·27046
25	0·22805	0·22813
30	0·19784	0·19794
35	0·17513	0·17525
40	0·15738	0·15752
45	0·14310	0·14324
50	0·13135	0·13149

This table can be used directly in testing significance; the 5 per cent. point is the lowest level of significance likely to be wanted, and for higher levels, such as the 1 per cent. point, the first term will provide an even closer approximation. The method of section 5 should be useful in many distribution problems involving points of discontinuity.

The value of g may in all cases be very easily obtained. If all the Fourier submultiples have been worked out, it is, as already defined,

$$\frac{x_1}{x_1 + x_2 + \dots + x_n}.$$

The denominator of this expression is, however, merely

$$\overset{2n+1}{\underset{r=1}{\mathrm{S}}} (u_r - \bar{u})^2.$$

In the case where the number of observations in the series is even, $(2n + 2)$, we need still only consider the n complete harmonic terms, and can obtain their sum as

$$\overset{2n+2}{\underset{r=1}{\mathrm{S}}} (u_r - \bar{u})^2 - \frac{(u_1 - u_2 + u_3 - \dots - u_{2n+2})^2}{2n + 2}.$$

The Arc Spectrum of Chlorine.

By KANAKENDU MAJUMDAR, M.Sc., Demonstrator, Physical Laboratory of the University of Allahabad.

(Communicated by M. Saha, F.R.S.—Received April 15, 1929.)

Introduction.

The arc spectrum of chlorine has hitherto been only partially investigated. In 1926, L. A. Turner* discovered the fundamental arc lines in the Schumann region due to the transition $4M_2(M_2 \leftarrow N_1)$. de Bruin† found a number of lines on the shorter wave-length side of the visible with the constant frequency difference of 530. More recently Laporte,‡ in a note to 'Nature,' announced the discovery by Asagoe of a set of arc lines between λ 4700–4200, which he ascribed to the transition $4M_2(N_1 \leftarrow N_2)$. Apparently some of these lines are identical with those of de Bruin.

Location of the Group $4M_2$ $(N_1 \leftarrow N_2)$.

The theories of spectra have now so far advanced that it is possible to predict and locate the exact position of groups of lines corresponding to definite transitions. In a recent paper,§ it has been shown that if we consider the arc spectra of a group of successive elements, as for example,

$$\text{Al, Si, P, S, Cl, A, K,} \qquad (1)$$

then the wave-numbers of the strongest lines of the elements due to the transition $N_1 \leftarrow N_2$ increase linearly with the atomic number. This fact is graphically represented in fig. 1 and has also been verified in other similar groups (*e.g.*, B, C, N, O, F, Ne, Na_3; Si^+, P^+, S^+, ..., ..., Ca^+).

In the group of elements we are considering, viz., Al to K, we have complete knowledge of the lines due to the transition $N_1 \leftarrow N_2$ of the elements Al, S, A and K. In the figure each dot represents a multiplet or the frequency of the strongest line in the multiplet. It will be seen that the average of these in the different elements lie almost on a straight line. Thus chlorine lying between

---

* 'Phys. Rev.,' vol. 27, p. 397 (1926).

† 'Amst. Proc.,' vol. 30, p. 20 (1927).

‡ 'Nature,' vol. 121, p. 1021 (1928).

§ Saha and Majumdar, 'Ind. J. Phys.,' vol. 3, p. 67 (1928).

S and A will have for the frequency of its average multiplet the value of $\nu = 11930$. The positions of the other groups can be located from a comparison of the positions of the corresponding groups in the spectra of atoms having the same electronic configuration. This is available in the spectrum of A^+ which has been analysed by de Bruin.* For comparison the frequencies of the ionised elements, Si^+, P^+, S^+, ..., ..., Ca^+ which have respectively the same electron structure as those of group (1) have also been plotted in the figure. Thus it is seen that the groups of lines of chlorine due to the transition $4M_2 (N_1 \leftarrow N_2)$ are expected to lie in the region λ 9300–7700.

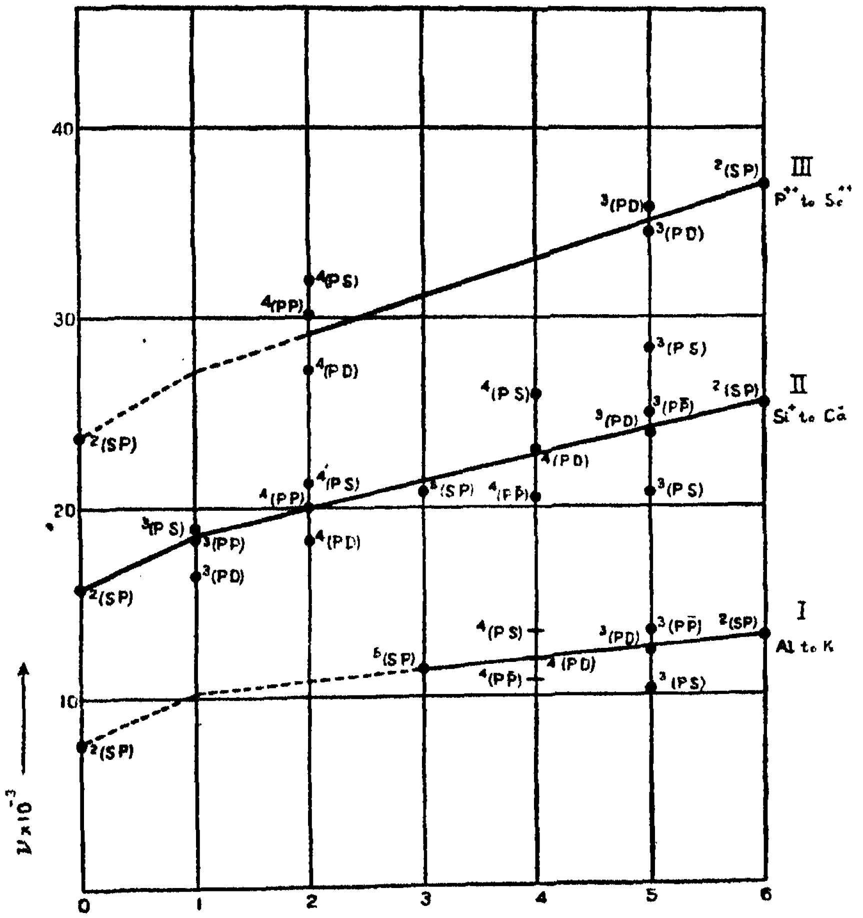

FIG. 1.

It is, therefore, clear that Laporte's identification of the group at λ 4700–4200 being due to $4M_2 (N_1 \leftarrow N_2)$ is wrong. These have to be identified as the higher Rydberg sequence, viz., due to the transition $4M_2 (N_1 \leftarrow O_2)$.

---

* 'Amst. Proc.,' vol. 31, p. 771 (1928).

With a view to discovering these predicted infra-red lines of chlorine, an investigation at this end of the spectrum was undertaken.

Experimental.

The experimental work proved to be more difficult than was at first supposed, not only on account of the difficulty of photographing this part of the spectrum with sufficient dispersion, but also on account of the great activity of chlorine specially when a discharge is passed through it. It was found that after running the chlorine tube for some time, the pressure of the gas in the tube diminished, thereby the nature of the discharge changed. This phenomenon is due to the fact that with the electrical stimulus chlorine acts readily with the material of the electrodes and forms chloride of the metal which deposits on the walls of the tube. Thus the pressure of the gas in the tube is reduced. Hence a tube permanently sealed was found to be unsuitable for the purpose. In order to overcome the difficulty the arrangement illustrated in fig. 2 was used. It consists of a pyrex glass tube 1·5 cm. in diameter with a capillary in the middle, the total length of the tube being 40 cm. Two side tubes EE carry the electrodes by means of molybdenum wires, which seal readily in the pyrex glass under vacuum. The electrodes were of nickel sheets bent into

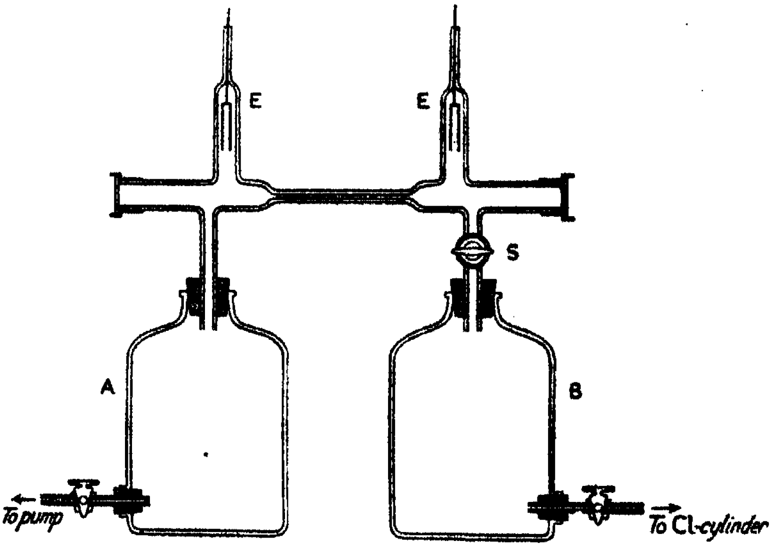

FIG. 2.

cylinders, this metal having been chosen as it was found that it was less acted on by chlorine than the other commonly used metals. The ends of the tube were provided with brass sockets carrying glass windows, which were placed at a sufficient distance from the electrodes to prevent the frequent deposit of the chloride on them. To maintain the pressure fairly constant for a sufficient length of time, the tube was kept connected to a bell-jar A, so that slight decrease in the amount of the gas did not alter the pressure appreciably. The pressure of the gas in the system was about 12 mm. The supply of chlorine was obtained from another bell-jar B connected to the tube through a stopcock S. This bell-jar was from time to time filled from a steel cylinder containing liquid chlorine at high pressure.

The tube was run by an induction coil, supplying about 100 watts at 20,000 volts. It was found that a transformer having a large current-carrying capacity was not suitable, as the action of chlorine on the electrodes increased greatly with the current in the tube. An oil-immersed plate condenser had to be put in parallel with the tube; otherwise the band spectrum of chlorine appeared strongly.

The spectrum was produced by means of a plane replica glass grating having about 15,000 lines to the inch. The photographic arrangement consisted of an Adam Hilger camera which is supplied with the constant-deviation spectrograph. Thus the dispersion in the first order was about 29 Å. per millimetre at λ 8000. Photographs were taken on neocyanin plates hypersensitised with ammonia, using neon lines as standards. The second order lines were cut off by means of Wratten orange filter. Exposures varied from 24 hours to 80 hours. Even with maximum exposures given, no lines could be obtained beyond λ 8700, though they are expected to be present. This is probably due to the fact that these infra-red sensitive dyes are rather unstable compounds and are very sensitive to heat. Long storage and climatic conditions are responsible for loss of sensitiveness. The lines due to oxygen and nitrogen appeared strongly on the plates. It has been noted before by previous workers that chlorine contains nitrogen and oxygen as impurities in sufficient quantities to make their line spectra prominent. These lines, however, served to check the wave-lengths of the chlorine lines measured.

Classification.

The structure of chlorine may be represented as follows :—

K_1						
2						
	L_1	L_2				
	2	6				
		M_1	M_2	M_3		
		2	5	(1)		
			N_1	N_2	N_3	N_4
			(1)	(1)	(1)	
				O_1	O_2	O_3
				(1)	(1)	

The following sets of terms with different configurations of electrons are thus obtained :—

Table I.

Electron configuration.	Terms (theoretical).	Terms (observed).
$5M_2$	$^2\overline{P}$	$^2\overline{P}$
$4M_2N_1$	^4P ^2P $^2\overline{D}$ ^2S	^4P
$4M_2N_2$	^4D $^4\overline{P}$ ^4S ^2D $^2\overline{P}$ ^2S $^2\overline{F}$ ^2D $^2\overline{P}$	^4D ^4S
$4M_2O_2$	Ditto	^4D $^4\overline{P}$ ^4S

As has been mentioned before, the lines in the Schumann region were obtained by Turner and may be identified as originating from the combination of the doublets of $5M_2$ with the quartet and doublet terms of $4M_2N_1$. The lines from the transitions $5M_2 (M_2 \leftarrow M_3)$ are also expected to lie near about these lines though more shifted towards the higher frequency side, but have not been observed. The infra-red lines found in the course of this work have been identified as belonging to the transition $N_1 \leftarrow N_2$ and are given in Table II in the form of multiplets. So far it has only been possible to discover ^4D and ^4S terms of the configuration $4M_2N_1$. The ^4P terms and the other doublet terms have not been identified and are possibly outside the region photographed. Table III contains the lines from the combination $(N_1 \leftarrow O_2)$ giving the higher

Table II.

$4M_2N_1$ $4M_2N_2$	$^4P_3$	(530)	$^4P_2$	(339)	$^4P_1$
$^4D_4$	(9) 11935·2				
(239)					
$^4D_3$	(12) 12174*		(4) 11644·8		
(216)					
$^4D_2$	—		(3) 11861·1		(5) 11522*
(135)					
$^4D_1$			(4) 11995·9		(2) 11657·9
$^4S_2$	(2) 13777·5		(1) 13246·4		(1) 12907·2

* Masked by the strong nitrogen groups at λ 8211–23 and at λ 8680–86 respectively.

Table III.

$4M_2N_1$ $4M_2O_2$	$^4P_3$	(530)	$^4P_2$	(339)	$^4P_1$.
$^4\bar{P}_3$	(10) 23015·6		(2) 22484·9		
(340)					
$^4\bar{P}_2$	(3) 23355·5		(8) 22825·1		(2) 22486·9
(375)					
$^4\bar{P}_1$			(3) 23200·6		(6) 22861·5
$^4D_4$	(9) 23504·2				
(−62)					
$^4D_3$	(3) 23442·4		(8) 22912·0		
(297)					
$^4D_2$	—		(6) 23209·2		(5) 22868·8
(253)					
$^4D_1$			(3) 23461·0		(6) 23123·7
$^4S_2$	(7) 23654·0		(6) 23123·7		(5) 22785·4

Rydberg sequence to the terms from $4M_2N_2$ configuration. Laporte has probably arrived at a similar analysis, for the region which he mentioned in his letter to 'Nature' coincides with that described here, but since his full paper is not available a comparison has not been made. The lines from the transition $4M_2(N_2 \leftarrow N_3)$ would lie still further in the infra-red, and have not been found.

Table IV contains the full list of new lines of chlorine measured in the infra-red, along with all the lines classified by the present analysis.

Table IV.

λ I.A.	I.	ν (vac.).	Combination.
			$4M_2(N_1 \leftarrow N_2)$
8696·8	0	11495·3	
8676·7	5	11522	$^4P_1 - {}^4D_2$
8585·2	4	11644·8	$^4P_2 - {}^4D_3$
8575·5	2	11657·9	$^4P_1 - {}^4D_1$
8428·6	3	11861·1	$^4P_2 - {}^4D_2$
8376·3	9	11935·2	$^4P_3 - {}^4D_4$
8333·9	4	11995·9	$^4P_2 - {}^4D_1$
8211·3	12	12175	$^4P_3 - {}^4D_3$
8202·0	1	12188·8	
8087·6	3	12361·3	
7883·5	0	12681·2	
7826·4	0	12773·7	
7758·7	1	12885·2	
7745·5	1	12907·2	$^4P_1 - {}^4S_2$
7720·3	0	12949·3	
7547·2	1	13246·3	$^4P_2 - {}^4S_2$
7256·2	2	13777·5	$^4P_3 - {}^4S_2$
6687·8	1	14948·5	
6661·9	2	15006·6	
6614·5	3	15114·1	
6487·1	3	15411·0	
6465·9	1	15461·5	
			$4M_2(N_1 \leftarrow O_2)$
4446·18	2	22484·9	$^4P_2 - {}^4\bar{P}_3$
4445·93	2	22486·9	$^4P_1 - {}^4\bar{P}_2$
4387·54	5	22785·4	$^4P_1 - {}^4S_2$
4379·91	8	22825·1	$^4P_2 - {}^4\bar{P}_2$
4372·95	6	22861·5	$^4P_1 - {}^4\bar{P}_1$
4371·55	5	22868·8	$^4P_1 - {}^4D_1$
4363·31	8	22912·0	$^4P_2 - {}^4D_3$
4343·66	10	23015·6	$^4P_3 - {}^4\bar{P}_3$
4323·36	6	23123·7	$\left\{\begin{matrix} ^4P_1 - {}^4D_2 \\ ^4P_2 - {}^4S_2 \end{matrix}\right.$
4309·03	3	23200·6	$^4P_2 - {}^4\bar{P}_1$
4307·43	6	23209·2	$^4P_2 - {}^4D_1$
4283·45	3	23355·5	$^4P_3 - {}^4\bar{P}_2$
4264·58	3	23442·4	$^4P_3 - {}^4D_3$
4261·19	3	23461·0	$^4P_2 - {}^4D_2$
4253·37	9	23504·2	$^4P_3 - {}^4D_4$
4226·42	7	23654·0	$^4P_3 - {}^4S_2$

Ionisation Potential.

The quarter D-terms from the configurations $4M_2N_2$ and $4M_2O_2$ forming a Rydberg sequence will have for their $^4D_4$-terms the values near about 22100 and 10530 respectively. Now since the frequency of the line $^4P_3 - {}^4D_4$ belonging to the transition $4M_2(N_1 \leftarrow N_2)$ is 11935, the term value of $^4P_3$ of configuration $4M_2N_1$ will be 34035. According to Laporte,* the frequency of the line $^2\bar{P}_2 - {}^4P_3$ due to the transition $4M_2(M_2 \leftarrow N_1)$ is 71947, which gives the value of $^2\bar{P}_2$ of the fundamental configuration $5M_2$ as 105980 in wave-number units. Since $^2\bar{P}_2$ is greater than $^2P_1$, this gives the ionisation potential of chlorine as 13·1 volts.

Comparison with the Solar Wave-lengths.

In order to find out if these infra-red lines of chlorine occur in the sun, the following comparison has been made. The evidence, however, seems to be indecisive.

Table V.

Chlorine wave-length.	Intensity.	Classification.	Solar wave-length.†	Intensity.
8678·7	5	$^4P_1 - {}^4D_2$	—	
8585·2	4	$^4P_2 - {}^4D_3$	8585·58	−2
8575·5	2	$^4P_1 - {}^4D_1$	8575·73	−2
8428·6	3	$^4P_2 - {}^4D_2$	8428·08	−2
8376·3	9	$^4P_3 - {}^4D_4$	8376·38	−2 Atm.
8333·9	4	$^4P_2 - {}^4D_1$	8333·89	−2
8211·3	12	$^4P_3 - {}^4D_3$	8211·19	−2 Atm.
7745·5	1	$^4P_1 - {}^4S_2$	—	
7547·2	1	$^4P_2 - {}^4S_2$	—	
7256·2	2	$^4P_3 - {}^4S_2$	7256·13	−2 Fe ?

The author wishes to express his indebtedness to Prof. Meghnad Saha, D.Sc., F.R.S., under whose direction and guidance this work has been carried out. His thanks are also due to Mr. S. C. Deb, M.Sc., for much useful help in the experiments.

Summary.

The spectrum of chlorine has been photographed in the region λ 6400 to 8700, and the lines obtained have been identified as belonging to the transition $4M_2(N_1 \leftarrow N_2)$. The group of lines occurring at λ 4200–4500 originates from the combination $4M_2(N_1 \leftarrow O_2)$, giving the higher Rydberg sequence to the terms of the configuration $4M_2N_2$. The ionisation potential has therefore been calculated as 13·1 volts.

---

* *Loc cit.*

† "Revision of Rowland's Preliminary Table of Solar Wave-lengths," by St. John and others.

On the Numerical Solution of Equations with Complex Roots.

By R. A. Frazer, B.A., B.Sc., and W. J. Duncan, B.Sc., A.M.I.Mech.E.

(Communicated by H. Lamb, F.R.S.—Received April 26, 1929.—Revised June 1, 1929.)

1. *Introduction.*—Parts I and II of the present paper give a brief description of two methods, which are believed to be substantially novel, for the numerical resolution of equations with complex roots. As regards rapidity of computation, the methods will probably be found inferior to others such as Aitken's extension of Bernoulli's method,[*] or the root-squaring method as improved by Brodetsky and Smeal.[†] On the other hand, a feature of the alternatives proposed is that arithmetical errors need not be cumulative. Certain further merits will be suggested in due course.

Part III contains a résumé of Bairstow's variant of the root-squaring method, and Part IV deals with successive approximation to a quadratic factor. The substance of these parts has already appeared in aeronautical publications, but may not be familiar to the general scientific public.

PART I.—"TEST FUNCTION" METHOD.

2. *General Description.*—The underlying principle is very simple. Suppose that an equation has a pair of roots $\alpha \pm \beta$, where α is real and β is either real or pure imaginary. If the roots of the equation be decreased by the real quantity α, then the modified equation will have the pair of equal and opposite roots $\pm \beta$. The occurrence of equal and opposite roots is indicated by the vanishing of a certain "test function." The use of this function[‡] thus permits the determination of α, and an explicit formula for β can readily be obtained.

3. *Construction of the Test Function.*—Suppose that the original equation, on reduction of its roots by the real quantity μ, becomes

$$f(z) \equiv p_0 z^n + p_1 z^{n-1} + p_2 z^{n-2} + \dots + p_{n-1} z + p_n = 0. \qquad (1)$$

If μ is such that (1) has the pair of equal and opposite roots $\pm \beta$, then

---

[*] 'Proc. Roy. Soc. Edinburgh,' vol. 46, p. 289 (1926).

[†] 'Proc. Camb. Phil. Soc.,' vol. 22, p. 83 (1924).

[‡] For an account of these "test functions" see Frazer and Duncan, 'Roy. Soc. Proc.,' A, vol. 124, p. 642 (1929).

$f(\beta) = f(-\beta) = 0$. For equations of even degree (*e.g.*, $n = 2m$) it follows that

$$p_0 y^m + p_2 y^{m-1} + p_4 y^{m-2} + \dots + p_{2m-2} y + p_{2m} = 0, \tag{2}$$

$$p_1 y^{m-1} + p_3 y^{m-2} + \dots + p_{2m-3} y + p_{2m-1} = 0, \tag{3}$$

where y has been substituted for β^2. Analogous relations hold good for equations of odd degree.

Any form of the eliminant of (2) and (3) may be adopted as the test function T. The standard form of T is the determinant obtained by the application of Sylvester's dialytic method of elimination, but others may be more convenient for computation. Some of the alternatives will be indicated hereafter.

When T vanishes, y is a common root of equations (2) and (3), and the explicit expression of this root in terms of the coefficients can be derived by a process of "partial elimination."[*]

The method of Jelinek[†] may be regarded as a special case of the test function method. Jelinek substitutes the roots of (2) in the expression on the left of (3) and varies μ until (3) is satisfied. Evidently this process amounts to the use of a test function, but the treatment developed in the present paper is more general, and is believed to be more convenient.

The detailed application of the test function method to quartic, sextic and octic equations will now be considered.

(*a*) *The Quartic.*—In this case (2) and (3) become

$$p_0 y^2 + p_2 y + p_4 = 0, \tag{4}$$

$$p_1 y + p_3 = 0. \tag{5}$$

Hence

$$\mathrm{T}_3 = \begin{vmatrix} p_1 & p_0 & 0 \\ p_3 & p_2 & p_1 \\ 0 & p_4 & p_3 \end{vmatrix} = p_1 p_2 p_3 - p_1^2 p_4 - p_3^2 p_0, \tag{6}$$

and from (5),

$$y \equiv \beta^2 = -p_3/p_1. \tag{7}$$

(*b*) *The Sextic.*—The equations for y are

$$p_0 y^3 + p_2 y^2 + p_4 y + p_6 = 0, \tag{8}$$

$$p_1 y^2 + p_3 y + p_5 = 0. \tag{9}$$

---

[*] Frazer and Duncan, *loc. cit.*, § 6.

[†] 'Die Auflösung der höheren numerischen Gleichungen,' Leipzig, 1865.

The standard determinantal form of the test function given by the dialytic method of elimination is

$$T_5 = \begin{vmatrix} p_1 & p_0 & 0 & 0 & 0 \\ p_3 & p_2 & p_1 & p_0 & 0 \\ p_5 & p_4 & p_3 & p_2 & p_1 \\ 0 & p_6 & p_5 & p_4 & p_3 \\ 0 & 0 & 0 & p_6 & p_5 \end{vmatrix} \tag{10}$$

Another form of the test function is

$$T_5' = \begin{vmatrix} p_1 & p_0 & 0 \\ p_3 & p_2 & p_1 \\ p_5 & p_4 & p_3 \end{vmatrix} \times \begin{vmatrix} p_1 & p_0 & 0 \\ p_5 & p_4 & p_3 \\ 0 & p_6 & p_5 \end{vmatrix} - \begin{vmatrix} p_1 & p_0 & 0 \\ p_3 & p_2 & p_1 \\ 0 & p_6 & p_5 \end{vmatrix}^2, \tag{11}$$

and y is given by

$$y \begin{vmatrix} p_1 & p_0 & 0 \\ p_3 & p_2 & p_1 \\ 0 & p_6 & p_5 \end{vmatrix} + \begin{vmatrix} p_1 & p_0 & 0 \\ p_5 & p_4 & p_3 \\ 0 & p_6 & p_5 \end{vmatrix} = 0. \tag{12}$$

Probably the simplest of all the forms of the test function is

$$T_5'' = (p_0 y_1^3 + p_2 y_1^2 + p_4 y_1 + p_6)\,(p_0 y_2^3 + p_2 y_2^3 + p_4 y_2 + p_6), \tag{13}$$

where y_1 and y_2 are the roots of the quadratic

$$p_1 y^2 + p_3 y + p_5 = 0. \tag{14}$$

When T_5'' vanishes, at least one of its factors must vanish, and the corresponding value of y ($\equiv \beta^2$) must obviously be *real*. Thus, if the roots of (14) are complex the assumed value of μ is certainly incorrect, and the computation of T_5'' may be unnecessary. Clearly, the two factors of (13) can always be dealt with separately.

(*c*) *The Octic.*—Here the standard test function is

$$T_7 = \begin{vmatrix} p_1 & p_0 & 0 & 0 & 0 & 0 & 0 \\ p_3 & p_2 & p_1 & p_0 & 0 & 0 & 0 \\ p_5 & p_4 & p_3 & p_2 & p_1 & p_0 & 0 \\ p_7 & p_6 & p_5 & p_4 & p_3 & p_2 & p_1 \\ 0 & p_8 & p_7 & p_6 & p_5 & p_4 & p_3 \\ 0 & 0 & 0 & p_8 & p_7 & p_6 & p_5 \\ 0 & 0 & 0 & 0 & 0 & p_8 & p_7 \end{vmatrix} \tag{15}$$

The expression corresponding to (11) is

$$T_7' = \begin{vmatrix} p_1 & p_0 & 0 & 0 & 0 \\ p_3 & p_2 & p_1 & p_0 & 0 \\ p_5 & p_4 & p_3 & p_2 & p_1 \\ p_7 & p_6 & p_5 & p_4 & p_3 \\ 0 & p_8 & p_7 & p_6 & p_5 \end{vmatrix} \times \begin{vmatrix} p_1 & p_0 & 0 & 0 & 0 \\ p_3 & p_2 & p_1 & p_0 & 0 \\ p_5 & p_4 & p_3 & p_2 & p_1 \\ 0 & p_8 & p_7 & p_6 & p_5 \\ 0 & 0 & 0 & p_8 & p_7 \end{vmatrix} - \begin{vmatrix} p_1 & p_0 & 0 & 0 & 0 \\ p_3 & p_2 & p_1 & p_0 & 0 \\ p_5 & p_4 & p_3 & p_2 & p_1 \\ p_7 & p_6 & p_5 & p_4 & p_3 \\ 0 & 0 & 0 & p_8 & p_7 \end{vmatrix}^2, \qquad (16)$$

and y is given by

$$y \begin{vmatrix} p_1 & p_0 & 0 & 0 & 0 \\ p_3 & p_2 & p_1 & p_0 & 0 \\ p_5 & p_4 & p_3 & p_2 & p_1 \\ p_7 & p_6 & p_5 & p_4 & p_3 \\ 0 & 0 & 0 & p_8 & p_7 \end{vmatrix} + \begin{vmatrix} p_1 & p_0 & 0 & 0 & 0 \\ p_3 & p_2 & p_1 & p_0 & 0 \\ p_5 & p_4 & p_3 & p_2 & p_1 \\ 0 & p_8 & p_7 & p_6 & p_5 \\ 0 & 0 & 0 & p_8 & p_7 \end{vmatrix} = 0. \qquad (17)$$

In actual computation it may be found convenient to transfer the fourth rows to the leading position, for then the minors of the elements in the first rows are identical in the two determinants.

Both T_7 and T_7' are rather laborious in use, and a more convenient test function is

$$T_7'' = (p_1y_1^3 + p_3y_1^2 + p_5y_1 + p_7)(p_1y_2^3 + p_3y_2^2 + p_5y_2 + p_7), \qquad (18)$$

where y_1 and y_2 are the roots of the quadratic,*

$$y^2 \begin{vmatrix} p_1 & p_0 & 0 \\ p_3 & p_2 & p_1 \\ 0 & p_8 & p_7 \end{vmatrix} + y \begin{vmatrix} p_1 & p_0 & 0 \\ p_5 & p_4 & p_3 \\ 0 & p_8 & p_7 \end{vmatrix} + \begin{vmatrix} p_1 & p_0 & 0 \\ p_7 & p_6 & p_5 \\ 0 & p_8 & p_7 \end{vmatrix} = 0. \qquad (19)$$

Equation (19) is a partial eliminant of equations (2) and (3) with $m = 4$. The actual treatment of T_7'' in relation to the nature of the roots of (19) would be strictly parallel to that already detailed for the sextic.

4. *Illustrative Application to a Particular Sextic.*—Let the equation for solution be

$$z^6 + 3z^5 + 20z^4 + 3z^3 + 2z^2 + 4z + 5 = 0. \qquad (20)$$

The following table contains the values of the coefficients, and of T_5 for a series of values of μ, the real quantity by which the roots of (20) are reduced. The details of the calculations of the coefficients by Horner's process are omitted.

---

* Frazer and Duncan, *loc. cit.*, equation (31).

Table I.

μ.	p_0.	p_1.	p_2.	p_3.	p_4.	p_5.	p_6.	$T_5 \times 10^{-4}$.
0	1	3·0	20·0	3·0	2·0	4·0	5·0	−1·32
0·1	1	3·6	21·65	11·32	4·1315	4·57156	5·42503	−4·956
0·3	1	4·8	25·85	30·24	16·4315	8·30608	6·63102	−27·62
0·45	1	5·7	29·7875	46·8974	33·6988	15·6383	8·36217	−2·103
0·46	1	5·76	30·074	48·0947	35·1237	16·3264	8·52194	+4·107
0·47	1	5·82	30·3635	49·3034	36·5846	17·04347	8·68879	14·22
0·5	1	6·0	31·25	53·0	41·1875	19·375	9·23435	53·50
1·0	1	9·0	50·0	133·0	176·0	118·0	38·0	27824·0

Fig. 1 is a preliminary graph of T_5 on a base of μ, while fig. 2 shows the result of more detailed exploration for the range 0·45 to 0·47. The approximate value of α for one pair of roots of the sextic is seen to be 0·454. By means of equation (12) the corresponding value of $y\ (\equiv \beta^2)$ is found to be $-0{\cdot}343$. Thus $\beta = \pm 0{\cdot}586i$; and a pair of roots of the sextic is approximately $0{\cdot}454 \pm 0{\cdot}586i$, corresponding to the quadratic factor $z^2 - 0{\cdot}908z + 0{\cdot}549$.

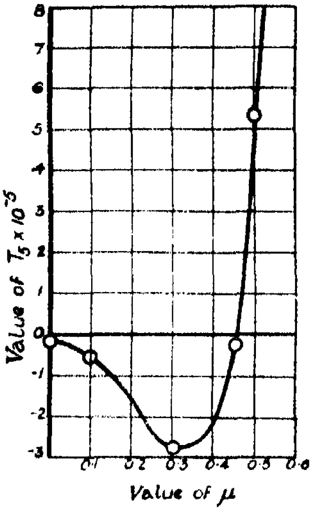

Fig. 1.

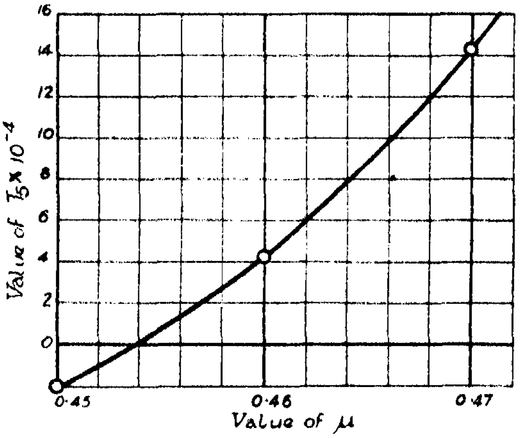

Fig. 2.

Bairstow's process of successive approximation (see Part IV) is now applied, and a more accurate value for the factor found to be

$$z^2 - 0{\cdot}91036z + 0{\cdot}55862, \tag{21}$$

so that the roots are

$$0{\cdot}45518 \pm 0{\cdot}59282i. \tag{22}$$

The actual time taken by a computer, not experienced in the method, to obtain this result was 3 hours.

When the sextic (20) is divided by the quadratic factor (21) the quotient is the quartic

$$z^4 + 3\cdot91036z^3 + 23\cdot0012z^2 + 21\cdot7549z + 8\cdot9557 = 0. \qquad (23)$$

The roots of (23) are found by means of the test function T_3. Values of the coefficients and of the test function are given in the following table.

Table II.

μ.	p_0.	p_1.	p_2.	p_3.	p_4.	T_3.
0	1	3·91036	23·0012	21·7549	8·9557	1346·5
−0·1	1	3·51036	21·8882	17·268	7·0064	942·3
−0·5	1	1·91036	18·6356	1·1865	3·4022	28·4
−0·51	1	1·87036	18·5789	0·8143	3·39226	15·8
−0·523	1	1·81836	18·5070	0·3322	3·38481	−0·12
−0·53	1	1·79036	18·4691	0·0734	3·38339	−8·4

A graph shows that a close approximation to the value of α is $-0\cdot5228$ and equation (7) gives $\beta^2 = -0\cdot1867$. Hence an approximation to a pair of roots is $-0\cdot5228 \pm 0\cdot432i$, and the corresponding quadratic factor is $z^2 + 1\cdot0456z + 0\cdot4600$. Bairstow's process now gives the more correct expression

$$z^2 + 1\cdot0458z + 0\cdot45815. \qquad (24)$$

By division the second factor of (23) is

$$z^2 + 2\cdot86456z + 19\cdot5472. \qquad (25)$$

The complete solution of (20) is accordingly

$$+0\cdot4552 \pm 0\cdot5928i,$$

$$-0\cdot5229 \pm 0\cdot4298i,$$

$$-1\cdot4323 \pm 4\cdot1828i.$$

5. *Singular Cases of the Test Function Method.*—Singular cases arise when two or more pairs of roots of the equation have the same mean value (*e.g.*, there are roots of the forms $\alpha \pm \beta_1$, $\alpha \pm \beta_2$). Such cases are not of much practical importance, but present some points of interest. The octic equation will be taken as an example.

Suppose, firstly, that merely two pairs of roots have the same mean value α.

Then obviously both of the roots y_1 and y_2 of the quadratic (19) must cause the expression

$$p_1y^3 + p_3y^2 + p_5y + p_7$$

to vanish. Each of these roots determines a value of β^2, so that four roots of the octic are found.

Next, suppose that three pairs of roots have the same mean value α. Since T_7'' vanishes for three distinct values of y, these must be the roots of

$$p_1y^3 + p_3y^2 + p_5y + p_7 = 0. \tag{26}$$

The three roots of (26), which are necessarily all real, determine the three relevant values of β^2.

Lastly, let all four pairs of roots have the same mean value. Then the cubic equation (26) has four distinct roots, and is thus an identity. Hence

$$p_1 = p_3 = p_5 = p_7 = 0, \tag{27}$$

and the four values of β^2 are the roots of the quartic

$$p_0y^4 + p_2y^3 + p_4y^2 + p_6y + p_8 = 0. \tag{28}$$

It will be seen that the singular cases present no difficulty when the test function T_7'' is adopted. On the other hand, the determinantal forms (15) and (16) of the test function become nugatory. Since in the singular cases more than one value of y corresponds to a certain value of α, it follows that the equation (17) must be indeterminate, and both of the determinants involved must vanish. Thus, all the determinants of the following matrix must vanish :—

$$\left\Vert \begin{matrix} p_1 & p_3 & p_5 & p_7 & 0 & 0 \\ p_0 & p_2 & p_4 & p_6 & p_8 & 0 \\ 0 & p_1 & p_3 & p_5 & p_7 & 0 \\ 0 & p_0 & p_2 & p_4 & p_6 & p_8 \\ 0 & 0 & p_1 & p_3 & p_5 & p_7 \end{matrix} \right\Vert \tag{29}$$

If

$$T_6 = \begin{vmatrix} p_1 & p_0 & 0 & 0 & 0 & 0 \\ p_3 & p_2 & p_1 & p_0 & 0 & 0 \\ p_5 & p_4 & p_3 & p_2 & p_1 & p_0 \\ p_7 & p_6 & p_5 & p_4 & p_3 & p_2 \\ 0 & p_8 & p_7 & p_6 & p_5 & p_4 \\ 0 & 0 & 0 & p_8 & p_7 & p_6 \end{vmatrix} \tag{30}$$

it follows, on expansion in the elements of the last column, that T_6 vanishes. Also

$$T_5 = \begin{vmatrix} p_1 & p_0 & 0 & 0 & 0 \\ p_3 & p_2 & p_1 & p_0 & 0 \\ p_5 & p_4 & p_3 & p_2 & p_1 \\ p_7 & p_6 & p_5 & p_4 & p_3 \\ 0 & p_8 & p_7 & p_6 & p_5 \end{vmatrix} \tag{31}$$

is one of the determinants of the matrix (29), and therefore vanishes. Thus, when the quantity α is once repeated

$$T_7 = T_6 = T_5 = 0. \tag{32}$$

The graph of T_7 on a base of μ would in such a case touch the axis of abscissæ, and fail to give a precise value for α; but the graph of T_5 would cut the axis and give the needed definition. More generally, in the case of an equation of degree n, if the same value of α is associated with s pairs of roots, the test function T_{n-2s+1} may be adopted. The corresponding values of β^2 are obtained from the roots of a partial eliminant of the equations (2) and (3) of degrees s in y.

Whenever a singular case arises the determination of the remaining non-singular roots is facilitated. For example, suppose that a sextic has roots with a repeated real part α. When the roots have been diminished by α, the equation is

$$p_0z^6 + p_1z^5 + p_2z^4 + p_3z^3 + p_4z^2 + p_5z + p_6 = 0, \tag{33}$$

which must be identical with

$$p_0(z^2 - y_1)(z^2 - y_2)(z^2 - x_3z - y_3) = 0. \tag{34}$$

On identification of the coefficients in (33) and (34) the following results are obtained :—

$$x_3 = -p_1/p_0, \tag{35}$$

$$y_3 = -p_1p_6/p_0p_5. \tag{36}$$

Thus all the roots are at once calculable.

PART II.—GRAPHICAL SOLUTION.

6. *General Description.*—In this method the coefficient of z and the constant term in a quadratic factor of the equation are determined directly as the co-ordinates of a point of intersection of a pair of plane curves.

Suppose that $(z^2 - \xi z - \eta)$ is a quadratic factor of the equation, and let z_1 and z_2 be the roots of the quadratic

$$z^2 - \xi z - \eta = 0. \tag{37}$$

Whenever z *has one of these values*

$$z^2 = \xi z + \eta \tag{38}$$

$$z^3 = \xi z^2 + \eta z = (\xi^2 + \eta) z + \xi\eta \tag{39}$$

$$z^4 = (\xi^2 + \eta) z^2 + \xi\eta z = (\xi^3 + 2\xi\eta) z + \eta(\xi^2 + \eta), \tag{40}$$

etc.

The formula for z^n is

$$z^n = \phi_{n-1} z + \eta\phi_{n-2}, \tag{41}$$

where ϕ_n is a function of ξ and η, which obviously satisfies the recurrence relation

$$\phi_n = \xi\phi_{n-1} + \eta\phi_{n-2}. \tag{42}$$

Inspection of the first few members of the series suggests the formula

$$\phi_n = \Sigma \frac{|\underline{n-r}}{|\underline{r}\,|\underline{n-2r}} \xi^{n-2r}\eta^r, \tag{43}$$

which can be established by induction. A formula equivalent to (43) is quoted by Bairstow* with a different application in view.

When the foregoing expressions for the powers of z are substituted in the original equation a result of the form

$$f_1(\xi, \eta) z + f_2(\xi, \eta) = 0 \tag{44}$$

is obtained, and this must be valid when z has either of the values z_1, z_2 since these are, by hypothesis, roots of the equation. Hence

$$f_1(\xi, \eta) = 0, \tag{45}$$

and

$$f_2(\xi, \eta) = 0. \tag{46}$$

If ξ and η be treated as co-ordinates in a plane, the equations (45) and (46) define a pair of curves whose *real* intersections determine the quadratic factors of the equation.

In practice it is convenient to use a pair of equations derived from (45) and (46) rather than these equations themselves. By a process of partial elimination* equations of any desired degree in ξ or in η can be obtained; in particular, explicit expressions for ξ in terms of η, and of η in terms of ξ, can always be found, but these latter forms are not always convenient. Quartic and sextic equations will now be considered in detail.

---

* L. Bairstow, Appendix to "Investigations Relating to the Stability of the Aeroplane," 'Reports and Memoranda No. 154 of the Advisory Committee for Aeronautics,' October, 1914. Bairstow attributes the formula to Encke.

(*a*) *The Quartic.*—Let the equation be

$$p_0 z^4 + p_1 z^3 + p_2 z^2 + p_3 z + p_4 = 0. \tag{47}$$

On substitution from (38)–(40) it appears that

$$f_1(\xi, \eta) \equiv p_0(\xi^3 + 2\xi\eta) + p_1(\xi^2 + \eta) + p_2\xi + p_3 = 0, \tag{48}$$

and

$$f_2(\xi, \eta) \equiv p_0\eta(\xi^2 + \eta) + p_1\xi\eta + p_2\eta + p_4 = 0. \tag{49}$$

Equation (48) can be written

$$\eta = -(p_0\xi^3 + p_1\xi^2 + p_2\xi + p_3)/(2p_0\xi + p_1). \tag{50}$$

Multiply (48) by η and (49) by ξ, and subtract; the resulting equation can be written

$$\xi = (p_1\eta^2 + p_3\eta)/(p_4 - p_0\eta^2). \tag{51}$$

The curves (50) and (51) can be plotted very readily. It may be noted that (50) has the asymptote $\xi = -p_1/2p_0$, and (51) the asymptotes $\eta = \pm (p_4/p_0)^{\frac{1}{2}}$.

(*b*) *The Sextic.*—The equation to be solved is

$$p_0 z^6 + p_1 z^5 + p_2 z^4 + p_3 z^3 + p_4 z^2 + p_5 z + p_6 = 0. \tag{52}$$

In this case

$$\begin{aligned} f_1(\xi, \eta) = {} & (3p_0\xi + p_1)\eta^2 + (4p_0\xi^3 + 3p_1\xi^2 + 2p_2\xi + p_3)\eta \\ & + (p_0\xi^5 + p_1\xi^4 + p_2\xi^3 + p_3\xi^2 + p_4\xi + p_5) = 0, \end{aligned} \tag{53}$$

$$\begin{aligned} f_2(\xi, \eta) = {} & p_0\eta^3 + (3p_0\xi^2 + 2p_1\xi + p_2)\eta \\ & + (p_0\xi^4 + p_1\xi^3 + p_2\xi^2 + p^3\xi + p_4)\eta + p_6 = 0. \end{aligned} \tag{54}$$

Equation (53) is a quadratic for η and the corresponding curve can accordingly be plotted without difficulty. Multiply (53) by $\xi\eta$ and (54) by $(\xi^2 + \eta)$ and subtract. The result is the following quadratic for ξ

$$(p_0\eta^3 + p_6)\xi^2 + (p_1\eta^3 - p_5\eta)\xi + (p_0\eta^4 + p_2\eta^3 + p_4\eta^2 + p_6\eta) = 0. \tag{55}$$

This equation may be adopted as the equation of the second of the intersecting curves in place of (54), but certain spurious intersections will be introduced. These, however, can immediately be recognised, since they will necessarily lie on the parabola $\xi^2 + \eta = 0$.

There is actually some advantage in the use of equations which are quadratic in one of the co-ordinates, for, since merely *real* intersections of the curves are sought, those ranges of the variables which lead to imaginary roots of the quadratics are immediately ruled out as irrelevant. Explicit formulæ for ξ and η can be obtained without difficulty, but they are complicated and considerably more laborious in use than the equations (53) and (55). The explicit formula for ξ may, however, be quoted. It is

---

* See Frazer and Duncan, *loc. cit.*, § 6.

$$\xi = \frac{(p_3 + \gamma\eta + 2p_5/\eta) - (p_1 - p_0\gamma/\beta)(\eta + \delta/\beta)}{\eta(\beta - 2p_0) + p_0\delta/\beta - p_2 + \gamma(p_1 - p_0\gamma/\beta)/\beta}, \tag{56}$$

where

$$\beta = p_0 + p_6/\eta^3 \tag{57}$$

$$\gamma = p_1 - p_5/\eta^2 \tag{58}$$

$$\delta = p_2 + p_4/\eta. \tag{59}$$

Formulæ equivalent to (51) and (56) are given by Bairstow for use in his version of the root-squaring method of solution (see Part III).

7. *Illustrative Application to a Particular Sextic.*—The graphical method

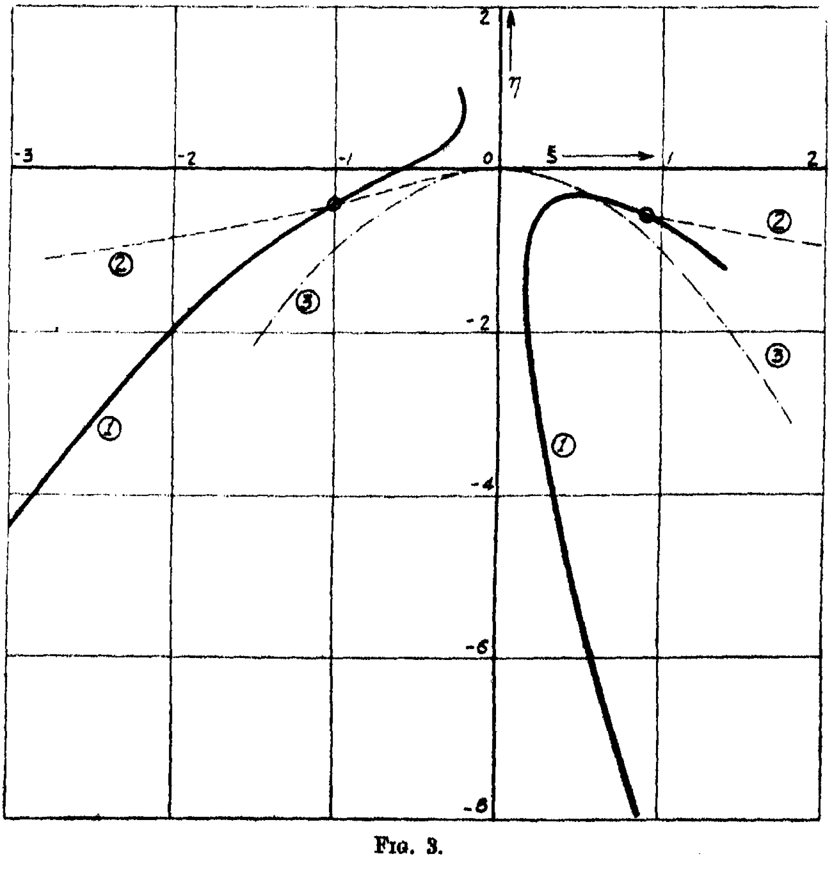

FIG. 3.

will be applied to the equation (20) which has already been solved by the test function method.

A preliminary plotting is given in fig. 3, where the curve No. 1 corresponds to (53) and curve No. 2 to (55). For completeness the parabola $\xi^2 + \eta = 0$ (curve No. 3) is also represented. It will be seen that of the three intersections of No. 1 and No. 2 which appear in the diagram, one lies on the parabola, and is, therefore, spurious. Large scale plottings in the neighbourhoods of the two genuine intersections indicated are given in figs. 4 and 5.

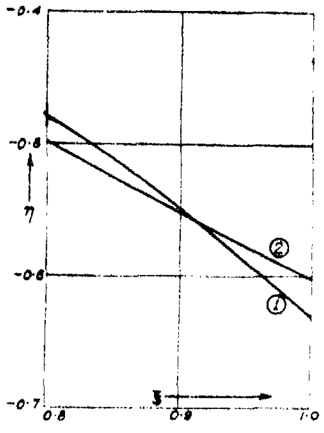

FIG. 4.

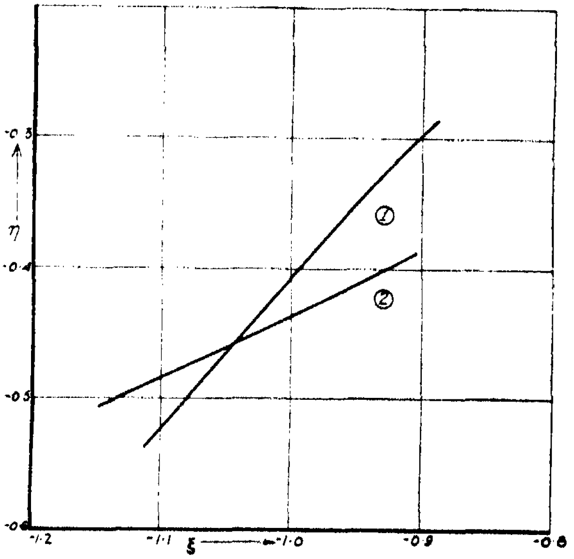

FIG. 5.

The following approximate quadratic factors are obtained

$$z^2 - 0\cdot910z + 0\cdot559,$$

$$z^2 + 1\cdot045z + 0\cdot458.$$

The approximations can be improved by the method of Part IV and the third factor obtained by division. Actually the above approximations are very close to the truth (*cp.* (21) and 24)).

PART III.—NOTE ON THE ROOT-SQUARING METHOD.

8. *Bairstow's Variant.*—The principal difficulty in the application of the root-squaring method in its earlier forms lies in the determination of the amplitudes of the complex roots. The scheme of Brodetsky and Smeal (*loc.*

cit.), based on the use of an infinitesimal transformation, successfully disposes of this defect, but it may be opportune here to refer to an alternative process due to Bairstow, which makes use of equations obtained incidentally in Part II of the present paper. In his method the moduli are determined in the ordinary way, and the corresponding amplitudes are then obtained without ambiguity by an application of formulæ (51), (56), or their appropriate generalisations.

PART IV.—SUCCESSIVE APPROXIMATION TO A QUADRATIC FACTOR.

9. *General Description.*—The following very useful method of improving the accuracy of a quadratic factor of an equation is due to Bairstow. In principle it is similar to Newton's method of obtaining a real linear factor by successive approximations.

Suppose that $(z^2 - \xi z - \eta)$ is known to be an approximate quadratic factor of the equation $f(z) = 0$. Divide $f(z)$ by $(z^2 - \xi z - \eta)$, and let the quotient be $Q_1(z)$ and the remainder $R_1 z + R_0$. Next divide $Q_1(z)$ by the same quadratic factor, and let the remainder be $R_3 z + R_2$. Then the corrections to be added to ξ and η are

$$\delta\xi = \begin{vmatrix} R_1, & R_3 \\ R_0, & R_2 \end{vmatrix} \Big/ \begin{vmatrix} R_3, & R_2 + \xi R_3 \\ R_2, & \eta R_3 \end{vmatrix} \tag{60}$$

$$\delta\eta = - \begin{vmatrix} R_1, & R_2 + \xi R_3 \\ R_0, & \eta R_3 \end{vmatrix} \Big/ \begin{vmatrix} R_3, & R_2 + \xi R_3 \\ R_2, & \eta R_3 \end{vmatrix} . \tag{61}$$

The process must be continued until the remainders R_1 and R_0 are sufficiently small. Once a near approximation has been attained, it will be found that R_2 and R_3 remain almost constant, and it becomes unnecessary to recalculate them at each step.

10. *Proof.*—The following proof of the method is a slight modification of that given by Bairstow in R. & M. 154.* Let $\alpha + \beta$ and $\alpha - \beta$ be approximations to a pair of roots of the equation. Then the corresponding approximate quadratic factor is $(z - \alpha)^2 - \beta^2$ and

$$f(z) = Q_1(z)\{(z-\alpha)^2 - \beta^2\} + R_1 z + R_0. \tag{62}$$

Substitution of the values $\alpha + \beta$ and $\alpha - \beta$ for z in (62) gives

$$f(\alpha + \beta) = R_1(\alpha + \beta) + R_0, \tag{63}$$

$$f(\alpha - \beta) = R_1(\alpha - \beta) + R_0. \tag{64}$$

---

* See footnote, p. 76.

Hence

$$2\beta R_1 = f(\alpha+\beta) - f(\alpha-\beta), \tag{65}$$

$$2R_0 = f(\alpha+\beta) + f(\alpha-\beta) - 2\alpha R_1. \tag{66}$$

Now, by the definition of R_2 and R_3:

$$Q_1(z) = Q_2(z)\{(z-\alpha)^2 - \beta^2\} + R_3 z + R_2. \tag{67}$$

Hence the equation (62) becomes

$$f(z) = Q_2(z)\{(z-\alpha)^2 - \beta^2\}^2 + (R_3 z + R_2)\{(z-\alpha)^2 - \beta^2\} + R_1 z + R_0. \tag{68}$$

Differentiate the last equation with respect to z, and then put $z = \alpha \pm \beta$. The resulting equations are

$$f'(\alpha+\beta) = 2\beta\{R_3(\alpha+\beta) + R_2\} + R_1, \tag{69}$$

$$f'(\alpha-\beta) = -2\beta\{R_3(\alpha-\beta) + R_2\} + R_1. \tag{70}$$

Suppose that the correct values of the pair of roots considered are $\alpha + \delta\alpha \pm (\beta + \delta\beta)$. Provided that $\delta\alpha$ and $\delta\beta$ are sufficiently small, and that the differential coefficients $\partial R_1/\partial\alpha$, etc., are not all zero, it will be legitimate to retain merely the linear terms in the Taylor expansions for R_1 and R_0. Hence

$$R_1 + \frac{\partial R_1}{\partial\alpha}\delta\alpha + \frac{\partial R_1}{\partial\beta}\delta\beta = 0, \tag{71}$$

and

$$R_0 + \frac{\partial R_0}{\partial\alpha}.\,\delta\alpha + \frac{\partial R_0}{\partial\beta}.\,\delta\beta = 0. \tag{72}$$

By equations (65), (66), (69) and (70) the differential coefficients $\partial R_1/\partial\alpha$, etc., can be expressed in terms of R_2 and R_3. Upon substitution, (71) and (72) become

$$R_1 + 2\delta\alpha(R_2 + \alpha R_3) + 2\beta\delta\beta R_3 = 0 \tag{73}$$

$$R_0 - 2\delta\alpha\{(\alpha^2 - \beta^2)R_3 + \alpha R_2\} + 2\beta\delta\beta R_2 = 0. \tag{74}$$

Now $\xi = 2\alpha$ and $\eta = \beta^2 - \alpha^2$, so that

$$2\delta\alpha = \delta\xi,$$

$$2\beta\delta\beta = \delta\eta + \tfrac{1}{2}\xi\delta\xi.$$

With these substitutions (73) and (74) become

$$(R_2 + \xi R_3)\delta\xi + R_3\delta\eta + R_1 = 0, \tag{75}$$

$$\eta R_3\delta\xi + R_2\delta\eta + R_0 = 0. \tag{76}$$

Solution of the last equations leads to the formulæ (60) and (61).

11. *Numerical Illustration.*—In the solution of the equation (20) by the test function method, the approximate quadratic factor $z^2 - 0{\cdot}9078z + 0{\cdot}5494$ was obtained.

It is found that

$$R_1 = 0{\cdot}240 \qquad R_0 = 0{\cdot}140$$

$$R_3 = 43{\cdot}16 \qquad R_2 = -5{\cdot}89.$$

Hence by (62) and (63)

$$\delta\xi = 0{\cdot}009,$$

$$\delta\eta = -0{\cdot}0125,$$

and the corrected quadratic factor is $z^2 - 0{\cdot}9168z + 0{\cdot}5619$.

On a repetition of the divisions,

$$R_1 = 0{\cdot}0747 \qquad R_0 = -0{\cdot}140$$

$$R_3 = 44{\cdot}89 \qquad R_2 = -6{\cdot}598.$$

Whence

$$\delta\xi = -0{\cdot}00644,$$

$$\delta\eta = 0{\cdot}00328.$$

The third approximation to the quadratic factor is accordingly $z^2 - 0{\cdot}91036z + 0{\cdot}55862$. On division of (20) by this expression, $R_1 = -0{\cdot}0001$ and $R_0 = -0{\cdot}0028$. This approximation was judged sufficient for the purpose in view.

12. *Conclusion.*—As regards the practical utility of the methods suggested in Parts I and II of the present paper, it may be remarked that both permit a determination of merely a single pair of roots quite independently of the remainder. This may be a distinct advantage, since in some physical problems the interest is confined to particular pairs of roots. Moreover the computer has frequently a rough knowledge of such roots at the commencement of the calculation. For example, in dynamical problems, the real part α of a complex root determines the damping of an oscillation of the system, and its order of magnitude will usually be obvious. Thus, in an application of the test function method, the range of values of μ for trial is not large. A further feature of the test function method is that it can be applied without difficulty to cases in which roots are approximately, or exactly, duplicated.

High Frequency Fatigue.

By C. F. Jenkin and G. D. Lehmann.

(Communicated by Sir Richard Glazebrook, F.R.S.—Received May 4, 1929.)

I.—Summary.

The object of these researches was to determine the effect of the frequency of alternation of stress on the fatigue limits of various metals. The work was carried out in the Engineering Laboratories, Oxford. Tests were made on rolled, normalised and hardened steel; rolled aluminium; annealed copper and normalised armco iron. The ordinary frequency employed in fatigue tests is 50 periods per second. Jenkin* in 1924 carried out tests up to 2000 periods per second and in the research described in this paper tests were made at frequencies up to 20,000 periods per second. In all the higher frequency tests the specimen consisted of a bar supported at the nodes, and vibrating freely. Jenkin used an electro-magnetic method to produce the vibrations, but this will not work for very high frequencies and a new method had to be invented. In the experiments now described fluctuations of air pressure acting directly on the specimen were used to make them vibrate and a number of methods were tried before a successful apparatus was evolved. The apparatus consists essentially of the two blowers used to vibrate the specimen. Each blower consisted of a small adjustable resonating chamber, into which air was admitted by a throttle valve in the back, while the front was closed by one face of the specimen. The position of the specimen was so arranged that as it vibrated to and fro it alternately released the air pressure or allowed it to mount up in the chamber.

The strains were calculated on the assumption that the bar vibrated freely and the only measurement necessary was the amplitude of vibration at the centre of the bar. Lord Rayleigh† has shown how the strains may be calculated for a long, thin vibrating bar. But using the method of vibrating by air, the bars had to have a moderate width and for the highest speeds they had to be short, so that Lord Rayleigh's theory was no longer sufficiently accurate. The experiments would have been impossible but for the assistance of Prof. Love, who explained how the known theory could be applied to bars of moderate width, such as could be used in our apparatus.

---

* 'Roy. Soc. Proc.,' A, vol. 109, p. 119 (1925).

† 'Sound.'

The results obtained were very interesting. In Jenkin's experiments the largest increase of the fatigue limit was only 15 per cent. but he pointed out that much larger rises were to be expected at higher frequencies. In the present tests increases of fatigue limit up to 60 per cent. have been recorded. It has also been found that the fatigue limit does not increase indefinitely with the frequency but reaches a maximum value, and in some tests was shown actually to fall at the highest frequencies. The greatest drop obtained beyond the maximum fatigue limit was about 9 per cent. of the maximum. This fall might have occurred for the other metals also, if they had been tested at still higher frequencies.

II.—INTRODUCTION.

This research on high frequency fatigue in rolled, normalised and hard steels, rolled aluminium, annealed copper and normalised armco iron was carried out in the Engineering Laboratories, Oxford. The cost of the apparatus was defrayed by a grant from the Engineering Research Board of the Department of Scientific and Industrial Research.

The necessity for some work in this field has been realised since 1911 when Hopkinson* published the results of some tests on mild steel carried out at about 116 periods per second. As these were not considered to be conclusive further work was done by Jenkin (*loc. cit.*) who, while showing that in Hopkinson's tests the effects of speed were exaggerated, confirmed his anticipation that the fatigue limit increased with the rate of alternation. Jenkin also showed that at higher speeds the effect was becoming considerable and that still more striking effects were to be expected if the speed of alternation could be further increased. He used an electrical method, with which he reached 2000 periods per second, but failed to obtain sufficient power to break specimens at higher frequencies.

The higher frequencies reached in the present paper were obtained by using fluctuations of air pressure acting directly on the test pieces. Preliminary investigations were made upon the possibility of adapting the accepted methods of sounding organ reeds, but in these little power is developed† as the small amplitudes required only develop stresses well below the elastic limit, whereas for materials stressed to the fatigue limit considerable power is required to overcome hysteresis.‡ Therefore trial experiments were made to find a method which would develop more power. For simplicity, cantilever bars were used in these preliminary tests instead of free-free bars, which are the most desirable form of test piece.*

---

* 'Roy. Soc. Proc.,' A, vol. 86, p. 131 (1911).

† Lehmann, 'Sound' (Pressure in Organ Pipes).

‡ Gough, 'Fatigue of Metals,' p. 129, etc.

III.—THE EVOLUTION OF THE APPARATUS.

The first apparatus designed was based on a suggestion by Prof. B. P. Haigh, viz., that the pressure variations in a convergent-divergent throat could be used as a source of power. The design of apparatus I is shown in fig. 1. The throat

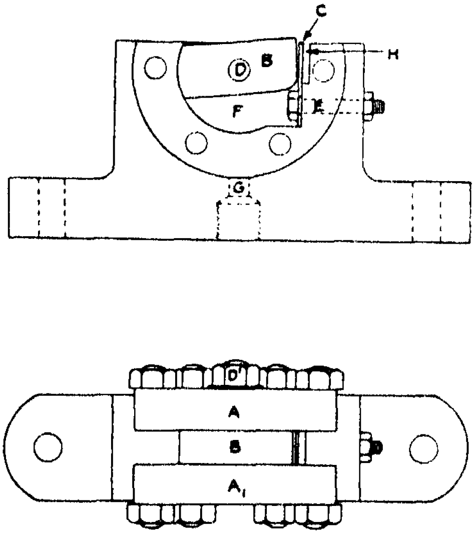

FIG. 1.

is formed by the two parallel semicircular plates A and A_1, the revolving plate B and the cantilever specimen C. The plate B could be turned about the axle D and fixed by the nut D′, thus adjusting the position of the throat along the length of the specimen. The width of the throat could also be altered by moving the plate B upon its axle D, the diameter of the hole in B being made slightly larger than the diameter of the rod. The specimen C was held in position by the bolt E. When the two cover plates A and A_1 were bolted in position a chamber F was formed at the base of the specimen. The high pressure air entered this chamber through the orifice G in the base of the apparatus. The reed was just free to vibrate between the two cover plates.

By adjusting the position and width of the throat, and the air pressure, the combination developing maximum power was found, which was again increased considerably by covering the small chamber H at the back of the specimen with a plate. The specimen then acted as a valve opening and closing this auxiliary chamber, into which air entered by leaking between the walls A, A_1, and the specimen. In this way an aluminium specimen was successfully broken in fatigue at approximately 5000 periods per second. But difficulties were experienced in starting the specimen vibrating, as the throat width had to be made so small that the specimen struck the opposite edge.

---

* Jenkin, *loc. cit.*

The design of the next apparatus (apparatus II) is shown in fig. 2. The air enters the chamber B (formed by the plate C, the cantilever specimen D and the two circular plates A and A_1) through the adjustable orifice E. The specimen D was adjusted so that when it vibrated it would act as a valve opening and

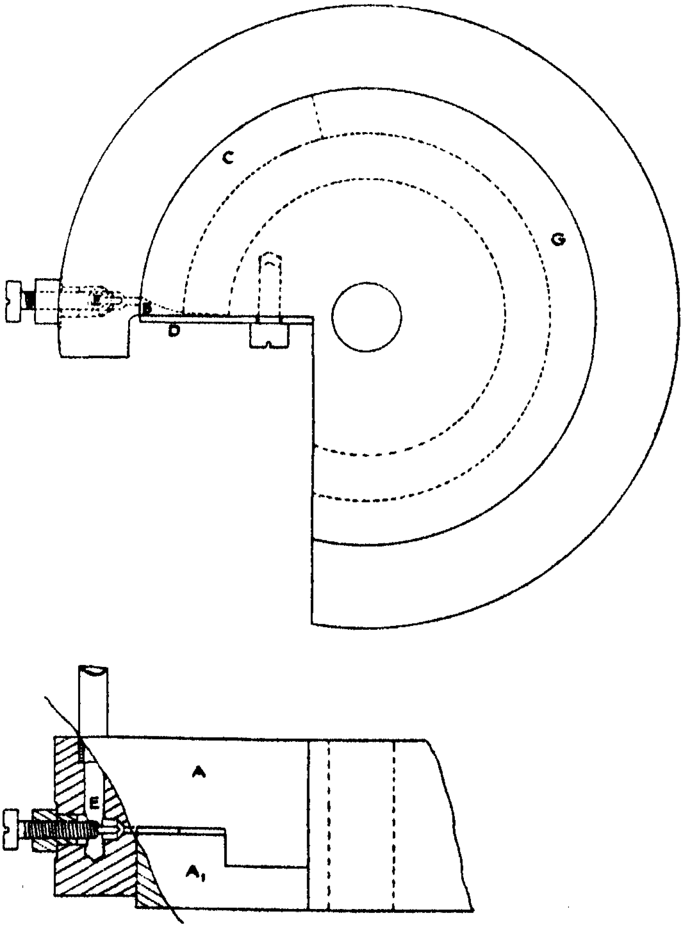

Fig. 2.

closing the chamber B. The position of the back of the chamber could be changed, by moving the sliding steel plate C in its groove G. A series of experiments were then made upon the orifice size and the volume of the chamber to obtain maximum power. From these sufficient data were collected from which to design the third apparatus in which the same method was applied to specimens supported as free-free bars. Using apparatus II some steel specimens were stressed to fracture at 5000 periods per second, but the stresses developed were unknown, as the specimens were of cantilever form and not of uniform cross section. One important disadvantage of this type of apparatus was that with the single blower used the stresses developed were not equalised upon the two faces of the specimen, as the deflection away from the blower was greater than that towards it. The specimen would therefore sometimes take a "permanent set" away from the chamber, and failing to function as a valve the vibrations would cease.

The original form of the next apparatus (apparatus III), which was designed

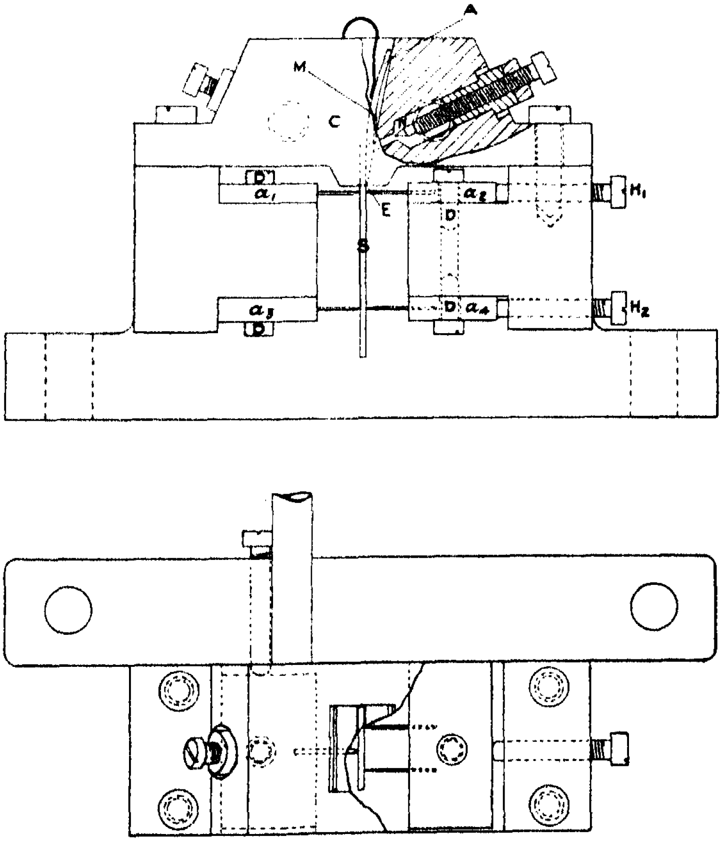

FIG. 3.

to equalise the stresses on the two faces of the specimens by using multiple blowers, is shown in fig. 3. (This was the first apparatus designed to stress free-free bars.)

The blowers were situated at the end of the specimen above the nodes. The front faces of the chambers were formed by the specimen S (fig. 3), the tops by a plate A and the back and sides by the machined gap in the nozzle block C. The cover plates were adjustable and were held in position by the small screws J (fig. 4). The slot K (fig. 4) allowed of a vertical motion, and the horizontal movement was obtained by adjusting the two fine screws L. The rubber lining M at the back of the cover plate took up the required motion without increasing the chamber area. The movement of the specimen was again

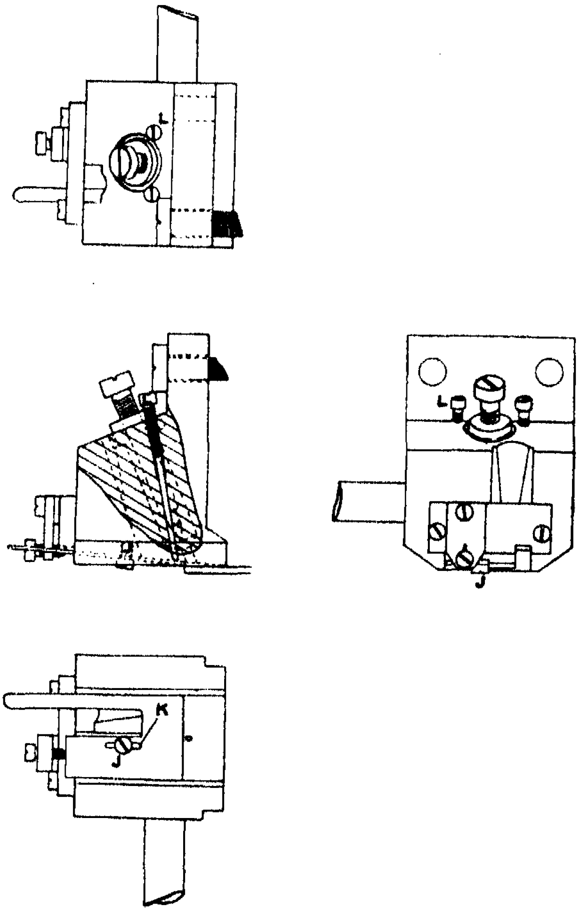

FIG. 4.

used to open and close the chamber, which was charged through the adjustable orifice N in the block C. As this must not touch the specimen, there was always a small air leak at E. But the motion at this point being very minute the gap could be made extremely small. Various devices for reducing this leak without damping the specimen were tried, the most successful being pads of vulcanised rubber.

Using this apparatus considerable power was developed with a single nozzle chamber. With two nozzles an increase of power was obtained, but the adjustment of the cover plates was very difficult, any small upward motion of the specimen due to one blower would cause the specimen to touch the cover plate of the other and the vibrations to cease.

A series of experiments were made upon the most efficient methods of supporting the specimen at the nodes. These are explained in detail in section IV. At this stage while experimenting with a jet of air delivered from a small orifice in the centre of a flat disc, it was noticed that when a plate was placed close to the disc a negative pressure was produced between the plate and the disc, while at points further away the effect was reversed. The positions depended upon and varied with the air pressure, the size of the disc and the orifice. There was therefore somewhere between the points a position of instability surrounded by zones of potential high and low pressure. A trial showed that a specimen placed in this position could be made to vibrate.

Apparatus IV (fig. 5) shows the form designed to produce vibration by this method. The specimen is shown in position between the two blowers B and B_1. The air entered along the tube C, and escaped between the faces of the specimen and the heads of the blowers. The positions of the blowers were adjusted by sliding in the block A.

This type of apparatus had the following manifest advantages over its predecessor :—

(*a*) Simplicity of design and manufacture.

(*b*) Simplicity of setting—no microscopic adjustments of cover plates.

(*c*) In the previous type, the power developed depended upon the specimen acting as a valve for the outlet of the air, so that a large amplitude or a very critical adjustment of the cover plate was necessary. But in this method a small movement of the specimen was sufficient to start vibrations. The blowers could therefore be placed at its centre (fig. 5), where, although the amplitude is only 60·6 per cent. of the amplitude at the free antinodes, there is more room.

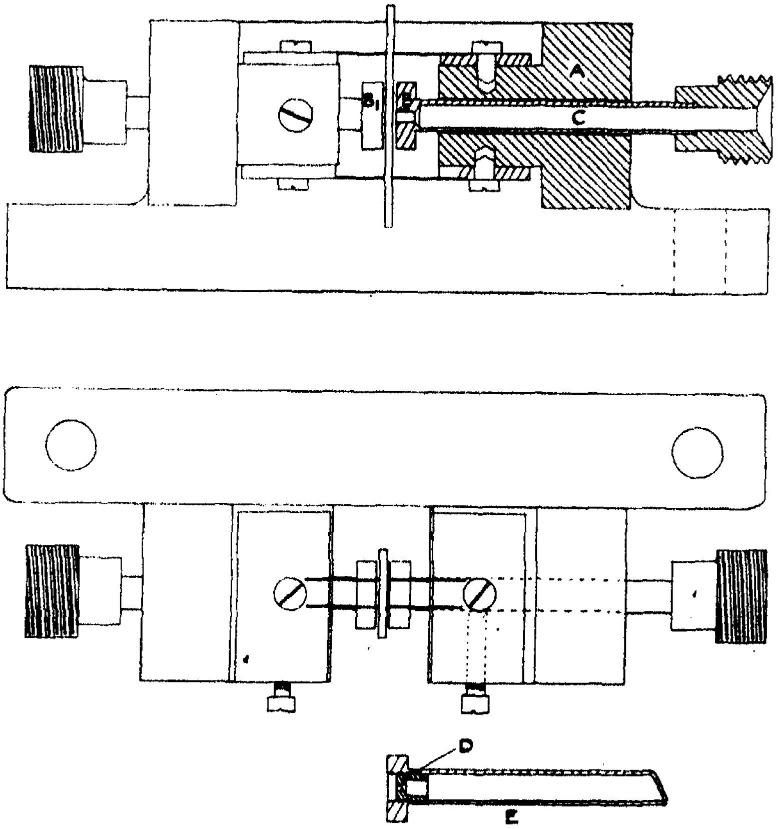

Fig. 5.

(*d*) Following from (*b*) a double blower could easily be used giving more power and an equalised maximum compression and tension upon the two faces of the specimen.

The blowers B and B_1 were now replaced by the type shown at E in fig. 5 in the heads of which a chamber was formed by the adjustable orifice holder D. The specimen was again made to act as a valve. By this means more power was developed and a series of experiments were carried out:—

(i) Varying the blower head diameter (B) from 0·253 inch to 0·5 inch.

(ii) Varying the orifice diameter in the orifice holder D from 0·5 mm. to 2·5 mm.

(iii) Varying the depth of the chamber from 0 to 0·5 inch.

(iv) Varying the diameter of D from 0·125 inch to 0·375 inch.

The amplitudes obtained were plotted against these variables, giving an extremely interesting series of curves. The graph (fig. 6) shows a typical example which seems to show that some resonance of the type developed by Hartmann and Trolle* in their air jet generator was present.

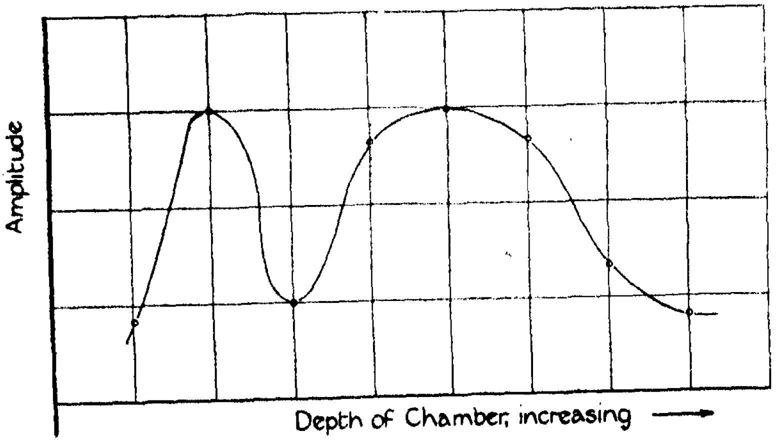

Fig. 6.

The next apparatus (apparatus V), designed from the knowledge obtained by these experiments, is shown in fig. 7. This contains all the essential parts of the final type of apparatus without any of the refinements which were made later. The specimen A is shown in position with one of the oscillatory chambers B. The distance of the face of chamber B from the specimen was regulated

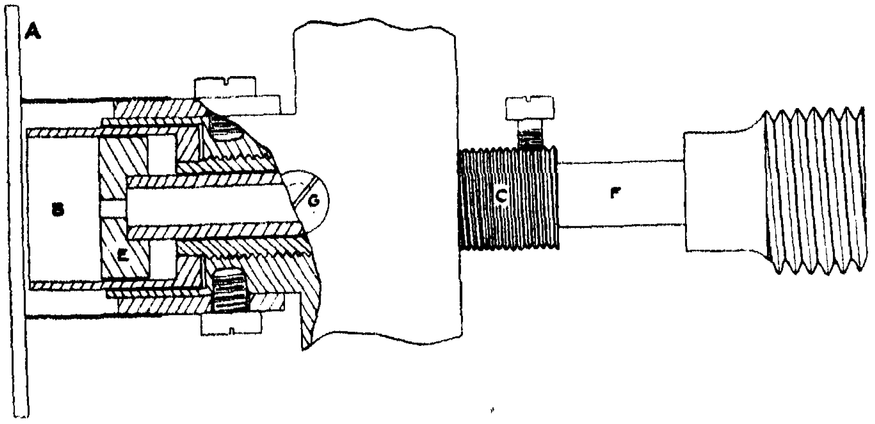

Fig. 7.

---

* "The Air Jet Generator," 'J. Sci. Inst.,' vol. 4 (1927).

by revolving the screw thread C, which was locked in any position by tightening G. The plunger E, which is a sliding fit in the oscillatory chamber B, contains a small orifice 1½ mm. diameter at its centre. This plunger could be adjusted horizontally by sliding the tube F in the screwed tube C. F is connected to the high pressure air supply by a flexible tube.

Fig. 8 (apparatus VI) shows the final form of the apparatus which is an improved type of apparatus V, designed to stress specimens of varying lengths and widths. The blowers were adjusted by moving the milled nut B, and locked in position by the milled nut C. The plungers could be moved in and out in the oscillatory chambers by rotating the milled head D.

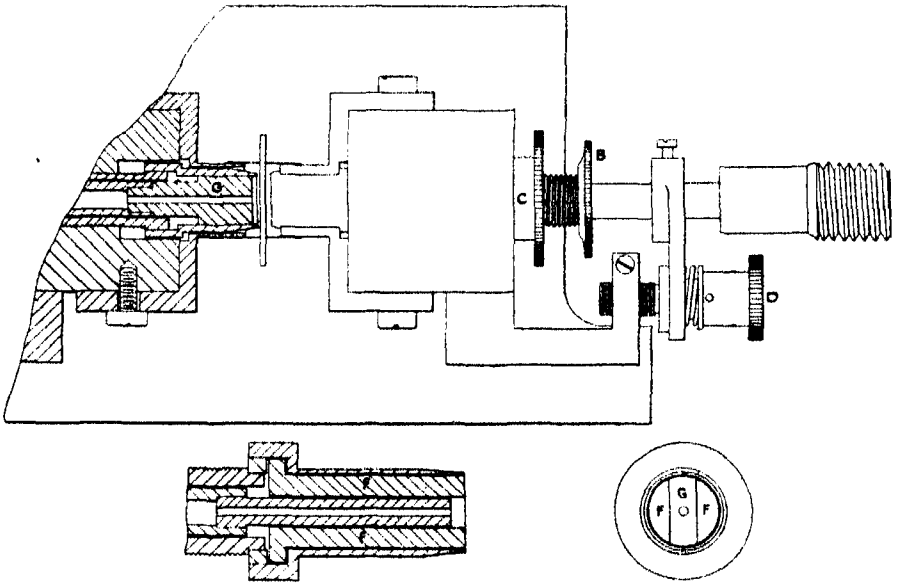

Fig. 8.

When the specimen is vibrating fluctuations of pressure occur in the small chamber, from which the air is periodically released by the specimen acting as a valve, and recharged through the orifice. The exact action is uncertain but it appears as if all that was necessary to develop power was an approximate adjustment between the volume of the chamber and the size of the orifice, fluctuations of pressure will then occur which are out of phase with the motion of the specimen. But in addition to the simple throttle action some form of resonance occurred similar to that described by Hartmann and Trolle (*loc. cit.*).

There is a limit to the frequency obtainable with this apparatus. To obtain appreciable power a certain minimum amplitude of vibration is necessary. With very short specimens, strain hysteresis begins and power must be supplied at amplitudes lower than this minimum. Under these conditions vibration cannot be started. The weaker the material the lower is the above frequency limit. This limit was reached for some of the material tested.

IV.—Supporting the Specimen.

Steel needles were used to support the first specimens of the free-free type. The preliminary design is shown in fig. 3, a_1, a_2, a_3 and a_4 are four plates fixed to the apparatus by the four set screws D and arranged so that the centres of each pair are the same vertical distance apart as the nodes of the specimen. The two plates a_1 and a_3 carry one needle each at their mid-points and the plates a_2 and a_4 two needles each, so placed that they are one-quarter of the breadth of the specimen from each of its sides (as shown in the plan view, fig. 3). The specimen had six small punch marks made at the nodes, two on one face and four on the other. The plate a_1 was fixed. The plates a_2 and a_4 were adjustable horizontally at right angles to the plane of the face of the specimen, while the plate a_3 was made adjustable horizontally on a plane at right angles to this. In this way the needles could be made to move up to the specimen and hold it in position by entering the punch marks on its faces. The pressure exerted was regulated by the two screws H_1 and H_2. This arrangement failed after the specimen had been vibrating for some time, the needle points either becoming blunted or else digging into the specimen. Figs. 9A and 9B show

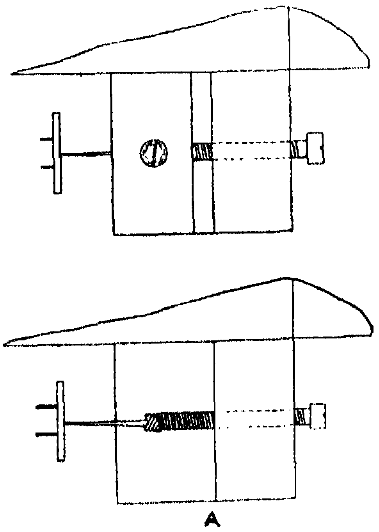

Fig. 9A.

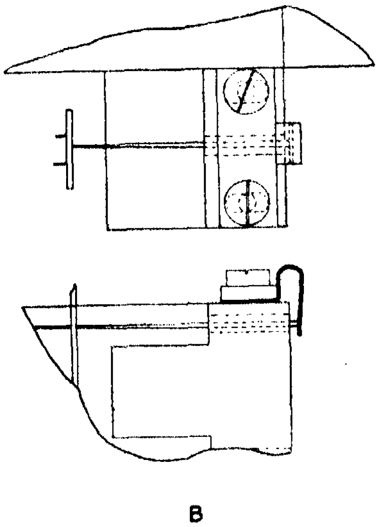

Fig. 9B.

the further modifications made to overcome this defect. The first modification is shown in fig. 9A where the needles are each held in position by a separate screw, with a hollow top made to fit the butt end of the needle which was ground hemispherical. In the next modification, fig. 9B, the circular butt of the needle was supported by springs. Each of these methods worked, but did not overcome the fault of the original apparatus, so modifications at the point of contact were considered next. In the first place the points of the needles were ground in the holes made on the specimen, until both were rounded and smooth (when viewed under a microscope), next the contacts were changed to annular rings by using spherically-ended needles in V-shaped holes, and finally the contact areas were reduced by grinding two parallel faces on each needle (fig. 10A). These methods were all improvements upon the original, but the needles were inclined to jamb in the holes. To overcome this a small hole was bored right through the specimen and a needle of larger diameter was placed as shown in fig. 10B. This was better but was still unsatisfactory, and finally needles were abandoned for the wire supports shown in fig. 10C. Wires of 10/1000 inch diameter were soldered into position through the specimen. In the earlier experiments three wires were used, two through one node and one through the other, but in the final form two wires were placed at each

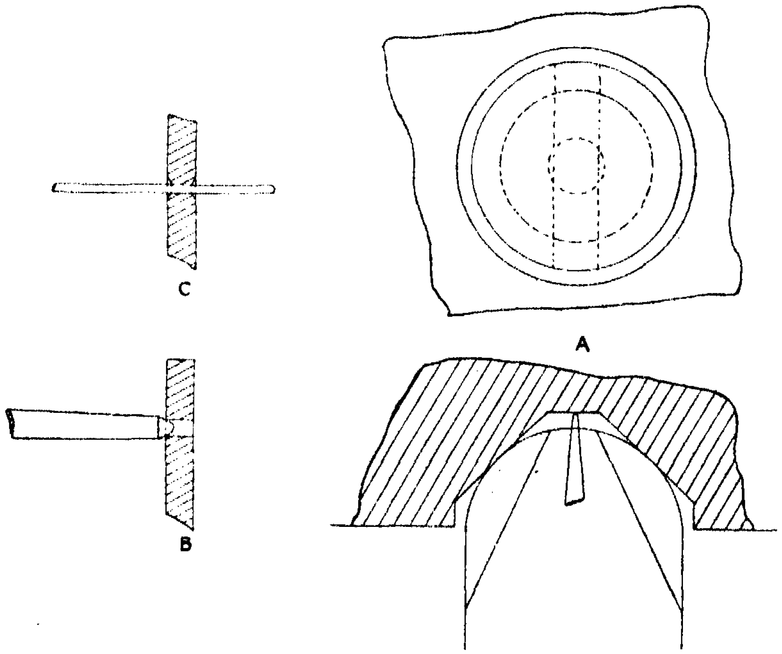

Fig. 10.

node arranged so that they were also at the nodes for anticlastic bending. With the aluminium and duraluminium specimens the wires could not be soldered. To fix them a copper wire of 0·0048 inch diameter was wound around the steel wire until a length 1·5 times the thickness of the specimen was covered. This was then completely covered with solder, forming a barrel-shaped bead of 0·02 inch diameter upon the supporting wire, which was then placed in a hole drilled in the specimen, so that the bead of solder protruded an equal distance upon each side of the specimen. The solder was then riveted over into the two countersinks, which had been made on each side of the hole drilled in the aluminium. This method answered very satisfactorily.

V.—The Air Supply.

The compressed air was supplied by a 7-h.p. air compressor driven by an electric motor. The output air from the compressor was circulated through a cooler and then taken to an air container. From here, after passing through a glass wool trap, it was taken through flexible tubing to the two blowers. The air-pressure was regulated by a throttle valve in conjunction with a pressure-gauge.

While some of the aforementioned apparatus was being made two other types were designed. In the first a jet of air was made to drive a disc while at the same time passing through the disc to impinge on a reed, thus causing it to vibrate. An automatic speed-regulator was arranged so that the frequency of the jet of air was kept the same as that of the reed, but out of phase with it. The second was made to work on the principle of the acoustic generator,* in which the vibrating reed was made to form the back of the pulsator chamber. Neither of these apparatus was made as the other types worked successfully, but some of the principles developed in them were incorporated in apparatus IV.

VI.—Calculation of Strains in a Vibrating Beam.

Rayleigh's theory for the stresses in a long thin beam is given in Jenkin's paper and need not be reproduced here. The final result may be written :—

$$R = u_1 a m^2 \, 8\cdot 49/6\cdot 49, \quad . \quad . \quad . \quad . \quad . \quad \text{Formula A}$$

where R = extreme fibre strain (at centre of beam) ; $2a$ = thickness of beam ; u_1 = amplitude of vibration at the centre of beam ; $\frac{1}{2}ml = 2\cdot 365$ radians ; l = whole length of beam.

---

* Hartmann and Birgit Trolle, *loc. cit.*

When the present research was begun this theory was applied to calculate the stresses in the relatively wide bars used in the apparatus which has been described, and a large number of tests were made on copper, duraluminium, steel and aluminium. Later it was realised that anticlastic bending would introduce serious errors. Their importance was therefore investigated and it seemed likely that this type of air machine would have to be given up, as it was improbable that bars could be made to vibrate of such a size that anticlastic curvature could be neglected. At this stage the authors asked the advice of Prof. Love: he explained that the known theory does not avail to obtain corrections for wide bars (plates) and how it may be applied to bars of moderate width. A small modification in apparatus VI enabled bars of these widths to be vibrated. The oscillatory chambers B (fig. 7) which were cylindrical for the wide specimens were now narrowed by the addition of the sliding blocks F (fig. 8), which were kept vertical by the rectangular plungers G carrying the orifices. A narrow chamber was thus formed which could be completely closed by the specimen.

The following note on the mathematical theory of vibration of a bar of moderate width was supplied by Prof. Love. The idea of the theory of transverse vibrations of a bar is that the bar may be divided in imagination into a large number of short lengths or "elements," each of which is strained, at any instant, in the same way as a bar, held bent by opposing couples, these couples being adjusted so that the curvature of the central line of the bar at the centre of the element is that which would be produced statically by the couples associated with the element. In other words: the curvature of the central line is known from the theory as given by Lord Rayleigh, and the strain in the element is the same as if the element were a bar bent to a uniform curvature equal to that of the central line at the centre of the element. The strain in a bar bent to a given uniform curvature is, of course, known.

According to this idea let u denote the displacement of a point of the central line, the axis of z in fig. 11A, in the direction of the axis of x. u is a certain function of z.

The displacement of any particle of the bar in the central plane of x and y is $u_0 + \frac{1}{2}k\sigma(x^2 - y^2) = u_1$, say, where u_0 is the value of u at the origin and k is the value of $\partial^2 u/\partial z^2$ at the origin. Also σ is the value of Poisson's ratio for the material (one-third or one-quarter for most solids).

Let the bar be of length l and let E be Young's modulus for the material. Let ρ be the density and $2a$ the thickness. The frequency of the gravest symmetrical mode of oscillation is $n/2\pi$ where $3n^2\rho/Ea^2 = m^4$, and m is the smallest root of the equation

$$\tanh \tfrac{1}{2}ml + \tan \tfrac{1}{2}ml = 0.$$

The value of ml/π is $1\cdot50562$ approximately.

The formula expressing u in terms of z and t is

$$u = \text{C}\,(\cosh \tfrac{1}{2}ml \cos mz + \cos \tfrac{1}{2}ml \cosh mz) \cos nt,$$

where C is an arbitrary constant, which must be small.

It follows that

$$u_1 = u_0\left\{1 - \tfrac{1}{2}\sigma\frac{\cosh \frac{1}{2}ml - \cos \frac{1}{2}ml}{\cosh \frac{1}{2}ml + \cos \frac{1}{2}ml} m^2 (x^2 - y^2)\right\}.$$

Now if $2b$ is the breadth of the bar, and u_1 is observed for $x = 0$, $y = b$, the formula giving u_0 is

$$u_0 = u_1\bigg/\left[1 + \tfrac{1}{2}\sigma\frac{\cosh \frac{1}{2}ml - \cos \frac{1}{2}ml}{\cosh \frac{1}{2}ml + \cos \frac{1}{2}ml} m^2b^2\right].$$

The greatest strain in the bar is

$$au_0m^2 (\cosh \tfrac{1}{2}ml - \cos \tfrac{1}{2}ml)/(\cosh \tfrac{1}{2}ml + \cos \tfrac{1}{2}ml) \quad . \ . \text{ Formula B}$$

It should be noted that u_1 is the amplitude measured at the side of the specimen and is due to direct and anticlastic bending.

VII.—MEASUREMENTS.

Measurements had to be made of (i) the amplitude—to calculate the strains, (ii) the frequency, and (iii) the time to fracture.

(*a*) *The Amplitude.*

To measure the amplitude the specimen was illuminated from the front and the length of line made by the vibration of a bright speck on the surface was measured. A bright light shining upon the flat edge of the specimen would show on the surface various very small spots of light, so small as to have no appreciable size even when seen under a magnification of 150 diameters. For some tests a minute bead of gold, as described in Jenkin's paper (*loc. cit.*), was used. When the specimen started to vibrate this spot formed a bright line of light whose length was easily measured accurately. Measurements were made with a microscope fitted with a Beck micrometer eyepiece—consisting of two hair lines, which could be adjusted to the two ends of the line of light, and the length read on a micrometer scale. Object glasses of different focal lengths were used according to the amplitude of the vibrations which were to be measured.

An experiment was made to see whether the specimen was vibrating equally about its zero position. For this four small arms were fitted to the face of the apparatus, to which very small springs were attached, joined diagonally by two pieces of 40 gauge copper wire. The two bottom arms could be rotated through about 20°. By this means the small V made by the intersection of the wires could be moved about the face of the specimen. The wires were made to touch each other and could be adjusted so that they nearly touched the face of the specimen. The spot of light reflected in the gold bead was then arranged so that it was at the intersection of the two wires and the specimen was started vibrating. When the spot of light was in focus the two wires were only just out of focus and the point of intersection could be plainly seen. The two hair lines were then placed at the ends of the line of light. From this it was found that the amplitudes on each side of the V were equal, and therefore the maximum positive and negative stresses on the two faces of the specimen were equal. The nodes of the specimen were also viewed during this test and it was seen that there was no lateral motion of the complete specimen.

(b) *Time.*

Time measurements were made by means of a stop clock started and stopped by hand.

(c) *Frequency.*

The size of the specimens to give the required frequencies were calculated and stroboscopic tests were made up to 10,000 periods per second as a check upon these figures. The direct and calculated results differed slightly showing that E increased with the frequency.* For making stroboscopic observations a telescope was fitted at the side of and at a small angle to the measuring microscope. A hole was cut in the supporting plate at the back of the apparatus, so that the top of the specimen could be illuminated from behind and viewed from the front. The illumination consisted of a 4-volt straight filament lamp A (fig. 11), shielded by a sheet of black paper in which a very fine vertical slit E had been cut. The lamp was mounted so that the vertical filament was directly behind the slit E, which was brought to a focus at C (at the side of the specimen S), by a lens. The image and the specimen, which was partly obscuring it, was then viewed through the telescope F. M was a small high-speed motor, fitted with a spindle geared to a counter and a brass disc D around a circumference of which 100 holes 0·01 inch diameter had been drilled. The source of illumination A was placed directly behind the disc. When the specimen was vibrating, but the disc stationary, the illumination viewed through a hole in D was seen as a band of light shaded on one side by the vibrating specimen. The disc was then started rotating and the speed adjusted until a nearly stationary black band replaced the shaded area in the slit of light. The frequency of the specimen was then the same as or some multiple of the number of holes passing the light per second.

---

* E was assumed constant in all stress calculations. Any increase in E would accentuate the slope of the curves.

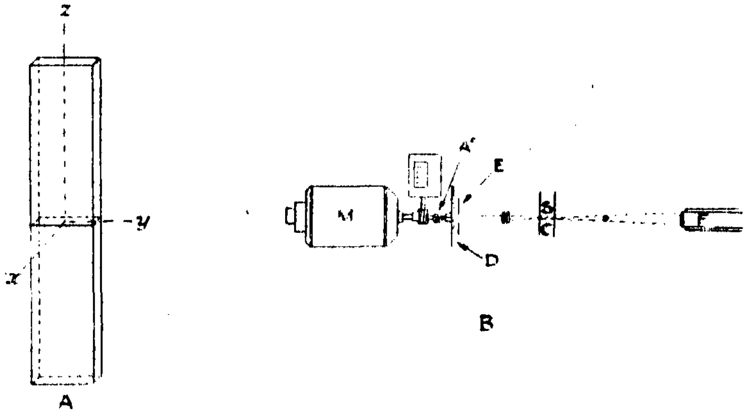

FIG. 11.

VIII.—MATERIALS TESTED.

The four materials tested were copper (annealed), 0·11 per cent. carbon steel (both in the rolled and normalised conditions), 0·89 per cent. carbon steel (hardened) aluminium (as rolled) and armco iron (normalised). These materials were selected because most of the researches of the Fatigue Sub-Committee of the Aeronautical Research Committee had been carried out on them, and also because they gave a good range of variations in crystalline structure.

(*a*) *Heat Treatment.*

Copper.—The copper strips were cut into lengths and carefully straightened by gentle blows with a wooden mallet and then annealed for half an hour at 600° C. in an electric furnace. The straight rods were put into one limb of a hard glass U-tube, the other limb of which was filled with scrap copper wire. Dried hydrogen was passed very slowly through the tube as it lay in the furnace, entering by the side filled with scrap copper. At the end of the period the tube was taken out of the furnace and allowed to cool. There were slight traces of oxidation in the first inch of the scrap wires but none on the test pieces.

Steels.—The 0·11 per cent. carbon steel was cut into lengths, straightened like the copper and then normalised by heating for half an hour at 880° C. and then cooling. The straight strips were put into a piece of iron gas pipe fitted with caps and packed with kieselguhr. The whole was heated in an electric furnace and then taken out and allowed to cool in the air. The strips when removed from the kieselguhr were silver grey.

The 0·86 per cent. carbon steel was required in a "hardened" condition. The strips were cut into the required lengths and the necessary holes for the wires were drilled. They were then strung together on a wire and put in a bath of a molten salt in the furnace. The furnace temperature was held at 800° C. for 15 minutes, after which the string of specimens were removed and quickly plunged into a bath of cold water. The salt prevented oxidation by forming a film around them, which cracked away immediately they were immersed in water. Care was taken that each specimen was well separated from the others, so that the cooling was rapid and equalised over the surfaces. After quenching the specimens were a dull grey. Subsequent examination showed that this treatment had not been satisfactory. A microphotograph showed that the carbon had not been fully dissolved before quenching. The tensile tests confirm this.

Armco Iron.—When the armco iron specimens were treated in the same way as the 0·11 per cent. carbon steel, a film of oxide was formed over the faces of the specimens. To prevent this they were packed in a thin layer of kieselguhr, then in a very fine copper gauze, after which they were placed in a tube and surrounded with kieselguhr. Care had to be taken that the strips did not actually touch the copper as when this happened they became copper plated. The tube was then heated to 950° C. for half an hour in the electric furnace, after which it was taken out of the furnace and allowed to cool. The specimens upon removal from the tube were found to be silver grey without any signs of oxidation.

(*b*) *Brinell Hardness Numbers.*

The microscopic brinell tests were made with balls of 2 and 1·2 mm. diameter and loads varying with the materials tested.

Hard steel, $P/D^2 = 30$.

Rolled steel, normalised steel, $P/D^2 = 10$.

Copper, aluminium, $P/D^2 = 5$.

Hardness Numbers.

	As rolled.	**After treatment.**
0·86 per cent. C steel	245	550
0·11 per cent. C steel	200	101
Armco iron	—	84·9
Copper	—	38·1
Aluminium	38·1	—

IX.—TESTING PROCEDURE.

For each recorded test a fresh specimen was put into the apparatus, the air turned on, and a small adjustment made until the desired amplitude viewed through the microscope was obtained. The amplitude was then kept steady by small further adjustments if necessary. The position of the oscillatory chambers and plungers were fixed before the air was turned on so that to regulate the amplitude only a small movement of either the oscillatory chambers (by rotating the milled nut B, fig. 8) or of the plungers G (by rotating the milled nut D, fig. 8) was needed.

At the lowest frequencies used, *i.e.*, 600 periods per second, the time for 10,000,000 periods was 4¾ hours approximately, while at the highest frequency, 20,000 periods per second, the time required was only 8 minutes 20 seconds. At the low speeds failure was gradual: the first sign being a decrease in the frequency and the amplitude, owing to the increase of the natural period of vibration of test piece with the formation of the crack. If more power was turned on and the amplitude increased the note became lower and lower until the specimen was completely broken in half. The specimen could therefore be stopped at any stage and the cracks could be viewed from the very initial stages of hair crack until the final stage of fracture. But with the very high speeds, no lowering of the note could be heard, and upon the formation of a very fine crack the specimen ceased to vibrate.

Using the final form of apparatus (fig. 8) the amplitude could be very easily regulated. This was done in five ways, by adjusting (i) the distance of the oscillatory chambers from the specimen, (ii) the distance of the plunger from the face of the oscillatory chamber, (iii) the pressure, (iv) the size of the oscillatory chambers, (v) the size of the orifice.

Adjustments (i), (ii) and (iii) could be done very simply during the test.

Upon moving the oscillatory chamber away from the specimen, after a certain position was reached the pressure reading remained constant and the vibrating specimen did not touch the walls of the chamber.* Further movement of the chamber away from the specimen gradually increased the amplitude to a maximum after which there was a small decrease and then suddenly the vibrations stopped. By increasing the pressure this maximum amplitude could be increased. All tests were carried out with the oscillatory chamber approximately at this position of maximum amplitude, only the final slight adjustment being made by a movement of the oscillatory chamber out of this position. Both sides of the apparatus were always moved in step. Very fine adjustments of the amplitude could be made by movements of the plungers. There was found to be with each material certain settings of the adjustments (i)–(iii) when the amplitude was unstable, *i.e.*, increasing rapidly when the unstable adjustment was reached. When, however, it was necessary to take readings at this amplitude the position of instability could be changed by altering adjustments (iv) or (v).

X.—TEMPERATURE.

Jenkin (*loc. cit.*) showed that specimens running at temperatures above normal were appreciably stronger than those tested at room temperatures. In the present paper it was assumed that the temperature of the test pieces was kept at 15° C. which was the temperature of the air blast blowing past them.

XI.—RESULTS.

The results are given in Tables I to VII. The strains were calculated from formula (B), p. 97. As fatigue limits are usually expressed in terms of stress, not strain (the stress being calculated from the strain on the assumption that the material is elastic), stress readings are placed beside the strain figures, calculated from an assumed value of E. It is probable that E increases with the frequency, but for all readings an average value of E (checked by stroboscopic readings at some frequencies) was used.

Figs. 12 to 17 show the variations of the fatigue limit with the frequency (plotted as periodic time).

The thickness and breadths of the specimens tested are given at the head of each table. For each material tests were made on the following lengths: 7·25 cm., 3·24 cm., 2·395 cm., 1·96 cm. and 1·695 cm.

---

* During recorded tests the specimen was not allowed to touch the walls of the oscillatory chambers while vibrating.

Normalised Steel, 0·11 per cent. carbon. (Fig. 12.)

$E = 30 \times 10^6$ lb./sq. in. $\sigma = 0{\cdot}286$.

Tensile strengths of strip as used :—

Maximum Load/Original Area = 22·5 tons/sq. in.

Breaking Load/Reduced Area = 32 tons/sq. in.

Brinell hardness number of strip as used, 101.

Specimen : Thickness, 0·109 cm. ; breadth, 0·3 cm.

Table I.

Specimen number.	No. of cycles.	Formula A.		Formula B.		Frequency.	Remarks.
		Strain.	Stress.	Strain.	Stress.		
	× 10⁶.	× 10⁻⁴.	tons/sq. in.	× 10⁻⁴.	tons/sq. in.		
NS. 37	4·8			9·34	12·84	1,100	Unbroken
NS. 39	1·14			12·96	17·81	1,100	Broken
NS. 38	8·74			10·89	14·99	1,100	Broken
NS. 40	11·82			10·70	14·72	1,100	Unbroken
Fatigue limit…………		10·92	15·03	10·89	14·99	1,100	
NS. 47	9·9			11·86	16·30	5,500	Unbroken
NS. 48	7·09			12·33	16·98	5,500	Broken
NS. 49	6·48			12·73	17·52	5,500	Broken
NS. 50	6·28			12·33	16·98	5,500	Broken
NS. 51	10·01			12·14	16·7	5,500	Broken
Fatigue limit…………		12·24	16·84	12·14	16·7	5,500	
NS. 30	0·60			15·38	21·18	10,000	Broken (3 wires)
NS. 31	0·63			15·38	21·18	10,000	Broken (4 wires)
NS. 32	10·35			12·86	17·69	10,000	Broken
NS. 33	3·61			14·29	19·65	10,000	Broken
NS. 34	5·50			13·22	18·20	10,000	Broken
NS. 35	15·00			12·69	17·43	10,000	Unbroken
NS. 36	6·40			13·04	17·92	10,000	Broken
Fatigue limit…………		13·04	17·93	12·86	17·69	10,000	
NS. 45	4·62			13·88	19·1	15,000	Broken
NS. 43	5·71			13·34	18·38	15,000	Broken
NS. 42	9·67			13·07	17·99	15,000	Broken
NS. 46…	13·7			12·82	17·63	15,000	Unbroken
Fatigue limit…………		13·42	18·49	13·07	17·99	15,000	

Fatigue limit at 50 periods per second = 14·2 tons/sq. in. approximately.

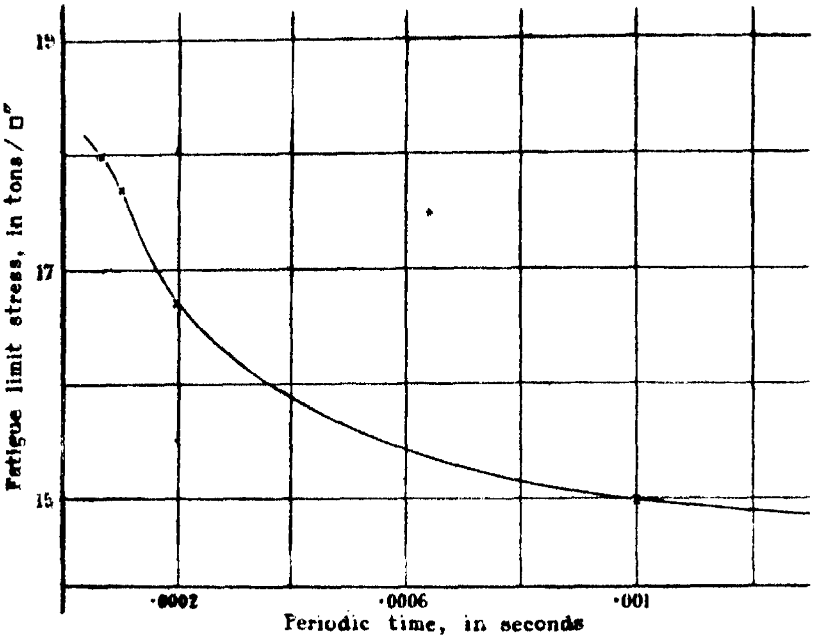

Fig. 12.

Early tests on wide specimens (see p. 96).

Normalised steel, 0·11 per cent. carbon (as in Table I).

Specimen thickness, 0·109 cm.; breadth, 1·27 cm.

Table II.—(Formula A.)

Specimen number.	No. of cycles.	Stress.	Frequency.	Remarks.
	$\times 10^6$	Tons/sq. in.		
NS. 10	4·53	16·4	1,100	Broken
NS. 12	5·75	16·12		Broken
NS. 18	8·45	15·85		Broken
Fatigue limit		15·85		
NS. 17	6·06	18·8	5,500	Broken
NS. 19	7·24	18·25		Broken
NS. 21	4·75	19·12		Broken
NS. 23	5·28	19·21		Broken
NS. 25	6·55	18·37		Broken
NS. 29	12·29	18·1		Unbroken
Fatigue limit		18·2		
NS. 4	15·09	19·7	10,000	Unbroken
NS. 5	21·10	18·39		Unbroken
NS. 8	10·15	23·05		Unbroken
NS. 7	6·64	23·15		Broken
NS. 9	5·17	23·95		Broken
Fatigue limit		23·05		

Rolled Steel, 0·11 per cent. Carbon. (Fig. 13.)
$E = 30 \times 10^6$ lb./sq. in. $\sigma = 0{\cdot}286$.

Tensile strength of strip as used :—

Ultimate strength, 43 tons/sq. in.

Brinell hardness number of strip as used, 200.

Specimen : Thickness, 0·109 cm. ; breadth, 0·3 cm.

Table III.

Specimen number.	No. of cycles.	Formula A.		Formula B.		Frequency.	Remarks.
		Strain.	Stress.	Strain.	Stress.		
	$\times 10^6$.	$\times 10^{-4}$.	tons/sq. in.	$\times 10^{-4}$.	tons/sq. in.		
R. 31	6·94			17·28	23·74	1,100	
R. 32	8·52			16·84	23·15	1,100	Broken
Fatigue limit..............		16·87	23·19	16·84	23·15	1,100	
R. 37	4·16			17·91	24·65	5,500	Broken
R. 38	10·50			17·45	24·00	5,500	Broken
R. 39	10·56			17·38	23·88	5,500	Unbroken
Fatigue limit..............		17·57	24·18	17·45	24·00	5,500	
R. 43	0·61			23·58	39·25	10,000	Broken
R. 44	7·99			18·41	25·35	10,000	Broken
R. 45	7·55			18·08	24·85	10,000	Broken
R. 46	11·10			17·79	24·60	10,000	Broken
R. 47	12·00			17·79	24·60	10,000	Unbroken
Fatigue limit..............		18·19	25·00	17·79	24·60	10,000	
R. 49	0·45			24·17	33·2	15,000	Broken
R. 50	2·18			20·94	28·8	15,000	Broken
R. 51	5·40			19·30	26·58	15,000	Broken
R. 52	9·45			18·41	25·34	15,000	Broken
R. 53	18·35			18·29	25·15	15,000	Unbroken
Fatigue limit..............		19·59	26·95	18·38	25·25	15,000	

Fatigue limit at 50 periods per second = 22·7 tons/sq. in. approximately.

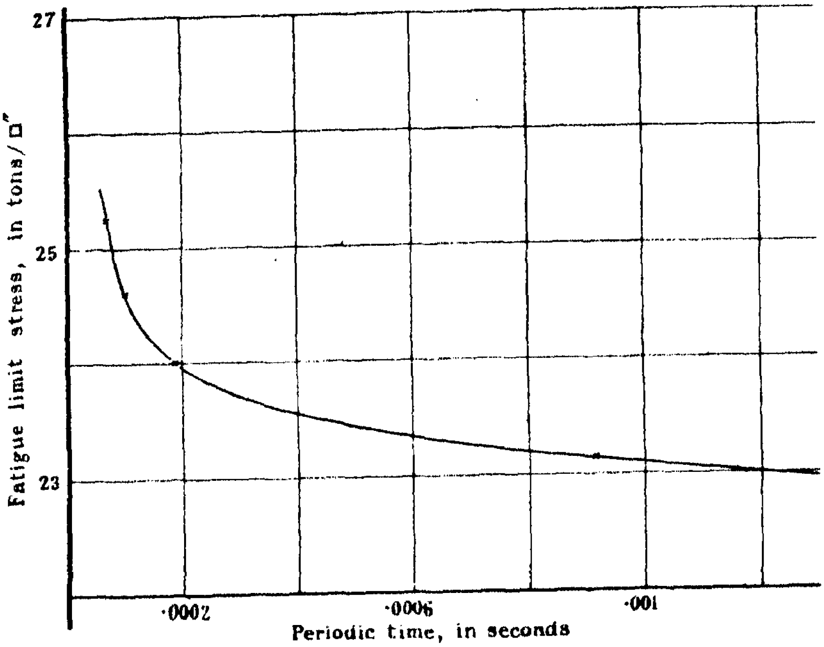
27
25
23
Fatigue limit stress, in tons/□″
·0002
·0006
·001
Periodic time, in seconds

FIG. 13.

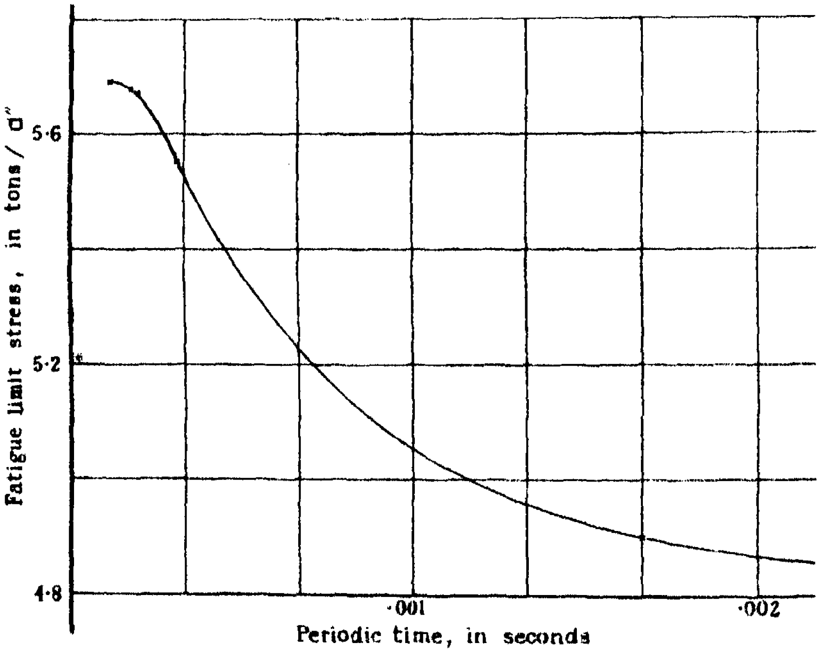
5·6
5·2
4·8
Fatigue limit stress, in tons/□″
·001
·002
Periodic time, in seconds

FIG. 14.

Annealed Copper. (Fig. 14.)

$E = 16{\cdot}4 \times 10^6$ lb./sq. in.[*] $\sigma = 0{\cdot}33$.[†]

Tensile strength of strip as used :—

Ultimate strength 14·78 tons/sq. in.

Brinell hardness number of strip as used, 38·1.

Specimen : Thickness, 0·0876 cm. ; breadth, 0·3 cm.

Table IV.

Specimen number.	No. of cycles.	Formula A.		Formula B.		Frequency.	Remarks.
		Strain.	Stress.	Strain.	Stress.		
	$\times 10^6$.	$\times 10^{-4}$.	tons/sq. in.	$\times 10^{-4}$.	tons/sq. in.		
C. 32	0·78			8·95	6·54	660	Broken
C. 33	1·66			7·82	5·72		Broken
C. 34	4·67			6·84	5·0		Broken
C. 35	11·68			6·48	4·74		Unbroken
Fatigue limit...............		6·70	4·91	6·69	4·90	660	
C. 41	0·45			8·64	6·32	3,200	Broken
C. 42	3·01			8·06	5·9	3,200	Broken
C. 43	4·73			7·66	5·61	3,200	Broken
C. 44	10·2			7·52	5·50	3,200	Unbroken
Fatigue limit.....		7·66	5·61	7·59	5·55	3,200	Broken
C. 47	1·2			10·99	8·04	5,900	Broken
C. 48	1·09			11·72	8·58	5,900	Broken
C. 50	5·98			8·04	5·88	5,900	Broken
C. 51	4·6			8·04	5·88	5,900	Broken
C. 52	5·9			7·87	5·76	5,900	Broken
C. 53	12·5			7·74	5·66	5,900	Unbroken
Fatigue limit............ ...		7·93	5·80	7·76	5·68	5,900	
C. 57	3·93			8·44	6·18	8,800	Broken
C. 58	11·19			7·55	5·68	8,800	Unbroken
C. 59	6·67			7·93	5·8	8,800	Broken
C. 60	10·0			7·77	5·69	8,800	Broken
Fatigue limit...............		8·04	5·88	7·77	5·69	8,800	

Fatigue limit at 50 periods per second = 4·79 tons/sq. in.

The fatigue limit strengths obtained in these tests are slightly lower than those obtained by Jenkin for the same frequency. This may be due to the circumstances that the copper was heat treated in a slightly different way; and while, for the test published in this paper, the temperature was 15° C., for those of Jenkin the temperature was slightly higher.

---

[*] Jenkin.

[†] Kaye and Laby.

Rolled Aluminium. (Fig. 15.)

$E = 9\cdot6 \times 10^6$ lb./sq. in.* $\sigma = 0\cdot36$.\*

Tensile strength of strip as used :—

Ultimate strength 6·4 tons/sq. in.

Brinell hardness number of strip as used, 38·1.

Specimen : Thickness, 0·102 cm. ; breadth, 0·3 cm.

Table V.

Specimen number.	No. of cycles.	Formula A.		Formula B.		Frequency.	Remarks.
		Strain.	Stress.	Strain.	Stress.		
	$\times 10^6$.	$\times 10^{-4}$.	tons/sq. in.	$\times 10^{-4}$.	tons/sq. in.		
AR. 36	10·0	9·70	4·11	9·68	4·1	900	Unbroken
AR. 37	4·51			10·88	4·61	5,000	Broken
AR. 38	9·22			10·69	4·53	5,000	Broken
AR. 39	10·0			10·60	4·49	5,000	Unbroken
Fatigue limit		10·80	4·58	10·69	4·53	5,000	
AR. 51	1·44			13·6	5·76	9,200	Broken
AR. 53	11·04			10·88	4·61	9,200	Unbroken
AR. 54	2·83			12·39	5·25	9,200	Broken
AR. 57	3·11			11·52	4·88	9,200	Broken
AR. 58	11·19			11·19	4·74	9,200	Broken
Fatigue limit		11·48	4·86	11·19	4·74	9,200	
AR. 45	1·69			16·45	6·92	14.100	Broken
AR. 46	3·58			13·00	5·51	14,100	Broken
AR. 47	2·47			14·04	5·95	14,100	Broken
AR. 48	2·54			13·55	5·74	14,100	Broken
AR. 50	5·30			11·99	5·08	14,100	Broken
AR. 52	10·0			11·49	4·86	14,100	Unbroken
Fatigue limit		12·13	5·14	11·74	4·97	14,100	
AR. 60	2·2			13·21	5·60	18,400	Broken
AR. 61	3·31			12·88	5·45	18,400	Broken
AR. 63	15·43			11·51	4·88	18,400	Unbroken
AR. 64	7·35			11·85	5·02	18,400	Broken
Fatigue limit		12·31	5·22	11·85	5·02	18,400	

Fatigue limit at 50 periods per second = 3·75 tons/sq. in. approximately.

---

* 'Aluminium, Facts and Figures.'

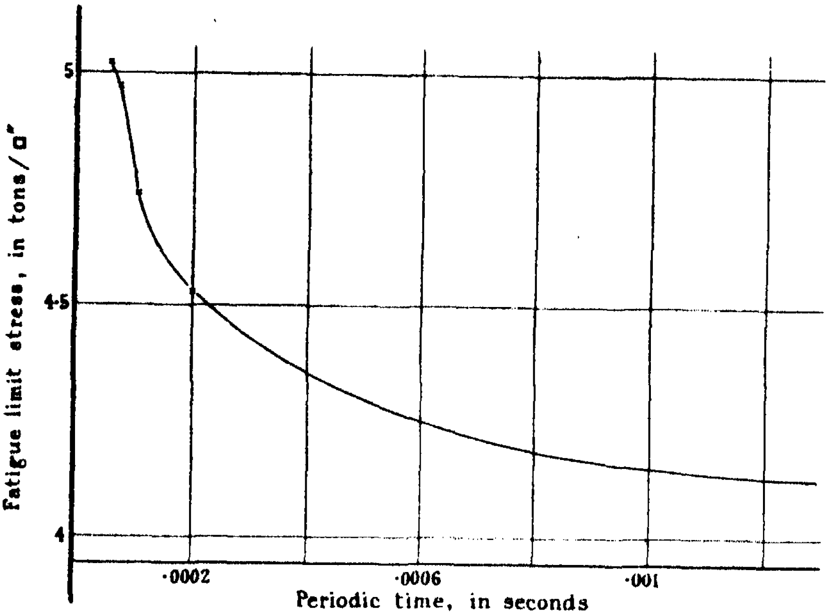
Fatigue limit stress, in tons/□"
5
4·5
4
·0002
·0006
·001
Periodic time, in seconds

Fig. 15.

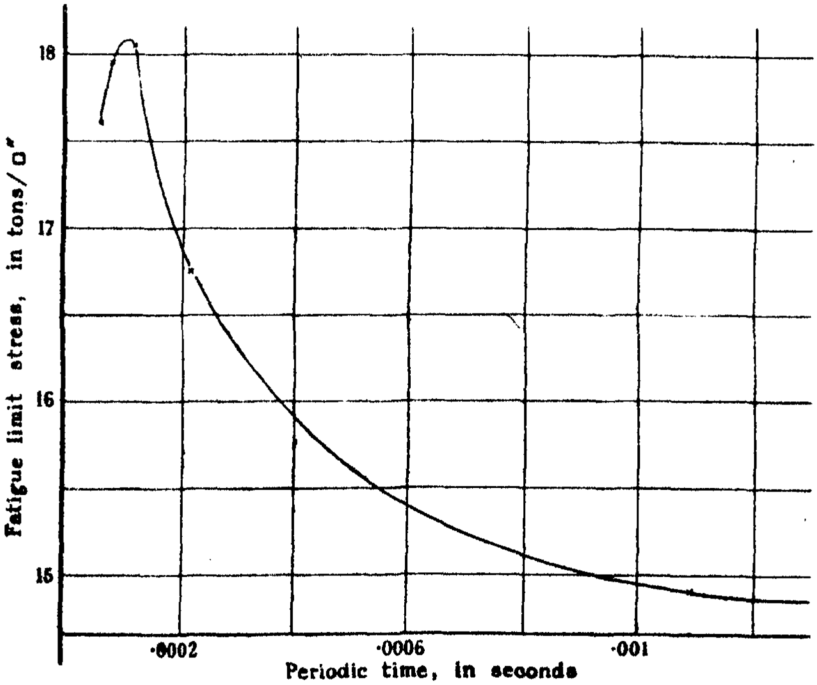
Fatigue limit stress, in tons/□"
18
17
16
15
·0002
·0006
·001
Periodic time, in seconds

Fig. 16.

Normalised Armco Iron. (Fig. 16.)

$E = 29{\cdot}85 \times 10^6$ lb./sq. in.[*] $\sigma = 0{\cdot}285$.[†]

Tensile strength of strip used :—

Ultimate strength 20·05 tons/sq. in.

Brinell hardness number of strip as used, 84·9.

Specimen : Thickness, 0·091 cm. ; breadth, 0·3 cm.

Table VI.

Specimen number.	No. of cycles.	Formula A.		Formula B.		Frequency.	Remarks.
		Strain.	Stress.	Strain.	Stress.		
	$\times 10^6$.	$\times 10^{-4}$.	tons/sq. in.	$\times 10^{-4}$.	tons/sq. in.		
A. 2	1·4			12·24	16·3	920	Broken
A. 3	3·71			11·49	15·30	920	Broken
A. 4	6·06			10·23	14·95	920	Broken
Fatigue limit		11·22	14·97	11·2	14·93	920	
A. 8	3·52			13·34	17·78	4,600	Broken
A. 9	3·89			12·99	17·31	4,600	Broken
A. 10	6·02			12·58	16·75	4,600	Broken
A. 11	9·8			12·58	16·75	4,600	Broken
Fatigue limit		12·64	16·86	12·58	16·75	4,600	
A. 13	3·15			15·09	20·1	8,400	Broken
A. 14	3·00			15·09	20·01	8,400	Broken
A. 15	5·33			14·11	18·82	8,400	Broken
A. 16	6·24			13·82	18·43	8,400	Broken
A. 17	8·72			13·55	18·05	8,400	Broken
Fatigue limit		13·78	18·35	13·55	18·05	8,400	
A. 19	1·86			15·59	20·75	12,400	Broken
A. 20	3·68			14·40	19·2	12,400	Broken
A. 21	5·41			13·93	18·59	12,400	Broken
A. 22	7·95			13·47	17·95	12,400	Broken
A. 23	7·75			13·47	17·95	12,400	Broken
A. 24	14·90			13·24	17·65	12,400	Unbroken
Fatigue limit		13·81	18·4	13·47	17·95	12,400	
A. 25	1·49			15·29	20·35	16,500	Broken
A. 26	5·01			13·95	18·6	16,500	Broken
A. 27	6·24			13·51	18·01	16,500	Broken
A. 28	11·62			13·20	17·6	16,500	Broken
A. 29	14·13			12·92	17·22	16,500	Unbroken
Fatigue limit		13·61	18·18	13·20	17·6	16,500	

Fatigue limit at 50 periods per second = 13·75 tons/sq. in. approximately.

---

[*] ‘Dep. Sci. Ind. Res., Eng. Res., No. 1, Special Report.’

[†] Aeronaut. Res. Com. Elasticity and Fatigue Sub-Committee, EF. 178, “Variation of Poisson's Ratio.”

Hard 0·86 *per cent. C steel.* (Fig. 17.)

$E = 30 \times 10^{6}$ lb./sq. in. $\sigma = 0{\cdot}286$.

Tensile strength of strip as used* :—

Ultimate strength 50 tons/sq. in.

Brinell hardness number of strip as used = 550.

Specimen : Thickness, 0·099 cm. ; breadth, 0·3 cm.

Table VII.

Specimen number.	No. of cycles.	Formula A.		Formula B.		Frequency.	Remarks.
		Strain.	Stress.	Strain.	Stress.		
	$\times 10^{6}$.	$\times 10^{-4}$.	tons/sq. in.	$\times 10^{-4}$.	tons/sq. in.		
HS. 21	11·01			19·94	27·42	5,000	Unbroken
HS. 19	1·7			23·10	31·8	5,000	Broken
HS. 20	2·52			21·64	29·8	5,000	Broken
HS. 24	6·6			20·63	28·42	5,000	Broken
HS. 23	4·5			20·78	28·59	5,000	Broken
Fatigue limit		20·52	28·23	20·46	28·19	5,000	
HS. 13	1·41			25·94	35·66	9,200	Broken
HS. 14	11·0			23·44	32·25	9,200	Unbroken
HS. 17	4·2			24·20	33·3	9,200	Broken
HS. 15	5·76			23·61	32·5	9,200	Broken
Fatigue limit		23·88	32·86	23·48	32·3	9,200	
HS. 12	4·03			24·16	33·2	13,600	Broken
HS. 11	18·37			22·90	31·5	13,600	Unbroken
HS. 10	10·92			23·18	31·85	13,600	Broken
HS. 9	9·4			23·27	32·0	13,600	Broken
Fatigue limit		23·75	32·68	23·18	31·85	13,600	
HS. 2	1·46			36·03	49·6	18,200	Broken
HS. 4	1·82			25·44	35·0	18,200	Broken
HS. 5	4·5			22·68	31·2	18,200	Broken
HS. 6	6·28			21·65	29·8	18,200	Broken
HS. 7	13·1			21·07	29·0	18,200	Unbroken
Fatigue limit		22·05	30·35	21·38	29·4	18,200	

Fatigue limit at 50 periods per second = 20 tons/sq. in. approximately.

---

* The heat treatment was unsatisfactory (see p. 100).

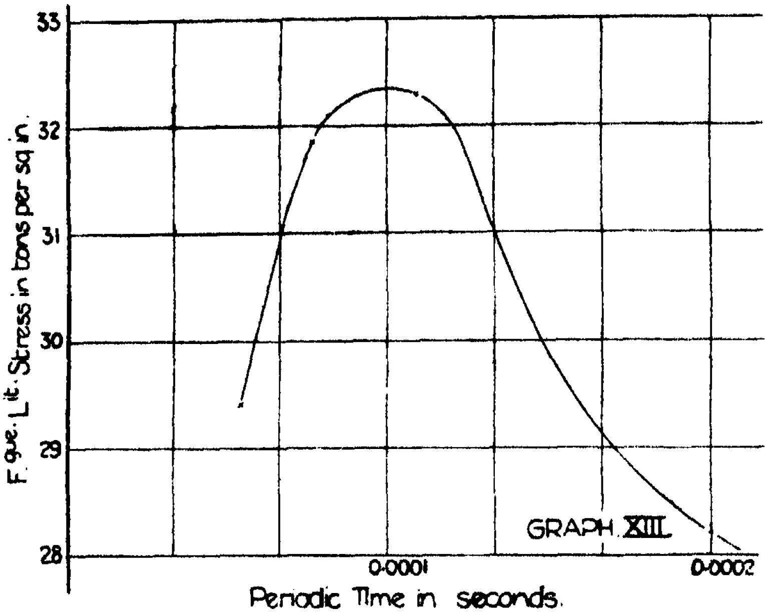

Fig. 17.

The following table summarises the results :—

Material.	Critical frequency.*	Maximum fatigue limit.	Ratio Maximum F.L. to Ultimate Tensile stress.	Ratio F.L. at 50 ∼ to Ultimate Tensile stress.	Maximum increase above F.L. at 50 ∼ .
	Approx.	tons/sq. in.			per cent.
Normalised 0·11 per cent. C. steel	20,000	>17·99	>0·799	0·631	>26·7
Rolled 0·11 per cent. C. steel	>20,000	>25·25	>0·588	0·528	>11·5
Annealed copper	10,000	5·59	0·385	0·324	18·8
Rolled aluminium	20,000	5·02	0·785	0·586	33·9
Normalised armco iron	10,000	18·1	0·903	0·685	31·6
Hardened 0·86 per cent. C. steel	10,000	32·4	0·658	0·400	62

* The critical frequency is the frequency at which the F.L. was the maximum.

Figs. 18 to 23 show the comparisons between fatigue limit stress calculated from formulæ (A) and (B). The stresses calculated from (A) which neglects anticlastic bending, increase more rapidly with the frequency than those calculated from (B). The differences below 1000 periods per second are very small. The frequencies are plotted as periodic time on a logarithmic scale.

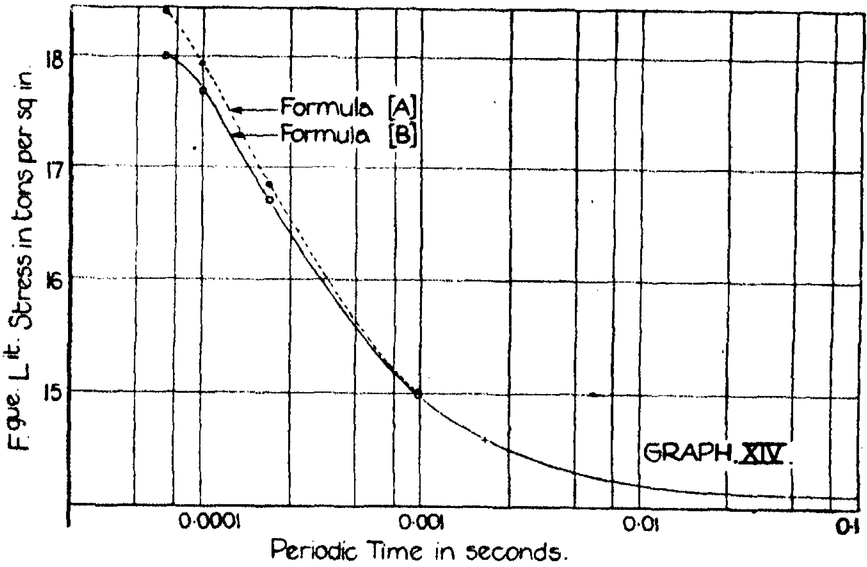

FIG. 18.—Normalised 0·11 per cent. C steel.

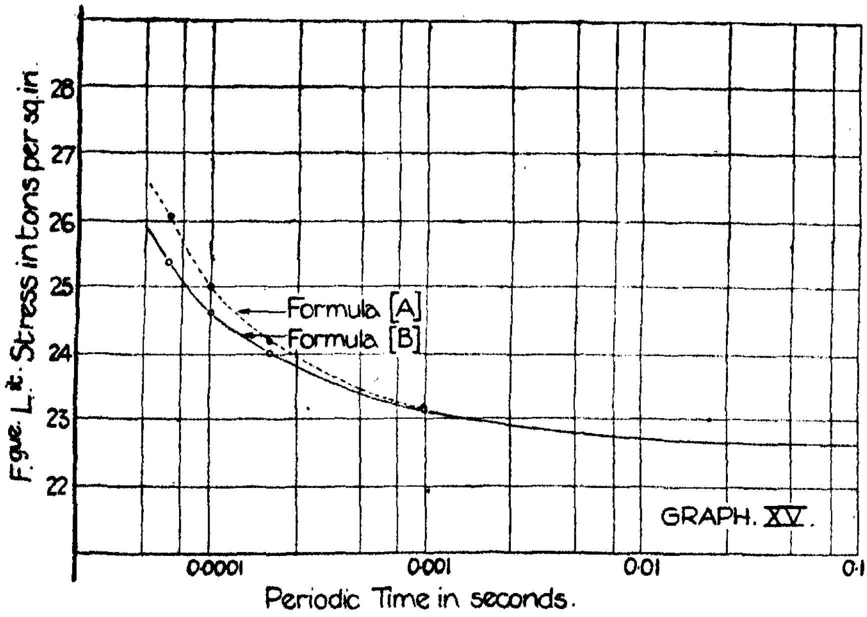

FIG. 19.—Rolled 0·11 per cent. C steel.

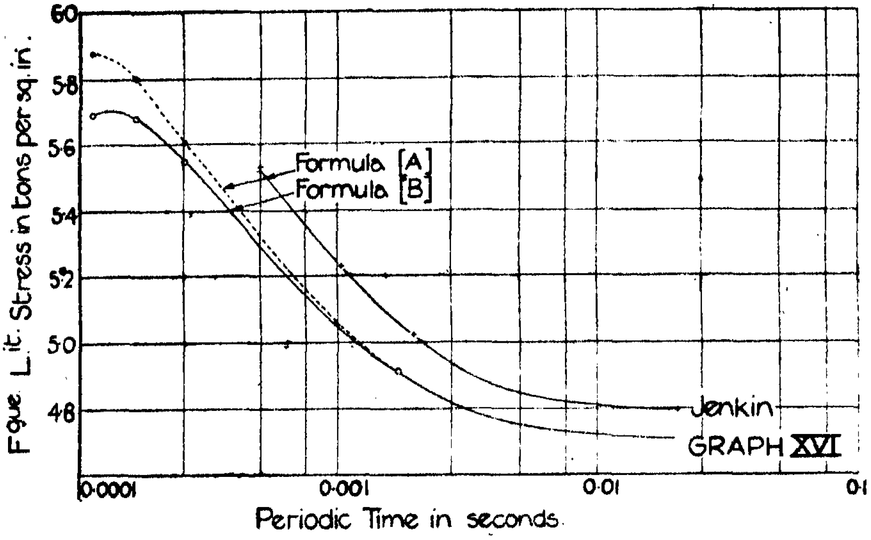

FIG. 20.—Copper.

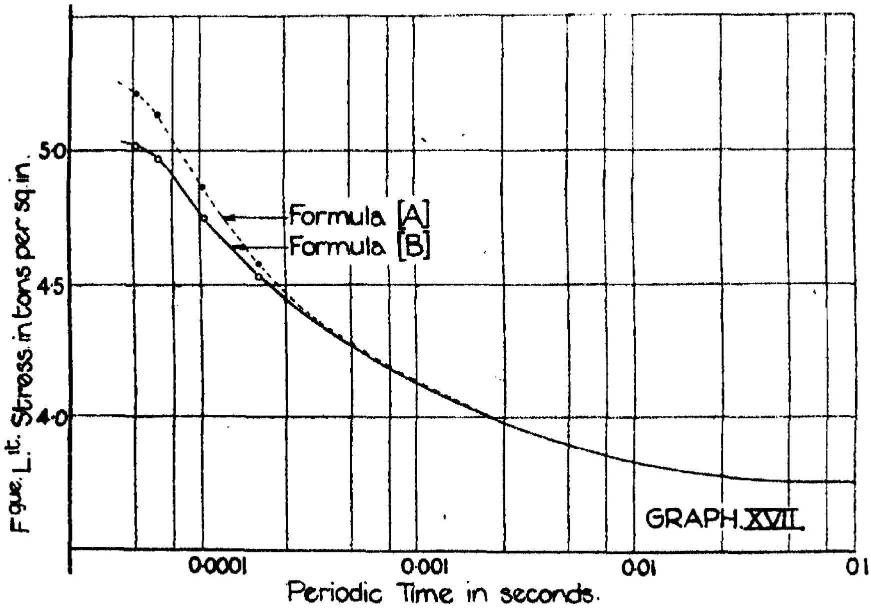

FIG. 21.—Rolled Aluminium.

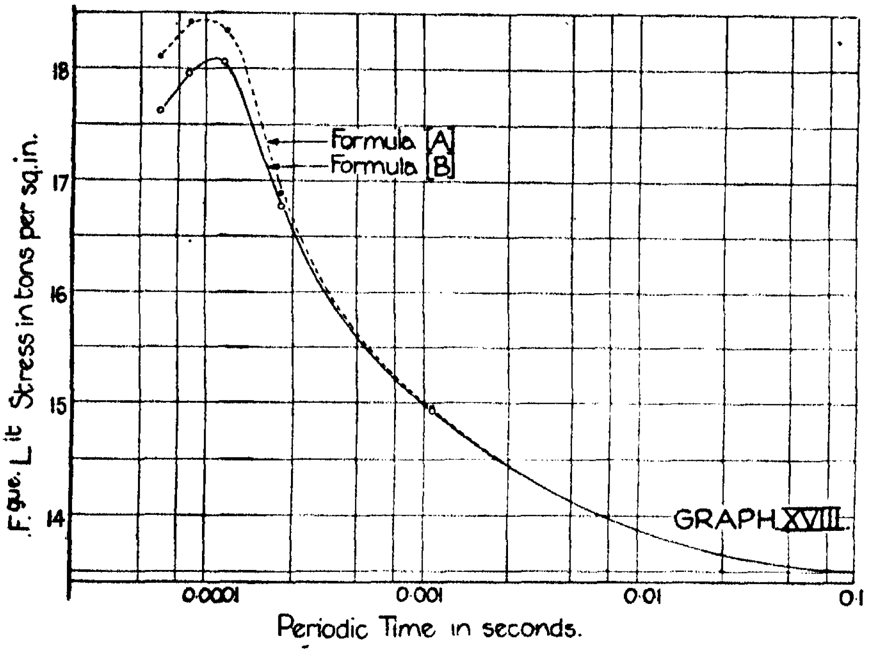

Fig. 22.—Armco Iron.

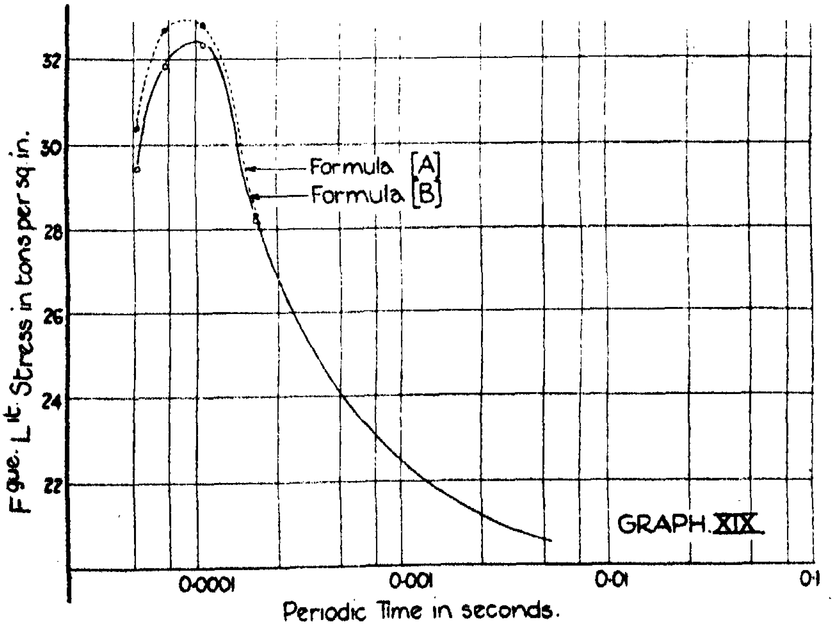

Fig. 23.—Hard 0·86 per cent. C steel.

Fig. 24 shows the large errors due to anticlastic bending when too wide bars are used (such as those in the original test). Curve I is for a bar of 1·27 cm. wide, using formula (A) which neglects anticlastic bending. Curve II is for a bar of 0·3 cm. wide using formula (B) which makes anticlastic bending corrections for narrow bars.

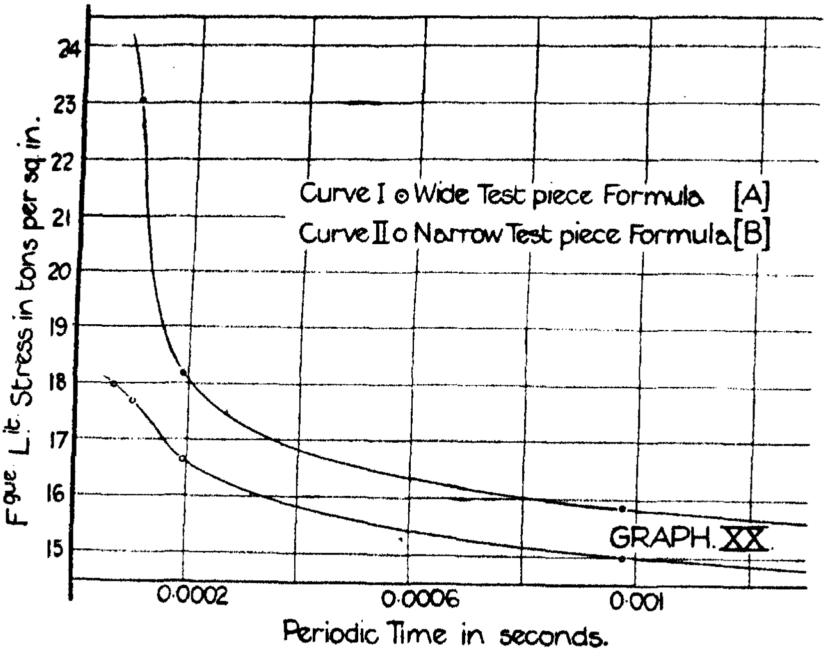

Fig. 24.—Normalised 0·11 per cent. C steel.

Further Tests.

Brinell hardness tests (*vide* p. 100) and microscopic investigations of the fractures were made on the specimens. But as these were not part of the original programme they were not carried out very systematically, and a fuller investigation on these points is required to establish the results with certainty. Only a few results were recorded, but these are very suggestive. Brinell tests were made on the annealed copper, normalised mild steel and normalised armco iron specimens of the fracture. The microscopic Brinell tests do not give a real hardness, because the hardness of the broken specimen presumably varies from a maximum at the surface to a minimum at the core, which being unstressed remains nearly unaltered. The hardening on the surface also varies along the length of the specimen and is a maximum at the crack. Nor are the results directly comparable, because it was not possible to measure the hardnesses at the same distances from the fracture. They show, however, that the Brinell hardness number of the fractured specimens rises with the frequency, and for armco iron drops again at the highest frequencies, the maximum Brinell figure occurring at a lower frequency than the maximum fatigue limit.

A few microscopic examinations of the fractures were made from which it appeared that the fractures of the mild steel bars at the highest frequencies, beyond the maximum fatigue limit, were inter-crystalline, whereas at all lower frequencies they ran across the crystals. Too few samples were examined to determine this point with certainty.

Control Tests.

Three additional tests were made to investigate whether the results obtained were affected by :—

(i) The stiffness of the supporting wires.
(ii) The size of the blowers.
(iii) The sharp corners of the specimens.

(i) The effect due to the stffness of the supports would be greatest with the lightest material vibrating at the highest frequency, *i.e.*, for the shortest aluminium specimens. Tests were therefore carried out with aluminium specimens stressed at 18,400 periods per second, using supporting wires of 0·006 inch diameter, instead of 0·01 inch diameter wires used throughout the recorded tests. These tests showed no appreciable change in the calculated fatigue limit.

(ii) Tests were carried out with blowers of different sizes, so that the area subject to air pressure varied. There was no appreciable change in the calculated fatigue limit.

(iii) Specimens of hard steel (frequency 18,200 periods per second) were made with the edges microscopically rounded. When these were tested the fatigue limit was very slightly greater than that obtained for the specimens with sharp edges. The rise in fatigue limit, however, was very small, and might be due to a very small decrease in frequency. The fatigue limit/periodic time curve at that point being nearly vertical, and very small change in frequency will give an appreciable change in fatigue limit.

XII.—DISCUSSION.

In comparing the results for different metals it is necessary to remember that the maximum frequencies obtained were not the same. The same length and breadth test pieces were used, so that the frequency depended upon Young's modulus, the density of the material and the thickness of the specimen (*vide* p. 96). An examination of the graphs show that the fatigue limit of all the metals rise as the frequency increases, but that a frequency is reached when this rise ceases, and in the normalised armco iron and the hardened high carbon steel the fatigue limit actually fell again at the highest frequencies. The maximum rise in fatigue limit for any material is about 60 per cent. above the value at 50 periods per second, and the greatest drop in the fatigue limit is about 9 per cent. of the maximum. The Brinell hardness of the metal near the fracture also rises with the frequency (*vide supra*) and for normalised armco iron shows a drop at the highest frequencies. The maximum Brinell figure, however, occurs at a lower frequency than the maximum fatigue limit. This hardening has been observed before and was referred to in Dr. Aitcheson's* paper on "Cold Work and Fatigue," where he also states that the hardening due to cold working on a material is limited in extent† and may be reversed and softening occur, so that the Brinell‡ value is lower than that for the original material. Possibly this effect of excessive cold work may be connected with the drop in the Brinell figures and even the drop in fatigue limit.

The results given in this paper may be criticised from several points of view :—

(i) The apparent change in the fatigue limit may be due to the mathematical analysis of the strains. The formula used may not give a sufficiently accurate approximation to the true strains as the length of the test piece decreases.

(ii) The shape of the bent bar may be affected by the forces applied by the air.

(iii) The shape of the bent bar may be affected by the method of support.

(iv) The mathematical theory assumes that the metals are perfectly elastic, which is known not to be exactly true at such high stresses.

(i) With regard to the first objection, we necessarily rely on Prof. Love's theory, but it seems unlikely that the complex form of the graphs can be due to any systematic error.

(ii) The forces required to vibrate the bar are so small that its shape when bent must be almost exactly that assumed by a free bar. These forces may be estimated from the work they do in overcoming hysteresis. Making reasonable approximations it can be shown that the effects of the forces will not increase for the shorter specimens. Again the complex form of the graph confirms this.

---

* 'Aeronaut. Res. Com. Rep. and Memo., No. 923,' M. 27, May, 1924.

† *Cf.* Beilby's 'Aggregation of Flow of Solids,' p. 151.

‡ Rosenhain and Fry, 'J. Inst. Met.,' p. 11 (1919).

(iii) The control tests show that the effect of the supports was negligible.

(iv) Imperfect elasticity may affect the shorter bars more than longer, thus producing a systematic error.

In conclusion the authors wish to thank Prof. A. E. H. Love for the essential mathematical theory; Messrs. Thos. Firth & Sons, Messrs. Arthur Lee & Sons, and The Armco International Corporation, for supplying the special materials rolled to the sizes required; Amalgam, Ltd., for supplying a suitable salt for hardening the steel; and Messrs. Bruntons for supplying a very fine steel wire.

Gaseous Combustion at High Pressures.—Part XIII. *The Molecular Heats of Nitrogen, Steam, and Carbon Dioxide at High Temperatures.*

By D. M. Newitt, Ph.D., D.I.C.

(Communicated by W. A. Bone, F.R.S.—Received May 11, 1929.)

The only information available concerning the internal energy of gases at temperatures higher than 2000° C. or so is that provided by the results of explosion experiments in which the energy liberated during the combustion serves to raise the products and any other gases that may be present in the medium to some definite maximum temperature. By varying the proportions of the reacting gases, or by adding suitable quantities of some diluent gas, this temperature may be varied between comparatively wide limits.

In a previous paper* of this series the method of calculating the mean maximum temperature attained during a gaseous explosion in a closed vessel was discussed, and those calculated from our experiments for theoretical CO-air and H_2-air explosions at initial pressures of between 3 atmospheres and 175 atmospheres were given. At Prof. Bone's request I have recently reviewed and analysed the mass of data accumulated during these researches, together with others resulting from the supplementary experiments described herein, with a view to seeing how far it is possible to deduce, not only a quantitative estimate of the energy distribution at the moment of maximum pressure in typical explosions at high pressures, but also the mean heat capacities of the various explosion products over a temperature range from 15° C. up to various definite points between 2600° and 3000° C. The results of this investigation are described in the present paper.

---

* Part X, 'Roy. Soc. Proc.,' A, vol. 119, p. 464 (1928).

It may be well to recall that in such explosions the energy developed is distributed at any moment between (*a*) kinetic energy in the products, (*b*) potential energy of either "dissociated products" or of unburnt gas, and (*c*) that lost by radiation and conduction to the walls of the containing vessel.

The effect of both (*b*) and (*c*) is to lower the maximum pressure attained; but whilst (*b*) is solely a property of the gases concerned and of the temperature and pressure, (*c*) depends, not only upon such properties of the gases as conductivity and chemi-luminescence, but also upon the shape and size of the containing vessel, the nature of its surface and the position of the point of ignition.

The magnitude of the heat losses due to all causes usually represents an important fraction of the total heat of combustion and must be estimated accurately before a proper energy balance can be deduced from the explosion data. The direct measurement of these losses presents formidable difficulties and although many attempts have been made the problem cannot yet be said to have been successfully solved. The indirect methods usually employed take into account some fraction only of the heat losses, neglecting the remainder, and are based upon assumptions of somewhat doubtful validity. A critical survey of the results of specific heat calculations based upon explosion methods indicates the possibility of greater errors on this account than are sometimes supposed unless the experimental conditions are known to be such as will minimise the losses referred to.

Our knowledge of the radiation emitted during explosions in closed vessels is still very imperfect. Prof. W. T. David found by direct measurement in a cylindrical vessel of diameter 30 cm. and height 30 cm.—that in the explosion of a 25·4 per cent. hydrogen-air mixture 0·5 per cent. of the energy liberated was lost by radiation up to the moment of attainment of maximum pressure; for a 9·8 per cent. coal gas air mixture the corresponding quantity was 7·0 per cent. That radiation loss in carbonic oxide-oxygen explosions may sometimes involve as much as 10 per cent. of the total energy liberated has recently been shown by Garner and Johnson.

Very little quantitative work appears to have been done on the effect of initial pressure upon the absolute amount of chemi-luminescence resulting from gaseous combustion under explosive conditions. David has shown that in the case of a 15 per cent. coal gas-air mixture fired at initial pressures of ½ and 1½ atmospheres, respectively, the total energy lost by radiation up to the moment of attainment of maximum pressure was 3·3 per cent. of the heat of combustion at the lower, and 2·5 per cent. at the higher, pressure. This would seem to indicate an increase in the opacity of the medium with increasing pressure, an observation in line with the results of our experiments over a much wider pressure range.

In this connection a most noticeable feature in all our explosion experiments is the progressive increase with pressure of the ratio of maximum to initial pressure for any given mixture. Thus, for example, comparing the two mixtures $2H_2 + O_2 + 4N_2$ and $2CO + O_2 + 4CO$ the ratio increases are as follows :—

	Atmospheres.						
Initial pressure :	3.	10.	50.	75.	100.	125.	150.
$2H_2 + O_2 + 4N_2$—							
P_{m_b}/P_{i_b}	7·8	7·98	8·0	8·14	8·27	8·36	8·36
T_m° K	2585°	2630°	2650°	2695°	2728°	2745°	2760°
$2CO + O_2 + 4CO$—							
P_{m_b}/P_{i_b}	8·03	8·36	8·53	8·93	8·95	9·04	9·07
T_m° K	2710°	2820°	2873°	3010°	3018°	3050°	3072°

When the initial pressure is increased from 3 to 150 atmospheres the increase of ratio is 7·2 per cent. for the hydrogen mixture and no less than 11·4 per cent. for the carbonic oxide mixture. Furthermore, experiments carried out in these laboratories furnish support for the view that, in the case of carbonic oxide-oxygen explosions the ultra-violet radiation emitted is, at high pressures, partly absorbed by any excess of the combustible gas or by nitrogen present as a diluent, and that the amount absorbed increases with increase of pressure. In so far as the absolute amount of radiation varies with pressure, a corresponding change will be produced in the amount of kinetic energy found in the products of combustion ; and it therefore becomes possible to estimate, from the change in kinetic energy with pressure, the magnitude of the total radiation emitted.

The importance of the heat losses due to conduction in the calculation of specific heats from explosion data has long been recognised. Both Berthelot and Vieille and Mallard and Le Chatelier applied corrections to their experimental results on this account; the former, by employing explosion vessels of different sizes and thus varying the surface/volume ratio, and the latter by a graphical method applied to the pressure-time records of their explosion. Recently Bjerrum and Siegel have estimated the heat losses due to conduction in these experiments by observing the change in the ratio of maximum to initial pressure caused by increasing the initial gas density and assuming the heat losses to be inversely proportional to such increase.

So far, in nearly every instance, the principle has been adopted of minimising the heat losses by using explosion vessels as large as is practicable (*i.e.*, with a small surface/volume ratio) having regard to the pressures involved. Pier, Bjerrum and Siegel for example, worked with a spherical bomb of 35 litres capacity having a surface/volume ratio of 0·14; but whereas Pier and Siegel employed initial pressures of 1 or 2 atmospheres, Bjerrum used pressures as low as 0·25 atmospheres, thereby sacrificing in some measure the advantage due to the size of his explosion vessel and introducing heat losses estimated in some cases to be as much as 19 per cent.

Hopkinson, David and Maxwell and Wheeler have carried out explosions at relatively low initial pressures in bombs having highly polished inner surfaces, a device which reduces considerably the amount of radiation absorbed by the walls.

There is another, and in some respects perhaps a better, way of dealing with the problem, namely, by working at relatively high pressures; because, although in high pressure explosions it is not practicable either to employ vessels of large capacities or to maintain their inner surfaces in a highly polished condition, the relative heat losses can be diminished asymptotically merely by increasing the initial pressure of the medium, and at exceedingly high pressures they can be reduced to an absolute minimum. Hence estimations of the energy distribution at the maximum temperature in such high pressure explosions have a special interest for comparative purposes.

The Experimental Data and their Analysis.

The experimental data which I have selected for the purpose of calculating the mean molecular heats (C_v) of carbon dioxide, steam, or nitrogen have all been derived from explosions at high initial pressures (i) of theoretical hydrogen-oxygen mixtures diluted with either argon or nitrogen or (ii) of carbonic oxide-oxygen mixtures containing excess of the combustible. I have restricted myself to explosions in which the initial pressure was at least 50 atmospheres, the explosion period (t_m) did not exceed 0·025 second, and the pressure-time curve was quite free from any vibrational disturbance at the maximum pressure. It will be seen later that, with the particular media referred to, this imposed certain limits (namely, 2600°–3000° K.) upon the maximum explosion temperatures considered; and therefore it should be understood that in each case the mean molecular heat value deduced from the experimental results refers to a temperature range between 15° C. and the particular maximum explosion temperature in question.

The experiments were all carried out in a steel bomb having a spherical explosion chamber of 3 inches diameter (capacity 240 c.c.), the explosive mixture being ignited by the electrical fusion of a thin platinum wire. Pressures were recorded by means of a Petavel manometer and its optical accessories. Full details of the experimental method are contained in the earlier papers to which reference should also be made for a description of the apparatus employed. In calculating heat losses in explosions an assumption first made by Bjerrum, namely that for any given mixture they are inversely proportional to the initial pressure, has been adopted, with the proviso (which I consider necessary) that one pressure is no more than double the other. On such assumption, the total heat loss for a 88 hydrogen–12 oxygen mixture fired at 100 atmospheres initial pressure is found to be 2 per cent. of the total heat of combustion, whilst for the same mixture fired at 50 atmospheres initial pressure it would be about one and a half times as great, the explosion time being 0·005 second in both cases.

It may be pointed out that this method of applying a correction for heat losses conceals any variation of the internal energy of the gases that is solely a function of pressure.

The Molecular Heat (C_v) *of Nitrogen.*—The method employed for calculating from explosion data the molecular heat of nitrogen depends upon the assumption that the molecular heat of the monatomic argon is independent of temperature, and that the increase in its energy of translation per 1° rise in temperature is 1·5 R or 2·977 cals. per gram-molecule. By exploding a series of $2H_2 + O_2$ mixtures diluted on the one hand with argon and on the other with the diatomic gas in varying proportions, it is possible to obtain by interpolation the composition of pairs of mixtures which on explosion will attain the same mean maximum temperature. If the heat losses up to the moment of attainment of maximum pressure were either negligible or equal to one another the heat capacities of the two diluents could be equated and the molecular heat of the nitrogen found directly. Actually the heat losses differ and the apparent value of the molecular heat so obtained is too large by an amount proportional to the difference. If, for example, the two mixtures $2H_2 + O_2 + aA$ and $2H_2 + O_2 + bN_2$ on explosion at an initial pressure of P atmospheres and a temperature of T° C. both attain the same mean maximum temperature $T_m°$, then if the heat losses for the two mixtures are the same the mean molecular heat of the nitrogen between T° and $T_m°$ (C_{vN_2}) will be given by $2{\cdot}977a/b$. If, however, the equivalent heat loss for the argon diluted mixture is H calories and for the nitrogen diluted mixture is H′ calories, then

$$2{\cdot}977a + H = C_{vN_2}b + H' \qquad (1)$$

and

$$C_{vN_2} = \{2{\cdot}977a + (H - H')\}/b.$$

To obtain the true mean molecular heat it is necessary to carry out a second series of explosions of mixtures $2H_2 + O_2 + xN_2$ at some other initial pressure, say P′ atmospheres. If the composition of the mixture giving on explosion at P′ atmospheres a mean maximum temperature of $T_m°$ is $2H_2 + O_2 + cN_2$* and the equivalent heat loss is H′ calories, then

$$2{\cdot}977a + H = C_{vN_2}c + H'', \qquad (2)$$

and from equations (1) and (2)

$$C_{vN_2} = (H'' - H')/(b - c).$$

If P′ does not differ greatly from P the respective heat losses may be taken as inversely proportional to the initial pressure, and the true mean molecular heat of nitrogen is then directly obtained from the apparent values :—

$$C_{vN_2} = 2{\cdot}977a\,(P_c - P'b)/bc\,(P - P'). \qquad (3)$$

Accordingly two series of nitrogen diluted $2H_2 + O_2$ mixtures were exploded at initial pressures of 75 and 100 atmospheres respectively, and a series of argon diluted mixtures at an initial pressure of 100 atmospheres, with results which are summarised in Tables I to III, where

P_m/P_i = ratio of the observed maximum pressure to the observed initial pressure.

P_{m_b}/P_{i_b} = ratio of P_m to P_i each corrected for deviations from the gas laws.

t_m = time in seconds for the attainment of maximum pressure.

$T_m°$ K. = mean maximum temperature actually attained in the explosion.

---

* A small correction is necessary due to the difference in the degree of dissociation of steam caused by changing the pressure from P to P′ atmospheres.

Table I.—$2H_2 + O_2 + xA$ Mixtures Fired at $P_i = 100$ atmospheres.

Initial mixture.			t_m secs.	P_m/P_i.	P_{m_b}/P_{i_b}.	T_m° K.
$2H_2 + O_2$.	Argon.	Diatomic gases.*				
per cent.	per cent.	per cent.				
24·6	72·2	3·2	0·02	8·90	8·32	2620
28·1	69·2	2·7	0·02	9·55	8·98	2860
29·1	68·2	2·7	0·02	9·70	9·13	2920
30·0	67·6	2·4	0·015	9·95	9·39	3010
34·2	63·5	2·3	0·005	10·60	10·0	3255

* Any hydrogen or oxygen in excess of the theoretical proportions together with any adventitious nitrogen and oxygen contained in the argon are included under the heading of diatomic gases.

Table II.—$2H_2 + O_2 + xN_2$ Mixtures Fired at $P_i = 100$ atmospheres.

Initial mixture.		t_m secs.	P_m/P_i.	P_m/P_{i_b}.	T_m° K.
$2H_2 + O_2$.	N_2.*				
per cent.	per cent.				
36·6	63·4	0·025	7·65	7·21	2370
37·5	62·5	0·025	7·70	7·26	2395
40·4	59·6	0·015	8·17	7·75	2578
43·5	56·5	0·005	8·65	8·25	2785
42·8	56·2	0·005	8·70	8·32	2815
43·6	56·4	0·005	8·90	8·44	2860
45·9	54·1	0·005	8·85	8·51	2900
49·4	50·6	0·005	9·25	8·95	3085
49·8	50·2	0·005	9·20	8·92	3085
53·3	46·7	<0·005	9·60†	9·35	3270

* Any hydrogen or oxygen in excess of the theoretical proportions is included in the nitrogen.
† The pressure-time record showed marked secondary vibrations.

Table III.—$2H_2 + O_2 + xN_2$ Mixtures Fired at $P_i = 75$ atmospheres.

Initial mixture.		t_m secs.	P_m/P_i.	P_{m_b}/P_{i_b}.	T_m° K.
$2H_2 + O_2$.	N_2.				
per cent.	per cent.				
33·3	66·7	0·015	6·68	6·42	2085
37·1	62·9	0·010	7·45	7·17	2365
40·5	59·5	0·010	8·03	7·71	2575
44·8	57·2	0·005	8·34	8·01	2700
47·1	52·9	0·005	8·96	8·60	2950

From an inspection of results it will be seen that the upper temperature limit is determined by the nitrogen diluted mixtures at $P_i = 100$ atmospheres (Table II), for when the nitrogen content fell below about 50 per cent. the explosions were so violent that vibrations were set up in the recording manometer, and it became difficult to measure with sufficient accuracy the recorded maximum pressure. On the other hand, the lower temperature limit was found to depend on the argon diluted mixtures (Table I) because when the argon content exceeded 72 per cent. the explosion time, and consequently the heat losses, increased rapidly as the mixture was made progressively weaker. Taking these facts into consideration no attempt has been made to calculate molecular heats at temperatures below 2600° nor above 3000° K. Within these limits the explosion times never exceeded 0·025 second and the pressure-time records were free from secondary vibrations.

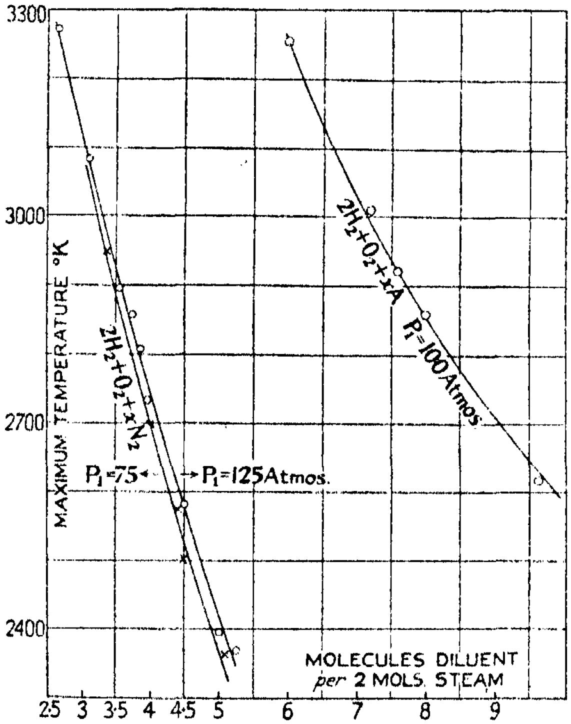

FIG. 1.

The curves in fig. 1 show graphically the relation between the mean maximum temperature and the amount of diluent in the initial mixture for the three series of experiments. By interpolation of the results the composition of equivalent mixtures at temperature intervals of 100° between 2600° and 3000° K. have been found and are recorded in Table IV.

Table IV.—Composition of Equivalent Mixtures at Various Temperatures.

Temperature ° K.	$2H_2 + O_2 + xN_2$.		$2H_2 + O_2 + xA$.
	P_i=75 atmospheres.	P_i=100 atmospheres.	P_i=100 atmospheres.
3000	x = 3·23	x = 3·30	x = 7·12
2900	3·47	3·55	7·72
2800	3·74	3·84	8·36
2700	4·02	4·14	9·07
2600	4·28	4·44	9·86

From the composition of such equivalent mixtures the apparent mean molecular heats of nitrogen at the various temperatures have been calculated in the manner explained (Table V).

Table V.—Apparent Mean Molecular Heat of Nitrogen.

Temperature ° K.	P_i = 75 atmospheres.	P_i = 100 atmospheres.
289 to—		
3000	6·56	6·42
2900	6·63	6·47
2800	6·66	6·48
2700	6·72	6·52
2600	6·86	6·61

The decrease in the value of the apparent mean molecular heat with increase of initial pressure is due to the relatively smaller heat loss at the higher pressure. Assuming the heat loss to be inversely proportional to the initial pressure the true mean molecular heats as calculated from the above figures by means of equation (3) are as follows :—

Table VI.—True Mean Molecular Heat of Nitrogen.

Temperature ° K.	C_{vN_2}.
289 to—	
3000	6·01
2900	5·99
2800	5·96
2700	5·94
2600	5·87

The Mean Molecular Heat of Steam.

From a knowledge of the heat of combustion of hydrogen, the degree of dissociation of steam and the mean molecular heat of nitrogen it is possible to calculate from the results recorded in Tables II and III the mean molecular heat of steam. Before this can be done, however, it is necessary to determine the heat loss in order that the distribution of energy at the moment of attainment of maximum pressure may be known. This is best done by calculating from pairs of equivalent mixtures fired at different initial pressures a series of apparent values for the molecular heats and then determining from them the true value on the assumption that the heat loss is inversely proportional to the initial pressure.

The method of carrying out the calculation may best be shown by an actual example. By reference to Table IV it will be seen that a mixture of composition $2H_2 + O_2 + 3 \cdot 74N_2$ fired at an initial pressure of 75 atmospheres and a mixture of composition $2H_2 + O_2 + 3 \cdot 84N_2$ fired at 100 atmospheres each attained a maximum temperature of 2800° K. In the former case, the steam in the products at T_m was dissociated to the extent of 1·7 per cent. and in the latter case to 1·5 per cent. Taking 57,500 calories as the heat of combustion of hydrogen to steam, at the moment of maximum pressure (temperature) this energy is distributed as follows :—

For the Mixture $2H_2 + O_2 + 3 \cdot 84N_2$.

To the steam	$C_{vH_2O} \times (0 \cdot 985) \times 2511$ calories.
To the nitrogen	$5 \cdot 96 \times 1 \cdot 920 \times 2511$ calories.
To the products of dissociation	$5 \cdot 96 \times 0 \cdot 022 \times 2511$ calories.
Chemical energy in dissociated products	862 calories.
Heat lost to the vessel	h calories.

And $C_{vH_2O} + h/(0 \cdot 985 \times 2511) = 11 \cdot 15$ calories.

For the Mixture $2H_2 + O_2 + 3 \cdot 74N_2$.

To the steam	$C_{vH_2O} \times 0 \cdot 983 \times 2511$ calories.
To the nitrogen	$5 \cdot 96 \times 1 \cdot 87 \times 2511$ calories.
To the products of dissociation	$5 \cdot 96 \times 0 \cdot 025 \times 2511$ calories.
Chemical energy in dissociated products	977 calories.
Heat lost to vessel	h' calories.

$C_{vH_2O} + h'/(0 \cdot 983 \times 2511) = 11 \cdot 40$ calories.

These quantities may be termed the apparent mean molecular heats ; they differ from the true molecular heats by amounts proportional to the respective heat losses.

The terms containing h and h' depend for any particular mixture upon the shape of the explosion vessel, its surface/volume ratio, the position of the point of ignition, and the initial pressure at which the mixture is fired. Assuming h and h' in the above example to be inversely proportional to the initial pressure the true mean C_v value between 289° and 2800° K. is found to be 10·40 calories.

By calculating in a similar manner for the remaining equivalent mixtures given in Table IV the following results are obtained :—

Table VII.—Apparent and True Mean Molecular Heats of Steam at Constant Volume.

Temperature ° K.	Apparent mean molecular heat.		$C_{v}H_2O$.
	P_i = 75 atmospheres.	P_i = 100 atmospheres.	
289 to—			
3000	11·10	10·95	10·50
2900	11·28	11·07	10·44
2800	11·40	11·15	10·40
2700	11·68	11·34	10·32
2600	12·14	11·67	10·25

The Mean Molecular Heat of Steam and Carbon Dioxide calculated from results of Experiments with Mixtures of Composition $2H_2 + O_2 + 4N_2$ *and* $2CO + O_2 + 4CO$ *Fired at various Initial Pressures.*

In Part X of this series the mean maximum temperatures attained on the explosion of mixtures of composition $2H_2 + O_2 + 4N_2$, $2CO + O_2 + 4N_2$ and $2CO + O_2 + 4CO$ were calculated and are recorded in Tables III, IV and VI (*q.v.*). The results showed that for all three mixtures there was a rapid rise of temperature as the initial pressure was progressively increased from 3 to 50 atmospheres, and that thereafter in the case of the carbonic oxide mixtures the maximum temperature continued to rise steadily but slowly with increase of pressure up to 150 atmospheres. The hydrogen series was anomalous in that the temperature after rising from 2585° at 3 atmospheres to 2700° at 100 atmospheres then remained constant to 125 atmospheres, and subsequently fell to 2660° at 150 atmospheres ; the discontinuity observed between 50 and 75 atmospheres is due to the fact that beyond 50 atmospheres an explosion vessel (bomb No. 3) of greater strength had to be employed, and although its internal dimensions were the same as those of the bomb employed at the lower pressures (bomb No. 2) the cooling effects of its more massive walls introduced a disturbing factor.

The explanation of the fall of temperature observed in the case of the hydrogen mixtures was at first sight not obvious; the pressure-time records were consistent and any abrupt change in the specific heat of steam due to increase of density appeared inadmissible. A re-examination of the results pointed to the possibility of an error in the determination of the hydrogen-air isotherm at the higher pressures. This isotherm had been measured initially in the bomb apparatus, pressures being observed by means of a standard Bourdon tube gauge calibrated against a dead weight pressure balance at the National Physical Laboratory; and it had subsequently been redetermined in a special apparatus installed for the purpose up to a pressure of 50 atmospheres. More recently Mr. G. A. Scott working in these laboratories has completed the measurements up to 150 atmospheres, and the new values reveal the existence of the suspected error in the earlier determinations amounting to 2·6 per cent. at 150 atmospheres. The new values for the compressibility factors are as follows :—

Pressure (atmospheres)	90	120	150
Compressibility factor	0·981	0·970	0·957

Using these values the mean maximum temperatures have been recalculated for initial pressure of 75 atmospheres and upwards and the results are recorded in Table VIII.

Table VIII.—Initial Mixture $2H_2 + O_2 + 4N_2$.

P_i atmospheres	75	100	125	150
T_m° K.*	2695°	2728°	2745°	2760°

* These temperatures are the mean of the temperatures calculated by means of equations (2) and (3).

In deducing the mean molecular heat of steam from these results it must be borne in mind that the maximum temperature is progressively changing with increase of initial pressure, and that the heat losses are becoming relatively smaller as the initial pressure increases.

The apparent molecular heats for the series calculated in the manner already described are as follows :—

Pressure	50	75	100	125	150
Temperature ° K.	2650°	2695°	2728°	2745°	2760°
Apparent C_v	12·27	11·76	11·40	11·18	11·04

Under ideal conditions (*i.e.*, such that no heat is lost during the experiment) and assuming molecular heats to be independent of pressure a series of explosions of similar mixtures at different initial pressures should give rise to progressively increasing maximum temperatures, the increase of temperature being due to a diminution of the dissociation with increase of pressure; in the case under consideration the dissociation of steam, however, is insufficient to alter materially the temperature attained.

Taking the heat loss to be inversely proportional to the initial pressure the results set forth in Table IX are obtained.

Table IX.—Mean Molecular Heat of Steam Calculated from the Results of $2H_2 + O_2 + 4N_2$ Explosions.

Pressure (atmospheres).					
150.	125.	100.	75.	50.	
11·04	10·34	10·32	10·32	10·42	
2760°	2835°	2824°	2825°	2815°	
	11·18	10·30	10·21	10·45	Mean temperature 2816° K.
	2745°	2813°	2820°	2808°	
		11·40	10·32	10·53	Average mean molecular heat of steam = 10·41.
		2728°	2827°	2806°	
			11·76	10·74	
			2695°	2785°	
				12·27	
				2650°	

In the Table the figures to the left of the heavy line are the actual maximum temperatures and the apparent mean molecular heats calculated therefrom. To the right of the line are the corrected temperatures and molecular heats obtained by taking successive pairs of mixtures. It will be seen that with the exception of the results at 50 atmospheres the agreement between the figures is good, and that the average of the results confirms the figure already found (Table VII) for the C_v of steam at 289°–2800° K. They furthermore afford justification for the assumption made in the earlier part of the paper in respect of the relation between initial gas density and heat loss. It should be pointed out in this connection, however, that the agreement between the values for the molecular heat found at the same temperature but at different pressures is not proof of the independence of molecular heat on pressure, since the method of calculating heat losses would conceal any such variation.

The Mean Molecular Heat (C_v) *of Carbon Dioxide.*

The results of a series of explosions of the mixture $2CO + O_2 + 4CO$, between initial pressures of 50 and 150 atmospheres are available for this purpose ; this series is well adapted for the calculation of molecular heats since the explosion times are identical at all the pressures in question and dissociation of the carbon dioxide is almost completely suppressed and may be neglected.

In carrying out the calculations the mean of the temperatures obtained by correcting the maximum pressures, according to the two methods described in the previous paper, have been taken (*loc. cit.*), the temperatures being read off from a smooth curve drawn between the points.

The apparent and true mean molecular heats of carbon dioxide so obtained are set forth similarly in Table X.

Table X.—Apparent and True Mean Molecular Heats of Carbon Dioxide.

Pressure (atmospheres).				
150.	125.	100.	50.	
12·40	11·45	11·40	11·43	
3072°	3182°	3180°	3171°	Mean temperature 3173 ° K.
	12·59	11·35	11·43	
	3050°	3178°	3168°	Average mean molecular heat of carbon dioxide 11·42.
		12·90	11·47	
		3018°	3163°	
			14·33	
			2873°	

Discussion of Results.

The values for the mean molecular heat of nitrogen over the temperature range 289°–2600° to 3000° K. are in general higher than those found by Pier (corrected). Thus, whereas his results may be represented by the empirical equation

$$C_v = 4\cdot85 + 0\cdot000375\,T,$$

mine are better represented by

$$C_v = 4\cdot87 + 0\cdot000387\,T.$$

The following comparative figures indicate the magnitude of the differences :

Temperature ° K.	Author. C_{vN_2}.		Pier (corrected). C_{vN_2}.
	Experiment.	Calculated.	Calculated.
3000	6·01	6·03	5·98
2900	5·99	5·99	5·94
2800	5·96	5·95	5·91
2700	5·94	5·92	5·86
2600	5·87	5·88	5·82

My results for the molecular heat of steam and carbon dioxide are somewhat higher than those of Pier at corresponding temperatures.

For comparative purposes the results of some of the best molecular heat determinations for nitrogen, steam and carbon dioxide extending over a wide temperature range are shown in fig. 2. From these curves it will be seen that

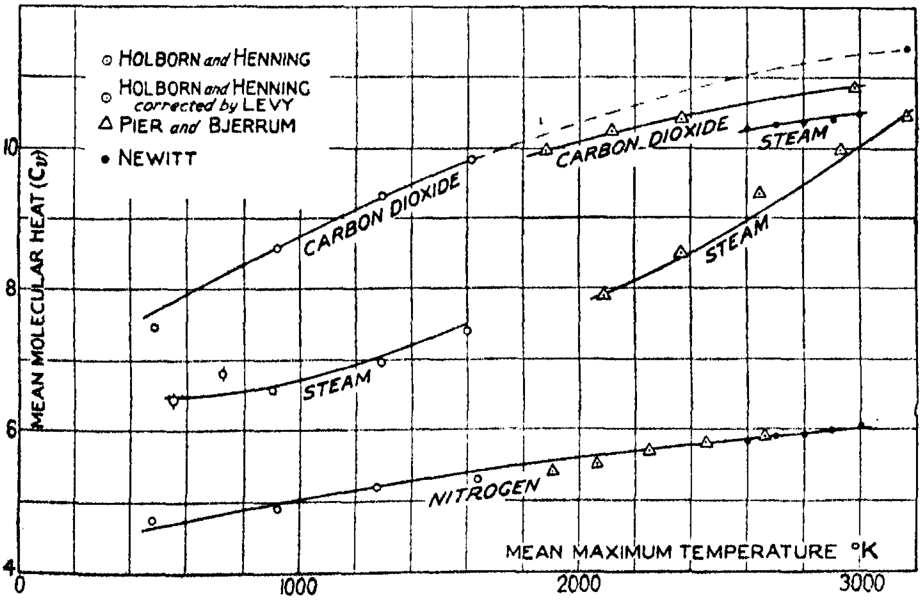

Fig. 2.

in the case of steam the results are by no means concordant. There is a region of temperature between 1600° and 2000° K. which has not been covered by any of the methods so far employed. The results of Holborn and Henning between 800° and 1600° K. suggest that Pier and Bjerrum's values over the range 2000° to 3000° K. may be low; in this connection it may be mentioned that Callendar has drawn attention to systematic errors in Holborn and Hennings results between 800° and 1400° K. which may make them as much as 10 per cent. too low. Taking these facts into consideration my values do not seem inconsistent with those found by Holborn and Henning at temperatures between 300° and 1600° K.

In conclusion my thanks are due to Prof. W. A. Bone for his advice in the preparation of the paper, to Dr. D. T. A. Townend for assistance in carrying out some of the experiments, and to Mr. G. A. Scott for a number of compressibility measurements; the investigation has been aided by grants made by the Department of Scientific and Industrial Research to the Imperial College for the work.

The Absorption Coefficient for Slow Electrons in Mercury Vapour.

By Robert B. Brode, University of California, Berkeley, California, U.S.A.

(Communicated by F. A. Lindemann, F.R.S.—Received May 18, 1929.)

The effective cross-sectional area of an atom is defined in this paper as that area within which a passing electron is deflected so that it can no longer go through a system of slits defining a beam of electrons. The sum of all of these areas in a cubic centimetre of the gas defines the absorption coefficient, the reciprocal of which is the mean free path. The absorption coefficient is a function of the atom studied and the velocity of the electron. It may also depend on the geometry of the apparatus which defines the maximum angle of deflection. From the agreement of the results obtained by several observers with different limiting angles, the variation of the observed absorption coefficient with the size of the limiting angle appears to be small. The absorption coefficient is computed from the equation

$$I = I_0 e^{-\alpha x p},$$

where I is the electron current at the end of the path, I_0 the current at the beginning of the path, x the path length, p the pressure of the gas and α the absorption coefficient.

Apparatus.—For the measurement of the absorption coefficient a modification of Ramsauer's original apparatus* was used. The same modification was previously used for the measurement of the absorption coefficient in other gases giving results in good agreement with those by Ramsauer's more complicated apparatus.†

Another change in this apparatus was in the source of electrons. K. Cole‡ has shown that with a filament in the centre of a cylinder with a fine longitudinal slit in the side, a very fine beam of electrons can be produced. The apparent sharpness of the beam was due in part to the focussing action of the magnetic field. A further advantage of this source was found at potentials where ionisation takes place. The space charge about the filament was changed by this, but the distribution of current was unchanged due to the symmetry of the apparatus. The same fraction of the total emission still left through the slit as at lower potentials.

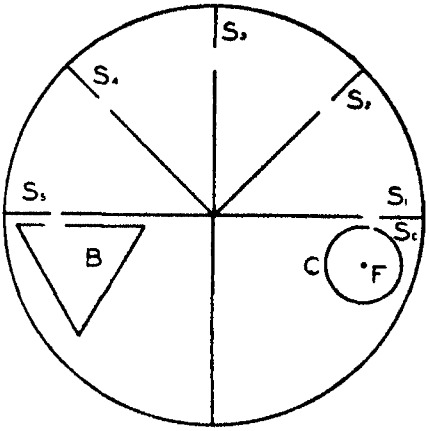

Fig. 1.

A cross-section of the apparatus is shown in fig. 1. The mean radius of the path in which the electrons moved was 15·0 mm. The slit in the cylinder, S_c, was 0·20 mm. wide and 5 mm. high. The slit S_5 was 1·0 mm. wide and 10 mm. high. The other slits were all 2·0 mm. wide and 10 mm. high. The cylinder C had a radius of 3·5 mm. The filament F was a 3 mill tungsten wire 15 mm. long. The filament was held centred by circular quartz insulators at each end of the cylinder C. A small hole in each insulator allowed the filament conductor to pass through. The filament leads were kept as close together as possible to avoid magnetic effects of the filament current. A small effect was observed in the currents that arrived at B when the direction of the filament current was reversed. The values of the absorption coefficient computed from data obtained when the direction of the filament current was unchanged, were identical with those obtained when the filament current was reversed. The filament current was about 0·5 ampere.

---

* 'Ann. Physik,' vol. 64, p. 513 (1921).

† Brode, 'Phys. Rev.,' vol. 25, p. 636 (1925).

‡ 'Phys. Rev.,' vol. 28, p. 781 (1926).

Electrons were accelerated from the filament to the cylinder C. This current was measured by a microammeter and was of the order of 10 microamperes. The current from B passed through a high sensitivity galvanometer to the lead that came from the remainder of the apparatus. The lead then went to another high sensitivity galvanometer. When working with low velocity electrons, galvanometers of a sensitivity of about 10^{-11} amperes per division were used. For higher velocity electrons galvanometers with a shorter period and a sensitivity of about 10^{-10} amperes were used.

The earths field was neutralised by a large pair of square coils. A solenoid 30 cm. long and 15 cm. in diameter was placed so that its centre was coincident with the centre of the apparatus and its axis perpendicular to the plane of the apparatus shown in fig. 1. The magnetic field required to bend a beam of electrons into a given circular path depends directly on the velocity of the electrons or on the square root of the potential through which the electron has passed. Plotting the current used to produce the magnetic field against the square root of the potential applied to the electrons should give a straight line passing through the origin. Using only the points for potentials between 200 and 400 volts where contact E.M.Fs. were negligible, the slope of the line was determined. When the current producing the magnetic field was known, the velocity of the electrons in square root of volts could then be determined.

Two furnaces were used for controlling the temperature. One heated the apparatus and the other heated the mercury in a tube connected to the apparatus. The electrical heating wires for the furnaces were wound so that no magnetic field was produced. Reversing 5 amperes in the furnaces did not produce an observable change in the magnetic field required to bring a beam of slow electrons into the collecting box. The furnaces were constructed so that about an hour was required before a constant temperature was reached. This had the advantage that fluctuations in the heating current which was taken from the power lines produced effects so small that the temperature could easily be held constant to a quarter of a degree. The temperature was measured by means of copper-constantan thermocouples attached to copper cylinders that were in contact with the glass walls of the apparatus. The walls of the furnaces were also made of copper so as to ensure uniformity of temperature throughout the furnace. The thermocouples were calibrated by comparison with a Bureau of Standards certificated thermocouple. Temperatures were read to 0·1° C. by means of a potentiometer.

The metal parts of the apparatus were constructed of tantalum as the metal used must be non-magnetic and must not alloy with mercury. Tantalum also has the advantage of being reasonably easy to work and readily spot welded. The apparatus was supported on tungsten seals through Pyrex glass. Each of these seals was protected by a pair of guard rings. A Pyrex bulb with a tube projecting from one end for the purpose of holding the mercury, enclosed the apparatus. The tube was evacuated by a mercury diffusion pump and baked for 8 hours at 500° C. The metal parts were then glowed to a bright yellow by an induction furnace. A small amount of carefully distilled mercury was then slowly distilled into the tube and the tube sealed off from the pumps.

Method.—The apparatus was maintained at a temperature which was from 20° to 50° C. above that of the mercury. The pressure was corrected for thermal effusion and reduced to an equivalent pressure at 0° C. The temperature of the mercury was varied from —5° C. to 30° C. For temperatures below room temperature the furnace about the mercury was replaced by a cooling bath of water, ice or brine and ice. The pressure of the mercury vapour was determined from the vapour pressure data given in Landolt and Bornstein's table of physical constants. The International Critical Tables give values about 10 per cent. lower for corresponding temperatures, which would result in values of the absorption coefficient about 10 per cent. larger.

In making observations the accelerating potential was fixed. The magnetic field was then varied slowly. The current to the galvanometer connected to B rose rapidly to a maximum when the field corresponding to the accelerating potential was reached. This maximum deflection was recorded as I. At the same time the deflection of the other galvanometer that measured the total current coming from the slit was recorded as M. These measurements were repeated throughout the range of velocities studied keeping the temperature, *i.e.*, the pressure, as constant as possible. Changing the temperature values of M and I are obtained for different pressures from which the absorption coefficient could be computed.

This current M was taken to be proportional to I_0, the initial current of electrons that would have reached the collecting box had it not been for gas molecules in the path of the electrons. From the equation $I = I_0 e^{-axp}$, it should be possible to measure I_0 by making either x or p zero. If one makes the path length zero the definition of the limiting angle of deflection changes and also many electrons will be caught in the collecting box that would never have reached it due to the geometry of the apparatus. Reducing the pressure to zero will cause the emission of the filament to change due to the change in temperature and due to possible changes in the emitting surface. To ensure measurements being made under the same conditions measurements of I and I_0 should be made nearly at the same time. Taking the emission through the slit in the cylinder as proportional to I_0 these difficulties are avoided. If KM is substituted for I_0 and the value of $\alpha x p$ solved for, then

$$\alpha x p = \log (\mathrm{M}/\mathrm{I}) + \log \mathrm{K}.$$

If log (M/I) is plotted as a function of p the points will fall on a straight line whose slope is αx provided K is independent of the pressure. Fig. 2 shows some

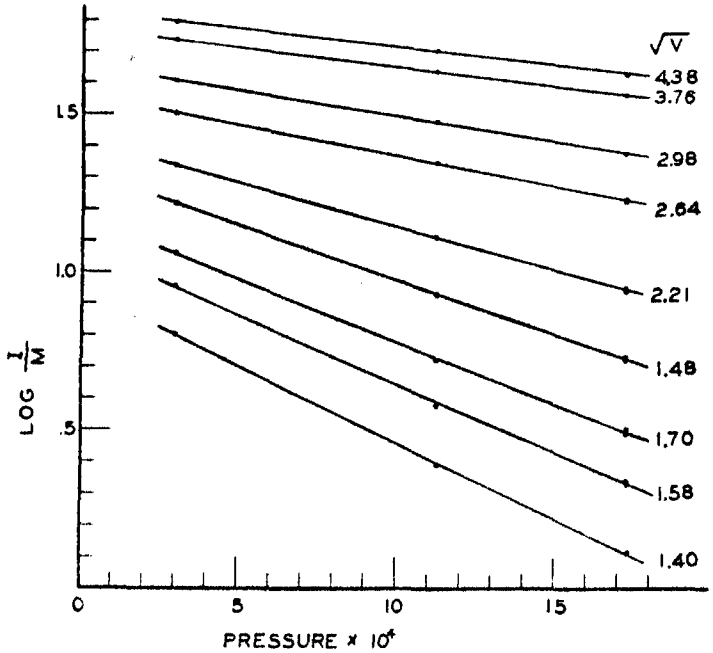

FIG. 2.

of the observed points which clearly indicates that K is independent of the pressure. The failure of all of the lines to meet at a point where p is zero means that the proportionality factor K is a function of the velocity.

The ratio of the current at the beginning of the path to that at the end of the path is under some conditions a function of the current density in the beam. If very large current densities are used the beam will spread due to the mutual repulsion of the electrons. If ionisation takes place there may be more scattering if the value of α for the ion is larger than that of the atom.

Due to the accumulation of ions along the beam the scattering may be decreased by the positives pace charge of the ions. Metastable atoms along the path may also influence the absorption coefficients by having an absorption coefficient different from that of the atom investigated. For all of these effects the amount of the additional influence is proportional to the current, and hence the loss of electrons due to scattering in any element of length is proportional to the square of the current. The scattering in an element of length of the path dx is

$$dI = (I\alpha p + I^2\beta p)\,dx,$$

β is the absorption coefficient for the amount of additional scattering material produced by unit current at unit pressure. Solving for I in terms of M gives

$$\frac{1}{I} = \frac{1}{KMe^{-\alpha xp}} + \frac{\beta(1 - e^{-\alpha xp})}{\alpha p e^{-\alpha xp}},$$

M is varied by changing the temperature of the filament and the values of I observed as a function of M. At values of M above 10^{-7} amperes I was not a linear function of M. From the above equation it can be seen that if the reciprocal of I is plotted as a function of the reciprocal of M the result should be a straight line whose slope is the reciprocal of $Ke^{-\alpha xp}$. This was found to be true for currents up to 10^{-4} amperes. For convenience in measurement the currents were kept below 10^{-7} amperes where I was proportional to M.

Results.—For each velocity six observations were made at six different pressures. Instead of using the graphical method the data was treated analytically. The value of α was calculated for each of every possible pair of observations. The average of these is shown in fig. 3. Above 10 volts the values of α in no cases differed more than 5 per cent. from the average value. Below 10 volts the data were not as consistent although the values did not differ more than 10 per cent. from the average value.

The absorption coefficient for slow electrons in mercury vapour did not show a Ramsauer effect, *i.e.*, small values of α for low velocity electrons. The value of α was large at 0·5 volt, the lowest velocity studied and decreased rapidly with increasing velocity. A small change in this decrease was observed at about 5 volts. A minimum was reached at 20 volts followed by a maximum at 35 volts from which the value of α decreased monotonously with increasing velocity to 400 volts the limit of the measurements.

Discussion.—The results of this measurement of the absorption coefficient for slow electrons in mercury vapour are compared with the results of other

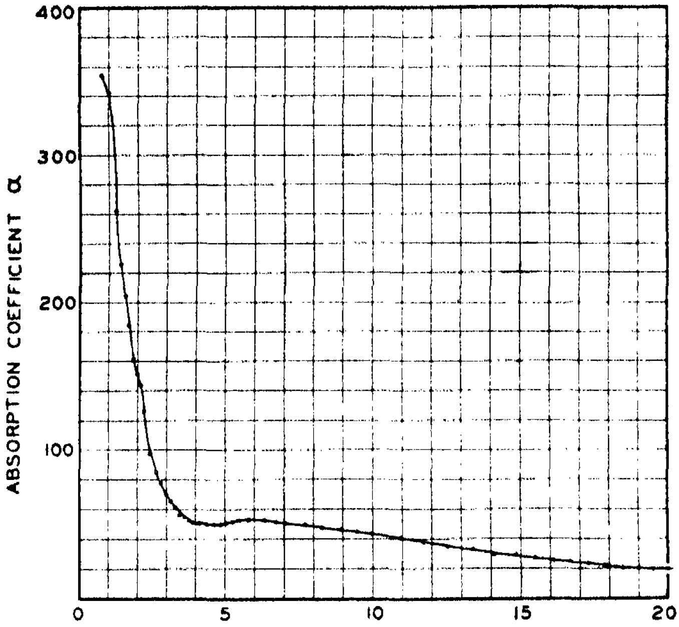

Fig. 3.

observers in fig. 4. Although the first measurements of the absorption coefficient in mercury vapour* were made with a very much simplified apparatus, the results at low velocities are in good agreement with the present result. Due to the form of this apparatus secondary and scattered electrons could not be kept from the collector at the end of the path. The possibility of errors due to this was mentioned in the discussion of these first measurements. It now appears that the results of these first measurements are too small above about 15 volts, which is what would be expected as a result of secondary and scattered electrons.

Maxwell's†‡ measurements although a little lower than the present results, are in best agreement as far as the details of the variation of the shape of the curve with velocity. He observed a break in the curve at about 5 volts, in the vicinity of the first resonance potential. Although the minimum at about 20 volts and the maximum at about 35 volts are observed by Maxwell, he

---

* Brode, 'Roy. Soc. Proc.,' A, vol. 109, p. 397 (1925).

† 'Proc. Nat. Acad. Sci.,' vol. 12, p. 509 (1926).

‡ Maxwell's own data given for the free path of electrons in mercury vapour at a pressure of 3 baryes at a temperature of 75° C. For the purpose of comparison his data has been reduced to absorption coefficients at 1 mm. of Hg at 0° C.

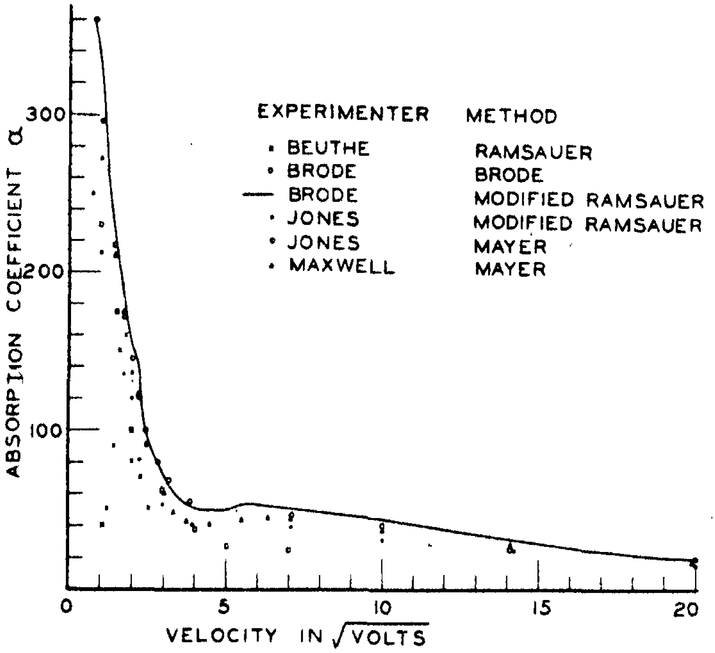

Fig. 4.

ascribes them to the influence of secondary electrons. Due to the magnetic field in the present apparatus the secondary electrons cannot start at the beginning of the path and reach the collecting box. The maximum at 35 volts is here shown to be due to a real variation in the absorption coefficient.

The measurements of Beuthe* although made with a Ramsauer type of apparatus are in complete disagreement with other observers. The construction of his apparatus was such as to make evacuation difficult. The pressure of the mercury vapour was maintained by a constriction so narrow that the rate of diffusion of the vapour out of the region containing the apparatus was small compared with the rate of evaporation. This constriction was also effective in preventing the escape of foreign gas coming off the walls of the apparatus. Due to waxed seals and brass metal parts the apparatus could not be baked out. Beuthe was unable to take consistent measurements with his apparatus. The value of the absorption coefficient decreased with the length of time the filament had been in operation until negative values were obtained. Beuthe ascribes these influences to the formation of large numbers of negative ions in the mercury vapour. It seems more reasonable to ascribe his difficulties to foreign gases accumulating in the apparatus.

---

* 'Ann. Physik,' vol. 84, p. 949 (1927).

Jones* has measured the absorption coefficient for slow electrons in mercury vapour by both a modified form of the Ramsauer apparatus and a modification of the apparatus used by Mayer.† His results do not agree well for the two methods. The values obtained by the Mayer method are in excellent agreement with the results reported here. By use of a special source of electrons he seems to have eliminated the secondary electrons and his curves indicate that there is no maximum at about 35 volts. This would appear to check the statement of Maxwell that the maximum at about 35 volts was not real but was due to secondary electrons. Jones, however, made no measurements in the region between 15 and 50 volts and was not justified in concluding from his data that Maxwell's assumption was correct.

Summary.

The absorption coefficient has been measured in mercury vapour for electrons with velocities corresponding to from 0·5 to 400 volts. No indication was found for small values of the absorption coefficient, *i.e.*, long free paths, at low velocities. A change in slope of the curve was observed at about 5 volts, a minimum at about 20 volts and a maximum at 35 volts.

---

* 'Phys. Rev.,' vol. 32, p. 459 (1928).

† 'Ann. Physik,' vol. 64, p. 451 (1921).

A Mechanism of Gelatinisation.

By FRANCIS L. USHER, The University, Leeds.

(Communicated by R. Whytlaw-Gray, F.R.S.—Received May 29, 1929.)

[PLATES 4, 5.]

In seeking to account for the transition of certain liquids to rigid jellies three main lines of explanation have been put forward, namely, (1) a micellar theory according to which the process consists in the separation of a dissolved or dispersed substance in the form of interlacing fibrils which are generally supposed to be associated with some of the solvent, any free solvent remaining enmeshed in the network so produced; (2) a theory which assumes a modification of the properties of the solvent in the neighbourhood of the disperse phase so as to produce rigidity of the whole system, without requiring any particular spacial arrangement of the solid units; and (3) an emulsion theory, which regards jellies as emulsions of two partially miscible liquid phases possessing an interfacial tension. Of these three theories, the last-named fails to provide a theoretically satisfactory explanation of the mechanical properties of jellies; it would only account for rigidity when the disperse phase occupied the major part of the total volume, and is not supported by any direct experimental evidence. The micellar theory, on the other hand, is supported in certain cases—for example, in that of sodium stearate in water, where a solid phase separates in the form of tenuous crystals—by direct ultramicroscopic observations, and a similar fibrillar structure is often assumed when no such arrangement is actually visible.* It has also been shown† that some of the elastic properties of jellies of gelatin and of cellulose acetate are best accounted for by this theory. Within the last few years an important class of reversible jellies, chiefly metallic oxides, has been investigated, and their properties have been extensively studied and described in a series of papers published from the Kaiser-Wilhelm Institut at Dahlem. In one of the earliest of these papers,‡ describing some ultramicroscopic observations of gelatinising ferric oxide sols, it was concluded that the formation of the jelly was not caused by any actual contact between the particles of ferric oxide, which remained more or less uniformly distributed in the liquid, the only apparent difference between the jelly and the sol which gave rise to it being the absence of brownian movement in the former. This observation, if correct, is evidently consistent with the second theory and definitely negatives the first. Further, measurements of the viscosity, at different rates of shear, of a number of sols, some of which are capable of gelatinising, and of suspensions of starch grains in an indifferent organic liquid* can be explained by assuming the existence of a layer of liquid adherent to the surface of the particles, its thickness being diminished as the rate of shear increases. Finally, Porter and Hedges† have pointed out that their observations on the distribution of suspended particles of gamboge under gravity can be expressed in terms of Porter's general formula of osmotic pressure if the effective volume of the particles is taken to be considerably greater than that actually measured.

---

* Darke, McBain and Salmon, 'Roy. Soc. Proc.,' A, vol. 98, p. 395 (1921); Seifriz, 'Colloid Symposium Monograph,' vol. 3, p. 285 (1925); McBain, 'J. Phys. Chem.,' vol. 30, pp. 231, 312 (1926).

† Poole, 'Trans. Faraday Soc.,' vol. 21, p. 114 (1925), and vol. 22, p. 82 (1926).

‡ Schalek and Szegvari, 'Kolloid Z.,' vol. 33, p. 326 (1923).

Apart from the possibility that a number of different explanations may be needed to account for the production of various kinds of jellies, it may be noted that, up to the present, direct observation has pointed to a fibrillar structure in some soap jellies and to an absence of structure in certain jellies formed from oxide sols. The object of the present paper is to show that sols which owe their stability to an electric charge may be expected to give rise to jellies when that charge is reduced, and to present some experimental evidence for this view.

Gelatinisation through the Action of Electrolytes.

Assuming that the stability of an aqueous suspension is due to an electric charge arising from the dissociation of molecules—whether autogenous or adsorbed—in the surface of the particles of the disperse phase, ions of one sign remaining in the surface while those of the other sign are in the surrounding liquid, the distribution of the volume charge due to the latter must conform to some kind of exponential law,‡ the exact form of which will depend on assumptions which for the present purpose need not be considered. An essential feature of the state of things presumed to exist is that the addition of a foreign electrolyte will produce one of two effects; if the surface molecules ionise completely, the total charge due to the ions, while remaining of constant magnitude, will behave as though concentrated near to the surface of the particles, or, if the ionisation is partial and reversible, the charge will be diminished owing to recombination of the ions. In either case the result must be to lessen the distance to which two particles may approach one another before they experience a given force of repulsion. When only a trace of electrolyte is present the thickness of the ionic atmosphere* is considerable, and that component of the joint kinetic energy of two particles which is parallel to the line of their approach is neutralised before they make contact or come within the range of molecular attraction; whereas in the presence of a sufficient quantity of an electrolyte the outer atmosphere shrinks to a thin shell very close to the surface of the particles (or else the total charge is reduced), so that the work required to produce contact becomes small compared with the kinetic energy, and coalescence ensues whenever a collision provides an opportunity for it. At some stage between these extreme conditions of complete stability and complete instability it must happen that the kinetic energy of the particles only just enables them to approach within the range of the molecular attractive force, and this leads to an interesting consequence. In fig. 1 (*a*) represents two particles which have just succeeded in making contact, the outer dotted line denoting the extent of the residual ionic field of force. If now a third particle collides with this binary aggregate, in order to make contact with both particles—as in (*b*)—it must possess kinetic energy sufficient to carry it through a portion of the field belonging to each, whereas it requires only about half this energy to enable it to make contact with one only, as in (*c*).

---

* Hatschek, 'Kolloid Z.,' vol. 13, p. 88 (1913); Humphrey and Hatschek, 'Proc. Phys. Soc.,' vol. 38, p. 274 (1916); Hatschek and Jane, 'Kolloid Z.,' vol. 39, p. 300 (1926), and vol. 40, p. 53 (1926).

† 'Trans. Faraday Soc.,' vol. 18, p. 91 (1922).

‡ Gouy, 'J. Physique,' vol. 9, p. 457 (1910); Debye and Hückel, 'Physik Z.,' vol. 24, p. 185 (1923).

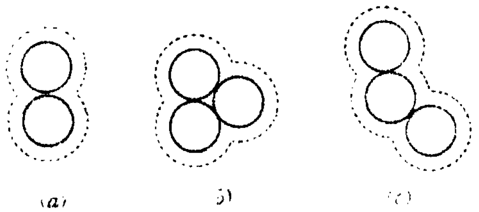

FIG. 1.

Thus over a certain limited range of electrolyte concentration collisions will result in the formation of linear aggregates rather than of compact clusters, and if sufficiently close together they will naturally tend to form a tangled network holding the liquid in its meshes. Actually, since all the particles do not possess the mean kinetic energy determined by the temperature of the system these conditions are not exactly fulfilled, so that while some particles will be unable to make contact at all, others will succeed in making contact with two simultaneously; but on the whole there will be a strong tendency to the open linear formation.

---

* That is, the thickness of some definite fraction of the outer charge, *e.g.*, nine-tenths: strictly speaking, the whole charge always extends to the outer boundary of the solution.

Experimental.

Most or all of the jellies hitherto examined have been made from sols in which the individual particles have been either too small or of insufficient optical density to be visible in the ultramicroscope, but if the view outlined above is correct gelatinisation should occur under suitable conditions in the case of sols having larger and visible particles. Although jellies can be prepared quite easily, for example, by adding the proper proportion of common salt to sols of prussian blue or copper ferrocyanide in which the larger particles can be individually distinguished, the majority are too small to be resolved, and in such cases no direct evidence of structure can be obtained. In order to see exactly what takes place and to avoid any ambiguity in interpretation, it is necessary to use material containing no particles below the limit of resolvability and to view it through an ordinary microscope by transmitted light. For this purpose a fairly uniform suspension of gamboge in water was prepared by fractional centrifuging, the final product having particles of a radius about 4×10^{-5} cm., and no appreciable number of a smaller size. Portions of this suspension were mixed with solutions of sodium chloride so that the final concentrations were known, and the mixtures were examined under a microscope, using a Pointolite lamp with a Wratten C filter. Trouble was caused by the particles attaching themselves to the slides and cover slips in the presence of the electrolyte, and since they frequently arranged themselves in long straight rows—presumably along slight fissures or scratches in the glass surface—a method was sought by which this might be avoided. The use of quartz in place of glass was found to be of no advantage, and the method finally adopted was to coat the inner surfaces of slide and cover glass with a thin film of acid sodium stearate; this substance is practically insoluble in water, and did not sensibly impair the illumination. It was found to prevent entirely the attachment of particles to the glass in rows. A ring of rubber solution round the cover glass was used to prevent evaporation. The slides were examined, usually for about half an hour at a time, at frequent intervals during 3 weeks. The following is a summary of the observations:—

A. *Gamboge mounted in water.*—Only single particles were seen, and these remained in vigorous brownian movement during the whole period.

B. *Decinormal hydrochloric acid.*—Large compact stationary clusters separated by patches of nearly clear liquid, with isolated particles fixed to the slide. In this case no brownian movement was detected at any time, and no obvious change occurred over the period of examination.

C. *Twentieth-normal sodium chloride.*—These slides showed at first only single particles in brownian movement; later a few doublets were formed, some of which were observed to break up.

D. *Decinormal sodium chloride.*—As with the preceding specimen only single particles were seen at first, afterwards many doublets and triplets and some simple rows of four and five particles. With more than three particles, however, there was always a strong tendency to branch.

E. *Fifth-normal sodium chloride.*—The appearance of this slide was very similar to that of D. There was a large number of simple rows of four particles.

F. *Normal sodium chloride.*—With this concentration the appearance was much more complex. Singles, doublets and triplets were at first numerous, but quickly gave place to larger combinations. Some of the latter, although they appeared at first sight to be compact, on turning round became resolved into long branched structures.

G.—A drop of the gamboge suspension was placed on a slide and normal sodium chloride drawn in alongside of it, so that the behaviour of the particles could be examined in an electrolyte solution at concentrations ranging downwards from a little less than normal. After 24 hours a part of the field showed strings of particles, attached at both ends, stretching obliquely from cover glass to slide. These strings were observed to be in irregular wavy motion, and their character was only determined by careful focussing.

General.

It was found that in solutions of sodium chloride of less than decinormal strength little or no permanent union between particles occurred, and that in stronger solutions the various stages of complexity reached were chiefly determined by the length of time allowed for the action of the electrolyte. A particular field in slide D, for example, was watched continuously for half an hour when first prepared, without a single permanent union between particles being observed, although when examined 24 hours later many doublets and triplets were seen. In slide E, where the electrolyte was twice as concentrated, many such unions were noticed during an equal period. This behaviour would be expected if the effect of increasing the electrolyte concentration is to increase the proportion of collisions resulting in cohesion. Extended observation of the brownian movement within small aggregates showed that, with decinormal salt, such movement hardly ever brings about closer packing of the particles, whereas with normal salt it does so. Triplets, for example, were seldom seen with their constituent particles in a straight line, but generally in the former case one of the particles, pivoting on the middle, was observed to swing about so as frequently to make apparent contact with the third without, however, adhering to it. On the other hand, in a normal solution permanent triangular combinations were frequently seen.

The importance of the brownian movement of entire aggregates is difficult to estimate since, although sometimes permanent contact between such aggregates was seen to occur, this may have been caused by slight accidental movements of the liquid. With the suspensions used for these experiments the brownian movement of aggregates containing more than 10 particles must have been very slight, although this would not be true of suspensions of much smaller particles, such as occur in the majority of stable sols. On the other hand the brownian movement of the individual particles in an aggregate appears to be of great importance in determining the final character of the system. Aggregates which in the first instance are tenuous usually bend about so that, if the electrolyte is sufficiently concentrated, the free ends often become permanently joined to other parts of the same aggregate, and in this way the general structure, initially filamentous, tends to become more compact. The process is fairly rapid in seminormal salt, and either absent or so slow as to escape notice in decinormal. When the suspensions were fairly concentrated, separate aggregates were sometimes observed to unite by the accretion of single particles, doublets, or triplets whose own brownian motion enabled them to link up the larger aggregates; and since the latter had often undergone a certain amount of internal packing, a common type of structure was a collection of loosely packed and comparatively large aggregates united by much more slender filaments, leaving lacunæ of clear liquid.

The stability of aggregates towards mechanical disturbance appears to depend on the concentration of the electrolyte present. In the weaker solutions of sodium chloride an aggregate was sometimes observed to lose one or two particles in consequence of a collision, whereas in the stronger solutions more severe disturbance was necessary. Thus in slide G, where the final electrolyte concentration was probably about third-normal, the building up of aggregates occupied 22 days, by which time no brownian movement was detectable; slight pressure on the cover glass, however, caused shearing of the aggregates with the production of a large number of single particles, which then continued in rapid brownian movement for many days.

Formation of Gels from Suspensions.

It is evident from the observations recorded above that it should be possible, by using electrolyte solutions of suitable concentration, to convert sols containing visible particles of typically lyophobic substances into rigid systems possessing the mechanical properties of jellies such as those formed from sols usually classed as emulsoid. Further, since the characteristic gel structure appears to depend on the formation of more or less linear aggregates, the factor which sets a lower limit to the proportion of the solid phase necessary to permit gelatinisation should be the product of the radius of the particles and their numerical concentration, rather than the total volume of solid. Thus if with particles of a certain radius a rigid gel requires 20 per cent. by volume of the solid phase, one should obtain a geometrically similar structure with only 0·2 per cent. of the substance when the particles have one-tenth the radius of the former. Since in practice the arrangement shows no more than a general tendency to linearity, the lower limit of volume concentration cannot be strictly proportional to the square of the radius of the particles, but should at least vary directly with it. So far as the present observations go, this expectation is fulfilled.

For the purpose of these experiments a liquid system was considered to have gelatinised if a test tube half an inch in diameter containing it could be laid on its side without any flow taking place. Gels satisfying this test have been made from gamboge suspensions containing 14 per cent. by volume of the solid, with common salt in concentration ranging from 0·22 to 0·42-normal. A specimen of one of these gels in a sealed tube has been kept for 14 months without showing any visible change in its properties. No stable gel could be prepared with a smaller proportion of gamboge which, however, being the coarser residues from the fractional centrifuging previously referred to, contained particles all larger than 4×10^{-5} cm.

With cadmium sulphide a much smaller proportion of solid can be used. A sol of cadmium sulphide prepared by passing hydrogen sulphide through the thoroughly washed precipitate suspended in water was treated with varying quantities of sodium chloride, and was found to gelatinise if the concentration of electrolyte was between centinormal and decinormal. Thus in a mixture in which the final concentration of cadmium sulphide was 1·51 per cent. by volume, decinormal sodium chloride caused gelatinisation immediately, twenty-fifth-normal in 2 minutes, and fiftieth-normal after several hours. Corresponding to the gradual contraction of filamentous aggregates observed microscopically, a general contraction of the entire gel was noticed in many instances, the upper surface of the gel settling down and leaving clear liquid above it. Fig. 2 (Plate 4) shows a photograph of five cadmium sulphide gels after standing for 48 hours; the sodium chloride concentrations (from left to right) were normal, quarter-, tenth-, twenty-fifth-, and fiftieth-normal. It will be seen that the two last-named specimens showed no contraction, and that in the three others the degree of contraction increased with the concentration of electrolyte.

The examination of prepared gels under the microscope usually gives no useful information, on account of the high numerical concentration of the particles making it impossible to distinguish the details of the structure. On the other hand the formation of purely filamentous aggregates at the dilutions necessary for satisfactory microscopic examination requires a very long time, and it has been found convenient to use for this purpose such electrolyte concentrations as would lead to the production of a contractile gel. The photographs shown in figs. 3, 4, and 5 were taken (with a "Micca" photographic eyepiece) after the structure had developed so far as to stop brownian movement. Fig. 3 (Plate 4) shows gamboge in 0·4-normal sodium chloride photographed with a Zeiss "AA" objective to give a general view of the structure, which is distinctly dendritic. Fig. 4 (Plate 5) shows a more highly magnified part of the same field photographed with a Leitz 2 mm. apochromatic lens, showing the comparatively open nature of the aggregates. Fig. 5 (Plate 5) is a high power photograph of gamboge in 0·25-normal sodium chloride, and fig. 6 (Plate 5) shows the effect of decinormal hydrochloric acid in giving rise to large isolated compact aggregates.

Conclusion.

It has been shown that suspensions of typically lyophobic materials such as gamboge and cadmium sulphide can be caused to gelatinise when mixed with sodium chloride solutions of suitable concentrations. The process has been followed microscopically with the first-named substance, and found to consist in the union of single particles to form expanded aggregates which eventually link up (if a sufficient proportion of the solid is present) to form an irregular and essentially open structure. The degree of compactness ultimately

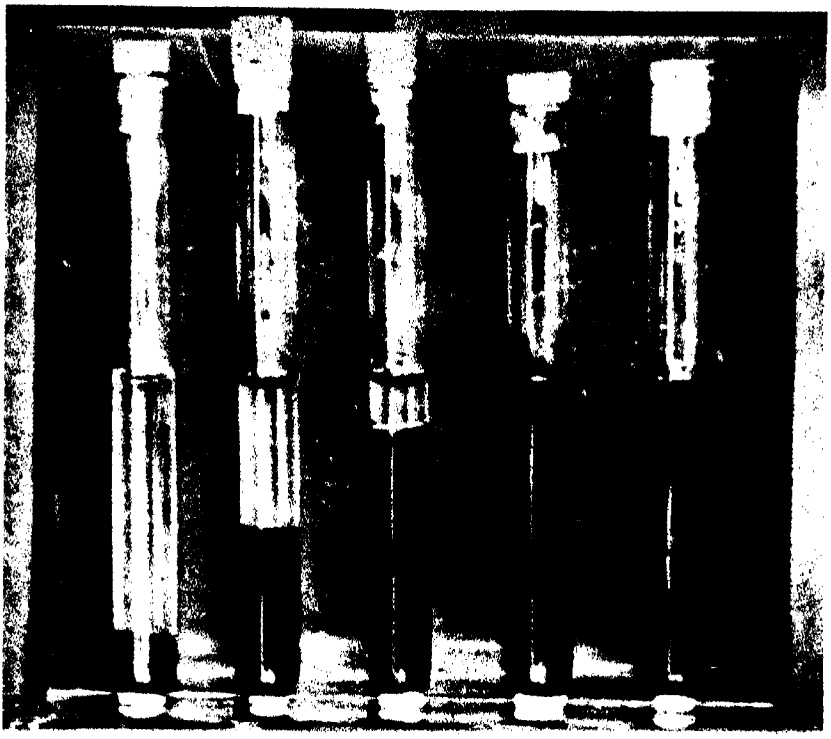

Fig. 2.

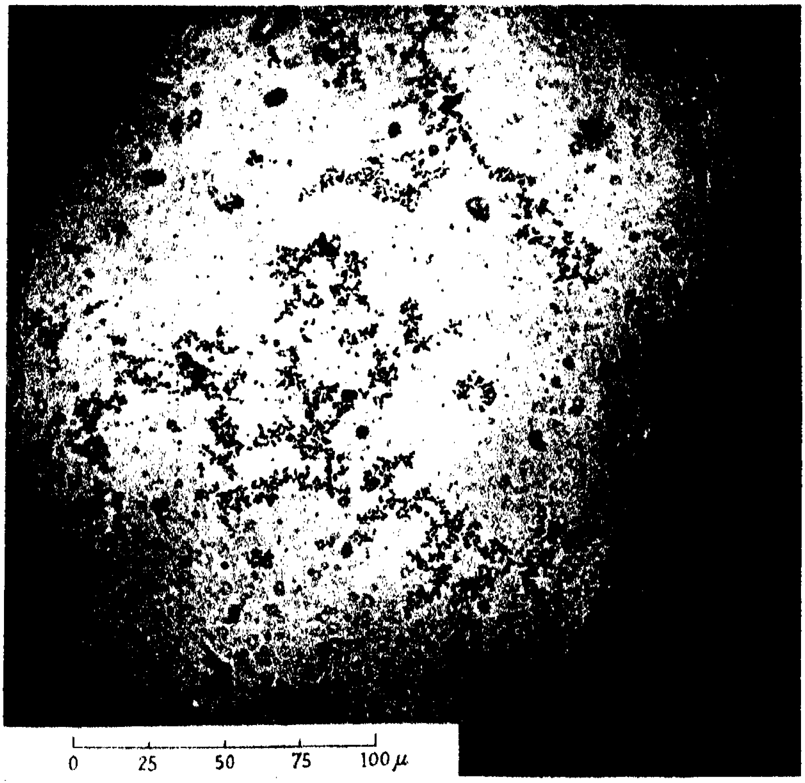

Fig. 3.

(*Facing p.* 150.)

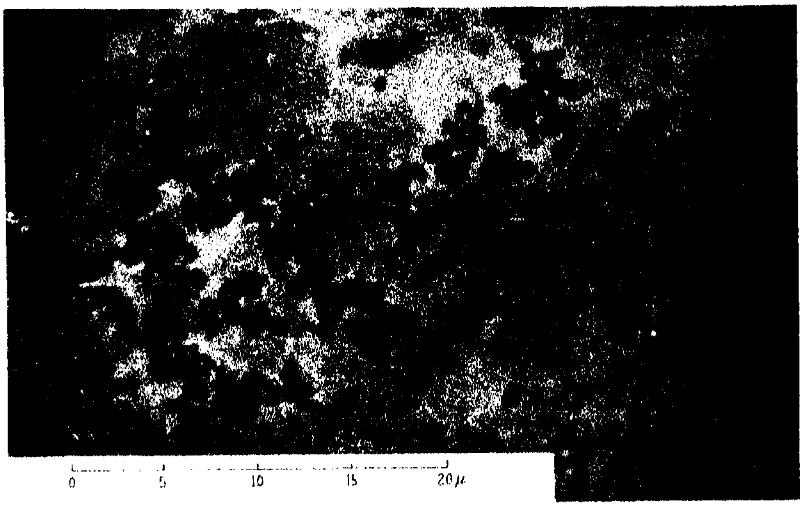

Fig. 4.

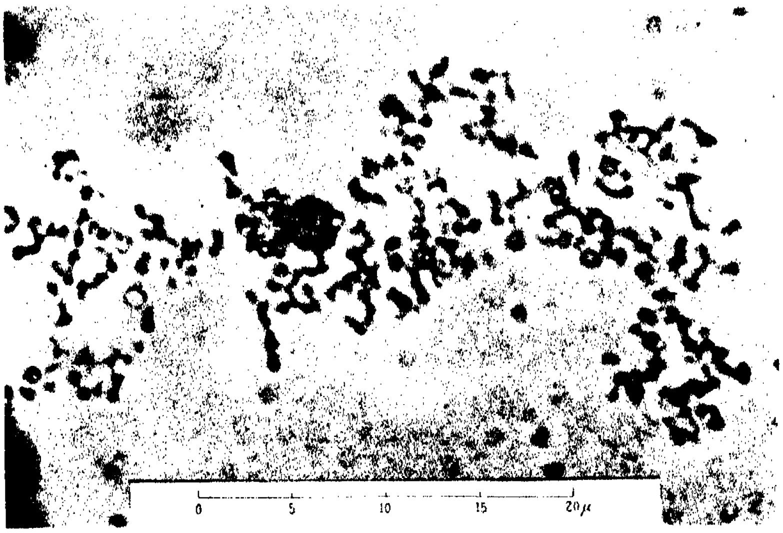

Fig. 5.

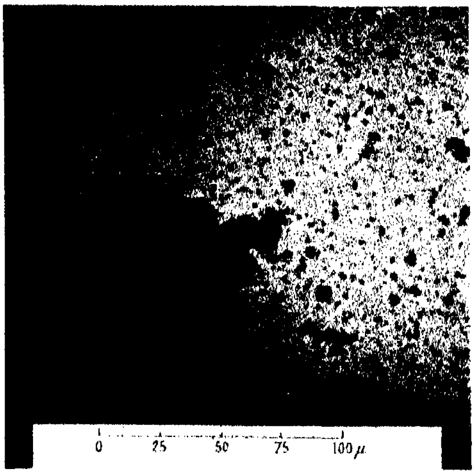

Fig. 6.

attained has been found to depend on the electrolyte concentration, the packing itself being partially due to internal brownian movement in initially linear aggregates. It is clear that if the solid framework of a rigid two-phase system becomes thickened in consequence of such internal packing, the system itself must become physically heterogeneous, and this appears to be an adequate explanation of the "syneresis" characteristic of such gels as are now being discussed. When the electrolyte is sufficiently concentrated the particles unite to form dense aggregates so rapidly that there are not enough available for linking these up into a coherent structure, and the result is a more or less dense "precipitate." A gel is therefore to be regarded as an intermediate stage in the formation of a precipitate, a stage which, however, is realised only when the volume of the solid phase bears a large enough proportion to that of the liquid, and in the presence of a suitable electrolyte at a concentration lying between rather narrow limits. The conclusions drawn by Schalek and Szegvari in the paper already referred to do not necessarily follow from their published observations. Ferric oxide sols are well known to contain at first amicrons only, and the particles seen by these authors were comparatively large crystals which had grown in the course of time from some of the original amicrons. It is suggested that the larger visible particles played no active part in the process of gelatinisation, which on the contrary was due to the union of the still invisible amicrons. It is interesting to note that Schalek and Szegvari succeeded in photographing a ferric oxide gel in which local packing of the solid (syneresis) was taking place, although naturally they were unable to observe the mechanism which produced this condition.

It is desirable to point out that the mechanism of gelatinisation discussed in this paper is considered to hold good for colloidal systems which can be induced to gelatinise by the addition of a suitable electrolyte, and not for turgescible substances like gelatin or agar. Moreover, an entirely different explanation is required for gels (rubber, cellulose esters etc.) formed in non-ionising liquids.

The Second Order Wave Equations of the Spinning Electron.

G. TEMPLE, Ph.D., Imperial College, 1851 Exhibition Research Student.

(Communicated by S. Chapman, F.R.S.—Received June 12, 1929.)

§ 1. *Introduction.*

In a previous paper† the author attempted to cast Dirac's wave equations into a tensorial form, but the results obtained were unsatisfactory as the first order equations (A) were expressed in terms of a third rank tensor, $\gamma^{\mu\nu}{}_{\alpha}$, whose significance remained obscure. In fact, tensors of the required character are not provided by the special theory of relativity, and it is not difficult to convince one's self by actual trial that there does not exist any system of equations (for a 4-vector wave function) which is equivalent to Dirac's first order equations.

It is, however, possible to construct a system of equations which is equivalent to Dirac's second order equations. This is evident from the form of the second order equations (I) of the paper cited above, for, by making the tensor $\beta_{\alpha\sigma\tau\nu}$ antisymmetric in all four suffixes, these equations are reducible to a 4-vector form. The object of this paper is to give the general theory of a system of second order equations satisfied by a wave tensor of the first rank. Vectorial notation is employed in preference to tensorial notation to facilitate comparison with the procedure of electrodynamic theory.

§ 2. *Genesis of the Wave Equations.*

A simple modification of Maxwell's equations for a super-dispersive medium yields a system of second order equations of the same form as the relativistic wave equation for free space. Starting with a wave vector **s** and a wave scalar σ we form the derived vectors

$$\mathbf{h} = \operatorname{curl} \mathbf{s} \quad \text{and} \quad \mathbf{e} = -\operatorname{grad} \sigma - \dot{\mathbf{s}}/c, \tag{2.1}$$

and write the wave equations for free space as

and

$$\left.\begin{aligned} \operatorname{curl} \mathbf{h} - \dot{\mathbf{e}}/c &= -\omega^2 \mathbf{s}, \\ \operatorname{div} \mathbf{e} &= -\omega^2 \sigma, \end{aligned}\right\} \tag{2.2}$$

---

† 'Roy. Soc. Proc.,' A, vol. 122, p. 352 (1929).

where, as before, ω denotes $2\pi m_0 c/h$. It is clear that these equations may be written in tensorial form, the components of the wave-tensor s^* being s_1, s_2, s_3 and σ/c. These equations yield the divergence relation

$$\operatorname{div} \mathbf{s} + \dot{\sigma}/c = 0, \tag{2.3}$$

and the Schrödinger-Gordon equation

$$\nabla^2\phi = \ddot{\phi}/c^2 + \omega^2\phi, \tag{2.4}$$

where ϕ stands for $\mathbf{s}$ or σ.

Guided by the form of Larmor's action function for an electromagnetic field we find that the wave equations (2.2) may be derived from the Lagrangian function

$$\omega^2(\sigma^*\sigma - \mathbf{s}^* . \mathbf{s}) + (\mathbf{e}^* . \mathbf{e} - \mathbf{h}^* . \mathbf{h}), \tag{2.5}$$

in which the asterisks denote conjugate complex quantities.

It is now a simple matter to form the corresponding equations for a region under the influence of an electromagnetic field with vector potential A and scalar potential V. We introduce the vector operator

$$\left.\begin{aligned} \mathbf{p} &= (h/2\pi\iota)\nabla + (e/c)\,\mathrm{A} \\ \text{and the scalar operator}\qquad \mathrm{D} &= -(h/2\pi\iota c)\,\partial/\partial t + (e/c)\,\mathrm{V} \end{aligned}\right\}, \tag{2.6}$$

and with them form the derived vectors,

$$\mathrm{G} = \mathbf{p}_\wedge \mathbf{s} \quad\text{and}\quad \mathrm{F} = -\,\mathbf{p}\sigma + \mathrm{D}\mathbf{s}. \tag{2.7}$$

We take the general Lagrangian function to be

$$\mathrm{L} = m_0c^2(\sigma^*\sigma - \mathbf{s}^* . \mathbf{s}) + (\mathrm{F}^* . \mathrm{F} - \mathrm{G}^* . \mathrm{G}), \tag{2.8}$$

and by varying $\mathbf{s}^*$ and σ^* we deduce the general wave equations,

$$\left.\begin{aligned} \mathbf{p}_\wedge \mathrm{G} + \mathrm{D}\mathrm{F} &= m_0^2c^2 . \mathbf{s}, \\ \text{and}\qquad \mathbf{p} . \mathrm{F} \qquad &= m_0^2c^2 . \sigma. \end{aligned}\right\} \tag{2.9}$$

§ 3. *Non-commutative Properties of the Operators.*

The characteristic feature of Dirac's theory is its use of the non-commutative properties of the operators p and D to symbolise the properties of the electron due to its spin. These properties are summarised by the following equations, (3.1) to (3.6), in which κ denotes $(he/2\pi\iota c)$ and **E**, **H** are the electric and magnetic intensities defined by

$$\mathbf{E} = -\operatorname{grad} \mathrm{V} - \partial \mathbf{A}/c\,\partial t, \quad \mathbf{H} = \operatorname{curl} \mathbf{A}.$$

$$\mathbf{p}_\wedge \mathbf{p}\sigma = \kappa\sigma\mathbf{H}. \tag{3.1}$$

$$\mathbf{p} \,.\, \mathbf{p}_\wedge \mathbf{s} = \kappa \mathbf{s} \,.\, \mathbf{H}, \tag{3.2}$$

$$\mathbf{p}\mathrm{D}\sigma - \mathrm{D}\,\mathbf{p}\sigma = -\kappa\sigma\mathbf{E}, \tag{3.3}$$

$$\mathbf{p} \,.\, \mathrm{D}\mathbf{s} - \mathrm{D}\mathbf{p} \,.\, \mathbf{s} = -\kappa\mathbf{s} \,.\, \mathbf{E}, \tag{3.4}$$

$$\mathbf{p}_\wedge \mathrm{D}\mathbf{s} - \mathrm{D}\mathbf{p}_\wedge \mathbf{s} = \kappa\mathbf{s}_\wedge \mathbf{E}, \tag{3.5}$$

$$\mathbf{p}_\wedge [\mathbf{p}_\wedge \mathbf{s}] = \mathbf{p}\,(\mathbf{p} \,.\, \mathbf{s}) - (\mathbf{p} \,.\, \mathbf{p})\,\mathbf{s} + \kappa\mathbf{s}_\wedge \mathbf{H}. \tag{3.6}$$

By making use of these properties the following relations may be deduced from the wave equations (2.9) :—
the divergence equation,

$$m_0^2c^2\,(\mathbf{p} \,.\, \mathbf{s} - \mathrm{D}\sigma) = \kappa\,(\mathbf{H} \,.\, \mathbf{G} - \mathbf{E} \,.\, \mathbf{F}), \tag{3.7}$$

corresponding to (2.3), and the generalised form of the Schrödinger-Gordon equations (2.4) for the spinning electron,

$$\left.\begin{aligned} -(\mathbf{p} \,.\, \mathbf{p})\,\sigma + \mathrm{D}^2\sigma - m_0^2c^2 \,.\, \sigma &= \kappa\mathbf{s} \,.\, \mathbf{E} - \mathrm{D}\mu \\ -(\mathbf{p} \,.\, \mathbf{p})\,\mathbf{s} + \mathrm{D}^2\mathbf{s} - m_0^2c^2 \,.\, \mathbf{s} &= \kappa\,(\sigma\mathbf{E} - \mathbf{s}_\wedge \mathbf{H}) - \mathbf{p}\mu \end{aligned}\right\}, \tag{3.8}$$

where μ denotes $(\mathbf{p} \,.\, \mathbf{s} - \mathrm{D}\sigma)$.

§ 4. *The Charge and Current Density.*

The charge density ρ and the current density $\mathbf{j}$ are determined by the equations

$$\rho = -\partial \mathrm{L}/\partial \mathrm{V} \quad \text{and} \quad \mathbf{j} = \partial \mathrm{L}/\partial \mathbf{A}, \tag{4.1}$$

whence

$$\rho = -(e/c)\,(\mathbf{s} \,.\, \mathbf{F}^* + \mathbf{s}^* \,.\, \mathbf{F}), \tag{4.2}$$

and

$$\mathbf{j} = -(e/c)\,(\sigma\mathbf{F}^* + \sigma^*\mathbf{F}) - (e/c)\,(\mathbf{s}_\wedge \mathbf{G}^* + \mathbf{s}^*{}_\wedge \mathbf{G}). \tag{4.3}$$

From these equations it follows at once that

$$\begin{aligned} \operatorname{div} \mathbf{j} + \dot{\rho}/c = &- ec^{-2}(\dot{\mathbf{s}} \,.\, \mathbf{F}^* + \mathbf{s} \,.\, \dot{\mathbf{F}}^*) - ec^{-1}(\sigma \operatorname{div} \mathbf{F}^* + \mathbf{F}^* \,.\, \operatorname{grad} \sigma) \\ &- ec^{-1}(\mathbf{G}^* \,.\, \operatorname{curl} \mathbf{s} - \mathbf{s} \,.\, \operatorname{curl} \mathbf{G}^*) + \text{conjugate}. \end{aligned}$$

Hence

$$\begin{aligned} (hc/2\pi\iota e)\,(\operatorname{div} \mathbf{j} + \dot{\rho}/c) = &\,(\mathbf{F}^* \,.\, \mathrm{D}\mathbf{s} - \mathbf{s} \,.\, \mathrm{D}^*\mathbf{F}^*) - (\mathbf{F}^* \,.\, \mathbf{p}\sigma - \sigma\mathbf{p}^* \,.\, \mathbf{F}^*) \\ &- (\mathbf{G}^* \,.\, \mathbf{p}_\wedge \mathbf{s} + \mathbf{s} \,.\, \mathbf{p}^*{}_\wedge \mathbf{G}^*) - \text{conjugate}. \end{aligned}$$

It appears from the wave equations (2.9) that the right-hand side equals

$$\mathbf{F}^* . (-\mathbf{p}\sigma + \mathrm{D}\mathbf{s}) - \mathbf{s} . (\mathbf{p}^* \wedge \mathbf{G}^* + \mathrm{D}^*\mathbf{F}^*) + m_0^2c^2\sigma^*\sigma - \mathbf{G}^* . \mathbf{G} \\ - \text{conjugate}$$

$$= m_0^2c^2(\sigma^*\sigma - \mathbf{s}^* . \mathbf{s}) + \mathbf{F}^* . \mathbf{F} - \mathbf{G}^* . \mathbf{G} - \text{conjugate}$$
$$= \mathrm{L} - \mathrm{L}^* = 0.$$

Hence ρ and $\mathbf{j}$ satisfy the equation of continuity

$$\operatorname{div} \mathbf{j} + \dot{\rho}/c = 0. \tag{4.4}$$

The preceding expressions, (4.2) and (4.3), for ρ and $\mathbf{j}$ may be transformed so as to exhibit their relation to the polarisation and magnetisation. The expressions for these vectors are

$$\mathbf{P} = \kappa(\sigma^*\mathbf{s} - \sigma\mathbf{s}^*) \quad \text{and} \quad \mathbf{M} = \kappa\mathbf{s} \wedge \mathbf{s}^*. \tag{4.5}$$

We find that

$$\rho = (\kappa/c)(\sigma\dot{\sigma}^* - \mathbf{s} . \dot{\mathbf{s}}^* - \sigma^*\dot{\sigma} + \mathbf{s}^* . \dot{\mathbf{s}}) - \operatorname{div} \mathbf{P} \\ + 2(e^2/c^2)\mathrm{V}(\sigma\sigma^* - \mathbf{s} . \mathbf{s}^*) + (e/c)(\sigma\mu^* + \sigma^*\mu), \tag{4.6}$$

$$\mathbf{j} = -\kappa(\sigma\nabla\sigma^* - \mathbf{s}\nabla\mathbf{s}^* - \sigma^*\nabla\sigma + \mathbf{s}^*\nabla\mathbf{s}) + \partial\mathbf{P}/c\partial t \\ + \operatorname{curl} \mathbf{M} + 2(e^2/c^2)\mathbf{A}(\sigma\sigma^* - \mathbf{s} . \mathbf{s}^*) + (e/c)(\mathbf{s}\mu^* + \mathbf{s}^*\mu), \tag{4.7}$$

with the convention that

$$\mathbf{s}\nabla\mathbf{s}^* = s_1\nabla s_1^* + s_2\nabla s_2^* + s_3\nabla s_3^*.$$

§ 5. *Plane Waves.*

An illustration of these results is provided by the system of plane wave represented by

$$\sigma = b \exp(2\pi\iota/h)(\mathbf{n} . \mathbf{r} - \mathrm{W}t),$$
$$\mathbf{s} = \mathbf{B} \exp(2\pi\iota/h)(\mathbf{n} . \mathbf{r} - \mathrm{W}t),$$

where b is a constant scalar and $\mathbf{B}$ a constant vector. The wave equations for free space are satisfied if

$$\mathrm{W}^2/c^2 = m_0^2c^2 + n^2,$$

and

$$b . \mathrm{W}/c = \mathbf{B} . \mathbf{n}.$$

The charge density is

$$\rho = 2e\mathrm{W}c^{-2}(b^*b - \mathbf{B}^* . \mathbf{B}),$$

and the current density is

$$\mathbf{j} = 2e\mathbf{n}/c . (b^*b - \mathbf{B}^* . \mathbf{B}),$$

whence the velocity of the charge is

$$\mathbf{v} = c\mathbf{j}/\rho = c^2\mathbf{n}/\mathrm{W}.$$

The polarisation and magnetisation are respectively

$$\mathbf{P} = \kappa(b^*\mathbf{B} - b\mathbf{B}^*) \quad \text{and} \quad \mathbf{M} = \kappa\mathbf{B}_\wedge\mathbf{B}^*,$$

and they are connected by Frenkel's kinematic relation

$$c\mathbf{P} = \mathbf{v}_\wedge\mathbf{M}.$$

§ 6. *Conclusion.*

The theory sketched in this paper reproduces the general features of Dirac's theory by employing the non-commutative properties of the operators **p** and D to introduce the spin corrections into the Schrödinger-Gordon equation. The nature of these corrections is indicated by the equation—

$$\Omega\sigma \doteqdot 2\kappa\mathbf{s}\,.\,\mathrm{E} + \frac{h^2e}{4\pi^2m_0c^2}(\mathrm{E}\,.\,\mathrm{grad}\,\sigma + \mathbf{H}\,.\,\mathrm{curl}\,\mathbf{s}),$$

which is deduced from equations (3.7) and (3.8) by writing Ω for the uncorrected operator

$$-(\mathbf{p}\,.\,\mathbf{p}) + \mathrm{D}^2 - m_0^2c^2,$$

and by neglecting the small terms.

The Ultra-Violet Spectrum of Magnesium Hydride.—II. The Many-Lined γ-System.

By R. W. B. Pearse, A.R.C.S., B.Sc., D.I.C., Demonstrator of Physics, Imperial College of Science and Technology.

(Communicated by A. Fowler, F.R.S.—Received June 10, 1929.)

Introductory.

During the course of investigation of the bands at λλ 5622, 5211 and 4845, emitted by the magnesium arc in hydrogen at low pressures, Prof. A. Fowler* observed that they were always accompanied by a further band at λ 2430 and by series of double lines in the region λ 2940 to λ 3100. These features of this spectrum seemed to merit further study in view of the important part played by the spectra of other molecules with 13 electrons (CN, BO, BeF, CO^+, $N_2{}^+$) in the classification of molecular energy levels.† Further, MgH is one of the interesting series of hydrides (BeH, MgH, CaH, ZnH, CdH, HgH) which show a pair of excited P states, with doublet separation increasing with molecular weight, closely resembling the lowest ^2P state of the preceding monovalent atoms (Li, Na, K, Cu, Ag, Au).

An account of an analysis of the band at λ 2430 was given in a previous paper;‡ the present paper deals with the series of double lines. For convenience the system in the visible region is referred to as the α-system, the one represented by the band at λ 2430 as the β-system, and that about to be described as the γ-system.

The α-system was first analysed in the form of P, Q and R branches by Heurlinger,§ using Fowler's measures. Several of the bands were later remeasured and analysed in the light of more recent quantum theory by W. W. Watson and P. Rudnick,‖ who detected an isotope effect of the magnitude to be expected theoretically for an emitter MgH. The electronic transition involved is of the type classed as $^2P \rightarrow {}^2S$.[*]

---

* 'Phil. Trans.,' A, vol. 209, p. 447 (1909). This paper contains a full list of wave-lengths of the lines of these bands. Many of the strongest lines were identified with absorption lines in the spectra of sun-spots.

† The subject of molecular electron states and their similarity to atomic states is discussed by Mulliken in a recent paper, 'Phys. Rev.,' vol. 32, p. 186 (1928). Full references to earlier papers are given.

‡ 'Roy. Soc. Proc.,' A, vol. 122, p. 442 (1929).

§ 'Dissertation,' Lund (1918).

‖ 'Astrophys. J.,' vol. 63, p. 20 (1926); 'Phys. Ref.,' vol. 29, p. 413 (1927).

The β-system is very similar to the α-system except that fewer bands appear, and was found by the writer to have the same final level. It was also classed as a $^2P \rightarrow {}^2S$ transition.

The γ-system is very different, showing no prominent heads, but appearing as an almost continuous background of very close lines stretching throughout the spectrum from λ 5000 to below λ 2100. Against this the sharply defined heads of the α and β-systems, degraded to the violet, stand out clearly. The background reaches a maximum of intensity in the region λ 3100 to λ 3500, and between λ 2940 and λ 3100 the structure becomes more open showing series apparently composed of double lines. Heads, degraded to the red and composed of relatively weak lines, can be detected at λλ 3100, 2940, 2720, 2640 and 2567. Unfortunately, much of the system near the origin is masked by the strong magnesium lines which fall in this region.

Measurements.

Plates for measurement were obtained using a quartz spectrograph of the Littrow type (Hilger's E.1). This instrument has a dispersion ranging from 2·3 A./mm. at λ 2400 to 6·3 A./mm. at λ 3240. The wave-lengths were calculated with reference to the values given by Burns[†] for the iron arc. The reductions to wave-numbers *in vacuo* were made with the aid of Kayser's "Tabelle der Schwingungszahlen."

The Vibrational Structure of the System.

The distribution of band origins about the origin of a system is usually represented by an equation of the form

$$\nu_0 = \nu_e + \omega'_0(n' + \tfrac{1}{2}) - \omega'_0 x'(n + \tfrac{1}{2})^2 - \omega''_0(n'' + \tfrac{1}{2}) + \omega_0{}''x''(n'' + \tfrac{1}{2})^2,$$

where ν_e represents the wave-number for the origin of the system, ω_0 the frequency of vibration for vanishing amplitude and zero rotation, and x a small constant arising from the anharmonic nature of the oscillation of the molecule. Integral values are given to n' and n''. Single primes refer to the initial state and the double primes to the final electronic state of the molecule.

---

[*] Mulliken, 'Phys. Rev.,' vol. 32, p. 388 (1928) and previous papers of the series. The notation used here is that used by Mulliken. Following Hund, many writers now use Σ, Π, Δ, Φ ... and σ, π, δ, φ ... for molecular states and molecular electron configurations, retaining S, P, D, F ... *s*, *p*, *d*, *f* ... for atoms only.

[†] 'Lick Observatory Bulletin,' No. 247 (1913).

Half integral values within the brackets are required in theory by the new quantum mechanics of Heisenberg and the wave-mechanics and also empirically to describe the isotope effect.

The correct assignment of values of n to the bands of this system was rendered somewhat difficult by the weakness of the heads of the bands, the considerable overlapping of bands of neighbouring sequences and the interference of strong Mg and Mg^+ lines. Under these circumstances an analysis of the rotational structure of the strongest bands was first made, and then every possible assignment of origins considered by the direct method described by W. C. Pomeroy.*

The heads at λλ 3100, 2940, 2720, 2640, 2567 were found to be formed by the R branches of simple bands consisting of R and P branches only. These bands are relatively strong and the branches can be traced for considerable distances towards the red among the many weaker lines. It was determined that the bands at λλ 2720, 2640, 2567 possessed the same final vibrational level, and that their initial levels were in progression n, $n + 1$, $n + 2$. The band at λ 2940 appeared to have no vibrational level in common with the others, but the one at λ 3100 showed the same initial level as that at λ 2720. The simplest assignment of n' and n'' satisfying an equation of the above form, and fulfilling these conditions is (1, 0), (2, 0), (3, 0) for the first three bands, (0, 1) for the fourth and (1, 3) for the fifth. This allocation of quantum numbers was finally justified by a study of the isotope effect which was measurable in the case of several of the bands. Further support was also given by the fact that other bands whose positions could be calculated from the data so far obtained were subsequently identified among the remaining data.

Two cases arise in which the positions of other bands may be readily predicted from data on three known bands in a system. In the first the three bands lie on a progression; that is, all have the same final or initial vibrational level, and from the known positions of lines of corresponding rotational states in these bands, the positions of the lines of the same rotational states in other bands of the progression may be calculated approximately. Thus, knowing the wave-numbers of R (15) in the (1, 0), (2, 0) and (3, 0) bands the wave-numbers of R (15) in the (0, 0) and (4, 0) bands may be obtained. In the other case, the bands form three corners of a square in the vibrational (n', n'') table and from the lines of the same rotational state in these bands, the corresponding lines of the band at the fourth corner may be calculated accurately by use of the combination principle. Thus

---

* 'Phys. Rev.,' vol. 29, p. 63 (1927).

$$(d', b'')\,\mathrm{R}\,(15) = (d', a'')\,\mathrm{R}\,(15) - (c', a'')\,\mathrm{R}\,(15) + (c', b'')\,\mathrm{R}\,(15).$$

This method has been described in detail by W. Jevons,[*] who first drew the author's attention to it in this form.

The wave-numbers of the origins of the bands analysed, calculated from the rotational data, are shown in Table I, and may be represented by the equation :

$$\nu_0 = 35904\cdot5 + 1138\cdot4\,(n' + \tfrac{1}{2}) - 9\cdot5\,(n' + \tfrac{1}{2})^2 - 1702\cdot2\,(n'' + \tfrac{1}{2}) + 34\cdot2\,(n'' + \tfrac{1}{2})^2.$$

The strongest bands lie on a rather wide Condon parabola as is usual where a large change of vibrational frequency takes place during the electron transition.

Table I.—Band-origins of the γ-system.

n' \ n''	0	1	2	3
0	35628·9	33993·6	32425·3	30932·6
1	36747·8	35114·0		32051·8
2	37848·2			
3	38930·6			

The Rotational Structure of the Bands.

The bands analysed consist of a single R and a single P branch, with one line missing at the origin. The wave-lengths and wave-numbers of the lines classified are given in Tables II to IX. Owing to the large change which takes place in the rotational constant B during the electron transition the head formed by the turning back of the R branch occurs very near the origin of each band and is thus composed of weak lines. Another effect of this rapid turning back of the R branch is to cause it to run along closely in step with the P branch, the two together presenting the appearance of a doublet series as described by Fowler. There are no doublets in the usual sense.

This simple structure is that characteristic of the type of transition classed as $^1\mathrm{S} \rightarrow {}^1\mathrm{S}$. If the system is to be assigned to the molecule MgH which has an odd number of electrons (13) the electron levels should be double and the

---

[*] 'Roy. Soc. Proc.,' A, vol. 112, p. 414 (1926).

Table II.—Structure of the (0, 0) Band.

j_n	R branch.		P branch.	
	λ air.	ν.	λ air.	ν.
0				
1				
2			2808·179	35599·79
3			09·802	579·24
4			11·853	553·29
5			14·037	525·70
6	2807·813	35604·44	16·581	493·60
7	09·451	583·68	19·580	455·86
8	11·163	562·01	22·687	416·84
9	13·340	534·49	26·187†	372·98
10	15·827	503·11	30·012	325·17
11	18·599†	468·20	34·167	273·39
12	21·763	428·43	38·647	217·72
13	25·136	386·14	43·407	35158·77
14	28·853†	339·64	............*	....
15	32·947	288·58	............*	....
16	37·321	234·18	............*	....
17	42·001	176·16	65·648	34885·90
18	46·975†	35114·71	72·011	808·62
19	............*	....	78·667	728·13
20	57·932	34980·08	85·630	644·34
21	63·844	907·88	2892·908	557·19
22	70·160†	831·07	2900·513	466·59
23	76·653	752·45	08·429	372·78
24	83·508	669·84	16·620	276·25
25	90·672	583·92	25·126	176·59
26	2898·160†	494·57	33·970	34073·57
27	2905·915	402·52	43·047	33968·49
28	13·995	307·13	52·484	859·91
29	22·364	208·89	62·200	748·86
30	31·059	34107·41	72·234	634·94
31	............*	....	82·504	519·12
32	49·226	33897·32	2993·105	399·91
33	58·737	788·36	3004·022	279·04
34	....	....	15·122†	156·52
35	78·667	562·30		

* Indicates that line is blended with or obscured by a line of the Mg or Mg^+ spectrum.
† Indicates line blended with another band line.

transition therefore $^2S \rightarrow {}^2S$. Evidence of this multiplicity would lie in the detection of a close-spaced doubling in each line, the doubling increasing in magnitude with the rotational energy as in the violet CN bands. This, however, has not been detected. Since, however, a $^2S \rightarrow {}^2S$ system with the doublets unresolved would appear identical with a $^1S \rightarrow {}^1S$ system the experimental data do not decide between the alternative interpretations of a $^1S \rightarrow {}^1S$ transition or a $^2S \rightarrow {}^2S$ transition with fine structure doubling less than 3·0 cm.$^{-1}$ even at such high rotations as $j = 30$. Such a small value is not unlikely

Table III.—Structure of the (1, 0) Band.

j_k.	R branch.		P branch.	
	λ air.	ν.	λ air.	ν.
0	2719·826	36756·20		
1	19·561	759·77	2721·323	36735·84
2	19·561	759·77	22·565	719·22
3	19·826	756·20	24·199	697·19
4	20·428	748·06	26·028	672·57
5	21·323	735·84	28·217	643·16
6	22·565	719·22	30·697	609·93
7	24·051	699·19	33·430	573·27
8	25·872	674·67	36·545	531·64
9	28·020	645·80	39·892	487·02
10	30·471	612·91	43·584	437·69
11	33·210	576·21	47·585	384·86
12	36·266	535·36	51·906	327·73
13	39·620	490·64	56·507	267·15
14	43·292	441·81	61·410	202·72
15	47·260	389·18	2766·624	36134·49
16	51·534	332·66	............*	....
17	56·092	272·36	............*	....
18	61·004	208·04	............*	....
19	2766·179	36140·31	............*	....
20	............*	....	............*	....
21	............*	....	............*	....
22	............*	....	2812·167	35549·32
23	............*	....	19·580	455·86
24	............*	....	27·310	358·93
25	............*	....	35·547	256·22
26	2810·956	35564·63	44·095	35150·26
27	18·599	468·20	............*	....
28	26·416	370·11	62·088	34929·29
29	34·574	268·32	71·489	814·95
30	43·088	35162·72	81·191	697·72
31	............*	....	2891·220	577·36
32	60·868	34944·19	2901·498	454·88
33	70·160	831·07	12·046	330·09
34	79·768	714·86	22·871	202·95
35	89·615	596·57	33·970	34073·57
36	2899·768	475·44	45·321	33942·26
37	2910·166	352·27	56·989	808·33
38	20·806	227·13	68·943	672·21

* Indicates that line is blended with or obscured by a line of the Mg or Mg^+ spectrum.

for the light molecule MgH, but there are reasons, considered later, for assigning the system to the ionised molecule MgH^+ and this being an even molecule, would require it to be $^1S \rightarrow {}^1S$.

Term Structure.

The notation throughout is that adopted by Mulliken,[*] in his well-known series of papers, for the systematic interpretation of the empirical data on

---

[*] 'Phys. Rev.,' vol. 32, p. 388 (1928), and previous papers.

Table IV.—Structure of the (2, 0) Band.

j_k.	R branch.		P branch.	
	λ air.	ν.	λ air.	ν.
0	2640·795	37856·12		
1	40·490	860·49		
2	40·490	860·49	2643·408	37818·71
3	40·795	856·12	44·863	797·91
4	41·419	847·18	46·616	772·88
5	42·343	833·96	48·678	743·47
6	43·549	816·70	51·090	709·12
7	45·060	795·11	53·773	671·02
8	46·872	769·22	56·781	628·36
9	48·970	739·31	60·000	582·82
10	51·390	704·87	63·568	532·48
11	54·092	666·49	67·429	478·14
12	57·105	623·78	71·600	419·65
13	60·416	576·96	76·076*	357·07
14	63·996	526·45	80·802	291·23
15	67·904	471·53	85·882	220·68
16	72·092	412·76	91·233	146·69
17	76·582	350·01	2696·876	37068·96
18	81·375	283·25	2702·830	36987·31
19	86·460	212·67	09·072	902·10
20	91·852	138·15	15·605	813·33
21	2697·526	37060·07	22·420	721·18
22	2703·506	36978·07	29·577	624·91
23	09·765	892·65	37·011	525·43
24	16·314	803·72	44·710	422·98
25	23·161	711·19	52·745	316·66
26	30·307	615·12		
27	37·723	515·92		
28	45·468	412·92		
29	53·483	306·93		

* Indicates line blended with another band line.

band spectra in terms of Hund's* electron spin theory of molecular states.

In the present paper only S type states have to be considered. These are characterised by the fact that the component of orbital electronic angular momentum parallel to the internuclear axis, denoted by σ_k, is zero.† As in the case of atoms the electrons orient themselves so that all are parallel or anti-parallel to any one, giving a resultant spin electronic angular momentum denoted by s. The values 0, $\frac{1}{2}$, 1, ... for s give rise to singlet, doublet, triplet, ... states.

---

* 'Z. Physik,' vol. 43, p. 805 (1927), and previous papers.

† In Mulliken's most recent papers σ_k is denoted by σ_l. For S, P, D, ... levels $\sigma_l = 0, 1, 2, \dots$.

Table V.—Structure of the (3, 0) Band.

j_k.	R branch.		P branch.	
	λ air.	ν.	λ air.	ν.
0	2567·336	38939·22		
1	67·150	942·04	2568·728	38918·12
2	67·150	942·04	69·833	901·39
3	67·510	936·58	71·332	878·71
4	68·155	926·80	72·991	853·64
5	69·079	912·79	74·988	823·51
6	70·286	894·52	77·285	788·92
7	71·783	871·89	79·882	749·87
8	73·571	844·89	82·753	706·80
9	75·662	813·35	85·923	659·37
10	78·055	777·33	89·354	608·13
11	80·731	737·12	93·100	552·36
12	83·683	692·89	2597·158	492·28
13	86·928	644·34	2601·482	428·16
14	90·479	591·38	06·114	359·86
15	94·311	534·37	11·046	287·42
16	2598·437	473·19	16·221	211·69
17	2602·866	407·72	21·702	131·80
18	07·585	338·22	27·499	38047·66
19	12·581	264·91	33·604	37959·48
20	17·859	187·77	39·948	868·27
21	23·458	106·29	46·616†	772·88
22	29·329	38021·20	53·550	674·16
23	35·489	37932·35	............*	....
24	41·926	839·94	68·298	465·82
25	48·678†	743·47	76·076†	357·14
26	55·680	643·96	84·192	244·11
27	62·978	540·79	2692·568	128·28
28	70·556	434·28	2701·173†	37009·99
29	78·423	324·34	10·160	36887·28
30	86·584	210·96	19·380	762·21
31	2695·017	37094·53	28·899	633·99
32	2703·719	36975·15	38·669	503·31
33	12·699	852·80	48·733	369·67
34	21·971	727·22	59·054	233·63
35	31·480	599·39		
36	41·274	468·63		

* Indicates that line is blended with or obscured by a line of the Mg or Mg^+ spectrum.
† Indicates line blended with another band line.

In general s interacts with the rest of the molecule in one of two ways, called by Hund "case a" and "case b." In case a, which can only occur with $\sigma_k > 0$, s is coupled magnetically with σ_k and oriented to form a component along the internuclear axis denoted by σ_s, which takes the values $-s$, $-(s-1)$, ... s. The total electronic angular momentum about the axis is denoted by σ, which is therefore equal to $\sigma_k + \sigma_s$. The resultant of σ and the nuclear angular momentum is the total angular momentum and is denoted by j. The

Table VI.—Structure of the (0, 1) Band.

j_k	R branch.		P branch.	
	λ air.	ν.	λ air.	ν.
0	2940·193	34001·45		
1	39·763	006·43	2941·882	33981·94
2	39·502	009·45	43·278	965·82
3	39·763	006·43	45·007	945·88
4	40·252	34000·72	46·962	923·36
5	41·127	33990·67	49·226	897·32
6	42·259	977·58	51·913	866·47
7	43·698	960·98	54·871	832·56
8	45·489	940·33	58·090	795·74
9	47·570	916·36	61·688	754·93
10	49·962	888·86	65·551	710·73
11	52·695	857·50	69·741	663·17
12	55·725	822·79	74·268	611·93
13	59·052	784·77	79·075	557·71
14	62·706	743·10	84·208	499·98
15	66·703	697·64	89·639	439·13
16	70·928	649·71	2995·380	375·05
17	75·514	597·86	3001·432	307·75
18	80·390	542·90	07·798	237·25
19	85·587	484·51	14·484	163·54
20	91·072	423·11	21·434	087·26
21	2996·885	358·29	28·713	33007·74
22	3002·973	290·65	36·291	32925·37
23	09·349	220·13	44·193	839·91
24	16·090	145·88	52·318	752·49
25	23·075	33069·31	60·761	662·15
26	30·359	32989·82	69·515	569·00
27	37·911	907·81	78·545	473·48
28	45·767	822·94	3087·867	375·44
29	53·900	735·52	...........*	...........*
30	62·315	645·57	3107·340	172·56
31	71·003	553·22	17·474	32067·98
32	79·947	458·70	27·852	31961·59
33	89·179	361·69	38·497	853·18
34	3098·647	262·81	49·415	742·76
35	3108·282	162·81	60·578	630·65
36	18·240	32060·10	71·975	517·01
37	28·435	31955·63	83·599	401·93
38	38·824	849·87	95·421	285·77
39	49·415	742·76	3207·447	168·46
40	60·258	633·85	19·680	050·05

* Indicates that line is blended with or obscured by a line of the Mg or Mg^+ spectrum.

different values of σ for any state of nuclear rotation give rise to the multiplet components. The values of j are $|\sigma|$, $|\sigma + 1|$, ...

In case *b*, which always holds for S states, the forces on s due to molecular rotation are large compared with those between s and σ_k, the spin axis is only loosely coupled to the rest of the molecule and makes a constant angle only with j. Under these circumstances the total angular momentum excluding

Table VII.—Structure of the (1, 1) Band.

j_k.	R branch.		P branch.	
	λ air.	ν.	λ air.	ν.
0	2846·262	35123·50		
1	46·057	126·03		
2	46·057	126·03	2849·116	35088·31
3	46·262	123·50	50·952*	065·72
4	46·649*	116·86	............*	....
5	47·616	106·80	55·179	35013·81
6	48·740	092·95	57·635	34983·72
7	50·253	074·32	60·502	948·66
8	51·983	35053·05	63·640	910·36
9	............*	....	67·070	868·60
10	56·449	34998·34	70·794	823·37
11	59·107	965·71	74·867	774·04
12	62·088	929·29	79·210	721·59
13	65·385	889·10	83·842	665·82
14	68·968	845·53	88·807	606·24
15	72·862†	799·01	94·077	543·23
16	77·036	747·82	2899·601	477·43
17	81·540	693·52	2905·479	407·67
18	86·323	636·03	11·620	335·11
19	91·411	575·08	18·064	259·29
20	2896·818	510·55	24·826	180·09
21	2902·481	443·21	31·796	098·84
22	08·429	372·78	39·198†	34012·97
23	14·720	298·60	46·772	33925·55
24	21·276	221·63	54·651	835·08
25	............*	....	62·858	741·37
26	35·199†	34059·30	71·311	645·38
27	42·612	33973·51	80·090	546·28
28	50·214	885·97	89·123†	444·90
29	58·232	794·13	98·394	341·50
30	66·474	700·24		
31	74·934	604·41		
32	83·830	504·23		
33	93·105	399·91		

* Indicates that line is blended with or obscured by a line of the Mg or Mg^+ spectrum.
† Indicates line blended with another band line.

spin, denoted by j_k is quantised and takes the values $j_k = |\sigma_k|, |\sigma_k + 1|, \ldots$ The different orientations of s then give rise to the values of $j = |j_k - s|, \ldots, |j_k + s|$ for the total angular momentum.

In ^1S states $s = 0$; $\sigma_k = 0$; and therefore $j = j_k = 0, 1, 2 \ldots$ and represents the nuclear angular momentum alone.

In ^2S states $s = \frac{1}{2}$; $\sigma_k = 0$ and therefore $j_k = 0, 1, 2, \ldots$, and $j = j_k \pm \frac{1}{2}$.

In the tables showing the P and R branches of the bands, the lines have been numbered according to their j_k values. If the levels are ^1S these values are also the j values. If they are ^2S then each line is a very close pair having $j = j_k \pm \frac{1}{2}$ respectively.

Table VIII.—Structure of the (0, 2) Band.

j_k.	R branch.		P branch.	
	λ air.	ν.	λ air.	ν.
0				
1				
2				
3				
3				
5				
6				
7				
8				
9				
10			3108·282	32162·81
11			12·500	119·23
12			16·985	073·02
13	3099·827	32250·54	21·810	32023·44
14	3103·150	216·00	26·912	31971·20
15	07·084	175·21	32·503	914·13
16	11·226	132·38	38·043	857·79
17	15·616	087·11	44·022	797·21
18	20·305	32038·89	50·344	733·40
19	25·298	31987·71	56·944	667·07
20	30·546	934·08	63·821	598·23
21	36·116	877·37	70·987	526·83
22	41·969	817·99	78·440	452·90
23	48·097	756·05	86·172	376·58
24	54·493	691·67	3194·170	298·02
25	61·173	624·70	3202·455	217·05
26	68·163	554·93	10·976	134·21
27	....	....	19·680	31050·05
28	82·861	409·22	28·839	30961·97
29	90·576	333·27	38·107	873·36
30	3198·565	255·01		
31	3206·749	175·25		
32	15·186	093·44		
33	23·875	31009·65		
34	32·713	30924·87		
35	41·825	837·95		

Using the form of rotational energy function given by the wave mechanics* for the rigid rotator with free axis, the rotational terms in wave-number units may be represented by

$$F(j_k) = Bj_k(j_k + 1) \ldots$$

for a ^1S state, and by

$$F(j_k) = Bj_k(j_k + 1) \pm c(j_k + \tfrac{1}{2}) \ldots$$

where c is a small constant,† for a ^2S state.

---

* *Cf.* E. Schrödinger, " Collected Papers on Wave Mechanics," p. 35.

† *Cf.* Mulliken, ' Phys. Rev.,' vol. 32, p. 399 (1928). The values of c given for CaH and OH are 0·0225 and 0·11. In Mulliken's paper the empirical term $\pm cj_k$ was used, the form $\pm c(j_k + \frac{1}{2})$ is that due to Van Vleck, ' Phys. Rev.,' vol. 33, p. 467 (1929), and has a theoretical basis.

Table IX.—Structure of the (1, 3) Band.

j_k.	R branch.		$\dot{\mathrm{P}}$ branch.	
	λ air.	ν.	λ air.	ν.
0				
1				
2				
3			3122·936	32011·90
4			25·298	31987·71
5			27·852	961·59
6			30·546	934·08
7			....	....
8	3122·936	32011·90	36·885†	869·55
9	24·705	31993·78	40·329	834·61
10	26·912*	971·20	44·022	797·21
11	....	....	48·097	756·05
12	31·883	920·45	52·330	713·41
13	34·820	890·55	56·944	667·07
14	38·043	857·79	61·769	618·74
15	41·580	821·93	66·916	567·36
16	45·322	784·07	72·349	513·29
17	49·415*	742·76	78·018	457·08
18	53·746	699·17	83·961	398·37
19	58·299	653·47	90·162	337·33
20	63·160	604·84	3196·638	273·85
21	68·163*	554·93	3203·336	208·46
22	73·683	500·04	10·311	140·66
23	79·351*	443·90	17·522	31070·87
24	85·230	385·86	24·981	30999·01
25	91·341	325·76	32·713†	924·87
26	3197·687	263·60	40·631	849·31
27	3204·278	199·29		
28	10·976*	134·21		
29	17·612*	31065·48		
30	25·320	30995·76		
31	32·713	924·87		
32	40·323	852·24		

* Indicates line blended with another band line.

On account of the imperfect rigidity of a molecule an additional term becomes necessary at large j_k values to allow for the "expansion" of the molecule at high rotations; this takes the form shown in the equation

$$\mathrm{F}(j_k) = \mathrm{B}j_k(j_k+1) - \mathrm{D}\{j_k\ (j_k+1)\}^2 \ldots$$

For the state of no vibration it has been shown theoretically* that

$$\mathrm{D}_0 = 4\mathrm{B}_0{}^3/\omega_0{}^2.$$

---

* 'Bulletin Nat. Res. Council U.S.,' No. 57, "Molecular Spectra in Gases," article by Birge, p. 172.

The P and R branches result from the transitions $\Delta j_k = \pm 1$ and are defined by

$$P(j_k) = F'(j_k - 1) \rightarrow F''(j_k)$$
$$R(j_k) = F'(j_k + 1) \rightarrow F''(j_k).$$

Values of the quantities $\Delta_2 F'(j_k)$ and $\Delta_2 F''(j_k)$ defined by :—

$$\Delta_2 F'(j_k) = F'(j_k + 1) - F'(j_k - 1)$$
$$\Delta_2 F''(j_k) = F''(j_k + 1) - F''(j_k - 1)$$

are obtained from the following combinations of lines

$$\Delta_2 F'(j_k) = R(j_k) - P(j_k)$$
$$\Delta_2 F''(j_k) = R(j_k - 1) - P(j_k + 1).$$

Values thus obtained represent the " observed " values of Tables X and XI. The " calculated " values are those obtained from the above form of rotational energy term using the values of B_n and D_n indicated in the tables. These values of B_n and D_n were calculated in each case from several of the observed values of the Δ_2F's. The calculated values fit the observed values well except for small regular departures which occur at very small and very large values of j_k. The departures at high j_k values may be explained as due to neglect of higher power terms in the rotation function. The departures at low values of j_k are not simple, and the data are not sufficiently accurate for an attempt to represent them by an additional term.

The values of B_n' and B_n'' obtained may be represented by the equations

$$B_n' = 4 \cdot 3020 - 0 \cdot 0492\,(n + \tfrac{1}{2}) - 0 \cdot 0050(n + \tfrac{1}{2})^2,$$
$$B_n'' = 6 \cdot 3782 - 0 \cdot 1854\,(n + \tfrac{1}{2}).$$

The values of D_n' and D_n'' do not show definitely a regular variation with n. The mean values are therefore compared with the values calculated from the values of B_0', ω_0' and B_0'', ω_0''.

$$D_n' = 2 \cdot 16 \times 10^{-4}, \quad 4B_0'^3/\omega_0'^2 = 2 \cdot 46 \times 10^{-4},$$
$$D_n'' = 3 \cdot 45 \times 10^{-4}, \quad 4B_0''^3/\omega_0''^2 = 3 \cdot 58 \times 10^{-4}.$$

The values of the moments of inertia I_0 and internuclear distance r_0 are

$$I_0' = 6 \cdot 439 \times 10^{-40} \text{ gm. cm.}^2, \quad r_0' = 2 \cdot 02 \times 10^{-8} \text{ cm.}$$
$$I_0'' = 4 \cdot 343 \times 10^{-40} \text{ gm. cm.}^2, \quad r_0'' = 1 \cdot 65 \times 10^{-8} \text{ cm.}$$

Table X.—Comparison of Observed and Calculated Values of $\Delta_2F'(j_k)$.

v'.	0.				1.				2.				3.		
	$B_0'=4\cdot2762$. $D_0'=2\cdot143\times10^{-4}$.				$B_1'=4\cdot2165$. $D_1'=2\cdot239\times10^{-4}$.				$B_2'=4\cdot1480$. $D_2'=2\cdot186\times10^{-4}$.				$B_3'=4\cdot0682$. $D_3'=2\cdot060\times10^{-4}$.		
j_k.	Calc.	Obs.—Calc.			Calc.	Obs.—Calc.			Calc.	Obs.—Calc.			Calc.	Obs.—Calc.	
		(0, 0).	(0, 1).	(0, 2).		(1, 0).	(1, 1).	(1, 3).		(2, 0).				(3, 0).	
1	25·65		−1·16		25·29	−1·64			24·88				24·40	−0·48	
2	42·73		+0·90		42·14	−1·58			41·45				40·65	0·00	
3	59·79		+0·76		58·95	+0·06	−1·17		57·99				56·88	+0·99	
4	76·81		+0·55		75·73	−0·24			74·49	−0·18†			73·07	+0·09	
5	93·79		−0·11		92·45	+0·24	+0·54		90·96	−0·47			89·22	+0·06	
6	110·70	+0·14	+0·41		109·13	+0·21	+0·10		107·36	+0·22			105·31	+0·29	
7	127·56	+0·26	+0·86		125·73	+0·25	−0·07		123·69	+0·41			121·35	+0·67	
8	144·34	+0·83†	+0·25		142·25	+0·93	+0·44		139·94	+0·93			137·30	+0·79	
9	161·02	+0·49	+0·41		158·68	+0·11			156·11	+0·38			153·17	+0·81	
10	177·60	+0·34	+0·53		175·00	+0·22	−0·03		172·18	+0·21			168·94	+0·26	
11	194·09	+0·72	+0·24		191·22	+0·14	+0·45		188·14	+0·21			184·62	+0·14	
12	210·45	+0·36	+0·41		207·31	+0·32	+0·39		203·97	+0·16			200·18	+0·44	
13	226·67	+0·70†	+0·39		223·26	+0·29	+0·02		219·67	+0·22†			215·61	+0·57	
14	242·77		+0·35		239·08	+0·01	+0·21	−0·03	235·23	0·00			230·92	+0·60	
15	258·72		−0·21		254·73	−0·04	+1·05†	−0·36	250·65	+0·20			246·07	+1·01	
16	274·51		+0·15	+0·28	270·22		+0·17	+0·56	265·89	+0·18			261·08	+0·43	
17	290·12	+0·14	−0·01	−0·22	285·54		+0·31	+0·14	280·96	+0·19			275·92	0·00	
18	305·56	+0·53†	+0·09	−0·07	300·65		+0·27	+0·15	295·85	+0·09			290·59	−0·04	
19	320·80		+1·17	−0·16	315·58		+0·21	+0·56	310·55	+0·02			305·08	+0·34	
20	335·85	−0·11	0·00	0·00	330·29		+0·17	+0·70	325·05	−0·23			319·37	+0·13	
21	350·68	+0·01	−0·13	+0·48	344·79		−0·40	+1·68	339·32	+0·47			333·46	−0·05†	
22	365·30	−0·82†	−0·02	−0·21	359·06		+0·75	+0·32	353·37	−0·20			347·34	−0·30	
23	379·68	−0·01	+0·54	−0·21	373·07		−0·02	+0·04	367·18	+0·04			360·99	−0·42	

24	393·83	−0·24	−0·44	−0·18		386·85		−0·30	0·00	380·75	0·00			374·41	−0·29	
25	407·71	−0·38	−0·45	−0·06		400·35			+0·54	394·07	+0·47			387·60	−1·27†	
26	421·34	−0·34	−0·52	−0·62		413·58	+0·79	+0·34	+0·71	407·09				400·53	−0·68	
27	434·69	−0·66	−1·26	−2·04		426·53		+0·70		419·87				413·19	−0·67	
28	447·77	−0·55	−0·27	−0·52		439·18	+1·64	+0·89		432·35				425·59	−1·29†	
29	460·54	−0·51				451·53	+1·84	+1·10		444·53				437·71	−0·65	
30	473·02	−0·55	−0·01			463·55	+1·45			456·40				449·52	−0·27	
31	485·17		+0·07			475·25	+0·94			467·95				461·04	−0·50	
32	497·02	+0·39	+0·09			486·62	+2·69			479·16				472·26	−0·42	
33	508·51	+0·81	0·00			497·62	+3·36			490·04				483·14	0·00	
34	519·67		+0·38			508·28	+3·63			500·56				493·69	−0·09	
35	530·47		+1·69			518·56	+4·44			510·73				503·91		
36	540·92		+2·17			528·46	+4·72			520·52				513·78		
37	550·97		+2·73			537·97	+5·97			529·93				523·28		
38	560·65		+3·45			547·07	+6·85			538·94				532·41		
39	569·93		+4·37			555·77				547·55				541·17		
40	578·80		+5·00			564·03				555·75				549·52		

† Indicates that one of the lines from which $\Delta_2F(j_k)$ was obtained is a blend.

Table XI.—Comparison of Observed and Calculated Values of Δ_2F'' (j_k).

v''.	0.					1.				2.				3.			
	$B_0''=6\cdot2855$. $D_0''=3\cdot406\times10^{-4}$.					$B_1''=6\cdot0968$. $D_1''=3\cdot357\times10^{-4}$.				$B_2''=5\cdot9148$. $D_2''=3\cdot456\times10^{-4}$.				$B_3''=5\cdot7292$. $D_3''=3\cdot567\times10^{-4}$.			
j_k.	Calc.	Obs.—Calc.				Calc.	Obs.—Calc.			Calc.	Obs.—Calc.			Calc.	Obs.—Calc.		
		(0, 0).	(1, 0).	(2, 0).	(3, 0).		(0, 1).	(1, 1).	(2, 1).		(0, 2).	(1, 2).	(2, 2).		(0, 3).	(1, 3).	(2, 3).
1	37·70		—0·72		—0·07	36·58	—0·98	—1·39†		35·48				34·37			
2	62·81		—0·23		+0·52	60·92	—0·37	—0·61		59·10				57·24			
3	87·68		—0·46		+0·72	85·24	+0·85			82·68				80·08			
4	112·88		+0·16	—0·22	+0·19	109·49	—0·38	+0·20		106·21				102·86			
5	137·82		+0·36	+0·22	—0·06	133·67	+0·73	—0·53		129·66				125·55			
6	162·66		—0·09	+0·28	+0·26	157·77	+0·67	+0·37		153·01				148·16			
7	187·41	+0·19	+0·16	+0·93	+0·31	181·75	+0·09	+0·84		176·26				170·66			
8	212·02	—1·52†	+0·16	+0·28	+0·50	205·62	+0·43	+0·10		199·38				193·02			
9	236·49	+0·35	+0·49	+0·25	+0·27	229·36	+0·24	+0·32		222·37				215·24			
10	260·81	+0·29	+0·13	+0·36	+0·18	252·94	+0·25			245·20				237·31			
11	284·96	+0·43	+0·22	+0·22	+0·10	276·34	+0·59	+0·41		267·85				259·18			
12	308·93	+0·50	+0·18	+0·49†	+0·04	299·57	+0·22	+0·32		290·31				280·86			
13	332·69		—0·06	—0·14	+0·34	322·60	+0·21	+0·45		312·57				302·33		—0·62	
14	356·22		—0·07	+0·06	+0·70	345·39	+0·25	+0·48		334·60				323·66		—0·47	
15	379·52			+0·25	+0·17	367·97	+0·08	+0·23		365·39				344·55		—0·05	
16	402·57	+0·11		+0·01	0·00	390·29	—0·40	+1·05†		377·93	+0·07			365·28		—0·43	
17	425·35	+0·21		+0·10	+0·17	412·35	+0·11	+0·36		399·19	—0·01			385·71		—0·01	
18	447·83	+0·20		+0·08	+0·41	434·12	+0·20	+0·11		420·16	—0·12			405·85		—0·42	
19	470·03	+0·34†		—0·10	—0·08	455·60	+0·04	+0·34		440·81	—0·15			425·68		—0·37	
20	491·89			—0·39	+0·64	476·76	+0·01	—0·52		461·15	+0·33			445·16		—0·15	
21	513·43	+0·06		+0·01	+0·18	497·59	+0·15	—0·01		481·15	+0·03			464·30		—0·12	
22	534·62	+0·48		—0·02	—0·03	518·07	+0·31	—0·39		500·79	0·00			483·08		—0·02	
23	555·43	—0·61†		—0·33	—0·05	538·20	—0·04	—0·50		520·07	—0·10			501·46		—0·43	

24	575·86	0·00		+0·13	−0·65	557·95	+0·03	−0·72		538·94	+0·06			519·44		−0·41
25	595·89	+0·38			−0·06	577·29	−0·41	−1·04		557·41	+0·05			537·01		−0·46
26	615·51	−0·08			−0·32	596·23	−0·40			575·46	−0·81			554·14		
27	634·69	−0·03	+0·65		−0·72	614·74	−0·36	−0·34		593·07	−0·11			570·81		
28	653·42	+0·24	−0·07		+0·09	632·81		−0·80		610·23	−0·89			587·01		
29	671·68	+0·51	+0·71		+0·39	650·41	−0·03			626·91				602·73		
30	689·46	+0·31	+1·50		+0·89	667·55	−0·01			643·10				617·93		
31	706·74	+0·76	+1·10		+0·91	684·20	−0·22	−0·60		658·78				632·62		
32	723·52		−0·06		+1·34	700·32	−0·28	−0·03		673·94				645·77		
33	739·75	+1·05	+1·49		+1·77	715·94	0·00			688·57				660·36		
34	755·44		+2·06			731·01	+0·03			702·64				673·38		
35	770·56		+2·04			745·53	+0·27			716·13				685·81		
36	785·11		+3·13			759·46	+1·42			729·04				697·62		
37	799·06		+4·17			772·82	+1·51			741·34				708·82		
38	812·40					785·57	+1·60			753·02				719·47		
39	825·10					797·69	+2·13			764·06				729·26		
40	837·16					809·19	+3·76			774·45				738·48		

† Indicates that one of the lines from which $\Delta_2F(j_k)$ was obtained is a blend.

The Isotope Effect.

If one of the atoms forming a molecule possesses isotopes, then the wavelengths of the light emitted by the similar molecules formed from the different isotopes differ slightly. There is first of all a very small shift of the whole band system due to change of the orbital electronic energy, but as a rule the mass of the molecule is so great compared with that of the electron that this cannot be observed. Then each band as a whole suffers a vibrational isotope displacement. This for the (n', n'') band is given approximately[*] by :—

$$\Delta\nu^n = \nu_2{}^n - \nu_1{}^n = (\rho - 1)\,[\,(\omega_0')\,(n' + \tfrac{1}{2}) - (\omega_0'')_1\,(n'' + \tfrac{1}{2})\,]$$
$$- (\rho^2 - 1)\,[\,(\omega_0'x')_1\,(n' + \tfrac{1}{2})^2 - (\omega_0''x'')_1\,(n'' + \tfrac{1}{2})^2\,],$$

where ν^n represents the distance of the band origin from the origin of the system and for a diatomic molecule

$$\rho = \sqrt{\mu_1/\mu_2}, \quad \text{where} \quad \mu_{1,2,\ldots} = \mathrm{M}_{1,2,\ldots}\mathrm{M}'/(\mathrm{M}_{1,2,\ldots} + \mathrm{M}').$$

$\mathrm{M}_{1,2}$, ..., are the atomic weights of the isotopes and M′ the atomic weight of the combining atom.

By a slight rearrangement the equation may be written in the form

$$\Delta\nu^n = (\rho - 1)\,\nu_1{}^n + (\rho - \rho^2)\,[\,(\omega_0'x')_1\,(n' + \tfrac{1}{2})^2 - (\omega_0''x'')_1\,(n'' + \tfrac{1}{2})^2\,],$$

which is more convenient for calculation, especially as the second part of the expression is usually small compared with the first, and may often be neglected. It cannot be neglected here[†] on account of the high value of $\omega_0''x''$.

Each line of the band is then subject to a rotational isotope displacement given approximately by

$$\Delta\nu^m = \nu_2{}^m - \nu_1{}^m = (\rho^2 - 1)\,\nu_1{}^m,$$

where ν^m is the distance of the line from the origin of the band and ρ is as defined above. For magnesium there are three isotopes of weights 24, 25, 26, in order of abundance 7 : 1 : 1. Taking 24 as M_1 the other isotopes yield the following values for $(\rho - 1)$ and $(\rho^2 - 1)$:—

	25	26
$(\rho - 1)$	−0·000800	−0·001539
$(\rho^2 - 1)$	−0·001600	−0·003077

---

[*] For the derivation of this equation and further details of the isotope effect see the article by Loomis, chap. V, of the 'U.S. National Research Council Report' on "Molecular Spectra in Gases."

[†] *Cf.* A. Elliott, 'Roy. Soc. Proc.,' A, vol. 123, p. 641 (1929), on the isotope effect in the band spectrum of chlorine.

Using these values of $(\rho - 1)$ and $(\rho^2 - 1)$ together with the equation for the band origins given above, the isotope separations for the (0, 2) and (0, 1) bands have been calculated and are compared with the observed values in Table XII.

Table XII.—Comparison of Observed and Calculated Values of Isotope Separations.

(0, 2) band.—$\nu_0 = 32429 \cdot 6$. $\nu'' = 3474 \cdot 9$. $\Delta\nu_{25}'' = 2 \cdot 61$. $\Delta\nu_{26}'' = 5 \cdot 02$.

ν Isotope 24.	Classification.	Observed separations.		Calculated separations.	
		Isotope 25.	Isotope 26.	Isotope 25.	Isotope 26.
31877·37	R (21)	3·53	6·75	3·49	6·72
857·79	P (16)	3·29	6·74	3·51	6·78
797·21	P (17)	3·35	6·45	3·62	6·97
756·05	R (23)	3·60	6·75	3·69	7·09
733·40	P (18)	3·84	6·88	3·72	7·16
691·67	R (24)	3·78	—	3·79	7·29
667·07	P (19)	3·61	6·69	3·83	7·37
409·22	R (28)	—	8·03	4·24	8·16
255·01	R (30)	5·02	—	4·49	8·63
217·05	P (25)	4·48	8·10	4·55	8·75
175·25	R (31)	3·77	8·03	4·62	8·98

(0, 1) band.—$\nu_0 = 33995 \cdot 0$. $\nu'' = 1909 \cdot 5$. $\Delta\nu_{25}'' = 1 \cdot 47$. $\Delta\nu_{26}'' = 2 \cdot 83$.

ν Isotope 24.	Classification.	Observed separations.		Calculated separations.	
		Isotope 25.	Isotope 26.	Isotope 25.	Isotope 26.
33743·10	R (14)	1·48	2·46	1·86	3·61
649·71	R (16)	1·86	4·11	2·02	3·89
611·93	P (12)	2·11	4·14	2·08	4·01
597·86	R (17)	1·96	3·93	2·11	4·05
499·98	P (14)	1·76	4·25	2·26	4·35
464·51	R (19)	2·23	4·47	2·28	4·40
439·13	P (15)	2·38	—	2·36	4·54
423·11	R (20)	2·08	4·79	2·39	4·59
375·05	P (16)	2·45	4·84	2·46	4·74
358·29	R (21)	2·23	4·49	2·49	4·79
237·25	P (18)	2·68	—	2·68	5·16
163·54	P (19)	2·88	—	2·80	5·39
007·74	P (21)	2·82	5·52	3·05	5·87

The Electron States.

The α- and β-systems of the molecule MgH are both classed as $^2P \rightarrow {}^2S$ transitions and have the same final ^2S state. The γ-system is of the $S \rightarrow S$

type of transition and has no state common with the other systems. These transitions are illustrated diagrammatically in the accompanying figures.

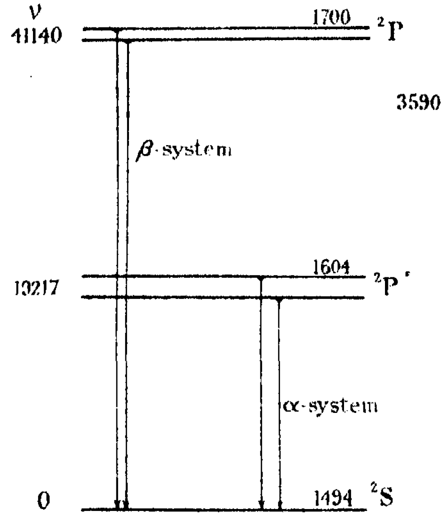

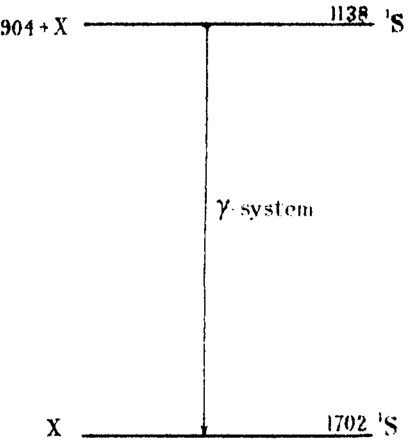

FIG. 1. FIG. 2.

FIG. 1.—Diagram showing the relations between the electron levels involved in the α- and β-systems.

FIG. 2.—Diagram showing the relation between the electron levels involved in the γ-system.

The diagrams are to scale except for the doublet separations which have been increased about 100 times. The quantity above each level on the right is the approximate value of ω_0 for that level. The numbers on the left represent the electronic energy in wave-number units associated with each level.

There remains to be considered the possible relationship of these two new levels to the three already known. For this purpose the various constants for the five levels are collected together in Table XIII.

The values for the vibrational constants show definitely that the two new S levels are quite distinct from the ^{2}S level of the α- and β-systems. A similar position has been reached by W. W. Watson* and E. Bengtsson† who find no connection between the two S levels of the many-lined ultra-violet system of BeH and the final ^{2}S level of the green band. The values of ω_0 also seem to rule out the suggestion that these two levels are two ^{2}S states of the MgH molecule either both above or both below that of the α- and β-systems; and

---

* 'Phys. Rev.,' vol. 32, No. 4, p. 606 (1928).

† 'Nature,' vol. 123, No. 3101, p. 529 (1929).

Table XIII.—Constants* for the Molecular Electron States.

Level.	Energy. cm.$^{-1}$.	ω_0.	$\omega_0 x$.	E_n cm.$^{-1}$.	$I_0 \times 10^{40}$.	$r_0 \times 10^8$.
^2S	0	1493·5	31·25	17100	4·86†	1·74†
^2P	19217	1603·5	34·75	17700	4·62†	1·70†
^2P	41140	1700 ?	38 ?	19000 ?	4·54‡	1·69‡
$^1S''$	X	1702·2	34·2	21200	4·34	1·65
$^1S'$	35904·5 + X	1138·4	9·5	34200	6·44	2·02

* Column 1 contains the designation of the level; column 2 the electronic energy of the level, that of the ^2S level being taken as zero; columns 3 and 4 the vibrational constants already defined; column 5 a rough calculation of the energy required for dissociation of the molecule vibrationally, E_n = maximum value of $\omega_0 n - \omega_0 x n^2 = \omega_0{}^2/4\omega_0 x$: column 6 the moment of inertia of the molecule, $I_0 = h/8\pi^2 c B_0 = 27 \cdot 70/B_0 \times 10^{-40}$ gm. cm.^{2}; and column 7 the internuclear distance $r_0 = \sqrt{I_0/\mu}$ where $\mu = M_1 M'/(M_1 + M') \times 1 \cdot 650 \times 10^{-24}$ gm.

† These values are taken from Table I of the 'Constants of Diatomic Molecules,' Birge, 'Int. Crit. Tables,' vol. 5, and are in terms of the Old Mechanics. To reduce to New Mechanics $I_0 \alpha/2B_0$ should be subtracted from I_0 and $r_0 \alpha/4B_0$ from r_0. Values of α are not given so these quantities cannot be calculated, but judging from the $^1S''$ level they are of the order of 0·06 and 0·02 respectively.

‡ These values are calculated from the value of B found for the initial state of the λ 2430 band. This was the only band sufficiently strong for analysis so that a value for α could not be obtained. These values, therefore, are not in terms of the New Mechanics.

to place one on either side would at once raise the objection that the many possible combination systems indicated by such an arrangement are not found although falling in regions convenient for observation.

The alternative explanation, as pointed out by Watson in the case of the BeH systems, is that the many-lined system is due to the ionised molecule. Direct proof of this is difficult to obtain. Examination of the lines with an interferometer would be required to establish that the lines do not exhibit the small doubling to be expected for a $^2S \rightarrow {}^2S$ transition in the MgH molecule, and experimental work on the production of the spectrum in the arc can give no very decisive evidence. At the same time this explanation raises no objections of very definite nature so far as the writer can see, and even suggests an explanation of one or two experimental points observed when photographing the spectrum. Thus it was found that the γ-system was more sensitive to change of pressure of the hydrogen in the arc chamber than the other two systems, and that its intensity relative to them varied considerably. Lower pressure seemed to favour the production of the γ-system in much the same way that it favours the production of the Mg^+ lines, until depletion of the hydrogen entered as a factor at very low pressures and diminished the intensity of the whole band spectrum. Further it should be recorded that under the conditions at which the spectrum was best obtained the Mg^+ lines at λλ 2790·8, 2798·0 ($3\,^2D_{2,3} \rightarrow 3\,^2P_{1,2}$), 2928·6, 2936·5 ($4\,^2S \rightarrow 3\,^2P_{1,2}$) and 3104·8 ($5\,^2F \rightarrow 3\,^2D$) were approaching the principal pair at λλ 2795·5, 2802·7 ($3\,^2P_{2,1} \rightarrow 3\,^2S$) in intensity and were among the strongest in the spectrum, showing that considerable numbers of Mg^+ ions in various stages of excitation were present.

Interpreting the γ-system as a $^1S \rightarrow {}^1S$ transition in the molecule MgH^+, the following speculations as to the course of events during the emission of the spectrum may be made. Union of a Mg^+ ion with a hydrogen atom in its normal state[*] yields a MgH^+ molecule in the higher ^1S state. The variation with internuclear distance of the force between the atoms in this state is evidently very different from that existing in any of the other states, for ω_0 is much smaller and $\omega_0 x$ very much smaller. This points to a weaker but much more uniform field for this state. A rough calculation of the energy required to dissociate the molecule vibrationally in each state shows that it is greater for this state than for any of the others. The larger number of vibrational states existing at this level shown by the strength of the $n'' = 0$ progression and by the fact that this system extends down to below λ 2000 seems compatible with the view that combination takes place at this level. From this initial ^1S state an electron transition brings the molecule to the final ^1S state where the value of ω_0 is found to approach *close* to that for the highest ^2P state of the normal MgH molecule, and the value of $\omega_0 x$ is of the order 30–35 shown by all the other states. If the excited electron in the ^2P state is so far out that it is "as good as ionised" this approach of the constants receives a natural explanation. The moving in of the electron in the ionised molecule increases the attraction between the nuclei as shown by the value of ω_0, but decreases the uniformity of the field as measured by $\omega_0 x$ so greatly that the energy for dissociation is also decreased. This electron therefore appears to be closely concerned in the "binding" of the molecule. The moving in of the electron in the neutral molecule changes the values of the constants very little, suggesting that this electron does little to hold the atoms together. It falls to two lower levels, giving rise to the lower ^2P and the ^2S state of the molecule.[†] The sudden cessation of the P and R branches of the λ 2430 band and of the

---

[*] The Balmer series is not prominent in the spectrum although early members are sometimes seen in flashes. The secondary spectrum of hydrogen (due to H_2) is also not apparent in the visible region, but on a plate taken with a vacuum spectrograph, the bands at λ 1600—λ 1400 appeared.

[†] The transition $^2P \rightarrow {}^2P$ to be expected has not yet been recorded, but it is not likely to be conspicuous on account of the instability of the upper level and the close approach of the values of B_0 for these levels.

C band of CaH may find an explanation in the fact that the upper state is on the border of ionisation.

Summary.

(1) The bands of the many-lined ultra-violet (γ) system of magnesium hydride have been measured in the region λ 2560 to λ 3240.

(2) Vibrational quantum numbers have been assigned to the bands. The band origins are represented by the equation

$$\nu_0 = 35904 \cdot 5 + 1138 \cdot 4 (n' + \tfrac{1}{2}) - 9 \cdot 5 (n' + \tfrac{1}{2})^2 - 1702 \cdot 2 (n'' + \tfrac{1}{2}) + 34 \cdot 2 (n'' + \tfrac{1}{2})^2.$$

This equation shows that neither of the electron states involved is identical with any of those involved in the α- and β-systems of MgH.

(3) The rotational structure has been analysed and found to be of the simple type—one P and one R branch with one line missing at the origin—characteristic of the $^1S \rightarrow {}^1S$ type of transition. Using a rotational term of the form

$$F(j_k) = B_n j_k (j_k + 1) - D_n [j_k (j_k + 1)]^2,$$

the following values of B_n and D_n were found

$$B_n' = 4 \cdot 3020 - 0 \cdot 0492 (n' + \tfrac{1}{2}) - 0 \cdot 0050 (n' + \tfrac{1}{2})^2$$
$$B_n'' = 6 \cdot 3782 - 0 \cdot 1854 (n'' + \tfrac{1}{2}).$$

Mean value $D_n' = 2 \cdot 16 \times 10^{-4}$, mean value $D_n'' = 3 \cdot 45 \times 10^{-4}$.

(4) The isotope effect was measured in the case of the (0, 1) and (0, 2) bands and observed values found to be in good agreement with those calculated on the assumption that the bands are emitted by the diatomic molecule MgH (or MgH^+), Mg having isotopes of atomic weights 24, 25, 26.

(5) The electron levels involved in the α-, β- and γ-systems of magnesium hydride are discussed, and reasons advanced for assigning the γ-system to the ionised molecule MgH^+.

In conclusion, the author wishes to express his thanks to Prof. A. Fowler for continued interest in the progress of the investigation, and to Dr. W. Jevons and Assist.-Prof. H. Dingle for helpful suggestions and criticism.

On the Criterion for Stability of a Layer of Viscous Fluid Heated from Below.

By A. R. Low, M.A.

(Communicated by L. N. G. Filon, F.R.S.—Received May 22, 1929.)

1. An analogy has been drawn by the present writer* between Bénard's problem of the modes of instability of a layer of viscous fluid initially at rest under gravity between horizontal plane boundaries heated below and cooled above, and Prof. G. I. Taylor's problem of the modes of instability of a viscous fluid initially in steady cyclic motion under inertia forces between concentric circular cylinders rotating with constant unequal angular velocities.

Rayleigh obtained a solution of Bénard's problem for two boundaries with no tangential forces between boundary and fluid,† while in Taylor's problem‡ there are two boundaries with no slip.

Dr. Harold Jeffreys § reduced Bénard's problem to the solution of a linear differential equation of the sixth order with constant coefficients, but remarked that the eliminant of the arbitrary constants of integration from the six boundary conditions, three at each boundary, would be a determinant of the sixth order, many complex quantities being involved, and proceeded to obtain approximate values of the criterion for stability by a method of finite differences. Among other results he obtained a criterion for two boundaries of no slip maintained at different constant temperatures which is the analogue of Taylor's problem, but his critical value was only about two-thirds of the corresponding value found from Taylor's analysis.

The writer confidently expected a much closer numerical agreement, and Prof. Taylor suggested the work undertaken in the present paper, of verifying the result.

In the meantime, Dr. Jeffreys has devised a method of solving the differential equation by expressing the sixth derivative of the assumed solution as a Fourier series, had amended the boundary conditions and has discussed the writer's analogy which he has put on a formal mathematical basis. His new value of the criterion for stability agrees closely with the value calculated from Taylor's analogous condition, the figures being 1709·5 and 1706 respectively.

---

* 'Nature,' vol. 115, p. 289 (1925).

† Rayleigh, 'Collected Papers,' vol. 6, p. 432 (1916).

‡ G. I. Taylor, 'Phil. Trans.,' A, vol. 223, p. 289 (1923).

§ H. Jeffreys, 'Phil. Mag.,' vol. 2, pp. 833–844 (1926).

In the present paper the formal solution of Jeffreys' differential equation is obtained by the usual methods without prohibitive complication.

The critical values given by the vanishing of the eliminant are computed for three cases, two surfaces of free slip, one surface of free slip and one of no slip, and two surfaces of no slip, in all cases the boundaries being kept at constant temperatures. The figures are 651, 1108 and 1706*, the first being in agreement with Rayleigh and Jeffreys, the second being a new result and the third agreeing closely with the critical value as calculated by Jeffreys for Taylor's analogous problem.

2. Slight alterations have been made in the notation for the sake of lightening the analytical expressions. In the investigation, equilibrium with a uniform negative temperature gradient upward, defining the undisturbed temperature $T = \beta\zeta$ in terms of the height above the lower boundary, was found by Rayleigh to be stable until a certain numerical value of β depending on the depth of the layer and the physical constants of the fluid was reached. At this value of β a slight disturbance produces a departure from the equilibrium distribution of temperature T. This departure is assumed to have the form

$$\Delta T = Z \sin(2\pi\xi/\lambda) \sin(2\pi\eta/\mu).$$

ξ, η, ζ being the co-ordinates in space, Z a function of the vertical co-ordinate ζ only; further $1/\lambda^2 + 1/\mu^2 = b^2/4h^2$, defining b, h being the depth of the layer.

3. Jeffreys' differential equation, satisfied by Z throughout the fluid becomes, on putting $z = \pi b\zeta/h$,

$$\{(D^2 - 1)^3 + (p^2 + 1)^3\} Z = 0, \tag{1}$$

where $D = d/dz$, κ = thermometric conductivity, ν = kinematic viscosity,

$$(p^2 + 1)^3 = g\alpha\beta' h^4/\kappa\nu\pi^4 b^4 = E/E_0\pi^4 b^4.$$

($\beta' = -\beta$ is used to avoid negative constants), $\alpha\beta' h = (\rho_2 - \rho_1)/\rho$ = the relative increase of density from bottom to top, $E = g(\rho_2 - \rho_1)h/6$ = the apparent energy per unit volume stored against gravity by the top-heavy distribution of the fluid, $E_0 = \kappa\nu\rho/6h^2$, a quantity depending on the physical constants and of the dimensions of energy per unit volume.

This permits of the immediate interpretation of the criterion of instability as the apparent amount of energy per unit volume stored in the fluid, beyond which the equilibrium becomes unstable.

---

* Corrected value 1704·4.

4. Proceeding now to solve equation (1) it may be factorised as follows,

$$(D+\iota p)(D-\iota p)(D+\iota q e^{\iota\gamma})(D-\iota q e^{\iota\gamma})(D+\iota q e^{-\iota\gamma})(D-\iota q e^{-\iota\gamma})Z=0, \quad (2)$$

where

$$q^4=p^4+3p^2+3, \qquad \tan 2\gamma=\sqrt{3}\,(p^2+1)/(p^2+3).$$

For brevity put $c=\cos\gamma$, $s=\sin\gamma$, $c'=\cos 2\gamma$, $c''=\cos 3\gamma$, $c'''=\cos 4\gamma$, etc.

The general solution and its first four derivatives may be written

$$Z=A_1e^{\iota pz}+A_2e^{-\iota pz}+A_3e^{q(c+\iota s)z}+A_4e^{-q(c+\iota s)z}+A_5e^{q(c-\iota s)z}+A_6e^{-q(c-\iota s)z},$$

$$Z'=\iota p(A_1e^{\iota pz}-A_2e^{-\iota pz})+q(c+\iota s)[A_3e^{q(c+\iota s)z}-A_4e^{-q(c+\iota s)z}]$$
$$+q(c-\iota s)[A_5e^{q(c-\iota s)z}-A_6e^{-q(c+\iota s)z}],$$

$$Z''=-p^2(A_1e^{\iota pz}+A_2e^{-\iota pz})+q^2(c'+\iota s')[A_3e^{q(c+\iota s)z}+A_4e^{-q(c+\iota s)z}]$$
$$+q^2(c'-\iota s')[A_5e^{q(c-\iota s)z}+A_6e^{-q(c-\iota s)z}],$$

$$Z'''=-\iota p^3(A_1e^{\iota pz}-A_2e^{-\iota pz})+q^3(c''+\iota s'')[A_3e^{q(c+\iota s)z}-A_4e^{-q(c+\iota s)z}]$$
$$+q^3(c''-\iota s'')[A_5e^{q(c-\iota s)z}-A_6e^{-q(c-\iota s)z}],$$

$$Z^{\text{iv}}=p^4(A_1e^{\iota pz}+A_2e^{-pz})+q^4(c'''+\iota s''')[A_3e^{q(c+\iota s)z}+[A_4e^{-q(c+\iota s)z}]$$
$$+q^4(c'''-\iota s''')[A_5e^{q(c-\iota s)z}+A_6e^{-q(c-\iota s)z}].$$

5. Grouping conjugate factors and expressing the result as the sum of even and odd functions

$$Z=a_2\cos pz+a_4(e^{qcz}C_0+e^{-qcz}C_0)+a_6(e^{qcz}S_0-e^{-qcz}S_0)$$
$$+a_1\sin pz+a_3(e^{qcz}C_0-e^{-qcz}C_0)+a_5(e^{qcz}S_0+e^{-qcz}S_0),$$

$$Z'=-a_2p\sin pz+a_4q(e^{qcz}C_1-e^{-qcz}C_{-1})+a_6q(e^{qcz}S_1+e^{-qcz}S_{-1})$$
$$+a_1p\cos pz+a_3q(e^{qcz}C_1+e^{-qcz}C_{-1})+a_5q(e^{qcz}S_1-e^{-qcz}S_{-1}),$$

$$Z''=-a_2p^2\cos pz+a_4q^2(e^{qcz}C_2+e^{-qcz}C_{-2})+a_6q^2(e^{qcz}S_2-e^{-qcz}S_{-2})$$
$$-a_1p^2\sin pz+a_3q^2(e^{qcz}C_2-e^{-qcz}C_{-2})+a_5q^2(e^{qcz}S_2+e^{-qcz}S_{-2}),$$

$$Z'''=a_2p^3\sin pz+a_4q^3(e^{qcz}C_3-e^{-qcz}C_{-3})+a_6q^3(e^{qcz}S_3+e^{-qcz}S_{-3})$$
$$-a_1p^3\cos pz+a_3q^3(e^{qcz}C_3+e^{-qcz}C_{-3})+a_5q^3(e^{qcz}S_3-e^{-qcz}S_{-3}),$$

$$Z^{\text{iv}}=a_2p^4\cos pz+a_4q^4(e^{qcz}C_4+e^{-qcz}C_{-4})+a_6q^4(e^{qcz}S_4-e^{-qcz}S_{-4})$$
$$+a_1p^4\sin pz+a_3q^4(e^{qcz}C_4-e^{-qcz}C_{-4})+a_5q^4(e^{qcz}S_4+e^{-qcz}S_{-4}),$$

where

$$C_{\pm n}=\cos(\psi\pm n\gamma), \qquad S_{\pm n}=\sin(\psi\pm n\gamma), \qquad \psi=qsz,$$

further

$$\phi=pz, \qquad Q=qcz,$$

and at a boundary where $\zeta=h/2$, $z=\pi b\zeta/h=\pi b/2$

$$\psi=qsb\pi/2, \qquad \phi=pb\pi/2, \qquad Q=qcb\pi/2.$$

All the quantities involved are now real for real values of z.

Later it will be convenient to write these relations in the form

$$
\begin{aligned}
Z &= a_2 Z_2 + a_4 Z_4 + a_6 Z_6 + a_1 Z_1 + a_3 Z_3 + a_5 Z_5, \\
Z' &= a_2 Z_2' + a_4 Z_4' \dots\dots\dots\dots\dots\dots + a_5 Z_5', \\
&\dots\dots\dots\dots\dots\dots\dots\dots\dots\dots\dots\dots \\
Z^{iv} &= a_2 Z_2^{iv} + a_4 Z_4^{iv} + \dots\dots\dots\dots\dots + a_5 Z_5^{iv}.
\end{aligned}
$$

6. There must be six boundary conditions available to determine the six arbitrary coefficients. In the problems under consideration there are two dynamical conditions and one thermal condition at each boundary. Let u, v, w be the components of the motion of instability.

Considering first the dynamical conditions, the condition $w = 0$ leads to $\nabla^2 T = 0$. At a surface of free slip the conditions $\partial u/\partial\xi = \partial v/\partial\eta = 0$ lead to $\partial^2 w/\partial\zeta^2 = 0$, thence to $\partial^2 \nabla^2 T/\partial\zeta^2 = 0$. At a surface of no slip the conditions $u = 0$, $v = 0$, $w = 0$ lead to $\partial u/\partial\xi = \partial v/\partial\eta = \partial w/\partial\zeta = \partial \nabla^2 T/\partial\zeta = 0$.

Transforming from ζ to z, these conditions become :—

At a fixed plane surface......	$Z'' - Z = 0$	(3)
With no slip................	$Z''' - Z' = 0$	(4)
With free slip	$Z^{iv} - Z'' = 0$	(5)

Conditions (3) and (5) were first given by Rayleigh, and condition (4) by Jeffreys.

Rayleigh assumed, as thermal conditions, that both boundaries were maintained at different constant temperatures, which is at once expressed by

$$Z = 0. \quad (1)$$

Conditions (3) and (1) apply to both surfaces. Condition (4) or condition (5) may apply to either surface. Denoting the groups of conditions (1 3 4) and (1 3 5) by *a* and *b*, there are three cases :—

aa (1 3 4) at both surfaces,
bb (1 3 5) at both surfaces,
ab (1 3 4) at one surface,
(1 3 5) at the other surface.

Problem *bb* was solved by Rayleigh, and his result was obtained by Dr. Jeffreys and in the present paper in different ways.

Problem *aa* was solved by Dr. Jeffreys to a close approximation, and in the present paper more exactly.

Problem *ab* is solved in the present paper.

It is to be noted that a free fluid surface (under gravity) is a surface of zero tangential forces, further since the velocities are small quantities, say of the first order, the differences of level at a free surface are, at most, small quantities of the second order, by Bernoulli's relation. Hence no distinction need be made between a free fluid surface and a horizontal rigid plane surface of free slip to the order of approximation employed.

7. Considering first Rayleigh's problem, (*bb*), two horizontal plane boundaries, maintained at constant unequal temperatures and with free slip between boundary surface and fluid, yield the conditions at both boundaries,

$$Z = 0, \qquad Z'' - Z = 0, \qquad Z^{\text{iv}} - Z'' = 0$$

reducing at once to

$$Z = 0, \qquad Z'' = 0, \qquad Z^{\text{iv}} = 0.$$

Where the same condition holds at both boundaries, the odd and even parts of the expressions can be made to disappear independently by taking the origin midway between the boundaries, where $\zeta = \pm h/2$, $z = \pm pb\pi/2$.

Eliminating a_2, a_4, a_6 and a_1, a_3, a_5 in separate groups, the conditions of consistency are obtained in the form of third order determinants equated to zero. Dividing the second row by q^2, the third row by q^4 and multiplying the first column by q^4, we get

$$\begin{vmatrix} q^4 \begin{smallmatrix}\cos\\ \sin\end{smallmatrix} \phi & e^{Q}C_0 \pm e^{-Q}C_0 & e^{Q}S_0 \mp e^{-Q}S_0 \\ -p^2q^2 \begin{smallmatrix}\cos\\ \sin\end{smallmatrix} \phi & e^{Q}C_2 \pm e^{-Q}C_{-2} & e^{Q}S_2 \mp e^{-Q}S_{-2} \\ p^4 \begin{smallmatrix}\cos\\ \sin\end{smallmatrix} \phi & e^{Q}C_4 \pm e^{-Q}C_{-4} & e^{Q}S_4 \mp e^{-Q}S_{-4} \end{vmatrix} = 0$$

the upper symbols being taken for the even solution, the lower symbols for the odd solution.

On reduction of the even solution we get,

$$(e^{2Q} + 2\cos 2\psi + e^{-2Q})\,(q^4 + 2q^2p^2\cos 2\gamma + p^4)\sin 2\gamma \cos\phi = 0.$$

The only physical solution is given by

$$\cos\phi = 0, \quad \phi = pb\pi/2 = (2n+1)\pi/2, \quad pb = 2n+1$$

where n is any integer.

Subject to this relation a minimum value has to be found for

$$(p^2+1)^3b^4 = \mathrm{E}/\pi^4\mathrm{E}_0 = (2n+1)^4(p^2+1)^3/p^4.$$

Clearly pb must be as small as possible numerically so that $n = 0$, $pb = 1$, which together with the minimum condition gives readily

$$p^2 = 2, \qquad p = \sqrt{2}, \qquad b = 1/\sqrt{2}, \qquad \mathrm{E}_{\mathrm{min.}}/\mathrm{E}_0 = 3^3 \,.\, 2^{-2} \,.\, \pi^4 = 651$$

in agreement with Rayleigh and Jeffreys. The type of unstable flow is shown diagrammatically in fig. 1A.

The writer was anticipated in obtaining this result by his colleague Capt. D. Brunt of the Meteorological Office, who had noted that $Z = \cos pz$ satisfied the differential equation (1) by virtue of satisfying $(D^2 + p^2)\, Z = 0$, $D^2 + p^2$ being an obvious factor, and further can be made to satisfy the boundary conditions $Z = 0$, $Z'' = 0$, $Z^{\mathrm{iv}} = 0$ at $z = \pm\, pb\pi/2$ by making $pb = 1$, thus obtaining Rayleigh's solution in a simple way.

8. Taking the lower symbols for the odd conditions we get in a similar manner $Z = \sin \phi = \sin pz$, and at the boundaries,

$$\begin{aligned} \sin \phi &= 0 \\ pb\pi/2 = \phi &= n\pi \\ pb &= 2n. \end{aligned}$$

The smallest integral value of n for which pb does not vanish is unity, hence

$$pb = 2 \qquad \mathrm{E}_{\mathrm{min.}}/\mathrm{E}_0 = 3^3 2^2 \pi^4.$$

This is 16 times larger than for the even solution and is not the critical solution. These conditions are produced by two circuits in the motion of instability (fig. 1B) mirror images of each other in the median plane, which is then dynamically equivalent to a surface of free slip since the tangential forces over it evidently vanish by symmetry.

From paragraph 3 it is seen that E is proportional to $\beta' h^4$ (for a given fluid with fixed values of α, κ, ν) so that halving the effective depth increases the required temperature gradient 16 times. For a given temperature gradient β, the minimum value of E is therefore the same for odd and even solutions of depth h and $2h$, and with one and two circuits respectively, and the odd solution is transformable into the even solution by change of scale and origin.

Fig. 1A shows diagrammatically the configuration of the motion of instability for Rayleigh's case, with a single circuit of flow in depth, but with mirror image circuits on either side. The motion is further assumed to be two-dimensional for simplicity of representation as this does not affect the critical value of E (*cp.* Rayleigh, *loc. cit.*).

Fig. 1B shows the configuration which produces the conditions of the odd

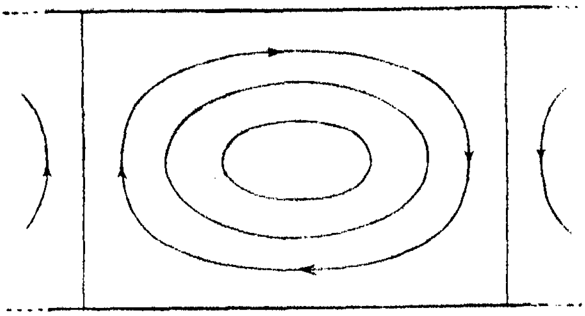

Fig. 1A.

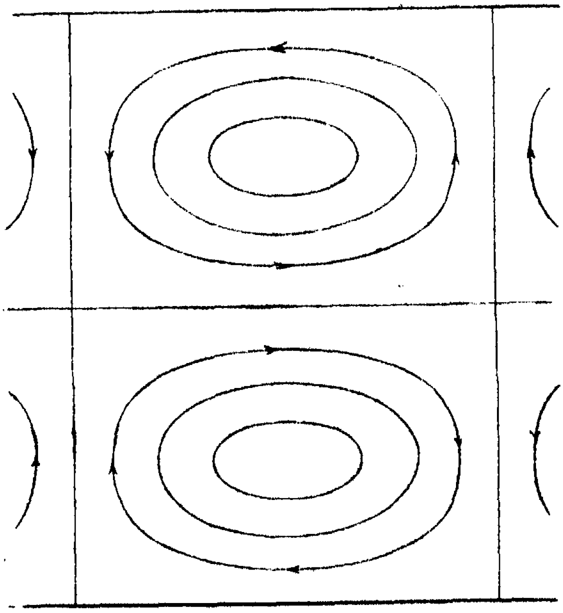

Fig. 1B.

solution, with twice the total depth, but with two circuits in depth so that the effective depth is unaltered. According to Rayleigh's commentary the former type would prevail in the long run as it has a larger increment in time for a given set of conditions, but the latter type is physically possible and would be set up by a suitable disturbance.

9. Considering next the case of two rigid boundaries with no slip; the conditions at both boundaries are

$$Z = 0, \quad Z'' = 0, \quad Z''' - Z' = 0 \quad \text{(case } aa\text{)}.$$

Taking the origin midway between the boundaries and eliminating a_2, a_4, a_6 and a_1, a_3, a_5 in separate groups we get,

$$0 = \begin{vmatrix} q^2 \begin{smallmatrix}\cos\\ \sin\end{smallmatrix} \phi, & e^{Q}C_0 \pm e^{-Q}C_0, & e^{Q}S_0 \mp e^{-Q}S_0 \\ -p^2 \begin{smallmatrix}\cos\\ \sin\end{smallmatrix} \phi, & e^{Q}C_2 \pm e^{-Q}C_{-2}, & e^{Q}S_2 \mp e^{-Q}S_{-2} \\ \pm pq(q^2+1) \begin{smallmatrix}\sin\\ \cos\end{smallmatrix} \phi, & \begin{matrix} e^{Q}(q^2C_3 - C_1), \\ \mp e^{-Q}(q^2C_{-3} - C_{-1}), \end{matrix} & \begin{matrix} e^{Q}(q^2S_3 - S_1) \\ \pm e^{-Q}(q^2S_{-3} - S_{-1}) \end{matrix} \end{vmatrix},$$

taking as before the upper symbols for the even solution and the lower for the odd solution.

10. With the upper symbols, after reduction, we get,

$$\begin{aligned} \cos\phi\{[(q^4+q^2-p^2)\sin\gamma + p^2q^2\sin 3\gamma](e^{2Q}-e^{-2Q}) \\ + [(q^4-q^2-p^2)\cos\gamma + p^2q^2\cos 3\gamma]\, 2\sin 2\psi\} \\ + \sin\phi\, qp(p^2+1)(e^{2Q}+e^{-2Q}+2\cos 2\psi)\sin 2\gamma = 0, \end{aligned}$$

whence

$$\begin{aligned} pb\pi/2 &= \phi \\ &= \tan^{-1}[\{(q^4+q^2-p^2)\sin\gamma + p^2q^2\sin 3\gamma + \varepsilon_1\}/\{qp(p^2+1)\sin 2\gamma\,(1+\varepsilon_2)\}]. \end{aligned}$$

where

$$\begin{aligned} \varepsilon_1 &= [(q^4-q^2-p^2)\cos\gamma + p^2q^2\sin 3\gamma]\, 2\sin 2\psi/(e^{2Q}-e^{-2Q}), \\ \varepsilon_2 &= 2(\cos 2\psi + e^{-2Q})/(e^{2Q}-e^{-2Q}). \end{aligned}$$

It will be noted that b appears implicitly in Q, $\sin 2\psi$, and $\cos 2\psi$ and through them in ε_1, ε_2.

The convergence is, however, rapid owing to the magnitude of $e^{2Q} > 100$ near the minimum value of E, as appeared during the computations.

As p varies from zero to infinity, $-\tan\phi$ varies from infinity to $\sqrt{3}$, and $pb\pi/2 = \phi$ varies from $\pi/2 + n\pi$ to $2\pi/3 + n\pi$, where n has any integral value.

Putting $n = 0$ and plotting b as a function of p the pb curve lies between the hyperbolas $pb = 1$, and $pb = 4/3$.

The minimum value of $E/E_0 = (p^2+1)^3 b^4\pi^4$ subject to the condition $pb = 2\phi/\pi$, is most conveniently computed by assuming a series of values of p and tabulating the corresponding values of q, γ, and the first approximations for ϕ and b; then, using the values of b so found to evaluate ε_1, ε_2, second approximations are found for ϕ and b. Fig. 2A shows diagrammatically the flow for the two dimensional type of instability.

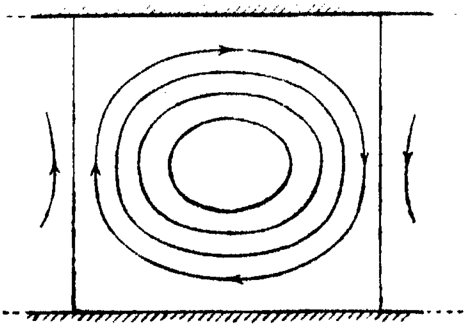

FIG. 2A.

The following values have been computed :—

EVEN SOLUTION.

1st approximation (neglecting ε_1, ε_2).

p	1·1	1·2	1·3	1·4	1·5
b..........	1·139	1·052	0·977	0·912	0·855
E/E_0	1767	1731	1726	1747	1788

2nd approximation.

b..........	1·137	1·049	0·974	0·914	0·852
E/E_0......	1756	1716	1709	1726	1763

3rd approximation.

p	1·285	
b..........	0·9846	
E/E_0......	1706*	minimum by interpolation.

11. Considering now the odd terms, the first approximation gives $\cot \phi' = -\tan \phi$ where the accent denotes the odd solution, whence $\phi' = \phi + \pi/2 + n\pi$. Putting $n = 0$ we get, for boundaries at $\pm h$

$$p b \pi = \phi' = \phi + \pi/2 > \pi$$
$$< \pi + \pi/6$$

or

$$1 < pb < 7/6,$$

the pb curve in this case lying between the hyperbolas $pb = 1$ and $pb = 7/6$.

---

* Corrected value 1704·4.

The value of Q is now $qbc\pi$ instead of $qbc\pi/2$ and e^Q is found to exceed 10^2, so that neglect of e^{-Q} in comparison with e^Q leads to an error of the order of 10^{-4}, and the first approximation is sufficient for all practical purposes. The following values have been computed to the first approximation only.

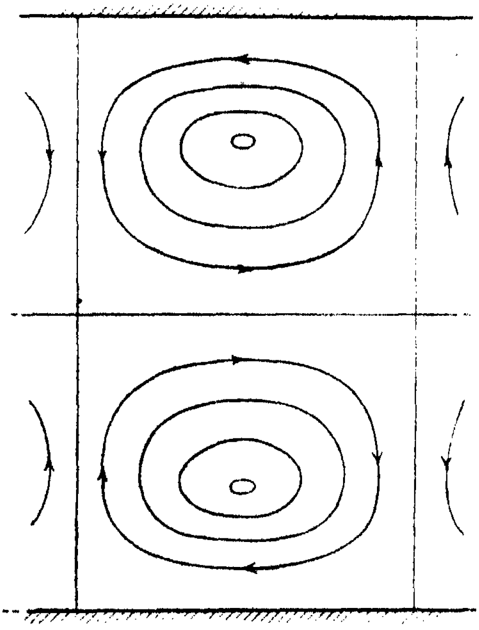

FIG. 2B.

ODD SOLUTION.

1st approximation.

b..........	1·025	0·944	0·874	0·815	0·762
E/E_0......	1180	1123	1108	1112	1130

The minimum value is nearly 1108, the corresponding value of p is 1·3.

Two vertically superposed circuits of flow, mirror images of each other in the median plane, produce the conditions of a free surface at steady temperature since clearly $Z = 0$ and tangential forces $= 0$ by symmetry. For comparison with the even solution the total depth is taken as $2h$, and the depth per circuit as h (fig. 2B).

The odd solution thus satisfies the conditions of case (ab) paragraph 6.

Using the values of p and b already found for minimum E/E_0 the coefficients a_1, a_2, a_3, a_4, a_5, a_6 have been computed, the relative values being—

$$a_2/75\cdot22 = a_4/4\cdot591 = -a_6/0\cdot0693$$

$$a_1/569\cdot0 = a_3/3\cdot064 = a_5/3\cdot507.$$

Putting a_1 and a_2 arbitrarily as unity, the curves of Z regarded as a function of ζ/h are drawn in figs. 3A and 3B. The first term which is simple harmonic and the other terms which are affected by exponential factors are plotted separately. It is seen how rapidly the effect of the latter terms falls off as the distance from the solid boundary increases.

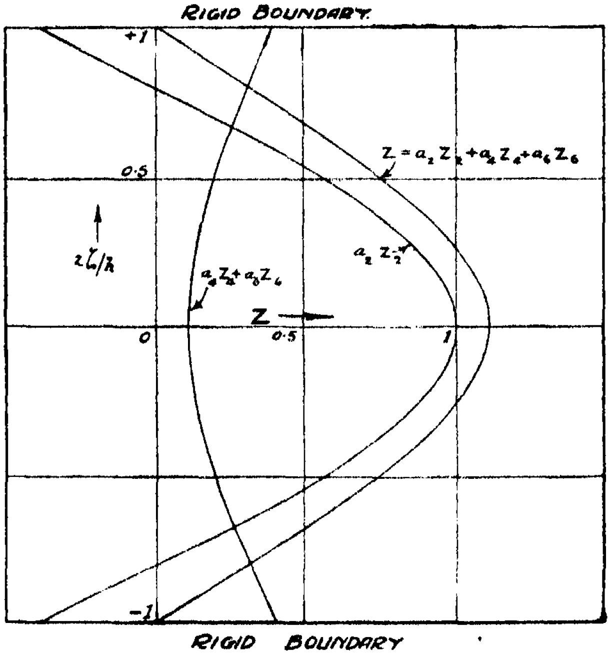

FIG. 3A.

At the boundary their sum is equal and opposite to the simple harmonic term. At distance $h/2$ it has fallen, in the even case, to about 5 per cent. for one boundary and by addition to about 10 per cent. for both boundaries. At distance h it has fallen, in the odd case, to about 1 per cent. for each boundary but the values are of opposite sign and their sum vanishes at the surface separating the two circuits.

In the problems of paragraphs 7 and 8, we have $Z = \cos\phi$, $Z = \sin\phi$ respectively, but as these are elementary curves they have not been drawn.

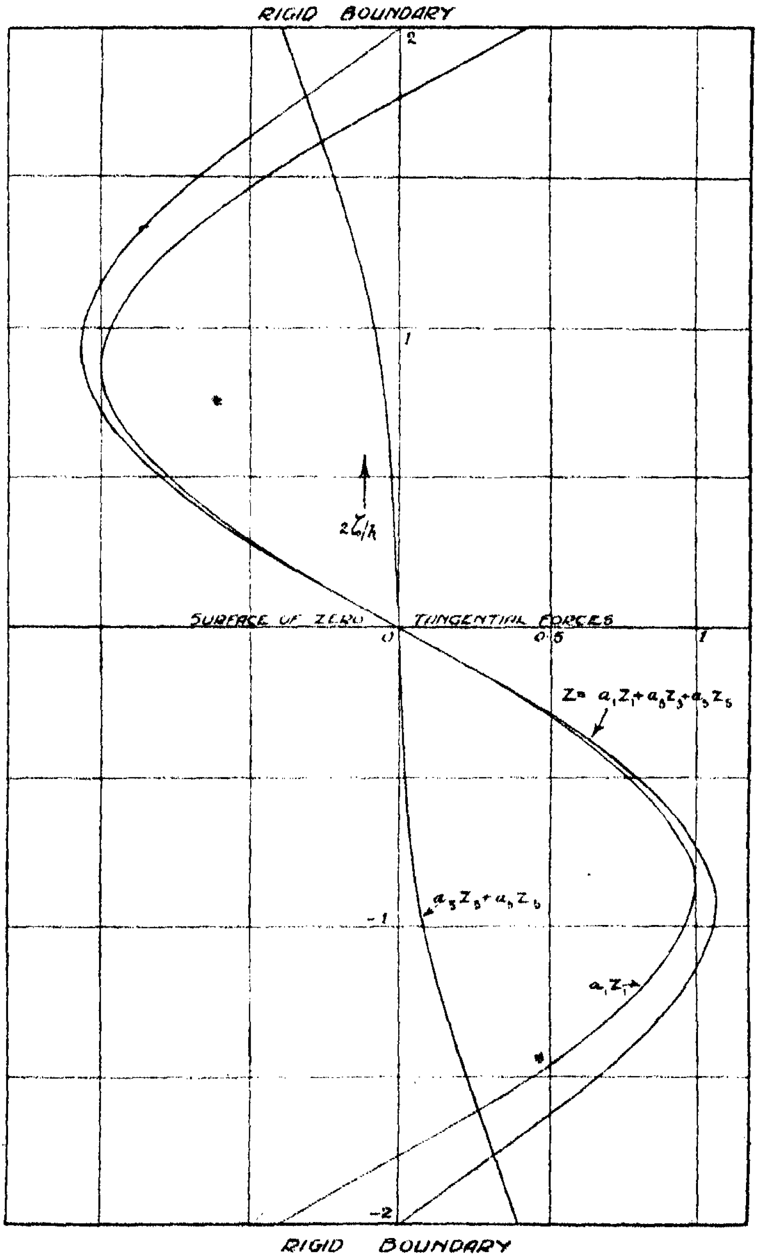
RIGID BOUNDARY
2
1
$2\zeta/h$
SURFACE OF ZERO TANGENTIAL FORCES
0
0·5
1
$Z = a_1Z_1 + a_3Z_3 + a_5Z_5$
$a_3Z_3 + a_5Z_5$
-1
a_1Z_1
-2
RIGID BOUNDARY

FIG. 3B.

12. The direct solution of the case *ab* with the origin midway between the rigid surface and the free surface, gives the eliminant in the form

$$\begin{vmatrix} Z_2 & Z_4 & Z_6 & 0 & 0 & 0 \\ 0 & 0 & 0 & Z_1 & Z_3 & Z_5 \\ Z_2'' & Z_4'' & Z_6'' & 0 & 0 & 0 \\ 0 & 0 & 0 & Z_1'' & Z_3'' & Z_5'' \\ Z_2'''-Z_2' & Z_4'''-Z_4' & Z_6'''-Z_6' & -Z_1'''+Z_1' & -Z_3'''+Z_3' & -Z_5'''+Z_5' \\ Z_2^{iv} & Z_4^{iv} & Z_6^{iv} & Z_1^{iv} & Z_3^{iv} & Z_5^{iv} \end{vmatrix} = 0.$$

Expressing this as the sum of products of pairs of 3rd order minors, one of each pair taken from columns 1, 2, 3 and the complementary minor from columns 4, 5, 6, there are in general ${}_6C_3 = 20$ pairs, but owing to the two rows of zeros in each set of three columns all but ${}_2C_1 = 2$ of the products are zero.

The eliminant reduces to

$$-\begin{vmatrix} Z_2 & Z_4 & Z_6 \\ Z_2'' & Z_4'' & Z_6'' \\ Z_2^{iv} & Z_4^{iv} & Z_6^{iv} \end{vmatrix} \times \begin{vmatrix} Z_1 & Z_3 & Z_5 \\ Z_1'' & Z_3'' & Z_5'' \\ Z_1'''-Z_1' & Z_3'''-Z_3' & Z_5'''-Z_5' \end{vmatrix}$$

$$+\begin{vmatrix} Z_1 & Z_3 & Z_5 \\ Z_1'' & Z_3'' & Z_5'' \\ Z_1^{iv} & Z_3^{iv} & Z_5^{iv} \end{vmatrix} \times \begin{vmatrix} Z_2 & Z_4 & Z_6 \\ Z_2'' & Z_4'' & Z_6'' \\ Z_2'''-Z_2' & Z_4'''-Z_4' & Z_6'''-Z_6' \end{vmatrix} = 0$$

These four minors are identical in form with the four minors of paragraphs 7 and 9, but the boundary value of z is halved, and with it the boundary values of ϕ, ψ and q, which must be replaced by $\phi/2$, $\psi/2$, $q/2$.

On substituting these values the expression above for the eliminant is transformable identically into the odd solution of paragraph 9.

The reductions are somewhat lengthy but quite elementary and need not be given here.

13. Dr. Jeffreys has introduced a new type of boundary condition, namely, that the boundary is non-conducting and gives an analytical expression which becomes in the present notation $Z' = 0$. This seems to preclude any steady flow of heat with a constant temperature gradient and to render the phenomenon a transient one, unless it may be regarded as a limiting case of perfect transmission of heat from the boundary.

Assuming, in the first place, that the flow of heat is steady so that the heat reaching the boundary through the fluid equals the heat transmitted from the boundary to the ultimate sink, and that the latter quantity is proportional to the temperature difference between boundary and sink, while the former quantity, as before, is proportional to the temperature gradient in the fluid at the boundary, then we have

$$\partial \mathrm{T}/\partial z = \mathrm{K}\,(\mathrm{T} - \mathrm{T}_0),$$

where T is the steady boundary temperature and T_0 is the constant temperature of the sink.

In the disturbed state

$$\partial\,(\mathrm{T} + \Delta\mathrm{T})/\partial z = \mathrm{K}\,(\mathrm{T} + \Delta\mathrm{T} - \mathrm{T}_0)$$

where $\mathrm{T} + \Delta\mathrm{T}$ is the disturbed temperature at the boundary.

Hence

$$\partial \Delta\mathrm{T}/\partial z = \mathrm{K}\,\Delta\mathrm{T},$$

which in the present notation reduces on dropping a common factor to

$$Z' = \mathrm{K}Z.$$

If K becomes very large this condition approaches $Z = 0$, Rayleigh's boundary condition. If K becomes very small the condition approaches $Z' = 0$, Jeffreys's adiabatic condition.

Numbering this condition (2) in the scheme of para. 6, the possible combinations at a boundary surface are the old combinations (1 3 4) and (1 3 5) designated *a*, *b*, as in para. 6 and the new combinations (2 3 4), (2 3 5) which may be designed as *c*, *d*.

The possible pairs at two surfaces are *aa*, *bb*, *cc*, *dd*, *ab*, *ac*, *ad*, *bc*, *bd*, *cd*, ten in all. The odd and even solutions of *cc*, *dd* are separable and present no new difficulty.

Taking as before the plane of symmetry in the odd solutions as a surface of free slip and constant temperature subject to boundary conditions *b*, the odd solutions of *cc*, *dd*, give solutions of *cb*, *db*. Since the odd solution of *aa* transforms identically into the direct solution of *ab* (para. 12) it seems probable that the odd solutions of *cc*, *dd*, will be identical with the solutions of *cb*, *db*, but this has not been verified by direct transformation.

There remain three cases, *ac*, *ad*, *cd*. In cases *ac* and *cd* there are two conditions common to both boundaries, and the eliminants reduce to the sum of two products of complementary third order minors, as in case *ab* of para. 12.

The case *ad* has been considered by Jeffreys but the solution has not been completed. It is the least tractable of all, since there is only one condition common to both boundaries and the number of pairs of complementary minors reduces from ${}_3C_6$ only to ${}_2C_5 = 10$, of which two pairs have already been reduced above.

The third order minors are expressible in terms of the second order minors obtained from the matrix

$$\left\| \begin{array}{ll} e^{Q}C_0 \pm e^{-Q}C_0 & e^{Q}S_0 \mp e^{-Q}S_0 \\ e^{Q}C_1 \mp e^{-Q}C_{-1} & e^{Q}S_1 \pm e^{-Q}S_{-1} \\ e^{Q}C_2 \pm e^{-Q}C_{-2} & e^{Q}S_2 \mp e^{-Q}S_{-2} \\ e^{Q}C_3 \mp e^{-Q}C_{-3} & e^{Q}S_3 \pm e^{-Q}S_{-3} \\ e^{Q}C_4 \pm e^{-Q}C_{-4} & e^{Q}S_4 \mp e^{-Q}S_{-4} \end{array} \right\|$$

Denoting them by $\overline{01}$, $\overline{12}$, $\overline{23}$, $\overline{13}$, etc., for the upper signs and $\underline{01}$, $\underline{12}$, $\underline{23}$, $\underline{13}$ for the lower signs, we find on reduction,

$$\overline{01} = \overline{23} = \underline{12} = \underline{24} = (e^{2Q} - e^{-2Q}) \sin \gamma + 2 \sin 2 \psi \cos \gamma,$$

$$\underline{01} = \underline{23} = \overline{12} = \overline{24} = (e^{2Q} - e^{-2Q}) \sin \gamma - 2 \sin 2 \psi \cos \gamma,$$

$$\overline{02} = \overline{24} = \underline{13} = (e^{2Q} + e^{-2Q} + 2 \cos 2\psi) \sin 2 \gamma,$$

$$\underline{02} = \underline{24} = \overline{13} = (e^{2Q} + e^{-2Q} - 2 \cos 2\psi) \sin 2 \gamma,$$

$$\overline{03} = 14 = (e^{2Q} - e^{-2Q}) \sin 3\gamma + 2 \sin 2\psi \cos 3\gamma,$$

$$\underline{03} = \overline{14} = (e^{2Q} - e^{-2Q}) \sin 3\gamma - 2 \sin 2\psi \cos 3\gamma,$$

$$\overline{04} = (e^{2Q} + e^{-2Q} + 2 \cos 2\psi) \sin 4\gamma,$$

$$\underline{04} = (e^{2Q} + e^{-2Q} - 2 \cos 2\psi) \sin 4\gamma.$$

With these identities and recurrence relations, the eliminant of case *ad* can be expanded, and the minimum value found by computation, which may be lengthy.

The writer has not carried further this new problem which indeed lies outside the scope of his analogy and has been discussed here only on account of the attention given to it by Dr. Jeffreys.

14. The writer would acknowledge the advances made by Dr. Jeffreys in generalising Rayleigh's treatment of Bénard's problem, and in establishing formally the mathematical expression of the analogy with Taylor's problem.

The physical basis of the writer's analogy is the replacement of κ, measuring the diffusion of heat, by ν, measuring the diffusion of vorticity.

To render the analogous problems identical in mathematical detail the distribution through the fluids of the apparent energy of instability must be the same.

This is clearly so when the radii and angular velocities of the cylinders in Taylor's experiment are large compared with their differences since the energy is a function of ω and r of which the gradient may be considered linear throughout a small range of the variables, while the curvature of the boundaries has no sensible effect beyond setting up the inertia field. Jeffreys has given his demonstration of equivalence under these conditions.

But the numerical value of the criterion for instability is very nearly constant through the whole range of angular velocities in Taylor's first case where there is one circuit of unstable motion in the depth of the fluid, and it only begins to diverge when the second case with two circuits in depth has set in.

The physical explanation appears to be that the total apparent energy of the instability is the deciding factor, and that a departure from a linear gradient of energy per unit volume is of quite secondary importance.

If it were possible to impose an arbitrary variable gravitational field a general mathematical analogue of Taylor's problem could be constructed.

It is worth remarking that in Taylor's second case the larger circuit is giving out energy on a relatively large scale while the smaller circuit is absorbing energy on a smaller scale.

15. These solved problems of instability have the essential characteristic that the initial state of (rest or) steady motion, and the motion of instability have no common co-ordinate of velocity, as shown by the table.

		Steady state.	Motion of instability.
Rayleigh	3 dimensional case ..	$0,\ 0,\ 0$	$u,\ v,\ w$
	2 dimensional case ..	$u,\ 0,\ 0$	$0,\ v,\ w$
Taylor	....	$0,\ v,\ 0$	$u,\ 0,\ w$

In such cases the motion of instability is in effect treated as steady.

Where the motion of instability and the initial steady motion involve a common velocity co-ordinate the former is no longer steady; the difficulties of the problem then become much greater, and have so far defeated all attempts at solution.

The Determination of Molecular Forces from the Viscosity of a Gas.

By H. R. Hassé, Professor of Mathematics, The University, Bristol, and W. R. Cook, M.Sc., The University, Bristol.

(Communicated by S. Chapman, F.R.S.—Received May 30, 1929.)

The investigations of the kinetic theory of gases fall into two groups, those dealing with the deviations from Boyle's law as given by the second virial coefficient of the equation of state, and those dealing with the transport phenomena of viscosity, diffusion, and conduction of heat. In both cases the investigations are in so complete a form that there only remains the problem of working out the application of the results of the theory to particular models intended to represent the mutual action of the molecules.

In the case of the equation of state it has been shown by Lennard-Jones that it is possible to carry out the necessary numerical calculations for the molecular model in which the repulsive force between two molecules is of the form λr^{-n}, where r is the distance between any two molecules, and the attractive force is of the form μr^{-m}. The results of this work have been developed in a series of papers* in which various values of m and n have been found suitable for particular cases, and the corresponding force constants λ and μ have been determined.

In the case of the transport phenomena the variation of the viscosity of a gas with temperature has provided a simple method of testing the adequacy of any particular model, and those models in which (1) the field of force is repulsive and varies as r^{-n}, and (2) the repulsive field is concentrated in an elastic sphere of definite radius to which is added a *weak* attractive field have been employed by Maxwell and Sutherland respectively in the attempt to satisfy the experimental results.

The calculations for the Sutherland model have been carried out for an attractive field, not restricted in magnitude, varying as r^{-5} by the authors of this paper,† and the values obtained for the force constant of this field differ considerably from those obtained by the use of the approximate Sutherland formula.

The next step is clearly to take the molecular model used by Lennard-Jones, and to determine the law of variation of viscosity with temperature for this case. The investigation contained in this paper has been undertaken primarily in order to compare the values of the force constants determined by the variation of viscosity with temperature with those obtained from the deviations from Boyle's law, and further in order to obtain a formula for the viscosity which is based on a model in which an elastic sphere plays no part.

---

* Lennard-Jones, 'Roy. Soc. Proc.,' A, vol. 106, p. 463 (1924), vol. 107, p. 157 (1925), and Lennard-Jones and Cook, *ibid.*, vol. 112, p. 214 (1926).

† Hassé and Cook, 'Phil. Mag.,' vol. 3, p. 978 (1927).

The calculations necessary to arrive at the formula for the viscosity of a gas based on Lennard-Jones' molecular model are so lengthy that it has only been possible to complete them for a particular pair of values of m and n. In order to carry out the comparison of the values of the force constants as stated above m must be taken equal to 5, and then in order to make the calculation as simple as possible we must take $n = 9$. Hence the problem dealt with in this paper is the working out of a formula for the viscosity of a gas when the molecular repulsive force varies as r^{-9}, and the attractive force varies as r^{-5}. At the same time certain aspects of the general case will be considered as they arise.

The starting point is the formula for the coefficient of viscosity η given by Chapman* in the form

$$\eta = \frac{5}{4h^3M^2}\left(\frac{2\pi}{hM}\right)^{3/2}\frac{1+\varepsilon}{\pi R_{11}}, \tag{1}$$

where $h = (2RT)^{-1}$, R being the gas constant, and R_{11} is defined by

$$R_{11} = 2\pi\int_0^\infty V^7 e^{-\frac{hMV^2}{2}}\,dV\int_0^\infty \sin^2\theta\cos^2\theta\,d(p^2), \tag{2}$$

where V is the relative velocity of any two molecules, each of mass M, before an encounter, $\pi - 2\theta$ is the angle through which the relative path is deflected by the encounter, and p is the length of the perpendicular from the centre of either molecule on the direction of V.

The value of the correcting factor $1 + \varepsilon$ depends on the values of m and n in the law of force between the molecules, and for the case considered in this paper its value may be taken as unity, since for a repulsive force in which $n = 9$ its value is 1·004, while for an attractive force in which $m = 5$ its value is unity. When both repulsive and attractive forces are acting we may expect its value to lie between 1 and 1·004.

It must be remembered that (1) only applies to temperatures high enough to ensure that no multiple collisions occur, and hence that there is no possibility of molecular aggregation.

---

* Chapman, 'Phil. Trans.,' A, vol. 216, p. 279 (1915).

1. *The Theory of the General Case.*

The first stage in the investigation is the calculation of θ as a function of p and V, which is to be obtained from the dynamics of an encounter between two molecules. The polar equation of the relative orbit of two masses m_1 and m_2 under the attractive force μr^{-m} and the repulsive force λr^{-n} is

$$\left(\frac{1}{r}\frac{dr}{d\theta}\right)^2 + 1 = \frac{r^2}{p^2} - \frac{2(m_1+m_2)}{m_1 m_2}\frac{r^2}{p^2 \mathrm{V}^2}\left\{\frac{\lambda}{(n-1)r^{n-1}} - \frac{\mu}{(m-1)r^{m-1}}\right\},$$

which, if we put

$$r\xi = p, \quad (m_1+m_2)\lambda = m_1 m_2 \lambda', \quad (m_1+m_2)\mu = m_1 m_2 \mu',$$

becomes

$$\left(\frac{d\xi}{d\theta}\right)^2 = 1 - \xi^2 - \frac{2}{\mathrm{V}^2}\frac{\lambda'}{n-1}\left(\frac{\xi}{p}\right)^{n-1} + \frac{2}{\mathrm{V}^2}\frac{\mu'}{m-1}\left(\frac{\xi}{p}\right)^{m-1}.$$

Again, if we write

$$a^{n-1}\lambda' = p^{n-1}\mathrm{V}^2, \quad b^{m-1}\mu' = p^{m-1}\mathrm{V}^2, \quad \xi = ay, \quad \text{and} \quad k = (a/b)^{m-1}, \tag{3}$$

the above differential equation for ξ becomes

$$a^2\left(\frac{dy}{d\theta}\right)^2 = 1 - a^2y^2 - \frac{2}{n-1}y^{n-1} + \frac{2}{m-1}ky^{m-1}, \tag{4}$$

and θ is to be obtained by integration with respect to y between the limits 0 and t, where t is the least root of the equation

$$1 - a^2t^2 - \frac{2}{n-1}t^{n-1} + \frac{2}{m-1}kt^{m-1} = 0, \tag{5}$$

and corresponds to the apse of the relative orbit.

From (4) and (5) we have, putting $t = \sin\chi$,

$$\begin{aligned} a^2t^2\cos^2\chi\left(\frac{d\chi}{d\theta}\right)^2 = \cos^2\chi &+ \frac{2t^{n-1}}{n-1}\sin^2\chi\,(1-\sin^{n-3}\chi) \\ &- \frac{2kt^{m-1}}{m-1}\sin^2\chi\,(1-\sin^{m-3}\chi). \end{aligned} \tag{6}$$

For $m = 5$, $n = 9$, (6) gives

$$\theta = at\int_0^{\frac{1}{2}\pi} d\chi\,[1 + \tfrac{1}{4}t^8(s^2+s^4+s^6) - \tfrac{1}{2}kt^4s^2]^{-\frac{1}{2}}, \tag{7}$$

where $s \equiv \sin\chi$, so that θ is a function of a for a given value of k, since t is given in terms of a and k from (5).

Equation (5) plays an important part in the second stage of the investigation which is concerned with the integration with respect to p^2 in (2). It is convenient to change the variable in this integration to a^2 so that from (3) we have

$$\int_0^\infty \sin^2\theta\cos^2\theta\, d\,(p^2) = \left(\frac{\lambda'}{V^2}\right)^{\frac{2}{n-1}} \int_0^\infty \sin^2\theta\cos^2\theta\, d\,(a^2). \tag{8}$$

In the general case it would probably be necessary to take t as the variable instead of a, where from (5)

$$a^2 = t^{-2}\left(1 - \frac{2}{n-1}\,t^{n-1} + \frac{2k}{m-1}\,t^{m-1}\right),$$

so that, corresponding to the range of a from 0 to ∞, the range of t will be t_1 to 0, where t_1 is given by

$$1 - \frac{2}{n-1}\,t_1^{\,n-1} + \frac{2k}{m-1}\,t_1^{\,m-1} = 0, \tag{9}$$

and, since $n > m > 0$, it is easily shown that there is only one positive value t_1 satisfying this equation.

The value of $d\,(a^2)/dt$ is now required, which is

$$2t^{-3}\left(1 + \frac{n-3}{n-1}\,t^{n-1} - \frac{m-3}{m-1}\,kt^{m-1}\right),$$

and changes sign or not in the range $0 < t < t_1$ according as

$$E \equiv 1 - \frac{(n-3)\,(n-m)}{(n-1)\,(m-1)}\,t_2^{\,n-1}$$

is greater or less than zero, where $(n-3)\,t_2^{\,n-m} = (m-3)\,k$. Further, the change of sign, if it occurs, takes place at two values t_3, t_4 in the range.

For example, $m = 5$, $n = 9$, gives $t_2^{\,4} = \frac{1}{3}k$, $E = 1 - k^2/12$, so that $d(a^2)/dt$ changes sign or not in the range $0 < t < t_1$ according as $k^2 \gtrless 12$. Again $m = 5$, $n = 13$ gives $t_2^{\,8} = \frac{1}{5}k$, $E = 1 - \frac{5}{3}t_2^{\,12}$, so that the change of sign takes place or not according as $k^3 \gtrless 45$. Thus there is always a critical value of k, and the calculation proceeds quite differently for values of k above and below this critical value. In the first case, since da^2/dt changes sign at t_3 and t_4, the integration with respect to t has to be split up into the ranges 0 to t_3 and t_4 to t_1, while in the second case da^2/dt does not change sign so that the interval of integration is the whole range 0 to t_1.

The calculation of θ in the general case from (6), and the integration with respect to a in (8), determines

$$\int_0^\infty \sin^2\theta\cos^2\theta\, d\,(a^2)$$

as a function of k for given values of m and n, which integral will be denoted by $(2\pi)^{-1}\,\mathrm{I}_2(n, m\,;\,k)$*. There remains the integration with respect to V in the calculation of R_{11} from (2), which gives

$$\mathrm{R}_{11} = \int_0^\infty \mathrm{V}^7 e^{-\frac{h\mathrm{MV}^2}{2}} \left(\frac{\lambda'}{\mathrm{V}^2}\right)^{\frac{2}{n-1}} \mathrm{I}_2(n, m\,;\,k)\,d\mathrm{V},$$

where from (3)

$$k = \left(\frac{a}{b}\right)^{m-1} = \frac{\mu'}{\mathrm{V}^2}\left(\frac{\mathrm{V}^2}{\lambda'}\right)^{\frac{m-1}{n-1}}.$$

If we write $h\mathrm{MV}^2 = z^2$, and put $m_1 = m_2 = \mathrm{M}$ we find that

$$\mathrm{R}_{11} = \left(\frac{2}{h\mathrm{M}}\right)^{4-\frac{2}{n-1}} (\lambda')^{\frac{2}{n-1}} \int_0^\infty z^{7-\frac{4}{n-1}} e^{-z^2}\,\mathrm{I}_2(n, m\,;\,k)\,dz, \tag{10}$$

where

$$k = \frac{\mu'}{(\lambda')^{\frac{m-1}{n-1}}}\left(\frac{2z^2}{h\mathrm{M}}\right)^{\frac{m-n}{n-1}}, \quad \text{and} \quad \lambda' = \frac{2\lambda}{\mathrm{M}}, \qquad \mu' = \frac{2\mu}{\mathrm{M}}. \tag{11}$$

In the particular case of $m = 5$, $n = 9$,

$$\mathrm{R}_{11} = \left(\frac{2}{h\mathrm{M}}\right)^{15/4} (\lambda')^{1/4} \int_0^\infty z^{13/2} e^{-z^2}\,\mathrm{I}_2(k)\,dk, \tag{12}$$

and $k = \mu h^{\frac12}/\lambda^{\frac12}$, where $\mathrm{I}_2(k)$ has been written instead of $\mathrm{I}_2(9, 5\,;\,k)$.

Before leaving the general case, it is of interest to consider the case of k small, which would correspond to a *weak* attractive field of the type μr^{-m} superposed on a repulsive field of the type λr^{-n}.

It is evident from (6) that in this case θ will differ from its value when k is zero by a term involving the first power of k, and that this is also true as regards the value of a^2, whence it follows that $\mathrm{I}_2(n, m\,;\,k)$ may be taken as a linear function of k so that from (10) and (11)

$$\mathrm{R}_{11} = \left(\frac{2}{h\mathrm{M}}\right)^{4-\frac{2}{n-1}} (\lambda')^{\frac{2}{n-1}} \int_0^\infty z^{7-\frac{4}{n-1}} e^{-z^2}\,\mathrm{F}(z)\,dz, \tag{13}$$

where

$$\mathrm{F}(z) \equiv \mathrm{I}_2(n, m\,;\,0) + \mathrm{A}\mu'\left(\tfrac{1}{2}h\mathrm{M}\right)^{\frac{n-m}{n-1}} (z^2)^{\frac{m-n}{n-1}} (\lambda')^{\frac{1-m}{n-1}},$$

and A is a numerical constant depending on the values of m and n. The integrals in (13) can be expressed in terms of Γ functions, so that

$$\eta = \frac{5}{8}\left(\frac{\pi\mathrm{M}}{2h}\right)^{\frac12} (h\lambda)^{-\frac{2}{n-1}} \Big/ \mathrm{D}, \tag{14}$$

where

$$\mathrm{D} = \Gamma\left(4 - \frac{2}{n-1}\right)\mathrm{I}_2(n, m\,;\,0) + \mathrm{A}\mu'\left(\frac{h\mathrm{M}}{2}\right)^{\frac{n-m}{n-1}} (\lambda')^{\frac{1-m}{n-1}}\,\Gamma\left(3 - \frac{3-m}{n-1}\right),$$

---

* The notation is introduced as an extension of that given by Chapman, 'Mem. Proc. Manchester Lit. Phil. Soc.,' vol. 66 (1922).

in which the additional term in D due to the *weak* attractive field can be calculated when A has been determined.

The variation of η with the temperature, which is of chief interest, can be easily obtained since this depends only on h, $= (2\mathrm{RT})^{-1}$, and we have from (14)

$$\eta = \mathrm{BT}^{\frac{1}{2}+\frac{2}{n-1}} \Big/ \left(1 + \mathrm{ST}^{\frac{m-n}{n-1}}\right), \tag{15}$$

where

$$\mathrm{B} = \frac{5\,(\pi \mathrm{M})^{\frac{1}{2}}\,\mathrm{R}^{\frac{1}{2}+\frac{2}{n-1}}}{2^{\left(3-\frac{2}{n-1}\right)}\,\lambda^{\frac{2}{n-1}}\,\Gamma\left(4-\frac{2}{n-1}\right)\mathrm{I}_2\,(n,\, m\,;\, 0)}, \tag{16}$$

and S may be called a generalised Sutherland constant.

For $n = \infty$, this gives the ordinary Sutherland formula, while for $m = 3$ we have Lennard-Jones'* formula

$$\eta \propto \frac{\mathrm{T}^{3/2}}{\mathrm{T}^{\frac{n-3}{n-1}} + \mathrm{S}'}$$

where the dependence of S on n and m has been indicated by using the symbol S′ for this constant.

The difficulty in applying (15), or any special case of it, is that it gives no indication of the error involved in the approximation by which it was obtained, so that it is necessary to have an accurate formula for the viscosity of a gas before any satisfactory comparison with experiment can be made.

2. *Calculation for the Special Case* $m = 5$, $n = 9$.

The case of $m = 5$, $n = 9$, lends itself to trigonometrical treatment by putting $k = 2 \tan \alpha$, $at = \sec \alpha \sin \phi$ whence we obtain from (5),

$$a^4 = (\sec^3 \alpha \sin^4 \phi)/2\,(\sin \alpha \pm \cos \phi),$$

so that, taking the positive sign, ϕ will range from 0 to $\frac{1}{2}\pi + \alpha$ as a ranges from 0 to ∞.

Since

$$\frac{d\,(a^2)}{d\phi} = \left(\frac{\sec^3 \alpha}{8}\right)^{\frac{1}{2}} \frac{\sin \phi\,(4 \sin \alpha \cos \phi + 1 + 3 \cos^2 \phi)}{(\sin \alpha + \cos \phi)^{3/2}},$$

it vanishes when

$$3 \cos \phi = -2 \sin \alpha \pm (4 \sin^2 \alpha - 3)^{\frac{1}{2}},$$

so that for $\alpha < 60°$, corresponding to $k^2 < 12$, $d\,(a^2)/d\phi$ is always positive.

---

* 'Roy. Soc. Proc.,' A, vol. 106, p. 441 (1924).

For values of $\alpha \leqslant 60°$, θ is to be determined from (7), which now reads

$$\theta = \sin\phi \int_0^{\frac{1}{2}\pi} \mathrm{D}^{-\frac{1}{2}}\, d\chi, \tag{17}$$

where

$$\mathrm{D} \equiv 1 + (\sin\alpha + \cos\phi)^2 (s^2 + s^4 + s^6) - 2\sin\alpha\,(\sin\alpha + \cos\phi)\, s^2,$$

for given values of α and ϕ.

The integral in (8) with respect to a^2 then becomes

$$\left(\frac{\sec^3\alpha}{8}\right)^{\frac{1}{2}} \int_0^{\frac{1}{2}\pi+\alpha} \sin^2\theta\cos^2\theta\, \frac{\sin\phi\,(4\sin\alpha\cos\phi + 1 + 3\cos^2\phi)}{(\sin\alpha + \cos\phi)^{3/2}}\, d\phi, \tag{18}$$

which integral is $(2\pi)^{-1}\,\mathrm{I}_2(k)$, the integral with $\cos^2\theta$ in place of $\sin^2\theta\cos^2\theta$ being denoted by $(2\pi)^{-1}\,\mathrm{I}_1(k)$. This latter integral occurs in the kinetic theory of diffusion, and in any case its calculation serves as a useful check on the numerical work, as its integrand clearly oscillates less rapidly than that of $(2\pi)^{-1}\,\mathrm{I}_2(k)$, so that $\mathrm{I}_1(k)$ is easier to obtain accurately.

The case of $\alpha = 0$ was worked out in some detail, and it was found that by taking 5° intervals in the integration with respect to χ in (17) the values of θ so obtained were correct to within 1 second of arc. In the integration in (18) 5° intervals were also taken and the values $\mathrm{I}_1(0) = 2{\cdot}39263$, $\mathrm{I}_2(0) = 1{\cdot}03797$, were obtained, in the calculation of which the general difference formula for numerical integration was always used in preference to the 6-ordinate rule or to Weddle's rule. Chapman* has given 2·4000, and 1·0435 for the values of these integrals, and it seems probable that the difference is due to the use by Chapman of Simpson's rule for the numerical integration combined with the fact that 9° intervals were taken in the integration with respect to ϕ, as the values of θ obtained agreed very well with those given by Chapman.

The values of $\mathrm{I}_1/2\pi$ and $\mathrm{I}_2/2\pi$ were then calculated for values of α at 5° intervals from 0° to 60°, and the results are given in the following table.

---

* Chapman, 'Mem. Proc. Manchester Lit. Phil. Soc.,' vol. 66 (1922).

Table I.

α. °	$I_1/2\pi$.	$I_2/2\pi$.
0	0·38080	0·16520
5	0·36504	0·15474
10	0·35325	0·14722
15	0·34700	0·14424
20	0·34886	0·14827
25	0·36286	0·16301
30	0·39543	0·19360
35	0·45675	0·24586
40	0·56231	0·32205
45	0·73297	0·40754
50	0·98228	0·44926
55	1·23697	0·44778
60	1·32953	0·50824

Taking the values from $\alpha = 0°$ to $\alpha = 45°$, those for k ($= 2 \tan \alpha$) at intervals of 0·25 were obtained by numerical interpolation.

Table II.

k.	$I_1/2\pi$.	$I_2/2\pi$.
0	0·38080	0·16520
0·25	0·35947	0·15108
0·50	0·34766	0·14435
0·75	0·34972	0·14929
1·00	0·37066	0·17059
1·25	0·41584	0·21165
1·50	0·49001	0·27171
1·75	0·59603	0·34269
2·00	0·73297	0·40754

An accuracy of five decimal places was aimed at throughout the calculation, and to ensure this all the refinements of the calculus of differences were employed, the intervals of the variable in the numerical integration in (17) and (18) were often halved, and sometimes halved again, and for special small ranges of integration the integrand had often to be expanded in series and integrated term by term. Up to $\alpha = 45°$ no great difficulty was experienced in reaching this accuracy, but it is clear that the calculation becomes a much more serious matter as α approaches the critical angle 60°, and it is in the range 45° to 60° that the calculation presents the greatest difficulties. Table I shows that in this range I_1 increases very rapidly, and that I_2 has a maximum followed by a minimum. This behaviour of I_2 was noticed in the corresponding calculation for the Sutherland model* ($n = \infty$, $m = 5$), and it was there suggested that it might be a characteristic of this model, but unfortunately it occurs again in the case of $m = 5$, $n = 9$.

The above applies only to the range $0° < \alpha < 60°$, *i.e.*, for $k^2 < 12$. For $k^2 > 12$, the procedure is somewhat different. We first of all take b as the variable instead of a from (3), and then write $b^2 = \gamma^2\sqrt{2}$, so that, since $k = (a/b)^4$ for $m = 5$,

$$\int_0^\infty \sin^2\theta\cos^2\theta\, d(a^2) = (2k)^{\frac{1}{2}} \int_0^\infty \sin^2\theta\cos^2\theta\, d(\gamma^2). \tag{19}$$

If we put $kt^4 = 2x^2$, then (5) for $m = 5$, $n = 9$ becomes

$$2\gamma^2 x = 1 + x^2 - k'^2 x^4, \tag{20}$$

where $k' \equiv k^{-1}$, and x is finally to be taken as the variable instead of γ^2.

With these changes in notation, θ is from (7) determined by the equation

$$\theta = (2\gamma^2 x)^{\frac{1}{2}} \int_0^{\frac{1}{2}\pi} d\chi\, \mathrm{D}'^{-\frac{1}{2}}, \tag{21}$$

where

$$\mathrm{D}' \equiv 1 - x^2 s^2 + k'^2 x^4 (s^2 + s^4 + s^6).$$

The advantage of this method is that it enables us to connect the calculations with those for the Sutherland model ($n = \infty$, $m = 5$) in so far as in the limiting case $k' = 0$, ($k \rightarrow \infty$) the value of the integral in (19) with respect to γ^2 is known.

Since $k^2 > 12$, it follows from (20) that γ^2 has a minimum when $x = x_1$, that it vanishes when $x = x_3$, and that the tangent at $x = x_1$ cuts the curve again when $x = x_2$, where these values are given by

$$6k'^2 x_1^2 = 1 - \sqrt{(1 - 12k'^2)}, \qquad 2k'^2 x_3^2 = 1 + \sqrt{(1 + 4k'^2)},$$

and

$$x_2 = \sqrt{(k^2 - 2x_1^2)} - x_1.$$

As γ^2 decreases from infinity to zero, it follows that x increases from 0 to x_1 and then increases from x_2 to x_3, so that the integration with respect to x has to be divided into two portions.

For the range $0 \leqslant x \leqslant x_1$, we write $x = x_1 \sin\beta$ and change the variable from γ^2 to β so that we have

$$\theta = \sqrt{(1 + x_1^2 \sin^2\beta - k'^2 x_1^4 \sin^4\beta)} \int_0^{\frac{1}{2}\pi} d\chi\, \mathrm{D}'^{-\frac{1}{2}},$$

---

* Hassé and Cook, *loc. cit.*

and the contribution of this range to the value of the integral with respect to γ^2 in (19) is

$$\frac{1}{2x_1}\int_0^{\frac{1}{2}\pi}\sin^2\theta\cos^2\theta\frac{\cos^3\beta}{\sin^2\beta}\{1-(x_1^2-1)\sin^2\beta\}\,d\beta. \tag{22}$$

For the range $x_2 \leqslant x \leqslant x_3$ the difficulties of the calculation become very pronounced, especially as $k' \to 0$, and the authors are indebted to Prof. G. N. Watson for providing the following method which made it possible to carry through the calculation for this range. The problem is to find the value of θ from (21), in which the integral

$$\mathrm{I} = \int_0^{\frac{1}{2}\pi} d\chi\,\{1 - x^2s^2 + k'^2x^4(s^2+s^4+s^6)\}^{-\frac{1}{2}}$$

occurs, when k' is small, x is large, and $k'x - 1$ is small, and the integrand has a maximum value in the range of integration. If we put $s \equiv \sin^2\chi = w$, the integral is

$$(2k'x^2)^{-1}\int_0^1 dw\,\{w(1-w)(w^3+w^2+w-w(k'x)^{-2}+(k'x^2)^{-2})\}^{-\frac{1}{2}}$$

and, since $1-(k'x)^{-2}$, and $(k'x^2)^{-2}$ are both small, the roots of the equation

$$w^3+w^2+w-w(k'x)^{-2}+(k'x^2)^{-2}=0$$

are approximately 0, 0, -1. The maximum value of the integrand being due to the existence of complex roots of small modulus of this equation, we take the exact values of these roots to be $\beta \pm i\gamma$, $-1-2\beta$ so that

$$\mathrm{I} = (2k'x^2)^{-1}\int_0^1 dw\,(w+1+2\beta)^{-\frac{1}{2}}[w(1-w)(\overline{w-\beta}^2+\gamma^2)]^{-\frac{1}{2}}.$$

This integral is transformed by the substitution

$$w/(1-w) = \lambda(1+t)/(1-t),$$

where λ is a positive constant to be determined, so that we have

$$(w-\beta)^2+\gamma^2 = \frac{\lambda(\Delta_1+2\Delta_2t+\Delta_3t^2)}{\{(1+\lambda)-t(1-\lambda)\}^2},$$

where

$$\lambda\Delta_1 = \lambda^2 - 2\beta\lambda(1+\lambda)+(\beta^2+\gamma^2)(1+\lambda)^2,$$
$$\lambda\Delta_2 = \lambda^2 - 2\beta\lambda^2+(\beta^2+\gamma^2)(\lambda^2-1),$$
$$\lambda\Delta_3 = \lambda^2 + 2\beta\lambda(1-\lambda)+(\beta^2+\gamma^2)(1-\lambda)^2.$$

If λ is chosen so that $\Delta_2 = 0$ making

$$\lambda^2 = (\beta^2 + \gamma^2)/\{(1 - \beta)^2 + \gamma^2\},$$

we find that, putting $t = \cos\psi$

$$\mathrm{I} = \frac{(k'x^2)^{-1}}{2(\Delta_1 + \Delta_3)^{\frac{1}{2}}} \int_0^{\pi} \frac{d\psi}{\sqrt{(1 - p^2 \sin^2\psi)}} \left[1 + 2\beta + \frac{\lambda\cos^2\frac{1}{2}\psi}{\sin^2\frac{1}{2}\psi + \lambda\cos^2\frac{1}{2}\psi}\right]^{-\frac{1}{2}},$$

where

$$2p^2 = \frac{2\Delta_3}{\Delta_1 + \Delta_3} = 1 - \frac{\beta^2 + \gamma^2 - \beta}{(\beta^2 + \gamma^2)^{\frac{1}{2}}\{(1 - \beta)^2 + \gamma^2\}^{\frac{1}{2}}}.$$

and finally

$$\begin{aligned} \mathrm{I} &= \frac{\sqrt{\lambda}}{2} \int_0^{\pi} \frac{d\psi}{\sqrt{(1 - p^2\sin^2\psi)}} \left[1 + \frac{\lambda/(1 + 2\beta)}{\lambda + \tan^2\frac{1}{2}\psi}\right]^{-\frac{1}{2}} \\ &= \frac{\sqrt{\lambda}}{2} \int_0^{\frac{1}{2}\pi} \frac{d\psi}{\sqrt{(1 - p^2\sin^2\psi)}} \left\{\left[1 + \frac{\lambda/(1 + 2\beta)}{\lambda + \tan^2\frac{1}{2}\psi}\right]^{-\frac{1}{2}} + \left[1 + \frac{\lambda/(1 + 2\beta)}{\lambda + \cot^2\frac{1}{2}\psi}\right]^{-\frac{1}{2}}\right\}. \end{aligned} \tag{23}$$

The expression in { } in this integral is a slowly varying monotomic increasing function of ψ, so that the largest value of the integrand occurs when $\psi = \frac{1}{2}\pi$.

For the integration with respect to x, we write

$$x = x_3 - (x_3 - x_2)\cos\phi,$$

whence

$$\int_{x_2}^{x_3} \cos^2\theta \sin^2\theta \, d(\gamma^2) = (x_3 - x_2) \int_0^{\frac{1}{2}\pi} \cos^2\theta \sin^2\theta \frac{d(\gamma^2)}{dx} \sin\phi \, d\phi. \tag{24}$$

The calculation of the values of the integrals

$$\mathrm{Y}_1 \equiv \int_0^{\infty} \cos^2\theta \frac{d(\gamma^2)}{dx} dx, \quad \mathrm{Y}_2 \equiv \int_0^{\infty} \sin^2\theta\cos^2\theta \frac{d(\gamma^2)}{dx} dx,$$

for the two ranges $0 \leqslant x \leqslant x_1$, and $x_2 \leqslant x \leqslant x_3$ separately, and for the whole range gave the following results for $k = 4, 6, 8, 10$, the values as $k \to \infty$ being already known.

Table III.

k.	(1st range).	(2nd range).	Y_1.	(1st range).	(2nd range).	Y_2.
4	0·11680	0·39419	0·51099	0·06922	0·12403	0·19325
6	0·10834	0·41461	0·52295	0·06671	0·12648	0·19319
8	0·10613	0·42359	0·52972	0·06600	0·12716	0·19316
10	0·10520	0·42778	0·53298	0·06570	0·12742	0·19312
∞	0·10366	0·44894	0·55260	0·06518	0·12739	0·19257

3. *Formula for the Viscosity for the Special Case.*

The calculations so far completed have given the value of $I_2(k)$ for certain values of k. In order to find the formula for the coefficient of viscosity it remains to carry out the integration with respect to z in (13). If this integral is denoted by $I(s)$, where $k = (zs)^{-1}$, then we have, since $s = \lambda^{\frac{1}{2}}/\mu h^{\frac{1}{2}}$,

$$R_{11} = 2\pi\,(2/M)^{4}\,(\lambda/h)^{\frac{1}{2}}\,I(s)/h^{4}s^{\frac{1}{2}},$$

whence from (1) the coefficient of viscosity η is given by

$$\eta = \tfrac{5}{32}\,(MRT/\pi)^{\frac{1}{2}}\,(\mu/\lambda)^{\frac{1}{2}}\,s^{\frac{1}{2}}/I(s), \tag{25}$$

where

$$s = (2RT\lambda)^{\frac{1}{2}}/\mu. \tag{26}$$

In order to calculate $I(s)$ it was found most convenient to replace the tabulation of $I_2(k)$ as a function of k by algebraic functions of k, and to use incomplete gamma functions for the integration. The range of k from 0 to ∞ was split up into four sections, and the following expressions were obtained :—

$$(0 \leqslant k \leqslant 1),\quad I_2(k) = 0\cdot16520 - 0\cdot06507k + 0\cdot02268k^2 + 0\cdot04778k^3,$$

$$(1 \leqslant k \leqslant 2),\quad I_2(k) = 0\cdot04084 + 0\cdot38639k - 0\cdot60454k^2 + 0\cdot44429k^3 - 0\cdot09639k^4,$$

$$(2 \leqslant k \leqslant 4),\quad I_2(k) = -7\cdot62945 + 11\cdot33735k - 5\cdot87922k^2 + 1\cdot33082k^3 - 0\cdot11046k^4,$$

$$(4 \leqslant k < \infty),\quad I_2(k) = 0\cdot27234k^{\frac{1}{2}} + 0\cdot00344 - 0\cdot00309k^{-\frac{1}{2}}.$$

The errors in the calculation of $I(s)$ arise from those due to the replacement of the tabulated values of $I_2(k)$ by these algebraic expressions. These latter errors are estimated to be less than 1 in 3100, 1 in 2700, 1 in 100 and 1 in 19000 for the four sections respectively, the large error in the third section being due to the existence of the maximum and minimum values of $I_2(k)$ already considered. The consequent errors $\Delta I(s)$ in $I(s)$ are given in the following table.

Table IV.

s.	$\Delta I(s)$.	s.	$\Delta I(s)$.	s.	$\Delta I(s)$.
0·10	0·0015	0·30	0·0036	0·50	0·0004
0·15	0·0072	0·35	0·0020	0·55	0·0003
0·20	0·0081	0·40	0·0011	0·60	0·0002
0·25	0·0060	0·45	0·0006	0·65	0·0001

In order to use (25), $s^{\frac{1}{2}}/\mathrm{I}(s)$ has been tabulated as a function of s in Table V, the accuracy of which can be determined from the errors given in Table IV, which shows that the large error in the third section dominates the situation for values of $s \leqslant 0 \cdot 4$.

Table V.

s.	$s^{\frac{1}{2}}/\mathrm{I}(s)$.	s.	$s^{\frac{1}{2}}/\mathrm{I}(s)$.	s.	$s^{\frac{1}{2}}/\mathrm{I}(s)$.	s.	$s^{\frac{1}{2}}/\mathrm{I}(s)$.
0·05	0·1102	0·55	1·7714	1·1	3·2254	2·2	4·4415
0·10	0·2181	0·60	1·9753	1·2	3·3763	2·4	4·6120
0·15	0·3306	0·65	2·1622	1·3	3·5126	2·6	4·7751
0·20	0·4359	0·70	2·3308	1·4	3·6381	2·8	4·9320
0·25	0·5529	0·75	2·4830	1·5	3·7551	3·0	5·0835
0·30	0·7030	0·80	2·6200	1·6	3·8656	3·2	5·2302
0·35	0·8886	0·85	2·7440	1·7	3·9707	3·4	5·3725
0·40	1·1005	0·90	2·8567	1·8	4·0714	3·6	5·5110
0·45	1·3261	0·95	2·9598	1·9	4·1684	3·8	5·6459
0·50	1·5533	1·00	3·0548	2·0	4·2621	4·0	5·7776

For a *weak* attractive field of the type μr^{-5}, so that s is large, the approximate value of $\mathrm{I}(s)$ is

$$0 \cdot 36534 - 0 \cdot 08294\, s^{-1} + 0 \cdot 01824\, s^{-2} + 0 \cdot 02706\, s^{-3},$$

whence, taking only the first two terms, we have from (25)

$$\eta = \tfrac{5}{32}\left(\frac{\mathrm{MR}}{\pi\lambda}\right)^{\frac{1}{2}} \frac{(2\mathrm{R}\lambda)^{\frac{1}{4}}\,\mathrm{T}^{\frac{3}{4}}}{0 \cdot 36534 - (0 \cdot 08294)\,\mu\,(2\mathrm{RT}\lambda)^{-\frac{1}{2}}}$$

so that, in comparison with (15) for $m = 5$, $n = 9$, the value of S is equal to

$$-\,0 \cdot 08294\,\mu/(0 \cdot 36534)\,(2\mathrm{R}\lambda)^{\frac{1}{2}}$$

being negative as in the case $m = 3$ discussed by Lennard-Jones.

In order to carry out the comparison between theory and experiment, equations (25) and (26) are written in the forms

$$\log\,(\eta \mathrm{T}^{-\frac{1}{2}}) - \log s^{\frac{1}{2}}/\mathrm{I}(s) = \log \tfrac{5}{32}\,(\mathrm{MR}/\pi)^{\frac{1}{2}} + \tfrac{1}{2} \log\,(\mu/\lambda), \qquad (27)$$

and

$$\tfrac{1}{2} \log \mathrm{T} - \log s = \log\,(\mu \lambda^{-\frac{1}{2}}) - \tfrac{1}{2} \log 2\mathrm{R}. \qquad (28)$$

Log $\eta \mathrm{T}^{-\frac{1}{2}}$ is plotted, on transparent paper, against log T from the experimental data for the various gases considered, and log $s^{\frac{1}{2}}/\mathrm{I}(s)$ is plotted against log s so that the scales of log $\eta \mathrm{T}^{-\frac{1}{2}}$ and of log $s^{\frac{1}{2}}/\mathrm{I}(s)$ are the same, while the scale of log s is twice that of log T. The two curves are moved, one over the other, the axes being kept parallel, until the experimental points lie as nearly as possible on the theoretical curve. To determine the best fit of the two curves, several attempts are made and the value of $\Sigma(p^2)$, where p is the perpendicular distance from an experimental point to the theoretical curve, is determined for each fit. With the actual scales adopted, in which 1 inch represents 0·1 both for $\log s$ and $\log s^{\frac{1}{2}}/\mathrm{I}(s)$, the unit for p was taken as 0·01 inch.

For each such fit a parallel transformation* with constants P, Q is therefore defined by

$$\log \eta \mathrm{T}^{-\frac{1}{2}} - \log s^{\frac{1}{2}}/\mathrm{I}(s) = \mathrm{Q}, \qquad \tfrac{1}{2}\log \mathrm{T} - \log s = \mathrm{P},$$

whence from (27) and (28) we have

$$\mathrm{Q} = \log \tfrac{5}{32}(\mathrm{MR}/\pi)^{\frac{1}{2}} + \tfrac{1}{2}\log(\mu/\lambda), \tag{29}$$

and

$$\mathrm{P} = \log(\mu/\lambda^{\frac{1}{2}}) - \tfrac{1}{2}\log 2\mathrm{R}, \tag{30}$$

from which μ and λ can be found.

The corresponding values of the "diameter" as defined by Lennard-Jones by the formula

$$\sigma_n = (2\lambda n/3(n-1)\,\mathrm{R})^{1/n-1},$$

can then be calculated, and in the cases where the index of the law of force is 9 or 5 the formula gives

$$\sigma = (\lambda/12\mathrm{R})^{1/8} \quad \text{and} \quad \sigma' = (\mu/6\mathrm{R})^{1/4}, \tag{31}$$

which make σ and σ' of the same order of magnitude.

4. *Results of Comparison with Experiment.*

1. *Argon.*—The values of the viscosity of argon have been given by Schmidt.† With the exception of that at the lowest temperature (89·9° absolute) these values can be made to give an excellent fit with the theoretical curve. The following table gives the results of five attempts, and shows the values of the constants of the transformation and the values of the force constants λ and μ for which the curves may be taken to fit. The values of the force constants found by Lennard-Jones from the equation of state for the same molecular model are included in the table for comparison with those obtained from viscosity.

---

* This method, originally due to Keesom, has been used by Lennard-Jones in his investigations in connection with the equation of state of a gas.

† Schmidt, 'Ann. Physik,' vol. 30, p. 400 (1909).

Table VI.—Results for Argon.

	P.	Q.	$\mu 10^{43}$.	$\lambda 10^{72}$.	$\Sigma(p^2)$.
1	1·270	$\bar{6}$·667	3·10	1·01	57
2	1·270	$\bar{6}$·660	3·20	1·08	51
3	1·273	$\bar{6}$·659	3·26	1·10	50
4	1·2635	$\bar{6}$·656	3·17	1·09	57
5	1·267	$\bar{6}$·657	3·20	1·09	60
Best fit, mean of 2 and 3			3·23	1·09	
From equation of state			1·62	1·01	

If the result for the lowest temperature is omitted a very good fit can be obtained which gives $\Sigma(p^2) = 15$, $P = 1\cdot2975$, $Q = \bar{6}\cdot677$, $\lambda\, 10^{72} = 1\cdot05$, $\mu\, 10^{43} = 3\cdot36$.

The viscosity was then calculated from the theoretical formula, using (*a*) the force constants as given by taking the best fit of the theoretical and experimental curves, and (*b*) the force constants as determined from the equation of state.

Table VII.—Viscosity of Argon.

T. (abs.)	$\eta\, 10^7$. (obs.)	$\eta\, 10^7$. (*a*).	$\eta\, 10^7$. (*b*).
456·4	3243	3212	3186
372·8	2751	2745	2756
286·3	2207	2216	2280
272·9	2116	2129	2203
252·8	1987	1993	2085
232·9	1854	1855	1965
212·9	1697	1711	1841
194·3	1575	1572	1722
168·7	1379	1373	1553
89·9	735·6	686·9	957·6

Fig. 1 shows the theoretical curve and the experimental points superposed on it so as to give the best fit.

2. *Hydrogen.*—The viscosity of hydrogen* has been measured by Markowski, Schmidt, and Kamerlingh Onnes, Dorsman and Weber over a wide range of temperature. The results of fitting the experimental data to the theoretical

---

* Markowski, 'Ann. Physik,' vol. 14, p. 742 (1904); Schmidt, *loc. cit.*; Kamerlingh Onnes, Dorsman and Weber, 'Comm. Phys. Lab. Leiden,' No. 134, *a* (1913).

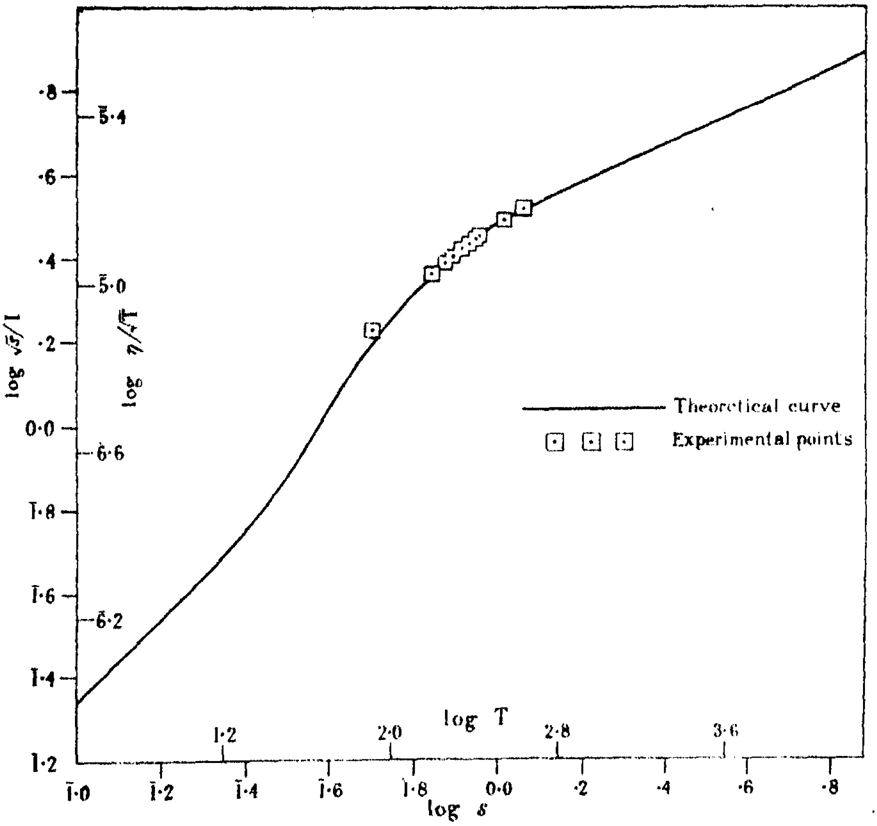

Fig. 1.—Superposition of Theoretical and Experimental Curves for Argon.

curve are given in Table VIII, together with the force constants as deduced from the equation of state, using the same molecular model.

Table VIII.—Results for Hydrogen.

	P.	Q.	$\mu 10^{44}$.	$\lambda 10^{78}$.	$\Sigma(p^2)$.
1	0·8065	$\bar{6}$·0315	3·45	1·06	295
2	0·810	$\bar{6}$·033	3·48	1·06	286
3	0·824	$\bar{6}$·040	3·60	1·06	285
4	0·818	$\bar{6}$·0355	3·41	1·03	302
Mean of 2 and 3			3·54	1·06	
From equation of state			2·54	0·92	

The values of the viscosity as calculated from the theoretical formula, (*a*) using the force constants determined above, (*b*) using those deduced from the equation of state, and (*c*) as given by Kamerlingh Onnes on the basis of the repulsive law of force varying as $r^{-11\cdot 2}$, are given in Table IX.

Table IX.—Viscosity of Hydrogen.

T (abs.).	$\eta 10^7$ (obs.).	$\eta\ 10^7\ (a)$.	$\eta\ 10^7\ (b)$.	$\eta\ 10^7\ (c)$.
457·3	1212	1226	1253	1207
373·6	1046	1060	1082	1052
287·6	877	878	896	875
273·0	844	846	863	843
261·2	821	820	836	816
255·3	802	806	822	803
233·2	760	756	770	757
212·9	710	708	722	709
194·4	670	664	676	666
170·2	609·3	603	614	608
89·63	392·2	380	388	389
70·87	319·3	320	328	329
20·04	105–111	111	125	137

3. *Nitrogen.*—In this case an almost exact fit was obtained for the following values of the constants, the experimental* data being taken from the work of Schmidt, Vogel, and Kia Lok Yen.

Table X.—Result for Nitrogen.

P.	Q.	$\mu\ 10^{48}$.	$\lambda\ 10^{78}$.
1·180	5·499	3·11	1·54
From equation of state …………………		1·82	1·58

4. *Air.*—The experimental data in the case of air are due to Vogel and Breitenbach† for the range of temperatures from 81·6° absolute to 575° absolute. Measurements of the viscosity of air have recently been made over the range from 288° absolute to 718° absolute by Edwards‡ in connection with a discussion of the experiments of Williams on the viscosity of air at high temperatures. The results of Breitenbach and Edwards, the latter being reduced to agree with the former at 15° C. are in good agreement, and have been used together

---

* Schmidt, *loc. cit.*; Vogel, 'Ann. Physik,' vol. 43, p. 1258 (1914); Kia Lok Yen, 'Phil. Mag.,' vol. 38, p. 582 (1919).

† Vogel, *loc. cit.*; Breitenbach, 'Ann. Physik,' vol. 5, p. 166 (1901).

‡ Edwards, 'Roy. Soc. Proc.,' A, vol. 117, p. 245 (1927); Williams, 'Roy. Soc. Proc.,' A, vol. 110, p. 141 (1926).

with those of Vogel for a determination of the force constants with the following result.

Table XI.—Results for Air.

	P.	Q.	$\mu\,10^{43}$.	$\lambda\,10^{72}$.	$\Sigma(p^2)$.
1	1·201	$\bar{6}$·5235	3·17	1·45	151
2	1·189	$\bar{6}$·5165	3·10	1·46	81
3	1·178	$\bar{6}$·511	3·02	1·46	93
4	1·1695	$\bar{6}$·508	2·94	1·45	127

The fit of the experimental and theoretical curves for the second determination in the above table is given in fig. 2, which shows that the fit is governed by the values at the lower temperatures, and that the values for the two highest temperatures show a distinct tendency to fall below the theoretical curve. The values given by Williams below 500° C. are quite inconsistent with the values for lower temperatures, though it is possible that those above 500° C.

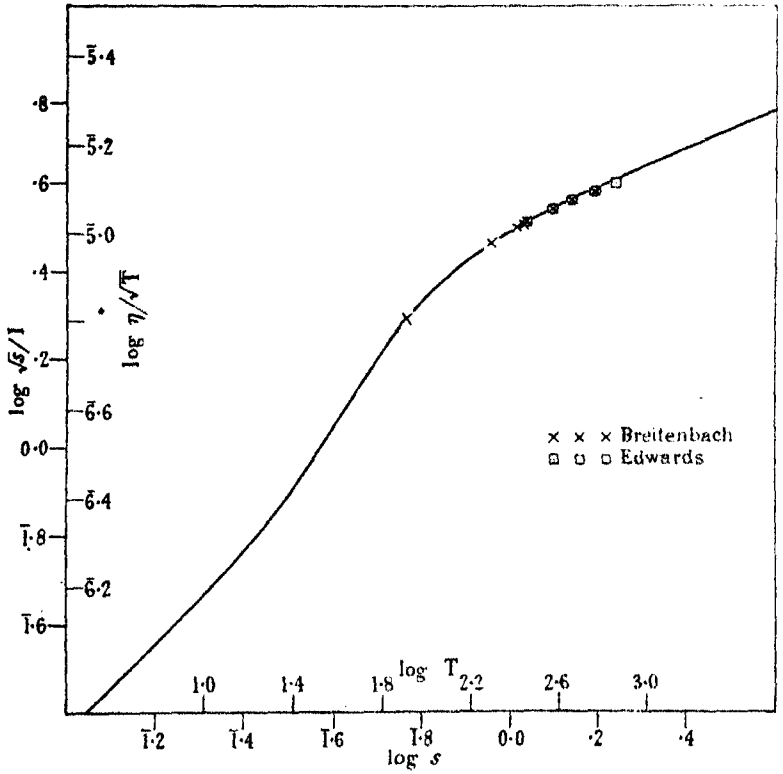

Fig. 2.—Superposition of Theoretical and Experimental Curves for Air.

would fit on to a smooth curve through the values given by Edwards, Breitenbach and Vogel for lower temperatures.

Further experimental results at temperatures up to 923° absolute have been given recently,[*] and the values are in fair agreement with those given by Williams, and therefore distinctly below the theoretical curve for $m = 5$, $n = 9$ given in the figure.

It seems, therefore, that $n = 9$ is not the correct value for the case of air, and that a higher value would have to be taken in order to obtain agreement with the experimental results at high temperatures which suggest a value in the neighbourhood of $n = 13$. All that has been shown in this paper is that between 80° and 500° absolute, the choice of $m = 5$, $n = 9$ is consistent with experiment, so that the case of air indicates very well the limitations of this choice, and the need for further calculations with a higher value of n.

5. *Carbon-dioxide.*—The viscosity of carbon-dioxide has been determined by Breitenbach and Vogel (*loc. cit.*) over a range of temperature from 194·6° absolute to 575·1° absolute, and the values of the force constants deduced are given in the following table, in which the fourth attempt to fit the experimental and theoretical curves gives the least value of $\Sigma\,(p^2)$.

Table XII.—Results for Carbon-dioxide.

	P.	Q.	$\mu\,10^{43}$.	$\lambda\,10^{72}$.	$\Sigma(p^2)$.
1	1·352	$\bar{6}\cdot5465$	8·67	5·42	678
2	1·337	$\bar{6}\cdot532$	8·65	5·79	498
3	1·3275	$\bar{6}\cdot527$	8·48	5·79	478
4	1·3155	$\bar{6}\cdot513$	8·55	6·24	470
5	1·301	$\bar{6}\cdot5045$	8·32	6·31	528

The large values of $\Sigma\,(p^2)$ show that the fits in this case are not at all good, which is due to the fact that the point corresponding to the lowest temperature cannot be made to fall on to the theoretical curve without readjusting the fit obtained from the other points. If this point is omitted, a very good fit can be obtained for which $\Sigma\,(p^2) = 10$, where $\mathrm{P} = 1\cdot387$, $\mathrm{Q} = \bar{6}\cdot567$, $\mu 10^{43} = 9\cdot27$, and $\lambda\,10^{72} = 5\cdot27$.

6. *Mercury Vapour.*—The viscosity of mercury vapour has recently been measured by Braume, Basch and Wentzel (*loc. cit.*) and the results are particularly interesting as they provide the *reductio ad absurdum* of the application

---

[*] Braume, Basch and Wentzel, 'Z. Phys. Chem.,' vol. 137, p. 178 (1928). The authors are indebted to Prof. A. O. Rankine for this reference.

of the approximate Sutherland formula. The value of S is found to be 942 whence, as the highest temperature is 880°, S/T is always greater than unity instead of being small as is demanded by the theoretical deduction of the formula.

It was found possible to obtain a fairly good fit for the region of the theoretical curve from $s = 0 \cdot 22$ to $s = 0 \cdot 29$, the results being given in the following table.

Table XIII.—Results for Mercury Vapour.

	P.	Q.	$\mu\, 10^{48}$.	$\lambda\, 10^{74}$.	$\Sigma(p^2)$.
1	2·0245	$\bar{5}$·662	5·14	8·59	53
2	2·016	$\bar{5}$·656	5·08	8·73	49
3	2·009	$\bar{5}$·6505	5·05	8·90	47
4	2·0065	$\bar{5}$·648	5·05	9·00	47
5	2·0035	$\bar{5}$·645	5·05	9·12	55
6	2·0000	$\bar{5}$·6405	5·07	9·35	65
Mean of 3 and 4			5·05	8·95	

7. *Neon.*—It did not prove possible to obtain agreement with experiment in the cases of helium and neon, for which the values of $\log \eta T^{-\frac{1}{2}}$ plotted against $\log T$ give approximate straight lines whose slopes indicate that the index n of the repulsive force should be 13. It is known that the viscosity of helium can be represented very accurately on the basis of a repulsive force alone with the index $n = 14 \cdot 6$ (*cf.* Jeans, 'Dynamical Theory of Gases,' 3rd ed., 1921, p. 286) down to a temperature of 15° absolute, so that there is very little chance of obtaining the value of the attractive force, which must be small compared with that of argon and nitrogen.

Similar remarks apply to neon, for which further experimental results are available in the recent work of Edwards.* These results have been combined with those calculated by Lennard-Jones† from experimental work on thermal conductivity to give the second column of Table XIV.

Equation (15), which for $n = 13$, $m = 5$, may be written

$$T^{\frac{2}{3}} + S = BT^{\frac{4}{3}}\eta^{-1},$$

giving a straight line for $T^{\frac{4}{3}}\eta^{-1}$ plotted against $T^{\frac{2}{3}}$, was then used to determine B and S, giving $B = 7 \cdot 085 \,.\, 10^{-6}$, and $S = 0 \cdot 52$. The small value of S may be held to confirm the assumption that the attractive field is weak, though its actual magnitude cannot be found until the value of the numerical constant A in (14) has been calculated for $n = 13$, $m = 5$. The value of the repulsive force constant λ can be determined from (16), and is equal to $3 \cdot 20 \,.\, 10^{-104}$, the corresponding "diameter" being $3 \cdot 91 \,.\, 10^{-8}$. The third column in Table XIV gives the viscosity as calculated from the formula with the above values of B and S, and shows a good agreement with the observed values except for the highest and lowest temperatures.

---

* Edwards, 'Roy. Soc. Proc.,' A, vol. 119, p. 578 (1928).

† Lennard-Jones, 'Roy. Soc. Proc.,' A, vol. 107, p. 157 (1925).

Table XIV.—Viscosity of Neon.

T (abs.).	$\eta\, 10^7$ (obs.).	$\eta\, 10^7$ (calc.).
91·66	1352	1404
194·7	2367	2344
198·7	2382	2376
273·1	2946	2946
288·1	3076	3054
373·1	3656	3635
457·5	4177	4170
575·1	4901	4863
717·6	5584	5642

5. *Discussion of Results.*

General Considerations.—The curve obtained from the theory gives the relation between $\log \{I(s)/s^{\frac{1}{2}}\}$ and $\log s$, and is seen from the figures to consist of two approximately linear portions for values of $\log s < \bar{1} \cdot 4$ ($s < 0 \cdot 25$), and $\log s > 0 \cdot 2$ ($s > 1 \cdot 6$) respectively, joined by a curved portion. The approximately linear portions correspond to the extreme cases where the viscosity is determined mainly by the attractive force and the repulsive force respectively, while along the curved portion neither of these forces can be said to play the dominating rôle. The curve is, of course, drawn for the values $m = 5$, $n = 9$ for which the calculation has been carried out, but the curve for any pair of values of m and n would necessarily consist of three portions to which the above description would apply.

The three portions correspond, in a sense, to low, moderate, and high temperatures so that, for example, values of the viscosity at temperatures high enough to bring the experimental points on to the right-hand linear portion of the theoretical curve should enable the index n of the repulsive force to be determined, and the choice of the index m of the attractive force would then be confirmed or not by a comparison of the theoretical and experimental results at lower temperatures. Conversely, values of the viscosity at temperatures low enough to bring the experimental points on to the left-hand portion of the curve would give the value of the index m.

In no case do the experimental values at present available cover a range wide enough to suggest appropriate values of m and n directly in this way, so that the choice of numerical values for these indices is largely a matter of trial and error, and the first result of this investigation has been to show what gases conform to the choice of $m = 5$, $n = 9$ for the range of temperature available.

The following table gives the range of values of s within which the theoretical and experimental curves are in agreement.

Table XV.

Gas.	Range of values of s.	Gas.	Range of values of s.
A	0·5–1·14	Air	0·6–1·6
N_2	0·6–1·4	CO_2	0·6–1·14
H_2	0·7–3·3	Hg vapour	0·22–0·29

Within the above limits of s it is clear that the errors, given in Table IV, in $I(s)$ are not large enough, except perhaps in the case of mercury vapour, to affect the calculation of the force constants.

A physical meaning may be given to the parameter s, which is non-dimensional, as follows.* If ϕ is the work done by the molecular forces between two molecules as they move from their equilibrium position to infinity, then it can be shown that for $m = 5$, $n = 9$, ϕ is equal to $\mu^2/8\lambda$. The average kinetic energy E of a molecule being equal to $\frac{3}{2}RT$, it follows that

$$s^2 = 2RT\lambda\mu^{-2} = E/6\phi.$$

If, therefore, ϕ is known for any gas from the results for the equation of state, and it is assumed that the critical values of s, in this case 0·25 and 1·6, do not alter very much as the values of m and n are changed, then the experimenter can obtain a rough guide as to the range of temperatures for which further experiments are required, for the above equation will give the temperatures T_1 and T_2 corresponding to the critical values of s. If ϕ is not known, but the experimental values of $\log \eta T^{-\frac{1}{2}}$ plotted against $\log T$ give an indication of the value of either T_1 or T_2, then the other temperature can be found from the above equation.

Again the above equation can be used to give an upper limit for the attractive fields in cases where the repulsive field dominates the situation. For this purpose we require the general result corresponding to $s^2 = E/6\phi$, which is

---

* What follows under the heading " General Considerations " is due to Prof. Lennard-Jones, who has very kindly read the paper in MS., and has made several suggestions for its improvement.

$$\frac{\mu^{n-1}}{\lambda^{m-1}} = \left[\frac{(m-1)(n-1)\phi}{n-m}\right]^{n-m} = \left(\frac{4E}{3}\right)^{n-m}\left(\frac{1}{s}\right)^{n-1}.$$

For example, in the case of hydrogen it is known that for $n = 11$, the graph of $\log \eta T^{-\frac{1}{2}}$ against $\log T$ gives approximately a straight line, showing that for the range of temperatures available the value of s must be greater than 1·6. Taking the lowest temperature 89·6° absolute for which there is a good agreement between theory and experiment, and putting $\lambda = 7{\cdot}19 \,.\, 10^{-80}$ as deduced from the viscosity data, the above equation for $n = 11$, $m = 5$ gives $\phi < 1{\cdot}68 \,.\, 10^{-15}$, and $\mu < 2{\cdot}41 \,.\, 10^{-44}$, in agreement with the values $\phi = 1{\cdot}23 \,.\, 10^{-15}$ and $\mu = 1{\cdot}98 \,.\, 10^{-44}$ as determined from the equation of state.

Similarly for helium, in which case $n = 14{\cdot}6$ is found to be the value of the index of the repulsive force from the viscosity data, we find, taking $m = 5$, $\lambda = 2{\cdot}414 \,.\, 10^{-117}$, and the lowest temperature as 20° absolute, that μ must be less than $2{\cdot}69 \,.\, 10^{-45}$, in agreement with the result given by the equation of state, according to which μ is $1{\cdot}90 \,.\, 10^{-45}$ for $m = 5$, $n = 14\frac{1}{3}$, and will be slightly less for $m = 5$, $n = 14{\cdot}6$.

Comparison with Values of Force Constants as Determined from the Equation of State.

It has been shown in the cases of argon, hydrogen, nitrogen, carbon-dioxide, air and mercury vapour that it is possible to get a fairly satisfactory agreement with experiment on the assumption that the mutual actions of the molecules are represented by repulsive and attractive forces of the types λr^{-9} and μr^{-5} respectively, and the values of the force constants λ and μ have been determined. This agreement only applies to a limited range of temperature, and in the cases of argon and CO_2 at the lowest temperature, and air at high temperatures, there is an indication of disagreement between theory and experiment.

The result of the comparison of the values of force constants with those obtained for the same law of molecular force from the equation of state is given in Table XVI.

The agreement in the values of λ determined by two such different methods is very striking, and goes far to justify the somewhat lengthy calculations

Table XVI.—Comparison of Force Constants.

Gas.	$\lambda\,10^{72}$.*	$\lambda\,10^{72}$.†	$\mu\,10^{43}$.*	$\mu\,10^{43}$.†
Argon	1·09	1·01	3·23	1·62
Nitrogen	1·54	1·58	3·11	1·82
Hydrogen	0·106	0·092	0·354	0·254

* From viscosity. † From equation of state.

involved in this paper. The repulsive force constants of argon and nitrogen* as obtained from viscosity have thus been brought into line with those obtained from the equation of state. There is, however, a real divergence between the values of the attractive force constants μ as given by the two methods.

The comparison may be made more complete by expressing the constants for the repulsive and attractive forces in terms of the "diameters" σ and σ' defined in (31), and by using the results found for $n = \infty$ (rigid sphere), $m = 5$ as given in the former paper by the present authors already referred to, in which a similar divergence in the values of μ was found.

Table XVII.—Comparison of "Diameters."

Gas.		$\sigma\,10^{8}$.*	$\sigma\,10^{8}$.†	$\sigma'\,10^{8}$.*	$\sigma'\,10^{8}$.†
$m = 5$ $n = 9$	Argon	7·12	7·05	14·1	11·8
	Nitrogen	7·43	7·46	13·9	12·2
	Hydrogen	5·32	5·23	8·10	7·45
$m = 5$ $n = \infty$	Argon	2·98	3·13	11·2	9·62
	Nitrogen	3·28	3·38	11·16	9·90

* From viscosity. † From equation of state.

This table shows that, keeping $m = 5$, both the agreement in σ and the disagreement in σ' are as pronounced for $n = 9$ as for $n = \infty$. This suggests that no change in the value of n would bring about agreement in the value of σ', that given from viscosity data being always much greater than that determined by the equation of state.

The suggestion that the fields of force determined by the two methods are not strictly comparable would seem to be ruled out by the fact that both investigations start from the same dynamical equations for the encounter between two molecules, the process of averaging over all such encounters being different in the two cases. Further it would be necessary to explain the agreement which has been found above for the repulsive force constants, an agreement which extends to the case of hydrogen, helium and neon, where the attractive forces as determined by the equation of state are weak compared with those of argon and nitrogen, so that an approximate formula of the type (15) can be used to determine the repulsive force constants. The results are given in the following table, in which those for hydrogen and helium are given by Lennard-Jones.

---

* Those for hydrogen have been shown to be in agreement for the repulsive force λr^{-11} by Lennard-Jones and Cook, *loc. cit.*

Table XVIII.—" Diameters " of Repulsive Forces.

Gas.	n.	$\sigma\, 10^8$.*	$\sigma\, 10^8$.†
Helium	$14\frac{1}{3}$	4·51	4·52
Hydrogen	11	3·128	3·105
Neon	13	3·91	3·88

* From viscosity. † From equation of state.

A possible explanation is that neither theoretical method is sufficiently sensitive, and that each allows considerable latitude in the attractive force constants without producing serious divergence from the observations. This suggestion is negatived (1) by a calculation of the coefficient of viscosity from force constants derived from the second virial coefficient, as is shown in the fourth columns of Tables VII and IX which give the results for argon and hydrogen, and (2) by the reverse procedure of calculating the second virial coefficient B_N from the values of the force constants derived from viscosity data. The result of this latter calculation for argon is given in Table XIX, and together with the former prove conclusively that each of the observed quantities is very sensitive to changes in the molecular field of force.

Table XIX.—Argon.

T (abs.).	$B_N 10^3$ (obs.).	$B_N 10^3$.*	$B_N 10^3$.†
673·1	0·6830	—1·589	0·6667
573·1	0·5008	—2·086	0·4979
473·1	0·2085	—2·930	0·2431
423·1	0·0520	—3·480	0·0609
373·1	—0·1917	—4·190	—0·1789
323·1	—0·4920	—5·136	—0·5053
273·1	—0·9861	—6·457	—0·9686

* From viscosity. † From equation of state.

Since it is mainly the attractive force on which the viscosity at "low" temperatures depends, it is possible that the differences found above in the values of this force constant are due to the fact that at these temperatures the viscosity formula (1) may require correction in order to take into account the effect of multiple collisions. Until some estimate of this effect can be made, it remains doubtful whether the differences in the value of μ are to be ascribed to it, or whether they indicate that the choice of the index m of the attractive force to be equal to 5 is incorrect. In this connection it is of interest to note that the omission of the results at the lowest temperature in the cases both of argon and carbon dioxide has not a large effect on the values obtained for λ and μ. This suggests that it is the value of the index m which is incorrect, and does not point to the necessity of any correction to the viscosity formula.

There seems to be no reason why this index should not vary with the gas, as is the case with n, so that, for example, its value is higher in the case of monatomic and lighter gases than in the case of diatomic and heavier gases. Theoretical considerations do not appear able as yet to give any indication of the correct value of m, and the method of trial and error involves lengthy calculations. Since, however, this is the only method available, it is very desirable that the work of calculating the formula for the viscosity for a further pair of values of m and n should be undertaken. The trigonometrical treatment used in the calculation for $m = 5$, $n = 9$ could be used for $m = 7$, $n = 13$, which seems likely to provide interesting results, but the choice of m and n would need careful consideration.

The Exclusion Principle and Aperiodic Systems.

By N. F. Mott, B.A., St. John's College, Cambridge.

(Communicated by R. H. Fowler, F.R.S.—Received June 14, 1929.)

Section I.—The exclusion principle of Pauli was introduced into the old quantum theory as an empirical fact that had been brought to light in the ordering of spectra. The new mechanics has provided some sort of explanation of the principle, for in a closed system with many electrons the mathematically possible stationary states can be separated into a number of groups, with the property that transitions between stationary states in different groups cannot occur. One of these groups is made up of the stationary states corresponding to wave functions that are antisymmetrical in the co-ordinates of the electrons. Apart from accidental degeneracies, the stationary states in different groups have different energy values. The exclusion principle then states that only energy values belonging to the antisymmetrical group are found in nature.

The exclusion principle has had great success not only in explaining the spectra of helium and of more complicated atoms, but also, under the form of the Fermi-Dirac statistics, in accounting for metallic conduction and ferromagnetism. In all these phenomena we are dealing with systems in stationary states, possessing energy values which are discrete, although they may lie very close together. Now, as was first emphasised by Oppenheimer,* we must also use antisymmetrical wave-functions to describe aperiodic phenomena, such as the collision between an electron and an atom. If we do not, we obtain probabilities for the formation of atoms whose wave-functions are not antisymmetrical, as we shall show in section 4, where we consider the collision between an electron and a helium atom. A helium atom described by a symmetrical wave-function would show a singlet series in place of the observed triplets and a triplet series in place of the observed singlets. The wave-functions of open systems are essentially degenerate; the symmetrical and antisymmetrical† solutions are *not* separated from one another by a finite energy difference; but for any arbitrary value of the energy (and of the other integrals of the motion) we can form a symmetrical *and* an antisymmetrical solution. This is a somewhat fundamental difference between open and closed systems. For closed systems containing two electrons there exist only the symmetrical and the antisymmetrical solution; but for open systems we might take any combination of the two. In fact, to describe an observable phenomenon such as a collision, the wave-function that it would first occur to us to use *is* a combination of the two. To fix our ideas we shall discuss the collision between two electrons. Our arguments could equally well be applied to the collision between an electron and a hydrogen atom, the problem originally discussed by Born; but the former is the simpler case, and perhaps illustrates our theory better.

---

* Oppenheimer, 'Phys. Rev.,' vol. 32, p. 361 (1928).

† For simplicity we discuss the case of only two electrons present.

We wish to observe the collision between two electrons; first of all, therefore, we must do two separate experiments to find out where these two electrons are. Suppose we observe one electron in the neighbourhood of a point A, and with momentum $\mathbf{p}_a$, and with its spin axis in a given direction.* There is, of course, an uncertainty in the position and momentum of the electron; we describe the result of our observations by a wave-function, which determines the probability of any position and momentum. If $\mathbf{r}$ be the space co-ordinate of the point A, then the wave-function is†

$$\phi_a(q) = \mathrm{A}_s(\chi) \exp\{-(\mathbf{a}-\mathbf{r})^2/\sigma^2 + i\mathbf{p}_a\mathbf{r}/h\},$$

where q is written for $\mathbf{r}$, s. In the neighbourhood of another point B we observe another electron. A and B are supposed to be a distance apart large compared to the uncertainty in the position of either electron. The wave-function for the second electron will then be

$$\phi_b(q) = \mathrm{A}_s(\chi') \exp\{-(\mathbf{b}-\mathbf{r})^2/\sigma^2 + i\mathbf{p}_b\mathbf{r}/h\}.$$

We shall suppose that $\mathbf{p}_a$ and $\mathbf{p}_b$ are such that the two wave-packets will, in the future, have a collision.

Now, the question is, what wave-function are we to use to describe the pair of electrons? We might be tempted to argue thus: let q_1 be the co-ordinates of the electron which we have located near A, and q_2 the co-ordinates of the electron that we have located near B; then the wave-function at time t_0 is

$$\phi(q_1, q_2, t_0) = \phi_a(q_1)\,\phi_b(q_2).$$

---

* We pass over the fact that there is at present no known experiment by which we can know the direction of the spin axis of a free electron; mathematically, we can form a wave-packet with a given direction for the spin axis.

† $\mathrm{A}_s(\chi)$ is the spin wave-function. s is a variable which can take four values, specifying the four components of Dirac's wave-function. χ is written for the two constants which determine the direction of the spin axis.

From the equations of motion ϕ is determined for all time, so that, at time t, the probability that we shall find electron (1) in the volume element* dq_1, and electron (2) in the volume element dq_2 is

$$|\phi(q_1, q_2, t)|^2 \, dq_1 \, dq_2.$$

The wave-function ϕ is a wave-function of the type used by Born† in his original paper on collisions. However, as was pointed out by Oppenheimer, the true wave function is not ϕ, but the antisymmetrical wave-function Φ, where

$$\Phi(q_1, q_2, t) = \phi(q_1, q_2, t) - \phi(q_2, q_1, t).$$

Now, at time $t = t_0$, and until the two wave-packets have collided, the probabilities represented by $|\phi|^2$ and by $|\Phi|^2$ are the same, since $\phi(q_1, q_2, t) \, \phi(q_2, q_1, t)$ vanishes for all q_1, q_2; but after the collision this is not necessarily the case, as we shall show. The antisymmetry of the wave-functions will affect the experimentally observable results.

Now, it is at first a little disconcerting to find that we have a wave-packet at A containing either electron (1) or electron (2), to find that, although we have located an electron at A, and know that no electron is anywhere near, yet we may not label that electron, electron number 1. However, let us remember that $|\Phi(q_1, q_2, t)| dq_1 \, dq_2$ means simply, the probability that, in the particular experiment which we are considering, we shall find one electron at q_1 and one electron at q_2. Now, it is only possible for us to know whether the electron at q_1 is the one which *was* in the neighbourhood of A, if $\phi(q_1, q_2, t) \, \phi(q_2, q_1, t)$ vanishes at the points and time considered. This will be so, for instance, if the collision is "classical," the wave-packets not having intermixed. And in this case it does not make any difference whether the wave-function used is ϕ or Φ. If, however, $\phi(q_1, q_2, t) \, \phi(q_2, q_1, t)$ does not vanish, then we do not know whether the electron at q_1 is the electron that was at A or not; and in this case a wave-function Φ such that $|\Phi(q_1, q_2)|^2$ was *not* symmetrical in q_1, q_2 would give us more information than we could obtain experimentally. Experimentally we can only observe that *an* electron is at q_1 and another electron at q_2; so that interchanging q_1 and q_2 should not alter the amplitude of the wave-function.

In this paper we shall discuss the collision between an electron and an atom. We shall throughout neglect the actual spin forces; the spin, to our approximation, merely affects the symmetry of the wave-functions. In section 2 we shall obtain a scattering law for a polarised or unpolarised beam of electrons falling on a hydrogen atom. In section 3 we shall discuss the scattering by an atom whose magnetic moment has been orientated in a given direction by a Stern-Gerlach experiment; we shall show that the scattered beam is polarised; that is to say, more spin axes point in one direction than another. We shall show, further, how this polarisation could be detected by a second scattering, analogously to the method discussed by the author in a previous paper.* In a later paper, the author hopes to discuss the collision between two free electrons.

---

* And with given spin direction.

† Born, 'Z. Physik,' vol. 38, p. 803 (1926).

Section 2.—We shall first discuss a two-electron problem, the collision between an electron and a hydrogen atom. We shall first form the unsymmetrical wave-function that describes the collision, after the method of Born,† and then form the antisymmetrical wave-function as described in section 1. Throughout this section we shall consider for simplicity that the energy of the incident electron is less than the first resonance potential of the atom, so that the collision is of necessity elastic.

First of all, let us neglect spin. Let $\mathbf{r}_1$ be the co-ordinate of the incident electron, and $\mathbf{r}_2$ of the atomic electron. We shall also make use of spherical polar co-ordinates r, θ, ϕ, and of cartesian co-ordinates xyz. Let $\phi(\mathbf{r})$ be the wave-function of the atom in its normal state. Then, as has been shown by Oppenheimer,‡ a solution w of the wave-equation exists, such that, for large r_1 *or large* r_2

$$w(\mathbf{r}_1, \mathbf{r}_2) \sim e^{ikz_1}\psi(\mathbf{r}_2) + f(\theta_1)\frac{e^{ikr_1}}{r_1}\psi(\mathbf{r}_2) + g(\theta_2)\frac{e^{ikr_2}}{r_2}\psi(\mathbf{r}_1). \tag{2.1}$$

This is the familiar solution of Born, but Born only considered the asymptotic form for large r_1. The last term in (2.1) corresponds to an interchange of the two electrons, the incident electron staying behind in the atom, and the atomic electron being knocked out. This term exists quite apart from any Pauli principle or resonance; in fact, on the old semi-classical Bohr picture of the atom, one can see that if the incident electron hit the atomic electron "dead on," it would probably stay behind and knock the other one out. If we do not believe in the Pauli principle, then the scattered intensity will be

$$|f|^2 + |g|^2,$$

$|f|^2$ being the number of electrons scattered in a given direction, $|g|^2$ the number knocked out in a given direction after an interchange. We could not, of course, distinguish experimentally between the two kinds.

---

* Mott, 'Roy. Soc. Proc.,' A, vol. 124, p. 425 (1929).

† Born, *loc. cit.*

‡ Oppenheimer, *loc. cit.*

We shall now introduce a spin co-ordinate. According to Dirac the wave-function of a single electron has four components ψ_1, ψ_2, ψ_3, ψ_4. We are neglecting relativity and spin forces; we may therefore neglect ψ_1, ψ_2 in comparison to ψ_3 and ψ_4, and further assume that ψ_3 and ψ_4 separately obey the Schrödinger wave-equation. There exists, therefore, a solution of the wave-equation of the form

$$\psi_s = A_s \psi, \qquad (s = 3, 4)$$

where ψ satisfies the Schrödinger wave-equation. The constants A_3, A_4 determine the direction of the spin axis of electron. Suppose now that χ, ω are the spherical polar co-ordinates of this direction. We shall write A_s as a function of these co-ordinates, $A_s(\chi, \omega)$. Then it has been shown by Darwin* that

$$\left.\begin{aligned} A_3(\chi, \omega) &= a \cos \tfrac{1}{2}\chi \\ A_4(\phi, \omega) &= a \sin \tfrac{1}{2}\chi \, e^{i\omega} \end{aligned}\right\}, \qquad (2.2)$$

The wave-function for two electrons in any field of force has 16 components, and may be written

$$\psi_{s_1 s_2}(\mathbf{r}_1, \mathbf{r}_2) \qquad (s_1 = 1, \ldots, 4, \quad s_2 = 1, \ldots, 4).$$

A suffix s is to be associated with each set of space co-ordinates, and may be thought of as a spin co-ordinate capable of four values. The condition for antisymmetry is

$$\psi_{s_1 s_2}(\mathbf{r}_1, \mathbf{r}_2) = -\psi_{s_2 s_1}(\mathbf{r}_2, \mathbf{r}_1). \qquad (2.3)$$

In the same way as for one electron, we neglect all but four of the 16 components and assume that each component satisfies the Schrödinger equation.

We shall obtain wave-functions and scattering laws for the case when the spin axis of the incident electron is in direction χ, ω; and of the atomic electron in the direction χ_0, ω_0. The incident beam of electrons would presumably be unpolarised; it is at present uncertain whether a completely polarised beam can be obtained. It is immaterial whether we assume that the spin axes, in an unpolarised beam, point in all directions at random, or whether we take an arbitrary direction in space, and consider that the spin axes of half the electron in the beam point parallel and half antiparallel. Either assumption leads always to the same experimental results. We shall make the former assumption; for an unpolarised beam, therefore, we shall average our scattering laws over all directions of χ, ω.

It is, however, possible to know the direction of the spin axis of an electron in a hydrogen atom, for it lies in the same direction as the magnetic moment, which can be determined by a Stern-Gerlach experiment. If, therefore, we are considering collisions with such atoms, we must take χ_0, ω_0 as the direction of the magnetic moment of the atom. If not, we must average over all χ_0, ω_0.

---

* Darwin, 'Roy. Soc. Proc.,' A, vol. 120, p. 621 (1928).

The non-symmetrical wave-function describing the collision is, then

$$\phi_{s_1 s_2}(\mathbf{r}_1, \mathbf{r}_2) = \mathrm{A}_{s_1}(\chi, \omega)\, \mathrm{A}_{s_2}(\chi_0, \omega_0)\, w(\mathbf{r}_1, \mathbf{r}_2), \tag{2.4}$$

where $w(\mathbf{r}_1, \mathbf{r}_2)$ is defined by (2.1).

The antisymmetrical wave-function, satisfying (2.3) is

$$\Phi_{s_1 s_2}(\mathbf{r}_1, \mathbf{r}_2) = \phi_{s_1 s_2}(\mathbf{r}_1, \mathbf{r}_2) - \phi_{s_2 s_1}(\mathbf{r}_2, \mathbf{r}_1). \tag{2.5}$$

The probability that an electron shall be found at $\mathbf{r}_1$, and another at $\mathbf{r}_2$, will then, per unit volume for each electron, be

$$\sum_{s_1 s_2} \Phi_{s_1 s_2}(\mathbf{r}_1, \mathbf{r}_2)\, \Phi^*_{s_1 s_2}(\mathbf{r}_1, \mathbf{r}_2).$$

Substituting from (2.2), (2.4), (2.5) we obtain for this probability

$$\begin{aligned} &|w(\mathbf{r}_1, \mathbf{r}_2)|^2 + |w(\mathbf{r}_2, \mathbf{r}_1)|^2 \\ &\qquad - \cos^2 \tfrac{1}{2}\bar{\chi} \cdot \{w(\mathbf{r}_1, \mathbf{r}_2)\, w^*(\mathbf{r}_2, \mathbf{r}_1) + w(\mathbf{r}_2, \mathbf{r}_1)\, w^*(\mathbf{r}_1, \mathbf{r}_2)\}, \end{aligned} \tag{2.6}$$

where

$$\cos \bar{\chi} = \cos \chi \cos \chi^0 + \sin \chi \sin \chi_0 \cos(\omega - \omega_0).$$

If now the initial beam is unpolarised, we must average over all directions χ, ω of the spin axes of the incident beam.† We obtain then

$$|w(\mathbf{r}_1, \mathbf{r}_2)|^2 + |w(\mathbf{r}_2, \mathbf{r}_1)|^2 - \tfrac{1}{2}\{w(\mathbf{r}_1, \mathbf{r}_2)\, w^*(\mathbf{r}_2, \mathbf{r}_1) + w(\mathbf{r}_2, \mathbf{r}_1)\, w^*(\mathbf{r}_1, \mathbf{r}_2)\}. \tag{2.7}$$

The scattering formula (2.7) does not depend on the direction of the magnetic moment of the hydrogen atom; it is true, therefore, whether this direction is known from a Stern-Gerlach experiment, or not.

It is interesting that (2.7) may be written

$$\tfrac{1}{4}\{3\,|w(\mathbf{r}_1, \mathbf{r}_2) - w(\mathbf{r}_2, \mathbf{r}_1)|^2 + |w(\mathbf{r}_1, \mathbf{r}_2) + w(\mathbf{r}_2, \mathbf{r}_1)|^2\}, \tag{2.8}$$

so that the true scattering law in any two electron problem is obtained by combining, in the ratio 3 to 1, the scattering laws obtained by using wave-functions respectively symmetrical and antisymmetrical in the space co-ordinates.

---

† We may, if we like, assume that the spin axes in the incident beam all point parallel or antiparallel to a given direction; we obtain the same result.

To obtain a scattering law from (2.8) we need simply the probability that an electron will be found at a point $\mathbf{r}_1$ so distant from the atom that $\psi(\mathbf{r}_1)$ may be taken as zero. We have simply to integrate (2.8) over all $\mathbf{r}_2$ space. For an unpolarised beam the scattering law is

$$\tfrac{1}{4}\{3\,|f(\theta)-g(\theta)|^2+|f(\theta)+g(\theta)|^2\},$$

a result already obtained by Oppenheimer.

Section 3.—We shall now consider the polarisation of a beam of electrons scattered by atoms whose spin axes have been orientated by a Stern-Gerlach experiment. We see from (2.6) that the probability that an electron will be scattered in a given direction depends on the orientation of its spin axes; therefore, in the scattered beam, the spin axes will not be distributed equally in all directions. This polarisation could be detected by letting the scattered beam fall on a second assembly of atoms, whose magnetic moments have been orientated in a known direction by a second Stern-Gerlach experiment. If the scattering by these second atoms depends on the direction of the magnetic moments of the first, then we can say that the beam is polarised.

This experiment is a three-electron problem, and the wave-function which we use must be antisymmetrical in all three.

Let χ_0, ω_0 be the direction of the magnetic moment of the first atom, χ_0', ω_0' of the second. Let $\psi(\mathbf{r})$, $\psi'(\mathbf{r})$ be the wave-functions of the two atoms, in the same space. The atoms are naturally a sufficient distance apart for us to be able to assume

$$\int \psi(\mathbf{r})\,\psi'(\mathbf{r})\,d\mathbf{r}=0.$$

We shall suppose that an electron must be scattered through an angle θ by the first atom if it is to hit the second atom. f and g are the amplitudes of the scattered waves (*cf.* (2.1)) for the first scattering, in the direction θ. f' and g' refer to the second scattering, in the direction θ'. We shall first form the unsymmetrical wave-function; assuming that electron 1 is the incident electron, that electron 2 was initially in the first atom, and electron 3 in the second, then the wave scattered by the second atom may be written

$$\begin{aligned}\phi(123)=\{&ff'\,\psi(2)\,\psi'(3)\,\mathrm{S}(1)+gf'\,\psi(1)\,\psi'(3)\,\mathrm{S}(2)\\&+fg'\,\psi(2)\,\psi'(1)\,\mathrm{S}(3)+gg'\,\psi(1)\,\psi'(2)\,\mathrm{S}(3)\}\\&\times \mathrm{A}_{s_1}(\chi,\omega)\,\mathrm{A}_{s_2}(\chi_0,\omega_0)\,\mathrm{A}_{s_3}(\chi_0',\omega_0'),\end{aligned}$$

where

$$\mathrm{S}(r)=e^{ikr}/r,$$

and S (1), etc., are written as shortened forms of S (r_1), etc.† Now, the antisymmetrical wave-function will be

$$\Phi\,(123) = \phi\,(123) - \phi\,(132) + \phi\,(312) - \phi\,(321) + \phi\,(231) - \phi\,(213).$$

To obtain the scattering law by the second atom, we must as before integrate $\Phi\,\Phi^*$ over all $\mathbf{r}_1$, $\mathbf{r}_2$, and integrate over all directions of the spin axes of the incident beam. We obtain, for the square of the amplitude of the scattered wave in the direction θ'

$$[ff^* + gg^* - \tfrac{1}{2}(fg^* + f^*g)][f'f'^* + g'g'^* - \tfrac{1}{2}(f'g'^* + f'^*g')] \\ - \tfrac{1}{2}(fg^* + f^*g - 2gg^*)\,(f'g'^* + f'^*g')\cos\bar{\chi},$$

where

$$\cos\bar{\chi} = \cos\chi_0\cos\chi_0' + \sin\chi_0\sin\chi_0'\cos(\omega_0 - \omega_0')$$

and

$$f' = f'(\theta'), \text{ etc.}$$

The scattered intensity does, therefore, depend on the angle between the magnetic moments of the two atoms. The function of θ

$$fg^* + f^*g - 2gg^*$$

may be taken as a measure of the polarisation of the first scattered beam; if it vanishes, the scattered beam is unpolarised.

Section 4.—We shall now consider the scattering by a helium atom. The wave-function of the helium atom in its normal state is symmetrical in the space co-ordinates, and antisymmetrical in the spin co-ordinates. The two spins lie antiparallel to one another. Neglecting the spin forces, therefore, the wave-function of the atom is

$$\psi\,(\mathbf{r}_1, \mathbf{r}_2)\,\{\mathrm{A}_{s_1}(\chi_0, \omega_0)\,\mathrm{A}_{s_2}(\chi_0', \omega_0') - \mathrm{A}_{s_2}(\chi_0, \omega_0)\,\mathrm{A}_{s_1}(\chi_0', \omega_0')\},$$

where χ_0, ω_0 are the polar co-ordinates of an arbitrary direction, and χ_0', ω_0' the opposite direction.

The unsymmetrical function $w(\mathbf{r}_3\,;\ \mathbf{r}_2, \mathbf{r}_1)$ of the space co-ordinates describing the collision will have the form

$$w\,(\mathbf{r}_3, \mathbf{r}_2, \mathbf{r}_1) \sim e^{ikz_3}\,\psi\,(\mathbf{r}_1, \mathbf{r}_2) + f(\theta)\,\frac{e^{ikr_3}}{r_3}\,\psi\,(\mathbf{r}_1, \mathbf{r}_2) \\ + g\,(\theta)\,\frac{e^{ikr_2}}{r_2}\,\psi\,(\mathbf{r}_3, \mathbf{r}_1) + g\,(\theta)\,\frac{e^{ikr_1}}{r_1}\,\psi\,(\mathbf{r}_2, \mathbf{r}_3).$$

---

† The first term is contributed by collisions without interchange; the second by an interchange at the first collision but not at the second, and so on.

The unsymmetrical function of space and spin co-ordinates is†

$$\phi(q_3\,;\ q_2, q_1) = w(\mathbf{r}_3\,;\ \mathbf{r}_2, \mathbf{r}_1)\,\{\mathrm{A}_{s_1}(\chi_0, \omega_0)\,\mathrm{A}_{s_2}(\chi_0', \omega_0') - \mathrm{A}_{s_2}(\chi_0, \omega_0)\,\mathrm{A}_{s_1}(\chi_0', \omega_0')\}\,\mathrm{A}_{s_3}(\chi, \omega), \quad (4.1)$$

where χ, ω is the direction of the spin axis of the incident electron.

We can see very clearly from this wave-function how the use of wave-functions which are not antisymmetrical gives a probability for the formation of symmetrical helium atoms. The scattered wave in (4.1) contains terms of the form

$$g(\theta)\frac{e^{ikr_2}}{r_2}\psi(\mathbf{r}_3, \mathbf{r}_1)\,\mathrm{A}_{s_1}(\chi_0, \omega_0)\,\mathrm{A}_{s_2}(\chi_0', \omega_0')\,\mathrm{A}_{s_3}(\chi, \omega),$$

which represents a scattered wave together with a symmetrical helium atom.

For the antisymmetrical wave-function describing the collision, we have

$$\Phi(q_1, q_2, q_3) = \phi(q_3\,;\ q_2, q_1) + \phi(q_2\,;\ q_1, q_3) + \phi(q_1\,;\ q_3, q_2).$$

We interpret this wave-function in exactly the same way as for hydrogen. Assuming, say, that r_3 is so large that $\psi(\mathbf{r}_1, r_3)$ vanishes, the scattered wave in (4.1) reduces to

$$\{f(\theta) - g(\theta)\}\frac{e^{ikr_3}}{r_3}\mathrm{A}_{s_3}(\chi, \omega)\,\{\mathrm{A}_{s_1}(\chi_0, \omega_0)\,\mathrm{A}_{s_2}(\chi_0', \omega_0') - \mathrm{A}_{s_2}(\chi_0, \omega_0)\,\mathrm{A}_{s_1}(\chi_0', \omega_0')\}.$$

The scattered wave, therefore, has the same spin axes as the incident wave; if the former is unpolarised, so is the latter; and the scattering law for a polarised or unpolarised beam is

$$|f(\theta) - g(\theta)|^2,$$

a result already obtained by Oppenheimer.

In conclusion, the author would like to express his thanks to Prof. Niels Bohr for many discussions on this subject.

Summary.

The collision between an electron and an atom is discussed. The wave-function must be antisymmetrical in the co-ordinates of all the electrons present. If the magnetic moments of the scattering atoms have been orientated by a Stern-Gerlach experiment, then the scattered beam of electrons will be polarised. It is shown how this polarisation could be detected.

---

† *Cf.* (2.4).

The Compton Scattering and the New Statistics.

By S. CHANDRASEKHAR, The Presidency College, Madras.

(Communicated by R. H. Fowler, F.R.S.—Received June 20, 1929.)

1. *Introduction.*

Great success has been achieved by Sommerfeld in the electron theory of metals by assuming that there are free electrons in them which obey the Fermi-Dirac statistics. It has been assumed in the case of univalent metals that on the average one electron per atom is free. In general, however, the valency electrons can be considered as free.* These free electrons will take part in the Compton scattering. The analysis of such a Compton effect reduces to the analysis of the collisions between radiation quanta and an electron gas. The general features of such a scattering was first considered by Dirac.† But he has assumed a Maxwellian distribution for the electrons which will not be applicable to the case under consideration, because the electrons in a conductor being degenerate do not obey the Maxwell's law, but the Fermian distribution.

In considering such a process we take it that the conservation of momentum and energy principles are satisfied for each particular collision just as in Compton's theory—only we are here dealing with moving electrons instead of stationary electrons which Compton considers. Thus electrons of different momenta components will produce different Compton shifts, and the intensity of any particular shift will depend on the number of electrons in that state. Thus we have to average for the radiation falling on an assembly of electrons whose momenta are distributed according to the Fermi-Dirac law.

The above is just a natural extension of Compton's theory. In this connection mention should be made of Jauncey's‡ theory of bound electrons whose arguments are essentially what we have put forward in the previous paragraph. But his theory has not been quite satisfactory because he has not assumed any definite distribution of the electrons.

---

* Rosenfeld, 'Naturw.,' p. 49 (1929).

† 'M.N.R.A.S.,' vol. 85, p. 825 (1925).

‡ 'Phys. Rev.,' vol. 25, p. 723 (1925).

2. *Compton scattering with Moving Electrons.*

Let m_x, m_y, m_z be the momentum of the scattering electron and g_x, g_y, g_z those of the quantum, g_t, m_t represent the masses of the electron and the quantum multiplied by the velocity of light c. If we take polar co-ordinates

$$g_x = h\nu \cos \theta/c \, ; \; g_y = h\nu \sin \theta \cos \phi/c \, ; \; g_z = \sin \theta \sin \phi \;\; g_t = h\nu/c. \qquad (1)$$

Then the conservation of momentum and energy gives

$$(m_u, g_u) - (m_u, g_u') = (g_u, g_u'). \qquad (2)$$

The above equation gives the frequency of the scattered quantum in terms of the initial momentum of the electron and the incident quantum, and the directions of the incident and scattered quanta.

Equation (2) reduces to

$$m_t - m_x \cos \theta' - m_y \sin \theta' = \frac{\nu}{\nu'}(m_t - m_x) - \frac{h\nu}{c}(1 - \cos \theta')\,, \qquad (3)$$

if we assume that the directions of the incident quantum is along the x axis and that of the scattered quantum in the xy plane. Here θ' is simply the angle of scattering.

3. *The Spectral-intensity Distribution Function.*

Before considering the case of scattering of monochromatic X-radiation, we will consider first the more general case when the incident radiation is continuous. Suppose we have such a pencil of radiation confined to a small solid angle $d\omega$ and let I_ν be the intensity per unit frequency range. Let this radiation be incident on an assembly of dn electrons of momentum m_x, m_y, m_z. Let the intensity of radiation scattered in the solid angle $d\omega'$ and frequency range ν' and $\nu' + d\nu'$ be given by

$$R(\nu')\, d\nu'\, d\omega'. \qquad (4)$$

Then it has been shown by Dirac (*loc. cit.*, equation (8)) that

$$R(\nu') = \frac{h^2}{m^2c^2} \,.\, dn \,.\, I_\nu\, d\omega \frac{\nu' F(a, b)}{\nu m_t}\,. \qquad (5)$$

Here ν' is to be regarded as a function of g_x', g_y', g_z' and m_x, m_y, m_z, being that frequency of the incident quantum which will be scattered by an (m_x, m_y, m_z) electron into the frequency range ν' to $\nu' + d\nu'$.

In the above equation $F(a, b)$ is a function which depends on the scattering law adopted and a and b the two invariants connected with the scattering process which as well as the initial momentum m_x, m_y, m_z of the electron and g_x, g_y, g_z of the quantum specify the collision.

Now for dn in equation (5), we have to put the Fermi-expression

$$dn = \frac{V}{h^3} \cdot G \cdot \frac{dm_x \, dm_y \, dm_z}{\exp(\Sigma m_x^2/2mkT)/A + 1}, \tag{6}$$

and integrate with respect to m_x, m_y, m_z. In the above equation A is the constant appearing in the Fermi-Dirac statistics. It has different values according as we consider a degenerate or a non-degenerate gas. When the system is non-degenerate A is a small positive quantity and then has the value

$$A = nh^3 \cdot (2\pi mkT)^{-3/2}/G. \tag{7}$$

A degenerate system corresponds to A being a large quantity and in that case

$$\log A = \left(\frac{3n}{4\pi G}\right)^{2/3} \cdot \frac{h^2}{2mkT}. \tag{8}$$

Then by equation (6)

$$R(\nu') = \frac{h^2}{m^2c^3} \cdot \frac{V}{h^3} \cdot G \iiint_{-\infty}^{\infty} \frac{I_\nu d\omega \nu' F}{\nu m_t} \cdot \frac{dm_x \, dm_y \, dm_z}{\exp(\Sigma m_x^2/2mkT)/A + 1} \tag{9}$$

$$= \frac{h^2}{m^2c^3} \cdot \frac{V}{h^3} \cdot G \int_0^{\infty} I_\nu \, d\omega \, \psi(\nu, \nu') \, d\nu. \tag{10}$$

Where

$$\psi(\nu, \nu') = \iint_{-\infty}^{\infty} \frac{\nu' F}{\nu m_t} \cdot \frac{dm_y \, dm_z}{\exp(\Sigma m_x^2/2mkT)/A + 1} \Big/ \frac{\partial \nu}{\partial m_x}. \tag{11}$$

Where m_x and $\partial\nu/\partial m_x$ are to be evaluated in terms of m_y, m_z and ν by means of equation (3)

$$(6) \quad \frac{\partial m_x}{\partial \nu} = \frac{mc}{\nu'(1 - \cos\theta')} - \frac{h}{c}, \tag{12}$$

and

$$m_x^2 + m_y^2 = \frac{\beta}{\gamma^2}\left[m_y - \frac{K\sin\theta'}{\beta}\right]^2 + \frac{K^2}{\gamma^2}\left(1 - \frac{\sin^2\theta'}{\beta}\right), \tag{13}$$

where

$$\beta = 1 - 2\nu\cos\theta'/\nu' + (\nu/\nu')^2, \quad \gamma = \nu/\nu' - \cos\theta',$$

$$K = -mc(\nu/\nu' - 1) + h\nu(1 - \cos\theta')/c. \tag{14}$$

Then

$$\psi(\nu, \nu') = \iint_{-\infty}^{\infty} \frac{F\left[\frac{1}{\nu(1 - \cos\theta')} - \frac{h\nu'}{mc^2\nu}\right] dm_y \, dm_z}{\frac{1}{A}\exp\left\{\frac{\frac{\beta}{\gamma^2}\left[m_y - \frac{K\sin\theta'}{\beta}\right]^2 + \frac{K^2}{\gamma^2} \cdot \left[1 - \frac{\sin^2\theta'}{\beta}\right] + m_z^2}{2mkT}\right\} + 1}. \tag{15}$$

Suppose now that the radiation is monochromatic, then the number of quanta scattered between the frequency range ν' and $\nu' + d\nu'$ into the solid angle $d\omega'$ is given by

$$\mathrm{R}(\nu') = \frac{h^2}{m^2c^3} \cdot \frac{\mathrm{V}}{h^3} \cdot \mathrm{G} \cdot \mathrm{I}_\nu \, d\nu \, dw \, \psi(\nu, \nu'). \tag{16}$$

So that the (spectral) distribution of intensity about the primary frequency ν is given by $\psi(\nu, \nu')$, which we shall now evaluate.

$$\psi(\nu, \nu') = 4\mathrm{F}_0 \left[\frac{1}{\nu(1 - \cos\theta')} - \frac{h\nu'}{mc^2\nu}\right] \iint_0^\infty \frac{dm_y \, dm_z}{\frac{1}{\mathrm{B}} \exp\left(\frac{\beta}{\gamma^2} \cdot \frac{m'^2_y + m_z^2}{2mk\mathrm{T}}\right) + 1}, \tag{17}$$

where

$$\left.\begin{aligned} m'_y &= m_y - \frac{\mathrm{K}\sin\theta'}{\beta} \\ \frac{1}{\mathrm{B}} &= \frac{1}{\mathrm{A}} \cdot \exp\left\{\frac{\mathrm{K}^2}{\gamma^2 \cdot 2mk\mathrm{T}} \cdot \left(1 - \frac{\sin^2\theta'}{\beta}\right)\right\} \end{aligned}\right\}. \tag{18}$$

If we introduce the new variables

$$y = m'^2_y \, \beta/\gamma^2 \cdot 2mk\mathrm{T}, \quad z = m_z^2/2mk\mathrm{T}.$$

Then

$$\begin{aligned} \psi(\nu, \nu') &= 2\mathrm{F}_0 \left[\frac{1}{\nu(1 - \cos\theta')} - \frac{h\nu'}{mc^2\nu}\right] \frac{\gamma \cdot mk\mathrm{T}}{\beta^{\frac{1}{2}}} \cdot \iint_0^\infty \frac{y^{-\frac{1}{2}} \cdot z^{-\frac{1}{2}} \cdot dy \, dz}{e^{y+z}/\mathrm{B} + 1} \\ &= 2\mathrm{F}_0 \left[\frac{1}{\nu(1 - \cos\theta')} - \frac{h\nu'}{mc^2\nu}\right] \cdot \frac{\gamma \cdot mk\mathrm{T}}{\beta^{\frac{1}{2}}} \cdot \mathrm{U}_0, \end{aligned} \tag{19}$$

where U_0 is the special case of the general Sommerfeld integral

$$\mathrm{U}_\rho = \frac{1}{\Gamma(\rho + 1)} \cdot \int_0^\infty \frac{u^\rho \, du}{e^u/\mathrm{B} + 1}, \tag{20}$$

which gives for $\rho = 0$*

$$\mathrm{U}_0 = \pi \log(\mathrm{B} + 1). \tag{21}$$

Hence we get our intensity distribution function

$$\psi(\nu, \nu') = 2\mathrm{F}_0 \left[\frac{1}{\nu(1 - \cos\theta')} - \frac{h\nu'}{mc^2\nu}\right] \cdot \frac{\gamma \cdot mk\mathrm{T}\pi}{\beta^{\frac{1}{2}}} \cdot \log(\mathrm{B} + 1). \tag{22}$$

Case I.—If B is large and positive we get

$$\begin{aligned} \psi(\nu, \nu') = 2\mathrm{F}_0 &\left[\frac{1}{\nu(1 - \cos\theta')} \cdot \frac{h\nu'}{mc^2\nu}\right] \cdot \frac{\gamma \cdot mk\mathrm{T}\pi}{\beta^{\frac{1}{2}}} \\ &\times \left[\log \mathrm{A} - \frac{\mathrm{K}^2}{\gamma^2 \cdot 2mk\mathrm{T}}\left(1 - \frac{\sin^2\theta'}{\beta}\right)\right], \end{aligned} \tag{23}$$

the value of log A being given by (8).

---

* Sommerfeld, 'Z. Physik,' vol. 47, p. 1 (1928), equation (31A).

An approximation of the above equation to an order of accuracy where the Compton-shift is neglected is

$$\psi(\nu, \nu') = \frac{\sqrt{2}\, F_0 \pi m k T}{\nu (1 - \cos \theta')^{\frac{1}{2}}} \cdot \left[\log A - \frac{(\nu' - \nu)^2}{a \nu^2}\right]. \tag{24}$$

where $a = 4kT(1 - \cos \theta')/mc^2$.

Case II.—If B is small due to the smallness of A we get, to the same order of accuracy as (24), the equation

$$\psi(\nu, \nu') = \frac{n}{h^3 . G} \cdot (2\pi m k T)^{-3/2} \cdot \frac{\sqrt{2} F_0 \pi m k T}{\nu (1 - \cos \theta')^{\frac{1}{2}}} \cdot e^{-(\nu' - \nu)^2 / a\nu^2}, \tag{25}$$

the one given by Dirac (*loc. cit.*, equation (13)).

Equation (25) gives an exponential distribution of intensity about the primary frequency for the scattered radiation. But equations (23) and (24) indicate that the distribution of intensity of the radiation scattered by a degenerate electron gas does not follow an exponential law but gives a parabolic distribution. This perhaps explains the rather broad structure of the Compton modified radiation.*

4. *The Compton effect.*

It is natural that the distribution of intensity predicted by equation (23) places the maximum peak of intensity at a place where the Compton's theory for a free-stationary electron predicts a line. Remembering that in any case $\nu/\nu' = 1$ the maximum frequency will be at a modified frequency where $K = 0$ where

$$K = -mc(\nu/\nu' - 1) + h\nu(1 - \cos \theta')/c = 0,$$

i.e., where

$$\lambda' - \lambda = h(1 - \cos \theta')/mc, \tag{26}$$

i.e., on an intensity-frequency graph the maximum occurs at a place corresponding to the Compton shift.

5. *The Effect of Temperature.*

If we consider the Compton scattering by an electron-gas, the distribution function of which depends on temperature, it would naturally be expected that the spectral intensity distribution function in the Compton scattering would also depend on temperature and Dirac's classical expression (25) does indicate this by the explicit appearance of the temperature factor in $\psi(\nu, \nu')$. But if we substitute the value of log A given by (8) in (23) we get

---

* Mr. J. W. Du Mond in a private communication to the author from the California Institute of Technology, Pasadena, has kindly pointed out that the above is the characteristic of the Compton-radiation from conductors. His paper in the May issue of the 'Physical Review' (vol. 33, p. 643) gives experimental details and theoretical calculations as well. He has independently derived the parabolic structure.

$$\psi(\nu, \nu') = 2F_0\left[\frac{1}{\nu(1-\cos\theta')} - \frac{h\nu'}{mc^2\nu}\right] \cdot \frac{\gamma . \pi}{\beta^{\frac{1}{2}}} \times \left[\tfrac{1}{8}\left(\frac{6}{\pi}n\right)^{2/3} h^2 - \frac{K^2}{\gamma^2} \cdot \left(1 - \frac{\sin^2\theta'}{\beta}\right)\right], \tag{27}$$

where all the temperature factors have cancelled out. Thus Compton-scattering by an *electron-gas* will not be influenced by temperature. Further the Compton scattering by the bound electrons will also not be influenced by the ranges of temperature available in the laboratory. Thus it appears that the *total* Compton scattering will not be affected by temperature.*

6. *The Effect of a Magnetic-field.*

We will consider the scattering by the conduction electrons only. When the scatterer is placed in a magnetic-field the distribution function for the electrons changes, and in that case the number of electrons in the momentum range m_x, m_y, m_z and $m_x + dm_x$, $m_y + dm_y$, $m_z + dm_z$ is given by the Pauli's expression†

$$dn = \frac{V}{h^3} \cdot \frac{dm_x \, . \, dm_y \, . \, dm_z}{\exp\left(\frac{\varepsilon_m}{kT} + \frac{\Sigma m_x^2}{2m_0 kT}\right)\Big/ A + 1}, \tag{28}$$

where $\varepsilon_m = mg\,\mu_0 H$; where $\mu_0 = -eh/4\pi m_0 c =$ a Bohr magneton, $g =$ the Lande factor, $H =$ the field strength.

For the summation over all the values of the quantum number m from $-j$ to $+j$ we have the relations

$$\left.\begin{aligned} \sum_{m=-j}^{+j} \varepsilon_m &= 0 \\ \sum_{m=-j}^{+j} \varepsilon_m^2 &= \tfrac{1}{3} G \mu^2 H^2 \end{aligned}\right\}. \tag{29}$$

To derive the spectral-intensity distribution function we have to substitute

---

* Since the writing of the above a report by Jauncey and Bowers has appeared (' Bull. Amer. Phys. Soc.,' vol. 4, p. 26 (1929)) giving experimental observations which support the above conclusions.

† ' Z. Physik,' vol. 41, p. 81 (1927).

(28) instead of (6) in equation (5) and carry out the integration as before. The final result as one can easily see is

$$\psi(\nu, \nu') = 2\mathrm{F}_0\left[\frac{1}{\nu(1-\cos\theta')} - \frac{h\nu'}{mc^2\nu}\right] \cdot \frac{\gamma \, . \, mk\mathrm{T}, \pi}{\beta^{\frac{1}{2}}}$$
$$\times\left[\log \mathrm{A} + \sum_{m=-j}^{+j} \frac{-\varepsilon_m}{k\mathrm{T}} - \frac{\mathrm{K}^2}{2\gamma^2 \, . \, mk\mathrm{T}}\left(1 - \frac{\sin^2\theta'}{\beta}\right)\right], \quad (30)$$

which on account of (29) becomes identical with (23). Thus it appears on Pauli's theory of the paramagnetism of an electron-gas that the scattering of such an assembly should not be influenced by the presence of a magnetic field. In this connection mention should be made of an experimental observation of Bothe* where he tried the influence of a magnetic field. The scatterer he used was paraffin, and he tried up the field strengths of the order of 20,000 Γ. But he could detect no influence.

Summary.

In this paper the Compton scattering by an electron-gas on the Fermi-Dirac statistics is considered. The theory predicts a distribution of spectral intensity not exponentially falling off about the maximum but *parabolically*. It places the peak of maximum intensity at a place where the Compton relation $\lambda' - \lambda = h(1 - \cos\theta')/mc$ is satisfied. Further, the theory indicates that there should be no influence of temperature or magnetic field in Compton scattering.

In conclusion the author wishes to express his thanks to Dr. R. H. Fowler, F.R.S., and Mr. N. F. Mott for kindly going through the manuscript and suggesting improvements.

---

* 'Z. Physik,' vol. 41, p. 872 (1927).

Regularities in the Arc Spectrum of Arsenic.

By K. R. Rao, D.Sc., Government of Madras Research Scholar, Imperial College of Science, London.

(Communicated by A. Fowler, F.R.S.—Received June 22, 1929.)

Introductory.

In the course of an investigation of the spectrum of arsenic under different conditions of excitation several regularities have been detected among the lines due to As I, and it is the purpose of the present paper to give an account of these.

Besides the very early work of Kayser and Runge, previous investigations on the analysis of the arc spectrum of arsenic consist chiefly of two contributions. Ruark, Mohler, Foote and Chenault* have made measurements of the critical potentials of As, and, with the aid of these and the recurring frequency differences pointed out by Kayser and Runge, have suggested an empirical scheme of terms which accounted for many of the more intense lines of the arc. But a large number of lines of wave-length below λ 2100 have not entered into the above scheme and remained unclassified. A study of the absorption by the normal vapour of arsenic failed to show any characteristic line absorption, for the vapour has been found to exhibit continuous absorption in the ultra-violet which spreads towards longer wave-lengths as the vapour pressure rises.

More recently, in the light of Hund's theory, McLennan and McLay† have partially identified, from the above scheme of combinations, the groups of lines arising from the transition of the electron from the $4p$ to the $5s$ orbit.

In the present investigation the spectrum has been extended to λ 1563. Several new lines have been added which have led to the identification of combinations due to the electron transitions from the deepest $4p$ state to the higher $5s$, $4p'$ and $4d$ states.

Observational Data.

The wave-lengths of the arc spectrum of arsenic recorded by Randall‡ extend from λ 10614 to λ 8823. The region 3119 A. to 2144 A. has been measured by Kayser and Runge. Below λ 2144 A. the measurements of

---

* 'Sci. Pap. Bur. Standards,' vol. 19, p. 463 (1924).

† 'Phil. Trans. R. S. Can.,' Sect. 3, vol. 21, p. 63 (1927).

‡ 'Astrophys. J.,' vol 34, p. 1 (1911).

L. and E. Bloch* are those of the spark spectrum. In this work the spectrum has been photographed between λ 8800 and λ 1370. The infra-red region has been investigated by a glass prism (Littrow type) spectrograph using hypersensitised neo-cyanine plates and giving an exposure of about 4 hours. But there is no trace of any lines in that region. The characteristic spectrum, as has been observed by previous investigators, begins at λ 3119. A few of the lines have been measured in the second order of a 10-foot grating of dispersion about 2·8 A. per millimetre, and these are distinguished in the tables by giving their wave-lengths to seven figures ; the error is believed to be less than 0·01 A. Between λ 2500 and λ 2000, the measurements have been made on photographs taken on Hilger quartz spectrographs, types E_1 and E_2. The vacuum spectrograph used for the Schumann region has a metre grating of 30,000 lines per inch and gives a dispersion of about 8·6 A. per millimetre. The lines are of very good definition. The standards adopted in reducing the vacuum plates are those of carbon λ 1930·94, λ 1656·27 and nitrogen λ 1745·26, 1742·74 and 1494·78, 1492·83. It is thought that the errors in the wave-lengths do not generally exceed 0·03 A.

Unlike that of nitrogen and phosphorus, the production of the arc spectrum of arsenic presents little difficulty. The ordinary arc between metallic arsenic contained in poles of carbon or aluminium served as a convenient source in most of these experiments. In investigating the Schumann region the arc in nitrogen, in the manner devised by Mr. E. W. H. Selwyn† and adopted by Prof. Fowler for Si‡ and by the writer for Ge§ and described in detail in these papers, has been used. The stream of nitrogen served also to prevent the formation of a deposit of the metal on the fluorite window, which had been a source of great trouble in several of these experiments. The spectrum taken by this method, however, extended only to λ 1650. For photographing below this region the arc *in vacuo* between carbon poles containing arsenic and the spark between metallic arsenic in hydrogen, at atmospheric pressure, have been used. These latter methods, however, produce lines due to the ionised atom in addition to those of the arc. Therefore in extending the classification below λ 1650 only those lines have been included which, by their appearance, are believed to be arc lines, and which further are supported by the equality of the frequency differences.

---

* 'J. Physique,' vol. 4, p. 622 (1914), and 'C. R.,' vol. 171, p. 709 (1920).

† 'Phys. Soc. Proc.' (Lond.) in course of publication.

‡ 'Roy. Soc. Proc.,' A, vol. 123, p. 422 (1929).

§ 'Roy. Soc. Proc.,' A, vol. 124, p. 465 (1929).

Analysis of the Spectrum.

The terms to be expected in the arc spectrum of arsenic may be represented in the usual way by the following table. The notation is the same as that used in the writer's paper on Ge I (*loc. cit.*). Similar terms arising from the same electronic configuration, but due to different states of the core, are distinguished by the super-scripts *a*, *b*, etc.

Table I.—Predicted Terms of As I.

3_1 3_2 3_3	4_1 4_2 4_3 4_4	5_1 5_2 5_3	Term prefix.	Terms.		
				Limit ^3P.	^1D.	^1S.
2 6 10	2 3		4*p*	^4S	^2D	^2P
2 6 10	2 2	1	5*s*	^4P ^2P	^2D	^2S
2 6 10	2 2 1		4*d*	^4F ^4D ^4P ^2F ^2D ^2P	^2G $^2F^a$ $^2D^a$ $^2P^a$ ^2S	$^2D^b$
2 6 10	1 4		4*p*′	^4P ^2P	^2D	^2S
2 6 10	2 2	1	5*p*	^4D ^4P ^4S ^2D ^2P ^2S	^2F $^2D^a$ $^2P^a$	$^2P^b$

The terms which have been identified are shown with the observed combinations in Table II. From the data it will be seen that doublet-quartet system inter-combinations are fairly strong in the spectrum of As I.

Table II.—Multiplets of As I.

4*p*	$^4S_2$	$^2D_2$	$^2D_3$	$^2P_1$	$^2P_2$
	(93500)*	82909·7	82587·4	75316·7	74855·5
	10590·3		*322·3*	*7270·7*	*461·16*
5*s* $^4P_1$ = 42808·0	50693·5 (15)	40102·0 (2)		32507·56 (2)	32046·38 (4)
915·8					
$^4P_2$ = 41892·2	51608·1 (15)	41018·0 (2)	40695·6 (4)	33423·91 (2)	32962·77 (4)
1287·7					
$^4P_3$ = 40604·5	52895·2 (15)	42305·4 (2)	41983·0 (4)		—
$^2P_1$ = 40366·8	53134·1 (5)	42543·2 (10)		34949·27 (7)	34488·12 (5)
1169·6					
$^2P_2$ = 38897·2	54603·3 (6)	44012·4 (4)	43690·5 (10)	36419·24 (6)	35958·09 (8)
$^2D_2$ = 32667·8	—	50241·9 (9)	49920·6 (4)	42648·6 (6)	42187·1 (5)
−19·1					
$^2D_3$ = 32686·9	60812·5 (3)	50224·0 (7)	49901·4 (10)		42167·0 (6)
$^2S_1$ = 28005·2		54901·6 (2) ?		47311·3 (4)	46850·6 (4)

* This value is derived from the ionisation potential.

Table II—(continued).

$4p$	$^4S_2$	$^2D_2$	$^2D_3$	$^2P_1$	$^2P_2$
	(93500)*	82909·7	82587·4	75316·7	74855·5
	10590·3	*322·3*	*7270·7*	*461·16*	
$4p'\ ^4P_3$ = 30751·9	62748·6 (6)	52158·3 (4)	51835·7 (1)		44102·4 (4)
−752·1					
$^4P_2$ = 29999·8	63502·2 (5)	—	52587·6 (2)	45315·9 (2)	44854·8 (3)
−477·3					
$^4P_1$ = 29522·5	63976·3 (3)	53387·7 (4)		45794·6 (2)	45333·2 (1)
$^2P_2$ = 26494·6		—	—	48822·4 (5)	48360·7 (4)
−1305·9					
$^2P_1$ = 25188·7		57719·7 (3)		50128·6 (6)	49667·4 (4)
$^2D_{2,3}$ = 28693·2		54215·5 (7)	53894·4 (4)	46624·0 (5)	46162·6 (6)
$^2S_1$ = 26916·8		55992·0 (1)		48400·8 (6)	47938·7 (5)
$4d\ ^4D_4$ = 26719·6 ?			55867·8 (4)		
59·9					
$^4D_3$ = 26779·5		56130·9 (5)	55807·9 (4)		48075·2 (2)
239·2					
$^4D_2$ = 27018·7		55889·4 (3)	55567·6 (2)	48298·6 (5)	47838·9 (3)
−34·4					
$^4D_1$ = 26984·3 ?		—		48332·4 (4)	
$4d\ ^2F_3$ = 29160·7		53749·6 (8)	53426·2 (5)		
1937·8					
$^2F_4$ = 27222·9			55364·5 (9)		
$^2D_2$ = 25202·3		57707·7 (2)	[57385]†	50114·0 (7)	49653·5 (6)
101·4					
$^2D_3$ = 25100·9		57808·5 (2)	57486·8 (4)		49754·6 (9)
$^2P_1$ = 20986·6		61922·6 (5)		54330·7 (4)	—
260·2					
$^2P_2$ = 20726·4		62182·4 (2)	61859·8 (5)	54591·1 (6)	54130·4 (6)
		Other regularities.			
α = 25582·8			57004·7 (2)	49733·8 (4)	
β = 23806·4			58781·4 (3)		51048·8 (7)
γ = 21380·3			61207·8 (3)		53474·5 (4)
δ = 19871·9				55444·7 (3)	54983·7 (1)
ϵ = 18902·7				56413·3 (2)	55953·5 (2)

* This value is derived from the ionisation potential.
† Close to a line of N I.

There can be little doubt as to the correct identification of the combinations $4p\ ^4S$, ^2D, ^2P with $5s\ ^4P$, ^2P. As McLennan and McLay have pointed out, the intervals of the various terms are perfectly in consonance with the corresponding values for the other elements N I, P I, Sb I of the same chemical group. The lines λλ 1972·64, 1937·68, 1890·53 are distinctly the strongest lines of the spectrum and can be no other than the resonance triplet $4p\ ^4S$—$5s\ ^4P$. Some difficulty was experienced in finding the other terms of the $5s$ state, particularly $5s\ ^2D$, for the line λ 2344·02 (ν 42648·6) had been recorded previously not as an arc line but as one of the spark. In the present experiments, however, it is easily observed in the ordinary arc where none of the other spark lines of As is present. The small interval of -19 cm.$^{-1}$ of the $5s\ ^2D$ term appears probable from a consideration of the corresponding value in O II.*

An interesting feature of the analysis is the detection of the $4p'$ group of terms. In As I, as in other spectra of this type, the term $4p'\ ^4P$ is inverted. The absence of the line $4p\ ^2D_3$—$4p'\ ^2P_2$ makes the assignment of the latter level somewhat doubtful but no other alternative was found. The level $4p'\ ^2D$ is presumably unresolved.

It was found extremely difficult to identify with any degree of certainty the $4d$ group of terms. Of these the doublet terms arising from the ^1D and ^1S states of the core give combinations lying further down in the ultra-violet below the region investigated, while the quartets depending on the ^3P state of the core have to be located only by weak inter-combination lines. An attempt has, however, been made to locate a few of these terms. But as there are no means of checking the correctness of these terms either by other combinations such as $4d \rightarrow 5p$ or at least by comparison with other similar spectra, the assignments cannot be said to be entirely definite. The pair $4p\ ^2D$—$4d\ ^2F$ is very strong on the plates and seems to be correctly identified.

Term Values.

It has not been possible to find the absolute values of the terms, as even two members of any series have not been identified. The values adopted in Table II are estimated by assuming $4p\ ^4S_2$ to be 93500 cm.$^{-1}$ which is derived from the ionisation potential of 11·54 volts found by Ruark and others for arsenic.

---

* A. Fowler, 'Roy. Soc. Proc.,' A, vol, 110, p. 476 (1926), also R. H. Fowler and Hartree, 'Roy. Soc. Proc.,' A, vol. 111, p. 83 (1926); Russell, 'Phys. Rev.,' vol. 31, p. 27 (1928).

The estimated probable error in this value is 0·5 volt which corresponds roughly to 4000 cm.$^{-1}$. The value adopted will at least serve as well as one arbitrarily chosen.

An interesting feature about the relative values of the $4p'$ and $5s$ terms deserves notice. In the spark spectra of this type, *e.g.*, O II,* F III,† S II,‡ Cl III § the corresponding p' group is much deeper than the s group, so that the so-called resonance triplet corresponds to the combination $mp\ {}^4\text{S}—mp'\ {}^4\text{P}$ and not $mp\ {}^4\text{S}—(m+1)s\ {}^4\text{P}$, while in the arc spectra, *e.g.*, N I,† As I and presumably Sb I the reverse is the case. This change in the relative values of the two groups of terms as we pass from the arc spectra to the spark may throw some light on the relative importance of the inner electron transition in spark spectra.

Finally, a general catalogue of the As arc lines is given in Table III, in which the last column indicates the classification of the lines. Measurements by Randall in the infra-red region have been omitted from the table. The following pair pointed out by Ruark and others may, however, be mentioned.

λ	ν	Δν	
8823·3	11330·6	916·0	$5s\ {}^4\text{P}_1—x$
9599·3	10414·6		$5s\ {}^4\text{P}_2—x$

The term x is probably one of the $5p$ group of terms.

---

* *Loc. cit.* and Bowen, 'Phys. Rev.,' vol. 29, p. 231 (1927).

† Bowen, 'Phys. Rev.,' vol. 29, p. 231 (1927), and Dingle, 'Roy. Soc. Proc.,' A, vol. 122, p. 144 (1929).

‡ 'Phys. Rev.,' vol. 32, p. 172 (1928); also 'Roy. Soc. Proc.,' A, vol. 122, p. 416 (1929).

§ 'Phys. Rev.,' vol. 31, p. 34 (1928).

Table III.—Catalogue of Lines of the As Arc Spectrum.

λ I.A. (int.).	ν (vac.).	Classification.		
		Doublets.	Inter-combinations.	Quartets and other combinations.
3119·576 (4)	32046·38		$4p\ {}^2P_2$—$5s\ {}^4P_1$	
3075·317 (2)	32507·56		$4p\ {}^2P_1$—$5s\ {}^4P_1$	
3032·845 (4)	32962·77		$4p\ {}^2P_2$—$5s\ {}^4P_2$	
2990·991 (2)	33423·91		$4p\ {}^2P_1$—$5s\ {}^4P_2$	
2898·702 (5)	34488·12	$4p\ {}^2P_2$—$5s\ {}^2P_1$		
2860·452 (7)	34949·27	$4p\ {}^2P_1$—$5s\ {}^2P_1$		
2780·197 (8)	35958·09	$4p\ {}^2P_2$—$5s\ {}^2P_2$		
2744·991 (6)	36419·24	$4p\ {}^2P_1$—$5s\ {}^2P_2$		
2492·89 (2)	40102·0		$4p\ {}^2D_2$—$5s\ {}^4P_1$	
2456·53 (4)	40695·6		$4p\ {}^2D_3$—$5s\ {}^4P_2$	
2437·22 (2)	41018·0		$4p\ {}^2D_2$—$5s\ {}^4P_2$	
2381·19 (4)	41983·0		$4p\ {}^2D_3$—$5s\ {}^4P_3$	
2370·80 (6)	42167·0	$4p\ {}^2P_2$—$5s\ {}^2D_3$		
2369·67 (5)	42187·1	$4p\ {}^2P_2$—$5s\ {}^2D_2$		
2363·04 (2)	42305·4		$4p\ {}^2D_2$—$5s\ {}^4P_3$	
2349·83 (10)	42543·2	$4p\ {}^2D_2$—$5s\ {}^2P_1$		
2344·02 (6)	42648·6	$4p\ {}^2P_1$—$5s\ {}^2D_2$		
2288·12 (10)	43690·5	$4p\ {}^2D_3$—$5s\ {}^2P_2$		
2271·39 (4)	44012·4	$4p\ {}^2D_2$—$5s\ {}^2P_2$		
2266·75 (2)	44102·4		$4p\ {}^2P_2$—$4p'\ {}^4P_3$	
2228·72 (3)	44854·8		$4p\ {}^2P_2$—$4p'\ {}^4P_2$	
2206·04 (2)	45315·9		$4p\ {}^2P_1$—$4p'\ {}^4P_2$	
2205·20 (1)	45333·2		$4p\ {}^2P_2$—$4p'\ {}^4P_1$	
2182·98 (2)	45794·6		$4p\ {}^2P_1$—$4p'\ {}^4P_1$	
2176·26 (1)	45935·9			
2165·57 (6)	46162·6	$4p\ {}^2P_2$—$4p'\ {}^2D_{2,3}$		
2144·14 (5)	46624·0	$4p\ {}^2P_1$—$4p'\ {}^2D_2$		
2138·53 (2)	46746·3			
2133·77 (4)	46850·6	$4p\ {}^2P_2$—$5s\ {}^2S_1$		
2124·06 (1)	47064·7			
2112·99 (4)	47311·3	$4p\ {}^2P_1$—$5s\ {}^2S_1$		
2089·68 (3)	47838·9		$4p\ {}^2P_2$—$4d\ {}^4D_2$	
2085·33 (5)	47938·7	$4p\ {}^2P_2$—$4p'\ {}^2S_1$		
2079·41 (2)	48075·2		$4p\ {}^2P_2$—$4d\ {}^4D_3$	
2069·79 (5)	48298·6		$4p\ {}^2P_1$—$4d\ {}^4D_2$	
2068·34 (4)	48332·4		$4p\ {}^2P_1$—$4d\ {}^4D_1$	
2067·13 (4)	48360·7	$4p\ {}^2P_2$—$4p'\ {}^2P_2$		
2065·42 (6)	48400·8	$4p\ {}^2P_1$—$4p'\ {}^2S_1$		
2047·58 (5)	48822·4	$4p\ {}^2P_1$—$4p'\ {}^2P_2$		
2025·36 (1)	49358·0			
2013·30 (6)	49653·5	$4p\ {}^2P_2$—$4d\ {}^2D_2$		
2012·74 (4)	49667·4	$4p\ {}^2P_2$—$4p'\ {}^2P_1$		
2010·05 (4)	49733·8			$4p\ {}^2P_1$—α
2009·21 (9)	49754·6	$4p\ {}^2P_2$—$4d\ {}^2D_3$		
2003·28 (10)	49901·4	$4p\ {}^2D_3$—$5s\ {}^2D_3$		
2002·53 (4)	49920·6	$4p\ {}^2D_3$—$5s\ {}^2D_2$		
λ vac.				
1995·45 (7)	50114·0	$4p\ {}^2P_1$—$4d\ {}^2D_2$		
1994·87 (6)	50128·6	$4p\ {}^2P_1$—$4p'\ {}^2P_1$		
1991·08 (7)	50224·0	$4p\ {}^2D_2$—$5s\ {}^2D_3$		
1990·37 (9)	50241·9	$4p\ {}^2D_2$—$5s\ {}^2D_2$		
1972·64 (15)	50693·5			$4p\ {}^4S_2$—$5s\ {}^4P_1$
1958·91 (7)	51048·8			$4p\ {}^2P_2$—β
1937·68 (15)	51608·1			$4p\ {}^4S_2$—$5s\ {}^4P_2$

Table III (continued).

λ I.A. (int.).	ν (vac.).	Classification.		
		Doublets.	Inter-combinations.	Quartets and other combinations.
1929·17 (1)	51835·7		$4p\,{}^2D_3$—$4p'\,{}^4P_3$	
1917·24 (4)	52158·3		$4p\,{}^2D_2$—$4p'\,{}^4P_3$	
1902·48 (2) Bi	52563·0			
1901·59 (2)	52587·6		$4p\,{}^2D_3$—$4p'\,{}^4P_2$	
1900·02 (1)	52631·0			
1890·53 (15)	52895·2			$4p\,{}^4S_2$—$5s\,{}^4P_3$
1882·03 (5)	53134·1		$4p\,{}^4S_2$—$5s\,{}^2P_1$	
1873·09 (4)	53387·7		$4p\,{}^2D_2$—$4p'\,{}^4P_1$	
1871·74 (5)	53426·2	$4p\,{}^2D_3$—$4d\,{}^2F_3$		
1870·05 (4)	53474·5			$4p\,{}^2P_2$—γ
1865·21 (3)	53613·3			
1860·77 (1)	53741·2			
1860·48 (8)	53749·6	$4p\,{}^2D_2$—$4d\,{}^2F_3$		
1855·48 (4)	53894·4	$4p\,{}^2D_3$—$4p'\,{}^2D_{2,3}$		
1853·29 (5)	53958·1			
1850·32 (6)	54044·7			
1847·39 (6)	54130·4	$4p\,{}^2P_2$—$4d\,{}^2P_2$		
1844·49 (7)	54215·5	$4p\,{}^2D_2$—$4p'\,{}^2D_{2,3}$		
1840·58 (4)	54330·7	$4p\,{}^2P_1$—$4d\,{}^2P_1$		
1831·80 (6)	54591·1	$4p\,{}^2P_1$—$4d\,{}^2P_2$		
1831·39 (6)	54603·3		$4p\,{}^4S_2$—$5s\,{}^2P_2$	
1821·44 (2)	54901·6		$4p\,{}^2D_2$—$5s\,{}^2S_1$?	
1818·72 (1)	54983·7			$4p\,{}^2P_2$—δ
1816·87 (2)	55039·7			
1813·18 (0)	55151·8			
1806·21 (9)	55364·5	$4p\,{}^2D_3$—$4d\,{}^2F_4$		
1803·60 (3)	55444·7			$4p\,{}^2P_1$—δ
1799·61 (2)	55567·6		$4p\,{}^2D_2$—$4d\,{}^4D_2$	
1798·71 (4)	55595·4			
1791·86 (4)	55807·9		$4p\,{}^2D_3$—$4d\,{}^4D_3$	
1789·94 (4)	55867·8		$4p\,{}^2D_3$—$4d\,{}^4D_4$	
1789·25 (3)	55889·4		$4p\,{}^2D_2$—$4d\,{}^4D_1$	
1787·20 (2)	55953·5			$4p\,{}^2P_2$—ϵ
1785·97 (1)	55992·0	$4p\,{}^2D_3$—$4p'\,{}^2S_1$		
1781·55 (5)	56130·9		$4p\,{}^2D_2$—$4d\,{}^4D_3$	
1780·61 (5)	56160·5			
1772·63 (2)	56413·3			$4p\,{}^2P_1$—ϵ
1768·07 (2)	56558·9			
1760·39 (1)	56805·6			
1758·62 (7)	56862·8			
1754·24 (2)	57004·7			$4p\,{}^2D_3$—α
1741·23 (3)	57430·7			
1739·53 (4)	57486·8	$4p\,{}^2D_3$—$4d\,{}^2D_3$		
1732·87 (2)	57707·7	$4p\,{}^2D_2$—$4d\,{}^2D_2$		
1732·51 (3)	57719·7			
1729·85 (2)	57808·5	$4p\,{}^2D_2$—$4d\,{}^2D_3$		
1724·84 (2)	57976·4			
1701·22 (3)	58781·4			$4p\,{}^2D_3$—β
1644·40 (3)	60812·5		$4p\,{}^4S_2$—$5s\,{}^2D_3$	
1633·78 (3)	61207·8			$4p\,{}^2D_3$—γ
1616·56 (5)	61859·8	$4p\,{}^2D_3$—$4d\,{}^2P_2$		
1614·92 (5)	61922·6	$4p\,{}^2D_2$—$4d\,{}^2P_1$		
1608·17 (2)	62182·4	$4p\,{}^2D_2$—$4d\,{}^2P_2$		
1593·66 (6)	62748·6			$4p\,{}^4S_2$—$4p'\,{}^4P_3$
1574·75 (5)	63502·2			$4p\,{}^4S_2$—$4p'\,{}^4P_2$
1571·34 (2)	63640·0			
1563·08 (3)	63976·3			$4p\,{}^4S_2$—$4p'\,{}^4P_1$

Summary.

The spectrum of arsenic has been investigated in the region λ 8800–λ 1370 and several previously unrecorded lines of As I have been measured. These have led to the identification of the combinations between the deepest set of terms, $4p\ {}^4S$, ${}^2D$, ${}^2P$ of As I, and the higher $5s$ and $4p'$ terms. Combinations with some of the terms of the $4d$ state have also been suggested. The resonance triplet is found to correspond to the combination $4p\ {}^4S$—$5s\ {}^4P$.

I wish to express my deep indebtedness to Prof. A. Fowler, F.R.S., for his continual interest and encouragement throughout the course of the investigation. My thanks are due also to the Andhra University and the Government of Madras for the award of a scholarship.

The Action of High Speed Cathode Rays on Acetylene.

By Prof. J. C. McLennan, F.R.S., M. W. Perrin, and H. J. C. Ireton.

(Received June 3, 1929.)

Introduction.

The effect of a silent electric discharge on acetylene was investigated by de Wilde and by P. and A. Thenard in 1874.* They found that a pale yellow solid was formed, together with an oily liquid in some cases. The solid on analysis was found to have the empirical formula of acetylene. The same product was obtained by Berthelot and Gandechon† as a result of the exposure of acetylene to ultra-violet light, and by Mund and Koch, and by Lind and Bardwell‡ by bombardment with alpha particles.

Only very small amounts of hydrogen were formed in the reaction and the product was presumed to be a polymer of acetylene. Mund and Koch's, and Lind and Bardwell's experiments both gave a value of nearly 20 for the number of molecules leaving the gas phase per ion-pair formed, and the latter assumed that the reaction could be represented by the following mechanism :—

---

* de Wilde, 'Ber. D. Chem. Ges.,' vol. 7, p. 352 (1874); Thenard, 'C. R.,' vol. 78, p. 219 (1874).

† 'C. R.,' vol. 150, p. 1169 (1910)

‡ Mund and Koch, 'Bull. Soc. Chim. Belg.,' vol. 34, p. 119 (1925); Lind and Bardwell, 'J. Am. Chem. Soc.,' vol. 48, p. 1556 (1926).

$$C_2H_2^+ + 19\,C_2H_2 \longrightarrow (C_2H_2)_{20}^+$$

$$(C_2H_2)_{20}^+ + \varepsilon \longrightarrow (C_2H_2)_{20}\ \text{(solid)}.$$

No solvent has been found suitable for determining the molecular weight of the polymer. Its molecular weight therefore cannot be determined directly.

On being heated, it decomposes with evolution of hydrogen and darkens in colour. It burns quietly with a luminous flame.

Coolidge* bombarded acetylene with high-speed electrons and by this means obtained the same product. The present investigation was carried out with a similar apparatus in order to investigate the kinetics of the reaction in greater detail.

Apparatus.

High voltage source for the operation of the cathode ray tube.

The cathode ray tube was operated by a transformer system similar to that described by Coolidge.† A diagrammatic sketch of the arrangement of the apparatus is shown in fig. 1. The mains of the 110 volt, 50 cycle current were connected in series with a variable resistance (A), an ammeter (B) and the primary of a 2 : 1 transformer (C). The secondary of this transformer supplied current to the primary of a 1 : 1 insulation transformer (D) having a secondary insulated for 125 KV. The primary of a 200 KV. Snook transformer (E) was fed by the secondary of transformer D. The case of the high tension transformer was insulated from ground and connected to the primary and to the middle of the secondary. One terminal of the secondary was connected to the cathode of the tube and the other was joined to earth through a milliammeter (F). This method of operation was a convenience since the window‡ of the cathode-ray tube and any apparatus connected to it could be grounded.

The storage batteries and the variable resistance (G) used in the filament circuit of the tube were placed in a galvanised iron box, the corners and edges of which were rounded off so as to cut down corona discharge. This box was placed on a suitably insulated stand. The current through the filament was controlled by means of an ebonite rod which passed into the box and was connected to the variable resistance.

---

* 'Science,' vol. 62, p. 441 (1925).

† 'J. Franklin Inst.,' vol. 202, p. 693 (1926).

‡ The windows were made of "resistal" foil, the composition of which, kindly given me by Sir Robert Hadfield, Bart., is as follows: 0·45 C, 3·15 Si, 0·85 Mn, 17·9 Cr, 26·0 Ni, 51·6 Fe per cent.

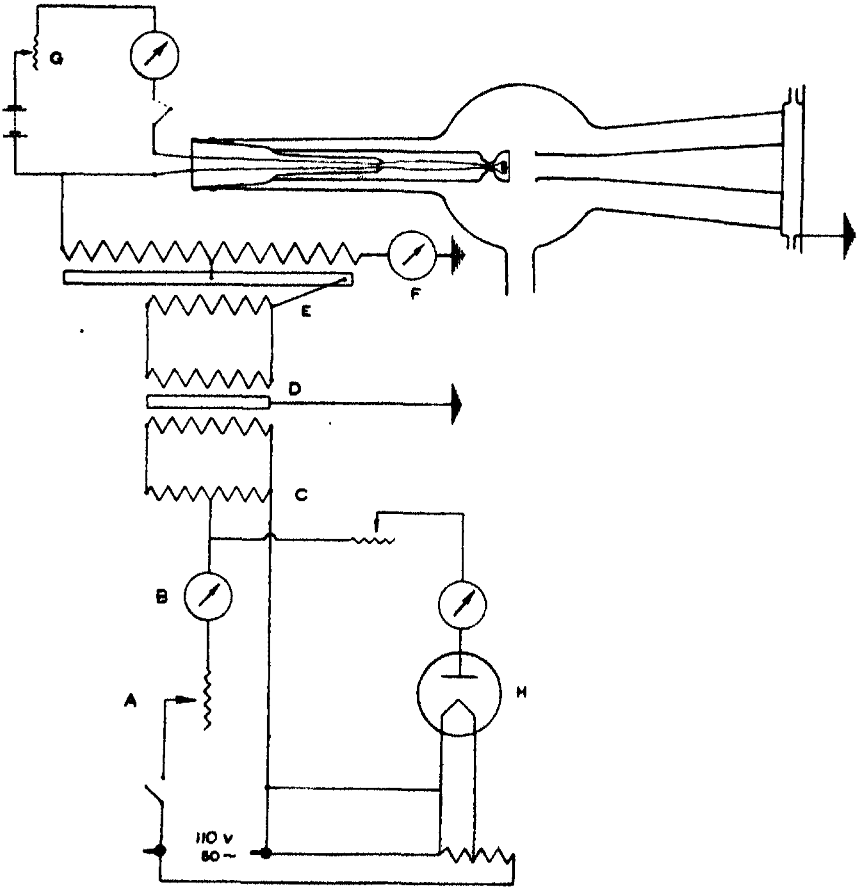

FIG. 1.

In order to decrease the voltage of that half of the wave not utilised by the cathode-ray tube and thus bring the " inverse " voltage below the " useful," a Tungar valve (H) was connected in parallel across the primary of the transformer C.

The voltage applied to the tube was measured by means of a standard Victor X-ray sphere gap.

Reaction Cell.

The reaction cell was a cylinder of pyrex glass waxed into an annular groove in a metal plate which was soldered to the front of the cathode-ray tube. A diagrammatic sketch is shown in fig. 2. Side tubes led from the cell to a manometer, to a gas reservoir and to a Hyvac oil pump respectively.

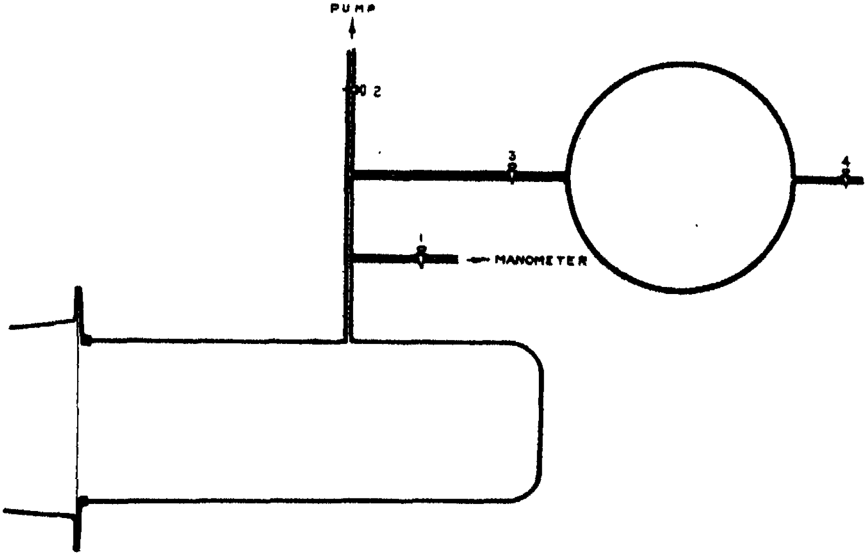

FIG. 2.

Preparation of Gas.

The acetylene was prepared by the action of distilled water on pure calcium carbide. The gas was purified by passing it through chromic acid and potassium hydroxide solutions and dried over phosphorus pentoxide. It was stored in the reservoir.

Experimental Procedure.

The whole system was exhausted as far as the tap (4), and a slow stream of acetylene passed through for some time. The system was then again exhausted and filled with acetylene, and this was repeated three times. The taps (3 and 4) connecting the reservoir to the reaction cell and to the generating system were then closed and some of the gas pumped out of the reaction cell until any desired pressure was obtained. This pressure was noted and then the tap (1) between the reaction cell and the manometer was also closed.

The acetylene was bombarded for a known time, usually varying between 5 and 30 minutes. During each experiment the voltage applied to the tube was kept constant and also the current through it. The latter was controlled by regulating the current in the filament circuit.

At the end of the bombardment the tap between the reaction cell and the manometer was opened and the change in pressure noted. This new pressure did not alter over a considerable time, and it was therefore assumed that there had been no appreciable thermal expansion of the gas, in agreement with the results obtained by McLennan and Greenwood.*

Results.

When the acetylene was bombarded no change in pressure occurred until the voltage across the tube exceeded 85 KV. A slight mist was then seen to form throughout the reaction cell after which a pale yellow, opaque deposit was formed on the walls and for a short distance along the tubes leading into the cell. This reaction was accompanied by a decrease in pressure.

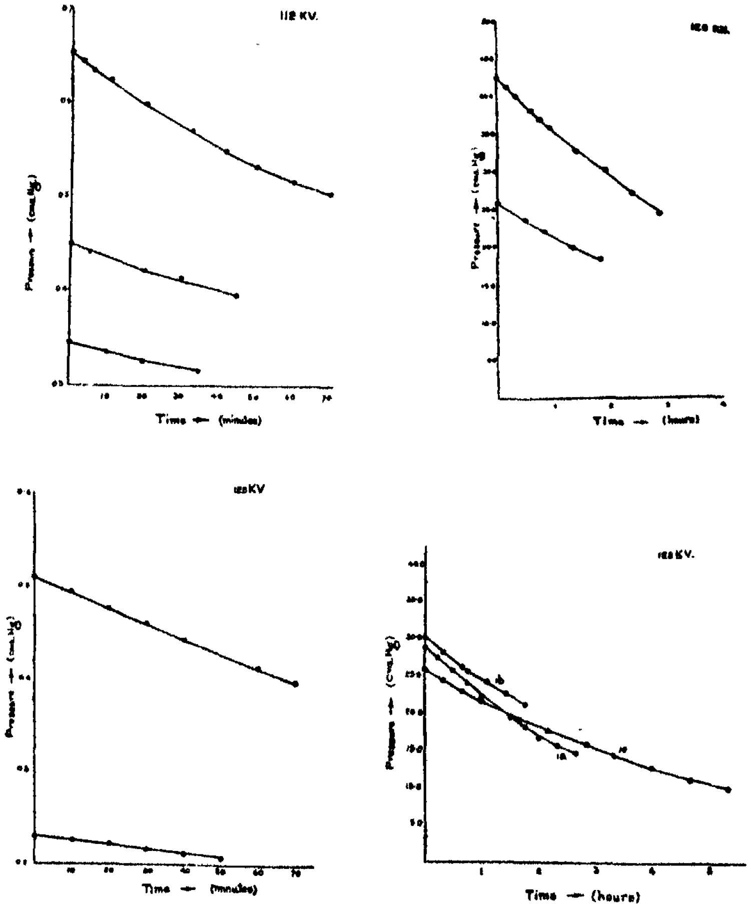

Fig. 3.—A–D.

---

* 'Roy. Soc. Proc.,' A, vol. 120, p. 283 (1928).

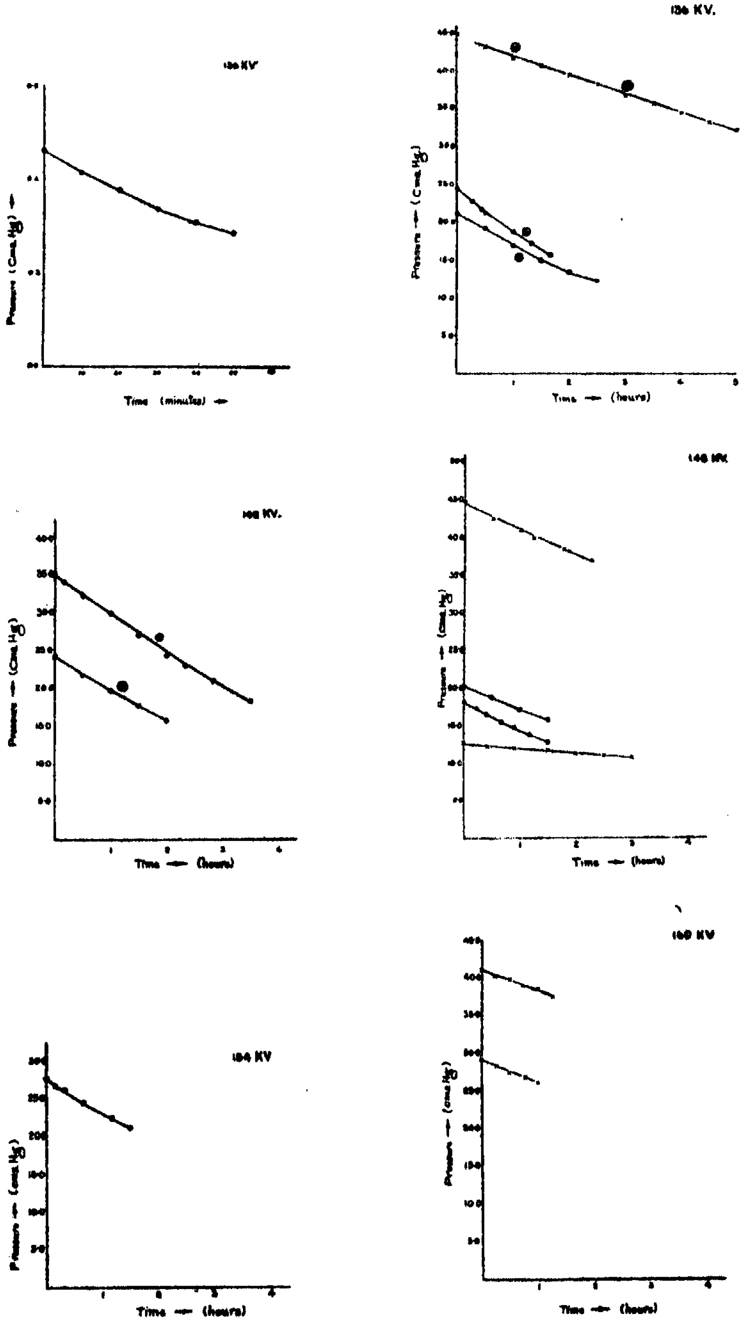
KV
Pressure → (Cms. Hg)
Time (minutes) →
KV.
Pressure → (Cms. Hg)
45.0
40.0
35.0
30.0
25.0
20.0
15.0
10.0
5.0
1
2
3
4
5
Time → (hours)
KV.
Pressure → (Cms. Hg)
40.0
35.0
30.0
25.0
20.0
15.0
10.0
5.0
1
2
3
4
Time → (hours)
KV
Pressure → (Cms. Hg)
1
2
3
4
Time → (hours)
KV
Pressure → (Cms. Hg)
Time → (hours)
KV
Pressure → (Cms. Hg)
40.0
35.0
30.0
25.0
20.0
15.0
10.0
5.0
1
2
3
4
Time → (hours)

FIG. 3.—E-J.

Table I.

112 KV.		120 KV.	
Time.	Pressure.	Time.	Pressure.
h. m.	cm.	h. m.	cm.
—	17·4	—	25·9
0 30	16·6	0 30	23·7
1 0	15·8	0 50	22·1
1 30	15·1	1 20	20·1
2 0	14·5	1 50	18·4
2 40	13·6		
—	16·75		
0 30	16·1	125 KV.	
1 0	15·5		
1 30	14·7	—	29·0
		0 15	27·5
—	39·8	0 30	25·9
0 30	37·9	0 45	24·1
0 50	36·7	1 0	22·4
1 20	35·0	1 30	19·6
1 50	33·2	1 45	18·2
2 20	31·5	2 0	16·8
2 30	31·0	2 20	15·7
		2 40	14·6
—	0·654		
0 3	0·644	—	30·2
0 6	0·634	0 20	28·2
0 10·5	0·624	0 40	26·3
0 20	0·597	0 45	25·8
0 32	0·570	1 5	24·2
0 41·5	0·548	1 25	22·6
0 50	0·532	1 45	21·2
0 60	0·517		
0 70	0·503	—	26·1
		0 20	24·5
—	0·450	0 40	23·1
0 5	0·442	1 0	21·7
0 20	0·423	1 30	19·1
0 30	0·414	2 0	17·6
0 45	0·396	2 40	15·9
		3 10	14·5
—	0·344	3 50	12·8
0 10	0·336	4 30	11·3
0 20	0·326	5 20	10·0
0 35	0·316		
		—	0·510
		0 10	0·493
120 KV.		0 20	0·476
		0 30	0·459
—	42·3	0 40	0·442
0 10	41·2	0 60	0·412
0 20	40·0	1 10	0·396
0 35	38·3		
0 45	37·0	—	0·230
0 55	35·9	0 10	0·226
1 25	32·8	0 20	0·222
1 55	30·2	0 30	0·216
2 25	27·2	0 40	0·212
2 55	24·5	0 50	0·208

Table I—(continued).

136 KV.

Time.	Pressure.
h. m.	cm.
—	24·5
0 15	22·8
0 25	21·8
0 30	21·3
1 0	18·7
1 20	17·2
1 40	15·8
—	21·3
0 30	19·2
1 0	17·0
1 30	15·0
2 0	13·5
2 30	12·1
—	44·9
0 30	43·3
1 0	41·9
1 30	40·6
2 0	39·5
2 30	38·2
3 0	36·9
3 30	35·7
4 0	34·4
4 30	33·2
5 0	32·1
—	0·432
0 10	0·408
0 20	0·388
0 30	0·370
0 40	0·356
0 50	0·344

142 KV.

Time.	Pressure.
—	34·9
0 10	34·1
0 30	32·2
1 0	29·8
1 30	26·8
2 0	24·2
2 20	22·9
2 50	21·0
3 30	18·1
—	24·3
0 30	21·8
1 0	19·7
1 30	17·7
2 0	15·6

148 KV.

Time.	Pressure.
h. m.	cm.
—	18·3
0 7	17·8
0 15	17·3
0 25	16·5
0 40	15·5
0 55	14·7
1 10	13·8
1 30	12·8
—	20·2
0 30	18·6
1 0	17·1
1 30	15·8
—	12·7
0 25	12·1
0 55	11·9
1 30	11·7
2 0	11·4
2 30	11·0
3 0	10·6
—	47·3
0 30	44·9
1 0	43·5
1 15	42·7
1 45	40·9
2 15	39·4

154 KV.

Time.	Pressure.
—	27·7
0 10	26·7
0 20	26·1
0 40	24·5
1 10	22·4
1 30	21·1

160 KV.

Time.	Pressure.
—	41·1
0 15	40·2
0 30	39·7
0 45	39·0
1 0	38·4
1 15	37·5
—	29·3
0 15	28·4
0 30	27·6
0 45	26·9
1 0	26·2

Since the reaction only occurred while the gas was bombarded, its course could be followed by the change in pressure after known intervals of time of exposure to the rays.

A series of such readings was obtained for different values of the voltage and the results are given in Table I. Curves for the readings at different applied voltages are shown in fig. 3. The values at the low pressures were determined by means of a McLeod gauge. The current through the tube was kept constant in all the experiments at a value of 0·13 milliamps.

In some cases a fresh supply of acetylene was let in to the reaction cell and a portion of the curve previously obtained was repeated. It was found that the presence of the deposit had no appreciable effect on the rate of change of pressure.

It will be seen that the slopes of some of the curves, namely those with readings marked by a cross (*vide* curves for potentials 136 and 148 KV.) are considerably less steep than those of others obtained with the same voltage applied to the tube. These results were obtained with a different window on the cathode-ray tube. Reference will be made to this again later.

After the walls of the cell had become well coated with the deposit the remaining gas was pumped out. No readable vapour pressure could be obtained on the manometer, and when the deposit was again bombarded there was no increase in pressure. The reaction was therefore irreversible.

The solid was scraped off the walls of the cell and examination under the microscope showed it to be a very fine translucent powder. The particles showed no evidence of crystalline structure and did not affect polarised light. No X-ray spectrum could be obtained from the powder. Its density was found by flotation in water-alcohol mixtures to be 0·97. Its refractive index was found* by immersing it in liquid of known refractive index by the method of Van der Kolke. The value obtained was $\mu_D = 1 \cdot 625 \pm 0 \cdot 005$.

The number of electrons crossing the cathode-ray tube could be calculated from the current measured by the milliammeter (F) in the transformer circuit (fig. 4). No information, however, could be obtained from this as to the proportion of the electrons passing through the window of the tube into the reaction cell, and hence as to the number of molecules of acetylene reacting for each electron. In order to measure this number the apparatus shown diagrammatically in fig. 4 was used. A brass cylinder (A) was soldered to the front of the cathode-ray tube. A side tube from it led to a mercury diffusion pump backed by a Hyvac oil pump. A Faraday cylinder (B) whose diameter was the same as that of the window of the tube was supported inside this cylinder by a brass rod waxed through an ebonite plug (C). The end of the Faraday cylinder was closed with a sheet of aluminium foil and was placed about 2 mm. from the window of the cathode-ray tube. The Faraday cylinder was connected to a microammeter (D), the other terminal of which was grounded. The outer cylinder was grounded. By this means a direct measure could be made of the electron current outside the cathode-ray tube. This was done for different values of the voltage applied to the tube and for different currents across it. The results are given for two windows in Table II. The curves

---

* With the kind assistance of Prof. T. L. Walker.

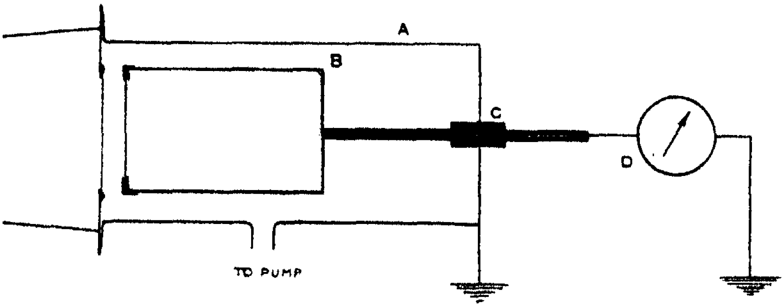

Fig. 4.

Table II.

Kilo-Voltage.	Current through tube (milliamps.).			Current through tube (milliamps.).		
	0·066	0·13	0·196	0·066	0·13	0·196
	External current (microamps.).			External current (microamps.).		
79	—	—	—	—	0·1	—
90	—	—	—	0·35	0·65	0·94
95	—	0·05	0·05	0·62 ; 0·65	1·35	1·45
101	0·05	0·1	0·12	1·1	1·55 ; 1·75	3·5
107	0·12	0·35	0·35 ; 0·4	—	2·15	—
108	—	—	—	1·95	2·8	4·05
110	—	—	—	—	—	4·5
112	0·35	0·4	1·0 ; 0·75	2·0 ; 2·45	3·95	7·7 ; 8·0
118	0·65	1·1	1·4	3·0 ; 3·1	4·9	8·0
125	0·75	1·65	1·98 ; 2·1	3·0 ; 3·95	5·4 ; 6·7	8·9
131	0·95 ; 1·1	2·25	2·97	3·2	—	—
136	1·3	2·9 ; 2·95	3·95	4·2 ; 4·6	7·7 ; 8·5	—
142	—	3·55	4·6	5·0 ; 5·5	10·3	—
145	—	—	5·15	—	—	—
148	1·95 ; 1·55	4·2	—	—	9·9	—
154	2·0	4·55	—	5·3	—	—
157	—	5·1	—	—	—	—
160	2·0	—	—	—	—	—

corresponding to these results are shown in figs. 5 and 6. The lower set of values was obtained using the window which had been found to give low values for the rate of change of pressure of the acetylene. In the calculations that follow, the results obtained with this window are not used.

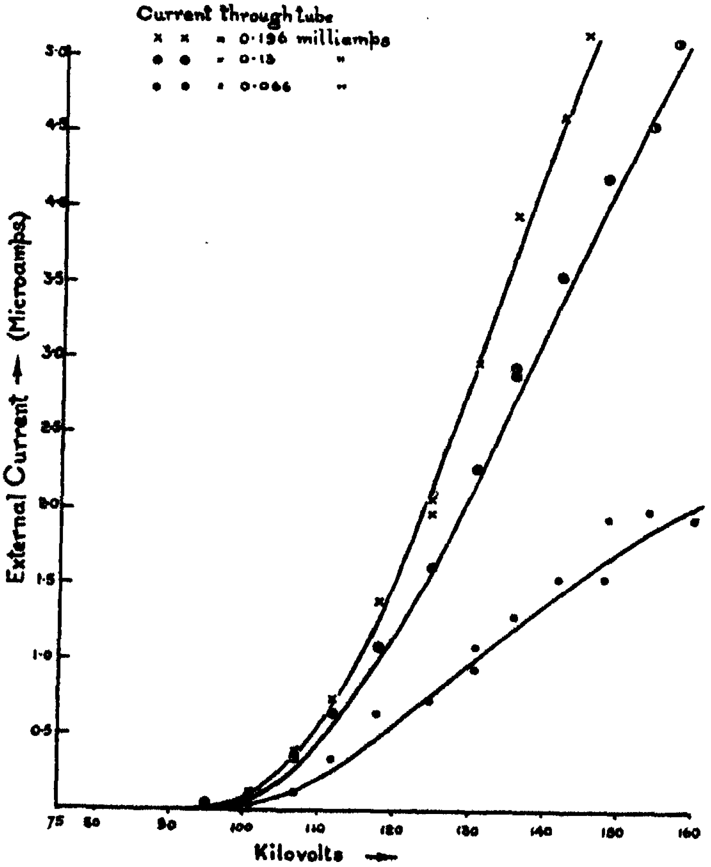

FIG. 5.

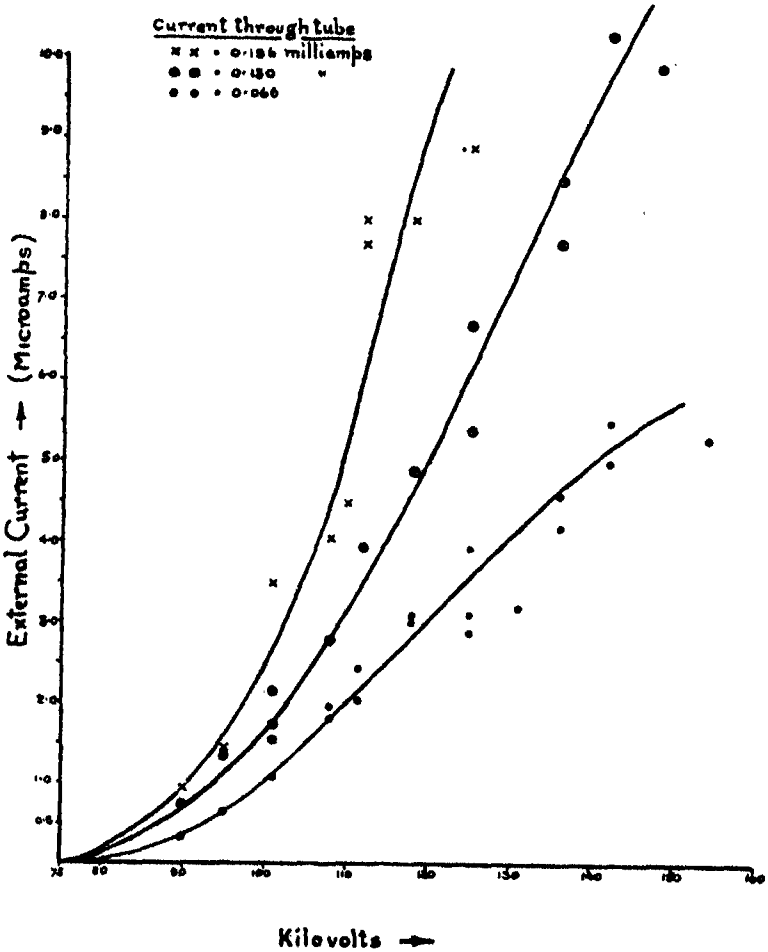

FIG. 6.

Conclusions.

Since the volume of the solid formed is negligible in comparison with the volume of the gas bombarded, the rate of the reaction can be followed by the rate of decrease in pressure in the reaction cell according to the equation

$$-\frac{dp}{dt} = kp^n \quad \text{or} \quad \log\left(-\frac{dp}{dt}\right) = n \log p + \log k,$$

where k is the velocity constant, and n the order of the reaction.

The rate of change of pressure at different values of the pressure was measured directly from the pressure-time curve by drawing tangents to the points. This is possible because the curvature is small in all cases.

The results for different values of the voltage are given below :—

112 KV.		120 KV.		125 KV.		136 KV.		142 KV.	
p.	*—dp/dt*.	*p*.	*—dp/dt*.	*p*.	*—dp/dt*.	*p*.	*—dp/dt*.	*p*.	*—dp/dt*.
cm.	mm. per min.	cm.	mm. per min.	cm.	mm. per min.	cm.	mm. per min.	cm.	mm. per min.
35	0·58	40	1·23	25	0·83	20	0·68	30	0·88
15	0·23	30	0·9	12·5	0·40	13·5	0·50	25	0·80
0·6	0·025	20	0·53	0·45	0·016	0·38	0·018	20	0·60
0·33	0·008	—	—	0·22	0·0045	—	—	—	—

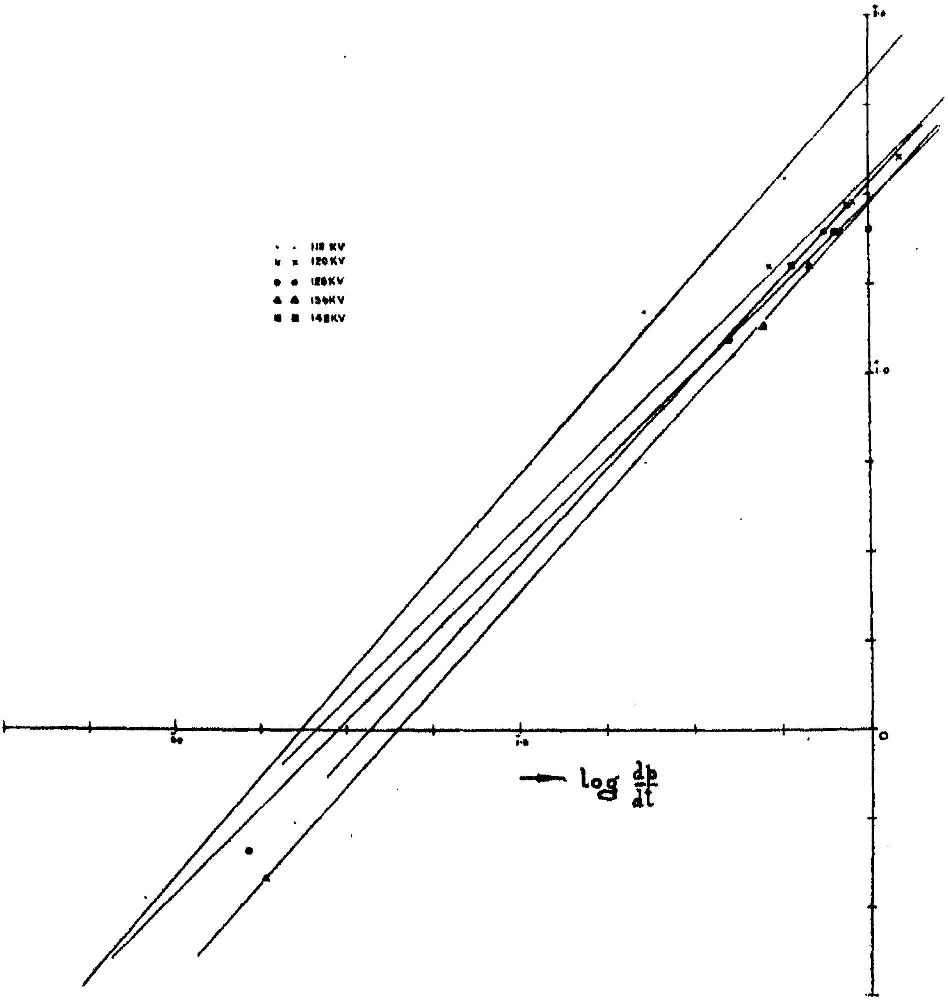

Fig. 7.

When the logarithms of p and $-dp/dt$ are plotted against each other as they are in fig. 7, a series of straight lines are obtained. The slopes of these lines give the value of the order of the reaction. They are found to be nearly unity over the whole pressure range.

The reaction is therefore apparently mono-molecular, the rate of change of pressure being proportional to the pressure.

The value of log k may be obtained from the values of the intercepts of the curves on the abscissa where $\log(-dp/dt) = 0$. Values so determined are given in Table III. It will be seen that there is a general increase in the value of k with increasing voltage applied to the tube.

Table III.

Volts.	log k.	k.
KV.		units : mm. and min.
112	2·36	0·023
120	2·41	0·026
125	2·47	0·0295
136	2·64	0·044
142	2·57	0·037

When these values of the velocity constant are plotted against the values of the voltage the curve obtained (fig. 8) indicates a linear relationship. Extrapolation of this curve to a zero value for the velocity constant gives a critical value of 80 KV. for the voltage. This is in agreement with the value for the

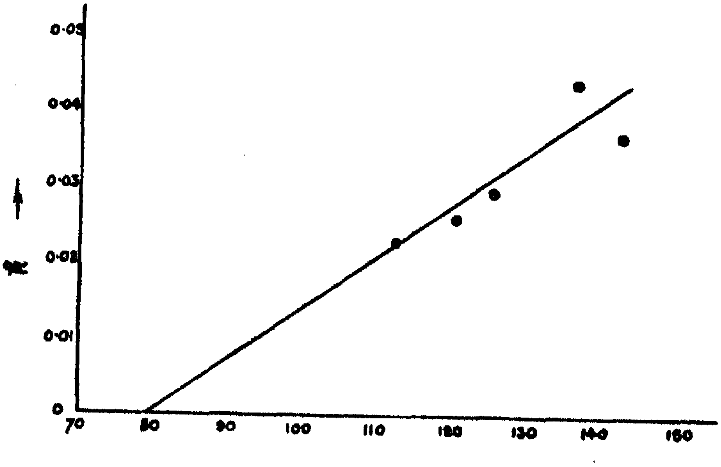

FIG. 8.

voltage at which a decrease in the pressure of the acetylene occurred when it was bombarded.

Therefore it would seem that the rate of the reaction is proportional to the pressure of the acetylene and that the velocity constant increases directly as the voltage.

If the results obtained for the number of electrons passing into the reaction cell are examined it will be seen that a voltage of between 70 and 80 KV. had to be applied to the tube before any electrons passed through the window. After a value of about 90 KV. had been reached the number passing through the window was nearly proportional to the voltage over the range investigated for any given value of the current through the tube. Reference may be made to the results obtained by McLennan and Greenwood (*loc. cit.*) on the decomposition of ammonia by cathode rays. They found that the percentage decomposition was proportional to the voltage applied to the tube which is in agreement with the connection found between the number of electrons passing through the window and the voltage.

We may assume that the number of molecules struck by any one electron is given by $\pi\sigma^2 r n_0 p/p_0$ where σ is the radius of the molecule, r is the range of the electron, n_0 is the number of molecules per cubic centimetre at standard pressure p_0, and temperature, and p is the actual pressure.

No very accurate statements can be made about the range of the electrons in the gas at different pressures as nothing is known about the distribution of velocities in the cathode-ray beam. The electrons also suffer deflections from their course in passing through the metal window, and some of them will be stopped by the walls of the reaction cell.

In order to make the calculation we may, however, take the range as being equal to the length of the reaction cell, namely 27·0 cm., for pressures below about 35 cm., and for voltages greater than 100 KV.

Then at a value of the pressure of, say, 12·5 cm., the number of molecules hit by an electron will be

$$\pi \times (10^{-8})^2 \times 27 \times 2{\cdot}7 \times 10^{19} \times 12{\cdot}5/76 = 3{\cdot}77 \,.\, 10^4.$$

Now at this pressure with a voltage of 125 KV. the rate of change of pressure was found to be 0·40 mm. per minute. The rate of change in volume at N.T.P. will therefore be

$$\frac{dv_0}{dt} = \frac{p\mathrm{T}_0}{p_0\mathrm{T}} \cdot \frac{dv}{dt}$$

$$= -\frac{\mathrm{VT}_0}{p_0\mathrm{T}} \cdot \frac{dp}{dt}.$$

The volume of the reaction cell was 805·5 c.c., therefore dv_0/dt will be $805 \cdot 5 \times 273 \div (76 \times 293) \times 0 \cdot 04 = 0 \cdot 395$ c.c. per minute. This is equivalent to the removal of $1 \cdot 1 \,.\, 10^{19}$ molecules from the gas per minute.

At this voltage the electron current as measured just outside the window was found to be 6·0 microamperes. This current flowing for 1 minute will give 360 microcoulombs. Since the charge on one electron is $1 \cdot 59 \,.\, 10^{-19}$ coulombs the above quantity of electricity is equivalent to $2 \cdot 26 \,.\, 10^{15}$ electrons.

Therefore $4 \cdot 9 \,.\, 10^3$ molecules enter into the reaction for every electron entering the gas. This number is of the same order as that previously found for the number of molecules hit by one electron.

It seems reasonable to assume that the reaction takes place between molecules some of which have been ionised by the cathode rays. On this hypothesis the number of ions formed, and hence the rate of the reaction, will be proportional to the number of electrons passing through the window of the cathode-ray tube.

Both these deductions are in agreement with the apparent order of the reaction and the dependence of the velocity constant on the voltage as found by experiment.

Summary.

A Coolidge cathode ray tube was set up and operated by a high tension transformer in a manner similar to that described by Coolidge. Acetylene was bombarded with known values of voltage applied to the tube, and with known current through it, and the pressure was noted at different times. A pale yellow solid was deposited on the walls of the reaction cell during the bombardment. The product had no measurable vapour pressure and on bombarding it there was no increase in pressure. When heated the solid turned black and burnt with a luminous flame. Its specific gravity and refractive index were measured. No X-ray spectrum could be obtained from it.

For any given voltage it was found that the rate of decrease of pressure of the acetylene was proportional to the pressure. The velocity constant of the reaction increased with increasing voltage.

The number of electrons passing through the window of the cathode ray tube was determined by collecting them in a Faraday cylinder placed close up to the window and measuring the current with a microammeter.

Calculation showed that the number of molecules of acetylene reacting is of the same order as the number of ions produced by each electron that passes through the window. The observed facts can be explained on the hypothesis that the reaction takes place following the ionisation of the acetylene by the cathode rays.

For the "resistal" windows used in our cathode-ray tubes I am indebted to Dr. Coolidge of The General Electric Company, Schenectady. For financial aid that enabled me to purchase a portion of the transformer equipment I am indebted to The Carnegie Corporation.

Kronecker's Fundamental Limit Formula in the Theory of Numbers and Elliptic Functions, and Similar Theorems.

By L. J. Mordell, F.R.S.

(Received May 25, 1929.)

1. Many important applications of analysis to number-theory require the study of a function $f(s)$ of a complex variable $s = \sigma + i\tau$ near a singular point $s_0 = \sigma_0 + i\tau_0$. The function $f(s)$ is frequently defined for $\sigma > \sigma_0$ by an infinite series, really a Dirichlet's series, the general term of which is a function of the variables of summation, *e.g.*, a quadratic form, raised to the power s. Thus the question of finding the number of classes of binary quadratic forms of given determinant, or the number of classes of ideals in a given field, depends upon the residue, say R, of an appropriate $f(s)$ at a simple pole s_0. A deeper question then suggested is that of finding

$$\lim_{s \to s_0} \left(f(s) - \frac{R}{s - s_0} \right).$$

In particular, Kronecker's fundamental formula arises when $f(s)$ is a homogeneous binary quadratic form in the variables of summation. Thus, let $a\ (\neq 0)$, b, c be any constants real or complex which are such that the roots ω_1, ω_2 of the quadratic form

$$\phi(x, y) = ax^2 + bxy + cy^2 = a(x - \omega_1 y)(x - \omega_2 y)$$

are neither real nor equal. We need only distinguish the two cases

$$\text{(I)} \quad I(\omega_1) > 0, \qquad I(\omega_2) < 0,$$
$$\text{(II)} \quad I(\omega_1) > 0, \qquad I(\omega_2) > 0,$$

as the others can be included by writing $-y$ for y. We write

$$2a\omega_1 = -b + i\Delta^{\frac{1}{2}}, \qquad 2a\omega_2 = -b - i\Delta^{\frac{1}{2}}, \qquad \Delta = 4ac - b^2,$$

so that the sign of $\Delta^{\frac{1}{2}}$ is fixed in case I, by the assumption $I(\omega_1) > 0$, and is immaterial in case II.

Put

$$f(s) = \sum_{m,n}{}' \phi(m, n)^{-s}, \tag{1.1}$$

where the summation refers to all integer values of m, n, the dash denoting, here and elsewhere, the exclusion of combinations such as $m = n = 0$. The many-valued function ϕ^s is defined as $e^{s \log \phi}$, where $\log \phi = \log|\phi| + i \arg \phi$. Throughout this paper, unless otherwise stated, we define the logarithmic function $\log \xi$ as follows. When ξ is a constant, the principal value given by $-\pi < \arg \xi \leqslant \pi$ is taken. If $\xi = \xi(x)$, for $-\infty < x < \infty$, is a continuous function of x which does not vanish for real values of x, its argument is defined as the continuous function of x which has some selected value at $x = +\infty$, *e.g.*, if

$$\xi(x) = a_0 x^r + a_1 x^{r-1} + \dots + a_r, \qquad \arg \xi(+\infty) = \arg a_0.$$

Also, $\xi(x, y)$, a function of two variables may be defined by first inserting the value of y and using $\xi(x, y) = \xi(x)$. With these definitions, the series (1.1) converges absolutely and uniformly for $\sigma \geqslant 1 + \delta > 1$ and defines $f(s)$ as an analytic function of s for $\sigma > 1$.

Let ω be a number such that $I(\omega) > 0$, and let $q \equiv e^{\pi i \omega}$. We write as usual

$$\theta_{11}'(0, \omega) = 2\pi e^{\pi i \omega/4} \prod_1^\infty (1 - e^{2n\pi i \omega})^3$$

$$= 2\pi q^{\frac{1}{4}} \prod_1^\infty (1 - q^{2n})^3.$$

Then if $I(\omega_1) > 0$, $I(\omega_2) < 0$, and a is a positive number (which involves no loss of generality),

$$\lim_{s \to 1} \left\{ f(s) - \frac{2\pi \Delta^{-\frac{1}{2}}}{s - 1} \right\} = \frac{2\pi\gamma}{\Delta^{\frac{1}{2}}} + \frac{2\pi}{\Delta^{\frac{1}{2}}} \log \frac{a}{\Delta} + \frac{8\pi}{3\Delta^{\frac{1}{2}}} \log 2\pi$$

$$- \frac{4\pi}{3\Delta^{\frac{1}{2}}} \log \theta_{11}'(0, \omega_1)\, \theta_{11}'(0, -\omega_2) \tag{1.2}$$

where γ is Euler's constant.

If, however, $I(\omega_1) > 0$, $I(\omega_2) > 0$, and a is a complex number,

$$\lim_{s \to 1} f(s) = -\frac{4\pi}{3\Delta^{\frac{1}{2}}} \log \frac{\theta_{11}'(0, \omega_1)}{\theta_{11}'(0, \omega_2)}. \tag{1.3}$$

We define

$$\log \theta_{11}'(0, \omega_1) = \log 2\pi + \tfrac{1}{4}\pi i \omega + \sum_{n=1}^{\infty} 3 \log (1 - e^{2n\pi i \omega_1}),$$

and similarly for the other theta functions, so that we are not necessarily taking the principal values of the logarithms of the theta functions. Also, as a definition,

$$\log \theta_{11}'(0, \omega_1)\, \theta_{11}'(0, -\omega_2) = \log \theta_{11}'(0, \omega_1) + \log \theta_{11}'(0, -\omega_2),$$
$$\log \theta_{11}'(0, \omega_1)/\theta_{11}'(0, \omega_2) = \log \theta_{11}'(0, \omega_1) - \log \theta_{11}'(0, \omega_2).$$

The formula (1.2) is Kronecker's well-known result which is so important in the applications of elliptic functions to the theory of numbers that it has long since found its way into the text books. A version of Kronecker's proof is given in Seguier's[*] book, and another proof is given in Weber's[†] book. Others have been given by Lerch, Franel, Landau, Epstein, Herglotz and Brix.[‡] Sometimes they impose unnecessary restrictions upon a, b, c, those of Kronecker, Seguier, Epstein, assuming that $\phi(m, n)$ has for its real part a definite quadratic form in m and n, while Weber and Landau assume that a, b, c are all real. Again, as in the accounts by Weber and Herglotz, they are sometimes of an informal character, without discussion of questions of convergence and the validity of certain operations. Epstein's proof has the great advantage that it gives the corresponding result when $\phi(m, n)$ is replaced by the similarly restricted quadratic form in any number of variables. Herglotz considers the question from the point of view of the analytic continuation of a function of a complex variable, but there is no generality about his method.

I have discovered a very simple and direct proof of Kronecker's formula, which in addition reveals the existence of the new formulæ (1.3), (2.6) and similar ones, and also permits of generalisation. Thus $\phi(m, n)$ may be replaced by any homogeneous binary form of degree $r > 2$ whose roots are all imaginary, or again by a homogeneous quadratic form in any number of variables which is such that simultaneous zeros are the only real values of the variables for which the form vanishes.

---

[*] 'Formes quadratiques et Multiplication complexe,' pp. 212–219, Berlin (1894).

[†] 'Lehrbuch der Algebra,' vol. 3, pp. 525–533, Braunschweig (1908).

[‡] Franel, 'Math. Ann.,' vol. 48, pp. 595–602 (1897) and vol. 52, pp. 529–536 (1899); Landau, 'J. r. angew. Math.,' vol. 125, pp. 64–182 (1903), this contains further detailed references as well as an interesting account of the earlier history of the subject; Epstein, 'Math. Ann.,' vol. 56, pp. 615–644 (1903) and vol. 63, pp. 205–216 (1907); Herglotz, 'Math. Ann.,' vol. 61, pp. 551–560 (1905); Brix, 'Monats. Math. Phys.,' vol. 21, pp. 309–325 (1910).

The explicit formulæ analogous to Kronecker's are in the first case expressed by means of a series of integrals. The results show incidentally that the function of s defined by the series for $\sigma > 1/r$ is analytic throughout the finite part of the s plane except possibly for simple poles given by $rs = 2, 1, -2, -4, -6, \ldots$, excluding, however, multiples of r from the right-hand side.

The results are more striking in the case of the general quadratic form. They are very simple and strictly analogous to those for the binary quadratic form.

§ 2. All these results are simple consequences of Poisson's summation formula, of which a particular case for one variable is as follows.* If $\mathrm{F}(x)$ and $\mathrm{F}'(x)$ are continuous for all real values of x and both tend to zero as $|x| \to \infty$, and if $\mathrm{F}(x)$ and $\mathrm{F}''(x)$ are such that $\int_{-\infty}^{\infty} \mathrm{F}(x)\,dx$ and $\int_{-\infty}^{\infty} |\mathrm{F}''(x)|\,dx$ both converge, then

$$\sum_{n=-\infty}^{\infty} \mathrm{F}(n) = \sum_{n=-\infty}^{\infty} \int_{-\infty}^{\infty} e^{2n\pi ix}\,\mathrm{F}(x)\,dx. \tag{2.1}$$

The proof is merely a question of integrating twice by parts the general term on the right-hand side.

I take first the formulæ (1.2) and (1.3). Write separately the terms in (1.1) for which $n = 0$. Then

$$f(s) = \sum_{m=-\infty}^{\infty}{}' (am^2)^{-s} + 2 \sum_{n=1}^{\infty} \sum_{m=-\infty}^{\infty} \phi(m, n)^{-s}. \tag{2.2}$$

Apply Poisson's summation formula to the last summation in m; the required conditions are obviously satisfied. This gives

$$f(s) = \sum_{m=-\infty}^{\infty}{}' (am^2)^{-s} + 2 \sum_{n=1}^{\infty} \sum_{m=-\infty}^{\infty} \int_{-\infty}^{\infty} \frac{e^{2m\pi ix}}{\phi(x, n)^s}\,dx. \tag{2.3}$$

Put $x = nx$ in the integral and write separately the term when $m = 0$. Hence

$$f(s) = 2a^{-s}\,\zeta(2s) + g(s) + g_1(s), \tag{2.4}$$

say, where

$$g(s) = 2 \sum_{n=1}^{\infty} \frac{1}{n^{2s-1}} \int_{-\infty}^{\infty} \frac{dx}{\phi(x, 1)^s}, \tag{2.5}$$

$$g_1(s) = 2 \sum_{n=1}^{\infty} \sum_{m=-\infty}^{\infty}{}' \frac{1}{n^{2s-1}} \int_{-\infty}^{\infty} \frac{e^{2mn\pi ix}}{\phi(x, 1)^s}\,dx.$$

It is now an easy matter to discuss the behaviour of $f(s)$ near $s = 1$.

---

* Mordell, 'J. London Math. Soc.,' vol. 4, part 4 (1929), *not yet published*.

Write

$$g_1(s) = 2 \sum_{n=1}^{\infty} \sum_{m=-\infty}^{\infty}{}' \frac{1}{n^{2s-1}} \int_{-\infty}^{\infty} e^{2mn\pi ix} \chi(x)\, dx$$

$$= 2 \sum_{n=1}^{\infty} \sum_{m=-\infty}^{\infty}{}' \frac{1}{n^{2s-1}} \mathrm{J}_{mn}.$$

Then $g_1(s)$, which is certainly defined by this series when $\sigma > 1$, is really an integral function of s. For if $|s| < \mathrm{M}$, say, so that we deal only with bounded values of s, on integrating twice by parts and noting $\sigma > 1$,

$$\mathrm{J}_{mn} = \frac{1}{(2mn\pi i)^2} \int_{-\infty}^{\infty} e^{2mn\pi ix} \chi''(x)\, dx$$

$$= O\left(\frac{1}{m^2 n^2}\right),$$

the constant implied being independent of s, n and m. Hence the series for $g_1(s)$ converges absolutely and uniformly for $\sigma > \delta > 0$. Another integration by parts shows then that $\mathrm{J}_{mn} = O\left(\frac{1}{m^3 n^3}\right)$, and so the new series for $g_1(s)$ converges absolutely and uniformly for $\sigma > -\frac{1}{2} + \delta > -\frac{1}{2}$, etc.
Hence as $s \to 1$,

$$g_1(s) = 2 \sum_{n=1}^{\infty} \sum_{m=-\infty}^{\infty}{}' \frac{1}{n} \int_{-\infty}^{\infty} \frac{e^{2mn\pi ix}}{\phi(x, 1)}\, dx + o(s-1),$$

the last term $o(s-1)$ denoting throughout a function of s vanishing for $s = 1$ and regular near $s = 1$. The integral

$$\int_{-\infty}^{\infty} \frac{e^{2mn\pi ix}}{\phi(x, 1)}\, dx = \frac{1}{a} \int_{-\infty}^{\infty} \frac{e^{2mn\pi ix}}{(x - \omega_1)(x - \omega_2)}\, dx$$

is a standard form and can be evaluated by deforming the path of integration into an infinite semicircle described above or below the real axis of x according as $m \geqslant 0$ or $m \leqslant 0$. The residue of the integrand at $x = \omega_1$ is

$$\frac{e^{2mn\pi i\omega_1}}{\omega_1 - \omega_2} = \frac{1}{2\pi i} \cdot \frac{2\pi a}{\Delta^{\frac{1}{2}}} e^{2mn\pi i\omega_1}.$$

Hence when $\mathrm{I}(\omega_1) > 0$, $\mathrm{I}(\omega_2) < 0$, so that ω_1 is in the upper half plane and ω_2 in the lower half plane,

$$\int_{-\infty}^{\infty} \frac{e^{2mn\pi ix}}{(x - \omega_1)(x - \omega_2)}\, dx = \frac{2\pi a}{\Delta^{\frac{1}{2}}} e^{2mn\pi i\omega_1} \quad \text{or} \quad \frac{2\pi a}{\Delta^{\frac{1}{2}}} e^{2mn\pi i\omega_2},$$

according as $m \geqslant 0$ or $m \leqslant 0$, since $\omega_1 - \omega_2 = i\Delta^{\frac{1}{2}}a^{-1}$. Hence

$$g_1(s) = \frac{4\pi}{\Delta^{\frac{1}{2}}} \sum_{n=1}^{\infty} \sum_{m=1}^{\infty} \frac{1}{n} e^{2mn\pi i\omega_1} + \frac{4\pi}{\Delta^{\frac{1}{2}}} \sum_{n=1}^{\infty} \sum_{m=1}^{\infty} \frac{1}{n} e^{-2mn\pi i\omega_2} + o(s-1).$$

The double series may be summed first for n as it is absolutely convergent, and so

$$\begin{aligned} g_1(s) &= -\frac{4\pi}{\Delta^{\frac{1}{2}}} \sum_{m=1}^{\infty} \log(1 - e^{2m\pi i\omega_1}) - \frac{4\pi}{\Delta^{\frac{1}{2}}} \sum_{m=1}^{\infty} \log(1 - e^{-2m\pi i\omega_2}) + o(s-1) \\ &= -\frac{4\pi}{3\Delta^{\frac{1}{2}}} \log\{\theta_{11}'(0, \omega_1)\, \theta_{11}'(0, -\omega_2)\} + \frac{i\pi^2}{3\Delta^{\frac{1}{2}}}(\omega_1 - \omega_2) \\ &\qquad + \frac{8\pi}{3\Delta^{\frac{1}{2}}} \log 2\pi + o(s-1). \end{aligned}$$

When, however, $I(\omega)_1 > 0$, $I(\omega_2) > 0$, then

$$\begin{aligned} g_1(s) &= \frac{4\pi}{\Delta^{\frac{1}{2}}} \sum_{n=1}^{\infty} \sum_{m=1}^{\infty} \frac{1}{n} e^{2mn\pi i\omega_1} - \frac{4\pi}{\Delta^{\frac{1}{2}}} \sum_{n=1}^{\infty} \sum_{m=1}^{\infty} \frac{1}{n} e^{2mn\pi i\omega_2} + o(s-1) \\ &= -\frac{4\pi}{\Delta^{\frac{1}{2}}} \sum_{m=1}^{\infty} \log(1 - e^{2m\pi i\omega_1}) + \frac{4\pi}{\Delta^{\frac{1}{2}}} \sum_{m=1}^{\infty} \log(1 - e^{2m\pi i\omega_2}) + o(s-1) \\ &= -\frac{4\pi}{3\Delta^{\frac{1}{2}}} \log\{\theta_{11}'(0, \omega_1)/\theta_{11}'(0, \omega_2)\} + \frac{i\pi^2}{3\Delta^{\frac{1}{2}}}(\omega_1 - \omega_2) + o(s-1). \end{aligned}$$

Take next

$$g(s) = 2\zeta(2s-1) \int_{-\infty}^{\infty} \frac{dx}{\phi(x, 1)^s}, \tag{2.6}$$

where

$$\sum_{1}^{\infty} \frac{2}{n^{2s-1}} = 2\zeta(2s-1) = \frac{1}{s-1} + 2\gamma + o(s-1).$$

The integral

$$J = \int_{-\infty}^{\infty} \frac{dx}{\phi(x, 1)^s} \tag{2.7}$$

is an analytic function of s near $s = 1$. When $I(\omega_1) > 0$, $I(\omega_2) > 0$ $R(s) > \frac{1}{2}$, the integral is seen to vanish on deforming the path of integration into an infinite semicircle below the real axis.

When $I(\omega_1) > 0$, $I(\omega_2) < 0$, we write

$$J = \int_{-\infty}^{\infty} \frac{dx}{\phi(x, 1)} - (s-1) \int_{-\infty}^{\infty} \frac{\log \phi(x, 1)}{\phi(x, 1)} dx + o(s-1).$$

Now

$$\int_{-\infty}^{\infty} \frac{dx}{\phi(x, 1)} = \frac{2\pi i a^{-1}}{\omega_1 - \omega_2}$$

$$\begin{aligned} \log \phi(x, 1) &= \log a + \log(x - \omega_1)(x - \omega_2) \\ &= \log a + \log(x - \omega_1) + \log(x - \omega_2). \end{aligned}$$

This holds for the principal values of the logarithms, if a is real, since for real values of x and ω_1, ω_2, with imaginary parts of opposite sign, $\arg(x-\omega_1)$ and $\arg(x-\omega_2)$ are of opposite sign.

Also

$$\int_{-\infty}^{\infty} \frac{\log(x-\omega_1)}{(x-\omega_1)(x-\omega_2)}\,dx = -\frac{2\pi i \log(\omega_2-\omega_1)}{\omega_2-\omega_1},$$

$$\int_{-\infty}^{\infty} \frac{\log(x-\omega_2)}{(x-\omega_1)(x-\omega_2)}\,dx = \frac{2\pi i \log(\omega_1-\omega_2)}{\omega_1-\omega_2},$$

and so

$$(\omega_1-\omega_2)\int_{-\infty}^{\infty} \frac{\log\phi(x,1)}{\phi(x,1)}\,dx = 2\pi i a^{-1}\log a + 2\pi i a^{-1}\log -(\omega_1-\omega_2)^2$$

$$= 2\pi i a^{-1}\log -a(\omega_1-\omega_2)^2 = 2\pi i a^{-1}\log\left(\frac{\Delta}{a}\right),$$

since $\omega_1-\omega_2 = i\Delta^{\frac{1}{2}}/a$. The equalities are again true for the principal logarithms since $\arg(\omega_2-\omega_1) < 0$, $\arg(\omega_1-\omega_2) > 0$. We can gather our results together, on noting that

$$2a^{-s}\zeta(2s) = \frac{\pi^2 a^{-1}}{3} + o(s-1),$$

and have in case I

$$f(s) = \frac{\pi^2 a^{-1}}{3} + \left(\frac{1}{s-1}+2\gamma\right)\left\{\frac{2\pi i a^{-1}}{\omega_1-\omega_2} - \frac{2\pi i a^{-1}\log(\Delta/a)}{\omega_1-\omega_2}(s-1)\right\}$$

$$+\frac{i\pi^2}{3\Delta^{\frac{1}{2}}}(\omega_1-\omega_2) - \frac{4\pi}{3\Delta^{\frac{1}{2}}}\log\{\theta_{11}'(0,\omega_1)\,\theta_{11}'(0,-\omega_2)\}$$

$$+\frac{8\pi}{3\Delta^{\frac{1}{2}}}\log 2\pi + o(s-1)$$

$$= \frac{2\pi}{(s-1)\Delta^{\frac{1}{2}}} + \frac{4\pi\gamma}{\Delta^{\frac{1}{2}}} + \frac{2\pi}{\Delta^{\frac{1}{2}}}\log\left(\frac{a}{\Delta}\right) + \frac{8\pi}{3\Delta^{\frac{1}{2}}}\log 2\pi$$

$$-\frac{4\pi}{3\Delta^{\frac{1}{2}}}\log\theta_{11}'(0,\omega_1)\,\theta_{11}'(0,-\omega_2) + o(s-1).$$

In case II the result is simpler, since $g(s) = 0$; whence

$$f(s) = -\frac{4\pi}{3\Delta^{\frac{1}{2}}}\log[\theta_{11}'(0,\omega_1)/\theta_{11}'(0,\omega_2)] + o(s-1).$$

I now prove that the only finite singularities of $f(s)$ are, in case I (as is well known) a simple pole at $s=1$, and in case II a simple pole at $s=\frac{1}{2}$.

First, J defined when $R(s) > \frac{1}{2}$ by (2.7) is really a meromorphic function of s existing over all the s plane. For J can be evaluated in finite terms by means of gamma functions on deforming the real axis of x into an infinite upper semicircle together with a cut from ω_1 to ∞ parallel to the real axis together with, in case II, a similar cut from ω_2 to ∞. Hence $\mathrm{J} = 0$ in case II as $\mathrm{J} = 0$ when $\mathrm{R}(s) > \frac{1}{2}$. We can, however, proceed as follows—

Write

$$\begin{aligned}(ax^2+bx+c)^{-s} &= \frac{f_0}{x^{2s}} + O\left(\frac{1}{x^{2s+1}}\right)\\ &= \frac{f_0}{x^{2s}} + \frac{f_1}{x^{2s+1}} + O\left(\frac{1}{x^{2s+2}}\right)\\ &= \frac{f_0}{x^{2s}} + \frac{f_1}{x^{2s+1}} + \frac{f_2}{x^{2s+2}} + O\left(\frac{1}{x^{2s+3}}\right), \text{ etc,}\end{aligned}$$

where $f_0 = a^{-s}$, $f_1 = -sba^{-s-1}, \ldots$, and if $|x| \geqslant \mathrm{N} = \mathrm{N}(a, b, c)$, say, these equations hold uniformly for bounded s, say $|s| < \mathrm{M}$. Write

$$\int_{-\infty}^{\infty} = \int_{-\infty}^{-\mathrm{N}} + \int_{-\mathrm{N}}^{\mathrm{N}} + \int_{\mathrm{N}}^{\infty}.$$

The middle integral represents an integral function of s. The end integrals, on taking the successive approximations to $\phi(x, 1)^s$, are seen to be analytic functions of s for $\sigma > \frac{1}{2}, 0, -\frac{1}{2}, \ldots$, successively, with possibly simple poles at $s = \frac{1}{2}, 0, -\frac{1}{2}, -\frac{3}{2}, \ldots$. However $s = 0$ cannot be a pole because of the value of f_1. The term f_3 will contain a factor $s + 1$, as is clear on putting $s = -1$ in the expansion. Hence $s = -1$, and so also $s = -2, -3, \ldots$, are not poles of the integral.

The zeta function $\zeta(2s-1)$ has a simple pole at $s = 1$ and simple zeros at $-\frac{1}{2}, -\frac{3}{2}, -\frac{5}{2}, \ldots$. Hence from (2.5), $g(s)$ has at most simple poles at $s = 1$ and at $s = +\frac{1}{2}$, with residues, in case I,

$$\int_{-\infty}^{\infty} \frac{dx}{\phi(x, 1)} \quad \text{and} \quad (\tfrac{1}{2}a^{-\frac{1}{2}} + \tfrac{1}{2}a^{-\frac{1}{2}})\, 2\zeta(0) = -a^{-\frac{1}{2}} \text{ respectively.}$$

In (2.4) we note that $2a^{-s}\zeta(2s)$ has a simple pole at $s = \frac{1}{2}$ with residue $a^{-\frac{1}{2}}$; hence, in case I, $s = \frac{1}{2}$ is not a pole of $f(s)$, while in case II, as $g(s) = 0$, $s = \frac{1}{2}$ is a simple pole with residue $a^{-\frac{1}{2}}$.

The formula in case II for the expansion near the pole $s = \frac{1}{2}$ may be obtained as follows; put $s = \frac{1}{2} + \rho$ and suppose that a is real and positive; then by (2.4)

$$\begin{aligned}f(s) = 2a^{-\frac{1}{2}-\rho}\zeta(1+2\rho) + 2\zeta(2\rho)\int_{-\infty}^{\infty} \frac{dx}{(ax^2+bx+c)^{\frac{1}{2}+\rho}}&\\ + 2\sum_{n=1}^{\infty}\ \sum_{m=-\infty}^{\infty}{}' \frac{1}{n^{2\rho}} \int_{-\infty}^{\infty} \frac{e^{2mn\pi ix}}{(ax^2+bx+c)^{\frac{1}{2}+\rho}}\, dx.&\end{aligned}$$

We have just seen that the middle term vanishes identically and that the double series is an integral function of ρ. The terms given by $m < 0$ vanish on deforming the path of integration into the lower half of an infinite circle. Since

$$a^{-\frac{1}{2}-\rho} = a^{-\frac{1}{2}}(1 - \rho \log a \ldots), \quad \zeta(1 + 2\rho) = \frac{1}{2\rho} + \gamma + \cdots$$

$$f(s) = \frac{a^{-\frac{1}{2}}}{\rho} + a^{-\frac{1}{2}}(2\gamma - \log a) + 2 \sum_{n=1}^{\infty} \sum_{m=-\infty}^{\infty}{}' \int_{-\infty}^{\infty} \frac{e^{2mn\pi i x}}{(ax^2 + bx + c)^{\frac{1}{2}}}\, dx + o(\rho).$$

Choose the notation for ω_1, ω_2 so that $|\arg(\omega_1 - \omega_2)| \leqslant \frac{1}{2}\pi$ and deform the path of integration into the upper half of an infinite circle together with a loop enclosing ω_1 and ω_2 both in the positive direction. Then

$$\int_{-\infty}^{\infty} \frac{e^{2mn\pi i x}}{(ax^2 + bx + c)^{\frac{1}{2}}}\, dx = \int^{\omega_2+,\,\omega_1+} = 2\int_{\omega_1}^{\omega_2} \frac{e^{2mn\pi i x}}{a^{\frac{1}{2}}[(x - \omega_1)(x - \omega_2)]^{\frac{1}{2}}}\, dx.$$

Put $x = \omega_1 + (\omega_2 - \omega_1)v$ where $0 \leqslant v \leqslant 1$, then

$$a^{\frac{1}{2}}[(x - \omega_1)(x - \omega_2)]^{\frac{1}{2}} = ia^{\frac{1}{2}}(\omega_2 - \omega_1)v^{\frac{1}{2}}(1 - v)^{\frac{1}{2}},$$

since the arguments of both sides lie between 0 and π. Hence

$$\int_{-\infty}^{\infty} \frac{e^{2mn\pi i x}}{(ax^2 + bx + c)^{\frac{1}{2}}}\, dx = \frac{2}{ia^{\frac{1}{2}}} \int_0^1 \frac{e^{2mn\pi i(\omega_1 + \overline{\omega_2 - \omega_1}v)}}{v^{\frac{1}{2}}(1 - v)^{\frac{1}{2}}}\, dv.$$

The right-hand side becomes on putting $v = \cos^2 \frac{1}{2}\theta$

$$\frac{2}{ia^{\frac{1}{2}}} \int_0^{\pi} e^{mn\pi i(\omega_1 + \omega_2) + mn\pi i(\omega_2 - \omega_1)\cos\theta}\, d\theta = \frac{2\pi}{ia^{\frac{1}{2}}} e^{mn\pi i(\omega_1 + \omega_2)} J_0[mn\pi(\omega_2 - \omega_1)]$$
$$= \frac{2\pi}{ia^{\frac{1}{2}}} e^{-\frac{mn\pi i b}{a}} J_0\left(\frac{mn\pi\Delta^{\frac{1}{2}}}{a}\right),$$

where J_0 is the usual Bessel function and so

$$f(s) = \frac{a^{-\frac{1}{2}}}{s - \frac{1}{2}} + a^{-\frac{1}{2}}(2\gamma - \log a)$$
$$- 2\pi i a^{-\frac{1}{2}} \sum_{n=1}^{\infty} \sum_{m=1}^{\infty} e^{-\frac{mn\pi i b}{a}} J_0\left(\frac{mn\pi\Delta^{\frac{1}{2}}}{a}\right) + o(s - \tfrac{1}{2}).$$

The double series converges absolutely, for

$$e^{mn\pi i(\omega_1 - \omega_2)} J_0[mn\pi(\omega_2 - \omega_1)] = O[e^{mn\pi i(\omega_1 + \omega_2) \pm mn\pi i(\omega_2 - \omega_1)}] = O(e^{-mnA}),$$
$$A > 0,$$

since $I(\omega_1) > 0$, $I(\omega_2) > 0$. Hence

$$f(s) = \frac{a^{-\frac{1}{2}}}{s - \frac{1}{2}} + a^{-\frac{1}{2}}(2\gamma - \log a)$$
$$- 2\pi i a^{-\frac{1}{2}} \sum_{n=1}^{\infty} d(n)\, e^{-n\pi i\frac{b}{a}} J_0\left(\frac{n\pi\Delta^{\frac{1}{2}}}{a}\right) + o(s - \tfrac{1}{2}) \qquad (2.6)$$

where $d(n)$ is the number of divisors of n. The condition

$$|\arg(\omega_2 - \omega_1)| \leqslant \tfrac{1}{2}\pi$$

is not necessary in (2.6).

§ 3. The corresponding results when the form $\phi(m, n)$ is replaced by the more general one

$$\chi(x, y) = ax^r + bx^{r-1}y + \ldots + ky^r = y^r\chi(x/y),$$

where $\chi(v) = 0$ has no real roots, follow easily in the same way.

Put now

$$h(s) = \sum_{n=1}^{\infty} \sum_{m=-\infty}^{\infty} \chi(m, n)^{-s},$$

so that the series converges absolutely when $\sigma > 2/r$. Then as in § 2, Poisson's summation formula gives

$$h(s) = \sum_{n=1}^{\infty} \frac{1}{n^{rs-1}} \int_{-\infty}^{\infty} \frac{dv}{\chi(v)^s} + \sum_{n=1}^{\infty} \sum_{m=-\infty}^{\infty}{}' \frac{1}{n^{rs-1}} \int_{-\infty}^{\infty} \frac{e^{2mn\pi iv}}{\chi(v)^s}\, dv.$$

The last doubly infinite series is seen to represent an integral function of s on integrating by parts as before. So

$$\int_{-\infty}^{\infty} \frac{dv}{\chi(v)^s}$$

is a meromorphic function of s whose only singularities are possibly simple poles at $s = 1/r, 0, -1/r, -2/r, -3/r, \ldots$, among which $s = 0, -1, -2 \ldots$, need not be included owing to the presence of factors $s, s+1, s+2, \ldots$, in the coefficients of v^{-rs-1}, $v^{-rs-s-1}$, $v^{-rs-2s-1}, \ldots$, respectively in the expansion of $\chi(v)^{-s}$ in descending powers of v. Also

$$\sum_{n=1}^{\infty} n^{1-rs} = \zeta(rs-1)$$

has a simple pole at $s = 2/r$ and simple zeros at $s = -1/r, -3/r, -5/r, \ldots$. Hence finally $h(s)$ is analytic throughout the finite part of the s plane except possibly for simple poles at $s = 2/r, 1/r, -2/r, -4/r, -6/r, \ldots$, excluding those values which are negative integers.

If the summation for n in $h(s)$ had been from $n = -\infty$ to ∞, excluding $m = n = 0$, the part $\sum_{m=-\infty}^{\infty} (am^r)^{-s}$ would introduce a pole at $s = 1/r$, already included.

It need hardly be remarked that the condition that $\chi(v)$ is a polynomial in

v is not essential for the application of Poisson's formula to the discussion of the function $h(s)$. The results will then depend upon the conditions imposed on $\chi(v)$.

§ 4. The case when $\phi(x, y)$ is replaced by a quadratic form in any number of variables is sufficiently illustrated by the ternary quadratic when we take

$$\phi(x, y, z) = ax^2 + by^2 + cz^2 + 2fgy + 2gzx + 2hxy,$$

where the constants $a, b, \ldots, f, g, \ldots$, are such that $x = y = z = 0$ are the only real values of x, y, z for which $\phi(x, y, z) = 0$. We write

$$f(s) = \Sigma' f(l, m, n)^{-s}, \tag{4.1}$$

the summation extending to all integer values of l, m, n, excluding

$$l = m = n = 0,$$

so that the series converges if $\sigma > \frac{3}{2}$. Put

$$\begin{aligned} f(s) &= \sum_{m,n=-\infty}^{\infty}{}' (bm^2 + cn^2 + 2fmn)^{-s} + 2 \sum_{l=1}^{\infty} \sum_{m,n=-\infty}^{\infty}{}' \phi(l, m, n)^{-s} \qquad (4.2) \\ &= f_1(s) + 2f_2(s). \end{aligned}$$

The term $f_1(s)$ represents a function of s analytic throughout the finite part of the s plane except for a simple pole at $s = 1$ or $s = \frac{1}{2}$. The last summation for m, n is transformed by Poisson's summation formula in two dimensions, namely

$$\sum_{-\infty}^{\infty} \sum_{-\infty}^{\infty} \mathrm{F}(m, n) = \sum_{-\infty}^{\infty} \sum_{-\infty}^{\infty} \int_{-\infty}^{\infty} \int_{-\infty}^{\infty} e^{2m\pi ix + 2n\pi iy}\, \mathrm{F}(x, y)\, dx\, dy.$$

I have given a proof* by integration by parts when

$$\frac{\partial^{a+b} \mathrm{F}(x, y)}{\partial x^a\, \partial y^b}, \quad a, b = 0, 1, 2,$$

excluding $a = b = 2$ are all continuous functions of x and y which tend to zero when either variable tends to $\pm\infty$, and

$$\int_{-\infty}^{\infty} \int_{-\infty}^{\infty} \left\{ |\mathrm{F}| + \left| \frac{\partial^2 \mathrm{F}}{\partial x^2} \right| + \left| \frac{\partial^2 \mathrm{F}}{\partial y^2} \right| + \left| \frac{\partial^4 \mathrm{F}}{\partial^2 x\, \partial^2 y} \right| \right\} dx\, dy$$

converges.

Hence

$$f_2(s) = \sum_{l=1}^{\infty} \sum_{m,n=-\infty}^{\infty} \int_{-\infty}^{\infty} \int_{-\infty}^{\infty} \frac{e^{2\pi i(my + nz)}\, dy\, dz}{\phi(l, y, z)^s}.$$

---

* Mordell, 'Proc. Camb. Phil. Soc.,' vol. 25 (1929), *not yet published*.

Put ly, lz for y and z and write separately the term with $m = n = 0$. Then

$$f_2(s) = \sum_{l=1}^{\infty} \frac{1}{l^{2s-2}} \int_{-\infty}^{\infty} \int_{-\infty}^{\infty} \frac{dy\, dz}{\phi(1, y, z)^s}$$
$$+ \sum_{l=1}^{\infty} \sum_{m,n=-\infty}^{\infty}{}' \frac{1}{l^{2s-2}} \int_{-\infty}^{\infty} \int_{-\infty}^{\infty} \frac{e^{2\pi i l(my+nz)}\, dy\, dz}{\phi(1, y, z)^s}.$$

The last part as in § 2 is clearly an integral function of s since integration by parts twice for either y or z introduces a factor l^2m^2 or l^2n^2 in the denominator, so that if $n = 0$ say, we need only integrate twice by parts for y.

The corresponding result for the homogeneous quadratic form $\phi(x_1, x_2, \dots x_\nu)$ of ν variables can be written as

$$\sum_{m_1 \dots m_\nu = -\infty}^{\infty}{}' \phi(m_1, m_2, \dots, m_\nu)^{-s} = \sum_{m_1, m_2 \dots m_{\nu-1} = -\infty}^{\infty}{}' \phi(m_1, m_2 \dots m_{\nu-1}, 0)^{-s}$$
$$+ \sum_{m_\nu = 1}^{\infty} \frac{2}{m_\nu^{2s-\nu+1}} \int_{-\infty}^{\infty} \int_{-\infty}^{\infty} \dots \frac{dx_1\, dx_2 \dots dx_{\nu-1}}{\phi(x_1, x_2 \dots x_{\nu-1}, 1)^s}$$
$$+ \sum_{m_\nu = 1}^{\infty} \sum_{m_1 \dots m_{\nu-1} = -\infty}^{\infty}{}' \frac{2}{m_\nu^{2s-\nu+1}} \int_{-\infty}^{\infty} \int_{-\infty}^{\infty} \dots \frac{e^{2\pi i m_\nu (m_1x_1 + m_2x_2 + \dots m_{\nu-1}x_{\nu-1})}\, dx_1\, dx_2 \dots dx_{\nu-1}}{\phi(x_1, x_2 \dots x_{\nu-1}, 1)^s}.$$

§ 5. The integrals occurring when the quadratic form is taken with ν variables will now be evaluated. Suppose first that the form is a positive definite one with real coefficients.

Put

$$\mathrm{I}_{\nu, s} = \int_{-\infty}^{\infty} \int_{-\infty}^{\infty} \int_{-\infty}^{\infty} \dots \frac{e^{2\pi i (m_1x_1 + \dots + m_{\nu-1}x_{\nu-1})}\, dx_1\, dx_2 \dots dx_{\nu-1}}{\phi(x_1, x_2, \dots, x_{\nu-1}, 1)^s} \tag{5.1}$$

so that § 4 deals with the case $\nu = 3$. It is proved that

$$\mathrm{I}_{\nu, \frac{1}{2}\nu} = \frac{\pi^{\frac{1}{2}\nu}}{|\Delta_\nu|^{\frac{1}{2}}\, \Gamma(\nu/2)}\, e^{-2\pi i \mathrm{R}},$$

where R is the root x_ν, taken with a negative imaginary part, of the equation $\Phi(x_1, x_2, \dots, x_{\nu-1}, x_\nu) = 0$, where Φ is the form adjoint to

$$\phi(x_1, x_2, \dots x_{\nu-1}, x_\nu);$$

that is

$$\phi(x_1, x_2, \dots, x_\nu) = \sum_{\mu=1}^{\nu} \sum_{\lambda=1}^{\nu} a_{\lambda\mu} x_\lambda x_\mu, \quad \Phi(x_1, x_2, \dots, x_\nu) = \sum_{\mu=1}^{\nu} \sum_{\lambda=1}^{\nu} \mathrm{A}_{\lambda\mu} x_\lambda x_\mu,$$

where $\mathrm{A}_{\lambda\mu}$ are the first minors in

$$\Delta_\nu = \begin{vmatrix} a_{11} & . & . & . & . & a_{1\nu} \\ . & . & . & . & . & . \\ . & . & . & . & . & . \\ a_{\nu 1} & . & . & . & . & a_{\nu\nu} \end{vmatrix}.$$

For apply a real linear transformation

$$x_1 = c_{11}y_1 + \dots + c_{1\,\nu-1}y_{\nu-1} + c_{1\,\nu},$$
$$\cdot\quad\cdot\quad\cdot\quad\cdot\quad\cdot\quad\cdot\quad\cdot\quad\cdot\quad\cdot\quad\cdot\quad\cdot\quad\cdot\quad\cdot\quad\cdot$$
$$\cdot\quad\cdot\quad\cdot\quad\cdot\quad\cdot\quad\cdot\quad\cdot\quad\cdot\quad\cdot\quad\cdot\quad\cdot\quad\cdot\quad\cdot\quad\cdot$$
$$x_{\nu-1} = c_{\nu-1\,1}\,y_1 + \dots + c_{\nu-1\,\nu-1}\,y_{\nu-1} + c_{\nu-1\,\nu},$$

which is such that

$$\phi(x_1, x_2, \dots, x_{\nu-1}, 1) = k(y_1^2 + y_2^2 + \dots + y^2_{\nu-1} + 1).$$

The set of values $c_{1\nu}, \dots, c_{\nu-1\,\nu}$, are the co-ordinates of the *centre* of the hyperquadric $\phi(x_1, x_2, \dots, x_{\nu-1}, 1) = 0$, and are given by

$$a_{\lambda 1}c_{1\nu} + a_{\lambda 2}c_{2\nu} + \dots + a_{\lambda\,\nu-1}c_{\nu-1\,\nu} + a_{\lambda\nu} = 0, \quad \lambda = 1, 2, \dots, \nu - 1.$$

Multiply by $c_{\lambda\nu}$ and add together the equations. Since

$$k = \phi(c_{1\nu}, c_{2\nu}, \dots, c_{\nu-1\,\nu}, 1),$$

we have

$$a_{\nu 1}c_{1\nu} + a_{\nu 2}c_{2\nu} + \dots + a_{\nu\,\nu-1}c_{\nu-1\,\nu} + a_{\nu\nu} - k = 0.$$

Eliminate the c's, whence $k\Delta_{\nu-1} = \Delta_\nu$, where $\Delta_{\nu-1}$ is the co-factor of $a_{\nu\nu}$ in Δ_ν.

The determinant $|c_{rs}|$ of the linear transformation is given by

$$\Delta_{\nu-1}|c_{rs}|^2 = k^{\nu-1}.$$

Hence

$$\mathrm{I}_{\nu,s} = \frac{1}{|\Delta_\nu|^{\frac12}k^{s-\nu/2}} = \int_{-\infty}^{\infty}\int_{-\infty}^{\infty}\int_{-\infty}^{\infty}\dots\frac{e^{2\pi i(\rho_1 y_1 + \rho_2 y_2 + \dots + \rho_{\nu-1}y_{\nu-1} + \rho_\nu)}\,dy_1\,dy_2, \dots, dy_{\nu-1}}{(y_1^2 + y_2^2 + \dots + y_{\nu-1}^2 + 1)^s},$$

where

$$m_1x_1 + \dots + m_{\nu-1}x_{\nu-1} = \rho_1y_1 + \rho_2y_2 + \dots + \rho_{\nu-1}y_{\nu-1} + \rho_\nu.$$

Since

$$\Gamma(s) = \xi^s\int_0^\infty e^{-t\xi}t^{s-1}\,dt \qquad \text{for } \xi > 0,$$

we can put

$$\mathrm{I}_{\nu,s}\Gamma(s)\Delta_\nu^{\frac12}k^{s-\nu/2}$$
$$= \int_0^\infty\int_{-\infty}^{\infty}\int_{-\infty}^{\infty}\dots e^{2\pi i(\rho_1y_1 + \dots + \rho_{\nu-1}y_{\nu-1} + \rho_\nu) - t(y_1^2 + \dots + y_{\nu-1}^2 + 1)}\,t^{s-1}\,dt\,dy_1, \dots, dy_{\nu-1}.$$

The justification is easy since the multiple integral converges absolutely when $\mathrm{R}(s) > \frac12(\nu - 1)$.

But

$$\int_{-\infty}^{\infty} e^{2\pi i\rho y - ty^2}\,dy = \pi^{\frac12}t^{-\frac12}e^{-\pi^2\rho^2/t},$$

where $t^{-\frac{1}{2}} > 0$, and so

$$\mathrm{I}_{\nu,s}\Gamma(s)\,\Delta_\nu^{\frac{1}{2}}\,k^{s-\nu/2} = \pi^{(\nu-1)/2}\int_0^\infty e^{2\pi i\rho_\nu - t - \pi^2(\rho_1^2 + \dots + \rho_{\nu-1}^2)/t}\,t^{s-(\nu+1)/2}\,dt$$

$$= 2\pi^{(\nu-1)/2}\,e^{2\pi i\rho_\nu}\int_0^\infty e^{-t^2 - \pi^2(\rho_1^2 + \dots + \rho_{\nu-1}^2)/t^2}\,t^{2s-\nu}\,dt.$$

This expresses $\mathrm{I}_{\nu,s}$ as a simple integral which can be evaluated in finite terms when $\nu = 2s$, since

$$\int_0^\infty e^{-t^2 - a^2/t^2}\,dt = \tfrac{1}{2}\pi^{\frac{1}{2}}e^{-2|a|}$$

if a is real. Hence

$$\mathrm{I}_{\nu,\nu/2}\Gamma(\nu/2)\,|\Delta_\nu|^{\frac{1}{2}} = \pi^{\nu/2}e^{2\pi i\rho_\nu - 2\pi(\rho_1^2 + \dots + \rho_{\nu-1}^2)^{\frac{1}{2}}}$$

or

$$\mathrm{I}_{\nu,\nu/2} = \frac{\pi^{\nu/2}}{|\Delta_\nu|^{\frac{1}{2}}\,\Gamma(\nu/2)}\,e^{-2\pi i\mathrm{R}},$$

say, where R must now be interpreted in terms of the general quadratic form. Note that

$$\phi(x_1, x_2, \dots, x_{\nu-1}, 1) = k(y_1^2 + y_2^2 + \dots + y_{\nu-1}^2 + 1),$$

$$m_1x_1 + \dots + m_{\nu-1}x_{\nu-1} + m_\nu = \rho_1y_1 + \dots + \rho_{\nu-1}y_{\nu-1} + \rho_\nu + m_\nu,$$

where m_ν is arbitrary. Express the condition of *tangency*, *i.e.*, that the contravariant of the linear form should vanish. The y forms give

$$\rho_1^2 + \dots + \rho_{\nu-1}^2 + (\rho_\nu + m_\nu)^2 = 0,$$

and we can take $m_\nu = -\rho_\nu - i(\rho_1^2 + \dots + \rho_{\nu-1}^2)^{\frac{1}{2}} = \mathrm{R}$. The x forms then give the value of R as in the enunciation of the theorem.

We also require the expansion of $\mathrm{I}_{\nu,s}$ in powers of $\lambda = s - \nu/2$ when $m_1 = m_2 = \dots = m_{\nu-1} = 0$. But now

$$\mathrm{I}_{\nu,s}\Gamma(s)\,|\Delta_\nu|^{\frac{1}{2}}\,k^{s-\nu/2} = 2\pi^{(\nu-1)/2}\int_0^\infty e^{-t^2}t^{2s-\nu}\,dt$$

$$= \pi^{(\nu-1)/2}\Gamma(s - \overline{\nu - 1}/2).$$

Hence

$$\mathrm{I}_{\nu,s} = \frac{\pi^{(\nu-1)/2}}{|\Delta_\nu|^{\frac{1}{2}}}\,\frac{\Gamma(\frac{1}{2} + \lambda)}{\Gamma\left(\frac{\nu}{2} + \lambda\right)}\,k^{-\zeta}$$

$$= \frac{\pi^{(\nu-1)/2}}{|\Delta_\nu|^{\frac{1}{2}}}\,\frac{\Gamma(\frac{1}{2})}{\Gamma(\nu/2)}\left\{1 + \lambda\frac{\Gamma'(\frac{1}{2})}{\Gamma(\frac{1}{2})} - \lambda\frac{\Gamma'(\nu/2)}{\Gamma(\nu/2)} - \lambda\log k\right\} + \dots,$$

and as $\zeta(2s - \nu + 1) = \dfrac{1}{2\lambda} + \gamma + \dots$

$$\mathrm{I}_{\nu,s}\zeta(2s-\nu+1) = \frac{\pi^{(\nu-1)/2}}{2\,|\Delta_\nu|^{\frac{1}{2}}}\,\frac{\Gamma(\frac{1}{2})}{\Gamma(\nu/2)}\left\{\frac{1}{\lambda} + \frac{\Gamma'(\frac{1}{2})}{F(\frac{1}{2})} - \frac{\Gamma'(\nu/2)}{\Gamma(\nu/2)} - \log k + 2\gamma\right\} + \dots.$$

We have hence for the expansion in powers of $s - \nu/2$,

$$\begin{aligned}f_{\nu-1}(s) = {} & \frac{\pi^{(\nu-1)/2}\Gamma(\frac{1}{2})}{|\Delta_\nu|^{\frac{1}{2}}\Gamma(\nu/2)}\frac{1}{s-\nu/2} \\ & + \frac{\pi^{(\nu-1)/2}\Gamma(\frac{1}{2})}{|\Delta_\nu|^{\frac{1}{2}}\Gamma(\nu/2)}\left\{\frac{\Gamma'(\frac{1}{2})}{\Gamma(\frac{1}{2})} - \frac{\Gamma'(\nu/2)}{\Gamma(\nu/2)} - \log\left(\frac{\Delta_\nu}{\Delta_{\nu-1}}\right) + 2\gamma\right\} \\ & + \frac{2\pi^{\nu/2}}{|\Delta_\nu|^{\frac{1}{2}}\Gamma(\nu/2)}\sum_{m=1}^{\infty}\sum_{m_1, m_2 \dots m_{\nu-1}=-\infty}^{\infty}\frac{1}{m}e^{-2\pi i m \mathrm{R}} \\ & + \sum_{m_1, m_2 \dots m_{\nu-1}=-\infty}^{\infty}{}' \phi(m_1, m_2 \dots m_{\nu-1}, 0)^{-\nu/2} + O(s-\nu/2), \quad (5.2)\end{aligned}$$

where R is the root with negative imaginary part of the equation

$$\Phi(m_1, m_2 \dots m_{\nu-1}, \mathrm{R}) = 0$$

where Φ is the form adjoint to $\phi(m_1, m_2 \dots m_{\nu-1}, m_\nu)$.

The summation for m gives $-\log(1 - e^{-2\pi i \mathrm{R}})$ and with this form (5.2) is practically Epstein's result.

In the general case, the result may be expected to take several forms in analogy with (1.2), (1.3). The evaluations of the integrals are still valid if the coefficients of ϕ are such that the real part of ϕ is a positive definite form. For near their real value in (5.1), $\mathrm{I}_{\nu, s}$ is an analytic function of the coefficients. The result (5.2) will still hold provided $|\Delta_\nu|^{\frac{1}{2}}$ is taken with a positive real part and $\log(\Delta_\nu/\Delta_{\nu-1})$ has its principal value.

The Kinetics of the Oxidation of Ethylene.

By H. W. THOMPSON and C. N. HINSHELWOOD, F.R.S.

(Received July 2, 1929.)

Introduction.

The idea of chain reactions has long been familiar in connection with photochemical changes, but experimental evidence that thermal changes sometimes occur by a chain mechanism has only recently been forthcoming. In chain reactions the first transformation yields a product endowed with excess of energy which initiates a further change, the cycle being repeated until the chain is broken by the destruction or deactivation of the active intermediate product in some secondary process. The conditions are particularly favourable to the operation of this chain mechanism in highly exothermic gaseous reactions.

Under certain circumstances, when enough energy is available, and possibly other more specific conditions are satisfied, each elementary reaction may induce more than one new reaction.* Thus the number of active centres present at any moment tends to increase, and would increase indefinitely unless the rate of deactivating processes, such as molecular collisions, or adsorption by the walls of the vessel, balanced the rate of production. If the number of fresh chains starting in unit time is greater than the number which can be broken, then explosion results; if, on the other hand, the two rates become equal, then a stationary state is established and the reaction proceeds with a measurable velocity depending on the length of the chains. The balance between the rate of production of fresh centres and the rate of deactivation depends upon the concentration. Thus there will be a quite definite pressure at which one rate begins to preponderate over the other. No matter how slow the reaction, if the first rate exceeds the second, the condition of the gas is unstable and explosion takes place after a certain lapse of time during which the chains develop. This time may be insensibly small, since many million molecular collisions occur in a second. Thus there is the appearance of a quite abrupt transition, at a definite concentration, from negligible reaction to explosion.

But any exothermic reaction, whether depending on a chain mechanism or not, becomes explosive when its velocity is so great that the temperature of the whole system rises. While, therefore, an abrupt transition is a characteristic criterion of a reaction involving "branching" chains, when the transition is gradual, and a purely "thermal" explosion terminates a region where rate increases steadily with concentration, other tests must be applied to determine whether or not the measurable reaction involves stable chains.

---

* Christiansen and Kramers, 'Z. Phys. Chem.,' vol. 104, p. 451 (1923); Semenoff, 'Z. Physik,' vol. 46, p. 109 (1927), and vol. 48, p. 571 (1928).

In photochemical reactions the well-known tests are examination of the number of molecules transformed for each quantum, and investigation of the sensitiveness of the reactions to inhibitors. In thermal reactions, retardation of the transformation by increased surface of the containing vessel, acceleration by inert gases which hinder the active centres from reaching the walls, and an abnormally great influence of pressure or temperature on the reaction rate all reveal the operation of a chain mechanism.

In the reaction between hydrogen and oxygen* at temperatures between 500° and 600° C. both unstable, explosive chains and stable chains appear to play a part. The former are recognised by the existence of sharp explosion limits which occur at certain concentrations, the latter by the remarkable influence on the reaction velocity in other regions of concentration of the various factors enumerated above.

It appeared of interest, therefore, to make a similar investigation of some other exothermic reaction, and for the purpose the interaction of oxygen and ethylene was chosen.

Method of Experiment.

Ethylene was prepared by allowing alcohol to drop into syrupy phosphoric acid kept at 220° C. It was found necessary to heat the acid to 230° before use, and to keep the temperature high during the preparation; otherwise troublesome amounts of ether are formed. After passage over glass wool soaked in concentrated caustic potash and over phosphorus pentoxide, the ethylene was condensed in a vessel surrounded by liquid air. One half was then distilled into a second vessel also kept in liquid air. After thorough evacuation of the apparatus, about one half of the second condensate was allowed to evaporate into a gas holder containing mercury. This thorough fractionation was carried out for safety, but as a matter of fact the second condensate appeared to be nearly pure ethylene, and evaporated completely without leaving any residue of ether. Oxygen was prepared from potassium permanganate and purified in the usual way in an all glass, previously evacuated apparatus.

---

* 'Roy. Soc. Proc.,' A, vol. 118, p. 170 (1928); vol. 119, p. 591 (1928); vol. 122, p. 610 (1929), and vol. 124, p. 219 (1929).

The experimental method of measuring the reaction velocity was the same as that described in previous papers.* Gas analyses were made in a " Bone and Wheeler " apparatus.

The Course of the Reaction.

The course of the oxidation of ethylene has been fully worked out by Bone and Wheeler,† who showed that all the varied relationships between the possible products can be adequately explained if the following series of changes is assumed :—

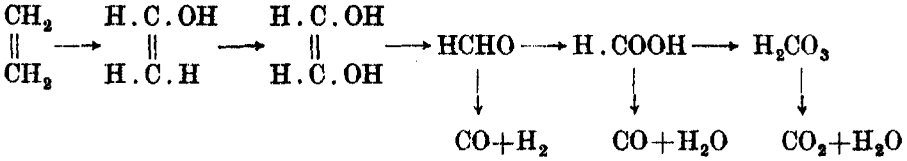

$$\begin{array}{ccccccccccc} CH_2 & & H.C.OH & & H.C.OH & & & & & & \\ \| & \longrightarrow & \| & \longrightarrow & \| & \longrightarrow & HCHO & \longrightarrow & H.COOH & \longrightarrow & H_2CO_3 \\ CH_2 & & H.C.H & & H.C.OH & & \downarrow & & \downarrow & & \downarrow \\ & & & & & & CO+H_2 & & CO+H_2O & & CO_2+H_2O \end{array}$$

The rates of oxidation and decomposition of a given intermediate product vary relatively to one another according to circumstances. Bone and Wheeler found, for example, that at the high temperature of the explosion the formaldehyde is decomposed more rapidly than it is oxidised, so that the reaction $C_2H_4 + O_2 = 2CO + 2H_2$ may take place almost quantitatively, while in the slow combustion at about 300° C. further oxidation of the formaldehyde occurs much more readily than the decomposition. Care must therefore be taken in investigating the kinetics of the oxidation to determine which reactions predominate under the particular experimental conditions.

The velocity was found to be conveniently measurable in vessels of silica or porcelain between 400° and 500° C., that is, about 100° lower than the union of hydrogen and oxygen. Whether the ratio of ethylene to oxygen was 1 : 1 or 1 : 2 the products of oxidation were preponderatingly those formed by the decomposition of formic acid, *i.e.*, the net result of the oxidation was $C_2H_4 + 2O_2 = 2CO + 2H_2O$. Some oxidation to carbonic acid took place, and in addition some formation of saturated hydrocarbon (see Table I) produced by a secondary decomposition. No trace of formaldehyde could be detected by Schryver's test at any stage of the reaction, which agrees with Bone's result‡ that formaldehyde decomposes almost instantaneously above 400° C.

The most convenient method of observing the progress of a reaction is to make continuous observations of the change of pressure. In a complex reaction like the oxidation of ethylene it is necessary to consider very carefully what relation the rate of pressure increase bears to the rate of disappearance of the primary reacting substances. In principle the two rates need not correspond, but it may in practice be possible to find a set of conditions under which one serves at least as an approximate measure of the other. The reaction $C_2H_4 + 2O_2 = 2CO + 2H_2O$ gives when complete an increase of pressure of one-third, but the reaction $C_2H_4 + 3O_2 = 2CO_2 + 2H_2O$ gives no increase. Thus with different proportions of the two gases the " end-point " of the reaction might be expected to vary considerably. It was found by trial that when the ratio was $C_2H_4 : 2O_2$ the pressure increase was 58 per cent. of that required for oxidation to carbon monoxide and steam, and when the ratio was $C_2H_4 : O_2$ or even $C_2H_4 : 3O_2$ the increase was almost exactly the same. Thus the relative proportions of oxygen and ethylene can be varied in this range without affecting the " end-point." For larger or smaller proportions of oxygen the end-point changes (Table II). Thus in experiments on the rate of reaction only the three ratios mentioned were used.

---

* 'J. Chem. Soc.,' vol. 125, p. 393 (1924); 'Roy. Soc. Proc.,' A, vol. 111, p. 245 (1926), vol. 118, p. 170 (1928).

† 'J. Chem. Soc.,' vol. 85, p. 1637 (1904).

‡ 'J. Chem. Soc.,' vol. 87, p. 910 (1905).

The total pressure increase for a ratio $C_2H_4 : 2O_2$ was found to be nearly proportional to the initial pressure. Thus the total pressure can be varied over a considerable range without affecting the course of the reaction very much (Table II).

For investigating the effect of such factors as temperature or initial total pressure on the rate of reaction it is desirable so to arrange matters that the proportions of the two reacting gases change as little as possible during an experiment. Since the preponderating reaction is $C_2H_4 + 2O_2 = 2CO + 2H_2O$, and since the initial interaction of ethylene with one molecule of oxygen probably determines the rate, the second molecule of oxygen being used up with much greater rapidity, a mixture of two volumes of oxygen and one of ethylene seemed the most suitable one to work with. Table I shows that with this proportion the oxygen and ethylene are in fact both used up together, there being little excess of one or other when the reaction is complete. Furthermore, the rate of increase of pressure for this mixture is a fairly good measure of the actual rate of disappearance of the ethylene. For example, in one experiment the products were withdrawn from the reaction vessel where the pressure had increased by half the amount corresponding to the " end-point." Analysis showed 16·4 parts of C_2H_4 to 5·8 CO_2, 30·2 CO and 4·5 CH_4. This must have come from $16 \cdot 4 + \frac{1}{2}(5 \cdot 8 + 30 \cdot 2 + 4 \cdot 5) = 36 \cdot 7$ parts of ethylene, half of which amounts to 18·3, compared with the 16·4 actually found. But there is not complete correspondence at every stage ; nor could this be expected.

The curve representing the increase of pressure plotted against time has the form characteristic of an autocatalytic reaction, a certain period of induction being evident, during which the rate of increase is abnormally small. This is quite probably due to the fact that at first oxygenated products are formed from the ethylene which do not give the full increase of pressure corresponding to the completed reaction. The induction is not, however, very marked.

Table I.

Analyses of Products of Reaction of Mixtures $C_2H_4 : 2O_2$.

—	200 mm. C_2H_4, 400 mm. O_2 at 402° C.	200 mm. C_2H_4, 400 mm. O_2 at 404° C.	100 mm. C_2H_4, 200 mm. O_2 at 409° C.	100 mm. C_2H_4, 200 mm. O_2 at 450° C. Reaction not quite completed.	100 mm. C_2H_4, 200 mm. O_2 at 450° C. Reaction not quite completed.
	per cent.	per cent.	per cent.	per cent.	per cent.
CO_2	19·6	19·2	18·6	16·95	16·4
O_2	2·9	1·7	2·0	12·65	12·55
C_2H_4	1·0	3·0	1·0	12·95	12·2
CO	66·1	64·4	59·6	49·2	43·7
Residue	10·3	11·7	18·8	8·3	15·2
Ratio CO/CO_2	3·37	3·34	3·22	2·90	2·67

	Analyses of Products at Half-way Stage for Mixture $C_2H_4 : 2O_2$.		Analyses of Products of Reaction for Mixtures $C_2H_4 : O_2$.		
—	200 mm. C_2H_4, 400 mm. O_2 at 404° C.	200 mm. C_2H_4, 400 mm. O_2 at 404° C.	200 mm. C_2H_4, 200 mm. O_2 at 450° C.	200 mm. C_2H_4, 100 mm. O_2 at 450° C.	100 mm. C_2H_4, 100 mm. O_2 at 450° C.
	per cent.	per cent.	per cent.	per cent.	per cent.
CO_2	5·8	6·9	10·2	12·0	12·5
O_2	43·1	43·2	8·0	6·0	6·9
C_2H_4	16·4	14·8	24·3	17·5	24·4
CO	30·2	28·3	38·8	44·9	41·2
Residue	4·5	6·9	18·7	19·6	15·0
Ratio CO/CO_2	5·2	4·1	3·53	3·74	3·29

Note.—All analyses are of the dry gaseous products.

Table II.—" End-points " for various Pressures of Ethylene and Oxygen.

	Temperature.	Initial pressure of ethylene.	Initial pressure of oxygen.	Total increase.	Increase as percentage of that required by the reaction $C_2H_4 + 2O_2 = 2CO + 2H_2O$.
(*a*)	° C.	mm.	mm.		
Ratio $C_2H_4 : 2O_2$ (used in most of the experiments)	400	200	400	112	56
	420	200	400	112	56
	440	200	400	115	57·5
	420	150	300	87	58
	440	150	300	91	60·7
	400	100	200	57	57
	420	100	200	57	57
	450	100	200	58	58
	480	50	100	28	56
	500	50	100	28	56
Ratio $C_2H_4 : O_2$	418	200	200	61	61
	430	200	200	58	58
	450	200	200	58	58
	441	150	150	50	66·5
	418	100	100	33	66
	441	100	100	36	72
	480	100	100	35	70
	502	55	55	19	69
Ratio $C_2H_4 : 3O_2$	450	100	300	59	59
	450	100	300	59	59
(*b*) Ratios not used in the experiments on reaction velocity—					
$3C_2H_4 : O_2$	430	300	100	12	24
	430	300	100	11	22
$5C_2H_4 : 3O_2$	430	250	150	31	41·3
	430	250	150	32	42·7
$3C_2H_4 : 5O_2$	430	150	250	78	62
	430	150	250	76	61

We conclude then that although the rate of pressure increase is not a very strict measure of the rate of disappearance of the ethylene, it is sufficiently nearly so for mixtures $C_2H_4 + 2O_2$, $C_2H_4 + O_2$ and $C_2H_4 + 3O_2$ to enable it to be used in an investigation of the influence on the rate of reaction of the total pressure, the temperature, and, within the range of ratios given, the relative proportions of the two gases. It may be stated at once that the influence of some of these factors is so marked that slight uncertainties about the relation of pressure change to ethylene consumption could not possibly affect the interpretation of the observations.

Existence of Explosive Limits between 400° *and* 500° *C.*

Experiments were made to ascertain whether any limits of concentration existed at which there was a sharp transition from slow reaction to explosion. Such limits occur with hydrogen and oxygen, but none could be found with oxygen and ethylene. In the course of the experiments the order of the addition of the two gases to the reaction bulb was varied, so that each gas might pass through all possible concentrations. At any of the higher temperatures an explosion occurred when the pressure was increased beyond a certain value but the reaction velocity increased continuously and rapidly up to this point.

Influence of the Total Pressure on the Rate of Reaction for Mixtures $C_2H_4 : 2O_2$.

The effect of total pressure on the rate is roughly that corresponding to a reaction of the third order ; the " order," although recorded in the following table as giving a convenient measure of the influence of pressure, is not to be regarded in a reaction of this kind as representing the actual number of molecules taking part in the change.

Temperature. 0° C.	Initial pressure of C_2H_4.	Initial pressure of O_2.	Time of half change.		" Order."
	mm.	mm.	′	″	
400	101	204	9	54	2·9
	199	402	2	42	
420	50	103	27	30	3·0
	152	301	2	56	
	104	195	5	35	3·25
	204	400	1	13	
440	100	200	3	3	3·7
	150	300	1	2	
	165	335	exploded		
480	51	98	3	9	3·5
	80	157	1	2	
	100	200	exploded		

Fig. 1 shows the logarithm of the time of half change plotted against the logarithm of the pressure for two series of experiments not recorded in the table. The slopes of the lines give orders of 3·4 and 3·0 respectively.

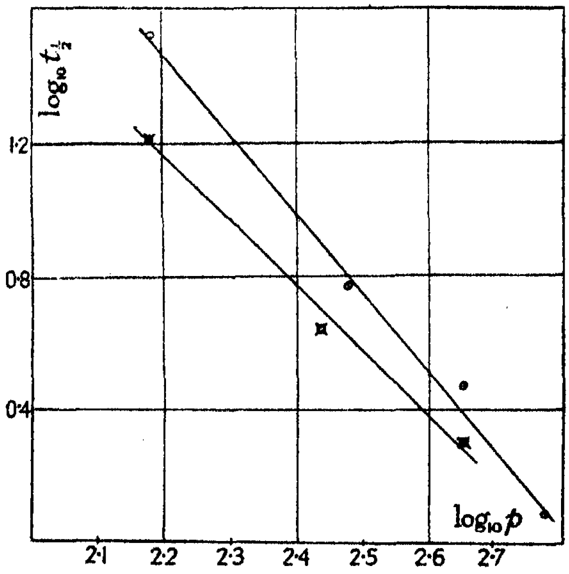

FIG. 1.

Influence of the Partial Pressures of Ethylene and Oxygen on the Rate of Reaction.

For reasons already explained mixtures within the range $C_2H_4 : O_2$ and $C_2H_4 : 3O_2$ were chosen as suitable for these experiments. The following tables contain detailed results of some typical experiments made in vessels of silica and porcelain respectively. The corresponding curves showing the complete course of the reaction for the different mixtures are also given in figs. 2A and 2B.

Although the oxygen pressure has some influence on the reaction velocity, that of the ethylene is far more pronounced. The rate seems in certain regions of pressure to be proportional to about the third power of the ethylene concentration.

Silica Bulb, 450° C.

C_2H_4 103 mm., O_2 199 mm.			C_2H_4 99 mm., O_2 200 mm.			C_2H_4 101 mm., O_2 299 mm.			C_2H_4 150 mm., O_2 200 mm.		
Time.		Per cent. change.	Time.		Per cent. change.	Time.		Per cent. change.	Time.		Per cent. change.
′	″		′	″		′	″		′	″	
1	55	8·8	1	50	8·9	1	16	8·2	0	28	8·8
2	55	17·6	2	51	17·9	2	6	16·4	0	43	17·6
3	56	26·3	3	53	26·8	2	50	24·6	0	56	26·3
5	15	36·0	4	58	35·7	3	28	32·8	1	10	35·0
7	34	52·6	6	10	44·7	5	27	49·2	1	24	43·9
9	15	61·4	7	35	53·6	6	35	57·4	2	0	61·4
11	10	70·2	11	20	71·5	8	2	65·6	2	55	79·0
13	36	79·0	18	25	89·4	9	54	73·8	3	42	88·0
			26	0	98·3	17	0	90·2	4	55	96·5
						35	0	100·0	6	20	100·0
									11	0	100·0

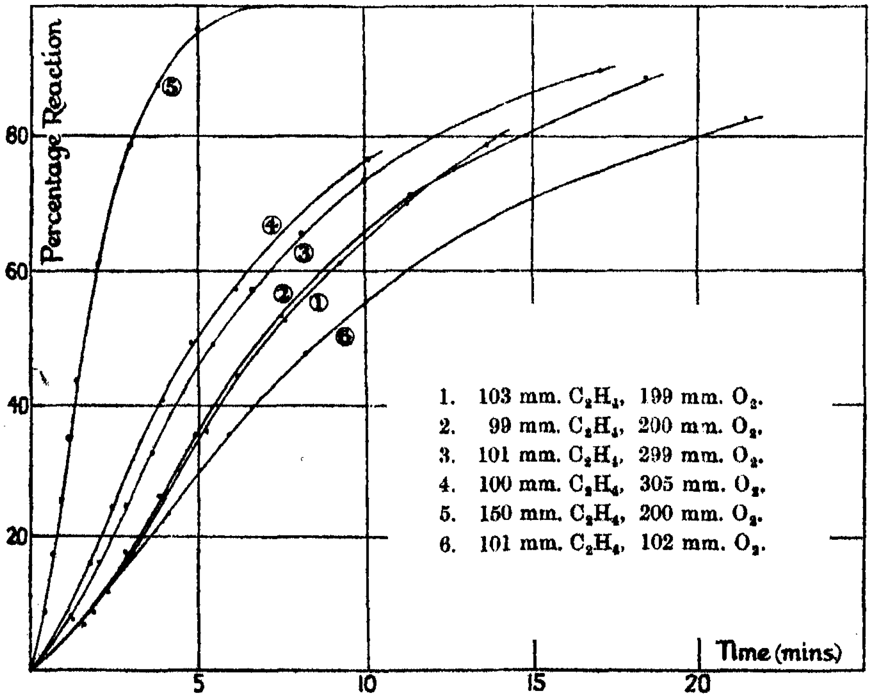

FIG. 2A.—Experiments in Silica Vessel at 450° C.

Porcelain Bulb, 450° C.

C_2H_4 200 mm., O_2 203 mm.		C_2H_4 103 mm., O_2 202 mm.		C_2H_4 101 mm., O_2 104 mm.	
Time.	Per cent. change.	Time.	Per cent. change.	Time.	Per cent. change.
′ ″		′ ″		′ ″	
0 26	22·0	1 20	8·8	2 15	14·7
0 35	33·9	1 56	17·6	3 46	35·3
0 48	50·9	2 30	26·3	4 15	44·1
0 55	59·4	3 2	35·0	5 25	58·8
1 4	67·8	3 40	43·9	7 0	79·5
1 30	84·8	6 9	70·2	9 40	88·2
1 53	93·2	7 42	79·0	12 22	97·0
3 15	96·7	13 55	94·8		
4 20	98·4	18 15	98·2		

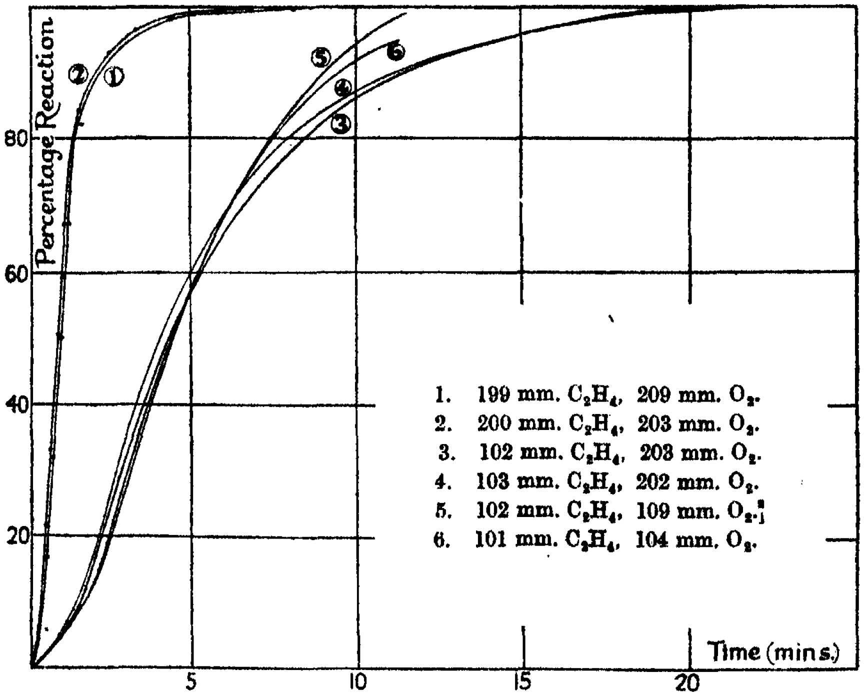

FIG. 2B.—Experiments in Porcelain Vessel at 450° C.

Influence of the Vessel Surface on the Reaction Velocity.

The rate of reaction is not very different in silica vessels and in porcelain vessels, as may be seen from the figures given above. It was investigated also in a porcelain vessel two-thirds filled with small pieces of porcelain.

If the reaction being studied were mainly on the surface a marked acceleration would be noticed, while a chain reaction might be substantially slowed down. Immediately ethylene was introduced to the packed vessel at 460° a rapid though small increase of pressure was observed, which continued for a short time after admitting the oxygen, and, as gas analyses showed, was due to the decomposition of the ethylene. This decomposition, although occurring to some extent in all the experiments is hardly measurable in an empty bulb. Thus when 300 mm. ethylene, a higher pressure than was generally used in the oxidation experiments, were allowed to remain at 450° C. for 30 minutes—longer than would be required for complete oxidation in the ordinary way—analysis showed that less than 2 per cent. had been decomposed. The decomposition is, however, very much accelerated by increasing the surface to the extent that packing the bulb with small pieces of porcelain allows.

It was therefore necessary to find some means of increasing the surface but less drastically. A silica bulb completely packed with spheres of silica about 1 cm. in diameter was used for this purpose.

In this vessel the reaction velocity as measured by the percentage of the total pressure increase occurring in a given time is far less than in an empty bulb. But it is not precisely the same reaction which is measured. The total pressure increase observed in the packed bulb is generally rather less than in the empty one, which indicates a greater proportion of the reaction giving carbon dioxide—since the latter occurs with no pressure change at all. However it is clear that the main reaction is considerably retarded, for analysis always showed considerable amounts of unchanged ethylene and oxygen after long periods. Thus in the empty bulb at 450° C. 100 mm. ethylene and 200 mm. oxygen would have combined completely in 10 minutes; in the sphere packed bulb there was 53·5 per cent. of ethylene after 30 minutes. Moreover, whatever process is really being measured in the packed bulb the one yielding carbon monoxide is occurring simultaneously, and if the total rate is less than in the empty bulb, then the rate of the reaction yielding carbon monoxide must be less still.

Thus it seems probable that there is a real retardation by increased surface, as in the combination of hydrogen and oxygen, which suggests the existence of reaction chains.

The Temperature Coefficient of the Reaction Velocity.

When the logarithm of the time of half change, $t_{\frac{1}{2}}$, is plotted against 1/T, the reciprocal of the absolute temperature, a straight line is usually found, the slope of which is determined by the heat of activation. With the combination of hydrogen and oxygen the slope varies both with temperature and pressure, being governed not only by the heat of activation but by the variable chain length. The "order" of the oxidation of ethylene does not vary much with temperature; thus the temperature coefficient of the rate cannot vary very much with pressure. The temperature coefficient is not very great, and its actual value varies slightly with the condition of the surface. Since any real variation in the value of the heat of activation might be of fundamental importance in understanding the mechanism of the reaction it seemed necessary to make determinations preventing as far as possible changes in the experimental conditions. With this object a whole series of experiments at different temperatures were made at in as rapid succession as possible. The temperatures were chosen in random order. Fig. 3 shows that the values for a given pressure lie on a curve which does not differ systematically from a straight line. The slopes vary slightly for the different pressures. The results are tabulated

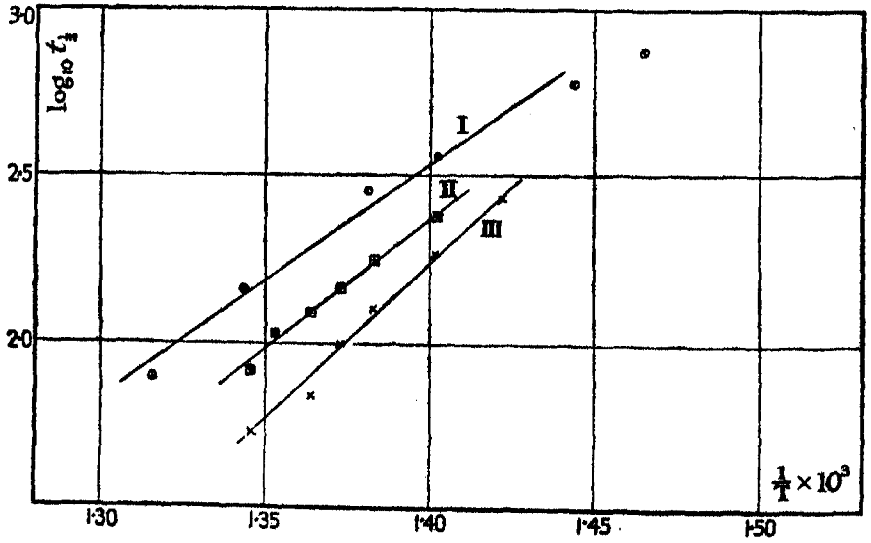

FIG. 3.—I, 100 mm. O_2, 200 mm. C_2H_4. II, 125 mm. O_2, 250 mm. C_2H_4. III, 150 mm. O_2, 300 mm. C_2H_4.

below. From the figures given E, the heat of activation, was calculated by the method of least squares.

100 mm. C_2H_4, 200 mm. O_2.		125 mm. C_2H_4, 250 mm. O_2.		150 mm. C_2H_4, 300 mm. O_2.	
T° (absolute).	$t_{\frac{1}{2}}$ (seconds).	T° (absolute).	$t_{\frac{1}{2}}$ (seconds).	T° (absolute).	$t_{\frac{1}{2}}$ (seconds).
(683)	(770)	713	244	703	276
(693)	(620)	723	180	713	169
713	369	728	148	723	128
724	290	733	125	728	100
744	146	739	107	733	70
763	78	743	83	743	54
E = 35,000 calories.		E = 37,000 calories.		E = 43,000 calories.	

Influence of Nitrogen and of Argon on the Rate.

A number of experiments were made to find whether nitrogen and argon cause an acceleration of the reaction similar to that which they cause in the union of hyrogen and oxygen. While the acceleration of the hydrogen-oxygen reaction is very great, that of the oxidation of ethylene is small and in certain respects erratic.

With 100 mm. ethylene and 200 mm. oxygen, 200 or 300 mm. argon or nitrogen appear to cause an appreciable acceleration, amounting to as much as one-third. But when the curves of pressure increase plotted against time are examined it becomes evident that this acceleration is due principally to a shortening of the induction period. After about the first 10 per cent. of the pressure increase, the course of the reaction is almost independent of whether argon is present or not. Nitrogen, however, appears to exert in addition a quite small accelerating effect over the greater part of the course.*

* To explain these results it would be necessary to understand what is taking place during the induction period.

If, as appears probable from the next section, the reaction is regarded as one in which chains are initiated by the formation of some kind of peroxide, the induction period may well depend upon the initial production of this body. The effect of argon in shortening the induction period seemed to depend upon the order in which the various gases were admitted to the reaction bulb, being greatest when oxygen was admitted last. It is conceivable that the varying conditions of concentration or even the varying degrees of adiabatic compression associated with different orders of admission of the gases might influence the initial concentration of the unstable substance upon which the establishment of the chains depends. This effect of the initial conditions, being small, somewhat variable, and temporary, can hardly be regarded as of fundamental importance. It should be noted that in the absence of the argon the order of admission of ethylene and oxygen had no influence.

Discussion.

Several characteristics of the reaction between ethylene and oxygen are difficult to explain without the assumption that the oxidation takes place by a chain mechanism.

The influence of pressure on the rate is very great, and the principal reaction seems to be retarded by increasing the surface of the vessel.

The partial pressure of the ethylene has far more effect on the rate than that of the oxygen. Indeed, with 100 mm. ethylene, increasing the pressure of the oxygen, from 100 mm. to 200 mm. causes no acceleration but actually a slight retardation. The effect of the pressure of the ethylene is probably greater than could be accounted for by any simple reaction mechanism not depending on the propagation of chains.

The influence of nitrogen and of argon on the rate yields no definite evidence either for or against the existence of chains. Apart from the effect on the induction period discussed in the last section the acceleration of the reaction caused by these gases is but slight. A definite acceleration would be expected if the foreign gas prevented chains from reaching the wall and there being broken. To account for the smallness of the observed effect it can be supposed that the chains are quite short, and that many of them are terminated in the gas phase without reaching the wall.

This supposition is supported to some extent by a consideration of the temperature coefficient. The heat of activation varies from 35,000 calories with 100 mm. ethylene and 200 mm. oxygen to 43,000 calories with 150 mm. ethylene and 300 mm. oxygen. If very long chains were involved the rate of reaction would be many times greater than that to be expected from the heat of activation on a theoretical basis. The initial activation process is probably bimolecular, but might be termolecular. It is easy to calculate from the relation between the rates of other reactions and their heats of activation that a bimolecular process, occurring at the same temperature and with the same rate as the combination of 100 mm. ethylene and 200 mm. oxygen, would have a heat of activation of about 38,000 calories. This is near enough to the observed values to show that a bimolecular process would not need to have its rate multiplied by many powers of 10, though there is nothing to show that chains of comparatively short length do not occur. If the initial process were termolecular, it would, for the same heat of activation, proceed about 10^3 to 10^4 times more slowly. Thus for the oxidation to take place at the observed rate chains of considerable length would have to be involved. The first alternative, a bimolecular activation process and comparatively short chains, is on the whole more plausible.

With regard to the process by which the reaction chains are initiated, the experiments which have been described lend support to views recently expressed by Egerton* and others on the nature of hydrocarbon combustion in general.

The most remarkable fact about the reaction is the rapid increase in rate with increasing pressure of ethylene, the pressure of the oxygen being relatively unimportant. It seems, therefore, that a high concentration of ethylene favours the propagation of chains while a high concentration of oxygen does not.

Egerton suggests that the initial process in the combustion of a hydrocarbon is the formation of an unstable peroxide. This provides active centres from which reaction chains proceed. On the other hand, there is no doubt that Bone's interpretation of the complete course of oxidation as a process of successive hydroxylation is essentially correct. The two views are not incompatible, and a combination of them suggests an explanation of the facts just mentioned. We may suppose that the initial act in the oxidation is a collision between ethylene and oxygen giving the unstable $C_2H_4 : O_2$. If this collides with another ethylene molecule the oxygen is shared and two active hydroxylated molecules, *e.g.*, $\begin{matrix} \text{CHOH} \\ \| \\ \text{CH}_2 \end{matrix}$, are produced, which continue the chain. If, however, the peroxide collides with oxygen it may either be decomposed or oxidised completely to stable products which do not happen to be effective in continuing the chain.

Summary.

The oxidation of ethylene between 400° and 500° C. is probably a chain reaction. The rate is affected by the total pressure approximately as in a reaction of the third order, the effect depending very much more on the partial pressure of the ethylene than on that of the oxygen. It is suggested that the first stage in the reaction is the formation of an unstable peroxide; if this reacts with more oxygen the chain ends, but if it reacts with ethylene unstable hydroxylated molecules are formed which continue the chain. The reaction is retarded by an increase in the surface exposed to the gas. From a consideration of the temperature coefficient and the influence of foreign gases on the rate of reaction it is concluded that the chains are probably not of great length.

---

* Egerton and Gates, 'J. Inst. Petroleum Tech.,' vol. 13, p. 281 (1927).

Observations of the Height of the Ozone in the Upper Atmosphere.—Part II.

By F. W. P. Götz, Dr. Phil. Nat. (Lichtklimatisches Observatorium, Arosa), and G. M. B. Dobson, D.Sc., F.R.S.

(Received July 3, 1929.)

Measurements to determine the height of the ozone layer over Arosa, extending over a period of 6 months, have been described in a former paper.* These observations have now been continued for another 6 months with the results given below.

It was previously stated, that the constant of the spectrograph, which gives the ratio of the two wave-lengths used which would be obtained if the instrument could be taken right outside the atmosphere, was subject to some uncertainty, and any error in the adopted value would cause an error in the heights deduced. Recent improved determinations of this constant show that the value used was too low, with the result that the heights previously published should be increased by about 18 km. This brings the heights found at Arosa into good agreement with those found by other observers, the average height being about 50 km.

It may be well to explain here the main cause of the change in the value of the constant used. The constant is obtained by plotting the intensity at the earth's surface of any wave-length, against the length of the light's path through the absorbing atmosphere and extrapolating to zero path-length. For the longer waves the extinction is mainly due to scattering by air and haze in the lower atmosphere, and the path-length is closely proportional to sec Z (where Z is the sun's observed zenith distance). For the shorter waves, which are absorbed by ozone in the upper air, the absorbing path is more nearly proportional to sec α, where α is given by the relation $\sin \alpha = \mathrm{R}/(\mathrm{R} + h) \, . \sin \mathrm{Z}$ (where R is the earth's radius and h is the height of the ozone layer). In the previous determinations of the constant in question, this difference in the treatment of the two wave-lengths was not taken into account. It will be noticed that sin α involves a knowledge of h—the height of the ozone layer—but fortunately this can be overcome by what is equivalent to successive approximation.

Fig. 1 shows the heights found at Arosa at different times of the year.

---

* 'Roy. Soc. Proc.,' A, vol. 120, p. 251 (1928).

There is some indication that the height is greater in the spring than at other times of the year, but this is not yet certain.

Fig. 2 shows the variation in the height of the ozone with the amount of ozone present. To eliminate the annual effects, the amounts of ozone are given as differences from the monthly mean values. While the accuracy of the observations is poor, it is clear that the average height is *not* lower when there is much ozone than when there is little ozone ; if anything, the reverse would appear to be more nearly true. This is the most important result of the observations, since most hypotheses which might be put forward to explain the connection between the changes in the amount of ozone and the meteorological conditions in the lower atmosphere would require that the average height should be lower when there was much ozone present, and *vice versâ.* Thus an obvious suggestion is that polar air currents in the upper troposphere carry air which is rich in ozone from polar to temperate regions, so that the changes in the amount of ozone occur in the upper troposphere, and that when there is much ozone this is due to ozone being present both at, say,

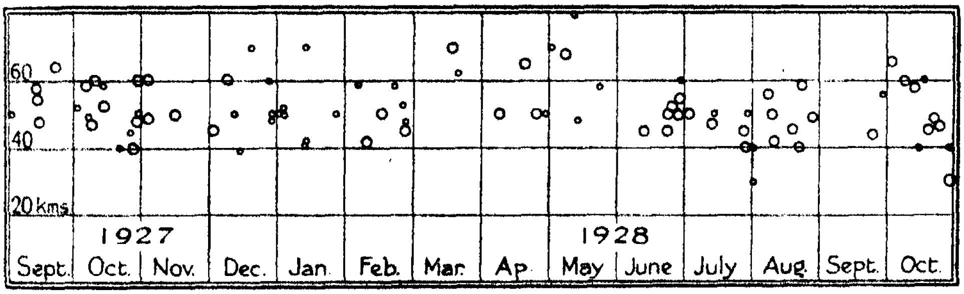

FIG. 1.

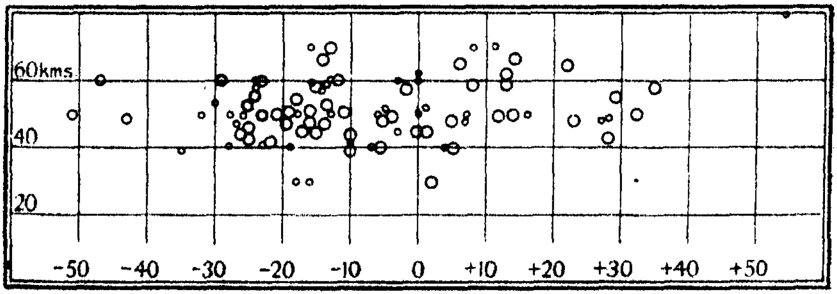

Difference of Ozone Value from Monthly Mean. *(Unit = 0·001 cm. of Ozone)*

FIG. 2.

(NOTE.—Small circles are less reliable observations.)

10 km. and 50 km. If such a hypothesis were true, the average height would evidently be much lower at times of much ozone than at times of little ozone.

The accuracy of such measurements as these depends on getting observations when the sun is low. The instruments at present in use were not primarily designed for this purpose and their "light-gathering power" is not very good; thus the exposures become very long when the sun is low, and in practice it is not possible to observe when the sun is less than 14° above the horizon. In the past these instruments were the only ones available for making a large number of observations, but as more suitable instruments are being obtained, the present observations will not be continued.

In conclusion, we should like to express our thanks to Mr. R. W. M. Gibbs, who has again measured all the spectra on which this work is based and computed the ozone values. We also wish to thank the Department of Scientific and Industrial Research for a grant for assistance with the large amount of computing work involved.

The Oxidation of Phosphine at Low Pressures.

By R. H. Dalton, Ramsay Fellow, and C. N. Hinshelwood, F.R.S.

(Received July 17, 1929.)

I.—*Introduction.*

In the recent developments of chemical kinetics there have been many indications of a type of reaction known as a chain reaction, in which each act of transformation gives rise to a product which, on account of its active chemical nature or high energy content, causes further molecules to be transformed without special activation. Under certain conditions the chain may "branch," and the number of centres from which reaction proceeds increases indefinitely unless the chains are broken. In a gaseous reaction there may be a definite concentration at which the rate of initiation of chains just begins to exceed the rate at which they are broken. At this point a stable condition ceases to be possible. However slow the reaction may be on one side of the limiting concentration, on the other side its rate increases continuously with time till explosion results. The acceleration may require an imperceptible fraction of a second only, since the time scale on which molecular collision processes occur is a very minute one.

The remarkable phenomenon to which this gives rise, namely an abrupt transition from negligibly slow reaction to explosion, is exemplified in the union of oxygen with phosphorus vapour* and with sulphur vapour† at low pressure, and in the combination of hydrogen and oxygen‡ under certain conditions. The present paper deals with a similar phenomenon in the oxidation of phosphine.

Chains may be broken by deactivation of molecules either in the gas phase or at the surface of the vessel. The first kind of deactivation becomes more prominent the higher the pressure, the second kind the lower the pressure. When explosion occurs abruptly on decreasing the pressure, it indicates that some process in the gas phase has ceased to break the chains as rapidly as they start; when there is a similar abrupt transition with increasing pressure, it indicates that the deactivating influence of the surface of the vessel has become inadequate.

It has long been known that mixtures of phosphine and oxygen explode when the pressure is reduced,§ and the influence of various factors on the critical pressure was studied by van't Hoff|| and van der Stadt,¶ but no theoretical explanation was then forthcoming. Regarded in the light of more recent work these results suggest that the oxidation of phosphine is a chain reaction. Further study of the reaction has been undertaken from this point of view. The first part of the work, which is described in this paper, shows that, in addition to the higher pressure limit, there is also a lower pressure limit, below which the rate of combination is quite negligibly slow but above which there is explosion. The nature of this limit has been experimentally investigated by introducing the gases at low pressure into a tube and compressing them until explosion occurred, separate experiments having shown that the rate of reaction at slightly lower pressures is negligibly small.

The formally simplest theory of the phenomenon is that chains are maintained by active intermediate products, which react alternately with oxygen

---

* Semenoff, 'Z. Physik,' vol. 46, p. 109 (1927).

† Semenoff and Rjabinin, 'Z. physikal. Chem.,' B, vol. 1, p. 192 (1928).

‡ Thompson and Hinshelwood, 'Roy. Soc. Proc.,' A, vol. 122, p. 610 (1929); vol. 124, p. 219 (1929); Gibson and Hinshelwood, 'Trans. Faraday Soc.,' vol. 24, p. 559 (1928).

§ The products of explosion are given by the equation $PH_3 + O_2 = HPO_2 + H_2$, unless oxygen is in excess, when the hydrogen is also burnt and H_3PO_3 is formed.

|| 'Études de Dynamique Chimique.'

¶ 'Z. physikal. Chem.,' vol. 12, p. 322 (1893).

and phosphine. The chains are supposed only to be broken when they reach the wall of the vessel. There is a certain small definite probability of their branching. As shown in section 8 the simple development of this theory leads to the result that at the critical pressure the following relation should hold approximately :—

$$p_{O_2} . p_{PH_3} . d^2 \left(1 + \frac{p_{N_2}}{p_{O_2} + p_{PH_3}}\right) = \text{constant.}$$

d is the diameter of the tube containing the gases, and p_{N_2} is the pressure of nitrogen, or any other inert gas present. This formula is analogous to that used by Semenoff* in connexion with the reaction between oxygen and phosphorus.

It describes the results qualitatively in that (*a*) there is an inverse relationship between the pressure of oxygen and that of phosphine at the explosion point, (*b*) the critical partial pressures are lowered by the presence of nitrogen or argon, (*c*) in the absence of inert gases the product $p_{O_2} . p_{PH_3}$ is inversely proportional to a power of the diameter which is nearer the second than any other integral power.

To obtain quantitative agreement the theory needs elaboration. In the absence of inert gases, p_{O_2} and p_{PH_3} are connected by a relation which is only approximately hyperbolic : when the walls of the tube in which the reaction occurs are covered with phosphoric acid to give a constant surface the curve obtained is symmetrical (fig. 2), but differs from a rectangular hyperbola in that $p_{O_2} . p_{PH_3}$ rises to a maximum for equal pressures. In a glass tube with the solid reaction products on the walls the curve is actually unsymmetrical (fig. 3), but this is probably due to changing nature of the surface caused by changing adsorption for different proportions of the two gases. The effect of inert gases is smaller than that predicted by the formula, though this gives the right order of magnitude (fig. 4). The deviation of the p_{O_2}, p_{PH_3} curve from strictly hyperbolic form can be attributed to mutual deactivation of the active intermediate products, while the discrepancy between the observed and calculated effect of the inert gas can be ascribed to a certain amount of deactivation by the inert gas itself or inhibitors introduced with it.

II.—*Preparation of Materials.*

The phosphine was generated by decomposition of phosphonium iodide with potassium hydroxide, and purified by passing over solid potassium hydroxide, and then through a trap cooled with solid carbon dioxide to free it from other hydrides of phosphorus. It was finally collected by freezing out in a liquid air trap, and allowed to evaporate into an evacuated container.

---

* 'Z. physikal. Chem.,' B, vol. 2, p. 161 (1929).

Oxygen was prepared by heating potassium permanganate, and purified by passage through a liquid air trap.

Commercial nitrogen and argon were purified by passage over hot active copper, solid potassium hydroxide and phosphorus pentoxide. The argon contained some nitrogen.

III.—*Experimental Procedure.*

The apparatus is illustrated in fig. 1. The gases were contained in reservoirs under known pressure and were admitted to the apparatus in small, accurately known portions by the pipettes P_1, P_2 and P_3. On their way to the reaction vessel, R, they passed through a long spiral, S, cooled with solid carbon dioxide, which served to control the humidity. The tubing connecting the pipettes with R was of small bore. By means of the three-way tap, A, the reaction vessel could be connected to the gas pipettes or the pumps, or could be cut off completely while the pipettes were connected to the pumps. The

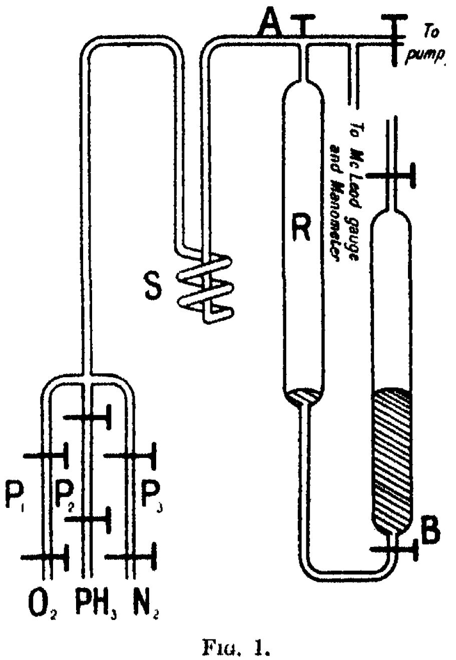

FIG. 1.

lower end of R was connected through a glass tube to a burette containing mercury by means of which the gases in R could be compressed until they exploded. The general procedure was to evacuate the apparatus to about 10^{-4} mm. of mercury, and then to add from the pipettes the desired quantities of the various gases, pumping out the connecting tubes between additions. The volume of R and the connecting tubes was known so that the pressures of the gases could be calculated. A correction was applied for the effect of cooling S.*

The tap A was then turned so as to close R, and the gases were compressed by raising the mercury slowly until the mixture exploded, as shown by a faint flash. The mercury was stopped instantly by closing the tap B. The decrease in volume of R was obtained from the burette readings, and the pressures at the instant of explosion could be calculated. Changes of temperature of a few degrees were found to have very little effect on the explosion limit, so that it was unnecessary to place the reaction vessel in a thermostat.

In the later experiments it was found advisable to introduce a few cubic centimetres of very strong phosphoric acid on top of the mercury. This had the advantage of controlling the humidity more accurately and giving more reproducible wall conditions, since it adhered to the glass and dissolved the products of the reaction. The acid used was made by dissolving phosphorus pentoxide in ordinary phosphoric acid, density 1·75, until a very viscous liquid was obtained which solidified slowly at temperatures below 20°. There was no indication that the acid dissolved any of the gases. The experiments made in presence of phosphoric acid were more reproducible and freer from complications than the earlier experiments, and hence will be given the principal consideration in the discussion.

IV.—*Dependence of Explosion Pressure on the Ratio of Phosphine to Oxygen.*

The results of the experiments in the tubes with walls covered with phosphoric acid are given in Table I. p_{O_2} and p_{PH_3} are the pressures at which explosion occurred. In all these experiments the phosphoric acid layer was

---

* The pressure in R was calculated from the pressure in the pipettes and the ratio of their volume to the total volume of the apparatus. In the formula used the term for the connecting tube was not its real volume but that which it appeared to have when S was cooled. This was determined by direct experiments in which gas at pressures large enough to be measured on a manometer was shared with R. The pressure of the second gas added was less than that calculated from the volume ratio, because of the presence of the first gas in R. Assuming that none of the first gas diffused back into the narrow connecting tube when the second was admitted, the correction was equal to the volume of the connecting tube times the pressure of the first gas.

Table I.

Series A. Diameter 1·95 cm.		Series B. Diameter 1·95 cm.				Series C. Diameter 1·0 cm.	
p_{O_2}.	p_{PH_3}.	p_{O_2}.	p_{PH_3}.	p_{O_2}.	p_{PH_3}.	p_{O_2}.	p_{PH_3}.
0·27	1·58	0·13	2·25	0·20	1·65	0·49	2·88
0·27	1·55	0·14	2·40	0·23	1·81	0·50	2·89
0·27	1·49	0·16	2·04	0·33	1·42	0·89	2·18
0·28	1·59	0·19	1·83	0·34	1·46	0·93	2·25
0·45	1·09	0·19	1·90	0·35	1·53	0·95	1·97
0·46	1·11	0·20	1·96	0·79	0·89	0·97	1·98
0·67	0·86	0·49	0·92	0·81	0·93	1·56	1·26
0·69	0·88	0·55	1·18	0·85	0·95	1·62	1·30
0·71	0·92	0·55	1·03	1·05	0·55	2·16	0·79
0·98	0·54	0·57	1·23	1·10	0·58	2·24	0·83
1·02	0·56	0·65	1·12	1·67	0·23	2·28	0·83
1·03	0·56	0·66	1·14	1·76	0·25	3·16	0·45
1·20	0·42	1·01	0·48	1·80	0·16	3·19	0·45
1·21	0·43	1·02	0·55	1·99	0·21	3·26	0·47
1·26	0·45	1·12	0·60	2·04	0·21		
1·50	0·25	1·16	0·39	2·08	0·18		
1·56	0·26	1·16	0·40	2·25	0·17		
		1·22	0·41	2·30	0·18		

first raised to the top of the reaction tube and lowered again, just before carrying out the determination, to ensure that the walls were covered. All pressures are expressed in millimetres of mercury. Series A and Series C are shown in fig. 2, where the dotted lines represent the form of curve expected from the simple theory.

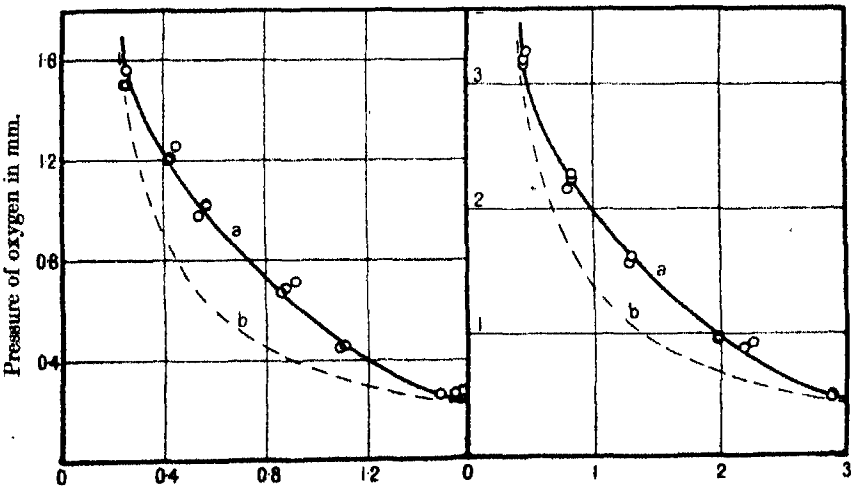

FIG. 2.—Explosion Pressures of Oxygen-Phosphine Mixtures. Left hand figure : Series A, 1·95 cm. tube, H_3PO_3 surface. Right-hand figure : Series C, 1 cm. tube, H_3PO_3 surface. The broken curves *b* are hyperbolas.

The curves are symmetrical with respect to p_{O_2} and p_{PH_3}, and of the same general form as a rectangular hyperbola. The central section is in general flatter than the hyperbola, although in some series the deviation was not much greater than the experimental error. It should be noted that in fig. 2 $p_{PH_3} \times p_{O_2}$ deviates from the 'hyperbolic' value by about the same percentage for the 1 cm. tube and the 1·95 cm. tube.

When one of the gases is at a very much higher pressure than the other the results are no longer symmetrical, the product being greater with high oxygen pressure (Table I, Series B). When the ratio p_{O_2}/p_{PH_3} is increased to 15 or 20 a point is reached where the mixture fails to explode at any pressure. This probably indicates deactivation of the active molecules by oxygen. Indeed, it is known that this factor must become important at high pressures of oxygen, since the work of van der Stadt proved the existence of an upper limit largely determined by the oxygen pressure. At high values of the ratio p_{PH_3}/p_{O_2}, on the other hand, the explosions become weaker and weaker until at ratios of about 17 they can no longer be detected, but there was no indication of a definite limit in this direction.

In starting a series of experiments after the apparatus had been unused for some hours it was always noticed that the explosion pressure gradually decreased during the first few explosions and then settled down to a fixed value with only random fluctuations. A number of attempts were made to discover the cause of this behaviour and if possible eliminate it, but without much success. The most probable explanation seemed to be that some substance produced by the explosion was retained to a small extent in the tube and promoted the initiation of chains in the following experiment. The removal in the first explosions of traces of an inhibiting substance which had accumulated in the tube on standing would give rise to a similar effect.

V.—*Influence of the Diameter of the Tube and the Nature of the Walls.*

In the earlier experiments, in which phosphoric acid was not present, the solid products of reaction were deposited on the walls of the tube. The surface thus covered was found to be less effective in breaking the chains than clean glass. After a number of explosions had taken place in a given tube the critical pressure became fairly steady, and the final value of $p_{O_2} \cdot p_{PH_3}$ was usually about half that for the clean tube. Some typical results of experiments made under these conditions are given in Table II and the corresponding curves in fig. 3.

It is seen that the curves are no longer symmetrical, except with the 1 cm.

Table II.

Series A. Diameter 3·6 cm.		Series B. Diameter 1·95 cm.		Series C. Diameter 1·0 cm.	
p_{O_2}.	p_{PH_3}.	p_{O_2}.	p_{PH_3}.	p_{O_2}.	p_{PH_3}.
mm.	mm.	mm.	mm.	mm.	mm.
0·20	1·33	0·57	1·39	0·77	3·51
0·21	1·37	0·59	1·45	0·80	3·63
0·35	1·00	0·73	0·91	0·81	3·66
0·35	0·99	0·75	0·94	0·82	3·80
0·55	0·58	0·80	0·52	1·21	2·22
0·56	0·59	0·81	0·52	1·26	2·25
0·60	0·47	0·83	0·28	1·68	1·65
0·66	0·49	0·87	0·57	1·73	1·67
0·68	0·49	0·90	0·58	2·23	1·03
0·77	0·35	0·91	0·30	2·37	1·12
0·79	0·35	1·03	0·14	4·50	0·54
0·94	0·18	1·06	0·14	4·82	0·57
0·95	0·18				
1·03	0·20	The results of this series are unusually erratic for an unknown reason.			
1·36	0·10				
1·39	0·10				
1·46	0·10				

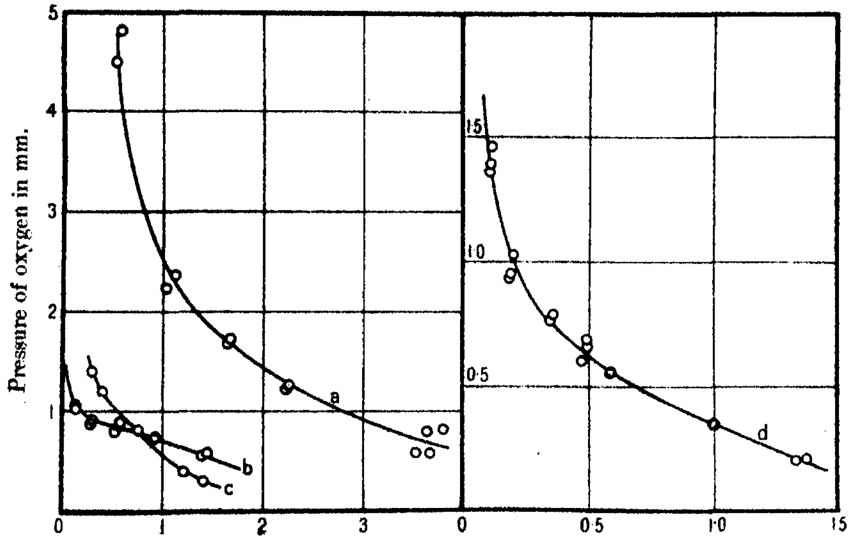

Fig. 3.—Explosion Pressures of Oxygen-Phosphine Mixtures. (*a*) 1 cm. tube; (*b*) 1·95 cm. tube; (*c*) 1·95 cm. tube, H_3PO_4 surface; (*d*) 3·6 cm. tube.

tube, and may show an inflection point near the middle. The mixtures explode more readily when oxygen is in excess than when phosphine is in excess. The mean value of $p_{O_2} \cdot p_{PH_3}$ is, however, not greatly different from its value in the experiments with phosphoric acid (fig. 3, curves *b* and *c*). It should be mentioned that while successive experiments at the same pressures were frequently in very good agreement, different series carried out at intervals of several days showed a considerable drift.

An attempt was made to obtain a series of results with completely clean walls by taking down the tube and washing it between experiments. It was found impossible, however, to get a reproducible surface in this manner, and the method was abandoned.

Experiments with a silica tube gave approximately the same results as those with glass tubes.

The asymmetry of the curve may be explained if it is assumed that the deactivating properties of the walls increase with the amount of phosphine adsorbed. This amount would be greatest at high ratios of phosphine to oxygen, where the explosion pressures are observed to be relatively higher. The liquid phosphoric acid surface would presumably not adsorb phosphine, but possess a specific deactivating property independent of the gas pressure, and hence would give symmetrical results. The high values of $p_{O_2} \cdot p_{PH_3}$ with surfaces of clean glass or silica would indicate that the latter adsorb phosphine strongly.

The effect of the diameter of the tube on the explosion pressure is shown in Table III, where the values of $p_{O_2} \cdot p_{PH_3}$, at the point where $p_{O_2} = p_{PH_3}$, are compared for different tubes. The theory predicts that this product times the square of the diameter should be constant for a given kind of surface. The square root of this quantity is given in the last column.

Table III.

Nature of Surface.	Diameter in cm.	$p_{O_2} \cdot p_{PH_3}$.	$\sqrt{p_{O_2} \cdot p_{PH_3} \cdot d^2}$.
Covered with H_3PO_4	1·95	0·59	1·5
	1·00	2·18	1·4
Glass coated with reaction products	3·6	0·29	1·9
	1·95	0·64	1·6
	1·8	0·91	1·7
	1·0	2·8	1·7

For the two tubes containing phosphoric acid the agreement is good. For the others the results with the smaller diameters agree but in the widest tube the gases are less explosive than the theory predicts. This is perhaps due to the existence of some deactivation in the gas phase, a factor which is naturally more important the greater the diameter.

VI.—*Influence of an Inert Gas.*

A series of determinations of the explosion pressure were made, in which various quantities of an inert gas were added, the ratio of oxygen to phosphine being kept constant. Some typical results are given in Table IV, and two typical curves in fig. 4. The lower lines show the relationship expected on the basis of the simple theory.

Table IV.

Series A. (With H_3PO_4)		Series B. (With H_3PO_4)		Series C. (Without H_3PO_4)		Series D. (With H_3PO_4)		Series E. (With H_3PO_4)	
Diameter 1·0 cm.		Diameter 1·95 cm.		Diameter 0·95 cm.		Diameter 1·95 cm.		Diameter 1·95 cm.	
$p_{O_2}/p_{PH_3} = 1\cdot39$.		$p_{O_2}/p_{PH_3} = 1\cdot20$.		$p_{O_2}/p_{PH_3} = 0\cdot91$.		$p_{O_2}/p_{PH_3} = 1\cdot40$.		$p_{O_2}/_{PH_3} = 1\cdot50$.	
p_{O_2}.	p_{Argon}.	p_{O_2}.	p_{Argon}.	p_{O_2}.	$p_{Nitrogen}$.	p_{O_2}.	$p_{Nitrogen}$.	p_{O_2}.	p_{Argon}.
1·62	0	0·73	0	1·64	0	0·85	0	1·08	0
1·62	0	0·73	0	1·62	0	0·85	0	1·02	0
1·38	1·15	0·75	0	1·23	3·43	0·89	0	0·85	0·52
1·37	1·17	0·77	0	1·22	3·35	0·84	0·56	0·83	0·50
1·22	2·71	0·69	0·64	0·97	5·95	0·81	0·53	0·77	1·11
1·19	2·75	0·67	0·63	0·97	5·90	0·74	0·49	0·75	1·10
1·12	5·14	0·65	0·61			0·74	1·05	0·71	1·70
1·09	4·68	0·60	1·04			0·73	1·05	0·69	1·58
		0·60	1·06			0·72	1·00	0·68	1·58
		0·59	2·38			0·67	1·66	0·65	2·09
		0·57	2·13			0·69	1·70	0·66	2·02
		0·54	2·11			0·64	3·24	0·67	2·86
								0·64	2·65
								0·63	2·53

The results show that in general the effect of the added gas is less than that calculated, but that the theory predicts the correct order of magnitude. On account possibly of the introduction of inhibitors with the inert gas the results are not very consistent; for example, in Series E of Table IV, the results are in fairly good agreement with the theory while in another series made under similar conditions the effect was decidedly too small. The fact that their influence is in general somewhat smaller than that expected may be due to a certain deactivating influence of the inert gases, which partially counteracts their normal influence of preventing the diffusion of the active molecules to the wall. Nitrogen seems to have a smaller influence than argon, suggesting, as seems probable, that it has more deactivating effect.

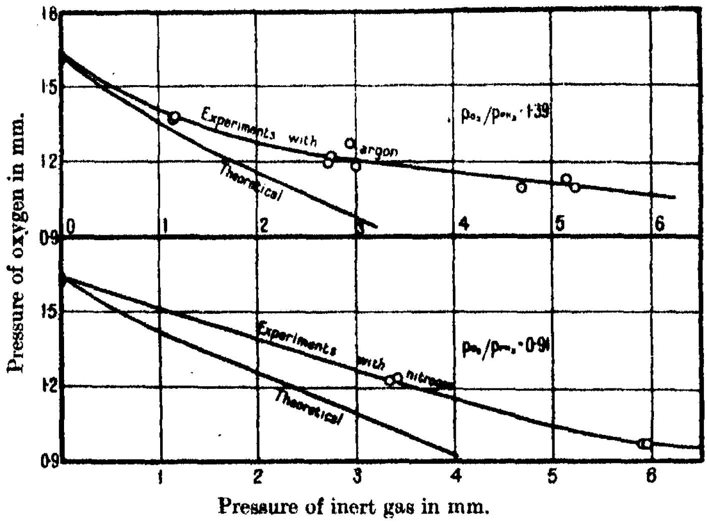

FIG. 4.—Influence of Inert Gasses on the Explosion Pressure.

VII.—*Rate of Reaction below the Explosion Pressure.*

To determine the extent of reaction below the explosion limit, a mixture was compressed nearly to the explosion point and allowed to stand overnight. On continuing the compression next morning the mixture exploded nearly at the expected point, thus showing that any reaction had been negligible in amount.

As a further proof of this point a mixture of phosphine and oxygen, at known pressures below the critical values, was allowed to stand over night. The phosphine was then frozen out with liquid air and the oxygen pumped off. The liquid air was then removed, and the pressure of the phosphine was found to be about 75 per cent. of its original value. In a blank experiment it was found that a loss of this amount was obtained even in the absence of oxygen, on account of the appreciable volatility of phosphine at the temperature of liquid air. Thus, in about 16 hours, no real reaction can be detected.

VIII.—*Simple Theory of the Lower Pressure Limit.**

The exact origin of the first centres from which chains are propagated does not affect the following considerations, which deal with the rate of increase of the chains when they are once started.

---

* Compare Semenoff, *loc. cit.*, whose method of treatment is followed in the first part of this discussion, but modified in the later part.

Let it be supposed that there are a certain number of molecules of activated oxygen, and that these act upon phosphine giving an active product, denoted by the symbol X_P, which reacts with oxygen to give another active product X_O. This in turn reacts with phosphine giving X_P again, and so on until the chain is broken by reaching the wall of the vessel.

In the course of a chain let there be n_1 collisions between X_O and PH_3, n_2 between X_O and O_2, n_3 between X_P and PH_3, and n_4 between X_P and O_2. Let $n_1 + n_2 + n_3 + n_4 = n$. Since X_O only appears when X_P disappears and vice versa, $n_1 = n_4$.

$$n_1/(n_1 + n_2) = p_{PH_3}/(p_{PH_3} + p_{O_2})\,;\quad n_4/(n_3 + n_4) = p_{O_2}/(p_{PH_3} + p_{O_2})$$

whence

$$n_1 = n_4 = \frac{p_{O_2} \cdot p_{PH_3}}{(p_{O_2} + p_{PH_3})^2} \cdot n.$$

By the Einstein-Smoluchowsky relation, the number of collisions suffered by a particle undergoing a mean displacement d is $1 \cdot 5d^2/\lambda^2$, where λ is the mean free path.

If we assume that every chain is terminated by the action of the wall of the tube, $n = 1 \cdot 5d^2/\lambda^2$, d being of the order of magnitude of the diameter of the tube. If some of the chains are "reflected" from the walls, this is equivalent to an increase in the effective diameter, so that the qualitative nature of the wall may be taken into account by multiplying d by a factor β, which varies from one kind of tube to another. Taking the mean free paths of all the kinds of molecule to be approximately equal, λ is inversely proportional to the total pressure, and thus may be written $\lambda_0/(p_{PH_3} + p_{O_2})$.

Substituting these values we find for n_1 or n_4 the expression

$$p_{O_2} \cdot p_{PH_3} \times 1 \cdot 5\ \beta^2 d^2/\lambda_0^2.$$

Suppose the probability that the chain branches at a given collision to be ν. Then the number of times on the average that the chains branch before their existence is ended is $\nu \cdot p_{O_2} \cdot p_{PH_3} \cdot \beta^2 d^2/\lambda_0^2$. If this average is much less than unity, the branching will not lead to explosion since there is less than an even chance that a new chain so produced will create another before it comes to an end. The condition for explosion is therefore that the above expression is of the order of magnitude unity. Thus at the critical pressure we have the relation $p_{O_2} \cdot p_{PH_3} \cdot \beta^2 d^2 = \text{constant}$. To take into account the presence of an inert gas, *e.g.*, nitrogen, the necessary modification of the above calculation is easily made and leads to the relation :—

$$p_{O_2} \cdot p_{PH_3} \cdot \beta^2 d^2 \left(1 + \frac{p_{N_2}}{p_{O_2} + p_{PH_3}}\right) = \text{constant}.$$

The above method of calculation is an approximate one only, since the condition for explosion is not quite rigidly formulated. A more accurate procedure, though one which does not give so clear a picture of the mechanism, is to write down equations for the rate of production and rate of removal of X_O and X_P, and find the condition where a "stationary state" just ceases to be possible. This leads to an equation reducible with certain approximations to the above simple form.

Thus we have :—

$$\frac{d\,[X_O]}{dt} = k_1\,F(c) + k_2\,[X_P]\,[O_2] - k_3\,[X_O]\,[PH_3] - K\,[X_O] = 0, \qquad (1)$$

$$\frac{d\,[X_P]}{dt} = \alpha\,k_3\,[X_O]\,[PH_3] - k_2\,[X_P]\,[O_2] - K\,[X_P] = 0. \qquad (2)$$

(1) expresses the fact that X_O is formed both spontaneously, in some way left undetermined, the rate being expressed simply by $k_1\,F(c)$, and by collision of X_P with oxygen in the chain; and that X_O is destroyed both by reaction with phosphine and by some process at the wall, the rate of the latter being $K\,[X_O]$.

(2) expresses similar facts about the production and destruction of X_P. α molecules of X_P are supposed on the average to be formed from one of X_O, thus introducing the condition that the chains can branch. α is greater than unity. No spontaneous production of X_P is allowed for, but it is easily shown that there is no loss in generality on this account. Solving for $[X_O]$ we obtain

$$[X_O] = \frac{k_1 k_2\,[O_2]\,F(c) + Kk_1\,F(c)}{(1-\alpha)\,k_2 k_3\,[PH_3]\,[O_2] + k_2\,K\,[O_2] + k_3\,K\,[PH_3] + K^2}.$$

Assuming perfect efficiency for the collisions between X_O and PH_3 and between X_P and O_2, we have $k_2 = k_3$; moreover K^2/k_2 is probably small, since k_2 is large. Introducing these simplifications, and equating the *denominator* to zero, we find that $[X_O]$ increases indefinitely, *i.e.*, the stationary condition ceases to be possible, when

$$(\alpha - 1)\,k_3\,[PH_3]\,[O_2] = K\,([O_2] + [PH_3]).$$

Since K, which determines the rate at which X_O and X_P reach the wall, for unit concentration of either, is for a given tube inversely proportional to the total pressure we have $K = K_0/([O_2] + [PH_3] + [N_2])$.

Thus

$$(\alpha - 1)\,k_3\,[PH_3]\,[O_2] = K_0\,([O_2] + [PH_3])/([O_2] + [PH_3] + [N_2]).$$

Since concentrations are proportional to partial pressures, this condition becomes

$$p_{O_2} \cdot p_{PH_3}\left(1 + \frac{p_{N_2}}{p_{O_2} + p_{PH_3}}\right) = \text{constant}$$

for a given tube, as above.

As has been shown in the course of the preceding sections the experimental results conform in a general way to this equation. The mutual deactivation of X_O and X_P, not taken into account in the simple theory, probably accounts for the fact that $p_{O_2} \cdot p_{PH_3}$, in the absence of an inert gas, is not constant but passes through a maximum at approximately equal proportions of oxygen and phosphine. The effect of inert gases has already been discussed.

It has also been mentioned that in the first few experiments of a new series there is an increase in the explosibility of the gases, apparently connected with the accumulation in the tube of traces of a substance which is only removed by long continued evacuation. The possible cause may be somewhat as follows. The velocity of a reaction in which branching chains occur can be expressed by an equation of the form* $F(c)/\{A(1-\alpha)+B\}$. $F(c)$ is some function expressing the rate at which reaction centres are formed spontaneously, *i.e.*, independently of chains already in existence, B depends upon various factors which break the chains, and A depends on the mechanism by which the chain is propagated from link to link, but not on the original method of starting. α is the number of fresh centres formed at each link of the chain. The condition for explosion is that B becomes less than $A(\alpha - 1)$. This expresses the fact that the deactivating processes no longer balance the effect of the branching. This condition does not involve $F(c)$, and thus appears to be independent of the exact way in which the first chains are initiated. Nevertheless, if $F(c)$ were absolutely zero, no chains would begin to be propagated and the question of their rate of increase would not arise. Thus, although the initial process does not enter explicitly into the condition for explosion, we tacitly assume that a number of chains sensibly greater than zero actually start spontaneously. It is possible that the initial increase of explosibility depends, therefore, on traces of some product which actually helps to provide the necessary minimum number of spontaneously originated chains without which the whole mechanism would fail to start. The explanation of the imperfect reproducibility of successive experiments may be similar.

---

* Christiansen and Kramers, 'Z. physikal. Chem.,' vol. 104, p. 451 (1923).

Summary.

The rate of reaction between oxygen and phosphine is negligibly small when the pressure is below a certain critical value. At this value an explosion occurs.

The abrupt transition can be explained by means of the theory that the oxidation is a chain reaction, the limiting pressure being that at which chains begin to multiply more rapidly than they are broken by the walls of the vessel.

A simple theory leads to the following relation between the partial pressures of the various gases at the explosion point :—

$$p_{O_2} \cdot p_{PH_3}\left(1 + \frac{p_{N_2}}{p_{O_2} + p_{PH_3}}\right) = \frac{\text{constant}}{d^2}$$

where d is the diameter of the cylindrical containing tube.

This equation expresses the following facts, which are in many ways analogous to those found by Semenoff for the oxidation of phosphorus vapour :—

(*a*) That there is an inverse relationship between the pressures of phosphine and of oxygen in the absence of an inert gas ;

(*b*) That the mixture explodes more readily in presence of argon or nitrogen ;

(*c*) That the product of the pressures of phosphine and oxygen at the explosion point is inversely proportional to the square of the diameter of the tube.

There are certain deviations from the behaviour predicted by the simple theory, namely, (*a*) that in the absence of an inert gas $p_{O_2} \cdot p_{PH_3}$ is not quite constant, but passes through a maximum when $p_{O_2} = p_{PH_3}$, and (*b*) that the inert gas has a somewhat smaller effect than that calculated ; further (*c*) in wide tubes the product $p_{O_2} \cdot p_{PH_3} \cdot d^2$ tends to rise. These quantitative deviations are attributed to the fact that some of the chains are broken in the gas, and not solely at the walls as the theory postulates.

The Spectrum of H_2: *The Bands Analogous to the Orthohelium Line Spectrum.—Part* II.

By O. W. Richardson, F.R.S., Yarrow Research Professor of the Royal Society, and K. Das, King's College, London.

(Received July 18, 1929.)

§ 1. It will be recalled that all the bands in this group of band systems end on an electronic level with total quantum number 2, which does not combine with the ground level of H_2. For this and other reasons, we call them the bands analogous to the orthohelium line spectrum since the $n = 2$ level of that spectrum does not combine with the ground level of He. Since our former paper* was written a number of new facts have come to light bearing on this group of band systems. These will now be briefly described.

§ 2. *The System formerly called* $3\,{}^3S \rightarrow 2\,{}^3S$, *now called* $2\,{}^3S' \rightarrow 2\,{}^3S$.

Important additions have been made to this band system which require a reconsideration of its structure. By making use of Poettker's† infra-red measurements Sandeman‡ has found three bands with initial vibrational levels lower than those of any of the bands which we discovered. This makes it necessary to change the numbering of the initial vibrational levels which we gave. The progressions to which we assigned the initial vibrational numbers $n' = 0$, 1 and 2 should be $n' = 2$, 3 and 4 respectively. The 3 new bands found by Sandeman are the $0' \rightarrow 0''$, $0' \rightarrow 1''$ and $1' \rightarrow 1''$. The new additions made by Sandeman to our former Tables XIII and XIV are collected in Table I. The wave numbers are given, followed by Gale, Monk and Lee's§ eye estimates of intensities, in brackets.

These additions make considerable changes in the interpretation of the constants of the initial levels of the system such as, for example, are given in Table XV, and in § 8, of the former paper. The formula $F_n'(m) = B_n'(m - \varepsilon)^2 + \beta_n'(m - \varepsilon)^4$, with $\varepsilon = -\frac{1}{2}$ represents the initial rotational term values to the accuracy of the observational data. We have recalculated the constants B_n' and β_n' by the same methods as before and keeping throughout to

---

* Richardson and Das, 'Roy. Soc. Proc.,' A, vol. 122, p. 688 (1929).

† 'Phys. Rev.,' vol. 30, p. 418 (1927).

‡ 'Proc. Roy. Soc., Edinburgh,' vol. 49, p. 245 (1929).

§ 'Astrophys. J.,' vol. 67, p. 89 (1928).

Table I.

n' ↓	m ↓	n''→	0	1	2	
0	0	R	11658·7 (0*b*)			Also 3′ 2″ R (5) = 12484·3 3′ 2″ P (6) = 11887·92 and the following substitutions :— 14881·60 for 14885·15 = 1′ 1″ R (4) 14524·51 for 12527·9 = 1′ 2″ R (4)
	1	P	539·0 (3*a*)			
		R	697·8 (6)			
	2	P	459·3 (2*c*)			
		R	722·7 (2)			
	3	P	367·1 (1*a*)			
		R	733·4 (2)			
	4	P	263·23			
		R	729·9 (1)			
	5	P	148·85			
		R	712·3 (00)			
	6	P	024·3			
		R				
	7	P	10891·4			
1	0	R	13718·4 (2)	11193·97		
	1	P	601·7 (4)	080·7		
		R	751·3 (7)	230·3 (0*b*)		
	2	P	518·9 (3)	004·3		
		R	767·2 (1)	11252·65		
	3	P	420·7 (4)	10916·0		
		R	765·9 (1*a*)	11261·17		
	4	P	307·9 (1*b*)	10816·1		
		R	747·28	11255·56		
	5	P	181·3 (0*a*)	10705·2		
		R				
	6	P	042·2 (00)			
		R				

Table I—(continued).

n' ↓	m ↓	n'' →	0	1	2	
2	1	P			10623·1	
		R			10762·9	
	2	P				
		R				
	3	P			10464·6	
		R			10788·8	
	4	P			367·8	
		R		13137·01		
	5	P			260·6	
		R	15576·06 (00*a*)	13100·07		
	6	P		12466·4 (00)		
		R				
	7	P		12319·5 (1*b*)'		

the formulæ of the old quantum mechanics with the result shown in Table II.

Table II.

n' →	0	1	2	3
$2\ B_{n}'$ →	53·08	50·05	47·00	43·99
β_{n}' →	− 0·0141	− 0·0138	− 0·0139	− 0·0128

The value of $B_0 = 26 \cdot 54$ requires the moment of inertia in the vibrationless state $I_0 = 10 \cdot 42 \times 10^{-41}$ gm. cm.^{2} and the internuclear distance $r_0 = 1 \cdot 119 \times 10^{-8}$ cm. The value of α (the constant in $B_n = B_0 - \alpha n$) is 1·515. The value of β_0' calculated from the theoretical relation $\beta_0' = -4\ B_0'^3/\omega_0^2$ is − 0·0165. The empirical way of determining β_0' is less accurate than the theoretical, and the agreement is of the kind which is usually obtained. By adding 0·4 which is $\frac{1}{4}$th of the mean second difference (with m) to the initial vibrational differences of the P (1) lines we obtain the following formula for the vibrational terms of the initial rotationless states

$$w_n = 2130 \cdot 0\, n - 66 \cdot 45 n^2 - 0 \cdot 433 n^3.$$

The negative coefficient of the third power term in n in this expression is unusual.

From these coefficients and the foregoing values of B_0 and α we have determined* the coefficients in the energy equation

$$U = K\xi^2 (1 + a\xi + b\xi^2 + \ldots)$$

for the upper level, obtaining

$$U \text{ (in volts)} = 5 \cdot 282\, \xi^2 - 9 \cdot 274\, \xi^3 + 11 \cdot 53\, \xi^4.$$

In these expressions U is the energy at internuclear distance r, $\xi = r/r_0 - 1$ and r_0 is the equilibrium internuclear distance. The corresponding equation for the final states of these bands and of the α, β, γ bands is

$$U \text{ (in volts)} = 6 \cdot 238\, \xi^2 - 10 \cdot 21\, \xi^3 + 12 \cdot 12\, \xi^4 - 13 \cdot 4\, \xi^5 + 15 \cdot 5\, \xi^6.$$

The graphs for both states are drawn in fig. 1. The ordinates are the values of U in volts and the abscissæ are the values of r/a, where a is the radius of the first Bohr circle for H. A few of the vibrational levels are indicated by the broken horizontal lines. This band system extends to $n' = 4$, but as the $n' = 4$ level appears to be perturbed it has not been used in extracting the data.

From fig. 1 we can determine the theoretical intensity distribution among the vibrational transitions of the band system by Condon's method (see Richardson and Davidson, *loc. cit.*, p. 46). The result is shown in fig. 2. In this figure the vibrational transitions are set out by the usual double entry method, the final states being set out horizontally and the initial states vertically. The figures in the body of the diagram are Gale, Monk and Lee's estimates of the intensities of the R (1) lines, which are representative of the intensities of the bands as a whole. (There are no actual measurements of the intensities of these infra-red lines.) The solid curve gives the location of the intensity maxima, the dotted continuation of it being estimated, and the intervening broken straight line the position of the minima. These are the actual empirical estimations as published by Sandeman (*loc. cit.*, p. 254). The positions of the maxima as determined by us from fig. 1 by Condon's method are shown by the crosses in fig. 2. It will be seen that the agreement with the

---

* The details of the method by which this is done are fully described by Richardson and Davidson in 'Roy. Soc. Proc.,' A, vol. 125, p. 23.

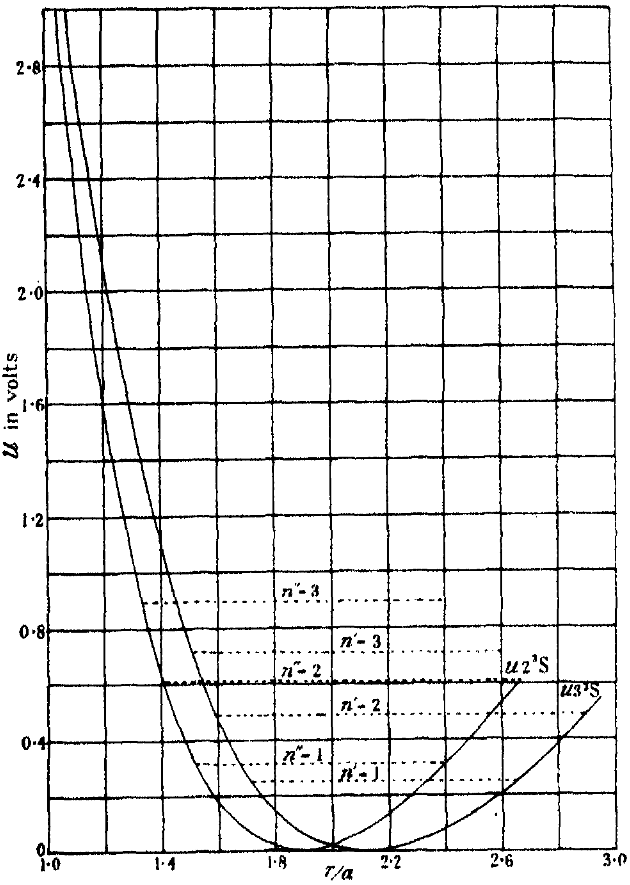

The level marked 3 ^3S in this figure is the level called 2 $^3S'$ in the present paper.

FIG. 1.

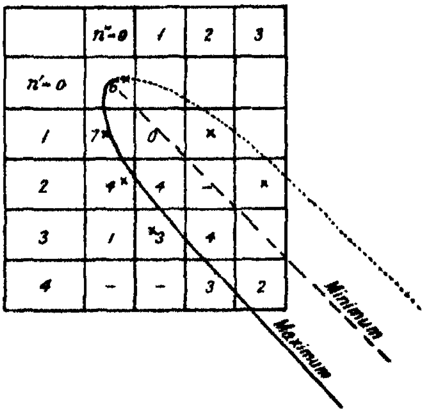

	$n''=0$	1	2	3
$n'=0$	6×			
1	7×	0	×	
2	4×	4	–	×
3	1	×3	4	
4	–	–	3	2

FIG. 2.

observed estimation by Sandeman is quite good. The divergence, such as it is, is similar to that found by Richardson and Davidson (*loc. cit.*, p. 46) for the band system—3′ B → 2′ S.

This agreement and the other reasons adduced by Sandeman lead us to the conclusion that there are no lower initial vibrational levels further out in the infra-red, and that the vibrational numbers have now been correctly assigned. It is therefore necessary to re-investigate the electronic status of this system. For the 0′ → 0″ band we have—

$$P(1) = \nu_0 + F'(0) - F''(1),$$

and $F'(0) = 6\cdot635$, $F''(1) = 75\cdot011$ giving $\nu_0 = 11607\cdot4$. Now the ν_e (electronic frequency), measured from the ground state of H_2+ which is the final product of ionisation, of the final $2\,{}^3S$ level is 29340 wave-numbers.* As the upper electronic level of these bands is 11607·4 *w.* nos. above this its ν_e is 17732·6. If this is equated to R/x^2 where R is Rydberg's constant the denominator x is 2·485. These values compare with the former $\nu_0 = 15597\cdot3$ $\nu_e = 13753$ and $x = 2\cdot825$ got with the wrong vibrational numbering of the bands. The new value of ν_e makes the equilibrium value $W(r_0)$ of the negative energy of this upper state equal to $W(H_2+) + \nu_e = 16\cdot16 + 2\cdot19 = 18\cdot35$ volts.

In our former paper we called the upper electronic level of this system $3\,{}^3S$. The reduction of the denominator from 2·825 to 2·485 makes the assignment of the principal quantum number 3 very doubtful. In fact, there are several reasons for thinking that this level is some kind of a new 2 S state. If we assume it to be a 2 S state we can calculate the heat of dissociation D (2 S) from the total negative energy $W(r_0) = 18\cdot35$ volts. This must be equal to the dissociation energy + the ionisation energy of the dissociation products. These are an unexcited and a 2-excited hydrogen atom. Thus $18\cdot35 = D(2\,S) + R + \frac{1}{4}R$ where R is Rydberg's constant in equivalent volts (13·54). This gives $D(2\,S) = 1\cdot42_5$ volts. On the other hand, if this upper state were taken to be a 3 S state we should have $18\cdot35 = D(3\,S) + R + \frac{1}{9}R$, the dissociated excited atom now having total quantum number 3. This would give $D(3\,S) = 3\cdot30_5$ volts. We can distinguish between these alternatives by estimating the heat of dissociation from the vibrational constants of the level. As there are only 5 vibrational levels of which the highest seems to be perturbed the extrapolation is rather long so that no great accuracy is to be expected. By using the graphical method we find $D = 2\cdot0$ volts. As the coefficient of n^3 in the expression for ω_n in terms of n is negative it would seem that $\omega_0^2/4x\omega_0$ should be an upper limit for D. The value of this is 2·1 volts.

---

* Richardson, 'Roy. Soc. Proc.,' A, vol. 113, p. 399 (1926).

These calculations definitely favour the view that this upper state is a 2 state so that provisionally we shall give it the symbol 2 ^{3}S′. In the notation used by Weizel* if the final state of the α β γ bands, which we denote by 2 ^{3}S, is $1s\sigma$. $2s\sigma$ $^3\Sigma$ the upper state of the present system is presumably $1s\sigma$. $2p\sigma$ $^3\Sigma$. It would thus correspond in the orthohelium system to the 2 ^{1}S state $1s\sigma$. $2p\sigma$ $^1\Sigma$, in the parhelium systems. Further evidence bearing on the principal quantum number of this state will be found in the next section.

§ 3. *A New Band System ending on* 2 ^{3}S.

This system lies in the blue, the stronger lines being distributed on each side of H_β. There are only P and R branches and it resembles the system 2 ^{3}S′ → 2 ^{3}S and the α, β, γ systems in having the R stronger than the P branches. It is not an extensive system, only 3 bands having been found. The wave numbers of the lines preceded by Kapuscinsky and Eymers'† measured intensities and followed by Gale, Monk, and Lee's‡ eye estimates, in brackets, are set out by the usual double entry method in Table II. A study of the properties of the lines as set out by Merton and Barratt§ shows that they possess the following features in common with the α and β bands :— The lines are given a greater intensity by Gale, Monk and Lee than by Merton and Barratt. This is especially the case for the lines with low rotational quantum numbers. The lines are enhanced at low pressures. They are depressed, particularly those with low rotational quantum numbers, by the condensed discharge. In some of the bands there is a tendency for helium to bring up the lines of higher quantum number ; others are unresponsive. None of them respond to the Zeeman effect. These are all features which characterise the α, β bands (see, for example, the tables of properties of the lines of the Q branches of the α bands given by Richardson in these Proceedings, vol. 113, p. 373 (1926)).

The lines show the alternation of intensity due to a 3 to 1 ratio in the weights of the consecutive rotational states which has been found to be characteristic of all the other bands of the H_2 spectrum. This is shown in Table III where the intensities of the P (2) lines are compared with $\frac{1}{6}$ of the sums of the intensities

---

* 'Zeits. f. Physik,' vol. 54, p. 321 (1929).

† 'Roy. Soc. Proc.,' A, vol. 122, p. 58 (1929).

‡ 'Astrophys. J.,' vol. 67, p. 89 (1928).

§ 'Phil. Trans.,' A, vol. 222, p. 369 (1922).

Table II.

n' ↓	m ↓	n''→	0		1	
0	0	R		20575·67 (3)		
	1	P	5·0	20459·24 (2)		
		R	73·7	20615·78 (9)		
	2	P	6·0	20376·15 (4)		
		R	10·8	20645·23 (3)		
	3	P	22·5	20285·06 (4)	? →	17780·37 (1*a*)
		R	34·5	20662·91 (6)		
	4	P	8·3	20185·85 (3)*		
		R		20668·61 (1)		
	5	P	9·5	20078·30 (2)†		
1	0	R	2·7	22722·65 (1)	5·5	20198·29 (3)
	1	P	15·1	22602·84 (2)	16·3	20081·77 (4)
		R	7·8	22761·81 (2)	18·5	20240·71 (5)
	2	P	7·3	22523·16 (2)	7·8	20008·60 (2)
	3	P	30·9	22431·10 (4)	16·2	19926·18 (5)

Final Rotational Term Differences.

	0′ 0″	1′ 0″
R (0) − P (2)	199·52	199·49
R (1) − P (3)	330·72	330·71
R (2) − P (4)	459·38	
R (3) − P (5)	584·61	

	1′ 1″
R (0) − P (2)	189·69
R (1) − P (3)	314·53

Initial Rotational Term Differences.

	0′ 0″
R (1) − P (1)	156·54
R (2) − P (2)	269·08
R (3) − P (3)	377·85
R (4) − P (4)	482·76

	1′ 0″	1′ 1″
R (1) − P (1)	158·97	158·94

? 2′ → 2″ R (1) = 19915·90 (00). ? 2′ → 2″ P (3) = 19616·95 (1*bh*).

* Given as 20184·63 in Gale, Monk and Lee's tables.

† Given as 20078·30 in Gale, Monk and Lee's tables.

of the P (1) and P (3) lines of each band, R (2) with $\frac{1}{6}$ {R (1) + R (3)} for the 0′ → 0″ band, R (0) with $\frac{1}{3}$ R (1) for the other two bands and $\frac{1}{3}$ P (3) with $\frac{1}{2}$ {P (2) + P (4)} for the 0′ → 0″ band. The agreement is satisfactory except in the case of R (2) and $\frac{1}{6}$ {R (1) + R (3)} for the 0′ → 0″ band. A com-

Table III.

	0′ → 0″	1′ → 0″	1′ → 1″		0′ → 0″		0′ → 0″		1′ → 0″	1′ → 1″
P (1) …………	5·0	15·1	16·3	P (2)* …………	6·0	R (1) …………	73·7	R (1) …………	7·8	18·5
P (3) …………	22·5	30·9	16·2	P (4) …………	8·3	R (3) …………	34·5			
$\frac{1}{6}$\{P (1) + P (3)\} ……	4·6	7·7	5·4	$\frac{1}{2}$\{P (2) + P (4)\} ……	7·2	$\frac{1}{6}$\{R(1) + R (3)\} ……	18·0	$\frac{1}{3}$ R (1) …………	2·6	6·2
P (2) …………	6·0	7·3	7·8	$\frac{1}{3}$ P (3) …………	7·5	R (2) …………	10·8	R (0) …………	2·7	5·5

parison of the intensities of the R (1), R (2), R (3) lines with those of P (3), P (4) and P (5) for this band suggests that R (2) is abnormally weak if it is correctly measured. The intensity measurements used are those of Kapuscinski and Eymers (*loc. cit.*).

The rotational term differences, such as F (2) — F (0), are given in Table II. The values, which are averages where there are more than one, of both the rotational and vibrational final term differences are collected, together with the mean values of the corresponding mean final term differences for the α, β, γ bands, in Table IV. In every case the values are identical within the accuracy of the measurements. This shows that the present bands have the same final electronic level ($2\,^3S$) as the α, β, γ bands and the band system described in § 2. It also shows that the numbering of the final vibrational levels given in Table II is correct.

Table IV.

Final Rotational Term Differences.

Vibrational level n''.	0	0	0	0	1	1
Rotational Term …………………	F(2)—F(0)	F(3)—F(1)	F(4)—F(2)	F(5)—F(3)	F(2)—F(0)	F(3)—F(1)
Mean value for present bands	$199{\cdot}50_5$	$330{\cdot}71_5$	459·38*	584·61*	189·69*	314·53*
Mean value for α, β, γ bands	199·50	330·77	459·43	584·64	189·74	314·54

Final Vibrational Term Differences.

Rotational level m.	0	1	2	3		
Vibrational term ………………	1″— 0″	* 1″ — 0″	1′ — 0″	1′ — 0″		
Value for present bands ………	2524·36	$2521{\cdot}08_5$	2514·56	2504·92		
Mean value for α, β, γ bands	$2524{\cdot}35_3$	$2521{\cdot}06_5$	2514·60	2504·85		

* Not mean values.

We now proceed to investigate the rotational structure of the upper levels of the bands. We adopt the rotational numbering of the lines shown in Table II where the value of m indicates the value at the final level, the lowest being $m = 0$. This is the same numeration as we used in the former paper. If F (m) denotes the rotational term value, with a single dash for initial and a double dash for final terms, we have

$$R(0) = \nu_0 + F'(1) - F''(0) \quad \text{and} \quad P(1) = \nu_0 + F'(0) - F''(1),$$

where $h\nu_0$ is the non-rotational part of the energy change.

Thus, $R(0) - P(1) = F'(1) - F'(0) + F''(1) - F''(0)$.

The values of the final term differences such as $F''(1) - F''(0)$ are well established and are given in Table VII on p. 705 of the former paper. For the lowest initial vibration state, numbered $n' = 0$ in Table II, we thus find $F'(1) - F'(0) = 49{\cdot}76_4$. Similarly from $R(1) - P(2) = F'(2) - F'(1) + F''(2) - F''(1)$ we find $F'(2) - F'(1) = 106{\cdot}80_3$ wave numbers. In this way we find the various level differences which are set out for the state designated $3\,{}^3S'$, $n = 0$ in fig. 3.

These terms are not capable of representation to the accuracy of the data by the expression $F(m) = B_0(m - \varepsilon)^2 + \beta_0(m - \varepsilon)^4$ with B_0, β_0 and ε constants; but such an expression comes very near to covering them. For example, the expression

$$F(m) = 28{\cdot}91\,(m + 0{\cdot}362)^2 - 0{\cdot}03324\,(m + 0{\cdot}362)^4$$

gives the following comparison between the calculated term differences and the directly observed term differences such as $F'(2) - F'(0)$ ($= R(1) - P(1)$) which involve no assumptions about the final levels.

Table V.

m	0	1	2	3	4	5
$F(m)$ calculated	3·79	53·52	160·37	322·55	538·07	804·11
$F(m+2) - F(m)$ calc.....	156·58	269·03	377·70	481·56		
$F(m+2) - F(m)$ obs.	156·54	269·08	377·85	482·76		

The agreement is satisfactory except at the last interval but we believe that the data cannot be forced into a complete fit with this formula.

To determine B_0 for small values of m we can employ another method. The effect of the 4th power term is small when m is small; so that we assume as a good approximation that this term can be neglected for values of m below 3. We then have simply $F(m) = B_0(m - \varepsilon)^2$ for $m = 0$, 1 and 2. With this we get $F(1) - F(0) = B_0(1 - 2\varepsilon) = 49{\cdot}76_4$ and $F(2) - F(1) = B_0(3 - 2\varepsilon) = 108{\cdot}80_3$. These give $B_0 = 28{\cdot}52$ and $\varepsilon = -0{\cdot}372$. These values compare reasonably with the values $B_0 = 28{\cdot}91$ and $\varepsilon = -0{\cdot}0362$ in the 2-term expression. It is quite likely that they are closer to the actual values near $m = 0$. The 3 third differences of the term values given for this level in fig. 3 give the following values of $-\beta$, viz.: 0·042, 0·038 and 0·018. These are not very constant but their average is close to the value $\beta = -0{\cdot}03324$ used in the 2 term expression. Anyhow, the data only allow of a rough guess at the magnitude of this constant by these methods. Its theoretical value from the formula $\beta_0 = -4B_0^3/\omega_0^2$ is $= -0 \cdot 019$, and the agreement is of about the kind to be expected.

For the higher vibrational upper level, called $n' = 1$ in Table II, by proceeding in the same way we obtain from $R(0) - P(1) = F'(1) - F'(0) + F''(1) + F''(0)$, etc., the level differences shown for the upper level designated $3\,{}^3S'$, $n = 1$ in fig. 3. In this case we only have the levels $m = 0$, 1 and 2 so that the 4th power term in $m - \varepsilon$ is of no interest. Assuming $F(m) = B_1 (m - \varepsilon)^2$ and proceeding as before we find $B_1 = 26 \cdot 34$ and $\varepsilon = -0 \cdot 509$. Thus at the $n = 1$ vibration level ε is practically equal to $-\frac{1}{2}$ as in the case of $2\,{}^3S$, $3\,{}^3P$, $4\,{}^3P$, $2\,{}^1S$ and many of the initial levels of the band systems which end on $2\,{}^1S$ (see Richardson and Davidson, 'Roy. Soc. Proc.,' A, vol. 123, p. 54, p. 457; vol. 124, p. 50, p. 69, 1929). Using $B_0 = 28 \cdot 52$ this value of B_1 leads to α (in $B_n = B_0 - \alpha n$) $= 2 \cdot 18$.

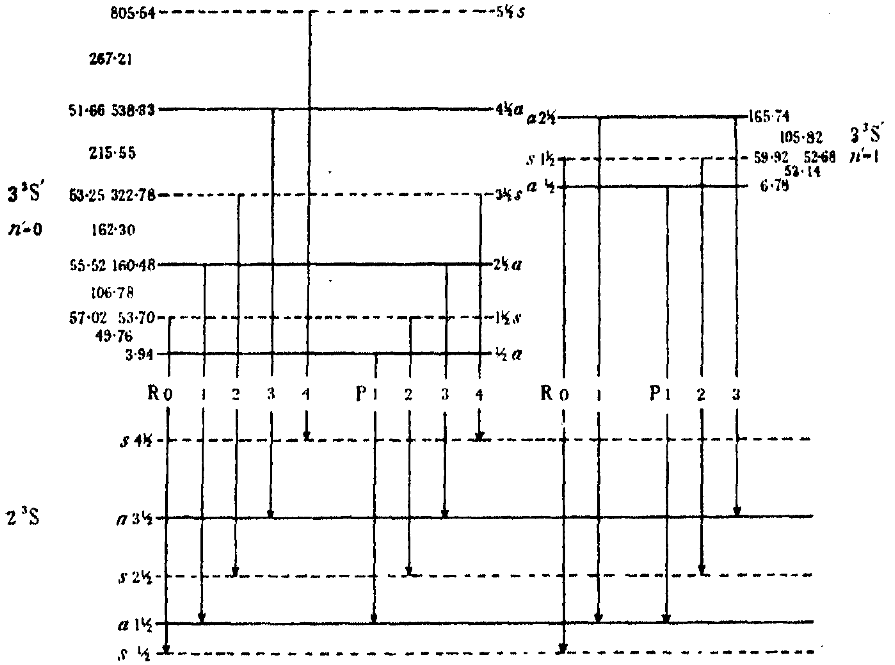

Fig. 3.

The values at the lowest level in fig. 3 are got by putting $F'(0) = B\varepsilon^2$ using $B_0 = 28 \cdot 52$, $\varepsilon_0 = -0 \cdot 372$ and $B_1 = 26 \cdot 34$, $\varepsilon_1 = -\frac{1}{2}$. It will be seen that for both the vibrational levels the rotational levels have alternately *a* and *s* character and that all transitions are from *s* to *s* or *a* to *a*. This together with $\Delta j = 0$ or ± 1 and the fact that the lowest level ($j = \frac{1}{2}$) has the *a* character determines all the transitions which occur including the absence of Q branches. The rotational structure is, in fact, the same as that of the upper level of the system considered in § 2, and which was described in the former paper (*loc. cit.*, p. 715). The strong lines are those which have *a* to *a* and the weak lines *s* to *s* transitions.

The final vibration numbers assigned to the bands in Table II are quite certain since they rest on well-established combinations. We also think that there is no reasonable doubt that the initial vibration numbers are correct. In the first place if the band with R (0) = 20575·67 were not the $0' \rightarrow 0''$ band there should be another strong band with R (1) in the neighbourhood of 18420 *w.* nos. It seems quite certain that no such band exists. The occurrence of a single strong $0' \rightarrow 0''$ band followed by all the rest weak or absent is a feature which is characteristic of and confined to $0' \rightarrow n''$ progressions in the α, β, γ systems. The $0' \rightarrow 0''$ band of the R′ P′ H_β system is comparable in intensity with but a little stronger than the band which we are calling $0' \rightarrow 0''$ of the present system; it is followed by a $0' \rightarrow 1''$ band represented by three very weak lines and the remaining bands of the progression absent. This is precisely similar to the present example where $0' \rightarrow 0''$ is strong, $0' \rightarrow 1''$ is represented by one weak line and $0' \rightarrow n'' > 1$ are all absent. In fact, if this were not a $0' \rightarrow n''$ progression it would be unique; because there is no progression in the whole number of systems, now exceeding 20, which have been arranged in the H_2 spectrum, in which $n' \rightarrow 0''$ is strong, n' to $1''$ is weak, and which is followed by no strength in the higher n'' bands ($n' \rightarrow n''$) which is not a $0' \rightarrow n''$ progression. Again the other progression is very similar to the $1' \rightarrow n''$ progression of the H_αQP′R′ system, which has $1' \rightarrow 1''$ a little stronger than $1' \rightarrow 0''$, both definitely weaker than $0' \rightarrow 0''$ and $1' \rightarrow 2''$ very much weaker than any of these.

The association of these bands as two progressions of the same system is justified by the values of B_0 and B_1 although the value of $\alpha = B_0 - B_1$ is perhaps rather large. However, the value of B_0 is not known very accurately so that α might be somewhat less than 2·18.

We can determine the non-rotational energy switch $h\nu_0$ from $P(1) = \nu_0 + F'(0) - F''(1)$. Putting $F''(1) = 75{\cdot}011$ $F'(0) = 3{\cdot}94$ this gives, from $0' \rightarrow 0''$ $P(1) = 20459{\cdot}24$, $\nu_0 = 20530{\cdot}41$. Similarly, from the upper vibrational level using $1' \rightarrow 0''$ $P(1) = 22602{\cdot}84$ and $F_1'(0) = 6{\cdot}78$ we have $\nu_1 = 22671{\cdot}17$. The difference $\nu_1 - \nu_0$ is $\omega_0 - x\omega_0 = 2140{\cdot}76$. As we have only two initial vibrational levels we cannot determine $x\omega_0$ but it is probably about 60. We can take ω_0 to be 2200 in round numbers with an uncertainty of one or two units at the third figure.

ν_0 measures the electronic switch from the upper electronic level of these bands to the level $2\,^3S$ which is 29,340 wave numbers below the ground state of H_2+; so that the electronic frequency ν_e of the upper level is $\nu_e = 29340 - 20530 \cdot 41 = 8810$ *w.* nos. If this term is equated to R/x^2 we have for the denominator $x = 3 \cdot 53$. From $\nu_e = 8810$ *w.* nos. we obtain the equilibrium value W (r_0) of the negative energy of the upper state of this system to be $= W(H_2+) + \nu_e = 16 \cdot 16 + 1 \cdot 09 = 17 \cdot 25$ volts.

The denominator 3·53 suggests that the upper level of this system is the next higher electronic level to the upper level of the system discussed in § 2 for which the denominator was $2 \cdot 48_5$. The values of B_0, B_1 and ω_0 for that level were 26·54, 25·03 and $2130 \cdot_0$. These compare with 28·52, 26·34 and about 2200 respectively for the upper level of the present system. As a rule these quantities are each smaller for higher members of the same set of electronic levels, but it is significant that the ratio B_0/ω_0 remains nearly constant (Mecke's rule) at about 0·0125 compared with 0·01297. A denominator of 3·53 would admit of a total electronic quantum number n either 3 or 4. If $n = 3$ the heat of dissociation calculated from W (r_0) by the method used at the end of § 2 is $2 \cdot 20_5$ in equivalent volts, if $n = 4$ it is $2 \cdot 86_4$. We cannot distinguish between these from internal evidence in the band system as in § 2 because we have only two upper vibrational levels, so that $x\omega_0$ is unknown. However, if this is the next higher electronic level corresponding to the upper level of the system of § 2 the proper choice is $n = 3$ since we decided that $n = 2$ for that system. In either event the vibrational stability, as measured by the heat of dissociation, is higher for the upper level of the present system. This is entirely reasonable on account of the larger values of B_0 and ω_0 and the smaller internuclear distance r_0. For these various reasons we have therefore decided to denote the upper electronic level of this system provisionally by the symbol $3\,^3S'$.

It should be added that there are two weak lines 19915·90(00) and 19616·95 (1 *bh*) in Gale, Monk and Lee's tables which may well be the R (1) and P (3) lines of the $2' \rightarrow 2''$ band of this system. The value of R (1) — P (3) has a defect of 0·13 *w.* no. which is about what is to be expected from an *h* line (probable blend). If these lines belong to the system they settle the value of $x\omega_0$ as 43 and ω_0 as 2184. If these are used to determine the heat of dissociation from $D = \omega_0/4x$ we find $D = 3 \cdot 43$ volts. This is in excess of the values got by assuming either $n = 3$ or $n = 4$, but if it is in excess by about the same proportion as the similarly calculated limit for the $2\ ^3S'$ level it would be more favourable to $n = 3$ than to $n = 4$.

§ 4. *Various Constants of $2\ ^3S'$ and $3\ ^3S'$.*

It is convenient to have these collected together. They are :—For $2\ ^3S'$:—$\nu_e = 17733$, denominator $= 2\cdot48_5$, $W(r_0) = 18\cdot35$, $D = 1\cdot42_5$, $\omega_0 = 2130$, $x\omega_0 = 67$, $B_0 = 26\cdot54$, $r_0 = 1\cdot119 \times 10^{-8}$, $\varepsilon = 0$, $\sigma = 0$. For $3\ ^3S'$:—$\nu_e = 8810$, denominator $= 3\cdot53$, $W(r_0) = 17\cdot25$, $D = 2\cdot20_5$, $\omega_0 = 2184$?, $x\omega_0 = 43$?, $B_0 = 28\cdot52$, $r_0 = 1\cdot114 \times 10^{-8}$, $\varepsilon =$ about $\frac{1}{8}$, $\sigma = 0$. ν_e, ω_0, $x\omega_0$, B_0 are in wave numbers, $W(r_0)$, D in volts, r_0 in cms. ν_e is measured from the ground state of the molecule ion, $W(r_0)$ is the equilibrium value of the negative energy (see p. 314). D is the heat of dissociation, ε is the constant in $F(j - \varepsilon)^2$ with j half integral and σ is the number of missing rotational levels.

§ 5. *Two New Progressions ending on $2\ ^3S$.*

In all the band systems hitherto found which have $2\ ^3S$ as the final state the bands arrange themselves in sequences with the strong bands having the same initial and final vibration quantum numbers ($n' = n''$) near the origin of the system ($n' = n'' = 0$). As n' increases there is a *tendency* for the strength to change over to $n' = n'' + 2$ at about $n' = 7$ in the $^3P \rightarrow 2\ ^3S$ bands, and at about $n' = 4$ in $2\ ^3S' \rightarrow 2\ ^3S$. We have now found a set of bands having $2\ ^3S$ as the final state which has the character of a well marked progression, *i.e.*, the vibrational transitions are from $n' \rightarrow n''$ where n' is constant and $n'' = 0, 1, 2, 3, 4$. As n' is unknown we denote it provisionally by y, a symbol which will also serve to indicate the progression. There is also another set consisting of a few lines of two bands only, perhaps hardly enough to merit the term progression, which we denote provisionally by $x \rightarrow n''$ or x for short. We are, however, describing these together as two progressions because we think that they are closely related.

The wave numbers of the lines preceded by Kapuscinski and Eymers' measures of their intensities and followed by Gale, Monk and Lee's eye estimates, in brackets, are given in Table VII. There are no strong lines in either progression. In x the strongest has an intensity of $20\cdot0$ in the scale of Kapuscinski and Eymers, whilst in y their highest measure is $15\cdot3$. However, this is a P (2) line and should be much weaker than the P (3) line of the same band which has a measure of $8\cdot6$. The properties assigned to it in

Merton and Barratt's tables (enhanced by the condensed discharge and by helium) are unusual in a P (2) line and R (0) is missing. It thus appears that this line is either abnormal or is covered up by some other line of unknown classification. Judging by Gale, Monk and Lee's eye estimates the strongest band of this progression is $y \rightarrow 3''$ which lies in the infra-red beyond Kapuscinski and Eymers' limit.

Below and between the wave numbers in Table VII are given the vibrational differences and at the bottom of the table are set out the corresponding differences for the Q branches of the H_α bands taken from Table I (p. 691) of our

Table VII.

n' ↓	m ↓	n'' →	0		1		2		3		4
x	0	R			18011·73 (1)						
	1	R		20·0	18035·41 (4)		15650·27 (1)				
						2385·14					
	2	R		2·6	18045·66 (1)						
	2	P			17821·99 (1)						
	3	P			17720·81 (1)		15351·49 (0)				
						2369·32					
	4	P			17608·81*(00)						

* Also R (3) of $0' \rightarrow 3''$ $3\,^1K \rightarrow 2\,^1S$.

y	0	R			19311·71 (00)				——14667·73 (0*h*)		
						2388·30		2255·68			
	1	R	21847·14 (0)		⌈19326·08 (0)	7·7	16940·99 (1)		14687·93 (4)		12564·0 (0*b*)
				2521·06		2385·09		2253·06		2123·93	
	2	R	21841·22 (1)	——	⌊19326·08 (0)	——			14700·79 (00)		
				2515·14		2378·42		2246·87			
	2	P	?21636·35 (1*a*)		19122·16 (00)	15·3	16743·17 (3)		——14495·86† (2)		
				2514·19		2378·99		2247·31			
	3	P			19011·51 (1)	8·6	16642·14 (2)		14404·38 (4)		12295·6 (3)
						2369·37		2237·76		2108·78	
	4	P					16532·87 (0*a*)		14307·13 (00)		12210·0 (0)
								2225·74		2097·13	

† Also P (4) of $3' \rightarrow 1''$ $2\,^3S' \rightarrow 2\,^3S$.

	0			2524·32		2388·26		2256·10		2126·86	
	1			2521·07		2385·12		2253·05		2123·85	
	2			2514·55		2378·80		2246·91		2117·78	
	3			2504·85		2369·41		2237·77		2108·83	
	4			2492·00		2357·06		2225·60		2096·57	

former paper. There are three blended lines whose wave numbers have defects of about 0·4 in y. These are R (0) of 3″ = 14667·73 (0h) — h is Gale, Monk and Lee's terminology for a probable blend — R (2) of 1″ = 19326·08 (0), which has to do duty also as R (1) of the same band, and P (2) of 3″ = 14495·86 (2) which is also $3' \rightarrow 1''$ P (4) of the system considered in § 2. The intervals affected by these are indicated by bars above the numbers. The agreement of the others with the corresponding final differences for the $2\,^3S$ level is within the accuracy of Gale, Monk and Lee's data except in two cases. The first is 21636·35 (1a) = P (2) of $y \rightarrow 0''$. The propriety of including this is doubtful; in fact, it is certain that most of it is something else. The other is $y \rightarrow 4''$ P (4) = 12210·0 (0). This gives the vibration interval $4'' - 3''$ for $m = 4$ as 2097·13 compared with 2096·57 from the former paper. However, it is quite uncertain what the true value of this interval is; there is, fortunately, no doubt about any of the others. In y four vibration intervals involve the wave numbers of missing R (m) lines. These have been got from the corresponding P ($m + 2$) lines by using the known final rotational term differences R (m) — P ($m + 2$) of $3\,^3P \rightarrow 2\,^3S$.

In Table VIII we set out the values of the final rotational term differences R (m) — P ($m + 2$) with the corresponding values from the α bands, taken from the former paper, immediately under them. The values in brackets involve a missing line whose wave number has been got from some other line by the vibrational combinations. When the status of the various lines is taken into account the agreement is quite satisfactory. Nearly all the real strength is believed to lie in the R (1) and P (3) lines and it is gratifying to find that the values for R (1) — P (3) are identical with those from the α system to the accuracy of the data. We believe that the identity of these rotational

Table VIII.

n' ↓		0	1	2	3	4
x	R (0) — P (2)		189·74			
y	R (0) — P (2)	(199·68)	189·55	(180·28)		
	R (0) — P (2) α	199·50	189·74	180·24		
x	R (1) — P (3)		314·60	298·78		
y	R (1) — P (3)		314·57	298·85	283·55	268·4
	R (1) — P (3) α		314·53$_5$	298·82	283·53$_5$	268·55
x	R (2) — P (4)		436·85			
y	R (2) — P (4)			(414·79)	393·66	(373·0)
	R (2) — P (4) α		436·91	415·03	393·71$_5$	372·74

terms together with that of the vibrational terms in Table VII establishes the reality of these bands beyond any doubt.

We have found some evidence of the existence of another set of branches, possibly Q, close to those of $x \rightarrow n''$. The lines are very faint and half of them coincide with stronger lines of other systems. This makes it difficult to decide whether these branches are real or not; so that it does not seem worth while to publish an account of them until they are supported by some additional evidence.

As to what these progressions are, it seems very probable that they constitute the $n' = 5$ and $n' = 6$ progressions of the system discussed in § 2 and denoted by $2\,{}^3S' \rightarrow 2\,{}^3S$. As we shall see this is borne out by an investigation of the vibrational and rotational structure of the initial levels of the bands and by the values of the resulting constants. We have pointed out already that the $n' = 4$ level had properties which deviated in some respects from those of the levels $n' = 0$, 1, 2 and 3. This was referred to in § 2 as an 'abnormality' at the $n' = 4$ level. This deviation is much more marked, if these bands belong to the system, at the $n' = 5$ level, and is carried on, with some rectification, into the $n' = 6$ level.

We turn first to the rotational structure of the initial levels. In both progressions we have both P and R branches ending on the well authenticated final levels of $2\,{}^3S$; so that there is no doubt about the j values of the initial levels and the actual level differences, except that we are confined entirely to three levels since we only have the lines R (0), R (1), R (2), P (2), P (3) and P (4). We assume the exclusion rules $\Delta j = 0, \pm 1$ and $s \rightarrow a$ or $a \rightarrow s$ not allowed which hold throughout the rest of this spectrum so far as it has yet been explored. The correctness of this is confirmed by the fact that the strength of these progressions lies in the R (1) and P (3) lines which end on $m = 1$ and 3 respectively. This shows that the alternation of intensity with a weight ratio of 3 to 1 is present as in the other bands of this spectrum. The data are too meagre for more than a rough estimate of this ratio in the present case.

From, for example, $P(m) = \nu_0 + F'(m-1) - F''(m)$, $m - 1 \rightarrow m$, we have $F'(m) - F'(m-1) = P(m+1) - P(m) + F''(m+1) - F''(m)$. The values of $F''(m)$ are given in the former paper. From them and the wave numbers of the P (m) lines we can thus calculate the values of the intervals $F'(m+1) - F'(m)$. In this way the data for $y \rightarrow 0''$ give $F'(2) - F'(1) = 77{\cdot}76$ and $F'(3) - F'(2) = 127{\cdot}15$. Such of the rotational terms of the H_2 band spectrum as are capable of being expressed by any known formula are covered by $F(m) = B(m - \varepsilon)^2 + \beta(m - \varepsilon)^4$ where B, β and ε are constants. We shall not get far wrong by assuming that the effect of the fourth power term will be small for m below 4 so we assume $F_n'(m) = B_n'(m - \varepsilon_n)^2$. Using this the two level differences give, for y, $2B' = 49 \cdot 39$ and $\varepsilon = -0 \cdot 0743$.

With the x progression we cannot proceed in precisely this way as the 0″ band is absent; but there are various other ways of obtaining the same information. The method adopted has been to calculate the wave numbers of the lines of the 0″ progression from those of the 1″ progression, using the final vibrational intervals of 2 ^3S, which are known with precision, and then proceed in the same way as we have outlined for y.

In Table IX we have set out in the last two columns, under $n' = 5$ for x and $n' = 6$ for y, the values of $F'(3) - F'(2)$, $F'(2) - F'(1)$, B′ and ε'

Table IX.

$n' \rightarrow$	0	1	2	3	4	5	6
$F'(3) - F'(2)$	157·73	148·73	139·46	130·64	127·27	136·56	126·91
$F'(2) - F'(1)$	105·77	99·57	93·58	87·52	83·68	87·10	77·96
B_n	25·98	24·58	22·94	21·56	21·80	24·73	24·48
$-\epsilon_n$	0·536	0·525	0·535	0·530	0·419	0·262	0·093
ν_0	11605·85	13669·65	15596·63	17386·52	19034·93	20505·00	21785·80
$\Delta_1 \nu_0$	2063·80	1926·98	1789·89	1648·41	1470·07	1200·80	
$-\Delta_2 \nu_0$		136·82	137·09	141·48	178·34	269·27	
$\Delta_3 \nu_0$		0·27	4·39	36·86	90·93		

obtained in this way. These are preceded by the corresponding quantities for the initial vibrational levels $n' = 0, 1, 2, 3, 4$ of the band system discussed in § 2, all extracted in the same way. Actually in constructing this table the R lines of the bands were used instead of the P lines. This accounts for the slight difference in the values for $n' = 6$ compared with the values got for y in the example just worked out. It will be seen that the values of all these quantities for $n' = 6$ are a smooth continuation of those for $n' = 0, 1, 2, 3$ and 4. The constancy of ε_n and the linearity of $F_n'(3) - F_n'(2)$, of $F_n'(2) - F_n'(1)$ and of B_n' as a function of n which holds for $n' = 0, 1, 2$ and 3 has already ceased at $n' = 4$ and the change at this level is in the direction and of such an amount as to point to the values found for $n' = 6$. The values found at the level x and put under $n' = 5$ do not lie on the same curve, the values of $F'(3) - F'(2)$, $F'(2) - F'(1)$ and B′ all being high. They are, however, not very far away and the value of ϵ for $n' = 5$ lies between the values for $n' = 4$ and $n' = 6$ at about the place to be expected. It seems highly probable, on this evidence, that these two progressions form the extension to the upper vibrational levels $n' = 5$ and $n' = 6$ of the system $2\,{}^3S' \rightarrow 2\,{}^3S$ considered in § 2.

This position is strengthened when we consider the wave numbers ν_0 of the origins of these progressions. These have been calculated, using $\nu_0 = R\,(0) + F''\,(0) - F'\,(1)$, $F'\,(1) = B_{n'}\,(1 - \epsilon_{n'})^2$ and $F''\,(0) = 8 \cdot 34_5$ (taken from the former paper), both for x and y and for all the progressions $n' = 0, 1, 2, 3$ and 4 of § 2. These have been set out under the respective values of n' in Table IX with those for x under $n' = 5$ and for y under $n' = 6$. The values of B_n and ϵ_n used in calculating $F'\,(1)$ are in each case those immediately above the respective value of ν_0. Below the values of ν_0 are given in succession the values of their 1st, 2nd and 3rd differences. Whilst the 3rd differences are far from constant they increase in a regular manner with n'. Thus, the vibrational properties agree with the rotational in placing these bands in the same system.

If these progressions are the $n' = 5$ and $n' = 6$ progressions of $2\,{}^3S' \rightarrow 2\,{}^3S$, the vibrational energy is approaching that required to dissociate the molecule $2\,{}^3S'$. The vibrational and rotational energy of the upper state of $21841 \cdot 22$, if it is $6' \rightarrow 0''$ of $2\,{}^3S' \rightarrow 2\,{}^3S$, is about 10430 *w.* nos. $= 1 \cdot 288$ volts. The next higher vibrational level would be about $0 \cdot 125$ volts above this and would lift the energy to just about the value for dissociation found in § 2, viz., $1 \cdot 42_5$ volts. It is hardly to be expected that this level will occur.

§ 6. *A New Band in the Yellow.*

This is only a single band but it contains one of the few remaining strong lines which are not classified. It has every appearance of being authentic, and, if so, its final state is the vibrational state $n'' = 1$ of $2\,{}^3S$. This makes it important as showing that there is at least one undiscovered system with some strength which ends on $2\,{}^3S$.

Gale, Monk and Lee's wave numbers followed by their eye estimates of intensities, in brackets, and preceded by Kapuscinski and Eymers' measured intensities of the lines are set out in Table X. The strong lines R (1) and P (3) are recorded as enhanced at low pressures by Merton and Barratt. The intensity measures show that the mean of $R\,(0) + R\,(2)$ is not far from $\frac{1}{3}$ of R (1) and that of $P\,(2) + P\,(4)$ is close to $\frac{1}{3}$ of P (3), showing that the alternation of intensity with a weight ratio of 3 to 1 is present. The final term differences $R\,(n) - P\,(m + 2)$ are set out in Table X above the corresponding term

Table X.

$m \rightarrow$	0	1	2	3
R (m)	14·2 17778·92 (4)	57·8 17812·31 (10)	14·1 17837·29 (3)	2·7 17853·78 (1)
P $(m+2)$	19·4 17589·17 (3)	33·5 17497·72 (5)	17400·48 (1)	
R $(m)-$P $(m+2)$	189·75	314·59	436·81	
[R $(m)-$P $(m+2)$] a	189·74	314·54	436·91	

differences for the $n'' = 1$ level of the α bands taken from the former paper and the numbers show a good agreement.

The initial rotational term differences for this band have been extracted by the method used in dealing with the x progression in § 5. They are $F'(4) - F'(3) = 204\cdot77$, $F'(3) - F'(2) = 151\cdot29$ and $F'(2) - F'(1) = 96\cdot81$. The successive differences of these numbers are 53·48 and 54·38. If we assume that $F'(m) = B'(m - \varepsilon')^2$ holds up to $m = 3$ as a sufficient approximation we obtain $B' = 27\cdot19$ and $\varepsilon' = -0\cdot28$. If we treat it as the second band $n' \rightarrow 1''$ of an n' progression of which the first $n' \rightarrow 0''$ does not occur the value of ν_0 for the progression is $20627\cdot_0$.

Up to the present we have not found any other bands which belong to the same system as this, and until this is done there will, of course, be a certain amount of doubt as to its reality.

§ 7. *The* α, β, γ *Band Systems.*

A paper has recently appeared by Finkelnburg and Mecke[*] which deals with the Q branches of this series of systems. The authors have added a few lines to the α system and made considerable additions to the β system, as these systems were described in our former paper. We think, however, that the validity of some of these additions is very doubtful, the new lines either having the wrong properties or giving bad combinations or both. In particular we think that in the β system the reality of the $\Delta n = n'' - n' = 3$ sequence and of the $n' = 5$ progression are both extremely doubtful. We are not yet prepared to discuss the details of the γ and higher systems, the elucidation of which is undoubtedly difficult. Finkelnburg and Mecke propose to call these systems the singlet systems of H_2, as they claim to have found[†] a triplet structure in the bands analogous to the parhelium line spectrum described by Richardson and Davidson. This means that either at the switch $1\,{}^1S \rightarrow 2\,{}^1S$, which occurs in the absorption spectrum of unexcited H_2, or at the switch $3\,^1A\ 3\,^1B\ 3\,^1C \rightarrow 2\,^1S$, which includes the strongest lines in the emission spectrum in the visible, there is a transition from triplet to singlet states, or else, that the ground state of H_2 is a triplet state. These alternatives all seem to us extremely improbable. Accordingly we prefer for the present to retain the symbols $m\,^3P \rightarrow 2\,^3S$ for the α, β, γ band systems, although no measurable triplicity of the lines has yet been found, as they recall the undoubted analogy between the spectrum of H_2 and the line spectrum of He, and the fact that there are no known transitions from the final states of these bands to the ground state of H_2.

---

[*] 'Zeits. f. Physik,' vol. 54, p. 198 (1929).

[†] Finkelnburg and Mecke, 'Zeits. f. Physik,' vol. 54, p. 597 (1929).

The Isotherms of Hydrogen, Carbon Monoxide and their Mixtures.

By Gordon A. Scott, B.Sc., D.I.C., High Pressure Gas Research Laboratories of the Imperial College of Science and Technology, London.

(Communicated by W. A. Bone, F.R.S.—Received May 22, 1929.)

Introduction.

In investigations involving gases at high pressures it is as essential to know the relative densities of the media concerned as it is their actual pressures. This demands a knowledge of the deviations from the ideal gas laws over wide ranges of pressure and temperature for each particular medium.

Although reliable data are available for the commoner single gases, with perhaps the exception of carbon monoxide, as yet little is known concerning the compressibility of mixtures, except generally that neither the Law of Partial Pressures nor the Law of Additive Volumes is strictly obeyed. In this connection the recent researches of Masson, Verschoyle, Bartlett, Keyes and their co-workers have been very informative, yet a great deal more work needs to be done before such lacunæ in our knowledge of such matters are filled.

An apparatus for determining the compressibility of gaseous media has been developed in the High Pressure Gas Research Laboratories at the Imperial College, London, under the direction of Prof. W. A. Bone; and some time ago at his suggestion the author commenced to determine the isotherms of hydrogen, carbon monoxide and mixtures of the two in the molecular proportions 2 : 1, 1 : 1, and 1 : 2, the first-named mixture being of importance in connection with the industrial synthesis of methyl alcohol. The present paper describes the apparatus and method employed as well as the results obtained over a pressure range up to 170 atmospheres at a temperature of 25° C.

The Isotherms of the Single Gases.

(*a*) *Hydrogen Isotherm.*—Although many investigators have studied the compressibility of hydrogen it would appear that no direct measuremets have been made at 25° C. In the recent work of Gibby, Tanner and Masson* carried out at this temperature, pressures were measured by comparison with hydrogen as the standard, and for this purpose an equation interpolated from Holborn and Otto's† figures was used, as follows :—

$$pv_A = 1 \cdot 090850 + 0 \cdot 656 \times 10^{-3} p + 0 \cdot 105 \times 10^{-6} p^2.$$

The isotherm determined in the present investigation is best expressed by the equation

$$pv_A = 1 \cdot 09090 + 0 \cdot 651 \times 10^{-3} p + 0 \cdot 033 \times 10^{-6} p^2,$$

which will be seen to be in close agreement with the interpolated Berlin equation.

(*b*) *The Carbon Monoxide Isotherm.*—The only researches hitherto carried out on the compressibility of carbon monoxide at high pressures were those of Natterer‡ and those of Amagat.§ In the former case the gas was compressed into a steel vessel at pressures up to 3000 atmospheres and then released by letting out successive quantities each occupying at atmospheric pressure 10 times the volume of the vessel, and measuring after each release of gas the resultant pressure. Unfortunately neither was the temperature of determination stated, nor are the figures suitable for comparison. In 1880 Amagat published a few relative figures only, covering a pressure range between 30 and 400 atmospheres, but apparently did not pursue the study of this gas in his later researches.

The equation expressing the isotherm determined in the present investigation is

$$pv_A = 1 \cdot 09196 - 0 \cdot 4393 \times 10^{-3} p + 3 \cdot 55 \times 10^{-6} p^2.$$

---

* 'Roy. Soc. Proc.,' A, vol. 122, p. 283 (1929).

† 'Z. Physik,' vol. 23, p. 77 (1924), and vol. 33, p. 1 (1925).

‡ 'Sitz. Wien Akad. and Pogg. Ann.' (1844 to 1855).

§ 'Ann. Chim. Phys.,' vol. 19, p. 345 (1880).

Experimental.

Apparatus and Method.—In principle the method employed was that first used by Natterer, afterwards by both Wroblewski and Witkowski, and more recently by Holborn in Berlin and Bartlett in the American Nitrogen Fixation Research Laboratories. It consisted in filling, at a known constant temperature, a vessel of known constant volume with the gas or mixture under investigation up to a given accurately measured pressure, and upon releasing the gas determining its volume at atmospheric pressure.*

It has an advantage over the alternative method of compressing a constant mass of the gas at constant temperature and determining its diminished volume at selected higher pressures in that the entity finally measured increases instead of diminishes with the degree of compression, so that the experimental error does not increase. The apparatus employed consisted essentially of the following parts: (i) a high pressure vessel; (ii) its filling system; (iii) a glass measuring system; (iv) an accurate pressure balance; and (v) a water bath fitted with a plate glass window and maintained at a constant temperature of 25° C. and in which the high pressure vessel and the glass measuring system were immersed.

(i) *The High Pressure Vessel* was a mild steel cylinder 30 cm. long, 7·5 cm. external diameter, with a bore of circular section 1 cm. in diameter running longitudinally through its entire length and capable of withstanding an internal pressure of 2000 atmospheres. One end was closed with a blank screw plug, whilst into the other end was screwed a needle valve. The desired accuracy for the *pv*-values of the gaseous media necessitated knowing precisely the volume (approximately 28 c.c.) of the vessel to *at least* 0·01 c.c., which corresponded with an error of 0·035 per cent. in the final values.

The direct use of mercury for the determination of this volume was precluded for several reasons which need not be discussed here. The method eventually adopted consisted in (*a*) evacuating the vessel down to below 0·01 mm. of mercury, (*b*) allowing air to flow into it from a glass bulb, and (*c*) measuring the quantity of mercury required to be admitted to the bulb in order to restore atmospheric pressure to the system. This method was found to be capable of giving concordant results of an accuracy depending upon the smallest quantity of mercury which could be added to produce a perceptible change in the pressure of the system. With the mercury jet in use this was found to be 0·006 c.c.

---

* It should be mentioned that all pressures in this paper are given in terms of standard atmospheres equivalent to 760 mm. of mercury measured at sea level in latitude 45° and at 0° C. In the High Pressure Laboratories of the Imperial College this pressure corresponds to 759·55 mm. of mercury at 0° C.

The arrangements for the operation are shown in fig. 1, which is self-explanatory. The high pressure vessel A in position in the water bath was first of all evacuated by means of a " Hyvac " pump attached at *m*, the vacuum being determined by the appearance in a discharge tube B. As soon as a vacuum of below 0·01 mm. was attained, the valve at A was shut and air allowed to enter the outside system. When thermal equilibrium had been attained, the system was closed from the outer atmosphere by turning tap *n* ; valve A was then opened and at the same time mercury was admitted into the bulb C (also immersed in the water bath) until atmospheric pressure had been restored in the system. By weighing the mercury so admitted the volume of the high pressure vessel was obtained. The mean of 12 determinations gave the value of 27·793 c.c.

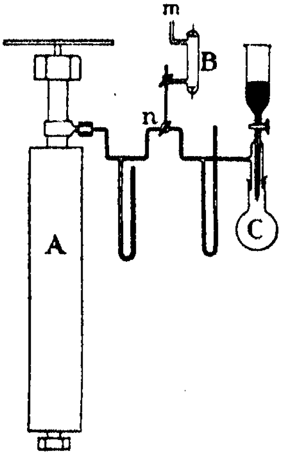

Fig. 1.

(ii) *The filling system* allowed of the compression (without any contamination) of pure gas into the high pressure vessel and the measurement of its pressure when so compressed. The essential parts (fig. 2) were the glycerine pump D and the mercury pump E.

The *glycerine pump* consisted of a cast-iron cylinder, D, of about 3 litres capacity into which the gas or gaseous mixture was admitted at slightly above atmospheric pressure from a 50-litre copper gas holder. A 50 per cent. mixture of glycerine and water (in which the gases are practically insoluble) was then pumped into the bottom of this cylinder, thus compressing the gas into the upper cylinder, E_1, of the mercury compressor. When the level of glycerine reached nearly to the top of the cylinder (as indicated by the amount pumped from the glycerine mixture reservoir) valve *q* was closed and valve *r* opened to allow the glycerine mixture to return to its reservoir, and at the same time to draw in a fresh supply of gas from the gas holder. In passing to the mercury pump the gas was dried by contact with redistilled and highly purified phosphorus pentoxide contained in the steel tube F. By repeating this operation a store of gas was obtained in the cylinder E_1, its pressure, indicated by the standard Bourdon gauge G, not exceeding 100 atmospheres which was the limit attainable by the glycerine pump.

The *mercury pump*, which operated on the same principle as the glycerine pump, consisted of two steel cylinders, an upper E_1 and a lower E_2, each of

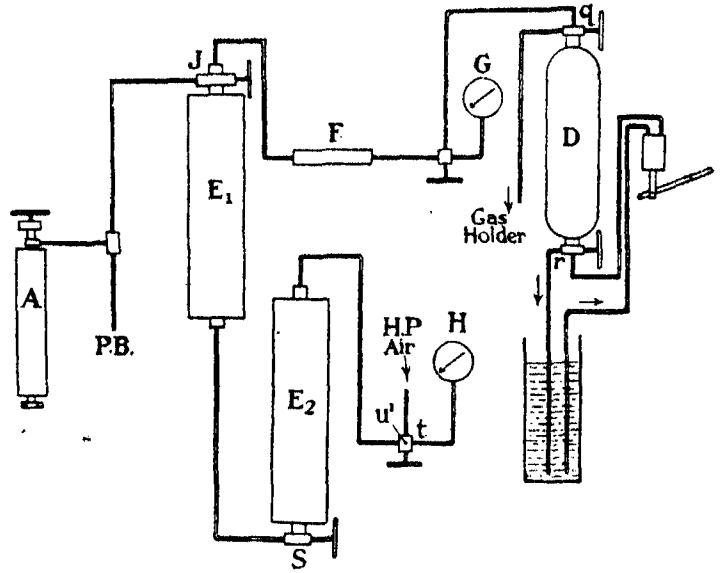

Fig. 2.

about 500 c.c. capacity and designed to withstand pressures of 2000 atmospheres. They were connected at their lower ends by a steel capillary which could be closed by a needle valve S. The gas in the upper cylinder (in this case already at 100 atmospheres pressure) was further compressed by raising the mercury from the lower cylinder with compressed air. This operation was controlled by a valve *t* to which was attached a standard Bourdon gauge H and a release valve *u*.

The high pressure vessel A was connected to the mercury pump by way of a capillary and 3-way piece to which was attached the pressure balance PB. The filling system could be shut off by closing valve J.

(iii) The *glass measuring system* (fig. 3) consisted of a series of three accurately calibrated gas burettes of 500 c.c., 300 c.c. and 100 c.c. approximate capacity respectively. Each terminated at the upper end in a short capillary tube and a 3-way tap sealed into a common horizontal capillary. At one end of this capillary a 2-way tap connected either to a U-tube manometer or to the outlet, while at the other end connection could be made to the high pressure vessel. The 100 c.c. burette was graduated throughout its entire length; the larger ones, however, were graduated only on short stems at their lower ends. Below the graduations in each case was sealed a vertical tube which served to show the approximate pressure of the gas in the burette. Each burette was also sealed at the base into a stout horizontal glass tube which connected by means of pressure tubing with a mercury reservoir. The mercury in the burettes was raised or lowered by means of water pressure or by suction.

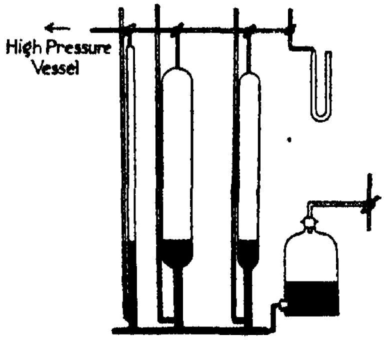

Fig. 3.

(iv) Pressures were measured by means of a *pressure balance* supplied by Messrs. Budenberg & Co.; the diameter of its piston was measured at the National Physical Laboratory and found to be 0·15946 inch which corresponds to a cross-section of 0·12884 sq. cm. For the purpose of the present investigation this value was accepted as the effective area at all pressures. By observing the movement of the piston with a cathetometer the balance was found to have a sensitiveness of 1 part in more than 20,000 at the highest pressures employed.

(v) The *water-bath* consisted of a galvanised iron tank 60 cm. long, 30 cm. wide and 80 cm. high. In it were mounted the high pressure vessel together with the burette system and its mercury reservoir. In the front of the tank a window of plate glass (50 cm. high, 30 cm. wide) was fitted through which the gas burettes could be read by a method whereby parallax was avoided. The water was maintained at a constant temperature of 25° C. by an ordinary thermostat control containing about 200 c.c. of xylene, thorough stirring being effected by means of a horizontal paddle wheel driven by a 1/25-h.p. electric motor. The temperature, which was chosen as being that most easily controllable in the region of the ordinary atmospheric temperature, was checked by a Beckmann thermometer, calibrated against a standard Charlottenberg thermometer.

Procedure.—In making a determination the high pressure vessel was first of all evacuated, then connected to the filling system and filled with gas from the mercury pump. When the gas had been in the high pressure vessel long enough to allow of the attainment of thermal equilibrium, the needle valve at A (fig. 2) was just closed and the pressure accurately measured by means of the pressure balance. The valve was then finally turned to "pressure tightness," the mercury pump shut off and the filling system disconnected.

The high pressure vessel was next connected to the glass measuring system and the gas allowed to expand slowly into the burettes, at the same time mercury being withdrawn from them at such a rate that the gas pressure could be maintained approximately at that of the atmosphere. When the burettes were full, the flow of gas was arrested and connection made by means of the 2-way tap with the U-tube manometer. By further adjustment the gas was brought accurately to atmospheric pressure and its volume read. Subsequently the burettes were refilled with mercury, the gas at the same time being expelled and collected in a gas holder. This operation was repeated until all the gas had been released from the high pressure vessel and its total volume measured. As the amount of gas to be released at any particular pressure was known approximately, the burettes were used in such an order that the final reading could be made in the 100 c.c. burette, which was graduated throughout its whole length.

Preparation of Gases.—(1) The hydrogen was obtained in cylinders through the kindness of the Osram (G.E.C.) Lamp Company and guaranteed to have a purity of 99·9 per cent. This was checked by chemical analysis and found to be correct.

(2) The carbon monoxide was prepared in these laboratories by dropping formic acid (95 per cent.) on to warm concentrated sulphuric acid. The gas after being scrubbed by passing through a 5-foot column of pumice sprayed with a 50 per cent. solution of caustic potash was collected in a large gas holder. Analysis showed it to have a purity of over 99·5 per cent. and to be quite free from both hydrogen and carbon dioxide, the only impurity being air. Since the compressibility of carbon monoxide differs but little from that of air, it was deemed justifiable to assume its compressibility to be unaltered by the presence of this very small air content.

It should be added that steps were taken to make sure that no perceptible iron carbonyl had been formed during the short time that the compressed gas was in contact with the walls of any steel cylinder or pressure vessel employed either during its compression or the subsequent compressibility determinations.

(3) The experimental mixtures of carbon monoxide and hydrogen in the proportion of 2 : 1, 1 : 1 and 1 : 2, respectively, were carefully made up in gas holders and samples taken before and after compression and also after release from the high pressure vessel. Their compositions were determined by chemical analysis and found to be unaltered.

Results.

Calculation.—If the absolute pressure recorded by the pressure balance be P_2 atmospheres and the total volume of the gas upon expansion and measured at atmospheric pressure (P_1) and t° C. be V_1; then if V_2 be the volume of the high pressure vessel

$$pv_A = (1 + \alpha t)\, P_2V_2/P_1V_1,$$

where pv_A is the pressure-volume product at P_2 atmospheres pressure and t° C. of a mass of gas occupying unit volume at 1 atmosphere and 0° C.; α being the coefficient of expansion of the gas at a constant pressure of 1 atmosphere and t the temperature of determination (25° C.). The value of α for the separate gases and their mixtures has been taken as 0·003662. This value holds well for hydrogen, and, although 0·0036688 was given by Regnault for carbon monoxide there appears to be little recent information in respect of this gas and the former value has therefore been adopted in each case. The only difference this has made is that the pv_A values for this gas are 0·0001 lower than they would have been, had Regnault's figure been employed.

A Typical Determination.—As illustrating the method of calculating pv_A values, the following figures in respect of a typical experimental determination of a point on the isotherm of the 66·3 per cent. hydrogen mixture, may be cited :—

Temperature of water bath (t)	25·00° C.
Pressure balance (reading)	90·242 atmospheres.
Barometer reading	752·65 mm.
Temperature	16·8° C.
Corrected to 0° C.	750·60 mm.
In terms of standard atmospheres (P_1)	0·9884 atmospheres.
Pressure of gas before release (P_2) (*i.e.*, Pressure balance reading + atmospheric pressure)	91·230 atmospheres.
Volume of gas released and measured at 25·00° C. and atmospheric pressure	2426·60 c.c.
Volume of high pressure vessel (V_2)	27·793 c.c.
Total volume of gas at 25° C. and atmospheric pressure (V_1)	2454·39 c.c.
Coefficient of expansion (α)	0·003662.

$$pv_A = (1 + \alpha t)\, P_2V_2/P_1V_1 = 1{\cdot}09155 \times 1{\cdot}0452$$
$$= 1{\cdot}1409 \text{ for the mixture at } 91{\cdot}230 \text{ atmospheres and } 25^\circ \text{ C.}^*$$

---

* Using the value of 91·230 for p in the experimental equation $pv_A = 1{\cdot}09109 + 0{\cdot}4626 \times 10^{-3}\, p + 0{\cdot}947 \times 10^{-6}\, p^2$ the value obtained is 1·14117.

Isotherms.—Between 50 and 60 experimental determinations of pv_A for each isotherm were made over the whole pressure range and plotted as ordinates against pressure as abscissæ (fig. 4). From smooth curves drawn through these points, values were read off at intervals of 10 atmospheres (Table I).

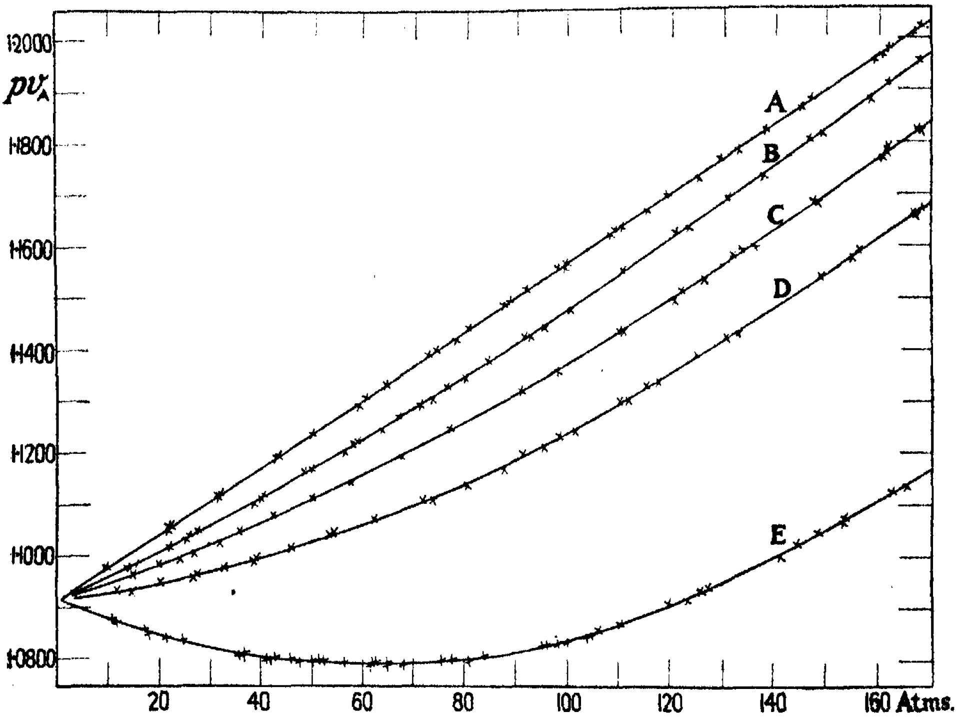

Fig. 4.—Isotherms at 25° C.

A, Hydrogen. B, 66·3 per cent. H_2, 33·7 per cent. CO. C, 51·7 per cent. H_2, 48·3 per cent. CO. D, 33·1 per cent. H_2, 66·9 per cent. CO. E, Carbon monoxide.

The isotherms so determined may be represented in the usual manner by equations of the form

$$pv_A = a + bp + cp^2,$$

where a, b and c are constants. The values of these constants (Table II) were found by the method of least squares which was applied to the figures in Table I.

Table I.—pv_A values at 25° C.

P (atmos.).	H_2.	66·3 per cent. H_2, 33·7 per cent. CO.	51·7 per cent. H_2, 48·3 per cent. CO.	33·1 per cent. H_2, 66·9 per cent. CO.	CO.
1	$1{\cdot}0915_5$	$1{\cdot}0915_5$	$1{\cdot}0915_5$	$1{\cdot}0915_5$	$1{\cdot}0915_5$
10	1·0973	1·0955	1·0945	1·0926	1·0876
20	1·1039	1·1005	1·0980	1·0942	1·0846
30	1·1103	1·1056	1·1022	1·0965	1·0823
40	$1{\cdot}1167_5$	1·1110	1·1065	1·0992	1·0806
50	1·1235	1·1165	1·1110	1·1023	1·0797
60	1·1300	1·1223	1·1155	1·1060	1·0790
70	1·1367	1·1280	1·1203	1·1095	1·0794
80	1·1432	1·1343	1·1257	1·1138	1·0801
90	1·1498	1·1405	1·1310	1·1184	1·0814
100	1·1563	1·1470	1·1370	1·1235	1·0836
110	1·1628	1·1537	1·1430	1·1293	1·0867
120	1·1694	1·1604	1·1492	1·1350	1·0906
130	1·1760	1·1675	1·1555	1·1411	1·0948
140	1·1826	1·1746	1·1625	1·1474	1·0997
150	1·1892	1·1820	1·1690	1·1540	1·1050
160	1·1959	1·1893	1·1760	1·1608	1·1106
170	1·2024	1·1965	1·1832	1·1677	1·1165

Table II.—$pv_A = a + bp + cp^2$.

	a.	$b \times 10^3$.	$c \times 10^6$.
H_2	1·09090	0·6511	0·033
66·3 per cent. H_2, 33·7 per cent. CO	1·09109	0·4626	0·947
51·7 per cent. H_2, 48·3 per cent. CO	1·09122	0·3281	1·28
33·1 per cent. H_2, 66·9 per cent. CO	1·09142	0·1514	1·88
CO...	1·09196	−0·4393	3·55

Volume Calculations from Isotherms.—For practical purposes it is often desirable to know the volume obtainable when a gas is released to atmospheric pressure from a vessel containing the gas at a known pressure. Such volumes referred to the volume of the vessel as unity are numerically equal to the density of the gas at the particular high pressure similarly referred to its density at atmospheric pressure and at the same temperature. For a gas obeying Boyle's Law such densities or volumes would be numerically equal to the pressure. It has been customary in these laboratories to make use of curves showing the differences of volume obtained on expansion above or below that which would be obtained for a "perfect" gas. Such values for the gases and mixtures herein studied are given in Table III and plotted in fig. 5.

Table III.—Difference between volume obtained on expanding gas from P atmospheres to 1 atmosphere and that which would be obtained for a "perfect" gas.

P (atmos.).	H_2.	66·3 per cent. H_2, 33·7 per cent. CO.	51·7 per cent. H_2, 48·3 per cent. CO.	33·1 per cent. H_2, 66·9 per cent. CO.	CO.
1	—	—	—	—	—
10	−0·05	−0·04	−0·03	−0·01	+0·03
20	−0·22	−0·16	−0·12	−0·05	+0·11
30	−0·51	−0·38	−0·28	−0·14	+0·26
40	−1·00	−0·70	−0·51	−0·28	+0·40
50	−1·42	−1·12	−0·88	−0·49	+0·55
60	−2·04	−1·64	−1·29	−0·79	+0·70
70	−2·78	−2·27	−1·80	−1·14	+0·78
80	−3·62	−3·01	−2·43	−1·60	+0·84
90	−4·55	−3·91	−3·14	−2·17	+0·84
100	−5·60	−4·84	−4·00	−2·85	+0·73
110	−6·75	−5·92	−5·06	−3·69	+0·49
120	−7·99	−7·12	−6·02	−4·60	+0·10
130	−9·34	−8·46	−7·22	−5·66	−0·39
140	−10·79	−9·91	−8·54	−6·83	−1·04
150	−12·32	−11·47	−9·97	−8·13	−1·76
160	−13·96	−13·17	−11·50	−9·57	−2·75
170	−15·68	−14·93	−13·18	−11·10	−3·81

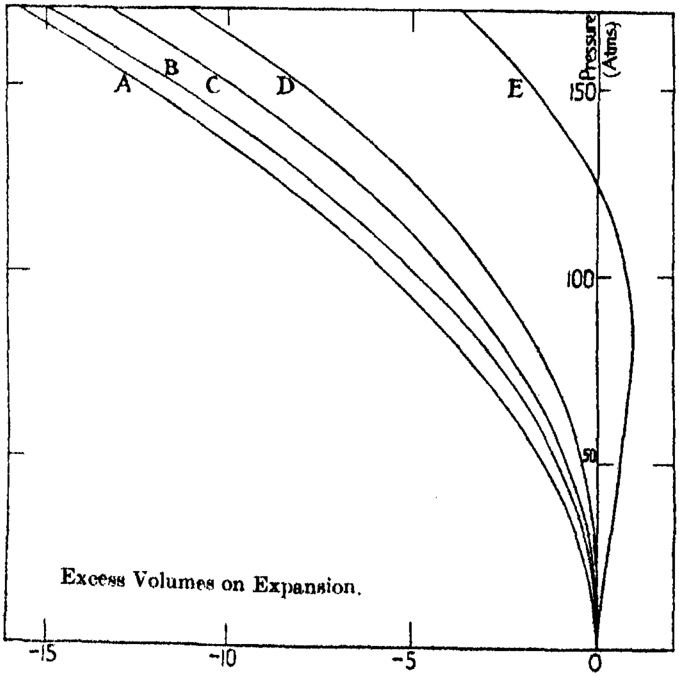

Fig. 5.

A, Hydrogen. B, 66·3 per cent. H_2, 33·7 per cent. CO. C, 51·7 per cent. H_2, 48·3 per cent. CO. D, 33·1 per cent. H_2, 66·9 per cent. CO. E, Carbon monoxide.

Discussion of Results.

The law, first enunciated by Dalton, that the pressure of a gaseous mixture is the sum of the pressures exerted by the constituents when each one occupies by itself the same volume as the mixture, cannot hold good at high pressures because (*a*) in a mixture the space between the molecules of one gas is occupied by those of the other (co-volume effect or Van der Waal's "*b*") and (*b*) there is likely to be an attraction of the molecules of one gas for those of the other. The first experimental disproof of this law at high pressures was that due to Andrews working on mixtures of nitrogen and carbon dioxide. Recently Masson and Dolley have tested this law in respect to the binary mixtures of argon, oxygen and ethylene up to 125 atmospheres pressure and have found that in nearly all cases the actual pressures of the mixtures are less than the sum of the pressures of the components acting separately.

An alternative version of this law is that the volume of a gaseous mixture is the sum of the volumes of the separate gases all measured at the same temperature and pressure. In this case conditions are such that the resultant cohesive forces operative in the gaseous mixture are different from those previously existing in the separate gases, then deviations from the law would be expected. Amagat was the first to enunciate this version of the law as an outcome of his work on the compressibilities of air, oxygen and nitrogen; he observed that the *pv*-values for air are related linearly to those of its component gases. It should be borne in mind, however, that the critical temperatures of oxygen and nitrogen are almost identical and that therefore it may be supposed that the cohesive forces acting between the molecules of each separate gas are similar and will not differ greatly from the force between a molecule of one gas and a molecule of the other. Masson and Dolley have found only small deviations (not exceeding 0·25 per cent.) from this law with a 50 : 50 oxygen-argon mixture where the compressibilities of the constituent gases are very similar. In the cases of oxygen-ethylene and argon-ethylene mixtures, however, where the gases have very different compressibilities, the volumes of certain of the mixtures exceeded the sum of the separate volumes by as much as 30 per cent.

In the present investigation it has been found that mixtures of hydrogen and carbon monoxide show deviations from both versions of the law. Deviations from the "additive volume" version are at once apparent from the curves in fig. 4, where it will be seen the isotherms for the mixtures lie considerably nearer the hydrogen isotherm than they would if a linear relationship with composition held good. Although the effect is marked, the numerical value is not great in the case of each mixture, the deviation above the additive volume increases from 0·35 per cent. at 30 atmospheres pressure up to 2 per cent., a maximum not having been reached in the present range of pressure.

Deviations from the "additive pressure" version of the law have also been calculated. The pressure of a mixture is greater than the sum of the pressures exerted by the separate component gases occupying the same volume by an amount which again increases over the whole range and reaches 10 atmospheres at 170 atmospheres.

Verschoyle* has determined the isotherms of hydrogen and nitrogen and some of their binary mixtures at temperatures of 0° and 20° C. over a pressure range up to 200 atmospheres.

In general he found deviations from both versions of the law, but as in the present investigation, considerably smaller than those observed by Masson and Dolley for ethylene mixtures. His isotherms were expressed in the usual form :

$$pv_A = a + bp + cp^2 ;$$

it was also noted that the constants b and c are not linear functions of the composition of the mixtures concerned. The behaviour of these mixtures shows a remarkable similarity to that of the hydrogen-carbon monoxide mixtures here studied, thus in fig. 6, the values of the constants b and c for the latter mixtures are plotted against composition, and lie on smooth curves closely resembling those of Verschoyle.

Bartlett† also has investigated the compressibility of hydrogen and nitrogen and of several mixtures of these gases at 0° C. and over a pressure range extending to 1000 atmospheres. His determinations were in very close agreement with those of Verschoyle at the same temperature and over the same pressure range. More recently he has extended the temperature range to 400° C. in respect of these single gases and a 3 : 1 mixture, finding that at temperatures above 300° C. the additive volume law is obeyed very closely.

Keyes and Burks‡ have studied the compressibility of nitrogen, methane and mixtures of those gases by an isometric method, and have observed similar divergences from both versions of the law.

From the theoretical aspect of the subject a noteworthy contribution has

---

[*] 'Roy. Soc. Proc.,' A, vol. 111, p. 552 (1926).

[†] 'J. Amer. Chem. Soc.,' vol. 49, p. 687 (1927), and vol. 50, p. 1275 (1928).

[‡] 'J. Amer. Chem. Soc.,' vol. 50, p. 1100 (1928).

been made by Lennard-Jones* who has based his calculations on the assumption that a molecule is surrounded by a spherically symmetrical field of force,

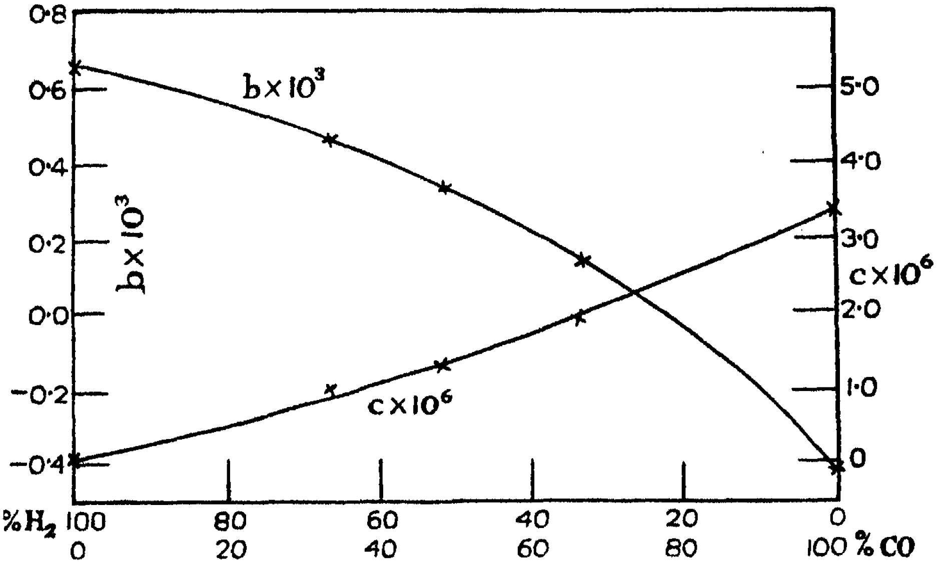

FIG. 6.

resulting from superposed repulsive and attractive forces. According to his theory " b " in the expression

$$pv_A = a + bp + cp^2$$

is some measure of the forces acting between two molecules of the gas concerned. In the case of a gaseous mixture the expression becomes

$$pv = a_m + b_m p + c_m p^2$$

and the value of the constant " b_m " is dependent upon the " b " factor for each single gas (*i.e.*, b_{11} and b_{22}) and also upon b_{12} which is a measure of the force acting between a molecule of the first gas and a molecule of the second. The relative effects of these three types of forces acting in a mixture of the two gases will depend upon the proportion in which the two gases are present. Lennard-Jones has obtained an expression combining b_{11}, b_{22} and b_{12} with b_m (the resultant effect of the three forces in determining the form of the isotherm of the mixture) as follows :—

$$b_m = b_{11}\,x_1^2 + 2x_1\,x_2\,b_{12} + b_{22}\,x_2^2,$$

---

* 'Roy. Soc. Proc.,' A, vol. 115, p. 334 (1927).

where x_1 and x_2 are the molecular proportions of the two gases in any mixture of them. Ascertaining by other means the value of b_{12}, it is possible to predict the value of b_m for any particular mixture of the two gases. On the other hand if b_m is obtained experimentally, b_{12} may be calculated and should be constant and independent of the composition of the mixture. Gibby, Tanner and Masson have investigated the isotherms of helium and hydrogen mixtures in the light of these considerations and have found close agreement with the views of Lennard-Jones.

In the present investigation the constant b_{12} for the force acting between a molecule of carbon monoxide and a molecule of hydrogen at 25° C. has been calculated from the isotherms of each experimental mixture. The values so derived for $b_{12} \times 10^3$ are 0·50, 0·51 and 0·62 as obtained from the three mixtures containing 66·3, 51·7 and 33·1 per cent. of hydrogen respectively, an agreement which may be considered satisfactory.

The investigation is being extended to cover a pressure range up to 1000 atmospheres, determinations also being made at temperatures other than 25° C.

Summary.

The isotherms of hydrogen, carbon monoxide and three mixtures of these gases containing 66·3, 51·7 and 33·1 per cent. of hydrogen respectively have been determined over a pressure range extending to 170 atmospheres at 25° C.

Each isotherm has been expressed in the form $pv_A = a + bp + cp^2$ and the values of a, b and c tabulated in each case.

The mixtures deviate from both the law of additive volumes and that of additive pressures and in general exhibit similar characteristics to those of hydrogen and nitrogen.

In conclusion I desire to express my best thanks to Prof. W. A. Bone for his advice and help during the investigation in his laboratories, and to the Department of Scientific and Industrial Research for grants which have enabled me to carry it out.

The Effect of a Transverse Magnetic Field on the Propagation of Light in vacuo.

By William H. Watson, Carnegie Research Fellow.

(Communicated by Sir Ernest Rutherford, P.R.S.—Received June 21, 1929.)

[Plate 6a.]

§ 1.

In modern physics there have developed two complementary—and apparently mutually contradictory—modes of description of radiation processes and of the motion of molecules, atoms, electrons and protons. How far can the parallelism in description of photons (light quanta) and members of the second group of entities be carried? It is now well known that the physical effects by which an entity is recognised are, in all cases, atomic and individual, *e.g.*, photoelectric and Compton effects, scintillation on a fluorescent screen, effect on a photographic plate. Such effects are quite naturally correlated with the concept of a moving particle with energy and momentum. On the other hand, the motion of these particles can only be completely described by the wave method. Except in the case of very long wireless waves, the waves are never observed directly as waves with periodic physical effects in space and time, and even in the case of the exception it seems probable that the periodicity observed is only a large scale phenomenon (for comparatively large numbers of particles). The development of the analogy between photons and entities of the second class (atoms, electrons, etc.) has already reached the stage where it is possible to give a wave description of the motion of the particles in all cases and to assign to the particles an energy-momentum four-vector within the limits of Heisenberg's principle. There remains, however, a fundamental distinction in current theory. All the entities in the second class have electromagnetic particle properties while none have been assigned to the photon. Electrons, ions, and protons have electric charge which is quantised in integral multiples of the electronic charge $\pm e$. Atoms possess the electromagnetic particle properties, magnetic moment and possibly electric moment, while molecules have magnetic and electric moments and mechanical moments of inertia. Since the photon is assumed to be electromagnetic in origin, and can produce electromagnetic effects, it is necessary to assign to it some electromagnetic character. The simplest particle properties which one can postulate are those of electric moment and magnetic moment; free electric charge is excluded by the fact that light is not deflected in a uniform electric or magnetic field.

The present investigation was carried out with the object of detecting, if possible, the existence of the magnetic moment of a photon. The Stern-Gerlach method of the non-uniform field involving the deflection of particles moving with velocity of light, presents obvious difficulties. The method actually adopted depends for its sensitiveness on the interference properties of light, and the principle was the following. Light was passed through a Fabry-Perot étalon placed in a strong magnetic field which was perpendicular to the direction of propagation of the light. A particle with a magnetic moment μ parallel or antiparallel to the field H, would undergo a change in energy $\Delta E = \pm \mu H$ on entering the field and in accordance with the principles of the quantum theory would experience a change in frequency $\Delta\nu = \pm \mu H/h$. This would involve an effective change in wave-length

$$\Delta\lambda = \pm \mu H \lambda^2/hc$$

and a change in the interference pattern formed by the interferometer of the type observed in the normal Zeeman effect.

§ 2. *Experimental Arrangement.*

The electromagnet which is capable of giving 10,000 gauss across a 2 cm. gap, is mounted in the centre of a wooden optical bench, 2·14 metres long, supported centrally on a specially stout table. The optical arrangement is practically that of Fabry and Buisson* and is shown in fig. 1. Light from a neon discharge tube (T) on one arm of the bench, passes through a lens (L_1) and nicol prism (N) to the interferometer (I) whose plates are parallel to the

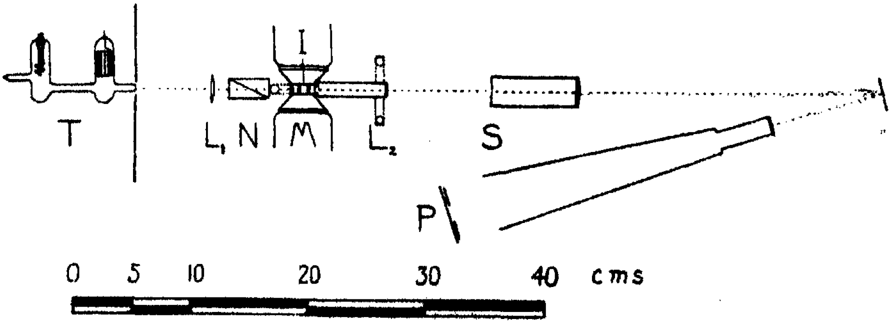

FIG. 1.

---

* 'J. Physique,' vol. 9, p. 129 (1910).

axis of the electromagnet (M). The interference pattern is then projected by an achromatic objective (L_2), of 17·5 cm. focal length, on the slit (S) of the collimator of a grating (G) spectrometer and the fringe system of the yellow line 5852 is examined in the eye-piece of the telescope or projected in the focal plane of a photographic camera (P). The collimator, grating and telescope or camera are set up separately on the bench, since in the presence of the powerful magnet an ordinary spectrometer table mounting cannot be used.

The interferometer has, after consultation with Messrs. Adam Hilger who made the instrument, been designed so as to occupy as little space as possible; it is shown in fig. 2. The plates are made of quartz, "half-silvered," and separated by a quartz ring distance piece, 1 cm. long, making optical contact at three places near the rim on each plate. The étalon lies without constraint in a copper tube which is fixed by four screws to the end of a brass box (fig. 3A) and into which it fits with a clearance of less than 0·5 mm. (see fig. 3B).

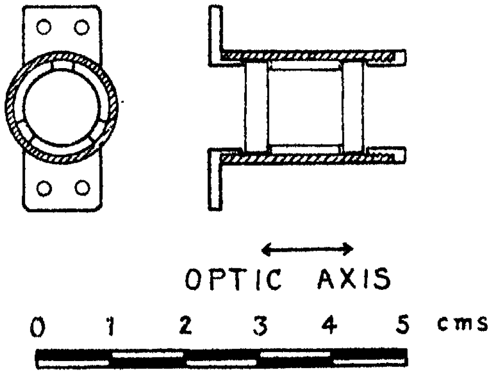

FIG. 2.

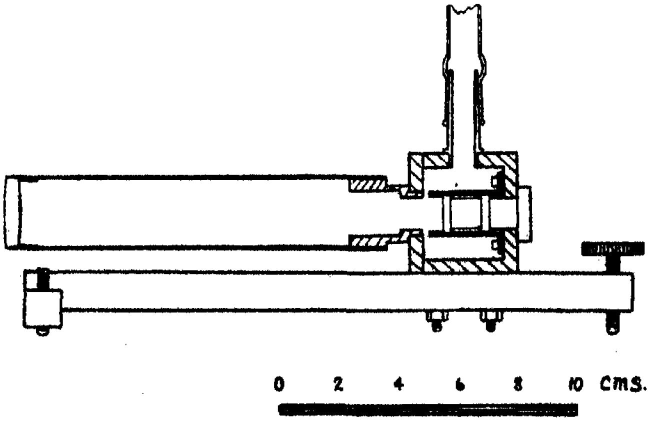

FIG. 3A.

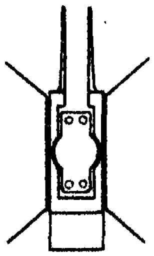

FIG. 3B.

This box is closed in front by a plate-glass window; the opposite face carries a brass tube closed by the objective lens L_2. Once the interferometer has been mounted, the box is cemented and screwed together and then connected via a tap, flexible glass tube system and a liquid air mercury trap to a vacuum pump. The box is mounted on a stout T-base supported by three levelling screws on the optical bench.

The light selected for observation is an intense line on the neon spectrum, a singlet, and exhibits a normal Zeeman effect; its colour makes it easy to observe visually, so facilitating adjustment. On the other hand, it is not efficient for photography even with panchromatic plates. The breadth of the line determines the limit of resolution possible for a theoretically infinite resolving power of the interferometer. Fabry* observed the value 324000 for this limit at ordinary temperatures and this accords with Lord Rayleigh's formula† for temperature broadening—the pressure of the gas was sufficiently low to be of negligible account in determining breadth. On the performance of étalons, Childs‡ gives data from which may be deduced by interpolation that the optimum resolving power of a 10 mm. étalon, silvered to 90 per cent. reflecting power, is about 560000 for λ 5852, that is, the fringe breadth is 0·061 of an order. Since on account of the breadth of the line we can only resolve 0·105 of an order, and since the étalon actually used was silvered to more than 90 per cent., it is evident that temperature breadth is the more important factor in determining the limits of resolution.

The source of light initially employed was a neon discharge tube of about 100 c.c. capacity, first with plane Al electrodes, and then with cylindrical Mo electrodes. These tubes were operated by a transformer at about 400 volts, passed 5 ma., and were immersed in an oil bath, light being taken from the tube by a window on the axis of the capillary positive column. Owing to cathodic sputtering and consequent disappearance of gas these tubes proved unsatisfactory. A more intense source of light was obtained by the use of a low voltage arc in neon. A Wehnelt cathode surrounded by a grid was used for starting the arc which afterwards maintained itself on the D.C. mains when no current passed through the filament. The positive column was 12 mm. diameter and the whole lamp in soda glass. The potential across the tube was 120 volts and currents up to 0·5 amp. could be passed without rendering the tube unduly hot; the oil bath was dispensed with, and a large screen was

---

[*] "Les applications des interférences lumineuses," p. 142.

[†] 'Phil. Mag.,' vol. 29, p. 274 (1915).

[‡] W. H. J. Childs, 'J. Sci. Inst.,' vol. 3, pp. 97, 129 (1925–6).

interposed to confine light to the axis of the apparatus (see fig. 1). Before being filled the tube was evacuated and baked out at 350° C. for 2 hours, then before sealing off it was run for some hours at varying currents up to 0·5 amp. being connected all the time with a charcoal tube immersed in liquid air. Good fringes were obtained with light from along the axis of the positive column with currents up to 0·3 amp. (see fig. 4, Plate 6).

The effect of the magnetic field on the optical apparatus may be discussed briefly :—

(i) Source of light—Zeeman effect negligible.

(ii) Étalon—

  (*a*) Change of temperature, see below.

  (*b*) Magnetostriction and magnetic double refraction—negligible.

  (*c*) Rotation of the plane of polarisation of the light if there is a component of the field parallel to the direction of propagation of the light.

(iii) Ring objective—this closes the evacuated box and is removed from the strong part of the field so the effect of the field on this lens must be negligible.

§ 3. *The Result of the Experiment.*

For λ 5852 the normal Zeeman effect in a field of 10,000 gauss is 0·161 Å.U., and this is the change in wave-length which would take place if the interferometer were μ, the magnetic moment of the photon, equal to 1 Bohr magneton ($9 \cdot 21 \,.\, 10^{-21}$ e.m.u.). On the other hand a separation in a normal Zeeman fringe pattern of a fraction q of an order would correspond to a change in wave-length $\Delta\lambda = \lambda^2 q/2 = 0 \cdot 171\, q$ Å.U., and therefore in this case a magnetic moment $\mu = 1 \cdot 06\, q\mu_B$. Hence the smallest magnetic moment completely resolvable by the apparatus is about $0 \cdot 1\ \mu_B$.

If the light when inside the interferometer is plane polarised with its electric vector perpendicular to H, the magnetic moments of the photons will be orientated parallel and antiparallel with H and we should expect the simple splitting of each fringe into two displaced fringes ⊥⊥, but if the plane of polarisation is not so orientated, we should expect the pattern ⊥⊥⊥, the relative intensity of the undisplaced to the displaced components being proportional to $\tan^2 \theta$, where θ is the angle between the plane of polarisation and H. If the magnetic moment sought for is too small to be resolved, but is nevertheless large enough to produce a measurable broadening of the fringes, this broadening should depend on the setting of the nicol, reaching maximum and minimum values respectively at orientations of the plane of polarisation 90° apart. Neither of these effects was observed; the only broadening which occurred could be accounted for by changes in the temperature of the étalon during the experiment.

The influence of change in temperature is two-fold—first, to increase the mean diameters of the rings, and secondly, if there is steady increase in temperature during the experiment, to produce an asymmetrical broadening of the fringes obtained with constant temperature. Since the coefficient of expansion of fused quartz is about $4 \,.\, 10^{-7}$ per degree C. a change in temperature of 1° C. involves a change in ring diameter corresponding to 0·014 of an order. This is the magnitude of the increase in the mean ring diameter observed in a photograph, with 90 minutes' exposure and field current 5 amperes; and all differences of ring diameter observed as between "field-off" and "field-on" exposures can be accounted for by temperature changes of this amount and of the proper sign. The corresponding increase in the breadth of the fringes in the case of temperature altering over the above interval during exposure, being 0·007 order, is less than 10 per cent. of the fringe breadth and is not measurable with certainty.

Fringe breadths were measured with a comparator on several plates and in no case was the broadening produced by the field observed to be greater than 10 per cent. of the fringe breadth, with a possible error of 10 per cent. Thus the maximum possible broadening which could fail to be revealed by the measurements was 20 per cent. of a fringe breadth, and fringe breadths were found to be about 0·140 order. That is, the maximum possible effect due to the photonic magnetic moment could not exceed an effective splitting displacement of $1/10 \times 0{\cdot}140$ order.

Therefore $\mu \ngtr 0{\cdot}014 \times 1{\cdot}06 \; \mu_B = 0{\cdot}015 \; \mu_B$.

It is unfortunate that it is impossible to gain the factor 50 necessary to detect a magnetic moment equal to that of the proton [$5 \,.\, 10^{-24}$ e.m.u.].

The result of this investigation may also be stated in terms of wave theory, viz., the alteration of the refractive index of vacuum by a magnetic field perpendicular to the direction of light-propagation is not greater than $4 \,.\, 10^{-11}$ per gauss.

In conclusion it may be pointed out that this experiment proves conclusively that the Zeeman effect is determined completely by the emitting atom in the field, and that no effect* is contributed by the propagation of the light from a region where the magnetic field is strong to a place where it is weak.

---

* Within the limits mentioned above.

Watson. *Roy. Soc. Proc., A, vol.* 125, *Pl.* 6A.

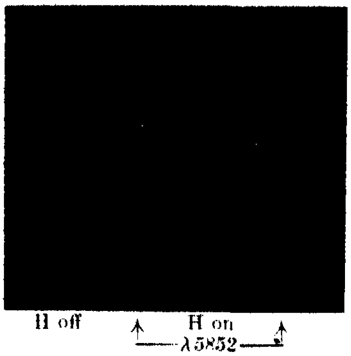

Fig. 4.

Thomson. *Roy. Soc. Proc., A, vol.* 125, *Pl.* 6B.

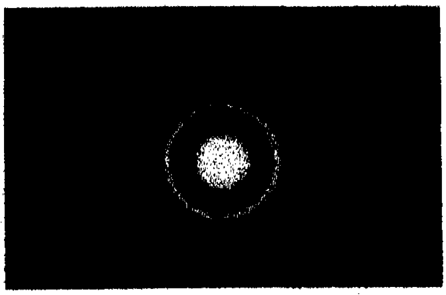

Diffraction Rings for spluttered Gold Film.

(*Facing p.* 350.)

I am indebted to Prof. Sir Ernest Rutherford for his interest in the work and to the various other workers in the Cavendish Laboratory for valuable technical advice and criticism. The grant by the Carnegie Trust of a research fellowship has made it possible for me to devote myself for a period completely to research. I take this opportunity of expressing my thanks, and of acknowledging the Trust's financial award to defray the cost of the étalon used in this work.

Summary.

It is reasonable to expect that photons may have some of the properties of electromagnetic particles. An experiment to detect the existence of the magnetic moment of a photon is described. This magnetic moment, if it exists, is less than $1 \cdot 4 \,.\, 10^{-22}$ e.m.u. The alteration in the refractive index of vacuum produced by a magnetic field perpendicular to the direction of light propagation does not exceed $4 \,.\, 10^{-11}$ per gauss.

Addendum.—The influence of a magnetic field component of 2500 gauss parallel to the direction of light propagation through the étalon has also been tested. To the limit of detection given above no effect on the interference pattern was observed.

Diffraction of Cathode Rays—III.

By G. P. Thomson, M.A., Professor of Natural Philosophy in the University of Aberdeen.

(Communicated by Sir Joseph Thomson, F.R.S.—Received June 26, 1929.)

[Plate 6b.]

This paper is a continuation of work described in these 'Proceedings,'* and the apparatus used was closely similar. The general method is to send a beam of cathode rays, of the order of 30,000 volts energy, through a thin film of crystalline material and examine the diffraction pattern formed by the action of the crystals on the de Broglie waves of the cathode rays. The patterns obtained are closely similar to those formed in the Hull-Debye-Scherrer method of X-ray analysis, thus in the case of a metal film containing a large number of small crystals orientated at random, they consist of a number of concentric rings, one corresponding to each spacing of crystal planes. The patterns are recorded by allowing the electrons which form them to strike a photographic plate and developing the plate in the ordinary way.

Preparation of Films.

The films used in the earlier work were made from beaten foil further thinned in a suitable reagent. These films when thin enough to show the effects, always had holes, and indeed were often more like a lacework of metal than a coherent film. Though they give in many cases very good rings, such films are quite unsuitable for quantitative work, especially as they generally show distinct orientation of the crystals in privileged directions. It was therefore decided to try again to make films by cathodic spluttering. I have been much helped by a suggestion made by M. F. Jolliot who pointed out to me the advantages of cellulose acetate as a base on which to splutter. The technique as now developed is as follows. A solution of pure cellulose acetate in acetone is clarified by filtering. Some of the solution is poured on to a clean glass plate, allowed to solidify, and stripped off; this is done in order to remove specks or dust particles from the plate. When the plate has warmed up again to room temperature enough solution is poured on to form a film, rather too thick to show interference colours but of that order. Round the edges of this film more solution is applied with a paint brush as the first lot dries. In this way a kind of picture frame is built up round the thin centre portion, which can be lifted off by means of the frame. It is then placed in a bell jar 3 or 4 cm. below a cathode of the metal to be spluttered. The spluttering is done with a current of 1–3 milliamps. with a dark space of about 1 cm. A thermionic valve is used to prevent back current from the induction coil. In most cases residual gas was used, but for aluminium the gas was 99 per cent. argon, obtained from the British Oxygen Company. In order to get films free from holes it was found necessary to make the cellulose acetate films, and transfer them to the bell jar, in a carefully sealed fume cupboard through which a stream of filtered air was drawn. Otherwise minute dust particles occurred on the surface of the cellulose acetate and the metal film was not continuous over them. When the spluttering has given a sufficient deposit, 5 minutes to an hour, the time being judged from the appearance of the surface, the composite film is removed from the bell jar and the cellulose acetate dissolved off in a bath of acetone. The metal film drifts away in the liquid, and must be washed by transferring it in a glass spoon to clean acetone; four dishes of acetone are used in succession to remove all traces of the cellulose acetate. A portion of the metal film is then caught on an aluminium disc with a hole 1–3 mm. in diameter through it. The film is manœuvred over the hole and sticks to the disc when removed from the acetone and dried. With practice the proportion of losses is surprisingly small considering that the films are of the order of 10^{-6} cm. thick and sometimes even less. The discs were made a standard size (1 cm. diameter) to fit a holder in the apparatus.

---

* Vol. 117, p. 600 (1928), and vol. 119, p. 651 (1928).

A variant of this method was to substitute a polished rock salt crystal for the cellulose acetate. This has previously been used by Rupp as a basis for his evaporated films. The spluttering in most cases was done in a stream of argon originally 99 per cent. pure and further purified by standing for an hour over a hot tungsten filament. The rock salt was removed by solution in brine. Films formed in this way were never so strong as those from cellulose acetate, they were difficult to mount and were never obtained free from holes. In some cases, however, they gave markedly better rings. However prepared, the films actually used were always highly transparent, sometimes almost invisible by transmitted light, in other cases showing appreciable colour. They could always readily be seen by light reflected at oblique incidence. They were too thin to show interference colours.

The cellulose acetate method has been applied to gold, silver, lead, iron, nickel, tungsten and aluminium, of which the first two and the last had been investigated before with films made by the thinning method. The rock salt method has been tried for nickel, lead, iron and aluminium.

Theory.—The theory may be briefly expressed as follows. Each spacing d of planes in the crystal will give a reflection at glancing angle θ where $2d \sin \theta = n\lambda$ and λ is given by de Broglie's expression $\lambda = hmv/\sqrt{1 - v^2/c^2}$, here v is velocity of the electron of mass m, and h is Planck's constant. This gives a deviation of the ray equal to 2θ, and if, as was always the case in these experiments, the crystals are arranged at random in the film, will lead to a ring of diameter $2\mathrm{L} \sin 2\theta$ on a plate at distance L. Since θ is small this becomes $\mathrm{D} = 2\mathrm{L}\lambda \, . \, n/d$. For a face-centred cubic crystal to which class belong the metals previously studied $n/d = \sqrt{h^2 + j^2 + k^2}/a$ where a is the cube side and h, j, k are integers which must be all even or all odd. If P is the measured voltage of the cathode rays it can be shown that $\mathrm{D}\sqrt{\mathrm{P}}\ (1 + \mathrm{P}e/1200mc^2)$ is constant for any ring.

Results.

Gold.—The films formed on cellulose acetate gave excellent rings in many cases, but a curious difference was noticed between the normal films, which were a pale green by transmitted light, and some occasionally obtained which were a pinkish purple. The latter indeed gave quite measurable rings but they were never really good. They were of the same size and arrangement as the others showing that there was no essential difference in the crystal structure. The pinkish films were generally found when the spluttering had been slow, and it seems possible that they contain layers of gas enclosed in the gold.

In all cases the pattern of rings was in complete agreement with the theory, as in the previous work, and the improved films brought out rings corresponding to higher values of the crystal indices. One of the plates used for the F curve determinations (see p. 364) is shown in Plate 6B.

Measurements showing rings for all possible value of $h^2 + j^2 + k^2$ up to 20 have been given in previous papers, though in some cases two close rings are unresolved, *e.g.*, those with radii in the ratio $\sqrt{19} : \sqrt{20}$. A few measurements for the higher rings are shown meaned in the table, the diameter of the ring corresponding to the (2, 2, 0) spacing being put equal to $\sqrt{8 \cdot 00}$ in all cases. In many cases several rings are too close to be resolved, but the agreement with a mean, weighted to allow for the number of planes co-operating to form each ring, is satisfactory.

Observed diameter (mean).	$\sqrt{24 \cdot 3}$.	$\sqrt{27 \cdot 5}$.	$\sqrt{35 \cdot 3}$.	$\sqrt{43 \cdot 6}$.	$\sqrt{51 \cdot 1}$.	$\sqrt{58 \cdot 5}$.
Corresponding planes .... Indices (h, j, k)	(4, 2, 2)	(5, 1, 1) (3, 3, 3)	(5, 3, 1) (6, 0, 0) (4, 4, 2)	(5, 3, 3) (6, 2, 2)	(4, 4, 4) (7, 0, 0) (5, 5, 1) (6, 4, 0)	(6, 4, 2) (7, 3, 1) (5, 5, 3)
$\sqrt{h^2 + j^2 + k^2}$	$\sqrt{24}$	$\sqrt{27}$	$\sqrt{35}$ $\sqrt{36}$	$\sqrt{43}$ $\sqrt{44}$	$\sqrt{48}$ $\sqrt{49}$ $\sqrt{51}$ $\sqrt{52}$	$\sqrt{56}$ $\sqrt{59}$
$\sqrt{h^2 + j^2 + k^2}$ weighted mean	$\sqrt{24}$	$\sqrt{27}$	$\sqrt{35 \cdot 4}$	$\sqrt{43 \cdot 5}$	$\sqrt{50}$	$\sqrt{57 \cdot 8}$

The individual measurements of diameters seldom differed by 1·0 from the means given. Using de Broglie's expression for the electron wave-length the value of "a" can be found, the speed of the electrons being calculated from the observed spark gap. The mean for the spluttered films is $a = 3 \cdot 99 \times 10^{-8}$, the X-ray value is $4 \cdot 06 \times 10^{-8}$. The agreement is somewhat better than for the thinned films which gave $4 \cdot 20 \times 10^{-8}$.

Silver.—The rings obtained with silver films were not so clear as those with gold, the greatest number of rings visible being six. The films were pale orange by transmitted light. Films of silver obtained by the thinning down method have previously been investigated by Ironside* who found good agreement with theory. The relative sizes of the rings measured with the present films are in good agreement with the face-centred cubic structure found with X-rays.

Lead.—The rings with this element are small because of the large size of the crystal cube (4·92 Å. by X-ray measurements), and also because high voltages have to be used, the rings disappearing below about 16,000 volts. Partly, no doubt, for this reason the rings $\sqrt{3}$ and $\sqrt{4}$ of the face-centred cubic structure are not resolved, but the films themselves are partly to blame, for the $\sqrt{8}$ and $\sqrt{11}$, $\sqrt{12}$ rings are also inseparable. These films were stretched quite tight over the aluminium mount, while the gold films usually showed folds. It seems possible that the lead films may have been stretched by surface tension beyond the elastic limit, and the crystal lattice deformed. If the inner ring D_1 is taken as $\sqrt{3}$, two other rings are visible of sizes $\sqrt{10 \cdot 4}$ and $\sqrt{20 \cdot 9}$. The first is probably a confusion of $\sqrt{8}$, $\sqrt{11}$, $\sqrt{12}$, the second the usual $\sqrt{19}$, $\sqrt{20}$ ring. The $\sqrt{4}$ ring is faint compared with the $\sqrt{3}$ in all spluttered films, and it seems reasonable to suppose that the size measured for the inner ring is little influenced by its presence. In spite of the poorness of the rings they show the right variation with voltage as is seen from the annexed table, the factor in brackets being a small relativity correction of not more than 2 per cent.

---

* 'Roy. Soc. Proc.,' A, vol. 119, p. 668.

P.	D_1.	$D_1\sqrt{P}(1+Pe/1200\, m_0c^2)$.
volts.	cms.	
15,800	1·53	194
18,100	1·50	204
23,300	1·28	198
27,000	1·16	194
27,300	1·18	198
28,400	1·16	199
34,500	1·06	200·5
36,600	0·98	192
42,000	0·96	201

If the ring is taken as $\sqrt{3}$, the value found for "*a*" is 4·99 Å., the X-ray value being 4·92; the discrepancy of less than 2 per cent. is within the probable error in view of the difficulty of measuring the rings. The films were of a brownish purple tinge.

The rock salt method was also tried using argon as gas, the temperature was high enough to begin to melt the lead. The films were very brittle but one was mounted. It gave excellent rings, very narrow and persisting even at voltages as low as 6000, but showing quite a different pattern from that of the familiar space-centred cube. The chief spacings calculated from four plates are as follows:--

Spacing in Å units	? circa 4·2 ?	2·88	2·59	2·23	1·68	1·48	1·29 1·25	1·11 0·99
Character of ring	Too near the central spot to be seen with certainty	faint	strong	diffuse	moderate	moderate	just resolved	faint

These spacings do not fit any probable structure for the metal and are probably due to a compound, perhaps $PbCl_2$.

Iron.—A number of films of this metal were prepared on cellulose acetate. They were very transparent and practically colourless by transmitted light. The rings for the most part were not very good, but the best were easily measurable. The two clearest rings in most cases had diameters in the ratio $1:\sqrt{2}$. Iron at ordinary temperatures forms body-centred cubic crystals.

For this system the first few rings are in the ratio $\sqrt{2}:\sqrt{4}:\sqrt{6}:\sqrt{8}$. Assuming that the rings observed are the first two of these, the size of unit cube can be calculated in the usual way. The mean of all the measurements on six films gives $a = 2\cdot78 \times 10^{-8}$ against $2\cdot87 \times 10^{-8}$ found by X-ray analysis. Taking measurements of the five clearest rings (3 films) the value is $2\cdot85 \times 10^{-8}$, so the discrepancy above is probably due to difficulty of measurement. Some of the films showed a ring at a mean value of $\sqrt{7\cdot2}$, this probably represents to $\sqrt{6}$ and $\sqrt{8}$ rings unresolved owing to their diffuseness. One film (No. 24, see p. 360) which though the densest optically gave fairly good rings, showed in addition to the $\sqrt{4}$ and a faint $\sqrt{2}$ ring, a ring which would correspond to $\sqrt{1\cdot3}$ on this scale. This cannot be due to the ordinary iron structure. Although the size of the third ring for this film agrees well with $\sqrt{4}$ for the ordinary iron structure, it is so much stronger than the $\sqrt{2}$ ring on the same plate that it is probably partly due to some other cause, presumably the structure which is causing the innermost ring.

This is confirmed by experiments with rock salt as base. Spluttering in argon a film was obtained which though very brittle was successfully mounted. It was brown in colour and rather dark, but gave two good rings. They corresponded well with the first and third of the above film, the second being absent. With only two rings the data are insufficient to enable one to tell whether this film is a new form of iron itself, or a compound with the rock salt or some impurity in the gas. The spacings are 2·55 and 2·90 Å.

Tungsten.—Transparent films were obtained by spluttering this metal in 99 per cent. argon on cellulose acetate. They showed only one very poor ring which does not agree in size with any to be expected from the known metal structure. They are probably compounds.

Aluminium.—Aluminium spluttered in argon on cellulose acetate gave good coherent films of optical density about 0·2. They were rather turbid in appearance and colourless. The rings were very poor, but appeared to fit fairly with the usual structure. Films spluttered on rock salt dissolved away entirely in the brine, the aluminium having probably reacted with the rock salt to form a chloride.

Nickel.—Pale brown films of nickel were obtained by the cellulose acetate method, they seemed thin enough but gave very poor rings, not measurable with certainty. Spluttering on rock salt crystals with polished or cleaved surfaces gave films similar in colour but extremely brittle and difficult to mount. None was ever obtained free from large tears. In spite of this they gave much better rings, easily measurable with accuracy. The rings showed a striking contrast to the familiar face-centred cubic pattern, though this is given in the tables as being the structure of nickel, and the experiments of Davisson and Germer with large crystals, and of Rupp with thin films, have confirmed the result by electron diffraction. Measurements were made with three films which gave the following spacings calculated in the usual way.

Plate	May 13 (1)	May 13 (2)	May 21 (1)	May 21 (2)	May 21 (3)	May 21 (4)	May 22 (1)	Mean.
Voltage	44,000	32,500	33,500	39,600	42,600	33,500	36,200	
Spacing in Å. Units—								
Ring 1	1·92	1·92	1·94	1·925	1·95	1·93	1·965	1·935
,, 2	1·465	1·46	1·52	1·48	1·49	1·42	1·475	1·473
,, 3	1·21	1·25	1·28	1·25	1·23	1·205	1·24	1·237
,, 4	—	1·14	1·18	—	—	—	—	1·16
,, 5	1·045	1·05	1·075	1·04	1·06	1·03	1·055	1·05
,, 6	—	—	0·936	0·938	—	—	—	0·937
,, 7	—	—	0·802	0·800	0·798	—	—	0·80
,, 8	—	—	0·6	—	—	—	—	0·6

A comparison of the mean spacings with Hull's curves showed that they corresponded at least roughly to hexagonal closest packing, some of the rings, which were rather diffuse, representing two or more spacings too close to be resolved. The second and third ring should be single and represent $(1, 0, \bar{1}, 2)$ and $(1, 1, \bar{2}, 0)$ respectively. From the latter "a" is found to be 2·474 Å., and then from the former $c = 4 \cdot 06$ Å. The ratio $c/a = 1 \cdot 64$, and is equal within the error of experiment to 1·633 the value for the close-packed arrangement.

Using these values we can calculate all the other spacings and the results for the inner rings are as shown :—

Plane.	NF.	Calculated spacing.	Spacings deduced from rings.	Appearance of ring.
$(10\bar{1}0)$	0·75	2·15	—	Trace of inner ring.
(0002)	1	2·025	1·935	Strong, rather diffuse.
$(10\bar{1}1)$	4·5	1·895		
$(10\bar{1}2)$	1·5	*1·473*	*1·473*	Moderate.
$(11\bar{2}0)$	3	*1·237*	*1·237*	Moderate.
$(10\bar{1}3)$	4·5	1·145	1·16	Faint.
$(10\bar{1}0)$	1·5	1·075	1·05	Moderate.
$(11\bar{2}2)$	6	1·06		
$(20\bar{2}1)$	4·5	1·04		
(0004)	1	1·01	—	—
$(20\bar{2}2)$	1·5	0·95	0·937	Diffuse.
$(10\bar{1}4)$	1·5	0·915		
$(20\bar{2}3)$	4·5	0·84	0·80	Diffuse.
$(21\bar{3}0)$	1·5	0·81		
$(21\bar{3}1)$	9	0·79		
$(11\bar{2}4)$	6	0·78		

The column NF gives the product of the phase factor F and the number of co-operating planes N, both calculated as for X-rays. It measures the strength of the effect to be expected, apart from a factor which gives a steady decrease of strength with increasing size. The agreement is as good as can be expected in view of the fact that the larger rings are composite.

Bredig and Allolio* have found a similar structure for nickel films spluttered in hydrogen, but with larger spacings. They calculate the density as 7·04 which is much less than that of nickel in bulk (8·9). Since both structures are close packed the difference seems inconsistent with the view that their films were pure nickel, and it is probable that they were a hydride or at least contained large quantities of hydrogen in the lattice.

The density calculated from the above measurements is 8·86 in good agreement with the ordinary value. The spluttering was done in the residual gas, but as this probably contained a good deal of hydrogen some films were made by spluttering in a stream of argon 99 per cent. pure and further purifying by standing for about an hour over heated tungsten. The films were very brittle, but there was no systematic difference in the size of the rings. Nickel thus resembles cobalt, its sister element, in crystallising alternatively in the two possible forms of closest packing. It may be mentioned that the rock salt became considerably heated during the spluttering, and even after taking out of the vacuum was too hot to handle. As far as could be seen from the rough measurements which alone were possible, the structure of the films deposited on cellulose acetate was the same as the above. The above is the first instance of the discovery of a new crystal structure by means of electron diffraction.

Lower Limit of Voltage for Rings.

In view of Rupp's† experiments in which he found good rings with electrons of only 180 volts energy it seemed of interest to determine the lowest voltages at which rings could be obtained with my films. In all cases with metal films the rings ceased to be visible below an energy of the order of 10,000 volts. At these voltages the rings appeared to merge into the background of scattered electrons. This background at large energies was very dark near the central spot, but became rapidly lighter as the distance from the centre increased. At the slower speeds the background was much more uniform, indicating a wider spread of the diffusely scattered electrons. If the film used was free from holes the centre spot became faint and disappeared at a voltage 2–4000 volts below that at which the rings vanished. The general impression is that the rings disappear because the diffuse scattering becomes too strong for them, and the intensity which was originally in the central spot gets spread diffusely over the whole field. It is not a question of failure to penetrate the film. I tried with a good gold film to see if any region existed at a lower voltage where the diffuse scattering was less, and used a high tension direct current generator of Evershed and Vignolles to produce the rays. This gave a beam which magnetic deflection showed to be highly homogeneous. With the film in place, however, it gave merely a uniform illumination over the range 7500–3500 volts as observed on the willemite screen and tested by photographing. It was possible to deflect the luminosity by a strong permanent magnet, so it was not due to soft X-rays. In another apparatus I was able to observe down to 1700 volts and the illumination was still uniform. Below this it was too feeble to see, and photographic observation requires special plates.

---

* 'Z. Phys. Chem.,' vol. 121, p. 41 (1927).

† 'Ann. Physik,' vol. 85, p. 981 (1928), and vol. 1, p. 773 (1929).

Photographs with a spluttered aluminium film over the range 1900–7000 volts show uniform illumination except for a minute spot due to a crack in the film.

The results of a series of observations on the lowest energy with which rings are obtainable are shown in the table. The values given are necessarily approximate, for the visibility of a faint ring is sometimes a matter of opinion, and in any case a good deal depends on hitting the right time of exposure, but the values given are probably accurate to about 1000 volts.

Metal.	Optical density of film.	Rings visible at	Rings invisible at	Estimated least voltage for rings.
Aluminium	(full of holes) film 10	11,000	10,150	10,500
	Film 8	11,600 doubtful 12,700 certain	—	11,600
Gold	Film 47	12,500	10,200	12,000
	Film 40 (rather thick and gave poor rings)	13,300 faint	—	13,300
Silver	Film 14, density 1·105	21,000	18,700 ?	20,000
	Film 12, density 0·334	15,000	—	14,000
Lead	Film 1, density 0·105	15,800 faint	—	15,500
	Film 8, density 0·972	27,300	24,000	27,000
Iron	Film 15, density 0·155	18,000	15,000	16,000
	Film 24,* density 0·195	22,500	21,000	22,000
	Film 19, density 0·053	21,800 16,000 barely	—	15,500
Compound formed by spluttering lead on rock salt	—	5,800	—	—

* This is the film discussed on p. 357.

The small value found for the last film may be compared with Ponte[*] result with films of zinc and cadmium oxides which gave good rings at 10,000 volts and apparently a good deal lower. It seems as if compounds will give rings at lower voltages than metals, but the iron film 24 is normal in this respect.

Effects with Slow Electrons.

These results could be brought into agreement with Rupp's if it were supposed that metals show a range of selective transparency for the range of electron energies used by him, about 180–300 volts, so that they could get through without excessive scattering. This idea was indeed suggested in his paper as a result of some experiments by Becker.[†] It therefore seemed worth while to try to repeat his results with the films made by spluttering on cellulose acetate. Rupp's films were made by evaporation on to polished rock salt and solution of the rock salt in brine.

The apparatus used was of the same general plan as that used for the fast electrons, with two main modifications. The distance from film to photographic plate was reduced from 20 or 30 cm. to 6·2 cm. and the gas discharge replaced by a hot oxide-coated filament, from which the electrons were driven by a battery of accumulators giving up to 300 volts. The pressure was kept as low as possible, but owing to the vapour from the plate and the joints there was generally a visible glow round the filament.

At these low voltages the Paget plates previously used are not very sensitive to electrons, and the effect of the light from the filament and glow was larger than that of the electron beam even when no film was present. Kodak process films were also tried but were no better. As Rupp had used oiled plates, I tried some Wellington plates of 450 H.D. speed number treated with a solution in ether of Everett tap grease. They were more than 10 times (but less than 20 times) as fast as Paget plates, judging by the length of exposure to give equal effects, and were relatively less sensitive to the light. They were better than the same plates treated with " Hyvac " oil. However, Schumann plates supplied by Hilger were considerably more than 10 times as fast again, and were therefore used.

In spite of repeated attempts no rings were found for films of gold or silver, but even when it seemed certain that none would be found, I persisted in the hope of being able to determine if the rays could penetrate the film with sufficiently little scattering to give a well defined central spot. As mentioned above at voltages between 2000 and 7000 the transmitted electrons are always completely diffused. The great difficulty was to avoid holes in the films. Films spluttered without the exclusion of dust almost always had holes visible under the microscope, and gave what were apparently well marked central spots with from 5 seconds to 1 minute exposure on a Schumann plate. Such spots were certainly due to electrons getting through the holes, and being slightly scattered by the residual gas. Even with films made in filtered air and apparently quite whole it is very difficult to be sure, for with such a film as many hours may be needed to give an effect as seconds without it, so that the minutest hole becomes important. In a number of cases such films gave, after several hours' exposure with about 5 milliamps. current, a "central spot" consisting of a group of small specks, obviously the result of invisible holes. One gold film (optical density 0·304 corresponding to about 85 Å. thickness) showed such an effect after 10 hours' exposure. Two or three seconds without the films would have given a good black patch, so the fraction of electrons transmitted by the sound parts of the films must be excessively minute. On the other hand, another gold film showed a faint spot after an hour's exposure; the film was examined and no holes could be seen, while from the size and shape of the spot it might have been genuine. A silver film gave a very faint and diffuse patch after 1 minute's exposure only.

---

[*] 'C. R.,' vol. 188, p. 244 (1929).

[†] 'Ann. Physik,' vol. 84, p. 779 (1927). The electrons observed by Becker to show selective transmission in the above range had all lost a large part of their energy, except in one doubtful experiment, and thus could hardly form an interference pattern. The two effects are probably quite distinct.

In a later paper Rupp (*loc. cit.*, 1929) states that the films are erratic in behaviour, and considers that the successful ones have small areas of extreme thinness which alone are operative. The above results are probably to be explained by supposing that in my films the thin areas are either entirely absent or too small to be effective, and that uniform films of about 10^{-6} cm. do not transmit slow electrons.

Regular and Diffuse Scattering.

There are two possible kinds of scattering which the electron waves may undergo. The one which gives rise to the rings is a scattering without loss of velocity, as shown by the magnetic deflection of the rings.* The other, which causes the diffuse background, is probably accompanied by transference of energy and in the language of particles may be spoken of as due to inelastic collisions, as opposed to the elastic collisions of the electrons which go to form the rings. It seems reasonable to suppose that as the original train of waves passes through the film, the amount of energy scattered at any point in the two ways is proportional to the energy of the wave train. But there is this difference, that rings will only be formed by electrons which have had a single scattering only, electrons which have had two elastic collisions, or one elastic and one inelastic, will alike appear in the diffuse background, unless the inelastic collision is so slight as not to deflect the electron beyond an angle of tolerance which depends on the arbitrary width assigned to the ring. Let us call the fraction of the energy of a wave train scattered elastically in a distance dx, k_1dx, and that scattered inelastically k_2dx. If the original intensity is A the intensity after penetrating a depth x of the film is $Ae^{-(k_1+k_2)x}$, the elastically scattered energy is $Ak_1e^{-(k_1+k_2)x}dx$ and of this a fraction $e^{-(k_1+k_2)(d-x)}$ emerges without further change, d being the thickness of the film. Thus the total ring intensity is $k_1 . A . de^{-(k_1+k_2)d}$.

---

* 'Roy. Soc. Proc.,' A, vol. 111, p. 651 (1928). It is there proved that the velocity of the electrons in the rings is the same as that in the central spot. The films used had numerous holes so electrons could get through to form the central spot without suffering loss of energy.

The total scattered intensity of all kinds is $A\{1 - e^{-(k_1+k_2)d}\}$, so the total diffuse intensity is $A\{1 - e^{-(k_1+k_2)d} - k_1de^{-(k_1+k_2)d}\}$.

The ring intensity has a maximum when $d = 1/(k_1 + k_2)$ but for the clearness of the rings a more important quantity is the ratio of ring to diffuse intensity. For small values of $(k_1 + k_2)d$, such as are given by good films the ratio is

$$\frac{k_1\{1 - (k_1 + k_2)d\}.}{k_2 + (k_1 + k_2)d . (k_1 - k_2)/2}.$$

This decreases as d increases, so that other things being equal, the thinner the film the clearer will be the rings, which is in agreement with observation. The ratio approaches the asymptotic value k_1/k_2 for very thin films, and if this is small no reduction in film thickness will give good rings. Thus the disappearance of the rings with slow electrons cannot necessarily be cured by reducing the thickness.

There appear to be no measurements of electron scattering through small angles for voltages near 10,000, but the measurements of the absorption and loss of velocity in electrons passing through metals show no sudden change at this point. The theory of nuclear scattering which has given good results with β-rays, would predict great differences between, for example, aluminium and gold, contrary to the experiments. This failure is not surprising, for the comparatively slow electrons used would be deflected by the outer regions of the atoms where the field of the nucleus has been largely neutralised by the surrounding electrons, and where atoms of widely different atomic number may have fields of force not greatly differing from one another.

It is more surprising that there should be so little variation with the thickness of the film. Thus in the case of lead for two films having optical densities in the ratio of 9·2 : 1 the limiting voltage only varied from 15,500 to 27,000, and in the case of silver a change from 14,000 to 20,000 volts corresponded to a change in density of 3·3 : 1. If the metals are reasonably pure the optical density is roughly proportional to the thickness in this range. If k_1/k_2 does not depend much on the speed, and the rings vanish at slow speeds because of excessive total scattering, the quantity which would determine their disappearance on the above theory is $(k_1 + k_2)\,d$. For deflections due to an electrostatic field the mean scattering angle of a particle varies inversely as the energy, but in the above example of lead $k_1 + k_2$ would have to vary inversely as about its fourth power. If one supposes that the scattering which masks the ring is mostly multiple, the determining factor is $\sqrt{d}$ (mean angle of deviation). This last would then vary inversely as the voltage squared in the case of lead. The other possible explanation of the disappearance of the rings is that k_1/k_2 decreases at low voltages. The fact that the central spot disappears, if the film is free from holes, at energies not much below those at which the rings vanish, supports the view that a large increase in total scattering occurs, and Rupp's experiments show that at very low speeds k_1/k_2 is still considerable, as otherwise rings could not be seen no matter how thin the films. If the greater visibility of rings due to compounds is general, the disappearance in the case of metals may be connected with the conductivity. It would be very interesting to have some experiments on the scattering of electrons in this range of speed.

Determination of " F " Curve.

The intensity of each of the rings will depend on a number of factors. The corresponding case for X-rays has been thoroughly investigated, and it has been found that the total radiation in a cone of semi-apex angle 2θ, *i.e.*, for planes at a glancing angle θ, is given by

$$R = kF^2\lambda^3 \frac{1 + \cos^2 2\theta}{2 \sin 2\theta} \,.\, \cos\theta \,.\, \frac{p\,.\,V}{2}$$

where V is the volume of the crystal, p is the number of planes giving the reflection and is obtained by permuting the crystal indices and their signs, λ the wave-length, k a factor corresponding to the X-ray scattering of a single electron and F a factor which represents the number of electrons to which each atom is equivalent in scattering power. F varies with θ because the scattered waves due to the several electrons will not be exactly in phase except when $\theta = 0$, and at other angles will interfere so that the combined amplitude is less than the sum of the separate amplitudes of the several electrons. For θ small, as in the present experiments, we may write for the linear density of scattered electrons on any ring $D = k'F^2 . p/\theta^2$ where k' is a constant for any single photograph. Since p is an easily calculable integer a measurement of D for various rings will enable us to compare the values of F for the angles θ to which the different rings correspond.

The necessary measurements and calculations have been made for diffraction patterns taken with two gold films. The experimental details are as follows. Two exposures were made on each plate with the times of exposure in a known ratio, in some cases 2 : 1 in others 3 : 1. In order to make the measurements of the times sufficiently accurate the intensity of the rays was reduced by a small magnet held near the fine tube till they gave suitable blackening with the shorter exposure 60 seconds in duration. Great care was taken to ensure that the discharge was running steadily and the pressure was kept constant by balancing the pump against an artificial leak. Plates were rejected for which there was any reason to suppose a change of conditions or on which the blackening did not lie within the range most suitable for photometric measurement. Four plates were selected for measurement, three made with one gold film and one with another. The first film was selected as giving specially good rings, the other was an average one.

The plates were developed in a Dobson tank to ensure equal development all over. The density was then measured in a Lindemann photometer made by the Cambridge Instrument Company. The measurements were made along corresponding radii of the two exposures of each plate and readings taken at 0·25 mm. intervals. The method of reduction was as follows. The densities (wedge readings) of a number of pairs of corresponding points of the two exposures were tabulated. From these a curve showing the relation between density and log It for the particular plate and the particular rays can be constructed as follows :—Each pair of densities is plotted with density as ordinate, and a *difference* in abscissa equal to log 2 or log 3 depending on the exposure ratio. Each pair of points is shifted parallel to the X axis until the whole lie on a smooth curve, which is the curve required. From this a second curve is drawn giving density against It, which in most cases was not far from a straight line through the origin. The second curve can be used to transform the measured densities into numbers of particles per unit area at any part of the plate.

In practice, owing to the large number of individual readings of density, the readings themselves were not transformed, but curves were drawn of the density along the radius, of which one is shown in fig. 1. The "background" of diffuse scattering is sketched in as shown by the smooth curve, and the area under each peak measured. This area was then reduced to (relative) number of particles by multiplying by the slope of the curve connecting density with

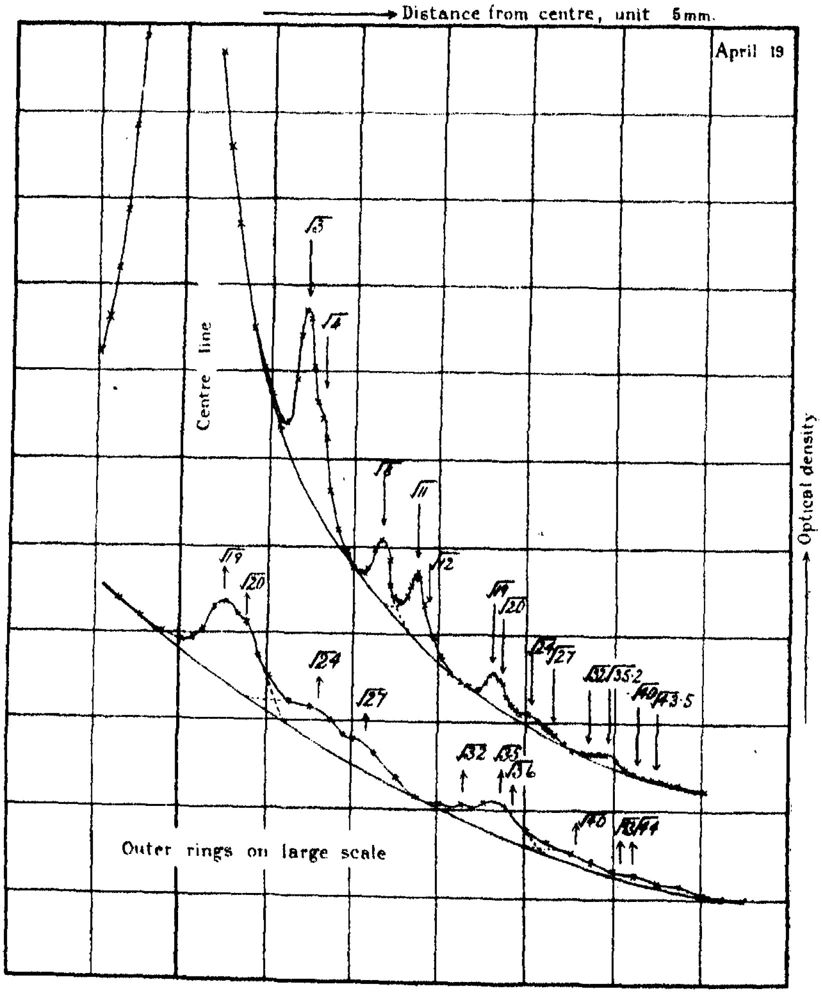

FIG. 1.

intensity, taken at a density corresponding to the centre of gravity of the area of the peak. This method, which was a great saving in labour, is justified by the relatively slight curvature of the density-intensity curve.

It will be seen that the above method makes no assumptions as to the characteristics of the plate, the calculations for a plate depending only on measurements made on that particular plate. It is indeed assumed that the blackening depends on the product, It, of intensity and time, but Ellis has shown that this law holds for the blackening produced by electrons, though, as is well known, it is not accurately true for that caused by light.

In many cases two or more rings were so close together that they were either not resolved at all, or if resolved overlapped to such an extent that the intensities corresponding to them could not be determined separately with any degree of accuracy. In such cases they were treated as one ring with a mean value of θ. The table shows the relative values of D thus obtained, that for the (2, 2, 0) ($\sqrt{8}$) ring being taken as 100 throughout. It will be seen that the four plates are in fair agreement and that the one at the higher voltage shows no appreciable difference from the others. Since the sizes of the rings

Ring $h^2+j^2+k^2$	p.		D in arbitrary units.					$h^2+j^2+k^2$ mean.	$F^2 = \frac{(h^2+j^2+k^2)D}{p}$.
			April 12 P=30500 Film 59.	April 19 P=30000 Film 59.	April 22 P=29000 Film 80.	April 29 P=49300 Film 59.	Mean D.		
3	8	14	467	525	534	537	518	3·4	126
4	6								
8	12		*100*	*100*	*100*	*100*	*100*	8	67
11	24	32	110	112	143	114	120	11·25	42·2
12	8								
16	6		—	—	(12)	—	—	16	(32)
19	24	48	54·2	55·2	52·2	43·5	51·3	19·5	20·8
20	24								
24	24	56	24·1	28·6	18	18·4	22·3	25·7	10·2
27	32								
32	12	90	17·1	20·6	20	16·6	18·6	35·0	7·2
35	48								
36	30								
40	24	72	7·1	6·7	—	5·3	6·4	42·3	3·8
43	24								
44	24								
48	8	192	12·0	—	—	8·0	10·0	54·6	2·8
49	6								
51	24								
52	24								
56	48								
59	72								

Film 59 had an optical density of 0·218, probable thickness 60 Å.
Film 80 had an optical density of 0·343, probably thickness 95 Å.

vary with the wave-length of the electrons, and hence with the voltage, F must vary with λ as well as θ. For X-rays it is a function of $\sin\theta/\lambda$ and is thus the same for any ring whatever the wave-length. Within the limits of experimental accuracy the same holds here.

The mean values of D have been used to calculate the relative values of $F^2 = \theta^2 . D/k'p$, the values of θ^2 being proportional to the squares of the ring radii, *i.e.*, to $h^2 + j^2 + k^2$. In the case of the compound rings the weighted mean was used for this quantity, which is given in the table.

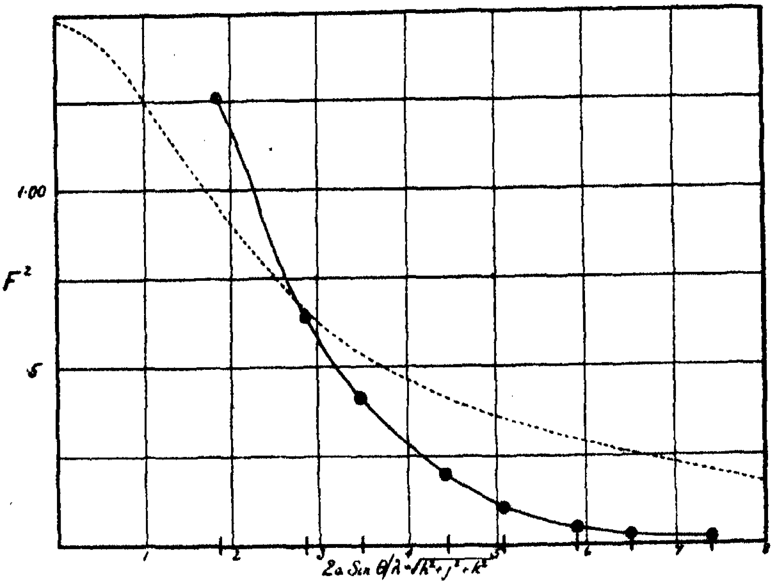

FIG. 2.—Full curve—electron scattering. ... Dotted curve—X-ray scattering. The ordinates of the two curves are in arbitrary units.

The value of F^2 is shown in fig. 2 plotted against $\sqrt{h^2 + j^2 + k^2}$, *i.e.*, $2a \sin\theta/\lambda$. It will be seen that it shows a rapid fall with increasing values of $\sin\theta/\lambda$, as is well known to occur for X-rays. This fall is to be expected on general considerations of interference. The closest distance of two atoms in a face-centred cube is $a/\sqrt{2}$, which is presumably the atomic diameter. For electrons diffracted through an angle 2θ, the path difference corresponding to scattering matter at the ends of a diameter is $a \sin 2\theta/\sqrt{2} = \sqrt{2}\, a \sin\theta$ since θ is small. It is thus equal to $\lambda\sqrt{h^2 + j^2 + k^2}/\sqrt{2}$. The effect of interference in reducing the intensity would become marked if this was about $\lambda/2$, *i.e.*, for a smaller value of $h^2 + j^2 + k^2$ than is available, so interference will be serious even for the (1, 1, 1) ring. If the scattering is due to the electrons which are distributed throughout the volume of the atom, the effect of interference will become more and more serious as the angle of diffraction increases, and this is what our curve shows. The shape of the curve will be governed by the relative amount of scattering caused by the electrons in the concentric shells of the atom, and it should thus be possible to check up on electron distribution curves such as those calculated by Hartree from wave mechanics considerations. This has in fact been done by Mott ('Nature,' May 11) in a note published while this work was being written up, using Dymond's data for the elastic scattering of helium to check the electron distribution in the atoms of that gas. It is hoped that these and similar experiments may lead to a better understanding of the nature of the "elastic" scattering which causes the rings.

It seemed of interest to compare the experimental curve with the corresponding curve for X-rays. No experiments are available for this curve for gold itself, but Bragg has shown that good agreement for the heavier elements is given by curves calculated from the electron distribution found from Thomas's formula. A curve calculated in this way* is shown dotted in fig. 2. It will be seen that the fall with increasing angle of diffraction is much less rapid than for the electrons, indicating that the mean position of the scattering material is nearer the centre of the atom than in the case of the electrons. This is not surprising in view of the much smaller penetrating power of the latter.

Incidentally the fact that the present method gives a smooth curve at all is strong evidence that the small crystals are distributed at random in the film. If there were any preferential directions some of the rings would be enhanced relative to the others. Thus in the original gold films made from leaf the (2, 0, 0) ring was stronger than the (1, 1, 1) because there was a slight tendency for a (1, 0, 0) axis to be perpendicular to the film. With the spluttered films the reverse is the case, because p is larger for the (1, 1, 1) and θ is smaller.

My sincere thanks are due to Mr. C. G. Fraser for the construction of much of the apparatus, and to Mr. J. D. McKay for his help in carrying out the experiments.

Summary.

1. A technique is described for making metal films of the order of 10^{-6} cm. thick approximately free from holes.

2. Cathode ray diffraction patterns for the following metals are described

---

* For the method of calculation see Bragg and West, 'Z. Krist.,' vol. 69, p. 136 (1928).

and discussed: gold, silver, lead, iron, nickel, and attempts with aluminium and tungsten.

3. Of these nickel shows an unexpected structure, namely, hexagonal closest packing, the rest give results in full agreement with the structures deduced by X-ray analysis for the metals, except for certain films formed from lead and iron which probably contained compounds.

4. The slowest speed of rays for which rings are visible is found for a number of films. For the metals the corresponding voltage varies from 10,500 to 15,500 thin films. It is only about 5800 for one of the films of compounds. For thicker films higher voltages are needed but the variation is not rapid.

5. Attempts to get rings with 300 volt electrons were unsuccessful.

6. By photometric measurements of the diffraction rings in gold a curve is deduced giving the variation of wave scattering with angle for the individual atoms, and analogous to the X-ray " F " curves. The curve falls much more steeply than the corresponding X-ray curve.

The Growth of Silver Iodide Films.

By U. R. Evans and L. C. Bannister.

(Communicated by Sir Harold Carpenter, F.R.S.—Received July 9, 1929.)

It is now well established that a large class of important chemical reactions is controlled by the growth of obstructive films, but our knowledge of the mechanism of the growth of such films—especially at low temperatures—is still very imperfect. The present paper describes a detailed study of a particularly instructive case of film-growth, the action of iodine on silver; this reaction was chosen because silver iodide films—in contrast with oxide films—reach visible thickness rapidly at ordinary temperatures. The optical properties of these films have already been studied by Wernick,* whilst much information regarding the velocity of film-growth has been obtained by Tammann,† by Kohlschütter and Krähenbühl,‡ and by Hartung.§ Tammann used the interference colour as the means of arriving at the thickness of the film; this method has certain unique advantages, but the more recent work of Tammann and Bockow* has indicated that—in the case of oxide-films at least—the particular form of the method employed gives values for the thickness differing widely from those obtained by the gravimetric method. Tammann expressed the relation between the thickness (y) and the time (t) by the parabolic equation $y^2 = 2pt$, where p is a constant. Kohlschütter and Krähenbühl, and also Hartung, used microgravimetric methods to determine the amount of iodine taken up, and obtained curves connecting thickness and time; these curves do not appear to follow the parabolic equation. All the experimenters mentioned used iodine vapour to attack the silver, but the concentration of iodine in the gas phase was not directly determined. In all cases the surfaces were prepared in air, and the possible effect of exposure to oxygen was not considered; yet in several of the reactions of copper and iron, pre-exposure to air or oxygen is known greatly to modify the result, owing to the fact that an oxide-film may become protective before reaching the thickness needed for interference colours.† It may be mentioned that after exposure to vapour, the colour produced on metallic specimens is usually not uniform, but indicates a greater film-thickness near the edge.

---

* 'Ann. Physik,' vol. 142, p. 560 (1871).

† 'Z. Anorg. Chem.,' vol. 111, p. 78 (1920), and vol. 123, p. 196 (1922).

‡ 'Z. Electrochem.,' vol. 29, p. 570 (1923).

§ 'J. Chem. Soc.,' p. 1349 (1926).

In the present research, it was decided to use a solution of iodine in an organic solvent; in this case, the concentration could be fixed or varied at will, and in general uniform colouration (*indicating uniform thickness*) could be obtained. Moreover, abrasion could be conducted, if required, below the surface of the solvent, instead of in air. Chloroform was found to be a suitable liquid, since, whilst freely dissolving iodine, it had no appreciable solvent action on a silver iodide film.

The special aims of the work were as follows :—

I. To ascertain the relation of thickness with colour.

II. To compare three other possible methods for measuring the amount of iodine taken up by silver, namely (*a*) micro-gravimetric, (*b*) nephelometric, and (*c*) electrometric, and to ascertain whether pre-exposure to air was a legitimate procedure.

III. To measure the rate of formation of silver iodide under different conditions of (1) solvent, (2) stirring-rate, (3) abrasive treatment, (4) temperature, and (5) concentration of solution.

---

[*] 'Z. Anorg. Chem.,' vol. 169, p. 42 (1928).

[†] Vernon, 'J. Chem. Soc.,' p. 2273 (1926); Evans, *ibid.*, p. 1020 (1927); Constable, 'Nature,' vol. 123, p. 569 (1929).

IV. In the light of the results, to consider the mechanism of the passage of the iodine through the iodide-films, and the nature of thin films in general.

Materials.—The silver used consisted of foil, 0·02 mm. thick. It was free from copper and lead, but contained 0·001 per cent. of iron. Kahlbaum's iodine was employed, and was dried at 100° C., mixed with potassium iodide and resublimed. The chloroform was purified by the method of Hantzsch and Hofmann* and kept in the dark. The abrasive used (except where otherwise stated) was carborundum powder, grade 3 F, previously washed free from chloride ; it was applied by means of a pad, made from linen, which had been soaked many times in boiling water and dried. A small bag was made by wrapping the carborundum powder in a piece of this linen, the loose ends of which were squeezed tightly into the end of a glass tube. It was then soaked in chloroform and rubbed over the silver surface, when the carborundum powder worked through the linen in the required quantity and produced a uniform abrasion. Residual abrasive was removed with clean cotton-wool.

I. *The Relation of Colour and Thickness.*

The assumption that the thickness of a solid film can be judged by dividing the thickness of the air-film required to give the same colour by the refractive index of the film-material has been the basis of nearly all the quantitative work of Tammann and his collaborators on the growth of films of oxides, sulphides, nitrides, chlorides, bromides and iodides ;† it has been used as an auxiliary method by Dunn.‡ Since, however, the assumption has been subjected to criticism, § it appears of general importance to ascertain whether the method is sufficiently accurate for ordinary use.

Portions of silver were prepared with carborundum, cut into strips 5 × 2 cm. accurately measured, kept in a desiccator for one hour, weighed on a microbalance, and immersed in iodine solution, with stirring, for different periods. They were then washed in chloroform, dried in a desiccator, reweighed, and the colour observed. The tint was in most cases uniform, except at certain thicknesses where the variation of colour with thickness is pronounced. The relation between weight-increment and colour is shown in columns 1 and 2 of Table A (see p. 374); the iodine-uptake at the central point of each range showing a typical colour is given in column 3. The uptake of iodine corresponding to this colour has been calculated in accordance with Tammann's assumption from the thicknesses of the air-films needed to give the nearest colour, as recorded in Rollett's tables;* these calculated numbers are shown in column 4.

---

* 'Ber. D. Chem. Ges.,' vol. 44, p. 1777 (1911).

† 'Z. Anorg. Chem.,' vol. 111, p. 78 (1920) ; vol. 123, p. 196 (1922) ; vol. 124, p. 25 (1922) ; vol. 128, p. 179 (1923) ; vol. 148, p. 297 (1925) ; vol. 156, p. 261 (1926).

‡ Dunn, 'Roy. Soc. Proc.,' A, vol. 111, p. 210 (1926).

§ Gale, 'J. Soc. Chem. Ind.,' vol. 43, p. 349 T (1924); Evans, 'Chem. Ind.,' vol. 45, p. 211 (1926) ; Jung, 'Z. Phys. Chem.,' vol. 119, p. 111 (1926).

The actual thicknesses of the silver iodide films—obtained by the two methods—are shown graphically in fig. 1; the individual determinations corresponding to different ranges are distinguished as crosses, circles and triangles. It is obvious that in the case of an abraded surface the term "film-thickness" requires definition. The numbers shown on the left-hand side of fig. 1 represent

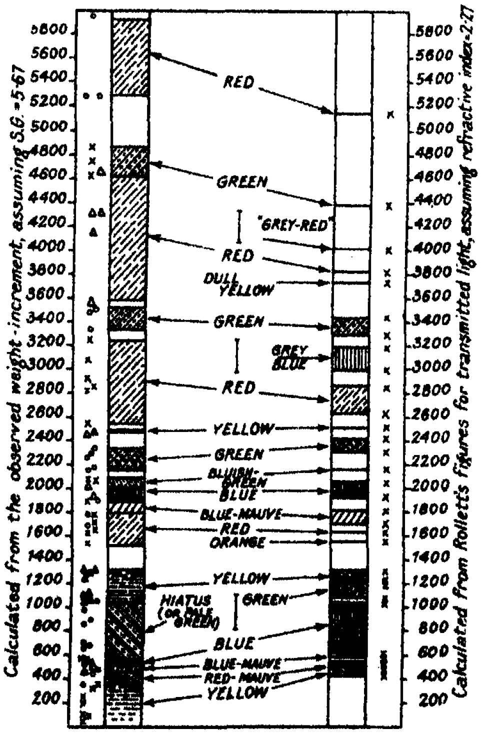

FIG. 1.—Thickness of Silver Iodide Layers in Ångström Units.

the thickness defined as "the average of the intercepts made by lines drawn normal to the *general* plane of the surface." If allowance is made for the

---

* 'Sitzb. Akad. Wien,' vol. 77, p. 229 (1878).

Table A.

(1) Iodine uptake. (mgms. per sq. dm.)	(2) Colour of iodised silver.	(3) Iodine uptake at centre of range showing typical colour.	(4) Iodine uptake at centre of range, as calculated by older colour method.
		mg./dm.^{2}	mg./dm.^{2}
0·21, 0·35, 0·44 0·64, 0·83, 1·00 1·11	Yellow I	Pale yellow.... 0·44 Brownish yellow 0·89	1·46 (brown)
1·13, 1·32, 1·38	Red mauve I	— 1·26	1·71
1·44, 1·55	Blue mauve I	— 1·50	1·82
1·68, 1·75, 1·77	Blue I	— 1·73	1·89
1·65, 2·06, 2·07 2·15, 3·01, 3·22	Hiatus (or pale green)	Bluish silver.... 2·13 Pure silver .... 2·49 Yellowish silver 2·85	Colours not represented in air-film sequence.
3·21, 3·31, 3·41 3·46, 3·74, 3·96 4·00, 4·03	Yellow II	Pale yellow........ 3·42 Yellow............... 3·62 Deep yellow .... 3·83	— 3·81 4·05
4·14	Yellow-red	— 4·37	4·76 (orange)
4·70, 4·91, 5·02 5·30, 5·50	Red II	Pale red .... 4·90 Red .... 5·10 Deep red........... 5·30	5·02 5·23
5·12, 5·48, 5·77	Blue mauve II	— 5·63	5·52
5·90, 6·14	Blue II	— 6·02	6·08
5·84, 6·36, 6·40	Blue green II	— 6·27	6·62
6·59, 6·71, 6·86 7·04, 7·19	Green II	— 6·89	7·02
7·49, 7·66	Yellow III	— 7·57	7·70
7·82, 8·62, 8·69 8·95, 9·46, 9·94	Red III	Pale red .... 8·35 Red .... 8·88 Impure red........ 9·41	8·10 (flesh red) 8·78 (" purpur ")
10·2, 10·6, 10·8	Green III	— 10·52	10·34
11·0, 12·7, 13·1 13·2, 14·3	Red IV	Pale red ....11·81 Red ....12·64 Impure red........13·42	11·76 (flesh red) 12·31
14·2, 14·6, 14·9	Green IV	— 14·55	13·45
16·2, 16·2, 18·2	Red V	— 17·20	15·78
18·8	Greenish grey	— —	—
23·5, 25·7	Reddish grey	— —	—

roughness, and the thickness is defined as " the average of the intercepts made by lines drawn normal to the *local* plane of the surface," smaller numbers would be obtained, and the agreement between optical and gravimetric results, at least for the lower thicknesses, would be even worse than that shown in the figure.

It will be seen that there are serious discrepancies between the gravimetric and optical methods of evaluating the thickness. Moreover in some places the character of the colours shown by iodide films is different from those shown by air films. For instance, in the iodide sequence a silvery " hiatus " occurs between the first order blue and the second order yellow, whilst in the air-colours there is a green interposed. This is quite to be expected. As indicated by one of us* elsewhere, a " perfect " film of *uniform thickness*, composed of a *highly transparent* substance on a *brightly reflecting base*, would be expected to give *narrow* absorption bands, and it is to be anticipated that, when the film thickness is increased sufficiently to make the first absorption band lie just beyond the red end of the visible spectrum, the second band would still lie outside the violet end ; at such thicknesses there will be no absorption within the visible region, explaining the silvery appearance of the iodised surface. With the air films, however, it follows from optical considerations that the absorption bands will be *broad*, the maxima being as well rounded as the minima ; before the first absorption band has passed beyond the red end of the visible spectrum, the second band begins to make an effect at the violet end ; there is thus a maximum reflection in the middle of the visible region, explaining the green colour. The breadths of the absorption bands must also greatly affect the " character " of the colour observed. It is true that even films on a metallic basis should show broad bands, if the films are imperfect or non-uniform, or, if they are composed of imperfectly transparent matter or if the basis is an imperfect reflector ; indeed, exceptional specimens of iodide-covered silver did show a faint green at the end of the first order. It is noteworthy that Constable,† during his study of the oxide-films on copper, obtained quite broad absorption bands, and normally observed a greenish colour between the first and second orders. Under such conditions, a rough proportionality between the air-thicknesses and the oxide-thicknesses is to be expected, and Constable obtained an approximate linear relation between the two thicknesses, although his investigations extended only to the middle of the second order. In the case of silver iodide films it is clear from fig. 1 that this proportionality does not exist; it is concluded, therefore, that in measuring the thickness of iodide films, the "Old Colour Method" is unreliable.

---

* Evans, 'Chem. Ind.,' vol. 45, p. 213 (1926).

† 'Roy. Soc. Proc.,' A, vol. 115, p. 570 (1927) ; vol. 117, p. 376 (1927).

Properly used, however, the observation of colours is of great service. When once the relation between thickness and colour has been recorded (as in Table A), these results may be used to gauge the film-thickness upon any new specimens which require examination. The colour indicates that the thickness must be between certain definite limits, and the middle value of this range (column 3) is adopted as the most probable value. Where the range is a narrow one, the maximum error is quite small; some colours, such as Red III and Red IV extend over a fairly broad range of thickness, but even here it is usually possible to subdivide the range—as indicated. This "New Colour Method," it should be noticed, ultimately depends on a comparison of iodide-colours with other iodide-colours, not of iodide-colours with air-colours; its validity does not rest on any special theory of the production of the tints, and only assumes the well-recognised fact that the thickness determines the colour. Indeed, with small specimens, the "New Colour Method" is a more accurate method than direct weighing, since the tint at the abnormal places such as the edges and points of support can simply be neglected, whereas in other methods such places introduce serious errors in all corrosion-research.

A number of calculations of error by the two methods have been made. Using the Newer Method, the maximum possible error over most colour-ranges is 4 to 7 per cent.; the average error of a random determination will usually be much less than this. On the other hand, in the hiatus zone, the error may well reach 20 per cent., and the method is here unreliable—as is also the case, for various reasons, in the first order yellow. The Older Colour Method involves serious inaccuracy; for instance, blue-mauve I (dark violet) is produced by an iodine-uptake of 1·50 mg. per sq. dm., but the calculation by the Older Method indicates 1·82 mg. per sq. dm., an error of 21 per cent. Errors of this sort of magnitude occur throughout the first order, but the percentage error is considerably smaller at greater thicknesses; it is clear, however, that the Newer Method gives a smaller maximum error.

In general, the Older Method gives values too low at great thicknesses and too high at small thicknesses. In their recent study of oxide-films, mainly of the first and second-order thickness, Tammann and Bockow* also find that this (older) form of the colour-method gives higher values than the gravimetric method; indeed in some cases their colour-value was 8 or 10 times their gravimetric value. They attribute the discrepancy to the existence of an invisible layer present on the metal before tinting, but in some cases the thickness of the layer which they assume as necessary to reconcile the results is very considerable, and it is perhaps a little difficult to understand why this layer should not in itself give tints.

---

* 'Z. Anorg. Chem.,' vol. 169, p. 42 (1928).

When obtaining the values recorded in Table A, a few measurements were made on silver abraded with a coarser abrasive (French emery paper No. 1). For thick films (second, third or fourth order colours) the relation of colour to weight increment was not found to be affected appreciably by the change of the abrasive. For very thin films (early-first-order), the character of the abrasive has a slight influence, although it required special experiments to establish it with certainty.

Two strips of silver were subjected to coarse and fine abrasion respectively, and placed in equal volumes of a very dilute solution of iodine (calculated as sufficient to give red-mauve I) for three weeks, after which time all the iodine had been taken up by the silver. Careful comparison showed the finely abraded piece to display a slightly more advanced colour, although no more iodine had been used than in the other piece. The experiment was repeated with a somewhat greater quantity of iodine, and the same result was obtained.

These results are most easily understood if it is remembered that Bowden and Rideal* found that abrasion increases the true surface, presumably by producing a network of cracks. Thus after coarse abrasion a limited amount of iodide has to be spread over a greatly increased surface, whilst with fine abrasion the cracks will be less extensive and narrower, and will more quickly become choked with iodide. Thus at low thicknesses, a given amount of iodine per unit area of apparent surface will produce a less advanced colour on a coarsely abraded surface than on a finely abraded surface. Clearly this will cease to be true when the film-thickness exceeds the depth at which the cracks are penetrable by iodine molecules.

Evidently the New Colour Method cannot be used with safety to follow the growth of very thin films on metal which has been abraded in an abnormal manner. But for metal abraded in the standard manner, the observation of colours combined with the results embodied in Table A, column 3, affords as accurate a means of judging the thickness as can be expected in view of the small quantities concerned. This method involves no optical assumptions (since the results of Table A rest directly on experiments), and is merely an indirect means of utilising the gravimetric procedure.

---

* 'Roy. Soc. Proc.,' A, vol. 120, p. 59 (1928); 'Nature,' vol. 112, p. 647 (1928).

II.—*Comparison of Gravimetric, Nephelometric and Electrometric Methods of Measuring the Iodine Uptake.*

Pieces of silver foil were abraded as usual, wiped, measured, weighed, exposed to iodine solution, washed, dried and reweighed. The gain in weight is shown in column (*a*) of Table B. A suitable portion of the foil was cut off, measured, and subjected to cathodic reduction in N/10 potassium nitrate solution with an E.M.F. of 2 volts, the strength of current at different times being noted. The interference colours quickly disappeared, being replaced by a chalky yellow appearance, which finally gave place to the black characteristic of reduced metallic silver. The current fell off with the time, and after reduction was complete, a small residual current, slowly decreasing, continued to flow (connected no doubt with the removal of hydrogen by diffusion or by combination with dissolved oxygen); the completion of reduction is shown by the disappearance of the last traces of yellow.

Table B.—First Methods.

The amount of iodine in mgms. per cm.^{2}.

(*a*) Micro-gravimetric.	(*b*) Electrometric.		(*c*) Nephelometric.
	Assumption (i).	Assumption (ii).	
0·058	0·059	0·033	0·050
0·053	0·049	0·033	0·044
0·034	0·041	0·027	0·029
0·022	0·023	0·017	0·017
0·021	0·016	0·011	0·010
0·014	0·012	0·008	0·009
0·013	0·014	0·010	0·011
0·011	0·007	0·004	0·007
0·006	0·004	0·003	0·004

From the number of coulombs needed to give complete reduction, the amount of iodide present could be calculated. The numbers shown in column (*b*) (i) of Table B are calculated on the assumption that the whole current is taken up in the reduction of the iodide, whilst those in column (*b*) (ii) are calculated on the assumption that the "residual current" (connected with changes other than the reduction of silver iodide) commences to flow from the first moment of immersion. Clearly the truth lies somewhere between the two values. This uncertainty renders the method in this form unsatisfactory, and the electrometric values show only general correspondence with the gravimetric values.

The amount of iodine brought into solution was also determined by adding silver nitrate and comparing the cloudiness with that formed in the same way from a known " standard " solution of potassium iodide. Since the unknown iodide solution contained nitric acid (a bye-product of the electrochemical process, and present in amount equivalent to the iodide) and also N/10 potassium nitrate, both of which affect the nephelometric comparison, these substances were also added in the appropriate quantities in making up the standards. This method of estimating amounts of iodide was found to be most sensitive when the concentration was 16–20 mgms. of iodine per litre, and accordingly this strength was aimed at in making the comparisons. Hence in the case of thick films an aliquot proportion of the electrolyte solution was taken for comparison, but when the films were very thin, the total volume of liquid used in the electrolysis vessel had to be diminished as far as possible ; for this reason, the tinted silver strip was rolled into a cylinder of diameter 0·5 cm. and placed for cathodic reduction in a small cylindrical glass cell containing 2 c.c. of electrolyte, a central platinum wire serving as anode.

The nephelometric determinations, shown in column (*c*) of Table B, give results somewhat lower than the gravimetric determinations ; special experiments showed the difference to be due to oxidation of part of the iodide to iodate, which subsequently interacts with the iodide in the now slightly acid solution to form free iodine. For this reason the process was modified as follows. The platinum anode was replaced by a strip of pure zinc externally short-circuited to the silver, thus eliminating the external source of E.M.F. The silver iodide was reduced as before, but no acid or iodate was produced, and thus the source of error was avoided. It was found that the time-current curve now obtained was of a different character and exhibited an inflection at the moment when the reduction of the iodide was complete. This, together with the fact that the residual current was smaller and more nearly constant, made the method of calculation more reliable and the results more accurate. Some results are given in Table C (see p. 380).

The nephelometric and electrometric methods are useful mainly in cases where it is desired to grind the metal under the solvent, avoiding exposure to air before tinting. The microgravimetric method necessarily involves exposure to air, and before it is legitimate in velocity work to use that method (or the newer colour method, which is merely an indirect use of the microgravimetric

Table C.—Improved Methods.

The amount of iodine in mgms. per cm.^{2}.		
(*a*) Microgravimetric.	(*b*) Electrometric.	(*c*) Nephelometric.
0·162	0·161	0·167
0·128	0·130	0·113
0·106	0·096	0·113
0·059	0·059	0·058
0·040	0·042	0·040
0·040	0·035	0·037
0·018	0·020	0·017
0·014	0·014	0·014
0·004	0·006	0·004
0·002	0·003	0·004

method) it is necessary to ascertain whether the pre-exposure to air affects the rate of growth of the films.

Accordingly different parts of a strip of silver were scratched with a knife point at different times, respectively 48, 27, 19, 3 hours, 1 hour, 5 minutes and 1 minute, previous to the moment of tinting. The abrasion was conducted under chloroform, but otherwise the silver was exposed to air in a desiccator until the time fixed for tinting arrived. The specimen was then re-immersed in chloroform, again scratched at a fresh place, and a solution of iodine in chloroform was added; the whole was then quickly mixed without allowing air to come into contact with the silver. This experiment was performed several times, the period of tinting being different in the various cases. It was found, after long pre-exposure to air, the tint reached seemed in some cases slightly less advanced than when air had been excluded altogether, or allowed to act for a short time only; but the effect was very small, and was not detectable when the period of aeration was less than 24 hours. Evidently any oxide produced by a short exposure to air imposes no appreciable hindrance on the diffusion of iodine to the metal.

Experiments using carborundum as the abrasive gave similar results. A strip of foil thus abraded, was washed in chloroform, kept in the desiccator for 3 hours and then placed in a glass cylinder containing chloroform, being held by means of a clip against the walls. One part only of the surface was then re-abraded below the chloroform level by means of the usual abrading pad. Immediately after re-abrasion, the iodine solution was introduced, and all air expelled. The whole was then mixed by inverting the cylinder, a glass bead being placed in the cylinder to promote stirring; after a suitable period the silver was withdrawn. No difference in colour was detected between the two parts, one only of which had been exposed to air after the abrasion.

In spite of this result, it still appeared possible that abrasion *in vacuo* might cause an increase in the uptake of iodine, because a liquid might penetrate better into cracks if these were not already filled with air; this difference might not be detected by the colour method, since any iodide formed in cracks below the general surface would hardly affect the colour. To test this point, two pieces of silver were abraded and exposed to air for 1 hour; one was introduced into the upper part of a vessel containing chloroform, and the vessel evacuated; the chloroform commenced to boil at ordinary temperature, thus assisting expulsion of air. After sufficient time had elapsed to eliminate all air, chloroform was allowed to enter and fill the vessel. The other specimen was then added and both tinted together. After removal, both pieces of silver exhibited exactly the same colour, and determinations of iodine content by gravimetric and nephelometric methods failed to detect any difference beyond the limits of experimental error.

The main conclusion to be drawn is that a short pre-exposure to air does not measurably affect the growth of iodide-films, and therefore that the microgravimetric method (which involves weighing in air) can be used instead of the more difficult nephelometric or electrometric methods.

Although pre-exposure to air at ordinary temperatures hardly affected the subsequent formation of iodide-films, it was found that a 30 minutes' exposure to air, at 400° C., considerably retarded the development of such films, whilst a preliminary heating *in vacuo*, with hydrogen as residual gas, had the opposite effect.

III.—*Velocity of Growth of Iodide Films.*

It is commonly considered that the increase of the thickness (y) with the time (t) is controlled by the rate of diffusion of the film-forming element (iodine), which is itself proportional to the concentration-gradient. Thus

$$\frac{dy}{dt} = \frac{K_D (C_0 - C_I)}{y},$$

where C_0 and C_I are the concentrations of free iodine at the outer and inner boundaries of the iodide film, and K_D a constant connected with the diffusivity. If the chemical combination of iodine and silver proceeds so quickly that C_I is kept small compared to C_0, this becomes

$$\frac{dy}{dt} = \frac{K_D C_0}{y} = \frac{k}{y},$$

the equation of a parabola. The more general case where the effect of a finite chemical velocity is taken into account has been discussed by one of the authors* elsewhere ; here the curve should be a straight line near the origin, gradually approximating to a parabola when y becomes large. In writing the equation $dy/dt = k/y$ in an integrated form $y^2 = 2kt + A$, most authors have assumed that if the time is so defined that $t = 0$ when $y = 0$, it follows that $A = 0$, and that y^2/t should be constant during a given experiment. This would be logical if the equation held good down to zero thickness ; clearly however it does not, for that would give an infinite value of dy/dt when $y = 0$, and chemical considerations would preclude an infinite velocity even in the absence of a film. Hence, whilst it may still be true that dy/dt is equal to k/y over the range of thicknesses easily investigated, this will cease to be true at very small thicknesses, and even over the range where the relation does hold the integration constant, A, need not in general be zero. Thus y^2/t will only become constant at such thicknesses that y^2 is large compared to A. Actually, however, some of the commonly neglected facts will tend to make A positive and others negative. The limitations imposed by chemical velocity—already referred to—will make it negative, but the fact that the effective area is greater at the instant of immersion than later on will tend to shift A in the positive direction ; finally the fact that the concentration of the liquid in contact with the film will tend first to fall with the time and then to rise again will affect A in a complicated manner. Actually in many of the cases examined, A is evidently small, but this could not have been predicted.

The external film-concentration C_0 will clearly depend on the concentration of free iodine in the liquid next to the film (C_L)

$$C_0 = K_p (C_L)^{m/n},$$

where m is the molecular state of free iodine in the film, n that in the solvent, and K_p is a constant which may provisionally be called the Partition Coefficient. Thus for a given solvent the rate of film-growth will increase with the iodine concentration ; indeed, if the molecular state be the same in the film and the liquid, y^2/t will be proportional to C_L, at ranges where A is small compared to y^2. C_L of course is the concentration of free (unsolvated) iodine molecules. For different solvents, containing the same total amount of iodine per litre, we may, on the whole, expect the violet solutions (where the iodine molecules are believed to be mainly unsolvated) to cause much quicker growth of films than the brown solutions (where there is believed to be much solvation); for solutions of identical colour, K_p will determine the film-growth.

---

* Evans, "Corrosion of Metals" (1926 edition), p. 14 (Arnold).

Experiments were performed to study the effect of different variables. In each series, all the factors were kept constant except one, which was varied.

(1) *Effect of Solvent.*—Specimens were abraded in the standard manner, immersed for different periods in solutions of iodine in six different solvents; all the solutions contained 0·553 grams iodine in 1 litre of *solvent.* The temperature was controlled at 15° C. in a thermostat; after withdrawing, washing and drying, the film-thickness was estimated by the New Colour Method. The curves obtained are shown in fig. 2. With ethyl acetate, ether and amyl acetate the measurements could not be carried to greater thicknesses than those shown, owing to the deposition of a yellowish powder; this occurrence made all measurements somewhat uncertain, and for the solutions mentioned it seemed difficult with confidence to express a relationship between thickness and time. The chloroform, hexane and benzene solutions showed approximate obedience to the parabolic relationship, since when y^2 was plotted against t, nearly straight lines were obtained. The order in which the solutions act is shown in Table D.

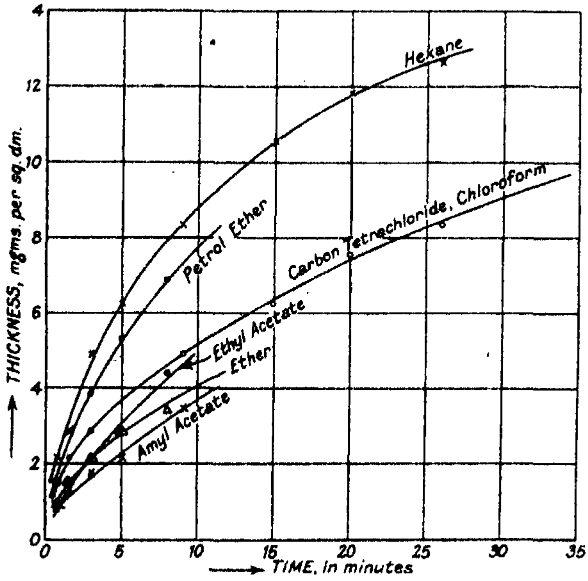

FIG. 2.

Table D.—Effect of Solvent.

Order of velocity of film-thickening.	Solvent.	Colour of solution.
1 (most rapid)	Hexane	Deep violet.
2	Petroleum ether	Red.
3, 4	Carbon tetrachloride	Deep violet.
	Chloroform	Reddish violet.
5	Benzene	Red.
6	Ethyl acetate	Brown.
7	Ether	Brown.
8 (slowest)	Amyl acetate	Brown.

The chloroform and carbon tetrachloride experiments were done simultaneously and specimens taken out at the same time always gave precisely the same colour. The brown liquids do produce slower action than the violet liquids, but petroleum ether falls out of place in the series, suggesting that some other factor (possibly K_p) is influencing the results.

It was found that commercially pure chloroform gave the same curve as the specially purified chloroform, but that commercial benzene containing thiophene gave a much quicker colouration than benzene free from thiophene.

(2) *Effect of Stirring.*—The previous experiments were performed in stagnant liquid, and there was reason to suppose that the consumption of iodine might affect the concentration in the liquid layer next to the iodide film. Experiments were carried out with very small specimens ($0 \cdot 7 \times 0 \cdot 7$ cm.) hung by glass hooks attached radially to a central glass axis which could be rotated; the speeds were varied from 8 to 50 revolutions per minute in different experiments. The solvent was chloroform, and as before the concentration was 0·553 gm. per litre, the temperature 15° C., and the abrasive treatment standard. The slowest stirring slightly increased the rate of thickening as compared with the stagnant experiments, and there was a perceptible further increase as the stirring was made more rapid. The effect, however, was slight, and was difficult to measure with certainty, since at the highest and lowest speeds uniform results were not obtained. Finally an intermediate speed of 16 revolutions per minute, which gave reproducible results, was adopted as standard for subsequent work; this was equivalent to a longitudinal velocity of 2 cm. per second.

The advantage of using very small specimens was that the alteration of concentration due to iodine-consumption could be avoided. The employment of such specimens was only rendered possible by the Newer Colour Method of measuring the thickness; the specimens used were far too small for the older methods, and in any case the irregularities around edges and points of support would have caused errors, had any of the other methods been utilised.

The fact that the motion increases the velocity of film-growth, shows that the thickening is controlled to some extent by passage across the "diffusion layer" of liquid, as well as by diffusion through the solid film; increased movement of the liquid is usually assumed to decrease the effective thickness of the diffusion layer. There is nothing specially surprising in the fact that diffusion through the liquid affects the velocity; in some organic reactions which proceed only at the surface of a metallic catalyst, Rideal* found that the velocity may be controlled entirely by diffusion through this layer, over a certain range of conditions.

(3) *Effect of Abrasion.*—Comparative experiments were performed with cold-rolled silver, and similar silver abraded with numerous different grades of carborundum and emery paper, and also with a rotary wire-brush, a steel point, and a steel blade. Experiments indicated that the abraded surface always ran through the sequence of tints more rapidly than the cold-rolled surface, and, as regards the later colours, it was found that coarse abrasion caused more rapid thickening than fine; in cases where the tinting was only carried on to the very early stages (early first-order colours) an *apparently*

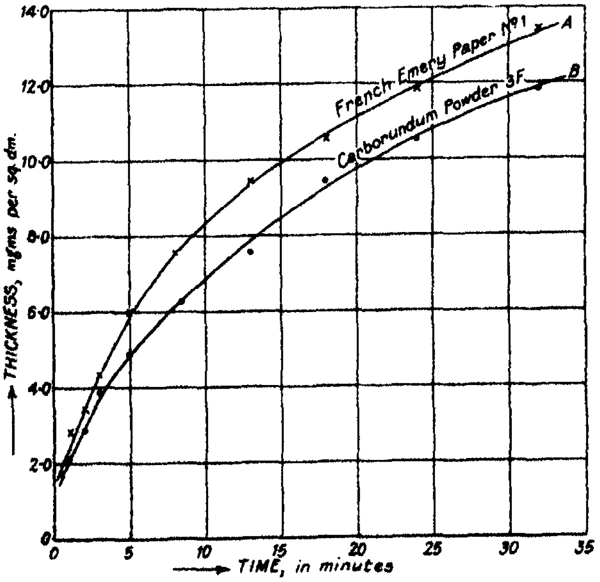

FIG. 3.

---

* 'Trans. Faraday Soc.,' vol. 19, p. 90 (1923).

contrary relation was obtained, fine abrasion giving a very slightly more advanced tint; this is due to the fact that for early tints the relation between colour and thickness varies slightly with the abrasive treatment, as already stated. Fig. 3 shows curves obtained after (A) Treatment with French emery paper No. 1; (B) "Standard" treatment with carborundum; the solvent was again chloroform, the concentration 0·553 gram per litre, the temperature 15° C., and the stirring-conditions "standard"; near the origin the curves are slightly inexact, as already explained.

(4) *Effect of Temperature.*—Measurements were carried out at different temperatures, the solvent being chloroform, the concentration 0·553 gram per litre, and the abrasive conditions and stirring-rate standard; each experiment was performed in duplicate. The values of y^2/t are shown in Table E; it will be noticed that they are far from constant, although approaching constancy at the higher values of y. The numbers placed in square brackets refer to the hiatus-zone where the thickness measurement is unreliable. The other thickness measurements have the accuracy mentioned early in the paper, but of course the percentage error on y^2 is double that on y. For the range of thickness between $y = 6$ and $y = 8$, the mean value of y^2/t is 2·60 at 0° C. and 5·26 at 35° C. Thus the rise of 35° C. merely doubles the velocity "constant"—indicating a somewhat low temperature coefficient.

Other sets of experiments carried out for longer periods, and a set of curves made at a concentration of 0·276 gm. per litre, also pointed to a low temperature coefficient.

(5) *The Effect of Concentration.*—Measurements were made at five different concentrations of iodine in chloroform, the temperature being 15° C., and the abrasive-conditions and stirring-rate standard; each experiment was carried out either in duplicate or triplicate. Experiments were also made at a concentration of 0·1105 gm. per litre; these were performed four times, but since the thickness lay during the greater period within the hiatus range, the results were considered inaccurate and are not included in the figures. The other curves are shown in figs. 4 and 5. In fig. 4 the thickness (y) is plotted against the time t, whilst in fig. 5, y^2 is plotted against t. These latter curves become fairly straight over the greater part of the range, indicating that $(y^2 - A)/t$ becomes fairly constant. The gradients of the straight portions are given in Table F. The ratios of the gradients, taking the gradient at standard concentration as unity, are shown in column 3 and the calculated ratios for different values of $m : n$ are given in columns 4, 5 and 6. The experimental ratio lies between that calculated for $m : n = 1 : 1$, and that calculated for 2 : 1, but

Table E.

First Experiment.				Second Experiment.			
Temperature 0° C.				Temperature 0° C.			
t.	y.	y^2.	y^2/t.	t.	y.	y^2.	y^2/t.
min.	mg. per sq. dm.			min.	mg. per sq. dm.		
0·53	1·26	1·59	3·00	0·73	1·50	2·25	3·08
0·95	1·73	2·99	3·15	2·03	[2·85]	[8·12]	[4·00]
1·48	[2·49]	[5·95]	[4·02]	4·57	3·62	13·1	2·87
3·32	3·42	11·70	3·52	7·85	4·90	24·0	3·06
5·88	3·83	14·67	2·49	12·77	6·27	39·3	3·08
8·98	4·90	24·0	2·67	18·63	6·89	47·4	2·54
15·03	6·27	39·3	2·62	23·0	7·57	57·2	2·49
20·95	7·57	57·2	2·73	26·43	7·57	57·2	2·16
Temperature 15° C.				Temperature 15° C.			
t.	y.	y^2.	y^2/t.	t.	y.	y^2.	y^2/t.
0·53	1·26	1·59	3·00	1·85	[2·85]	[8·12]	[4·39]
1·10	[2·49]	[5·95]	[5·41]	3·78	3·83	14·67	3·88
3·03	3·62	13·10	4·28	6·93	5·30	28·1	4·06
5·47	4·37	19·10	3·49	11·22	6·27	39·3	3·50
8·10	5·30	28·1	3·47	12·45	6·89	47·4	3·79
				16·15	7·57	57·2	3·54
Temperature 35° C.				Temperature 35° C.			
t.	y.	y^2.	y^2/t.	t.	y.	y^2.	y^2/t.
0·57	[2·49]	[5·95]	[10·4]	0·77	[2·49]	[5·95]	[7·66]
1·03	[2·85]	[8·12]	[7·9]	1·62	3·42	11·70	7·22
1·65	3·42	11·7	7·09	5·30	5·30	28·1	5·31
3·38	4·37	19·1	5·66	6·13	5·63	31·7	5·17
5·23	5·30	28·1	5·38	7·05	6·27	39·3	5·57
7·00	6·27	39·3	5·62	8·27	6·89	47·4	5·73
8·65	6·89	47·4	5·47	10·47	7·57	57·2	5·47
12·63	7·57	57·2	4·53	12·85	7·57	57·2	4·46

is much nearer to the former. It is concluded that the molecular condition of the free iodine within the film is for the most part the same as that in the liquid, but that if anything the proportion of the more complex molecules is actually rather greater in the film than in the solution. It is possible, however, that the fact that the change of concentration alters the velocity rather more quickly than would be expected on the assumption that

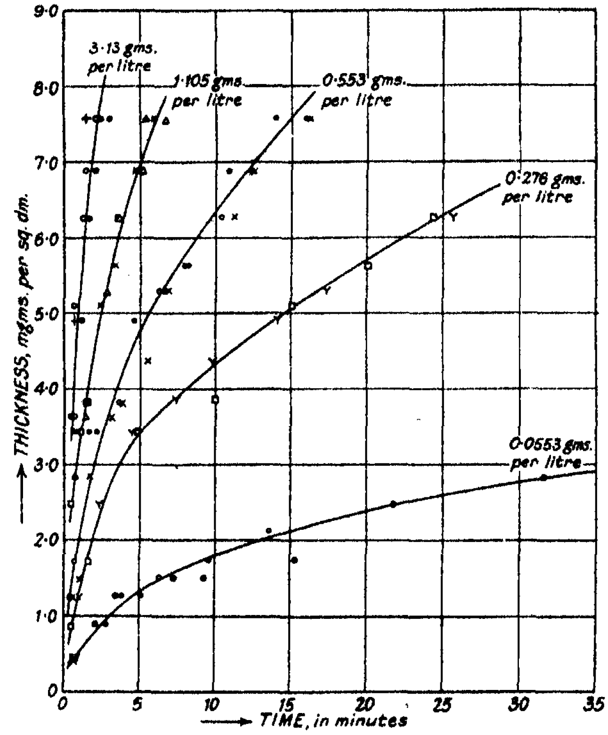
3·13 gms. per litre
1·105 gms. per litre
0·553 gms. per litre
0·276 gms. per litre
0·0553 gms. per litre
THICKNESS, mgms. per sq. dm.
9·0
8·0
7·0
6·0
5·0
4·0
3·0
2·0
1·0
0
0
5
10
15
20
25
30
35
TIME, in minutes

Fig. 4.

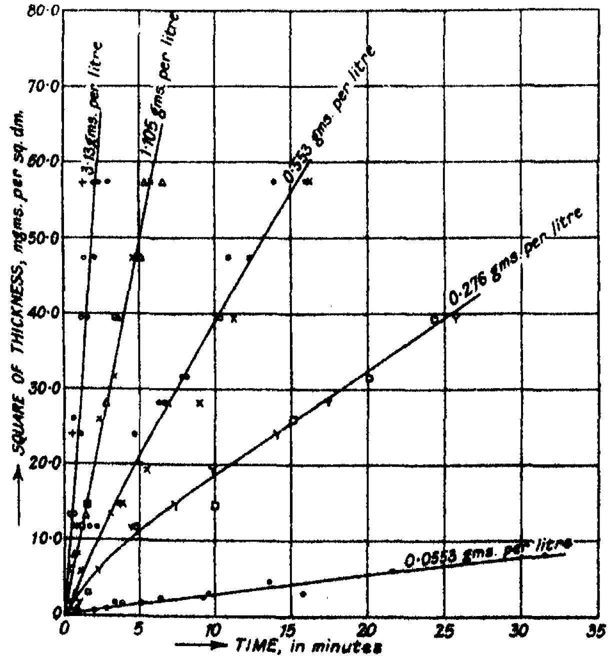
3·13 gms. per litre
1·105 gms. per litre
0·553 gms. per litre
0·276 gms. per litre
0·0553 gms. per litre
SQUARE OF THICKNESS, mgms. per sq. dm.
80·0
70·0
60·0
50·0
40·0
30·0
20·0
10·0
0
0
5
10
15
20
25
30
35
TIME, in minutes

Fig. 5.

$m : n = 1 : 1$ is attributable to the fact that the effect of diffusion over the liquid diffusion-layer becomes increasingly important as a disturbing factor as the dilution increases. However this may be, a comparison with the figures calculated for $m : n = 1 : 2$ completely dispels any idea that the iodine might exist as I_2 molecules in the liquid and single atoms in the film.

Experiments carried out for longer periods pointed in the same direction, although it is difficult to keep the concentration constant if the films are carried to considerable thicknesses. Other sets of curves were obtained with stagnant chloroform and with hexane solutions ; they also support the same conclusions.

Table F.

Concentration gms. per litre.	Gradient $mg^2 dm^{-4} min^{-1}$.	Ratio of gradients (standard concentration = unity).	Ratio calculated for—		
			$m : n = 1 : 1$.	$m : n = 1 ; 2$.	$m : n = 2 : 1$.
3·13	26·3	7·92	5·66	2·39	32·1
1·105	10·0	3·01	2·0	1·41	4·0
0·553	3·32	1·00	1·0	1·0	1·0
0·276	1·38	0·42	0·5	0·77	0·25
0·0553	0·27	0·081	0·1	0·32	0·01

Early Part of Curve.—Some experiments were made by the gravimetric method to follow the early part of the curve, below the point where the colours commenced ; as already explained, large specimens were needed for this method. In the short periods of immersion, the specimens were dipped in the solution, taken out and washed at once ; in the longer periods, specimens were kept in slow motion. Fig. 6 indicates the commencement of a curve at

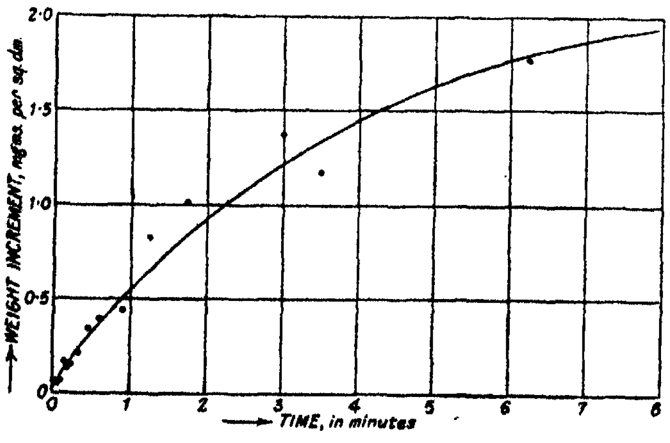

FIG. 6.

15° C., with 0·1105 gms. iodine per litre of chloroform, and standard abrasion; the range covered is largely the invisible and yellow I regions. The curve seems to commence as a nearly straight line, cutting the y axis at a finite angle (not tangentially, as the equation $y^2 = 2kt$ would imply), but at higher thicknesses it gradually passes into an approximately parabolic form ; perhaps the gradient of the initial portion indicates the velocity of combination of iodine with silver before the formation of a film begins to restrict access.

IV.—*Mechanism of Film Growth.*

The fact that the rate of thickening decreases with the thickness indicates that the process is essentially controlled by diffusion through the solid wall of iodide ; the perceptible departure from the parabolic law at the beginning of the curve and the effect of stirring are only what would be expected ; over the ranges where a linear relation holds between y^2 and t, diffusion is apparently the sole controlling factor.

In view of the recent work of Pfeil* on the oxidation of iron, it must not be assumed that the diffusion is due to the uptake of excess of iodine on the exterior. It is possible to imagine that excess of silver dissolves in the iodide layer on the interior surface, thus producing the concentration-gradient needed for diffusion. In this case the rôle of the iodine solutions would be merely to ensure that no excess of silver exists on the exterior surface. Provided the iodine concentration in the solution is sufficient to ensure this, the linear relation between y^2 and t would clearly be accounted for, but it will be noticed that the thickening-curve should be independent of the concentration of the solution, which is not the case. Clearly then Pfeil's mechanism cannot here hold good, and the diffusion must depend on passage of excess iodine inwards.

The results of varying the concentration indicate that iodine diffusing through the film exists in the same "effective" molecular state as in the solution. According to J. A. Müller,† the effective molecular state in both brown and violet solutions is I_2; certainly the general view is that it is not lower than I_2; if so, the diffusion through the film must be mainly as diatomic (or possibly polyatomic) molecules, certainly not as single atoms. Yet on steric grounds, it seems impossible to picture the passage of I_2 molecules—or larger molecules—through compact silver iodide. If, however, pores of sufficient size are present, diffusion of I_2 molecules is evidently possible. The marked influence of abrasion in increasing the rate of film-growth confirms the view that here we are dealing with diffusion through pores. Not only will the coarser abrasion leave the silver porous—a feature favourable to porosity in the silver iodide—but the internal stresses left behind will be favourable to fresh formation of cracks—as indicated in previous work.

---

* 'J. Iron Steel Inst.,' 1929.

† 'Bull. Soc. Chim.,' vol. 11, p. 1006 (1912).

The question then arises as to whether the solution, including solvent, enters the pores. This appears unlikely on several grounds, and the possibility appears to be completely excluded by the results obtained with different solvents. If the solvent entered the pores, the rate of growth of the film would be favoured by employing a solvent of low viscosity or high iodine-diffusivity. Actually, however, ether, which has a much lower viscosity* and higher iodine-diffusivity coefficient† than chloroform, produces a slower rate of film growth. Evidently the solvent does not itself enter the pores.

If then the iodine molecules enter the pores without the solvent, two possibilities remain :—

(1) They may diffuse as free molecules through relatively large channels; this is really gaseous diffusion.

(2) They may diffuse through pores just large enough to accommodate them, and in a sort of loose union with the silver iodide of the walls.

The first idea requires pores larger than are likely to exist, since the silver iodide behaves optically as a single phase. In any case such a mechanism would involve a high temperature coefficient; in cases where the parabolic relation holds good, the diffusion would be roughly proportional to the iodine vapour tension of the solution, and such vapour tensions rise sharply with the temperature, since they depend on the proportion of molecules which possess the necessary energy to escape from the liquid phase. Actually the temperature coefficient is far too low to admit of the idea of evaporation of free molecules.

If, however, the pores are very small, and the I_2 molecules pass through in loose union with the wall-substance, an iodine-molecule need possess no great energy to pass into a channel, and a comparatively low temperature-coefficient is easily understood, provided that there is some sort of affinity between the iodine and the iodide. Seeing that potassium iodide solutions can dissolve excess iodine as KI_3, and seeing that the prevailing views on the peptisation of silver halides postulate the attachment of extra halogen atoms or extra silver atoms to the halide surface, there is every reason to believe that the necessary affinity exists. It would seem therefore that the process is one of passage through channels of only a few molecular dimensions, and is a process intermediate in character between gaseous diffusion and diffusion in solid solution.

---

* Dorsey, 'International Critical Tables,' vol. 5, p. 11.

† Gróh and Kelp, 'Z. Anorg. Chem.,' vol. 147, p. 321 (1925).

Such an idea accords well with the ideas arising from the study of films of other kinds. It was at one time thought that the *steady* growth of films with time (exemplified* by Pilling and Bedworth's copper oxide films above 700° C.) depends on diffusion of the non-metal in solid solution through the material composing the film, but the "*jerky*" growth (such as Pilling and Bedworth found for copper exposed to oxygen at 500° C., or Vernon† found for aluminium at ordinary atmosphere) is due to the passage of the gas through definite cracks which appear at irregular intervals. Dunn,‡ however, has suggested that even in the case of steady growth "the structural units of the oxide are in a state of vibration," and "an oxygen molecule can only pass a structural unit provided that this possesses at the moment energy greater than a critical value causing a loosening of the oxide structure at the point." Feitnecht§ has brought forward evidence that passage of oxygen through copper oxide films may occur preferentially at the grain-boundaries of the oxide-grains; since many authorities, notably Tammann and Bredemeier,‖ consider that capillary channels exist along the grain-boundaries, it is possible that this may be really a special case of passage through pores.

Passing to the films formed at lower temperatures, recent results by one of the authors on corrosion and passivity¶ also indicate that usually the films are not continuous. Oxide-films of the interference-colour range on iron and copper are definitely less protective than the thinner films which are invisible whilst on the metal. But even the latter contain weak spots where penetration by ions can occur. These are of various degrees; the points where penetration by chlorine ions can occur are more closely studded than those where attack by sulphate ions commences. Penetration is also favoured by jagged places on the surface.

In such cases also the pores must be of dimensions small compared to the wave-length of light, since on heat-tinted specimens the film material apparently behaves optically as a single phase. The flow through the film must be a process midway in character between leakage through large apertures, and diffusion in solid solution, just as a " sol " is midway between a suspension and a true solution. As in osmosis, the facility to penetrate will not merely be a question of size ; affinity between the molecules penetrating and the substance penetrated will affect the ease of passage. This may assist the understanding of various cases which seem difficult to explain on the idea of ordinary diffusion in solid solution. Copper exposed to oxygen at ordinary temperatures yields films which cease to thicken before they produce colours ; it is necessary to apply heat before interference tints appear. But copper exposed to sulphur (or air containing hydrogen sulphide) at ordinary temperatures give sulphide films which pass readily through the sequence of interference tints. It is difficult to see why the oxide as such should be less capable of permitting diffusion in solid solution than the sulphide ; but it might easily be less liable to cracking. Quite often substances with large molecules act on metals, producing visible films ; benzene containing a trace of thiophene renders copper brown or mauve, but it is difficult to imagine the thiophene diffusing in solid solution through the film substance.

---

* 'J. Inst. Met.,' vol. 29, p. 544 (1923).

† 'Trans. Faraday Soc.,' vol. 23, p. 153 (1927).

‡ 'Roy. Soc. Proc.,' A, vol. 111, p. 203 (1926).

§ 'Z. Elektrochem.,' vol. 35, p. 142 (1929).

‖ 'Z. Anorg. Chem.,' vol. 142, p. 54 (1925).

¶ Evans, 'J. Chem. Soc.,' 1927, p. 1020; 1929, pp. 92, 111.

All the evidence points to the fact that the films under consideration are essentially porous, but that the leakage is most pronounced where the surface is rough or cracked or the film in a distended condition.

Summary.

Specimens of silver have been exposed to solutions of iodine in chloroform, and a study made of the relation between the weight-increment and the interference colour due to the iodide-film produced ; the assumption made by previous workers that the thickness of the film can be obtained by dividing the equivalent air thickness by the refractive index is shown to be inexact. Nephelometric and electrochemical methods of estimating the thickness of iodide films have been worked out and tested against the microgravimetric procedure. A " New Colour Method " is described, which for small specimens is more accurate than the direct microgravimetric method. It is found that a short pre-exposure to air does not sensibly interfere with the combination of iodine with silver.

The relation between the film-thickness (y) and time (t) has been studied under different conditions of solvent, stirring-rate, abrasive-treatment, temperature and concentration. Other things being equal, violet solutions act more rapidly than brown solutions, and coarsely abraded surfaces are attacked more rapidly than finely abraded surfaces. In general, there is a perceptible departure from the law $dy/dt = k/y$ at low thicknesses, but the

fact that y^2 becomes approximately a linear function of t as thickening proceeds indicates that the process is largely controlled by the rate of diffusion through the film. The effect of concentration indicates that the molecular state of the excess iodine in the film is not lower than I_2, but the small temperature coefficient excludes the idea of gaseous diffusion through large apertures. The effect of varying the solvent indicates that we are not dealing with pores through which the solvent can enter. It is concluded that the iodine passes through pores of a few molecular diameters in loose union with the silver iodide—a process intermediate in character between diffusion in solid solution and gaseous leakage through definite cracks. This idea agrees with conclusions drawn from work on films other than iodides.

The Electrical Conductivity Caused by Insoluble Monomolecular Films of Fatty Acid on Water.

By Prof. James W. McBain, F.R.S., and Dr. C. R. Peaker.

(Received June 24, 1929.)

Introduction.

The well-known researches on thin films of insoluble fatty substances on water have brilliantly demonstrated that such films are monomolecular and that the molecules are oriented with their polar groups in contact with the water. Thus stearic acid spreads on water with its carboxyl groups on the water surface. No one, however, has as yet investigated the possible dissociation of such fatty acids with formation of free hydrogen ions in the water, leaving the fatty ions behind in a monomolecular film on the surface.

Such dissociation need not and probably should not involve more than a small fraction of the molecules on the surface. One of us* has pointed out the enormous voltages which would be caused between a complete monomolecular layer of free ions and the charges of opposite sign, vastly exceeding the electromotive forces of vigorous chemical reactions. This and many other lines of evidence have led to the theory of "sparse surface dissociation,"[*] according to which a surface such as that of a colloidal particle may be largely covered or consist of undissociated molecules or adsorbed ion pairs, forming a double layer in the strict Helmholtz sense, but with a further portion of the surface covered only with unbalanced or singly adsorbed ions whose partners remain free and mobile somewhere in the solution.

---

* McBain, 'J. Phys. Chem.,' vol. 28, p. 706 (1924).

The fact that colloidal electrolytes, such as soap, exhibit a high conductivity showed that at least a portion of the double layer, if any on these colloidal particles, must be dissociated into free and mobile ions existing independently in the solution, leaving behind highly charged colloidal particles which, like the mobile ions, exhibit high conductivity by virtue of their free charges. This conception invalidates the application of the classical formulæ of the Helmholtz double layer which are all derived on the assumption that there are no free charges on the surface in the interface. Indeed it is very possible that the electrical double layer has nothing to do with electrokinetic phenomena, although its ion pairs may be of importance in stabilising colloid surfaces as, for example, through induced solvation.

Films of insoluble fatty acid on water afford an opportunity of testing the essential aspect of this modern conception of the existence of free mobile ions within the solution corresponding to free, unbalanced charges on the interface. We have measured here the conductivity due to these mobile ions and find that only about one-ninth of the monomolecular layer of stearic acid on water is dissociated. This extra conductivity, introduced by the insoluble film of fatty acid, may be termed "surface conductivity." This constitutes the first actual measurement of surface conductivity in absolute units.[†]

The Experimental Method.

The object was to measure the extra conductivity in the neighbourhood of the surface after coating with insoluble fatty acid, and to distinguish it clearly from any conductivity due to slight solubility of the fatty acid or impurities introduced therewith. These purposes are accomplished through the use of a conductivity vessel of special design as shown in fig. 1.

---

[*] Compare references in McBain, 'Colloid Symposium Monograph,' vol. 4, pp. 13 and 16 (1926); 'Kolloid-Z.,' vol. 40, p. 1 (1926). See also the formulations of Gouy ('J. Physique,' series 4, vol. 9, p. 457 (1910)), and of Stern ('Z. Electrochemie,' vol. 30, p. 508 (1924)), and the ionic structural mechanism of Mukherjee ('Phil. Mag.,' vol. 44, p. 321 (1922)).

[†] The absolute measurements of surface conductivity in the neighbourhood of optically polished glass surfaces in progress since 1919 (McBain and Darke, General Colloid Discussion, 'Trans. Farad. Soc.,' vol. 16, p. 150 (1921); 'Kolloid-Z.,' vol. 28, p. 239 (1921)) have now been completed by us for communication to the American Chemical Society.

The electrodes consist of two vertical platinum rings held concentrically by supports which in no wise tend to bridge the gap between them and which therefore do not introduce any surface conductivity of their own. It is a common fault in conductivity cells that they are partially short circuited by glass struts, or supports, or neighbouring glass walls, a source of error which seems never to have been suspected, even when cell "constants" have been recorded as varying appreciably with different solutions. The essential measurements are: (*a*) the conductivity of the water alone; (*b*) the conductivity of the water after introduction of the fatty acid but with the surface far removed from the electrodes; (*c*) the conductivity exhibited by the water when the surface is brought to the same level as the tops of the two electrodes; and (*d*) the conductivity with the surface in the same position after introduction of the fatty acid. In the design illustrated, measurements (*a*) and (*c*) could be repeated as often as desired until constant values were obtained before introducing fatty acid; thereafter the measurements (*b*) and (*d*) could be repeated indefinitely without opening the cell. This repetition is effected by pouring unwanted liquid into the side reservoir and pouring it back so as to fill the cell for such measurements as (*a*) and (*b*).

The outside platinum electrode was 1 cm. high and about 2 cm. in diameter, with about 1 or 2 mm. between it and the inner electrode, so that the area in square centimetres of the annular space between them is about equal to the volume between them in cubic centimetres. The platinum wires leading to the electrodes were covered with glass. A very great advantage of supporting the inner electrode from the ground-in joint at the top of the cell is the ease with which the electrodes may be taken apart for platinising and cleaning operations which otherwise were found to consume many weeks. Three cells were successively used, fig. 1 showing the final design for use with especially pure conductivity water which has not yet been available. The electrodes were well platinised, were reduced by using each as cathode, and were washed until the resistance of conductivity water placed in the cell remained constant.

The stearic acid used was a sample of stearic acid "Kahlbaum." This was extracted several times with hot conductivity water, allowed to dry on a filter paper in a desiccator, and finally recrystallised from distilled ether. The melting point of the stearic acid was 69·2° C.

The arrangement of the conductivity bridge was similar to that described by Jones and Josephs* with some modifications. Instead of the fixed-ratio slide wire used by them, we used a Kohlrausch type slide wire (Leeds and

---

* 'J. Am. Chem. Soc.,' vol. 50, p. 1049 (1928).

Northrup). The grounding resistance was another slide wire of the same type. The slide wire in the bridge circuit proper was carefully calibrated, and the necessary corrections applied to the bridge readings. The resistance of the box was adjusted so that the readings came about the centre of the slide wire.

The resistance box was of the five-dial type made by Leeds & Northrup. Coils of 1000 ohms and above were of the Curtis design. A Vreeland oscillator (Leeds & Northrup), supplying alternating current at a frequency of about 1000 cycles per second to the bridge network, was used. The oscillator was at a distance of 40–50 feet from the bridge. A one-stage vacuum tube amplifier was used in conjunction with the telephones. Two variable air condensers (caps. 0·001 and 0·00012 mfds.) were used to balance the capacity of the cell, the one of smaller capacity being used as a vernier. The region of silence in the telephones could be fixed very accurately (to 1/10,000 part of the length of the bridge wire).

Procedure and Calculation.

The cell was first filled with conductivity water to the point marked (*a*) in the figure and immersed in a thermostat, containing distilled water maintained at 25 ± 0·005° C. When the resistance became constant (R_1), water was spilled over into the side bulb until the tops of the electrodes were just in the surface. When the resistance again became constant (R_2), the water in the side bulb was run back into the main part of the cell, and another set of measurements on the resistance obtained. After obtaining a consistent series of values for R_1 and R_2 in this way, we were ready to start the second part of the experiment. After obtaining the last value for R_2, a small amount of stearic acid was put on the surface of the water through the side tube (A), thus not disturbing the electrodes at all. When the resistance became constant (R_3), the water in the side bulb was spilled back to fill the main part of the cell to point (*a*), and measurements taken until a constant resistance was obtained (R_4). Care was always taken to have visible crystals of stearic acid on the surface when measuring (R_3).

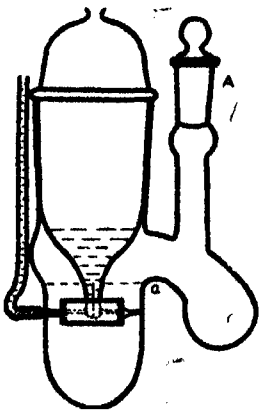

R_1 = resistance of cell filled with conductivity water; R_2 = resistance of cell filled to top of electrodes with conductivity water; R_3 = resistance of cell filled to same position with fatty acid present; this includes the resistance of the water, of the dissolved stearic acid, and any surface effects; R_4 =

resistance of cell filled with contaminated water; this includes the resistance of the water and of the dissolved stearic acid.

$1/R_3$ = conductivity of water + conductivity of dissolved stearic acid + "surface conductivity" (S).

Hence

$$1/R_3 = S + (1/R_2 \,.\, R_1/R_4). \qquad (1)$$

The equation can then be solved for S, since everything else is known. The calculations from a typical experiment are given in detail as follows: R_1 = 14,438 ohms; R_2 = 16,129 ohms; R_3 = 13,949 ohms; and R_4 = 12,816 ohms. Substituting in equation (1), S = 0·000001841 mhos. Conductivity of water = 1/14,438 = 0·00006200 mhos. Then per cent. increase in specific conductivity is

$$0{\cdot}000001841 \times 100 \div 0{\cdot}00006200 = 2{\cdot}7 \text{ per cent.}$$

The cell constant of this cell was 0·0226, so the conductivity of the surface is

$$2{\cdot}7 \times 0{\cdot}0226 \div (100 \times 14{,}438) = 0{\cdot}000000042_2 \text{ mhos.}$$

It is of great interest to calculate the surface conductivity in absolute units. Volume conductivity is always indicated by specific conductivity; that is, the conductivity in reciprocal ohms of a cube of solution placed between parallel electrodes 1 cm. square and 1 cm. apart. Similarly we must invent a specific surface conductivity in two dimensions instead of three (as regards the actual surface area), defining it as the conductivity in reciprocal ohms between two parallel electrodes 1 cm. long, placed 1 cm. apart on the surface. Hence, from the determination given above, since the area of the film between the electrodes is to the volume of liquid between the electrodes very nearly as 1 : 1, the specific surface conductivity (for 1 cm.^{3}) is

$$0{\cdot}000000042_2/1 = 0{\cdot}000000042_2 \text{ mhos./cm.}^2 = 4{\cdot}2 \times 10^{-8} \text{ mhos./cm.}^2.$$

Results and Discussion.

The following table records the results obtained with the different cells used.

The results demonstrate conclusively the existence of a conductivity in the neighbourhood of the monomolecular film of insoluble fatty acid. This is the first apparently unambiguous system that has been investigated. Surface conductivity has been surmised from the data of Stock, Miss Laing, Fairbrother, Briggs and Stamm, but in every case alternative explanations were possible

Table I.—Specific Surface Conductivity in mhos./cm.^{2} of a Surface of Water Carrying a Film of Stearic Acid at 25·00° C.

Cell.	R_1.	R_2.	R_3.	R_4.	Cell constant.	Per cent. increase.	Specific surface conductivity.
							(mhos./cm.^{2}).
‡1	4,618	4,805	4,409	4,289	0·00877	1·33	$4 \cdot 2 \times 10^{-8}$
‡2	14,438	16,129	13,949	12,816	0·0226	2·70	$4 \cdot 2 \times 10^{-8}$
‡3	10,137	10,576	10,153	9,964	0·00976	2·30	$2 \cdot 2 \times 10^{-8}$
						Mean	$3 \cdot 5 \times 10^{-8}$

and plausible. We have completed absolute measurements of surface conductivity of salt solutions in contact with known areas of optically polished glass. There excess conductivities likewise could equally well be explained as being merely due to a concentration of salt in the neighbourhood of the surface rather than as here unmistakably due to mobile ions complementing unbalanced charges in the surface proper. N. K. Adam* found that with palmitic acid, which is presumably far more soluble than stearic acid, not ½ per cent. of the molecules of palmitic acid placed upon his trough left the film to go into the water. This can only have been possible because of the acidity of his " water." Even with the more insoluble stearic acid, as will be seen, the amount which would dissolve in really pure water in a trough of the depth which Adam describes would be equal to the amount required for a monomolecular film upon the surface. Adam does not state the p_H or conductivity of the " water," but he does describe the clear cut results obtained when the acidity exceeded p_H 5·5.

Approximate evaluation of the true solubility of stearic acid is afforded by the data of Table I.† For example in cell ‡3, where the dissolved stearic acid raised the concentration of the water 980/963 fold, if the conductivity of the water ($0 \cdot 963 \times 10^{-6}$) is ascribed to H^+ and HCO_3^-, then the concentration of $H^+ = 2 \cdot 2 \times 10^{-6}$ N and of the stearate ion $= 7 \times 10^{-8}$ N, the solubility product being $15 \cdot 4 \times 10^{-14}$. If the dissociation constant be taken as $0 \cdot 8 \times 10^{-6}$, the dissociation is practically complete at this dilution and the total solubility is $4 \cdot 1 \times 10^{-7}$ N at 25° C.

There seem no other probable explanations of our measurements than that they are due to independent mobile hydrogen ions dissociated from the fatty film. If so, the fatty film is left with an equal and opposite electric charge. It is to these free charges, the mobile ions on the one hand and the sum of the unbalanced sessile charges on the other, that we ascribe all electrokinetic effects.*

---

* 'Roy. Soc. Proc.,' A, vol. 99, p. 342 (1921).

† Compare the corresponding calculation for palmitic acid at 90° by McBain and Taylor, Z. phys. Chem.,' vol. 76, p. 179 (1911).

Since the conductivity of the surface has been ascribed to the "mobile" ions of the double layer, it is of interest to calculate the number of such "mobile ions" per square centimetre. Considering the results for cell ‡2 in detail, let us assume that the conductivity of the water used in this experiment was due to (monobasic) carbonic acid. Then from the relation that $\Lambda = 1000\,k/\mathrm{C}$, where Λ = equivalent conductivity of H_2CO_3 solution (sum of mobility of H^+ (350) and HCO_3^- (70) at 25° C. = 420), k = specific conductivity of the water used, and C = concentration of hydrogen ion in gram equivalents per litre, we can calculate the value of C. This is

$$\mathrm{C} = \frac{1000 \times 0\cdot0226}{14{,}438 \times 420}.$$

Then the number of mobile hydrogen ions per square centimetre is given by

$$\frac{2\cdot7 \times 1000 \times 0\cdot0226 \times 6\cdot06 \times 10^{23}}{100 \times 1000 \times 1 \times 14{,}438 \times 420} = 6\cdot08 \times 10^{13}.$$

The total number of stearate molecules and ions per square centimetre for a "close-packed" monomolecular film, if each occupies $25\cdot1 \times 10^{-16}$ sq. cm. is 4×10^{14}. Thus the number of mobile hydrogen ions corresponds to about one-seventh of the stearate in the monomolecular film. (The number of mobile hydrogen ions per square centimetre, calculated as given above, is $3\cdot64 \times 10^{13}$ and $3\cdot20 \times 10^{13}$ for cells ‡1 and ‡3, respectively.)

The average value for the number of "mobile" ions, from the results of Table I, is $4\cdot64 \times 10^{13}$, corresponding to about one-ninth of a monomolecular film for a solution of p_H corresponding to a specific conductivity of about $1\cdot2 \times 10^{-6}$ mhos, at 25° C.

For the study of materials which do not spread spontaneously, a somewhat different design of cell could be used, consisting of two concentric rings of platinum, clamped between glass plates, coated with the substance to be studied. Such a cell would be perfectly general in its application to the measurements of "surface conductivity."

---

[*] For a quantitative verification of this point of view for the various kinds of soap systems see Laing, "A General Formulation of Movement in an Electrical Field: Migration, Electrophoresis and Electroosmosis of Sodium Oleate," 'J. Phys. Chem.,' vol. 28, p. 673 (1924).

Summary.

A monomolecular film of insoluble fatty acid on water consists partly of fatty ions whose corresponding hydrogen ions have dissociated into the aqueous layer. These free mobile hydrogen ions are revealed through the electrical conductivity which they impart to the aqueous layer in the neighbourhood of the surface. The specific surface conductivity at 25° C. in the neighbourhood of the monomolecular film of stearic acid is $3 \cdot 5 \times 10^{-8}$ mhos., corresponding to a dissociation of about one-ninth of the total stearic acid in the monomolecular layer on water of conductivity $1 \cdot 2 \times 10^{-6}$. The existence of the surface conductivity with its corollary of free mobile ions and corresponding charges left upon the interface lends support to the opinion that the Helmholtz double layer is not responsible for the electrokinetic phenomena, and that the classical formulæ are not strictly applicable, owing to the existence of unbalanced charges upon the interface.

A Quantitative Study of the Reflexion of X-Rays from Crystals of Aluminium.

By R. W. James, M.A., G. W. Brindley, M.Sc., and R. G. Wood, B.Sc., Manchester University.

(Communicated by W. L. Bragg, F.R.S.—Received July 5, 1929.)

1. It has already been shown* that the observed variations with temperature of the intensity of reflexion of X-rays from crystals of rock-salt and sylvine agree closely with those predicted by the theory of Debye,† as modified by Waller,‡ from the lowest temperature at which experiments have been made, that of liquid air, up to about 500° abs. Moreover, the absolute intensities of reflexion agree closely with those calculated theoretically, if the atomic scattering factors, F, are calculated from the Schrödinger charge-distributions for the atoms, obtained by the method due to Hartree.§ To obtain agreement, it is

---

* James and Firth, 'Roy. Soc. Proc.,' A, vol. 117, p. 62 (1927); Waller and James, *ibid.*, A, vol. 117, p. 214 (1927); James, Waller and Hartree, *ibid.*, A, vol. 118, p. 334 (1928); James and Brindley, *ibid.*, A, vol. 121, p. 155 (1928).

† 'Ann. Physik,' vol. 43, p. 49 (1914).

‡ Upsala Dissertation, 1925.

§ 'Camb. Phil. Soc. Proc.,' vol. 24, pp. 89, 111 (1928).

necessary to assume the existence of zero-point energy of an amount half a quantum for each degree of freedom, and the experiments may perhaps be considered as furnishing direct confirmation of such energy, since the differences between the intensities calculated with and without it are considerable. The work to be described in this paper was undertaken with a view to extending the investigations to a crystal of a metallic element. Aluminium at once suggested itself as suitable for this purpose, since it can be obtained in large single crystals, and since its coefficient of absorption for the X-rays employed in the experiments, Mo K_a, is small.

Experiments on the variation in the intensity of reflexion of X-rays from aluminium with temperature have already been made by Backhurst* and by Collins,† but their results are not in good agreement. Backhurst found a diminution of intensity with increasing temperature greater than that given by the original formula of Debye, while Collins found a smaller diminution. Both heated the crystal above the temperature of the laboratory, and such treatment is likely to alter the state of crystallisation, and perhaps to cause twinning. Backhurst reports that the intensity of reflexion from his crystal was permanently reduced as a result of the heating, which might have been due to twinning, or to more perfect crystallisation, with a consequent increase in extinction. To avoid these difficulties as far as possible, we have studied the temperature factor over the range from the temperature of liquid air, about 86° abs., to that of the laboratory. The alternate heating and cooling over this range appeared to produce no recrystallisation, and the intensity of reflexion at the laboratory temperature remained the same within the errors of experiment, throughout the work.

The work may be divided into two sections: (1) measurement at room temperature of the absolute intensities of a number of spectra by comparing them with a reflexion of known intensity from a standard rock-salt crystal; (2) comparative measurements at room temperature, and at the temperature of liquid air, to determine the temperature factor. From (1) the atomic scattering factors, F, at room temperature can be deduced, and these are finally compared with the values calculated theoretically from the Schrödinger charge-distributions, the F curves so obtained being corrected by means of the temperature factors deduced from (2).

---

* 'Roy. Soc. Proc.,' A, vol. 102, p. 340 (1922).

† 'Phys. Rev.,' vol. 24, p. 152 (1924).

2. *Experimental Work.*

Two single crystals of aluminium were used, which were very kindly given to us by Prof. G. I. Taylor, F.R.S., to whom we are also indebted for cutting and preparing the necessary faces upon them. On one crystal, A, a (111) face was cut, and on the other, B, a (100) face.

As a measure of the intensity of reflexion from a face, the integrated reflexion, ρ, is used, which is equal to $E\omega/I$, where E is the total energy reflected by the crystal as it rotates with uniform angular velocity ω through the small angular range over which it reflects, and I is the total energy incident in 1 second on the crystal face. In the experiments, I and ω are the same for the aluminium crystal and for the standard, so that it is only necessary to compare E for the spectrum whose intensity is required with that for the standard spectrum. This is in all cases the spectrum (400) of rock-salt, and the value of ρ for it is $98 \cdot 4 \,.\, 10^{-6}$ for molybdenum K_a.* It should be noticed that, since the (400) spectrum from rock-salt shows an appreciable amount of extinction, the values of ρ for it differ somewhat from crystal to crystal, so that the value given here refers only to the particular crystal used as the standard.

The method of determining the integrated reflexion has often been described, and it is not necessary to enter into details here. It consists in taking alternate readings of E for the spectrum to be measured, and for the standard. Twelve or 15 readings for each spectrum are usually taken in a comparison, together with an independent determination of the fraction of general radiation, so that a comparison may take nearly an hour to make. Care is taken to keep the filament current in the Coolidge bulb, and the applied voltage, as constant as possible, but variations still occur, which can only be smoothed out by taking a large number of readings. We give below, in Table I, the values of the integrated reflexions obtained in determining F. Each number represents a comparison made in the way just described. The cut faces are not exactly parallel to the crystal planes, so that a different value of the integrated reflexion is in general obtained if the crystal is turned through 180°.† The difference is only appreciable if the glancing angle of reflexion is small. For the spectra (111), (200), (222) and (400), observations have been taken in the two positions, the letters R and L against the numbers in Table I denoting whether the crystal faced right or left when mounted on the spectrometer. It can be shown that the true integrated reflexion is the mean of the values obtained in the left and right positions.

---

* James and Firth, *loc. cit.*

† W. H. Bragg, 'Phil. Mag.,' vol. 27, p. 881 (1914).

Table I.—Integrated reflexions from Al at 290° abs., in terms of NaCl (400) as 100.

Crystal A.

Spectrum.				
(111).	(222).	(333).	(444).	(555).
465·4 (L)	133·8 (L)	$26\cdot1_0$	4·95	1·41
465·4 (L)	132·9 (L)	$26\cdot4_5$	4·94	1·45
697·0 (R)	154·1 (R)	—	—	1·42
692·0 (R)	155·6 (R)	—	—	—
Means 580·0	144·1	$26\cdot2_8$	$4\cdot94_5$	$1\cdot43_3$

Crystal B.

Spectrum.			
(200).	(400).	(600).	(800).
428·5 (R)	85·2 (R)	12·24	$2\cdot07_6$
427·1 (R)	85·2 (R)	12·28	$2\cdot14_7$
440·2 (L)	86·3 (R)	12·20	—
445·6 (L)	88·1 (L)	—	—
440·9 (L)	87·0 (L)	—	—
450·2 (L)	—	—	—
Means 436·0	86·4	12·24	$2\cdot10_4$

The comparative measurements at the temperature of liquid air and at room temperature were made exactly as described in the paper on rock-salt.* The crystal was supported inside a thin walled Dewar flask, through the walls of which the incident and reflected X-ray beams passed. A comparison with the standard was first of all made, with the crystal in the flask, at room temperature. Liquid air was then poured in, until its level was just below that of the lower edge of the crystal-face. The crystal was supported in a metal holder which dipped well into the liquid air, so that the temperature of the crystal was kept uniform throughout by conduction. The comparison was repeated at the low temperature, and the crystal was finally allowed to regain the temperature of the room, another comparison being made later to ensure that no change either in the condition or in the setting of the crystal had occurred. The results of the measurements are given in Table II, and show the type of agreement obtained. The lower values of the intensities at room temperature as compared with those given in Table I are due to absorption in the walls of the flask.

---

* James and Firth, *loc. cit.*

Table II.—Comparative measurements at 290° abs. and 86° abs. Crystal in Dewar flask. Reflexions ρ_1 and ρ_2 in terms of NaCl (400) as 100.

Crystal A.

		(222).	(333).	(444).	(555).
$T_1 = 290°$		$86\cdot8$	$16\cdot84$	$3\cdot20$	$0\cdot91_2$
		$87\cdot1$	$16\cdot95$	$3\cdot25$	$0\cdot90_6$
		—	$16\cdot96$	$3\cdot26$	—
	ρ_1	$86\cdot9$	$16\cdot92$	$3\cdot23$	$0\cdot90_9$
$T_2 = 86°$		$99\cdot7$	$24\cdot23$	$6\cdot17$	$2\cdot47$
		$100\cdot9$	$24\cdot70$	$6\cdot46$	$2\cdot53$
		—	$24\cdot64$	$6\cdot32$	$2\cdot47$
		—	—	$6\cdot23$	—
	ρ_2	$100\cdot3$	$24\cdot52$	$6\cdot29_6$	$2\cdot49_1$

Crystal B.

		(400).	(600).	(800).	
$T_1 = 290°$		$56\cdot7$	$8\cdot21$	$1\cdot45_5$	
		$57\cdot0$	$8\cdot19$	$1\cdot43_0$	
		—	$8\cdot31$	$1\cdot42_5$	
	ρ_1	$56\cdot8_5$	$8\cdot23$	$1\cdot43_4$	
$T_2 = 86°$		$67\cdot8$	$13\cdot55$	$3\cdot48$	
		$68\cdot9$	$13\cdot40$	$3\cdot54$	
	ρ_2	$68\cdot3_5$	$13\cdot47$	$3\cdot51$	

3. *Discussion of the Results.*

The atoms in the crystal of aluminium lie on a face-centred cubic lattice, and the contributions of all of them to all the spectra are in phase. The integrated reflexion ρ for X-rays of wave-length λ, reflected at a glancing angle θ, is given by the formula

$$\rho = \frac{\mathrm{E}\omega}{\mathrm{I}} = \frac{\mathrm{N}^2\lambda^3}{2\mu}\cdot\frac{e^4}{m^2c^4}(\mathrm{F}_0e^{-\mathrm{M}})^2\,\frac{1+\cos^2 2\theta}{2\sin 2\theta}. \qquad (1)$$

N is the number of diffracting units per cubic centimetre of the crystal, and μ is the linear absorption coefficient. F_0 is the atomic scattering factor for the atom at rest. It is a function of the angle of scattering, and may be defined as the ratio of the amplitude scattered by the atom in any direction to that scattered in the same direction by a single classically-scattering electron under the same conditions, and it tends to a value equal to the number of electrons in the scattering atom for very small values of θ. The factor e^{-M} takes account of the heat motions of the atoms, and was first introduced by Debye. It can be shown that

$$M = 8\pi^2 \overline{u_x^2} (\sin^2 \theta)/\lambda^2, \tag{2}$$

where $\overline{u_x^2}$ is the mean-square displacement of an atom from the average position of the atomic plane to which it belongs, and is a function of the temperature. The quantity $F_0 e^{-M}$ is the scattering power for the average atom at the temperature under consideration; it will be denoted in what follows by F.

Using the known values of the atomic constants, and the observed values of ρ and θ, and putting $\mu = 14 \cdot 35$, the values of F for a series of spectra have been calculated from equation (1). The values of F for aluminium at room temperature, determined in this way, are given in Table III, column 5.

Table III.—Values of $F_0 e^{-M}$ at 290° abs. $\lambda = 0 \cdot 710$ Å.

Spectrum.	θ.	sin θ.	$(\sin \theta)/\lambda$.	$F = F_0 e^{-M}$.
	° ′			
111	8 43	0·1518	0·214 . 10^8	7·08
200	10 6	0·1754	0·247	6·63
222	17 40	0·3036	0·428	5·25
400	20 32	0·3508	0·494	4·46
333	27 6	0·4554	0·632	2·96
600	31 45	0·5262	0·742	2·24
444	37 23	0·6072	0·855	1·57
800	44 33	0·7016	0·988	1·08
555	49 23	0·7590	1·069	0·87

4. *Calculation of the Temperature Factor.*

Let quantities measured at the room temperature and at the temperature of liquid air be denoted by the suffixes 1 and 2 respectively. Then, if we neglect the small changes in θ, N and μ due to the change in the lattice spacing with temperature, we have from equation (1),

$$\log_e (\rho_2/\rho_1) = 2 (M_1 - M_2). \tag{3}$$

The values of $M_1 - M_2$ for the different spectra may therefore be calculated at once from the numbers in Table II. Now from equation (2), we have

$$M_1 - M_2 = 8\pi^2 \{(\overline{u_x^2})_1 - (\overline{u_x^2})_2\},$$

which, since $(\sin^2 \theta)/\lambda^2 = (h^2 + k^2 + l^2)/4a^2$, where h, k, l are the indices of the spectrum, and a the lattice constant, can be written

$$\frac{M_1 - M_2}{h^2 + k^2 + l^2} = \frac{2\pi^2}{a^2} \{(\overline{u_x^2})_1 - (\overline{u_x^2})_2\}. \tag{4}$$

Thus $(M_1 - M_2)/(h^2 + k^2 + l^2)$ should be constant, for a given pair of temperatures, for all spectra.

Table IV.

Spectrum.	$h^2+k^2+l^2$.	ρ_2/ρ_1.	$\log_e \rho_2/\rho_1$.	$2(M_1 - M_2)/(h^2+k^2+l^2)$.
222	12	1·154	0·1433	0·01194
400	16	1·202	0·1839	0·01150
333	27	1·450	0·3716	0·01376
600	36	1·635	0·4916	0·01365
444	48	1·944	0·6647	0·01385
800	64	2·439	0·8916	0·01395
555	75	2·741	1·0084	0·01345
			Mean	0·01373

In Table IV, the results of the measurements at the two temperatures $T_1 = 290°$ abs. and $T_2 = 86°$ abs. are summarised. The last column gives the values of $(M_1 - M_2)/(h^2 + k^2 + l^2)$, which are seen to be very nearly constant, except for the spectra (222) and (400). For these spectra the ratio ρ_2/ρ_1 is nearly unity, and the percentage change in its logarithm is large for a small change in its value; and also, as will be seen later, there is evidence that these spectra are affected to some extent by extinction. In obtaining the mean value in the last column of the table these spectra have therefore been neglected.

Calculation of M.—By comparing the intensities of the same spectrum at two different temperatures it is only possible to calculate the difference in M for the two temperatures. Under certain conditions, however, it is possible to determine M itself. Since this question has been dealt with at some length in a previous paper,[*] it is only necessary to give a brief outline here.

---

[*] Waller and James, *loc. cit.*

If $T > \Theta/2\pi$, where Θ is the "characteristic temperature" of the crystal, we may write

$$\overline{u_x^2} = \alpha + \beta T + \gamma/T + \delta/T^3. \qquad (5)$$

In this expression

$$\gamma = \frac{1}{12mk}\left(\frac{h}{2\pi}\right)^2,$$

where m is the mass of an atom of the lattice, k is Boltzmann's gas-constant, and h is Planck's constant. γ thus depends only on known constants, and can be evaluated at once. β and δ depend on the forces between the atoms of the lattice, but δ can be estimated with sufficient accuracy from an approximate formula, since the term containing it is small. α contains a factor $(L_\nu - \frac{1}{2}h\nu)$, where L_ν is the energy associated with the degree of freedom of frequency ν at the absolute zero of temperature. If this is half a quantum, as Planck suggested, and as the wave-mechanics requires, the term α vanishes. Under these conditions therefore, if β can be determined experimentally, M can be calculated. A knowledge of M will enable us to calculate the scattering power of the atom in a state of rest from the measured values of the scattering power at any temperature. It is therefore M which we wish to deduce from the experiments.

Now from equations (4) and (5),

$$\frac{M_1 - M_2}{h^2 + k^2 + l^2} = \frac{2\pi^2}{a^2}\left\{\beta(T_1 - T_2) + \gamma\left(\frac{1}{T_1} - \frac{1}{T_2}\right) + \delta\left(\frac{1}{T_1{}^3} - \frac{1}{T_2{}^3}\right)\right\} \qquad (6)$$

For aluminium, $m = 4{\cdot}47 \,.\, 10^{-23}$ gm., $\gamma = 1{\cdot}474 \,.\, 10^{-17}$, $\delta = -2{\cdot}3 \,.\, 10^{-14}$,* $a = 4{\cdot}05 \,.\, 10^{-8}$ cm. $(M_1 - M_2)/(h^2 + k^2 + l^2)$ has already been determined for the range from $T_1 = 290°$ to $T_2 = 86°$; its value is $6{\cdot}87 \,.\, 10^{-3}$. Substituting these values in equation (6), we find $\beta = 3{\cdot}218 \,.\, 10^{-21}$.

Assuming the existence of zero-point energy, so that $\alpha = 0$, we have finally, from equations (2) and (5),

$$M = (h^2 + k^2 + l^2)\{3{\cdot}87 \,.\, 10^{-5}\, T + 0{\cdot}177/T - 277/T^3\},$$

which gives for $T_1 = 290°$

$$M_1 = 0{\cdot}01182\,(h^2 + k^2 + l^2),$$

and for $T_2 = 86°$

$$M_2 = 0{\cdot}00496\,(h^2 + k^2 + l^2),$$

from which the value of M for any spectrum can be calculated.

---

* Calculated from an approximation due to Waller: $\delta = -\frac{113}{36}\frac{\Theta^2}{8\pi^2 A} \,.\, 10^{-16}$, where A is the atomic weight.

5. *Amplitude of the Heat Motions.*

Still assuming the existence of zero-point energy, it is now possible to calculate the root-mean-square displacements of the atoms at any temperature from equation (5). This gives

$$\overline{u_x^2} = 3\cdot218 \,.\, 10^{-21}\,\mathrm{T} + \frac{1\cdot474}{\mathrm{T}} \,.\, 10^{-17} - \frac{2\cdot3 \,.\, 10^{-14}}{\mathrm{T}^3}.$$

Substituting the values of T in this formula, and remembering that $\overline{u^2}$, the mean-square-displacement without reference to direction, is equal to $3\overline{u_x^2}$, we find

$$\text{at } \mathrm{T}_1 = 290^\circ \text{ abs., } (\overline{u_x^2})_1 = 9\cdot83 \,.\, 10^{-19} \text{ cm.}^2, \quad \sqrt{\overline{u^2}} = 0\cdot171 \text{ Å}.$$

$$\text{at } \mathrm{T}_2 = 86^\circ \text{ abs., } (\overline{u_x^2})_2 = 4\cdot13 \,.\, 10^{-19} \text{ cm.}^2, \quad \sqrt{\overline{u^2}} = 0\cdot111 \text{ Å}.$$

6. *Comparison with the Theoretical Value of M.*

The quantity β depends on the forces between the atoms in the lattice, and it is possible to give an expression for it in terms of the elastic constants of the crystal, as was done in the cases of rock-salt and sylvine. The necessary experimental values of the elastic constants are, however, not available for aluminium, and it is not possible to make the comparison in this way.

Debye (*loc. cit.*), in 1914, gave a theoretical expression for M, for the case of a cubic lattice consisting of one kind of atom. Waller (*loc. cit.*) later showed that Debye's value for M should be multiplied by two. In its amended form, Debye's formula is

$$\mathrm{M} = \frac{6h^2}{mk\Theta} \cdot \frac{\sin^2\theta}{\lambda^2} \left\{ \frac{\phi(x)}{x} + \tfrac{1}{4} \right\}, \tag{7}$$

in which h, m and k have the same significance as above. Θ is the "characteristic temperature" of specific heat theory, and $x = \Theta/\mathrm{T}$. $\phi(x)$ is a certain function evaluated in Debye's paper. The fraction 1/4 is added if zero-point energy is assumed to exist. Expression (7) may be put in the form

$$\frac{\mathrm{M}}{h^2 + k^2 + l^2} = \frac{3h^2}{2mk\Theta a^2} \left\{ \frac{\phi(x)}{x} + \tfrac{1}{4} \right\}, \tag{8}$$

where (hkl) on the left-hand side of the equation are the indices of the spectrum, and a is the lattice constant. From the figures given by Debye, the values of $\phi(x)/x$ are found to be 0·520 for $\mathrm{T}_1 = 290^\circ$, and 0·075 for $\mathrm{T}_2 = 86^\circ$. Taking for Θ the value 396°, as determined by Debye* from the specific heat, we find from (8)

$$(\mathrm{M}_1 - \mathrm{M}_2)/(h^2 + k^2 + l^2) = 7\cdot16 \,.\, 10^{-3}.$$

---

* 'Ann. Physik,' vol. 39, p. 789 (1912); see also Schrödinger, 'Phys. Z.,' vol. 20, p. 474 (1919).

The value determined from the experiments was $6 \cdot 87 \,.\, 10^{-3}$, and the agreement, which is within a little over 4 per cent., is probably as close as can be expected.

We may put the matter in another way by assuming the experimental values to be correct and using them to calculate the characteristic temperature for aluminium. We find in this way $\Theta = 403°$.

Determining the constants in Debye's expression for M in this way from the experimental numbers, we have

$$M = 0 \cdot 0155\,(h^2 + k^2 + l^2)\,\{\phi(x)/x + \tfrac{1}{4}\}. \tag{9}$$

The value of M, assuming the existence of zero-point energy, was calculated above in § 4. We may use Debye's formula to obtain the value of M for the case where the atoms are assumed to be at rest at the absolute zero of temperature. This is done simply by omitting the term $\frac{1}{4}$ in equation (9), which gives the following values :—

$$\text{for} \quad T_1 = 290°, \quad M_1 = 0 \cdot 00804\,(h^2 + k^2 + l^2),$$
$$\text{for} \quad T_2 = 86°, \quad M_2 = 0 \cdot 00116\,(h^2 + k^2 + l^2).$$

The corresponding root-mean square displacements are 0·141 Å. and 0·054 Å.

Calculation of the Theoretical F Curves for Aluminium.

It has been shown by Waller* that the coherent scattering by an atom, of X-rays of the order of wave-length used here, may be calculated from its Schrödinger charge-density distribution by supposing every element of the charge to scatter classically, and taking into account the interference between the radiation scattered from different parts of the atom. This is discussed in more detail in the paper on rock-salt,† to which reference may be made for details. To calculate the F curve for aluminium, it is necessary to know its charge distribution, and we have calculated this by the method of self-consistent fields, devised by Hartree.

Since aluminium is a good conductor of electricity, we must assume the atoms in the lattice to be ionised, but we cannot say whether they are singly, doubly, or triply ionised. The charge distribution has therefore been calculated for all three cases. Al^{+3} consists of a nucleus with a charge of +13, and 10 core electrons, made up of two 1_1, two 2_1, and six 2_2 electrons ; in Al^{+2}, the first

---

* 'Phil. Mag.,' vol. 4, p. 1228 (1927) ; see also Wentzel, 'Z. Physik,' vol. 43, pp. 1, 779 (1927), and Waller and Hartree, 'Roy. Soc. Proc., A, vol. 124, p. 119 (1929).

† James, Waller and Hartree, *loc. cit.*

3_1 electron of the M group is also present, and in Al^{+1}, a second 3_1 electron has been added. For the ions Al^{+2} and Al^{+1}, the fields corresponding to the distributions we have used are not strictly self-consistent. It has been assumed that the charge distribution due to the core electrons, as calculated for Al^{+3}, is not altered by the addition of the outer electrons. This assumption saves a very large amount of numerical work, and although not strictly true, must be very nearly so, since a very small fraction of the charge-distribution of the outer electrons lies within the region of the core, and it is certainly nearly enough true for the calculation of the F curves.

In fig. 1 the distributions for two Al^{+2} ions are shown. The centres of the atoms are at the points A and B, their distance apart being the distance of closest approach of two atoms in the aluminium lattice, 2·86 Å. The ordinates give the values of U(r), where U(r)dr is the amount of charge, expressed in terms of the electronic charge as unit, lying between distances r and $r + dr$ from the centre of the atom. The full curves give the distributions for Al^{+2}, the dotted ones, which only differ from the others at the larger values of r, are the distributions for Al^{+3}. It will be seen that the distributions for the two Al^{+3} ions do not overlap in the regions for which the charge-density is appreciable. If a corresponding diagram is drawn to show the relationship between neighbouring ions in the rock-salt lattice, it will be found that there is a considerable

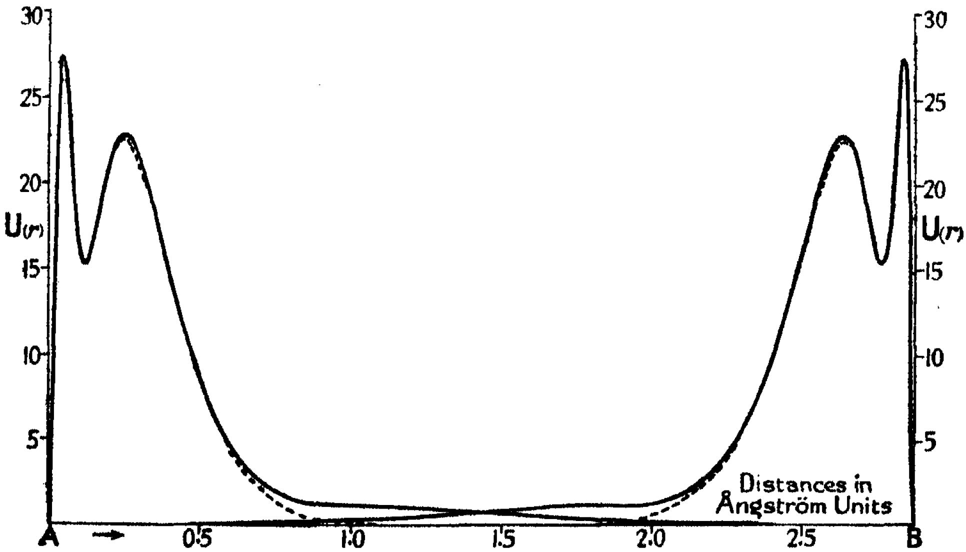

FIG. 1.—Charge Distribution for Al^{+2} and Al^{+3} placed at a distance apart equal to the distance of closest approach in aluminium lattice.

overlap between the charge distributions for the ions Na^+ and Cl^-, and the same is true for the ions K^+ and Cl^- in sylvine. It must be remembered that the distributions are calculated for the free ions in all these cases. When the ion is in a lattice, the field for the outer electrons must differ considerably from that for the same electrons when the ion is free, so that the corresponding charge distributions must be modified, and we can probably safely assume that whenever atoms are closely packed in a crystal lattice, there will be some overlap of the density distributions calculated for the corresponding free atoms. With this in mind, we see that if a charge-distribution corresponding to the ion Al^{+3} is placed at each point of the aluminium lattice, there will be a considerable amount of space available between them, into which the remaining three electrons belonging to each atom must go, although whether as valency electrons, attached to the atoms, or as free conductivity electrons, it is not possible to say without further knowledge. It is of interest to consider whether we can get any evidence on this point from X-ray measurements, and we shall return to this later.

The F_0 curves for the atoms at rest are calculated from the charge distributions by means of the formula

$$F = \int_0^\infty U(r) \frac{\sin \phi}{\phi} . dr$$

where $\phi = 4\pi r (\sin \theta)/\lambda$ the integral being evaluated numerically for a series of values of θ.

In fig. 2, the F_0 curves for the ions Al^{+1}, Al^{+2}, and Al^{+3} are given, together with the contributions of the different electron groups. It will be seen that the F_0 curves for the three ions differ appreciably only for values of $(\sin \theta)/\lambda$ smaller than about 0·2, the difference being due to the 3_1 electrons. Now the F_0 curve for the 3_1 group falls off extremely rapidly with increasing angle of scattering, owing to the fact that the greater part of its charge-distribution lies at distances from the centre of the atom greater than the wave-length of the X-rays. From fig. 2, it will be seen that, for the 3_1 electrons of Al^{+1}, the value of F_0 falls to zero for a value of $(\sin \theta)/\lambda$ equal to about 0·22, and that it then becomes negative, becoming positive again at about $(\sin \theta)/\lambda = 0{\cdot}44$, and thereafter decreasing slowly towards zero, but never again becoming negative. After the value of F_0 has once fallen to zero, it never again becomes numerically greater than about 0·05 for the two electrons together. The only appreciable contributions of the 3_1 electron to the F curve for the whole atom are for values of $(\sin \theta)/\lambda$ less than about 0·2. The negative contributions between 0·2 and 0·4 cause the F curve for Al^{+1} and, in a lesser degree, that for

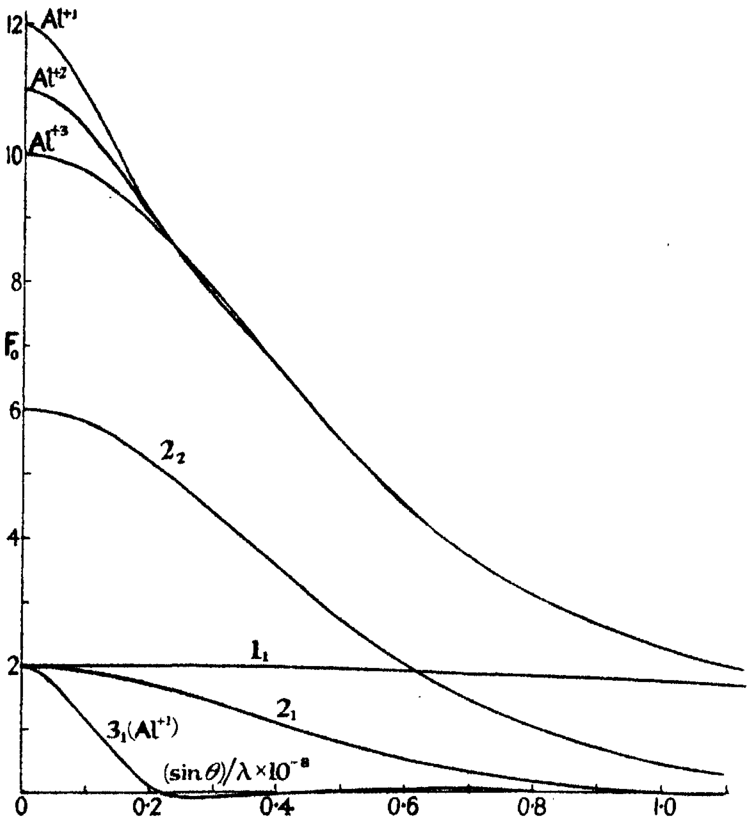

Fig. 2.—Contributions of the Electron Groups to F_0 for Aluminium.

Al^{+2} to lie below the F curve for Al^{+3} in that region, even although the latter ion contains fewer electrons. The F curve for 3_1 is, of course, calculated for the free ion; some distortion must be introduced when the ion is packed into the lattice, but it cannot be such as to alter materially the conclusion just reached, that the effective contributions of the 3_1 electrons are confined to quite small values of $(\sin \theta)/\lambda$.

For moderate values of $(\sin \theta)/\lambda$, the greatest contributions to F are from the 2_2 and 2_1 electrons, but for still larger values these become very small, and, for values greater than about unity, F is almost entirely due to the 1_1 electrons, which, being concentrated within a region small compared with the wave-length of the X-rays, give an F curve falling away very slowly for increasing angle of scattering. At the largest angle at which observations have been made in the present series of experiments, corresponding to scattering through about 100°, the contribution of the two 1_1 electrons to F is still 1·7. At angles of scattering of this order of magnitude the coherent scattering of molybdenum K radiation by aluminium is due almost entirely to the K electrons.

The values of F_0 for the three ions Al^{+1}, Al^{+2}, and Al^{+3} calculated from the charge distributions are given in Table V.

Table V.—Theoretical Values of F_0 for the different Al ions at rest.

$(\sin \theta)/\lambda$.	F.		
	Al^{+3}.	Al^{+2}.	Al^{+1}.
0·000	10·00	11·00	12·00
0·038	9·93	10·87	11·76
0·056	9·88	10·74	11·51
0·075	9·83	10·60	11·27
0·094	9·75	10·41	10·96
0·118	9·02	9·17	9·22
0·282	8·01	7·97	7·93
0·376	6·93	6·92	6·91
0·470	5·82	5·83	5·84
0·564	4·80	4·83	4·85
0·658	3·98	4·01	4·03
0·752	3·33	3·35	3·37
0·940	2·48	2·49	2·50
1·128	1·93	1·93	1·94
1·316	1·61	1·61	1·61
1·504	1·50	1·50	1·50
1·880	1·28	1·28	1·28

Comparison of the Theoretical F curves with Experiment.

The experimental curves deduced in § 3 may now be compared with the theoretical values discussed in the last paragraph. We must first reduce the theoretical F curves, which are, of course, calculated for the atom at rest, to correspond to the temperature 290° abs. at which the measurements of F were made. For this purpose, we use the temperature factors deduced in §§ 4 and 5 from the experimental results. The F_0 value for a spectrum (*hkl*) must be multiplied by a factor e^{-M}, where $M = 0{\cdot}01182\,(h^2 + k^2 + l^2)$ or $0{\cdot}00804\,(h^2 + k^2 + l^2)$, according to whether zero-point energy is assumed to exist or not.

In fig. 3 the group of curves A consists of the theoretical F curves for the three ions Al^{+1}, Al^{+2}, Al^{+3} when at rest. It is not possible on the scale of the diagram, to separate the curves, except for small values of $(\sin \theta)/\lambda$. Curves B and C show one of these F curves, that for Al^{+1}, reduced to a temperature of

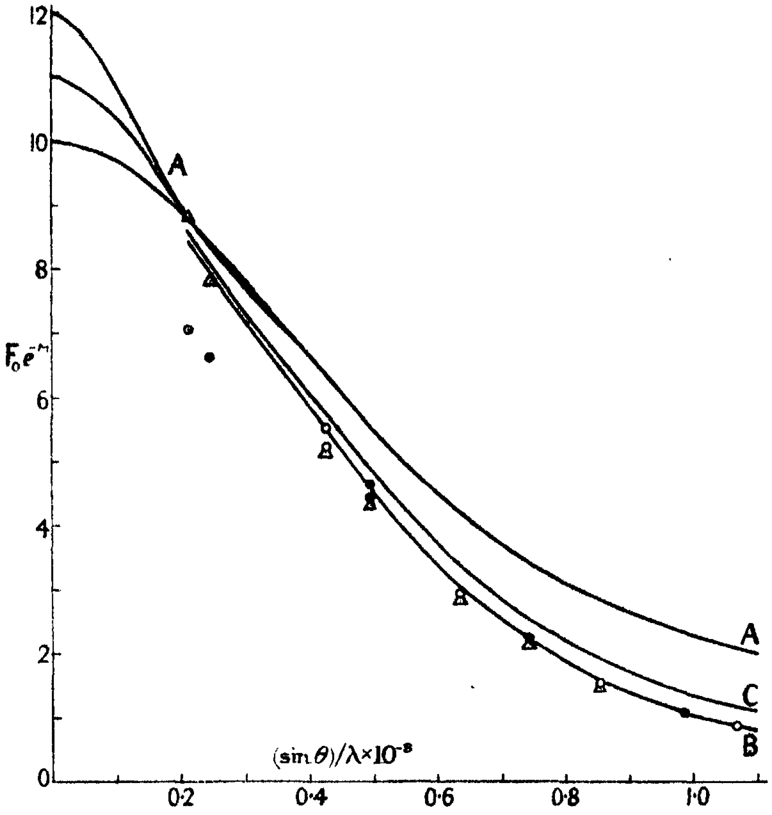

FIG. 3.

290° abs., B on the assumption that zero-point energy exists, C on the assumption that it does not. The observed values of F at 290° are shown in fig. 3 by means of circles; the plain circles indicate values from the (111) face on crystal A, the circles with a cross inside them, those from the (100) face on crystal B. In some cases there are two circles for the same value of $(\sin\theta)/\lambda$; the lower one is then the observed value of F, the upper ones will be considered later.

It will be seen that the points obtained from the two crystals lie on the same curve, except perhaps for very small angles, and also that, for large values of $(\sin\theta)/\lambda$, this curve agrees very closely indeed with the theoretical curve corrected to 290° abs. on the assumption that zero-point energy exists. The exactness of the agreement at large angles may be partly accidental, since it is scarcely to be hoped that all sources of error, whether in the measurement of F, or in the determination of the temperature factor, have been eliminated;

but it is satisfactory to find that, as in the cases of rock-salt and sylvine, the experimental results seem to decide definitely in favour of zero-point energy. The difference between the curves deduced with and without this energy should be considerably greater than experimental error. It will be noticed that the good agreement between the observed and calculated curves is confined to the larger values of $(\sin\theta)/\lambda$; for the smaller values there is a large discrepancy between them, the observed points being, in all cases, much too low, but for the moment we will confine the discussion to the large angles of scattering. As we have seen already, the F curves at such angles are due almost entirely to the innermost electrons. Now although there may be some uncertainty about the fields, and so about the distributions, for the outer electron groups, there is much less for the inner ones, and the theoretical F curves can probably be taken as correct for the large angles of scattering. We are therefore justified in using them to decide whether the experiments indicate zero-point energy or not. This was pointed out in the papers on rock-salt and sylvine, but a detailed analysis of the contributions of the different parts of the atom to the F curve was not actually given.

The Extinction Correction.

The low values of the observed F's at small angles are due to the fact that single crystals were used which were sufficiently perfect to make formula (1), which is only true for the ideal mosaic crystal, inapplicable to the strong reflexions. The question of extinction in single crystals has been dealt with by a number of writers,* and it is sufficient to state here that the existence in the crystal of fragments, large enough to produce appreciable absorption, which are at the same time nearly perfect in their lattice arrangement, has the effect of increasing the effective absorption coefficient at the reflecting angle by an amount proportional to the intensity of the reflexion. It is only for the strong reflexions that the effect is at all important; for the weaker ones there is a very small correction, an estimate of which can be obtained by assuming the F value for a strong spectrum, and calculating from it the extinction coefficient in the way which has frequently been described. In the present case it is the strong (111) and (200) spectra which are chiefly affected by extinction. The corrections are different for the spectra from the two faces, which are cut from different crystals. We have used the calculated values of F for these two spectra, and have worked out the extinction corrections for the higher orders from them. The corrected values are plotted in fig. 3, and are denoted by the upper of the two circles shown for the stronger spectra. It will be seen that the extinction correction brings the points for (222) and (400) on to the curves. The agreement between observed and calculated points is closer for Al than it was for K^+, Na^+ and Cl^-. This may be partly accidental, but it is perhaps worth noticing that, as we have seen above, the packing of the atoms in the aluminium crystal is such that the core electrons upon which the scattering at large angles depends, should not be greatly disturbed; so far as these electrons are concerned, the state of affairs approaches the condition in the free ion much more closely in the aluminium crystal than in rock-salt or sylvine. In Table VI are given the observed values of F corrected in this way for extinction, together with the calculated values corrected for temperature, with and without zero-point energy.

---

* *Cf.* Bragg, Darwin and James, 'Phil. Mag.,' vol. 1, p. 897 (1926).

Table VI.—Values of F_0e^{-M} at 290° abs.

Spectrum.	Calculated values.		Observed values, corrected for extinction.	Bearden's values.
	No zero-point energy.	With zero-point energy.		
111	8·57	8·46*	8·46	8·81
200	8·08	7·96*	7·96	7·81
222	5·79	5·53	5·52	5·17
400	4·91	4·62	4·65	4·34
333	3·42	3·09	2·99	2·85
600	2·56	2·24	2·24	2·16
444	1·93	1·61	1·57	1·48
800	1·38	1·08	1·08	—
555	1·15	0·87	0·87	—

* These values of F were used in calculating the extinction; the corrected observed values and the theoretical values are therefore made to agree.

It is interesting to compare the set of values of F obtained in this investigation with an entirely independent set, obtained by Bearden.* His values were also absolute values, but they were determined using powdered crystals, so that the errors due to extinction do not arise, although there are other difficulties inherent in the use of powdered crystals. It is not easy to be sure of the exact F values which he obtains, since he gives no table of numbers in his paper, but only a rather small-scale graph; measuring from the graph as accurately as possible, however, we obtain the set of values given in the last column of Table VI. Bearden measured more spectra than those we have tabulated, but we have confined our attention to the ones measured in the two sets of experiments. The corresponding points are plotted in fig. 3, and are denoted by triangles. At the smaller angles, Bearden's points, which are not affected by extinction, lie much above ours, but at higher angles where the values are comparable, the agreement on the whole is satisfactory, especially in view of the fact that an entirely different method was used, and that the determination was absolute. Our own points, in all cases in which extinction is negligible, lie above Bearden's, and this appears to be a systematic deviation. When the extinction correction is applied to our values, the difference between our curve and Bearden's between $(\sin \theta)/\lambda = 0\cdot2$ and $0\cdot6$ is accentuated. Bearden's curve falls more rapidly, and lies definitely below the theoretical curve, although at large angles the agreement between the two sets of numbers is quite close.

---

* 'Phys. Rev.,' vol. 29, p. 20 (1927).

The State of Ionisation of the Aluminium Atom.

We may now return to the question raised above as to whether it is possible to get any evidence from our measurements concerning the state of ionisation of the atoms in the aluminium lattice. The answer to this question appears to be quite definite. It is not possible to do so. Fig. 3 shows that the difference between the F curves for the three ions is quite inappreciable at all angles greater than those at which the (111) and (200) spectra appear, and the aluminium lattice gives no spectra at smaller angles. Even at these angles, the differences between the three F curves are smaller than the errors of experiment. For single crystals, in which extinction occurs, it is obviously quite out of the question to attempt to distinguish between the different cases, and the same would seem to be true for measurements with powdered crystals. The state of affairs may be summed up as follows. The intensities of reflexion to be expected theoretically from all three ions are identical, within very small limits, at all angles greater than those at which the (111) and (200) spectra occur; for these spectra, the differences in F for the different states of ionisation are not greater than about $0\cdot05$, and it cannot be claimed that any measurements yet made are accurate enough to decide between the possibilities with certainty.

In the above discussion, the outer electrons have been supposed to form part of the atoms, so that their charge distributions can be taken as spherically symmetrical about the atomic centre. In the actual crystal, however, some of the outer electrons are probably free conductivity electrons. We have nothing on which to base a calculation of the F's for such electrons, but we are probably safe in saying that a "free" electron of this kind will produce a smaller effect at all but very small angles than a 3_1 electron belonging to a definite atomic system. If the free electrons formed on the average anything in the nature of an electron lattice, we might perhaps expect that the spectra from different types of plane would not lie on the same curve, since the scattering from the electron lattice might help that from the atomic lattice in some cases and oppose it in others. This effect, if it exists, will however almost certainly be too small for measurement, and as we have seen, the F's from the different planes do, as a matter of fact, lie on one curve. It would appear to be impossible to get any direct evidence from experiments of this type concerning the existence of an electron lattice.

In conclusion we wish to express our thanks to Prof. G. I. Taylor, F.R.S., for his kindness in supplying us with the aluminium crystals used in this work, and to Dr. D. R. Hartree, who gave us the initial estimates of the fields for the calculation of the charge-distributions and also helped us with much advice during the calculations. We should also like to acknowledge our indebtedness to Prof. W. L. Bragg, F.R.S., who has helped us with his advice and criticism at all stages of the work. One of us (R.G.W.) is in receipt of a grant from the Department of Scientific and Industrial Research.

Summary.

The intensity of reflexion of X-rays by single crystals of aluminium has been studied at ordinary temperatures and at the temperature of liquid air, and the temperature-factor deduced from the results is found to agree well with the Debye-Waller theory.

From the temperature-factor, an estimate of the amplitude of the heat motions of the atoms in the aluminium lattice is obtained.

Absolute values of the atomic scattering power, F, for the aluminium atom are obtained at a number of angles of scattering, and these, when corrected by means of the measured temperature factor, are found to agree closely with the theoretical F curves for the atom at rest, obtained from the Schrödinger charge-distribution for Al calculated by Hartree's method. To obtain agreement, it is necessary to assume the existence of zero-point energy.

Curves are given showing the contributions of the different electron groups to the F curves, and it is found that, at all angles of scattering at which spectra can be obtained from the aluminium crystal, the values of F for the different possible states of ionisation of the aluminium atom differ by less than the errors of the experimental determination of F.

The Straggling of β-Particles.

By E. J. Williams, 1851 Exhibition Senior Research Student, Gonville and Caius College, Cambridge.

(Communicated by Sir Ernest Rutherford, P.R.S.—Received June 21, 1929 —Revised August 15, 1929.)

When a beam of electric particles is passed through a sheet of matter the energy of the individual particles is reduced. The loss of energy is not the same for all the particles so that particles incident on the foil with the same energy emerge with different energies. This dispersion of the energy caused by the foil is known as the "straggling" of the particles. The straggling of α-particles has been the subject of several experimental investigations, and the theory in this case was adequately developed by Bohr* in 1915. In the case of β-particles, however, the straggling was not experimentally investigated until quite recently and no theoretical treatment of the phenomenon has been given, the calculations of Bohr being, as he showed, applicable only to α-particles. The purpose of the work described in this paper is to develop a theory of the straggling of β-particles by thin foils and by means of it to interpret the results of experiment. The paper is arranged as follows.

In § 2 an account is given of the state of the experimental work on the subject, and in particular the effect of the complications introduced by "scattering" are considered. The formula derived by Bohr for the straggling of electric particles is given in § 3 and its inapplicability to β-particles demonstrated. The present calculations of the straggling of β-particles are given in § 4. The theory of the straggling of electric particles resolves itself into two parts. The first deals with the dynamics of collisions between electric particles and atoms, and is the same whether we are concerned with the straggling or some other phenomena such as ionisation or "stopping power." This may be called the fundamental theory and its requirements may be summarised in the function $\phi(Q)$ which expresses the frequency of collisions in which the electric particle loses energy of amount Q. The second part of the theory is the process of calculating the straggling by means of probability theory from the function ϕ. This may be regarded as the straggling theory proper and it is the main subject of § 4. When the present calculations were started it was intended to calculate the straggling on the basis of classical theory only, the value of the function ϕ on this theory being definitely known. However, after some practice with the type of calculation involved it was decided to calculate the straggling for other forms of ϕ. From the results obtained it is possible to deduce the straggling corresponding to any form which ϕ may reasonably have, and if a new theory leads to a value of ϕ different from the classical value, the straggling on the new theory may readily be determined. Alternatively this fuller treatment may be used for the reverse process of calculating from the observed straggling the value of ϕ to which it corresponds. This is considered to be the most convenient procedure and in § 5 the form of ϕ which explains the experimental results is deduced. This is compared in § 6 with the value of ϕ on classical theory. A brief outline is given in § 7 of certain new ideas concerning the nature of collisions of electric particles with electrons and atoms.

---

* 'Phil. Mag.,' vol. 30, p. 581 (1915).

§ 2. *Experimental Data.*

A large amount of experimental work has been done on the loss of energy by fast electrons in traversing matter, but unfortunately the results of most investigations are so complicated by the scattering suffered by the electrons that they are of little quantitative use. The usual experimental procedure is to place a material foil of known thickness in the path of a beam of electrons and observe the extent to which it reduces their number or velocity. Now unless the thickness of the intercepting foil is small compared with the total range of the incident electrons the electrons are so considerably scattered in traversing the foil that they describe tortuous and very unequal paths. As a result they lose varying amounts of energy corresponding to the different lengths of path in the foil. In this way the scattering gives rise to a spurious straggling effect, which, in most experiments, is of considerable magnitude and must be allowed for before the results can be compared with theory. This allowance, however, involves the problem of plural and multiple scattering and offers little prospect of an accurate solution, especially, as the problem is further complicated by the true straggling. In consequence of this difficulty, whether we desire information about the mean loss of energy or the straggling, we cannot make much use of those experiments in which the scattering effects are large and in our choice of experiments for comparison with theory we are limited to those in which there is little scattering effect to allow for. The scattering effect is less the smaller the thickness of the intercepting foil and the faster the β-particle. The order of magnitude of the effect for *thin* foils has been estimated and for light substances such as aluminium or mica it is found that provided the thickness of the intercepting foil is less than about a fifth of the total range of the particles the spurious straggling caused by scattering is small compared with the true straggling. A number of investigations have fortunately been made with foils of this thickness, using as fast electrons the natural β-particles from radioactive substances. In the recent experiments of P. White and G. Millington,* for instance, the foils used vary in thickness from a thirtieth to a sixth of the total range. The following is an outline of the kind of observations made in such experiments.

The loss of energy by the electrons is obtained by a magnetic analysis of the velocities of the emergent electrons. With semicircular focussing electrons emitted with the same velocity from a line source are brought into a line focus, and the position of this line, which may be recorded on a photographic plate, gives the velocity of the electrons. When the beam of electrons is intercepted by a thin foil the line appears in a different position corresponding to a smaller velocity. In addition to shifting the line as a whole the foil causes a broadening of the line into a band showing that the electrons which have the same incident velocity emerge from the foil with different velocities. This is the phenomenon of straggling. The distance from the undisplaced line to the point of maximum density on the displaced line measures the most probable loss of energy† and this is usually called the "peak displacement." Until recently the peak displacement was the only quantity that had been measured. Madgwick‡ (1926) appears to have been the first to make observations on the distribution of the velocities of the emergent electrons. Since then White and Millington have made extensive observations on the straggling and we are mainly dependent on their results for comparison with theory. White and Millington used a photographic method and measured the straggling by analysing with a photometer the intensity of the displaced line on their photographic plates.

§ 3. *The Calculations of Bohr.*

Consider the passage of a beam of particles of initial energy T through a thin material foil of thickness t. Let $\phi(Q)\,dQ$ represent the average number of collisions in which a particle loses energy between Q and $Q + dQ$ as it traverses the foil. (ϕ has already been referred to in the introduction.) $\phi(Q)$ is proportional to t since the foil considered is assumed to be thin. Then according to the formula derived by Bohr for the straggling of the particles, the probability $W(s)\,ds$ that a particle loses a total amount of energy between $(1+s)\Delta_m T$ and $(1+s+ds)\Delta_m T$, where $\Delta_m T$ is the mean loss of energy, is given by

---

* 'Roy. Soc. Proc.,' A, vol. 120, p. 701 (1928).

† For thin foils the loss of energy is proportional to the decrease in "$H\rho$."

‡ 'Proc. Camb. Phil. Soc.,' vol. 23, p. 920 (1926).

$$W(s)\,ds = \sqrt{(\Delta_m T^2/2\pi P)}\cdot \exp - (\Delta_m T^2 s^2/2P)\,ds, \tag{1}$$

where

$$\Delta_m T = \int_{Q_l}^{Q=Q_m} Q\,\phi(Q)\,dQ. \tag{2}$$

$$P = \int_{Q_l}^{Q=Q_m} Q^2\,\phi(Q)\,dQ, \tag{3}$$

and Q_l and Q_m are the limits of the range of values which Q may have, ϕ being 0 outside these limits.

This formula depends on certain assumptions about the function $\phi(Q)$ and it is valid only if the collisions from Q_l to Q_m can be divided into groups such that the number of collisions in each group is large at the same time as the difference between any two values of Q in the same group is small. To obtain a mathematical expression for this condition let Q and $Q+\delta Q$ define one of the groups into which the range of possible collisions is divided. Then the average number δA of collisions in this group is $\phi(Q)\,\delta Q$, whilst the fractional variation δf of Q for collisions in the group is of the order of $\delta Q/Q$. Now if the quotient $\delta A/\delta f$ is large, δQ may be chosen so that both δA and $1/\delta f$ are large, and the collisions for which the loss of energy is in the neighbourhood of Q may then be divided into groups in such a way that the assumption underlying the formula (1) is satisfied. The quotient $\delta A/\delta f$ is from the above expressions equal to $Q \times \phi(Q)$, so that (1) is applicable provided

$$Q\phi(Q) \gg 1. \tag{4}$$

Bohr used classical mechanics according to which the expression for $\phi(Q)$ for β-particles passing through free electrons initially at rest is

$$\phi(Q)_{\text{classical}} = (2\pi e^4 N/mv^2)t/Q^2 = kt/Q^2, \tag{5}$$

where

N = number of electrons per unit volume,
m = mass of electrons,
e = charge of electron,

and

v = velocity of β-particle.

The corresponding value λ of $Q\phi(Q)$ is

$$\lambda = (2\pi e^4 N/mv^2)t/Q = kt/Q, \tag{6}$$

and the condition of applicability of (1) becomes

$$\lambda = (kt/Q) \gg 1, \tag{4A}$$

λ varies inversely as $1/Q$ which means that the lighter the collisions the more accurate is their contribution to the total straggling represented in (1). The straggling as represented by (1) is, however, mainly due to the violent collisions as may be seen by evaluating the factor P for different ranges of Q (equation (3)). Accordingly in order that (1) may remain valid the condition (4A) must be satisfied for the largest values of Q. A β-particle may lose the whole of its energy in a collision so that the maximum value of Q is the energy, T, of the particle and the validity of (1) therefore requires

$$kt/\mathrm{T} \gg 1. \tag{4B}$$

For foils of thickness equal to about a fifth of the total average range of the particles—which is the thickest foil that is consistent with small scattering effect—the numerical value of kt/T is about 0·01 and the applicability of the formula (1) to the straggling is therefore out of the question. The condition of applicability would be far from being satisfied even if t were taken equal to the whole range. Since the condition (4A) is better satisfied the smaller the value of Q it is possible, as Bohr points out, to choose a value Q′ of Q so that (1) is applicable to the collisions for which $Q < Q'$. Bohr considered that the maximum value of Q′ is given by $\lambda = 1$, *i.e.*,

$$kt/Q' = 1, \qquad Q' = kt = \mathrm{S}. \tag{7}$$

In applying formula (1) to these collisions all we have to do is to substitute S for Q_m. The probability of a loss of energy between $(1 + z)\,\Delta_{\mathrm{S}}\mathrm{T}$ and $(1 + z + dz)\,\Delta_{\mathrm{S}}\mathrm{T}$ due to collisions for which Q is less than S is then given by

$$\mathrm{A}(z)\,dz = \sqrt{(\Delta_{\mathrm{S}}\mathrm{T}^2/2\pi\mathrm{P}_{\mathrm{S}})}\,\exp\left(-\Delta_{\mathrm{S}}\mathrm{T}^2z^2/2\mathrm{P}_{\mathrm{S}}\right)dz, \tag{8}$$

where

$$\Delta_{\mathrm{S}}\mathrm{T} = \int_{Q_l}^{\mathrm{S}} Q\,\phi(Q)\,dQ, \tag{9}$$

$$\mathrm{P}_{\mathrm{S}} = \int_{Q_l}^{\mathrm{S}} Q^2\,\phi(Q)\,dQ. \tag{10}$$

Using the classical expression for $\phi(Q)$ the probability of a collision for which $Q > \mathrm{S}$ is given by

$$\phi(> \mathrm{S}) = \int_{\mathrm{S}}^{Q_m} kQ^{-2}\,dQ\,t = 1 - \mathrm{S}/Q_m.$$

The maximum loss Q_m is equal to the energy, T, of the β-particle, and in all actual cases T is very large compared with S so that for all practical purposes the probability of a collision for which $Q > \mathrm{S}$ is unity. Bohr considered that the extra collision little affects the position of the maximum of the resultant distribution curve, in which case the peak-displacement is approximately equal to the loss of energy which corresponds to the maximum of the distribution A. This is given by (9) so that

$$\Delta_P T = \Delta_S T = \int_{Q_1}^{S} Q\phi(Q)\,dQ. \tag{9A}$$

For very small values of Q the value of $\phi(Q)$ is not given by (6) owing to the effects of atomic binding forces. In Bohr's theory of collisions this is allowed for and an evaluation of the integral for $\Delta_P T$ gives

$$\Delta_P T = (2\pi e^4 Nt/mv^2) . \log\{(1 \cdot 3\, v^2 Nt/4\pi\nu^2) - \log(1 - v^2/c^2) - v^2/c^2\} \tag{9B}$$

which is a formula familiar to workers in this field.

§ 4. *Present Calculations.*

(i) *General Case.*—In the calculations described in the previous section the position of the maximum of the curve representing the distribution of the losses of energy by the β-particle is roughly estimated. We shall now proceed to calculate accurately the complete straggling curve. In Bohr's calculations the classical expression for $\phi(Q)$ is used. We shall here consider the straggling for other forms of $\phi(Q)$ and in the following discussion $\phi(Q)$ does not necessarily stand for the classical value.

A general expression for the straggling involving an infinite series of integrals may readily be deduced and is given in Appendix (1). This general formula is, however, not very heplful and the following analysis though less direct shows the nature of β-ray straggling better, and the general formula it leads to represents the only way in which the straggling in particular cases may be calculated.

Following Bohr let us divide the possible collisions into two groups, one for which the energy, Q, lost in a collision is less than S, and the other for which Q is greater than S. S is here defined so that a β-particle traversing the foil suffers on the average one collision for which Q is greater than S, that is,

$$\int_S^{\infty} \phi(Q)\,dQ = 1. \tag{11}$$

Consider first the distribution of losses due to the collisions in the second group. Let E_B represent the total energy lost by a particle due to these collisions and let $B(E_B)\,dE_B$ represent the fraction of the particles for which E_B lies between E_B and $E_B + dE_B$. By definition of S the average number of these collisions per particle is one. From the theory of probability a thing which happens once on the average, under given conditions, has a probability $e^{-1}/n!$ of happening n times under those conditions. A fraction e^{-1} of the β-particles therefore suffer no collisions for which $Q > S$, and a fraction $e^{-1}/n!$ n such collisions. For the particles which suffer no such collisions $E_B = 0$ and their contribution, $B_0(E_B)$, to $B(E_B)$ may be mathematically expressed by

$$B_0(E_B) = 0, \quad E_B \neq 0; \qquad \int_{-0}^{+0} B_0(E_B)\, dE_B = e^{-1}. \tag{12.0}$$

A fraction e^{-1} of the particles suffer one collision each. This collision causes a loss of energy greater than S and the probability that the loss lies between E_B and $E_B + dE_B$ is equal to $\phi(E_B)\, dE_B$. Therefore if $\theta_1(E_B)$ represents the probability of a loss of energy E_B by particles which have suffered one collision

$$\theta_1(E_B) = 0, \quad E_B < S; \qquad \theta_1(E_B) = \phi(E_B), \quad E_B > S \tag{13.1}$$

and the contribution to $B(E_B)$ is given by

$$B_1(E_B) = e^{-1} \cdot \theta_1(E_B). \tag{12.1}$$

A fraction $e^{-1}/2!$ of the particles suffer two collisions each. These collisions are statistically independent since the only way in which the first collision can systematically control the second is for it to reduce the energy of the β-particle so appreciably that the value of $\phi(Q)$ is affected, and as we are dealing with thin foils for which the average loss of energy is small this effect may be ignored. It follows that the probabilities that the two collisions cause losses of energy Q_1 and Q_2 are $\theta_1(Q_1)$ and $\theta_1(Q_2)$ respectively, so that the probability of such a combination of losses is $\theta_1(Q_1) \times \theta_1(Q_2)$. If q is the energy lost in one, the probability that the sum of the losses due to the two is E_B is $\theta_1(q) \cdot \theta_1(E_B - q)$ and the total probability of a loss of energy between E_B and $E_B + dE_B$ due to all combinations is

$$\theta_2(E_B)\, dE_B = dE_B \int \theta_1(E_B - q) \cdot \theta_1(q)\, dq, \tag{13.2}$$

and the contribution to $B(E_B)$ is

$$B_2(E_B) = (e^{-1}/2!)\, \theta_2(E_B). \tag{12.2}$$

Consider now particles which have made $n - 1$ collisions and let $\theta_{n-1}(E_B)\, dE_B$ denote the probability that the $n - 1$ collisions cause a loss of energy between E_B and $E_B + dE_B$. Let each of these particles suffer one more collision each. As the collisions are independent the probability that this collision causes a loss of energy Q is $\theta_1(Q)$. The probability that n collisions cause a loss of energy between E_B and $E_B + dE_B$ is then (by the same argument as used in deriving (13.2)) given by

$$\theta_n(E_B)\,dE_B = dE_B\int \theta_{n-1}(E_B - q)\,\theta_1(q)\,dq. \tag{13.n}$$

The fraction of particles which suffer n collisions is $e^{-1}/n!$ so that the contribution to $B(E_B)$ from these is

$$B_n(E_B) = (e^{-1}/n!)\,\theta_n(E_B). \tag{12.n}$$

The value of $B(E_B)$ is the arithmetical sum of the contributions from all particles and is therefore given by

$$B(E_B) = B_0(E_B) + \sum_1^{\infty} B_n(E_B) = B_0(E_B) + e^{-1}\sum_1^{\infty}\theta_n(E_B)/n!. \tag{15}$$

Let us now consider the distribution of losses due to the collisions in the first group for which $Q < S$. Let E_A be the total energy lost by a particle due to these collisions, and let $A(E_A)\,dE_A$ be the fraction of the particles for which E_A is between E_A and $E_A + dE_A$. Bohr assumed the applicability of his straggling formula to this group in which case the distribution is given by (8). Bohr's formula is more applicable to the lighter collisions and the error in (8) may be estimated by dividing the collisions into two sub-groups one containing the more violent collisions, the other the lighter collisions. The distribution due to the more violent collisions, since they are few in number. may be obtained by a method similar to that used in deducing the distribution $B(E_B)$ for the collisions in the group $Q > S$. For the lighter collisions we may again use Bohr's formula. By combining those two distributions we obtain a distribution for the whole group which is more accurate than (8), since the new distribution involves the applicability of Bohr's formula only to a fraction of the collisions, and to that fraction for which it is most applicable. In this way by correcting (9) for the bulk of its error the total error may be estimated and the distribution $A(E_A)$ of losses due to the whole group may be evaluated with greater accuracy. The results for special cases show that the error in (8) is in most cases surprisingly small and $A(E_A)$ in any particular case may in this way be readily evaluated with sufficient accuracy for all practical purposes.

The next step is to combine the distribution of losses $A(E_A)$ due to collisions for which $Q < S$ with the distribution $B(E_B)$ due to the collisions for which $Q > S$. The energy E_A lost by a particle as a result of collisions in the first group is statistically independent of the energy, E_A, it loses due to those in the second group. The probability $P(E)\,dE$ of a resultant loss of energy between E and $E + dE$ due to all collisions is therefore given by

$$P(E) = \int A(E - \alpha)\, B(\alpha)\, d\alpha, \tag{15}$$

and this is the final formula for the straggling.

It might be pointed out here that in order to calculate the straggling in actual practice it is absolutely necessary to divide the collisions into two groups as has been done here. For the number of collisions of all kinds (including the lightest) is so large that it is impossible in practice to calculate the straggling without using a continuous calculus. On the other hand, owing to the fewness of the violent collisions—which nevertheless contribute much to the straggling—a continuous calculus cannot be applied to all collisions. The division into two groups is imperative, and the choice which underlies (15) is calculated to be the most convenient. It is fortunate that in most actual cases the two groups represented by (15) are fairly sharply defined, a continuous calculus being applicable to the first group with considerable accuracy whilst at the same time the second group contains so few collisions that the distribution for it may be evaluated arithmetically without undue labour. It might be pointed out that for α-particles the most violent collisions are sufficiently numerous to admit of a continuous calculus being applied to all the collisions ; this is the reason that Bohr's theory of straggling is applicable to α-particles.

(ii) *Straggling for* $\phi(Q) = kt/Q^2$.—The distributions A and B in (15) depend upon the function $\phi(Q)$, and we shall first consider the straggling which is required by the form of $\phi(Q)$ required by classical theory, viz.,

$$\phi(Q) = kt/Q^2. \tag{5A}$$

The corresponding value of S is given by $\int_S^{Q_m} kt\, dQ/Q^2 = 1$ so that

$$S = kt(1 - S/Q_m) = kt(1 - S/T),$$

Q_m being equal to the energy T of the particles. For thin foils S/T is generally less than 0·01 and for all practical purposes

$$S = kt. \tag{16}$$

Let us take S as unit of energy so that $Q = S \times x$. Then (5A) becomes

$$\phi(x) = 1/x^2, \tag{5B}$$ *

---

* $\phi(x)\,dx$ = probability that x is between x and $x + dx$

$$= \frac{kt}{Q^2}\,dQ, \text{ where } Q = Sx,$$

$$= \frac{S}{S^2x^2}\,S\,dx = \frac{dx}{x^2}.$$

and the probability of a loss of energy between yS and $(y+dy)$S due to the collisions in the second group (Q > S) becomes

$$\mathrm{B}(y) = \mathrm{B}_0(y) + e^{-1}\sum_{1}^{\infty}\theta_n(y)/n!. \tag{14B}$$

The formulæ for the terms in this series are given by (13) and their values for the classical form of ϕ are represented by the curves in fig. 1A. $\mathrm{B}_0(y)$ corresponds to the particles which suffer no collisions for which Q > S, and it is represented by an infinite ordinate at $y = 0$, its area of e^{-1} being represented by the adjacent broken lines. $\mathrm{B}_1(y)$ represents the particles which suffer one collision for which Q > S and is zero up to $y = 1$, and from $y = 1$ to $y = \mathrm{Q}_m/\mathrm{S}$ it is equal to e^{-1}/y^2, being zero again for values of y greater than Q_m/S.

The contribution to B(y) from the particles which suffer two collisions for which Q > S given by (12.2) becomes for $\phi(\mathrm{Q}) = kt/\mathrm{Q}^2$

$$\mathrm{B}_2(y) = \frac{e^{-1}}{2!}\int_1^{y-1}\frac{1}{(y-x)^2}\cdot\frac{dx}{x^2} = \frac{e^{-1}}{y^2}\left\{\frac{y-2}{y-1}+\frac{2}{y}\log(y-1)\right\}. \tag{13.2A}$$

This is represented by the curve B_2 in the figure. The curve starts at $y = 2$ since 2S is the minimum loss of energy for this group.

$\mathrm{B}_3(y)$ and subsequent terms in the series for B(y) were evaluated by experimental integration. Of these only B_3 is represented in the figure, the other terms being so small that they could hardly be distinguished from the axis. The series converges so rapidly that the total area of the curves for the terms after the third is less than 1/50th the area of those up to the 3rd, and for the terms after the 6th less than 0·0001 of that area.

The resultant distribution B(y) is represented by fig. 1B. The upper limit Q_m only affects this curve for values of y greater than Q_m/S. The height of the tail of the curve falls off very rapidly, being approximately proportional to $1/y^2$,* and is negligibly small after about $y = 10$. In view of this it is immaterial what the actual value of Q_m is, provided it is greater than about 10 S. We can make the more general statement that the curve B is independent of the value of $\phi(\mathrm{Q})$ for values of Q greater than about 10 S provided it does not *greatly* exceed kt/Q^2.

The distribution of losses, A, for collisions in the group Q < S is to a first approximation represented by (8) which for $\phi(\mathrm{Q}) = kt/\mathrm{Q}^2$ and using S as unit of energy, becomes

$$\mathrm{A}(z) = \sqrt{\{2\pi(1-\mathrm{Q}_l/\mathrm{S})\}^{-1}}\exp-\{z^2/2(1-\mathrm{Q}_l/\mathrm{S})\}, \tag{8A}$$

---

* Actually for large values of y the curve is represented by $(\overline{e^2-1}/e)/y^2$.

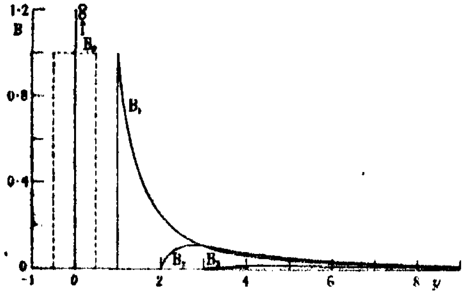

FIG. 1A.—B_0, B_1, B_2 and B_3 represent Classical Distribution of Losses due to 0, 1, 2 and 3 Collisions for which $Q > S$.

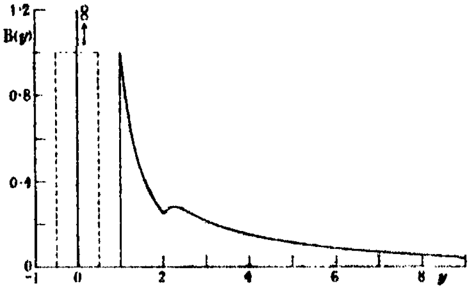

FIG. 1B.—Classical Distribution of Losses due to all Collisions for which $Q > S$.

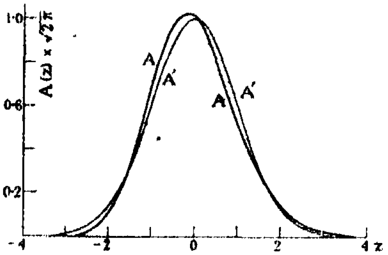

FIG. 1C.—A′ represents Distribution of Losses due to Collisions for which $Q < S$, assuming Bohr's formula. A is the same, corrected for inapplicability of Bohr's formula.

$z \times S$ representing the difference between the loss of energy and the mean loss $\Delta_S T$. If Q_l is small compared with S this formula becomes

$$A(z) = \sqrt{(2\pi)}^{-1} \exp - (z^2/2), \tag{8B}$$

and no longer contains Q_l. This result means that the distribution A is independent of the value of $\phi(Q)$ for values of Q much less than S.*

(8B) is represented by the curve A′ in fig. 1C. A correction must be applied to this owing to the incomplete applicability of Bohr's formula. This has been done in the manner already described, and the corrected distribution is represented by curve A in fig. 1C. (The origin $z = 0$ corresponds to the mean loss of energy $\Delta_S T$ which is given by (9).)

---

* In Bohr's theory of collisions the classical expression for $\phi(Q)$ is in fact not equal to kt/Q^2 for very small values of Q, being less than kt/Q^2 owing to the effect of atomic binding forces. However in view of this result provided this effect is not appreciable for values of Q greater than Q_l', where Q_l' is small compared with S, A (z) is independent of the effect and also of Q_l' and is given by (8B). If for instance $Q_l'/S = 1/4$, and $\phi(Q) = 0$ for $Q < Q_l'$—which is a gross exaggeration of the effect of atomic binding forces in actual cases—the corresponding half-maximum width of the distribution curve differs from that given by (8B) by only 5 per cent.

Having obtained the distributions A and B the resultant distribution P may be calculated from (15). This has been done by experimental integration and the resulting distribution which represents the straggling required by classical mechanics, is represented by the curve in fig. 2 and a table of the values of P is given in Appendix (2). This distribution may be regarded as either the distribution of the energies of the emergent particles or as the distribution of the energy losses in the foil. The choice only affects the calibration of the abscissæ. In the present paper we shall think of the straggling in terms of energy losses, and the abscissæ of fig. 2 are calibrated accordingly. The origin $y = 0$ corresponds to a loss of energy equal to $\Delta_S T$ which with S as unit of energy is, from (9), equal to $\log (S/Q_l)$.

Since the component distributions A and B are independent of the limits Q_l and Q_m the same must apply to the resultant distribution P. This is a very important feature of β-ray straggling. It means that the straggling is due to, and therefore represents, those collisions which cause losses of energy in the neighbourhood of S. Collisions for which Q is much greater than S only affect a distant part of the tail of the curve which is of no practical importance since such collisions are so rare. Collisions for which Q is much less than S on the other hand happen so frequently that for a given loss of energy, the statistical fluctuation is very small and there is no contribution to the straggling.

Since by using S as unit of energy the distributions A and B may be expressed without involving the value of k, or any variable factor such as the velocity v of the particles or the thickness t of the foil, the straggling in terms of S (as represented in fig. 2) is characteristic only of the index " -2 " of Q in the expression kt/Q^2 for $\phi(Q)$. The dependence of the straggling expressed in ergs on the quantities k, v, t, etc., is represented by the effect of these factors

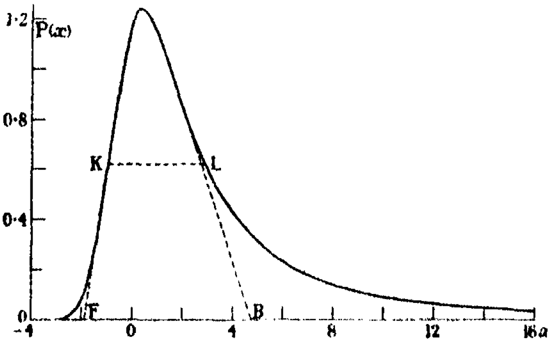

Fig. 2.—Straggling Curve calculated from Classical Theory. $\phi(Q) = kt/Q^2$.
Unit of abscissæ $= kt$.

on the unit S. This property introduces a great simplification into the treatment and expression of the results.

The magnitude of the straggling is proportional to S. S is given by (16) so that denoting the straggling by g

$$g \propto S \propto kt. \tag{17}$$

As a measure of the magnitude of the straggling we may take the width KL of the curve at half-maximum or the distance FB between the feet of the tangents at the points of inflexion. These are respectively equal to 3·8 S and 6·7 S (see fig. 2) so that

$$\begin{aligned} KL &= 3{\cdot}8\, kt \text{ (ergs)} \\ FB &= 6{\cdot}7\, kt. \end{aligned} \tag{17A}$$

The maximum of the distribution curve is situated at $y = 0{\cdot}16$ so that as the origin corresponds to a loss of energy $\Delta_S T$ which is equal to $S \times \log (S/Q_l)$ the peak-displacement is given by

$$\Delta_P T = S \times \log (S/Q_l) + 0{\cdot}16\, S = kt \,.\, \log (1{\cdot}2\, kt/Q_l). \tag{18}$$

If $\Delta_P T_1$, $\Delta_P T_2$ corresponds to t_1 and t_2 respectively, then

$$(\Delta_P T_1/t_1) - (\Delta_P T_2/t_2) = k \log (t_1/t_2), \tag{18A}$$

which is of interest since Q_l is eliminated and the value of k may be calculated from the variation of the peak displacement with t.

Bohr estimated $\Delta_P T$ to be equal to $\Delta_S T$ (§ 3) and as the numerical value of $\log (S/Q_l)$ is about 12 we see that Bohr's rough estimate is correct within about 1 per cent. The peak-displacement depends as much on Q_l as on S, and the presence of Q_l introduces issues which do not concern the straggling. In view of this and also the fact that the two phenomena are most conveniently discussed separately the peak-displacement will not be considered any further in the present paper except in connection with (18A).

(iii) *Straggling for* $\phi (Q) = k_n t/Q^n$, $1 < n < 3$.—Let us represent the general case by

$$\phi (Q) = k_n t/Q^n, \tag{19}$$

and we shall assume that this represents $\phi (Q)$ for values of Q between Q_l and Q_m. These limits have, of course, always to be introduced since if (19) were true for all values of Q from 0 to ∞ it would mean an infinite rate of loss of energy.

The straggling curves required by

$$\phi (Q) = k_{1\cdot 5} t/Q^{1\cdot 5} \tag{20}$$

and

$$\phi (Q) = k_{2\cdot 5} t/Q^{2\cdot 5} \tag{21}$$

have been calculated from the general formula (15) in the way already described for the case of $\phi(Q) = kt/Q^{2\cdot0}$. The calculated distributions are represented graphically in figs. 3A and 3C respectively.

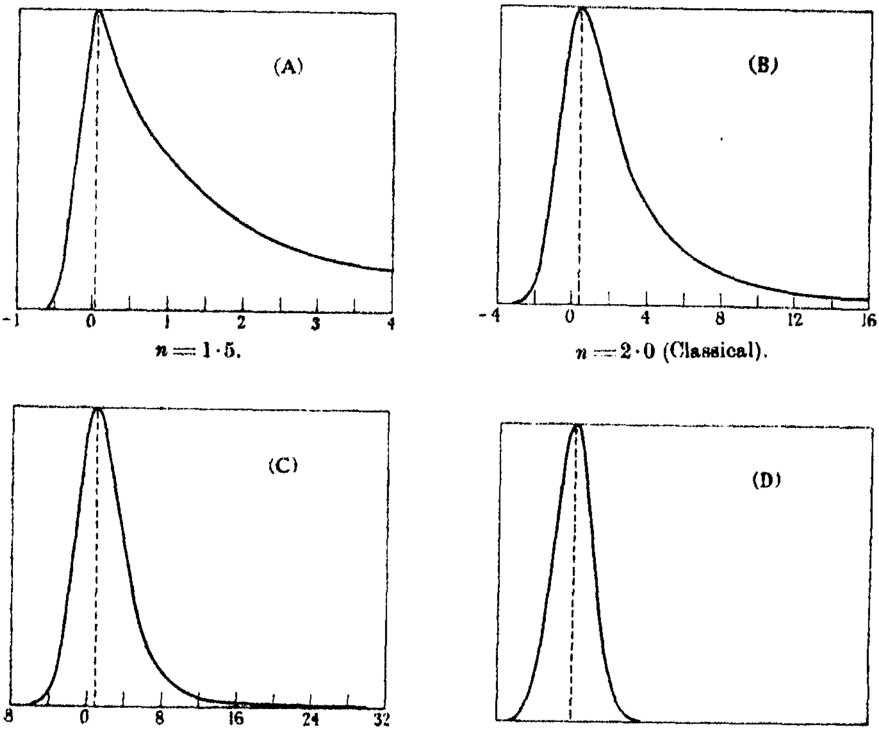

$n = 1\cdot5$.

$n = 2\cdot0$ (Classical).

$n = 2\cdot5$.

$n = 3\cdot0$.

FIG. 3.—Straggling calculated from $\phi(Q) = kt/Q^n$ for different values of n.

It was found in the case of $\phi(Q) = kt/Q^2$ that provided $Q_l \ll S \ll Q_m$ the straggling curve is independent of Q_l and Q_m, and that with S as unit of energy the curve is characteristic only of the index -2 of Q in $\phi(Q)$. The same theorem also holds for the more general case provided $1 < n < 3$, and each of the curves in fig. 3 which are plotted with S as unit of energy are characteristic only of the value of n they correspond to.

To prove this let S_n be the value of S. Then

$$\int_{S_n}^{Q_m} k_n t\, dQ/Q^n = 1, \quad \text{and} \quad S_n = \{k_n t/(n-1)\}^{1/(n-1)}\{1-(S_n/Q_m)^{n-1}\},$$

which if $S_n \ll Q_m$ and $n > 1$ becomes

$$S_n = \{k_n t/(n-1)\}^{1/(n-1)}. \tag{22}$$

Using this as unit of energy (19) becomes

$$\phi_n(x) = 1/x^n$$

and depends only on n. The distribution B (x) which represents collisions for which $Q > S_n$ depends on $\phi_n(x)$ and the limit Q_m. Q_m affects B (x) only for values of x greater than Q_m/S_n so that if $Q_m/S_n \gg 1$ the effect of Q_m is negligible and B (x) is dependent only on n.

The distribution A for collisions for which $Q < S$ using S as unit of energy becomes

$$A(y) = \sqrt{\{(3-n)/2\pi(n-1)\{1-(Q_l/S)^{3-n}\}}\exp\{-(3-n)\{1-(Q_l/S)^{3-n}\}y^2/2(n-1)\}, \tag{8c}$$

and if $n < 3$ and $Q_l \ll S$ this reduces to

$$A(y) = \sqrt{\{(3-n)/2\pi(n-1)\}}\exp\{-(3-n)y^2/2(n-1)\}, \tag{8D}$$

which depends only on n. Therefore provided $1 < n < 3$ and $Q_l \ll S \ll Q_m$ the resultant straggling which is a combination of the distributions A and B is independent of Q_l and Q_m and is characteristic of n only.

The magnitude of the straggling (g_n) is proportional to the unit S_n so that from (22)

$$g_n \propto S_n \propto (k_n t)^{1/(n-1)}. \tag{23}$$*

The constant of proportionality depends on n and may be obtained from the curves in fig. 3. The variation of the straggling with the thickness t of the foil is seen to depend on the value of n. This is a very useful property since it provides a very simple experimental method of determining the actual value of n.†

As regards the actual shape of the straggling curves (fig. 3) we notice that the

---

* If we assume to start with that the straggling is independent of the limits Q_l and Q_m this relation may readily be deduced as follows. Let $Q = x \times \alpha$. Then

$$\phi_n(x)\,dx = k_n t\,dx/\alpha^{n-1}x^n,$$

so that if $\alpha = (k_n t)^{1/(n-1)}$ then $\phi_n(x) = 1/x^n$. This only involves n so that the straggling being independent of Q_l and Q_m depends only on n if $(k_n t)^{(1/n-1)}$ is used as unit. The straggling in ergs is therefore proportional to $(kt)^{1/(n-1)}$.

† This is not a result that one would expect *a priori*. The average number of collisions a particle suffers in traversing a foil is proportional to t and as the probable fluctuation from the average is proportional to the square root of the average number one would expect the straggling to be proportional to $\sqrt{t}$, and in fact this law holds for α-particles whatever the value of n. For β-particles, however, increasing the thickness t of the foil not only increases the number of collisions but by increasing S increases the range of the collisions that are effective in producing straggling, and this accounts for the more rapid variation of g with t.

greater the value of n the more symmetrical the curves are, and in the limit $n = 3$ it can be shown that the distribution is symmetrical and Gaussian (3D). These curves have been drawn so that on the scale of the graph the distance from the maximum to the foot of the tangent at the point of inflexion on the steep side is the same in each case, and the different slopes on the right side therefore indicate the different degrees of asymmetry. For comparison with experiment it is convenient to have numerical measures of the asymmetry. For this purpose the ratios PL/PK, PB/PF and PR/PF are taken where KL is the width at half-maximum, R is the abscissa of the curve at a point where the height is one-fifth the maximum, and F and B are the points where the tangents at the points of inflexion intersect the axis. The variation of these ratios with n is shown in fig. 4.

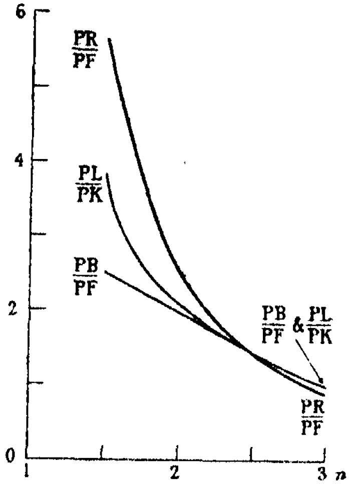

Fig. 4.—P = position of maximum of straggling curve. F = foot of tangent to steep side. B = foot of tangent to other side. LK = width at half maximum.

(iv) *Second Order Effects due to Finite Thickness of Foil.*—Second order effects arising from the finite thickness of the foil have been neglected in the above calculations. They include (1) the variation of ϕ (Q) due to primary straggling, (2) the change in path accompanying losses of energy, (3) change in path due to nuclear scattering. It is desirable that an estimate of the magnitude of these effects in actual experiments be made.

(A) *Variation of ϕ (Q).*—At any point within the foil the particles are straggled to some extent, and since ϕ (Q) increases with decreasing velocity those that have lost most energy lose energy at a faster rate during the remainder of their path through the foil. The straggling is thereby enhanced. If δv represents the heterogeneity of the particles half-way through the foil then the extra straggling δg is roughly equal to

$$\Delta T(v) - \Delta T(v + \delta v),$$

where ΔT_v is the average energy lost in traversing the foil by a β-particle of velocity v. ΔT varies roughly as $1/v^2$ so that $\delta g = \Delta T \times 2\delta v/v$ and its ratio to the true primary straggling g is $2\Delta T/g \cdot \delta v/v$. In the experiments of White and Millington $\Delta T/g$ is nearly constant and equal to 1·5, and the maximum value of $\delta v/v$ is 0·5 per cent. Therefore in an extreme case even, this kind of secondary straggling is only about 1/70th of the primary straggling and can be neglected.

(B) *Electron Scattering.*—A β-particle in losing energy Q to an electron is deflected through an angle θ of the order of $\sqrt{Q/T}$. If the deflection is away from the normal to the foil the average extra path travelled inside the foil due to this deflection is $\frac{1}{2}(\sec\theta - 1)t = \frac{1}{4}Qt/T$, and the extra energy lost is about $\Delta T \times Q/4T$, so that the total effective loss becomes $Q(1 + \frac{1}{4}\Delta T/T)$. In all actual cases $\frac{1}{4}\Delta T/T$ is never greater than about $1\frac{1}{2}$ per cent. and the effect is therefore negligible. Nuclear scattering greatly exceeds electron scattering so that the latter almost as often decreases the path of a particle as it increases it and the effect of electron scattering is actually much less than even the above estimate.

(C) *Nuclear Scattering.*—This is the most important of the second order effects. Let θ_m be the most probable angle of emergence from the foil of particles incident normally upon it. Then the most probable length of path in the foil is roughly equal to $t + \frac{1}{2}(\sec\theta_m - 1)t$. If all the particles had paths of this length the straggling, being proportional to the distance travelled by the particles, would be increased by $(1 + \sec\theta_m)/2$, and be given by

$$g_1 = g \times (1 + \sec\theta_m)/2.$$

Actually the particles traverse different lengths of path and the variation in path is of the order of $(\sec\theta_m - 1)t$, and the straggling δg caused by this effect alone is of the order of $\Delta T(\sec\theta_m - 1)$. As this straggling is independent of the true straggling the resultant straggling g_R is $\sqrt{g_1^2 + \delta g^2}$ (approximately) $= g\,\dfrac{1 + \sec\theta}{2}\sqrt{1 + (\delta g/g_R)^2}$. As representative of White and Millington's experiments we may take the case of $H\rho = 1677$, $t = 4$ mgms. of mica per square centimetre. For this case ΔT is about 8000 volts and the observed straggling g_R is about 5000 volts. C. E. Eddy* has made observations on the scattering by thin foils in this region and according to his results θ_m for this case is about 20°, so that

$$g\,(\text{obs.}) = g \times (1 + 1{\cdot}06/2) \times \sqrt{1 + 1/100},$$

from which g (corrected) $= 0{\cdot}96\,g$ (obs.). The correction is thus small. It cannot, however, be altogether neglected and a more accurate calculation of its magnitude has accordingly been made. The effect in a typical case is shown in fig. 5. Curve A is the classical straggling curve, and curve B is the same curve after allowing for the effect of scattering. In calculating curve B, the results obtained by Eddy for the scattering of β-particles were used. White and Millington pointed out that scattering produces an effective broadening of the source which produces an additional straggling effect. The magnitude of this effect has been evaluated and found to be less than 0·1 per cent. of the total scattering and therefore negligible.

---

* 'Proc. Camb. Phil. Soc.,' vol. 24 (1929).

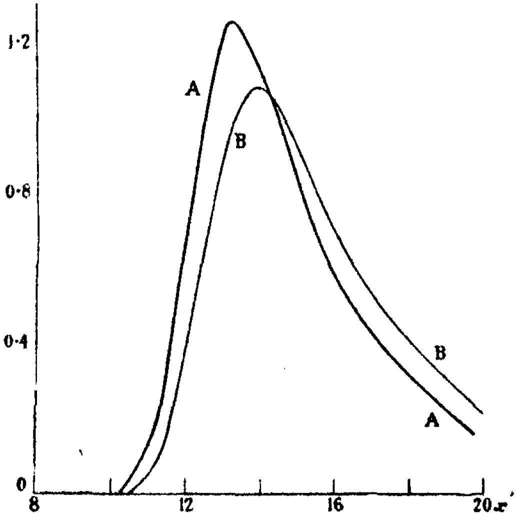

FIG. 5.—A = Classical Theoretical Straggling Curve for Mica Foil. $t = 0{\cdot}0057$ mgm./cm.², velocity of β-particle = $0{\cdot}75c$ — without scattering. B = Classical Straggling Curve for same case, allowing for scattering. $x' = 0$ corresponds to no loss of energy.

§ 5. *Interpretation of Experimental Results.*

The straggling depends upon the function $\phi(Q)$ and by means of the theoretical results obtained in the preceding section it is possible to determine the form of $\phi(Q)$ which corresponds to the experimental straggling. This may then be compared with the theoretical expressions for $\phi(Q)$.

From (23)

$$g \propto k^{1/(n-1)} \, . \, t^{1/(n-1)}, \tag{23}$$

so that n in the expression $\phi(Q) = kt/Q^n$ may be determined unambiguously from the variation of the straggling with the thickness of the foil. As measures of the magnitude of the straggling we take the width at half-maximum of the straggling curve (KL), and the distance between the feet of the tangents at the points of inflexion (FB). In their paper, White and Millington publish full details of their experimental results from which the values of KL and FB may be obtained. These are given in the following table.

Table I.

H_ρ.	T.	$\frac{\text{Velocity}}{c} = \beta$.	Thickness of foil, t.	KL.	FB.
	volts.		mgms./sq. cm.	volts.	volts.
1410	152,000	0·637	2·25	4460	7850
			2·65	5610	9200
			3·95	6500	9900
1677	205,000	0·701	2·25	3450	5330
			2·65	3450	5600
			3·95	5540	8840
			5·72	8400	12000
1938	262,000	0·751	2·25	2880	4100
			2·65	3600	5620
			3·95	6120	9080
			5·72	7600	11200

Four different thicknesses of foil were used and three different velocities of the β-particles. To find the variation with the thickness of the foil the values of KL and FB may be averaged over the velocities and the mean values are given in the next table, together with their ratio to the thickness of foil.*

Table II.

t.	$\overline{\text{KL}}$.	$\overline{\text{KL}}/t$.	$\overline{\text{FB}}$.	$\overline{\text{FB}}/t$.
2·25	360	1·60 ± 0·06	576	2·56 ± 0·15
2·65	420	1·59 ± 0·06	681	2·57 ± 0·09
3·95	605	1·53 ± 0·09	928	2·35 ± 0·20
5·72	900	1·57 ± 0·04	1345	2·35 ± 0·03

The probable errors given in this table are estimated from the fluctuations in the individual values. It is seen that both KL and FB are within experimental error proportional to the thickness of the foil. They are actually represented by

$$\text{KL} \propto t^{0\cdot97\pm0\cdot07}, \quad \text{FB} \propto t^{0\cdot90\pm0\cdot09},$$

the mean result being

$$g \propto t^{0\cdot94\pm0\cdot06}. \tag{24}$$

---

* In taking the mean value for the case of $H\rho = 1410$ allowance is made for the absence of observations for $t = 5\cdot72$.

It follows from (23) that $1/(n-1) = 0\cdot94 \pm 0\cdot06$ so that $n = 2\cdot06 \pm 0\cdot06$. When corrected for the effect of scattering this becomes $2\cdot11 \pm 0\cdot07$.

The fact that g can be represented by a single term in t shows that $\phi\,(\mathrm{Q})$ can be represented by a single term in Q.

The shape of the theoretical straggling curves is dependent only upon the value of n so that a comparison of the observed curves with the theoretical curves affords another method of determining n. In § 4 the ratios PL/PK, PB/PF, and PR/PF are used as measures of the shape of the curves and their values for different values of n are represented in fig. 4. White and Millington observed the straggling curves in 11 different cases and the values of the above ratios do not show any systematic variation with the thickness of the foils or velocity of the β-particles. This shows that over the range of the values of Q concerned $\phi\,(\mathrm{Q})$ is represented by a single term in Q, in agreement with the above result. The mean values of PL/PK, PB/PF and PR/PF for these curves are $2\cdot3_0$, $1\cdot9_1$, and $2\cdot8_2$, respectively. The corresponding values of n which may be read off the curves in fig. 4 are $1\cdot8_2$, $2\cdot1_2$ and $1\cdot9_2$, respectively, the mean value being $1\cdot9_7 \pm 0\cdot1$. The scattering affects the shape of the observed curves to some extent and after correcting for this effect the mean value of n is $1\cdot9_1 \pm 0\cdot1$. This value agrees satisfactorily with the value deduced from the variation of the magnitude of the straggling with the thickness of the foil. The mean of the two values is

$$n_{\text{obs.}} = 2\cdot0 \pm 0\cdot1, \tag{25}$$

so that

$$\phi\,(\mathrm{Q})_{\text{obs.}} = kt/\mathrm{Q}^{2\cdot0\pm0\cdot1}, \tag{26A}$$

k depends on the velocity of the β-particles and may be represented by κ/β^{ξ} where κ is a constant. The experiments of White and Millington cover only a small range of velocities ($0\cdot64c \rightarrow 0\cdot75c$) and the index ξ can only be roughly estimated. The actual value obtained, corrected for scattering, is $2\cdot0 \pm 0\cdot5$ so that

$$\phi\,(\mathrm{Q})_{\text{obs.}} = \kappa t/\beta^{2\cdot0\pm0\cdot5}\mathrm{Q}^{2\cdot0\pm0\cdot1}. \tag{26B}$$

The value of κ may be determined from the absolute magnitude of the straggling. For $n = 2$ the theoretical values of KL and FB are $3\cdot8kt$ and $6\cdot7kt$ respectively (equation (17A)) so that $\kappa = \mathrm{KL}\,.\,\beta^2/3\cdot8t = \mathrm{FB}\,.\,\beta^2/6\cdot7t$. The values of KL and FB for different thicknesses and velocities are given in Table I, and the mean values of κ calculated from these by means of the above relations are $(1\cdot97 \pm 0\cdot08) \times 10^5$ and $(1\cdot74 \pm 0\cdot10) \times 10^5$ respectively, the units being volts per gm. cm.^{2} sec.$^{-2}$. When corrected for scattering these become

$1 \cdot 85 \times 10^5$ and $1 \cdot 67 \times 10^5$ respectively and the mean value is $1 \cdot 77 \pm 0 \cdot 07 \times 10^5$. Substituting in (26B) we have

$$\phi(\mathrm{Q})_{\mathrm{obs.}} = 1 \cdot 77 \times 10^5 \, t/\beta^2\mathrm{Q}^2, \tag{26}$$

and this equation summarises the significance of the experimental results of White and Millington for straggling.

It is shown in § 4 that the straggling depends chiefly on the values of $\phi(\mathrm{Q})$ in the neighbourhood of $\mathrm{Q} = \mathrm{S}$. In the cases investigated by White and Millington S varies from about 700 to 2000 volts, and (26) accordingly applies to a region of values of Q between about 500 volts and 5000 volts, for β-rays of velocity about $0 \cdot 7c$ traversing mica.

From the observed straggling we are thus able to make a complete determination of the function $\phi(\mathrm{Q})$ for a certain region of values of Q. This cannot be done for the case of α-rays so that the straggling of β-rays gives much more information than the corresponding phenomenon for α-rays.

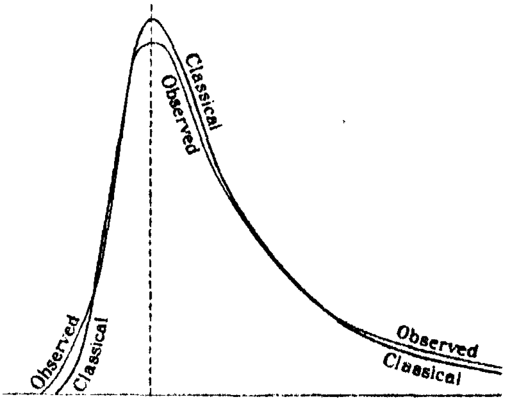

Fig. 6.—Comparison of shape of Observed Straggling Curve with Theoretical Classical Curve. Scale of observed curve = 2·3 × scale of theoretical curve. Ordinates adjusted so that areas are the same.

§ 6. *Comparison with Classical Theory, etc.*

The value of $\phi(\mathrm{Q})$ according to the classical theory of Thomson is

$$\phi(\mathrm{Q})_{\mathrm{classical}} = (2\pi e^4 \mathrm{N}/mv^2) \, t/\mathrm{Q}^2.$$

Substituting for e, etc., and expressing the distance t in grams of mica per square centimetre of superficial area, this becomes

$$\phi(\mathrm{Q})_{\mathrm{classical}} = 0 \cdot 767 \times 10^5 \, t/\beta^2\mathrm{Q}^2 \tag{27}$$

This expression for $\phi(Q)$ is of the same form $(\kappa t/\beta^2 Q^2)$ as the observed expression for $\phi(Q)$ given by (26), but the observed value of the constant κ is about 2·3 times greater than the classical value.* It is possible, by means of equation (18A), to determine the value of κ from the extent to which the observed variation of the peak-displacement $\Delta_P T$ with the thickness of the foil departs from a linear law. White and Millington pointed out that this departure is greater than is given by Bohr's formula for the peak-displacement—which assumes the classical value of κ. The value of κ which corresponds to their experimental results is actually 2·3 (± 0·3) times the classical value, and 1·7 (±0·6) times the classical value after allowing for the effect of scattering. The departure from a linear law is of the nature of a second order effect so that the experimental error is large and the value of κ obtained in this way agrees as well as might be expected with the value obtained from straggling.

The fact that the classical theory gives the index of Q in $\phi(Q)$ equal to 2 means that it explains within experimental error the shape of the observed straggling curve, and also the variation of the straggling with the thickness of the foil. The agreement between the shape of the observed and theoretical curve is shown in fig. 6, where the "mean" observed curve, and the classical theoretical curve are given. (The scale of the observed curve is 2·3 times greater than that of the classical curve.)

It is interesting to note that the index of Q on the classical theory depends directly on the law of force between the β-particle and the electrons. If we assume for instance that the law of force between two electrons is

$$F = ke^2/r^m, \tag{28}$$

it can be shown that

$$\phi(Q) = k'/v^{2/(m-1)}Q^{m/(m-1)}, \tag{28A}$$

so that $n = m/(m-1)$, which for the inverse square law gives $n = 2$. The observed value of ϕ holds for the range $500 < Q < 5000$ volts and the corresponding distance of closest approach is about 1×10^{-11} cms. (This is 20 times less than the de Broglie wave-length for the β-particles.) It should be mentioned that the interpretation of the value of n in terms of a law of force, whilst rigorous on classical ideas, is however not so on the new quantum theory.

---

* If an atomic electron which receives energy Q is initially free and at rest, the β-particle is deflected through an angle approximately equal to $\sqrt{(Q/T)}$. On these assumptions the present result corresponds to a scattering 2·3 times the classical scattering, for angles of scattering of the order of 5°.

The observed value of $\phi(Q)$ is $2 \cdot 3$ times the classical value so that

$$\phi(Q)_{\text{obs.}} = 2 \cdot 3ct/\beta^2 Q^2, \tag{26c}$$

where $c = 2\pi e^4 N/mc^2$. The classical expression (27) was deduced by J. J. Thomson on the assumption that the electrons in the matter traversed are at rest. If this is not the case and the electrons possess a mean kinetic energy ε the classical expression is

$$\phi(Q) = c(1 + 4\varepsilon/3Q)/\beta^2 Q^2 \tag{29}$$

and is $(1 + 4\varepsilon/3Q)$ times greater than Thomson's value.* If we assume the old quantum theory of electron orbits the value of this correcting factor for the range $500 < Q < 5000$, for β-particles traversing mica, varies from $1 \cdot 4$ to $1 \cdot 1$. It is therefore too small to increase the classical value appreciably and the bulk of the discrepancy remains. It is interesting to note in this connection that the width of the Compton modified line in the spectrum of scattered X-rays is on the old quantum theory attributed to the motion of the scattering electrons, and that the calculated width is much less than the observed width. To explain the actual width it is necessary to assume bigger velocities for the atomic electrons which would also increase the effect of the motion of the electrons on the straggling of β-particles. The factor in (29) which represents the effect of the motion of the electrons is, however, dependent on Q whilst the ratio of the observed ϕ to the value of ϕ given by Thomson's formula is nearly constant ($= 2 \cdot 3$) so that even if large velocities were postulated discrepancies would still remain.

The classical theory thus fails to give a quantitative explanation of the straggling of β-particles. It fails in a similar way to account for the straggling of α-particles, and also other phenomena connected with the passage of electric particles through matter such as ionisation and stopping power. The new quantum theory has not been quantitatively applied to these problems. An outline of certain concepts regarding collisions which the writer has found helpful in understanding and classifying the various phenomena connected with the loss of energy by moving electric particles is given in the next section. It is hoped to give a fuller account elsewhere.

---

* E. J. Williams, 'Manchester Memoirs,' vol 71, pp. 25–41 (1926); 'Nature,' vol. 119, p. 489 (1927). This formula is also involved in an independent calculation by L. H. Thomas of the effect of the motion of the atomic electrons on the stopping power for α-particles in 'Proc. Camb. Phil. Soc.,' vol. 23, p. 6 (1927).

§ 7. *The Nature of the Collisions of* α *and* β-*particles with Electrons.*

According to the theory which the writer proposes the collisions in which a moving electric particle loses energy to an atomic electron are of two distinct types. In the first type of collision only two bodies are essentially involved—the moving particle and the electron which acquires the energy. Any influence which the nucleus of the atom may have on the collision is incidental. This type of collision corresponds approximately to that conceived in classical theory. The second type of collision is one in which the whole atom is essentially involved. The nucleus plays an essential part and a collision of this type cannot take place between an electric particle and a free electron. In this type of collision the momenta acquired by the nucleus and electron, respectively, are comparable in magnitude. This is so even though the energy acquired by the electron is so large that the corresponding classical impact parameter is very much less than the electron-nucleus distance, under which conditions, on classical theory, the nucleus is too far away to be affected. The collision is thus not intelligible on classical theory.

Owing to the part played by the nucleus the deflection of the moving particle in the second type of collision does not correspond to the momentum acquired by the electron. C. T. R. Wilson* made observations on the deflection of β-particles caused by the production of "branches" and found that in 30 per cent. of such collisions the deflection of the β-particle is less than a tenth of the deflection corresponding to the momentum of the branch. This is the most direct experimental evidence for the second type of collision.

The two types of collision have a very close parallel in the processes of scattering and absorption of photons (radiation-quanta). Corresponding to the first type of collision is the Compton-effect which essentially is a two body collision between a photon and an electron. The second type of collision corresponds to the photoelectric absorption of a photon, which is a process that essentially involves the whole atom.† This correspondence between the effects of moving electric particles and photons is not inconsistent with the new quantum theory. In deriving on that theory the photoelectric and Compton effects of radiation no more is assumed about the radiation than its electromagnetic properties. The theory moreover makes no fundamental distinction between the perturbation of an atom by the electromagnetic field of radiation and the perturbation produced by the electromagnetic field of a moving particle. The latter may therefore result in effects which fundamentally are the same as the Compton and photoelectric effects of radiation.

---

* 'Roy. Soc. Proc.,' A, vol. 104, p. 203 (1923).

† A photon possesses no rest mass and completely disappears in photoelectric absorption; this does not happen to an electric particle in the corresponding type of collision.

A preliminary consideration of the phenomena connected with the loss of energy by electric particles on the basis of the above ideas has lead to the following classification :—

(1) The collisions chiefly concerned in the straggling, stopping power, and ionisation, for α- and β-particles, are of the Compton type. Their frequency and magnitude are roughly given by Thomson's classical theory, and more accurately by Bohr's classical theory if we assume that all the energy loss given by Bohr's formula is spent in ionising collisions.*

(2) The photoelectric type of collision is responsible for some of the "branch" collisions which occur in the paths of β-particles, and possibly for the excitation of the characteristic radiation of heavy elements by α-particles.

Summary.

The theoretical distribution of the losses of energy by β-particles traversing thin foils is calculated. The classical theory gives the *shape* of the observed distribution curves, but the *absolute magnitude* of the classical straggling is 2·3 times less than the observed. This means that collisions in which a fast β-particle loses energy of the order of a 1000 volts, are 2·3 times more frequent than is required by classical theory. A brief outline of certain new ideas concerning the nature of collisions is given.

I wish to express my thanks to Sir Ernest Rutherford, Dr. C. D. Ellis and Mr. R. H. Fowler for the interest they have taken in this work.

APPENDIX (1).—*General Formula for Straggling.*

The average number of collisions of all kinds suffered by a β-particle in traversing a foil is $\int_{Q_l}^{Q_m} \phi(Q)\,dQ$. If this be denoted by m then the probability that a particle suffers n collisions is $m^n e^{-m}/n\,!$. The probability $\phi_n(E)\,dE$ that the energy lost in n collisions is between E and E + dE is given by

$$\phi_n(E) = \int \phi_{m-1}(E - q)\,\phi(q)\,dq.$$

---

* See Gaunt, 'Proc. Camb. Phil. Soc.,' vol. 23, p. 732 (1927).

This is a reduction formula which determines $\phi_n(\mathrm{E})$ in terms of $\phi_1(\mathrm{E})$. ($\phi_1 = \phi$). Therefore if $\mathrm{P(E)}\, d\mathrm{E}$ is the total probability of a loss of energy between E and $\mathrm{E} + d\mathrm{E}$

$$\mathrm{P(E)} = \sum_{n=1}^{a} (m^n e^{-m}/n\,!) \times \phi_n(\mathrm{E}) + \mathrm{P}_0,$$

where P_0 is zero for $\mathrm{E} \neq 0$ and is equal to e^{-m} for $\mathrm{E} = 0$. This represents the straggling. In actual cases m is of the order of 1000 and an evaluation of the expression for P from this general formula is not practicable.

APPENDIX (2).—*Table of Values of* P *on Classical Theory* $[\phi(\mathrm{Q}) = (2\pi e^4 \mathrm{N}t/mv^2)/\mathrm{Q}^2]$.

x = (loss of energy − Δ_sT) ÷ $(2\pi e^4\mathrm{N}t/mv^2)$; maximum at $x = 0{\cdot}3$; maximum ordinate = 1·25.

x.	$\mathrm{P}(x) \times \sqrt{2\pi e}$.	x.	$\mathrm{P}(x) \times \sqrt{2\pi e}$.
−3·0	0·00	2·6	0·70
−2·5	0·01	3·0	0·59
−2·0	0·08	4·0	0·42
−1·6	0·22	5·0	0·32
−1·2	0·47	6·0	0·23
−0·8	0·76	7·0	0·18
−0·4	0·99	8·0	0·14
0·0	1·16	9·0	0·11
0·4	1·24	10·0	0·093
0·8	1·19	20	0·022
1·0	1·15	30	0·0095
1·4	1·04	40	0·0050
1·8	0·92	50	0·0032
2·2	0·79	100	0·0008

The Amount of Hydrogen and Oxygen present on the Surface of a Metallic Electrode.

By F. P. Bowden, International Research Fellow, Laboratory of Physical Chemistry, Cambridge.

(Communicated by T. M. Lowry, F.R.S.—Received June 24, 1929.)

In a previous communication* a study has been made of the potential changes which occur during the discharge of small quantities of electricity at metallic cathodes in an acid electrolyte. The electrode potential was, in general, more negative than the reversible hydrogen electrode, and it was found that over this range the potential change was a linear function of the quantity of electricity passed. This quantity was very small, 6×10^{-7} coulombs per square centimetre causing a change of 100 millivolts in the electrode potential at a mercury surface. This linear relation was found on all the metals investigated, but the quantity varied with the nature and condition of the surface, being greater the rougher the surface. Experiments with amalgams, and platinised mercury surfaces showed that this quantity was, to a first approximation, independent of the nature of the underlying metal and depended simply on the accessible area of its surface. It was suggested that this change in potential may be regarded as due to the deposition of more hydrogen dipoles to the surface, or alternatively to a flux of electricity across the interface causing a further deformation of the hydrogen dipoles already present on the surface.

Although the potential changes accompanying these additions to the surface have been studied, few measurements were made of the quantity of hydrogen initially present on the surface at the reversible hydrogen potential. It was considered probable that this was approximately a monatomic layer† but it was of some interest to investigate this point.

With most metals the problem is complicated by the passage of the metal ions into solution, the electrode potential at relatively positive potentials being controlled by this factor. It seemed possible that with a platinum electrode this would not occur; the metal should act merely as an inert electrode enabling the gas to come into electrical equilibrium with the electrolyte. In this case the electrode potential should be controlled by the nature and quantity of the gas present on its surface.

---

* Bowden and Rideal, 'Roy. Soc. Proc.,' A, vol. 120, p. 59 (1928).

† Bowden, 'Nature,' vol. 122, p. 647 (1928).

If a platinum electrode free from adsorbed hydrogen be immersed in a solution containing hydrogen ions, there should be a spontaneous deposition on the electrode, until the thermodynamic potential of the hydrogen is the same on the surface as in the electrolyte. This is of course true for all the components of the system. The quantity of hydrogen deposited is very small, and it is apparent that its measurement in this way is a matter of some difficulty. However, by removing the hydrogen electrolytically from the surface and studying the electrode potential as it changes from that of hydrogen to that of oxygen, it is possible to measure the quantities associated with the change. Similarly the quantity necessary to change the potential from that of oxygen to that of hydrogen can be measured. It is apparent that during the time required for the potential change, gas can be lost from the surface by evaporation or solution in the electrode or electrolyte. By controlling the experimental conditions and making the changes sufficiently rapid, these factors can be eliminated and a measure obtained of the quantity on the surface associated with this potential change. This paper is concerned with this measurement of quantity; the rate of loss from the surface will be considered later.

Apparatus.

The apparatus for measuring the rapidly changing potential of a single electrode as a small quantity of electricity is passed, has previously been described. It consists essentially of an Einthoven string galvanometer (period 1/300 second), with a moving film camera to photograph the movement of the fibre. The current for polarising the electrode was supplied by a 100 volt battery of small accumulators and the small currents used were measured by a milliammeter and a unipivot micro-ammeter. The test electrode was a square centimetre of bright platinum foil. This was carefully cleaned in acids and flamed, and one side coated with a thin layer of molten soda glass. On annealing and slowly cooling, this formed a protective insulating film over the back of the electrode. The cell used for the majority of the experiments is shown in fig. 1.

The test electrode A was sealed into the bottom of a small glass cylinder B, the other electrode of the cell being a platinum wire sealed into the tube C. The current from this electrode was led into the top of the cylinder by two symmetrical glass tubes D, the electrical resistance of which were equal so as to obtain uniform current density at the test electrode. The geometry of the apparatus prevented gas from the electrode at C diffusing into the cylinder. The potential of the test electrode was measured against the saturated calomel electrode E or against a hydrogen electrode; the latter consisted simply of a platinised platinum wire sealed into the side arm at F.

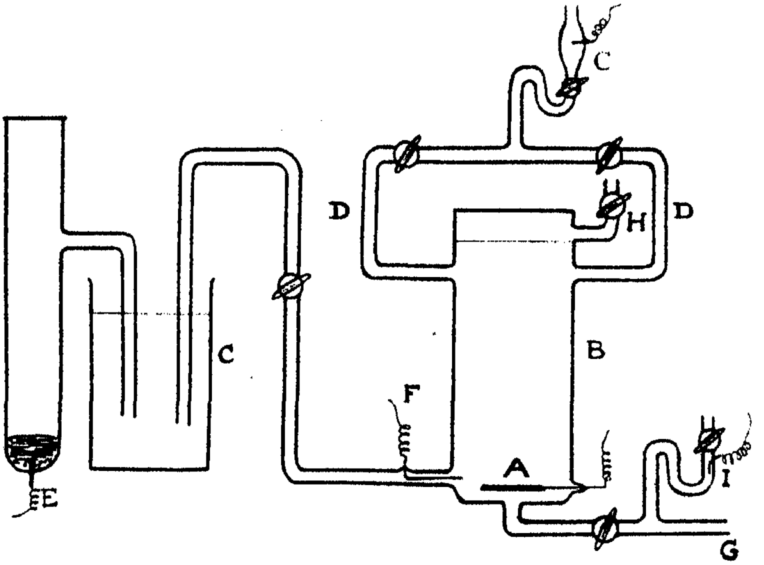

Fig. 1.—Apparatus.

The cell was filled with air-free electrolyte by means of the tube G. In the case of a hydrogen saturated electrolyte the solution was boiled out under reduced pressure and cooled in a hydrogen atmosphere. By means of a two-way tap on the storage flask, hydrogen was blown in through the tube G and out by H to displace air from the cell, and the electrolyte then admitted. An auxiliary anode I enabled the test electrode to be made cathodic as soon as it was wetted by the electrolyte. When the cell was filled and connection made with the main anode in C, this auxiliary electrode was disconnected. The electrolyte used throughout was N/5 sulphuric acid prepared from water redistilled in a silica still, and the sulphuric acid was purified by redistillation in pyrex glass.

Experimental.

It is apparent that in the time interval during which hydrogen and oxygen are being electrochemically removed or deposited at the electrode, a spontaneous loss of both may occur from the surface. The most probable methods of removal are: solution in the electrode or electrolyte; evaporation from the surface, probable as neutral molecules; and combination with one another to form water. The amount of this natural loss is a function of time, so that the total quantity of electricity which must be passed to change the electrode potential from that of hydrogen to that of oxygen should be greater when this time interval is long. A number of preliminary experiments were carried out to investigate this. At low current densities when the time for the change was long the quantity passed was dependent on the current density, being greater the lower the current density. At high current densities, however, when the change occurred in a fraction of a second, the total quantity of electricity to cause the change reached a limiting minimum value which was then independent of further increases in the current density. This indicates that at this point there is no longer time for the natural loss from the surface by solution and evaporation to be appreciable. The measurements described below were made under these conditions of high current density.

The experiments fall into two series : the first in solutions saturated with hydrogen, the second in solutions saturated with oxygen.

Electrolyte Saturated with Hydrogen.

The electrolyte was N/5 sulphuric acid freed from dissolved air and saturated with hydrogen. Several cases must be distinguished here and these are illustrated in fig. 2. For the sake of brevity only one example of each case is plotted, but several determinations of each have been made under widely varying conditions of current density and time of electrolysis. Provided the rate of deposition was sufficiently rapid, all these determinations were in substantial agreement.

(1) *Virgin Cathode. From Hydrogen to Oxygen.*—This is the case of an electrode which has been serving continuously as a cathode in a solution saturated with hydrogen. Hence no oxygen is present. The polarising current is then suddenly reversed and the potential forced rapidly from that of hydrogen to that of oxygen. The rapid change in the electrode potential is followed by photographing the rapid movement of the galvanometer fibre. The behaviour is illustrated by Curve I, fig. 2. The abscissa represents the coulombs passed, and the ordinate the potential of the electrode against a saturated calomel electrode. The current in this case was $2 \cdot 5 \times 10^{-2}$ amps. and the time required for the change about $0 \cdot 1$ seconds. The potential of the reversible hydrogen electrode on this scale is $-0 \cdot 3$ volts.

There is a rapid drop in the hydrogen overpotential (from $-0 \cdot 6$ to $-0 \cdot 3$ volts). This requires 6×10^{-6} coulombs or 2×10^{-6} coulombs per 100 millivolts, which agrees with the quantity found in previous work and which gives the area of the platinum as $3 \cdot 3$ times its apparent area. A considerably greater quantity of electricity must then be passed to cause any alteration, the potential changing linearly from − 0·3 volts to + 1·4 volts with a slight pause at the potential of + 0·37 volts. Actually the potential rises above + 1·6 volts to + 1·8 volts, but since the natural loss at this high overvoltage is comparable with the rate of deposition the graph is no longer linear over this latter portion. It is not plotted in fig. 2. The total quantity passed to cause this potential change from − 0·3 to + 1·6 volts was 3×10^{-3} coulombs.

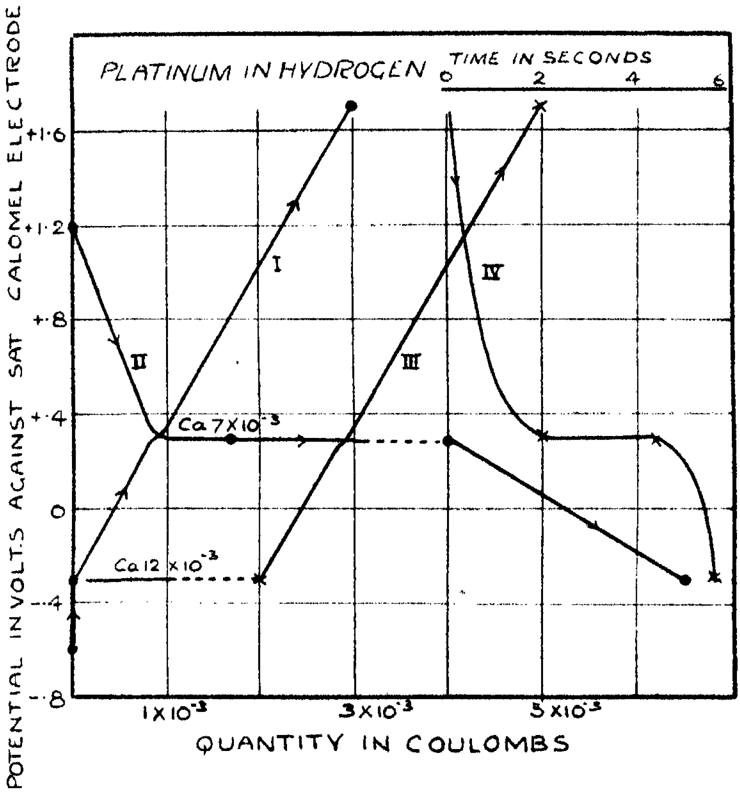

Fig. 2.

(2) *From Oxygen to Hydrogen.*—After holding the electrode anodic for a few seconds the current was then reversed, making the test electrode again the cathode. The behaviour is shown in Curve II. During the time taken for throwing over the switch the potential fell rapidly from + 1·9 volts to + 1·2 volts; at this point the current was reversed. The potential fell fairly rapidly to + 0·37 volts at which it remained constant while 7×10^{-3} coulombs were

passed. It then began to fall again linearly and after $2 \cdot 4 \times 10^{-3}$ coulombs were passed had reached the reversible hydrogen potential, at which it remained. Excluding the arrest at $+ 0 \cdot 37$ volts the number of coulombs passed to change the potential from oxygen to hydrogen was $3 \cdot 2 \times 10^{-3}$.

Further experiments showed that the length of the arrest at $+ 0 \cdot 37$ volts depended on the time for which the electrode had been held anodic. If this were short then the arrest was also very short, whilst if the electrode were made anodic for several seconds the arrest was even longer than that shown in the figure. The quantities causing the *change* in the potential were, however, independent of this factor and of the current density.

(3) *Used Cathode. From Hydrogen to Oxygen.*—The behaviour of a cathode which has been treated in this way, by being made alternately anodic and cathodic, differs in one or two interesting respects from a cathode which has never been made anodic. In the first place its activity for hydrogen deposition is greatly increased, high current densities causing very little overpotential. Secondly, on making it anodic the potential does not change immediately toward that of oxygen but remains at the reversible hydrogen potential for a considerable time and then changes in the normal way to that of oxygen. This behaviour is shown in Curve III. The length of this pause is dependent on the time for which the electrode has been made anodic and cathodic, but once the change has commenced, the quantity required to cause the change from hydrogen to oxygen is independent of these factors. The quantity found is 3×10^{-3} coulombs, which agrees with that found for a virgin cathode.

The explanation of this pause at the reversible hydrogen potential probably lies in the increased activity of the cathode. With a normal cathode the rate of supply of electromotively active hydrogen from gas bubbles adhering to the surface is small, so that if the potential change is rapid the potential can be forced from that of hydrogen to that of oxygen even when large hydrogen bubbles are still adhering to the surface. With a very active surface which rapidly catalyses the formation of active hydrogen from gaseous hydrogen, all the excess molecular hydrogen adhering to the surface must be used up before the potential can change. The experimental behaviour supports this view, a longer pause at the hydrogen potential occurring when the electrode has been made cathodic for a longer period. The reason for the increased activity of the cathode will be discussed later.

(4) *On Open Circuit.*—When the test electrode is made cathodic and the circuit then opened, the potential changes to that of the reversible hydrogen electrode and remains there indefinitely. The behaviour when it has been made

anodic for a short interval and the circuit opened is shown in Curve IV, fig. 2, the numbers at the top of the graph denoting the time in seconds. The potential falls from + 1·7 volts to that of the reversible hydrogen potential with a marked pause at + 0·37 volts. The length of the arrest at + 0·37 volts depends upon the time for which the electrode is made anodic.

Table I.

Time for which electrode was made anodic.	Time for which potential paused at + 0·37 volts.
seconds.	seconds.
1	3
2	5
4	15
10	50

If the electrode is made anodic for several minutes and the circuit then opened, the potential falls only slowly from the oxygen value and the general behaviour more nearly resembles that of an electrode in solutions saturated with oxygen.

Electrolyte Saturated with Oxygen.

(1) *Virgin Anode. From Oxygen to Hydrogen.*—The electrode is made the anode in a solution saturated with oxygen, no hydrogen being present. Even at low current densities the oxygen overpotential on platinum is high. If the decomposition potential of water is taken as 1·02 volts, the potential of the reversible oxygen electrode in this electrolyte should be + 0·92 volts on the saturated calomel scale. With a current of 10^{-2} amps. there is an overpotential of nearly 1 volt. The behaviour on reversing the current is shown in Curve I, fig. 3. The potential falls linearly and fairly rapidly to + 0·9 volts and then more slowly to + 0·37 volts. Here there is a long pause, after which the potential drops to that of the reversible hydrogen electrode. The initial portion of this curve + 1·8 to + 0·9 volts gives the quantity of electricity to establish the oxygen overpotential. This quantity is comparatively small and will be considered in more detail in a later section.

The length of the pause at + 0·37 volts depends upon the previous history of the electrode, being greater when it has been made anodic for long periods. Once the potential change begins, it drops comparatively rapidly to that of the hydrogen electrode. Excluding the arrest at + 0·37 volts, $2{\cdot}5 \times 10^{-3}$ coulombs were passed to change the potential from oxygen to hydrogen.

Open Circuit.—For an anode in oxygen-saturated solutions, the decay of potential on open circuit is very slow, taking many hours to fall from + 1·8 to + 0·62 volts. This is illustrated by Curve II, fig. 3. For convenience in comparing it with the other curves this is plotted on fig. 3, the ordinate again representing time. The period plotted corresponds to ca. 4 hours. The potential remains constant at + 0·62 volts. If the anode has been subject to very prolonged electrolysis the decay is even slower, taking several days to fall, but in each case the equilibrium value reached is + 0·62 volts.

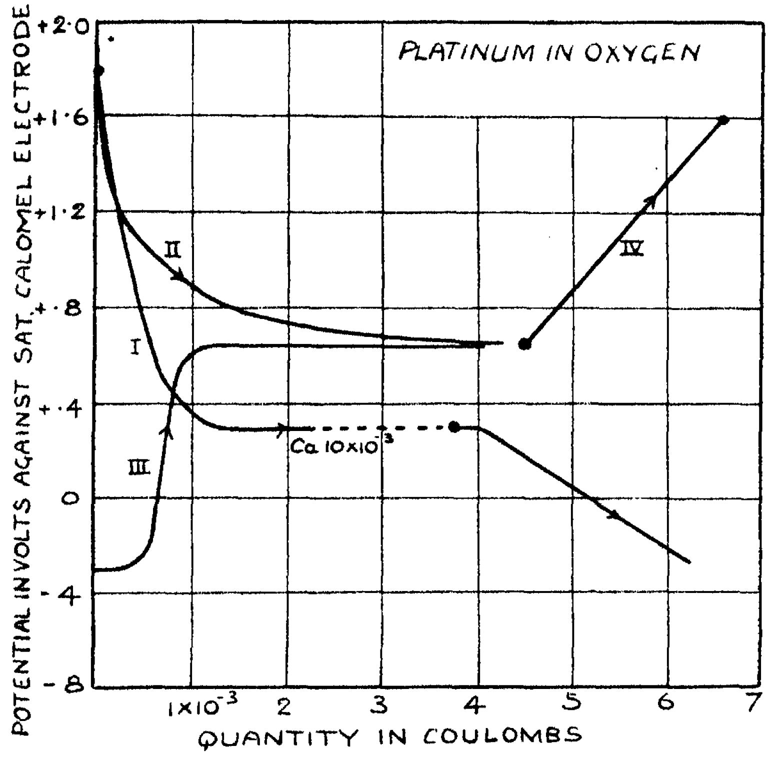

Fig. 3.

In Curve III, fig. 3, is shown the behaviour when the anode in this oxygen-saturated solution is made cathodic for a few seconds and the circuit then opened. The ordinate again represents time, the period in this case being 30 seconds. It pauses for a few seconds at the reversible hydrogen potential and then rises to + 0·62 volts, at which it remains constant. The length of the pause at the hydrogen potential depends upon the time for which the electrode is made cathodic, and, as suggested in the previous section, probably represents the time required for the excess hydrogen on the surface to become exhausted and allow the potential to change toward that of oxygen.

Curve IV, fig. 3, shows the behaviour when this electrode is again made anodic and the potential forced from $+0\cdot62$ to $+1\cdot8$. The potential rises linearly and $2\cdot1\times10^{-3}$ coulombs are required for the change.

Discussion of Results.

It is seen that the potential of the platinum electrode changes from that of hydrogen to that of oxygen or *vice versa* on the passage of ca. 3×10^{-3} coulombs per apparent square centimetre except for two arrests which occur at the potentials of $+0\cdot62$ and $+0\cdot37$ volts respectively. This quantity of 3×10^{-3} coulombs is to a first approximation independent of the previous history of the electrode, and, provided the rate of deposition is sufficiently rapid, is independent of the current density.

The length of the arrests, however, is dependent on the previous history of the electrode and becomes very long when the electrode has been made anodic for long periods. It is suggested that these arrests are due to the formation and solution of an oxide of platinum. The potential of $+0\cdot62$ volts is the equilibrium potential of this oxide in solutions saturated with oxygen. The potential of $+0\cdot37$ volts is the potential of this oxide in solutions saturated with hydrogen and probably corresponds to the reduction potential of the oxide to give platinum and water.

This would explain the behaviour of the potential in both oxygen and hydrogen solutions. For example in Curve I, fig. 2, the electrode has been cathodic in solutions saturated with hydrogen and there is no oxygen nor oxide present. On making it anodic, hydrogen is removed from the surface and the potential rises rapidly toward that of oxygen. There is a slight arrest at the potential of $+0\cdot37$ volts which would on the above hypothesis correspond to the commencement of oxide formation. The formation of platinum oxide from adsorbed oxygen is, however, a comparatively slow process compared with the rate at which oxygen is being deposited, and the potential rises rapidly as the deposited oxygen accumulates on the surface. It is of interest to note that on making the cathode anodic the potential slightly overshoots the value of $+0\cdot37$, returns to it and then rises rapidly to the oxygen potential. The arrest at this point is only short if the rate of deposition is rapid ; at low current densities when there is time for the oxide to form, the arrest is much more prolonged.

The behaviour when the electrode has been made anodic for long periods is shown by Curves II and IV, fig. 2. In this case there has been time for the formation of a complete oxide film so that there is a long arrest while this is being removed before the potential can change toward that of hydrogen. As shown in Table I, the length of this pause depends on the time for which the electrode has been made anodic. In oxygen-saturated solutions the behaviour is similar, the equilibrium potential being + 0·62 volts except in the case where the potential is being forced toward that of hydrogen and the oxide removed, when it is again + 0·37 volts.

Experiments with Oxidised Platinum.

Further evidence for the existence of an oxide at these potentials was obtained by experiments with oxidised platinum foil. A piece of bright platinum was dipped into strong nitric acid and heated white hot, the process being repeated several times. On immersion in oxygen saturated electrolyte, the potential was constant at + 0·62 volts. On immersion in hydrogen saturated electrolyte, the potential was ca. + 0·38 volts and fell rapidly to − 0·3 volts, the potential of the reversible hydrogen electrode. Measurements were also made with a platinum wire coated with a brown layer of oxide. This had been formed by burning platinum in oxygen at high temperatures and allowing the oxide to deposit on the wire. It had been found by chemical analysis to be PtO_2.* In oxygen-saturated electrolyte the potential remained constant at + 0·67 volts. In hydrogen-saturated electrolyte the potential remained steady for a long period at + 0·38 volts.

These experiments indicate that the arrests observed are due to platinum dioxide PtO_2 which is formed when the electrode is made the anode. When the electrode was made anodic for several days and the current then reversed, the potential paused at + 0·37 volts while 20×10^{-3} coulombs were passed. This shows that after conditions of prolonged electrolysis there is sufficient oxide on the surface to form several molecular layers.

It is to be expected that the alternate formation and reduction of this oxide would increase the activity of the electrode. This is found to be the case for both hydrogen and oxygen, the overpotential for a given current density being considerably decreased by this treatment. This increased activity slowly diminishes with time. It is possible that the low rate at which platinum catalyses the evolution of oxygen is in part due to this film of oxide, which under normal conditions is present on the surface. It suggests the possibility of making an active electrode by alternate oxidation and reduction which would function as a reversible oxygen electrode.

---

* Rideal and Wansbrough-Jones, 'Roy. Soc. Proc.,' A, vol. 123, p. 202 (1929).

At first thought it would appear that the reduction of an oxide film should cause a marked increase in the accessible area of the metal surface, but under the experimental conditions plotted in figs. 2 and 3 this is not the case. The time for which the electrode is made anodic is comparatively short so that the oxide layer is very thin, in many cases less than unimolecular; accordingly, the reduction of this to the metallic state can cause little change in the accessible area. It is only when the reduced metal atoms can form a loose network to a depth of many atoms that a marked increase in the accessible area can occur. The agreement between the quantity to change the potential from hydrogen to oxygen, when there is no oxide film to be reduced, with that required to change it from oxygen to hydrogen when oxide is reduced, indicates that the change in area is a second order effect. The catalytic activity can, however, be markedly increased by the oxidation and reduction of even a unimolecular layer.

Quantity of Electricity to Change Potential from Hydrogen to Oxygen.

The photographs of the movement of the galvanometer fibre show that, excluding the arrest due to oxide formation, the change of potential from hydrogen to oxygen or *vice versa* is practically linear with the quantity of electricity passed. The measured quantities associated with this change (exclusive of that due to oxide formation) are summarised in Table II.

Table II.

Electrode.	Direction.	Solution.	Current amps. $\times 10^{-4}$.	Quantity in coulombs.
Virgin cathode	Hydrogen to oxygen	Saturated with hydrogen	27	$4 \cdot 0 \times 10^{-3}$
,,	,, ,,	,, ,,	120	3·0
,,	,, ,,	,, ,,	308	3·2
,,	,, ,,	,, ,,	303	2·9
,,	,, ,,	,, ,,	2520	3·2
Used cathode	,, ,,	,, ,,	420	2·7
Used anode	Oxygen to hydrogen	,, ,,	930	2·5
Virgin anode	,, ,,	Saturated with oxygen	500	3·8
Used anode	,, ,,	,, ,, ...	500	3·0
Used cathode	Hydrogen to oxygen	,, ,, ...	380	2·5
			Mean	3·0

In spite of the varied experimental conditions the agreement is reasonably good and gives a mean value of 3×10^{-3} coulombs per apparent square centimetre.

By comparing the quantity of electricity necessary to cause a given change in the hydrogen overpotential with that required to cause the same change at a mercury surface the accessible area of the platinum electrode is estimated as $3 \cdot 3$ times its apparent area. If, as indicated by experiment, the accessible area of the electrode is not greatly changed by being made anodic, the coulombs passed to cause the potential to change from that of hydrogen to that of oxygen is 9×10^{-4} coulombs per square centimetre of accessible area.

The various interpretations which can be placed on this change may be considered. In the first place it might be regarded as due to the charging of a simple condenser formed by the double layer between the electrode and the electrolyte, without reference to any particular mechanism. It is found that 9×10^{-4} coulombs per square centimetre of accessible surface change the potential from $-0 \cdot 3$ volts to $+1 \cdot 7$ volts, *i.e.*, a change of 2 volts. Since the capacity of the condenser $= q/v = k/4\pi d$ the thickness d of the double layer can be calculated. Taking the dielectric capacity k of the double layer as unity the thickness required to give the observed capacity is $d = 1 \cdot 9 \times 10^{-10}$ cm. This value is improbable, since most considerations indicate that the thickness of the double layer is of atomic dimensions. If the dielectric medium were water having the same dielectric constant as water in bulk ($k = 80$), then $d = 1 \cdot 5 \times 10^{-8}$. This is of the right order, but it is improbable that a unimolecular layer of orientated water molecules would have the same dielectric constant as water in bulk. In view of the uncertainty on this point little reliance can be placed on this value for d. A more serious objection to this very simple view is that it disregards the chemical changes which are obviously occurring on the electrode surface. The exact mechanism of the gas electrode is still obscure, but it is almost certain that at a cathode where hydrogen ions are being discharged to form molecular hydrogen, there is hydrogen in some form adsorbed on the metal surface. Similarly at an anode where oxygen is being discharged, oxygen (or hydroxyl) in some form is adsorbed on the surface. A simple assumption to make as to the quantity is that it is a monatomic layer in each case. This could be packed on the metal in two ways, either as a complete envelope of gas atoms covering the surface and mutually touching one another, or alternatively as one gas atom adsorbed on each accessible metal atom. It was considered* that the latter method was the more probable. To change the potential from hydrogen to oxygen would necessitate the removal of this adsorbed hydrogen and its replacement by oxygen. If it is assumed that the adsorbed gas follows the metal packing, this quantity can be calculated. Taking the diameter of a platinum atom as $2\cdot5 \times 10^{-8}$ cms. (from the density), the number of hydrogens required to cover the metal surface is $1\cdot6 \times 10^{15}$. To remove this number from the surface as hydrogen ions requires $2\cdot7 \times 10^{-4}$ coulombs. To deposit an equivalent number of oxygens requires $2 \times 2\cdot7 \times 10^{-4}$ coulombs, since oxygen is divalent; so that the total quantity required to change the potential on this view would be $8\cdot1 \times 10^{-4}$ coulombs. If the gas were packed to form a complete envelope the quantity would be 16×10^{-4} coulombs. The quantity found experimentally is 9×10^{-4} coulombs, which is not sufficient for gas packing, but which is in good agreement with the quantity calculated on the assumption that a gas atom is adsorbed on or between each metal atom and that the potential change involves the displacement of the hydrogen by oxygen or *vice versa*. The linear form of the curves indicates that the transformation between these two processes is a gradual one, and at intermediate potentials it is probable that both are present on the surface. The rapidity with which the change is forced to take place makes this possible.

---

* 'Nature,' *loc. cit.*

There is some evidence from other sources that gas atoms adsorbed on a surface do not form a complete gas envelope but form a regular pattern on the lattice of the underlying surface. The work of Davisson and Germer on the diffraction of electrons indicated that gas adsorbed on a nickel surface followed the spacing of the nickel atoms.* Also Johnson† in a recent paper concludes that the adsorption of atomic hydrogen on glass reaches a saturation maximum when a complete surface layer is formed with a spacing between each hydrogen atom of ca. $1\cdot6 \times 10^{-8}$ cms.

Quantity of Electricity to Establish Oxygen Overpotential.

The last section is concerned with the quantity of electricity to change the potential from hydrogen to oxygen. The quantity to establish the hydrogen overpotential at a metallic cathode in solutions saturated with hydrogen has been considered in a previous communication; it is very small, ca. 6×10^{-7} coulombs per 100 millivolts. It is of some interest to measure the quantity necessary to establish the oxygen overpotential in solutions saturated with oxygen, and a number of measurements of this were made in a similar manner to that used for hydrogen. Provided that the potential is not made more negative than the reversible oxygen potential, the amount found is the same both for the growth and forced decay of the overpotential, and the potential change is a linear function of the amount passed.

---

* Davisson and Germer, 'Phys. Rev.,' vol. 30, p. 705 (1927); see also Germer, 'Z. Physik.,' vol. 54, p. 408 (1929).

† Johnson, 'Roy. Soc. Proc.,' A, vol. 23, p. 603 (1929).

The results of a number of experiments are summarised in the following table.

Current.	Method.	Quantity of electricity to cause change of 100 millivolts.
18×10^{-3}	Growth	$4 \cdot 6 \times 10^{-5}$ coulombs
18×10^{-3}	Decay	$4 \cdot 0$
3×10^{-4}	,,	$3 \cdot 8$
3×10^{-3}	,,	$3 \cdot 0$
3×10^{-5}	Growth	$3 \cdot 8$
		Mean .... $3 \cdot 8 \times 10^{-5}$ coulombs

To cause the same change in the hydrogen overpotential on this same platinum electrode required 2×10^{-6} coulombs; this gives a value for the accessible area of the platinum of $3 \cdot 3$ times its apparent area. If the accessible area of the electrode is not greatly changed on being made anodic, then in the case of of oxygen, 11×10^{-6} coulombs per square centimetre of accessible surface are required to cause a change of 100 millivolts in the overpotential. If the potential change is due to the formation of orientated oxygen dipoles in a similar manner to that suggested for hydrogen, the moment of the oxygen dipole can be calculated. 11×10^{-6} coulombs can deposit $6 \times 10^{23} \times 11 \times 10^{-6} / 2 \times 96450 = 3 \cdot 4 \times 10^{13}$ doublets.

Since $\Delta E = 4\pi \Delta n \mu$, $\frac{1}{3} \times 0 \cdot 1 \times 10^{-2} = 4 \times \pi \times 3 \cdot 4 \times 10^{13} \times \mu$, or $\mu = 7 \cdot 8 \times 10^{-19}$ e.s.u.

Mechanism of the Potential Change.

In this investigation of the potential changes which occur at an inert metal electrode in an acid electrolyte measurement is made of three quantities. The greatest of them is that required to change the potential from that of hydrogen to that of oxygen or vice versa. Provided the rate of deposition is sufficiently rapid this quantity is independent of the current density and of whether the electrolyte is saturated with hydrogen or oxygen. The magnitude of this quantity (9×10^{-4} coulombs per square centimetre of accessible area) and the general behaviour are consistent with the view that it involves the removal of a surface layer of one gas adsorbed on or between the metal atoms and its replacement by the other gas.

The second quantity is that associated with the change in the potential of a platinum cathode in an electrolyte saturated with hydrogen, as it is made more negative than the reversible hydrogen electrode. This has been studied in some detail for a number of metallic cathodes. We are here dealing with a hydrogen overpotential, and, provided the potential is never made greatly more positive than the reversible hydrogen electrode, the potential changes linearly with the quantity of electricity passed whether the electrode is being charged or discharged. The quantity of electricity associated with this change is small; 6×10^{-7} coulombs per square centimetre of accessible area causing a change of 100 millivolts in the overpotential.

The third quantity is that associated with the change in the potential of a platinum cathode in an electrolyte saturated with oxygen as it is made more positive than the reversible oxygen electrode. This corresponds to an oxygen overpotential, and it is again found that, provided the potential is not made greatly more negative than the reversible oxygen electrode, the potential changes linearly with the quantity of electricity passed whether the electrode is being charged or discharged. The quantity in this case is 11×10^{-6} coulombs per square centimetre of accessible surface for a change of 100 millivolts in the electrode potential.

The suggestion is that the change of potential from hydrogen to oxygen involves the removal and the deposition of a layer of gas adsorbed on the accessible metal atoms in the electrode surface. In the forces existing at the metal surfaces this adsorbed gas is deformed, forming dipoles orientated on the surface, the potential difference across the interface being controlled by the number and electric moment of these orientated dipoles. In the case of oxygen the orientation is with the positive end of the dipole towards the electrode, with hydrogen the orientation is reversed. Further changes in the potential, with the establishment of hydrogen or oxygen overpotential, are due to an increased deformation of these adsorbed dipoles with consequent increase in electric moment. Since the thickness of the double layer is of atomic dimensions a change of the potential difference between the electrode and the electrolyte of 100 millivolts means a change in the electric field in the double layer of 10^6 to 10^7 volts cm., and such a field is capable of producing the required deformation.

The exact nature of the adsorbed gas and the structure of the dipoles is not known with certainty. In the case of hydrogen the hydrogen ion, which is almost certainly hydrated, gains an electron from the metal surface and is finally evolved as molecular hydrogen gas. The detailed mechanism is not certain and the dipoles on the surface could be hydrogen ions, atomic hydrogen or molecular hydrogen. A suggestion has been made for hydrogen that it consists of a doublet of positive and negative ions orientated at the surface, a change in the potential on passage of electricity being due to the deposition of more dipoles or to a further distortion of those already present. For oxygen a similar mechanism may hold, the positive end of the doublet in this case being orientated toward the electrode. The doublet can be formed by oxygen or hydroxyl ions or more simply by a deformed oxygen atom.

It is of interest to note that when the test electrode has been made cathodic so that no oxygen is present on the surface and it is then made anodic, the potential rises linearly to a value considerably more positive than the reversible oxygen potential. This suggests that when deposition is very rapid many of the discharged ions are deformed, so that when the complete layer is established the potential corresponds to a considerable oxygen overpotential.

Summary and Conclusion.

A study has been made of the potential changes occurring at metallic electrodes in a dilute acid electrolyte as definite quantities of electricity are passed. Using a bright platinum electrode it is found that the quantity of electricity required to change the potential from that of hydrogen to that of oxygen or *vice versa* is 9×10^{-4} coulombs per square centimetre of accessible surface, *i.e.*, 9×10^{-9} gm. ions per square centimetre. Provided that the rate of deposition is rapid so that the loss by natural decay is inappreciable, this quantity is independent of the current density and the direction of the change. The quantity is in agreement with that calculated on the assumption that the potential change from that of oxygen to hydrogen involves the removal of an oxygen adsorbed on or between each accessible metal atom in the surface and its replacement by hydrogen. It is not sufficient to form a complete layer of gas atoms mutually in contact.

The quantities necessary to cause further changes in the electrode potential and establish the hydrogen and oxygen overpotentials respectively have also been measured and are considerably smaller. For hydrogen overpotential it is 6×10^{-7} coulombs, for oxygen overpotential 11×10^{-6} coulombs per 100 millivolts.

It is considered that the adsorbed oxygens and hydrogens are distorted by the forces existing at the metal surface with the formation of orientated dipoles, the potential difference across the interface being controlled by the number and electric moment of these dipoles. The further changes which occur in the electrode potential with the establishment of oxygen or hydrogen overpotential are due to an increased deformation of these adsorbed dipoles with consequent increase in the electric moment.

There is considerable evidence for the formation of a layer of platinum oxide on the surface of a platinum anode on which oxygen is being deposited.

The formation and reduction of a unimolecular layer of platinum oxide on a platinum surface produces little change in its accessible area but causes a marked increase in its catalytic activity.

It is with very great pleasure that I express my appreciation of the interest taken by Prof. T. M. Lowry, and my great indebtedness to Dr. E. K. Rideal for his valuable suggestions and stimulating encouragement, throughout the progress of this work.

Infra-Red Investigations of Molecular Structure. Part III.—*The Molecule of Carbon Monoxide.*

By C. P. Snow (Keddy Fletcher-Warr Student) and E. K. Rideal.

(Communicated by T. M. Lowry, F.R.S.—Received June 25, 1929.)

Introduction.

Although the infra-red bands of carbon monoxide have been known for years, they have not yet been resolved. In 1913 Burmeister found, among the many doublets which he measured, one due to CO with its centre at $4\cdot66\ \mu$, and from the Rayleigh-Bjerrum separation an approximation to the moment of inertia was made. The harmonic at $2\cdot35\ \mu$ was observed by Brinsmade and Kemble in 1917; Schaefer and Thomas added a second harmonic, at $1\cdot2\ \mu$, to the known bands; E. F. Lowry in 1924 tried to analyse Burmeister's doublet into the rotational fine structure which it must be supposed to have, but had no success.*

---

* Burmeister, 'Verh. d. D. Phys. Ges.,' vol. 15, p. 589 (1913); Brinsmade and Kemble, 'Proc. Nat. Acad. Sci.,' vol. 3, p. 420 (1917); Schaefer and Thomas, 'Z. Physik,' vol. 12, p. 330 (1923); Lowry, 'J. Opt. Soc. Amer.,' vol. 8, p. 647 (1924).

There has been some theoretical speculation based upon the scanty data of the vibration bands. Hettner[*] in 1920 showed the frequency relationships of the bands found by Burmeister and by Brinsmade and Kemble could be explained by the assumption that the $2 \cdot 35\ \mu$ band was an overtone of the $4 \cdot 66\ \mu$ band (in the paper published later in the same year which is the foundation of our theoretical knowledge of vibration-rotation spectra, Kratzer[†] did not include these frequencies as an example of the anharmony which he was able to prove for other molecules). Dennison[‡] compared the observed intensity ratios with a ratio calculated from a very rough approximation. The molecule has generally been assumed HCl-like, but for confirmation theory had to wait upon experiment.

In sharp contrast to the vibration-rotation bands, the electronic bands are known in much detail. The absence of multiplicity in some of the systems made their unravelling easier than in most molecules; hence there are now four band systems analysed and fitting into a consistent scheme[§] :—

$$2\,^3P—1\,^1S$$
$$2\,^1P—1\,^1S$$
$$1\,^3S—2\,^3P$$
$$2\,^1S—2\,^1P.$$

All the evidence shows that the ground state of the CO molecule is a completely normal ^1S state.

This normality itself made the study of the vibration-rotation bands worth while, for clearly, on grounds of stability alone, almost all " chemical " molecules exist when unexcited in a ^1S state. A complete knowledge of the ^1S state in the simplest possible case of a diatomic molecule is therefore a step towards the analysis of polyatomic " chemical " molecules. The one diatomic " chemical " molecule (NO) which is not normally in a ^1S state had already been worked on,[||] and the fine structure of its band found to differ from that of the HCl bands, as was expected from the ^2P (or odd electron) character of the ground state of NO. After this, the study of an HCl-like diatomic molecule was desirable as a test of theory.

The fundamental at $4 \cdot 663\ \mu$ has now been resolved; the first overtone at

---

[*] Hettner, ' Z. Physik,' vol. 1, p. 345 (1920).

[†] Kratzer, ' Z. Physik,' vol. 3, p. 289 (1920).

[‡] Dennison, ' Phil. Mag.,' vol. 1, p. 195 (1926).

[§] Birge, ' Phys. Rev.,' vol. 28, p. 1157 (1926); Mulliken, ' Phys. Rev.,' vol. 32, p. 186 (1928); see also R. C. Johnson and Asundi, ' Roy. Soc. Proc.,' A, vol. 123, p. 560 (1929).

[||] Snow, Rawlins and Rideal, ' Roy. Soc. Proc.,' A, vol. 124, p. 453 (1929).

2·345 μ has been plotted and the P branch partly resolved, although the low dispersion of the grating (945 lines per centimetre) made complete analysis impossible. The second overtone was in such an unfavourable place for our instrument that it was considered that nothing would be gained by measuring it.

Almost all the results obtained agree with those calculated for the vibration-rotation bands of a molecule in a ^1S state, acting as an anharmonic oscillator, and with the actual experimental values for the vibration frequency and constant of anharmony obtained from the electronic bands. And further, the inferences from the vibration-rotation bands are self-consistent; it is possible to describe the positions of the lines in the R and P branches of the fundamental by an expression which involves other, and independent, measurements.

It was mentioned in Part II that E. F. Lowry's failure to analyse the fundamental was probably caused by his working at one atmosphere pressure. Only indications of the fine structure were found upon our instrument at half an atmosphere, and those in the P branch, for the R branch is convergent. This convergence would have increased the improbability of Lowry's success, made unlikely enough by the high pressure. As his work shows care and a well-made instrument, we have not made any readings upon the band at one atmosphere pressure.

Experimental.

Instrument.—One slight modification has been made in the spectrometer described in Part I* of this series. It became frequently necessary for the apparatus to be manipulated by a single observer, and so a method for rocking the observation tubes into position from a distance has been used. One of the slotted discs which carry the tubes is connected to a sprocket wheel by an endless chain which binds the disc firmly; the wheel is mounted at one end of a stiff rod, 2 metres long, at the other end of which is a small rubber-tyred wheel. The rubber-tyred wheel is turned in order to rock the tubes. We are indebted to Mr. P. S. H. Henry, of this laboratory, for suggesting the device.

It is now possible to control the tubes and shutter from the galvanometer stool, and it requires only two or three steps to set the grating. There are disadvantages in solitary experiments where so many visual readings have to be made, but, as all the work had to be done at night, and most of it after midnight, there was no alternative.

Preparation of the Gas.—The gas was made from a mixture of formic acid and concentrated sulphuric acid. It was washed through sodium hydroxide solution several times, and was kept over water. It was run into the apparatus through drying tubes of phosphoric oxide in the way already described.

---

* Snow and Taylor, 'Roy. Soc. Proc.,' A, vol. 124, p. 442 (1929).

Observations.—The method of reading the galvanometer used in Part II was again made necessary by the smallness of the deflections, although for the fundamental these were of the order of 25 mm. and for the overtone considerably larger (70 mm.). Unless deflections are 100 mm. or more, there seems no justification for an averaging process, and accordingly many readings were taken at each point until the observer was satisfied that all irrelevant effects had been excluded. Late on calm nights three undisturbed readings often gave identical deflections and these were taken as establishing a point; usually, however, at least eight readings were needed, and the work was slow and tiring.

Before any readings were taken, the rock-salt end plates were taken out and polished, replaced, and the tubes tested for equality of transmission. Between $4 \cdot 4\ \mu$ and $4 \cdot 8\ \mu$ they transmitted equally to within 1 per cent. (actually no difference could be detected); but at $2 \cdot 4\ \mu$, the region of the overtone, the tube which throughout the experiment held the gas transmitted 4 per cent. more energy than the other. All the points where readings were to be taken were tested, and the 4 per cent. was found to be a constant difference throughout the region of the overtone. Accordingly, a linear correction was applied to the observed percentage in order to obtain the actual percentage absorption. The subsequent work then included :—

(i) A detailed study of the fundamental at $4 \cdot 663\ \mu$, with readings every 10 seconds of arc over the whole extent of the band, except in the further members of the R branch, where convergence makes fine structure disappear. During this work the carbon monoxide was at a pressure of 11 cm.

(ii) A similar study of the first overtone at $2 \cdot 345\ \mu$. In order that the absorption might be of reasonable intensity (10 to 20 per cent.), the pressure of the gas was increased to half an atmosphere.

(iii) The intensity of the fundamental at half an atmosphere's pressure of the gas was measured for purposes of comparison. This could have been calculated from the result of (i) upon the assumption of Beer's law; but it seemed preferable to do the experiment, as the margin of error in these intensity comparisons is small (see later).

Results.

Graphs.—Figs. 1 to 4 illustrate the sections of the experimental work. Fig. 1 is a representation of the fundamental of CO. Fig. 2 consists of straight lines drawn through experimental points taken in the neighbourhood of the centre of the band, and is included in order to show the nature of the results when finally decided on; both of these are derived from the readings of (i). The first harmonic, with its centre at 2·345 μ, is drawn in fig. 3, again by straight lines through experimental points, and fig. 4 is a rough sketch, upon a reduced scale, of the fundamental at half an atmosphere pressure. The observations (ii) and (iii) provided the material for these curves.

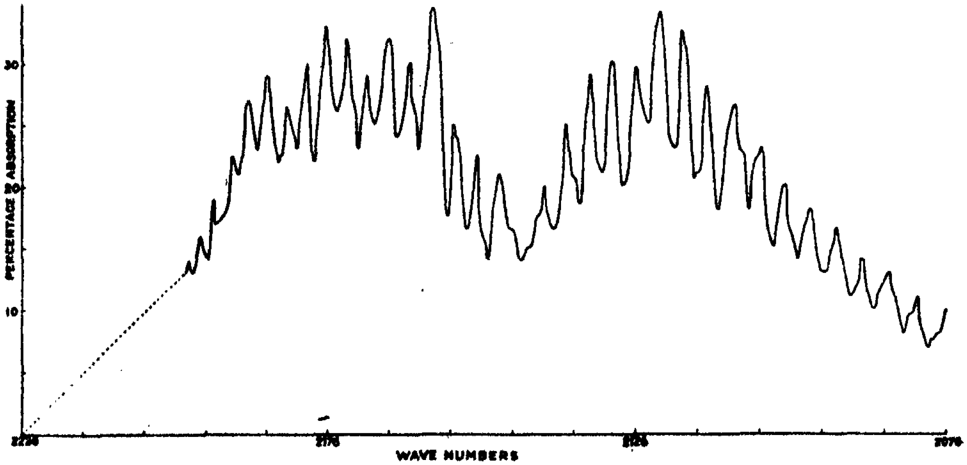

FIG. 1.

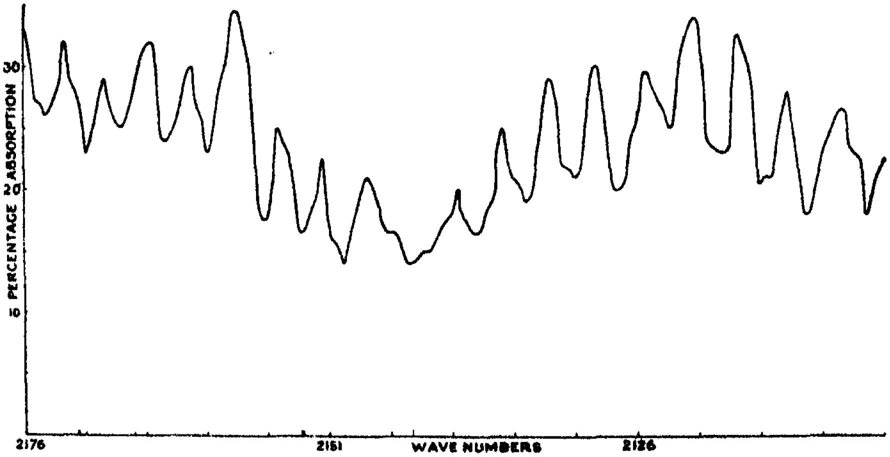

FIG. 2.

Fundamental.—The fundamental ($n'' = 0 \rightarrow n' = 1$, or $n'' = \frac{1}{2} \rightarrow n' = \frac{3}{2}$) consists of R and P branches, and no Q branch. The centre of the band is at 2144·0 cm.$^{-1}$ ± 0·4 cm.$^{-1}$ (4·663 μ). There are at least 30 members of the P branch, which shows definite divergence; convergence in the R branch is such that after the sixteenth member the separation is below the effective resolution of the instrument.

Like NO and HCl fundamentals, the band has a higher maximum of intensity in the R branch than in the P, an ordinary Boltzmann distribution effect.

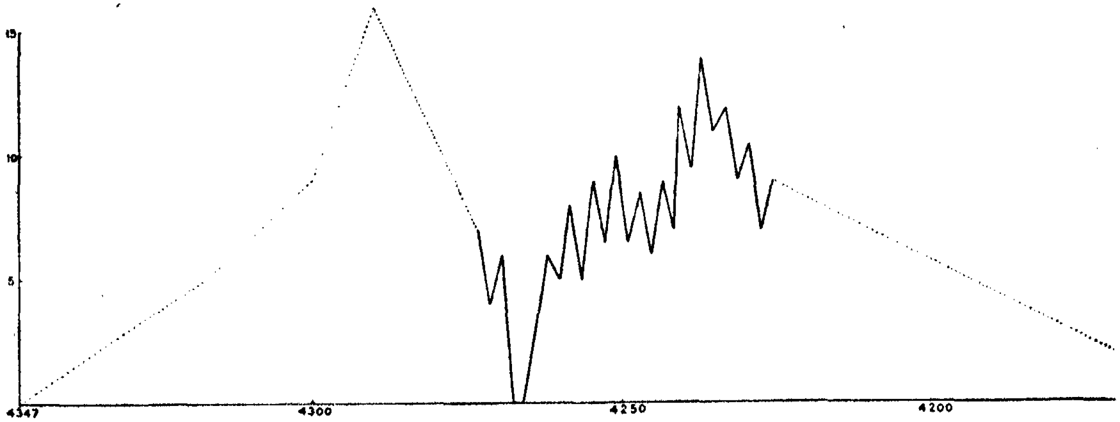

FIG. 3.

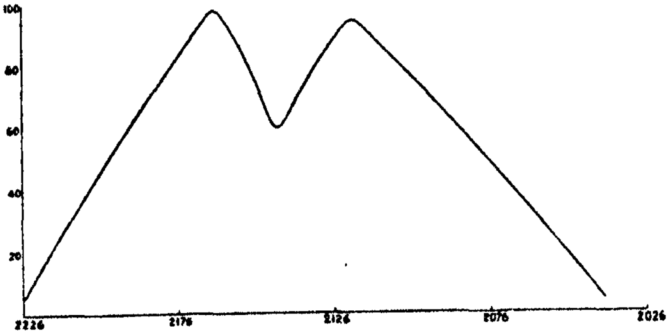

FIG. 4.

Overtone.—The overtone ($n'' = 0 \rightarrow n' = 2$, or $n'' = \frac{1}{2} \rightarrow n' = \frac{5}{2}$) has the same arrangement of the R and P branches, but without a Q branch. The centre of the band is at 4266 cm.$^{-1}$ ± 1 cm.$^{-1}$ (2·345 μ). The P branch has been resolved, partially at least, but the low dispersion of the grating at 2·3 μ has made it impossible to do more than to get indications of the fine structure of the convergent R branch.

The intensity relationship of the R to P branch in the overtone is the same as in the fundamental.

Interpretation of the Results.

General Character of the Bands.—The vibration-rotation bands of CO may be regarded as a ^1S—^1S transition, and the character of the curves agrees perfectly with this. As the molecule is a typical diatomic molecule with all its outer electrons paired (*i.e.*, $\sigma_l = 0$) we should expect no Q branch ; and, as in the case of HCl, no sign of a Q branch was found in the fundamental or in the overtone. We should also expect that there would be no missing lines ; and, in fact, no irregularity of any kind was observed near the centre of the band. Further, the energy of the rotator should be described by

$$E_r = Bm(m+1)$$

to a first approximation,* where B has its usual spectroscopic significance of $h/8\pi^2I$, or in cm.$^{-1}$, $h/8\pi^2Ic$, and m is any integer.

As will be shown later, this term enters into the complete expression for the anharmonic vibrator-rotator, and integral values of m describe the position of many of the rotation bands with exactness.

An interesting comparison can be made with the NO fundamental (and with the NO overtone, lately found). In NO we are dealing with a ^2P—^2P transition, and accordingly, with $\sigma_l = 1$†, a Q branch is probable ; it has been found experimentally that a Q branch is certainly present. For this molecule we have the same energy formula

$$E_r = Bm(m+1),$$

---

* It is perhaps useful here to make clear the use of the formulæ for the energy of a rotator. The first important suggestion was Schwarzschild's,

$$E_r = Bm^2 \text{ where } m \text{ had integral values.}$$

This formula was reconciled to the Selection Principle by Lenz and Heurlinger. The difficulty of the missing line (1 → 0, not to be confused with the missing Q branch) in HCl led to the adoption of half integral values for m in the formula.

With the help of the new mechanics Dennison found the expression for a rotator

$$E_r = Bm(m+1)$$

where for S molecules m has integral values and for P molecules half integral values. Now $Bm(m+1)$, where m is integral, differs only from Bm^2 where m is half integral, by the negligible constant B/4 ; the representation of the ^1S HCl rotator as Bm^2 with half quantum numbers is therefore a very close approximation to the formula deduced with the help of quantum mechanics. (See Schwarzschild, 'Sitzb. preuss. Akad. Wiss.,' vol. 1, p. 548 (1916) ; Lenz, 'Verh. deut. physik. Ges.,' vol. 21, p. 632 (1919) ; Heurlinger, 'Phys. Z.,' vol. 20, p. 188 (1919) ; Dennison, 'Phys. Rev.,' vol. 28, p. 318 (1926).).

† σ_l is the orbital angular momentum parallel to the axis of figure. The notation is fully described in Mulliken (*loc. cit.*), and referred to by Snow, Rawlins and Rideal (*loc. cit.*).

but *m* should have half integral values. The separations on each side of the Q branch are so small that with the present technique it would be unwarranted to make a pronouncement on the subject of the missing lines in NO, which would be expected theoretically; but curious irregularities in intensity have been observed around the Q branch. Until the centre of the band has been re-examined with greater dispersion and high intensity of incident radiation, this point will have to remain doubtful.

There is one result which also illustrates this difference between S—S and P — P transitions in vibration-rotation spectra. Working upon the comparatively large separations in the bands of methane, Cooley* found in each of the two fundamentals a Q branch which apparently obliterated the two lines on either side of it (the first lines of the P and R branches). This beautiful observation suggests at once a P—P transition with the ordinary selection rules and $\sigma = \sigma_s + \sigma_l = \frac{1}{2}$, and seems to be the first recorded case of a missing line, as opposed to a missing branch, in vibration-rotation spectra. It must not be thought that the suggestion is made that CH_4 is a P molecule; the molecule as a whole has such a marked resemblance to an inert gas that it must be thought of as in a ^1S state. What is suggested is the probability that particular vibrations may be looked upon as similar to P—P transitions in diatomic molecules. Even from these data it is not possible to give a positive answer to the question of the half integral formula, which remains nevertheless a theoretical necessity.

The Molecular Constants.—The convergence and divergence in the R and P branches of the fundamental make it necessary to use only the separations near the centre of the band for the calculation of the average moment of inertia of the unexcited molecule. The wave-number differences are :—

1—2	3·68 cm.$^{-1}$
1—1′	7·32 „
2′—1′	3·68 „

The agreement flatters the technique. Actually, each reading on the band is separated from the next by 0·47 cm.$^{-1}$, and therefore the separations are really only equal to the first place at best. The average $\delta\nu = 3\cdot68$ cm.$^{-1}$. I and *r* are obtained in the usual way, and the agreement of the results with those previously calculated from the unresolved doublets is brought out in the following table :—

---

* 'Astrophys. J.,' vol. 62, p. 73 (1925). See also Dennison, 'Astrophys. J.,' vol. 62, p. 84 (1925).

—	Infra-red fundamental fine structure.	Burmeister's doublet classical separation.	Lowry's doublet classical separation.	Classical separation of the overtone, Schaefer and Phillips.§
I	$1\cdot50 \times 10^{-39}$	$1\cdot47 \times 10^{-39}$	$1\cdot49 \times 10^{-39}$	$1\cdot48 \times 10^{-39}$
r	$1\cdot15 \times 10^{-8}$	$1\cdot147 \times 10^{-8}$	$1\cdot15 \times 10^{-8}$	$1\cdot149 \times 10^{-8}$

§ 'Z. Physik,' vol. 36, p. 399 (1926).

The value $1\cdot48 \times 10^{-39}$ has been generally accepted, and can be reconciled with most of the electronic data. Recent work by Asundi* suggests a smaller value, of the order of $1\cdot38 \times 10^{-39}$. In spite of the uncertainty of separations in bands as fine as these, it is most unlikely that the vibration-rotation bands can give this value ; the small separations, which make the fine structure so difficult to study, make the envelope a fair approach to the classical. This is shown by the results in the above table. The agreement of classical and quantum values when $\delta\nu$ is small is also shown very clearly in the work of Levin and Meyer on the vibration-rotation bands of hydrocarbons. As Asundi remarks, other criteria do not support the smaller value. The product of I_0 and ω_0, and the series relationships of internuclear distances, both require a value not smaller than $1\cdot45 \times 10^{-39}$ for I_0, and the same is true of all infra-red measurements so far made. Approximate values of $\delta\nu$, and consequently of I and r, can also be deduced from the data upon the fine structure of the overtone, although the accuracy is probably not better than a wave-number. The actual figures are :—

$P(7) \rightarrow P(6)$	$3\cdot6$ cm.$^{-1}$
$P(6) \rightarrow P(5)$	$3\cdot5$,,
$P(5) \rightarrow P(4)$	$3\cdot8$,,

The average $\delta\nu$ is equal to the value for the fundamental within the limits of error. There is an observed, if slight, difference between the $\delta\nu$'s of the HCl fundamental and overtone, caused by the more rapid coming into play of convergence in the overtone (see the energy expression later). The point has not yet been studied in detail, and is beyond verification at present for these small separations of CO.

Further molecular constants follow directly from the positions of the centre of the fundamental and of the centre of the overtone. The vibration frequency of the fundamental is given by

---

* 'Roy. Soc. Proc.,' A, vol. 124, p. 277 (1929).

$$\omega_1 = \omega_0 (1 - x),$$

and that of the overtone by

$$\omega_2 = 2\omega_0 (1 - 2x).$$

If the experimental values of ω_1 and ω_2, 2144 and 4266, are substituted, then

$$\omega_0 x = 11,$$
$$\omega_0 = 2155.$$

The values deduced from the electronic bands are

$$\omega_0 x = 12 \cdot 7,$$
$$\omega_0 = 2155.$$

Although the accuracy of these results from electronic bands is of a higher order than we can hope for, it is pleasing to find that the infra-red can make some attempt at a quantitative statement of the most important of the constants of the normal state of a molecule. Such assurance was needed if investigations of triatomic molecules were to be undertaken with any confidence, for in this field there is as yet no information from electronic bands to act as a standard.

It should be noticed that, for the sake of consistency with the electronic figures, we assume the transitions $n = 0 \rightarrow n = 1$ and $n = 0 \rightarrow n = 2$ for fundamental and overtone. Half integral quantum numbers alter the value of ω_0 to $\omega_0/(1 - x)$. There is no independent criterion to judge between the two values in the present inaccurate state of specific heat data. If the difficulty is borne in mind, there should be no confusion.

The Potential Function of the Molecule.—The constant x is a measure of the anharmonic character of the vibrations, and from it we are led to a search for the potential function of the molecule considered as an anharmonic vibrator. Where the vibration is harmonic, $E = nh\omega_0$, and the potential function is $V = Kx^2$.* We have $E = nh\omega_0 (1 - nx_{\text{anh.}})$ and it is required to find the modification imposed upon the potential function.

(1) In the most general case, the potential function is

$$V = \tfrac{1}{2}K_1 x^2 + \tfrac{1}{3}K_2 x^3 + \tfrac{1}{4}K_3 x^4 \ldots,$$

---

* This x (the finite displacement of the nuclei) is not to be confused with the molecular constant.

when x is the variable describing the finite displacement of the nuclei, and has no reference whatever to the x used above. For the harmonic vibration the corresponding expression is $V = Kx^2$. The constants K_1, K_2, K_3 are characteristic of the particular potential function considered ; the numerical coefficients are merely for convenience of differentiation to the form

$$\ddot{x} = K_1 x + K_2 x^2 + K_3 x^3 \ldots\ldots$$

By combining this function with the kinetic function $T = \frac{1}{2}\mu\dot{x}^2$ Hettner was able to solve for x by the relations

$$x = A \cos 2\pi\omega t + \frac{K_2 A^2}{6K_1} \cos 4\pi\omega t + \left(\frac{K_2^2}{6K_1^2} + \frac{K_3}{4K_1}\right)\frac{A^3}{8} \cos 6\pi\omega t - \frac{K_2 A^2}{2K_1}$$

$$\omega = \omega_0 \left\{1 - \frac{A^2}{24}\left[\frac{10K_2^2}{K_1} - \frac{9K_3}{K_1}\right]\right\} = \omega_0 (1 - x_{\text{anh.}})$$

$$K_1 = 4\pi^2\mu\omega_0^2 \quad \text{and} \quad A^2 = nh/2\pi^2\mu\omega_0,$$

[to close approximations : A is the amplitude of vibration] and these two constants can be obtained without consideration of the positions of the band lines as convergence and divergence become effective, but for K_2 and K_3 a complete knowledge of the fine structure is necessary.

An interesting comparison can be made of the K_1 of CO and of C — O in CO_2. The figures are for these molecules :—

		ω_0	K_1	
CO molecule ..	C — O	2155	184×10^4	
In CO_2	C — O	2315	151×10^4	calculated by Dennison (*loc. cit.*).
In HCHO	C — O	1550		from electronic bands, Henri and Schou.*

K_1 expresses the binding forces between the atoms, and is seen to vary from molecule to molecule. The modification of the force fields is a hitherto untouched problem which must become of importance as soon as the theory of the polyatomic molecule is developed. HCHO is added to the list in the hope that information upon the K may soon be to hand from the work which has been reported from New York.† It clearly is a favourable case for the beginning of theoretical attack.

(2) With a knowledge of the fine structure, the potential function can be completely expressed. The most convenient way is that due to Kratzer (*loc.*

---

* Henri and Schou, 'Z. Physik,' vol. 49, p. 774 (1928).

† Salant and West, 'Phys. Rev.,' vol. 33, p. 640 (1929).

cit.), who altered the form of the general function in such a way as to show the inter-ionic attractive (Coulomb) forces and repulsive forces of the kind shown below.

For an anharmonic vibrator

$$V = -\frac{e^2}{r}\left(1 + \frac{\beta}{r} + \frac{\gamma}{r^2} + \frac{\delta}{r^3}\cdots\right),$$

where r is the distance between the nuclei. In the equilibrium position $r = r_0$. Kratzer's transformation is effected by putting $r/r_0 = \rho$, and $\xi = \rho - 1$. Then

$$V = -\frac{e^2}{r_0}\chi\left(\alpha + \frac{1}{\rho} - \frac{1}{2\rho^2} + c_3\xi^3 + c_4\xi^4\cdots\right).$$

We know that

$$\left(\frac{dV}{d\rho}\right)_{r=1} = 0,$$

and also

$$\left(\frac{d^2V}{d\rho^2}\right)_{\rho=1} = \frac{e^2}{r_0}\chi,$$

and because infinitely small amplitude of vibration corresponds to the frequency ω_0, then

$$(2\pi\omega_0)^2 = \frac{1}{\mu}\left(\frac{d^2V}{dr^2}\right)_{r=r_0} = \frac{1}{\mu r_0^2}\left(\frac{d^2V}{d\rho^2}\right)_{\rho=1} = \frac{1}{\mu r_0^2}\cdot\frac{e^2}{r_0}\chi.$$

That is,

$$-e^2\chi/r_0 = 4\pi^2\omega_0^2\mu r_0^2,$$

and the constants α, c_3, c_4, can be derived from the experimental data when the positions of many of the lines of the fine structure are known. This application was first carried out by Kratzer, using Imes'* results for HCl, and is now used upon the CO fundamental (see next section).

It is easy to pass from the Kratzer function to the more general one, and to substitute K_2, K_3 from the constants c_3, c_4. It is necessary to put $x = r - r_0$, and we have

$$\begin{aligned} V &= \tfrac{1}{2}K_1x^2 + \tfrac{1}{3}K_2x^3 + \tfrac{1}{4}K_3x_4\ldots \\ &= \tfrac{1}{2}K_1(r-r_0)^2 + \tfrac{1}{3}K_2(r-r_0)^3 + \tfrac{1}{4}K_3(r-r_0)^4\ldots \end{aligned}$$

since

$$\rho = r_0/r = \tfrac{1}{2}K_1r_0^2(\rho-1)^2 + \tfrac{1}{3}K_2r_0^3(\rho-1)^3 + \tfrac{1}{4}K_3r_0^4(\rho-1)^4.$$

Hence

$$\tfrac{1}{3}K_2r_0^3 = c_3$$

$$\tfrac{1}{4}K_3r_0^4 = c_4.$$

---

* 'Astrophys. J.,' vol. 50, p. 251 (1919).

From the fine structure it is thus possible to find K_2 and K_3; from these constants the theoretical intensity, according to the correspondence principle, of fundamental and overtone can be calculated in a manner which was originally due to Dennison. This is done later.

(3) A logical extension of Kratzer's type of potential function has recently become popular, and has the merits of simplicity and an obvious physical significance. It consists of writing the potential function as two terms only, one of which represents the attractive forces and the other the repulsive. That is,

$$V = e^2 (c_1/r^p + c_2/r^q),$$

p may usually be assumed to be equal to 1, and it is then easy from our value of $\omega_0 x$ to find q, for

$$2\omega_0 x = B_0 (\tfrac{11}{12} pq + \tfrac{1}{8} (p-q)^2 + p + q + 1)$$

from which

$$q \doteqdot 4,$$

a very reasonable result for a quasi-polar molecule like CO.

Knowing p and q, we can make an estimate of D_0, the dissociation energy per molecule, for

$$2\pi\omega_0 = \sqrt{D_0 pq/I}$$

[or the same result may be obtained in the more usual way from

$$D_0 = h \int_0^{\omega_n} \omega_n \, dn = hc \frac{\omega_0^2}{4\omega_0 x}.$$

Found in this way D, the dissociation energy per gm. mol., is equal to 11·2 volts, in fair agreement with the electronic spectral quantity of 11 ± 0·5 volt, or the chemical value of 11 volts. The possibility arises of expressing the potential function of the molecule graphically. In fig. 5 this is carried out; the upper curve is the potential function e^2c/r, representing the attractive forces, the lower curve e^2c_2/r^4, is the function

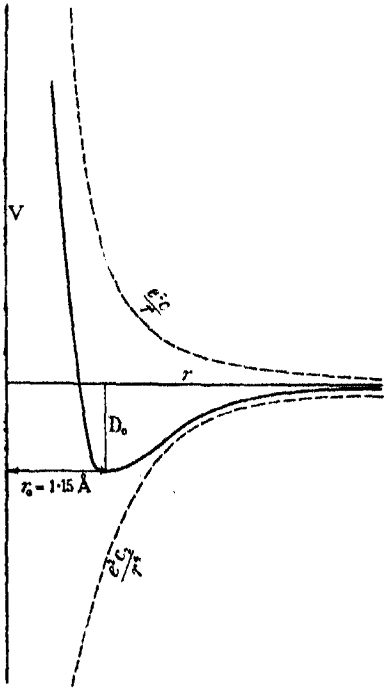

FIG. 5.

of the repulsive forces, and their sum (the heavy curve) is the complete potential function of the CO molecule. The minimum is, of course, the position of stability of the molecule, with $r_0 = 1 \cdot 15$ Å. The form of the curve gives a picture of the anharmonic nature of the vibrations.

The Formula for the Band Lines.

(1) As soon as Imes had established the convergence in the R branch of hydrogen halides the simple Schwarzschild formula, with its equidistant lines, was not adequate for the vibration-rotation band of a diatomic molecule.

From his potential function, already discussed, and the kinetic function

$$T = \tfrac{1}{2} I_0 (\dot{\rho}^2 + \rho^2 \dot{\phi}^2),$$

where ϕ is a cyclic co-ordinate describing the rotational azimuth.

Kratzer obtained the Hamilton Jacobi equation

$$\frac{1}{2I_0} p_\rho^2 + \frac{p_\phi^2}{\rho^2 2I_0} + V = E,$$

where

$$p_\rho = I_0 \dot{\rho}, \qquad p_\phi = I_0 \rho^2 \dot{\phi}.$$

We have the quantum conditions

$$p_\phi = mh/2\pi = p$$

$$nh = \oint p_\rho d\rho = \oint \sqrt{2I_0E - 2I_0V - \frac{p^2}{\rho}}\, d\rho.$$

If the value of the potential function is substituted in this,

$$nh = \oint \sqrt{2I_0E + I_0 \frac{e^2}{r_0} \chi \left(2a + \frac{2}{\rho} - \frac{1}{\rho^2}\left[1 + \frac{m^2h^2}{4\pi I_0 e^2 K/r_0}\right] + 2c_3\xi^3 + \ldots\right)}\, d\rho.$$

From this Kratzer obtained a general formula for the stationary states of a vibrator-rotator. The expression is

$$E_m^n = E_0^n - m^2 a_n h + hB_0 (m^2 - m^4 u^2),$$

where

$$E_0^n = nh\omega_0 [1 - (\tfrac{3}{2} + K) nu]$$

$$a_n = \tfrac{3}{4} nu \,.\, 2B_0 (1 + 2c_3).$$

$$u = \frac{h}{2\pi \sqrt{I_0 e^2 \chi / r_0}} = \frac{2B_n}{\omega_0},$$

$$K = \tfrac{15}{2} c_3 + \tfrac{3}{2} c_4 + \tfrac{15}{4} c_3^2.$$

From the term $m^2 a_n h$ and the term in m^4, the convergence and divergence of the lines is expected; the terms were explained as caused by "coupling" between vibration and rotation. The lines are defined by the difference between two such stationary states, $E_{m''}^{n''}$ and $E_{m'}^{n'}$, when, for the fundamental, $n' = 1$, $n'' = 0$, and for the overtone, $n' = 2$, $n'' = 0$, and when $\Delta m = \pm 1$ (for ${}^1S$ molecules, probably the only class for which the expression is strictly valid). Kratzer himself found the constants a_1 and a_2 and from these α, c_3, c_4, by using Imes's values for two corresponding lines in the R and P branches, say $\omega_{m,\,m-1}^{n,\,0}$, $\omega_{m-1,\,m}^{n,\,0}$, where

$$\omega_{m,\,m-1}^{n,\,0} = (E_m^n - E_{m-1}^0)\,h = E_0^n/h - m^2 a_n + (m - \tfrac{1}{2})B_0 - \{m^4 - (m-1)^4\}\,B_0 u^2/h$$

and

$$\omega_{m,\,m-1}^{n,\,0} = E_0^n - (m-1)^2\,a_n - (m - \tfrac{1}{2})\,B_0 + \tfrac{1}{2}\{m^4 - (m-1)^4\}\,B_0 u^2.$$

Then

$$S_m = \omega_{m,\,m-1}^{n,\,0} + \omega_{n-1,\,n}^{n,\,0} = 2E_0^n/h - [m^2 + (m-1)^2]\,a_n.$$

Thus from the positions of the two chosen corresponding lines, R (m) and P (m), a_n follows at once. If it is substituted in the formula for other lines R (m_1), P (m_1), etc., it is possible to test the accuracy with which a_n so obtained fits the general case. This was done with considerable success for the fundamental and overtone of HCl, and for the fundamentals of HBr and HF. When half integral quantum numbers were introduced in order to remove the difficulty of the missing line 1 → 0, the data, theoretical and experimental, for the HCl bands were made consistent and complete; and, as has been already mentioned, the replacement of m $(m + 1)$ for m has caused only the slightest readjustment.

A similar method has been used upon the CO fundamental. In order to find a_n by substitution, R (4) and P (4) were chosen, as the first lines where deviations from the unmodified δr of 3·68 cm.$^{-1}$ are to be seen. The positions of these lines are :—

$$R\,(4) = 2158{\cdot}79 \text{ cm.}^{-1}$$

$$P\,(4) = 2129{\cdot}14 \text{ cm.}^{-1},$$

i.e.,

$$S_4 - 2E_0^n/h = 0{\cdot}50$$

$$= [m^2 - (m-1)^2]\,a_1$$

where

$$m = \tfrac{9}{2}$$

$$a_1 = 0{\cdot}016.$$

The table below shows the wave-numbers of the remaining lines of the band and the comparison of S_m so found with S_m calculated by the use of $a_1 = 0{\cdot}016$.

When it is remembered that the interval between successive readings is 0·45 to 0·48 cm.$^{-1}$, it will be seen that the agreement is usually within experimental error, except for the far members of the bands. Here there is increasing

m.	R.	P.	S_{exp}.	S_{calc}.
$\frac{3}{2}$	2147·89	2140·53	4288·42	4288·38
$\frac{5}{2}$	2151·58	2136·88	4288·46	4288·30
$\frac{7}{2}$	2155·30	2133·21	4288·51	4288·13
$\frac{9}{2}$	2158·79	2129·14	4287·93	4287·93
$\frac{11}{2}$	2162·25	2125·30	4287·55	4287·62
$\frac{13}{2}$	2165·64	2121·50	4287·14	4287·20
$\frac{15}{2}$	2169·13	2117·80	4286·93	4286·82
$\frac{17}{2}$	2172·69	2113·85	4286·54	4286·33
$\frac{19}{2}$	2175·98	2109·80	4285·78	4285·91
$\frac{21}{2}$	2179·27	2105·75	4285·02	4285·22
$\frac{23}{2}$	2182·50	2101·75	4284·25	4284·10
$\frac{25}{2}$	2185·70	2097·65	4283·35	4283·81
$\frac{27}{2}$	2188·70	2093·50	4282·20	4282·91
$\frac{29}{2}$	2191·59	2089·45	4281·04	4282·04
$\frac{31}{2}$	2194·41	2085·40	4279·81	4281·20
$\frac{33}{2}$	2196·76	2080·95	4277·71	4280·10

Note.—The limit of accuracy of the experimental figures above is, at the best, confined to the first place.

difficulty in deciding on the position of the heads of bands, and the probable inaccuracy is higher.

From a_1 other constants are at once available. Thus :—

$$a_1 = \tfrac{3}{2}u\,2\mathrm{B}\,(1 + 2c_3)$$

$$2c_3 = \frac{0{\cdot}016}{3u\mathrm{B}} - 1$$

$$= 0{\cdot}58$$

$$c_3 = 0{\cdot}29.$$

And

$$(\tfrac{3}{2} + \mathrm{K})\, u = x_{\mathrm{anh.}} = 11/2155, \text{ so that } \mathrm{K} = 1\cdot34,$$

and, since

$$\mathrm{K} = \tfrac{15}{2}\, c_3 + \tfrac{3}{2}\, c_4 + \tfrac{15}{4}\, c_3{}^2, \qquad c_4 = -\, 0\cdot77.$$

The constant α cannot be obtained without a detailed knowledge of the fine structure of the overtone; however, we can assume it to be of the order of $0\cdot001$. Then the Kratzer potential function will be

$$\mathrm{V} = (2\pi\omega_0)^2\, \mu r_0{}^2 (\alpha + 1/\rho - 1/2\rho^2 + 0\cdot29\, \xi^3 - 0\cdot77\, \xi^4 + \ldots).$$

where ω_0, μ, r_0 are known and α is very small.

Since

$$(2\pi\omega_0)^2\, \mu r_0{}^2\, c_3 = \tfrac{1}{3}\mathrm{K}_2\, r_0{}^3$$

$$\tfrac{1}{3}\mathrm{K}_2 = (2\pi\omega_0)^2\, \mu c_3/r^0,$$

and similarly

$$\tfrac{1}{4}\mathrm{K}_3 = (2\pi\omega_0)^2\, \mu\, c_4/r_0{}^2.$$

From the numerical values of K_2 and K_3 there is found an expansion of the usual kind:

$$\mathrm{V} = -\, 92 \times 10^4\, x^2 + 15\cdot6 \times 10^{12}\, x^3 - 30\cdot5 \times 10^{20}\, x^4 + \ldots$$

where $x = r - r_0$.

(2) If the terms in powers of r higher than the first of the Kratzer function are added, then the coefficient of the sum may be taken as the c_2 of the expression

$$\mathrm{V} = e^2 (c_1/r^p + c_2/r^q).$$

A fairly close numerical approach to the representation of the CO molecule is

$$\mathrm{V} = \frac{-\, e^2}{(2\pi\omega_0)^2\, \mu r_0{}^3} \left(\frac{1}{r} - \frac{0\cdot60\, r_0}{r^4}\right).$$

It is from these values of c_1 and c_2 that the graph of the components of the potential function included in the last section were obtained.

But without any knowledge of c_1 and c_2 it is now practicable to describe the positions of the band lines, from the molecular constants ω_0, x and B simply. This advance depends upon the formula for the energy states of a vibrator rotator

$$\mathrm{E} = \omega_0 (1 - nx) + \mathrm{B}_n m\, (m + 1)\, [1 - u^2 m\, (m + 1)].$$

When

$$\mathrm{B}_n = \mathrm{B}_0 (1 - \alpha n)$$

$$\alpha = 2\mathrm{B}_0 (p + q)/\omega_0.$$

The expression is a quantum mechanical modification of the Kratzer formula; the resemblance in form will be revealed on examination.

Because of its quantum mechanical basis, the expression needs whole number values of m for a ^1S molecule. For convenience n is also regarded as integral, as the choice of the vibration quantum number does not affect the fine structure. From differences between two such states, where $n' = 1$ in the upper and $n'' = 0$ in the lower, and where m has integral values and changes only by ± 1, positions of the lines in the R and P branches of the fundamental of CO can be found. These are tabulated below, and compared with experiment.

	R branch.		P branch.	
	Calculated.	Observed.	Calculated.	Observed.
(1)	2147·86	2147·89	2140·53	2140·53
(2)	2151·46	2151·58	2136·82	2136·88
(3)	2154·93	2155·30	2133·01	2133·21
(4)	2158·49	2158·79	2129·22	2129·14
(5)	2162·00	2162·25	2125·42	2125·30
(6)	2165·47	2165·64	2121·59	2121·50
(7)	2168·93	2169·13	2117·68	2117·81
(8)	2172·33	2172·69	2113·76	2113·85
(9)	2175·70	2175·98	2109·82	2109·80
(10)	2179·04	2179·27	2105·83	2105·75
(11)	2182·31	2182·50	2101·81	2101·75
(12)	2185·65	2185·70	2097·79	2097·65
(13)	2188·87	2188·79	2093·72	2093·50
(14)	2191·97	2191·59	2089·57	2089·45
(15)	2194·93	2194·41	2085·42	2085·40
(16)	2196·89	2196·76	2081·17	2080·95
(17)	2199·12	2198·74	2076·87	2076·45

Apart from R (14) and P (17) when the bands have flat topped heads and $\delta\nu$ is accordingly difficult to measure, the correspondence of theory and experiment is remarkable. [See, however, note on page 477.]

It would be interesting to test the expressions on an overtone (where $n' = 2, 3, \ldots$) for which quantitative wave-number positions could be determined, *e.g.*, HBr, where the size of the separations would make accurate work easy. There is no doubt that for CO the energy function, obtained as it is from independent data, gives a satisfactory account of experimental fact.

There is the possibility of beginning from the experimentally-found lines, substituting in the expression, and either of fitting the constants μ, B_n, etc., or by a laborious algebraic transformation of arriving at the constants of the potential function. As the Kratzer method was available and had the merit of greater ease, this process was considered redundant.

Intensity of Fundamental and Overtone.

A method has been devised by Dennison (*loc. cit.*) for the theoretical comparison of the intensities of fundamental and overtone. He begins from the well-known relation between the absorption coefficient α_ω of a band ω_i, and the Einstein probability coefficient A_0^i from ω_i to the normal state

$$A_0^i = \frac{g_0}{g_i}\,\omega_i^2 K \int a_\omega \, d\omega,$$

where g_0 and g_i are the *a priori* probabilities of the normal state and where K is independent of ω_i. Then, if ρ_i^2 is adopted as a measure of intensity,

$$\rho_i^2 = \frac{A_0^i}{\omega_i^2} = \frac{g_0}{g_i} K \int_0^\infty a_\omega \, d\omega.$$

It is necessary to approximate for $\int a_\omega \, d\omega$. When absorption bands of the same molecule (and due to a vibration of the electric moment in the same direction for the bands compared, as must be the case in a diatomic molecule) are compared, the integral may be replaced by the absorption coefficient at corresponding points, *e.g.*, the maxima of the bands, $(a_\omega)_{\max}$ or for P (m) or R (m) in each band, (a_ω) P (m) or (a_ω) R (m).

Dennison's theoretical estimate of ρ_i^2 depends upon the assumption of central forces acting upon the nuclei and defining their behaviour, an assumption which is only strictly true for diatomic molecules. If each nucleus is regarded as a centre of effective change, then the change in electric moment is directly proportional to the displacement of the nuclei. Thus, if E_i is the amplitude of change of the electric moment, the following relation is given by the correspondence principle (and will only be completely valid for large quantum numbers)

$$A_0^i \, (h\omega_i) = g E_i^2 \omega_i^4$$

and

$$\rho_i^2 = A_0^i / \omega_i^2 = E_i^2 \omega_i \text{ (constant)}.$$

The amplitude of the change of electric moment is taken in the upper state rather than in average value of the CO state in the transition. This, of course, introduces the usual kind of correspondence principle ambiguity.

Using the constants of Hettner's approximate solution of the energy equations we have, from the foregoing,

$$\rho_1^2 = A_0^2 \omega_0,$$

$$\rho_2^2 = (K_2/6K_1)^2 (4A_0^4)(2\omega_0) = \tfrac{2}{9}(K_2/K_1)^2 A_0^4 \omega_0,$$

where

$$A_0^2 = h/2\pi^2 \mu \omega_0,$$

i.e.,

$$\frac{\rho_1^2}{\rho_2^2} = \frac{1}{\tfrac{2}{9}(K_2/K_1)^2 A_0^2}.$$

For CO, K_2 and K_1 have already been calculated, and A_0 follows from the molecular constants. Substitution gives

$$\rho_2^2/\rho_1^2 = 0 \cdot 032.$$

The measured ratio with which this is to be compared comes from the ratio of the absorption coefficients at corresponding points on the two bands. The choice of the corresponding points is not easy. Dennison took the maxima of the bands, but this may introduce a serious practical inaccuracy. Since $a_\omega = \log(I_0/I_t)$, and since I_t (for the fundamental) is in most of these comparisons of the order of 5 to 10 per cent., it is clear that a small error in I_t will considerably influence the ratio I_0/I_t. Even the most careful of intensity measurements could contain an error of 1 per cent. in an absorption of 95 per cent., and hence the a_ω for the maximum of the fundamental cannot be relied upon. In the table below the maxima of the P branches and also P (4), (5) (6) for each band are compared.

	Fundamental $\log I_0/I_t$.	Overtone $\log I_0/I_t$.	$\frac{\rho_1^2}{\rho_2^2}$ (measured).
P max.	100/5·5	100/86	0·05
P (3)	100/10	100/92	0·037
P (5)	100/9	100/92	0·034
P (6)	100/10	100/92·5	0·035

There is a marked improvement of the correspondence between theory and practice for the lower values of a_ω.*

The measurements of absorption on which the above figures depend were made upon the same pressure of CO (½ atmosphere) for both fundamental and overtone. At this pressure the positions of the intensity maxima for the individual bands of the fine structure are very difficult to fix and the values are given only in an attempt to improve the practice of an interesting theoretical point. No greater faith can be put in the figures than to say that they are of the right order. It can be said that the values of the intensity of the fine structure bands, calculated from the fundamental at 11 cm. pressure by assuming Beer's law, are in fair agreement with the observations.

---

* Recently a method has become available for the theoretical comparison of intensities, based upon the quantum mechanical solution of a perturbed oscillator. For CO the ratio so obtained is rather smaller than that given by the older method.

Alternating Intensities.

There are certain irregularities in the fine structure of the fundamental, notably R (4), R (5), R (6) and P (5) and P (6). Although at some points the variations in intensity suggest alternation, they are not part of a regular alternating system, because, for example, P (5) is weak and P (7) is strong. Probably, as the variations are small (not more than 4 per cent.) the effect is due merely to the occasional missing of a maximum in the breadth of the difference between observations.

It is now certain that there cannot be regular alternating intensities in any bands save those due to a completely symmetrical molecule X_2. The slight indications of alternation noticed in high numbers of the P and R branches of the NO fundamental must be caused by some similar instrumental reason; they were said at the time to be irregular and to be at the most of the order of 4 per cent. The only definite case of marked alternation in vibration-rotation bands is given in Levin and Meyer's[*] observation on acetylene and ethylene, when the symmetrical systems of CH–CH and CH_2–CH_2 are concerned.

Summary.

(1) The vibration-rotation band ($n'' = \frac{1}{2} \rightarrow n' = \frac{3}{2}$) of CO has been resolved completely. Its centre is at 2144 ± 0·4 cm.$^{-1}$, it has no Q branch and the separations of lines converge on the side of higher frequency and diverge on the lower side. The overtone ($n'' = \frac{1}{2} \rightarrow n' = \frac{5}{2}$) has been plotted, and partially resolved.

(2) The general character of vibration-rotation bands carried by ^1S molecules is discussed, and the CO bands are shown to be consistent with the scheme.

(3) The molecular constants deduced from the vibration-rotation bands are compared with those from the electronic bands. The values are :—

---

[*] Levin and Meyer, 'J. Opt. Sci. Amer.,' vol. 16, p. 137 (1928).

	Vibration-rotation.	Electronic.
ω_0	2155	2155
$\omega_0 x$	11	12·7
I	$1 \cdot 50 \times 10^{-39}$	No definite
r	$1 \cdot 15 \times 10^{-8}$	values as yet.

(4) From the positions of the band lines, the constants of potential functions have been determined, and the data are found to give excellent concordance when the method first applied by Kratzer is used. Later, the constants of the general potential functions are included in a theoretical method for the determination of the ratio of the intensities of overtone and fundamental; the value obtained is found to be quite near the ratio experimentally determined.

(5) The potential function can also be expressed as

$$V = e^2 (C_1/r + C_2/r^4).$$

This result is represented graphically. From this basis it is possible to describe the band lines by an expression which contains only I, ω_0, and x, constants external to the convergence or divergence within the bands. The method successfully accounts for most of the experimental results upon the position of the band lines.

(6) The question of alternating intensities is mentioned, and it is suggested that the only vibration-rotation bands showing this effect are those of the symmetrical molecules of acetylene and ethylene.

(7) The detailed character of the bands agrees so well with the theory of the ^1S diatomic molecule as to make it theoretically possible completely to describe the vibration-rotation bands of this type of molecule.

Acknowledgments.

We are glad to thank the Keddey Fletcher-Warr Studentship Board, who made it possible for one of us (C.P.S.) to engage in this work; and to make personal acknowledgment to Prof. Lowry, for his interest in it, and for much help in presentation; to Sir Robert Robertson, for encouragement in many ways; to Dr. A. M. Taylor, for help and criticism at all stages of the work; to Prof. D. R. Hartree, for advice and interest. Lastly, we should like to express thanks to Dr. R. de L. Kronig, for the benefit of the clarity of thought and knowledge of molecular spectroscopy given to us in the course of a series of lectures and several conversations.

The Structure of the Band Spectrum of Helium.—VI.

By Prof. W. E. Curtis, D.Sc., and A. Harvey, B.Sc., Armstrong College,
Newcastle-upon-Tyne.

(Communicated by T. H. Havelock, F.R.S.—Received July 10, 1929.)

1. *Introductory.*

Much progress in the analysis and interpretation of the helium band spectrum has been made since the publication of Part V of this series about a year ago.* Nearly a hundred new branches have been identified, many of them relatively weak and arising from vibrational states of the molecule, and all derived from electronic levels belonging to known sequences. The most important development has been in connection with the interpretation of these levels. It was pointed out by one of us† that the He_2 spectrum affords the first clear evidence of the existence of electronic levels additional to those characteristic of atoms, and suggestions as to a possible correlation of these with the predictions of Hund were put forward in V. Weizel independently arrived at the same conclusion at about the same time, and has succeeded in accounting for all the known types of He_2 term on the basis of Hund's theory.‡ He has also given an explanation of certain peculiarities of the rotation term differences by postulating a change of coupling of the electronic orbital angular momentum. Dieke,§ working on similar lines, has accounted for the anomalous appearance and intensities of the branches of some of the bands. There have been several other publications, to which reference will be made later, giving details of a number of new bands and remeasurements of some already known. A brief résumé of the above results may help to make what follows more intelligible.

2. *The Electronic Levels.*

The feature of Hund's theory which is of fundamental importance in the interpretation of the He_2 spectrum is his deduction that the non-central field due to the two separated nuclei should give rise to term sequences additional to those familiar in atoms under the names S, P, D, etc. He concludes that the electronic orbital angular momentum (quantum number l) may be coupled to the inter-nuclear axis, so that a new quantum number (σ_l) appears which may have any integral value between 0 and l. Thus we should expect the three atomic levels S, P, D, to be resolved in the molecule into six, namely, $\sigma\Sigma$ ($l = 0, \sigma_l = 0$); $\pi\Sigma$ ($l = 1, \sigma_l = 0$) and $\pi\Pi$ ($l = 1, \sigma_l = 1$); $\delta\Sigma$ ($l = 2, \sigma_l = 0$); $\delta\Pi$ ($l = 2, \sigma_l = 1$) and $\delta\Delta$ ($l = 2, \sigma_l = 2$). The notation employed here is that of Dieke. A comparison with those of Mulliken and Weizel is given in Table I, the empirical system previously in use being also included. Weizel's is too elaborate to be generally useful, but has the advantage of specifying the state of each of the four electrons of the molecule. The letters s, p, d represent the l values and σ, π, δ the σ_l values of the individual electrons, whilst Σ, Π, Δ correspond to the resultant σ_l values of the whole electron system.

---

* The previous papers of this series have appeared in these 'Proceedings' as follows: I, vol. 101, p. 38 (1922); II, vol. 103, p. 315 (1923); III, vol. 108, p. 513 (1925); IV, vol. 118, p. 157 (1928); V, vol. 121, p. 381 (1928).

† 'Nature,' vol. 121, p. 907 (1928).

‡ 'Z. Physik,' vol. 51, p. 328 (1928); vol. 52, p. 175 (1928); vol. 54, p. 321 (1929).

§ 'Nature,' vol. 123, p. 716 (1929).

Table I.—Comparison of Notations.

Empirical	S, ${}_p\mathrm{He}_2$	S, ${}_o\mathrm{He}_2$	[U, ${}_o\mathrm{He}_2$]	P, ${}_o\mathrm{He}_2$
Mulliken	${}^1\mathrm{S}^\mathrm{s}$	${}^3\mathrm{S}^\mathrm{s}$	${}^3\mathrm{S}^\mathrm{p}$	${}^3\mathrm{P}^\mathrm{p}$
Weizel	$(1s\sigma)^2 p\sigma . s\sigma^1 \Sigma$	$(1s\sigma)^2 p\sigma . s\sigma^3 \Sigma$	$(1s\sigma)^2 p\sigma . p\sigma^3 \Sigma$	$(1s\sigma)^2 p\sigma . p\pi^3 \Pi$
Dieke	$\sigma^1 \Sigma$	$\sigma^3 \Sigma$	$\pi^3 \Sigma$	$\pi^3 \Pi$

Empirical	Z, ${}_o\mathrm{He}_2$	$\left.\begin{matrix}\mathrm{X}\\\mathrm{Y}\end{matrix}\right\}$, ${}_o\mathrm{He}_2$	D, ${}_o\mathrm{He}_2$
Mulliken	${}^3\mathrm{S}^\mathrm{D}$	${}^3\mathrm{P}^\mathrm{D}$	${}^3\mathrm{D}^\mathrm{D}$
Weizel	$(1s\sigma)^2 p\sigma . d\sigma^3 \Sigma$	$(1s\sigma)^2 p\sigma . d\pi^3 \Pi$	$(1s\sigma)^2 p\sigma . d\delta^3 \Delta$
Dieke	$\delta^3 \Sigma$	$\delta^3 \Pi$	$\delta^3 \Delta$

The X and Y levels have been shown by Weizel to be the b and a levels* of $\delta\Pi$, and are therefore bracketed together. The terms ortho and par which have previously been used to denote the two systems of helium bands may now be replaced† by the customary notation for triplet and singlet levels. All the

---

* Levels having j odd are here labelled a and those having j even b, in accordance with present usage. It should be noted that these designations differ in some cases from those employed in the previous papers of this series.

† See Monk and Mulliken, 'Nature,' vol. 124, p. 91 (1929).

Σ-type levels have only one set of rotation states (A, j odd). The rest have two distinct sets (A, j odd, and B, j even).

One of the predicted levels, $\pi\Sigma$, to which the empirical designation U has been attached, has not hitherto been observed. We believe that we have now identified this, and shall describe below a number of new bands having 2U as final level. This probably completes the electronic term scheme so far as the visible spectrum is concerned. But there are many striking peculiarities of the rotation terms which call for comment.

In the earlier stages of this work, which concerned the S, P, and D levels, it was found that the rotation terms could be well represented by a formula of the type $F(j) = Bj^2 - \beta j^4$, j being half-integral. This as a rule held so accurately that it was possible to calculate a trustworthy value for the vibration frequency ω from the constants B and β ($\omega = 2\sqrt{B^3/\beta}$). The levels which were subsequently discovered, and in particular the Z type, showed very pronounced deviations from this formula, especially for low j values, so that it was not found possible to calculate the terms. Moreover, the intensity distribution between the branches was frequently very peculiar, and their interpretation difficult. Thus for example, Dieke, Takamine and Suga* denoted the three branches of the bands $3Y \rightarrow 2P$ by Q, R and S (S representing the transition $(j+2) \rightarrow j$), but purely on account of their appearance. The combination differences provided no justification for this, and it is now clear that they are actually P, Q and R of a somewhat exceptional type. Again, the same workers labelled the two branches which they found in $Z \rightarrow P$ bands as P and Q, also on account of their appearance. In one case, however, $3\,{}^3Z \rightarrow 2\,{}^3P$, we had found traces of a third (P) branch which if genuine would point to Q and R as the true designations, and there is now no doubt, in view of the developments described below, that this is the correct view.

The explanation of these and other anomalies was first given by Weizel. He showed that they result from a loosening of the coupling between the electronic orbital angular momentum and the inter-nuclear axis as the rotational angular momentum increases, whereby the former ceases to be strictly quantised with respect to the latter, and develops a mean component ρ ($\times\ h/2\pi$) along the axis of rotation. The first term in the expression for the rotational energy then becomes $B(\sqrt{j(j+1) - \sigma_i^2} - \rho)^2$, as in the well-known Kramers-Pauli formula, except that in this case ρ varies with j. This uncoupling effect should become more marked as j increases and also as n (the principal electronic quantum number) increases. The former factor accounts for the anomalous course of some of the branches and the latter for the marked difference in appearance of certain bands belonging to the same electronic sequence. Weizel succeeded in obtaining on this basis a semi-quantitative explanation of the more striking peculiarities of the rotation terms, in particular of the behaviour of their second differences, and established the identification of empirical with theoretical terms set out in Table I.

---

* 'Z. Physik,' vol. 49, p. 637 (1928).

Dieke has traced the uncoupling process somewhat further, to the stage at which l is coupled to the axis of rotation and there is a corresponding quantum number (ρ, an integer). He pointed out that the peculiar distribution of intensity between the branches of some of the bands could be accounted for, and assigned values of ρ which would be attained for complete uncoupling from the nuclear axis. He gave the following table showing the correlation of the terms in the two extreme cases.

Table II.—Classification of He_2 Terms (Dieke).

	$l = 0$.	$l = 1$.			$l = 2$.				
Case I	$\sigma\Sigma_a$	$\pi\Sigma_b$	$\pi\Sigma_a$	$\pi\Pi_b$	$\delta\Sigma_a$	$\delta\Pi_b$	$\delta\Pi_a$	$\delta\Delta_b$	$\delta\Delta_a$
σ	0	0	1	1	0	1	1	2	2
Case II	σ_0	π_1	π_0	π_{-1}	δ_2	δ_1	δ_0	δ_{-1}	δ_{-2}
ρ	0	1	0	−1	2	1	0	−1	−2
Empirical	S_a	....	P_a	P_b	Z	X	Y	D_b	D_a

The process of transition from Case I to Case II is particularly well exhibited in the group of terms for which $l = 2$, which Dieke calls a δ complex. Thus for $n = 3$ Case I applies, at any rate when j is small, for $n = 4$ the transition has commenced, for $n = 5$ it is well advanced, and for $n = 6$ practically completed, although in the last case data for the Y and D terms are lacking. The transition process is very clearly seen, and the ρ values are at once obvious, from an inspection of the rotation term differences for all the states of the He_2 molecule. These are tabulated in Table III and discussed in the following section.

3. *The Rotation Term Differences.*

The helium bands consist of two distinct non-combining systems, designated par and ortho by analogy with He, and probably also having singlet and triplet fine structure. In each system the five types of electronic level already mentioned have been found, and the bands fall into two groups according to their final states. One of these terminates on the 2S level, with initial levels 3P, 4P, etc., and the other on the 2P level, with initial levels 3S, 4S, . . ., 3Z, 4Z, . . ., 3XY, 4XY, . . ., 3D, 4D, . . . The 2S and 2P levels are thus common to a number of bands, and their rotation term differences are therefore well determined. The other differences tabulated are as a rule derived from one band only, but will usually be reliable to within a few tenths of a wave-number. The vibrational states have been left out of consideration entirely, since although a large number of the resulting bands have been observed they are comparatively weak, and the data derived from them would consequently have been much less reliable and complete than that derived from the main (*i.e.* vibrationless) bands.

The data have been drawn from so many sources, and such various methods have been applied to them for the extraction of the required differences, that it is impossible to give full details of their derivation. A few words of explanation may be useful, however. Whenever possible the differences have been obtained in the usual manner, by combining corresponding lines of the P and R branches. In an S → P type band, for instance,

$$P(j) = S_a(j-1) - P_b(j), \quad \text{and} \quad R(j) = S_a(j+1) - P_b(j),$$

neglecting the electronic terms, which disappear in forming the differences.

Hence $\Delta(j)$ for the S level $= S_a(j+1) - S_a(j-1) = R(j) - P(j)$ and $\Delta(j)$ for the P_b level $= P_b(j+1) - P_b(j-1) = R(j+1) - P(j-1)$. The Q branch is derived from the P_a level, thus :—

$$Q(j) = S_a(j) - P_a(j),$$

and to derive the P_a differences four lines must be combined, thus

$$\Delta(j) \text{ for } P_a \text{ level} = Q(j-1) - Q(j+1) + R(j) - P(j).$$

Again, we may have only Q and R branches present, as in the Z → P bands, where $Q(j-1) = Z_a(j-1) - P_a(j-1)$, and $R(j) = Z_a(j+1) - P_b(j)$. In this case $\Delta(j)$ for the Z_a level is given by $R(j) - Q(j-1) + \{P_b(j) - P_a(j-1)\}$, the difference in brackets being readily obtainable from the S → P bands.

Finally, there are several cases of single branches, as for example the R branch of $5\,{}^1Z \rightarrow 2\,{}^1P$, where one set of differences involved is already known. The other can then be found exactly as described above for the Q branch of an S → P band. Differences derived in this way from one branch only are enclosed in brackets in the table, and are naturally of somewhat less weight than those resulting from straightforward combination of two branches. Known blends and perturbations are denoted by * and † respectively. The table contains all the term differences at present known, including those derived from the new bands described below.

The chief conclusions which may be drawn from the data set out in the table below can be summarised as follows :—

(1) In the same electronic sequence for a given value of j the term differences tend towards a definite limiting value as n increases. This is reached fairly quickly in certain cases (*e.g.* S, P_a, Z) whilst in others the process is more gradual (*e.g.* P_b, D_b). In one case, D_a, only two levels ($n = 3$ and 4) have been observed as yet, but the beginning of the same process is apparent.

(2) So far as can be judged from the data at present available these limiting values are identical in all cases, although they are not in general associated with the same j values. They are as follows, the accuracy of estimation being probably a few tenths of a wave-number except for the last two :—

70·9 127·5 183·4 239·0 293·5 347·0 399·5 451

(3) The ${}_o\mathrm{He}_2$ and ${}_p\mathrm{He}_2$ differences behave in exactly the same manner, although the data for the latter are much less complete. Both tend to sensibly the same limiting values ; the initial values, however, are quite appreciably different.

(4) The j's associated with the limiting values are not identical, but the $(j - \rho)$'s are, if the ρ's assigned by Dieke are used. For example, for the S levels the j's in question are 2, 4, 6, etc. This applies also to the P_a and Y levels, and $\rho = 0$ for all three. But for the X and Z levels the j's are 3, 5, 7, . . . and 4, 6, 8, . . . respectively, and Dieke assigns $\rho = 1$ and 2 to these levels. The D_b and D_a values are rather fragmentary but behave as they should if $\rho = -1$ and -2 in agreement with Dieke. There is a discrepancy in the case of P_b, for which he concludes ρ to be -1. If this were so the differences should increase with n as in the case of the D's, but actually they diminish, and the corresponding j values are one unit higher than those of the S levels. Both of these facts point to $\rho = +1$, and this is supported by the behaviour of the new (U) level which we have found, and which behaves as though $\rho = -1$. We have therefore interchanged Dieke's ρ values for the P_b and U levels.

The interpretation of these results is in the main quite simple. The general course of the differences is to be attributed to the tendency as j and n increase

Table III.—Rotation Term Differences

l = 0.

ρ	Term	j = 1	2	3	4	5	6	7	8	9	10	11	12
0	2S		75·80		136·18		196·08		255·30		313·60		370·77
	3S		72·20		129·70		186·79		243·21		298·78		353·20
	4S		70·95		128·19		184·59		240·71		295·46		349·24
	5S		(70·93)		127·98*		183·76		242·23	†	292·46		347·97
	6S		70·88		126·67	†	184·76		239·59		293·86		

l = 1.

1	$2P_b$			101·98		160·06		217·55		274·26		329·98	
	$3P_b$			99·25		155·58		211·35		266·44		320·55	
	$4P_b$			97·35		151·80	†	208·84		261·55		315·00	
	$5P_b$		†	96·97		150·29		205·07		258·84		[312·54]	
	$6P_b$			92·83		146·19		199·09		[252·41]		305·09	
	$7P_b$			90·36		143·07		[196·43]		[250·18]		303·97	
	$8P_b$			87·03		139·83		[193·95]					
	$9P_b$			{84·86}		{136·18}							
	$10P_b$			{85·89}									
0	$2P_a$		73·34		131·65		189·54		246·82		303·24		358·58
	$3P_a$		71·67		128·69		185·35		241·32		296·49		350·57
	$4P_a$		71·22		127·99		184·15		|244·61| |238·10|	†	|290·41| |296·92|		348·39
	$5P_a$		70·77		|129·02| |125·48|	†	|185·98| |192·44|		239·59		294·14		347·58
	$6P_a$		70·90		127·91		183·44		239·11		294·32		346·93
	$7P_a$		70·92		127·67		183·56		239·11		293·58		347·40
	$8P_a$		70·79		127·63		183·49		238·97		293·67		346·99
	$9P_a$		70·75		127·86		183·04		238·85				
	$10P_a$		71·12		127·35		183·95		237·62				
−1	2U	41·11		95·72		150·04		203·08		256·72		308·54	

l = 2.

2	$3Z_a$		(45·08)		89·03		138·49		190·19		242·44		294·61
	$4Z_a$		(26·64)		77·42		131·05		185·27		239·62		293·41*
	$5Z_a$		?		72·50*		128·42		180·77*	†	240·80*		293·48
	$6Z_a$		?		71·40		126·02	†	183·38		238·90		292·90
1	$3X_b$			92·11		144·73		197·25		249·70		301·69	
	$4X_b$			85·37*		136·48*		189·40		242·62*		295·88	
	$5X_b$			75·32		129·55		184·48		239·42		293·65	
	$6X_b$					126·95		183·15		238·85		293·22	
0	$3Y_a$		80·52 ?		153·16		210·42		263·90		315·20		365·21
	$4Y_a$		99·88		152·41		199·94		248·54		298·74		350·17
	$5Y_a$		(78·59)		(132·25)		(184·88)		(239·33)		(293·55)		
−1	$3D_b$			105·42		164·70		228·01		279·97		335·59	
	$4D_b$			112·50		173·76*		231·89		288·35		342·93	
	$5D_b$			122·82		180·87		237·29					
−2	$3D_a$				135·65		195·58		254·78		312·81		369·44
	$4D_a$				149·87*		216·35		278·76		336·76		391·55

The meaning of the symbols employed is as follows :—

Differences derived from blends marked *. Values of *j* for which perturbations occur indicated by †; the two neighbouring differences are equally displaced in opposite directions.

Differences derived from one branch only are enclosed in brackets or so described under "derivation."

[ ] from P branch only, ( ) from Q, { } from R.

| | indicates that the perturbed level is apparently split into two.

[F $(j+1)$ − F $(j-1)$] for $_o\text{He}_2$.

$l = 0$

13	14	15	16	17	18	19	20	Derivation.
	426·66		481·05		534·03			Means from “ main series.” 16, 18 from two bands only—
	(406·38)							3 $^3S \rightarrow 2\,^3P$ (Curtis I).
	(401·50)							4 $^3S \rightarrow 2\,^3P$ (Curtis I).
	[400·93]							5 $^3S \rightarrow 2\,^3P$ (Weizel).
								6 $^3S \rightarrow 2\,^3U$ (Imanishi).

$l = 1$

384·61		437·98		489·92		540·13		Weighted means from bands ending in 2 ^3P_b.
378·63		425·41		475·81				
367·39		418·55						
[364·88]		415·02		462·75				
357·31		408·50						
358·82								P.R. branches of “ main series ” (Curtis III).
	412·74		465·50		516·93			Weighted means from bands ending in 2 ^3P_a.
	403·40		455·33					
	401·05		452·16					
	400·39		452·53					
	399·85							Q branches of “ main series ” (Curtis III).
359·16		408·60						Means from $^3S \rightarrow 2\,^3U$. 13, 15 from 4 $^3S \rightarrow 2\,^3U$ only (Table IV).

$l = 2$

	346·23		396·85		446·25*		494·09*	R branches of Z→P bands (Curtis).
	346·67*		403·46	†	439·41			(Curtis).
	345·72		398·60 ?		449·70 ?			(Weizel).
	346·40		399·39 ?					(Weizel).
352·91		408·42		452·49				3 $^3X \rightarrow 2\,^3P$ (Curtis).
348·44		399·80		450·97*		499·61		4 $^3X \rightarrow 2\,^3P$ means Dieke-Weizel ; 17, 19 Weizel only
347·10								5 $^3X \rightarrow 2\,^3P$ means from Q & R branches (Table V).
346·82		399·27		450·15				6 $^3X \rightarrow 2\,^3P$,, ,, ,, (Dieke—see text).
	413·70		461·15		507·28			3 $^3Y \rightarrow 2\,^3P$ (Dieke).
	(401·21)		(451·10)					4 $^3Y \rightarrow 2\,^3P$ (Table V) ; 14 and 16 from Dieke.
								5 $^3Y \rightarrow 2\,^3P$ (Table V).
380·60		441·66						3 $^3D_b \rightarrow 2\,^3P$ (Curtis).
395·95		447·36		496·98		544·16*		4 $^3D_b \rightarrow 2\,^3P$ (Dieke).
								5 $^3D_b \rightarrow 2\,^3P$ (Weizel).
	424·07							3 $^3D_a \rightarrow 2\,^3P$ (Curtis).
	448·77		493·91		541·77			4 $^3D_a \rightarrow 2\,^3P$ (Dieke).

Table III—(continued). Rotation term

$l = 0$.

ρ	Term	$j = 2$	3	4	5	6	7	8	9	10	11	12	13
0	2S	76·42		137·64		197·98		258·19		316·97		375·01	
	3S	72·85		[131·22]		187·42		243·92		299·84		354·30	
	4S	71·05		127·45		183·98		(239·75)		(294·35)			

$l = 1$.

1	$2P_b$		101·72		159·39		216·46		273·10		328·66		383·01
	$3P_b$		99·05		156·01		211·68		266·79		320·45		
	$4P_b$		98·19		153·95		208·95		263·92		[317·20]		|369·89|
	$5P_b$		96·46*		152·05		206·01		260·24		318·62		365·58
	$6P_b$		95·03*		149·90		203·12		257·57		311·21		362·61
	$7P_b$		92·37*		145·48**		205·22*		260·97*				
	$8P_b$		91·90		147·08		203·84		{259·87}				
0	$2P_a$	73·06		130·98		188·70		245·52		301·66*		356·84	
	$3P_a$	71·24		128·58		184·82		241·07		299·02		350·11	
	$4P_a$	71·03		127·93		183·95		239·90		294·36		348·24	
	$5P_a$	—		127·46		183·92		239·06*		293·89*		348·05	
	$6P_a$	69·17*		127·30		183·56		238·78		294·05		346·95	
	$7P_a$	70·49*		127·37		183·66*		239·30*		293·29		346·78	
	$8P_a$	70·31		127·55		183·17		239·19		293·24		346·37	
−1	$2U_b$	Not observed.											

$l = 2$.

2	$3Z_a$	42·10		86·50		136·80		189·10		242·17		295·12	
	$5Z_a$				†	118·47		184·59		239·09		293·23	
1	$3X_b$		90·80		143·05		195·44		247·95		300·42*		351·86
0	$3Y_a$	94·84 ?		154·50		209·81		261·58		311·68*		361·27	
−1	$3D_b$		107·16		167·10		225·86		282·56		338·53		392·24
	$4D_b$		(117·07)		(177·51)		(234·78)		(290·98)		(345·25)		(397·69)
	$5D_b$		(122·79)		(182·04)		(237·65)		(292·56)		(345·96)		(398·15)
−2	$3D_a$			138·32		199·50		260·09		319·18		376·50	
He_2^+		70·9		127·5		183·4		239·0		293·5		347·0	

The meaning of the symbols employed is as follows:—

Differences derived from blends marked *. Values of j for which perturbations occur indicated by †; the two neighbouring differences are equally displaced in opposite directions,

Differences derived from one branch only are enclosed in brackets or so described under "derivation."

[ ] from P branch only, ( ) from Q, { } from T.

| | indicates that the perturbed level is apparently split into two.

Differences F $(j + 1) - $ F $(j - 1)$ for $_p$He$_2$.

$l = 0$

14	15	16	Derivation.
431·88			Adopted values, "main series" (Curtis III). 12 and 14 from $7^1P \rightarrow 2^1S$ and $8^1P \rightarrow 2^1S$ (Weizel).
[407·40]			$3^1S \rightarrow 2^1P$ (Dieke).
			$4^1S \rightarrow 2^1P$ (Weizel).

$l = 1$

	436·00		Weighted means from bands ending in 2^1P_b.	
				(Curtis III).
				(Curtis III).
	{416·83}		PR branches of	Weizel).
			"second series")	(Weizel).
				(Imanishi).
				(Imanishi).
410·68			Weighted means from bands ending in 2^1P_a.	
				(Curtis III).
401·01				(Curtis III).
403·81			Q branches of	(means, Curtis III and Weizel).
400·64			"second series"	(Weizel).
				(Imanishi).
398·45				(Imanishi).
	Not observed.			

$l = 2$

347·41		398·80	$3^1Z \rightarrow 2^1P$. Means from Q and R branches (Curtis V and Dieke).
346·46		398·50	$5^1Z \rightarrow 2^1P$ (Dieke).
	402·56		$3^1X \rightarrow 2^1P$ means (Curtis V and Dieke).
408·83*			$3^1Y \rightarrow 2^1P$ (Dieke).
			$3^1D_b \rightarrow 2^1P$ means (Dieke and Weizel). $4^1D_b \rightarrow 2^1P$ (Curtis, Table V). $5\ D_b \rightarrow 2^1P$ (Dieke—see text).
			$3^1D_a \rightarrow 2^1P$ means (Dieke and Weizel) ; 12, from 1 only.
399·5		451	Mean estimated limiting values.

for the coupling of l to the nuclear axis to break down, and coupling to the rotation axis to be substituted. When this process is completed the effective value of j is changed to $j - \rho$, and the differences will correspond to a lower or higher j value according to whether ρ is positive or negative. The matter is to some extent complicated by a variation in the value of the moment of inertia with n to which part of the change in the differences is due. Conversely, an increase in the differences is not necessarily due to a decrease in the moment of inertia, but may be due to the development of a negative ρ, and this is no doubt the explanation of the apparently anomalous behaviour of the D terms which has been previously remarked (see IV, p. 168, and V, p. 389).

It is to be noted that the final $(j - \rho)$ values for the terms themselves are odd (those given refer to the differences $F(j+1) - F(j-1)$), corresponding to terms antisymmetric in the nuclei, which are the only ones theoretically possible.

The limiting values of the term differences must evidently be those characteristic of the He_2^+ ion, since they correspond to the complete removal of an electron; they will naturally be identical for all sequences, and should be the same for ${}_pHe_2$ and ${}_oHe_2$ as observed, since the two systems differ only in the orientation of the spin of the optical electron. Weizel has found a similar approach to constancy in the vibration frequencies of the various sequences, so that we now have both vibrational and rotational constants for the He_2^+ ion. They are

$$\omega = 1628 \text{ cm.}^{-1}, \quad B = 7\cdot105 \text{ cm.}^{-1}, \quad I = 3\cdot898 \times 10^{-40}, \quad r_0 = 1\cdot087 \text{ A.}$$

Apart from the theoretical interest attaching to these regularities, they are of very great assistance in the further analysis of the spectrum. The majority of the lines still unallocated to bands are probably due either to higher levels of the known electronic sequences or to vibrational levels associated with known electronic levels. The latter type are readily identified from their similarity to the corresponding $0 \rightarrow 0$ bands, and from the existence of combination relationships. The former sometimes present difficulty because of the fading out of branches with increasing n. In the $n\text{Z} \rightarrow 2\text{P}$ bands, for instance, the P branch is extremely weak for $n = 3$ (${}_oHe_2$) and has not been observed in any other case. For $n = 4$ the Q branch is much weaker than the R, and for $n = 5$ the former is only fragmentary. In ${}_pHe_2$ only $3\text{Z} \rightarrow 2\text{P}$ has been identified, but Dieke, Imanishi and Takamine* give a single branch which they designate $5\,{}^1\text{Z} \rightarrow 2\,{}^1\text{P}$ from its position and appearance. The identification cannot be checked by combination differences, and they remark that the numeration is doubtful. We have derived a set of initial differences for this branch on the assumption that the final state is $2\,^1P_b$, and find that these fit into the table (*q.v.*) very well as $5\,^1Z$ differences. Changing the numeration in either direction gives distinctly less satisfactory results. The designation and numeration of the branch may therefore be regarded as verified, and we have incorporated the $5\,^1Z$ differences derived from it in Table III.

---

* 'Z. Physik,' vol. 54, p. 834 (1929).

In the same paper (p. 832) two associated branches apparently belonging to the 6δ complex of ${}_o He_2$ are tabulated, but not further identified. They are of P- and Q-form, and the combination differences show that the final states are $2P_b$ and $2P_a$ respectively. The initial differences (see Table III under $6\,^3X$) are very close to the standard values and require that ρ should be either 0 or $+1$. In the former case the branches would be P and Q of the Y level, and in the latter Q and R of the X level. The question is easily settled by considering the intensity distribution in these two types of band. In the Y type the appearance of the branches is fairly normal, the P branch being the weakest; we have for example only been able to observe P(2) and P(4) in $5\,^3Y \rightarrow 2\,^3P$. In the X type the P branch fades out as n increases, whilst the Q and R branches take on the appearance of P and Q branches, exactly as here. Further, the course of the branches corresponds closely with that to be expected for 6X, and not at all with the expected 6Y. We therefore identify the branches in question as the Q and R branches of $6\,^3X \rightarrow 2\,^3P$.

From similar considerations we conclude that the branch designated $5\,^1D_a \rightarrow 2\,^1P$ in the above paper is actually the Q branch of $5\,^1D_b \rightarrow 2\,^1P_b$. On the latter view, and on no other so far as we can see, a set of initial differences is obtained which fall into place in the scheme. The second differences correspond well with those of $5\,^3D_b$, and the first line, Q (2) (not observed by D., I., and T.) was predicted and found at 24044·95. It is a blend with Q (7) of the band labelled $5\,^1\delta_v \rightarrow 2\,^1P$, where it is of abnormally high intensity. The absence of the P and R branches presents no difficulty, since the Q branch of $5\,^1D_b \rightarrow 2\,^1P$ should be the strongest.

4. *New Bands having $2\,^3U$ as Final State.*

Merton and Pilley* gave the first measurements of a band in the green (near λ 5350) which is enhanced in the cathode glow of an uncondensed discharge as compared with the positive column of the condensed discharge. This, together with an associated band at λ 4950, was remeasured by Fujioka* and again by Imanishi† using greater dispersion. Both workers agree that these two bands have a common final state; the initial term differences are also closely similar to one another, but Imanishi was able to show that they were not identical as Fujioka considered was possibly the case. None of the states involved were identified.

---

* 'Roy. Soc. Proc.,' A, vol. 109, p. 267 (1925).

The final term differences are quite unlike any previously observed, but the initial differences of λ 5350 are evidently those of 5 ^{3}S. The actual values are as follows :—

ΔF′ from λ 5350....	71·40	127·74	183·87	242·38†
	292·60†	350·06	404·58	457·56
ΔF′ from 5 ^{3}S → 2 ^{3}P	70·93	127·98*	183·76	242·23†
	292·46†	347·97	400·93	—

The first five values are in good agreement, and the same perturbation occurs in both, so that the initial term of λ 5350 must certainly be 5 ^{3}S. The last three do not agree, and the lines in question have probably been wrongly identified on account of the preceding perturbation. The obvious inference that the initial term of λ 4950 may be 6 ^{3}S (which has not been observed) is confirmed by the agreement of the separation of corresponding lines of the two bands (~ 1486 cm.$^{-1}$) with the calculated separation of 5 ^{3}S and 6 ^{3}S (~ 1484 cm.$^{-1}$). From the known value (4713) of the electronic term 5 ^{3}S we obtain for the final term of the two bands 23396, corresponding to an effective quantum number 2·16. The principal quantum number of the final term is therefore 2, and since the missing term U would combine with S to give P and R branches as observed in these bands, it is natural to identify the final term with 2U. This is confirmed by comparing the final differences with those of 2 ^3P_b. It is found that the means of $\Delta(j+1)$ for 2 ^3P_b and $\Delta(j-1)$ for 2 ^{3}U give practically the He_2^+ differences, as shown below :—

j	2	4	6	8	10	12
$\Delta(j+1)$, 2P	101·98	160·06	217·55	274·26	329·98	384·61
$\Delta(j-1)$, 2U	41·10	95·65	149·96	203·65	256·79	308·56
Means	71·54	127·86	183·76	238·96	293·39	346·59
$\Delta(j)$, He_2^+	70·9	127·5	183·4	239·0	294·5	347·0

The theoretical significance of this relation is not obvious, but it is sufficiently striking to establish a close connection between 2 ^3P_b and 2 ^{3}U and strongly suggests that ρ is numerically equal in the two cases but opposite in sign. That is to say, the new term 2 ^{3}U may safely be identified with $2\pi{}^3\Sigma$ for which ρ would be -1 for complete uncoupling.

---

* 'Z. Physik,' vol. 52, p. 657 (1928).

† 'Sci. Pap. Inst. Phys. & Chem. Res.,' Tokyo, No. 189, p. 237 (1929).

The term $2\pi{}^3\Sigma$ should also combine with the other S terms and with the X, Y, Z, and D terms, and the resulting bands may in some cases be calculated from the lines of known bands. In the case of 4 ^{3}S → 2 ^{3}U, for example, the bands 4 ^{3}S → 2 ^{3}P, 5 ^{3}S → 2 ^{3}U, and 5 ^{3}S → 2 ^{3}P are already known, so that for corresponding lines we have

$$2\,{}^3\mathrm{U} - 4\,{}^3\mathrm{S} = (2\,{}^3\mathrm{U} - 5\,{}^3\mathrm{S}) + (2\,{}^3\mathrm{P} - 4\,{}^3\mathrm{S}) - (2\,{}^3\mathrm{P} - 5\,{}^3\mathrm{S}).$$

We have found the following bands by this method: 4 ^{3}S → 2 ^{3}U (P and R branches), 4 ^{3}Z → 2 ^{3}U (R branch, P not observed), 4 ^{3}X → 2 ^{3}U (Q branch) and 4 ^{3}Y → 2 ^{3}U (P branch, R not observed). The calculated and observed values are in good agreement, and the latter are set out in Table IV.

Table IV.

4 ^{3}S → 2 ^{3}U. $4\sigma\,{}^3\Sigma \rightarrow 2\pi\,{}^3\Sigma$.

j.	P branch.			R branch.			Notes.
	I.	λ (air) I.A.	ν (vac.).	I.	λ (air) I.A.	ν (vac.).	
0	—	—	—	1	6293·52	15885·04	
2	2—	6309·86	15843·89	3*	81·50	915·43	* R (2) blend with P (14) 3 ^{1}Y → 2 ^{1}P.
4	2	19·58	819·56	3	68·66	948·05	
6	3—	28·26	797·84	3*	55·10	982·64	* R (6) blend with P (2) 3 ^{1}Y → 2 ^{1}P.
8	3	35·86	778·89	2+	40·75	16019·38	
10	3	42·33	762·78	3—*	25·60	058·16	*R (10) blend with R (15) 3 ^{1}X → 2 ^{1}P.
12	2	47·61	749·67	1	09·94	098·83	
14	1	51·64	739·67	1—	6193·64	141·19	
16	1	54·51	732·59				

4 ^{3}Z → 2 ^{3}U. $4\delta\,{}^3\Sigma \rightarrow 2\pi\,{}^3\Sigma$.

j.	P branch.			R branch.			Notes.
	I.	λ (air) I.A.	ν (vac.).	I.	λ (air) I.A.	ν (vac.).	
0				1— —	6125·88	16319·73	
2				3—	31·62	304·47	
4				3	38·43	286·64	
6		Not	observed	3	45·62	267·34	
8				3+	52·57	248·97	
10				2+	58·98	232·06	
12				1+	64·76	216·82	

Table IV—(continued).

$4\,^3Y \rightarrow 2\,^3U$. $4\,^3X \rightarrow 2\,^3U$. $4\delta\,^3\Pi \rightarrow 2\pi\,^3\Sigma$.

j.	P branch.			Q branch.			R branch.	Notes.
	I.	λ (air) I.A.	ν (vac.).	I.	λ (air) I.A.	ν (vac.).		
2	1 — —	6101·21	16385·73	2*	6096·87	16397·39	Not observed	Q (2) blend with Q (9) $3\,^1D \rightarrow 2\,^1P$.
4	2 —	6099·70	389·79	2	6100·72	387·04		
6	1	98·83	392·13	2	05·73	373·61		
8	2 —	6100·27	388·26	2	11·09	359·24		
10	1 —	03·25	380·25	2	16·28	345·37		
12	3*	06·49	371·56	1	21·03	332·69		P (12) blend with Q (5) $3^1\,D \rightarrow 2\,^1P$.
14	2* —	10·13	361·82	1 —	25·03	322·03		P (14) blend with Q (2) $3^1\,D \rightarrow 2\,^1P$.

Combination Differences from above Bands, $2\,^3U\,(j+1) - 2\,^3U\,(j-1)$.

Band.	$j = 1$	3	5	7	9	11	13	15	17	Derivation.
$4\,^3S \rightarrow 2\,^3U$	41·15	95·87	150·21	203·75	256·60	308·49*	359·16	408·60	—	$R(j-1) - P(j+1)$.
$5\,^3S \rightarrow 2\,^3U$	41·09	95·69	149·97	203·73	256·66	308·52	361·18	412·42	462·65	$R(j-1) - P(j+1)$.
$6\,^3S \rightarrow 2\,^3U$	41·10	95·60	149·95	203·57	256·91	308·60	(361·61)	412·47	462·37	$R(j-1) - P(j+1)$.
$4\,^3Z \rightarrow 2\,^3U$	41·90	95·25	150·35	203·64	256·53	308·65	—	—	—	Employing $4\,^3Z\ \Delta\,^1F_8$ from table.
$4\,^3Y \rightarrow 2\,^3U$	—	95·82	150·07	203·81	256·55	307·43*	359·91**	—	—	Employing $4\,^3Y\ \Delta\,^1F_8$ from table.
$4\,^3X \rightarrow 2\,^3U$	—	95·72**	149·91*	203·77	256·49*	308·54	359·10	—	—	Employing $4\,^3X\ \Delta\,^1F_8$ from table.

$5\,^3S \rightarrow 2\,^3U$ and $6\,^3S \rightarrow 2\,^3U$ are from Imanishi's measurements, and the differences 13, 15, 17 are probably in error as noted in the text.

We have calculated the bands $4\,^3D \rightarrow 2\,^3U$, $7\,^3S \rightarrow 2\,^3U$ and $6\,^3S \rightarrow 2\,^3P$, but only fragments of the first appear on our plates. With heavier exposures there should be no difficulty in obtaining them. The band $3\,^3S \rightarrow 2\,^3U$ and the complex $3\,^3\delta \rightarrow 2\,^3U$ will lie round about 10000 A.; we have observed some emission in this region, but the dispersion we used was not sufficient to determine its nature, There should also be a series of bands $n\,^3U \rightarrow 2\,^3S$. These cannot be calculated, but a rough estimate of the position of $3\,^3U \rightarrow 2\,^3S$ may be obtained from the effective quantum number (2·16) of $2\,^3U$ and its probable change. That of $3\,^3U$ may be taken as about 3·1, which would place $3\,^3U \rightarrow 2\,^3S$ round about λ 4360. We have observed a band of structure rather like λ 5350 in this region on an old plate the dispersion of which is too small to permit of analysis.

As already remarked, the nS → 2U series of bands is enhanced in the cathode glow in comparison with the condensed discharge. The same is true of the

nS → 2P series, so that it would appear that the conditions in the cathode glow favour the production of S states of the molecule.

5. *New Bands having* 2P *as Final State.*

(*a*) 4 ^{3}Y → 2 ^{3}P.—This band consists of P, Q and R branches ; the Q behaves like that of 3 ^{3}Y → 2 ^{3}P in running to a head on the high frequency side, but reaches it earlier (about $j = 9$ instead of 13). Dieke, Imanishi and Takamine have recently published an analysis of this band with which we agree, except as regards the first P and Q lines. Our P (2) differs from theirs by 13·63 cm.$^{-1}$, but is supported by a Q (1) which gives the correct final combination difference, whereas they do not list a Q (1). Reference to the other known band with the same initial term, 4 ^{3}Y → 2 ^{3}U, would be expected to settle the question, but it happens that there are lines in positions corresponding to both interpretations. Theirs seems very unlikely, however, as it introduces a serious discontinuity into the P branch of this band whilst it is quite regular if our values are adopted.

(*b*) 5 ^{3}Y → 2 ^{3}P.—The tendencies observed in the two preceding bands of this series have here progressed a stage further. Most of the strength is now in the Q branch, which turns still earlier, near $j = 5$, so that one may expect that 6 ^{3}Y → 2 ^{3}P will be virtually a single (Q) branch band degraded to the low frequency side.

(*c*) 5 ^{3}X → 2 ^{3}P.—Here the R branch is predominant but is practically of Q-form. The Q branch is of P-form and only a trace of the P branch remains. These features are seen to represent a further development of the characteristics of 3 ^{3}X → 2 ^{3}P and 4 ^{3}X → 2 ^{3}P, and are carried a stage further in 6 ^{3}X → 2 ^{3}P (see section 3).

(*d*) 4 ^{1}D$_b$ → 2 ^{1}P.—The Q branch of this band is an obvious series just outside the R head of 3 ^{3}P → 2 ^{3}S (λ 4650, first member of " main series of doublets "), but the P branch falls inside the latter and has only recently been identified. In comparison with 3 ^{1}D$_b$ → 2 ^{1}P the P branch is closing up (tending to Q type), the Q branch opening out (tending to R type) and the R branch beginning to fade out. These tendencies are exactly the reverse of those observed in the X → P series, as would be expected from the opposite sign of ρ in the two cases.

We also analysed 3 ^{1}D → 2 ^{1}P, but the results need not be given since they are in agreement with those of Weizel and Dieke subsequently published. We found that the Q branch, 3 ^{1}D$_b$ → 2 ^{1}P$_b$, tended towards a second head at the end of its course, and this led us to re-examine 3 ^{3}D$_b$ → 2 ^{3}P$_b$, for which the existing data did not disclose this behaviour. We were able to extend this Q branch by three lines, and it then showed the same peculiarity. The new lines are Q (14), (16) and (18), at the wave-numbers 17467·30 (blend), 17471·64 and 17474·06 respectively.

Table V.

$4\,{}^3\mathrm{Y} \rightarrow 2\,{}^3\mathrm{P}$. $4\delta\,{}^3\Pi \rightarrow 2\pi\,{}^3\Pi$.

j.	P branch.			Q branch.			R branch.		
	I.	λ (I.A.) air	ν (vac.).	I.	λ (I.A.) air.	ν (vac.).	I.	λ (I.A.) air.	ν (vac.).
1				2	4436·62	22533·35			
2	7*	4442·32	22504·44				5	4422·71	22604·32
3				2+	31·36	560·12			
4	8	42·78	502·13				8	12·89	654·55
5				8	27·28	580·92			
6	6	44·30	494·45				8	05·14	694·41
7				10	25·24	591·32			
8	2	47·80	476·77				6	4399·14	725·34
9				9	24·93	592·92			
10	2−	52·84	451·29				4	94·37	750·03
11				8	25·77	588·63			
12	0−	59·06	419·98				2	90·49	770·15
13				5	27·46	579·98			
14	0−−	65·70	386·64				1	87·32	786·59
15				5	29·73	568·43			
16		[73·09]	[349·68]				0−	84·76	799·87
17				1	32·57	553·95			

* P (2) blend with P (21) of $4\,{}^3\mathrm{D} \rightarrow 2\,{}^3\mathrm{P}$.
[ ] from Weizel, private communication.

$5\,{}^3\mathrm{Y} \rightarrow 2\,{}^3\mathrm{P}$. $5\delta\,{}^3\Pi \rightarrow 2\pi\,{}^3\Pi$.

j.	P branch.			Q branch.			R branch.		
	I.	λ (I.A.) air.	ν (vac.).	I.	λ (I.A.) air.	ν (vac.).	I.	λ (I.A.) air.	ν (vac.).
1				2	3981·92	25106·46			
2	1	3986·55	25077·25				2	3974·12	25155·74
3				3	81·08	111·71			
4	0−−	90·34	053·46				2	69·37	185·82
5				4	80·99	112·31			
6							1+	65·45	210·72
7				4	81·73	107·65			
8							1−	62·03	232·49
9				3+	82·92	100·16			
10							0−	58·98	251·92
11				1+	84·45	090·47			

Table V—(continued).

$5\,^3X \rightarrow 2\,^3P$. $5\delta\,^3\Pi \rightarrow 2\pi\,^3\Pi$.

j.	P branch.			Q branch.			R branch.		
	I.	λ (I.A.) air.	ν (vac.).	I.	λ (I.A.) air.	ν (vac.).	I.	λ (I.A.) air.	ν (vac.).
1							5+*	3983·84	25094·34
2				0—	3988·49	25065·10			
3	1	3995·55	25020·83				5	83·51	096·44
4				0	92·75	038·32			
5	0	4004·51	24964·82				5+*	83·84	094·34
6				1	97·62	007·81			
7	0—	14·17	904·76				4+	84·65	089·23
8				1	4002·91	24974·78			
9							4	85·83	081·83
10				1	08·50	939·94			
11							3—	87·33	072·39
12				0*	14·37	903·46			
13							3—*	89·13	061·03
14				0—	20·45	865·83			

* R (1) and R (5) coincide.
R (13) blend with R (9) of $4\,^1P \rightarrow 2\,^1S$.
Q (12) blend with Q (5) of $5\,^3Z \rightarrow 2\,^3P$.

$4\,^1D \rightarrow 2\,^1P$. $4\delta\,^1\Delta \rightarrow 2\,\pi\,^1\Pi$.

j.	P branch.			Q branch.			R branch.		
	I.	λ (I.A.) air.	ν (vac.).	I.	λ (I.A.) air.	ν (vac.).	I.	λ (I.A.) air.	ν (vac.).
1							2	4615·18	21661·66
2				2	4621·39	21632·57			
3							2+	05·78	705·86
4				4	18·11	647·92			
5	2	4633·78	21574·74				3	4595·91	752·46
6				3	14·25	666·04			
7	2	36·11	563·86				4	86·18	798·65
8				4	10·35	684·36			
9	5	38·46	552·98						
10				2	06·55	702·24			
11	2—	40·69	542·58						
12				2	03·03	718·83			
13	2	42·97	532·00						
14				1	4599·92	733·51			
15	1+	46·04	517·78						

P (13) gives a combination difference 1 ν out, but there is no other line in the neighbourhood.

Table V—(continued).

Combination Differences from above Bands.

$F_a''(j+1) - F_b''(j)$

Band.	$j = 2$	4	6	8	10	12	14	16	Derivation.
$4\,^3Y \rightarrow 2\,^3P$	44·20	73·63	103·09	132·42	161·40	190·17	218·16	245·92	$R(j) - Q(j+1)$.
$5\,^3Y \rightarrow 2\,^3P$	44·03	73·51	103·07	132·33	161·45	—	—	—	$R(j) - Q(j+1)$.
$5\,^3X \rightarrow 2\,^3P$	44·27	73·50	103·05	—	—	—	—	—	$Q(j) - P(j+1)$.
	44·06	73·68	103·12	132·42	161·42	189·96	(218·21)	(245·78)	Means from $\left\{\begin{matrix} 3S \\ 4S \end{matrix}\right\} \rightarrow 2P$.

$F_b''(j) - F_a''(j-1)$

$4\,^3Y \rightarrow 2\,^3P$	28·91*	57·99	86·47	114·55	141·63	168·65	193·34	—	$Q(j-1) - P(j)$.
$5\,^3Y \rightarrow 2\,^3P$	29·21	58·25	—	—	—	—	—	—	$Q(j+1) - P(j)$.
$5\,^3X \rightarrow 2\,^3P$	29·24*	58·12	86·53*	114·45	141·89	168·93*	195·20*	—	$R(j-1) - Q(j)$.
	29·37	58·01	86·50	114·48	141·90	168·79	194·54	...	Means from V.

$F_b''(j) - F_a''(j-1)$

$4\,^1D_b \rightarrow 2\,^1P$	29·09	57·94	86·44	114·29	—	—	—	—	$R(j-1) - Q(j)$.
	—	58·01	86·39	114·56	142·30	168·91	—	—	See note below.

$F_a''(j+1) - F_b(j)$

$4\,^1D_b \rightarrow 2\,^1P$	—	73·18	102·18	131·38	159·76	186·83	215·73	—	$Q(j) - P(j+1)$.
	43·98	73·22	102·02	131·00	159·57	187·90	(215·59)	—	See note below.

The $2\,^1P$ values given for comparison are from our analysis of $3\,^1D \rightarrow 2\,^1P$.

6. *Unidentified Bands.*

It will be seen from Table III that most of the He_2 terms up to $n = 5$, and some beyond, have now been found. It seems probable that when the existing scheme is completed up to this point all the chief lines of the spectrum will have been accounted for. We propose to discuss briefly in this section some of the problems of analysis which remain to be solved.

(*a*) *The* 4δ *Complex of* $_p He_2$.—This comprises the bands having as initial states $4\,^1Z$, $4\,^1X$, $4\,^1Y$, $4\,^1D_b$, $4\,^1D_a$, and as final states $2\,^1P$; the wave-numbers of the origins should increase in the order given. Of these only the band $4\,^1D_b \rightarrow 2\,^1P$ has been identified (see Table V). Most of the others probably fall amongst the very strong band $3\,^3P \rightarrow 2\,^3S$ (λ 4650) and its associated vibrational bands. We have searched the region very thoroughly and have found many pairs of lines giving the $2\,^1P$ combination differences. Some are no doubt accidental but a number are certainly genuine; yet we have not been able to arrange them as satisfactory branches. One attempt is given in Table VI. The final combination differences are reasonably good, but the branches are very irregular.

Table VI.

j.	P branch.			Q branch.			R branch.		
	I.	λ (air) I.A.	ν (vac.).	I.	λ (air) I.A.	ν (vac.)	I.	λ (air) I.A.	ν (vac.).
1							10*	4625·43	21613·57
2				4	4631·71	21584·27			
3	2	4614·14	21540·43				5	19·07	643·33
4				4	31·46	585·41			
5	5	47·22	512·25				3	12·61	673·67
6				8	31·06	587·31			
7	2	53·13	484·90				2	04·45	712·06
8				6	28·84	597·64			
9	0	57·07	466·76				2*	4595·88	752·54
10				9*	26·03	610·77			
11	2*	60·51	450·89						

* P (11) blend with R (11) of $3\,^3P^2 \rightarrow 2\,^3S^2$.
* Q (10) blend with R (11) of $3\,^3P \rightarrow 2\,^3S$.
* R (1) blend with R (13) of $3\,^3P \rightarrow 2\,^3S$.
* R (9) blend with R (5) of $4\,^1D \rightarrow 2\,^1P$.

Combination Differences from above Band. Final Differences, $F''(j+1) - F''(j-1)$.

$j = 1$	2	3	4	5	6	7	8	9	10	Derivation.
	43·84		73·16		102·41		130·88		159·88	$Q(j) - P(j+1)$.
	43·98		73·22		102·02		131·00		159·57	$2\,^1P_b(j) - 2\,^1P_a(j+1)$.
29·30		57·92		86·36		114·42		141·77		$R(j) - Q(j+1)$.
(29·09)		58·01		86·39		114·56		142·30		$2\,^1P_a(j) - 2\,^1P_b(j+1)$.

Initial Differences, $F'(j+1) - F'(j-1)$.

		102·90		161·42		227·16		285·78		$R(j) - P(j)$.

The 2^1P values given for comparison are from our analysis of $3\,^1D \rightarrow 2\,^1P$.

It is worthy of remark that apart from the band $4\,{}^1D_b \rightarrow 2\,{}^1P$ the only strong lines in the region 21620–90 look very like a branch, although the intervals are somewhat irregular.* This is possibly the Q branch of $4\,{}^1D_a \rightarrow 2\,{}^1P_a$, but we can find no P or R branch associated with it. Again, a group of lines round 21585 looks very like the expected R branch of $4\,{}^1X \rightarrow 2\,{}^1P_a$. It seems very probable that the difficulty of analysis is due to the existence of large perturbations in some at least of the initial terms.

(*b*) *The* 5δ *complex of* ${}_p\mathrm{He}_2$.—This falls in the region 23700–24250 ($\lambda\lambda$ 4220–4120), and so far only the R branch of $5\,{}^1Z \rightarrow 2\,{}^1P_b$ and the Q branch of $5\,{}^1D_b \rightarrow 2\,{}^1P_b$ have been identified. The P branch of the latter has been calculated, but does not appear on our plates, perhaps because they are too weak. The other expected branches and their appearance are as follows :—$5\,{}^1X \rightarrow 2\,{}^1P$, Q and R branches of P- and Q-form ; $5\,{}^1Y \rightarrow 2\,{}^1P$, three normal branches, P being the weakest ; $5\,{}^1D_a \rightarrow 2\,{}^1P$, P branch of R-form. There are thus six branches expected, two of each type, and this is precisely what has been observed, but the interpretation nevertheless presents some difficulties.

The outstanding peculiarity of the six observed branches is that they compose two complete bands (designated $5\,{}^1\delta_u$ and $5\,{}^1\delta_v \rightarrow 2\,{}^1P$ by Dieke) precisely identical with one another and separated by about 10 cm.$^{-1}$. Only one such band, $5\,{}^1Y \rightarrow 2\,{}^1P$, is to be expected, and we must first identify this before attempting an explanation of the other. The combination results indicate that the initial levels are odd and have $\rho = 0$, both characteristics of $5\,{}^1Y$. The only observable difference between the two bands is the lower intensity of the P branch† of $5\,{}^1\delta_v \rightarrow 2\,{}^1P$ relative to that of $5\,{}^1\delta_u \rightarrow 2\,{}^1P$. It appears to be characteristic of the higher members of the $Y \rightarrow 2P$ bands that the P branch is distinctly weaker than the Q and R, and we therefore take $5\,{}^1\delta_v$ to be the $5\,{}^1Y$ level. On this view there should be two lines, Q (1) and P (2), additional to those tabulated. If Q (1) is assumed to be a blend with Q (3), as is quite reasonable, there is an unallocated line at 24024·45 in the correct position for P (2). Also, the initial differences fit quite satisfactorily into the scheme as $5\,{}^1Y$.

The difficulty with the other band, $5\,{}^1\delta_u \rightarrow 2\,{}^1P$, is that if its three branches are genuinely associated as P, Q and R, ρ must be zero for the initial level, and there is no place in the scheme for this, which would be virtually an extra Y level. But if the R branch is disregarded for the moment the P and Q can be readily accounted for as the Q and R of $5\,^1X \rightarrow 2\,^1P$, which would be expected to have just this appearance, and $\rho = +1$ as required for the X level. The R branch which is left over may then be interpreted as the P branch of $5\,^1D_a \rightarrow 2\,^1P_b$, which according to Dieke should probably be of R-form. The only serious objection to this scheme appears to be the improbability of the latter branch falling in such a position that it gives $2\,^1P$ differences in combination with the Q and R branches of $5\,^1X \rightarrow 2\,^1P$. This is very unlikely to be fortuitous; it is more likely that there may be some theoretical reason for it, but we have none to propose. The parallelism of the pairs of branches presents no difficulty, since for $n = 5$ the initial terms may all be so close to the limiting He_2^+ values that this would naturally occur. For the same reason, and also because of the uncertainty as to the correctness of the interpretation, they have not been included in Table III. The observed branches are plotted in fig. 1, and the empirical and proposed designations are also indicated.

---

* 21626·37 (5), 43·34 (5+), 58·11 (4), 73·67 (3), 87·10 (4).

† This was hardly measurable on our plates, but we had analysed the other five branches in exactly the same way as Dieke, Imanishi and Takamine.

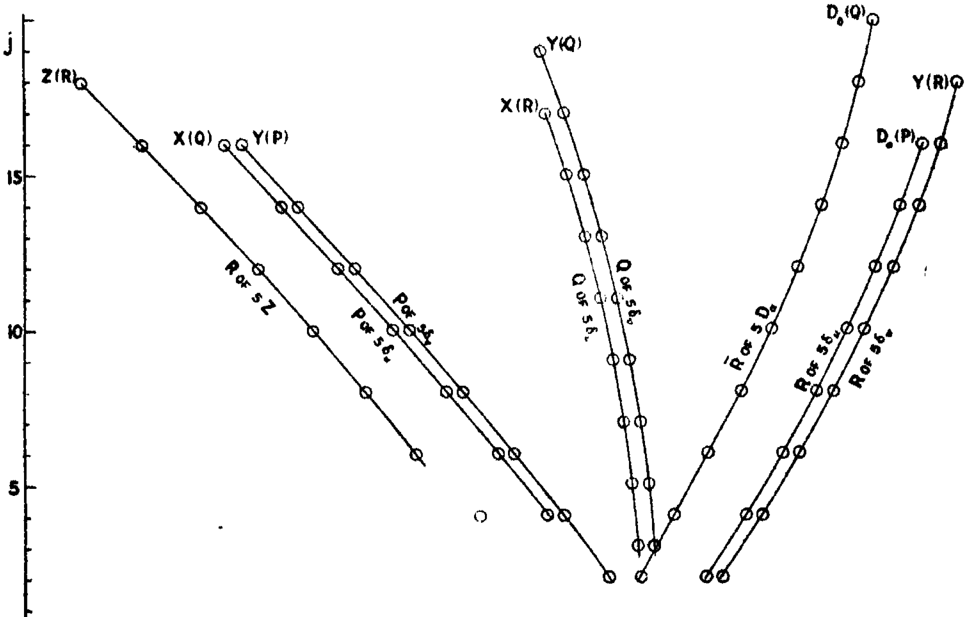

FIG. 1.—The 5δ complex of $_pHe_2$.

Our proposed designations are given at the end of each branch, and those of Dieke, Imanishi and Takamine at the side.

(*c*) ***Branches near*** λ 3340.—During the measurements on the "main series of doublets," $n\,^3P \rightarrow 2\,^3S$ (see III), three branches were noted which have not yet been interpreted. The approximate wave-numbers are as follows :—

29913·75 (0)
961·82 (1−)
30007·27 (1+)
050·09 (2−)
091·44 (2+)
130·29 (2)
167·56 (2−)
202·56 (1)

29898·59 (1)
942·27 (1+)
982·73 (1)
30021·09 (0+)
057·76 (0)

30125·51 (0)
154·79 (0)
177·69 (0)
197·64 (0)
211·69 (0)
221·57 (0)
227·60 (0)

The wave-numbers are greater than any of the known terms in this spectrum except 2 ^{3}S (34302) and 2 ^{1}S (31958), so that one of these two is probably the final term. The latter gives an initial effective quantum number of about 8·0, but in view of the relative weakness of the $_p$He$_2$ system this possibility may be ruled out. If 2 ^{3}S is the final term the initial effective quantum number would be about 5·0. This suggests 5 ^{3}U as a possibility for the initial term, but we have not been able to establish this, or to find any relation between the branches. More accurate measurements on stronger plates are desirable.

We wish to express our indebtedness to the Department of Scientific and Industrial Research for a grant which made this work possible.

Summary.

A comparison of all the He$_2$ rotation term differences at present obtainable shows that in each electronic sequence they tend to a set of limiting values which are the same in all cases and which must be those characteristic of the He$_2^+$ ion. These limiting values are identical for the ortho and par systems of bands, and the molecular constants of He$_2^+$ are calculated from them. The data also lead to a classification of the term sequences which is in agreement with that recently proposed by Dieke, and provide evidence which is of great assistance in the identification of hitherto unobserved terms.

Eight new bands are described, four of which involve a type of level predicted by Hund but not previously recognised ; with the discovery of this the theoretical term scheme is completed for ortho-He$_2$. New interpretations, based upon the above regularities in the rotation differences, are proposed for several bands recorded by other workers, and some of the remaining problems of analysis are discussed.

A "Spinning Target X-Ray Generator" and its Input Limit.

By Alex Müller.

(Communicated by Sir William Bragg, F.R.S.—Received July 15, 1929.)

Introduction.

It is desirable in many X-ray investigations that the specific intensity of the X-rays should be increased. By specific intensity is meant the amount of energy emitted in a second from the unit area of the focus in the X-ray generator. A limit for the specific input is soon reached in an ordinary X-ray tube owing to the intense heating in the focus and the consequent deterioration of the target surface. How the limit of input depends upon the material, size of the focus and dimensions of the anticathode has been shown by the writer in a previous note.*

The designers of X-ray tubes have already tried to avoid this limitation, and one of the methods suggested was to keep the target moving and so to carry the heat away from the spot where it is produced.

This method has never been used in practice for the following reasons. The designers have always tried to produce X-ray tubes of the sealed-off type, *i.e.*, tubes in which the necessary low pressure is permanent and no pumps are required. The cooling of such tubes is bound to rely at least to the greatest extent upon radiation, and this is a most serious drawback when a large energy input is applied such as is contemplated here.

The situation alters at once if the restriction of the sealing-off is dropped, for it is then possible not only to use this method of relative motion, but also to carry the heat away by the far more efficient water cooling. There are, of course, certain technical difficulties connected with the design of such an instrument, an obvious one is the maintenance of the low pressure inside the generator. This difficulty has proved to be not too serious owing to the very efficient pumps which are nowadays available.

Other difficulties may arise when the specific input is raised beyond certain limits. It may for instance be impossible to focus a very intense cathode ray beam into a small area, or even if the cathode rays could be concentrated the efficiency of the X-ray conversion may decrease. So far as the writer is aware there are no theoretical reasons why this should occur in the region of energy densities dealt with here. In fact the experiments show that it is possible to produce considerably higher specific intensities than those which have hitherto been obtained.

---

* 'Roy. Soc. Proc.,' A, vol. 117, p. 30 (1927).

The chief problem seems to be the heating of the target, and the object of this paper is to give an estimate of the extent to which the specific input can be raised when the focus is produced on a moving target. The experimental details of a generator built on this principle and the results obtainable with such an apparatus will be described in a separate paper.

General Remarks.

At first sight it might be anticipated that a reduction of the thickness of the target would help. It has been shown in the previous note (*loc. cit.*) that such a reduction is impracticable. The results of the calculations given here are based on the assumption that the target is a sheet with a plane surface and infinite dimensions. The expressions for the limiting input do not therefore contain any parameters referring to the shape or size of the anticathode. From the short analysis in the Appendix to this paper it can be seen how the expressions for the input limit are obtained and how a limitation of the size of the target affects this limit. For a practical discussion these more general equations are of no interest.

Definition of the Focus.

The same analytical expression for the heat inflow in the focus will be used as in the previous note

$$\text{INFLOW} = \text{A} \,.\, e^{-\text{B}\,.\,r^2}.$$

This equation expresses the fact that in the focus centre, *i.e.*, $r = 0$, the inflow of heat reaches a maximum and drops rapidly for increasing distances from the focus centre. The radius of the focus is defined by the distance δ at which the inflow drops to $\frac{1}{2}$ of its maximum. δ can be measured on pin hole photographs of the focus. The constants A and B have the following values :—

$$\text{A} = \text{W} \,.\, \ln 2/\pi\delta^2, \qquad \text{B} = \ln 2/\delta^2.$$

W is the total amount of heat per second which is flowing into the target. This quantity can be measured for instance by observing the temperature rise in the cooling water by a constant flow method. ln2 is the natural log of 2.

The Maximum Input.

For the sake of comparison we give first the expression for the maximum input when the target is at rest. This equation has already been given in the previous note (*loc. cit.*).

(*a*) *Target at Rest.*—

$$W_{\text{max.}}\ (\text{rest}) = 17\cdot 8 \times (T - T_0) \times \kappa \times \delta$$

T = melting point of the target material in Centrigade.
T_0 = temperature of the cooling water in Centigrade.
κ = thermal conductivity at the melting point in gr.-cal. sec.$^{-1}$ cm.$^{-1}$ Centigrade^{-1}.
δ = radius of the focus spot in centimetres.
$W_{\text{max.}}$ (rest) = maximum input in watts.

Taking for an example a focus of 0·1 cm. diameter we find that $W_{\text{max.}} = 0\cdot 75$ kilowatt for a copper target. Experiment shows that this is approximately the input which under these conditions the anticathode will stand without melting.

(*b*) *Moving Target.*—For the moving target it is found that:

$$W_{\text{max.}}\ (\text{moving}) = 17\cdot 0 \times (T - T_0) \times \kappa \times \delta \times \sqrt{\delta \,.\, \frac{\rho \,.\, c}{\kappa} \,.\, v}.$$

ρ = density of the material in gr.-cm.$^{-3}$.
c = specific heat in gr.-cal. gr.$^{-1}$ Centigrade^{-1}.
v = velocity of the target surface in cm. sec.$^{-1}$.
$W_{\text{max.}}$ (moving) = maximum input in watt.

This expression can only be applied to the calculation of the input limit if the numerical value of the term under the square root is large compared with unity. This term is a pure number and has no dimensions. From the two equations we find for the ratio of the two maxima:

$$\frac{W_{\text{max.}}\ (\text{moving})}{W_{\text{max.}}\ (\text{rest})} = \frac{17\cdot 0}{17\cdot 8}\sqrt{\delta \,.\, \frac{\rho c}{\kappa} v} \sim \sqrt{\delta \frac{\rho c}{\kappa} v}.$$

Supposing for example that we want to increase the maximum energy density 10 times, *i.e.*, instead of 0·75 kilowatt we have 7·5 kilowatt with the moving target, the focus diameter and the material being the same as before; then $\rho c/\kappa$ is approximately 1 for copper, $2\delta = 0\cdot 1$ cm. and $\sqrt{\delta\, \rho c v/\kappa} = 10$. Hence v is about 2000 cm. sec.$^{-1}$. Such a velocity can be easily obtained in a mechanical system. A point at the periphery of a disc of say 15 cm. diameter moves with this velocity if the disc makes approximately 2500 revolutions per minute, and a generator fitted with such a moving target will give the required result.

There is, however, a point which has to be borne in mind. It was assumed in the calculations that an infinite sheet moves with the velocity v. In the case of a revolving disc any point which is at a given time in the focus will return there after one revolution, *i.e.*, will be subjected to a periodic heating, whereas the calculations are based on a non-periodic process. The calculations are nevertheless valid provided it can be shown that the temperature of any such point drops to a small value before it is again subjected to the cathode ray bombardment. An approximate calculation shows that this actually happens with the spinning copper disc mentioned in the foregoing example.

The calculation is made as follows. We take a temperature distribution such as is actually obtained when the generator is working, and at a given time shut the cathode rays off. From this time onward we calculate the temperature T_t at the point which when $t = 0$ is in the focus centre. The calculation gives :

$$T_t - T_0 = (T_{\text{max.}} - T_0)\bigg/\left(1 + \frac{4 \ln 2}{2 \cdot 5}\,\frac{\kappa}{\rho c \delta^2}\,.\,t\right).$$

In the foregoing example where $2\delta = 0 \cdot 1$ cm., $\rho c/\kappa \sim 1$

$$T_t - T_0 = (T_{\text{max.}} - T_0)/(1 + 450\,.\,t),$$

i.e., in 1/50 of a second the temperature in the focus drops to 1/10 of its maximum. During this time the disc has made 0·8 of a revolution. This means that we are entitled to use the theoretical expression for calculating the maximum input in this case.

An X-ray generator with a rotating anticathode has been built and the results obtained so far are quite satisfactory. The details of the design will be described, and the results obtained will be given in a separate paper. A short analysis of the necessary calculations is given in the Appendix.

In conclusion the writer wishes to thank Sir William Bragg for the interest he has taken in this work.

APPENDIX.

For the sake of comparison the maximum input is first calculated when the target is at rest. We assume first that the target is a rectangular block of finite dimensions. At the end we make the transition to an infinite sheet. A similar calculation has been done before for a target with cylindrical boundaries (*loc. cit.*).

(*a*) ***Anticathode at Rest.***—The following problem has to be solved :

$$(1) \qquad \frac{\partial^2 T}{\partial x^2} + \frac{\partial^2 T}{\partial y^2} + \frac{\partial^2 T}{\partial z^2} = 0,$$

$$\text{for} \quad x = \pm a, \quad \frac{\partial T}{\partial x} = 0\,;$$

$$\text{for} \quad y = \pm b, \quad \frac{\partial T}{\partial y} = 0\,;$$

$$\text{for} \quad z = 0, \qquad T = T_0\,;$$

$$\text{for} \quad z = l, \quad \kappa \frac{\partial T}{\partial z} = A \,.\, e^{-B(x^2+y^2)}\,;$$

$$A = W \ln 2/\pi\delta^2, \qquad B = \ln 2/\delta^2.$$

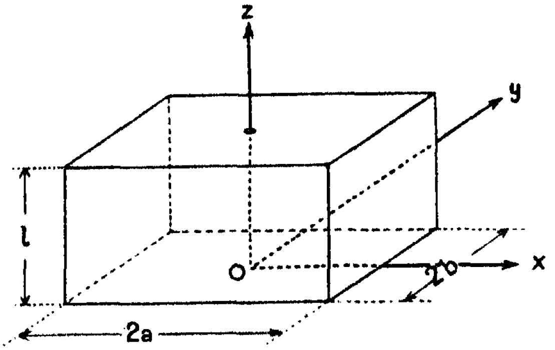

FIG. 1.

We put

$$(2) \qquad T - T_0 = \sum_1^\infty \sum_1^\infty a_{mn} \,.\, \cos \pi \frac{mx}{a} \,.\, \cos \pi \frac{ny}{b} \,.\, \sinh c_{mn} z + \bar{a} \,.\, z,$$

$$m = 1, 2, 3, \ldots, \qquad n = 1, 2, 3, \ldots,$$

in order to satisfy (1) we must have

$$c_{nm} = \pi \sqrt{m^2/a^2 + n^2/b^2}.$$

If a and b are large compared with δ, then $\frac{\partial T}{\partial z_{(z=l)}}$ is practically zero when $x = a$ or $y = b$. We have therefore :

$$(3) \qquad \bar{a} = -\sum_1^\infty \sum_1^\infty a_{m.n} \,.\, \cos (m\pi) \,.\, \cos (n\pi) \,.\, \cosh (c_{nm} l) \,.\, c_{nm}$$

and

$$(4) \quad \kappa \frac{\partial T}{\partial z_{(z=l)}} = \sum_1^\infty \sum_1^\infty a_{nm} \,.\, c_{nm} \,.\, \cosh (c_{nm} l) \,.\, \left\{ \cos \pi \frac{mx}{a} \,.\, \cos \pi \frac{ny}{b} - \cos \pi m \,.\, \cos \pi n \right\}$$
$$= A e^{-B(x^2+y^2)}.$$

From (4) we find

$$a_{mn} = \frac{\mathrm{A}}{\mathrm{B}} \cdot \frac{\pi}{\kappa \,.\, a \,.\, b} \cdot \frac{\exp\left[-\tfrac{1}{4}\pi^2 (m^2/a^2 + n^2/b^2)/\mathrm{B}\right]}{c_{nm} \,.\, \cosh (c_{nm} l)}.$$

This combined with (2) and (3) gives the complete solution of the problem. The temperature in the focus is :

$$\mathrm{T}_f - \mathrm{T}_0 = \frac{\mathrm{A}}{\mathrm{B}} \cdot \frac{\pi}{\kappa a b} \sum_1^\infty \sum_1^\infty \exp\left[-\tfrac{1}{4}\pi^2 (m^2/a^2 + n^2/b^2)/\mathrm{B}\right]$$
$$\times \{\tanh c_{nm} l / c_{nm} - l \,.\, \cos \pi m \,.\, \cos \pi n\}.$$

By the same process which has been given in the previous paper we find for an infinite sheet $l = a = b = \infty$ $l/a \,.\, b = 0$,

$$\mathrm{T}_f - \mathrm{T}_0 = \frac{\mathrm{W}}{\kappa \delta} \frac{\sqrt{\ln 2}}{2\sqrt{\pi}}.$$

(W measured in gr.-cal. sec.) or if T is the melting temperature of the target material and $\mathrm{W}_{\text{max.}}$ (rest) the maximum input now expressed in watts :

$$\mathrm{W}_{\text{max.}}\ (\text{rest}) = \frac{2\sqrt{\pi}}{0{\cdot}2389\sqrt{\ln 2}} \,.\, (\mathrm{T} - \mathrm{T}_0) \,.\, \kappa \,.\, \delta,$$

which is the formula given in the first part of the paper.

(*b*) *Moving Anticathode.*—The rigorous solution for a revolving disc of finite dimensions would be difficult to obtain. For our purpose it is quite sufficient to assume that the target is a moving rectangular strip. The expression given in the first part of this paper will then be obtained by extending the boundaries to infinity.

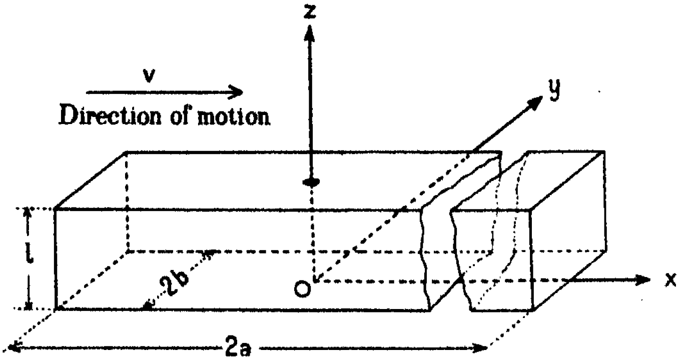

FIG. 2.

We have to solve the following problem :

$$(5)\qquad \frac{\partial^2 T}{\partial x^2}+\frac{\partial^2 T}{\partial y^2}+\frac{\partial^2 T}{\partial z^2}=\frac{\rho c}{\kappa}\cdot\frac{\partial T}{\partial t},$$

$$\frac{\partial T}{\partial y}=0 \text{ for } y=\pm b\,;\quad T=T_0 \text{ for } z=0,$$

$\partial T/\partial z$ = very small for any point at a big distance from the focus. Further :

$$(6)\qquad \kappa\frac{\partial T}{\partial z}=A\exp\left[-B\left([x-vt]^2+y^2\right)\right] \text{ for } z=l.$$

The following expression is a solution which conforms with the boundary conditions provided the momentary position of the focus is not far away from the centre of the target surface, or in other words not too near to the ends of the strip.

$$(7)\quad T-T_0=\sum_1^\infty\sum_1^\infty A_{mn}\cos\pi\frac{ny}{b}\,.\,\exp\left[-i\frac{\pi m(x-vt)}{a}\right]\sinh\left(\alpha_{mn}+i\beta_{mn}\right)z+\bar{a}z.$$

The term $\bar{a}z$ contributes nothing to the final result under the present conditions, we neglect it therefore from the beginning. The constants α_{mn} and β_{mn} have to satisfy the following equations :

$$\alpha_{mn}{}^2-\beta_m{}^2=\pi^2\left(m^2/a^2+n^2/b^2\right)$$

$$2\alpha_{mn}\beta_{mn}=-\rho c/\kappa\,.\,m/a\,.\,\pi\,.\,v.$$

We put

$$c_{mn}{}^2=\pi^2\left(m^2/a^2+n^2/b^2\right)$$

$$\bar{c}_m=\pi\, m/a\;\rho c/\kappa\,.\,v,$$

And find

$$\alpha_{mn}=\sqrt{\tfrac{1}{2}(c_{mn}{}^2+\sqrt{c_{mn}{}^4+\bar{c}_m{}^2}}$$

$$\beta_{mn}=-\tfrac{1}{2}\,\bar{c}_m/\alpha_{mn}.$$

We next have to calculate the coefficients A_{mn} in (7). Separating (7) into the real and imaginary part we obtain in the usual way two independent solutions of the differential equation which we multiply with a_{mn} and b_{mn} respectively. These constants are now real quantities which we have to calculate. The boundary condition (6) implies that $\partial T/\partial z$ is an even function of both $(x-vt)$ and y. All the $\sin\{\pi(x-vt)\,.\,m/a\}$ terms in (7) have therefore to vanish. This fixes the ratio b_{mn}/a_{mn}. The explicit boundary condition becomes

$$\kappa\sum_1^\infty\sum_1^\infty a_{mn}\frac{(\alpha_{mn}{}^2+\beta_{mn}{}^2)(\cosh^2(\alpha_{mn}l)-\sin^2\beta_{mn}l)}{\alpha_{mn}\cos\beta_{mn}l\cosh\alpha_{mn}l-\beta_{mn}\sin\beta_{mn}l\,.\,\sinh\alpha_{mn}l}\,.\,\cos\pi\frac{yn}{b}\,.\,\cos\pi\frac{(x-vt)}{a}m$$

$$=A\exp\left[-B\left((x-vt)^2+y^2\right)\right],$$

and from this we obtain in the usual way:

$$a_{mn} = \frac{A}{B}\frac{\pi}{\kappa . a . b} e^{-\frac{C_{mn}^2}{4B}} . \frac{\alpha_{mn} \cos \beta_{mn} l . \cosh \alpha_{mn} l - \beta_{mn} \sin \beta_{mn} l . \sinh \alpha_{mn} l}{(\alpha_{mn}^2 + \beta_{mn}^2)(\cosh^2 \alpha_{mn} l - \sin^2 \beta_{mn} l)} .$$

Therefore for $T_f - T_0$ in the focus

$$(8) \quad T_f - T_0 = \frac{A}{B} . \frac{\pi}{\kappa . a . b} \sum_1^\infty \sum_1^\infty e^{-\frac{C_{mn}^2}{4B}} . \frac{\alpha_{mn} \sinh \alpha_{mn} l . \cosh \alpha_{mn} l - \beta_{mn} \sin \beta_{mn} l . \cos \beta_{mn} l}{(\alpha_{mn}^2 + \beta_{mn}^2)(\cosh^2 \alpha_{mn} l - \sin^2 \beta_{mn} l)} .$$

This expression turns into the one which is found for the target at rest if we put $\beta_{mn} = 0$.

(8) is the complete solution of our problem with the restriction mentioned at the beginning of this section. In the above form the solution is not suited for numerical calculations. We find a much simpler form if we extend the boundaries to infinity. This by itself is not sufficient. If, however, we assume further that $\delta\rho c v/\kappa$ is large compared with unity we find that the infinite series in (8) can be written in form of a simple double integral

$$T_f - T_0 = \frac{W}{\kappa\delta} \frac{2 (\ln 2)^{3/2}}{\pi^2 \sqrt{\delta\rho c v/\kappa}} \int_0^\infty \int_0^\infty e^{-s_1^2} . e^{-s_2^2} \frac{1}{\sqrt{s_2}} \, ds_1 \, ds_2 .$$

These integrals can easily be evaluated and we find

$$T_f - T_0 = \frac{W}{\kappa\delta} \frac{1}{\sqrt{\delta\rho c v/\kappa}} \frac{2 (\ln 2)^{3/2}}{\pi^{3/2}} \Gamma(5/4) .$$

If by T we again denote the melting point of the target material we find for the limiting input $W_{\text{max.}}$ (moving) in watts

$$W_{\text{max.}} \text{ (moving)} = \frac{1}{0 \cdot 2389} \cdot \frac{\pi^{3/2}}{2 (\ln 2)^{3/2} \, \Gamma(5/4)} . (T - T_0) . \kappa . \delta . \sqrt{\delta\rho c v/\kappa}$$

which is the equation given in the first section of this paper.

(*c*) *Time Factor.*—The last part deals with the decrease of the focus temperature with time. We have

$$\frac{\partial^2 T}{\partial x^2} + \frac{\partial^2 T}{\partial y^2} + \frac{\partial^2 T}{\partial z^2} = \frac{\rho c}{\kappa} \frac{\partial T}{\partial t} ,$$

$$\frac{\partial T}{\partial x} = 0 \text{ for } x = \pm a ; \quad \frac{\partial T}{\partial y} = 0 \text{ for } y = \pm b ; \quad T = T_0 \text{ for } z = 0,$$

and

$$T - T_0 = (T_{\text{max.}} - T_0) \exp [- ln 2 \, (x^2 + y^2)/\delta^2] \text{ for } z = l \text{ and } t = 0.$$

It has to be borne in mind that in the first part we assumed that the energy inflow was given by Ae^{-Br^2}, here we assume that the temperature distribution is of the same type. The calculation will nevertheless be sufficiently correct provided we give the proper numerical value for $\bar{\delta}$. This value can easily be obtained by using the calculations in the previous paper. We find for a point in the target surface which is at a distance r from the focus centre the temperature

$$\mathrm{T}_r - \mathrm{T}_0 = (\mathrm{T}_f - \mathrm{T}_0)\,\frac{\displaystyle\int_0^\infty e^{-s^2}\,\mathfrak{J}_0(2\sqrt{\ln 2}/\delta\,.\,s\,.\,r)\,.\,ds.}{\displaystyle\int_0^\infty e^{-s^2}\,ds}.$$

If we call $\bar{\delta}$ the particular value of r for which

$$\frac{\mathrm{T}_r - \mathrm{T}_0}{\mathrm{T}_f - \mathrm{T}_0} = \tfrac{1}{2},$$

we get the following equation for $\bar{\delta}$

$$\tfrac{1}{2} = \frac{\displaystyle\int_0^\infty e^{-s^2}\,\mathfrak{J}_0(2\sqrt{\ln 2}/\delta\,.\,s\,.\,\bar{\delta})\,.\,ds}{\displaystyle\int_0^\infty e^{-s^2}\,ds}.$$

The integral can be developed in a series of $(\bar{\delta}/\delta)^2$ and the numerical value obtained by successive approximations is

$$(\bar{\delta}/\delta)^2 = 2{\cdot}5.$$

For solving our problem we put

$$\mathrm{T} - \mathrm{T}_0 = \sum_1^\infty\sum_1^\infty\sum_1^\infty a_{mnp}\cos\pi\frac{mx}{a}\,.\,\cos\pi\frac{ny}{b}\sin\frac{\pi}{2}\frac{2p+1}{l}z\,.\,e^{-\mu t}$$

$$\mu = \frac{\pi^2\,.\,\kappa}{\rho c}\left(\left(\frac{m}{a}\right)^2 + \left(\frac{n}{b}\right)^2 + \left(\frac{2p+1}{2l}\right)^2\right).$$

The calculation of the time factor depends essentially upon the temperature distribution in the immediate neighbourhood of the focus. The distribution in the bulk of the material is of little importance. The only condition which we have to impose is that the temperature gradient falls off with increasing distance from the focus centre. Such a distribution is obtained by putting $p = 0$ in the above equation. We now adjust the constants such as to satisfy the boundary conditions and find

$$a_{mn0} = \frac{(\mathrm{T}_{\max.} - \mathrm{T}_0)}{\ln 2\,.\,a\,.\,b}\,\pi\,.\,\exp\left[-\frac{\pi^2\bar{\delta}^2}{4\ln 2}\left(\left(\frac{m}{a}\right)^2 + \left(\frac{n}{b}\right)^2\right)\right]$$

$$\mathrm{T} - \mathrm{T}_0 = \frac{(\mathrm{T}_{\max.} - \mathrm{T}_0)}{a\,.\,b\,.\,\ln 2}\,.\,\pi\,.\,\bar{\delta}^2\,.\,\sum_1^\infty\sum_1^\infty\exp\left[-\frac{\pi^2\bar{\delta}^2}{4\ln 2}\left(\frac{m^2}{a^2} + \frac{n^2}{b^2}\right)\right]$$

$$\times\exp\left[-\frac{\pi^2}{\rho c}\kappa\left(\frac{m^2}{a^2} + \frac{n^2}{b^2} + \frac{1}{4l^2}\right)\cdot t\right].$$

Extending the limits to infinity we finally obtain

$$T - T_0 = (T_{\text{max.}} - T_0)/(1 + t\,.\,4\ln 2/\rho c\,.\,\kappa\,1/\overline{\delta^2})$$

and by substitution of δ^2 **arrive at the expression given in the first part of the paper.**

ERRATA.

A few minor misprints and errors in the previous paper (*loc. cit.*) may be corrected here—

p. 31.—is very small compared with 1 *instead of* compared with l

p. 32.— $\int_0^a \mathfrak{C}_0{}^2\left(\frac{\lambda_n}{a}r\right)r\,.\,dr = \frac{a^2}{2}\mathfrak{C}_0{}'^2(\lambda_n)$. *instead of* $\frac{a^2}{2}\mathfrak{C}_0{}'(\lambda_n)$.

p. 32.—Formula (6) $\dfrac{1}{\cosh\left(\frac{\lambda_n}{a}l\right)}$ *instead of* $\dfrac{1}{\cos\left(\frac{\lambda_n}{a}l\right)}$.

p. 36.— $\sigma = \delta/a$ *instead of* $/\delta a$.

p. 37.—Formula (21) tanh βx under integral *instead of* tan βx.

p. 38.— e^{-x^2} × series (" multiplied with series ") ***instead of*** e^{-x^2} **series.**

p. 38.— $\theta = \frac{1}{2}\beta - \frac{1}{6}\beta^3 + \frac{2}{15}\beta^5 - \frac{17}{105}\beta^7 \ldots$ ***instead of*** $\frac{4}{15}\beta^5 - \frac{34}{105}\beta^7 \ldots$.

p. 38.— $\int_0^\infty e^{-x^2-2n\beta x}\,dx$ ***instead of*** $\int_0^\infty e^{-x^2-n\beta x}\,.\,dx$.

p. 39.— $\theta = \frac{\sqrt{\pi}}{2} - \frac{1}{\beta}ln^2 - \frac{1}{2\beta^3}\sum_1^\infty\frac{(-1)^\kappa}{\kappa^3} + \frac{1\,.\,3}{2^2\beta^5}\,.\,\sum_1^\infty\frac{(-1)^\kappa}{\kappa^5}$, etc.,

instead of $+\frac{1}{2\beta^3}\sum_1^\infty\frac{1}{\kappa^3} - \frac{1\,.\,3}{2^2\beta^5}\frac{1}{\kappa^5}$, etc.

(The numerical coefficients of the corresponding series are correct.)

The Melting Point of Palladium.

By F. H. Schofield, B.A., B.Sc., Physics Department, National Physical Laboratory, Teddington, Middlesex.

(Communicated by Sir Joseph Petavel, F.R.S.—Received June 25, 1929.)

I. *Introduction.*

The melting point of palladium is a convenient reference point for the measurement of high temperatures. In fixing a scale of temperature the aim is, of course, to approximate as closely as possible to the thermodynamic scale. From the absolute zero up to moderately high temperatures this ideal scale is realised most directly and accurately through the medium of the gas thermometer. However, with increase of temperature beyond a certain limit, the experimental difficulties of gas thermometry multiply rapidly, so that ultimately it becomes necessary to adopt another basis for obtaining the scale. This is conveniently found in the laws governing the radiation from a black body, which have a sound theoretical foundation and permit the use of measuring instruments of precision.

The establishment of a practical scale of temperature on the lines above indicated has been the subject of considerable discussion between the national standardising laboratories of Germany, Great Britain and the United States of America. As a result, proposals for the definition of an " International Temperature Scale " were submitted to the 7th General Conference* of Weights and Measures, and approved by them. In effect, the basis of the scale up to the melting point of gold is the gas thermometer,† and beyond this temperature the Wien or Planck law‡ of radiation with an agreed value for the constant c_2. Owing to the difficulty of absolute measurements of radiation, no attempt has so far been made to place the radiation scale on an independent basis by fixing the other constant in the Wien or Planck equation. Consequently the scale is defined, for the present, relatively to a fixed point on the thermodynamic scale, as given by the gas thermometer, namely the melting point of gold (1063° C.).

---

* 'Comptes rendus des Séances, Sept. Conférence générale des poids et mesures,' Paris, 1927.

† The scale is actually defined by the assignment of certain values to the melting or boiling points of a number of pure substances, and by prescribed means of interpolation between these temperatures, the whole being based on work with the gas thermometer.

‡ The definition adopts the Wien law as confined to monochromatic visible radiation. When thus limited the two laws become practically identical.

While the radiation scale of temperature is thus completely defined by the values assigned to one fixed point and the constant c_2, it is useful to place on record the values of other fixed points in terms of the scale. Determinations of this kind serve to indicate the degree of reproducibility of the scale, and, where the values are sufficiently well established, may afford secondary standards for its realisation. Of such fixed points the most important is the melting point of palladium, a determination of which is described in this paper.

II. *Description of Method.*

For the purpose of realising the radiation scale of temperature as above defined, it has been found to be convenient to work with monochromatic, or nearly monochromatic, radiation in the visible portion of the spectrum, employing a photometer designed to measure the relative intensities of such radiation from black body radiators at different temperatures. The instrument most commonly used is the Holborn-Kurlbaum type of the disappearing-filament pyrometer. This can be fitted with a spectrometer so as to deal with monochromatic radiation or with a filter transmitting as narrow a band of radiation as possible. The latter type has the advantage of simplicity, and apparently also of ease and accuracy of setting, but the wave-length to which its transmission is to be assigned, involves a somewhat troublesome calculation. The "effective wave-length"* of the filter for any two temperatures is defined as that wave-length for which the ratio of the integral luminosities, viewed through the filter, of black bodies at these temperatures is equal to the ratio of their radiation intensities. The limiting value of this wave-length when the two temperatures approach each other has been shown by Foote† to be given by

$$\lambda_L = \int_0^\infty \mathrm{TVJ}\, d\lambda \div \int_0^\infty (\mathrm{TVJ}/\lambda)\, d\lambda,$$

where for any wave-length T, V and J are respectively the percentage transmission of the glass, the visibility coefficient‡ for the eye and the relative energy of a black body. It may be added that the relation between the limiting effective wave-length and temperature is generally so nearly linear as to allow the effective wave-length for a temperature interval of several hundred degrees to be taken as the mean of the limiting effective wave-lengths for the two extreme temperatures of the range.

---

* Hyde Cady and Forsythe, 'Phys. Rev.,' vol. 6, p. 70 (1915); 'Astrophys. J.,' vol. 42, p. 294 (1915).

† Foote, 'Bull. B.S.,' vol. 12, p. 483 (1915); see also Henning, 'Z. Instr.,' vol. 45, p. 530 (1925).

‡ For recent values see Gibson and Tyndall, 'Bull. B.S.,' vol. 19, p. 131 (1923).

The advantages of working in different parts of the spectrum have been discussed by Forsythe* and in the present investigation the Corning glass (high transmission red 53 per cent.) has been employed in a thickness of 5 mm. This has an effective wave-length for the gold-palladium interval of $0 \cdot 656\ \mu$. The form of pyrometer used does not differ essentially from those used elsewhere† and therefore calls for no detailed description. It should, however, be mentioned that the Bureau of Standards kindly presented the Laboratory with several of their pyrometric type of lamp having a cylindrical glass envelope closed with optically flat ends. These lamps have proved to be of great assistance, since they allow a high magnification without distortion. In order to determine the ratio of the radiation intensities at the two melting points, a rotating sector was employed, of such aperture that, for the wave-length above-mentioned, the radiation from a black body at the higher melting point was reduced by it to be about equal to that at the lower melting point. The sector consisted of a disc of planished steel, 35 cm. in diameter, with two accurately cut radial slots with bevelled edges, and its effective aperture was found by direct measurement‡ with a probable accuracy of $\pm 0 \cdot 5$ per cent. The rotating sector could be interposed in the pyrometer system just in front of the pyrometer lamp and rotated at speeds of the order of 3500 revolutions per minute in order to eliminate flicker effects.

We describe below, in detail, the experimental procedure adopted in order to obtain black-body radiator at the two melting points. No special originality is claimed for most of the devices adopted, the experience of previous investigators having been freely utilised.

III. *Experimental Procedure.*

In the present investigation three methods of realising a black-body have been employed, differing from each other as regards the type of enclosure or the method of measuring its temperature. The first method consists in the use of a tubular furnace with a series of diaphragms giving an inner chamber the temperature of which is indicated by the melting, inside the chamber, of a wire of a pure metal, *e.g.*, gold or palladium. In the second method a black-body chamber in the form of a stopped-down tube is inserted into an ingot of pure metal and the radiation is observed either at the melting or freezing point of the metal. In the third method the black-body radiator consists of a hollow cone made up from the pure metal in the form of foil, and the radiation from the interior of the cone is observed during its collapse on melting. For convenience the three methods are referred to respectively as the " wire," " ingot " and " cone " methods.

---

* 'J. Opt. Soc. Amer.,' p. 85 (1921); see also Henning and Heuse, 'Z. Physik,' vol. 32, p. 799 (1925).

† See, *e.g.*, Forsythe, 'Astrophys. J.,' vol. 43, p. 295 (1916); Worthing and Forsythe, 'Phys. Rev.,' p. 163 (1914); Fairchild and Hoover, 'J. Opt. Soc. Amer.,' p. 543 (1923).

‡ The discs were cut and measured by the Metrology Dept., Nat. Phys. Lab.

" *Wire* " *Method.*—The general practice is to employ a radiator formed by stopping down a furnace tube consisting of some highly refractory material with a heating element in contact with its outer surface. For the material of the latter platinum is very convenient and this may be applied to the tube in various ways, *e.g.*, a spiral winding of wire, or of ribbon, or a complete sheathing of thin foil. With the spiral winding a variable spacing of the wire or ribbon, or in the case of the ribbon a variable width,* may be used to counteract the cooling effects of the ends and give a reasonable length near the centre of the furnace at a constant temperature. The objection to a fixed compensation of this type is that it may not be equally effective at temperatures so widely separated as the melting points of gold and palladium, which are some 500° C. apart. It is preferable, therefore, to provide for a variable regulation of temperature distribution.

In the present case this has been done by means of auxiliary heating coils. After experiment with several different types, the arrangements shown in fig. 1 were adopted. The main furnace tube of alundum was wrapped with a sheath of platinum foil 42 cm. long which at the ends was 0·0025 cm. thick and at the central portion 25 cm. long, was 0·0037 cm. thick. The sheath was made up by welding on to a sheet of platinum of the first stated thickness an extra sheet of half the thickness, the ends of the latter being deeply serrated so as to avoid an abrupt change of resistance where the sheets were joined.† A permanent grading of the heating element was thus provided, so chosen that it was of itself insufficient to counteract the cooling effect of the ends. In addition there were inserted into each end of the furnace the auxiliary heaters shown. These consisted of alundum tubes spirally grooved and wound with platinum wire 0·5 mm. in diameter. A bifilar system of winding the heaters was adopted, in order that both leads should emerge from one end. For this purpose two parallel longitudinal cuts were made through the screw thread on the outside of the tube as shown in section in fig. 2. Starting from the centre of the wire, the winding of one half of the wire was commenced in the end section of the thread until, on reaching the gap *a*, it returned on itself in the next groove and similarly at *b*, and so on until the other end of the heater was reached. Each half of the wire was thus wound on a separate half, formed by the cuts *a* and *b*, of the tube. The ends of the wires, after being anchored through holes in the tube, were led out of the furnace inside a twin bore alundum sheath. A compact assembly was thus obtained, which could easily be moved about in the furnace without interfering with the other wires threaded through it. The heaters above described gave two methods of temperature adjustment, namely those afforded by movement of the heater and the variation of the heating current. Incidentally it may be remarked that any system of the type described tends to be rather unstable

---

* See, *e.g.*, Coblentz Art. on " Radiation," in vol. 4, " Dictionary of Applied Physics " (Macmillan & Co.); Ferguson, ' Phys. Rev.,' vol. 12, p. 81 (1918); Waidner and Burgess, ' Bull. B.S.,' vol. 00, p. 163 (1907).

† See Hoffmann and Meissner, ' J.X.Z.,' vol. 60, p. 201 (1919).

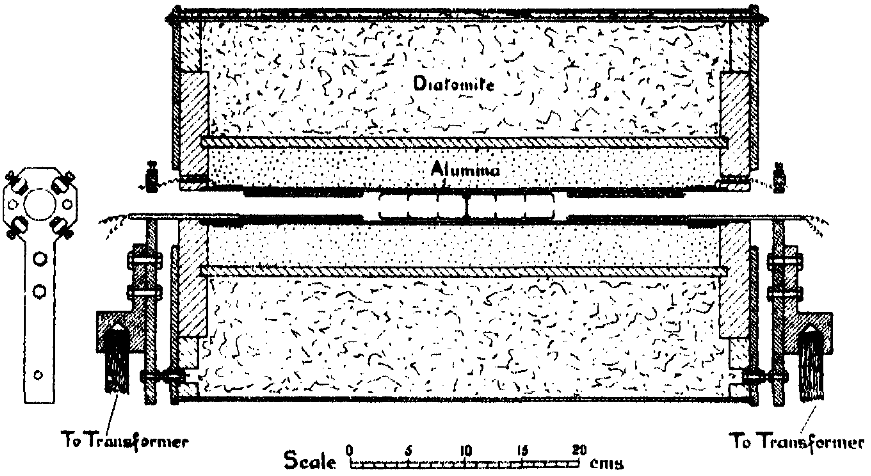

FIG. 1.

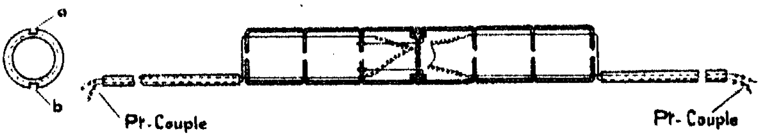

FIG. 2.

owing to the large temperature coefficient of resistance of platinum. Thus if the current through one of the auxiliary heaters is raised, this will cause a local heating of the contiguous portion of the main heating element. The resistance of this portion will consequently be raised while the current through the element being hardly affected, the local heating will tend to be enhanced. For the reasons indicated the adjustments are more easily effected when the heating elements consist of a material, like nichrome, of low temperature coefficient.

However, the arrangement described enabled an adjustment to be made without much trouble so that the temperature distribution inside the first two cavities on each side of the central disc (see figs. 1 and 2) did not vary by more than 1° C. The exploration was carried out by means of a thermocouple threaded through the furnace, the junction of the couple being butt-welded so that it would readily pass through the small hole in the central disc. It will be observed that a symmetrical arrangement of diaphragms is employed giving a radiating enclosure on each side of the central disc. The diaphragms were formed by cutting central holes* about 3 mm. in diameter in the bases of the alundum "thimbles," which were about 20 mm. in diameter. Smaller holes were also provided for threading through the two pairs of thermocouples, one pair passing from each end of the furnace into the innermost chamber nearest that end. A ridge was cast on each side of the central disc so that it interlocked with the neighbouring thimbles, thus preventing access of direct radiation from the furnace walls to the chambers. The disc was wired to one of the thimbles and each assembly of three thimbles, one with the wired-on disc, could readily be withdrawn from the furnace for replacement of the specimens of gold or palladium used for a melting point determination. The specimens, consisting of wire 0·5 mm. in diameter, were connected across the arms of one of the couples. The usual process of observing the melting points was followed. This consisted in raising the temperature of the furnace at a steady rate, not exceeding 1° C. per minute and taking successive readings of the four thermocouples, two of which had specimens of gold or palladium joining their arms and two of which had the usual welded junctions. In fig. 2, for purposes of clearness, only one of each type of couple is shown. On reaching the melting point the two former couples (which we may call the "melt-couples") remained constant in E.M.F., while the other couples (referred to below as the "control-couples") continued to rise. Usually the rise of the control-couples continued for about 2° C. before the circuits of the other couples broke on complete fusion of the metal, but in all cases the melting point was taken as that temperature at which the halt in the E.M.F. value of the melt-couple was first detected. The furnace was then adjusted to remain constant at this temperature, as given by the control-couple, while readings with the optical pyrometer were taken. A specimen set of observations on the two pairs of control- and melt-couples is given in fig. 3.

---

* *Cf.* arrangement adopted by Hoffmann and Meissner (*loc. cit.*).

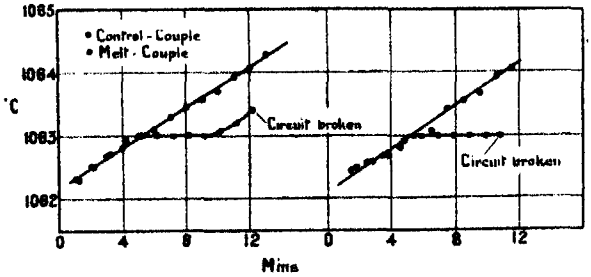

FIG. 3.

The following additional particulars of the apparatus may also be given. The leads to the main furnace winding consisted of 16 platinum wires of 0·5 mm. diameter. These, after being twisted round the foil on the tube, passed out in four batches to the electrode shown, both in elevation and section, in fig. 1. Here they were gripped by metal blocks working in holes in the electrode and clamped by the screws shown. The current required to maintain such a furnace at a steady temperature of 1550° C. was about 90 amps. in the main winding and 4 amps. in the auxiliary windings.

The observations taken with the apparatus above described, and also with similar furnaces and radiators of less elaborate construction, are dealt with in Section IV below.

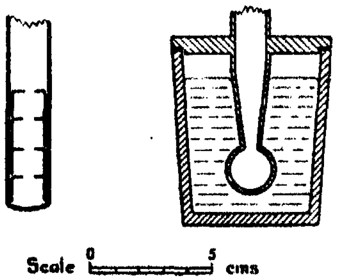

FIG. 4.

"*Ingot*" *Method.*—This method has so far been used only for the melting point of gold. A section of the ingot, about 2000 gms. in weight, with a black-body radiator in position, is shown in fig. 4. The radiator referred to is similar in shape to that employed by Hoffmann and Meissner and was made of pure china clay.* Another type of radiator used is also shown in fig. 4. This consisted of a thin-walled silica sheath with a number of perforated alundum thimbles arranged to act as diaphragms. In addition to the radiator a sheathed thermocouple (not shown in fig. 4) was inserted into the ingot.

---

* Made by a casting process by the Metallurgy Dept., National Physical Laboratory.

In making an experiment the usual procedure of observing a melting or freezing point was followed: namely, of raising or lowering the temperature of the furnace at a certain rate and taking of readings of temperature against time both with the thermocouple and optical pyrometer. A specimen of a freezing curve taken in this way is shown in fig. 5. The high purity obtainable with gold,* its freedom from oxidation and high latent heat combine to give a very sharp freezing or melting point which is readily distinguishable by the readings of an optical pyrometer as well as by the more sensitive indications of a thermocouple. The average period at constant temperature in the present experiments was about 20 minutes, which afforded ample time for the optical observations. The results are dealt with in Section IV below.

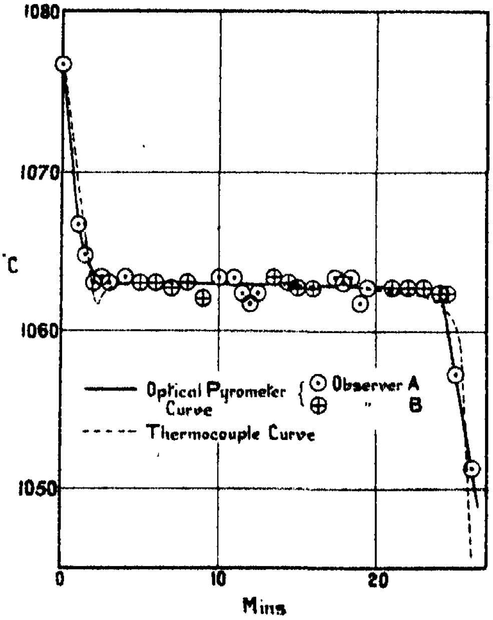

Fig. 5.

"*Cone*" *Method.*—Several experimenters have made use of thin sheet metal to form the walls of a black-body enclosure, the object generally being to obtain the emissivity of the metal by comparison of the radiation intensity from the internal and external surfaces of the enclosure. Thus Mendenhall[*] used two electrically-heated strips so juxtaposed as to give a narrow-angled wedge, Worthing[†] used a hollow filament with a minute observation hole, and Ives[‡] a larger cylinder of platinum foil with a longitudinal slit. In all these cases the heat was supplied by the passage of an electric current through the walls of the enclosure.

---

* The specimen used in these experiments was of pure assay gold supplied by Messrs. Johnson, Matthey & Co., and stated to be of 99·99$_9$ per cent. purity.

Where, as in the present case, the object is merely to make a single brightness determination of the radiation from a black-body at the melting point of the metal, direct electric heating, with the obvious limitations of shape which it imposes, may be dispensed with and the metallic envelope placed inside the usual tubular type of furnace. This has been done in the experiments here described, the shape chosen being that of a hollow cone. The thickness of the foil used in making up the cone was 0·004 cm. and the assembly for insertion in the furnace took several slightly differing forms of which two are illustrated in fig. 6. In one of these the cone was contained in an alundum thimble with a sighting hole in the bottom, which also served as a "stop" on the rather wide-angled cone. In the other arrangement a very narrow angled cone and a thicker-walled container were used, the latter generally consisting of "mabor" material, though graphite[§] could be employed in the case of gold. A hole parallel to the axis was provided in this container, so as to allow a thermocouple exploration after the assembly had been inserted into the central region of the tubular furnace shown in fig. 1. The central block was fairly short, but was flanked on either side by extra blocks which served as radiation shields (see fig. 6).

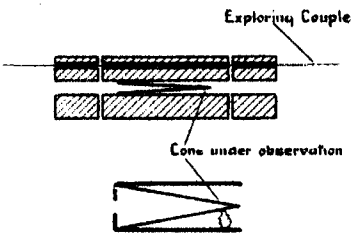

FIG. 6.

The process of observing the melting point consisted in taking simultaneous readings with the optical pyrometer, sighted into the cone, and with a thermocouple in its vicinity, *e.g.*, in the longitudinal hole shown in fig. 6. When the cone commenced to collapse on melting there appeared a black crescent-shaped patch of growing size, corresponding with the increasing area of unobstructed view through the furnace. It was found that, during the period of melting, the pyrometer readings remained sensibly constant.

---

[*] 'Astrophys. J.,' vol. 33, p. 91 (1911).

[†] 'Phys. Rev.,' vol. 10, p. 377 (1917).

[‡] 'J. Franklin Inst.,' vol. 197, p. 147 (1924).

[§] Roberts, 'J. Opt. Soc. Amer.,' p. 723 (1925).

A specimen series of readings with a thermocouple and pyrometer is given in fig. 7.

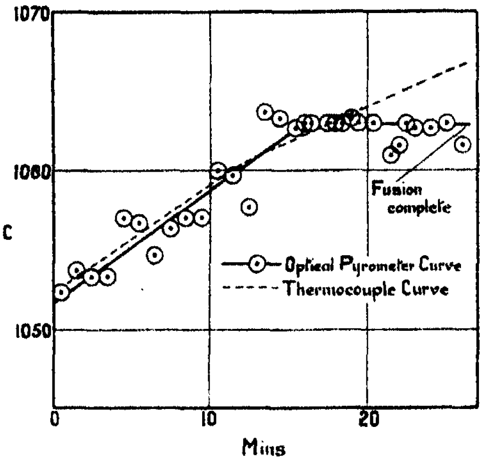

FIG. 7.

IV. *Summary of Results.*

As has already been indicated, the measurements made in the present investigation take the form of :—

(1) A determination of the current in the pyrometer lamp required to give a match in brightness, at a particular wave-length, with a black-body held at the melting point of gold.

(2) A similar measurement in the case of palladium, employing a rotating sector to reduce the brightness to about the same intensity as at the gold point.

These measurements enable the ratio of brightness, for a particular wave-length, of a black body at the two melting points to be determined, or, expressing the result in another way, enable a definite value to be assigned to the melting point of palladium, on the basis of an assumed value for the melting point of gold and the constant c_2.

Dealing first with the measurements at the gold point, the "ingot" method appears to give, as would be expected, the most reliable determinations. A summary of the observations obtained with this method is given in Table I,

Table I.—Gold Point Observations by "Ingot" Method.

(Pyrometer reading expressed in temperature relative to mean value of the series assumed to be 1063° C.)

Freezing points.		Melting points.		Type of radiator.
Rate of fall of furnace.	Pyrometer reading.	Rate of rise of furnace.	Pyrometer reading.	
° C./min.	° C.	° C./min.	° C.	
4·5	1063·0	4·5	1063·0	Bulb (fig. 4).
4·5	61·0	5·0	63·5	
4·0	63·0	4·5	62·5	
4·0	62·5	6·0	63·5	
6·5	63·0	5·0	62·5	
6·0	63·0	8·0	63·0	
4·5	63·0	7·5	63·0	
4·0	62·5	3·5	63·0	
—	—	5·0	62·5	
4·0	1063·5	8·5	1063·0	Diaphragmed tube (fig. 4).
7·0	61·5	8·5	63·0	
5·5	63·0	8·0	63·5	
6·0	63·0	7·0	63·5	
6·5	63·5	2·0	62·5	
6·0	63·0	8·5	63·0	
2·5	63·0	8·5	63·5	
5·5	62·5	8·5	62·5	
6·0	63·0	6·0	62·5	

the values being expressed in terms of temperature, relatively to the mean value of the whole series, assumed to be 1063° C. It will be noted that the considerable variations of the rate of cooling or heating, as the case may be, and the change in the type of radiator appear to have no appreciable effect on the values obtained. The observations summarised in Table I were obtained early in the investigation. At its conclusion, a repetition of the experiments with a larger ingot and a new radiator gave a result identical with that of the former series.

The values given by the "cone" and "wire" methods are summarised in Table II and are expressed in terms of temperature, taking as standard the mean value found by the ingot method and assumed to be 1063° C. Comparatively few observations were taken with the latest type of apparatus in view of the satisfactory results given by the "ingot" method and the close agreement of the latter with the mean of the numerous experiments carried out with earlier arrangements of the "cone" and "wire" methods. The mean values just referred to are given in the table.

Table II.—Gold Point Observations by "Cone" and "Wire" Methods.

(Pyrometer reading expressed in temperature relative to mean value given by "ingot" method (Table I) and assumed to be 1063° C.)

Rate of rise of furnace.	Pyrometer reading.	Range of values.	Remarks.
° C./min.	° C.		
0·6	1063·5		Cone method (individual readings with narrow cone, fig. 6).
0·8	64·0		
0·6	64·0		
0·4	62·0		
0·6	62·0		
0·9	63·5		
Mean..........	1063·5	±1° C.	
—	1064·0	± 2° C.	Cone method (mean of 13 determinations with wide cone, fig. 6).
0·2	1063·5		Wire method (individual readings with arrangement in figs. 1 and 2).
0·2	63·0		
0·4	64·0		
0·3	62·5		
0·2	63·5		
Mean..........	1063·5	± 1° C.	
—	1063·5	± 5° C.	Wire method (mean of 71 readings with miscellaneous arrangements of diaphragms).

In the case of the palladium, owing mainly to difficulties with the refractory materials, satisfactory results have not, so far, been obtained with the "ingot" method. The values given by the "wire" and "cone" methods, in their latest forms, are set out in Table III, together with the means of the values given by earlier work. Column 2 of the table gives the apparent temperatures, viewed through the sector, of the black body, held at the palladium point, while column 3 gives the true temperatures calculated from the Wien relation:

$$1/T_1 - 1/T_2 = (\lambda/c_2) \log R.$$

T_1 and T_2 being the true and apparent temperatures in absolute measure, λ the effective wave-length, R the transmission value of the sector, and c_2 being taken, as 1·432 cm. degrees. The range of values (± 3° C.) found at the palladium point is somewhat greater than at the gold point. This is to be accounted for, partly at any rate by the fact that any error of observation when using the sector to obtain a reading of apparent temperature in the neighbourhood of 1063° C. becomes approximately doubled when converted

Table III.—Determination of Melting Point of Palladium by "Cone" and "Wire" Methods).

(Constant $c_2 = 1\cdot432$ cm. degrees.)

Rate of rise of furnace.	Temperature.			Remarks.
	Apparent (with sector).	True.	Range of values.	
° C./min.	° C.	° C.		
0·7	1064·5	1552·5		Cone method (narrow-angled cone, see fig. 6).
1·6	66·5	56·5		
1·6	66·0	55·5		
0·7	65·5	54·5		
0·9	66·5	56·5		
0·7	66·5	56·5		
0·4	67·5	58·0		
0·8	67·5	58·0		
0·9	65·0	55·5		
0·8	65·5	54·5		
Mean	1066·$_1$	1555·$_8$	± 3° C.	
0·8	1067·5	1558·0*		Wire method (see figs. 1 and 2).
0·7	65·5	54·5*		
0·9	65·5	54·5*		
0·5	65·5	54·5*		
0·7	64·0	52·0		
0·4	65·0	53·5		
0·8	65·0	53·5		
0·8	66·0	55·5		
0·8	66·5	56·5		
0·4	65·5	54·5		
Mean	1065·$_6$	1554·$_5$	± 3° C.	
—	1065·$_7$	1554·$_5$	± 5° C.	Wire method (mean of 28 experiments with miscellaneous arrangements of diaphragms).

* Sample of palladium from Bureau of Standards (No. 138). All other specimens from Messrs. Johnson, Matthey & Co.

into a true temperature in the neighbourhood of 1550° C. Thus if the range of variation in setting up a black body at both the gold and palladium points were taken to be ± 1° C. and the range of observational error ± 1° C., then the total range of error at the gold point would be of the order of ± 2° C. and at the palladium point of the order of ± 3° C. In the case of the "wire" method the control-couple enables the furnace to be maintained at the temperature of the observed melting point for an indefinite period, so that readings can be taken with and without the sector. This would lead to a reduction of the observational error, but on the other hand there would be some risk of change in the pyrometer lamp when run at high temperature. In order to avoid this risk and for the purpose of obtaining a comparison with the " cone " method, which does not allow sufficient time for the taking of readings with and without the sector, the recent observations with the " wire " method have been obtained with a sector only.

From the experiments summarised in Table III the value of the melting point of palladium on the International Temperature Scale ($c_2 = 1\cdot432$ cm. degrees; M.P. of gold = 1063° C.) may be taken as 1555° C. to the nearest 1° C. The accuracy of this determination is estimated to be of the order of ± 2° C.

V. *Comparison with Previous Work.*

It is of interest to compare the value found in the present investigation for the melting point of palladium with those given by previous work of a similar nature. In Table IV are set out the values of the melting point as determined by radiation methods at the following laboratories, viz., Nela Research Laboratory (Nela), Physikalisch-Technische Reichsanstalt (P.T.R.), Bureau of Standards (B.S.), National Physical Laboratory (N.P.L.). The figures have been reduced to a common value of the constant c_2, namely, $1\cdot432$ cm. degrees, as prescribed for the International Temperature Scale.*

Table IV.—Melting Point of Palladium.

($c_2 = 1\cdot432$ cm. degrees ; M.P. of gold = 1063° C.)

Laboratory.	Reference.	Melting point on International Temperature Scale.
		° C.
Nela	Hyde and Forsythe, 'Astrophys. J.,' vol. 51, p. 245 (1920).	1557
P.T.R.	Hoffmann and Meissner, 'Ann. d. Physik,' vol. 60, p. 201 (1919).	1556
B.S.	Fairchild, Hoover and Peters, 'B.S. Jour. of Research,' vol. 2, p. 931 (1929).	1553·6
N.P.L.	Present paper (1929)	1555

The table shows the high degree of reproducibility obtained with this melting point. It seems probable that the agreed value of 1555° C. taken as the melting point for the purposes of the International Temperature Scale† is not in error by more than 2° C.

---

* Comptes rendus des Séances, Sept. Conférence générale des poids et mesures, Paris, 1927.

† *Loc. cit.*

For comparison with a direct determination of the melting point on the thermodynamic scale, reference may be made to the gas thermometer work of Day and Sosman* which yielded a value of 1549° C. with an estimated accuracy of ± 2° C.

Though of less fundamental importance, it is of interest to recall that, by extrapolation from the sulphur boiling point of his parabolic formula for the platinum resistance thermometer, Callendar† obtained the value of 1550° C. for the melting point. He had previously given a value of 1062° C. for the melting point of gold, as had Heycock and Neville, also using a platinum thermometer. These values are in remarkable agreement with the most recent determinations.

In conclusion, the author desires to record his indebtedness to the Director of the National Physical Laboratory, and to Dr. Kaye, the Superintendent of the Physics Department, for their interest in the work and the ample facilities provided. He is also much indebted to Mr. B. J. Gibbs, B.Sc., lately an Observer in the Physics Department, who constructed the greater part of the apparatus and rendered valuable assistance with the observations.

---

* 'Amer. J. Sci.,' vol. 29, p. 93 (1910).

† 'Phil. Mag.,' vol. 47, p. 191 (1899); see also Burgess and Le Chatelier "Measurement of High Temperatures" (John Wiley & Sons, New York), pp. 199, *et seq.*

Gaseous Combustion in Electric Discharges. Part IV.—The Effect of Moisture upon the Cathodic Combustion of Carbonic Oxide Detonating Gas.

By G. I. Finch and D. L. Hodge, Imperial College of Science.

(Communicated by W. A. Bone, F.R.S.—Received July 12, 1929.)

Introduction.

It has been shown previously in Part III* of the present series that the combustion of carbonic oxide "detonating gas"† is determined by a prior ionisation of both constituent gases; and further that, whereas carbonic oxide can be and is burnt directly by oxygen in the absence of, and therefore without the intervention of, either moisture or metal atoms, the presence of such metal atoms sputtered from the cathode by the passage of the discharge actively promotes cathodic combustion by the overcoming of the electrostatic forces of repulsion existing between similarly charged ions of carbonic oxide and oxygen.

It has been shown by Bone and his co-workers‡ that, though the rigidly dried "detonating gas" can be ignited, provided a sufficiently powerful condenser discharge be employed, and is then capable of propagating flame (though combustion may be incomplete), the presence of even a minute quantity of steam not only renders the mixture much more readily ignitable, but also increases the velocity of flame progagation and ensures practically complete combustion. Hitherto, however, experiments have afforded but little direct evidence as to the precise nature of the mechanism of the rôle played by moisture in promoting combustion, and the present work was carried out with the object of attempting to throw some light upon this question. For this purpose the investigation has been confined to an experimental study of the combustion of the moist "detonating gas" in the cathode zone of a direct current discharge, because, as has been previously shown, the conditions can then be easily and accurately controlled over a considerable range without introducing disturbing phenomena, such as heat and catalytic action, which might otherwise tend to obscure the real issues. In the experiments described herein we have succeeded in realising conditions in which the ratio of the rate of combustion of the " detonating gas " containing a given partial pressure of steam, to the current passed by the discharge, is, in the absence of sputtered metal atoms, proportional to the number of steam molecules, and hence electrically charged steam molecules, within the cathode zone.

---

* 'Roy. Soc. Proc.,' A, vol. 124, p. 303 (1929).

† For the sake of brevity a mixture of carbonic oxide and oxygen in their combining proportions will be referred to in what follows as the "detonating gas."

‡ 'Roy. Soc. Proc.,' A, vol. 110, p. 634 (1926).

Experimental.

The experiments were carried out in the circulation apparatus previously described in Part III, the partial pressure of water vapour in the " detonating gas " being kept constant throughout each series of experiments by means of a suitably diluted sulphuric acid solution, with which the concentrated sulphuric acid and phosphoric anhydride employed for the purpose of the " dry " experiments had been replaced. The caustic potash solution, which served to remove the product of combustion, was also diluted until its vapour pressure was approximately equal to that of the sulphuric acid solution in use.

Platinum, silver, gold, palladium, tantalum and tungsten were employed as cathodes. Magnesium and aluminium were found to be unsuitable for the purpose of these experiments as their use rendered the discharge unsteady.

The Discharge.

The addition of moisture to the dry " detonating gas " exerts a profound influence upon the appearance of the direct current discharge. Whereas in the case of the dry medium, gas pressure, current and gap width, either singly or together, could be varied, over a wide range without combustion being set up in the positive column of the discharge, it was found that the range of such conditions within which the combustion of the " detonating gas " was purely cathodic was narrowed down considerably by the presence of moisture, such effect being far more pronounced in the case of combustion at freely sputtering than at non-sputtering cathodes. For this reason, in the experiments to be described below, the gap width was reduced to 0·6 mm. A reduction much below this value was not considered advisable, owing to the risk of the cathode glow being distorted thereby.

The Experimental Results.

Throughout each series of experiments, the results of which are set forth below, the partial pressure of water vapour remained constant, whereas the *total pressure within the apparatus decreased as combustion and removal of* carbon dioxide proceeded. Thus, in each experiment, the percentage concentration of water vapour increased over a wide range with decreasing pressure. In all, five series of experiments were carried out, the corresponding partial pressures of water vapour being 0, 1, 3, 7 and 15 mm.

The metals employed as cathode materials can be divided into free- and non-sputterers. The experimental results obtained with the metals of the former class are set forth in Table I. As previously, c/i denotes the ratio of cubic centimetres of gas at N.T.P. burnt per minute to the current in milliamperes. *The two extreme right-hand columns of the table contain the ranges of pressure* and current over which combustion was purely cathodic in the presence of moisture. On exceeding these limits positive column combustion was set up. The results incorporated in the second column of the table are taken from Part III. The values of c/i are practically independent of the total gaseous pressure.

Table I.—Cathodic Combustion of Carbonic Oxide Detonating Gas.

Cathode material.	c/i when partial pressure of moisture in mm. is					Maximum moisture content. Per cent. by volume.	Limits of total pressure range. mm.	Limits of current range. Milliamperes.
	0	1	3	7	15			
Pt	0·24	—	0·23	0·23	0·23	37	40–120	1·46–2·92
Ag	0·29	0·19	0·20	0·17	0·17	30	35–120	1·46–2·92
Au	0·25	—	0·20	0·20	0·21	27	20–110	2·18–3·65
Pd	0·23	—	0·20	0·21	0.20	33	45–105	1·46–2·92

The results obtained with tantalum and tungsten, which metals were selected for the purpose of these experiments as typical of the non-sputtering class, are recorded in fig. 1 (tantalum), in which the relationship found between c/i and the total gaseous pressure, p, is recorded graphically for five different partial pressures of moisture (0, 1, 3, 7 and 15 mm.), and in figs. 2 (tantalum) and 3 (tungsten) where the observed values of c/i are plotted against the water vapour contents of the " detonating gas " expressed in per cent. by volume for a similar range of partial pressures of moisture. Since, with any given partial pressure of moisture, the total gas pressure determines the percentage content of water vapour, the pressure limits between which the experiments were carried out can be derived directly from the curves. The total current range within which combustion was purely cathodic was between 1·46 and 4·0 milliamperes in the case of tantalum, and between 2·18 and 4·37 milliamperes in the case of tungsten. The dotted sections of the curves have been obtained by extrapolation from the experimental results.

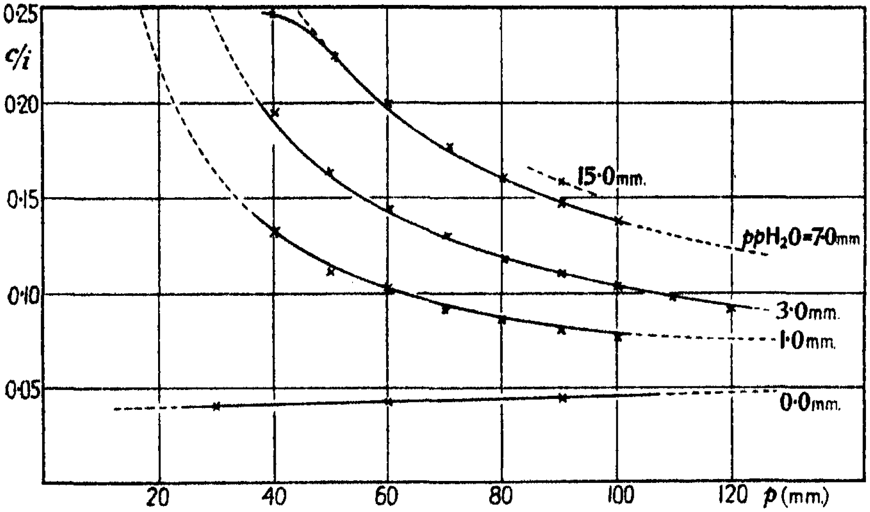

FIG. 1.—Cathodic Combustion of 2CO + O_2 at Tantalum.

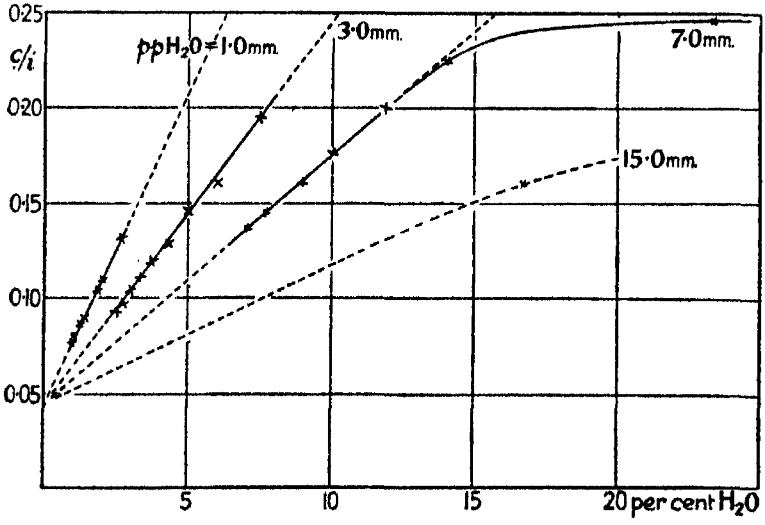

FIG. 2.—Cathodic Combustion of 2CO + O_2 at Tantalum.

Discussion of the Results.

It will be convenient to consider in the first place the results obtained at the non-sputtering type of cathode. It will suffice to base the discussion upon the results obtained with tantalum, as the main facts established in the cases of both this metal and tungsten are similar.

Fig. 1, in which the relationships found between c/i and the total gaseous pressure for the five different partial pressures of water vapour examined are recorded graphically, shows that, for each partial pressure of above 1·0 mm. of water vapour, the relationship between c/i and the total gaseous pressure, p, can be expressed over a wide range of conditions by the equation

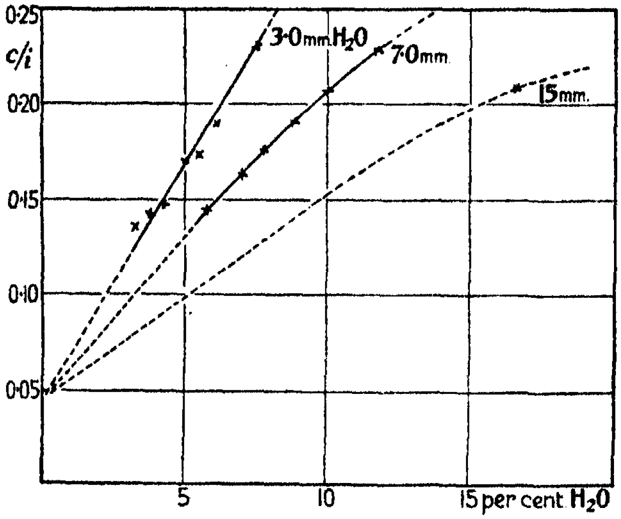

FIG. 3.—Cathodic Combustion of $2CO + O_2$ at Tungsten.

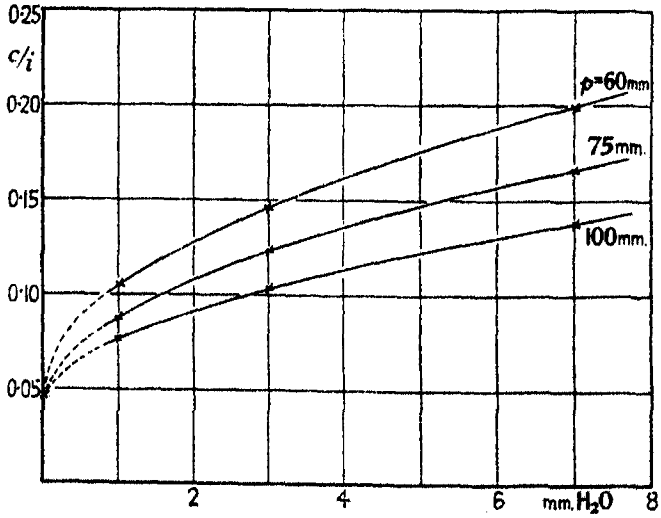

FIG. 4.—Cathodic Combustion of $2CO + O_2$ at Tantalum.

$$(c/i - 0\cdot045) \, . \, p = a,$$

where a is a constant, the value of which depends upon the partial pressure of moisture. Thus c/i and p are hyperbolically related. The values of a are 3·1, 5·9 and 9·1 when the partial pressures of steam are 1, 3 and 7 mm. respectively. Now in Parts I and III* it was shown that c/i is a constant which is practically independent of the pressure, and further, that cathodic combustion occurs only between charged molecules and is proportional to the number of such molecules within the cathode zone. Moreover, it has also been established in Part III that the cathode fall of potential in dry "detonating gas" is independent of both current and gas pressure; a result which is in agreement with that established by Warburg† who found that the cathode fall of potential is independent of the magnitude of the current through, and of the pressure of, the gas. Therefore, the number of ions, and also the total number of molecules, both charged and otherwise, within the cathode zone is determined solely by the current traversing the discharge. Hence, *ceteris paribus*, the volume occupied by the cathode glow of the type of discharge employed in our experiments increases proportionally with the current, but decreases hyperbolically with the gas pressure. Visual observations of the change in volume of the cathode zone with current and pressure afford a rough confirmation of this conclusion. Similarly, since throughout each experiment the partial pressure of water vapour was kept constant and was therefore independent of the total gas pressure, the number of steam molecules in the cathode zone likewise decreased hyperbolically with the pressure. Hence the value of the ratio c/i for the cathodic combustion of a "detonating gas" mixture, containing a given partial pressure of moisture at a non-sputtering cathode is, in effect, independent of the total gaseous pressure (except in so far as a change in pressure varies the number of steam molecules within the cathode zone), but proportional to the number of steam molecules within the cathode zone.

The full facts relating to the cathodic combustion of carbonic oxide "detonating gas" established by the results of this investigation and the conclusions which can be drawn therefrom may now be stated and set forth as follows :—

In the first place, other conditions remaining unchanged, the rate of cathodic combustion is determined solely by the current passed by the discharge, a result which agrees with those previously obtained with electrolytic gas (Part I)* and dry "detonating gas" (Part III) which, in the case of the latter mixture, as shown in Part III of this series, leads to the conclusion that such combustion involves the prior ionisation of both constituents of the combustible mixture.

---

* 'Roy. Soc. Proc.,' A, vol. 111, p. 257 (1926), and vol. 124, p. 303 (1929).

† 'Conduction of Electricity through Gases,' by Sir J. J. and G. P. Thomson, 3rd ed., p. 242 (1928).

The most remarkable new fact brought to light, however, is that moisture, while promoting combustion at non-sputtering cathodes, actually retards combustion at cathodes composed of the freely sputtering metals, platinum, silver, gold and palladium. In the case of platinum, however, the amount of such retardation is practically within the limits of experimental error.

The maximum retarding effect is fully attained when the partial pressure of moisture in the gaseous mixture is approximately 3 mm. (and probably less; in the case of silver, 1 mm.); higher concentrations of moisture, up to 15 mm., having no additional slowing down effect upon the rate of cathodic combustion. In view of the facts that moisture promotes combustion at non-sputtering cathodes, and that, provided the partial pressure of the moisture is constant, such acceleration is proportional to the number of steam molecules within the cathode zone, we can only conclude that at freely sputtering cathodes the rôle played by moisture in bringing about the union of carbonic oxide and oxygen ions is almost completely subordinated to that played by sputtered metal atoms. The most probable explanation of the mechanism of the cathodic combustion of moist "detonating gas" mixtures which we can put forward at the moment, and which takes into account all the facts hitherto established, is the following:—

(i) CO and O_2 are ionised, becoming positively charged and are then kept apart by electrostatic forces of repulsion.

(ii) In dry "detonating gas," negatively charged sputtered metal atoms overcome such repulsion, in the manner previously outlined in Part III, and thus enable combustion to proceed.

(iii) In moist "detonating gas" mixtures burning at freely sputtering cathodes, steam molecules are attracted by, and form clusters on, such sputtered metal atoms.

(iv) Such clusters, by acting in a similar manner to sputtered metal atoms in the cathodic combustion of dry "detonating gas," overcome the electrostatic forces of repulsion existing between ions of like charge and thus enable combustion to proceed.

(v) The combustion promoting action of the sputtered metal atoms is gradually reduced, though only to a comparatively small extent, as the number of steam molecules which associate with them increases, until a limit, corresponding to a partial pressure of moisture of about 3 mm., is reached, beyond which the clustering of additional steam molecules on the metal atoms has no further effect in reducing the activity of the latter.

Sputtered metal particles thus virtually drain the cathode zone of separate individual steam molecules, and the number of negatively charged particles available for the overcoming of electrostatic repulsion between ions of like charge is thus independent of (1) the total gas pressure, (2) the partial pressure of moisture contained in the mixture, and hence also (3) of the amount of moisture actually present within the cathode zone.

A further noteworthy feature disclosed by these experiments is the fact that the moisture content of "detonating gas" can be increased to as much as, and possibly more than, 37 per cent. without any further decrease in the value of c/i obtained at sputtering cathodes beyond that already brought about by approximately 3 per cent. in a mixture of which the partial pressure of the moisture content is 3 mm. It would be difficult to explain this fact satisfactorily on lines other than those outlined above, *i.e.*, that sputtered metal atoms, by forming clusters with steam molecules, and thus virtually draining the cathode zone of such molecules, in effect reduce by aggregation the number of separate individual water particles within the cathode zone to that of the sputtered metal atoms with which they become associated.

Thus, at a sputtering cathode the value of the ratio c/i is mainly determined by the numbers within the cathode zone of sputtered metal atoms and of suitable ions capable of combining when once their mutual electrostatic repulsion is overcome by means of such metal particles, only a comparatively small amount of combustion being due to the direct union of ions of dissimilar charge. Owing to cluster formation with the sputtered metal atoms, moisture has little effect upon the rate of combustion, beyond slightly retarding it, such retardation reaching a maximum when the moisture vapour partial pressure is approximately 3 mm. This rate of combustion is then practically independent of (1) the total gaseous pressure, (2) the partial pressure of steam, and hence (3) of the amount of moisture within the cathode zone.

When the discharge traverses moist "detonating gas" there are, within the cathode zone at a non-sputtering cathode, neutral molecules and positively charged ions, of carbonic oxide, oxygen and water vapour, together with steam molecules which are negatively charged as a result of the capture of electrons, and also a comparatively small number of negatively charged oxygen and, probably, still fewer (if, indeed, any) negatively charged carbonic oxide ions.

Promotion of combustion by moisture of the "detonating gas" at non-sputtering cathodes must be confined to negatively charged steam molecules, because neither neutral nor positively charged steam can assist in overcoming the repulsion between the positively charged ions of the combustible gases.

In the case of cathodic combustion at non-sputtering cathodes, we have found that steam exerts a dilution effect upon combustion which becomes pronounced at concentrations above about 12 per cent. of moisture. This observation is capable of ready explanation, because in the absence of sputtered metal atoms, upon which steam molecules can cluster to form comparatively large aggregates, the individual ionised steam molecules must share proportionately with carbonic oxide and oxygen ions in carrying the current, with the result that, as this steam concentration increases, the number of combustible gaseous ions must decrease in proportion.

Although, for any given partial pressure of steam within the limits stated above, the value of c/i varies hyperbolically with the total gaseous pressure, and is therefore proportional to the number of steam molecules within the cathode zone, the same relationship does not hold when the partial pressure of moisture is increased and the number of steam molecules within the cathode zone brought to the same value as before by suitably increasing the total gas pressure (figs. 2 and 4).

Within the cathode zone the number of water molecules and the total number of gaseous molecules (which latter is, as we have shown above, a function of the current alone), and hence also the number of combustible molecules, are in both cases the same. And since it has also been shown that the rate of combustion is virtually independent of pressure but proportional to the number of steam molecules within the cathode zone, it follows that the reduction in the value of c/i resulting from an increase in the partial pressure of water vapour can only be due to the increased *concentration* or density of packing of steam molecules, *i.e.*, the number of steam molecules contained in unit volume. It may therefore be reasonably concluded that the reduction in the value of c/i which is brought about by an increase in the partial pressure of moisture, when all other material conditions, such as percentage concentration and number of water and combustible molecules within the cathode zone remain unchanged, is due to a reduction in the number of separate individual water particles within the cathode zone resulting from cluster formation, which process will naturally be favoured by the increased density of packing of water molecules attendant upon an increase in the partial pressure of moisture.

Summary.

In the foregoing experiments it has been shown that :—

(i) An electric discharge can be passed through moist carbonic oxide "detonating gas" mixtures in such a manner that combination takes place at a rate which is determined solely by the current passed by the discharge.

(ii) Over a well-defined range of gas pressure, gap width and current, combustion is purely cathodic, *i.e.*, confined to the cathode zone ; such range is, however, considerably narrower in moist "detonating gas" mixtures than in the dry gas.

(iii) The rate of such cathodic combustion is directly proportional to the current.

(iv) Combustion of moist "detonating gas" mixtures occurring at freely sputtering cathodes is practically independent of the total gas pressure.

(v) Combustion occurring at a freely sputtering cathode, is reduced by the presence of steam, the maximum such reduction being brought about by a moisture partial pressure of approximately 3 mm. Higher partial pressures (up to 15 mm.) or concentrations of moisture above about 3 per cent. and up to 37 per cent. have no further effect.

(vi) The rate of combustion at non-sputtering cathodes is accelerated by the presence of moisture ; and, further,

(vii) for any given partial pressure of moisture the ratio of the rate of combustion to current is hyperbolically related to the total gaseous pressure, combustion increasing with decrease in pressure.

(viii) The relative accelerating effect of moisture upon the rate of combustion at non-sputtering cathodes decreases with increasing partial pressure of moisture, *i.e.*, with the number of steam molecules contained in unit volume.

From these facts it may be concluded that (i) the combustion of moist "detonating gas" mixtures is determined by a prior ionisation of the constituent molecules of the gas. (ii) at freely sputtering cathodes (*a*) steam molecules within the cathode zone condense on, and form clusters with sputtered metal atoms ; (*b*) the combustion promoting activity of such clusters is somewhat less than that of a sputtered metal atom free from moisture ; (*c*) such clusters promote combustion by neutralising the electrostatic forces of repulsion existing between positively charged ions. (iii) Combustion occurring at non-sputtering cathodes is (*a*) proportional to the number of separate individual moisture particles (clusters) within the cathode zone, such number depending upon the number of steam molecules within the cathode zone and contained in unit volume, and (*b*) effected by the overcoming of electrostatic forces of repulsion between positively charged ions by negatively charged moisture. (iv) At both classes of cathode a small amount of combustion is due to the direct union of ions of dissimilar charge, the negative ions consisting for the most part of oxygen molecules which have captured electrons.

One of us (D.L.H.) wishes to thank the London County Council for a grant which has enabled him to devote his full time to this research. We also wish to thank the Government Grants Committee of the Royal Society for a grant with which the cost of some of the apparatus employed in this investigation was defrayed.

An X-Ray Investigation of the Structure of Naphthalene and Anthracene.

By J. Monteath Robertson.

(Communicated by Sir William Bragg, F.R.S.—Received April 3, 1929.)

[Plates 7 and 8.]

In the present paper an attempt is made to develop a geometrical structure factor which will account for the intensity distribution in the various spectra of naphthalene and anthracene. Such an attempt is surrounded by many difficulties owing to the relatively low symmetry of the crystal systems (monoclinic), the complicated nature of the molecules, and uncertainties regarding the laws of reflection of X-rays from organic crystals. Recently, however, Dr. Müller has investigated the structure of a long chain hydrocarbon* making the simplification of treating a carbon atom and its attendant hydrogen atoms as one scattering centre for X-rays. The success of this investigation makes it seem probable that an approximate structure may likewise be obtained for some of the more complicated aromatic compounds.

The simple organic compounds of this type (benzene, cyclohexane) are very often liquids or low melting solids that call for a specialised and difficult technique in any investigation of their crystal structure. Good crystals of naphthalene and anthracene, however, are easily obtained. Moreover the crystal structure of these compounds has already been investigated very fully by Sir William Bragg, both by the ionisation spectrometer* and photographic methods.† The author has had the privilege of assisting in some of this later work, and the present paper is a continuation of these investigations.

---

* 'Roy. Soc. Proc.,' A, vol. 120, p. 437 (1928).

1. *Experimental Methods and Results.*

The rotating crystal photographic method has been used in this work, and the results are classified in Tables I to III according to a method previously used by the author.‡ The indices of the reflecting planes are referred to unit monoclinic cells of the following dimensions :—

	a.	*b*.	*c*.	*β*.	Space group.	Molecules per unit cell.	Density.
Naphthalene	8·34	5·98	8·68	122° 44′	C_{2h}^{5}	2	1·152
Anthracene	8·58	6·02	11·18	125° 0′	C_{2h}^{5}	2	1·250

Bernal's method of interpretation was employed.§ The intensity estimates given in the Tables I to III have been made in the manner previously described by the author (*loc. cit.*), but they must only be regarded as approximate. They are, however, usually sufficient for the purposes of this paper. Most of the results in the tables are derived from the analysis of overlapping oscillation photographs taken about the *b* axis, but the {0*k*0} reflections, and certain others, have been taken from photographs about the *a* and *c* axes. It was found most convenient in this work to employ Cu Kα and Kβ radiation and a small circular camera. When necessary in the oscillation photographs the Kβ radiation was removed by means of a nickel filter. Some of the rotation photographs are reproduced in Plates 7 and 8. The naphthalene photographs are more difficult to take owing to the rate at which a small crystal volatilises, and so in general a larger crystal and somewhat less accurate setting had to be employed than for anthracene, but this drawback did not lead to any ambiguity in the interpretation of the results. The striking similarity between corresponding photographs of naphthalene and anthracene is at once apparent, and points to similarity of underlying structure. We see that the length of the b axis in the two crystals is almost identical; but while the c axis is considerably longer in anthracene than in naphthalene (layer lines closer together) yet the intensity maxima occur at almost exactly the same points on the plates. The significance of this result has already been discussed by Bragg (*loc. cit.*). It indicates a recurrence of the same periodicity in the two structures.

---

* 'Proc. Phys. Soc.,' vol. 34, p. 33 (1921); vol. 35, p. 167 (1923); and "X-Rays and Crystal Structure," p. 229 (1925).

† 'Z. f. Krist.,' vol. 66, p. 22 (1927); 'Nature,' vol. 121, p. 327 (1928).

‡ 'Roy. Soc. Proc.,' A, vol. 118, p. 711 (1928).

§ 'Roy. Soc. Proc.,' A, vol. 113, p. 117 (1926).

2. *Space Group and General Structure Factor.*

A survey of the tables shows that in the case of both naphthalene and anthracene the $\{h0l\}$ planes are halved when h is odd, the $\{010\}$ is halved and there are no other halvings. The only space group in the monoclinic system which accounts for these facts is C_{2h}^5 in the prismatic class.* But this space group requires four asymmetric molecules to complete the necessary symmetry, and only two molecules are present in the unit cells of naphthalene and anthracene. Hence if all the halvings found are true halvings we must ascribe a centre of symmetry to the molecules of naphthalene and anthracene in the crystalline state, which is the only possible molecular symmetry in this space group.

It often happens that the determination of a space group depends upon the determination of the crystal class, regarding which only superficial evidence may be available. Thus it is sometimes possible to avoid the assumption of molecular symmetry by relegating the crystal to a lower symmetry class which does not require it. In the present example, however, if the $\{010\}$ halving is real, there is no space group available in any of the lower symmetry classes that will account for the halvings found. It therefore becomes necessary to assume a centre of symmetry in these molecules.

Let us now consider the space group C_{2h}^5 in more detail with a view to the development of a geometrical structure factor. First of all suppose there are four asymmetric molecules in the unit cell, and let (x, y, z) be the co-ordinates of any point (atom) on one of the molecules referred to the a, b and c crystal axes as axes and any lattice point as origin. Then the co-ordinates of the equivalent points on the four molecules are as follow,

$$\left.\begin{array}{llll} x, & y, & z; & \qquad\qquad\qquad\qquad\qquad\text{A} \\ x+\frac{1}{2}, & -y+\beta, & z; & \text{reflected molecule}\qquad\qquad\;\;\text{B} \\ -x+\alpha, & y+\frac{1}{2}, & -z+\gamma; & \text{rotated molecule}\qquad\qquad\quad\;\text{C} \\ -x+\frac{1}{2}+\alpha, & -y+\frac{1}{2}+\beta, & -z+\gamma; & \text{reflected rotated molecule D} \end{array}\right\}, \quad (1)$$

---

* Compare Astbury and Yardley, 'Phil. Trans. Roy. Soc.,' A, vol. 224, p. 221 (1924).

where α, β and γ are parameters which have to be determined. It is not in general possible to represent the positions of a molecule and its mirror image by means of two points unless the molecule itself has certain symmetry properties, *e.g.*, a centre of symmetry. But suppose the molecules have certain approximate symmetry properties, and that we can thus represent their positions approximately by means of points, then with such a representative point as origin the positions of the four molecules in the unit cell are denoted by the following co-ordinates :—

$$\left.\begin{array}{llll} 0, & 0, & 0 & \ldots\ldots\ldots \text{A} \\ \frac{1}{2}, & \beta, & 0 & \ldots\ldots\ldots \text{B} \\ \alpha, & \frac{1}{2}, & \gamma & \ldots\ldots\ldots \text{C} \\ \frac{1}{2}+\alpha, & \frac{1}{2}+\beta, & \gamma & \ldots\ldots\ldots \text{D} \end{array}\right\}. \qquad (2)$$

It can readily be seen that when and only when $\alpha = \frac{1}{2}$, $\beta = \frac{1}{2}$, $\gamma = 0$, the number of molecules is reduced to two. A coinciding with D, and B with C at the points (0, 0, 0) and ($\frac{1}{2}$, $\frac{1}{2}$, 0). Introducing those values for α, β and γ the general co-ordinates (1) now become

$$\begin{array}{l} \left.\begin{array}{llll} x, & y, & z & \ldots\ldots\ldots \text{A} \\ \multicolumn{3}{l}{\text{Centre of symmetry}} & \\ -x, & -y, & -z & \ldots\ldots\ldots \text{D} \end{array}\right\} \\ \left.\begin{array}{llll} x+\frac{1}{2}, & \frac{1}{2}-y & z & \ldots\ldots\ldots \text{B} \\ \multicolumn{3}{l}{\text{Centre of symmetry}} & \\ \frac{1}{2}-x, & y+\frac{1}{2}, & -z & \ldots\ldots\ldots \text{C} \end{array}\right\} \end{array} \qquad (3)$$

A and D lying on one molecule with a centre of symmetry at (0, 0, 0) and B and C on the second molecule with a centre of symmetry at ($\frac{1}{2}$, $\frac{1}{2}$, 0). The molecule BC can be derived from AD either by a reflection in the ac plane or by a rotation about the b axis, accompanied by a shift of $\frac{1}{2}a$, $\frac{1}{2}b$. We have thus determined α, β and γ by making use of the fact that there are only two molecules in the unit cell.

The geometrical structure factor for any plane $\{hkl\}$ may be written

$$S = \left| \sum_{r=1}^{r=m} \sum_{h=1}^{h=n} A_{pr}\, e^{2\pi i (x_{pr} h/a + y_{pr} k/b + z_{pr} l/c)} \right|, \qquad (4)$$

where A_{pr} is the reflecting power and (x_{pr}, y_{pr}, z_{pr}) the co-ordinates of the pth atom in the rth molecule in a unit cell built up of m molecules that each contain n atoms. For this purpose it is convenient to restrict the term

" molecule " to mean the asymmetric crystal unit, which in the present example consists of one-half of the chemical molecule. For mathematical purposes we thus divide the chemical molecule into two crystal units which are centro-symmetrical with respect to each other, and the general co-ordinates of equivalent points on these crystal units referred to a centre of symmetry as origin are given in (3). We can now carry the summation of the structure factor over the molecules, using these general co-ordinates. On simplifying the result we obtain the following two expressions, which are quite general and apply to any crystal of space group C_{2h}^5 which contains two molecules in the unit cell.

$$S = \sum_{h=1}^{h=n} 4A_p \cos 2\pi (x_p h/a + z_p l/c) \, . \cos 2\pi y_p k/b \qquad (5)$$

when $(h + k)$ is even

and

$$S = \sum_{h=1}^{h=n} 4A_p \sin 2\pi (x_p h/a + z_p l/c) \, . \sin 2\pi y_p k/b \qquad (6)$$

when $(h + k)$ is odd.

The remaining summation has now to be taken over that group of n atoms which make up the crystal unit.

3. *Form and Orientation of the Molecules.*

It is hardly possible to proceed further without some guiding principles as to the form and orientation of the molecules of naphthalene and anthracene in the crystal. In this connection Bragg has shown (*loc. cit.*) that all the evidence indicates that the long axes of the molecules lie along the c axes of the crystals. When we pass from naphthalene to anthracene, a, b and β, remain nearly the same, but the c axis increases in length by 2·5 A.U., which is just what is required to accommodate the atoms forming an extra ring, if it be of the dimensions found in the diamond or graphite structure. Again Bragg has shown that the characteristic appearance of the c axis photographs lead to the same conclusion, and by making a statistical investigation of the intensities of the reflections in anthracene by plotting against a given l index a number representing the sum of the intensities of all reflections from planes having this index, he obtains a curve with sharp maxima at 4·2 and 8·7. These numbers divided into the length of the c axis (11·18) give 2·66 and 1·28, which correspond closely to the two periodicities in the molecule, if it consists of three rings of the diamond pattern placed along the c axis. If the indices of the planes are referred to any direction in the crystal other than the c axis, this periodic property is not shown. In fig. 1 this curve is drawn again from the revised data now available in Tables I to III, and is compared with the corresponding curve for naphthalene. A number is assigned to each reflection* (v.s. = 7, s. = 6, ... v.w. = 1) and for all planes with a given l index these numbers are added together and plotted on the curve, the horizontal scale being l/c. This scale measures the reciprocal of the periodicity, if any, occurring along the c axis of the crystal, and the same periodicity in the two crystals will be indicated by maxima on the curves appearing at the same point on the horizontal scale.

The similarity of the curves is at once apparent, and we see that in both naphthalene and anthracene there are distinct maxima at 0·38 and 0·78 on the reciprocal scale, giving a periodicity of 2·63 A.U. and 1·28 A.U. for both crystals along the direction of the c axis. The fact that the curve for naphthalene lies wholly above the anthracene curve is due only to the experimental defect of using a larger crystal of naphthalene which in general gave stronger reflections than were obtained from anthracene.

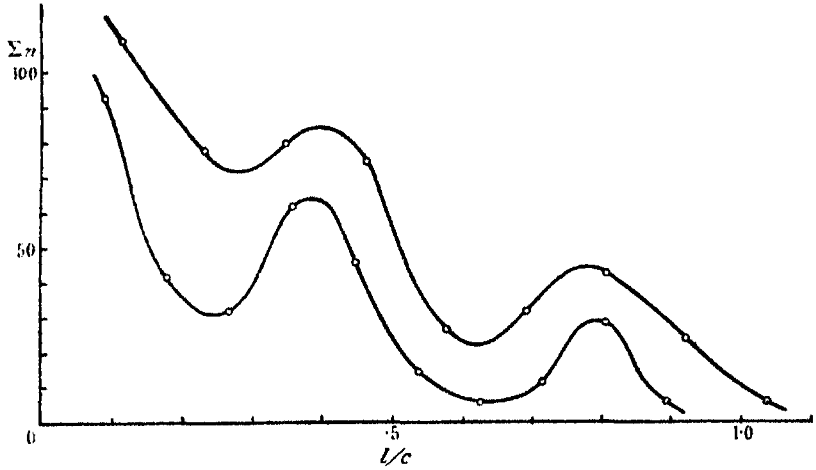

FIG. 1.

Thus quite apart from any ideas based on the chemical structure of the molecule, we have distinct evidence of a fundamental periodicity along the c axis of amount 1·28 A.U. in both naphthalene and anthracene. We can proceed to outline the structure somewhat further from general considerations of the X-ray results alone before entering on a detailed mathematical discussion.

---

* These numbers are approximately a linear function of the logarithm of the intensity. Compare 'Roy. Soc. Proc.,' A, vol. 118, p. 711 (1928).

The crystal unit of naphthalene contains five carbon and four hydrogen atoms, and the anthracene unit contains seven carbon and five hydrogen atoms. We will neglect the hydrogen atoms for the moment, or rather regard each scattering centre for X-rays as consisting of one carbon atom and its attendant hydrogen atom, if any. It is evident that the only reasonable structure for these crystals must be obtained by placing the five scattering centres of the naphthalene unit, and the seven scattering centres of the anthracene unit, at equal distances of about 1·28 A.U. along the *c* axis. Such an arrangement leaves a gap of (8·68 – 4 × 1·28) = 3·56 A.U. between the last scattering centre in one naphthalene molecule and the first scattering centre of the next identical molecule, if these two centres happen to lie in line along the *c* axis. The corresponding gap for anthracene is (11·18 – 6 × 1·28) = 3·50 A.U.

So far we have not discussed the lateral distribution of the scattering centres in a plane at right angles to the *c* axis. Fig. 2 (*a*) and (*b*) shows a projection of the structure thus far obtained for naphthalene and anthracene in the *ac* plane of the crystals.

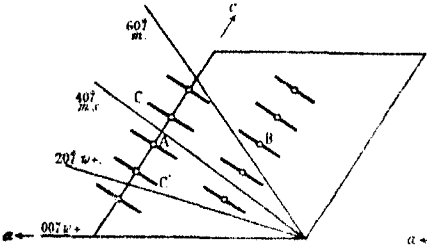

Fig. 2 (*a*).—Naphthalene.

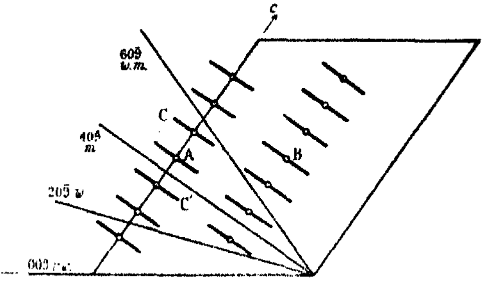

Fig. 2 (*b*).—Anthracene.

The diagrams are drawn to scale and the short thick lines mark the trace of the planes perpendicular to the *c* axis in which the scattering centres lie, the distance between these planes being 1·28 A.U. There are centres of symmetry at A and B. The molecule B can be derived from A either by a reflection in the plane of the paper, or by a rotation of 180° about an axis perpendicular to the plane of the paper, in each case accompanied by a shift of *a*/2, *b*/2. Each molecule, A and B, consists of two crystal units which are derived from each other by an inversion through the centre of symmetry at A or B. If we located a scattering centre at one extremity of any of the short thick lines of A (say at C) there would be another similar scattering centre at the other extremity of the corresponding line on the other side of A, belonging to the other crystal unit (at C′). If for example we located a scattering centre at one extremity of each of the short lines, there would be a similar centre at every other extremity and the two rows taken together would form the chemical molecule, $C_{10}H_8$ or $C_{14}H_{10}$.

We next observe that the relation of the axial ratios and the β angle to the periodicity is such that the third line of scattering centres of the A molecule is approximately in line with the first line of centres in the B molecule, in a direction perpendicular to the *c* axis. This is more nearly true of anthracene than of naphthalene. We now draw in the traces of certain $\{h07\}$ and $\{h09\}$ planes, which are all perpendicular to the plane of the paper. The intensities of the reflections from these planes are all enhanced relative to the reflections from the $\{h06\}$ and $\{h08\}$ planes, for example, because of the fundamental periodicity. But we observe that the reflection from the (407) in naphthalene, and from the $(40\bar{9})$ plane in anthracene is stronger than that from any of the other $\{h07\}$ or $\{h09\}$ planes. Now if the scattering centres were so distributed perpendicularly to the paper that they projected into the points indicated by the small circles in the diagrams, or approximately into these points, it is evident that there would be no good reason for this particular enhancement of the reflections from the $(40\bar{7})$ and $(40\bar{9})$ planes. It can be seen from the diagrams that the reflections from the various planes would be nearly all equally strong. But if the scattering centres were distributed in some manner along the short thick lines it is at once evident that the reflections from the $(40\bar{7})$ and $(40\bar{9})$ planes, the traces of which are nearly parallel to these lines, would be stronger than the reflections from the other planes. In the case of these other planes, $(60\bar{7})$ or $(60\bar{9})$, $(20\bar{7})$ or $(20\bar{9})$, and particularly (007) or (009), the reflections would be weakened by the fact that the scattering centres are distributed across the planes.

We thus require to assume that the scattering centres are distributed in some manner along the short thick lines in the diagrams, or in other words it is probable that the "plane" of the molecule lies nearer to the *ac* than to the *bc* plane of the crystal. Bragg has pointed out (*loc. cit.*) that the form of the crystal and the absence of the (100) plane as a natural face make it likely that this is the case. On making a model after the diamond pattern it is found that the molecules lock together much better when their plane makes a small angle with the *ac* plane.

From the results we have so far considered we might be led to assume some simple two-dimensional model in the *ac* plane, containing nearly flat hexagon rings such as are assigned to the graphite structure. The possibility of such a simple structure, however, is limited by the following considerations. Fig. 3 shows a view along the c axis of naphthalene or anthracene, the ovals being taken to represent roughly an end view of the region occupied by the scattering centres. We know that the molecule B at $(\frac{1}{2}, \frac{1}{2}, 0)$ exactly subdivides the primitive translation A A′. If the molecule contained an approximate plane of symmetry parallel to the ac plane, as represented in fig. 3 (a), then, in general reflections from planes with the indices $(h+k)$ an odd number should be weak.* A survey of the Tables I to III shows that any such general tendency is very small or absent in the case of naphthalene or anthracene. Rotation photographs about this axis, the (001), (110) zone, show a slight weakening of the intermediate layer lines, but this is mainly due to the absence of $\{h0l\}$ reflections when h is odd, a fact which we have already made use of in determining the space group, and which only indicates the presence of a reflected molecule somewhere on the line pq. As the reflections from the general planes are not sensibly weakened when $(h+k)$ is odd, and as we know that the molecule B exactly subdivides AA′, we must conclude that the molecule does not exhibit even an approximate plane of symmetry in the ac plane, and we are led to some such structure as is shown in fig. 3 (b).

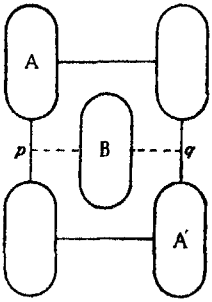

Fig. 3 (a).

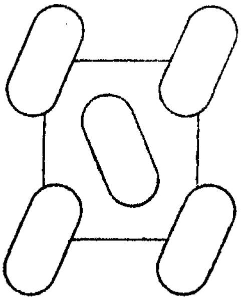

Fig. 3 (b).

4. *The Structure Factors for Naphthalene and Anthracene.*

We must now extend the expressions (5) and (6) over the scattering centres of the naphthalene and anthracene crystal units, being guided in the choice of parameters by the general considerations outlined above. Our present conception of the structure, however, would lead to expressions containing too many variables to be useful, and so it is necessary to simplify matters by assuming a certain degree of uniformity in the structure. We can do this in a very plausible way by supposing the scattering centres to lie in two rows parallel to the c axis, as indicated in fig. 4, which now replaces the more general diagram of fig. 2. Our assumption, then, is that the crystal unit* consists of a chain-like structure parallel to the c axis. We have definite evidence of the periodicity in this direction; but by placing the atoms in two rows we are making an assumption which can only be justified by the results of the investigation. There is, of course, much independent evidence in favour of such a structure; the tetrahedral properties assigned to the carbon atom in chemistry, the known structure of the diamond, and the results of Müller's work on the long chain hydrocarbons.

---

* Compare 'Roy. Soc. Proc.,' A, vol. 118, p. 711 (1928).

Fig. 4 represents the general case of such a structure, projected on to the ac plane. The periodicity along the c axis, which we know to be approximately equal to 1·28 A.U., is denoted by t. The direction a' is perpendicular to the b and c axes, and makes an angle of $(\beta - 90°)$ with the a axis. Two centro-symmetrical crystal units are shown in the diagram. Each unit contains n scattering centres, represented by points. The outer row (odd numbers)

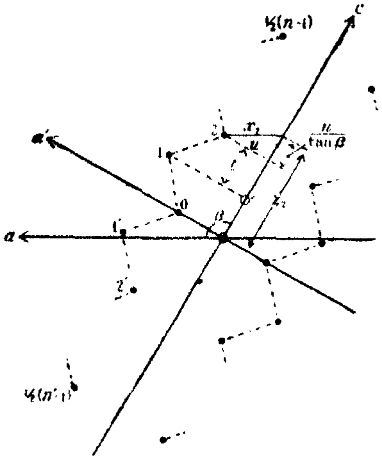

FIG. 4.

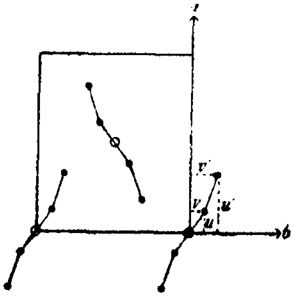

FIG. 5.

---

* Any n of the two chains of n points each, shown in fig. 4, which are not centro-symmetrical to each other may be chosen as the "crystal unit." The selection of the particular points numbered $\frac{1}{2}(n' - 1), \ldots, 2', 1', 0, 1, 2, \ldots, \frac{1}{2}(n - 1)$, and reference to them as the crystal unit is a matter of convenience, which simplifies the following mathematical treatment without affecting the results. We might, for example, choose the outlying row (odd numbers) together with the inlying row (even numbers) from the opposite side of the centre of symmetry, and using their co-ordinates, obtain the same final result.

contains $\frac{1}{2}(n-1)$ points, and the inner row (even numbers) contains $\frac{1}{2}(n+1)$ points. For any closed-ring structure (naphthalene, anthracene) n is always odd, and the number of rings is $\frac{1}{2}(n-1)$. (When the number of rings is odd (benzene, anthracene) the centre of symmetry 0 must be shifted to 0′, opposite an outlying point.) Fig. 5 is a view of this structure looking along the c axis. A is the projection of the row ..., 0, 2, ... in fig. 4, and B the projection of the row ..., 1, 3, ... We shall now define the positions of these rows by making u and v the rectangular co-ordinates of A, referred to the a' and b axes and the centre of symmetry 0 as origin; u' and v' will be the corresponding co-ordinates of B.

In order to formulate the structure factor for the general case we may now write down the co-ordinates (x, y, z) of the n scattering centres which make up the crystal unit, referred to the crystallographic axes a, b and c as axes, and the centre of symmetry 0 as origin. From figs. 4 and 5,

$$\left.\begin{array}{lll}
x_{(n'-1)/2} = x_0 & y_{(n'-1)/2} = y_0 & z_{(n'-1)/2} = \frac{1}{2}(n-1)t + u/\tan\beta \\
\vdots & \vdots & \vdots \\
x_{2'} = x_0 & y_{2'} = y_0 & z_{2'} = 2t + u/\tan\beta \\
x_{1'} = u'/\sin\beta & y_{1'} = v' & z_{1'} = t + u'/\tan\beta \\
x_0 = u/\sin\beta & y_0 = v & z_0 = -u/\tan\beta \\
x_1 = u'/\sin\beta & y_1 = v' & z_1 = t - u'/\tan\beta \\
x_2 = x_0 & y_2 = y_0 & z_2 = 2t - u/\tan\beta \\
\vdots & \vdots & \vdots \\
x_{(n-1)/2} = x_0 & y_{(n-1)/2} = y_0 & z_{(n-1)/2} = \frac{1}{2}(n-1)t - u/\tan\beta
\end{array}\right\} \quad (7)$$

We can now carry the summations (5) and (6) over these co-ordinates obtaining terms of the type

$$4A_1 \cos 2\pi\left[\frac{2tl}{c} + u'\left(\frac{hc - la\cos\beta}{ac\sin\beta}\right)\right] . \cos 2\pi\frac{v'\kappa}{b}$$

and

$$4A_1 \sin 2\pi\left[\frac{2tl}{c} + u'\left(\frac{hc - la\cos\beta}{ac\sin\beta}\right)\right] . \sin 2\pi\frac{v'\kappa}{b},$$

A_1 being the reflecting power of the centre (x_1, y_1, z_1). In order to simplify the expressions it is convenient to write

$$A = 2\pi(hc - la\cos\beta)/ac\sin\beta; \quad B = 2\pi k/b; \quad C = 2\pi l/c.$$

A, B and C thus depend only upon the indices and crystallographic constants, and their values can be written down for any plane. A list of these values for a number of planes calculated from the crystallographic data for naphthalene is given in Table IV, and from the anthracene data in Table V.

On completing the summations of (5) and (6), the final results can be expressed in the following simple forms,

$$\frac{kS}{8} = S' = \gamma \cdot \cos Au \cdot \cos Bv \cdot \left[\frac{\sin \frac{1}{2}(n+1)Ct}{2 \sin Ct}\right] + \cos Au' \cdot \cos Bv' \cdot \left[\frac{\sin \frac{1}{2}(n-1)Ct}{2 \sin Ct}\right] \quad (8)$$

when $(h+k)$ is even, and

$$S' = \gamma \cdot \sin Au \cdot \sin Bv \cdot \left[\frac{\sin \frac{1}{2}(n+1)Ct}{2 \sin Ct}\right] + \sin Au' \cdot \sin Bv' \cdot \left[\frac{\sin \frac{1}{2}(n-1)Ct}{2 \sin Ct}\right] \quad (9)$$

when $(h+k)$ is odd.

The results are not altered by shifting the centre of symmetry from 0 to 0′ when $\frac{1}{2}(n-1)$ (the number of rings) is odd. It will be seen that the sine factors in the square brackets in the above expressions are simply Müller's "chain factors"* for the two rows of scattering centres, the periodicity in each case being $2t$, and the number of centres $\frac{1}{2}(n+1)$ and $\frac{1}{2}(n-1)$ respectively.

In these expressions γ replaces A_{even}, the reflecting powers of the scattering centres on the inner row nearest the centre of symmetry, when the reflecting powers of the other centres on the outer row have all been put equal to unity. The need for this differentiation of the scattering centres is apparent when we consider the chemical structure of compounds like naphthalene and anthracene.

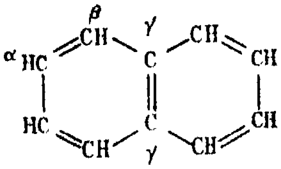

Naphthalene.

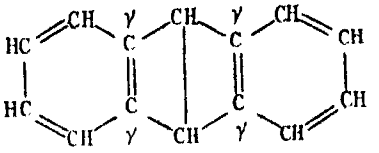

Anthracene.

The centres marked γ consist of a carbon atom only, whereas the other centres consist of the group $\geqslant$CH. Thus considering the atomic numbers involved we might expect γ to be equal to 6/7, the reflecting powers of the other centres being taken as unity. There is a discontinuity at the end positions, the α-positions of naphthalene, or the $\frac{1}{2}(n-1)$ positions of the general case, where the scattering centres again consist of the group $\geqslant$CH. In deriving the general expressions this small irregularity has been neglected, but in the particular cases of naphthalene and anthracene it is easy to take account of it by using the cosine expansions of the chain factors,* and attaching γ only to the centres indicated by the chemical structure. As n is only 7 for anthracene and 5 for naphthalene, the cosine expansions are generally the most convenient for computations, and have been used in the remainder of this paper. For naphthalene we find

---

* *Loc. cit.*

$$S' = \cos Au \,.\, \cos Bv \,.\, [\tfrac{1}{2}\gamma + \cos 2Ct] + \cos Au' \,.\, \cos Bv' \,.\, \cos Ct \qquad (10)$$

when $(h + k)$ is even, and

$$S' = \sin Au \,.\, \sin Bv \,.\, [\tfrac{1}{2}\gamma + \cos 2Ct] + \sin Au' \,.\, \sin Bv' \,.\, \cos Ct \qquad (11)$$

when $(h + k)$ is odd ; and for anthracene

$$S' = \cos Au \,.\, \cos Bv .\, [\gamma \cos Ct + \cos C3t] + \cos Au' \,.\, \cos Bv' .\, [\tfrac{1}{2} + \cos Ct] \quad (12)$$

when $(h + k)$ is even, and

$$S' = \sin Au \,.\, \sin Bv \,.\, [\gamma \cos Ct + \cos 3Ct] + \sin Au' \,.\, \sin Bv' \,.\, [\tfrac{1}{2} + \cos Ct] \quad (13)$$

when $(h + k)$ is odd.

Table IV.—Naphthalene.

$$A = 51{\cdot}31\,h + 26{\cdot}67\,l\,;\ B = 60{\cdot}20\,k\,;\ C = 41{\cdot}48\,l.$$

Values of A (in °).

	h →	0.	1.	2.	3.	4.
l	5	133·4	184·7	236·0	287·3	338·6
↓	4	106·7	158·0	209·3	260·6	311·9
	3	80·0	131·3	182·6	233·9	285·3
	2	53·3	104·7	156·0	207·3	258·6
	1	26·7	78·0	129·3	180·6	231·9
	0	0	51·3	102·6	153·9	205·2
	$\bar{1}$	− 26·7	24·6	76·0	127·3	178·6
	$\bar{2}$	− 53·3	− 2·0	49·3	100·6	151·9
	$\bar{3}$	− 80·0	− 28·7	22·6	73·9	125·2
	$\bar{4}$	−106·7	− 55·4	− 4·1	47·3	98·6
	$\bar{5}$	−133·4	− 82·0	− 30·7	20·6	71·9
	$\bar{6}$	−160·0	−108·7	− 57·4	− 6·1	45·2
	$\bar{7}$	−186·7	−135·4	− 84·1	− 32·8	18·6
	$\bar{8}$	−213·4	−162·1	−110·7	− 59·4	− 8·1
	$\bar{9}$	−240·0	−188·7	−137·4	− 86·1	− 34·8

---

* Generally,

$$\sin r\alpha/2 \sin \alpha = \cos \alpha + \cos 3\alpha + \dots + \cos (r - 3)\, \alpha + \cos (r - 1)\, \alpha \qquad (r \text{ even})$$

$$= \tfrac{1}{2} + \cos 2\alpha + \dots + \cos (r - 3) \dots \alpha + \cos (r - 1)\, \alpha \qquad (r \text{ odd}).$$

Table IV—(continued).

Values of C terms in structure factor for $t = 1·28$ A.U.

		$7/2 + \cos 2Ct$.	$\cos Ct$.
l ↓	0	1·429	1·000
	1	0·150	0·600
	2	−0·415	−0·279
	3	1·178	−0·935
	4	0·856	−0·844
	5	−0·558	−0·079
	6	0·553	0·749
	7	1·347	0·980
	8	−0·206	0·427
	9	−0·136	−0·466

Table V.—Anthracene.

$A = 51·22\,h + 22·55\,l$; $B = 59·80\,k$; $C = 32·21\,l$.

Values of A (in °).

	h →	0.	1.	2.	3.	4.
l ↓	5	112·8	164·0	215·2	266·4	317·6
	4	90·2	141·4	192·6	243·9	295·1
	3	67·7	118·9	170·1	221·3	272·5
	2	45·1	96·3	147·5	198·8	250·0
	1	22·6	73·8	125·0	176·2	227·4
	0	0	51·2	102·4	153·7	204·9
	$\bar{1}$	− 22·6	28·7	79·9	131·1	182·3
	$\bar{2}$	− 45·1	6·1	57·3	108·6	159·8
	$\bar{3}$	− 67·7	− 16·4	34·8	86·0	137·2
	$\bar{4}$	− 90·2	− 39·0	12·2	63·5	114·7
	$\bar{5}$	−112·8	− 61·5	− 10·3	40·9	92·1
	$\bar{6}$	−135·3	− 84·1	− 32·9	18·4	69·6
	$\bar{7}$	−157·9	−106·6	− 55·4	− 4·2	47·0
	$\bar{8}$	−180·4	−129·2	− 78·0	− 26·7	24·5
	$\bar{9}$	−203·0	−151·7	−100·5	− 49·3	1·9

Values of C terms in structure factor for $t = 1·28$ A.U.

		$\gamma \cos Ct + \cos 3Ct$.	$\frac{1}{2} + \cos 2Ct$.
l ↓	0	1·857	1·500
	1	0·090	0·631
	2	−0·272	−0·466
	3	0·505	0·116
	4	−1·534	1·364
	5	−0·969	1·112
	6	0·598	−0·205
	7	−0·553	−0·297
	8	0·731	0·996
	9	1·677	1·427
	10	−0·395	0·248

5. *Discussion of the Structure Factors in Relation to some Simple Models.*

We have now to determine what values of u, u', v and v' in the expressions for the structure factors will account for the outstanding variations in the intensities of the reflections observed in naphthalene and anthracene. The matter is complicated by uncertainties regarding the laws of reflection in the case of carbon compounds. The crystals of naphthalene and anthracene most likely belong to the "imperfect" type. No change was observed in the intensities of the principal reflections when a powder photograph was compared with the single crystal photographs. The expression for the integrated reflection in the case of an imperfect crystal may be written briefly

$$\rho = \mathrm{K}f^2\mathrm{S}^2\mathrm{PT},$$

where K represents constants independent of θ, the angle of reflection. f is the atomic structure factor which for the carbon atom decreases continuously and at first very rapidly with increasing θ, according to Ponte's measurements on diamond.* S is the geometrical structure factor we are at present considering. P is equal to $(1 + \cos^2 2\theta)/\sin 2\theta$, which also decreases with increasing θ, while T is the temperature factor, which is unknown for these crystals, but which will consist of some function of θ and the indices of the reflecting plane. The chief point to notice is that while S is a very rapidly oscillating function with respect to θ, the remaining part of the expression most probably decreases fairly continuously with increasing θ. Thus, if among the orders of a certain plane, one reflection is enhanced or diminished relative to its neighbours, the discontinuity should be shown by a marked change in the value of the structure factor for that order. The more nearly alike are the orders in spacing, the more accurate the result will be. When the planes to be considered have less than two indices in common the result is more doubtful, as Müller has pointed out (*loc. cit.*), owing to the operation of the unknown temperature factor.

A first approximation has already been obtained for t. The task of evaluating the remaining parameters, however, is a somewhat difficult one, and it is perhaps best to proceed by first discussing some simple models. In this way we may hope at least to limit the range of possible values which have to be considered. At present we will make γ equal to unity, *i.e.*, all the scattering centres are supposed to be of equal weight.

We may note that in all the expressions (8) to (13) the first term, containing u and v, always refers to the first row of scattering centres, or those nearest to the centre of symmetry, and the second term, containing **u' and v'**, refers to the outlying row.

---

* 'Phil. Mag.,' vol. 3, p. 195 (1927).

Consider first the case when u and u' are very small or zero. This applies to any structure in which the "plane" of the molecule is near the bc plane (which we have already found from general considerations to be unlikely). For the {001} planes B is also zero, and in the general case (8) becomes

$$S'_{00} = \frac{\sin \frac{1}{2}(n+1)Ct}{2 \sin Ct} + \frac{\sin \frac{1}{2}(n-1)Ct}{2 \sin Ct} = \frac{1}{2} \cdot \frac{\sin \frac{1}{2} nCt}{\sin \frac{1}{2} Ct}$$

$$= \tfrac{1}{2} + \cos Ct + \cos 2Ct + \ldots + \cos \tfrac{1}{2}(n-1)Ct. \qquad (8\text{A})$$

This is Müller's chain factor for a row of n scattering centres placed along the c axis, the periodicity being t. ($C = 2\pi l/c$.)

We may use this expression to examine the intensities of the reflections from the different orders of the cleavage planes (001) in naphthalene and anthracene. In naphthalene, for example, when t is in the neighbourhood of 1·28 there is a very strong maximum in the value of the structure factor between the sixth and seventh orders, as we expect. There is disagreement, however, with the observed facts in the following respects. The structure factor is found to diminish continuously from the first to about the fourth order, and then to rise to a figure which is near the possible maximum (all atoms in phase) at the seventh order. Actually there is observed a slight increase in intensity at the third order with respect to the second order. Further, the second observed maximum at the seventh order is not nearly the possible maximum, because much stronger reflections can be found from neighbouring planes with nearly as large spacings, *e.g.*, the (407). We cannot improve matters by varying the value of t around the figure 1·28. Such changes only shift the principal maximum away from the seventh order. We must conclude that u and u' differ appreciably from zero. Similar arguments can be applied to anthracene, with the same results.

In order to obtain a first approximation to the structure there are a number of models which we might consider, as, for example, a simple dipole model, in which the crystal unit would consist of only one row of scattering centres defined by the co-ordinates u and v. It is easier, however, to consider a structure in which there is only one parameter to vary. This may be done by making use of a simple hexagon model, in which the radius of the hexagon rings, and the distance from centre to centre around the rings, is denoted by r. Comparison with fig. 4 shows that

$$t = \tfrac{1}{2}\sqrt{3}r.$$

If ψ is the angle which the plane of the flat hexagon makes with the *ac* plane (compare fig. 5) then

$$u' = 2u = r\cos\psi,$$
$$v' = 2v = r\sin\psi.$$

The approximate value we have obtained for t can be used to calculate r. The only unknown quantity which remains is ψ. On varying ψ from 0° to 60° calculation shows that in the neighbourhood of 30° a fairly good general agreement is obtained between the values of the structure factor and the intensity variations for certain groups of $\{h1l\}$ planes. The groups of planes selected for calculation have closely similar spacings and the reflections all occur within a region of about 2 mm. on the photographic film. The method will be illustrated in the next section. It is sufficient at present to state the values of u, u', v and v' corresponding to $t = 1\cdot28$ and $\psi = 30°$, and employ these as a first rough approximation. From the relations given above we find

$$u = 0\cdot64 \text{ A.U.} \qquad u' = 1\cdot28 \text{ A.U.}$$
$$v = 0\cdot37 \text{ A.U.} \qquad v' = 0\cdot74 \text{ A.U.}$$

These results apply to both naphthalene and anthracene.

It may be stated here that, making independent variations in the parameters, the result of a good deal of further computation with various sets of reflections show that the value of u (referring to the first row of centres) probably does not differ much from the value given above by the hexagon model. A somewhat larger value is generally indicated. It is found, similarly, that not much improvement can be obtained by changing the value of v' (referring to the second row); and the approximate values, $u = 0\cdot74$ and $v' = 0\cdot80$ A.U. are used in the following discussion for the further calculation of the remaining variables u' and v. Other values of u and v' around 0·74 and 0·80 A.U. have, of course, been tested, but for brevity detailed reference to these calculations is omitted, the method, in general, being that used in the next section.

6. *Detailed Examination of the Parameters in the General Structure Factors.*

We may now try to make a more general determination of the values of the remaining unknown quantities in the structure factor expressions in a way which is not dependent upon any particular model. The approximations so far obtained will serve to limit the ranges of the parameters which need be discussed.

First consider the $\{h00\}$ planes. The structure factors reduce to expressions which contain only u and u'. For naphthalene we have

$$S'_{h00} = \cos Au \,.\, [\tfrac{1}{2}\gamma + 1] + \cos Au' \qquad (10\text{A})$$

and for anthracene

$$S'_{h00} = \cos Au \,.\, [\gamma + 1] + \tfrac{3}{2} \cos Au', \qquad (12\text{A})$$

h being always even. The value of γ can be taken as 6/7.

Unfortunately, owing to the halving, not much of data is available in this series of reflections (orders of the (200)). In both naphthalene and anthracene we find a strong (200), and a very much weaker (400). In naphthalene the (600) is at least as strong as the (400), while in anthracene the (600) is certainly stronger, probably two or three times as strong, as the anthracene (400). Bearing in mind the very rapid diminution of the intensity of reflection with increasing angle of incidence, we might expect that while the value of the structure factor for the (400) should be less than for the (200), the value for the (600) should be considerably greater, in both cases.

The following table gives the square of the structure factor for varying values of u' ($u = 0{\cdot}74$ A.U.) for naphthalene.*

Naphthalene.

Square of Structure Factor.

		200 v.s.	400 w. +.	600 w. +.
u' ↓	1·28	17	326	3
	1·35	28	219	26
	1·40	36	155	69
	1·45	44	106	137
	1·50	52	71	228
	1·55	59	45	335
	1·60	65	28	462
	1·65	69	17	562

We see that there is reasonable agreement with the observed results when u' is in the region of 1·55 A.U. This is considerably greater than the value obtained from the hexagon model, viz., $u' = 1{\cdot}28$ A.U. However, we obtain confirmation of this high value from the corresponding calculations for anthracene, using (12A). The results are given below.

---

* Before squaring, the structure factors are multiplied by a constant factor f in order to make the possible maximum (all atoms in phase) equal to 1000. For naphthalene, $f = 13{\cdot}0$, and for anthracene, $f = 9{\cdot}4$.

Anthracene.

Square of Structure Factor.

		200 v.s.	400 v.w.	600 w.
u'	1·28	26	299	0
↓	1·35	40	190	14
	1·40	51	125	52
	1·45	62	78	120
	1·50	72	46	214
	1·55	80	25	328
	1·60	88	11	462
	1·65	93	5	574

The weaker (400), as compared with naphthalene, is predicted by these results. A similar value of u', probably about 1·55 A.U., will account for the observed intensity variation.

In making use of this general method of obtaining approximate values for the parameters, it must be clear that we can only hope to obtain an account of the more outstanding variations in the intensities of sets of related reflections. Exact intensity measurements are not available; and if they were, the various corrections which would have to be applied are to a large extent unknown. Bearing these limitations in mind, we can proceed to check our results by calculating the structure factor for the orders of the (001) reflection and certain other $\{h0l\}$ reflections. These calculations only involve the quantities we have already approximately determined, viz.:—

$$t = 1 \cdot 28 \text{ A.U.}, \quad u = 0 \cdot 74 \text{ A.U.}, \quad u' = 1 \cdot 55 \text{ A.U.}$$

For naphthalene we have

$$S'_{h0l} = \cos Au \,.\, [\tfrac{1}{2}\gamma + \cos 2Ct] + \cos Au' \,.\, \cos Ct \qquad (10\text{B})$$

and for anthracene

$$S'_{h0l} = \cos Au \,.\, [\gamma \,.\, \cos Ct + \cos 3Ct] + \cos Au' \, [\tfrac{1}{2} + \cos 2Ct] \qquad (12\text{B})$$

as h is always even owing to the space group halving.

For the orders of the cleavage plane we get the following results:—

Naphthalene.			Anthracene.		
Order.	Observed intensity.	Square of structure factor.	Order.	Observed intensity.	Square of structure factor.
001	v.s.	59	001	v.s.	33
002	s.	22	002	m.s.	13
003	s.+	215	003	w.m.	8
004	m.s.	162	004	m.	241
005	abs.	4	005	w.m.	131
006	w.—	50	006	v.w.	0
007	w.+	79	007	abs.	13
008	v.w.	54	008	v.w.—	10
009	v.w.	17	009	v.w.	18

Our structure thus accounts for the strong first maximum at the third and fourth orders, and the weaker secondary maximum at the seventh and ninth orders in naphthalene and anthracene respectively. The value of the structure factor for the first few orders, however, appears to be rather small. The results can be somewhat improved by using a slightly smaller value for u'. But the general agreement is probably as good as we can expect.

It has already been observed that among the $\{h07\}$ and $\{h09\}$ planes in naphthalene and anthracene, a very strong maximum of intensity occurs at the ($40\bar{7}$) and ($40\bar{9}$) reflections. This result can now be examined by calculating the structure factor for these planes. As the reflections no longer constitute successive orders of a given plane, the comparison is less reliable. But we expect the relatively great strength of the reflections from the ($40\bar{7}$) and ($40\bar{9}$) planes in naphthalene and anthracene to be accounted for by an extra large structure factor. The results are set out below.

Naphthalene.				Anthracene.			
hkl.	*d.*	Intensity observed.	Square of structure factor.	*hkl.*	*d.*	Intensity observed.	Square of structure factor.
007	1·04	w. +	77	009	1·02	v.w.	18
$20\bar{7}$	1·19	w.+	0	$20\bar{9}$	1·17	w.	65
$40\bar{7}$	1·24	m.s.	795	$40\bar{9}$	1·24	m.	853
$60\bar{7}$	1·15	m.	160	$60\bar{9}$	1·17	w.m.	88

The general agreement is again good. We cannot expect to be able to account for the intensity variations in weak reflections with any degree of accuracy in such sets of planes. It may be noted here, however, that for a number of naphthalene $\{h0l\}$ planes, some of which give strong reflections, the structure factor does not explain the intensity variations. Thus for the ($20\bar{1}$), which is a natural face on the crystal, and gives a strong reflection, the value of the squared structure factor is as low as 7. This plane, of course, has a large spacing, and the small angle of incidence will cause a very great relative enhancement of the observed intensity compared to planes like those discussed above. Other strong reflections from planes with large spacings like the (001) have also comparatively small structure factors. These difficulties will be referred to again.

We have not yet discussed the parameters v and v' which define the position of the rows of scattering centres with respect to the b axes of the crystals. The determination of these quantities is more difficult, because owing to the shorter *b* axis we have less data concerning reflections from planes involving the *k* index. Thus we observe a moderately strong reflection from the (020) plane in naphthalene and anthracene, but no higher orders are recorded with certainty. The spacings of these higher orders are so small that the observations must be doubtful in any case, with the present experimental technique.

The result of a considerable amount of computation regarding the general $\{hkl\}$ planes, however, leads to the conclusion that v' probably does not differ much from the hexagon model value at $\psi = 30°$, viz., $v' = 0{\cdot}80$ A.U. Adopting this value for v' we may try and find what value of v will explain some outstanding intensity variations in the $\{h10\}$ and $\{h20\}$ reflections in naphthalene and anthracene. In the case of both crystals there is a prominent maximum of intensity at the (410) and (320) reflections. The following table gives the square of the structure factor for naphthalene $\{h10\}$ planes for varying values of v. ($v' = 0{\cdot}80$.)*

Naphthalene.

		110 v.s.+.	210 s.	310 w.m.	410 m.s.	510 w.
v	$+0{\cdot}3$	240	81	137	14	111
↓	± 0	262	12	146	42	130
	$-0{\cdot}3$	240	5	137	85	111
	$-0{\cdot}5$	203	40	123	118	80
	$-0{\cdot}7$	156	75	102	152	44

We see that when $v \doteq -0{\cdot}7$ A.U. we get a reasonable account of the intensity distribution. (The negative sign means that A, in fig. 5, lies in the upper quadrant to the left of the origin.)

For the $\{h20\}$ planes the results are as follows :-

Naphthalene.

		120 s. ?.	220 m.	320 m.s.	420 v.w.
v	$+0{\cdot}3$	378	25	1	205
↓	± 0	162	34	123	306
	$-0{\cdot}3$	36	25	441	205
	$-0{\cdot}5$	8	13	663	85
	$-0{\cdot}7$	2	3	780	7

---

* The general expressions (10) and (11) for naphthalene, and (12) and (13) for anthracene, are used for these calculations, putting C = 0. We must, of course, employ the values of u and u' already found. It is unfortunately not possible to make a completely independent determination of v owing to the absence of reliable data on the (020) series of reflections referred to above.

In this case there is reasonable agreement when $v \doteqdot -0\cdot 3$ A.U. It should be noted that when reflections like the (120) or (021) are recorded on rotation photographs about the b axis, a correction ought to be applied to the observed intensity to compensate for the relatively longer time during which the plane is in a reflecting position in the course of a rotation, compared to reflections from planes of larger ξ, lying further out on the film. No such correction has been attempted on the present rough estimates of intensity.

The results for anthracene are very closely similar. In the case of the $\{h10\}$ planes we find $v \doteqdot 0\cdot 7$ A.U. as before.

Anthracene.

		110 v.s.+.	210 v.s.	310 w.+.	410 m.s.	510 v.w.
v	$-0\cdot 5$	188	22	88	125	56
↓	$-0\cdot 7$	146	57	73	159	29

But the $\{h20\}$ planes point to the smaller value, $v \doteqdot -0\cdot 3$ A.U.

Anthracene.

		120 s. ?.	220 m.	320 m.s.	420 abs.
v	$-0\cdot 3$	56	23	458	182

It may be added that when v' is given other values in the neighbourhood of $0\cdot 8$ A.U., v still always requires some small negative value to account for the intensities of these reflections.

The values $v' = 0\cdot 8$ and $v = -0\cdot 3$ A.U. predict a moderately strong (020) with rapidly decreasing higher orders in naphthalene and anthracene, which is confirmed by the available data. Larger negative values of v greatly enhance the (040) and (060) with respect to the (020). We are thus led to favour the smaller negative value in these determinations of v, viz., $v = -0\cdot 3$ A.U. The calculations for the $\{0k0\}$ series with this value of the parameter are given below, p. 564. ($v' = 0\cdot 8$ A.U.)

In this way we are led to the following values for the parameters in the case of both naphthalene and anthracene, as determining the best approximation that can be obtained under the limitations of uniformity assumed on p. 551.

$$u \doteqdot 0\cdot 74\,; \quad u' \doteqdot 1\cdot 55\,; \quad v \doteqdot -0\cdot 3\,; \quad v' \doteqdot 0\cdot 8\,; \quad t \doteqdot 1\cdot 28\,;$$

	Naphthalene.			Anthracene.	
	Intensity observed.	Square of structure factor.		Intensity observed.	Square of structure factor.
020	m.s.	182	020	m.s.	162
040	w. or abs.	49	040	w. or abs.	71
060	w. or abs.	2	060	w. or abs.	1
080	*	12	080	*	1

* Beyond experimental limits.

all the values being expressed in A.U. It should be noted that in no case do the intensity variations in any of the sets of reflections discussed above lead us to assume a value for any of these quantities for naphthalene which differs from the corresponding value found for anthracene. The structures may be assumed to be alike, within the experimental limits of this investigation.

We may conclude by applying the data to the calculation of the structure factor for some groups of general {*hkl*} planes, which, while not having two indices in common, yet occupy not very dissimilar positions in the crystal, and whose spacings are practically identical. These groups of planes all reflect within regions of about 2 mm. on the photographic film, and while the reflections overlap on a rotation photograph, they can be separated and estimated from the oscillation photographs. These and similar groups of general planes were used for obtaining the best first approximation with the hexagon model. We cannot, of course, put much weight on the results for the weaker reflections, and can only look for a very general type of agreement. (See p. 565.)

It will be seen that there is a fairly general agreement with the observed results except in the case of the {*hkl*} and {*hkl*} planes. The structure factor for these planes must usually be small owing to the low values of the C terms when $l = 1$ (*cf.* Tables IV and V). Yet a number of these planes give relatively strong reflections. There does not seem to be any simple way of overcoming this difficulty in terms of our present conception of the structure. The discrepancies may have to be put down to the operation of the several unknown factors which enter into the expression for the intensity of reflection, or we may require to make a small departure from the assumption that the scattering centres forming the crystal unit are grouped in two rows. A discussion of these questions is beyond the scope of this paper, the purpose of which is to give the best approximation that can be obtained under the limitation of the uniformity which we have assumed and already defined.

Naphthalene.

hkl.	*d.*	Intensity observed.	Square of structure factor.	*hkl.*	*d.*	Intensity observed.	Square of structure factor.
$21\bar{3}$	2·56	m.	43	$22\bar{3}$	2·06	s.+	169
$11\bar{3}$	2·54	s.	61	$12\bar{3}$	2·05	m.+	140
$31\bar{2}$	2·49	abs.	1	$32\bar{2}$	2·03	w.	2
112	2·45	w.+	1	122	2·00	v.w.	4
$31\bar{1}$	2·45	s.	26	$32\bar{1}$	2·00	m.s.	12
211	2·41	v.w.	7	221	1·98	m.	1

Anthracene.

hkl.	*d.*	Intensity observed.	Square of structure factor.	*hkl.*	*d.*	Intensity observed.	Square of structure factor.
$31\bar{2}$	2·58	v.w.	6	$32\bar{2}$	2·07	w.	0
$21\bar{4}$	2·54	w.+	14	$22\bar{4}$	2·05	m.s.	164
$31\bar{3}$	2·52	v.m.	2	$32\bar{3}$	2·04	w.	3
211	2·52	abs.	3	221	2·04	w.m.	0
$11\bar{4}$	2·47	m.s.	61	$12\bar{4}$	2·01	m.—	231
$31\bar{1}$	2·44	m.s.	14	$32\bar{1}$	2·00	m.s.	8
$31\bar{4}$	2·32	*m.*	113	$32\bar{4}$	1·93	m.—	353

7. *Discussion of Results.*

We may now record our results by means of a few diagrams, drawn to scale. Fig. 6 shows the relation of five molecules viewed along the c axis, the centre one being the inversion of the others (a BC molecule). The small black points represent the positions of the rows of scattering centres in naphthalene and anthracene, obtained from the final value we found for the parameters, viz. :—

$$u = 0{\cdot}74\,; \quad u' = 1{\cdot}55\,; \quad v = -0{\cdot}3\,; \quad v' = 0{\cdot}8\,; \quad t = 1{\cdot}28 \text{ A.U.}$$

The small open circles are inserted for comparison, and represent the position of the centres of the carbon atoms in the remarkable structure put forward by Bragg for these compounds (‘X-rays and Crystal Structure’, 1925, p. 238). This structure is the end view of the strictly tetrahedral carbon-ring structure found in diamond, the distance of approach of the carbon centres being that of graphite, 1·50 A.U. When we consider the approximation we have made in treating the carbon and hydrogen atom together as one scattering centre for X-rays, there seems little doubt that Bragg's structure is essentially correct. In terms of the equations used in this paper the parameters of Bragg's structure (referring to the centres of the carbon atoms) are

$$u = 0\cdot75\,;\quad u' = 1\cdot25\,;\quad v = 0\,;\quad v' = 0\cdot71\,;\quad t = 1\cdot23 \text{ A.U.}$$

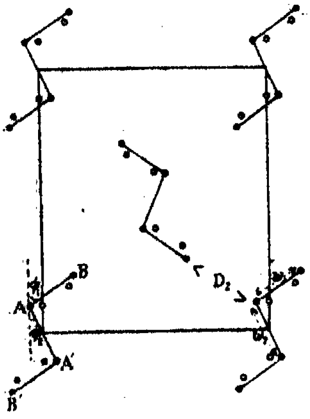

FIG. 6.

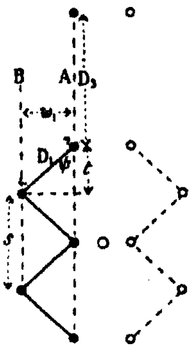

FIG. 7.

Fig. 7 is a side view of the chain structure in the naphthalene crystal unit, the projection being in the plane of the chain. The molecule, $C_{10}H_8$, consists of two such units, the second (shown in broken lines) being obtained by an inversion through the centre of symmetry at O.

It is interesting to examine the dimensions of the crystal unit and molecule, which can readily be calculated from the values of the parameters given above, and to compare the results with the corresponding dimensions found by Müller for the long chain hydrocarbon $C_{29}H_{60}$. For convenience Müller's notation is used in these diagrams; the meaning of the symbols will be clear from inspection. ω_1, the distance between two rows in the crystal unit (A and B) may be compared with Müller's ω. We require a second symbol, ω_2, to denote the distance, measured through the centre of symmetry, between the inner two rows in neighbouring crystal units of any one molecule (A and A'). Similarly, for the angle between the plane of the two rows and the symmetry plane of the crystal, ϕ_1 refers to the two rows A and B in the crystal unit, and ϕ_2 to the two rows in neighbouring units across the centre of symmetry (A and A'). Perhaps neither of these angles can be compared with Müller's ϕ, where the hydrocarbon molecule consists of two rows only. The following relations can be readily deduced, remembering that (u, v) and (u', v') are the co-ordinates of A and B respectively, referred to the origin 0, and the a' and b axes.

$$s = 2t$$

$$\omega_1 = \sqrt{\{(u - u')^2 + (v - v')^2\}}$$

$$\omega_2 = 2\sqrt{\{u^2 + v^2\}}$$

$$D_1 = \sqrt{\{t^2 + \omega_1{}^2\}}$$

$$D_2 = \sqrt{\{(\tfrac{1}{2}a \sin \beta - u - u')^2 + (\tfrac{1}{2}b + v - v')^2\}}$$

$$D_3 = c - 4t \text{ (naphthalene)}$$

$$= c - 6t \text{ (anthracene)}$$

$$\psi = \text{arc tan } (\omega_1/t)$$

$$\text{Zig-zag angle} = (180^\circ - 2\psi)$$

$$\phi_1 = \text{arc tan } \{(v - v')/(u - u')\}$$

$$\phi_2 = \text{arc tan } (v/u)$$

$$\text{Angle of “ warp ” in molecule} = 180^\circ - (\phi_1 + \phi_2).$$

In the following summary the values calculated for these quantities for naphthalene and anthracene are given (they are the same for the two crystals unless otherwise stated). The figures which follow in square brackets with prefix *M* are Müller's corresponding determinations for the long-chain hydrocarbon $C_{29}H_{60}$. It should be pointed out that our figures are probably subject to uncertainties at least as great as those mentioned by Müller, although they are given here in the form of the best approximations. The uncertainty is greatest for the quantities involving v and v'. Owing to the method we adopted of selecting the best values of the parameters required to explain the chief features in the intensities for given series of reflections, it is not easy to state the precise limits for our determinations.

Distance between two consecutive scattering centres on either row of the crystal unit :—

$$s = 2 \cdot 56 \text{ A.U.} \quad [M \quad s = 2 \cdot 537 \text{ A.U. error approx. } \tfrac{1}{2} \text{ per cent.}]$$

Distance between two consecutive centres in the chain :—

$$D_1 \doteqdot 1 \cdot 9 \text{ A.U.} \quad [M \quad 2 \cdot 0 > D_1 > 1 \cdot 8 \text{ A.U.}]$$

Distance between two rows in the molecule :—

$$\left.\begin{array}{l} \omega_1 \doteqdot 1 \cdot 37 \text{ A.U.} \\ \omega_2 \doteqdot 1 \cdot 60 \text{ A.U.} \end{array}\right. \quad [M \quad 1 \cdot 6 > \omega > 1 \cdot 2 \text{ A.U.}]$$

Zig-zag angle :—

$$(180^\circ - 2\psi) \doteqdot 86^\circ. \quad [M \quad 76^\circ < (180^\circ - 2\psi) < 92^\circ.]$$

(Tetrahedral value of the zig-zag angle $= 109\tfrac{1}{2}^\circ$.)

Angle between the plane of two rows and the symmetry plane in the crystal :—

$$\begin{matrix} \phi_1 \doteqdot 54^\circ \\ \phi_2 \doteqdot 22^\circ \end{matrix} \quad [M \quad 23^\circ < \phi < 30^\circ]$$

Angle of "warp" in the molecule :—

$$180^\circ - (\phi_1 + \phi_2) \doteqdot 104^\circ. \quad (\text{Tetrahedral value} = 125\tfrac{1}{4}^\circ.)$$

Distance of nearest approach between two centres on two neighbouring molecules (placed sideways) :—

$$D_2 \doteqdot 2\cdot 3 \text{ A.U.} \quad [M \quad 3\cdot 6 < D_2 < 3\cdot 9 \text{ A.U.}]$$

Distance of nearest approach between two centres on two neighbouring molecules (placed end to end) = gap between the ends of two consecutive molecules in the crystal (measured in the direction of the c axis).

$$\begin{matrix} D_3 \text{ (naphthalene)} = 3\cdot 56 \text{ A.U.} & [M \quad D_3 \doteqdot 4\cdot 0 \text{ A.U.} \\ D_3 \text{ (anthracene)} = 3\cdot 50 \text{ A.U.} & \text{gap} = 3\cdot 09 \text{ A.U.}] \end{matrix}$$

The close relations between many of the dimensions of the crystal units of naphthalene and anthracene and those of the hydrocarbon $C_{29}H_{60}$ are quite remarkable when we consider how different the substances are in their crystalline form and chemical constitution. These relations seem to afford strong evidence that the tetrahedral properties of the carbon atom are maintained in aromatic structures.

8. *Summary.*

1. The crystal structures of naphthalene and anthracene have been examined in detail by the rotating crystal photographic method, and approximate estimates of intensities made. The results are classified in Tables I to III.

2. The space group is C_{2h}^5 in each case, the unit cells containing two molecules, which therefore possess a centre of symmetry. The geometrical structure factor in its general form is developed for these conditions.

3. General and statistical considerations of the reflections indicate a periodic structure parallel to the c axes of the crystals, and an estimate of the periodicity is made. It is also shown that the scattering centres lie nearer the ac than the

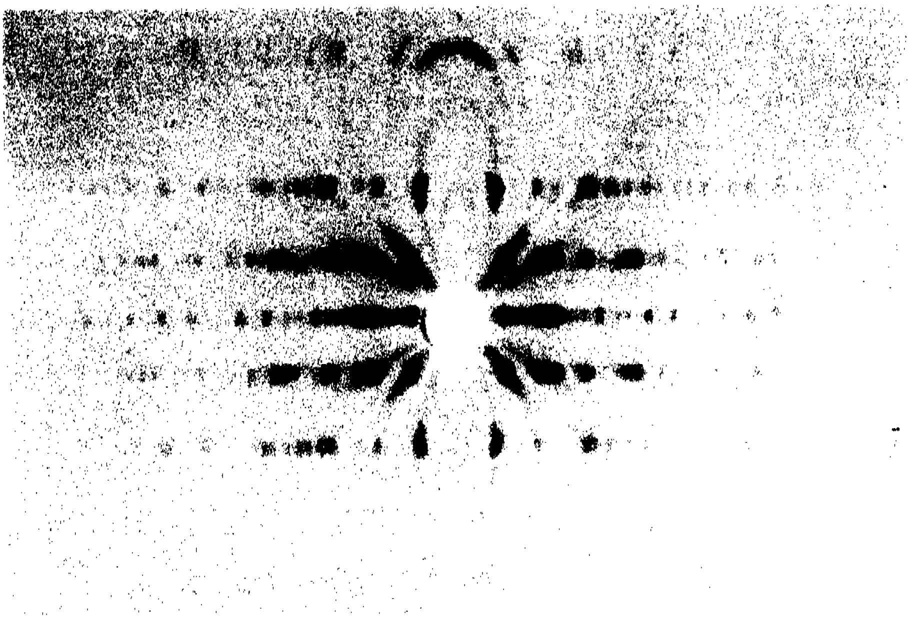

Naphthalene—Rotation about *b* axis.

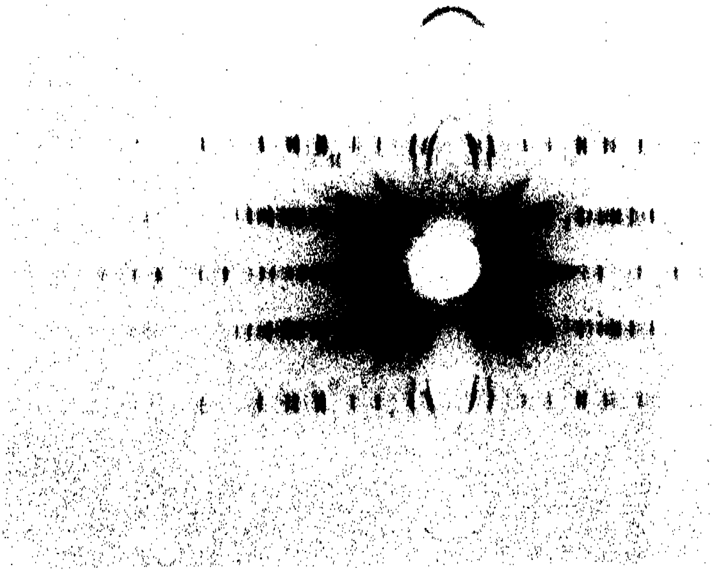

Anthracene—Rotation about *b* axis.

(Facing p. 508.)

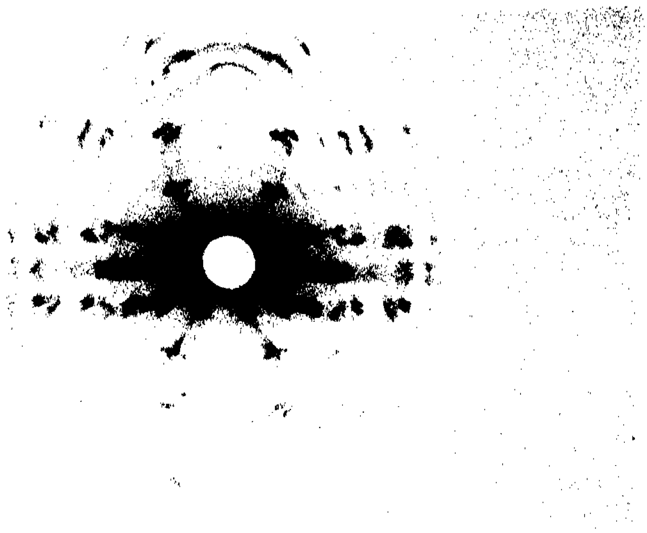

Naphthalene—Rotation about *c* axis.

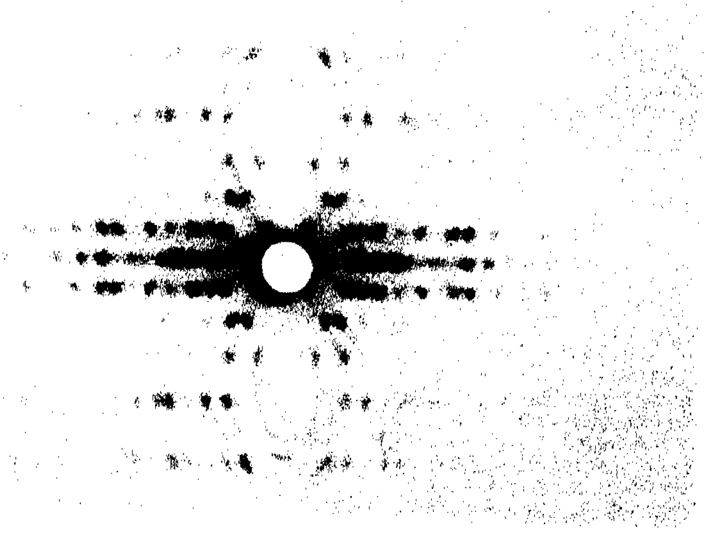

Anthracene—Rotation about *c* axis.

be planes, but no simple structure with a plane of symmetry parallel to the *ac* plane is possible.

4. The assumption is then made that the scattering centres (each regarded as consisting of a carbon atom and its attendant hydrogen atom if any) lie in two uniform rows parallel to the *c* axes of the crystals, thus forming a chain-like structure. With this limitation of the parameters it is possible to develop a compact geometrical structure factor for the general case of *n* scattering centres.

5. The special cases of naphthalene and anthracene are discussed in relation to some simple models, and results are obtained which serve to limit the range of the parameters for the general discussion.

6. Detailed examination of the parameters is made, and the values found which give the best account of the intensity variations in the principal spectra of naphthalene and anthracene, independently of any model structure, the only limitation being the assumption of uniformity in 4. The two structures are found to be the same, within the limits of experimental error.

7. The dimensions and relations of the molecules of naphthalene and anthracene, as calculated from the final values of the parameters, are found to differ only slightly from those of Bragg's tetrahedral structure. The chain structure is further shown to be very closely similar in many of its dimensions to the chain structure of the hydrocarbon $C_{29}H_{60}$, as determined by Müller. Evidence is thus afforded that the tetrahedral properties of the carbon atom are maintained in these aromatic structures.

In conclusion I again wish to express my thanks to Sir William Bragg for his unfailing encouragement and interest in the whole of this work, and for the facilities placed at my disposal in the Royal Institution for carrying it out. Among my co-workers at the Davy Faraday Laboratory I am particularly indebted to Dr. Müller for his valuable advice on many points. To the Carnegie Trust and the Commonwealth Fund I am indebted for fellowships which made it possible for me to carry out the work, and to the Chemical Society for a grant.

The Spark Spectrum of Thallium, Tl II.—Term Analysis.—Fine Structure of Lines.[*]

By Prof. J. C. McLennan, F.R.S., A. B. McLay, Ph.D., and M. F. Crawford, M.A.

(Received September 4, 1929.)

The spectral structure of Thallium II was investigated last year by Smith,[*] by Rao, Narayan and Rao, and by McLennan, McLay and Crawford.[†] The $6s^2\,{}^1S$, $6s7s\,{}^{3,1}S$, $6s6p\,{}^{3,1}P$ and $6s6d\,{}^{3,1}D$ terms were established by Smith and the authors with exact agreement. Rao, Narayan and Rao found these triplet terms, also $6s5f\,{}^3F^0$, and tentatively $6s^2\,{}^1S_0$ and $6s7p\,{}^3P_2{}^0$. In all three communications the location of one or more components of a $6p^2\,{}^3P$ term was suggested.

The term notation used above was proposed by Russell, Shenstone and Turner.[‡] It has been employed throughout this paper.

The authors' study of the thallium spark spectrum was confined previously to the ultra-violet region. It was continued this year in that, in the visible and in the near infra-red regions. Spectra of the spark in air between thallium metal electrodes were photographed from λ 8500 A. to λ 1850 A. with Hilger glass and quartz prism spectrographs. The introduction of variable inductance in the secondary of the spark circuit served, in a manner already described, to facilitate the differention of Tl^+ lines and those of neutral or more highly ionised atoms. Spectra of a condensed oscillatory discharge between aluminium terminals in an evacuated quartz tube that contained heated thallium vapour were photographed also from λ 7000 A. to λ 2100 A. Hilger E.1 spectrographs, one with a glass and one with a quartz optical train, were employed. The Tl^+ lines in the discharge tube spectra could be readily distinguished from others by their behaviour with change of pressure in the tube.

---

[*] [Mr. Crawford was enabled to participate in this investigation through the award of a studentship to him by the National Research Council of Canada, and I desire to record my thanks to the Council for a grant in aid of this investigation.—J. C. McL.]

[†] Smith, 'Proc. Nat. Acad. Sci.,' vol. 14, p. 951 (1928); Rao, Narayan and Rao, 'Ind. J. Phys.,' vol. 2, p. 467 (1928); McLennan, McLay and Crawford, 'Trans. R. Soc. Can.,' vol. 22, p. 241 (1928).

[‡] 'Phys. Rev.,' vol. 33, p. 900 (1929).

The wave-lengths of the spark in air were very broad and often quite diffuse in character. But most of those of the tube discharge were exceptionally sharp and admirably suited for measurement. Lines of Tl^+ between λ 7000 A. and λ 2100 A. were measured therefore on plates taken when the latter source was used. Neon and iron international standard lines and copper spark lines* were chosen for comparison wave-lengths from which dispersion formulæ were calculated. Lack of coincidence between the spectrum of the light from the thallium tube and that of the source of standard lines was evident on most of the plates. But carbon, cadmium and mercury† impurity wave-lengths were identified in the thallium spectrum and were measured. The differences between our measured values of these and the best accepted ones for them were used in plotting a correction curve. It was quite smooth over the whole wave-length range studied. It is believed, therefore, that the corrected wave-numbers of the thallium lines are accurate probably to within 0·2 cm.$^{-1}$. Wave-lengths of the spark in air from λ 7000 A. to λ 2100 A. were measured also from argon‡ comparison lines, and one below λ 2100 A. from copper spark lines. The accuracy of measurement is questionable, but the error in the wave-numbers should not exceed 1 or 2 cm.$^{-1}$.

In the course of the research a very important feature of the thallium spark spectrum was noticed, namely, fine structure of many of its lines. The resolution into components of a few intense ones was first observed in the spectrum of the spark when large inductance was used. But much clearer patterns were obtained for these and for many of the lines of medium intensity on the plates taken when the discharge tube was used as a source. The magnitudes of the line separations in numerous cases were found to be much greater than any reported on hitherto in an atomic spectrum. Since the spectrographs we were using were not suited for special investigation of fine structure of lines the results are probably far from being complete yet. But some interesting and fairly certain conclusions have been drawn already from a consideration of the line patterns that have been obtained up to the present. They will be put forward after a discussion of the ordinary term structure, whose analysis was primarily the object of the research.

---

* Shenstone, 'Phys. Rev.,' vol. 29, p. 380 (1927).

† Carbon—Fowler and Selwyn, 'Roy. Soc. Proc.,' A, vol. 120, p. 312 (1928); cadmium—Cd I, Kayser, "Hauptlinien," 1926, and Cd II, Salis, 'Ann. Physik,' vol. 76, p. 145 (1925); mercury—Hg I, Kayser, "Hauptlinien," 1926, and Hg II, Paschen, 'Sitz. Preuss. Akad. Wiss.,' 1928, p. 536.

‡ Meissner, 'Z. Physik,' vol. 39, p. 172 (1928).

All the evaluated energy levels of Thallium II (disregarding fine structure) with their designations, the n^* values of representative $6snx$ terms, and the triplet term intervals are given in Table I. The classified wave-lengths, with observed fine-structure components and their intensities, and the intensity sum for each term combination are recorded in Table II. The unweighted mean wave-number of each multiple line was used in the calculation of term values. The ionisation potential, $6s^2\,{}^1S$—$6s\,{}^2S$ was estimated to be approximately 165,700 cm.$^{-1}$ or 20·5 volts for Tl II by applying a simple Rydberg formula to the two members of the $6snd\,{}^3D$ series. This value is probably very nearly correct, since the corresponding ^3D terms of the iso-electronic Hg I* are almost Rydbergian. The Rydberg denominators (n^* values) given in Table I were arrived at by taking the absolute value of $6s^2\,{}^1S$ to be 165,700.

Table I.

Level.	
$6s^2\,{}^1S_0$	0
$6s6p\,{}^3P_0^0$	49452*
$6s6p\,{}^3P_1^0$	52393*
$6s6p\,{}^3P_2^0$	61726*
$6s6p\,{}^1P_1^0$	75661
$6s7s\,{}^3S_1$	105226
$6s7s\,{}^1S_0$	107997
$6s6d\,{}^1D_2$	115161
$6s6d\,{}^3D_1$	116147*
$6s6d\,{}^3D_2$	116431*
$6s6d\,{}^3D_3$	116828*
$6p^2\,{}^3P_0$	117408*
$6s7p\,{}^3P_0^0$	119362*
$6s7p\,{}^3P_1^0$	119577*
$6s7p\,{}^3P_2^0$	122030*
1_1^0	·122380
$6p^2\,{}^3P_1$	125338*
$6s7p\,{}^1P_1^0$	126205
$6p^2\,{}^1D_2$	128818
$6s5f\,{}^3F_3^0$	136116*
$6s5f\,{}^3F_2^0$	136216*
$6s5f\,{}^3F_4^0$	136231*
$6s5f\,{}^1F_3^0$	136264
$6s7d\,{}^1D_2$	136892
$6s7d\,{}^3D_1$	137928*
$6s7d\,{}^3D_2$	138054*
$6s7d\,{}^3D_3$	138205*

Intervals (higher J's first).		
$6s6p\,{}^3P^0$	9333	2941
$6s7p\,{}^3P^0$	2453	215
$6s6d\,{}^3D$	397	284
$6s7d\,{}^3D$	151	126
$6s5f\,{}^3F$	115	−100
$6p^2\,{}^3P$	……..	7950

N* of 6sN*x* Terms.

	$n = 6$.	$n = 7$.
$^3S_1$		2·694
$^1S_0$	1·628	2·758
$^3P_1^0$	1·968	3·085
$^1P_1^0$	2·208	3·334
$^1D_2$	2·947	3·904
$^3D_2$	2·985	3·985
$^3F_2^0$	3·852	
$^1F_3^0$	3·860	

There can be little doubt that the Tl II terms given in Table I have been identified correctly. All the classified lines in Table II, except the faintest ones and some below λ 1600 A., were proved to be Tl^+ ones by excitation experiments. The irregular doublet law applies quite well to the $6s^2$—$6s6p$, $6s6p$—$6s6d$, $6s6p$—$6p^2$ and $6s7s$—$6s7p$ transitions of Hg I, Tl II and Pb III.* The progression of the n^* values in each of the $6snx$ series is qualitatively similar to that in the corresponding series of Hg I, with a single exception in the case of the $6snp\,^1P^0$ one. But the reality of $6s7p\,^1P^0$ of Hg I is very questionable. $6s5f\,^3F$ is partially inverted in Tl II, as it is in Pb III. The $^3P_2$ and $^1S_0$ terms that should complete the $6p^2$ group have not been identified. The apparent absence of $6s6p\,^3,\,^1P^0$—$6p^2\,^3P_2$ combinations is especially peculiar but constitutes an anomalous feature that has been encountered in the analogous Zn I, Cd I, Hg I and Pb III spectra.† The term designated $1_1{}^0$ in Table I should be either $^3P_1{}^0$, $^1P_1{}^0$ or $^3D_1{}^0$ of the complex group $5d^9\,6s^2\,6p$. The intensities of its combinations support the first-mentioned choice.

---

* Fowler, "Series in Line Spectra" (1922); Paschen-Goetze, "Seriengesetze in Linienspectren" (1922); Sawyer, 'J.O.S.A. & R.S.I.,' vol. 13, p. 431 (1926).

The fine structure of Thallium II lines will be considered now in some detail. It will be seen from Table II that a number of them were resolved into components. The values of the wave-numbers indicate that resolution was obtained apparently only when the separations were 1 cm.$^{-1}$ or greater.

A few fine-structure term intervals were deduced directly by a wave-number analysis of the line components. Thus each of the terms $6s7s\,^3S_1$, $6s7p\,^3P_1{}^0$, $6s7p\,^3P_2{}^0$ and $6s7d\,^3D_1$ were found to be two-fold from two or more line patterns. The fact that the doublet separations were very large, 5·0, 4·0, 3·5 and 2·5 cm.$^{-1}$ respectively, tended to confirm the view that the maximum number of components for any of them was two. The moment I of Tl^+ atoms must be equal therefore to $\frac{1}{2}$, if the Back-Goudsmit‡ vector relation $F = J + I$ is valid. Here J is the usual resultant moment of the electrons, I is an intrinsic moment of the atom, that should be constant for all its electronic states, and F is the final resultant moment of the atom, each expressed in units of $h/2\pi$. The vector equation was deduced empirically by Goudsmit and Back from observed fine structure of Bi I lines. The selection rule $\Delta F = \pm 1$ or 0, with $0 \rightarrow 0$ forbidden also, in a transition was found by them to hold throughout in Bi I. It is subsidiary, of course, to the selection rules for J and L.

A number of fine structure patterns of Tl II have been interpreted on the basis that the vector relation was valid, that the selection rule for F was obeyed

---

* Rao, Narayan and Rao, *loc. cit.*

† Sawyer and Beese, 'Nature,' vol. 116, p. 936 (1925); Ruark, 'J.O.S.A. & R.S.I.' vol. 11, p. 199 (1925); Sawyer, 'J.O.S.A. & R.S.I.,' vol. 13, p. 431 (1925); Smith, 'Nature,' vol. 123, p. 566 (1929).

‡ 'Z. Physik,' vol. 43, p. 321 (1927) and vol. 47, p. 174 (1928).

Table II.

Author.	λ (I.A.).	ν.	I.	I (sum).	Classification.
Ml.	7072·7	14135	3	3	$6s7s\,{}^3S_1$ —$6s7p\,{}^3P_0^0$
,,	6968·52	14346·3	1	8	$6s7s\,{}^3S_1$ —$6s7p\,P_1^{0*}$
,,	6966·43	14350·6	6		
,,	6964·10	14355·4	1		
,,	6950·45	14383·6	5	5	$6s7s\,{}^1S_0^0$ — 1_1^0
,,	6888·85	14512·2	2	2	1_1 —$6s7d\,{}^1D_2$
,,	6727·2	14861	0	0	$6s7p\,{}^3P_2^0$—$6s7d\,{}^1D_2$
,,	6430·50	15546·6	1	1	1_1^0 —$6s7d\,{}^3D_1$
,,	6378·27	15673·9	2	2	1_1^0 —$6s7d\,{}^3D_2$
,,	6289·6	15895	0	0	$6s7p\,{}^3P_2^0$—$6s7d\,{}^3D_1$
,,	6239·46	16022·6	3	5	$6s7p\,{}^3P_2^0$— $6s7d\,{}^3D_2$*
,,	6238·49	16025·1	2		
,,	6181·44	16173·0	2	12	$6s7p\,{}^3P_2^0$—$6s7d\,{}^3D_3$*
,,	6180·09	16176·8	10		
,,	5950·77	16799·9	4	20	$6s7s\,{}^3S_1$ — $6s7p\,{}^3P_2^{0*}$
,,	5949·57	16803·3	9		
,,	5949·04	16804·8	7		
,,	5828·71	17151·7	5	8	$6s7s\,{}^3S_1$ — 1_1^{0*}
,,	5826·78	17157·4	3		
,,	5774·08	17314·0	3	5	$6s7p\,{}^3P_1^0$—$6s7d\,{}^1D_2$*
,,	5772·88	17317·6	2		
,,	5490·48	18208·3	8	8	$6s7s\,{}^1S_0$ —$6s7p\,{}^1P_1^0$
,,	5448·70	18347·9	3	4	$6s7p\,{}^3P_1^0$—$6s7d\,{}^3D_1$*
,,	5447·61	18351·6	0		
,,	5446·84	18354·2	1		
,,	5410·99	18475·8	5	8	$6s7p\,{}^3P_1^0$—$6s7d\,{}^3D_2$*
,,	5409·93	18479·4	3		
,,	5384·96	18565·1	3	5	$6s7p\,{}^3P_0^0$—$6s7d\,{}^3D_1$*
,,	5384·20	18567·7	2		
,,	5183·10	19288·1	3	6	$6s6d\,{}^3D_3$ —$6s5f\,{}^3F_3^0$
,,	5182·06	19292·0	3		
,,	5156·4	19388	0	0	$6s6d\,{}^3D_2$ —$6s5f\,{}^3F_2^0$
,,	5152·23	19403·7	20	20	$6s6d\,{}^3D_3$ —$6s5f\,{}^3F_4^0$
,,	5143·58	19436·3	3	3	$6s6d\,{}^3D_3$ —$6s5f\,{}^1F_3^0$
,,	5078·65	19684·8	20	20	$6s6d\,{}^3D_2$ —$6s5f\,{}^3F_3^0$
,,	5053·08	19784·4	3	6	$6s6d\,{}^3D_2$ —$6s5f\,{}^3F_2^0$
,,	5052·34	19787·3	3		
,,	5040·57	19833·5	2	2	$6s6d\,{}^3D_2$ —$6s5f\,{}^1F_3^0$
,,	4981·28	20069·6	18	18	$6s6d\,{}^3D_1$ —$6s5f\,{}^3F_2^0$
,,	4770·85	20954·8	2	3	$6s6d\,{}^1D_2$ —$6s5f\,{}^3F_3^0$
,,	4770·58	20956·0	1		
,,	4765·78	20977·1	6	10	$6s7s\,{}^3S_1$ —$6s7p\,{}^1P_1^{0*}$
,,	4764·62	20982·2	4		
,,	4748·01	21055·6	1	1	$6s6d\,{}^1D_2$ —$6s5f\,{}^3F_2^0$
,,	4737·12	21104·0	20	20	$6s6d\,{}^1D_2$ —$6s5f\,{}^1F_3^0$
,,	3381·74	29562·1	5	12	$6s6p\,{}^1P_1^0$—$6s7s\,{}^3S_1$*
,,	3381·12	29567·5	7		
,,	3091·66	32335·7	18	18	$6s6p\,{}^1P_1^0$—$6s7s\,{}^1S_0$
,,	2530·82	39501·0	7	16	$6s6p\,{}^1P_1^0$—$6s6d\,{}^1D_2$*
,,	2530·67	39503·4	9		
,,	2469·07	40488·8	4	7	$6s6p\,{}^1P_1^0$—$6s6d\,{}^3D_1$*
,,	2468·95	40490·8	3		
,,	2451·82	40773·7	4	10	$6s6p\,{}^1P_1^0$—$6s6d\,{}^3D_2$*
,,	2451·72	40775·3	6		
,,	2394·60	41747·9	4	4	$6s6p\,{}^1P_1^0$—$6p^2\,{}^3P_0$
,,	2298·16	43499·6	6	25	$6s6p\,{}^3P_2^0$—$6s7s\,{}^3S_1$*
,,	2298·08	43501·4	10		
,,	2297·88	43504·9	9		
,,	2012·27	49679	3	3	$6s6p\,{}^1P_1^0$—$6p^2\,{}^3P_1$

Table II—(continued).

Author.	λ (I. vac.).	ν.	I.	I (sum).	Classification.
M2.	1908·64	52393	20	—	$6s^2\,{}^1S_0$ —$6s6p\,{}^3P_1^0$
,,	1892·72	52834	16	—	$6s6p\,{}^3P_1^0$—$6s7s\,{}^3S_1$
,,	1881·15	53159	12	—	$6s6p\,{}^1P_1^0$—$6p^2\,{}^1D_2$
,,	1871·42	53435	4	—	$6s6p\,{}^3P_2^0$—$6s6d\,{}^1D_2$
,,	1837·55	54420	4	—	$6s6p\,{}^3P_2^0$—$6s6d\,{}^3D_1$
,,	1827·95	54706	12	—	$6s6p\,{}^3P_2^0$—$6s6d\,{}^3D_2$
,,	1814·80	55102	25	—	$6s6p\,{}^3P_2^0$—$6s6d\,{}^3D_3$
,,	1798·46	55603	6	—	$6s6p\,{}^3P_1^0$—$6s7s\,{}^1S_0$
,,	1792·87	55776	12	—	$6s6p\,{}^3P_0^0$—$6s7s\,{}^3S_1$
,,	1633·16	61231	3	—	$6s6p\,{}^1P_1^0$—$6s7d\,{}^1D_2$
,,	1593·19	62767	6	—	$6s6p\,{}^3P_1^0$—$6s6d\,{}^1D_2$
,,	1572·03	63612	10	—	$6s6p\,{}^3P_2^0$—$6p^2\,{}^3P_1$
,,	1568·52	63754	12	—	$6s6p\,{}^3P_1^0$—$6s6d\,{}^3D_1$
,,	1561·59	64038	15	—	$6s6p\,{}^3P_1^0$—$6s6d\,{}^3D_2$
* ,,	1538·13	64014	12	—	$6s6p\,{}^3P_1^0$—$6p^2\,{}^3P_0$
,,	1499·37	66695	12	—	$6s6p\,{}^3P_0^0$—$6s6d\,{}^3D_1$
,,	1490·52	67091	10	—	$6s6p\,{}^3P_2^0$—$6p^2\,{}^1D_2$
C.	1370·88	72946	4	—	$6s6p\,{}^3P_1^0$—$6p^2\,{}^3P_1$
,,	1330·41	75165	2	—	$6s6p\,{}^3P_2^0$—$6s7d\,{}^1D_2$
,,	1321·72	75659	7	—	$6s^2\,{}^1S_0$ —$6s6p\,{}^1P_1^0$
,,	1317·77	75886	2	—	$6s6p\,{}^3P_0^0$—$6p^2\,{}^3P_1$
,,	1308·50	76423	2	—	$6s6p\,{}^3P_1^0$—$6p^2\,{}^1D_2$
,,	1307·66	76472	0	—	$6s6p\,{}^3P_2^0$—$6s7d\,{}^3D_2$
,,	1183·59	84489	1	—	$6s6p\,{}^3P_1^0$—$6s7d\,{}^1D_2$
,,	1167·49	85653	0	—	$6s6p\,{}^3P_1^0$—$6s7d\,{}^3D_2$

M1.—McL., McL. and C., this investigation.
M2.—McL., McL. and C., 'Trans. Roy. Soc. Can.,' vol. 22, p. 241 (1928).
C.—Carroll, 'Phil. Trans. Roy. Soc. Lond.,' A, vol. 225, p. 357 (1926), wave-lengths and intensities.

* Fine structure interpreted in Table III.

and that I = ½. They are collected together, each in multiplet form, in Table III. A qualitative rule for the intensities of combinations between JF terms was derived from the completely resolved patterns, Nos. 1 and 2. It is apparently analogous in every respect to the one for intensities in ordinary multiplets between LJ terms if L is replaced by J and J by F. The rule was then assumed to hold throughout and was found very useful when interpreting partially resolved line patterns. If, in one of the latter, the two theoretically strongest (or weakest) components were not resolved, the single line observed is recorded twice in Table III. If a theoretically strong and a weak component were unresolved the single line is used in the position of the stronger and the position of the weaker one is indicated by a dotted line. The observed intensities of the components are enclosed in brackets after the wave-number in the table.

The terms, whose doublet structures have been determined from an analysis of the patterns in Table III, with the intervals in cm.$^{-1}$ to the nearest half unit

Table III.—Fine Structure Multiplets.

		1. $6s6p\ ^3P_2^0$.		2. $6s7p\ ^3P_2^0$.	
	F	1½	2½	1½	2½
$6s7s\ ^3S_1$	½	43499·6 (9)		16804·8 (7)	
	1½	43504·9 (6)	43501·4 (10)	16799·9 (4)	16803·3 (9)

		3. $6s7p\ ^3P_1^0$.		4. 1_1^0.	
	F	½	1½	½	1½
$6s7s\ ^3S_1$	½	14350·6 (6)	14355·4 (1)	17157·4 (3)	....
	1½	14346·3 (1)	14350·6 (6)	....	17151·7 (5)

		5. $6s6p\ ^1P_1^0$.		6. $6s7p\ ^1P_1^0$.	
	F	½	1½	½	1½
$6s7s\ ^3S_1$	½	29562·1 (5)	....	20982·2 (4)	....
	1½	....	29567·5 (7)	....	20977·1 (6)

		7. $6s7d\ ^3D_2$.		8. $6s7d\ ^3D_3$.	
	F	1½	2½	2½	3½
$6s7p\ ^3P_2^0$	1½	16025·1 (2)	....	16176·8 (10)	
	2½	....	16022·6 (3)	16173·0 (2)	16176·8 (10)

		9. $6s6d\ ^1D_2$.		10. $6s7d\ ^3D_2$.	
	F	1½	2½	1½	2½
$6s7p\ ^3P_1^0$	½	17317·6 (2)		18479·4 (3)	
	1½	....	17314·0 (3)	....	18475·8 (5)

		11. $6s7p\ ^3P_1^0$.		12. $6s7p\ ^3P_0^0$.
	F	½	1½	½
$6s7d\ ^3D_1$	½	18354·2 (1)	18351·6 (0)	18567·7 (2)
	1½	18351·6 (0)	18347·9 (3)	18565·1 (3)

		13. $6s6d\ ^1D_2$.		14. $6s6d\ ^3D_1$.		15. $6s6d\ ^3D_2$.	
	F	1½	2½	½	1½	1½	2½
$6s6p\ ^1P_1^0$	½	39501·0 (7)		40490·8 (3)	....	40773·7 (4)	
	1½	....	39503·4 (9)	....	40488·8 (4)	....	40775·3 (6)

and the number of patterns from which each was derived, are given in Table IV. A negative interval indicates that the term is inverted, *i.e.*, the component with larger F value is deepest.

It may be shown also that the terms $6s7p\,^3P_0^0$, $6s7s\,^1S_0$ and $6p^2\,^3P_0$ are very probably single-valued in agreement with theory. $^3P_0^0$ was assumed, of course, to be one-fold in forming pattern No. 11, Table III. But the correctness of the assumption is supported by the fact that the $^3D_1$ intervals deduced from that multiplet and from No. 12 are equal within the observational error. The combinations of $^1S_0$ with $6s6p\,^1P_1^0$, $6s7p\,^1P_1^0$ and 1_1^0 and that of $^3P_0$ with $6s6p\,^1P_1^0$ were observed to be single lines (see Table II). Since each of the above three terms with J = 1 have very small separations (see Table IV) the observed lines may be considered to be unresolved doublets if $^1S_0$ and $^3P_0$ are single valued.

Table IV.—Fine Structure Term Intervals.

Term.	$\Delta\nu$.	No. of patterns.
$6s6p\,^3P_2^0$	3·5	1
$6s6p\,^1P_1^0$	−0·5	1
$6s7s\,^3S_1$	5·0	6
$6s6d\,^1D_2$	2·0	1
$6s6d\,^3D_1$	−1·5	1
$6s6d\,^3D_2$	1·0	1
$6s7p\,^3P_1^0$	4·0	4
$6s7p\,^3P_2^0$	3·5	3
1_1^0	−0·5	1
$6s7p\,^1P_1^0$	$<$ −0·5	1
$6s7d\,^1D_2$	0·5	1
$6s7d\,^3D_1$	−2·5	2
$6s7d\,^3D_2$	0·5	2
$6s7d\,^3D_3$	4·0	1

A number of single faint lines classified in Table II fit into the fine structure wave-number scheme quite well if each is taken to be the theoretically strong line of a multiplet, whose fainter ones were not observed. The four very intense wave-lengths of the $6s6d$—$6s5f$ transition were too broad on our plates to be resolved into components. No attempt has been made, therefore, to deduce the structure of any of the $6s5f$ terms, although the fact that they have structure is evident from the magnitudes of the separations in patterns of $6s6d$—$6s5f$ lines of medium intensity.

It would not be wise perhaps to draw any detailed conclusions of a theoretical or empirical nature from the results of the fine-structure investigation reported above. But it seems certain that the observations are consistent with the validity of the Back-Goudsmit vector equation $F = J + I$, that the selection rule $\Delta F = \pm 1$ or 0 holds and that $I = \frac{1}{2}$ for Tl II. It is interesting to note that Schüler and Brück* recently found the same value for I for Tl I. The equality of the moments for neutral and singly-ionised thallium atoms strongly supports the generally accepted view that I is associated with the nucleus and is possibly its spin moment.

A point that should be of great theoretical importance is the fact that the magnitudes of fine-structure separations in Tl II lines are generally very much greater than any known for Tl I lines.† The patterns of lines of the latter spectrum were not resolved on our plates. Of added interest in this connection was the lack also of resolution into components of any wave-lengths that were classified by the authors in Tl III.‡ Their separations must be very small too.

A special investigation of fine structure of thallium spark wave-lengths is being planned. We hope by such a study to confirm the conclusions put forward above for structure in Tl II, to detect if possible structure in Tl III lines and to be able to extend the knowledge of the problem in general.

The closely related problem of the Zeeman-effect analysis of the thallium line patterns is being studied already in this laboratory by Mr. Durnford. He kindly photographed the line λ 5950 A. without magnetic field for us in the second order of a 3-metre concave grating. We measured the separations of its three components from his plates, since the two strong ones were unresolved on ours. The authors take this opportunity of thanking him for his assistance.

---

* 'Z. Physik,' vol. 55, p. 575 (1929).

† Back, 'Ann. Physik,' vol. 70, p. 333 (1923); Ruark and Chenault, 'Phil. Mag.,' vol. 50, p. 947 (1925); Mohammed and Mathur, 'Phil. Mag.,' vol. 5, p. 1111 (1928).

‡ 'Roy. Soc. Proc.,' A, vol. 125, p. 50 (1929).

A Robust Microbalance of High Sensitivity, Suitable for Weighing Sorbed Films.

By Prof. JAMES W. McBAIN, F.R.S., and Dr. H. G. TANNER, Stanford University, California.

(Received July 12, 1929.)

The sorption balance of McBain and Baker may be made of high degree of sensitivity, but the total weight which it will then support is correspondingly diminished. For weighing a monomolecular film on a comparatively heavy plane surface it is necessary to use a balance of beam type. A balance sensitive to 4×10^{-9} grams can be made sufficiently compact to be placed in a horizontal tube so that it may be used over a wide range of temperatures and pressures including the conditions necessary for freeing from sorbed material the surfaces to be weighed. Such a balance may be so designed that the volumes of the two halves of the balance are equal and unaffected by buoyancy. If, likewise, there be placed upon the two sides of the balance equal volumes of the same substance but of different area of surface, the differential change of weight caused by adsorption will be measured directly. A final desideratum is that the balance should be of null point type and free from any kind of hysteresis.

Steele and Grant* described a microbalance made of fused quartz which was sensitive to 4×10^{-9} grams and was capable of weighing 0·1 gram with an accuracy of 1×10^{-7} gram. Added improvements were described by Gray and Ramsay.† Aston‡ simplified the design of the beam and made a balance specially adapted to the determination of gas densities. Stock and Ritter§ made a further modification by replacing the fused quartz knife-edge with a pair of needle points. They also described a null-point balance in which a magnetised steel needle was sealed horizontally within the beam. The magnetic field from a bar magnet held vertically over the centre of the balance was used to compensate changes in level of the beam. The intensity of this controlling magnetic field was varied either by altering the distance between the bar magnet and the balance, or by increasing the field of the bar magnet electrically.

---

* Steele, 'Nature,' vol. 84, p. 428 (1910); Steele and Grant, 'Roy. Soc. Proc.,' A, vol. 82, p. 580 (1909).

† 'Roy. Soc. Proc.,' A, vol. 84, p. 536 (1911).

‡ 'Roy. Soc. Proc.,' A, vol. 89, p. 439 (1913).

§ 'Z. Physik. Chem.,' vol. 119, p. 333 (1926).

Stock and Ritter did not use this balance for precision measurements nor did they discuss its obvious weaknesses.

The balance whose construction is described below is a modification of all of the balances mentioned above. The essential changes are in the use of carborundum crystal points for the points of support and in the magnetic control arrangement.

The use of a pair of sewing needle points for the line of support, as suggested by Stock and Ritter, has the advantage over a knife-edge support of much greater ease of construction for a given degree of precision. On the other hand, a cement of some sort must be used to attach the needles to the glass or fused quartz beam. A cement capable of binding iron to fused quartz and able to withstand temperatures up to 400° is not available. Furthermore, needles are corrodible, and their magnetic characteristics variable. Fused quartz points might be used, but the material is brittle and difficult to shape into a satisfactory bearing point.

From the standpoint of sharpness, non-corrodibility, permanency, and freedom from magnetic effects, carborundum crystal points were selected as ideal balance points. The only difficulty in the way of their use was to find a method of attaching them to fused quartz. This proved easy when it was found that pyrex and carborundum seal to each other perfectly. A graded joint from fused quartz to pyrex was easily accomplished, and carborundum could then be attached to the pyrex. Heating the carborundum point to the fusion point of pyrex does not affect it in the least.

The magnetic arrangement differed essentially from that suggested by Stock and Ritter. A short piece of soft iron wire sealed within a tube of fused quartz was attached vertically to the centre of the beam. A horizontal disc shaped coil of wire was placed above and a little to one side of this vertical pin. When an alternating current (60 cycles) was passed through the coil, the iron pin on the beam was inclined toward the centre of the coil, and this inclination was proportional to the current flowing through the coil. If, therefore, a weight has caused the pin to be inclined away from the coil, adjustment of the current in the coil can bring the pin back to its former position.

There are several advantages of this arrangement over the arrangement used by Stock and Ritter who employed a more or less permanently magnetised needle in conjunction with a bar magnet. In the first place, the position taken by the soft iron pin in the alternating magnetic field is one of stable equilibrium, a principle which is applied in the construction of most of the alternating current measuring instruments. Secondly, the alternating magnetic field leaves no appreciable residual magnetism in the soft iron pin, and therefore the effect of the earth's magnetic field and other magnetic disturbances is minimised.

Originally direct current was intended to be used in a coil wound along the axis of the coil. Reversing the direction of the current through the coil would tilt the balance in the opposite direction. The use of direct current in such a coil, however, was found to produce erratic effects in the zero point of the balance, because of the hysteresis of the iron pin and the resultant position the pin would take in the earth's field. The alternating current magnet eliminates this uncontrolled systematic error.

The details of construction of the balance are as follows :—

A fused quartz rod 1·1 mm. in diameter and 22 cm. long was selected for the beam of the balance. It was laid on two carborundum grind stones (No. 112). Carborundum stones were used in preference to graphite (Gray and Ramsay) and asbestos (Stock and Ritter) because no contamination of the fused quartz rod resulted when the latter was heated to the softening point in contact with carborundum. Two stones were preferred to one because whenever a temperature higher than the softening temperature of fused quartz was required, the part to be heated could be moved to the crack between the stones and, since it was not in contact with the stone, could be heated to the fusion temperature of silica. Since most of the work must be done around the middle of the beam, spot fusions could be made between the stones without the beam sagging.

At the centre of the beam and at right angles to it were welded two silica rods 4 mm. long and of the same diameter as the beam. The first one can be attached with no special difficulty, but, in order to prevent it from sagging while the junction is being heated for attachment of the second rod, both the side rods were supported between the carborundum stones by small fused quartz fibres. When this operation is finished, the two side rods should lie in the same plane with the beam and be at right angles to it. Appropriate scratches on one of the carborundum stones are helpful in assisting with the alignment.

With the stones placed close together and the side rods lying in the groove between the stones a stem is built up vertically at the centre of the intersection. This is done by adding small bits of silica and fusing each addition to the preceding one. When a stem about a millimetre high has been built up, a fused quartz tube capable of holding snugly a piece of No. 24 soft iron wire 2 cm. long may be welded on to it without disturbing the beam and the side arms. After this weld is made, the iron wire is put into the tube and the tube is sealed off.

The next operation is to attach the carborundum crystal points. To the ends of the fused quartz side rods are fused tiny beads of pyrex. The dimensions are so small that thorough mixing of the pyrex and silica is readily accomplished merely by heating for a few seconds in a small oxy-hydrogen flame. A small amount of pyrex is then fused to each of the carborundum crystals. This may be accomplished by holding the crystal with nickled brass forceps in an air-hydrogen flame while it is touched with a pyrex fibre. As much surplus pyrex as possible should be removed. The crystal is then attached to one of the side rods, using an air-hydrogen flame.

Each end of the beam is then bent upwards. This is done by holding the balance upside down and applying a small oxy-hydrogen flame to the beam 1 centimetre in from each end. Gravity will cause the extremity to assume the desired position.

Holding the balance in the normal horizontal position the beam arms are bent slightly downward at points close to the centre. Application of an oxy-hydrogen flame at the desired place of bend until the beam sinks by the action of gravity accomplishes this. The purpose of bending the beam arms downward is to lower the centre of gravity of the balance below the line of support. Final adjustment of the position of the centre of gravity is made by resting the balance on a silica plate elevated above the carborundum stones to an appropriate height so that on heating the beam arm it will sink until its outer end rests on one of the stones. The adjustment was continued until the time of complete oscillation was between 10 and 15 seconds. A small bead of pyrex was fused to the tip of each arm of the beam. This tip of pyrex permitted platinum subsequently to be attached rigidly to the beam.

If the alignment of the balance is satisfactory and the period of oscillation great enough to give the desired sensitivity, the balance may be made to oscillate about a mean horizontal position (if it does not already do so) by fusing short pieces of pyrex fibres to the lighter end of the beam.

Before the platinum pieces were attached, some preliminary observations of the balance were made.

The balance points rested upon a piece of optically polished fused silica. A small glass case enclosed the balance, and this in turn was placed within an ordinary chemical balance case. Later a bell jar was used in order to enable pressure changes as well as gas composition effects to be studied. The apparatus was set up on a concrete pier built through a hole in the basement floor.

The position of a tiny bubble in one end of the beam relative to the cross hairs in a cathetometer furnished a reference or " zero " point for the balance. Observing this zero point for a few days showed erratic changes. The magnitude of the change from an approximate calibration amounted to 1×10^{-5} gram, which amount is very high considering that the balance was designed to weigh accurately at least to 1×10^{-7} gram. To account for these changes in the zero point various investigations were undertaken. Another balance was constructed, a duplicate of the first one except that no iron pin was attached to the beam. However, the zero point of the second balance was likewise very erratic, proving that the action of the earth's magnetic field on the iron pin of the balance was not the cause of the changes observed. Since a change in level of the pier upon which the apparatus rested was suspected, a silica fibre pendulum was suspended so that its movements could be watched relative to the movements of the balance beam. Although the pendulum did move about a mean vertical position relative to the cathetometer, the direction of movement of the pendulum did not always agree with the direction of movement of the balance, assuming the cause of their motions to be due to changes in level of their common support. The major cause of the zero point shift finally proved to be due to electrostatic charges on the balance and on objects near it. This accounted for the movements of the pendulum also. The disturbance was practically eliminated by adopting a suggestion, due to Sir William Ramsay, of placing uranium oxide near the balance. The radiations emanating from it are sufficient to ionise the air in the vicinity and conduct away stray electric charges from the balance.

To provide a convenient means of regulating the current through the balance control coil 110 volts of 60 cycle current was passed through a 40-watt lamp in series with a resistance of 330 ohms, the latter being provided with a sliding contact through which current was tapped off passing in series through the balance coil and milliammeter to the other end of the 330-ohm resistance coil. Moving the sliding contact back to this end before the circuit is broken anywhere reduces the magnetic fluctuations sufficiently slowly so that residual magnetism in the balance pin is negligible.

Because of the demagnetised condition of the pin, magnetic shielding of the balance is not necessary, provided strong magnets or large pieces of iron are not brought close to the balance. Machines using large alternating current must also be kept away from the balance because the intense fluctuating magnetic fields from them would induce an alternating current in the balance control coil which would disturb the zero point of the balance. This effect was observed when a mercury vapour lamp standing near the balance was started.

One other source of disturbance not previously mentioned is that of radiometer effects. The balance must be protected from radiations, particularly when one end of the balance has on it a piece of foil and the other end a wire. On one occasion it was noticed that a small flashlight shining on the foil several feet away produced a large movement of the balance.

Application to the Weighing of Adsorbed Films on Platinum.

The use of the balance is illustrated in the following account of preliminary measurements of the adsorption of toluene on platinum foil. A platinum wire and a platinum foil of exactly equal weight (and therefore volume) are spot-welded with a trace of pyrex glass to the silica beams. Since their centres of gravity were symmetrically placed on the two sides of the balance, all effects other than the difference in exposed surface (31·1 sq. cm.) were eliminated.

To calibrate the balance, riders were made from portions of a long uniform fibre of fused silica, the distance of the rider from the carborundum points being measured with a cathetometer and the amounts of current required to restore the balance to its original position being recorded. A sensitive balance is not required since a monomolecular film of toluene covering $23 \cdot 8 \times 10^{-16}$ sq. cm. per molecule would weigh as much as $2 \cdot 0 \times 10^{-6}$ gram. For preliminary experiments the balance complete with coil was placed within a bell jar, and nitrogen was passed for some hours when the zero point was determined. Thereafter the nitrogen supply bubbled through toluene kept at 0°. Equilibrium was only obtained several hours after shutting off the current of toluene laden nitrogen. To restore the balance to its null position required 58 milliamps, which corresponded to a weight of $6 \cdot 7 \times 10^{-6}$ gram or 3·5 times the calculated weight of a monomolecular layer of toluene. After prolonged exposure to the atmosphere, repetition of the treatment with nitrogen bubbling through toluene at 0° gave a weight of $3 \cdot 9 \times 10^{-6}$ gram (twice the weight of a monomolecular film) which remained constant for an additional 24 hours. After the balance with its platinum wire and foil was taken out and heated to dull redness in an atmosphere of hydrogen, it was replaced in the bell jar. First, pure hydrogen was passed, then it was bubbled through toluene at 0° for 2 hours, giving a weight of $1 \cdot 4 \times 10^{-6}$ gram or 0·7 of a monomolecular layer the next day. Although the zero of the balance was accidentally disturbed, the highest weight, even when the hydrogen was passed through toluene at room temperature, did not exceed $1 \cdot 8 \times 10^{-6}$ gram.

These determinations do not with certainty exceed a true monomolecular layer on account of the previous treatment of the platinum and because the foil when viewed under the microscope appeared pitted and scratched. Bowden and Rideal* showed from electrometric data that specimens of rolled nickel had an accessible area which was from two to five times the geometric area. Sand-papered surfaces were found to have ten times their apparent area, and nickel surfaces which had been alternately oxidised and reduced had an accessible area 46 times the apparent area. Likewise sorption and desorption of gases makes platinum brittle and probably increases its porosity.

Incidentally it may be here recorded that when a bead of platinum resting on a piece of fused silica was heated in an oxy-hydrogen flame, upon withdrawal of the flame the bead cooled and then spontaneously became incandescent for a moment, indicating the escape of gases sorbed at higher temperatures from the flame. This platinum " blick " resembles the well-known silver " blick " and seems to have been hitherto unnoticed.

Excluding data for porous bodies and for those with tarnished, rough, or absorbing surfaces, the few adsorption data which remain incompatible with the monomolecular thickness were obtained from studies of vapours at or near saturation concentrations. It is questionable whether it is legitimate to consider a vapour molecularly homogeneous when it is near saturation. In this condition there will be present " liquid nuclei " or " embryonic droplets " which upon striking a solid surface will not in general rebound. The time required for one of these nuclei to accumulate sufficient energy to vibrate loose like a single molecule might be comparatively long, and, pending this accumulation, it may waste away by evaporation of its constituent molecules. It seems probable, however, that these liquid nuclei would hold together for a much longer time when adsorbed upon a solid surface than they would in the free condition. The molecule or molecules that are in actual contact with the molecules of the surface will be strongly polarised thereby, and through chain effect this polarisation will be transmitted in diminished degree through all the successive molecules to the outside of the cluster. If evaporation from the surface be retarded compared to the rate of evaporation of these nuclei in the free condition, then the concentration of these nuclei upon the surface will be out of all proportion to that in the vapour and might form a more or less complete monoparticulate film of these molecular clusters. Such a film would simulate a multimolecular film, but no forces are postulated as operating other than between molecules in actual contact. This point of view is wholly different from the classical concept of a thick compressed adsorbed film caused by a wide range of molecular attraction extending out from the surface molecules of the solid.

---

* Bowden, 'Nature,' vol. 122, p. 647 (1928); F. P. Bowden and E. K. Rideal, 'Roy. Soc. Proc.,' A, vol. 120, p. 80 (1928).

Summary.

A robust and compact microbalance, capable of use under very varied conditions, sensitive to 4×10^{-9} gram, and capable of weighing at least 0·3 gram, is described. The two crystal points of carborundum on which the balance rests are superior to a knife edge in sharpness, hardness and chemical inertness.

Preliminary experiments on the adsorption of toluene vapour gave results several times higher than that corresponding to a monomolecular film for a true plane surface, but this was offset by the irregular surface of the platinum actually employed. A conception is put forward which would explain higher values of adsorption without reference to the classical assumption of a thick compressed film and providing an alternative to the hypothesis of multimolecular layers built up by superposition of monomolecular layers.

Further Studies on Intertraction.

By Sir ALMROTH E. WRIGHT, M.D., F.R.S.

(Received May 8, 1929.)

[PLATES 9 and 10.]

PART I.—REHEARSAL, CRITICISM AND AMPLIFICATION OF THE ORIGINAL EXPERIMENTS ON VERTICAL AND HORIZONTAL INTERTRACTION BETWEEN SERUM AND SALT SOLUTION.

Introduction.—The original experiments on intertraction in which serum coloured with eosin was imposed upon a heavier salt solution and uncoloured serum upon coloured salt solution were carried out in plane walled "intertraction cells" made from two microscopic slides placed from 1 to 1·5 mm. apart and cemented together by plasticene or pitch. In experiments thus conducted the intertraction pictures obtained are complicated by changes produced by the surrounding fluid in the ascending and descending pseudopodial processes; and by the diffusion of albumen and eosin, or eosin and salt outwards from the pseudopodial processes into the surrounding fluid. Moreover, certain significant features of the intertraction picture are only obscurely seen when they are viewed through too thick a sheet of fluid.

It will be necessary here to describe a little more fully what is seen in intertraction cells.

The disturbing complications in the case where coloured serum is superposed upon a 5 per cent. salt solution are as follows* :—The serum as it is drawn down into the subjacent salt solution gradually loses water and the albumens thus rendered heavier gravitate to the butt end of the pseudopodial processes with the result that these thin out in the middle, and develop bulbous extremities. And they, now weighted down as they are with inspissated albumens, fall heavily to the floor of the containing vessel. While these events are in progress eosin and albumen are continuously diffusing out from all the pseudopodia into the surrounding salt solution with the result that both the eosin and the albumen are soon dispersed evenly throughout the whole body of fluid.

Corresponding changes are seen when uncoloured serum is superposed upon a coloured 5 per cent. salt solution. Here* the ascending pseudopodia becoming by the intraction of water specifically lighter than the surrounding serum, thin out in the middle and expand at the ends and then are carried up to the surface. And at the same time the eosin and salt diffuse out from the pseudopodia into the serum, with the result that we have everywhere an equable mixture of eosin, salt and albumen.

---

* These are well seen in photograph No. 1, 'Roy. Soc. Proc.,' A, vol. 114, Pl. 41.

Method of conducting the experiments on vertical intertraction in such a manner as to avoid the complications introduced by (a) *alterations in the specific gravity of the pseudopodial contents, and* (b) *diffusion from the pseudopodia into the surrounding fluid.*

(1) By employing as a subjacent fluid coloured or uncoloured salted serum in the place of a simple 5 per cent. coloured or uncoloured salt solution, the gravitational ascent and descent of the pseudopodial contents and the consequent distortion of the pseudopodia and also much of the diffusion can be avoided.

The required salted serum is conveniently made by adding one volume of a saturated (25 per cent.) salt solution to four volumes of serum. (Descending and ascending vertical intertraction obtained by this method are well shown in 'Roy. Soc. Proc.,' A, vol. 114, Pl. 41, figs. 3a and 3b, and 4a and 4b.)

(2) The complications introduced by diffusion of dissolved colouring matter can be entirely avoided by employing in the place of the eosin-coloured serum or salt solution, suspensions of red blood corpuscles in serum and salt solution, or suspensions of Indian ink in serum or salted serum.†

(3) The blurring which is introduced into the picture when one ridge of pseudopodial processes is ranged up behind another can be avoided by conducting intertraction experiments in the compartments of a slide cell.‡

---

* These are well seen in photographs 2a and 2b, 'Roy. Soc. Proc.,' A, vol. 114, Pl. 41.

† In making a suspension of Indian ink in salted serum the ink is, in order to avoid agglutination of the particles, first suspended in the serum, the required salt solution being added afterwards.

Further it requires to be noted in connexion with all the suspensions employed in intertraction experiments that if the constituent particles are not sufficiently fine or are agglutinated by the salt solution employed they will gravitate to the extremities of the descending pseudopodial processes producing the same bulbous swelling as is produced in experiments with serum by the descent of the inspissated albumen, etc.

‡ A slide cell is made by cutting narrow strips of paper 1 inch in length, dipping these into hot vaseline, laying them down transversely upon the ordinary (1 × 3 inch) microscopic slide and then superposing upon this a hot slide. The slide cell may conveniently be divided up by strips into four compartments, and the paper used for the slips may conveniently be 1/6th to 1/8th mm. in thickness. Further, since microscopic slides are

It will be seen that most of the photographs which illustrate this paper are photographs of experiments made in slide cells.

The fact that we have in vertical intertraction a conjunction of descending and ascending intertraction is particularly well brought out on Plate I in photographs 1a, 1b and 1c.

Methods of Demonstrating Horizontal Intertraction.

Uncomplicated vertical intertraction having been brought into view by the devices just described it remained to devise methods for the demonstration of horizontal intertraction. Any or all of the four following methods may be employed for this purpose.

(*a*) We take a slide cell, lay it down on the bench and introduce into one of its compartments from its nearer side sufficient concentrated salt solution to fill it half full. We then, keeping the slide cell horizontal, turn the further side of the slide cell to us, and fill up the remainder of the compartment with a suspension of red blood corpuscles or Indian ink in serum. In a few moments a fringe or a close palisade of red or black streamers will be seen invading the salt solution (Photograph 2).

Much more picturesque and striking methods of demonstrating horizontal intertraction are the following.

(*b*) We take a square cover glass and we then, in preparation for setting it afloat, draw its four edges lightly across a block of plasticene. We then place a very minute fragment of the plasticene on the centre of the cover glass and press down a disc of filter paper very firmly upon it. This done we impregnate the paper disc with defibrinated blood or with serum containing a heavy charge of red blood corpuscles or Indian ink. Any excess of fluid beyond what the disc can absorb is then removed by blotting with filter paper. We now take any convenient shallow vessel and fill into it a concentrated salt solution and then set our cover glass afloat, turning the side which carries the filter paper disc downwards. After the lapse of a moment or two, black or red streamers will bud out all round the filter paper disc; and these, growing rapidly, will emerge from under the cover glass and be carried out far over the surface of the salt solution in the manner shown in Photograph 3.

(*c*) We take as before a serum suspension of red blood corpuscles or Indian ink and now, using for the purpose a capillary pipette with a stem bent at a

generally, as can be discovered by spinning them on a flat bench, convex on one face and concave on the other, it is advisable in making slide cells to dispose the slides with their convex faces directed upwards.

right angle and drawn out into a filiform point, impose a drop of this suspension upon the naked surface of a concentrated salt solution. Immediately the interior of the drop will begin to shape itself into horizontal streamers and these will gradually dispose of themselves into a pattern resembling a multiradiate star (Photograph 3).

(*d*) By the aid of a cork cutter we cut out a number of discs from a sheet of filter paper, and then using a smaller sized cork cutter cut out the central area of each disc. The filter paper rings thus obtained are dipped into melted paraffin wax and are laid one over the other upon a microscopic slide. We then take another slide, heat it in the flame and then press it down upon these rings in such a way as to weld them together, and make sure that our miniature lifebuoy—as we may call it—shall float upon an even keel.

We now set our paraffined paper lifebuoy afloat upon a saturated salt solution and then, using again a pipette drawn out into a filiform point, introduce a serum suspension of red blood corpuscles or of Indian ink into the hollow of the lifebuoy using only just enough to cover the included salt solution. Here, as in the experiment with the filter paper discs, red or black horizontal streamers will bud out from the circumference of the ring, and will be carried out over the subjacent salt solution (Photograph 5).

Experiments showing the conditions which determine, in the case where serum is deposited on the surface of a heavier salt solution, the development of descending apart from horizontal; or as the case may be, horizontal apart from vertical intertraction; or both forms of intertraction in conjunction.

The more important conditions which determine the development of these several varieties of intertraction are the following:—

1. Mechanical obstacles may definitely bar horizontal intertraction. Such obstacles present themselves when as in intertraction cells and slide cell compartments disposed in the vertical plane the overlying covers the whole of the underlying fluid, and abuts directly upon the walls of the containing vessel. Here horizontal intertraction being excluded, only descending intertraction can occur.

Horizontal intertraction is mechanically impeded also when an obstacle, such for example as a cover glass fixed upright in plasticene is set up in the path of a film or of a system of horizontal streamers of serum spreading out over the surface of salt solution. The serum on meeting such an obstructing cover glass will be banked up against it and will be drawn down all along its face in the form of a palisade of descending pseudopodial processes. The horizontal intertraction which is in progress being here obstructed, vertical intertraction substitutes itself for it.

The same thing occurs where we impose serum upon a heavier salt solution in the form of a large drop. Then the central portion of the drop will because it is confined horizontally give vertical intertraction.

2. A second operating force which determines the kind of intertraction obtained is the greater or less specific gravity of the salt solution chosen as a substratum.

The influence of varying gravitational resistance can be best studied by aid of the procedures which serve for the demonstration of horizontal intertraction. Making use of any of these we find that where saturated salt solution is employed as a substratum only horizontal intertraction is obtained. When, on the other hand, a salt solution which is only just heavier than the superimposed serum is employed, both descending and horizontal intertraction come into view simultaneously. Again in such cases horizontal intertraction may be obtained in the first phase of the experiment, and in the second phase horizontal may give place to vertical intertraction, this change over being no doubt brought about by the serum having by loss of water become heavier, and the subjacent salt solution by dilution lighter. In other cases again the pseudopodial processes may from the outset be carried down diagonally from a floating disc of serum producing a pattern resembling a hen coop.

The effect exerted by gravitational resistance upon vertical intertraction is exhibited in photographs 6 and 7.

3. A third operating force which determines the direction of intertraction is the attractive or repulsive force exerted by the walls of the containing vessel. The influences here in question are in reality those exerted by the concave or convex curvature of the fluid which lies alongside the wall of the containing vessel. These—and here I only resume what I said in my previous papers—may be studied by taking a vessel with naked and another with paraffined glass walls, filling into these, let us say, 8 per cent. salt solution and then in each case letting coloured serum flow gently down the walls on to the surface of the salt solution.

In the case where the serum flows on to the surface of salt solution from naked glass walls it will immediately be banked up against the wall and will run round in the form of a crescentic rim. Pseudopodial processes will now descend all along this rim forming a palisade, and horizontal intertraction will manifest itself only at the point where the serum has been run in, and then only in the case where the serum is not sufficiently rapidly absorbed into the meniscus.

Where the serum flows off from paraffined walls on to the surface of the salt solution it will, if little in quantity, be immediately conveyed away in the form of a system of radiating striæ. When a more generous quantum of serum is fed in, it will flow out over the salt solution in the form of a continuous film—a film from the confines of which streamers will presently emerge. Descending intertraction will here be obtained only at those points where the serum happens, owing to its not being sufficiently rapidly conveyed away by horizontal intertraction, to accumulate in sufficient amount to indent the surface of the salt solution.

Conditions almost identical with those just described can be provided by using a somewhat deep crystallising dish and tilting it up so that its upper wall makes an acute and its lower wall an obtuse angle with the surface of the contained 8 per cent. salt solution. If we now allow serum to flow in from the overhanging wall it will be held up in the re-entrant angle and only descending intertraction will be obtained. If, on the other hand, serum is run down the wall which slopes away from the salt solution the serum will be carried out over the surface of the salt solution by horizontal intertraction.

PART II.—PSEUDOPODIAL INTERTRACTION BETWEEN ALCOHOL AND WATER, AND BETWEEN WATER AND SALT SOLUTION.

It has been sufficiently brought out above that pseudopodial intertraction is obtainable when serum and salt solution are brought into apposition. Further, as was mentioned in the first of my papers on pseudopodial intertraction, such intertraction can be obtained not only with serum but also with other albuminous fluids, and not only with albuminous solutions superposed on salt but also with albuminous solutions superposed upon sugar and other crystalloids. Further pseudopodial intertraction is, as was shown by my sometime fellow worker, C. G. Schoneboom,* obtained also when solutions of crystalloids of carefully chosen strengths are brought into apposition. And there can in such cases—this also was pointed out by Schoneboom—by careful graduation of the strength of the superimposed solution be obtained in succession: pseudopodial penetration, rapid diffusion with delimiting rectilinear wave front, and the classical similarly delimited slow diffusion of the text-books.

The relation between these different forms of interpenetration obviously invited further investigation; and so did the question as to whether pseudopodial intertraction could be obtained when alcohol is superimposed upon water, and water upon solutions of salt and other crystalloids.

---

* 'Roy. Soc. Proc.,' A, vol. 101 (1922).

Experiments showing that Pseudopodial Intertraction can be obtained between Alcohol and Water.

We take a slide cell and fill the four compartments, which we may label A, B, C and D, half full with water, and then, first sealing the compartments below with melted paraffin, fill the upper halves of the compartments with suspensions of Indian ink in 25, 50, 75 and 100 per cent. alcohol respectively. We then seal the upper ends of the compartments (Photograph 6).

In compartment A the pseudopodial interpenetration begins in the course of a few minutes ; in compartments B and C there comes into view first a narrower or broader band of what we may call molecular or diffusional interpenetration ; a little later ascending and descending pseudopodial processes make their appearance at the upper and lower borders of that narrower or broader band. In compartment D we have a band of diffusional interpenetration delimited as in B and C by horizontal lines of demarcation. This band continues to broaden out slowly for half to three-quarters of an hour. By this time, when as we may assume the mixture of alcohol and water in this intermediate zone bears the required gravitational and surface tension relation to the alcohol above and the water below, ascending and descending pseudopodial processes make their appearance passing up or down from the upper or lower, or more usually both up and down from both the limiting surfaces of the diffusional band. Photograph 6, which was taken 10 minutes after the experiment was set up, shows in compartment A well-developed pseudopodial intertraction ; in compartments B and C less advanced pseudopodial supervening upon a preliminary diffusional interpenetration ; and in D a band of diffusional interpenetration only.

Horizontal pseudopodial intertraction between alcohol and water can also be obtained. It may be demonstrated by the aid of any of the procedures described in Part I of this paper.

It will, for the reason that this immediately brings up certain questions of principle, be well to begin with the procedure in which a naked drop of alcohol is imposed upon the naked surface of water.

When an alcoholic suspension of Indian ink is superimposed upon water in sufficient quantity to form a complete cap over the surface and to abut against the walls of the containing vessel, further horizontal spreading is, of course, definitely barred. When, on the contrary, a drop of undiluted alcoholic suspension is imposed upon a water-surface of larger extent, there is exerted upon it an unresisted horizontal traction. The drop is by consequence explosively disrupted. With a small drop a purely lateral explosion is witnessed; with a larger one—for here the alcohol cannot be sufficiently rapidly conveyed off over the face of the water—downward are added to lateral explosions. Similar but less violent explosions follow when weaker alcoholic Indian ink suspensions—suspensions which may contain only 1 per cent. of alcohol—are imposed upon the surface of water.

Such explosive disruptions being, of course, fatal to the development of pseudopodial intertraction figures a small amount of an agar agar solution was added to the subjacent water by way of a counteracting resistance. By this device typical pseudopodial intertraction figures are obtained with alcoholic suspensions of Indian ink containing a maximum of 2½ per cent. of alcohol.

Better than the method just mentioned is the method of reducing the disruptive forces exerted by water by lowering its surface tension by the addition of soap, lysol, or bile salts. Imposed by means of a capillary pipette upon water thus treated, Indian ink suspended in 50 per cent. or even higher percentages of alcohol gives beautiful intertraction figures (Photograph 4).

Of course, what applies to a naked drop of alcohol placed upon a naked water surface applies also to a drop of alcohol encircled by a paraffined paper ring floating on water. Strong alcohol filled into the centre of such a ring produces a perfect fusillade of lateral and downward explosions which drive the lifebuoy hither and thither over the surface of the water. When, however, the surface tension of the surrounding water has been duly reduced by the addition of soap, or bile salts, and when at the same time the surface tension of the alcoholic suspension has been duly increased by watering it down until it contains not more than 25 per cent. of alcohol, typical horizontal pseudopodia bud out all round the lifebuoy and develop into long streamers.

When we pass to the filter paper disc method we pass, as reflexion shows, to conditions essentially different from those just dealt with. For in the filter paper disc the intracting forces of the water are antagonised by the mechanical resistance offered by the texture of the paper. In correspondence to this excellent intertraction figures are obtained with filter paper discs impregnated with even full strength alcoholic suspensions of Indian ink (Photograph 11).

The device of adding soap or bile salts to water for promoting the development of pseudopodial interpenetration operates, of course, also in experiments on vertical and horizontal intertraction carried out in the slide cell,

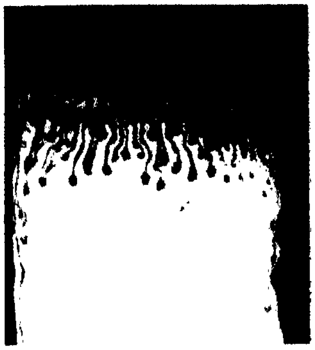

FIG. 1A.

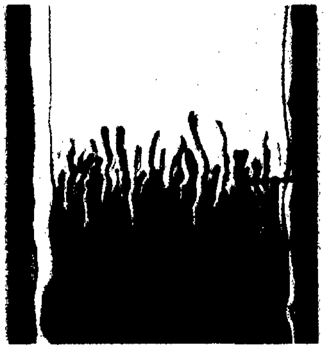

FIG. 1B.

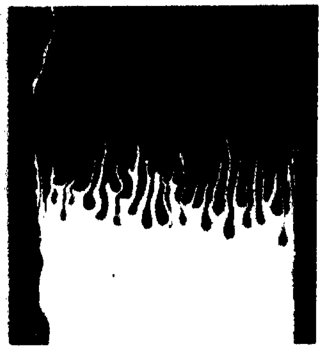

FIG. 1C.

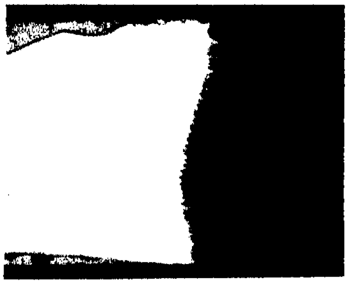

FIG. 2.

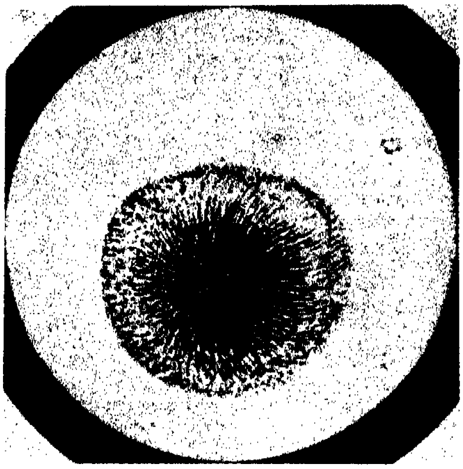

FIG. 3.

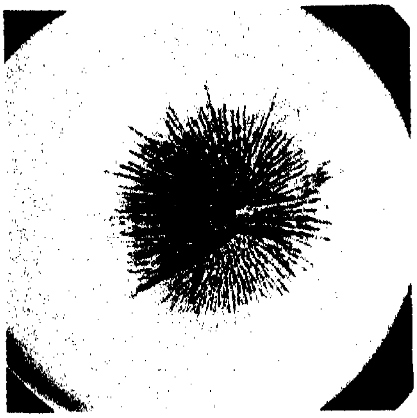

FIG. 4.

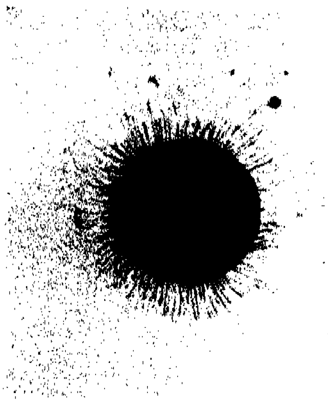

FIG. 5.

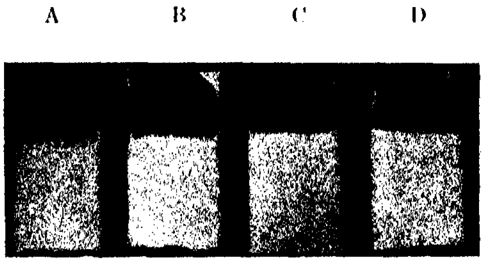

FIG. 6.

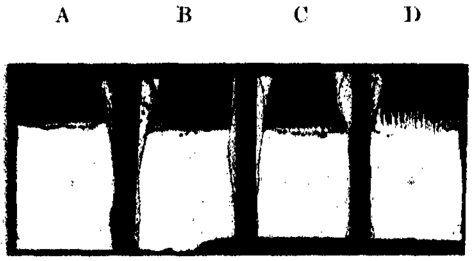

FIG. 7.

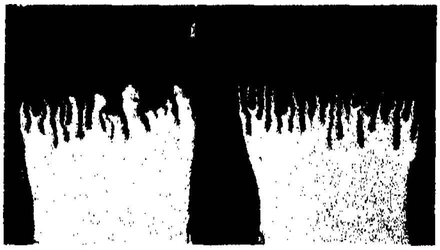

FIG. 8.

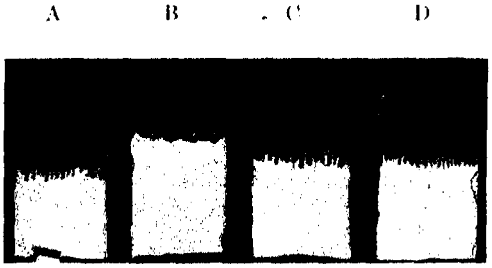

FIG. 9.

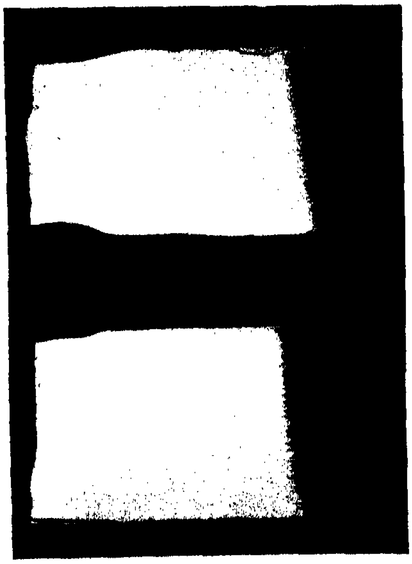

FIG. 10

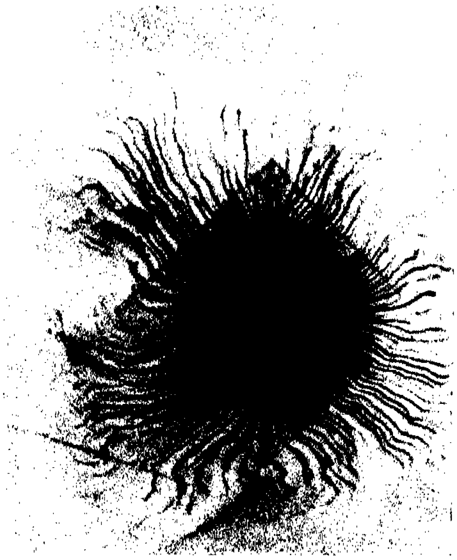

FIG. 11.

and, judging from measurements of the height to which intertracting fluids rise in one and the same capillary tube, there would appear to be a certain optimum difference of surface tension for optimum pseudopodial intertraction. For when the difference of surface tension of the attracting fluids is very great, pseudopodial interpenetration is retarded, and the same holds true when the surface tensions of the fluids involved have been brought almost to parity. Illustration of the influence of the addition of bile salts or soap upon the development of vertical intertraction is furnished by photographs 8 and 9.

Intertraction between Salt Solutions and Sugar Solutions and Water.

Intertraction takes place also between salt solutions and sugar solutions and water. There is a close analogy between pseudopodial intertraction between water and alcohol and that between salt solutions and water. To begin with, when a naked drop of a watery suspension of Indian ink is imposed upon the surface of a saturated salt solution it is instantly disrupted.

We might here, remembering what applies to intertraction between alcohol and water, have surmised that intertraction would have been obtained from naked or encircled drops of watery suspensions of Indian ink by simply diluting down the subjacent salt solution. And again we might, arguing from the fact that intertraction is obtained when filter paper discs impregnated with alcoholic suspensions of Indian ink are imposed upon a water surface, have anticipated that a filter paper disc impregnated with a watery suspension of Indian ink would have given intertraction when set afloat upon a saturated salt solution, Neither anticipation is realised for the reason that particles of Indian ink are under the influence of strong salt solutions instantly agglutinated and immobilised. When however, as in a slide cell placed vertically, the surface of contact between the salt and the suspension is restricted, and when in addition agglutination is held in curb by diluting both the salt solution and the Indian ink suspension, pseudopodial intertraction is as is witnessed by photograph No. 7.

The photograph in question shows the following:—With a 10 per cent. dilution of salt in compartment A of the slide cell there is obtained during a very long period of waiting only a band of diffusional interpenetration—further development being here arrested by the agglutination and immobilisation of the particles of Indian ink on the line of junction with the salt. In compartment B containing 7½ per cent. salt solution there are indications of intertraction, and in compartments C and D containing respectively 5 and 2½ per cent. salt solution there is well developed intertraction.

But even when working in slide cells with diluted suspensions of Indian ink and salt solutions there is some difficulty in obtaining vertical intertraction, and greater difficulty still in obtaining horizontal intertraction.

On pondering these difficulties it suggested itself that, notwithstanding the fact that the employment of weak salt solutions is obligatory when dealing with Indian ink, it might still be possible to obtain with such solutions both vertical and horizontal intertraction and to obtain these results both regularly and quickly. The method that suggested itself was to diminish the surface tension of the watery Indian ink suspension employed so as to facilitate intertraction. This idea furnished, in point of fact, the solution of this particular technical problem. With suspensions of Indian ink to which a modicum of bile salts has been added, both horizontal and vertical intertraction are obtained with quite weak salt solutions.

Photograph No. 9 represents an experiment in which in compartments A and B Indian ink suspensions with added bile salt were superimposed upon 1½ and 2½ per cent. salt solutions; simple watery suspensions of Indian ink were superimposed upon the same salt solutions while in compartments C and D. Photograph 10 shows horizontal intertraction obtained by bringing a suspension of Indian ink in water containing bile salts into apposition with weak saline solutions.

Attention will be drawn in a moment to the issue of control experiments in which water was superimposed upon watery suspensions of Indian ink to which bile salts or soap had been added.

But, first, brief reference may be made to intertraction between sugar solutions and water. All that requires to be said is that typical vertical and horizontal intertraction can be obtained by accoupling suspensions of either Indian ink or formalised red corpuscles with glucose solutions. Better results are obtained with 5, 10 and 20 per cent. glucose solutions than with the inconveniently viscid more concentrated solutions.

Points of a more general order.

It remains to refer to the issue of the control experiments referred to above. In the experiments in question in which water was superposed in slide cells upon watery suspensions of Indian ink containing graduated quantities of bile salts or soap, intertraction was never obtained. This, if it finds confirmation, would seem to make havoc of the theory which accounts for the development of tears on the walls of vessels containing fairly strong alcohol, by assuming that a fluid of robuster surface tension (such as wine from which alcohol has evaporated) will by virtue of its superior tensional strength engulf a fluid of more tender surface tension (such as wine possessing its full quantum of alcohol).

Finally, the following may to be said by way of summary. Inasmuch as the experiments recorded above have established (1) that alcohol and water, and water and salt and sugar solutions, attract each other in such a manner as to conquer gravitational resistance, and (2) that by tampering with the surface tension of one or other of the accoupled fluids molecular diffusion can be converted into intertraction, it would now seem legitimate to take up the position that slower or more rapid molecular diffusion, pseudopodial intertraction, hygroscopic attraction, the formation of tears in vessels containing moderately concentrated alcohol, and finally the osmosis through semi-permeable membranes of water in solutions of crystalloids and of alcohol into water are closely cognate phenomena, due in each case to a reciprocal attraction of either a solute for a solvent, or of one fluid for another.

In conclusion I have to acknowledge with gratitude much assistance from R. M. Fry in carrying out the experiments, and have to thank him also for the photographs which illustrate the paper.

EXPLANATION OF PHOTOGRAPHS.

PLATE 9.

No. 1A.—Vertical (descending and ascending) intertraction obtained by superimposing serum containing red blood corpuscles upon serum containing 10 per cent. of salt.

No. 1B.—Vertical (descending and ascending) intertraction obtained by superimposing serum upon serum containing 10 per cent. of salt and particles of Indian ink. The transverse line on the right in the photograph shows the original dividing line between the fluids.

No. 1C.—Vertical (descending and ascending) intertraction obtained by superimposing serum with Indian ink upon serum containing 10 per cent. salt; the original dividing line between the fluids is indicated by the transverse line on the right of photograph.

No. 2.—Horizontal intertraction between serum containing Indian ink and 12 per cent. salt solution.

No. 3.—Horizontal intertraction obtained by superimposing a suspension of red corpuscles in serum upon a saturated salt solution.

No. 4.—Horizontal intertraction obtained by superimposing a naked drop of a suspension of Indian ink in 25 per cent. alcohol upon water containing bile salts.

No. 5.—Horizontal intertraction obtained by floating a paraffined ring upon salt solution and filling into the interior of the ring serum containing red blood corpuscles.

PLATE 10.

No. 6.—Vertical intertraction obtained by superimposing upon water, Indian ink suspended in a 25 per cent., 50 per cent., 75 per cent. and 100 per cent. alcohol, the order being from left to right.

No. 7.—Vertical intertraction obtained by superimposing a watery suspension of Indian ink upon 10 per cent., 7·5 per cent., 5 per cent. and 2·5 per cent. salt solution, the order being from left to right.

No. 8.—Vertical intertraction. In the left-hand compartment a suspension of Indian ink in 50 per cent. alcohol has been superposed upon water. In the right-hand compartment the same suspension has been superimposed upon water containing soap.

No. 9.—Vertical intertraction. In the two left-hand compartments a suspension of Indian ink in water has been superimposed upon 1½ per cent. and 2½ per cent. salt solutions. In the two right-hand compartments a suspension of Indian ink in water containing bile salt has been superimposed upon the same strength of salt solution.

No. 10.—Horizontal intertraction. Here a suspension of Indian ink in water containing bile salt has been placed side by side with 2½ per cent. and 1½ per cent. salt solutions.

No. 11.—Horizontal intertraction. Here a disc of filter paper impregnated with a suspension of Indian ink in absolute alcohol has been set afloat upon water.

Notes on a Differential Equation which occurs in the Two-Dimensional Motion of a Compressible Fluid and the Associated Variational Problems.

By H. BATEMAN, F.R.S.

(Received April 27, 1929—Revised June 28, 1929.)

1. *Introduction.*

In two recent papers* Prof. G. I. Taylor and Dr. C. F. Sharman have discussed the flow of a compressible fluid by an experimental method and have formulated tentatively the criterion that no irrotational solution of the equations of motion exists when the velocity of the fluid at any point of the field of flow exceeds the local velocity of sound. They remark, however, that there appears at present to be no theoretical ground for supposing that this hypothesis is true in general. In this connection it may be pointed out that there is a change in type of the governing partial differential equation when the local velocity of sound is exceeded and the question naturally arises whether the problem is properly put when such a change occurs and the usual boundary conditions are retained. In order to present this question more definitely we take the case of steady motion in two dimensions and denote the velocity components at the point (x, y) by u, v, respectively and the density of the fluid by ρ. The equation of continuity is then

---

* 'Roy. Soc. Proc.,' A, vol. 121, p. 194 (1928); 'Aeronautical Research Committee,' R.M., 1196 & 1195.

$$\frac{\partial}{\partial x}(\rho u) + \frac{\partial}{\partial y}(\rho v) = 0. \tag{1}$$

When the pressure, p, is a function of the density and gravity is the only external force, Bernoulli's equation takes the form

$$\int \frac{dp}{\rho} + \tfrac{1}{2}(u^2 + v^2) + \Omega = C \tag{2}$$

where Ω is the potential energy per unit mass and C is constant along a stream-line. Since the motion is steady we may write

$$u\frac{\partial C}{\partial x} + v\frac{\partial C}{\partial y} = 0 \tag{3}$$

and so we have the equation

$$\frac{1}{\rho}\frac{dp}{d\rho}\left(u\frac{\partial \rho}{\partial x} + v\frac{\partial \rho}{\partial y}\right) + u\left(u\frac{\partial u}{\partial x} + v\frac{\partial v}{\partial x}\right) + v\left(u\frac{\partial u}{\partial y} + v\frac{\partial v}{\partial y}\right) + u\frac{\partial \Omega}{\partial x} + v\frac{\partial \Omega}{\partial y} = 0 \tag{4}$$

Writing $dp/d\rho = c^2$, where c is the "local velocity of sound,"* we have the differential equation

$$(c^2 - u^2)\frac{\partial u}{\partial x} - uv\left(\frac{\partial v}{\partial x} + \frac{\partial u}{\partial y}\right) + (c^2 - v^2)\frac{\partial v}{\partial y} = u\frac{\partial \Omega}{\partial x} + v\frac{\partial \Omega}{\partial y} \tag{5}$$

which is derived from (4) by combining it with the equation of continuity. When the motion is irrotational we may write $u = \frac{\partial \phi}{\partial x}$, $v = \frac{\partial \phi}{\partial y}$, and, if the effect of gravity is neglected, the equation takes the form

$$(c^2 - u^2)\frac{\partial^2 \phi}{\partial x^2} - 2uv\frac{\partial^2 \phi}{\partial x \partial y} + (c^2 - v^2)\frac{\partial^2 \phi}{\partial y^2} = 0. \tag{6}$$

In this case C can be regarded as a constant and c can be expressed in terms of u and v with the aid of the relation connecting the pressure and density and Bernoulli's equation. The resulting equation for ϕ may be regarded as the governing partial differential equation for irrotational flow; it may be transformed into a linear equation

---

* This is merely a convenient name. If, however, a small disturbance having the character of travelling waves is superposed on the original flow so as to give a new irrotational flow satisfying the hydrodynamical equations the quantity c can be regarded as the velocity of these waves relative to the fluid at the point (x, y).

$$A \frac{\partial^2 \chi}{\partial u^2} + 2H \frac{\partial^2 \chi}{\partial u \, \partial v} + B \frac{\partial^2 \chi}{\partial v^2} = 0 \tag{7}$$

by taking u and v as independent variables and making use of Legendre's transformation

$$\chi = ux + vy - \phi, \qquad x = \partial\chi/\partial u, \qquad y = \partial\chi/\partial v. \tag{8}$$

The coefficients A, B, H are respectively $c^2 - v^2$, $c^2 - u^2$, uv. According to the usual convention* a differential equation of this type is said to be elliptic, hyperbolic or parabolic according as $AB - H^2$ is positive, negative or zero, and these adjectives may be applied also to the original non-linear equation.† The character of the equation depends, then, on the sign of the expression

$$(c^2 - u^2)(c^2 - v^2) - u^2v^2 = c^2 - u^2 - v^2 = c^2 - q^2, \text{ say,}$$

and so there is a critical velocity, given by the equation $u^2 + v^2 = c^2$, at which there is a change in the character of the equation. When adiabatic conditions prevail, so that the relation between p and ρ is

$$p/p_0 = (\rho/\rho_0)^\gamma$$

where p_0, γ and ρ_0 are constants, the relation between c and q may be expressed in the form

$$\frac{c^2}{a^2} = \left(\frac{\rho}{\rho_0}\right)^{\gamma - 1} = 1 - \frac{\gamma - 1}{2a^2}(u^2 + v^2 - U^2) \tag{9}$$

where U and a are constants. If we suppose that at infinity $u = U$, $v = 0$, we have also $c = a$, $\rho = \rho_0$, so that ρ_0 can be regarded as the density and a as the velocity of sound for the fluid at an infinitely great distance from the origin, that is, in the undisturbed steady stream.

The critical velocity in the present case is given by the equation

$$q^2 = a^2 - \tfrac{1}{2}(\gamma - 1)(q^2 - U^2). \tag{10}$$

---

* See A. G. Webster, " Partial Differential Equations of Mathematical Physics," ch. 6.

† S. Bernstein, 'Math. Ann.,' vol. 59, p. 21 (1904). In this paper and in 'Comptes Rendus,' vol. 137, p. 778 (1903), a discussion is given of the analytical character of the solutions of an equation $F(x, y, z, p, q, r, s, t) = 0$ in which F is analytic in its arguments and satisfies the inequality $4 \frac{\partial^2 F}{\partial r \, \partial t} - \left(\frac{\partial F}{\partial q}\right)^2 > 0$. When this condition is satisfied the equation is said to be of elliptic type. The notation used here is explained in § 2. The general theorem relating to the analytic character of the solution was announced by Hilbert, 'Congrès Internationales Mathématiciens,' Paris (1900).

If $U = 0\cdot 6a$, $\gamma = 1\cdot 4$, we have

$$2\cdot 4\, q^2 = 2\cdot 144\, a^2,$$

so that the critical value of q is less than a.

2. *Supplementary Conditions of Elliptic Type.*

A knowledge of the type of an equation is important when an attempt is made to find supplementary conditions which will make the problem of solution one which is properly put so that there is indeed a solution and only one.

For an equation of elliptic type these conditions usually take the form of a condition of regularity in a region R bounded by one or more closed curves and a simple boundary condition on each of these curves. When the equation is linear and of type (7) a solution χ is said to be regular in R when χ, $\partial\chi/\partial u$, $\partial\chi/\partial v$, $\partial^2\chi/\partial u^2$, $\partial^2\chi/\partial v^2$ and $\partial^2\chi/\partial u\,\partial v$ are continuous functions of u and v in a region R in the uv-plane. When the equations is the more general equation $F(x, y, z, p, q, r, s, t) = 0$ where F is analytic in its arguments and $p = \partial z/\partial x$, $q = \partial z/\partial y$, $r = \partial^2 z/\partial x^2$, $s = \partial^2 z/\partial x\,\partial y$, $t = \partial^2 z/\partial y^2$, Bernstein assumes in his general theorem that the derivatives of z to the first three orders are finite and continuous. He then proves that z is an analytic function[*] of x and y. He shows, moreover, that a hyperbolic equation, such as $s = F(x, y, z, p, q)$, admits solutions which are not analytic functions of x and y and that a parabolic equation, such as $r = F(x, y, z, p, q)$, admits solutions which are analytic in x but not analytic in y. For a linear equation of elliptic type $r + t = F(x, y, z, p, q)$, where F is analytic in its arguments, the solution z is analytic when its derivatives up to the second order are known to be finite and continuous. This theorem, which is due to Lutkemeyer[†] and Holmgren[‡] is an extension of a similar theorem proved by Picard[§] for the case of a linear equation. Turning now to a consideration of appropriate boundary conditions we first consider equation (7). The boundary condition which usually occurs is that either χ or its normal derivative $\partial\chi/\partial\nu$ is assigned on the boundary.[||] If there is more than one boundary it may happen that the value of χ is assigned on one and the value of $\partial\chi/\partial\nu$ on the other, or it may happen that the value of χ or $\partial\chi/\partial\nu$ is assigned on both.

---

[*] This means that z can be expanded in a series of powers of $x - x_0$, $y - y_0$ in the neighbourhood of a point $(x_0\, y_0)$ where it is regular, the series being convergent for $|x - x_0| < k$, $|y - y_0| < k$ where k has some suitable value.

[†] Dissertation, Göttingen (1902).

[‡] 'Math. Ann.,' vol. 57, p. 409 (1903).

[§] 'C. R.,' vol. 121, p. 12 (1895); 'J. École Polytechnique,' cap. 60, p. 89 (1890); see also Paraf, 'Thèse,' Paris (1892).

[||] When the value of χ is assigned the problem is called the problem of Dirichlet; according to S. Bernstein, 'Math. Ann.,' vol. 69, p. 126 (1910), this problem is properly put for any *elliptic equation of type (6) with analytic coefficients* when the curve C in the (x, y)-plane is convex.

Such boundary conditions, combined with the condition of regularity in the region R, will be called *conditions of elliptic type.* The conditions which occur naturally in connection with a partial differential equation of hyperbolic type and render the problem capable of unique solution are often quite different. The characteristics* that satisfy the differential equation

$$A\,dv^2 - 2H\,du\,dv + B\,du^2 = 0 \tag{11}$$

play an important part.† They generally form two families of curves $\Gamma_1(u, v) = \text{constant}$, $\Gamma_2(u, v) = \text{constant}$. In one type of problem‡ which is properly put the values of χ and $\partial\chi/\partial\nu$ are assigned on a curve C, which need not be closed, and it appears that the values which are really needed for the determination of χ at a point (u_0, v_0) are those associated with a portion of C cut off by the characteristic curves through the point (u_0, v_0). This is not the only type of problem for a hyperbolic equation which is properly put and a general description of properly formulated problems for such an equation cannot at present be given. The question we are interested in at present is whether a problem can be properly formulated when the conditions are of elliptic type and the equation is wholly or partly of hyperbolic type. A study of this question will be commenced in the later sections of this paper by a consideration of some examples. Boundary conditions for a region R in the (u, v)-plane are of little interest in hydrodynamics§ but the characteristic curves in this plane have been used with some success in the treatment of hydrodynamical problems by Steichen and Prandtl.‖

The problems of hydrodynamics relate generally to a region S in the *xy*-plane and we shall now turn to a consideration of the equation (6) in such a region.

3. *An Associated Variational Problem.*

In many cases the supplementary conditions which must be associated with a partial differential equation to render the solution unique and existent are indicated by an associated problem in the "Calculus of Variations." This rule must not be regarded as an infallible guide as there are many dangers and difficulties but it will, at any rate, be useful to see what information can be derived by replacing the hydrodynamical equations by a variational problem.

---

* See Webster, *loc. cit.*

† They also play an important part in hydrodynamics when $U > a$.

‡ This is known as Cauchy's problem, a method of solution being indicated by Riemann. For an extensive discussion of Cauchy's problem for hyperbolic equations reference may be made to Hadamard's lectures on the subject.

§ A few cases may occur when q is constant along a given line or $v = 0$.

‖ A. Steichen, 'Dissertation,' Göttingen (1909). A brief account of this work is given in Ackeret's article on the dynamics of gases in "Handbuch der Physik," vol. 7.

Let us first consider a simple variational principle of type

$$\delta \iint G(q)\, dx\, dy = 0 \tag{12}$$

where $q^2 = u^2 + v^2$ and $u = \partial\phi/\partial x$, $v = \partial\phi/\partial y$. When ϕ is varied so that the variation $\delta\phi$ is zero over any boundary which is not a stream-line the Eulerian equation is

$$\frac{\partial}{\partial x}\left(\frac{\partial G}{\partial u}\right) + \frac{\partial}{\partial y}\left(\frac{\partial G}{\partial v}\right) = 0,$$

or

$$q^2 G'(q)\left[\frac{\partial^2\phi}{\partial x^2} + \frac{\partial^2\phi}{\partial y^2}\right] + [qG''(q) - G'(q)]\left[u^2\frac{\partial^2\phi}{\partial x^2} + 2uv\frac{\partial^2\phi}{\partial x\,\partial y} + v^2\frac{\partial^2\phi}{\partial y^2}\right]$$

This equation is elliptic, hyperbolic or parabolic according as $G'(q)\ G''(q)$ is positive, negative or zero. For adiabatic conditions the appropriate form of G is

$$G(q) = [2a^2 + (\gamma - 1)(U^2 - q^2)]^{\frac{\gamma}{\gamma-1}}. \tag{13}$$

Another case of interest is that in which the relation between p and ρ is of Earnshaw's type

$$p = \alpha - \beta/\rho$$

where α and β are constants. In this case

$$c^2 = u^2 + v^2 + a^2 - U^2 = u^2 + v^2 + b^2, \text{ say}$$

where $c = a$, $u = U$, $v = 0$ at infinity. The partial differential equation is

$$(v^2 + b^2)\frac{\partial^2\phi}{\partial x^2} - 2uv\frac{\partial^2\phi}{\partial x\,\partial y} + (u^2 + b^2)\frac{\partial^2\phi}{\partial y^2} = 0$$

and the variational problem is

$$\delta \iint (u^2 + v^2 + b^2)^{\frac{1}{2}}\, dx\, dy = 0. \tag{14}$$

If we write $\phi = bz$, where x, y and z are rectangular co-ordinates of a point in space, the integral in (14) can be interpreted as b times the area of a surface and the partial differential equation becomes that of a minimal surface and is elliptic if $b^2 > 0$, *i.e.*, if $U^2 < a^2$.

In this case the analogy between the equilibrium of a soap film and the motion of the fluid may be useful. The problem of Plateau for the soap film is to find a continuous soap film with a given boundary or with a number of prescribed boundaries. The conditions are in this case elliptic because the value of z is prescribed round the boundary of a region S in the xy-plane and the solution is required to be regular in this region. It seems, however, that a solution does not always exist when such conditions are imposed. This may be seen for example, by considering the case of a region S bounded by concentric circles when z has prescribed constant values on the circles.[*] The required surface is then, presumably, a surface of revolution and must be a catenoid, the surface formed by the revolution of a catenary about its directrix. Considering, then, a section of the surface by a plane through the axis of symmetry, the problem is to draw a catenary to pass through two given points in this plane and to have the axis as directrix. It is known, however, that it is not always possible to draw such a catenary.[†] With certain positions of the two points two catenaries can be drawn and in a particular case only one. When only one catenary can be drawn the film joining the two circles in space is unstable. When the two catenaries can be drawn, one corresponds to a stable film and the other to an unstable film. In this latter case the requirement of an absolute minimum enables us to decide which solution of the boundary problem corresponds to the physical conditions.

In this case, although we are dealing with an elliptic equation and elliptic conditions, the problem may not be properly put.[‡] It is true that the boundary conditions are not precisely those which usually occur in hydrodynamics[§] but we should be on the look out for similar failures in hydrodynamical problems, and in the discussion of these problems it may be worth while to adopt the methods of the Calculus of Variations. This means that we should omit one boundary condition and consider the family of regular solutions satisfying the other, determining, if possible, the " singular solution " which corresponds to the envelope of the catenaries through one point. Attention should be paid also to any discontinuous solutions which might correspond to the Goldschmidt solution, which consists of two lines perpendicular to the axis and the portion of the axis between them. It is this solution which furnishes the surface of minimum area when there is only one catenary joining the two points.

---

[*] This means that the soap film is required to terminate on two given circles in space.

[†] See Todhunter, " Researches in the Calculus of Variations " ; G. A. Bliss, " Calculus of Variations " (Open Court Publishing Co., Chicago) ; Forsyth, " Calculus of Variations " (1927), p. 480.

[‡] The essential difference between this case and Bernstein's case (the simple Dirichlet problem) is that there are two boundaries.

[§] In hydrodynamics the value of ϕ is generally assigned on one boundary and that of its normal derivative on the other.

[*Note added September*, 1929.—Variation problems of type

$$\delta \iint \mathrm{F}(u, v)\, dx\, dy = 0, \qquad u = \frac{\partial \phi}{\partial x}, \ v = \frac{\partial \phi}{\partial y}$$

have been considered recently by Bernstein[*] and Haar.[†] Bernstein regards the problem as regular when

$$\frac{\partial^2 \mathrm{F}}{\partial u^2}\frac{\partial^2 \mathrm{F}}{\partial v^2} > \left(\frac{\partial^2 \mathrm{F}}{\partial u\, \partial v}\right)^2,$$

for the Eulerian partial differential equation is then of elliptic type, and if also $\frac{\partial^2 \mathrm{F}}{\partial u^2} > 0$, the second order variation of the integral is positive. The question of the existence of a solution of the simple Dirichlet problem for a curve C in the (x, y)-plane, which is not wholly convex, depends on the value of a certain index α determined by the form of the function F. It is interesting to note that a critical value of α (for which the problem may not be soluble) occurs for the function F corresponding to Earnshaw's law, but not for the function F corresponding to the adiabatic law.

Haar shows that a variation problem of this type is associated with an adjoint problem of the same type. It is easy to verify that when the function F is of the type considered in § 3, the function F for the adjoint problem is also of this type.]

The appeal to the variation problem has proved rather disappointing because no immediate clear answer has been obtained to the question of the existence of a solution; moreover, the variational problem seems to suggest that the conditions are of elliptic type even when the associated partial differential equation is of hyperbolic type. It is possible, however, that the difficulties introduced by the "envelope" may occur before the equation becomes of hyperbolic type. If this is the case it is hard to see immediately what happens physically. Does the motion become rotational or cease to be steady?

The association of a partial differential equation with a variational principle is sometimes useful because direct methods are now being used for the solution of problems in the Calculus of Variations. The method of Rayleigh and Ritz may be regarded as a typical direct method; it is essentially a method of

---

[*] 'Ann. École Normale,' vol. 29, p. 431 (1912).

[†] 'Math. Ann.,' vol. 100, p. 481 (1928).

approximation in which a suitable finite series of orthogonal functions is used as an approximation to the desired function and the minimum problem is so reduced to an algebraic minimum problem in which the variables are the unknown coefficients in the series. This method has been used with considerable success and can be readily extended to the case in which there are several unknown functions. Sometimes much labour can be saved by modifying the variational problem, indeed, experience tells us that the variational problem associated with a given partial differential equation is by no means unique. Some attention may be paid, then, to the study of the different possible variation problems, so that a suitable choice may be made when it is necessary to make lengthy computations. [An announcement has just appeared of a book by Dr. Lichtenstein, 'Grundlagen der Hydromechanik,' Berlin (Springer), 1929, in which the derivation of the hydrodynamical equations from Hamilton's Principle is discussed in some detail, and special attention is paid to the case in which there are waves of discontinuity as in the work of Zemplen, 'Math. Ann.,' vol. 61, p. 437 (1905).—*Added September*, 1929.]

4. *Variational Principles giving the Equations of Vortex Motion.*

In view of the importance in modern physics of variational problems it seems worth while to review the progress which has been made in the derivation of the hydrodynamical equations for non-viscous flow from a variational principle and to add some new results. We may adopt as a guiding principle the property that, when the hydrodynamical equations are satisfied, the integrand in the variational principle is a linear function of the pressure.[*] This is true in the cases already considered. Making first a slight extension of Clebsch's theorem[†] we derive the hydrodynamical equations for an inviscid compressible fluid from a variational principle

$$\delta \int \mathrm{L}\, dx\, dy\, dz\, dt = 0 \tag{15}$$

in which

$$\mathrm{L} = f(\rho) - \rho\left[\frac{d\phi}{dt} + \alpha\frac{d\beta}{dt} - \tfrac{1}{2}(u^2 + v^2 + w^2)\right] \tag{16}$$

---

[*] Reference may be made to a paper by R. Hargreaves, "A Pressure-Integral as Kinetic Potential," 'Phil. Mag.,' September, 1908.

[†] Crelle, vol. 56 (1859); see also M. J. M. Hill, 'Q. J. Math.,' vol. 17 (1881); 'Camb. Trans.,' vol. 14 (1883); Lamb, "Hydrodynamics," pp. 229–230.

and

$$u = \frac{\partial \phi}{\partial x} + \alpha \frac{\partial \beta}{\partial x}, \quad v = \frac{\partial \phi}{\partial y} + \alpha \frac{\partial \beta}{\partial y}, \quad w = \frac{\partial \phi}{\partial z} + \alpha \frac{\partial \beta}{\partial z} \tag{17}$$

$$\frac{d}{dt} = \frac{\partial}{\partial t} + u \frac{\partial}{\partial x} + v \frac{\partial}{\partial y} + w \frac{\partial}{\partial z}.$$

If a boundary B is always in contact with the same particles of fluid no restrictions need be laid on the variations of the quantities ϕ and β on this boundary except that they must be small, but if there is a boundary B which is not always in contact with the same particles of fluid, the variations of ϕ and β should vanish on this boundary.*

The Eulerian equations of the Calculus of Variations give (1) the equation of continuity

$$\frac{\partial \rho}{\partial t} + \frac{\partial}{\partial x}(\rho u) + \frac{\partial}{\partial y}(\rho v) + \frac{\partial}{\partial z}(\rho w) = 0,$$

(2) the equations

$$\frac{d\alpha}{dt} = 0, \quad \frac{d\beta}{dt} = 0,$$

which imply that the vortex lines move with the fluid so as to consist always of the same particles, and (3) the equation

$$\frac{d\phi}{dt} + \alpha \frac{d\beta}{dt} - \tfrac{1}{2}(u^2 + v^2 + w^2) = f'(\rho),$$

which, when combined with the other equations, indicates that the dynamical equations

$$\rho \frac{du}{dt} = -\frac{\partial p}{\partial x}, \quad \rho \frac{dv}{dt} = -\frac{\partial p}{\partial y}, \quad \rho \frac{dw}{dt} = -\frac{\partial p}{\delta z}$$

are satisfied if the pressure, p, is given by the equation

$$p = -\rho f'(\rho) + f(\rho).$$

It should be noticed that when all these equations are satisfied the quantity L is equal to p.

The variational principle may be used in many equivalent forms. A simple equivalent form of L is

$$\mathrm{L} = -\rho \left[\frac{\partial \phi}{\partial t} + \alpha \frac{\partial \beta}{\partial t} + \tfrac{1}{2}(u^2 + v^2 + w^2) \right] + f(\rho),$$

---

* In the non-stationary case this seems to suggest that the values of ϕ and β should be prescribed both at the beginning and end of the interval of integration with respect to t. If the motion is not periodic, the boundary conditions suggested by the variation problem are not quite those which would be expected from physical considerations.—(*Added September*, 1929.)

but the first form is preferable because it can be used also in the case when u, v, w, ϕ, α, β and ρ are varied independently. The Eulerian equations then give the equations (17) in addition to the others.

When the motion under consideration is steady the variational principle may be taken in the form

$$\delta \iiint \mathrm{L}\, dx\, dy\, dz = 0,$$

and, of course, the time derivative may be omitted in the expression for d/dt. When the motion is to be irrotational β may be set equal to zero and then ϕ becomes the velocity potential. The variational principle then indicates that the value of ϕ should be prescribed on a boundary which is not a locus of stream-lines. This is precisely the type of boundary condition which occurs in hydrodynamics when the velocity of translation at infinity and the total circulation are prescribed. When the motion is not restricted to be irrotational the quantities ϕ and β should have assigned values on a boundary not made up of stream-lines. This introduces a slight difficulty because the quantities ϕ and β associated with a given velocity field are not unique; indeed, we may write $\phi + \alpha\beta$ in place of ϕ and $-\alpha$ in place of β. An attempt must therefore be made to write the expressions for u, v, w in a standard way and the plan we propose is to introduce a quantity s such that*

$$u = \frac{\partial \phi}{\partial x} \pm \dot{s}\frac{\partial s}{\partial x}, \quad v = \frac{\partial \phi}{\partial y} \pm \dot{s}\frac{\partial s}{\partial y}, \quad w = \frac{\partial \phi}{\partial z} \pm \dot{s}\frac{\partial s}{\partial z}, \quad \frac{d\dot{s}}{dt} = 0 \tag{18}$$

where $\dot{s} = ds/dt$. These equations may be derived from a variational principle

$$\delta \iiint \mathrm{L}\, dx\, dy\, dz = 0$$

where

$$\mathrm{L} = f(\rho) - \rho\left[\frac{d\phi}{dt} - \tfrac{1}{2}(u^2 + v^2 + w^2) \pm \tfrac{1}{2}\dot{s}^2\right] \tag{19}$$

and the quantities s, ϕ, u, v, w and ρ are to be varied independently. The pressure equation is now

$$\int \frac{dp}{\rho} + \tfrac{1}{2}(u^2 + v^2 + w^2 \pm \dot{s}^2) = \text{constant} \tag{20}$$

---

* The quantity s is not unique for we may write $s \pm \mathrm{F}'(\dot{s})$ in place of s and $\phi + \dot{s}\mathrm{F}'(\dot{s}) - \mathrm{F}(\dot{s})$ in place of ϕ. The chief advantage of the present plan is that $\dot{s}$ has a definite value and is generally zero at infinity. This makes the values of ϕ and s quite definite at infinity except for additive constants.

and the boundary condition is that ϕ and s should have prescribed values on a boundary not composed of stream-lines. In the case of the two-dimensional flow of an incompressible fluid the condition $d\dot{s}/dt = 0$ implies that $\dot{s} = g(\psi)$ where ψ is the stream-function and we have

$$\frac{\partial^2\psi}{\partial x^2} + \frac{\partial^2\psi}{\partial y^2} = \frac{\partial v}{\partial x} - \frac{\partial u}{\partial y} = \mp \frac{\partial(\dot{s}, s)}{\partial(x, y)} = \mp g'(\psi)\frac{\partial(\psi, s)}{\partial(x, y)} = \mp g'(\psi)\, g(\psi).$$

In the special case when $g(\psi) = \lambda e^{-h\psi}$ where λ and h are constants the equation reduces to one solved by Liouville.* When the upper sign is taken throughout the solution is†

$$e^{-2h\psi} = \frac{4}{\lambda^2 h^2}\frac{\left\{\left(\frac{\partial\sigma}{\partial x}\right)^2 + \left(\frac{\partial\sigma}{\partial y}\right)^2\right\}}{(\sigma^2 + \tau^2 + 1)^2}$$

where $\sigma + i\tau = F(x + iy)$ and F is an arbitrary function. In particular, if $r^2 = x^2 + y^2$, there is a solution of type

$$e^{h\psi} = -\frac{\lambda hr}{2}\left\{\left(\frac{r}{a}\right)^n + \left(\frac{a}{r}\right)^n\right\} = \lambda/\dot{s}$$

and when $n = 1$ the component velocities u, v are given by the expressions

$$u = -\frac{2y}{h(a^2 + r^2)}, \qquad v = \frac{2x}{h(a^2 + r^2)}$$

which are very like those for a line vortex but have the advantage that they do not become infinite at the origin. We also have

$$\phi = \frac{2}{h}\tan^{-1}\frac{y}{x}, \qquad s = -a\tan^{-1}\frac{y}{x}, \qquad \dot{s} = -\frac{2a}{h(r^2 + a^2)}.$$

When the lower sign is taken throughout the corresponding distribution of velocity is

$$u = -\frac{2y}{h(a^2 - r^2)}, \qquad v = \frac{2x}{h(a^2 - r^2)}$$

giving infinite values‡ of u and v on the circle $r = a$. There are thus two types of vortex motion, one in which the upper sign is taken throughout and another in which the lower sign is taken throughout. Brodetsky§ has worked out several cases of vortex motion of the second type and infinite values of the velocity are not exceptional. We shall devote our attention, then, to vortex *motion of the first type.*

---

* 'Liouville's Journal,' vol. 18, p. 71 (1853). The general solution of Liouville is quoted and used by S. Brodetsky, 'Proc. Interna. Congress Applied Mechanics,' Delft, p. 374 (1924).

† G. W. Walker, 'Roy. Soc. Proc.,' A, vol. 91, p. 410 (1915).

‡ It should be noticed that in this case $\phi = -\frac{2}{h}\tan^{-1}\frac{y}{x}$, $s = a\tan^{-1}\frac{y}{x}$, $\dot{s} = \frac{2a}{h(a^2 - r^2)}$

§ *Loc. cit.*

Now in the case under consideration $\dot{s}$ is zero at infinity and we may expect in general that when s varies like an angle over the circle of infinite radius that $\dot{s}$ will be zero even though u and v have finite limiting values.

On the assumption that $\dot{s}$ is zero at infinity and that adiabatic conditions prevail, the pressure equation (20) takes the form

$$\frac{a^2}{\gamma-1}[(\rho/\rho_0)^{\gamma-1}-1]+\tfrac{1}{2}(u^2+v^2+\dot{s}^2-U^2)=0$$

where a is the velocity of sound at infinity. As before

$$c^2=dp/d\rho=a^2(\rho/\rho_0)^{-\gamma 1}$$

and so $u^2+v^2=c^2$ when

$$u^2+v^2=\frac{2a^2}{\gamma+1}+\frac{\gamma-1}{\gamma+1}(U^2-\dot{s}^2).$$

This equation shows that when the motion is rotational and of the first type the local velocity of sound and velocity of flow at a point become equal for a smaller velocity of flow than when the flow is irrotational and the velocity at infinity is the same as before.*

This result indicates that when the irrotational solution fails on account of the velocity of flow becoming equal to the local velocity of sound the flow probably does not change over to a rotational flow of the first type because this would only make matters worse and give a velocity of flow greater than the local velocity of sound over a larger area. It is more likely that there will be a local production of waves and a consequent departure from steady motion. It is possible, too, that adiabatic conditions may no longer prevail.

5. *Hyperbolic Equations with elliptic boundary conditions.*

We shall first consider the hyperbolic equation

$$\frac{\partial^2 V}{\partial x\,\partial y}=0$$

and shall enquire whether there is a solution which takes an assigned value

---

* For rotational motion of the second type the word smaller must be replaced by larger. I see no good reason at present for completely excluding rotational motion of the second type if the infinite velocities do not actually occur in the field of flow but correspond to singularities enclosed by the boundary.

$F(\theta)$ on the unit circle $x = \cos\theta$, $y = \sin\theta$ and can be expressed in the form $V = f(x) + g(y)$ where $f(x)$ and $g(y)$ are expressible as power series

$$f(x) = \sum_{n=0}^{\infty} \alpha_n x^n, \qquad g(y) = \sum_{n=0}^{\infty} \beta_n y^n$$

which converge within the circle and on its circumference. If the given function $F(\theta)$ can be expressed as a Fourier series

$$\begin{aligned} F(\theta) &= a_0 + a_1\cos\theta + a_2\cos 2\theta + \dots \\ &\quad + b_1 \sin\theta + b_2 \sin 2\theta + \dots \end{aligned}$$

we should have

$$F(\theta) = f(\cos\theta) + g(\sin\theta).$$

Now it is clear that a term like $b_2 \sin 2\theta$ cannot be expressed in the form $\Sigma\beta_n \sin^n\theta$ for the series

$$2\sin\theta\left[1 - \frac{1}{2}\sin^2\theta - \frac{1\cdot 1}{2\cdot 4}\sin^4\theta \dots\right],$$

which looks as if it might be suitable for the purpose, represents $2\sin\theta|\cos\theta|$ instead of $2\sin\theta\cos\theta$. When $b_2 = 0$, $b_4 = 0$, . . ., there may, indeed, be a solution but this solution is not unique because $1 - x^2 - y^2$ is a regular solution which is zero at all points of the unit circle $x^2 + y^2 = 1$, and has continuous first derivatives throughout the circle, the second derivatives being finite.

By laying down the condition that V should be expressible as a power series we shall be requiring more than is necessary for physical problems. The conditions of regularity which are usually imposed relate to the continuity of the function and its first derivatives in the specified region and the finiteness of the second derivatives which occur in the differential equation.

6. *Elliptic region completely surrounded by a hyperbolic region.*

The effect of a change from the elliptic to the hyperbolic type may be illustrated by means of the partial differential equation.

$$\frac{\partial^2 V}{\partial r^2} + \frac{1}{r}\frac{\partial V}{\partial r} + \left(\frac{1}{r^2} - 1\right)\frac{\partial^2 V}{\partial\theta^2} = 0, \tag{6.1}$$

which is elliptic when $r < 1$ and hyperbolic when $r > 1$. We shall write $x = r\cos\theta$, $y = r\sin\theta$, and regard (x, y) as the rectangular co-ordinates of a point in a plane.

We seek a solution which is such that $V = f(\theta)$ when $r = a$ and is regular for $r < a$ in the sense that V, $\frac{\partial V}{\partial r}$ and $\frac{\partial V}{r\partial\theta}$ are continuous and $\frac{\partial^2 V}{\partial x^2} + \frac{\partial^2 V}{\partial y^2}$ finite.

If $f(\theta) = \cos n\theta$ there is a solution

$$V = \frac{J_n(nr)}{J_n(na)}\cos n\theta, \tag{6.2}$$

which satisfies the requirements if $J_n(na) \neq 0$. Now,* if $z^{(n)}$ is the smallest positive root of the equation $J_n(z) = 0$ we have $n^{-1}z^{(n)} > 1$ and as $n \to \infty$ it seems that $n^{-1}z^{(n)} \to 1$. Hence, when $a < 1$, that is, when the circle $r = a$ lies in the elliptic region, we have $J_n(na) \neq 0$ and there is certainly a solution of type (5.2), but when $a > 1$ and is equal to one of the quantities $z^{(n)}/n$ for which $J_n(na) = 0$ there is no regular solution of type $V = F(r) \cos n\theta$ which takes the value $\cos n\theta$ when $r = a$.

Again, when
$$f(\theta) = \sum_{n=0}^{\infty} (A_n \cos n\theta + B_n \sin n\theta)$$
and $a > 1$ there is a difficulty relating to the convergence of the series
$$V = \sum_{n=0}^{\infty} \frac{J_n(nr)}{J_n(na)} (A_n \cos n\theta + B_n \sin n\theta),$$
which gives the formal solution of the boundary problem. The behaviour of the nth term for large values of n may, in fact, be studied with the aid of the well-known asymptotic expressions† for $J_n(nr)$ for large values of n.

7. *A non-linear equation which changes in type.*

It now seems worth while to remark briefly on a non-linear equation which changes from the elliptic to the hyperbolic type as a point passes from one region to another. Let us form the equation with the general solution
$$x = f[z + \sqrt{(x^2 - y^2)}] + g[z - \sqrt{(x^2 - y^2)}] \tag{7.1}$$
where f and g are arbitrary functions of their arguments. These arguments are real when $x^2 > y^2$ and are complex when $x^2 < y^2$; hence we can expect a change from the elliptic to the hyperbolic type when the point (x, y) passes from the elliptic region, $x^2 < y^2$ (marked E in fig. 1) to the hyperbolic region,

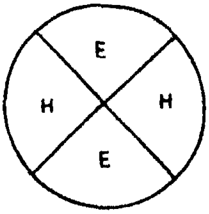

Fig. 1.

$x^2 > y^2$ (marked H in fig. 1). If we write $p = \frac{\partial z}{\partial x}, q = \frac{\partial z}{\partial y}, r = \frac{\partial^2 z}{\partial x^2}, s = \frac{\partial^2 z}{\partial x \partial y}$, $t = \frac{\partial^2 z}{\partial y^2}$, the differential equation is found to be
$$ar + 2hs + bt = c,$$

---

* See Watson's "Bessel Functions," pp. 485, 516.

† See Watson's "Bessel Functions."

where

$$a = y^2 - q^2 (x^2 - y^2), \qquad b = x^2 - p^2 (x^2 - y^2)$$
$$h = xy + pq (x^2 - y^2), \qquad cy = q \, [x^2 - y^2 - (px + qy)^2]$$

and it is easily found that

$$ab - h^2 = (y^2 - x^2)(py + qx)^2$$

so that the foregoing statements regarding the type of the equation are readily verified.

It is easily seen that there are particular solutions which are regular within the unit circle although the interior of the circle is partly elliptic and partly hyperbolic. A trivial solution of this type is $z = x$ and this is obtained by taking $f(u) = g(u) = \frac{1}{2}u$. Another interesting regular solution is obtained by writing

$$f(u) = g(u) = \tan^{-1} u.$$

This gives

$$z = (x^2 + \operatorname{cosec}^2 x - y^2)^{\frac{1}{2}} - \cot x.$$

When x is small $\operatorname{cosec}^2 x = x^{-2} + \frac{1}{3} + x^2/15 + \ldots \quad \cot x = x^{-1} + x/3 + \ldots$ and so

$$z = \tfrac{1}{6}x + \frac{187}{120} x^3 - \tfrac{1}{2}xy^2 - \ldots$$

the function z is thus regular at the origin. It is also single-valued in the unit circle because for a given value of x the greatest value of y^2 is $1 - x^2$ and with this value of y^2 the quantity under the square root is $2x^2 + \cot^2 x$, which is always positive.

This example shows that in some cases, at any rate, the elliptic type of boundary problem possesses a regular solution in the region enclosed by the boundary even though in this region the partial differential equation is partly of elliptic and partly of the hyperbolic type.

8. *Hyperbolic region.*

We shall now consider the equation

$$(1 - x^2) \frac{\partial^2 V}{\partial x^2} - 2x \frac{\partial V}{\partial x} = (1 - y^2) \frac{\partial^2 V}{\partial y^2} - 2y \frac{\partial V}{\partial y} \tag{8.1}$$

which is elliptic when $1 - x^2$ and $1 - y^2$ have different signs and hyperbolic when these quantities have the same sign. There is a particular solution of type

$$V = P_n(x) \, P_n(y),$$

but we shall find it more convenient to work with another type of solution which is readily obtained by expressing the last solution in the well-known form

$$P_n(x)\,P_n(y) = \frac{1}{\pi}\int_0^\pi P_n[xy + \cos\phi\sqrt{(1-x^2)(1-y^2)}]\,d\phi$$

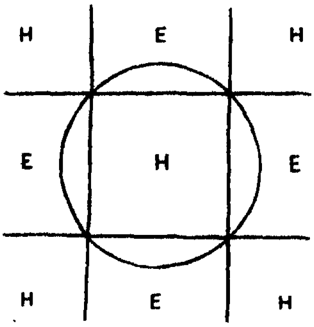

Fig. 2.

and generalising this into

$$V = \frac{1}{\pi}\int_0^\pi f[xy + \cos\phi\sqrt{(1-x^2)(1-y^2)}]\,d\phi.$$

Expanding $f(z)$ in a series of powers of z we obtain a solution of type

$$V = \sum_{n=0}^{\infty} a_n (x^2+y^2-1)^{n/2} P_n\left[\frac{xy}{(x^2+y^2-1)^{\frac{1}{2}}}\right]. \qquad (8.2)$$

Let us now consider a simple boundary problem for the realm bounded by the circle $x^2 + y^2 = 2$ which lies entirely in the elliptic region except that it passes through four points (1, 1), (1, −1), (−1, 1), (−1, −1) at which two elliptic regions and two hyperbolic regions are contiguous. At a point $x = \sqrt{2}\cos\theta$, $y = \sqrt{2}\sin\theta$ of this circle V takes the value

$$F(\theta) = \sum_{n=0}^{\infty} a_n P_n(\sin 2\theta)$$

the series being certainly convergent when the series

$$\sum_{n=0}^{\infty} n|a_n| \qquad (8.3)$$

is convergent.

When the coefficients a_n are unrestricted the series (8.2) does not necessarily represent a regular solution of the differential equation even though it is convergent. Let us suppose, for instance, that $a_n = 1$, that $x^2 + y^2 < 2$ so that $x^2 + y^2 - 1 < 1$ and that $(x^2 - 1)(y^2 - 1) < 0$ so that the argument of the Legendre function has a modulus less than unity, then

$$V = [1 - 2xy + (x^2 + y^2 - 1)]^{-\frac{1}{2}} = (x - y)^{-1}.$$

This solution is quite regular in the elliptic region defined by the foregoing inequalities but when it is continued into the hyperbolic region $x^2 < 1$, $y^2 < 1$, it gives a solution which is infinite on the line $x = y$. When, however, the coefficients a_n are such that the series (8.3) converges, the function V represented by the series (8.2) seems to be regular at all points of the circle $x^2 + y^2 \leqslant 2$ and represents a solution which takes the value $F(\theta)$ on the circumference. This function $F(\theta)$ is not a perfectly arbitrary function of θ, for it has the period π, but the chief point is that a solution with this boundary value exists and there is no evident reason for thinking that it is not the only solution.

The convergence of the series (8.2) when the series (8.3) converges may be inferred from the fact that when $x^2 < 1$ and $y^2 < 1$ the quantity $xy + \cos\phi \,.\, \sqrt{(1 - x^2)(1 - y^2)}$ can be regarded as the cosine of a real angle and so has a modulus less than unity or equal to unity. The equation

$$\begin{aligned} V_n \equiv (x^2 + y^2 - 1)^{n/2} \, P_n\left[\frac{xy}{(x^2 + y^2 - 1)^{\frac{1}{2}}}\right] \\ = \frac{1}{\pi}\int_0^{\pi} \left[xy + \cos\phi \sqrt{(1 - x^2)(1 - y^2)}\right]^n d\phi \end{aligned}$$

indicates, then, that*

$$\Bigg|(x^2 + y^2 - 1)^{n/2} P_n\left[\frac{xy}{(x^2 + y^2 - 1)^{\frac{1}{2}}}\right]\Bigg/ \leqq \Bigg| .$$

The convergence of the series in the elliptic region for which $(x^2 - 1)(y^2 - 1) < 0$, $x^2 + y^2 \ngtr 2$ follows from the fact that in this region

$$\Bigg| P_n\left[\frac{xy}{(x^2 + y^2 - 1)^{\frac{1}{2}}}\right]\Bigg/ \leqq \Bigg| .$$

At points $x = \cos\theta$, $y = \sin\theta$ on the circle $x^2 + y^2 = 1$ the solution (8.2) takes the value

$$f(\theta) = \sum_{n=0}^{\infty} \frac{1\cdot 3 \ldots 2n - 1}{2\cdot 4 \ldots 2n} a_n \sin^n 2\theta.$$

The function $f(\theta)$ is again of a special type but the boundary problem $V = f(\theta)$ at points of this circle still seems to possess a unique solution although the circle is almost wholly in the hyperbolic region. The points (1, 0), (0, 1), (−1, 0), (0, −1) on the circle belong, however, to the parabolic line which separates the elliptic and hyperbolic regions.

---

* The equation also gives $(1 - y^2)\dfrac{\partial Vn}{\partial y} = n[xV_{n-1} - yV_n]$ $(1 - x^2)\dfrac{\partial Vn}{\partial x} = n[yV_{n-1} - xV_n]$ and these relations may be used to discuss the convergence of the series for $\partial V/\partial x$ and $\partial V\partial/y$. When $y^2 = 1$ or $x^2 = 1$ the series (8.2) reduces to a simple power series.

When we consider a similar boundary problem for a circle $x^2+y^2=a^2$, which lies wholly within the hyperbolic region when $a^2<1$, the particular solutions of types $P_n(x)\,Q_n(y)$, $Q_n(x)\,P_n(y)$, $Q_n(x)\,Q_n(y)$ are now regular within the circle and there is every likelihood that if there is a solution with a prescribed boundary value $f(\theta)$, this solution will not be unique. Indeed, since Cauchy's problem generally* possesses a solution in the hyperbolic region it should be possible to find more than one regular solution with the prescribed boundary values.† In all the cases that have been considered the question of uniqueness requires further consideration.

9. *Hyperbolic region completely surrounded by an elliptic region.*

A particularly interesting case is furnished by the equation‡

$$(1-r^2)\frac{\partial^2 V}{\partial r^2}-2r\frac{\partial V}{\partial r}-\tfrac{1}{4}V-\frac{\partial^2 V}{\partial\theta^2}=0,$$

which is elliptic when $r>1$ and hyperbolic when $r<1$. The characteristics in this case are obtained by integrating the equation

$$(1-r^2)\,d\theta^2=dr^2,$$

and so are the circles of type $r=\cos(\theta-\alpha)$ where α is an arbitrary real constant.

The equation possesses an elementary solution

$$V=[\cos(\theta-\alpha)-r]^{-\frac{1}{2}}$$

which is infinite on the characteristic curve with parameter α, this solution may be generalised by multiplying by an arbitrary function $f(\alpha)$ and integrating between suitable limits. If $r=\cos\beta$ one integral of this type is

$$V=\frac{1}{\pi}\int_{\theta-\beta}^{\theta+\beta}[\cos(\alpha-\theta)-\cos\beta]^{-\frac{1}{2}}\,f(\alpha)\,d\alpha.$$

When $f(\alpha)=\cos n\alpha$, where n is an integer, we obtain the well-known particular solution

$$V=\frac{\cos n\theta}{\pi}\int_{-\beta}^{\beta}[\cos\omega-\cos\beta]^{-\frac{1}{2}}\cos n\omega\,d\omega=P_{n-\frac{1}{2}}(r)\cos n\theta,$$

where $P_m(r)$ is the Legendre function.

---

* When the prescribed values of V and $\partial V/\partial r$ are analytic functions of x and y. (See Hadamard, *loc. cit.*, ch. 2.)

† We may, for instance, add to any regular solution which satisfies the boundary condition, a new solution which is zero on the boundary and for which $\partial V/\partial r$ has a prescribed analytic value.

‡ This equation occurs naturally when Laplace's equation is transformed to toroidal co-ordinates.

If r and θ are regarded as polar co-ordinates, this solution is regular at the origin only when $n = 0$, for when $n > 0$, $\frac{\partial V}{\partial x}$ and $\frac{\partial V}{\partial y}$ are both infinite. If we are given that $V = 1$ on the circle $r = a$ there is a solution

$$V = \frac{P_{-\frac{1}{2}}(r)}{P_{-\frac{1}{2}}(a)}$$

regular in the circle if $P_{-\frac{1}{2}}(a) \neq 0$. Now

$$P_{-\frac{1}{2}}(a) = 1 - \left(\frac{1}{2}\right)^2 \frac{a-1}{2} + \left(\frac{1 \cdot 3}{2 \cdot 4}\right)^2 \left(\frac{a-1}{2}\right)^2 - \dots \qquad |a-1| < 2$$

and so if $0 \leqslant a \leqslant 3$ we have $P_{\frac{1}{2}-}(a) > 0$.

If $a < 1$ this is not the only solution that is regular in the circle $r \leqslant a$ for the differential equation

$$(1 - r^2)\frac{\partial^2 V}{\partial r^2} - 2r\frac{\partial V}{\partial r} - \frac{1}{4}V = 0$$

possesses a second solution*

$$S_{-\frac{1}{2}}(r) = \frac{1^2}{1!}\left(\frac{r}{2}\right) + \frac{3^2}{3!}\left(\frac{r}{2}\right)^3 + \frac{3^2 \,.\, 7^2}{5!}\left(\frac{r}{2}\right)^5 + \dots$$

which becomes infinite at $r = 1$ like $\log(1 - r)$. Consequently a more general solution which takes the value 1 on the circle $r = a$ is

$$V = \lambda \frac{P_{-\frac{1}{2}}(r)}{P_{-\frac{1}{2}}(a)} + \mu \frac{S_{-\frac{1}{2}}(r)}{S_{-\frac{1}{2}}(a)}$$

where λ and μ are constants whose sum is unity. When $1 < a < 3$ this second solution must be excluded since it is infinite on the circle $r = 1$. In this case the question of uniqueness is rather hard to decide because there may possibly be a solution which is zero on a characteristic $r = \cos(\theta - \alpha)$ and has at the same time zero first derivatives at all points of this curve. To satisfy the requirements of continuity, however, this solution of the partial differential equation would need to be regular at all points within the characteristic circle.

If we exclude the origin by a circle $r = b$ and consider a simple boundary problem for the annular region bounded by the circles $r = a$ and $r = b$ there will be regular solutions V satisfying the conditions

$$V = f(\theta) \text{ when } r = a, \qquad V = g(\theta) \text{ when } r = b,$$

provided that the functions $f(\theta)$ and $g(\theta)$ are suitably related. Thus, if

$$V = P_{m-\frac{1}{2}}(r) \cos m\theta$$

---

* See Forsyth, "Differential Equations," p. 241. The result is due to Heine.

where m is an integer, the boundary conditions are satisfied if

$$f(\theta) \equiv \mathrm{P}_{m-\frac{1}{2}}(a) \cos m\theta, \qquad g(\theta) \equiv \mathrm{P}_{m-\frac{1}{2}}(b) \cos m\theta.$$

Such a solution may fail to be unique when there is a solution $\mathrm{P}_{n-\frac{1}{2}}(a) \cos n\theta$, regular in the annulus and vanishing on both boundaries. This will be the case when $\mathrm{P}_{n-\frac{1}{2}}(a) = 0$ and $\mathrm{P}_{n-\frac{1}{2}}(b) = 0$. We shall now endeavour to show that this is not possible when $1 < a < 3$ because for such values of a we have always $\mathrm{P}_{n-\frac{1}{2}}(a) > 0$. Let us suppose that for some positive integral value of n we have

$$\mathrm{P}_{n-\frac{1}{2}}(a) > \mathrm{P}_{n-\frac{3}{2}}(a) > \dots \qquad > \mathrm{P}_{-\frac{1}{2}}(a) > 0.$$

The difference equation satisfied by the functions $\mathrm{P}_{n-\frac{1}{2}}(a)$ shows that

$$(n + \tfrac{1}{2})\, \mathrm{P}_{n+\frac{1}{2}}(a) + (n - \tfrac{1}{2})\, \mathrm{P}_{n-\frac{3}{2}}(a) = 2na\, \mathrm{P}_{n-\frac{1}{2}}(a) > 2n\, \mathrm{P}_{n-\frac{1}{2}}(a)$$

the inequality being valid for $a > 1$. Writing this inequality in the form

$$(n + \tfrac{1}{2})\, [\mathrm{P}_{n+\frac{1}{2}}(a) - \mathrm{P}_{n-\frac{1}{2}}(a)] > (n - \tfrac{1}{2})\, [\mathrm{P}_{n-\frac{1}{2}}(a) - \mathrm{P}_{n-\frac{3}{2}}(a)] > 0,$$

we see that it implies that $\mathrm{P}_{n+\frac{1}{2}}(a) > \mathrm{P}_{n-\frac{1}{2}}(a)$.

Now if $1 < a < 3$

$$\mathrm{P}_{\frac{1}{2}}(a) - \mathrm{P}_{-\frac{1}{2}}(a) = \frac{a-1}{2} - \frac{1\,.\,3}{2\,.\,4}\left(\frac{a-1}{2}\right)^2 + \frac{1\,.\,3^2\,.\,5}{2\,.\,4^2\,.\,6}\left(\frac{a-1}{2}\right)^3 - \frac{1\,.\,3^2\,.\,5^2\,.\,7}{2\,.\,4^2\,.\,6^2\,.\,8}\left(\frac{a-1}{2}\right)^4 - \dots$$

and the terms of this series decrease continually in magnitude as we proceed from left to right, therefore, when $1 < a < 3$ we have $\mathrm{P}_{\frac{1}{2}}(a) - \mathrm{P}_{-\frac{1}{2}}(a) > 0$, hence we may proceed by induction and prove that $\mathrm{P}_{n+\frac{1}{2}}(a) > 0$.

This result seems to indicate that if the circle $r = a$ lies in the region $1 < r < 3$ there is no solution of type $\mathrm{P}_{n-\frac{1}{2}}(r) \cos n\theta$ which is zero on both boundaries, though if $b < 1$ there may, perhaps, be a solution which is zero on the circle $r = b$.

It should be noticed also that there is no characteristic curve which lies entirely within the annular region and so it is not clear how the uniqueness of a solution can fail.

A new form of Calorimeter suitable for Determining Heats of Solution, with an Application to Worked and Annealed Metals.

By C. J. Smith, Ph.D., M.Sc., A.R.C.S., Lecturer in Physics, Royal Holloway College, London.

(Communicated by Prof. C. H. Desch, F.R.S.—Received August 2, 1929.)

Introduction.

In the course of a study of cold-worked metals it has been found desirable that some means should be devised for measuring the amount of energy stored in a metal when it is deformed beyond the elastic limit. During the process of cold-working a large part of the work done is converted into heat, but the change in properties of the metal is such as to indicate that its potential energy has been increased. The increase is known to be relatively small, and therefore difficult to measure. It should be possible to determine it by dissolving the cold-worked metal in a suitable solvent and finding the heat of solution, any difference between the result and the heat of solution of the same metal in a fully annealed or unworked condition then representing the increase of potential energy. Such a method has not hitherto been applied with success, on account of the insufficient accuracy of the usual calorimetric methods, and the object of the present paper is to describe a calorimeter on the continuous flow principle originally due to Callendar, having an increased sensitivity when used for such experiments. A few measurements of the heat of solution of cold-worked metals, and of the same metal in the annealed condition, are included. The results show that the potential energy stored in cold-working amounts, for the metals examined, only to about 1 per cent. of the heat of solution.

Some Earlier Types of Calorimeter.

The heat of solution of metals was a subject investigated by Salt* and Baker.† Baker employed a calorimeter in the form of a thin glass beaker of 500 c.c. capacity. This was supported inside a highly polished nickeled vessel, and the whole was screened from the influence of external fluctuations of temperature by surrounding it with a copper water jacket. The water was kept in motion by means of a stirrer. A copper lid was used to cover this enclosure. Such an apparatus has a considerable water equivalent, and this was determined by the method of mixtures.

---

* 'Rep. Brit. Assoc.,' 1898.

† 'Roy. Soc. Proc.,' A, vol. 196, p. 529 (1901).

Now when small differences are the subject of any piece of research the attempt should always be made to eliminate the possible errors, or at least reduce them to negligible amounts. Callendar* has shown that the errors of calorimetry can be largely avoided by the use of a continuous flow method. The present form of calorimeter was designed so that a continuous flow method could be utilised in helping to solve the present problem.

The Calorimeter.

The new calorimeter is shown in fig. 1. It consists of an inner tube A, which is made of very thin walled glass. This is surrounded by a somewhat larger tube B, the clearance between these two tubes being about 1·5 mm. By means of a glass tube spiral the tube B is joined to another tube C, which leads to an exit tube D. These tubes constitute the calorimeter proper, but to reduce heat losses to a minimum the whole is surrounded by a wide glass jacket fused to the calorimeter and exhausted by means of a mercury vapour pump, and closed hermetically at E. This calorimeter is surrounded by a copper jacket, through which water from a thermostat passes continuously.

The thermal reaction to be investigated takes place in the tube A, and the heat evolved is abstracted by means of a constant stream of water which is at the temperature of the thermostat, and enters the calorimeter at F. The water passes between the tubes A and B, where a spiral of copper wire serves to make it circulate around A. The tube A is made long in order to diminish the conduction of heat along it. The change in temperature of water when it has passed through the calorimeter is measured by means of a differential pair of platinum thermometers P_1 and P_2. The glass stirrer G facilitates the reaction and it should preferably just rest upon the bottom of the tube A, so that any solid matter is continuously moved until solution has taken place.

The Thermostat, Circulating Pump and Constant Flow Apparatus.

The thermostat is similar to that used by Callendar and recently described by the author.† No detailed description is therefore necessary in the present paper.

In continuous flow calorimetry, as well as in other methods, it is always advantageous to pass water at the temperature of the thermostat around

---

* 'Phil. Trans.,' A, vol. 199, p. 55 (1902).

† 'Roy. Soc. Proc.,' A, vol. 115, p. 564 (1927).

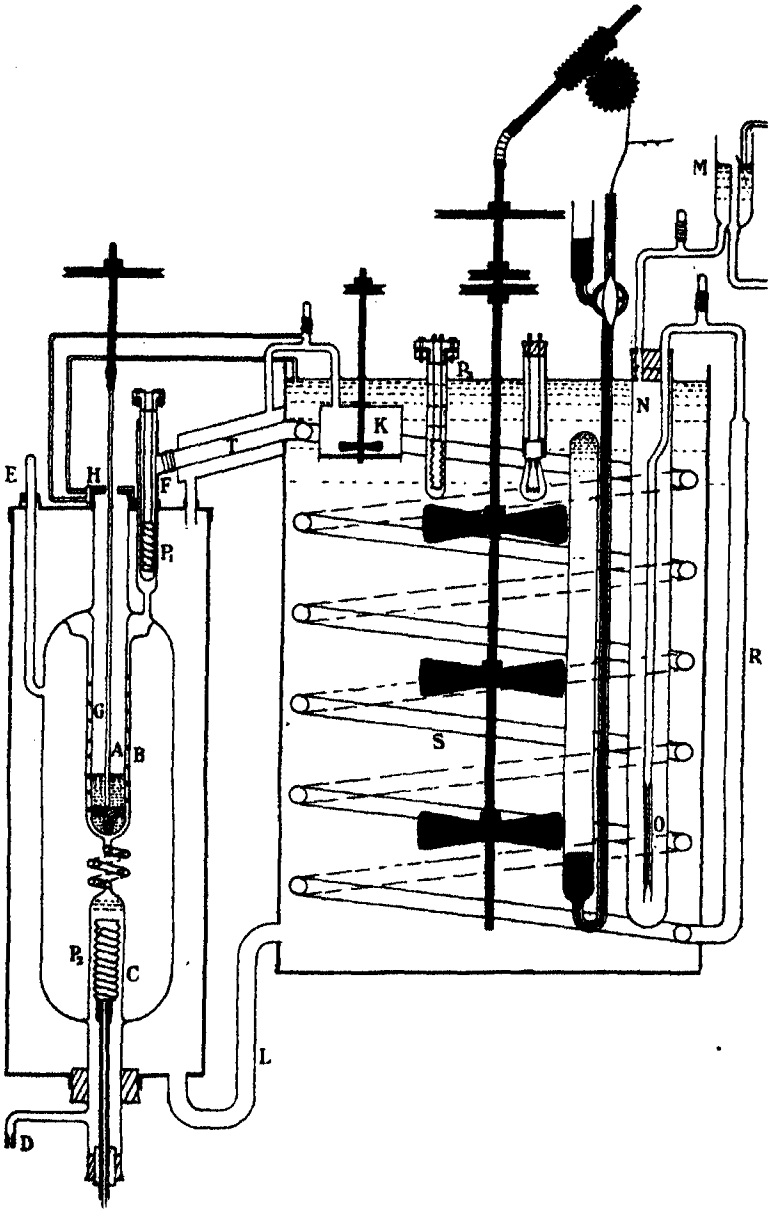

Fig. 1.

the outer walls of the glass calorimeter. This reduces the radiation losses to a minimum, since there is only a small temperature gradient (in this work it never exceeded 2° C.) between the calorimeter proper and its immediate surroundings. Such a flow of water is maintained by means of the pump K (fig. 1). Inside a cylinder of brass, which is open at its lower end but closed at the top except for a delivery tube which leads to the jacket of the calorimeter, a small revolving paddle is placed in such a way that an upward stream of water is maintained, the water returning to the calorimeter by way of the tube L.

A constant head of water is needed to provide a steady flow. The distilled water used in these experiments is supplied to the vessel M, as indicated, any excess finding an exit through an overflow tube. The water which is to be the calorimetric liquid passes from M to N, a long glass tube immersed in the thermostat, and flows through the capillary tube O, which serves to restrict the flow. This tube is about 1 mm. in diameter and 10 cm. long. Since the tube is maintained at a steady temperature the flow of water is kept constant, since the viscosity of water is not affected to any appreciable extent by small temperature changes. The water then passes along the wider tube in N, and although the temperature may now change this will not affect the constancy of flow because the tube is wide (5 mm.), so that the retarding forces due to viscosity become negligible. Leaving the thermostat the water passes along a wide glass tube R, and then flows through the lead spiral S, where it assumes the temperature of the thermostat. In transferring this water to the calorimeter along T the heat losses are made negligible by surrounding it with a wider tube containing water at the same temperature. The actual temperature of the water is recorded by means of a platinum thermometer P_3.

The pump K also supplies a stream of water which passes through a brass cover H, surrounding the otherwise open end of the calorimeter. In this way the convection currents in A are reduced, and since all the upper portion of A is at one and the same temperature, any heat loss along this part of the apparatus must be very small.

The Thermometers.

Of the three platinum resistance thermometers used in this investigation, the one which indicates the constancy of temperature in the thermostat is about 20 ohms in resistance, and is constructed in the usual manner.[*] The thermometers P_1 and P_2 also have a resistance of about 20 ohms, and since they are used differentially are constructed without the usual compensating leads. P_1 is enclosed in a glass tube because it remains in water at constant temperature. The construction of the thermometer P_2 presented considerable difficulties, since it had to be used to record the temperature of water which was changing continuously throughout an experiment. Accordingly, the usual glass sheath was not used, but the wire, having been wound on a mica frame, was insulated from the water by means of collodion. This substance was dissolved in ether and several coatings applied. Such a coating was able to withstand a pressure of 200 volts. Further, the thermal capacity of this thermometer was reduced to a minimum by using only the thinnest sheet of mica consistent with rigidity. The two leads from this thermometer passed along a glass supporting tube, the escape of water being prevented by means of sealing wax, placed as shown in the diagram, at the lower end of the mica.

---

[*] Lang, 'J. Sci. Inst.,' vol. 2, p. 228 (1925).

After some preliminary trials it was soon found that such a thermometer was not wholly satisfactory. Although several pieces of wire gauze were placed above the thermometer in order to mix the water, it was apparent that P_2 was not indicating the true mean temperature of the outflowing water. This difficulty was eventually overcome by rotating the thermometer so that it functioned as an efficient stirrer itself. The time of rotation was about 2 sec., and the method of imparting this motion to the thermometer and at the same time preventing an escape of water is shown in fig. 2. A phosphor bronze tube A is capable of rotating about its axis inside a steel collar C. The two faces of these tubes which are in contact are smeared with tap grease, there being an excess of grease in the small recess B. The whole is mounted in a steel framework. A small ball-race F and the spring S serve to keep the joint water-tight.

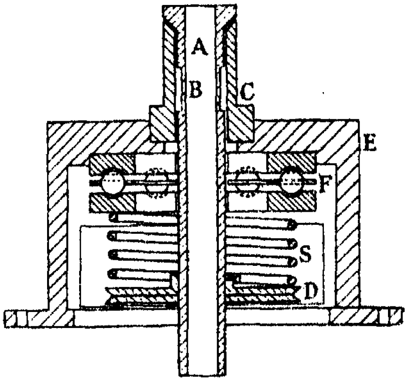

Fig. 2.

Calibration of the Thermometers.

The platinum resistance thermometer P_3 was calibrated in the usual way, and had a fundamental interval of six ohms. The thermometers P_1 and P_2 which constituted the differential pair, could not be calibrated in this manner owing to the wax used in the construction of P_2. The difference in resistance corresponding to a small rise in temperature (about 2° C.) was therefore determined, using the calorimeter as an ordinary continuous flow apparatus. A small heating coil was covered with sealing wax and placed in A. It was heated by means of a current supplied by a battery of three accumulators. The energy dissipated per second was calculated from observations on the potential difference across this coil and the current in it. This potential difference was measured by means of a Rayleigh potentiometer, using a Weston Cadmium cell as a standard of E.M.F. The current was deduced from observations on the potential difference across a standard one ohm coil included in the heating circuit.

The heat loss along the leads of the heating coil did not exceed the other experimental errors, for two determinations having the current twice the value in one as the other gave results which were consistent to within two parts in a thousand. In this particular piece of research it was not essential to calibrate the thermometers more accurately, since in the actual experiment the changes in temperature were nearly always identical.

The Preparation of the Copper, Zinc and Brass.

The copper which was used was specially prepared from electrolytic copper by Mr. E. A. Atkins, to whom I wish to express my appreciation for this very valuable assistance. The copper was supplied in the form of wire (22 S.W.G.). These annealed and hard-drawn copper wires broke under loads of 24 lb. weight and 49 lb. weight respectively. For the purpose of these experiments the copper wire was annealed *in vacuo* in a high frequency induction furnace, after having been cut into lengths of about 2 cm. The zinc, which was supplied commercially, was obtained in the form of sheet, the thickness of which was 0·1 mm. It was cut into pieces about 2 cm. long and 0·15 cm. wide. These were annealed in hydrogen at 380° C. for two hours. The brass wire was of the commercial variety (22 S.W.G.), and contained 62·4 per cent. of copper. It was cut into pieces about 2 cm. long, and annealed in hydrogen at 700° C. for two hours. No volatilisation of zinc from this brass was observed.

The Choice of a Solvent.

In work of this nature it is at once apparent that no gaseous products must be formed as a result of the chemical action between the metal and solvent. This fact at once precludes the use of such acids as sulphuric acid, and directs the choice towards nitric acid, bromine water, or such aqueous solutions as those of cupric ammonium chloride, although the gaseous products formed by the action of concentrated nitric acid on metal are, under suitable conditions, completely soluble in the acid.* Gladstone† showed, however, that nitric acid is not a suitable liquid when one wishes to compare the heat of dilution of an alloy with that of a mere mixture of the metals in the same proportion, because the products of the reaction are different.

---

* 'Roy. Soc. Proc.,' A, vol. 107, p. 422 (1925).

† 'J. Iron and Steel Inst.,' p. 497 (1923).

In his work Gladstone was able to use aqueous solutions of ferric ammonium chloride or cupric ammonium chloride, for the above objections cannot be raised against these, and the reaction was rapid. This latter condition was valid in his case, because the metals used were in the form of filings. In the present research these solutions were tried, but the reactions were so slow that these reagents were discarded.

In the experiments by Herschkowitsch[*] a solution of bromine in potassium bromide was used. A few preliminary experiments showed that a very strong solution was necessary, the solution which was finally used containing 231 grammes of bromine and 182 grammes of potassium bromide per litre. The amounts used in each experiment were copper 40·8 c.c., brass 40·8 c.c., and zinc 27·8 c.c., diluted with 26·7 c.c. water.

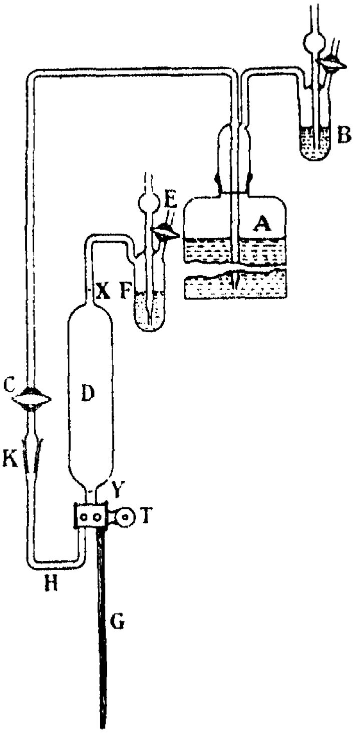

Fig. 3.

When dealing with such concentrated solutions of bromine, several difficulties are experienced. If the solution is stored in a large bottle and poured into a measuring jar prior to its transference to the calorimeter, some bromine is lost every time this operation is performed. Now the consequent change in the strength of the solution, whilst it may not be sufficient to produce a measurable change in the heat of the solution of any given metal, will produce errors owing to the existence of the heat changes which are associated with the diluting of the solution containing the final products of the reaction. In order to overcome these difficulties the apparatus shown in fig. 3 was constructed. The bromine solution is contained in a large bottle A, fitted with a conical glass joint held in position, as shown, by means of sealing wax placed around the outside of the joint. A delivery tube leading to the tap C extends to the bottom of the liquid: the glass trap B is made in the form shown, and contains bromine solution of the same strength as in A. When the solution is being delivered below C, the glass tap attached to B is closed, so that any air entering the space above the bromine solution in A is saturated with bromine vapour.

---

[*] 'Bull. Acad. Roy. Belge,' p. 1066 (1903).

The form of pipette used in this experiment is also shown in fig. 3. The bulb D was joined at its upper end to a glass trap F, similar to B; its lower end was attached to a two-way tap T. This tap was fitted with a long capillary tube G, which reached to the bottom of the calorimeter, and also with a tube H provided with a conical joint K. By opening the taps C, T, and E, the solution could be transferred to the pipette D. E was then closed and T turned so that the solution emptied itself through G: the air entering the pipette was saturated with bromine vapour, so that the strength of the solution coming from D was unaltered. Before actually transferring any solution to the calorimeter the pipette was washed out with the solution; suitably-placed marks, X and Y, enabled a known volume to be transferred to the calorimeter.

Details of Experimental Manipulation.

The metals and solution having been prepared, it was found that after a lapse of about two hours the temperature of the thermostat and calorimeter had become constant. At the beginning of the work it was decided to maintain a temperature of 20° C. in the thermostat, this being the temperature generally adopted in such experiments. The temperature could be maintained constant within 0·003° C. for periods of an hour at a time. The actual experiment only lasted thirty minutes, so that the temperature of the calorimeter could be considered constant.

The mass of water flowing per second was determined from observations on the mass of water which collected in a weighed conical flask over a period of five minutes. This flow was also constant to within 0·1 per cent., a fact which showed the constancy of the thermostat temperature, since a narrow tube controlled the flow of water. The fact that during an experiment the temperature of the water passing around A varied by 2° C. did not alter the rate of flow of the water was tested by observing the mass of water flowing under such conditions.

When in use the thermostat and calorimeter were surrounded by cotton wool, evaporation from the thermostat being prevented by covering the latter with a polished lid.

Before introducing the metal into the calorimeter a known quantity of it is allowed to remain in a glass tube resting on the outer jacket of the calorimeter; this tube rests under a layer of cotton wool. By raising the double-walled lid H the metal could be introduced into the calorimeter. The lid was then replaced in position, and 15 seconds after the introduction of the metal the spot of light from the galvanometer had moved nearly 1 cm. on a scale placed at 1 m. distance away from the galvanometer. This fact showed how rapidly the heat was transferred from the calorimeter vessel A to the thermometer P_2.

In measuring the difference in resistance between the two thermometers P_1 and P_2, it was decided to make observations at intervals of half a minute at those times when the temperature was changing rapidly. It was found possible, by sliding the jockey along the wire of a Callendar Griffiths bridge, to maintain the spot of light on the galvanometer scale so that its maximum excursion from the zero was not more than 1 cm.

The graph shown in fig. 4 is the result obtained by dissolving 0·500 gramme of annealed brass in 40·8 c.c. of the prepared solution. All the graphs which were obtained during these experiments were of the same shape. The area of the graph is a measure of the heat of solution. The following table is a synopsis of the results obtained :—

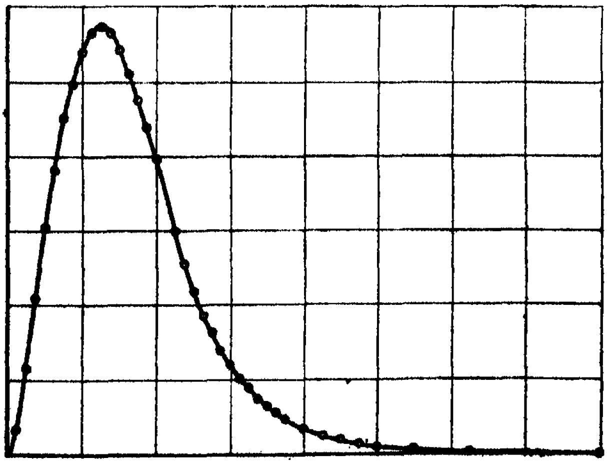

FIG. 4.

Metal.		Mass of Metal.	Volume of Solvent.	Heat of Solution (cals).			
				1	2	Mean.	Difference per gramme.
		Gramme.	c.c.				
Copper	Annealed	1·000	40·8	737	735	736	—
	Hard Drawn	1·000	40·8	747	746	746·5	10·5
Brass	Annealed	0·500	40·8	458	457	457·5	—
	Hard Drawn	0·500	40·8	462	462	462	9·0
Zinc	Annealed	0·300	27·8*	428	426	427	—
	Hard Drawn	0·300	27·8*	429	429	429	6·7

* In these two cases 26·7 c.c. of water were added in order to decrease the rate at which the metal dissolved.

The above table would indicate that the error in these experiments is about 0·3 per cent. The mean values, however, for the worked and annealed metals differ by about 1 per cent., so that it may safely be concluded that the difference which has been measured is a real one.

The author would like to take this opportunity of thanking Prof. C. H. Desch, F.R.S., for his guidance and encouragement during the course of these experiments, which were carried out in the Metallurgical Research Laboratory of the University of Sheffield.

APPENDIX.

The Potential Energy of Cold-Worked Metals.

By C. H. DESCH, F.R.S.

The direct determination of the energy stored in a metal during the process of cold-working is extremely difficult. The only satisfactory measurements are those of Farren and Taylor,* who determined the heat evolved during deformation, and found the difference between the total work done during the process and that converted into heat. Their results, re-calculated to give calories per gramme, are shown in the table below. Russell,† basing his calculations on the assumption that a part of the metal is actually liquified during deformation, arrived at a value of 2·27 calories-gramme for the energy stored in steel in its most severely cold-worked state. Spring‡ measured the difference of electrolytic potential between specimens of several metals in the annealed and cold-worked states respectively, and from his values the difference in energy has also been calculated and expressed as calories per gramme of metal. Although Spring's work was carried out with great care, it is open to the objection that measurements of electrolytic potential are unusually liable to be affected by chance differences of surface, and too much weight must not be assigned to the figures obtained. In the present investigation the differences in the heat of solution in bromine have been determined. This method has the disadvantage that the heat of solution is large compared with the differences of energy to be measured, so that the calorimetric method employed must be a delicate one, but this is compensated for by its freedom from large thermal losses, which make the direct determination of the heat evolved during deformation so troublesome.

---

* 'Roy. Soc. Proc.,' A, vol. 107, p. 422 (1925).

† 'J. Iron Steel Inst.,' p. 497 (1923).

‡ 'Bull. Acad. Roy. Belg.,' p. 1066 (1903).

The figures in the table show only a rough agreement as to the order of the quantities involved. In comparing the values obtained by different investigators, it must be remembered that the bars used by Farren and Taylor were only pulled in a tensile apparatus, the elongations being relatively small, whilst Spring and the author have used cold-drawn wires, the section of which has been reduced 95 per cent. or more. Microscopical examination and mechanical tests indicate that the later stages of cold-working have a more profound effect than the earlier, so that a much larger value might be expected if the method of direct measurement could be applied to wires during their passage through a series of dies. The values in the table have been obtained by multiplying the values of T_2-T_1 on p. 435 of Farren and Taylor's paper by the specific heat of the metal. The maximum value obtained in each series of experiments has been taken.

Metal.	Potential energy, expressed as calories per gramme of metal.			
	Smith.	Russell.	Spring.	Taylor and Farren.
Copper	10·5	—	—	0·073 (17 per cent. reduction).
Iron	—	2·27	—	0·144 (14 per cent. reduction.
Tin	—	—	0·43	—
Brass	9·0	—	—	—
Zinc	6·7	—	—	—
Aluminium, Polycryst.	—	—	—	0·083 (18 per cent. reduction).
,, single cryst.	—	—	—	0·11 (36·5 per cent. reduction).
Silver	—	—	2·09	—
Cadmium	—	—	0·83	—
Lead	—	—	0·27	—

Work on the determination of the heat of solution is being continued, and means will be adopted to increase the accuracy of the method.

Sulphide Colours on Metallic Copper.

By F. Hurn Constable, M.A., D.Sc., Ph.D., F.I.C., F.Inst.P., Fellow of St. John's College, Cambridge.

(Communicated by T. M. Lowry, F.R.S.—Received June 8, 1929.)

In view of the criticism of Tammann and Koster's investigations,* by Evans,† who remarks that they seem to have applied the interference theory to their results wrongly, it is evident that further investigation is necessary. The sulphide colour sequence differs considerably from the oxide sequence of colours, and spectrophotometric observations were made to trace the cause

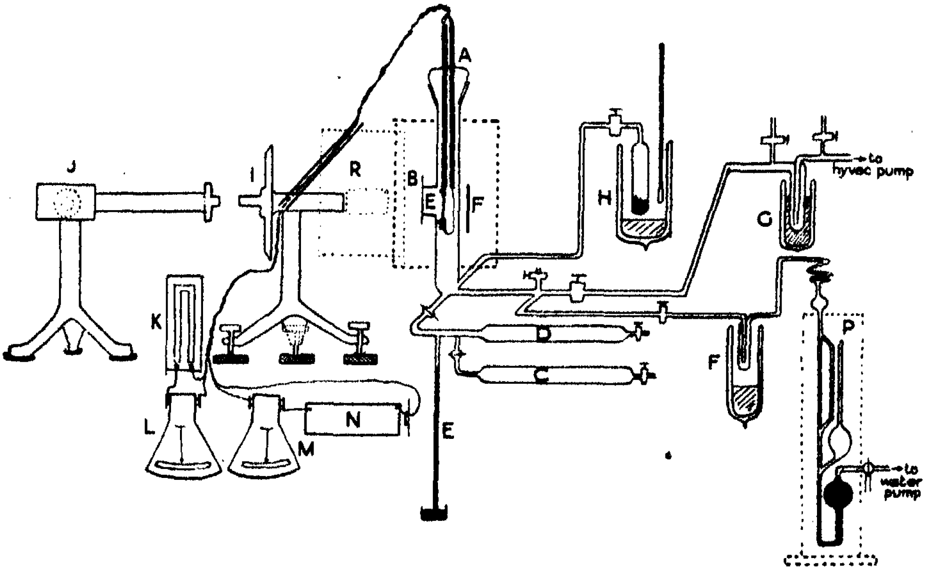

Fig. 1—Apparatus.—A, Ground joint admitting leads to the rod E supporting the copper film, enabling a known current to be passed through it via the ammeter M and resistance N, the voltage drop across the film being measured by the millivoltmeter L. B, Plane glass window through which the copper film may be observed through the spectrophotometer. C, Store for hydrogen sulphide. D, Chamber, with pressure gauge E, for mixing gases. F, Liquid air trap communicating with the McCleod gauge P. G, Liquid air trap protecting hyvac pump. H, Iodine, contained in a tube which may be cooled by liquid air, to obtain low pressures of iodine vapour in the apparatus. I, Nutting photometer to vary intensity of light from the comparison source F. J, Spectrometer with triply divided field. P, McCleod gauge for measuring pressure in reaction chamber. R, 400 c.p. Osram lamp illuminating the two rods E and F.

---

* 'Z. anorg. Chem.,' vol. 123, p. 220 (1922).

† 'Roy. Soc. Proc.,' A, vol. 107, p. 234 (1925).

of the divergence. The attack of a mixture of pure hydrogen sulphide and oxygen in equal volumes on pure metallic copper is rapid, and depends on the nature of the exposed surface, but the time for two complete colour sequences to be produced is of the order of three minutes. It is thus evident that no accurate photometric observations can be obtained, unless the progress of the reaction be stopped at various stages by removing reacting gases from the vessel by a pump. In practice it was found that there was some difficulty in getting complete sequences in this way. Thus it is necessary to slow down the rate of production of the colour sequences, and this was accomplished by coating the metal with an invisible oxide film. The cold activated metal was left in air for periods varying from 5 minutes to 1 hour. The oxide film so formed reduces very considerably the rate at which the colour sequences are produced, so that they may be observed conveniently with the spectrophotometer, in the apparatus here described, while the reaction is in progress. If the surface be exposed to air for too long a period, the brightness of the colour sequence is much diminished.

Apparatus.

The previous method* used for the study of oxide colours, suffers from the obvious disadvantage that the reaction has to be stopped to observe the colour of the oxide film by spectrophotometric means. The present apparatus was designed to enable spectrophotometric observations on the reflected light to be carried out as the reaction proceeds, while the resistance was obtained from a direct-reading millivoltmeter showing the potential difference across the copper film when a measured small current was passed through it.

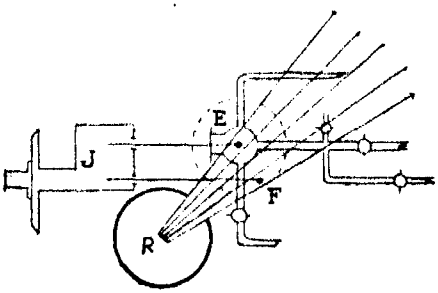

Fig. 2.—Arrangement of Light Source.

The spectrometer J (see fig. 2) was arranged in a mounting so that it could be moved, and replaced in exactly the same position. This is very necessary for the nutting photometer must be focussed before each experiment, because the movable supported film E cannot be replaced in exactly the same position, as flexibility in the connecting wires is desirable. Thus a photometer adjustment, focussing on E and moving F till the images of both coincide in the field of the instrument, is carried out at the commencement of each experiment before the spectrometer is placed in position. The standard F, reflecting white light, was made of burnished steel.

---

* *Cf.* 'Roy. Soc. Proc.,' A, vol. 117, p. 376 (1928).

The Sulphide Colours.

The copper films were uniformly activated *in situ* by alternate oxidation and reduction, as previously described (*loc. cit.* p. 207, fig. 2), and were allowed to cool in pure hydrogen gas. Pure hydrogen sulphide, saturated with water

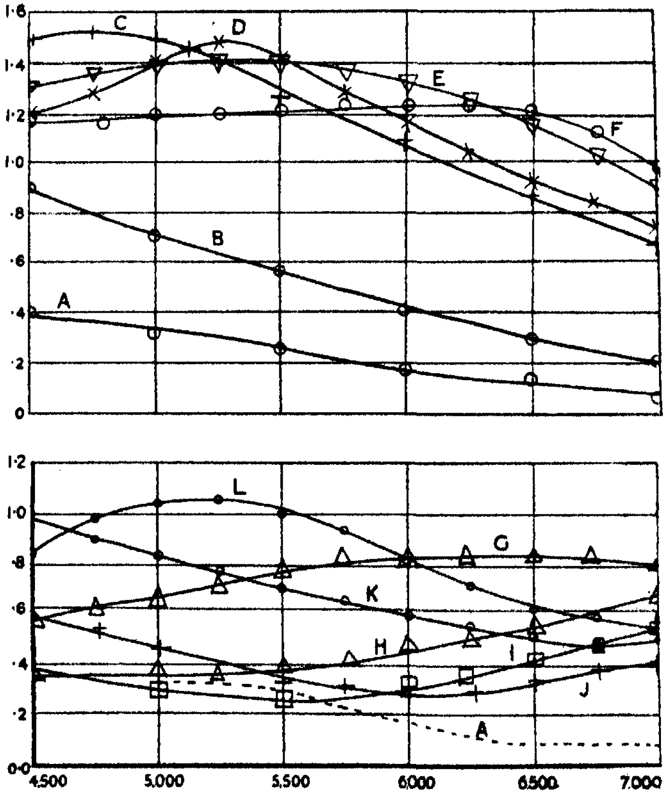

Fig. 3.—Spectrophotometer Observations on the Reflected Light.

A. Metal.
B. Slightly reddish.
C. Red brown.
D. Purple.
E. Bluish.
F. Bluish silver.
H. Greenish Silver.
I. Silvery white.
J. Yellowish.
K. Orange.
L. Reddish purple.

vapour was admitted from the vessel D into the reaction chamber, followed immediately by air. Observations were made with pressures of 5 cms. Hg hydrogen sulphide and 70 cms. Hg air, and the metal was exposed to air for 30 minutes before the reaction, so that during the five minutes that spectrophotometric observations were being made, the form of the intensity wave-length curve should not alter appreciably.

A beautiful sequence of colours was produced, and the resistances and corresponding conductivities, for each mean time interval for which the spectrophotometric observations were observed, were recorded.

The intensity wave-length curve for a given rod activated by three continued oxidations and reductions, gave a value for the area of the film approximately 2·4 times the plane area by the interference method; using this result with the known positions of the absorption bands, the refractive index of the mixed oxide sulphide film is 2.

Some difficulty was again experienced in getting a completely homogeneous film, and some films seemed to react quicker on the side with the more intense illumination. But in the main the evidence seemed to be against the photo-sensitiveness of the reaction. Of the results obtained only those with completely homogeneous films are recorded.

The typical curves in fig. 3 show the intensity wave-length curves for the reflected light from the copper film. The values of the equivalent air thickness calculated from λ_a and λ_r are plotted against the conductivity change of the film in fig. 4. The curves drawn in fig. 3 are plotted in fig. 4, curve I. Other

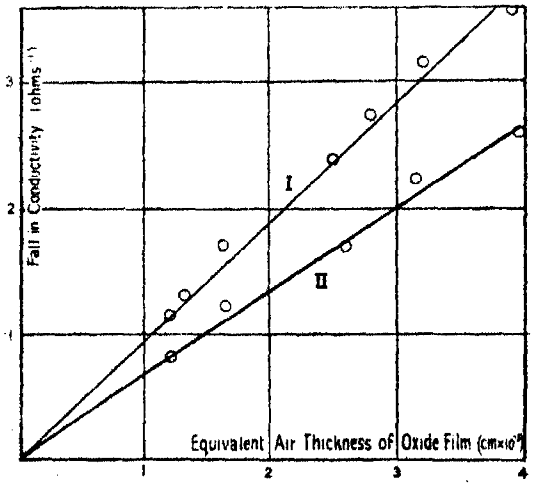

FIG. 4.—Fall in Conductivity with increase of Oxide Film Thickness.

curves were obtained with activated and sintered specimens of the metal (*e.g.*, curve II).

In these cases the fall in conductivity and the thickness of the film are directly proportional, and we have strong evidence that the interference colours are of a similar nature to those produced during the oxidation of copper.*

The principal conclusions obtained from the investigation are summarised below, some rough experiments being made with a series of copper surfaces to show the effect of an increasing partial pressure of oxygen. Fig. 5 shows that the reaction velocity is a maximum when the oxygen is somewhat in excess of the hydrogen sulphide. Experiments were made at temperatures up to 330° C.

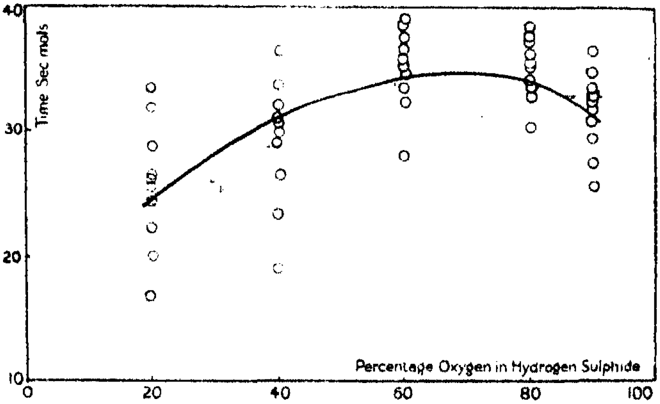

Fig. 5.—Reaction Velocity and Partial Pressure of Oxygen at 15° C.

My thanks are again due to Prof. T. M. Lowry, F.R.S., for his kindness in providing apparatus, and to the Government Grant Committee of the Royal Society, and the Research Fund of the Chemical Society for grants out of which some of the apparatus used was purchased.

Summary.

1. The colours produced when a mixture of hydrogen sulphide and oxygen or air act on copper are confirmed as true interference colours by spectrophotometric observations of the reflected light from films of increasing thickness.

2. The brightness of the silver colour of the first order is very characteristic of these sulphide colours, and the reflecting power of this film is considerably greater than that of the original metallic surface.

---

* 'Roy. Soc. Proc.,' A, p. 570 (1927).

3. If the copper surface be reduced at low temperature *in situ* before the reaction, and then air admitted for short periods, it is found that the rate of formation of the sulphide film is greatly reduced owing to the formation of an invisible oxide film (confirming Vernon's and Evans' conclusions). With long exposures to air before admitting hydrogen sulphide the colours formed became very dim, and scarcely a single order of colours could be gone through before blackness of the film supervened. High temperature reduction (about 600° C.) results in a copper surface, which can be exposed for hours with impunity, the rate of formation of sulphide colours being only very slightly decreased, owing to the slowness of low temperature oxidation of surfaces so prepared.

4. With a fully activated surface the maximum reaction velocity occurs with more oxygen present than is equivalent to the hydrogen sulphide.

5. Though there appears to be no temperature coefficient of reaction velocity over the range 0° to 180° C., the velocity of sulphide colour formation is enhanced at 200° C., and at 330° C. is very rapid, being six times faster than oxidation.

The Decomposition of Potassium Hydrogen Oxalate Hemihydrate.

By J. Hume, B.Sc., and J. Colvin, Ph.D., The University, Leeds.

(Communicated by R. Whytlaw-Gray, F.R.S.—Received July 27, 1929.)

In a previous communication, Topley and Hume* described the results obtained in an experimental study of the decomposition of calcium carbonate hexahydrate and showed that they could be most reasonably explained by assuming that reaction occurred only at the interface separating the two solid phases, $CaCO_3 . 6H_2O$ and $CaCO_3$. In addition it was assumed that this interface advanced through the crystalline particle with constant velocity in all directions; that is to say, the interface advanced as an expanding spherical surface, described about the nucleus† as centre. Since the latter assumption is inherently improbable, it was decided to investigate a reaction the interfacial nature of which would be beyond question and which would be susceptible to direct observation. After considerable search a suitable reaction was found in the decomposition of potassium hydrogen oxalate hemihydrate, *i.e.*,

---

* 'Roy. Soc. Proc.,' A, vol. 120, p. 211 (1928).

† Hume and Colvin, 'Phil. Mag.,' *in the press.*

$$2KHC_2O_4 . H_2O \longrightarrow 2KHC_2O_4 + H_2O.$$

The transition temperature of the hemihydrate, according to Hartley and others,* is in the neighbourhood of 6·4° C.

Experimental.

Suitable crystals of potassium hydrogen oxalate hemihydrate, in the form of clear thin plates, may be prepared by mixing equivalent solutions of potassium oxalate and oxalic acid, cooled to 3° C. Experiment showed that the most convenient concentrations were 18·4 gms. of potassium oxalate monohydrate in 100 c.cs. of water and 12·6 gms. of oxalic acid dihydrate in 320 c.cs. of water. In these concentrations there is no danger of separation of either of the solutes when the solutions are cooled to the temperature of mixing. The hemihydrate is thrown down in a few minutes; but the mixture requires to be kept at 0° C. for about 24 hours to give crystals of suitable size. Since potassium hydrogen oxalate is unstable in contact with its aqueous solution except in presence of potassium tetroxalate dihydrate,† a small quantity of this latter substance also separates with the hemihydrate crystals.

The crystals of hemihydrate when dried and examined microscopically appear as transparent plates of the shapes indicated in fig. 1, A, B. For convenience the edges of the crystal have been labelled with the letters *a*, *b*, *c* *d* and *e*. Above the transition temperature decomposition proceeds and is first evidenced by the appearance of black dots at the edges of the crystal. As these dots increase in size it can be seen that they are bounded in general by edges parallel to the edges of the crystal. Fig. 2, A, B and C are microphotographs showing this phenomenon as decomposition proceeds through a crystal. Since the interface separating the two phases is so distinct it becomes

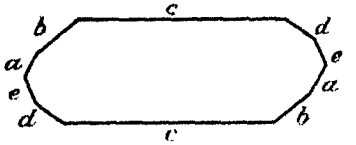

FIG. 1A.

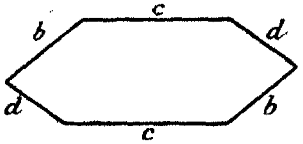

FIG. 1B.

---

* 'J. Chem. Soc.,' vol. 103, p. 1747 (1913).

† 'Amer. Chem. J.,' vol. 34, p. 153 (1905).

possible to measure the rate of advance by means of a travelling microscope, fitted with an eyepiece carrying a cross-wire.

Fig. 2a.

Fig. 2b.

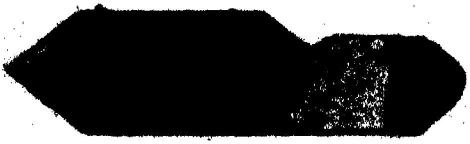

Fig. 2c.

The experimental method was as follows. Crystals of the hemihydrate were removed from their mother liquor, dried rapidly between filter paper, avoiding fracture so far as possible, and placed on a cover slip enclosed in a constant temperature cell attached to the stage of the microscope. A Zeiss travelling microscope fitted with a 17 mm. objective and a ×6 eyepiece was used for observation. When a suitable partially decomposed crystal was found, the coverslip was rotated until an edge of the interface coincided with the cross wire. In this way, the rates of advance of the different edges of the interface were determined.

Results.

Plotting the position of the interface against the time of observation shows clearly that the rate of advance is constant for any given edge. Two typical graphs are given in fig. 3, A and B. Almost the only variation from a straight line was of the type shown in the graphs, fig. 3, C and D. In these experiments, the advancing interface stopped completely for a time, as is shown by the horizontal portion of the curve, although the earlier and later portions are parallel straight lines.

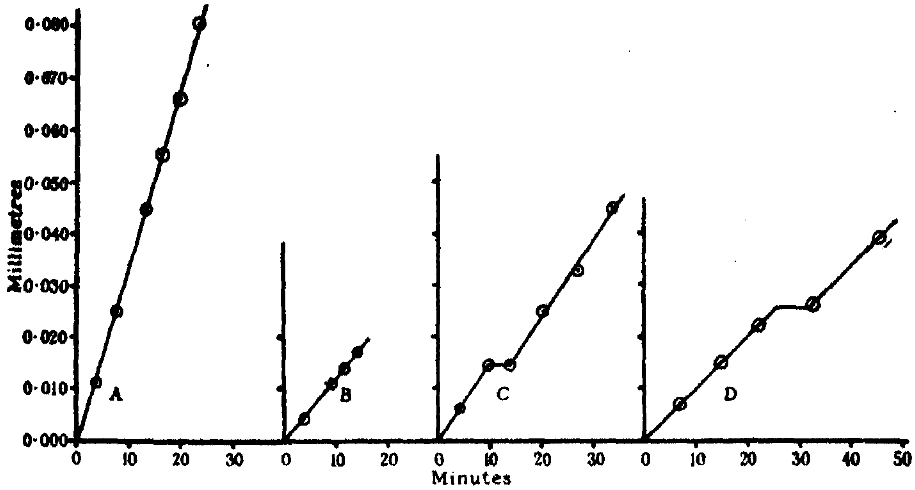

Fig. 3.

In the experimental method used, the crystals under observation were in contact with air containing water vapour the concentration of which was subject to some uncertainty. Before proceeding further it was therefore essential to determine to what extent the linear rate is affected by the presence of water vapour. To test this point, measurements of the rate were made on the same batch of crystals in the usual way in the microscope cell (Table I, series 1) and also with the crystals surrounded by phosphorus pentoxide (Table I, series 2). Finally the measurements were repeated under the most extreme conditions. A rapid stream of air—17 litres per hour—dried by phosphorus pentoxide and maintained at the temperature of the cell, was passed over the hemihydrate crystals, which were surrounded by phosphorus pentoxide (Table I, series 3). The results contained in Table I show that the presence of water vapour in the surrounding air produces no appreciable effect on the linear rate at the temperature of the experiments (20° C.).

Table I.

Edge of interface parallel to.		*a.*	*b.*	*d.*	*e.*
Linear rate in cms. sec.$^{-1}$ × 10^6	Series 1	1·30	1·50	2·33	2·08
	,, 2	1·43	1·75	—	—
	,, 3	—	1·67	1·83	1·83

In view of this result, the method used in series 1 was adopted for the subsequent work.

Measurements of the linear rate at 20° C. in directions perpendicular to the edges of the crystal were made and typical results are given in Table II.

Table II.

Edge of interface parallel to.	*a.*	*b.*	*c.*	*d.*	*e.*
Linear rate in cms. sec.$^{-1}$ × 10^6	1·54	1·75	1·48	2·77	2·57
	1·47	1·63	1·41	2·82	2·57
	—	1·61	1·40	2·71	—

Since each of the velocities tabulated above was measured on a different crystal—although all the crystals belonged to the same batch—it is evident that different velocities of advance are associated with the various directions in the crystal. Nevertheless in any one direction the rate is reasonably constant.

When two batches of crystals prepared in the same way as far as possible were examined, it was observed that there were more or less marked differences in the crystal habit. Hence comparison of the linear rates for the two batches was made. The mean rate for each edge in Table II, also the mean rates from Table IV, which were obtained with a second batch of crystals, are given in Table III.

Table III.

Edge of interface parallel to.		*a.*	*b.*	*c.*	*d.*
Linear rate in cms. sec.$^{-1}$ × 10^6	Series 1	1·50	1·66	1·43	2·76
	,, 2	1·61	2·12	3·86	3·29
Ratio of rates 1/2		0·93	0·78	0·57	0·84

Clearly the rates associated with the different directions in the crystal vary very considerably from batch to batch.

The Temperature Coefficient.

Since it was found impossible to prepare two batches of crystals which were perfectly comparable, the measurements necessary for the determination of the temperature coefficient of the linear rate were carried out on crystals taken from the same batch. The results of the measurements are given in detail in Table IV.

Table IV.

Edge of interface parallel to.	Rates in cms. sec.$^{-1}$ × 10^6.		
	b.	*c.*	*d.*
Temperature 20·0° C.	2·10	3·92	3·40
	2·17	3·88	3·83
	2·17	3·72	2·83
	2·08	3·92	3·42
	2·17	—	3·18
	2·00	—	3·45
	—	—	2·89
Temperature 24·83° C.	6·22	11·3	12·20
	7·00	10·7	11·1
	5·50	11·5	15·3
	6·67	—	16·7
	—	—	9·8

The mean rates for each edge and the temperature coefficient are given in Table V.

Table V.

Edge of interface parallel to.	Rates in cms. sec.$^{-1}$ × 10^6.		
	b.	*c.*	*d.*
Temperature 20·00°	2·12	3·86	3·29
Temperature 24·83°	6·35	11·2	13·0
Ratio	3·00	2·90	3·95

From Table V the energy of activation for edges parallel to the *c* face is 38,000 calories and for *d*, 49,000 calories. In addition, experiment has shown that in all probability the energy of activation is affected to a considerable extent by the changes in the crystal habit noted in different batches.

Discussion of Results.

Summarising the results of the previous sections, it has been shown that the reaction proceeds at the interface separating the solid phases, that the interface is bounded by edges parallel to the edges of the crystal, that each interfacial edge advances with a characteristic velocity, unaffected by the presence of water vapour and finally that the reaction possesses a high temperature coefficient.

In the course of the experimental work described in the preceding sections it was noted that the nuclei almost invariably form at the edges of the crystal, and preferentially at the corners. Cases of nuclei forming in the centre of a face were observed but these constituted a very small proportion of the total number.

Considering the data presented in Table III, it is highly probable that the differences in behaviour in the two batches are due to slight variations in the conditions during crystallisation and growth. Moreover the effect is specific to the various edges. That is to say, the ratio of the rates for corresponding edges is not a constant—*v*, Table III, line 3. Associated with this variation, there is a difference in the frequency of occurrence of any given interfacial edge, so that whilst one batch yields a large number of *c* edges, another batch yields very few. In many crystals the edges *a* and *e* are completely suppressed, yet in these, on decomposition, many *a* and *e* interfacial edges may occur. That is to say, suppression of crystal edges is not necessarily accompanied by suppression of corresponding interfacial edges. Since it was thought that the most probable cause of the differences in the linear rates from one batch of crystals to another was the adsorption and subsequent occlusion of either of the reactants, potassium oxalate or oxalic acid, by the crystals during growth, two batches were prepared, one in presence of excess of potassium oxalate and the other in presence of excess of oxalic acid. Microscopic examination of the two batches showed that the crystals were entirely different in habit and gave distinctly different rates on decomposition. In view of this, and since local changes in concentration are inevitable during the growth of the crystals, the constancy and reproducibility of the linear rate for any given interfacial edge for crystals from the same batch, are satisfactory.

The observation that the interface is bounded by edges parallel to the edges of the crystal has been made by Kohlschütter* in the case of the transformation of mercuric iodide. The association of characteristic linear rates of advance of the different interfacial edges may be compared with the occurrence of characteristic rates of growth of crystal faces, which have been measured by Bentivoglio.†

Having obtained convincing evidence that the reaction is interfacial in nature and that the interface advances at a linear rate, it became of great interest to determine the form of the curve obtained for a mass of decomposing crystals, in order to compare it with that obtained for the decomposition of calcium carbonate hexahydrate. In this latter reaction the linear advance of the interface was hypothetical and was not susceptible to direct observation.

---

* 'Koll. Z.,' vol. 42, p. 254 (1927).

† 'Roy. Soc. Proc.,' A, vol. 115, p. 59 (1927).

Experimental.

The most convenient method for determining the mass rate of decomposition is the spiral spring quartz fibre balance of the type described by Whytlaw-Gray and Topley.* In order to obtain a true measure of the extent of decomposition it is essential that the water liberated during the decomposition should be removed immediately from the mass of crystals. Under atmospheric pressure, the water remains entangled in the crystals and evaporates much more slowly than the true reaction rate ; hence the balance case must be evacuated. As we have indicated previously, the potassium hydrogen oxalate hemihydrate crystals are invariably mixed with a number of crystals of potassium tetroxalate dihydrate, the decomposition of which on the spring balance would lead to erroneous results. Fortunately it was shown that under the experimental conditions, no appreciable loss of water occurred from crystals of potassium tetroxalate dihydrate in 12 hours, a period more than sufficient for the complete decomposition of the hemihydrate.

Crystals were removed from the mother liquor, dried rapidly between filter paper and sized by sieving. A suitable quantity of the crystals was placed on the pan of the balance, which was then lowered into a thermostat maintained at 19·97 ± 0·01° C. After the lapse of 10 minutes in order to allow the establishment of temperature equilibrium the balance case was evacuated by a Pfeiffer oil pump through a stop-cock, which was closed when the pressure was sufficiently reduced. The readings of the extension of the spring, which were referred to a fixed reference point, were then commenced. The measurements of the extension were made by means of a travelling microscope, fitted with a 4½-inch objective, which allowed an accuracy of reading of 0·002 mm. The spring, which had a linear weight-extension curve had a sensitivity of 1·34 mm. per milligram.

Two series of experiments were carried out, firstly using phosphorus pentoxide in the balance case to absorb water vapour and secondly using a mixture of anhydrous copper sulphate with copper sulphate monohydrate to maintain a small but constant pressure of water vapour in the case.

The results of these experiments are best given graphically. Fig. 4, A and B,

---

* 'Phil. Mag.,' vol. 4, p. 873 (1927).

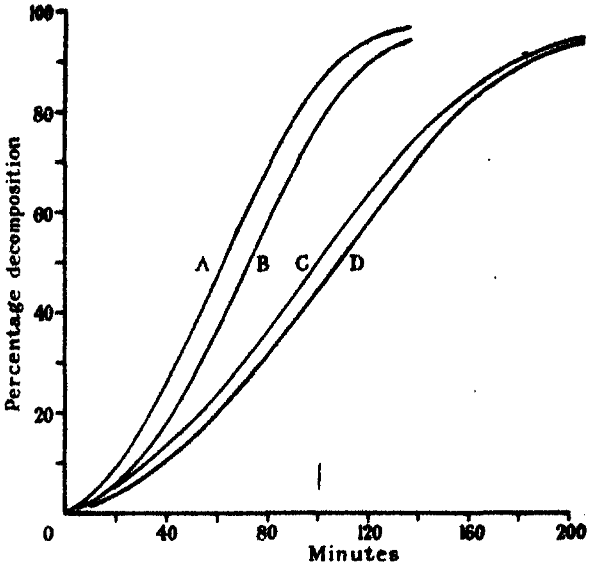

FIG. 4.

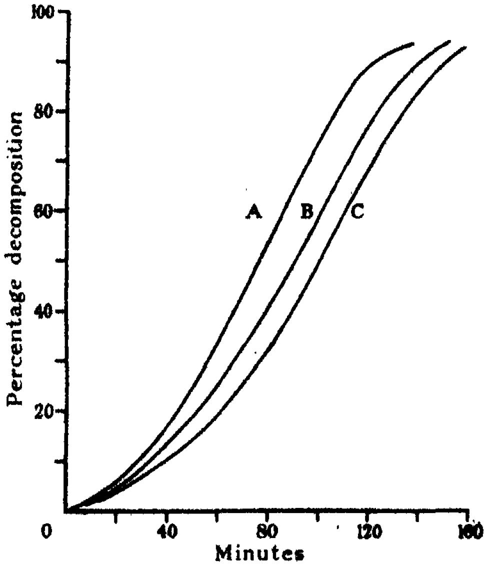

FIG. 5.

are curves obtained by using phosphorus pentoxide. Fig. 4, C and D, were obtained by using the mixture of anhydrous and monohydrated copper sulphate.

It was noted under the microscope that crystals which had been removed from their mother liquor, dried and kept in a dry test tube at 0° C., showed over a period of about 14 days, an increasing number of interfacial edges which stopped after a short advance. This effect was sought in the mass reaction on the spring balance and the curves, A, B and C, given in fig. 5, give the results of three runs, carried out, respectively, 2, 6 and 9 days after preparation of the crystals.

Discussion of Results.

In every case the curve is of the sigmoid type associated with many solid reactions.* Referring to fig. 4, curves A and B obtained using phosphorus pentoxide, have the same maximum slope although the curves are not coincident. Comparing these results with curves C and D, it is evident that in presence of the mixture $CuSO_4$–$CuSO_4 . H_2O$ the maximum slope of the curve is much lower and is attained after a much more prolonged induction period.

In the case of calcium carbonate hexahydrate, Topley and Hume derived values for the linear rate by solving the decomposition curves on the assumption that the spherical particles, in the advanced stage of decomposition are enclosed in a complete envelope of resultant. From a microscopic examination of the crystals of potassium hydrogen oxalate hemihydrate, it is clear that this procedure would not be justifiable. In the first place the crystals are plates of such thinness (0·02 mm.) that the reaction may be regarded as two-dimensional, *i.e.*, the fraction decomposed is simply that fraction of the upper surface of the crystal which has become opaque. Furthermore in the last stages of decomposition, the undecomposed area is bounded by rectilinear interfacial edges. Hence for simplicity it was decided to solve the decomposition curves by regarding the final stage as due to either (1) a contracting rectangle or (2) a contracting circle.

Case I. The Contracting Rectangle.—If the length of the crystal be m and its breadth n, and the mean linear rate of the advancing interface u, then D, the fraction decomposed is given by the expression

$$D = \frac{2u(t - t_0)}{m \, . \, n} \{m + n - 2u(t - t_0)\}, \tag{1}$$

where t is the time of observation and t_0, an arbitrary zero time, corresponding to an hypothetical state in which the rectangular crystal ($m \times n$) is bounded by a complete interfacial edge. By taking two points on the experimental curve, the equation may be solved for u, the linear rate.

---

* *Loc. cit.*

Solving curve A in this way, the value $u = 1 \cdot 27 \times 10^{-6}$ cms. sec.$^{-1}$ is obtained. This rate is much lower than that measured directly under the microscope for the same batch of crystals, namely, $2 \cdot 72 \times 10^{-6}$ cms. sec.$^{-1}$.

Case II. The Contracting Circle.—In this approximation the crystal, regarded for simplicity as a rectangle of length m and breadth n, is replaced by a circle of equal surface of radius a given by the expression

$$a = \sqrt{m \, . \, n/\pi}.$$

Then D, the fraction decomposed, is given by the expression

$$D = 2u\,(t - t_0)/a - u^2(t - t_0)^2/a^2, \tag{2}$$

where t and t_0 have the same significance as before. The values of u, obtained by solving curves A, B, C and D at 85 per cent. and 90 per cent. decomposition, are contained in Table VI.

Table VI.

Curve.	Absorbent.	Rate in cms. sec.$^{-1}$ × 10^6.
A	P_2O_5	2·31
B	P_2O_5	2·19
C	$CuSO_4$–$CuSO_4 . H_2O$	1·33
D	$CuSO_4$–$CuSO_4 . H_2O$	1·37

The mean rate observed directly is $2 \cdot 72 \times 10^{-6}$ cms. sec.$^{-1}$.

There is a noticeable difference between the linear rates in presence of phosphorus pentoxide and those in presence of $CuSO_4$–$CuSO_4 . H_2O$ as derived by expression (2). Now the one factor which has been changed in the two sets of experiments is the pressure of water vapour in the balance case. But it has been shown in a previous section that the linear rate is unaffected by the pressure of water vapour, hence the differences between the two sets of curves must be sought elsewhere. From this it must be concluded that the rate of nucleus formation is decreased by the presence of water vapour. Moreover the decreased rate of nucleus formation is supported by the more prolonged induction period, and by the diminished maximum slope, which are characteristic of curves C and D. Clearly the most important condition for the production of the state in which equation (2) is valid will be a high rate of nucleus formation. As this condition is best fulfilled in presence of phosphorus pentoxide it is to be expected that the solution of curves A and B should yield values of *u*, the linear rate, approximating most closely to those directly observed.

In view of the simplifying assumptions, the agreement between observed and calculated values is satisfactory and serves to justify the analogous procedure in the case of calcium carbonate hexahydrate, in which a contracting spherical envelope most closely accorded with the experimental conditions. In the analysis of the curves it is to be noted that the solution does not involve a knowledge of the zero time for the reaction. This is of great importance since the zero time is subject to great uncertainty owing to the irreproducibility of the rate of nucleus formation. This point has also been emphasised by Roginsky and Schulz* in a study of the decomposition of potassium permanganate in the solid state.

With reference to fig. 5, the direct observation that the number of stopped interfacial edges increases with the age of the dried crystals is confirmed by the progressively increasing length of the induction period preceding the attainment of the maximum rate of reaction. If this effect is to be attributed to the cracking of the crystals it must be recognised that these cracks are not comparable with the discontinuities produced by mechanical fracture of the freshly dried crystals, in that the cracks do not appear to be seats of nucleus formation.† In many cases a stopped interfacial edge will after a lapse of time begin to advance as a whole (*v.* fig. 3, C, D), which excludes the possibility of the advance being due to the formation of a new nucleus.

The energy of activation of the reaction appears to be of the order of 40,000 calories, which is close to that found by Topley and Hume for the decomposition of calcium carbonate hexahydrate. For this latter reaction, Kassel‡ has suggested that the high energy of activation may be explained by the reaction occurring in several stages with intermediate formation of lower hydrates. Whilst this is plausible in view of the large number of combined water molecules, it seems extremely unlikely that a similar explanation would be applicable to the dehydration of the potassium hydrogen oxalate hemihydrate.

---

* 'Z. Phys. Chem.,' vol. 138, p. 21 (1928).

† Hume and Colvin, *loc. cit.*

‡ 'J. Amer. Chem. Soc.,' vol. 51, p. 1136 (1929).

On the Turbulent Wake behind a Body of Revolution.

By L. M. Swain, M.A., Fellow of Newnham College, Cambridge.

(Communicated by L. Prandtl, For.Mem.R.S.—Received August 7, 1929.)

§ 1. Prof. Prandtl, in his paper* presented to the Second International Congress for Technical Mechanics, Zurich, 1926, shows that if certain assumptions are made, it is possible to obtain the equations of motion for the turbulent region behind a body, placed in a uniform stream, in such a form that they can be integrated. Taking the case, where the undisturbed stream is parallel to the axis of x, he shows that the interchange of momentum between the fluid particles, due to turbulence, may be allowed for by introducing into the equations of motion a term representing the "apparent stress" in the form $l^2\left(\frac{\partial u}{\partial y}\right)^2$, where u is the mean velocity at any point parallel to $0x$, y is distance from the axis of x and l is a length called by Prandtl "Mischungsweg" (mixing distance) or "mean free path"; it is not constant but varies from point to point. A form related to this was found by G. I. Taylor in his paper† on "Eddy motion in the atmosphere."

It has been pointed out by Jeffreys‡ that if A is the "apparent viscosity," the term introduced into the equation of motion by Taylor is $A\,\frac{\partial^2 u}{\partial y^2}$, whereas Prandtl introduces the term $\frac{\partial}{\partial y}\left(A\,\frac{\partial u}{\partial y}\right)$; further the difference between these two terms represents the momentum lost during migration owing to the differences of pressure. Taylor takes this loss into account. Prandtl assumes that for a first approximation the pressure may be treated as constant and hence no momentum is lost during migration and we get the form $\frac{\partial}{\partial y}\left(A\,\frac{\partial u}{\partial y}\right)$.

This form for the "apparent stress" does not however allow the equations of motion to be integrated, as l is an unknown function. Prandtl makes the further assumption, that for large Reynolds' numbers the motions in sections perpendicular to the direction of flow are mechanically and geometrically similar. With the aid of this assumption he shows that in the wake behind a solid body the "Mischungsweg" l is approximately proportional to the breadth of the wake. It is then possible to express l in such a form that the only undetermined factor in it is an absolute constant.

---

* 'Proceedings of the Second International Congress for Applied Mechanics, Zurich, 1926,' p. 62.

† 'Phil. Trans.,' A, vol. 215, p. 1 (1915).

‡ 'Proc. Camb. Phil. Soc.,' vol. 25, p. 20 (1929).

This paper deals with the wake behind a body of revolution. The two-dimensional case of the wake behind a cylindrical body has been worked out by H. Schlichting and his results will shortly be published in a German periodical; they are similar to those obtained in the case of the body of revolution. Prandtl (*loc. cit.*) in his paper obtains a first approximation to the motion for both cases, but the results obtained experimentally for the cylindrical body showed a slight deviation from those predicted theoretically; it appeared that as the body was approached the boundary of the wake lay outside the predicted boundary. The work in this paper was undertaken at Prof. Prandtl's suggestion to see whether a second approximation to the motion would give a wake lying outside that obtained from the first approximation; this appears to be the case. It is found that the boundary is of the form

$$y = \alpha x^{\frac{1}{3}} + \beta x^{-\frac{1}{3}},$$

where α, β are constants; the second term becomes more significant as the body is approached. The components of velocity at any point of the wake are also found.

§ 2. We consider a body of revolution held at rest with fluid streaming past it with velocity U. We take a fixed axis Ox along the direction of flow, the origin being some fixed point in the body on the axis of symmetry. The exact position of this point will be discussed later (p. 657). Distance perpendicular to the axis of symmetry is denoted by y.

At a great distance behind the body let the components of the mean velocity be $U + u$, v, where u, v are small compared with the undisturbed flow U. We assume further, as is usual in the theory of Prandtl's boundary layer, that the variation of the velocity perpendicular to Ox is large compared with that along Ox. As a first approximation to the apparent stress due to turbulence, we have $l^2 \left(\frac{\partial u}{\partial y}\right)^2$ and the variation of the pressure parallel to the axis of x is neglected. The equation of motion perpendicular to Oy may also be neglected in the first approximation. The justification for these assumptions will be discussed later (p. 656). The equations of continuity and for the motion parallel to Ox give respectively

$$\frac{\partial}{\partial x}(yu) + \frac{\partial}{\partial y}(yv) = 0, \qquad \text{(i)}$$

$$(U + u)\frac{\partial u}{\partial x} + v\frac{\partial u}{\partial y} = \frac{1}{y}\frac{\partial}{\partial y}\left[l^2 y \left(\frac{\partial u}{\partial y}\right)^2\right]. \qquad \text{(ii)}$$

Another equation which will be useful later is the "impulse equation"; it can, of course, be obtained by integrating (ii), but is more easily obtained directly.

Take a right-circular cylindrical surface in the liquid, everywhere at a great distance from the body and with its axis along Ox. The difference between the momentum entering and leaving this cylinder per unit time is equal to the resistance of the body. We thus obtain the equation

$$\rho\int_0^\infty \mathrm{U}^2 y\,dy - \rho\int_0^\infty (\mathrm{U}+u)^2 y\,dy - \rho\int_{-\infty}^{+\infty} v_\infty\,\mathrm{U}y\,dx = \tfrac{1}{2}\rho c_w \mathrm{F}\mathrm{U}^2$$

where $\frac{1}{2}\rho c_w \mathrm{FU}^2$ is the resistance of the body and v_∞ is the velocity perpendicular to Ox at a great distance from the body.

From (i) we have,

$$yv_\infty = -\int_0^\infty \frac{\partial}{\partial x}(yu)\,dy, \text{ since } v = 0, \text{ when } y = 0,$$

and hence

$$\begin{aligned}\int_{-\infty}^{+\infty} v_\infty\,\mathrm{U}y\,dx &= -\int_{-\infty}^{+\infty}\mathrm{U}y\,dx\int_0^\infty \frac{1}{y}\frac{\partial}{\partial x}(yu)\,dy,\\ &= -\int_0^\infty \mathrm{U}\,(\mathrm{U}+u-\mathrm{U})\,y\,dy,\\ &= -\int_0^\infty \mathrm{U}u\,y\,dy.\end{aligned}$$

Thus finally,

$$\int_0^\infty (u^2+\mathrm{U}u)\,y\,dy = -\tfrac{1}{2}c_w\mathrm{FU}^2. \qquad \text{(iii)}$$

Since the variation perpendicular to Oy is large compared with that along Ox, it is clear from (i) that v is small compared with u. Further if v' be the deviation from the mean velocity perpendicular to Ox, Prandtl shows in his paper that on the boundary of the turbulent region $y = b\,(x)$,

$$v' \propto \frac{\mathrm{D}b}{\mathrm{D}t} \propto \mathrm{U}\frac{\partial b}{\partial x},$$

and at any point

$$v' \propto l\frac{\partial u}{\partial y}, \quad \propto l\frac{\bar{u}}{b},$$

where $\bar{u}$ is a mean value of the velocity u and hence

$$\mathrm{U}\frac{\partial b}{\partial x} \propto l\frac{\bar{u}}{b}. \qquad \text{(iv)}$$

We now endeavour to deal with the equation of motion by the method of successive approximation. We require some quantity in terms of which we can measure the order of magnitude of the terms and it seems obvious that we should choose $1/x$, as we are dealing with motion far behind the body and hence $1/x$ will be small. With this assumption, the first approximation to the boundary of the turbulent region will be y equal to some power of x, say, $y = x^n$, where n has yet to be determined. We may then assume $u = x^r f\left(\frac{y}{x^n}\right)$ as a first approximation, where r has to be determined.

If we write $\eta = y/x^n$, (iii) gives as a first approximation

$$\int_0^\infty x^{2n+r} f(\eta)\,\eta\,d\eta = \text{const.},$$

$$x^{2n+r} = \text{const.},$$

and hence $2n + r = 0$ and so $u = x^{-2n} f(\eta)$.

We have further from (iv),

$$l x^{-3n} f(\eta) \propto x\mathrm{U}^{n-1},$$

and hence we see that

$$l \propto x^{4n-1}.$$

But we have seen that $l \propto b \propto x^n$ and hence

$$n = 4n - 1,$$

$$n = \tfrac{1}{3}.$$

Thus a first approximation to u is $x^{-\frac{2}{3}} f\left(\frac{y}{x^{\frac{1}{3}}}\right)$.*

We are now in a position to consider the magnitude of the various terms in (ii), regarded as powers of x. They are respectively

$$x^{-\frac{5}{3}},\ x^{-\frac{7}{3}},\ x^{-\frac{7}{3}},\ x^{-\frac{5}{3}}.$$

Hence for the first approximation equation (ii) may be taken in the simplified form

$$\mathrm{U}\frac{\partial u}{\partial x} = \frac{1}{y}\frac{\partial}{\partial y}\left[l^2 y\left(\frac{\partial u}{\partial y}\right)^2\right], \tag{v}$$

and the velocity may be written

$$u = \mathrm{U}\left(\frac{c_w \mathrm{F}}{x^2}\right)^{\frac{1}{3}} \chi_1\left(\frac{y}{b}\right).$$

This and subsequent forms are chosen so that results may easily be expressed in non-dimensional variables. We have further

$$l = c\,(c_w \mathrm{F} x)^{\frac{1}{3}},$$

---

* Prandtl (*loc. cit.*) arrives at this result by a slightly different method.

where c is an absolute constant and must be determined from the experiments. We further may write

$$u = \mathrm{U}\left(\frac{c_w\mathrm{F}}{x^2}\right)^{\frac{1}{3}}\chi_1\left(\frac{y}{[c_w\mathrm{F}x]^{\frac{1}{3}}}\right),$$

$$= \mathrm{U}\left(\frac{c_w\mathrm{F}}{x^2}\right)^{\frac{1}{3}}\chi_1(\eta),$$

where $\eta = y/(c_w\mathrm{F}x)^{\frac{1}{3}}$.

Substituting these expressions in (iii), we have

$$-\tfrac{2}{3}\chi_1 - \tfrac{1}{3}\eta\chi'_1 = \frac{c^2}{\eta}\frac{d}{d\eta}(\eta\chi_1'^2),$$

where $'$ denotes differentiation with respect to η, or integrating once

$$\eta^2\chi_1 + 3c^2\eta\chi_1'^2 = \mathrm{B}.$$

Now χ_1, χ_1' must both be finite on the axis of symmetry $\eta = 0$, hence $\mathrm{B} = 0$. Then by replacing η by $(3c^2)^{\frac{1}{3}}\eta$, the equation simplifies to

$$\begin{aligned}\eta\chi_1 + \chi_1'^2 &= 0,\\ \pm i\chi_1'/\chi_1^{\frac{1}{2}} &= \eta^{\frac{1}{2}},\\ \pm 2i\chi_1^{\frac{1}{2}} &= \tfrac{2}{3}\eta^{\frac{3}{2}} - 2\mathrm{A},\\ \chi_1 &= -(\tfrac{1}{3}\eta^{\frac{3}{2}} - \mathrm{A})^2.\end{aligned}$$

For the boundary conditions, we have

(*a*) $u = 0$ on the boundary of the turbulent region, $\eta = \eta_0$, say,

(*b*) resistance $\mathrm{W} = c_w\mathrm{F}\rho\mathrm{U}^2/2 = -2\pi\rho\int_{\eta=0}^{\eta=\eta_0}\mathrm{U}u\,y\,dy.$

We notice further that on the outer boundary $\dfrac{\partial u}{\partial y} = 0$ and on the axis of symmetry $\dfrac{\partial u}{\partial y} = 0$, while $\dfrac{\partial^2 u}{\partial y^2} \to \infty$, as a consequence of the form of χ_1.

From (*a*) we have immediately, $\eta_0^{\frac{3}{2}} = 3\mathrm{A}$, and from (*b*)

$$\tfrac{1}{2} = 2\pi\int_0^{\eta_0}\left(\tfrac{1}{3}\frac{\eta^{\frac{3}{2}}}{(3c^2)^{\frac{1}{2}}} - \mathrm{A}\right)^2\eta\,d\eta,$$

$$\frac{1}{4\pi} = (3c^2)^{\frac{2}{3}}\,\tfrac{2}{27}\,(3\mathrm{A})^{\frac{10}{3}}\int_0^1 z^{\frac{1}{3}}(z-1)^2\,dz, \quad \text{where} \quad z = \frac{\eta^{\frac{3}{2}}}{(3c^2)^{\frac{1}{2}}\,3\mathrm{A}},$$

and finally

$$\mathrm{A} = 0{\cdot}56\,(3c^2)^{-\frac{1}{5}}.$$

From (i) we have

$$vy = -\int^{y} \frac{\partial}{\partial x}(uy)\,dy,$$

$$v\eta = -(c_w\mathrm{F})^{1/3}\,x^{1/3}\int^{\eta} \eta\,\frac{\partial u}{\partial x}\,d\eta.$$

Thus, for the first approximation, we have

$$v = -\frac{1}{\eta}(c_w\mathrm{F})^{1/3}\,x^{1/3}\int^{\eta} \eta\,\frac{\partial}{\partial x}\left[\mathrm{U}\,(c_w\mathrm{F})^{1/3}\,x^{-2/3}\,\chi_1(\eta)\right]d\eta,$$

$$= \frac{\mathrm{U}}{3}(c_w\mathrm{F})^{2/3}\,x^{-4/3}\eta\chi_1,$$

since v is finite for $\eta = 0$.

The boundary of the turbulent region is

$$\eta = (3\mathrm{A})^{1/2},$$

or

$$y = 1\cdot 41\,(3c^2)^{1/2}\,(c_w\mathrm{F}x)^{1/3}.$$

§ 3. We now proceed to the second approximation and require first to see what form we must assume for u. The more accurate form of (iii) is

$$\int_0^{\infty}(\mathrm{U}u + u^2)\,y\,dy = \text{const.}$$

If we assume that the second order term in $u \propto x^m$, we see by evaluating the second order terms in the expression that $m \propto -\frac{4}{3}$.

We hence assume

$$u = \mathrm{U}\left\{\left(\frac{c_w\mathrm{F}}{x^2}\right)^{1/3}\chi_1(\eta) + \left(\frac{c_w\mathrm{F}}{x^2}\right)^{2/3}\chi_2(\eta)\right\}.$$

When we substitute this expression in (ii), it is clear that for the second approximation we retain terms of order $x^{-4/3}$. Now if l contained a term in $x^{-1/3}$, we should obtain a new term on the right-hand side of (ii) of order $x^{-4/3}$ by combining this part of l with the first approximation for u. Let us therefore write $l = c\,(c_w\mathrm{F}x)^{1/3} + c_1\,(c_w\mathrm{F})^{2/3}\,x^{-1/3}$ where c_1 is as yet undetermined. Substituting in (ii), we now get for the second approximation

$$4\chi_2 + \chi_2'\left[\eta + 6c^2\left\{\frac{\chi_1'}{\eta} + \chi_1''\right\}\right] + 6c^2\chi_2''\chi_1'$$
$$= -2\chi_1^2 - 6cc_1\left\{\frac{\chi_1'^2}{\eta} + 2\chi_1'\chi_1''\right\}.$$

If we multiply η as before by $(3c^2)^{\frac{1}{3}}$ and put in the value for χ_1, the equation becomes

$$2\eta\left(\tfrac{1}{3}\eta^{\frac{3}{2}} - \mathrm{A}\right)\chi_2'' + 3\left(\tfrac{1}{3}\eta^{\frac{3}{2}} - \mathrm{A}\right)\chi_2' - 4\eta^{\frac{1}{2}}\chi_2$$
$$= 2\eta^{\frac{1}{2}}\left(\tfrac{1}{3}\eta^{\frac{3}{2}} - \mathrm{A}\right)^4 + 2\,\frac{c_1}{c}\,\eta^{\frac{1}{2}}\left(\tfrac{1}{3}\eta^{\frac{3}{2}} - \mathrm{A}\right)\left(\tfrac{5}{3}\eta^{\frac{3}{2}} - 2\mathrm{A}\right),$$

or in terms of z

$$3z\,(z-1)\frac{d^2\chi_2}{dz^2} + 4\,(z-1)\frac{d\chi_2}{dz} - 8\chi_2 = 4\mathrm{A}^4\,(z-1)^4$$
$$+ 4\,\frac{c_1}{c}\,\mathrm{A}^2\,(z-1)\,(5z-2).$$

This is a hypergeometric equation, its complementary function is

$$\chi_2 = a_1\,\mathrm{F}\left(\frac{1+\sqrt{97}}{6},\ \frac{1-\sqrt{97}}{6},\ \tfrac{4}{3};\ z\right)$$
$$+ a_2 z^{-\frac{1}{3}}\,\mathrm{F}\left(\frac{-1+\sqrt{97}}{6},\ \frac{-1-\sqrt{97}}{6},\ \tfrac{2}{3};\ z\right),$$

where a_1, a_2 are constants and F denotes the hypergeometric function. It is found that the particular integrals corresponding to the two terms on the right-hand side are both polynomials in z. Their coefficients are easily evaluated by direct substitution. We finally get as the complete solution

$$\chi_2 = a_1\,\mathrm{F}\left(\frac{1+\sqrt{97}}{6},\ \frac{1-\sqrt{97}}{6},\ \tfrac{4}{3};\ z\right)$$
$$+ a_2 z^{-\frac{1}{3}}\,\mathrm{F}\left(\frac{-1+\sqrt{97}}{6},\ \frac{-1-\sqrt{97}}{6},\ \tfrac{2}{3};\ z\right)$$
$$+ 4\mathrm{A}^4\,(0{\cdot}0041 - 0{\cdot}259z + 0{\cdot}359z^2 - 0{\cdot}128z^3 + 0{\cdot}0227z^4)$$
$$+ 4\,\frac{c_1}{c}\,\mathrm{A}^2\left(\tfrac{1}{3} - \tfrac{7}{6}\,z + \tfrac{5}{6}\,z^2\right) \text{ approximately.}$$

If we assume that it still holds that $b \propto l$, we have the following boundary conditions :—

(*a*) u must be finite for $\eta = 0$, *i.e.*, for $z = 0$,

$$\left.\begin{array}{l}(b)\ u = 0 \\ (c)\ \dfrac{\partial u}{\partial y} = 0\end{array}\right\}\ \text{for the boundary } \eta = \eta_0\left[1 + \frac{c_1}{c}\,(c_w\mathrm{F})^{\frac{1}{3}}\,x^{-\frac{1}{3}}\right], \text{ or}$$
$$z = 1 + \tfrac{3}{2}\,\frac{c_1}{c}\,(c_w\mathrm{F})^{\frac{1}{3}}\,x^{-\frac{1}{3}}.$$

It follows from the form of χ_2 that for $\eta = 0$, $\dfrac{\partial u}{\partial y} = 0$, and $\dfrac{\partial^2 u}{\partial y^2} \rightarrow \infty$.

From (*a*), we have $a_2 = 0$.

From (b)

$$x^{-\frac{2}{3}}\chi_1\left(\eta_0+\eta_0\frac{c_1}{c}[c_w\mathrm{F}]^{\frac{1}{3}}x^{-\frac{2}{3}}\right)+(c_w\mathrm{F})^{\frac{1}{3}}x^{-\frac{4}{3}}\chi_2(\eta_0)=0 \text{ approximately,}$$

$$x^{-\frac{2}{3}}\left[\chi_1(\eta_0)+\eta_0\frac{c_1}{c}(c_w\mathrm{F})^{\frac{1}{3}}x^{-\frac{2}{3}}\chi_1'(\eta_0)\right]+(c_w\mathrm{F})^{\frac{1}{3}}x^{-\frac{4}{3}}\chi_2(\eta_0)=0,$$

$$\chi_2(\eta_0)=0,$$

or

$$\chi_2(z)=0 \quad \text{for } z=1.$$

The two particular integrals are zero for $z=1$, but the hypergeometric series $\mathrm{F}\left(\frac{1+\sqrt{97}}{6},\frac{1-\sqrt{97}}{6},\frac{4}{3};\ z\right)$ does not vanish there ; hence $a_1=0$.

From (c)

$$x^{-\frac{2}{3}}\left[\chi_1'(\eta_0)+\eta_0\frac{c_1}{c}(c_w\mathrm{F})^{\frac{1}{3}}x^{-\frac{2}{3}}\chi_1''(\eta_0)\right]+(c_w\mathrm{F})^{\frac{1}{3}}x^{-\frac{4}{3}}\chi_2'(\eta_0)=0,$$

$$\frac{c_1}{c}\eta_0\chi_1''(\eta_0)+(3\mathrm{A})^{-\frac{2}{3}}\tfrac{3}{2}z^{\frac{1}{3}}\left(\frac{d\chi_2}{dz}\right)_{z=1}=0,$$

and after some calculation this gives

$$c_1/c=0\cdot 60\ \mathrm{A}^2 \text{ approximately.}$$

Hence the outer boundary is

$$\eta=\eta_0\left(1+0\cdot 60\ \mathrm{A}^2(c_w\mathrm{F})^{\frac{1}{3}}x^{-\frac{2}{3}}\right),$$

or with the original magnitudes

$$y=1\cdot 41\,(3c^2)^{\frac{1}{3}}(c_w\mathrm{F}x)^{\frac{1}{3}}\left[1+0\cdot 187\,(3c^2)^{-\frac{1}{3}}(c_w\mathrm{F})^{\frac{1}{3}}x^{-\frac{2}{3}}\right.$$

For the second approximation, the additional term in the transverse velocity is given by

$$v\eta=\frac{\mathrm{U}}{3}(c_w\mathrm{F})x^{-2}\int^{\eta}\eta\,(4\chi_2+\eta\chi_2')\,d\eta$$

$$=\frac{\mathrm{U}}{3}(c_w\mathrm{F})\,x^{-2}\left[\eta\chi_2+\frac{2}{\eta}\int_0^{\eta}\eta\chi_2\,d\eta\right],$$

since v is finite for $\eta=0$. Hence v is easily evaluated since χ_2 is a polynomial in $\eta^{\frac{3}{2}}$.

Below are shown the graphs of u_1, u_2, v_1, v_2 where

$$u=\mathrm{U}\left\{\left(\frac{c_w\mathrm{F}}{x^2}\right)^{\frac{1}{3}}u_1+\left(\frac{c_w\mathrm{F}}{x^2}\right)u_2\right\},$$

$$v=\frac{\mathrm{U}}{3}\left\{\left(\frac{c_w\mathrm{F}}{x^2}\right)^{\frac{1}{3}}v_1+\left(\frac{c_w\mathrm{F}}{x^2}\right)v_2\right\},$$

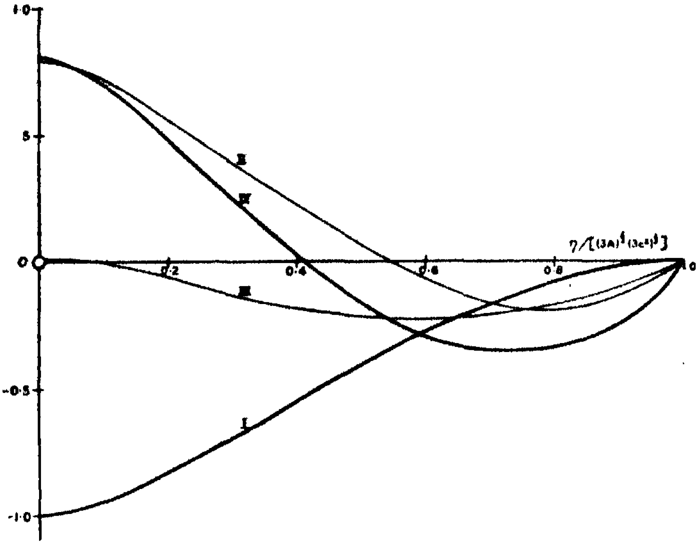

FIG. 1.

I is the curve u_1/A^2.
II is the curve of the quadratic in u_2/A^4 for the case $l \propto b$.
III is the curve of the quartic in u_2/A^4.
IV is the curve u_2/A^4 for the case $l \propto b$.

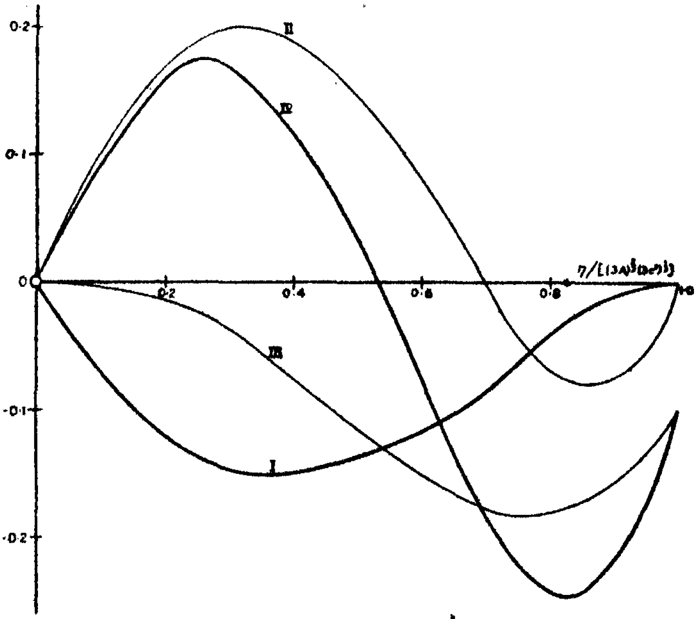

FIG. 2.

I is the curve $v_1/A^{\frac{8}{3}}$.
II is the curve of the quadratic in $v_2/A^{\frac{14}{3}}$ for the case $l \propto b$.
III is the curve of the quartic in $v_2/A^{\frac{14}{3}}$.
IV is the curve $v_2/A^{\frac{14}{3}}$ for the case $l \propto b$.

Lamb* found by means of Oseen's equations that for a sphere, the velocity in the wake along the axis varied as x^{-1} at a great distance from the body. This result has now been generalised by Goldstein† for any body of revolution. It must however be remembered that Oseen's equations give good approximations to the motion for small Reynolds' numbers, whereas the assumptions made in this paper hold for large Reynolds' numbers. It is known that the type of motion can abruptly change as the Reynolds' number is increased.

§ 4. We now return to the various assumptions made on p. 648. First as to the assumption that it is sufficiently accurate to take the " apparent stress " as $l^2\left(\frac{\partial u}{\partial y}\right)^2$. The complete vector form given by Prandtl‡ for the " apparent stress " in cartesian co-ordinates is

$$l^2\left[\left(\frac{\partial u}{\partial y}+\frac{\partial v}{\partial x}\right)^2-4\frac{\partial u}{\partial x}\cdot\frac{\partial v}{\partial y}+-+-\right]^{\frac{1}{2}}(\nabla\bar{v}+\bar{v}\nabla),$$

where $\bar{v}$ denotes the vector velocity.

The greatest possible orders of magnitude of $\frac{\partial u}{\partial y}$, $\frac{\partial u}{\partial x}$, $\frac{\partial v}{\partial y}$, $\frac{\partial v}{\partial x}$ are x^{-1}, $x^{-\frac{5}{3}}$, $x^{-\frac{5}{3}}$, $x^{-\frac{7}{3}}$ respectively. The additional terms that could occur in the x-equation of motion from $\nabla\bar{v}+\bar{v}\nabla$ are $\frac{\partial v}{\partial x}$, $2\frac{\partial u}{\partial x}$. They finally lead to terms

$$\frac{1}{y}\frac{\partial}{\partial y}\left[l^2 y\left\{\left(\frac{\partial u}{\partial y}+\frac{\partial v}{\partial x}\right)^2-+-+-\right\}^{\frac{1}{2}}\frac{\partial v}{\partial x}\right],$$

$$\frac{\partial}{\partial x}\left[2l^2\left\{\left(\frac{\partial u}{\partial y}+\frac{\partial v}{\partial x}\right)^2-+-+-\right\}^{\frac{1}{2}}\frac{\partial u}{\partial x}\right],$$

which are both at least of order x^{-3}. They will therefore not require to be taken into account until the third approximation is evaluated.

Secondly, the equation of motion perpendicular to Ox was neglected. It is clear that in this equation it will be sufficient to take the second factor in the " apparent stress " as $\frac{\partial u}{\partial y}$. The equation may then be written

$$(\mathrm{U}+u)\frac{\partial v}{\partial x}+v\frac{\partial v}{\partial y}=-\frac{1}{\rho}\frac{\partial p}{\partial y}+\frac{1}{y}\frac{\partial}{\partial y}\left(2l^2 y\frac{\partial u}{\partial y}\frac{\partial v}{\partial y}\right)$$
$$+\frac{\partial}{\partial x}\left(l^2\frac{\partial u}{\partial y}\left[\frac{\partial u}{\partial y}+\frac{\partial v}{\partial x}\right]\right)-2l^2\frac{\partial u}{\partial y}\frac{v}{y^2}. \quad \text{(vi)}$$

---

* Lamb, ' Hydrodynamics ' (5th ed.), p. 577.

† ' Roy. Soc. Proc.,' A, vol. 123, p. 216 (1929).

‡ Tollmien, ' Z. angew. Math. und Mech.,' vol. 6, p. 468 (1926).

The orders of magnitude of the terms are

$$x^{-\frac{7}{3}},\ x^{-3},\ x^{-3},\ \frac{\partial p}{\partial y},\ x^{-\frac{7}{3}},\ x^{-\frac{7}{3}},\ x^{-\frac{11}{3}},\ x^{-\frac{7}{3}}.$$

Hence $\partial p/\partial y$ is at least of order $x^{-\frac{7}{3}}$ and so p of order x^{-2}. Thus it is not necessary to take account of $\partial p/\partial x$ in the x-equation until the third approximation is reached. By keeping in the terms of order $x^{-\frac{7}{3}}$ in (vi) and integrating, we find

$$p_{\text{middle}} - p_{\text{boundary}} = 0{\cdot}07x^{-2}\,(c_w\mathrm{F})\,\rho\,\frac{\mathrm{U}^2}{2}.$$

The other point that was raised on p. 648 was the question of the position of the origin. It is to be some fixed point on the axis of symmetry. At very great distances from the body, no effect is produced by moving the origin a finite distance ε, as ε is then small compared with x. In general, if the exact position of the origin is left indeterminate, we must replace x by $x + \varepsilon$. From the first approximation to the boundary we should then get

$$\begin{aligned} y &\propto (x+\varepsilon)^{\frac{1}{3}}, \\ &\propto x^{\frac{1}{3}} + \tfrac{1}{3}\varepsilon x^{-\frac{2}{3}} + \dots, \end{aligned}$$

and hence an additional term that would come between the second and third approximations. Similarly we obtain for the velocity

$$\begin{aligned} u &= -\,\mathrm{U}\,\frac{(c_w\mathrm{F})^{\frac{2}{3}}}{(x+\varepsilon)^{\frac{2}{3}}}\left[\tfrac{1}{3}\,\frac{y^{\frac{3}{2}}}{(c_w\mathrm{F})^{\frac{1}{2}}\,(x+\varepsilon)^{\frac{1}{2}}} - \mathrm{A}\right]^2 \\ &= -\,\mathrm{U}\,\frac{(c_w\mathrm{F})^{\frac{2}{3}}}{x^{\frac{2}{3}}}\,(\tfrac{1}{3}\,\eta^{\frac{3}{2}} - \mathrm{A})\,\{(\tfrac{1}{3}\eta^{\frac{3}{2}} - \mathrm{A}) - \varepsilon x^{-1}\,(\eta^{\frac{3}{2}} - 2\mathrm{A})\}, \end{aligned}$$

and hence a term between the second and third approximations. We are thus left with an undetermined constant ε; this is ultimately to be expected and desired, as the shape of the body must effect u in the region nearer the body.

It seems clear that equation (i) can be solved to any order of approximation required. Each successive approximation will lead to a hypergeometric equation, of which only the particular integral, which will be a polynomial, will be admissible for the solution.

§ 5. In obtaining the second approximation, it might be assumed that l

still varies as $x^{\frac{1}{3}}$. This involves putting $c_1 = 0$. The second particular integral disappears and we have

$$\chi_2 = a_1 \mathrm{F}\left(\frac{1+\sqrt{97}}{6},\ \frac{1-\sqrt{97}}{6},\ \tfrac{4}{3};\ z\right) + a_2 z^{-\frac{1}{3}} \mathrm{F}\left(\frac{-1+\sqrt{97}}{6},\ \frac{-1-\sqrt{97}}{6},\ \tfrac{2}{3};\ z\right),$$
$$+ 4\mathrm{A}^4 (0 \cdot 0041 - 0 \cdot 259 z + 0 \cdot 359 z^2 - 0 \cdot 128 z^3 + 0 \cdot 0227 z^4).$$

As before $a_1 = 0$, $a_2 = 0$.

If we now assume the boundary to be given by

$$\eta = \eta_0 \left(1 + \frac{d}{c} (c_w \mathrm{F})^{\frac{1}{3}} x^{-\frac{2}{3}}\right),$$

or

$$z = 1 + \tfrac{3}{2} \frac{d}{c} (c_w \mathrm{F})^{\frac{1}{3}} x^{-\frac{2}{3}},$$

the condition (c) gives as before

$$\frac{d}{c} \eta_0 \chi_1''(\eta_0) + (3\mathrm{A})^{-\frac{2}{3}} \tfrac{3}{2} z^{\frac{1}{3}} \left(\frac{d\chi_2}{dz}\right)_{z=1} = 0,$$

leading to

$$\frac{d}{c} = 0 \cdot 22\ \mathrm{A}^2.$$

Hence the form of the boundary differs only in the magnitude of the numerical factor multiplying the power of $x^{-\frac{2}{3}}$. The forms for u, v are somewhat simplified.

It is possible to make a still more general assumption in obtaining the second approximation.

We write as before

$$l = c (c_w \mathrm{F} x)^{\frac{1}{3}} + c_1 (c_w \mathrm{F})^{\frac{2}{3}} x^{\frac{1}{3}},$$

but take for the outer boundary

$$\eta = \eta_0 \left[1 + \frac{e}{c} (c_w \mathrm{F})^{\frac{1}{3}} x^{-\frac{2}{3}}\right],$$

or

$$z = 1 + \tfrac{3}{2} \frac{e}{c} (c_w \mathrm{F})^{\frac{1}{3}} x^{-\frac{2}{3}},$$

where c_1, e are arbitrary constants.

We obtain the same form for χ_2 as that given above and find as before $a_1 = a_2 = 0$.

Condition (c) now gives us

$$\frac{e}{c} \eta_0 \chi_1''(\eta_0) + (3\mathrm{A})^{-\frac{2}{3}} \tfrac{3}{2} z^{\frac{1}{3}} \left(\frac{d\chi_2}{dz}\right)_{z=1} = 0,$$

leading to

$$3 \frac{e}{c} - 1 \cdot 91 \frac{c_1}{c} = 0 \cdot 66\ \mathrm{A}^2.$$

We can thus choose one of the constants e, c_1 arbitrarily and this leaves us with the desired freedom mentioned on p. 657.

In conclusion, the author would like to express her thanks to Prof. Prandtl both for originally proposing the problem and for many valuable suggestions while the work was in progress; she also had the opportunity of discussion with members of the Kaiser Wilhelm Institut für Strömungsforschung in Göttingen.

Summary.

The shape of the turbulent wake behind a body of revolution in a uniform stream is discussed and the distribution of the velocity in the wake is considered. The work is an extension of results given by Prof. Prandtl in his paper presented to the Second International Congress for Applied Mechanics, Zurich, 1926. The turbulent motion is assumed to introduce an "apparent stress" $l^2\left(\frac{\partial u}{\partial y}\right)^2$, where u is the mean velocity along the axis of x and y is distance perpendicular to that axis; l is a length called by Prandtl "Mischungsweg" (mixing distance). It is shown that $l \propto x^{\frac{1}{3}}$ and then using the approximations generally made in Prandtl's boundary layer theory, the equation of motion for the wake is obtained in such a form that it can be integrated by successive approximation. Taking the resistance of the body in a stream U to be $\frac{1}{2}\rho c_w \mathrm{F} \mathrm{U}^2$, the first approximation gives:—

(i) for the boundary of the turbulent region

$$y = 1\cdot41\,(3c^2)^{\frac{1}{3}}\,(c_w \mathrm{F} x)^{\frac{1}{3}},$$

where c is an absolute constant, which must be experimentally evaluated;

(ii) for the velocities,

$$u = \mathrm{U}\,(c_w \mathrm{F})^{\frac{1}{3}}\,x^{-\frac{2}{3}}\chi_1(\eta),$$

$$v = \frac{\mathrm{U}}{3}\,(c_w \mathrm{F})^{\frac{2}{3}}\,x^{-\frac{4}{3}}\eta\chi_1(\eta),$$

where $\chi_1(\eta) = -\left(\frac{1}{3}\eta^{\frac{3}{2}} - \mathrm{A}\right)^2$, $\eta = y/(c_w \mathrm{F} x)^{\frac{1}{3}}$, $\mathrm{A} = 0\cdot56\,(3c^2)^{-\frac{1}{2}}$. With the help of the second approximation, the boundary is obtained in the form

$$y = 1\cdot41\,(3c^2)^{\frac{1}{3}}\,(c_w \mathrm{F} x)^{\frac{1}{3}}\,\{1 + 0\cdot19\,(3c^2)^{-\frac{2}{3}}\,(c_w \mathrm{F})^{\frac{2}{3}}\,x^{-\frac{2}{3}}\},$$

and additional terms occur in u, v varying as $x^{-\frac{4}{3}}$, x^{-2} respectively. The correction to the boundary becomes more significant as the body is approached and gives a new boundary lying outside the original one.

Electron Scattering in Mercury Vapour.

By F. L. Arnot, B.Sc., Trinity College, Cambridge.

(Communicated by J. Chadwick, F.R.S.—Received August 12, 1929.)

Introduction.

When a beam of homogeneous electrons passes through a gas some of the electrons will collide with gas molecules, and be scattered out of the beam. The collision may be elastic, in which case the electron suffers only a change of direction (the loss of energy is inappreciable); or it may be inelastic, in which case the electron loses some of its energy besides being deflected. Thus if we examine the velocity distribution of the electrons scattered at a particular angle, θ, two main groups of electrons will be found, the elastic group and the inelastic group.

Except in the case of ionisation, the electron can only lose an appreciable amount of energy in discrete amounts corresponding to the excitation potentials of the gas. The inelastic group may therefore be subdivided into a number of groups corresponding to the different excitation potentials of the gas. The relative sizes of these subsidiary groups will depend upon the relative probabilities of excitation of the different states of the gas molecule. The probability of a collision resulting in a high state of excitation of the atom is usually small compared to the probability of a resonance or ionisation collision. Thus the inelastic group resolves itself into two main subsidiary groups; one group consists of the electrons which have ionised the atom, and the other group is composed of electrons which have caused resonance transitions in the atom.

The object of the experiments described in this paper is to find how the intensity of the elastic group and of the inelastic group varies with the angle through which the electrons are scattered. This will depend primarily upon the variation in the field of the atom with distance from the centre. Under any central field of force that decreases as we proceed outwards, the intensity of the elastic group per unit solid angle, I_e, will decrease as θ is increased. If the field falls off according to the inverse square law the relation between I_e and θ is given by the well known expression for the scattering of α-rays by a bare nucleus.

$$I_e \propto \text{cosec.}^4\, \theta/2.$$

If the field falls off according to some higher power of the distance, then I_e will not fall off with θ so steeply.[*] It is not possible to find a simple power law of force that is true for all parts of the atom. As we proceed outwards the law of force changes. Between the nucleus and the K-ring of electrons the inverse square law holds. Beyond the K-ring the partial shielding action of the inner electrons causes the field to fall off more sharply. The relation between I_e and θ will thus depend upon the velocity of the electrons; for the greater the velocity the more deeply will they penetrate into the atom.

Very little work has so far been done on the scattering of slow electrons. Langmuir and Jones[†] have obtained evidence by an indirect method that in a number of gases the electrons, after a single elastic or inelastic collision, are scattered through quite small angles. We should expect this result on any central field theory of the atom. They found that I_e falls off more steeply with θ as the velocity of the primary electron beam is increased. Dymond and Watson[‡] have made the first direct determination of the shape of the scattering curve for slow electrons. Using helium as the scattering gas, they found that I_e falls off with θ very much more gradually than would be expected if the field varied according to the inverse square law. As stated above this means that the outer field of the helium atom falls off according to some higher power of the distance than the square. Concerning the relative numbers of elastically and inelastically scattered electrons, they found that, for electrons of 200 volts energy, many more electrons were scattered elastically than inelastically at large angles; while at small angles the number of inelastically scattered electrons approximated in number to the elastically scattered electrons, and even exceeded the latter when the initial velocity of the electrons was raised to 400 volts.

Mott[§] has recently worked out the theoretical scattering curve for the elastically reflected electrons in helium on the basis of the wave mechanics, and finds that this fits very well with Dymond and Watson's experimental curve. During the progress of the present work a paper has appeared by Harnwell[||] in which a rough qualitative measurement of the scattering in He, Ne, H_2 and N_2, has been made. The present investigation deals with the angular scattering of electrons of about 80 volts energy in mercury vapour.

---

[*] See Darwin; 'Phil. Mag.,' vol. 27, p. 499 (1914).

[†] Phys. Rev.,' vol. 31, p. 357 (1928).

[‡] 'Roy. Soc. Proc.,' A, vol. 122, p. 571 (1929).

[§] 'Nature,' vol. 123, p. 717 (1929); also 'Proc. Camb. Phil. Soc.,' vol. 25, p. 304 (1929).

[||] 'Phys. Rev.,' vol. 33, p. 559 (1929). See also correction in letter to Editor, 'Phys. Rev.,' vol. 34, p. 162 (1929).

Experimental.

The apparatus is shown in a vertical section in fig. 1. Electrons from the oxide-coated platinum filament, F, were accelerated through the collimating cylinder, C, passing through the holes, H, each of 1 mm. in diameter. The Faraday cylinder, K, and its outer shield, Z, were supported on the bent quartz tube, T, passing through a wax joint in the ground glass stopper, G. The quartz tubing was coated on the outside with tin-foil connected to the shield, Z. By rotating the ground glass stopper, G, the Faraday cylinder could thus be set at any angle to the electron beam. The distance between the slit S_1 and the centre of the bulb was 1 cm., S_1 was 0·25 mm. wide and 5 mm. long and S_2 was 0·25 mm. wide and 1 mm. long. By applying retarding potentials between the Faraday cylinder and the shield, Z, the velocity distribution of the electrons scattered at any angles could be determined.

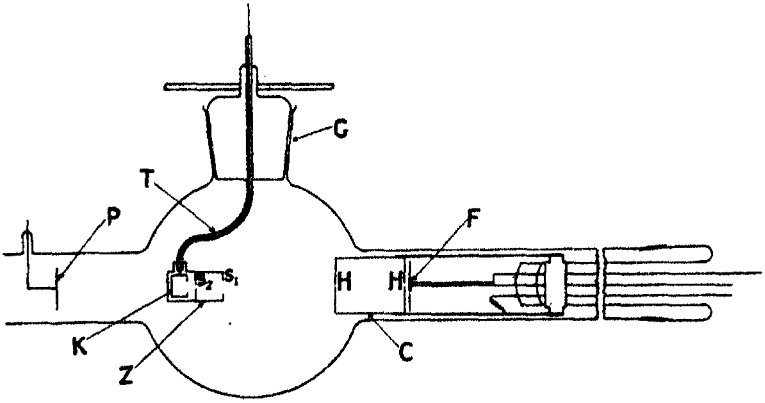

Fig. 1.

The inside of the bulb and the portion of the outlet tube up to the plate, P, were coated with magnesium by evaporating a small piece of magnesium wire on which was wound a nickel heating coil. A small wire not shown in the figure was sealed through the bulb and bent so as to press firmly on the magnesium coating. Tests showed that a good contact was made. The inside coating of the bulb, the shield, Z, and the plate, P, were all connected to one side of a galvanometer, the other side being connected to the cylinder, C. This ensured that the scattering took place in a practically field-free space, while the galvanometer recorded the intensity of the electron beam. The horizontal and vertical components of the earth's magnetic field were balanced out separately by means of large Helmholtz coils. The filament and Helmholtz coils were run off independent storage batteries of large capacity so as to ensure these currents being constant.

The apparatus was exhausted through a liquid air trap by means of a mercury diffusion pump backed by a rotary Gaede pump. The air pressure inside the apparatus was probably well below 10^{-5} mm. of Hg, the McLeod gauge reading zero. The apparatus was perfectly tight showing no rise in pressure over night. During a run the pumps were kept going with no liquid air on the mercury vapour trap. The pressure of mercury vapour inside the apparatus was therefore that corresponding to room temperature,* *i.e.*, about 10^{-3} mm. of Hg. The mean free path of an electron at this pressure is about 30 cms., so that the probability of an electron making two collisions in the bulb before entering the Faraday cylinder was very small.

The electron beam which could always be clearly seen was quite sharp and passed through the bulb with practically no divergence, its diameter of cross section being about 1 mm. Incidentally it may be mentioned that the oxide-coated filament, which was covered with a dark positive-ion sheath, a fraction of a millimetre in thickness, emitted electrons not uniformly but in quite sharp beams which showed practically no tendency to diverge. The filament emissions used varied for different runs from 0·2 to 2·0 milliamps. The strength of the electron beam varied from 1 to 10 microamps.

During each reading of the electrometer, which was worked at a sensitivity of 1,600 mm. per volt, the strength of the electron beam as recorded by the galvanometer was noted. The electrometer readings were then divided by the galvanometer readings so as to correct for any variation in the strength of the beam. As a rule this variation was only a few per cent. At different times throughout the experiment several runs were made with liquid air on the mercury vapour trap. In each case these tests showed that there was present only a single sharp electron beam represented by a peak at 0°. There was therefore no appreciable scattering of the primary electrons from the walls of the bulb. In these tests the retarding potential between the Faraday cylinder and the shield, Z, was between 20 and 40 volts for 80 volt electrons. If the retarding potential was reduced below about 12 volts quite large currents were obtained at all angles due to secondary electrons from the plate P (or the shield Z for angles near zero) being specularly reflected from the walls of the bulb (see below).

Angles were read by a protractor and arm attached to the ground glass joint, G, to an accuracy of about 1°. When the Faraday cylinder was set to receive electrons scattered at an angle θ, then owing to the finite width of the slits S_1 and S_2 (0·25 mm.) electrons scattered between $\theta + 1{\cdot}5^\circ$ and $\theta - 1{\cdot}5^\circ$ were collected. The error introduced by the length of the slits varies with θ, being 3° when θ is zero, and zero when θ is 90°.

---

* As the main object of the experiments was to observe the relative scattering, the temperature was not measured for each run.

Tests of the homogeneity of the primary electron beam were made by setting the Faraday cylinder at $\theta = 0^\circ$ and applying retarding potentials between it and the shield, Z. It was found that about 95 per cent. of the electrons had a velocity within one volt of the mean.

Results :—(1) *Velocity Distribution at a Fixed Angle.*

Fig. 2 shows the velocity distribution of electrons scattered at 10°. The electron current to the Faraday cylinder in arbitrary units is plotted against the retarding potential in volts. The initial velocity of the primary electron beam was 82 volts. It will be seen that there are three main groups of electrons :—

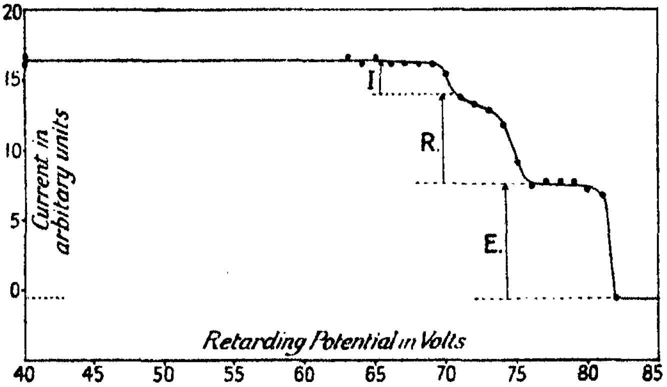

Fig. 2.

(1) Those which have been elastically scattered, represented in magnitude by the ordinate E.
(2) Those which have, in the process of being reflected by the atom, excited it to the resonance or some higher level. This group is represented by R.
(3) Those which on being scattered have ionised the atom, represented by I.

The resonance potential of mercury vapour is about 5 volts and the ionisation potential 10·4 volts. The position of the kinks agrees quite well with these values. The curve continues quite flat down to a retarding potential of about 12 volts, when it begins to rise steeply showing the presence of a large group of very slow electrons. These are mainly secondary electrons originating from the slits and from the point where the primary beam strikes the shield Z (or the plate P for larger angles). Their presence causes no trouble as they can be completely eliminated by a retarding potential of about 15 volts.

For retarding potentials greater than that of the primary beam a small positive current was observed. This is due partly to positive ions diffusing out of the path of the electron beam to the slit S_2 where they are then accelerated into the Faraday cylinder, and partly to a photo-electric effect from the Faraday cylinder. In the angular distribution curves (see below) this positive current was, except at large angles, so small compared to the negative current that it could be neglected. At small angles it was less than the experimental error involved in reading the negative currents ; at large angles ($\theta > 40°$) a reading of this positive current was taken at each angle, and the negative current corrected accordingly.

The flat top to the kink at ($V_0 - 10\cdot5$) volts, representing the group of electrons which have made ionising collisions, is interesting ; for it implies that when an 80 volt electron, in being scattered through 10°, ionises a mercury atom practically no energy is carried away by the ejected electron. If the ejected electron had an equal probability of carrying away any fraction of the excess energy we should expect a very gradual rise beginning when the retarding potential was 10·5 volts less than the initial velocity of the primary beam, and extending down to zero retarding potential.

When the primary electron causes ionisation of the atom it must interact closely with the ejected electron. On classical momentum considerations the amount of energy that the primary electron gives to the ejected electron will depend upon the angle through which the primary electron is scattered. If it is scattered through a small angle it can give the ejected electron only a small amount of energy. We cannot treat this problem quantitatively because of the binding force between the electron and the atom, but we know that if the ejected electron carries away a large fraction of the excess energy the primary electron should be scattered through a large angle. It is hoped later to investigate this point more fully, and if possible to obtain a relation between the angle through which the primary electron is scattered and the fraction of the excess energy carried away by the ejected electron.

(2) *Angular Distribution of Scattered Electrons.*

Readings were taken at intervals of 5° on both sides of the electron beam. By this means the angular zero could be determined to within an accuracy of half a degree. At each angular setting two readings were taken, (1) with a retarding potential of $(V_0 - 3)$ volts, and (2) with a retarding potential of $(V_0 - 40)$ volts, where V_0 is the initial velocity of the primary electron beam. The first reading gives the elastically reflected electrons, and the difference between the two readings gives the inelastically reflected electrons. The latter includes, besides the electrons that have made excitation collisions, also those that have made a collision resulting in ionisation. The length of path for collision is a function of the angle of scattering. The effective length of path is the length of the electron beam intercepted by the beam entering the Faraday cylinder, which is defined by the slits S_1 and S_2. If d is the width of this beam where it intersects the electron beam at the centre of the bulb, then the effective length of path for collision is $d/\sin\theta$. We must therefore multiply each angular reading by $\sin\theta$. The value of d is 0·75 mm.

Fig. 3 is a typical curve showing the angular distribution of the elastically and inelastically scattered electrons. The velocity of the primary beam was 82 volts. It will be seen that the number of electrons scattered at an angle θ decreases rapidly as θ is increased. The elastic scattering curve falls off more sharply than it does in helium, for the same velocity of the primary beam.* We may explain this by assuming that the outer field of the mercury atom falls off according to a lower power of the distance than does that of the helium atom.

The electrons that have made inelastic collisions fall off more sharply than do the electrons that have been elastically scattered, the curves crossing each other at a certain value of θ. Below this value there are more inelastically scattered electrons, while at larger angles there are more elastically scattered electrons. This point has been carefully checked with quite consistent results. The value of θ where the curves cross is 15° for 82 volt electrons.

In their general characteristics these results for mercury-vapour are in accord with those of Dymond and Watson for helium. The main difference is that in mercury vapour the curves cross for much lower values of the velocity of the primary beam. To make the curves cross at 5° in helium the velocity of the primary beam must be raised to over 400 volts. Owing to the scarcity

* See Dymond and Watson, *loc. cit.*

of the experimental data at present available, and to the lack of any satisfactory theoretical treatment of the inelastically scattered electrons, it is difficult to

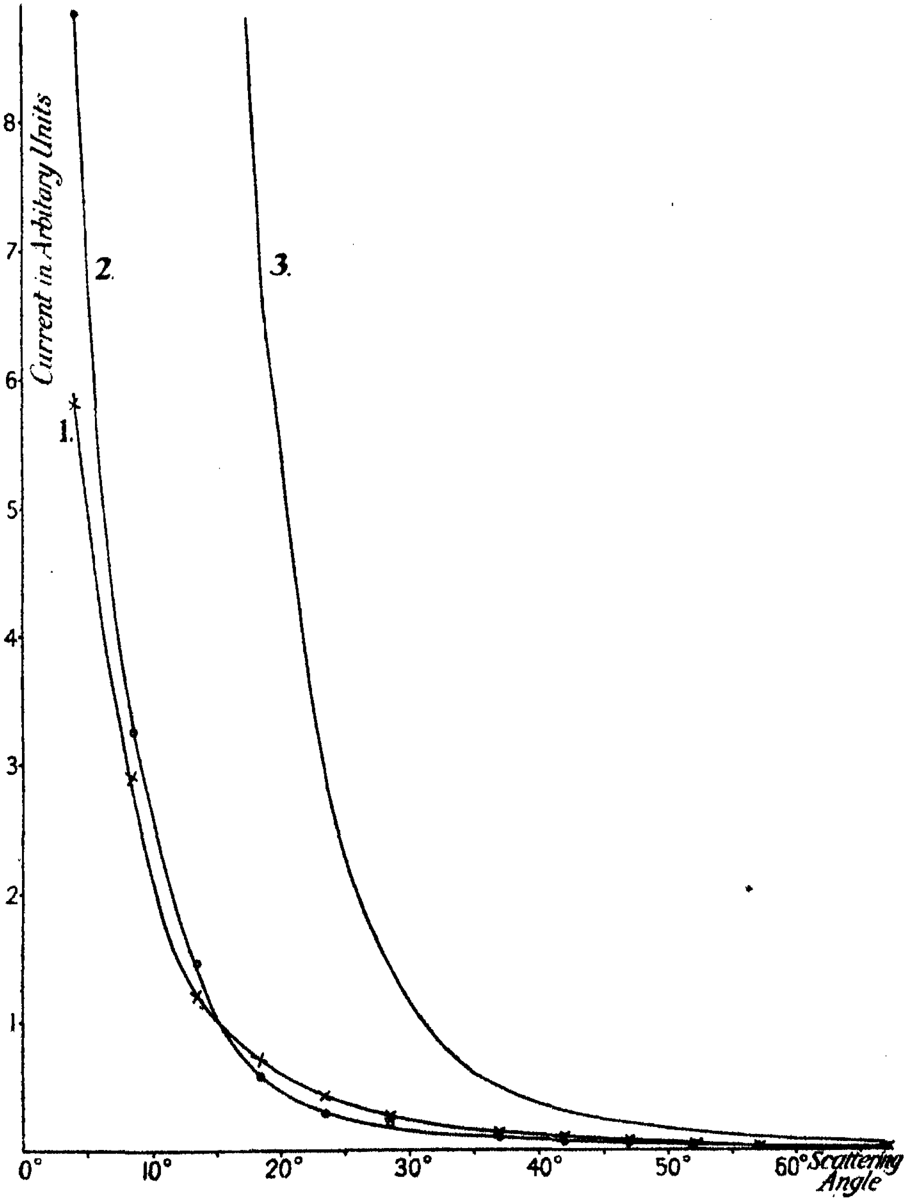

FIG. 3.—(1) Elastic Collision; (2) Inelastic Collision; (3) Coulomb Scattering Curve.

say what is the significance of this. It may be connected with the very much lower value of the excitation potentials in mercury vapour. The results of

Dymond and Watson show that as the velocity of the primary beam is increased the probability of an impact being inelastic increases, and the point where the curves cross moves to greater angles. One might expect then that the same effect as is obtained by increasing the velocity of the primary beam might be produced by employing a gas, such as mercury vapour, which has lower excitation potentials.

At angles greater than 55° there appear to be present about equal numbers of elastically and inelastically scattered electrons. At these large angles, however, the currents are so small that very little reliance can be placed upon these results. The difficulty of measuring these currents is still further increased by the presence of the positive drift for which correction must be made (see above). All that can be said definitely is that neither the elastic nor the inelastic curve shows any tendency to rise again. Readings were taken to 130°.

The ordinates of fig. 3 are in arbitrary units, and therefore the curves only show the relative scattering per unit solid angle. The absolute value of the scattered current at any angle may be obtained from fig. 3 by multiplying the ordinate at that angle by $3 \cdot 2 \times 10^{-12}$. The value so obtained is the current received by the Faraday cylinder in amperes. This value is for an electron beam of $2 \cdot 06 \times 10^{-6}$ amps., and a vapour pressure of $0 \cdot 0012$ mm. of Hg.* If $d\omega$ is the effective solid angle subtended by the Faraday cylinder at the point of collision, and i_θ is the current received by the Faraday cylinder when set at an angle θ to the electron beam, then the total scattered current is given by

$$\frac{2\pi}{d\omega}\int_0^\pi i_\theta \sin\theta \, d\theta.$$

We must therefore multiply the ordinates of fig. 3 by $2\pi \sin \theta d\theta/d\omega$, and numerically integrate the curves so obtained. The value of $d\theta$ is 3° and the value of $d\omega$ is $7 \cdot 2 \times 10^{-4}$ of the total solid angle around the point of collision. A certain error is introduced owing to the necessary extrapolation of the curves to zero angle. The error introduced by the extrapolation to 180° is negligible. On carrying out this integration we find the value of the total scattered current to be $1 \cdot 87 \times 10^{-9}$ amp. for the elastically scattered electrons, and $1 \cdot 94 \times 10^{-9}$ amp. for the inelastically scattered electrons. We see that inelastic collisions and elastic collisions are about equally probable under these conditions. The ratio

---

* Corresponding to a temp. of 20° C. Obtained from the International Critical Tables, vol. 3, p. 206.

$$\frac{\text{Inelastic collisions}}{\text{Elastic collisions}} = \frac{1 \cdot 94 \times 10^{-9}}{1 \cdot 87 \times 10^{-9}} = 1 \cdot 04.$$

Adding the currents for the elastically scattered and the inelastically scattered electrons we obtain the total scattered current $= 5 \cdot 7 \times 10^{-9}$ amp. The whole of this scattered current is due to collisions in a path of 0·75 mm. (see above). By dividing the total scattered current by the current in the electron beam we obtain the probability of collision in a path of 0·75 mm. The value obtained is $1 \cdot 85 \times 10^{-3}$. The mean free path of an electron in mercury vapour at a pressure of 0·0012 mm. of Hg. is therefore about 40 cms.

In fig. 3 is also drawn the theoretical curve for elastic scattering by a pure Coulomb field. This is given by the function cosec.^{4} $\theta/2$, where θ is the angle of scattering. In the figure this curve is fitted to the experimental curve at 90°. The Coulomb scattering curve actually falls off very much more steeply than does the experimental curve, but owing to both curves being so steep this difference in slope is not very marked in the figure. It is, however, clearly brought out by the following table, in which the ordinates of the Coulomb scattering curve have been proportionately reduced so as to fit the experimental elastic curve at $\theta = 15°$.

θ	5°.	10°.	15°.	20°.	25°.
Experimental curve	910	430	210	120	74·0
Coulomb curve	16,700	1,100	210	67	2·8

It is obvious from this table that the experimental readings could not be fitted to the Coulomb curve, but it is interesting to note that the elastic scattering curve for mercury vapour deviates less violently from the inverse square law scattering curve than does the curve for helium given by Dymond and Watson. This implies that the outer field of the mercury atom resembles a Coulomb field far more closely than does that of the helium atom.

In conclusion I wish to express my thanks to Sir Ernest Rutherford and Mr. P. M. S. Blackett for their interest and many helpful suggestions during the course of this work; also to Dr. Chadwick for his helpful criticism of this paper.

The Crystal Structure of Ice between 0° C. and −183° C.

By William Howard Barnes, M.Sc., Ph.D.
(Ramsay Memorial Fellow for Canada, 1927–29.)

(Communicated by Sir William Bragg, F.R.S.—Received August 13, 1929.)

[Plates 11, 12.]

1. *Introduction.*

The research described in this paper on the Crystal Structure of Ice was undertaken for various reasons.

In the first place data on the subject in the literature are very conflicting, as is also the case for those on the crystallography of ice. As the available structures for ice were appearing in text-books and elsewhere as representing the true facts it was deemed advisable to redetermine the structure in an effort to find why the existing models are so dissimilar and if possible to arrive at a structure on which more reliance could be placed.

It was hoped also that if the uncertainty regarding the structure and crystallographic features of ice could be eliminated valuable data might be available for such problems as the physical properties of ice, constitution of water, flow of glaciers and anomalous meteorological haloes. And further with the rapid advances that the subject of Ice Engineering is making in Canada the question of the arrangement of the oxygen and hydrogen atoms in the crystal of ice is of more than passing interest to workers in that field.

This paper contains brief surveys of the data available on the crystal structure and crystallography of ice. Two sections on new experimental work are presented, the first dealing with single crystal rotation, oscillation, and Laue photographs leading to a complete structure for ice, and the second describing a series of powder photographs testing the structure at various temperatures between 0° C. and −183° C. The positions of the diffracting centres in the unit cell of ice have been determined with great certainty. Estimated intensities agree satisfactorily with values calculated for either oxygen atoms or divalent oxygen ions at these positions. Certain arguments, partly of an hypothetical nature, are put forward in an attempt to show that the structure probably is ionic in nature, and to find the most probable positions of the hydrogen ions. Finally a short discussion is included on certain relevant points arising in connection with this work. The bearing of the model proposed for ice on various other subjects is not included, partly because of its hypothetical nature, and also because further experimental work is in contemplation.

II. *Literature Survey on the Crystal Structure of Ice.*

Previous experimental work* on the crystal structure of ice includes Laue photographs taken by Rinne in 1917 and interpreted by Gross in 1919, spectrographic data published by St. John in 1918, and powder measurements made by Dennison in 1921. In addition, Sir William Bragg, on theoretical grounds, proposed a structure in 1922. Finally, Aminoff in 1921 added the hydrogen atoms to the structure of Gross in an attempt to calculate the radius of the hydrogen atom, and some experimental work has been carried out at Leiden† to which the writer has been unable to find a reference.

Rinne's photographs were obtained by selecting an optically homogeneous piece of ice from a frozen water surface and passing the X-ray beam through it at right angles to the freezing face. The sample was kept frozen with liquid air. From the symmetry of the spots on his photographs (which is that of space group D_6), in conjunction with the crystallographic data of Nordenskiold,‡ Rinne concludes that ice is dihexagonal pyramidal. He gives the axial ratio ($c : a$) as about 1·6.

Gross carried these deductions further by taking a duplicate photograph of rock salt, determining the wave-lengths giving rise to the spots on the ice photograph, and comparing relative intensities. He decides that ice is dihexagonal bipyramidal (space group $D_{6h}{}^4$) with two molecules in the unit cell. The dimensions of the unit cell are given as

$$c_0 = 5 \cdot 53 \text{ Å}. \qquad a_0 = 3 \cdot 46 \text{ Å}. \qquad c : a = 1 \cdot 62.$$

This cell is shown in fig. 1. The co-ordinates of the oxygen atoms are 0, 0, 0; $\frac{1}{3}, \frac{2}{3}, \frac{1}{2}$. These equivalent points do not correspond to a possible arrangement in either $C_{6v}{}^4$ (dihexagonal pyramidal) or $D_{6h}{}^4$ (dihexagonal bipyramidal), and as a matter of fact, the space group cannot be determined from these data alone. One set of possible equivalent points for $C_{6v}{}^4$ is $\frac{1}{3}, \frac{2}{3}, U$; $\frac{2}{3}, \frac{1}{3}, U + \frac{1}{2}$, and for $D_{6h}{}^4$ $\frac{1}{3}, \frac{2}{3}, \frac{1}{4}$; $\frac{2}{3}, \frac{1}{3}, \frac{3}{4}$. Either of these is compatible with the structure proposed. In $C_{6v}{}^4$ U is an undetermined parameter, which in $D_{6h}{}^4$ is equal to $\frac{1}{4}$.

---

* Rinne, 'Ber. Verh. Ges. Wiss. Math.-Phys.,' vol. 69, p. 57 (1917); Gross, 'Centr. Min. Geol.,' p. 201 (1919); St. John, 'Proc. Nat. Acad. Sci.,' vol. 4, p. 193 (1918); Dennison, 'Phys. Rev.,' vol. 17, p. 20 (1921); Bragg, W. H., 'Proc. Phys. Soc. London,' vol. 34, p. 98 (1922); Aminoff, 'Geol. För. Förh.,' vol. 43, p. 389 (1921).

† Astbury and Bragg, 'Annual Rep. Chem. Soc.,' vol. 21, p. 232 (1924).

‡ Nordenskiold, 'Pogg. Ann.,' vol. 114, p. 612 (1861).

The additional symmetry required by the latter space group is contained in the molecule.

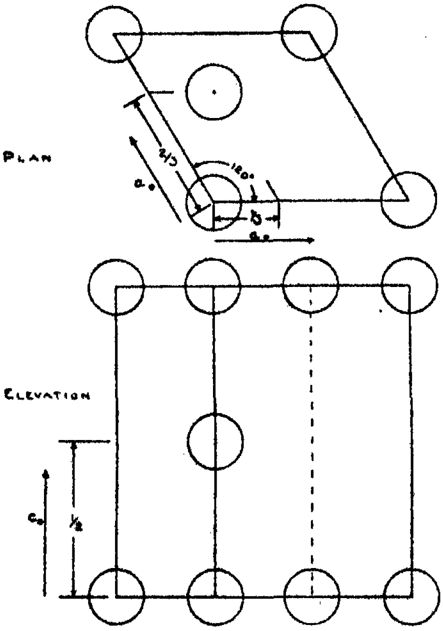

FIG. 1.

Aminoff places the hydrogen atoms in the unit cell of Gross at the points $0, 0, P$; $0, 0\,(1 - P)$; $\frac{1}{3}, \frac{2}{3}, (\frac{1}{2} - P)$; $\frac{1}{3}, \frac{2}{3}\,(\frac{1}{2} + P)$.

St. John's spectrographic photographs were obtained by oscillating single crystals of ice over known angular ranges. The specimens were obtained by allowing a pan of water to freeze slowly in an unheated room during the winter. The temperature at which the photographs were taken was about —15° C.

Dennison carried out his powder experiments at —183° C. A lime glass capillary containing water was frozen by plunging it into liquid air. The tube was rotated continuously during exposure to X-rays.

Sir William Bragg deduced his structure by taking the hexagonal alternative to the diamond structure, replacing each carbon atom by an oxygen ion, and altering the dimensions of the cell by a factor proportional to the ratio between the densities of ice and diamond. The hydrogen ions were placed on the lines joining the oxygen centres, one of the former between each pair of the latter.

The structures of St. John, Dennison, and Bragg are similar in that they agree on four molecules in a unit cell with construction points 0, 0, 0;

$\frac{1}{3}, \frac{2}{3}, U$; $\frac{1}{3}, \frac{2}{3}, \frac{1}{2}$; $0, 0, (\frac{1}{2} + U)$. Bragg gives the parameter U as $\frac{1}{8}$. It is undetermined in the investigations of St. John and Dennison. The space group is not mentioned. The unit cell is shown in fig. 2, the spheres representing the positions of the oxygen centres.

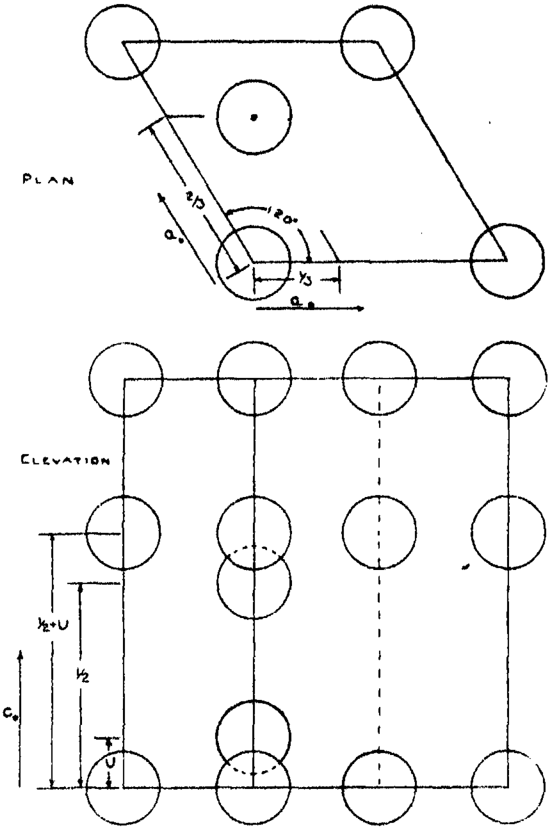

FIG. 2.

The dimensions of this cell, according to the different observers, are set forth in Table I.

Table I.

Observer.	c_0 (Å).	a_0 (Å).	$c : a$.
St. John	6·65	4·74	1·403
Dennison	7·32	4·52	1·617
Bragg	7·34	4·52	1·63

The structures of Dennison and Bragg are practically identical, and intensity calculations for Bragg's structure agree, in general, with estimations recorded by Dennison.

In reviewing these data it will be seen that they reduce to three structures, those of Rinne, Gross, and Aminoff; St. John; Dennison and Bragg. Furthermore, these structures are entirely distinct from one another. To quote Wyckoff,[*] "the sets of axes of these units are not merely rotations of one another through angles of 30° or integral multiples of one another; there is consequently a serious conflict among the reported experimental data on ice. Because of the danger of twinning in the crystals used in making both the Laue photographs and the spectrometer measurements, the powder data are the most reliable. These data alone are probably insufficient to establish the structure of ice; consequently nothing definite can be considered as known about its atomic arrangement."

III. *Literature Survey on the Crystallography of Ice.*

The literature on the crystallography of ice is so voluminous that a complete survey would be out of all proportion to the work with which this paper primarily is concerned. A very complete review of the data is to be found in Dobrowolski's "Historja Naturalna Lodu"[†] from which more than one hundred references to the subject may be obtained.

There seems to be little doubt that ice most commonly crystallises in the hexagonal system.[‡] Against this Mügge[§] claims to have found trigonal symmetry for the basal plane, and this is supported by a number of other observations[||] purporting to show that ice should be classed as rhombohedral. In addition a few specimens have been examined that appear to be cubic.[¶]

---

[*] "The Structure of Crystals," p. 266 (1924).

[†] p. 121 (1923).

[‡] See for example:—Bentley, 'Monthly Weather Review,' p. 212 (1901) and Aug., Sept., Oct., Nov., Dec. (1907); Smithson, 'Annals Philos.' vol. 5, p. 340 (1823); Secchi, 'Bull. meteorol. Osserv. Coll. Romano,' vol. 15, p. 73 (1876); Ledolt, 'Sitz.-Ber. K.-K. Akad. Wiss. Wien. Math.-nat.,' vol. 7 (1851); Tyndall, "The Form of Water in Clouds and Rivers, Ice and Glaciers," London (1876); Holland, 'Nature,' vol. 39, p. 295 (1889).

[§] Mügge, 'Centrl. Mineral,' p. 137 (1918).

[||] See for example:—Clarke, 'Trans. Camb. Phil. Soc.,' vol. 1, p. 209 (1822); Brewster, 'Phil. Mag.,' III, vol. 4, p. 245 (1834); Abich., 'Pogg. Ann.,' vol. 146, p. 475 (1872).

[¶] See for example:—Haüy and Romé de l'Isle (quoted by Smithson, *loc. cit.*); Barendrecht, 'Z. Phys. Chem.,' vol. 20 (1896); Wallérant 'Bull. Soc. Franç. Minéral, vol. 31, p. 217 (1908).

FIG. 3.

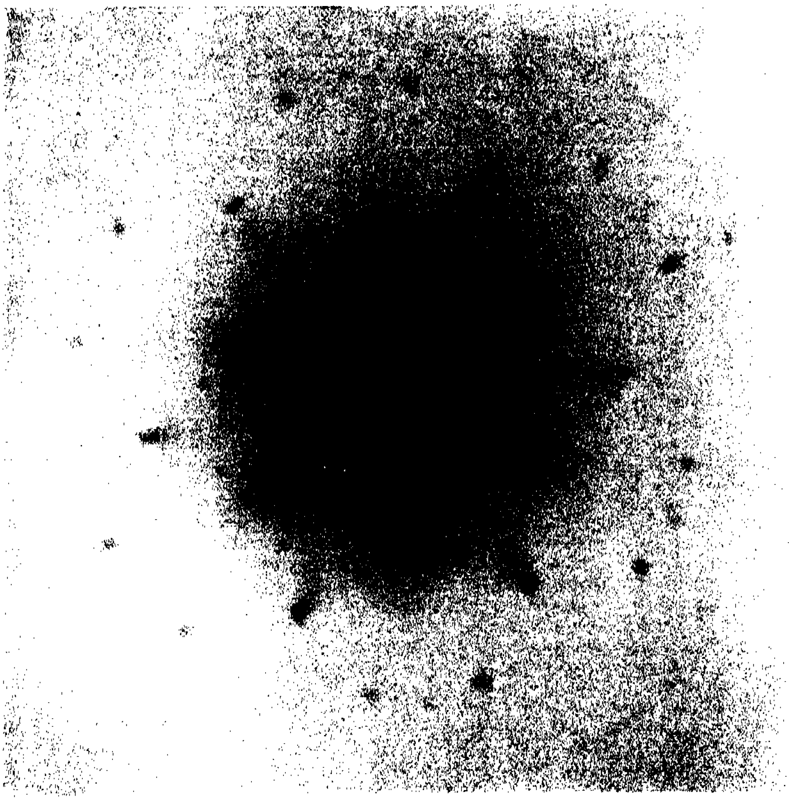

FIG. 6.

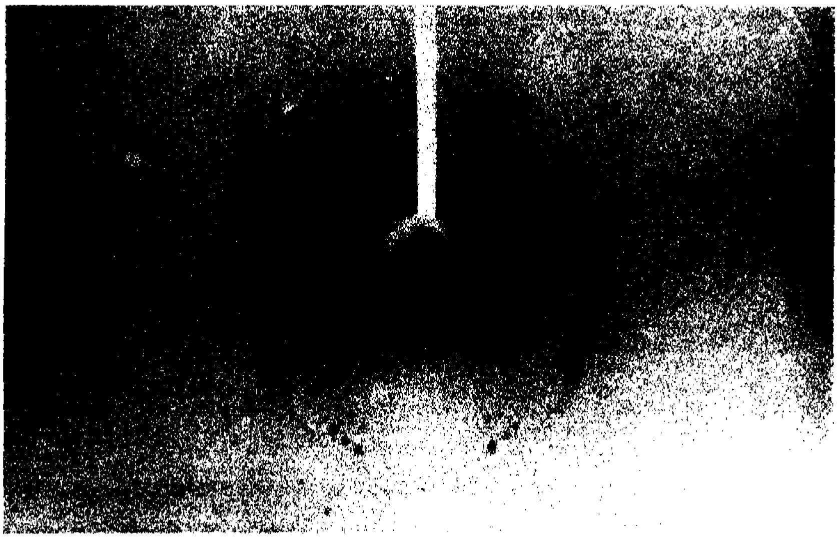

FIG. 4.

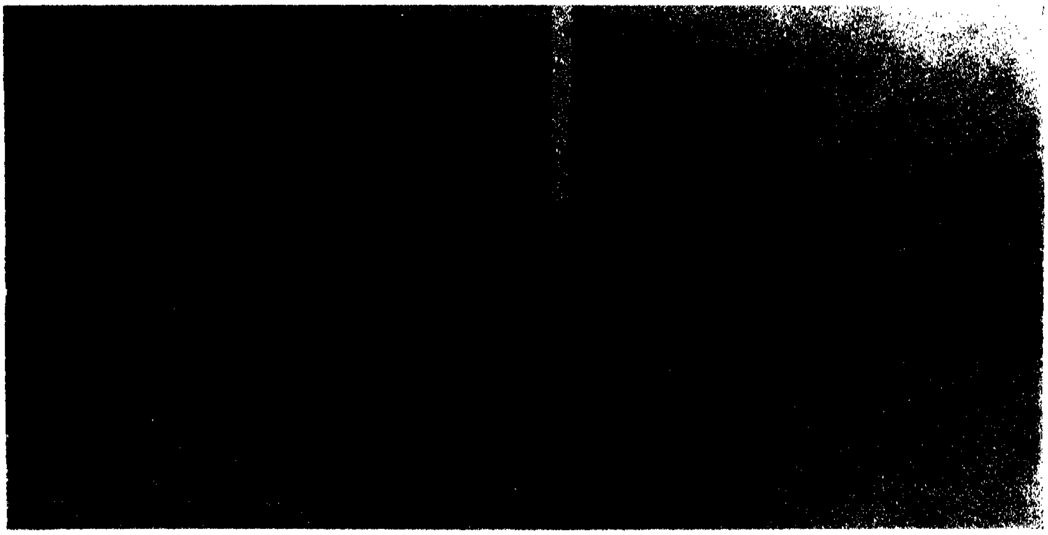

FIG. 5.

FIG. 11.

Nordenskiold (*loc. cit*) places ice in the dihexagonal pyramidal class of the hexagonal system with an axial ratio ($c : a$) of 1·617 or 1·400 depending on how he identifies the faces present on his crystal. Kenngott* calculates this ratio as 1·633, 1·622, and 1·589 from data of Clarke, Galle, and Smithson, respectively.

The disagreement among the reported observations can be emphasised very well by an examination of the data furnished by various crystallographic authorities who, it is assumed, have reached their conclusions after a critical survey of the available papers. Thus,† Groth and Dobrowolski give it as ditrigonal pyramidal; Lewis as hexagonal bipyramidal; and Dana as hexagonal, probably hemimorphic (dihexagonal pyramidal) with $c : a = 1 \cdot 4026$.

From this it appears that, although ice is probably hexagonal, it is impossible to place it in a particular class with any certainty. Leaving out of consideration the high pressure modifications of Tamman and Bridgman,‡ ice may be capable of exhibiting polymorphism under ordinary conditions.

IV. *Part I.—Single Crystal Rotation, Oscillation, and Laue Photographs of Ice.*

Apparatus.—The rotation and oscillation photographs to be described later were obtained with a Müller spectrograph and circular camera. The camera was adapted for use at temperatures below zero in the following way. The camera itself was enclosed in a coil of lead tubing packed in wool. The lower end of the coil dipped into an ebonite tray fixed at the bottom of the camera. A constant stream of methylated spirits was allowed to flow through a worm packed in a mush of solid carbon dioxide and methylated spirits and then through the coil around the camera into the ebonite tray. From the tray it overflowed into a receiver. The bottom of the camera was practically closed by a brass tray fixed to the goniometer arcs. This brass tray was bathed with the methylated spirits in the ebonite tray and rotated with the arcs. The top of the camera was closed with an ebonite cover.

The X-ray tube was of the gas-filled type used by Shearer and described by Bragg.§ The anticathode was of copper. A filter of nickel foil was used when desirable to remove the K_β line from the radiation.

---

* Kenngott, 'N. Jahrb. f. Mineral,' vol. 2, p. 184 (1886).

† Groth, "Chemische Krystallographie," vol. 1, p. 66 (1906); Dobrowolski, *loc. cit*, Lewis, "Crystallography," p. 403 (1899); Dana, "Descriptive Mineralogy," p. 205 (1892).

‡ Tamman, 'Z. phys. Chem.,' vol. 72, p. 609 (1910); Bridgman, 'Proc. Amer. Acad.,' vol. 47, p. 439 (1912).

§ "X-rays and Crystal Structure," p. 34 (1924).

Ice Crystals.—All attempts to grow single crystals of ice with well developed faces failed. Only needles could be obtained.

The crystals finally employed in this investigation were found in commercial, artificially frozen, ice by Mr. Green and the writer while preparing experiments for a lecture on " Ice " by Sir William Bragg at the Royal Institution. This ice is made up of small prisms, each of which, on examination in polarised light, proved to be a single crystal. Fig. 3 (Plate 11) is a photograph of a piece of this ice, the largest prism visible having a cross-sectional diameter of about 2·5 cms.

These prisms were mounted with one of the crystallographic axes coinciding with the axis of rotation of the spectrograph by means of α-angles calculated from random rotation photographs.* This method of setting had to be resorted to because Laue photographs showed that the faces present on the prisms in the ice block were not true crystallographic ones and even the long axis of the prisms did not coincide with the long crystallographic (c) axis.

Photographs.—Complete rotation photographs about the c and a axes are shown in Plate 12, figs. 4 and 5, respectively, that about the c axis being somewhat mis-set.

A complete set of photographs for 10° oscillations about the a axis over a range of 90° was made. Since there is no ambiguity in the identification of spots on the c axis rotation photograph it was unnecessary to take oscillations about this axis.

Laue photographs (see Plate 11, fig. 6) with the X-ray beam perpendicular to the basal plane were obtained from samples of naturally frozen ice. This ice was grown on the surface of a basin of water exposed to the atmosphere during cold weather. Clear, flawless areas were selected, small specimens cut from them, and the X-ray beam sent through them at right angles to the freezing face.

The temperature of the air in the camera during the rotation and oscillation photographs was about −20° C. The specimens for the Laue photographs were kept frozen with solid carbon dioxide (−78·5° C.).

Radius of Circular Camera.—The radius of the circular camera was standardised from rotation photographs of rock salt and mica. The value obtained was $2\cdot85_5$ cms. with an accuracy of about 1 per cent.

Dimensions of Unit Cell, Number of Molecules per Cell, and Space Group.—The symmetry of the Laue photographs (fig. 6) is that of space group D_6, so that the crystal at once can be referred to hexagonal axes.

---

* Bernal, 'Roy. Soc. Proc.' A, vol. 113 (1926).

From the rotation photographs the dimensions of the unit cell are

$$a_0 = 4{\cdot}53_5\ \text{Å}. \qquad c_0 = 7{\cdot}41\ \text{Å}. \qquad c : a = 1{\cdot}634.$$

The volume of this cell is equal to $1{\cdot}320 \times 10^{-22}$ cc.

Taking the density of ice at 0° C. as 0·9168[*] and the coefficient of cubical expansion as 0·00016,[†] the density at —20° C. is equal to 0·9196.

The number of molecules per unit cell is given by $\rho V/NM$, where ρ is the density at —20° C., V is the volume of the cell, N is the mass of the hydrogen atom ($1{\cdot}65 \times 10^{-24}$), M is the molecular weight (18); and it is equal to four.

The oscillation photographs proved the absence of reflections from the following planes :—

0001 0003 0005 0007

$11\bar{2}1$ $11\bar{2}3$ $11\bar{2}5$ $11\bar{2}7$

$22\bar{4}1$ $22\bar{4}3$ $22\bar{4}5$

$03\bar{3}1$ $03\bar{3}3$ $03\bar{3}5$

$14\bar{5}1$ $14\bar{5}3$

0004 $01\bar{1}4$ $02\bar{2}4$ $03\bar{3}4$ $04\bar{4}4$

$10\bar{1}4$ $11\bar{2}4$ $12\bar{3}4$ $13\bar{4}4$ $14\bar{5}4$

$20\bar{2}4$ $21\bar{3}4$ $22\bar{4}4$ $23\bar{5}4$

It thus appears that

$mm\overline{2m}l$ is halved when l is odd,
$03\bar{3}l$ is halved when l is odd,
$14\bar{5}l$ is halved when l is odd,
$hkil$ is halved when l is equal to 4.

Since the symmetry of the Laue photograph is that of space group D_6 the possible space groups for ice are D_{3h}, D_6, C_{6v}, and D_{6h},[‡] because these four appear as D_6 in a Laue photograph.

An examination of these space groups shows that, of the observed halvings, those of $mm\overline{2m}l$ are alone characteristic of a space group, so that the other missing reflections must be associated with the particular positions of the diffracting centres in the unit cell.

Of the possible space groups D_6 can be eliminated because no case in this group is possible with $mm\overline{2m}l$ halved when l is odd. $C_{6v}{}^4$, which does show this halving, is impossible with four molecules in the unit cell.

The number of possible space groups is thus reduced to two, namely, $D_{3h}{}^4$ (ditrigonal bipyramidal) and $D_{6h}{}^4$ (dihexagonal bipyramidal).

---

[*] Barnes, H. T., "Ice Engineering," p. 25 (1928).

[†] Barnes, H. T., *loc. cit.*, p. 46.

[‡] Astbury and Yardley, 'Phil. Trans.,' A, vol. 224 (1924).

For each of these two space groups the following two sets of equivalent points are possible* :—

1. $0, 0, \mathrm{U};\ 0, 0, \tfrac{1}{2} - \mathrm{U};\ 0, 0, \tfrac{1}{2} + \mathrm{U};\ 0, 0, \bar{\mathrm{U}}$.
2. $\tfrac{1}{3}, \tfrac{2}{3}, \mathrm{U};\ \tfrac{1}{3}, \tfrac{2}{3}, \tfrac{1}{2} - \mathrm{U};\ \tfrac{2}{3}, \tfrac{1}{3}, \tfrac{1}{2} + \mathrm{U};\ \tfrac{2}{3}, \tfrac{1}{3}, \bar{\mathrm{U}}$.

In D_{3h}^4 the molecule must be given a triad axis of symmetry perpendicular to the (0001) plane. In D_{6h}^4 the molecule must possess three planes of symmetry parallel to the $(11\bar{2}0)$ planes and intersecting in a triad axis perpendicular to the (0001) plane.

A possible choice between the two space groups is made later.

Geometrical Structure Factor.—Substituting the co-ordinates of the first set of equivalent points given above in the general expression for the geometrical structure factor and simplifying, the following expression for the structure factor is obtained :

$$\mathrm{S} = 2 \cos 2 \pi \mathrm{U} l \, (1 + e^{\pi i l}) \quad \ldots\ldots\ldots\ldots\ldots\ldots\ldots \quad (1)$$

From this equation, when l is odd, S is equal to zero, so that no reflections should be observed from any planes in which l is odd. Actually, with the exception of the halvings already mentioned, all planes reflect when l is odd. Consequently, this structure factor, and the set of equivalent points from which it is derived, cannot represent the positions of the diffracting centres in ice.

Substitution of the second set of equivalent points leads to the following expression for the geometrical structure factor :

$$\begin{aligned} \mathrm{S} = {} & e^{2\pi i \left(\frac{h+2k}{3}\right)} \{e^{2\pi i l \mathrm{U}} + e^{-2\pi i l \mathrm{U}} \,.\, e^{\pi i l}\} \\ & + e^{2\pi i \left(\frac{2h+k}{3}\right)} \{e^{-2\pi i l \mathrm{U}} + e^{2\pi i l \mathrm{U}} \,.\, e^{\pi i l}\} \qquad (2) \end{aligned}$$

Putting $h = k = m$, equation (2) becomes

$$\begin{aligned} \mathrm{S} & = e^{2\pi i m}\, 4 \cos 2\pi \mathrm{U} l \, (1 + e^{\pi i l}) \\ & = 0, \text{ when } l \text{ is odd,} \\ & = e^{2\pi i m}\, 8 \cos 2 \pi \mathrm{U} l, \text{ when } l \text{ is even.} \qquad (3) \end{aligned}$$

This agrees with the observation that $mm\overline{2m}l$ is halved when l is odd.

Equation (3) is a convenient form of (2) to use for the determination of the unknown parameter U, because reflections from all planes for which l is equal to 4 are missing.

---

* Wyckoff, "An Analytical Expression of the Results of the Theory of Space Groups," pp. 159 and 169 (1922).

Substituting $l = 4$, equation (3) becomes

$$S = e^{2\pi i m}\, 8 \cos 8\pi U.$$

Now, since S must be zero in this case

$$\cos 8\pi U = 0$$

since $e^{2\pi i m}$ has a finite value.

Hence $U = x/16$, where $x = 1, 3, 5, 7, 9, 11, 13$, or 15.

An examination of the structures arising for all these values of x shows that they reduce to two, because identical arrangements are obtained when x is equal to 1, 7, 9, or 15, and when x is equal to 3, 5, 11, or 13. Therefore, it is necessary only to decide between $x = 1$ and $x = 3$.

When $x = 1$ the distance between two centres such as ($\frac{1}{3}$, $\frac{2}{3}$, U) and ($\frac{1}{3}$, $\frac{2}{3}$, $\frac{1}{2}$ − U) is equal to $\frac{3}{8}\,c_0$ (2·78 Å), while for $x = 3$ it is equal to $\frac{1}{8}\,c_0$ (0·92 Å.). Now the diameter of an oxygen atom is of the order of 1·20 Å. and that of a divalent oxygen ion is about 2·64 Å.* Even if some uncertainty exists with respect to the accuracy of these values, it will be seen that, when $x = 3$, the resulting distance is too small, particularly since no addition for the hydrogen atoms has been made to the oxygen radii given.

It follows, therefore, that the value of the parameter U is $\frac{1}{16}$. The equivalent points of the diffracting centres in the unit cell of ice are thus

$$\tfrac{1}{3},\ \tfrac{2}{3},\ \tfrac{1}{16}\ ;\ \tfrac{1}{3},\ \tfrac{2}{3},\ \tfrac{7}{16}\ ;\ \tfrac{2}{3},\ \tfrac{1}{3},\ \tfrac{9}{16}\ ;\ \tfrac{2}{3},\ \tfrac{1}{3},\ -\tfrac{1}{16}.$$

This unit cell is shown in fig. 7. The spheres represent the positions of the diffracting centres at these equivalent points.

Substituting $\frac{1}{16}$ for U in equation (2), the structure factor becomes

$$S = 2i \sin \frac{\pi l}{8} \left\{ e^{2\pi i\left(\frac{h+2k}{3}\right)} - e^{2\pi i\left(\frac{2h+k}{3}\right)} \right\} \tag{4}$$

when l is odd, and

$$S = 2 \cos \frac{\pi l}{8} \left\{ e^{2\pi i\left(\frac{h+2k}{3}\right)} + e^{2\pi i\left(\frac{2h+k}{3}\right)} \right\}, \tag{5}$$

when l is even.

By the necessary substitutions it will be seen that these expressions agree with all the observed halvings.

Intensity Estimations.—The estimation of the intensities of the spots appearing on the a axis rotation photographs was made visually.

---

* See Glocker, Materialprüfung mit Röntgenstrahlen," p. 274 (1927).

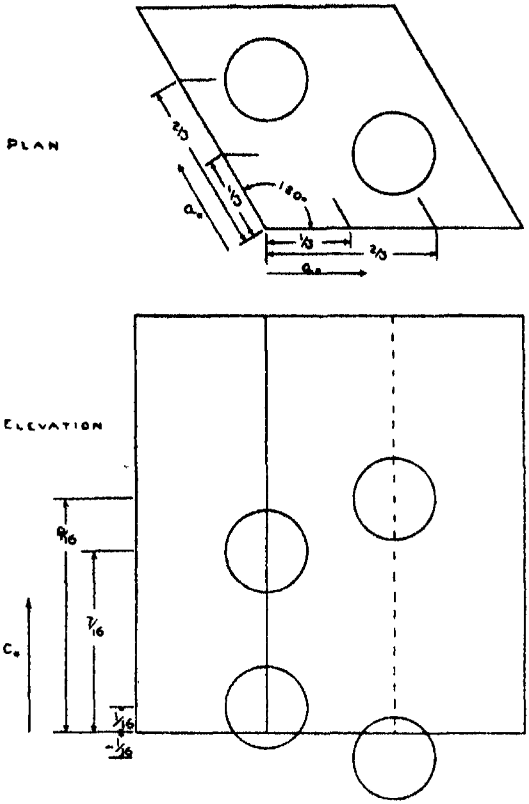

FIG. 7.

Assuming all the scattering to be due to the oxygen atoms (or ions), integrated intensities were calculated with the accepted expression

$$I \propto NS^2F^2 \frac{1 + \cos^2 2\theta}{\sin 2\theta} \frac{1}{D}, \tag{6}$$

where

I is the integrated intensity,

N is the number of planes co-operating to give a particular spot,

S is the geometrical structure factor calculated with expressions (4) and (5) above,

$1 + \cos^2 2\theta/\sin 2\theta$ is the polarisation and Lorentz factor,

θ is the glancing angle,

F is the variation of the scattering power with $\sin\theta$ calculated from Hartree's data* for the oxygen atom and for the divalent oxygen ion,

---

* 'Phil. Mag.,' vol. 50, p. 289 (1925).

D is a correction taking into account the obliquity of the diffracted rays to the film, and the obliquity of the various planes to the axis of rotation. Its values were obtained for the various spots from a chart prepared by Cox and Shaw* in this Laboratory.

Visual estimations of intensity do not represent the true integrated intensities for the following reason. Suppose a comparison to be made between two spots of the same uniform shade of grey but of different areas. On a visual estimation both spots would be given the same value (say, medium) whereas the integrated value for the one with larger area would be greater than that for the one of smaller area. For this reason calculated integrated intensities must be corrected for the relative areas of the spots to give values comparable with those estimated by eye.

On the films employed for intensity estimations the individual spots were of fairly uniform intensity and their areas were practically constant for any one layer line. The average area of spots on the various layer lines was found and expression (6) for the calculated intensities was multiplied by A_0/A_x, where A_0 is the average area of spots on the zero line, and A_x is the average area of spots on the xth layer line. The numerical values were 0·71 for the first layer line and 0·50 for the second layer line, taking the average area on the zero line as 1·00.

The estimated and calculated values for the intensities are set forth in Table II. The first column gives the indices of the planes producing the spots. Where two or more sets of indices are bracketed together it means that those planes give rise to spots which are not separable on the complete rotation films employed for the visual estimations. Column 2 gives the observed intensities while columns 3 and 4 show the values calculated, in 3 for scattering by divalent oxygen ions and in 4 by normal oxygen atoms. One or other of these forms of oxygen has to be assumed for the purpose of calculation. The columns of calculated intensities do not differ very much from one another and both agree well enough with the observed values to confirm the positions of the diffracting centres in the unit cell. The calculations for the ionic structure agree slightly better with observed intensities and reference to this will be made later.

A few points about some of the individual calculations for Table II should be noted.

In the first place all visual estimations were made before the calculations were commenced in order that there should be no unconscious bias affecting

---

* Unpublished results.

Table II.

Zero Line.

Plane.	I. (Observed.)	I. (Ionic, calculated).	I. (Atomic, calculated).
0002	Very strong	4920	3100
$01\bar{1}0$	Very strong	2780	1750
$01\bar{1}3$	Strong	2950	1800
$01\bar{1}1$	Strong	1960	1190
$01\bar{1}2$	Medium strong	1290	750
$02\bar{2}3$	Medium strong	888	568
$01\bar{1}5$	Medium	580	417
$02\bar{2}0$	Medium	475	298
0006 $03\bar{3}2$	Medium	377	291
$02\bar{2}1$	Medium	354	218
$03\bar{3}0$	Medium (minus)	340	251
$02\bar{2}5$ $01\bar{1}6$	Weak medium	288	264
$01\bar{1}8$ $03\bar{3}6$	Weak	63	115
0008 $02\bar{2}7$	Weak	57	99
$04\bar{4}3$	Weak	52	92
$04\bar{4}5$	Weak	41	100
$02\bar{2}6$	Very weak	23	25
$04\bar{4}0$ $04\bar{4}1$	Very weak	21	32
$01\bar{1}7$	Very weak	18	23
$02\bar{2}8$	Very very weak	16	37

First Layer Line.

Plane.	I. (Observed.)	I. (Ionic, calculated).	I. (Atomic, calculated).
$10\bar{1}0$	Very strong	8600	5320
$10\bar{1}3$	Very strong	5300	3080
$10\bar{1}1$	Very strong	4700	2860
$11\bar{2}2$	Strong	2900	1780
$11\bar{2}0$	Strong	2800	1680
$10\bar{1}2$	Strong	2500	1470
$10\bar{1}5$ $12\bar{3}2$	Medium strong	1085	770
$11\bar{2}6$ $13\bar{4}0$ $13\bar{4}1$	Weak medium	270	275
$12\bar{3}0$	Weak medium	260	166
$12\bar{3}5$ $13\bar{4}2$	Weak medium	234	252
$12\bar{3}1$	Weak medium	190	128
$13\bar{4}3$	Weak medium	140	192
$11\bar{2}8$ $12\bar{3}7$ $14\bar{5}0$	Medium weak	133	300
$13\bar{4}5$	Weak	123	256
$10\bar{1}6$	Weak	75	66
$14\bar{5}2$	Weak	62	146
$10\bar{1}8$	Weak	49	89
$10\bar{1}7$	Weak	28	33
$12\bar{3}6$	Very weak	21	33

Table II—(continued).

Second Layer Line.

Plane.	I. (Observed).	I. (Ionic, calculated).	I. (Atomic, calculated).
$20\bar{2}3$	Medium strong	1800	1170
$20\bar{2}0$	Medium strong	825	512
$20\bar{2}2$	Medium	750	460
$21\bar{3}3$	Medium	695	512
$20\bar{2}1$	Medium	550	347
$20\bar{2}5$	Medium	435	398
$21\bar{3}0$	Weak medium	290	188
$22\bar{4}0$	Weak medium	270	246
$20\bar{2}6$ $21\bar{3}5$	Weak medium	248	285
$21\bar{3}1$	Weak medium	230	150
$22\bar{4}2$	Weak medium	200	204
$21\bar{3}2$	Weak medium	195	135
$20\bar{2}8$ $22\bar{4}6$	Weak	68	159
$23\bar{5}3$	Weak	60	136
$21\bar{3}7$	Weak	5	11
$23\bar{5}0$ $23\bar{5}1$	Very weak	43	78
$21\bar{3}6$	Very weak	25	38
$23\bar{5}2$	Very weak	21	44
$20\bar{2}7$	Very weak	20	35

the intensity estimations of any of the spots. No alterations in the estimated values were made after the calculated values were obtained.

The values calculated for ($20\bar{2}0$) and ($20\bar{2}1$) were divided by 2 because these spots occurred in pairs on the film due to slight mis-setting of the crystal. The visual estimations were made on only one of each pair so that the number of co-operating planes was half that in the general expression. The values for ($21\bar{3}7$), ($23\bar{5}3$) and ($20\bar{2}8$) were divided by four (instead of by two) because their areas were about four times (instead of twice) the average of those on the zero line. These planes give rise to the last three spots on the second layer line.

An examination of Table II shows that the agreement between observed values and those calculated (particularly for an ionic lattice) is very satisfactory. Theoretically the lowest calculated value in any group of spots having the same visual designation should be higher than the highest value calculated for the next group in a lower category visually.

The only divergences from this rule for the ionic lattice are for ($01\bar{1}3$) and ($21\bar{3}7$). On the basis of calculated values, ($01\bar{1}3$) should be placed in the "very strong" group instead of "strong," and ($21\bar{3}7$) should be "very very weak" instead of "weak." These discrepancies are not serious because it is difficult to estimate grades of blackness close to the centre of the film [$(01\bar{1}3)$], and the estimation of relative areas becomes very uncertain at the end of the second layer line [$(21\bar{3}7)$].

For the atomic lattice the disagreement with the rule given above is rather more marked. On the basis of calculated values the following planes should be raised one group in the column of visual estimations : $(03\bar{3}0)$, $(02\bar{2}8)$, $(14\bar{5}0)$, $(12\bar{3}6)$, $(20\bar{2}8)$, (2350), while $(02\bar{2}5)$, $(13\bar{4}5)$, and $(14\bar{5}2)$ should be raised two. These anomalies are in addition to the two noted for the ionic lattice which are also present in the column of atomic values.

The reason for the difference between the two sets of calculations is to be found in the fact that the F-curve for atomic oxygen (8 electrons), is higher than that for the oxygen ion (10 electrons) for large values of $\sin \theta$, although it is lower of course by 2 units for $\sin \theta$ equal to zero.

Caution must be exercised in deciding between the atomic and ionic lattice because, although the agreement is somewhat better for the ionic, it must be remembered that two electrons from the hydrogen atoms in the atomic lattice have not been taken into consideration.

It is to be noted, however, that ice has a very small coefficient of expansion (0·00016) and an enormous energy of dissociation, both of which properties indicate a lattice exceptionally resistant to thermal and electrical influence.

Consequently the ionic type of lattice seems to be the more probable so far as the evidence goes.

Finally, regardless of whether the lattice is considered to be of an ionic or atomic type, the agreement between observed and calculated intensities completely establishes the positions for the diffracting centres given above.

The Complete Structure.—Having now determined the positions of the diffracting centres it becomes of interest to consider all possible arrangements of H_2O molecules about these centres in an attempt to find that which is most probable.

It has been shown above that the space group for ice is either D_{3h}^4 or D_{6h}^4, in the first of which the molecules must possess a three-fold axis of symmetry perpendicular to the (0001) plane, and in the second the molecules must in addition be given three symmetry planes parallel to $(11\bar{2}0)$ intersecting in the triad axis.

Considering each molecule of H_2O by itself there is only one general arrangement compatible with a triad axis in the molecule. The symmetry must be possessed by the oxygen atom (or ion) and the hydrogens must be placed on the three-fold symmetry axis. Six special cases satisfying these conditions are conceivable ; three in which the oxygen and hydrogen exist as atoms and three as ions.

The atomic arrangements, in addition to the evidence already quoted against them, are improbable with the dimensions found for the unit cell. Three cases can be considered. In one the hydrogen atoms are placed one above and one below the oxygen atoms. In the other two both hydrogens are placed above (or below) the oxygen atom. In the first case the unit cell would have to contain two hydrogen atoms on the axis through the points $(\frac{1}{3}, \frac{2}{3}, \frac{1}{16})$ and $(\frac{1}{3}, \frac{2}{3}, \frac{7}{16})$ and between these centres. Taking the diameter of the oxygen atom as about 1·20 Å. the distance available is about 1·58 Å. Now the radius of the (1, 1) orbit of the hydrogen atom is of the order of 0·54 Å,* so that a distance of about 2·16 Å. is necessary for this arrangement.

The other two cases require four hydrogen atoms to be placed between the oxygen atoms at $(\frac{1}{3}, \frac{2}{3}, \frac{1}{16})$ and $(\frac{1}{3}, \frac{2}{3}, \frac{7}{16})$ in one, and between the oxygen atoms at $(\frac{2}{3}, \frac{1}{3}, -\frac{1}{16})$ and $(\frac{2}{3}, \frac{1}{3}, \frac{9}{16})$ in the other. Following the same line of argument as before, the distance required in each case is 4·32 Å. and those available are respectively 1·58 Å. and 3·43 Å.

Three arrangements similar to those considered above are conceivable in an ionic lattice. In these cases, however, the space required by the hydrogen ions will be very much less, so that all three arrangements can be considered as possible. They are represented at A, B and C in fig. 8. The oxygen ions are represented by pyramids on equilateral bases in order to emphasise the three-fold symmetry and to distinguish between molecules pointing up and down in the cell. In A the protons are placed on opposite sides of the oxygen ions, while B and C represent the two possible ways of placing them on the same side of the oxygen ions. The dotted ellipses localise the individual H_2O units.

An inspection of these three diagrams shows that not one of them is very probable. As already indicated the most likely arrangement of the hydrogens and oxygens in ice will be that which is the most symmetrical and electrically balanced. From the point of view of electrostatic forces alone the H_2O units shown at A, B and C in fig. 8 are not in equilibrium with one another.

There remains one other way of considering the relative arrangement of hydrogen and oxygen atoms (or ions). It is shown at D in fig. 8, and is reached by considering the symmetry of each oxygen atom in relation to those by which it is surrounded.

An examination of the structure arising from the placement of oxygen atoms at the equivalent points proposed for ice shows that each is surrounded by four others situated at the points of a regular tetrahedron around the first

---

* Andrade, " The Structure of the Atom," p. 194 (1927).

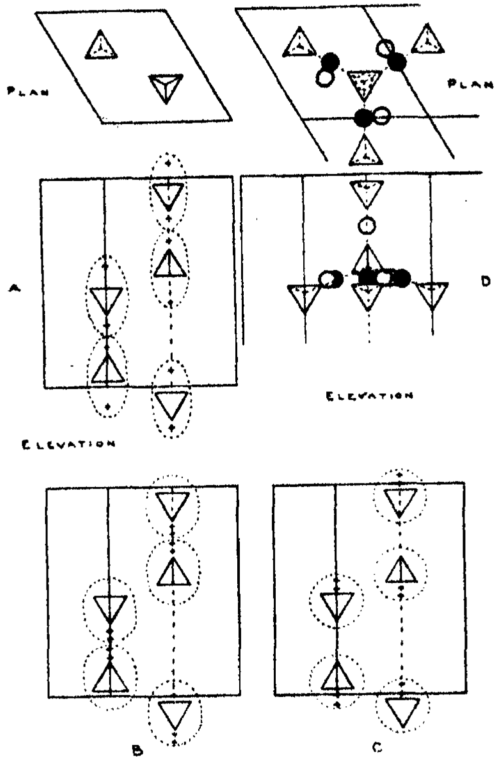

Fig. 8.

as centre. A three-fold axis of symmetry perpendicular to the (0001) plane thus passes through each oxygen atom. Now if hydrogens are placed symmetrically between the oxygen atoms, one of the former between each pair of the latter, this symmetry can still be maintained. There will also be twice as many hydrogens as oxygens in the structure, which, of course, is a necessary condition.

At D in fig. 8 two cases are considered in which the positions of the hydrogens are indicated by black and white spheres respectively. The hydrogen placed on the triad axis through the oxygen atom must be common to each arrangement in order not to upset the three-fold symmetry. The three black spheres represent the positions of hydrogens on the lines joining the oxygen centres. This arrangement introduces three symmetry planes parallel to $(11\bar{2}0)$ intersecting in the triad axis. This is the molecular symmetry required by space group D_{6h}^4. If the hydrogens are displaced to the positions occupied by the white spheres these planes of symmetry are lost, but the arrangement still has a three-fold axis of symmetry perpendicular to the (0001) plane. This is the molecular symmetry required by space group D_{3h}^4.

There is sufficient space in both of these structures for either an ionic or atomic arrangement. In neither case is there any reason for moving the hydrogens off the lines joining the oxygen centres. This latter is obviously the more symmetrical and probable arrangement. The arguments in favour of an ionic structure have already been given.

From this it follows that ice belongs to one of the space groups D_{3h}^4 or D_{6h}^4; that D_{6h}^4 is the more probable with one hydrogen placed on the line joining each pair of oxygen centres and half-way between them ; and that the structure probably is ionic in nature.

The complete structure is shown in fig. 9. Eight unit cells are represented, the boundaries of one being indicated by A, B, C, D, E, F, G, H, and its four molecules by 1, 2, 3, 4. The oxygen ions are represented by the tetrahedra,

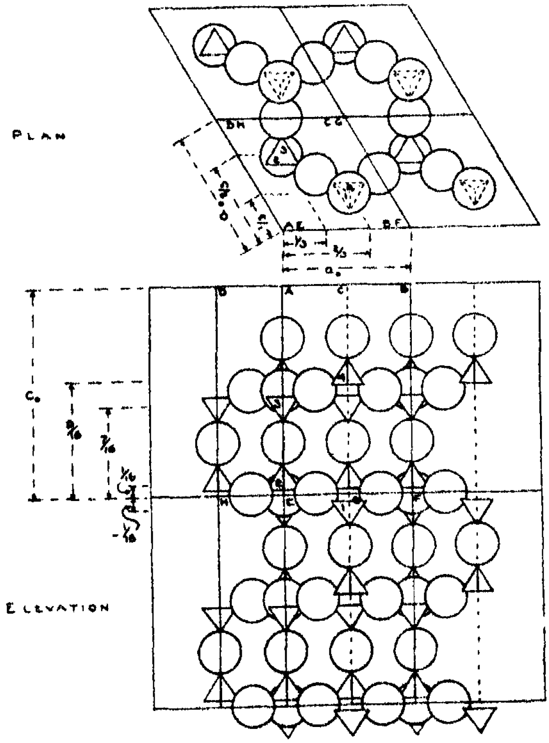

FIG. 9.

while the protons are placed at the centres of the spheres. Tetrahedra are employed to emphasise the molecular symmetry required by space group $D_{6h}{}^4$, and the difference between molecules pointing up and those pointing down in the cell. The dimensions of the tetrahedra are not to scale. If the oxygen ions are given a diameter of 2·64 Å. a drawing of the structure of ice is too confusing and a three-dimensional model is necessary to show the structure.

IV. *Part II.—Powder Photographs of Ice at Temperatures between 0° C. and —183° C.*

Apparatus.—The powder camera employed for these measurements is shown in fig. 10. Briefly the method used was as follows. Methylated spirits from a constant temperature bath were allowed to flow continuously through a thin-walled copper tube passing through the centre of the camera. A very uniform layer of frost grew on the outside of this tube. The frost layer was kept at a uniform thickness of about 1·5 mm. by means of a sharp edge. The tube was rotated continuously during exposure and, by previous adjustment, the frost on one side of the tube coincided with the axis of the camera. Powder lines were thus obtained on one half of the circular film. The camera was then moved to a second, previously determined and fixed, position in which the other side of the frost covered tube was in the X-ray beam. The powder lines were thus obtained on the other half of the film.

For temperatures between 0° C. and —78·5° C the constant temperature reservoir consisted of a transparent Dewar flask constructed with a glass spiral tube connecting the inner with the outer wall in such a way as to allow the liquid to pass out of the bottom of the flask. A nozzle making a loose fit in the top of the copper tube connected the reservoir with the powder spectrograph. The temperature in the reservoir was kept constant to 2° or 3° C. by regulating the flow into it of two streams of methylated spirits, one at room temperature and the other after passing through a mush of solid carbon dioxide and methylated spirits.

A temperature of about — 78° C. was obtained by passing methylated spirits through the tube in the camera directly after passing through a worm packed in solid carbon dioxide and methylated spirits.

Because of the increasing uncertainty about the temperature of the frost sample with decreasing temperature, the photograph at liquid air temperature (— 183° C.) was taken kindly by Dr. Müller in a special camera of his own. Distilled water in a small glass capillary was frozen by immersion in liquid air. The tube was rotated continuously during exposure to X-rays and was kept

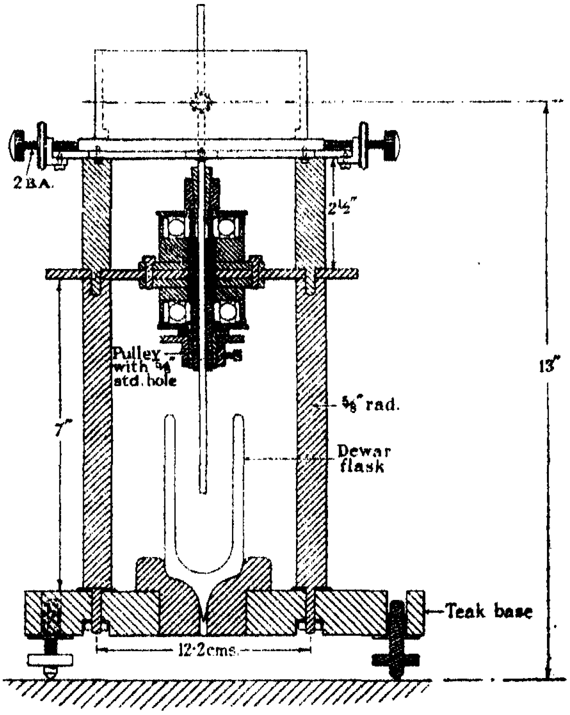

Part Sectional Elevation

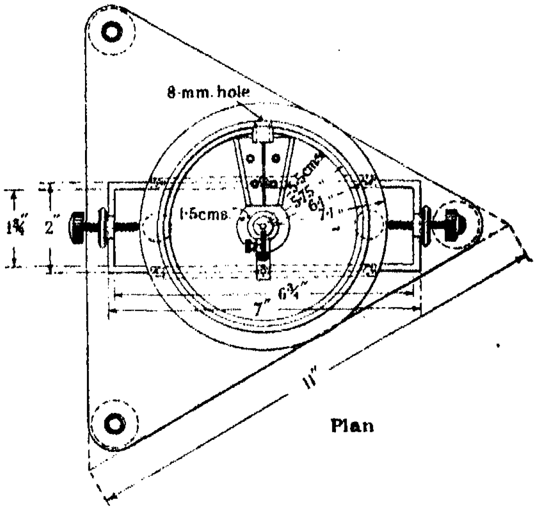

Plan

Fig. 10.

at the desired temperature by allowing a constant drip of liquid air to fall on it.

All the photographs were taken with a copper anticathode in the X-ray tube. The K_β line was removed from the radiation by a filter of nickel foil.

Results.—Photographs were taken with the sample at about − 9° C., − 13° C., − 78° C., and − 183° C. The one at liquid air temperature is shown in fig. 11 (Plate 12). The others are identical with it and the structure is the same as that found in the single crystal study at − 20° C. described in IV. Part I above.

The spacings giving rise to the lines on the photograph at − 183° C. were calculated and compared with those for a cell of dimensions: $a_0 = 4\cdot466$ Å., $c_0 = 7\cdot293$ Å. ($c : a = 1\cdot633$). The agreement for those planes involving a measurement of about 3 cms. on the film is better than 1 per cent., while for those involving measurements of more than 6 cms. the agreement is to within 2 or 3 parts in 1,000. The reason for selecting these cell dimensions will be brought out in the Discussion later.

V. *Discussion.*

A check on the dimensions found for the unit cell of ice in the single crystal studies described in Section IV, Part I, is afforded by calculating ideal values at various temperatures. This was done by assuming four molecules per cell and taking the density of ice at 0° C. as 0·9168 and the coefficient of cubical expansion as 0·00016. The value for the ratio $c : a$ (1·633) was assumed to be correct. The largest source of error in the measurements is the radius of the circular camera. But an error in this factor would introduce an error of the same relative magnitude into the values of both c_0 and a_0 so that the $c : a$ ratio is not affected by the accuracy with which the radius is known.

Values for the cell dimensions calculated on this basis are shown in Table III.

Table III.

Temperature (° C.).	a_0 (Å.).	c_0 (Å.).
0	4·51	7·36
−20	4·50	7·355
−183	4·466	7·293

The values at − 20° C. ($a_0 = 4\cdot50$; $c_0 = 7\cdot355$) agree with those found from the single crystal rotation photographs ($a_0 = 4\cdot53_5$; $c_0 = 7\cdot41$) to better than 1 per cent. This is about the accuracy with which the camera radius was determined.

That these ideal values are very near the truth is shown by the very good agreement obtained between spacings observed for the lines on the powder photograph at − 183° C. and those calculated with the dimensions of the unit cell at this temperature given in Table III. (See Section IV, Part II.) This indicates that the discrepancy between the values found at − 20° C. and those of Table III at this temperature is to be found in the value for the camera radius. Confirmation is obtained from the fact that although the powder photographs at − 9, − 13, and − 78° C. and at − 183° C. were taken on two different spectrographs, values of 2θ show very good agreement, whereas both sets are from 1 to 2 per cent. higher than those calculated for the corresponding spots on the single crystal rotation photographs.

Because of the danger of inadvertently employing twinned crystals a few remarks about the ice specimens should be made. An examination of the individual prisms from which the rotation photographs were obtained showed that, in large specimens containing small ellipsoidal cavities in their interior, the general shape and orientation of these cavities was always the same for any one specimen. Examination of individual prisms in polarised light showed no evidence of the presence of more than one crystal.

That the samples of natural ice used for the Laue photographs were single crystallographic units is shown by the fact that rotation photographs about the *a* axis, obtained with the same specimens from which the Laue pictures were obtained, are identical with those furnished by the prisms of commercial ice. This evidence is borne out by the fact that the symmetry of the Laue photographs is the same as that found by Rinne.

The series of powder photographs at various temperatures described in Section IV, Part II, shows that the structure of ice does not change between 0° C. and − 183° C. Consequently although the Laue photographs were taken of specimens at − 78·5° C. the symmetry is the same as that at − 20° C., the temperature at which the rotation photographs were made.

The structure for ice proposed in this paper is practically identical with those of Dennison and Sir William Bragg. If the corner of the latter's unit cell be moved from the point (0, 0, 0) in his complete structure to the point ($\frac{2}{3}$, $\frac{1}{3}$, $\frac{9}{16}$) the resulting cell is the same as that found in the present investigation.

Rinne's deduction of the symmetry as dihexagonal pyramidal depends on Nordenskiold's crystallographic data, which are meagre and uncertain. The structure proposed by Gross is based probably on insufficient data, and that due to Aminoff is dependent on that of Gross. It is more difficult to reconcile the dimensions of St. John with those found in the present work. The experimental work of St. John was carried out with great care, and since the publication of Dennison's values, he has remeasured his plates and found no reason for altering the dimensions given in his paper. The powder photographs described in the present paper were undertaken with a view to testing the structure at about -15° C. (St. John) and -183° C. (Dennison) because of the possibility that the two investigators worked with different modifications of ice. Although no change in structure has been found between 0° C. and -183° C. the mass of conflicting crystallographic data in the literature on ice makes it possible that different modifications may exist under slightly different conditions. Otherwise no explanation can be offered for the dimensions found by St. John.

Since the divalent oxygen ion has the same number of electrons as neon, their electronic configurations probably are similar. The structure of neon is given schematically by Main Smith as (2,224). It is possible that the tetrahedral nature of the symmetry exhibited by the oxygen ions in the structure for ice proposed in this paper is due to the arrangement of the four (2, 2) orbits about the nucleus.

VI. *Acknowledgments.*

Grateful acknowledgment is made to the National Research Council of Canada and to the Ramsay Memorial Fellowship Trust for the award of the Canadian Ramsay Memorial Fellowship for 1927–28 and 1928–29, which made possible the research described in this paper.

The writer takes this opportunity also of expressing his thanks to the Managers of the Royal Institution for permission to carry out this work in the Davy Faraday Research Laboratory; to Sir William Bragg for his interest and encouragement; to Dr. A. Müller, Dr. I. E. Knaggs, and Mr. E. G. Cox for much valuable assistance; and to Dr. Ancel St. John for his courtesy in allowing the writer to spend a week in his laboratory in New York discussing this problem and making use of his files before sailing for England in 1927.

Finally, this paper on ice would be incomplete without an expression of appreciation to Prof. H. T. Barnes for the inspiration derived from an uninterrupted correspondence containing much prized encouragement and interest in a problem so closely associated with his own work.

---

[*] "Chemistry and Atomic Structure," p. 196 (1924).

VII. *Summary.*

1. An investigation of the structure of ice by means of X-rays and single crystals is described.

2. Brief literature surveys of data on the crystal structure and crystallography of ice are included.

3. The types of apparatus, and crystals employed, are indicated.

4. The interpretation of Laue photographs, single crystal rotation photographs about the principal crystallographic axes, and oscillation photographs, is carried out.

5. The space group is found to be D_{6h}^4 (dihexagonal bipyramidal) or D_{3h}^4 (ditrigonal bipyramidal) with the probability in favour of the former.

6. The dimensions of the unit cell are found to be $a_0 = 4 \cdot 53_5$ Å., $c_0 = 7 \cdot 41$ Å., $c : a = 1 \cdot 634$.

7. The number of molecules per unit cell is four.

8. The geometrical structure factor for two sets of possible equivalent points is given, and one set is shown to be incompatible with observed halvings.

9. The equivalent points for the diffracting centres in the unit cell are found to be $\frac{1}{3}, \frac{2}{3}, \frac{1}{16}$; $\frac{1}{3}, \frac{2}{3}, \frac{7}{16}$; $\frac{2}{3}, \frac{1}{3}, \frac{9}{16}$; $\frac{2}{3}, \frac{1}{3} - \frac{1}{16}$.

10. Intensity calculations for the proposed structure are shown to agree with visually estimated intensities.

11. The placing of the hydrogen atoms is discussed.

12. Arguments in favour of an ionic lattice are put forward.

13. A complete structure for ice is proposed.

14. The accuracy of the cell dimensions is indicated.

15. A series of powder photographs are shown to prove that no change in the structure of ice takes place between 0° C. and — 183° C.

The Behaviour of Electrolytes in Mixed Solvents. Part I.—The Free Energies and Heat Contents of Hydrogen Chloride in Water—Ethyl Alcohol Solutions.

By J. A. V. Butler, D.Sc., and C. M. Robertson, Ph.D., University of Edinburgh.

(Communicated by J. Kendall, F.R.S.—Received July 2, 1929.)

Introduction.

Previous studies on the effect of a change of medium on the properties of dissolved electrolytes have aimed at correlating the behaviour of the electrolyte with the mean physical properties, *e.g.*, dielectric constants, of the medium. While this approach may be justified in the case of solvents containing molecules of only one kind, it is not sufficient to regard a mixed solvent as a uniform medium affecting the dissolved ions solely through the effect of its dielectric constant on the electric forces between them. For the electric fields of ions exert a differential attraction on molecules possessing different degrees of polarisability and since the more polarisable molecules must tend to congregate round the ions, the properties of the latter cannot depend solely on the mean properties of the medium. Studies on the behaviour of ions in such cases will throw light on the interaction between ions and solvent molecules.

The present paper gives the results of measurements of the free energies and heat contents of hydrogen chloride in water-alcohol solutions, obtained by determining the electromotive forces of cells of the type :—

$$H_2\,(g) \;\Big|\; \underset{\text{water-alcohol}}{HCl\,(m), \qquad AgCl\,(s)} \;\Big|\; Ag$$

The free energy change in the cell reaction :

$$\tfrac{1}{2}H_2\,(g) + AgCl\,(s) = HCl\,(m) + Ag$$

is given by

$$\Delta F = -\,EF = -\,23{,}074\ E \text{ calories}, \tag{1}$$

where E is the electromotive force, and F the electrochemical equivalent. Knowing the temperature coefficient of E, the heat content change in the reaction can be found by the use of the Gibbs-Helmholtz equation :

$$\Delta H = -\,EF + FT\,(dE/dT). \tag{2}$$

The electromotive forces of this cell were therefore determined at 15°, 25° and 35°, using a series of solvents containing 25, 50, 75, 95 and 100 mols. per cent. alcohol, and in each solvent a series of hydrogen chloride concentrations up to $m = 1$.*

The free energy of transfer of hydrogen chloride from a solution (1) to a solution (2) is given by

$$\Delta F_{(1)\rightarrow(2)} = -(E_2 - E_1) F. \tag{3}$$

We can thus obtain the free energies of transfer of hydrogen chloride—

(1) in a given solvent from one concentration to another,

(2) at a given concentration from one solvent to another,

and, making use of the temperature coefficients, the corresponding changes in heat content.

In ideal completely dissociated solutions the free energy of transfer of a mol. of a binary electrolyte from a concentration m_1 to a concentration m_2 in a given solvent is given by

$$\Delta F_{m_1 \rightarrow m_2} = -(E_2 - E_1) F = 2RT \log m_2/m_1.$$

In actual solutions these free energy changes are expressed in terms of the activities as determined by the equation:

$$\Delta F_{m_1 \rightarrow m_2} = -(E_2 - E_1) F = 2RT \log a_2/a_1, \tag{4}$$

the values being defined by the condition that $a_1 = m_1$ in the limit, at very small concentrations.

If E_0 is the value of E_1 when $a_1 = 1$ (*i.e.*, in a solution of unit activity) we have

$$E_0 = E_2 + 2RT/F \log a_2, \tag{5}$$

and if we define E_0' by

$$E_0' = E_2 + 2RT/F \log m_2, \tag{6}$$

it is evident that E_0' becomes equal to E_0 when $a_2 = m_2$, *i.e.*, at very small concentrations.

The value of E_0 is thus obtained by determining from the experimental data the values of E_0' and extrapolating to zero concentration. The manner in which the extrapolation was carried out is described at a later stage.

The mean activity coefficients are defined by the equation $a_2 = \gamma_2 m_2$, so that by (5):

$$2RT/F \,.\, \log \gamma_2 = E_0 - (E_2 + 2RT/F \,.\, \log m_2)$$

or

$$\log \gamma_2 = F(E_0 - E_0')/2RT. \tag{7}$$

---

* In this paper m is the number of gram-molecules of hydrogen chloride in 1000 grams of the solvent.

EXPERIMENTAL.

1. *Preparation of Materials and Electrodes.*

Alcohol.—Commercial absolute alcohol was allowed to stand for a week over freshly burnt quicklime in 4-litre flasks, which were shaken every day.* The alcohol was then refluxed on a water bath for 8 hours and then slowly fractionated, the middle portion being collected separately. The corks used were covered with tin foil to protect them from alcohol vapour. The distillate was protected from water vapour by calcium chloride tubes and was stored in amber-coloured winchesters.

The product had a density $D_4^{25} = 0\cdot78496$, and refractive index $n_D^{20} = 1\cdot36145$.

Hydrogen Chloride and Solutions.—Concentrated "A.R." hydrochloric acid was diluted with distilled water to specific gravity 1·10 and distilled from a Pyrex flask having a ground glass stopper. The side tube was plugged into a condenser with glass wool, no corks being used, and the constant boiling acid was collected in a resistance glass bottle. The composition of the distillate, determined by precipitation as silver chloride, was within 0·1 per cent. of that given by Hulett and Bonner.†

The weaker alcoholic solutions were prepared by diluting the weighed amount of the constant boiling acid with the calculated amounts of water and alcohol. The more concentrated solutions were prepared by passing dry hydrogen chloride gas into the solvent.

Hydrogen chloride was prepared by the action of pure concentrated sulphuric acid on pure dry sodium chloride. The gas was passed through a wash-bottle containing concentrated sulphuric acid, then through a tube a metre long containing phosphorus pentoxide and finally through a tube tightly packed with glass wool to remove any particles of phosphorus pentoxide which might possibly have been carried over. The gas was passed into the solvent which was kept cold in an ice bath to retard esterification and protected from atmospheric moisture by calcium chloride tubes.

Since, as Kailan‡ has shown, this solution is not stable, owing to the slow formation of ethyl chloride and water, alcoholic solutions were used immediately after preparation and a fresh solution prepared for each experiment.

Hydrogen.—Hydrogen was prepared from pure "AsT" zinc and hydrochloric acid (1 : 3) in a generator of the type designed by T. W. Richards.* The gas was passed through three towers, each 50 cms. high, containing glass pearls moistened with a saturated solution of sodium hydroxide, and finally through a tube containing phosphorus pentoxide before being admitted into the bubbler.

---

* Danner, 'J. Amer. Chem. Soc.,' vol. 44, p. 2832 (1922).

† 'J. Amer. Chem. Soc.,' vol. 31, p. 390 (1909).

‡ 'Monatschr.,' vol. 28, p. 559 (1907).

Silver-silver Chloride Electrodes.—Silver chloride electrodes prepared by the method of McInnes and Parker† were found to give values lower than the accepted values in aqueous solutions by about a millivolt, and different batches prepared at different times gave discordant values, differing at the most by 1 millivolt. Accordingly the method of Lewis‡ and Noyes and Ellis§ was adopted.

The platinum gauze electrodes (5 × 15 mms.) were plated with silver in a silver cyanide solution (1 gram $AgNO_3$, 2 grams KCN and 100 c.c. water) for 4 hours, using a current of 6 milliamperes per electrode. They were then washed and allowed to stand in water overnight, after which they were coated with a stiff paste of precipitated and washed silver hydroxide and dried in an oven at 150°. The coated electrodes were then heated in an electric oven for 6 hours at 450°, whereby the brown silver oxide was converted into shining white, finely divided metallic silver. Silver chloride was deposited on this by electrolysing in 0·1 *m* hydrochloric acid for 5 hours, using 4 milliamperes per electrode. Electrodes prepared in this way showed agreement within 0·1 millivolts, and remained constant for several days at least. In one case a batch of electrodes remained constant for 2 months.

While this investigation was in progress Randall and Young‖ published an exhaustive research on the reproducibility of silver-silver chloride electrodes, in which they state conclusions which agree with our own experience, namely, that the McInnes type of electrode is unreliable, while the Noyes type can be readily reproduced.

Hydrogen Electrodes.—These consisted of platinum foil (5 × 15 mms.), cleaned by immersion in boiling concentrated hydrochloric acid. Platinum black was deposited by electrolysing in a solution of pure chloroplatinic acid containing 1·3 per cent. platinum, using an auxiliary platinum electrode as anode. The electrodes were rotated for 1 minute, during which a thin deposit was formed, just sufficient to hide the glint of platinum underneath. They were then washed with water and made the cathode for 2 minutes in 0·1 *m* hydrochloric acid. After washing thoroughly with water they were transferred to a corked test-tube containing the same solution as that in which they were to be used. Electrodes prepared in this way could be reproduced without any trouble.

---

* 'Carnegie Inst. Publ.,' no. 56, p. 19 (1906).

† 'J. Amer. Chem. Soc.,' vol. 37, p. 1445 (1915).

‡ 'J. Amer. Chem. Soc.,' vol. 28, p. 166 (1906).

§ 'J. Amer. Chem. Soc.,' vol. 39, p. 2532 (1917).

‖ 'J. Amer. Chem. Soc.,' vol. 50, p. 989 (1928).

2. *Apparatus and Procedure.*

The hydrogen saturator and experimental cell employed are shown in fig. 1. The saturator, S, consisted of a straight tube about 35 cms. long, slightly inclined, containing a solution of the same composition as that in the cell. Its capacity was about 140 c.c. and the change in composition caused by the passage of hydrogen in an experiment was negligible. The experimental cell consisted of two tubes, A and B, containing the hydrogen electrodes and the silver chloride electrodes respectively, connected by a wide tube C. The hydrogen entered at H. The object of this design was to prevent the diffusion of hydrogen into the vicinity of the silver chloride electrodes, since it was found that, in the more concentrated solutions, it was impossible to obtain steady electromotive forces when this was allowed to take place.

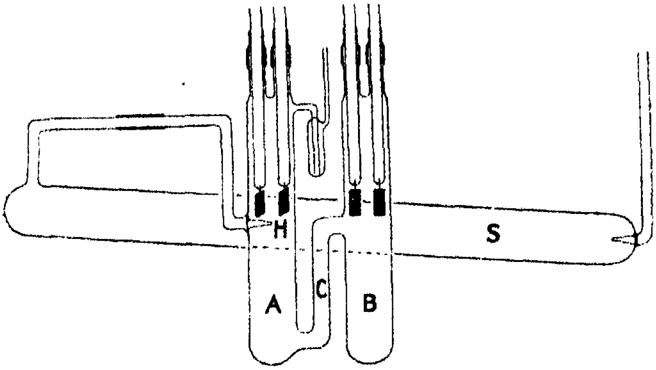

Fig. 1.—Electrode Vessel and Saturator.

In setting up a cell, freshly prepared electrodes were washed three times in stoppered test-tubes with the solution to be used, allowing them to stand in the solution for half-an-hour each time. The cell and saturator were then filled with the solution as quickly as possible, and the electrodes transferred to the cell and fixed in position by short lengths of rubber tubing. The cell was placed in the thermostat at 15° and a vigorous stream of hydrogen passed for 30 minutes. The stream was then reduced to a few bubbles per minute and left on over-night. In the morning the flow of hydrogen was readjusted and measurements taken every 30 minutes until they remained constant to about 0·00005 volts for an hour. The temperature was then raised to 25° and measurements continued. When the electromotive force had remained constant for an hour the temperature was raised to 35° and the procedure repeated.

The electromotive forces were measured by means of a Tinsley Vernier potentiometer reading directly to 0·01 millivolt. The standard Weston cell used for calibrating the instrument was also made by Tinsley and had been recently standardised by the National Physical Laboratory. Precautions were taken to avoid thermoelectric effects and also to avoid stray currents from the thermostat heating circuits by earthing the thermostat.

The thermostat was electrically heated and controlled, and the temperatures remained constant to ± 0·01°.

3. *Experimental Data.*

The following table gives the actual electromotive forces determined in one experiment. The silver electrode forms the positive pole of the cell.

Table I.

Cell :—

H_2 | 0·30 *m* HCl in 50 mol. per cent. alcohol AgCl (*s*) | Ag

Barometer, 760·5 mms. E.M.F.'s in volts.

Temperature.	Time from first reading.	Electrodes.			
		1—3.	1—4.	2—3.	2—4.
	hours.				
15°	0	0·26105	0·26101	0·26092	0·26090
	½	0·26129	0·26127	0·26121	0·26118
	1	0·26136	0·26134	0·26129	0·26127
	1½	0·26145	0·26143	0·26137	0·26135
	2	0·26145	0·26145	0·26137	0·26135
	2½	0·26144	0·26142	0·26136	0·26134
25°	3	0·25384	0·25382	0·25378	0·25374
	3½	0·25409	0·25404	0·25404	0·25402
	4	0·25411	0·25406	0·25406	0·25404
	4½	0·25411	0·25407	0·25407	0·25404
	5	0·25417	0·25413	0·25413	0·25408
	5½	0·25418	0·25414	0·25410	0·25406
35°	6	0·24566	0·24560	0·24560	0·24550
	6½	0·24569	0·24568	0·24565	0·24561
	7	0·24571	0·24569	0·24577	0·24573
	7½	0·24574	0·24574	0·24570	0·24568

The mean of the final measurements at each temperature were taken and corrected to a standard hydrogen pressure of 760 mm. by means of the equation

$$\Delta E = \frac{RT}{2F} \log \frac{760}{P'},$$

where $P' = P - p'$, P being the mean atmospheric pressure during the course of the experiment and p' the total vapour pressure of the solution. The following vapour pressures of water-alcohol mixtures, obtained by graphic interpolation from the data in the Landolt-Börnstein Tabellen, were employed in making this correction.

Table II.—Vapour Pressures of Alcohol-water Mixtures in mms. Hg.

Mols. per cent. alcohol.	0.	25.	50.	75.	95.	100.
15°	12·8	26·2	28·2	32·0	34·2	34·5
25°	23·7	48·6	51·3	57·6	59·8	60·2
35°	42·0	85·7	91·2	99·3	101·7	104·2

Two series of measurements were obtained with 0·01 *m* and 0·1 *m* solutions in the whole series of solvents. In water-alcohol solutions the differences were within 0·4 millivolts but in absolute alcohol agreement was not so good, the two cells differed 0·6 millivolts in 0·1 *m* and 1·0 millivolt in 0·01 *m* solutions. In these cases the mean of the two final figures are given. The corrected final values of the electromotive forces in the whole series are given in Table III.

Measurements of this cell have been made by Harned and Fleysher* at 25° for the two concentrations 0·01 and 0·1*m* in solvents containing 0, 25, 50, 75 and 100 mols. per cent. alcohol, also in the 50 mols. per cent. alcohol from 0·001 to 2·5 *m* and in absolute alcohol from 0·001 to 3·62 *m*. Our determinations are in good agreement with Harned and Fleysher's in water-alcohol solutions but differ considerably from their measurements in absolute alcohol. While their results agree with ours in this solvent at 1·0 *m*, they are higher by 8 millivolts at 0·1 *m* and 17 millivolts at 0·01 *m*. Since the presence of water raises the electromotive force in dilute solutions, it is probable that their absolute alcohol was not sufficiently dry.

---

* 'J. Amer. Chem. Soc.,' vol. 47, p. 82 (1925).

Table III.—Electromotive forces in volts of the cell $H_2 \mid \underset{m}{\text{HCl}}, \text{AgCl} \mid \text{Ag}$.

m.	15°.	25°.	35°.	$dE/dT \times 10^6$ at 25°.
25 mols. per cent. alcohol.				
0·01	0·4358	0·4361	0·4356	−1
0·025	0·3935	0·3927	0·3910	−125
0·05	0·3627	0·3606	0·3583	−220
0·1	0·3306	0·3281	0·3246	−300
0·15	0·3135	0·3105	0·3065	−350
0·3	0·2818	0·2778	0·2730	−440
0·6	0·2479	0·2431	0·2375	−520
1·0	0·2195	0·2141	0·2080	−575
50 mols. per cent. alcohol.				
0·01	0·4065	0·4033	0·3991	−370
0·05	0·3386	0·3331	0·3268	−590
0·1	0·3091	0·3034	0·2967	−620
0·3	0·2619	0·2550	0·2473	−730
0·6	0·2285	0·2209	0·2128	−785
1·0	0·2006	0·1926	0·1841	−825
75 mols. per cent. alcohol.				
0·01	0·3627	0·3563	0·3489	−690
0·05	0·2983	0·2902	0·2816	−835
0·1	0·2704	0·2622	0·2531	−865
0·3	0·2248	0·2156	0·2060	−940
0·6	0·1921	0·1825	0·1724	−985
1·0	0·1624	0·1524	0·1422	−1010
95 mols. per cent. alcohol.				
0·01	0·2835	0·2752	0·2660	−875
0·05	0·2212	0·2119	0·2020	−960
0·1	0·1932	0·1839	0·1739	−965
0·3	0·1468	0·1374	0·1278	−950
0·6	0·1098	0·1013	0·0924	−870
1·0	0·0763	0·0691	0·0617	−730
100 mols. per cent. alcohol.				
0·01	0·1982	0·1938	0·1888	−470
0·025	0·1672	0·1621	0·1566	−530
0·05	0·1445	0·1390	0·1331	−570
0·1	0·1197	0·1144	0·1087	−550
0·3	0·0859	0·0806	0·0749	−550
0·6	0·0646	0·0591	0·0534	−560
1·0	0·0465	0·0405	0·0344	−605

While this investigation was in progress Woolcock and Hartley* measured the same cell at 25° from 0·0003 *m* to 1·2 *m* in absolute alcohol only. Their results were also lower than Harned and Fleysher's and they concluded that the alcohol used by the latter contained traces of moisture. Our results agree with Woolcock and Hartley's at 0·01 *m* and 1·0 *m* but between these limits are about 3 millivolts higher.

---

* 'Phil. Mag.,' vol. 5, p. 1133 (1928).

Calculation of Derived Quantities.

1. *Values of* E_0.—According to (6) E_0 is the value of E_0' when $m = 0$. Lewis and Randall* recommend plotting E_0' against $\sqrt{m}$ and extrapolating graphically to zero concentration. In order to make use of this method it is desirable to have electromotive forces at low values of *m*, and these values are necessarily much more subject to experimental error than those at higher concentrations. Since the difficulty of working with low concentrations is greater in alcoholic than in aqueous solutions, we have adopted a method, which is a development of that recently given by D. I. Hitchcock,† which enables the extrapolation from higher concentrations to be performed with more confidence. From (7) we have

$$E_0' = E_0 - \frac{2RT}{F} \log \gamma,$$

where γ is the activity coefficient corresponding to E_0'. Now it is generally recognised that the variation of $\log \gamma$ with the concentration can be approximately represented by an equation containing two terms, one proportional to $\sqrt{m}$, the other to *m*. Thus if

$$\log \gamma = -a\sqrt{m} + bm$$

we may put

$$E_0' = A\sqrt{m} - Bm + E_0, \tag{8}$$

where $A = \frac{2RT}{F} a$ and $B = \frac{2RT}{F} b$.

With aqueous solutions Hitchcock employed a second derived quantity

$$E_0'' = E_0' - A\sqrt{m},$$

making use of the theoretical value of A, as given by the Debye-Hückel theory. If equation (8) holds, E_0'' should vary practically linearly with *m*, and the extrapolation to zero concentration is easily performed. With alcoholic solutions we are first faced with the difficulty that no theoretical values of A are available. We accordingly made use of our data to obtain the most plausible values of the constants A and B, by the solution of simultaneous equations of the type (8) in which the experimental values of E_0' at the different values of m were inserted. In order to obtain the most plausible values, making use of all our measurements, Legendre's method of least squares was employed.*

---

* 'Thermodynamics," p. 334 (1923).

† 'J. Amer. Chem. Soc.,' vol. 50, p. 2076 (1929).

While equation (8), with the constants so obtained, was capable of reproducing the values of E_0' within the experimental error, in solutions containing more than 50 mols. per cent. of water, in the more alcoholic solutions there were considerable deviations and it became evident that a simple equation of the type (8) was incapable of giving the course of the curve with sufficient precision. Accordingly the values of $E_0'' = E_0' - A\sqrt{m}$, obtained by making use of the "most plausible values" of A, were plotted against m and the nearly linear curve obtained was directly extrapolated to $m = 0$ (fig. 2).

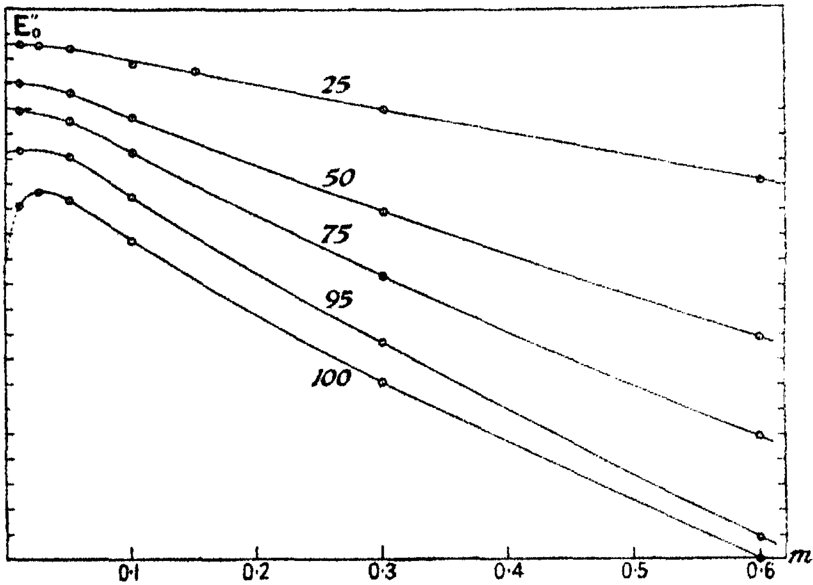

FIG. 2.—Extrapolation of E_0'' at 25° to infinite Dilution.
(Vertical Scale, 1 division = 0·005 volt.)

In pure alcohol this procedure was also inadequate, since the curve for E_0'' deviates widely from linearity at small concentrations. We were therefore forced to make a direct extrapolation of E_0' in this case. Our values of E_0' at 25° can be directly extrapolated to the value which Hartley and Woolcock (*loc. cit.*) obtained, and since they obtained a much greater number of readings at low concentrations we have adopted their figure and determined the values of 15° and 35° in the same way.

---

* Whittaker and Robinson, "The Calculus of Observations," p. 209 (1924).

Tables IV and V give the most plausible values of A and B, and the final values of E_0 for the different solvents.

Table IV.—Most Plausible Values of A and B.

Mols. per cent. alcohol.	15°.		25°.		30°.	
	A.	B.	A.	B.	A.	B.
25	0·0605	0·0431	0·0658	0·0458	0·0702	0·0478
50	0·1085	0·0776	0·1164	0·0816	0·1240	0·0851
75	0·1426	0·0912	0·1505	0·1064	0·1647	0·1145
95	0·1610	0·1281	0·1685	0·1262	0·1832	0·1303
100	0·2062	0·1178	0·2163	0·1171	0·2391	0·1316

Table V.—Values of E_0 and dE_0/dT.

Mols. per cent. alcohol.	15°.	25°.	35°.	$-(dE_0/dT)$.
0	0·2286	0·2226	0·2158	640
25	0·2012	0·1928	0·1845	835
50	0·1676	0·1554	0·4430	1230
75	0·1196	0·1053	0·0883	1570
95	0·0383	0·0215	0·0028	1780
100	−0·0620	−0·0760	−0·0912	1460

2. *Free Energy, Heat Content and Entropy Changes.*

The free energy and heat content changes in the cell reaction are obtained by the use of equations (1) and (2). The entropy change in the reaction is given by

$$\Delta S = F \cdot \frac{dE}{dT} = \frac{-\Delta F + \Delta H}{T}. \tag{9}$$

Table VI gives the values of these quantities for the ideal solution of unit activity. Tables VII and VIII give the values at 25° of ΔF and ΔH in actual solutions. The free energy and heat content changes in the transfer of the electrolyte from one solution to another are easily obtained by subtracting the corresponding values.

The free energy changes in the transfer of electrolyte from a given solvent to water in the ideal solution, $\Delta F_0{}^\circ$ (*i.e.*, corresponding to infinite dilution), are

Table VI.—Free Energy, Heat Content and Entropy Changes in the Cell Reaction in Ideal Solutions.

Mols. per cent. alcohol.	$-\Delta F_0$.			$-\Delta H_0$.	$-\Delta S_0$.
	15°.	25°.	35°.	25°.	25°.
0	5275	5136	4979	9548	14·77
25	4642	4449	4257	10180	19·27
50	3867	3586	3300	12030	28·38
75	2760	2430	2037	13200	36·23
95	884	496	65	12720	41·07
100	−1431	−1753	−2104	8274	33·69

Table VII.—Free Energy Changes in the Cell Reaction (−ΔF) at 25°.

m.	Composition of solvent (mols. per cent. alcohol).					
	0.	25.	50.	75.	95.	100.
0·01	10708	10063	9307	8221	6350	4472
0·025	—	9061	—	—	—	3740
0·05	8902	8320	7686	6696	4889	3207
0·1	8127	7571	7001	6050	4243	2640
0·3	6887	6410	5884	4975	3170	1860
0·6	—	5609	5097	4211	2337	1364
1·0	5376	4940	4444	3516	1594	934

Table VIII.—Heat Content Changes in the Cell Reaction (−ΔH) at 25°.

m.	Composition of solvent (mols. per cent. alcohol).					
	0.	25.	50.	75.	95.	100.
0·01	9490	10070	11850	12970	12370	7710
0·025	9440	9920	—	—	—	—
0·05	9390	9830	11740	12440	11490	7160
0·1	9310	9640	11270	12000	10880	6420
0·3	9250	9440	10900	11440	9700	5640
0·6	—	9190	10500	10990	8320	5220
1·0	—	8890	10120	10460	6620	5100

Table IX.—Mean Activity Coefficients of HCl in Aqueous and Alcoholic Solutions at 25°.

m.	Composition of solvent (mols. per cent. alcohol.)					
	0.	25.	50.	75.	95.	100.
0·01	0·910	0·876	0·803	0·756	0·717	0·524
0·05	0·836	0·763	0·630	0·547	0·492	0·328
0·1	0·801	0·719	0·561	0·472	0·424	0·242
0·3	0·763	0·638	0·480	0·390	0·350	0·158
0·6	0·770	0·626	0·465	0·371	0·352	0·120
1·0	0·817	0·661	0·486	0·400	0·397	0·104

given in fig. 3. The free energies of transfer from one concentration to another are best expressed in terms of the activity coefficients. The values of the activity coefficients at 25°, as determined by (7) are given in fig. 4. The values for aqueous solutions are those selected by Scatchard after examining all the available data. We have not calculated the corresponding activity coefficients at 15° and 35°, but they can easily be obtained from the data given if required.

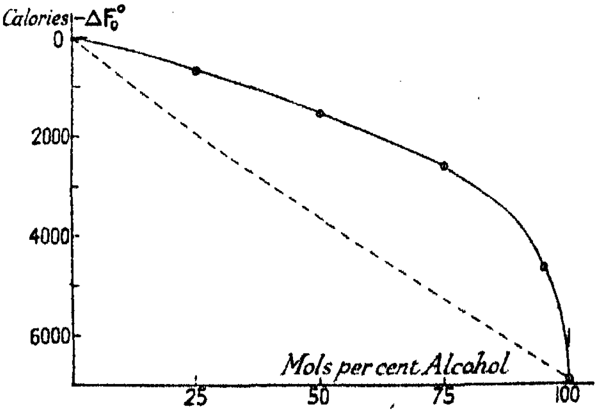

Fig. 3.—Free Energy of Transfer from Alcoholic Solutions to Water in Ideal Solution at 25°.

Fig. 5 shows how the heat content change in the formation of hydrogen chloride in the cell varies with the composition of the solvent in the ideal solution and at a number of constant concentrations. The heat content changes in its

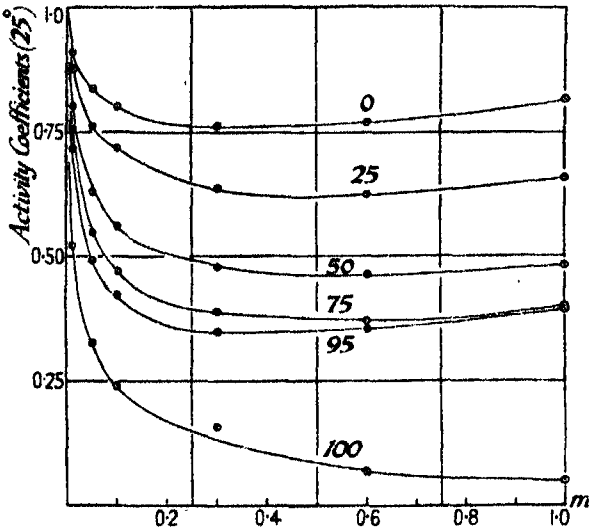

FIG. 4.—Activity Coefficients of Hydrogen Chloride in Water-alcohol Solutions. (Composition of Solvent in mols. per cent. Alcohol.)

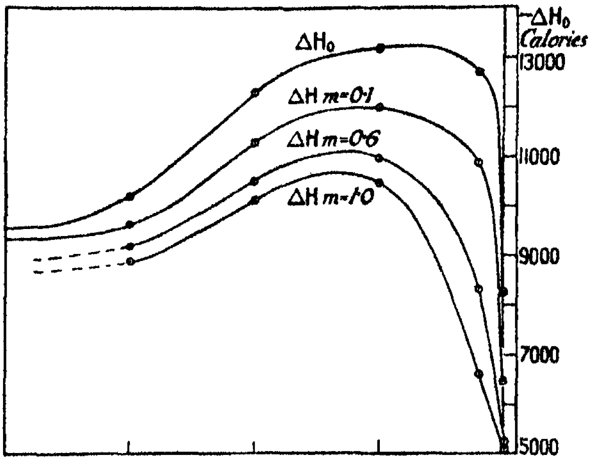

FIG. 5.—Variation of Heat Content Change of Cell Reaction (−ΔH) with Composition of Solvent.

transfer from the ideal solution (*i.e.*, infinite dilution) to the stated concentrations in each of the solvents are given in fig. 6.*

---

* The data given for aqueous solutions are derived from the following papers: 25°, Scatchard, 'J. Amer. Chem. Soc.,' vol. 47, p. 641 (1925); 15° and 35°, Noyes and Ellis, *ibid.*, vol. 39, p. 2532 (1917).

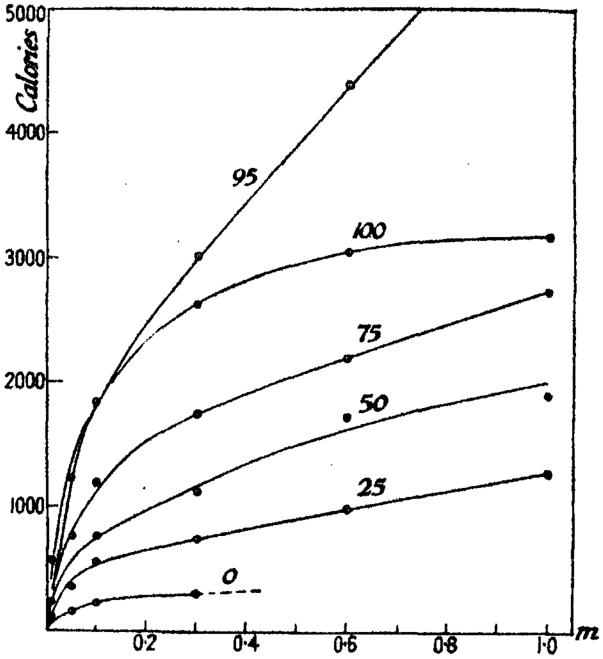

Fig. 6.—Heat Content Changes (ΔH) in Transfer of Hydrogen Chloride from Ideal Solution (infinite dilution) to Concentration *m*. (Composition of Solvent in mols. per cent. Alcohol.)

Discussion.

The free energies of hydrogen chloride in water-alcohol mixtures are best discussed under two headings: (1) the variation of the free energy in ideal solutions (ΔF_0) with the composition of the solvent; (2) the variation of the activity coefficients with concentration in each solvent.

The curve for $\Delta F_0°$ which has been obtained (fig. 3) is similar in form to that derived by Scatchard* from the somewhat fragmentary measurements of Harned and Fleysher (*loc. cit.*) by means of an extrapolation based on theoretical values of A and on values of B interpolated from those required by the more complete measurements in 0, 50 and 100 per cent. alcohol.

The free energy of transfer of ions from water to another solvent† in ideal solution, regarded as the difference between the electrostatic work of charging spherical ions in the two media, is given by

$$\Delta F_0° = \Sigma \frac{e^2}{2r}\left(\frac{1}{D} - \frac{1}{D_0}\right) \qquad (10)$$

---

* 'J. Amer. Chem. Soc.,' vol. 47, p. 2098 (1925).

† Debye and Hückel, 'Phys. Z.,' vol. 24, p. 305 (1923); Scatchard, *loc. cit.*

where r is the radius of an ion of charge e and D_0 and D are the dielectric constants of water and the other solvent. The dashed line (fig. 3) represents the requirements of this equation assuming a constant ionic radius, determined by the values required to fit the two ends of the curve. It is evident that this simple equation is not adequate.

The deviation might be ascribed to a number of effects, between which the experimental evidence is unable to distinguish. In the first place, the ionic radius may be variable, but since any reasonable variation of this factor could not account for more than a small part of the deviation, we must look for some other principal effect. While the expression

$$\Delta F = \Sigma \frac{e^2}{2r} \cdot \frac{1}{D}$$

may give the free energy of charging ions in a uniform medium of dielectric constant D, it is probably inadequate in a mixed solvent. Here, under the influence of the electric fields, the more polarisable molecules must tend to congregate round the ions* and the work of charging will then correspond to a medium containing a greater proportion of these molecules than is present in the bulk of the solvent. It can be seen in fig. 3 that the free energies of transfer do correspond to the values calculated for a greater water content.

Scatchard (*loc. cit.*) has ascribed the form of the curve to the almost complete formation of the hydrated ion H_3O^+. In order to obtain the effect of this hydration on the free energy of transfer, he adds to the theoretical value ΔF°_0 given by (10), the term RT log α_w corresponding to the free energy change in the transfer of a molecules of water from water to the given solvent (α_w being the activity of water in this solvent). In this way he obtains reasonable agreement with the experimental curve, which he regards as evidence in favour of the formation of the monohydrate H_3O^+. This procedure does not seem to be justified, for we have to deal only with the transfer of HCl from one solvent to another, and the effect of hydration can only be equal to the difference between the free energies required to remove water from the two solvents if the free energy change of the union of the hydrogen ion with a water molecule is independent of its surroundings. This may or may not be the case.

A third possibility is that hydrogen chloride may be incompletely dissociated even at small concentrations in alcoholic solutions so that part of the variation of the free energy on adding alcohol is due to the formation of undissociated molecules. This possibility, which is in accordance with the conclusion drawn from their electromotive force measurements at very low concentrations, in pure alcohol, by Woolcock and Hartley (*loc. cit.*) is also supported by our measurements of the heat contents discussed below. It is impossible on the present evidence to distinguish the magnitude of these various effects.

---

* Butler, 'J. Phys. Chem.,' vol. 33, p. 1015 (1929).

The variation with concentration of the activity coefficients in the various solutions, although not precisely represented by the constant A and B (Table IV), is nevertheless approximately defined by these constants, which may be taken to indicate, to a first approximation, the effect of change of solvent on the form of the curve. According to the theory of Debye and Hückel* the constant A, which expresses the electric interaction between the ions, should vary as $1/D^{3/2}$.

Fig. 7 shows that this proportionality does approximately hold. It is to be remembered that the constant for each curve is obtained empirically from the experimental data without reference to any theory, and without the use of the extrapolated value of E_0. The constant B of the formula which corresponds to the coefficient of the linear term of the Debye-Hückel equation, passes through a maximum in the vicinity of 95 per cent. alcohol. The significance of this is not clear. In Hückel's derivation, B is a function of the dielectric constant lowering produced by the electrolyte in the solvent. We have no information as to what this effect may be in mixed solvents.

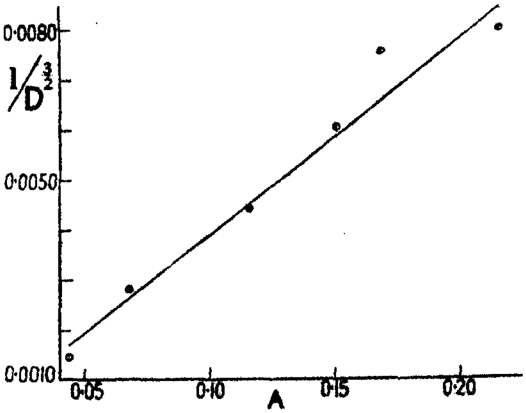

FIG. 7.

The curves for the heat content changes in the cell reaction (fig. 5), which differ by a constant amount from the partial heats of solution of hydrogen chloride in the same solutions, show a marked maximum in the vicinity of 90

---

[*] *Loc. cit.*, and Hückel, 'Phys. Z.,' vol. 26, p. 93 (1925).

per cent. alcohol. The significance of these curves can be seen by considering the transfer of hydrogen chloride from pure alcohol to a series of solvents containing increasing quantities of water. As the percentage of water increases there is first a large heat evolution, but in the solutions containing greater proportions of water a progressive heat absorption occurs. The heat evolution caused by the addition of water is readily accounted for by the hydration, chemical or physical, of the ions. It does not appear to be possible to account for the subsequent heat absorption on the basis of any physical interaction between the ions and the solvent. It could be explained if hydrogen chloride were only partially dissociated in alcoholic solutions. On adding small quantities of water, the affinity of the ions or dipole molecules for water molecules would give rise to a heat evolution. Subsequent additions would cause the necessary dissociation of the hydrogen chloride molecules and there would be a heat absorption on this account.

Fig. 6 shows that the effect of change of concentration on the heat content of hydrogen chloride varies greatly with the composition of the solvent, the effect being greatest in 95 per cent. alcohol. This behaviour is in harmony with the effects which have already been discussed. If the ions hold a water sheath by their electric fields, the greatest change of condition will be brought about by a change of concentration of hydrogen chloride, when only a small proportion of water is present. For when the water present is largely congregated round the ions, the addition of a further quantity of hydrogen chloride will cause a material redistribution, with a correspondingly large heat effect. The degree of ionisation also would probably depend very greatly on the concentration in a case where the ions have to compete for the amount of water available.

In conclusion we may emphasise the very large effect of the addition of traces of water on all the properties of hydrogen chloride in pure alcohol. This effect is the greater the smaller the amount of electrolyte present. This gives independent support to the conclusion that there is some kind of interaction between the hydrochloric acid and the water, and that the hydrochloric acid is more completely " saturated " by a given amount of water, the smaller its concentration. The curves for the temperature coefficients of the electromotive force show the same effect (fig. 8) and are of some interest because dE/dT is proportional to the entropy change in the reaction. The entropy change, like the heat content, goes through a maximum at a high proportion of alcohol, and the maximum is displaced to the right as the concentration of hydrochloric acid decreases.

We hope to make further measurements to ascertain whether the behaviour of hydrogen chloride is similar to that of other strong electrolytes.

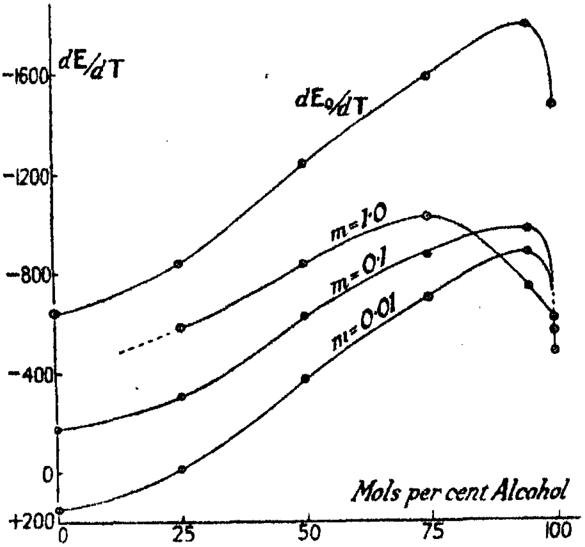

Fig. 8.—Variation of Temperature Coefficients of Cell with Composition of Solvent.

We desire to express our indebtedness to Imperial Chemical Industries, Ltd., for a grant which permitted the purchase of the potentiometer and certain other pieces of apparatus employed in this investigation, and to Sir James Walker, F.R.S., for his assistance in the provision of facilities and for his interest in the work.

Summary.

1. The electromotive forces of the hydrogen-silver chloride cell have been determined at 15°, 25° and 35° in a series of solutions of hydrogen chloride in water-alcohol mixtures.

2. From the measurements the variation of the free energies and heat contents of hydrogen chloride with (1) the composition of the solvent, (2) the concentration of the electrolyte, are calculated.

3. The free energies indicate that in solutions containing only a small proportion of water, the latter is largely associated with the electrolyte. The heat effects have maximum values in the region 90–95 per cent. alcohol. The most probable explanation of this behaviour is that hydrogen chloride is not completely dissociated in alcoholic solution and the addition of water increases the degree of dissociation.

The Rate of Emission of Alpha Particles from Radium.

By F. A. B. Ward, B.A., Sidney Sussex College, Cambridge, C. E. Wynn-Williams, Ph.D., Exhibition of 1851 Senior Student, and H. M. Cave, M.A., Exhibition of 1851 Scholar of Queen's University, Kingston.

(Communicated by J. Chadwick, F.R.S.—Received August 12, 1929.)

1. *Introduction.*

The number of disintegrations taking place per second in a gram of radium is a constant of great importance in quantitative radioactive work, and an accurate knowledge of its value is accordingly essential. This constant, which is usually denoted by Z, has been the subject of numerous researches, but the results, even of comparatively recent measurements, have been disappointingly inconsistent. A discussion of the methods employed and the results obtained has been recently given in a paper by Braddick and Cave,[*] so that it is unnecessary to discuss them at length here. The most direct way of measuring Z is to determine the number of α-particles emitted per second by a known mass of radium : this may be done either (*a*) by measuring the charge carried by the particles emitted within a known solid angle, or (*b*) by directly counting the number of particles emitted within a known very small solid angle.

The most recent measurements by the " total charge " method are those of Jedrzejowski[†] and of Braddick and Cave. The former used sources of radium (B + C) prepared in a special way and measured the charge by a quartz piezo-electrique ; a value for Z of $3 \cdot 50 \times 10^{10}$ was obtained. Braddick and Cave, using active deposit sources, and measuring the charge by the Townsend compensation method obtained a value of $3 \cdot 69 \times 10^{10}$.[‡] The discrepancy between these two results obtained by similar methods remains at present unexplained.

---

[*] 'Roy. Soc. Proc.,' A, vol. 121, p. 367 (1928).

[†] 'Ann. Physique,' vol. 9, p. 128 (1928).

[‡] The mean value of Z from the sixteen experiments was given as $3 \cdot 68_2 \times 10^{10}$ in this paper. A subsequent re-examination of the corrections necessary for non-uniform distribution of active matter over the sources used, the effect of the radium B γ-rays in the ionisation chamber (which was lined with brass 0·5 mm. thick) and the absorption of the γ-rays in the glass sheath used to support the standard source, has resulted in raising the mean value of Z for the sixteen experiments to $3 \cdot 69_6 \times 10^{10}$.—H.J.J.B. and H.M.C.

Determinations by the direct counting method have led to even more widely separated values. Two methods of counting α-particles have been used, the electrical method in which the ionization due to a particle is magnified many thousand times by collision, and the scintillation method. Using the electrical method and observing visually the throws of the electrometer, Hess and Lawson[*] in 1918 made a long series of experiments with active deposit sources. The value obtained for Z was $3 \cdot 72 \times 10^{10}$. Geiger and Werner in 1924[†] used both methods of counting with sources of radon. The scintillation method gave a value for Z of $3 \cdot 40 \times 10^{10}$ and the electrical method $3 \cdot 48 \times 10^{10}$.

The present determination by the direct counting method makes use of an entirely new type of counter, due to Greinacher,[‡] which is free from the objections of other types. In this counter the ionization produced by a single α-particle is linearly amplified by triode valves, there being no ionization by collision. We find from our experiments that $Z = 3 \cdot 66 \times 10^{10}$ α-particles per second per gram of radium. This can be directly compared with Braddick and Cave's value of $3 \cdot 69 \times 10^{10}$, for the same radium standard was used in both experiments and the type of source and the method of γ-ray comparison was the same.

2. *Experimental.*

General Description of the Experiment.—Apart from the different type of counter the general method of the experiment was the same as that of other workers who have used the direct counting method. A radioactive source was used which could be compared with a radium standard by γ-ray measurements, and the number of α-particles emitted from this source within a very small solid angle was counted over a known length of time. For accurate comparison the source should be of nearly the same activity as the standard available (*i.e.*, in our case about 6 mgm. of radium), and in order to give a convenient rate of counting with such a source the solid angle must not exceed about 10^{-7}. The solid angle was defined by an aperture about 2 mm. in diameter placed at the end of an evacuated brass tube some $2 \cdot 6$ metres long, at the other end of which was the source.

The Accurate Counting of α-particles.—An ideal α-ray counter would record separately every α-particle incident upon it, and would record nothing else.

---

[*] 'Wien. Akad. Ber.,' vol. 127, p. 405 (1918).

[†] 'Z. Physik,' vol. 21, p. 187 (1924); Tätigkeitsber, 'Phys. Tech. Reichsanstalt,' vol. 47 (1924), and 'Verh. D. Phys. Ges.,' vol. 12, p. 12 (1924).

[‡] 'Z. Physik,' vol. 36, p. 364 (1926), and vol. 44, p. 319 (1927).

Actual counters fall short of this ideal in several respects, which may be briefly tabulated as follows :—

(1) β and γ-rays may be recorded as well as α-rays.
(2) The efficiency of counting is less than 100 per cent., *i.e.*, particles are occasionally missed.
(3) Close pairs of particles are not resolved, *i.e.*, a group of particles entering in rapid succession may be counted as a single particle.
(4) Large natural effects may be present.

The scintillation method of counting suffers from defect (2) ; the inefficiency may be due to the screen or the observer, or to both.

The problem before the designer of an electrical counter is to detect an α-particle by the small ionization produced along the few centimetres of its path in a gas. An α-particle produces some 10^4 pairs of ions per centimetre in air and the total charge on these is some 5×10^{-15} coulomb. This charge could be detected by a sensitive electrometer, but for such sensitivity the time of swing would be long, so that anything like rapid counting would be entirely impossible. If rapid counting is desired some form of amplification of charge is essential. In all electrical counters used until recently this amplification was produced by ionization by collision, a factor of 10^3 to 10^5 being obtained by this means. Such counters may suffer in varying degree from all four defects mentioned above, and it is very difficult to eliminate them, though they can be reduced by suitable choice of experimental conditions.

Greinacher,[*] in 1926, first succeeded in recording α-particles by using valve amplification alone, and the method has also been used by Ortner and Stetter[†] and by Ramelet.[‡] One of the chief advantages possessed by such a " valve counter " is that the amplification is linear and the final deflection of the recording instrument is proportional to the initial ionization. Largely for this reason it can be made practically free from the above defects. Intense β and γ-radiation does in fact interfere with the counting of α-rays, but under the conditions of such experiments as the present this radiation is far too weak to give any observable effect. It is difficult to see how such a counter could fail to count an incident α-particle since it does not depend on a " trigger action " as do other electrical counters. The effective " resolving power " in time, for the valve counter, is high, since it is possible to make the amplification of charge as great as 10^9 times or even more if required, thus permitting the use of an instrument of comparatively low sensivity but quick response for recording. In the present experiment all the α-particles entering the ionization chamber have very nearly the same residual range (about 4 cm.), and from the geometrical conditions they all follow parallel paths, so that every particle produces practically the same ionization in the chamber. Thus the deflections for different particles should be uniform in size, and they were, in fact, observed to be so. A very close pair gave a deflection of twice the normal size and pairs 1/100th second apart were completely resolved; pairs with separation between these limits gave a "kick" easily recognizable as a double on the photographic record. In fig. 1 a short section of an actual record is reproduced showing the different types of kicks. The natural effects in this type of counter may be made very small. In our experiments the natural effect was due solely to slight radioactive contamination of the chamber. It usually amounted to 2 or 3 particles a minute. With a valve counter it is therefore possible to make the counting of α-particles a matter of precision even at a mean rate of 8 particles a second. The uncertainties in counting up the photographic record were no more than ± 1 part in 500.

---

[*] *Loc. cit.*

[†] 'Phys. Z.,' vol. 28, p. 70 (1927), and 'Z. Physik,' vol. 54, p. 449 (1929).

[‡] 'Ann. d. Phys.,' vol. 86, p. 871 (1928).

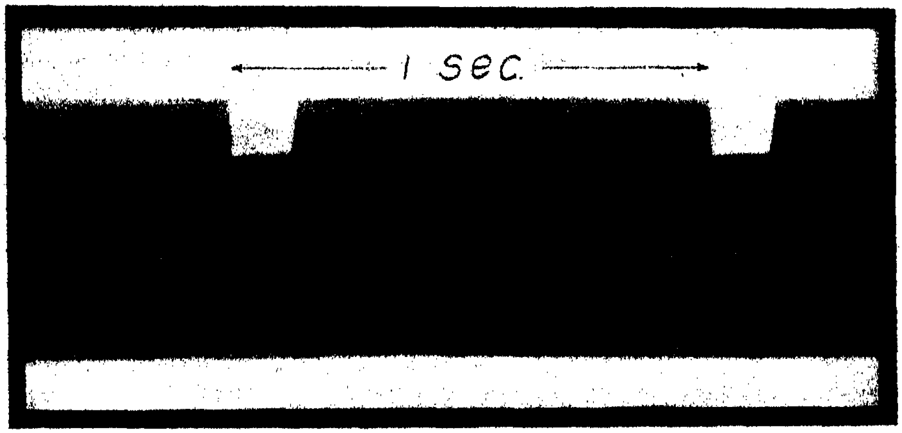

FIG. 1.—Record of α-particles with valve counter. Near the extreme left two particles about 1/100th second apart are seen to be completely resolved. The second kick towards the right from these is about twice the normal height and represents two particles. The fourth to the right from this shows two particles not quite resolved. Near the extreme right three particles have entered in rapid succession.

The fact that in such a counter the deflection of the recording instrument is proportional to the initial ionization is a very great advantage. Because of this it will distinguish between different types of rays, for example between an H-particle and an α-particle, for the ionization produced per centimetre path by an H-particle is only about one-quarter of that produced by an α-particle. As was pointed out by Greinacher the valve counter should prove a powerful instrument in the investigation of the artificial disintegration of the elements and it is for this purpose that it has been developed. It was decided, however, as a trial of its possibilities, to apply it first in the present experiment where large numbers of α-particles had to be counted at as rapid a rate as possible. For the reasons outlined above it has proved very suitable for this work.

Description of the Valve Counter.—The counter consisted essentially of an ionization chamber, a valve amplifier and a recording instrument. In the preliminary experiments telephones were used for detection, but in the actual measurements an Einthoven galvanometer was used with photographic recording, the telephones being retained for control purposes. A 5-valve amplifier, with resistance-capacity coupling throughout, was used ; for recording with the Einthoven galvanometer alone, three, or at most four, valves would have been sufficient. With five valves the total quantity amplification factor was about 10^9.

Fig. 2 shows a section through the ionization chamber and the box containing the first valve. The chamber itself took the form of a shallow cylinder 6 mm. deep. The opening through which the α-rays entered was 10 mm. in diameter and was covered with aluminium foil of stopping power equivalent to 2 mm.

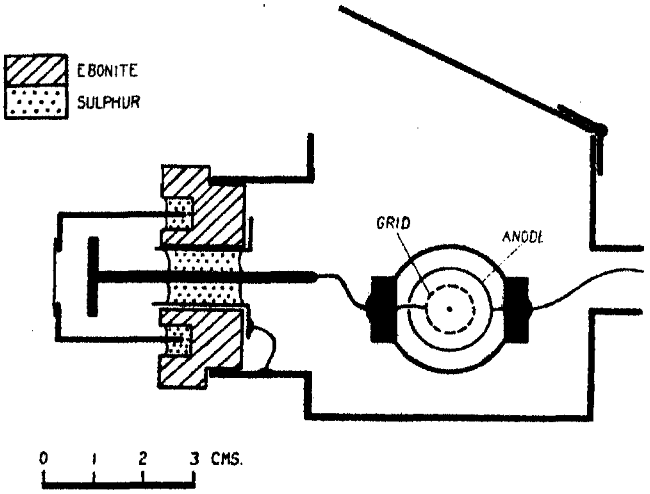

Fig. 2.

of air. When an α-particle enters the chamber, ions from 6 mm. of the α-ray track are collected by a field of about 300 volts per centimetre on to an electrode which is connected directly to the insulated grid of the first valve, the time of collection being about 10^{-3} seconds. The charge leaks away in a time of the same order, depending on the capacity and leak resistance of the insulated grid system; for maximum sensitivity the capacity should be as small and the resistance as large as possible. To fulfil these conditions a Marconi V24 was used for the first valve, as in this valve the grid lead is brought out to a separate cap to reduce inter-electrode capacity. The effect of a single α-particle is thus to raise the potential of the grid of this valve by some 10^{-4} volts for some 1/500th second. The resulting change of anode potential is communicated to the grid of the next valve and so on throughout the amplifier; the change in anode current of the last or output valve deflects the recording instrument. The output valve was an LS5 and the three intermediate amplifying valves were a DEH 610 and two DE 5b (all Marconi). In order to protect the apparatus as completely as possible from electrical and mechanical disturbances, to which it was very sensitive, the whole amplifier together with the filament heating batteries was enclosed in a metal box some 50 cm. cube, which was suspended from the roof of the room by four long metal springs. The leads from the anode batteries were brought in through holes in the box, and, at the point where each entered, a 2 μfd condenser was connected between the lead and the box to short-circuit high-frequency disturbances and prevent them from reaching the amplifier. Before these precautions were adopted, trouble had been experienced from a powerful induction coil in a neighbouring room.

The output circuit was as shown in fig. 3. The steady component of the anode current of the output valve was prevented from passing through the galvanometer by a choke-capacity filter-circuit, and high-frequency "swish" was reduced by a shunt condenser of 0·1 μfd. A variable shunt, S, was connected across the fibre of the Einthoven galvanometer. After the passage of an α-particle, the 2 μfd condenser is left charged, and this charge then leaks away through the resistances in series with it; the 100,000 ohm resistance is included to make this discharge slow. The effect on the shape of the kick recorded by the galvanometer is shown roughly in fig. 4.

In each case the area below the zero line must be equal to that above it since, over the whole time of recording of a particle, $\int i \, . \, dt = 0$. By increasing the time of leak the amplitude of the "back-kick" is reduced. While a large back-kick might be no disadvantage in some types of experiment, it would make the counting up of the records a little more troublesome in the present ones where particles followed in such rapid succession that often a second particle would be recorded during the back-kick due to a first. The deflection for the second would consequently start from well below the normal zero line.

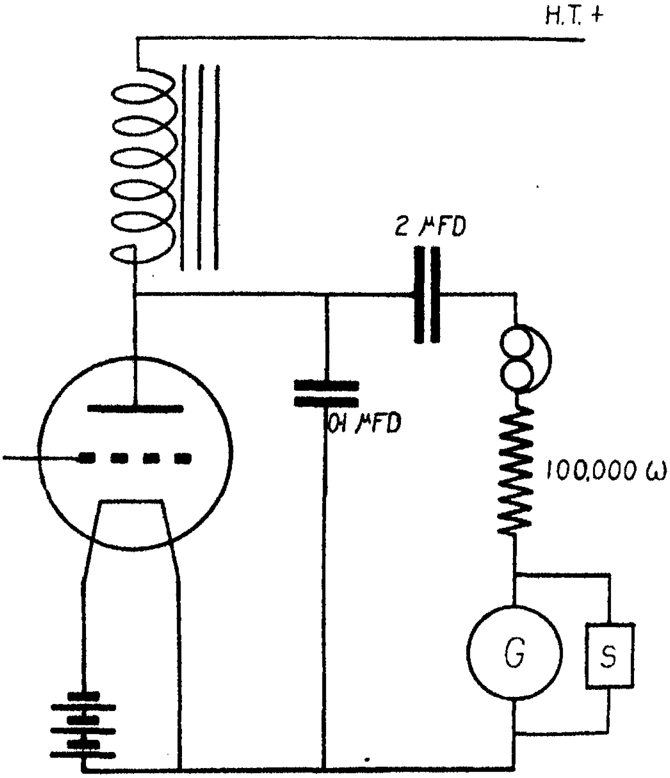

FIG. 3.

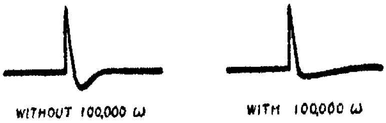

FIG. 4.

Photographic Recording.—A special camera was built for the photographic recording. It was in general somewhat similar to the cameras used in electrocardiographs, but special provision was made for accurate focussing and for dealing with considerable lengths of bromide paper—up to 400 feet at a time.

The light from the Einthoven galvanometer was condensed on to a slit by a cylindrical lens. The width of the slit was about 1/12th mm., and its distance from the eye-piece of the galvanometer was about 30 cms. The bromide paper was wound past the slit by rubber-covered rollers at a rate of 5 cms. per second. A small shutter, worked by an electric clock, cast a shadow on one edge of the record at 1-second intervals, thus providing a time-scale, and a similar shutter on the other edge marked every 100 seconds. The records were made on rolls of Kodak Rapid Platino-Matt bromide paper, 400 feet long and 1½ inches wide. The long records were easy to examine when this paper was used; any kind of gloss was found to be extremely irritating to the eyes.

The long roll of bromide paper was developed in the laboratory dark room. It was wound, sensitive side out, on to specially made frames of wood impregnated with paraffin wax, each frame taking about 25 feet of paper. Development was effected by immersing the whole frame in a large shallow dish of developer. Fixing was done in a similar dish and after washing and drying the sections of the record were joined together again in their proper sequence by short lengths of gummed paper and the complete record was then counted. Counting was done visually, the observer passing the record slowly in front of him and recording each kick observed on a mechanical counter actuated electromagnetically by means of a battery and tapping key.

Definition of the Solid Angle.—The source, A (fig. 5) was waxed on to a threaded brass carrier B which could be screwed on to the end of the brass rod C which was supported by wax H. The whole system could be readily removed through the ground glass joint D. The cap E served to catch recoil atoms, and fitted over the source without touching it; it was covered with a thin film of collodion of stopping power for α-rays equivalent to about 1 mm. of

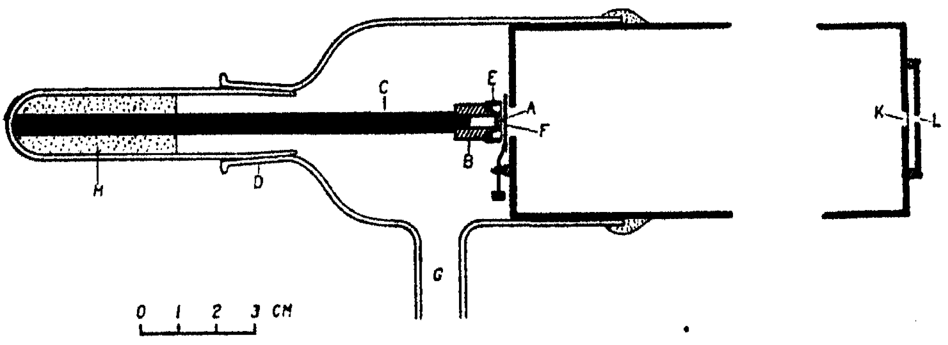

Fig. 5.

air. The aperture at the end of the brass tube could be covered by a small shutter F which was worked from outside by means of a magnet. The apparatus was exhausted through the side tube G. The other end of the tube was closed by a brass disc with a central hole K, 4 mm. in diameter, covered by a mica window of stopping power for α-rays equivalent to 8 mm. of air. The defining aperture L was placed immediately outside this window, between it and the ionization chamber of the counter. The aperture was made by a method described by Hess and Lawson.* A hole was first drilled in a steel plate 1 mm. thick and this hole was then turned out to a conical shape with a specially made countersink drill. The steel was then hardened and the hole ground with carborundum on a copper bit of the same taper (about 1 in 10) as the countersink. During the grinding process the hole was periodically examined under a microscope until it was satisfactory. When mounted in position, the smaller end of the hole faced the radioactive source, the solid angle thus being accurately defined by the area of this end and its distance from the source. Two different apertures were used in the course of the experiments. Their diameters were 1·660 mm. and 1·774 mm. respectively. The distance from source to aperture was usually 261·4 cm., with minor variations in different experiments.

Effects of Scattering.—It is assumed in the calculations that if ω be the solid angle subtended by the aperture at the source, the fraction of the total number of particles which pass through the aperture is $\omega/4\pi$. This fraction may be modified by scattering of the particles. The scattering may occur in the foil covering the source, in the residual gas in the tube, or at the walls of the tube. The end mica window was so close to the aperture that its scattering effect can be entirely neglected.

Scattering in the foil covering the source was investigated both theoretically and experimentally. The defining aperture subtended an angle of about 2′ at the source, and calculation shows that if a source emitting α-particles of 7 cm. range is covered with a uniform sheet of absorbing material of stopping power equal to 1 cm. of air, practically every particle from the source will be scattered through an angle greater than this. It can, however, be shown that under these conditions the number of particles scattered into the beam is closely equal to the number scattered out of it. As irregularities in the thickness of the absorbing sheet might interfere with this equality, the point was tested experimentally. In one series of experiments the "source" end of the tube was closed by a brass disc with a central hole covered with a mica window of 1·8 cm. stopping power, the source being placed immediately outside this window. About 13,000 particles were counted under these conditions, the value of Z deduced from these being $3 \cdot 62 \times 10^{10}$. The mean value for Z from 79,000 particles counted with the source inside the tube, and with no mica in front of it, was $3 \cdot 66 \times 10^{10}$. Both of these numbers, particularly the smaller, are subject to a small uncertainty due to probability variations in the number of particles counted, and the whole discrepancy between them might be due to this cause. It seems certain that the effect of the mica cannot be more than 2 per cent. at most, so that the effect of the collodion film covering the source in later experiments must therefore be very small, as its stopping power was only about 1 mm., and from its method of preparation it should be reasonably uniform in thickness.

---

* *Loc. cit.*

Scattering in the residual gas in the tube was investigated by performing experiments at different pressures which were measured by a calibrated viscosity gauge. The brass tube was evacuated from one end, but the gauge was attached near the middle, so as to give a reading representing the mean pressure in the tube.

Twenty-eight thousand particles were counted at a pressure of 1/100th mm. of mercury and gave a value of $3 \cdot 68 \times 10^{10}$ for Z; 52,000 counted at a pressure of about 7×10^{-4} mm. gave a value of $3 \cdot 66 \times 10^{10}$. It is evident, therefore, that the gas scattering is not serious, for it is very difficult to see how an increase in the pressure of the gas could cause an increase in the number of particles observed. The discrepancy between the above two numbers must therefore be ascribed to probability fluctuations, and we can be confident that the effect of scattering in the gas is negligible.

The effect of scattering at the walls of the tube was eliminated by five stops inside the tube. These were placed so that, on looking through the defining aperture, no portion of the wall surface could be seen except the few centimetres before the first stop. No particles could then reach the aperture either from the source by reflection at the walls or from radioactive contamination on the walls.

The Time Scale.—All times in a single experiment were taken from an electric clock controlled by a master pendulum clock. The electric clock recorded seconds and 100's of seconds on two separate dials; contacts on the clock actuated the electromagnets making the second and 100-second marks on the photographic record, and hence the exact time of every mark was known. The instant at which emanation was pumped from the source was taken as the zero of time and the clock started then. A record was kept of the time on the clock at which each γ-ray reading was taken.

Radioactive Sources.—The sources used were exactly similar to those used by Braddick and Cave* in their measurement of the total charge carried by the α-particles ; the preparation of the sources is described in detail in their paper. The radioactive material—the active deposit of radium—was deposited upon the inside of a shallow glass cup 4 mm. in diameter. Owing to the method of preparation, no active matter could be deposited on the back or sides of the cup. Careful experiments showed that the source was entirely free from occluded emanation.

Measurement of the Strength of the Source.—The strength of the source was measured by comparing its γ-ray activity with that of a standard radium source by means of a γ-ray electroscope surrounded by 2 cm. of lead ; either source or standard could be placed in a position accurately defined by observation through a microscope. Under these conditions the γ-rays by which the comparison is carried out are due almost entirely to radium C. From the γ-ray measurements and the α-ray count the rate of emission of α-particles from the radium C in the *standard* source (and hence from the radium itself with which it is in equilibrium) can be calculated. In the actual experiment the source had to be used, not in the standard position, but in a position inside the exhausted tube. To find its strength under these conditions, the following procedure was adopted. The decay of the source was first followed by its γ-rays while it was in the standard position. The source was then transferred as rapidly as possible into the holder in the tube, and its decay again followed during the time in which the α-particles were being recorded. At the close of the experiment it was withdrawn and replaced in the standard position and more measurements taken. If the γ-ray readings are plotted, a curve is obtained with two discontinuities. From this broken curve the ratio of the γ-ray activities of the source in the two different positions can be found ; the actual procedure adopted is described below. From this "position ratio" and the comparison of the decaying source with the standard source, with both in the standard position, the activity of the decaying source expressed in milligrams of radium is known throughout the experiment. All readings of the electroscope were, of course, corrected for natural leak, which amounted on the average to about 1 per cent. of the activity due to the standard source.

Determination of the Position Ratio.—The actual procedure adopted to find the position ratio as accurately as possible was as follows. The theoretical decay curve for the radium C in radium active deposit was plotted on a large sheet of squared paper (sheet *a*), the logarithm of the amount of radium C being plotted as ordinate against the time as abscissa. The experimental points corresponding to the activity of the source in the standard position were plotted in the same manner on a second sheet of paper (sheet *b*), and those corresponding to the activity in the firing position on a third (sheet *c*). All three sheets were then superposed and by observing with transmitted light both sets of points and the theoretical curve could be seen at the same time. By a process of adjusting the three sheets the best fit of both sets of points to the theoretical curve was obtained. In doing this, care was taken to keep the time scale of sheet *c* coincident with the time scale of sheet *b*, but the time scale of the two might be displaced with respect to that of sheet *a* as is discussed below. When the best fit has been obtained the amount of vertical displacement between any ordinate on sheet *b* and the numerically equal ordinate on sheet *c* then gives at once the logarithm of the position ratio. The values found for a given position ratio in separate trials always agreed to within 1 part in 500 and usually to within 1 part in 1000.

---

* *Loc. cit.*

[In practice it is found that, for active deposit sources prepared as these were, the actual decay is usually rather slower than the theoretical, apparently due to a disturbance of the equilibrium by the conditions of exposure to the emanation. It is found, however, that the decay curve observed experimentally is, over the time interval concerned, of the same shape as the theoretical curve over a rather earlier time interval, so that, by taking arbitrarily a zero of time rather later than the actual one, the points can be made to fit the theoretical decay curve quite accurately. This is to be expected, since, at any instant after the radium A has all decayed, the subsequent shape of the curve is determined uniquely by the ratio of radium B to radium C at that instant. This ratio changes from the equilibrium ratio by a factor of three during the interval with which we are concerned, so there are wide limits within which the equilibrium may be disturbed and yet give the same radium B to radium C ratio at some selected time after removal from the emanation as that occurring after a different interval in a normally decaying source. The subsequent shape of the curve must then be identical in each case. It has been definitely shown that the slow decay is not due to the presence of occluded emanation.]

Method of Evaluating Z from the results.—If the source is at any instant of strength x mgm., it is emitting particles at the rate of $Zx/10^3$ per second.

Therefore the number of particles emitted between times t_1 and t_2 is

$$\int_{t_1}^{t_2} \frac{Zx}{10^3}\,dt = \frac{Z}{10^3}\int_{t_1}^{t_2} x\,dt.$$

The number of these which reach the counter is

$$\frac{\omega}{4\pi}\cdot\frac{Z}{10^3}\int_{t_1}^{t_2} x\,dt = \text{N, say.}$$

Therefore

$$Z = 4\pi N\,.10^3/\omega\int_{t_1}^{t_2} x\,dt.$$

x can be evaluated from the γ-ray readings. If m be the mass of radium in the standard, G_0 its γ-ray activity in the standard position, G the activity of the decaying source at any instant, μ the position ratio, then

$$x/m = \mu G/G_0 \quad\text{or}\quad x = m\mu\,.\,G/G_0.$$

Therefore

$$Z = 4\pi N G_0\,10^3/m\mu\omega\int_{t_1}^{t_2} G\,dt.$$

μ is evaluated as described above and $\int_{t_1}^{t_2} G\,dt$ is equal to the area under the graph between the appropriate time limits, G being measured in the same units (div./min. of electroscope) as G_0.

Procedure in a Single Experiment.—While the source was being prepared, γ-ray readings of the activity of the standard were taken and the natural leak of the electroscope was determined. The active deposit source was then placed in the standard position and its decay followed by its γ-rays for a time depending on its initial strength, after which it was transferred to its position inside the tube. The pumps were immediately started, and when the pressure had fallen to 1/1,000th mm. the small shutter was brought in front of the source, and the recording camera was started and run for 3 minutes to obtain the " natural " count. The shutter was then drawn aside and the α-rays from the source recorded for about 35 minutes. The shutter was then closed again and a second control record taken for 3 minutes. Air was then let into the apparatus, the source removed and replaced in the standard position, and its decay followed for a further 15 minutes or so. Finally a further set of readings was taken on the standard source, and the natural leak redetermined. The strength of the source was usually about 10 mgm. when the recording of the α-particles was started ; by the end of the count it had decayed to about 5 mgm. Under such conditions about 15,000 particles would be recorded on some 350 feet of bromide paper in the 35 minutes.

3. *Results.*

A table is given showing the results of seven separate experiments.

Table of Results.

Number of experiment.	G_0 in div./min. of electroscope.	Position ratio.	γ-ray integral in div./min. × sec.	Solid angle $\frac{}{4\pi}$	Number of α-particles.	Z.
1	20·90	1·428	10,941	$2\cdot521 \times 10^{-8}$	4,320	$3\cdot59_2 \times 10^{10}$
2	21·14	1·574	20,630	2·520	8,980	$3\cdot63_4$
3	11·27	1·085	25,762	2·519	14,784	$3\cdot70_9$
4	14·60	1·437	22,660	2·519	13,131	$3\cdot66_3$
5	11·40	1·132	22,250	2·517	13,115	$3\cdot69_6$
6	11·18	1·135	37,291	2·517	22,204	$3\cdot65_2$
7	11·39	0·988	28,338	2·879	16,442	$3\cdot64_1$
				Weighted mean	……..	$3\cdot66_3 \times 10^{10}$

The second column gives the values of G_0, the rate of leak of the electroscope with the standard source; the values have been corrected (as described later) for the small absorption of the γ-rays in the glass sheath supporting the source, as well as, of course, for natural leak; the γ-ray integral given in the fourth column is also corrected for natural leak. The number of α-particles given in the sixth column is the number actually counted, less a correction (usually about 0·6 per cent.) for the natural effect, which was determined in each experiment as described before. The values of Z in the last column are obtained from the formula given above.

$$Z = 4\pi N G_0 \,.\, 10^3/m\mu\omega \int_{t_1}^{t_2} G\,dt.$$

The experiments fall into three groups. In experiments 1 and 2 the source was outside the brass tube with a mica window of 1·8 cm. stopping power in front of it, and the pressure in the tube was about 1/100th mm.; in experiments 3 and 4 the source was inside the tube and the pressure in the tube about 1/100th mm.; in experiments 5, 6 and 7 the source was again inside and the pressure about 7×10^{-4} mm.

The mean of experiments 5, 6 and 7, which were taken under the best conditions, gives a value of $3\cdot66_0 \times 10^{10}$ for Z, and the weighted mean of the whole seven experiments gives a value of $3\cdot66_3 \times 10^{10}$. Each experiment was weighted in proportion to the number of particles counted. We therefore take $Z = 3 \cdot 66 \times 10^{10}$ α-particles per second per gram of radium as the value given by our experiments.

In estimating the strength of the source a small correction had to be applied for the absorption of the α-rays from the standard in the thin glass sheath, 0·4 mm. thick, which supported it. This was investigated experimentally by observing the rate of leak of the electroscope with the standard source in its usual glass sheath and in a thicker sheath. From these measurements the absorption was estimated to be 1·0 per cent. per millimetre of glass,—in good agreement with the results found by Rutherford and Chadwick* for γ-rays from radium (B + C) filtered through 1 cm. of lead. The correction to be applied to G_0 was accordingly + 0·4 per cent.; the corrected values of G_0 are given in the table.

The effect of the γ-rays from radium B in the source has to be considered. According to measurements by Slater,† and to the recent measurements of Irene Curie‡ by a different method, the γ-ray ionization produced in an all-lead electroscope through 20 mm. of lead by the radium B in a source where it is in equilibrium with radium is 0·4 per cent. of the total, the rest being due to radium C. The radium B and radium C in the standard source were both in equilibrium with the radium there, but in the decaying source the ratio radium B/radium C was on the average about 0·4 times the equilibrium value over the time during which the measurements were made; the total correction to be applied for the effect of radium B in the standard and the decaying source is thus $-0 \cdot 4 + 0 \cdot 16$ per cent. or $-0 \cdot 24$ per cent. with an all-lead electroscope. Our electroscope was not all of lead, but consisted of a cube of aluminium with a spherical cavity; the minimum thickness of aluminium was 6 mm., and the whole cube was surrounded with 20 mm. of lead. The effective thickness of lead was thus more than 20 mm., and since the relative ionization due to the radium B rays is 2 or 3 times smaller for a lead electroscope lined with aluminium than for an all-lead electroscope,§ the correction for the radium B γ-rays becomes accordingly less than 0·1 per cent., which is practically negligible.

Limits of Accuracy.—Some uncertainty in the counting up of the records arose from the fact that the contamination particles recorded by the counter did not give kicks of uniform size, for these particles had paths of different lengths in the ionization chamber. Consequently it was occasionally difficult to decide whether a kick should be counted as one or two particles. Also there were a very few cases where such a large number of particles entered in rapid succession that it was difficult to tell to within one, how many the complicated response of the galvanometer represented. In counting up the records the uncertainties due to these causes amounted on the average to about ± 1 part in 500.

---

* 'Proc. Phys. Soc.,' vol. 24, p. 141 (1912).

† 'Phil. Mag.,' vol. 44, p. 300 (1922).

‡ 'C.R.,' vol. 188, p. 64 (1929).

§ Chalmers, 'Phil. Mag.,' vol. 6, p. 745 (1928).

The standard clock controlling the electric clock was tested against Greenwich time signals and found to be accurate to within 1 part in 10,000. The solid angle could be measured to about 1 part in 1,000.* The steel rule used in measuring the distance from source to diaphragm and the travelling microscope used in measuring the diameter of the diaphragm were both calibrated against the same standard metre belonging to the Laboratory. The probable error in the γ-ray measurements was less than ½ per cent. in any single experiment. An unavoidable source of uncertainty lies in the fact that only a finite number of particles can be counted, and that the number is subject to the probability variation in the emission. A total of 92,000 particles was counted and the probable error in the mean derived from counting this number, as usually defined, is just under 0·3 per cent. We estimate that the probable error in the value of Z from our experiments is about 0·5 per cent. assuming the value of the standard to be accurately known. The laboratory radium standard used throughout has been compared with the National Standard by the National Physical Laboratory and found to be equivalent in γ-ray activity to 6·38 mg. radium; this number is subject to the usual small uncertainties associated with the setting up and comparison of radium standards.

4. *Discussion.*

Although the absolute value of our result is subject to a small uncertainty, due to the uncertainty in the value of the radium standard, comparisons can be made more accurately with the results of other experiments made in this laboratory in which the same radium standard has been used. We refer to the experiments of Braddick and Cave, in which the total charge carried by the α-particles from radium was measured, and to the experiments of

---

* As defined geometrically. An uncertainty exists owing to the fact that α-particles penetrate the extreme edge of the aperture. It is difficult to determine accurately the appropriate correction for this effect. In this experiment, however, the correction is estimated to lie between 0 and −0·3 per cent. In view of the uncertainty of its exact value, the correction has not been applied, the results being based on the geometric value of the solid angle.

Watson and Henderson* on the heating effect of radium and its products. The value of Z found by Braddick and Cave was $3 \cdot 69 \times 10^{10}$, while our value is $3 \cdot 66 \times 10^{10}$. The difference between the two numbers lies just within the limits of error of the two experiments. As has been pointed out, the relative accuracy of these two experiments should be high, even though their absolute accuracy is less certain, since in both of them those measurements which introduce the greatest uncertainty into the result, *i.e.*, the γ-ray measurements, were carried out in a practically identical manner. Also exactly the same type of radioactive source was used in both experiments. If unrecognised systematic errors be involved in these measurements we should expect them to be about the same for both experiments and therefore not to affect the relative accuracy of the two. Taking these considerations into account it seems doubtful whether the whole discrepancy between the two results can be ascribed to experimental error. In the experiments of Braddick and Cave what is really measured is not Z but Ze, and Z is deduced by using Millikan's value of e, the electronic charge, whereas in the present experiments Z is determined directly. If therefore the accepted value of e were too low, the discrepancy between the two results might be explained. Some recent careful experiments have given values of e some ½ per cent. higher than the Millikan value, and if this higher value be adopted the results of the above experiments would be brought into close agreement.

Conversely it is obvious that two experiments such as the present afford a fairly direct method of determining the electronic charge—the method having in fact been used by Rutherford as early as 1908. The value of e from the present experiment and that of Braddick and Cave is $4 \cdot 81 \times 10^{-10}$ E.S.U. Unfortunately, no claim to high accuracy can be made for this result, partly on account of experimental errors and partly on account of the unavoidable uncertainty involved in having counted only a moderate number of particles in the direct counting experiments.

A discussion of the work on the heating effect was given by Braddick and Cave, and their result was shown to agree well with the latest work on the heating effect carried out in this laboratory by Watson and Henderson.† It was concluded that there was no need to assume any additional source of energy in radioactive disintegration other than the known radiations, and, considering the limits of accuracy, this conclusion is confirmed by the present work. It may be pointed out that the agreement between the results of Watson and Henderson and those of Braddick and Cave is independent of the value assumed for e.

---

* 'Roy. Soc. Proc.,' vol. 118, p. 318 (1928).

† *Loc. cit.*

5. *Summary.*

The number of α-particles emitted per second by 1 gram of radium has been determined by a direct counting experiment with a new type of electrical counter in which the whole of the amplification was produced by triode valves. The amplification was linear, so that the counting of α-rays was undisturbed by the presence of β-rays. It was found possible to count with accuracy at a high rate, *i.e.*, about 500 particles per minute. Approximately 10^5 α-particles were counted, and the value found for the rate of emission from radium was $3 \cdot 66 \times 10^{10}$ α-particles per second per gram of radium, in good agreement with the value of $3 \cdot 69 \times 10^{10}$ recently found by Braddick and Cave, and with recent measurements of the heating effect of radium and its products.

It is a pleasure to thank Sir Ernest Rutherford, who suggested the problem, for his interest and encouragement, and Dr. Chadwick for much helpful advice. We also wish to thank Mr. G. R. Crowe, who prepared the radioactive sources. The work has been made possible for one of us (F.A.B.W.) by a grant from the Department of Scientific and Industrial Research, to which we wish to express our thanks.

INDEX TO VOL. CXXV. (A)

Acetylene, action of cathode rays (McLennan and others), 246.
Alpha particles, emission from radium (Ward and others), 713.
Aluminium crystals, X-ray reflexion (James and others), 401.
Anthracene and naphthalene, structure by X-rays (Robertson), 542.
Arnot (F. L.) Electron Scattering in Mercury Vapour, 660.
Arsenic, regularities in arc spectrum (Rao), 238.

Bannister (L. C.) *See* Evans (U. R.).
Barnes (W. H.) The Crystal Structure of Ice between 0° C. and −183° C., 670.
Bateman (H.) Notes on a Differential Equation which occurs in the Two-Dimensional Motion of a Compressible Fluid and the Associated Variational Problems, 598.
Beta-particles, straggling (Williams), 420.
Bowden (F. P.) The Amount of Hydrogen and Oxygen present on the Surface of a Metallic Electrode, 446.
Brindley (G. W.) *See* James and others.
Brode (R. B.) The Absorption Coefficient for Slow Electrons in Mercury Vapour, 134.
Butler (J. A. V.) and Robertson (C. M.) The Behaviour of Electrolytes in Mixed Solvents, 694.

Calorimeter for determining heats of solution (Smith), 619.
Cathode rays, diffraction (Thomson), 352.
Cave (H. M.) *See* Ward and others.
Chandrasekhar (S.) The Compton Scattering and the New Statistics, 231.
Chlorine arc spectrum (Majumdar), 60.
Colvin (J.) *See* Hume and Colvin.
Compressible Fluid, differential equation in two-dimensional motion (Bateman), 598.
Compton scattering and new statistics (Chandrasekhar), 231.
Constable (F. H.) Sulphide Colours on Metallic Copper, 630.
Cook (W. R.) *See* Hassé and Cook.
Crawford (M. F.) *See* McLennan and others.
Curtis (W. E.) and Harvey (A.) The Structure of the Band Spectrum of Helium, VI, 484.

Dalton (R. H.) and Hinshelwood (C. N.) The Oxidation of Phosphine at Low Pressures, 294.
Das (K.) *See* Richardson and Das.
Davidson (P. M.) *See* Richardson and Davidson.
Desch (C. H.) *See* Smith (C. J.)
Dobson (G. M. B.) *See* Götz and Dobson.
Duncan (W. J.) *See* Frazer and Duncan.

Electrode, metallic, hydrogen and oxygen present (Bowden), 446.
Electrolytes in mixed solvents (Butler and Robertson), 694.
Electron scattering in mercury vapour (Arnot), 660.

Electron, spinning, wave equations (Temple), 152.
Electrons, slow, absorption coefficient in mercury (Brode), 134.
Ethylene, kinetics of oxidation (Thompson and Hinshelwood), 277.
Exclusion principle and aperiodic systems (Mott), 222.
Evans (U. R.) and Bannister (L. C.) The Growth of Silver Iodide Films, 370.

Fatigue, high frequency (Jenkin and Lehmann), 83.
Films of fatty acid on water (McBain and Peaker), 394.
Finch (G. I.) and Hodge (D. L.) Gaseous Combustion in Electrical Discharges, IV, 532.
Fisher (R. A.) Tests of Significance in Harmonic Analysis, 54.
Fluorescence of mercury (Rayleigh), 1.
Frazer (R. A.) and Duncan (W. J.) On the Numerical Solution of Equations with Complex Roots, 68.

Gaseous combustion at high pressures, XIII (Newitt), 119.
Gaseous combustion in electric discharges (Finch and Hodge), 532.
Gelatinisation, mechanism (Usher), 143.
Götz (F. W. P.) and Dobson (G. M. B.) Observations on the Height of the Ozone in the Upper Atmosphere, II, 292.

Harmonic analysis, tests of significance (Fisher), 54.
Harvey (A.) *See* Curtis and Harvey.
Hassé (H. R.) and Cook (W. R.) The Determinations of Molecular Forces from the Viscosity of a Gas, 196.
Helium, band spectrum (Curtis and Harvey), 484.
Hinshelwood (C. N.) *See* Dalton and Hinshelwood, *and* Thompson and Hinshelwood.
Hodge (D. L.) *See* Finch and Hodge.
Hume (J.) and Colvin (J.) The Decomposition of Potassium Hydrogen Oxalate Hemihydrate, 635.
Hydrogen molecules, energy functions (Richardson and Davidson), 23.
Hydrogen spectrum, *orthohelium bands* (Richardson and Das), 309.

Ice, crystal structure (Barnes), 670.
Infra-red investigations of molecular structure (Snow and Rideal), 462.
Intertraction (Wright), 587.
Ireton (H. J. C.) *See* McLennan and others.
Isotherms of hydrogen and carbon monoxide (Scott), 330.

James (R. W.), Brindley (G. W.) and Wood (R. G.) A Quantitative Study of the Reflexion of X-Rays from Crystals of Aluminium, 401.
Jenkin (C. F.) and Lehmann (G. D.) High Frequency Fatigue, 83.

Kronecker's fundamental limit formula (Mordell), 262.

Lehmann (G. D.) *See* Jenkin and Lehmann.
Low (A. R.) On the Criterion for Stability of a Layer of Viscous Fluid Heated from Below, 180.

McBain (J. W.) and Peaker (C. R.) The Electrical Conductivity caused by Insoluble Monomolecular Films of Fatty Acid on Water, 394.
McBain (J. W.) and Tanner (H. G.) A Robust Microbalance of High Sensitivity, suitable for weighing Sorbed Films, 579.

McLay (A. B.) *See* McLennan and others.

McLennan (J. C.), McLay (A. B.) and Crawford (M. F.) The Spark Spectrum of Thallium, 50, 570.

McLennan (J. C.), Perrin (M. W.) and Ireton (H. J. C.) The Action of High Speed Cathode Rays on Acetylene, 246.

Magnesium hydride, ultra-violet spectrum (Pearse), 157.

Magnetic field and propagation of light (Watson), 345.

Majumdar (K.) The Arc Spectrum of Chlorine, 60.

Mercury vapour, fluorescent and phosphorescent excitation (Rayleigh), 1.

Microbalance, suitable for sorbed films (McBain and Tanner), 579.

Molecular forces from gas viscosity (Hassé and Cook), 196.

Mordell (L. J.) Kronecker's Fundamental Limit Formula in the Theory of Numbers and Elliptic Functions, and Similar Theorems, 262.

Mott (N. F.) The Exclusion Principle and Aperiodic Systems, 222.

Müller (A.) A Spinning Target X-Ray Generator and its Input Limit, 507.

Naphthalene and anthracene, structure by X-rays (Robertson), 542.

Newitt (D. M.) Gaseous Combustion at High Pressures, XIII, 119.

Numerical solution of equations with complex roots (Frazer and Duncan), 68.

Ozone in upper atmosphere (Götz and Dobson), 292.

Palladium, melting point (Schofield), 517.

Peaker (C. R.) *See* McBain and Peaker.

Pearse (R. W. B.) The Ultra-Violet Spectrum of Magnesium Hydride, II, 157.

Perrin (M. W.) *See* McLennan and others.

Phosphine, oxidation at low pressures (Dalton and Hinshelwood), 294.

Potassium hydrogen oxalate hemihydrate, decomposition (Hume and Colvin), 635.

Rao (K. R.) Regularities in the Arc Spectrum of Arsenic, 238.

Rayleigh (Lord). Fluorescent and Phosphorescent Excitation of Mercury Vapour by the Resonance Frequency and Lower Frequencies, 1.

Richardson (O. W.) and Das (K.) The Spectrum of H_2; The Bands analogous to the Orthohelium Line Spectrum, II, 309.

Richardson (O. W.) and Davidson (P. M.) The Energy Functions of the H_2 Molecules, 23.

Rideal (E. K.) *See* Snow and Rideal.

Robertson (C. M.) *See* Butler and Robertson.

Robertson (J. M.) An X-Ray Investigation of the Structure of Naphthalene and Anthracene, 542.

Schofield (F. H.) The Melting Point of Palladium, 517.

Scott (G. A.) The Isotherms of Hydrogen, Carbon Monoxide and their mixtures, 330.

Silver iodide films, growth (Evans and Bannister), 370.

Smith (C. J.) A new form of Calorimeter suitable for determining Heats of Solution, with an Application to Worked and Annealed Metals, 619. With appendix by Desch (C. H.), 628.

Snow (C. P.) and Rideal (E. K.) Infra-Red Investigations of Molecular Structure, III, 462.

Spectrum, arc, of arsenic (Rao), 238.

Spectrum, arc, of chlorine (Majumdar), 60.

Spectrum, band, of helium (Curtis and Harvey), 484.

Spectrum, energy functions of H_2 molecules (Richardson and Davidson), 23.
Spectrum of H_2, Orthohelium bands, II (Richardson and Das), 309.
Spectrum, spark, of thallium (McLennan and others), 50, 570.
Spectrum, ultra-violet, of magnesium hydride (Pearse), 157.
Sulphide colours on metallic copper (Constable), 630.
Swain (L. M.) On the Turbulent Wake behind a Body of Revolution, 647.

Tanner (H. G.) *See* McBain and Tanner.
Temple (G.) The Second Order Wave Equations of the Spinning Electron, 152.
Thallium, spark spectrum (McLennan and others), 50, 570.
Thompson (H. W.) amd Hinshelwood (C. N.) The Kinetics of the Oxidation of Ethylene, 277.
Thomson (G. P.) Diffraction of Cathode Rays, III, 352.

Usher (F. L.) A Mechanism of Gelatinisation, 143.

Viscous fluid heated from below, stability (Low), 180.
Viscosity of gas, molecular forces (Hassé and Cook), 196.

Wake behind body of revolution (Swain), 647.
Ward (F. A. B.), Wynn-Williams (C. E.) and Cave (H. M.) The Rate of Emission of Alpha Particles from Radium, 713.
Watson (W. H.) The Effect of a Transverse Magnetic Field on the Propagation of Light in vacuo, 345.
Williams (E. J.) The Straggling of β-Particles, 420.
Wood (R. G.) *See* James and others.
Wright (Sir Almroth E.) Further Studies on Intertraction, 587.
Wynn-Williams (C. E.) *See* Ward and others.

X-ray generator, input limit (Müller), 507.

END OF THE ONE HUNDRED AND TWENTY-FIFTH VOLUME (SERIES A).

I. A. R. I. 75.

IMPERIAL AGRICULTURAL RESEARCH
INSTITUTE LIBRARY
NEW DELHI.

Date of issue.	Date of issue.	Date of issue.
४.१.५		
७.२.५		